

























**AERONAUTICS**

---

**FOURTEENTH ANNUAL REPORT**

OF THE

**NATIONAL ADVISORY COMMITTEE  
FOR AERONAUTICS**

---

**1928**

---

INCLUDING TECHNICAL  
REPORTS Nos. 283 to 308



UNITED STATES  
GOVERNMENT PRINTING OFFICE  
WASHINGTON : 1929

ADDITIONAL COPIES  
OF THIS PUBLICATION MAY BE PROCURED FROM  
THE SUPERINTENDENT OF DOCUMENTS  
U.S.GOVERNMENT PRINTING OFFICE  
WASHINGTON, D. C.  
AT  
\$1.25 PER COPY (PAPER COVERS)

## LETTER OF SUBMITTAL

---

*To the Congress of the United States:*

In compliance with the provisions of the act of March 3, 1915, establishing the National Advisory Committee for Aeronautics, I submit herewith the fourteenth annual report of the committee for the fiscal year ended June 30, 1928.

The attention of the Congress is invited to Part V of the committee's report presenting an outline of the present state of aeronautical development. It is encouraging to note from the committee's report that not only has aeronautic progress been at an accelerated rate within recent years but the progress has been greater in 1928 than in any single previous year. The significance of this to the American people and to the advancement of civilization can but faintly be pictured in the light of the amazing development that has characterized the first 25 years of aviation.

This country may well be proud of the contributions it has made to this remarkable development, and I am satisfied that continued support of proven policies will assure the further progress of American aviation. I concur in the committee's opinion that there is need for continuous prosecution of scientific research in order that this progress may continue at the maximum rate.

CALVIN COOLIDGE

THE WHITE HOUSE,  
*December 6, 1928.*





## LETTER OF TRANSMITTAL

---

NATIONAL ADVISORY COMMITTEE FOR AERONAUTICS,  
*Washington, D. C., November 20, 1928.*

MR. PRESIDENT: In compliance with the provisions of the act of Congress approved March 3, 1915 (Public, No. 271, 63d Cong.), I have the honor to transmit herewith the fourteenth annual report of the National Advisory Committee for Aeronautics for the fiscal year ended June 30, 1928.

The year 1928 marks the twenty-fifth anniversary of the first flight of an airplane. It is fitting that the Nation should pause to reflect on the wonderful development of aeronautics in the first quarter of a century of aviation. Improvement in the performance, efficiency, reliability, and safety of aircraft has been made at an accelerated rate within recent years, and it is noteworthy that in this, the twenty-fifth anniversary year, the progress should have been greater than in any previous year.

The National Advisory Committee for Aeronautics has jurisdiction over the scientific study of the fundamental problems of flight and is proud of the contributions it has made to this remarkable record of progress.

The status of the committee as a Government organization and the character of its functions have enabled it to attract the best scientific talent in aeronautics to service on its subcommittees without compensation and this has largely been responsible for the comprehensive character and general effectiveness of its research programs.

Attention is invited to Part V of the committee's report presenting an outline of the present state of aeronautical development. Emphasis is placed upon the need for continuous prosecution of scientific research in order that there may be continuous improvement in the safety and efficiency of aircraft both for military and civil purposes.

Respectfully submitted.

JOSEPH S. AMES,  
*Chairman.*

THE PRESIDENT,  
*The White House, Washington, D. C.*

## CONTENTS

---

Letter of submittal.....	Page III
Letter of transmittal.....	v
Fourteenth annual report.....	1

### PART I. ORGANIZATION

Functions of the committee.....	2
Organization of the committee.....	3
Meetings of the entire committee.....	3
The executive committee.....	3
Subcommittees.....	4
Quarters for committee.....	5
The Langley Memorial Aeronautical Laboratory.....	6
The Office of Aeronautical Intelligence.....	7
Financial report.....	8

### PART II. GENERAL ACTIVITIES

Method of analysis of aircraft accidents.....	9
Coordination of study of air-navigation problems.....	10
Consideration of aeronautical inventions.....	11
Relations with the aircraft industry.....	12
The Daniel Guggenheim Fund for the Promotion of Aeronautics.....	13
Conference of representatives of educational institutions actively engaged in aeronautical education.....	14
Coordination of aeronautical research in universities.....	14
Cooperation with British Aeronautical Research Committee.....	15
Cooperation of Army and Navy.....	15
Investigations undertaken for the Army and the Navy.....	16
American airship development.....	17

### PART III. REPORTS OF TECHNICAL COMMITTEES

Report of committee on aerodynamics.....	20
Report of committee on power plants for aircraft.....	33
Report of committee on materials for aircraft.....	48

### PART IV. TECHNICAL PUBLICATIONS OF THE COMMITTEE

Summaries of Technical Reports.....	58
List of Technical Notes issued during the past year.....	66
List of Technical Memorandums issued during the past year.....	67
List of Aircraft Circulars issued during the past year.....	70
Bibliography of aeronautics.....	71

### PART V. PRESENT STATE OF AERONAUTICAL DEVELOPMENT

Progress in technical development.....	72
Aerodynamics.....	72
Airplane structures.....	75
Airships.....	77
Aircraft engines.....	78
Summary.....	79
Conclusion.....	80



## TECHNICAL REPORTS

		Page
No. 283.	A Preliminary Investigation of Supercharging an Air-Cooled Engine in Flight. By Marsden Ware and Oscar W. Schey.....	81
No. 284.	The Comparative Performance of Roots Type Aircraft Engine Superchargers as Affected by Change in Impeller Speed and Displacement. By Marsden Ware and Ernest E. Wilson..	93
No. 285.	A Study of Wing Flutter. By A. F. Zahm and R. M. Bear.....	107
No. 286.	Aerodynamic Characteristics of Airfoils—V. By National Advisory Committee for Aeronautics .....	135
No. 287.	Theories of Flow Similitude. By A. F. Zahm.....	185
No. 288.	Pressure Distribution Over a Rectangular Monoplane Wing Model Up to 90° Angle of Attack. By Montgomery Knight and Oscar Loeser, jr.....	195
No. 289.	Forces on Elliptic Cylinders in Uniform Air Stream. By A. F. Zahm, R. H. Smith, and F. A. Louden.....	215
No. 290.	Water-Pressure Distribution on a Seaplane Float. By F. L. Thompson.....	233
No. 291.	Drag of C-Class Airship Hulls of Various Fineness Ratios. By A. F. Zahm, R. H. Smith, and F. A. Louden.....	249
No. 292.	Characteristics of Five Propellers in Flight. By J. W. Crowley, jr., and R. E. Mixson.....	265
No. 293.	Two Practical Methods for the Calculation of the Horizontal Tail Area Necessary for a Statically Stable Airplane. By Walter S. Diehl.....	289
No. 294.	The Measurement of Maximum Cylinder Pressures. By Chester W. Hicks.....	309
No. 295.	The Variation in Engine Power with Altitude Determined from Measurements in Flight with a Hub Dynamometer. By W. D. Gove.....	321
No. 296.	Pressure Distribution Tests on PW-9 Wing Models from -18° through 90° Angle of Attack. By Oscar E. Loeser, jr.....	333
No. 297.	Reduction of Observed Airplane Performance to Standard Conditions. By Walter S. Diehl..	355
No. 298.	Effect of Variation of Chord and Span of Ailerons on Rolling and Yawing Moments in Level Flight. By R. H. Heald and D. H. Strother .....	383
No. 299.	Investigation of Damping Liquids for Aircraft Instruments. By G. H. Keulegan.....	403
No. 300.	The Twenty-foot Propeller Research Tunnel of the National Advisory Committee for Aeronautics. Fred E. Weick and Donald H. Wood.....	427
No. 301.	Full Scale Tests of Wood Propellers on a VE-7 Airplane in the Propeller Research Tunnel. By Fred E. Weick .....	443
No. 302.	Full Scale Tests on a Thin Metal Propeller at Various Tip Speeds. By Fred E. Weick.....	463
No. 303.	An Investigation of the Use of Discharge Valves and an Intake Control for Improving the Performance of N. A. C. A. Roots Type Supercharger. By Oscar W. Schey and Ernest E. Wilson .....	477
No. 304.	An Investigation of the Aerodynamic Characteristics of an Airplane Equipped with Several Different Sets of Wings. By J. W. Crowley, jr., and M. W. Green.....	487
No. 305.	The Gaseous Explosive Reaction—A Study of the Kinetics of Composite Fuels. By F. W. Stevens.....	501
No. 306.	Full-Scale Wind-Tunnel Tests of a Series of Metal Propellers on a VE-7 Airplane. By Fred E. Weick.....	519
No. 307.	The Pressure Distribution Over the Horizontal and Vertical Tail Surfaces of the F6C-4 Pursuit Airplane in Violent Maneuvers. By R. V. Rhode.....	537
No. 308.	Aircraft Accidents. By Special Subcommittee of the National Advisory Committee for Aeronautics .....	557

## NATIONAL ADVISORY COMMITTEE FOR AERONAUTICS

3841 NAVY BUILDING, WASHINGTON, D. C.

---

JOSEPH S. AMES, Ph. D., *Chairman*,  
Provost Johns Hopkins University, Baltimore, Md.  
DAVID W. TAYLOR, D. Eng., *Vice Chairman*,  
Washington, D. C.  
CHARLES G. ABBOT, Sc. D.,  
Secretary Smithsonian Institution, Washington, D. C.  
GEORGE K. BURGESS, Sc. D.,  
Director Bureau of Standards, Washington, D. C.  
WILLIAM F. DURAND, Ph. D.,  
Professor Emeritus of Mechanical Engineering, Stanford University, California.  
JAMES E. FECHET, Major General, United States Army,  
Chief of Air Corps, War Department, Washington, D. C.  
WILLIAM E. GILLMORE, Brigadier General, United States Army,  
Chief, Matériel Division, Air Corps, Wright Field, Dayton, Ohio.  
EMORY S. LAND, Captain, United States Navy,  
Bureau of Aeronautics, Navy Department, Washington, D. C.  
CHARLES F. MARVIN, M. E.,  
Chief, United States Weather Bureau, Washington, D. C.  
WILLIAM A. MOFFETT, Rear Admiral, United States Navy,  
Chief, Bureau of Aeronautics, Navy Department, Washington, D. C.  
S. W. STRATTON, Sc. D.,  
President Massachusetts Institute of Technology, Cambridge, Mass.  
ORVILLE WRIGHT, Sc. D.,  
Dayton, Ohio.

---

GEORGE W. LEWIS, *Director of Aeronautical Research*.

JOHN F. VICTORY, *Secretary*.

HENRY J. E. REID, *Engineer in Charge, Langley Memorial Aeronautical Laboratory, Langley Field, Va.*

JOHN J. IDE, *Technical Assistant in Europe, Paris, France*.

---

### EXECUTIVE COMMITTEE

JOSEPH S. AMES, *Chairman*.

DAVID W. TAYLOR, *Vice Chairman*.

CHARLES G. ABBOT.  
GEORGE K. BURGESS.  
JAMES E. FECHET.  
WILLIAM E. GILLMORE.  
EMORY S. LAND.

CHARLES F. MARVIN.  
WILLIAM A. MOFFETT.  
S. W. STRATTON.  
ORVILLE WRIGHT.

JOHN F. VICTORY, *Secretary*.







NATIONAL ADVISORY COMMITTEE FOR AERONAUTICS  
SEMIANNUAL MEETING APRIL 18, 1929

*Left to right:* J. F. VICTORY, Secretary; DR. W. F. DURAND; DR. ORVILLE WRIGHT; DR. G. K. BURGESS; BRIG. GEN. W. E. GILLMORE; MAJ. GEN. J. E. FECHET; DR. JOSEPH S. AMES, Chairman; DR. D. W. TAYLOR, Vice Chairman; CAPT. E. S. LAND; REAR ADMIRAL W. A. MOFFETT; DR. S. W. STRATTON; DR. G. W. LEWIS, Director of Aeronautical Research; DR. CHARLES F. MARVIN. (One member absent—DR. CHARLES G. ABBOT.)



# FOURTEENTH ANNUAL REPORT

## OF THE

# NATIONAL ADVISORY COMMITTEE FOR AERONAUTICS

---

WASHINGTON, D. C., November 20, 1928.

*To the Congress of the United States:*

In accordance with the act of Congress approved March 3, 1915, establishing the National Advisory Committee for Aeronautics, the committee submits herewith its fourteenth annual report for the fiscal year 1928.

The year 1928 marks the twenty-fifth anniversary of the first successful flight of an airplane, designed and built by the Wright brothers and flown at Kitty Hawk, N. C., December 17, 1903. The quarter of a century that has intervened has witnessed remarkable progress in the development and use of aircraft for military and civil purposes. During recent years the rate of progress has been accelerated. During the year 1928 greater progress was made than in any single year since the first successful flight of man in a power-driven heavier-than-air flying machine.

This report is submitted in five parts. Part I describes the organization of the committee, states its functions, outlines the facilities available under the committee's direction for the conduct of scientific research in aeronautics, explains the activities and growth of the Office of Aeronautical Intelligence in the collection, analysis, and dissemination of scientific and technical data, and presents a financial report of expenditures during the fiscal year ended June 30, 1928.

In Part II of this report the committee describes its general activities, including the coordination of the study of air-navigation problems, the analysis of aircraft accidents, the consideration of aeronautical inventions and designs, the coordination of aeronautical research in universities, and the cooperation with other governmental agencies and with the industry.

In Part III the committee presents the reports of its standing technical subcommittees on aerodynamics, power plants for aircraft, and materials for aircraft, which include statements of the organization and the functions of each and of the progress of investigations conducted under their general cognizance in laboratories, governmental and private.

In Part IV the committee presents summaries of the Technical Reports published during the past year and enumerates by title the Technical Notes, Technical Memorandums, and Aircraft Circulars issued.

In Part V the committee presents its views as to the present state of aeronautical development with special reference to the technical development of aircraft. The report closes with a summary of the progress made during the past year and of the factors that have contributed to the advancement of American aeronautics.

# PART I

## ORGANIZATION

---

### FUNCTIONS OF THE COMMITTEE

The National Advisory Committee for Aeronautics was established by act of Congress approved March 3, 1915. The organic act charged the committee with the supervision and direction of the scientific study of the problems of flight with a view to their practical solution, the determination of problems which should be experimentally attacked, and their investigation and application to practical questions of aeronautics. The act also authorized the committee to direct and conduct research and experimentation in aeronautics in such laboratory or laboratories, in whole or in part, as may be placed under its direction.

Supplementing the prescribed duties of the committee under its organic act, its broad general functions may be stated as follows:

First. Under the law the committee holds itself at the service of any department or agency of the Government interested in aeronautics, for the furnishing of information or assistance in regard to scientific or technical matters relating to aeronautics, and in particular for the investigation and study of fundamental problems submitted by the War and Navy Departments with a view to their practical solution.

Second. The committee may also exercise its functions for any individual, firm, association, or corporation within the United States, provided that such individual, firm, association, or corporation defray the actual cost involved.

Third. The committee institutes research, investigation, and study of problems which, in the judgment of its members or of the members of its various subcommittees, are needful and timely for the advance of the science and art of aeronautics in its various branches.

Fourth. The committee keeps itself advised of the progress made in research and experimental work in aeronautics in all parts of the world, particularly in England, France, Italy, Germany, and Canada.

Fifth. The information thus gathered is brought to the attention of the various subcommittees for consideration in connection with the preparation of programs for research and experimental work in this country. This information is also made available promptly to the military and naval air organizations and other branches of the Government, and such as is not confidential is immediately released to university laboratories and aircraft manufacturers interested in the study of specific problems, and also to the public.

Sixth. The committee holds itself at the service of the President, the Congress, and the executive departments of the Government for the consideration of special problems which may be referred to it.

By act of Congress approved July 2, 1926 (Public, No. 446, 69th Cong.), and amended March 3, 1927 (Public, No. 748, 69th Cong.), the committee was given an additional function. This legislation created and specified the functions of an Aeronautical Patents and Design Board, consisting of an Assistant Secretary of War, an Assistant Secretary of the Navy, and an Assistant Secretary of Commerce, and provided that upon favorable recommendation of the National Advisory Committee for Aeronautics the Patents and Design Board shall determine questions as to the use and value to the Government of aeronautical inventions submitted to any branch of the Government. The legislation provided that designs submitted to the board should be referred to the National Advisory Committee for Aeronautics for its recommendation and this has served to impose upon the committee the additional duty of considering on behalf of the Government all aeronautical inventions and designs submitted.



### ORGANIZATION OF THE COMMITTEE

The committee has 12 members, appointed by the President. The law provides that the personnel of the committee shall consist of two members from the War Department, from the office in charge of military aeronautics; two members from the Navy Department, from the office in charge of naval aeronautics a representative each of the Smithsonian Institution, the United States Weather Bureau, and the United States Bureau of Standards; and not more than five additional persons acquainted with the needs of aeronautical science, either civil or military, or skilled in aeronautical engineering or its allied sciences. The law further provides that all members as such shall serve without compensation.

On December 13, 1927, Maj. Gen. Mason M. Patrick, formerly Chief of the Air Corps, was relieved from membership on his retirement from active service in the Army, and Maj. Gen. James E. Fechet, his successor as Chief of the Air Corps, was, on January 6, 1928, appointed to succeed him as a member of the National Advisory Committee for Aeronautics.

Dr. Charles G. Abbot, Secretary of the Smithsonian Institution, was, under date of June 29, 1928, appointed a member of the committee to fill the vacancy caused by the death in February, 1927, of Dr. Charles D. Walcott.

The entire committee meets twice a year, the annual meeting being held in October and the semiannual meeting in April. The present report includes the activities of the committee between the annual meeting held on October 20, 1927, and that held on October 18, 1928.

The organization of the committee at the close of the past year was as follows:

Joseph S. Ames, Ph. D., chairman.

David W. Taylor, D. Eng., vice chairman.

Charles G. Abbot, Sc. D.

George K. Burgess, Sc. D.

William F. Durand, Ph. D.

Maj. Gen. James E. Fechet, United States Army.

Brig. Gen. William E. Gillmore, United States Army.

Capt. Emory S. Land, United States Navy.

Charles F. Marvin, M. E.

Rear Admiral William A. Moffett, United States Navy.

S. W. Stratton, Sc. D.

Orville Wright, Sc. D.

### MEETINGS OF THE ENTIRE COMMITTEE

The semiannual meeting of the entire committee was held on April 19, 1928, at the committee's headquarters in Washington, and the annual meeting on October 18, 1928, also at the committee's headquarters. At these meetings the general progress in aeronautical research was reviewed and the problems which should be experimentally attacked were discussed. Administrative reports were submitted by the secretary, Mr. John F. Victory, and by the Director of the Office of Aeronautical Intelligence, Dr. Joseph S. Ames.

At both the annual and the semiannual meetings Doctor Ames, as chairman of the executive committee, presented detailed reports of the research work being conducted by the committee at the Langley Memorial Aeronautical Laboratory, Langley Field, Hampton, Va., and exhibited charts and photographs showing the methods used and the results obtained in the more important investigations.

The election of officers was the concluding feature of the annual meeting. The officers of the committee were reelected for the ensuing year, as follows: Chairman, Dr. Joseph S. Ames; vice chairman, Dr. David W. Taylor; chairman executive committee, Dr. Joseph S. Ames.

### THE EXECUTIVE COMMITTEE

For carrying out the work of the Advisory Committee the regulations provide for the election annually of an executive committee, to consist of seven members, and to include in addition any member of the Advisory Committee not otherwise a member of the executive



committee, but resident in or near Washington, and giving his time wholly or chiefly to the special work of the committee. The present organization of the executive committee is as follows:

Joseph S. Ames, Ph. D., chairman.  
 David W. Taylor, D. Eng., vice chairman.  
 Charles G. Abbot, Sc. D.  
 George K. Burgess, Sc. D.  
 Maj. Gen. James E. Fechet, United States Army.  
 Brig. Gen. William E. Gillmore, United States Army.  
 Capt. Emory S. Land, United States Navy.  
 Charles F. Marvin, M. E.  
 Rear Admiral William A. Moffett, United States Navy.  
 S. W. Stratton, Sc. D.  
 Orville Wright, Sc. D.

The executive committee, in accordance with general instructions of the Advisory Committee, exercises the functions prescribed by law for the whole committee, administers the affairs of the committee, and exercises general supervision over all its activities.

On November 25, 1927, the executive committee, on invitation of Admiral Moffett, held a meeting at the naval aircraft factory, Philadelphia, and following the meeting inspected the aircraft carrier, U. S. S. *Saratoga*, which was at the Philadelphia Navy Yard at that time.

The executive committee has organized the necessary clerical and technical staffs for handling the work of the committee proper. General responsibility for the execution of the policies and the direction of the activities as approved by the executive committee is vested in the Director of Aeronautical Research, Mr. George W. Lewis. He has immediate charge of the scientific and technical work of the committee, being directly responsible to the chairman of the executive committee, Dr. Joseph S. Ames. The secretary, Mr. John F. Victory, is ex officio secretary of the executive committee, directs the administrative work of the organization, and exercises general supervision over the expenditures of funds and the employment of personnel.

#### SUBCOMMITTEES

In order to facilitate the conduct of its work the executive committee has organized nine standing subcommittees, as follows:

Aerodynamics.  
 Power plants for aircraft.  
 Materials for aircraft.  
 Problems of air navigation.  
 Aircraft accidents.  
 Aeronautical inventions and designs.  
 Publications and intelligence.  
 Personnel, buildings, and equipment.  
 Governmental relations.

The organization and work of the technical committees on aerodynamics, power plants for aircraft, and materials for aircraft are covered in the reports of those committees in Part III of this report.

The committee on problems of air navigation and the committee on aircraft accidents have recently been established in response to needs which have been gradually increasing during the past few years. A statement as to the organization, functions, and activities of the committee on problems of air navigation is included under the subject of coordination of study of air navigation problems in Part II of this report, while an account of the activities leading to the establishment of the committee on aircraft accidents will be found under the subject of methods of analysis of aircraft accidents, and the work of the committee on aeronautical inventions and designs is included under the subject of the consideration of aeronautical inventions, also in Part II.



Statements of the organization and functions of the administrative committees on publications and intelligence; personnel, buildings, and equipment; and governmental relations, follow:

#### COMMITTEE ON PUBLICATIONS AND INTELLIGENCE

##### FUNCTIONS

1. The collection, classification, and diffusion of technical knowledge on the subject of aeronautics, including the results of research and experimental work done in all parts of the world.
2. The encouragement of the study of the subject of aeronautics in institutions of learning.
3. Supervision of the Office of Aeronautical Intelligence.
4. Supervision of the committee's foreign office in Paris.
5. The collection and preparation for publication of the Technical Reports, Technical Notes, Technical Memorandums, and Aircraft Circulars of the Committee.

##### ORGANIZATION

Dr. Joseph S. Ames, chairman.  
Prof. Charles F. Marvin, vice chairman.  
Miss M. M. Muller, secretary.

#### COMMITTEE ON PERSONNEL, BUILDINGS, AND EQUIPMENT

##### FUNCTIONS

1. To handle all matters relating to personnel, including the employment, promotion, discharge, and duties of all employees.
2. To consider questions referred to it and make recommendations regarding the initiation of projects concerning the erection or alteration of laboratories and offices.
3. To meet from time to time on the call of the chairman and report its actions and recommendations to the executive committee.
4. To supervise such construction and equipment work as may be authorized by the executive committee.

##### ORGANIZATION

Dr. Joseph S. Ames, chairman.  
Dr. David W. Taylor, vice chairman.  
Prof. Charles F. Marvin.  
John F. Victory, secretary.

#### COMMITTEE ON GOVERNMENTAL RELATIONS

##### FUNCTIONS

1. Relations of the committee with executive departments and other branches of the Government.
2. Governmental relations with civil agencies.

##### ORGANIZATION

Prof. Charles F. Marvin, chairman.  
Dr. David W. Taylor.  
John F. Victory, secretary.

#### QUARTERS FOR COMMITTEE

The headquarters of the National Advisory Committee for Aeronautics are located in the rear of the eighth wing, third floor, of the Navy Building, Eighteenth and B Streets NW., Washington, D. C., in close proximity to the Army and Navy air organizations. This space has been officially assigned for the use of the committee by the Public Buildings Commission. The administrative office is also the headquarters of the various subcommittees and of the Office of Aeronautical Intelligence.



Field stations of the committee are the Langley Memorial Aeronautical Laboratory, at Langley Field, Hampton, Va., and the office of the technical assistant in Europe is located at the American Embassy in Paris.

The scientific investigations authorized by the committee are not all conducted at the Langley Memorial Aeronautical Laboratory, but the facilities of other governmental laboratories and shops are utilized as well as the laboratories connected with institutions of learning whose cooperation in the scientific study of specific problems in aeronautics has been secured.

#### THE LANGLEY MEMORIAL AERONAUTICAL LABORATORY

The Langley Memorial Aeronautical Laboratory is operated under the direct control of the committee. It is located at Langley Field, Va., on a plot of ground set aside by the War Department for the committee's use. The laboratory was started in 1916 coincident with the establishment of Langley Field.

The laboratory is organized with five divisions, as follows: Aerodynamics division, power plants division, technical service division, flight operations division, and property and clerical division. The administration of the laboratory is under the immediate direction of an engineer in charge, Mr. Henry J. E. Reid, subject to the general supervision of the officers of the committee.

The laboratory consists of seven buildings—a research laboratory building, containing the administrative offices, the technical library, the photographic laboratory, and the headquarters of the aerodynamics, power plants, technical service, and flight operations divisions; two aerodynamical laboratories, one containing a wind tunnel of the standard type and the other a variable-density wind tunnel, each laboratory being complete in itself; two engine dynamometer laboratories of a semipermanent type, both equipped to carry on investigations in connection with power plants for aircraft; an airplane hangar with a repair shop and facilities for taking care of airplanes used in flight research; and a service building, containing an instrument laboratory, drafting room, machine and woodworking shops, and storeroom.

In addition to the above, the laboratory equipment includes a propeller research tunnel in which a velocity of 100 miles per hour may be obtained in a 20-foot air stream.

During the past year the committee has rebuilt the interior structure of the variable-density wind tunnel, which was destroyed by fire on August 1, 1927, the design of the tunnel being changed to an open-throat type. With the experience gained in wind-tunnel design since the construction of the variable-density tunnel in 1922, it was possible to incorporate features which resulted in greater efficiency from the standpoint of power required, ease of operation, accessibility of apparatus, and quality of air flow. The new construction is entirely of metal and all wiring is in conduit, thus eliminating the fire hazard.

A research balance of an entirely new design to insure greater reliability, accuracy, and adaptability for model tests, is being assembled outside of the tunnel for adjustment before its installation. In the meantime, however, drag tests have been made with the auxiliary drag balance which was not destroyed by the fire, and a series of pressure distribution tests with special recording instruments has been made at 20 atmospheres pressure.

In line with the improvement in efficiency of the variable-density tunnel a step was taken toward the utilization of the waste air. A high-speed wind tunnel has been designed and constructed, using the injector principle to create the flow. The waste air from the variable-density tunnel is thus utilized to produce speeds in excess of 1,200 feet per second or 800 miles per hour in the test chamber, which is 12 inches in diameter. Before this tunnel is placed in operation, however, a study will be made to determine the most efficient form of chamber.

To carry on more efficiently the study of ice formation in flight a 6-inch wind tunnel was built with means for refrigerating the air. In this tunnel a study of the conditions for ice formation will be made with a view to determining means for preventing the formation of ice on aircraft.



Recognition by the Government of the necessity of satisfying the increasing demand for new and accurate knowledge on the fundamental problems of flight has made possible the development of the Langley Memorial Aeronautical Laboratory as an efficient research organization numbering 168 employees at the close of the fiscal year 1928. The work of the laboratory is conducted without interference with military operations at the field. In fact, there is a splendid spirit of cooperation on the part of the military authorities, who by their helpfulness in many ways have aided the committee materially in its work.

#### THE OFFICE OF AERONAUTICAL INTELLIGENCE

The Office of Aeronautical Intelligence was established in the early part of 1918 as an integral branch of the committee's activities. Its functions are the collection, classification, and diffusion of technical knowledge on the subject of aeronautics to the military and naval air services, aircraft manufacturers, educational institutions, and others interested, including the results of research and experimental work conducted in all parts of the world. It is the officially designated Government depository for scientific and technical reports and data on aeronautics.

Promptly upon receipt, all reports are analyzed, classified, and brought to the special attention of the subcommittees having cognizance and to the attention of other interested parties through the medium of public and confidential bulletins. Reports are duplicated where practicable, and distributed upon request. Confidential bulletins and reports are not circulated outside of Government channels.

To handle efficiently the work of securing and exchanging reports in foreign countries, the committee maintains a technical assistant in Europe, with headquarters at the American Embassy in Paris. It is his duty to visit the Government and private laboratories, centers of aeronautical information, and private individuals in England, France, Italy, Germany, and other European countries, and endeavor to secure for America not only printed matter which would in the ordinary course of events become available in this country, but more especially to secure advance information as to work in progress and any technical data not prepared in printed form and which would otherwise not reach this country. John Jay Ide, of New York, has served as the committee's technical assistant in Europe since April, 1921.

The records of the committee show that during the past year copies of technical reports were distributed as follows:

Committee and subcommittee members.....	1, 398
Langley Memorial Aeronautical Laboratory.....	1, 984
Paris office of the committee.....	4, 596
Army Air Corps.....	2, 254
Naval Air Service, including Marine Corps.....	4, 062
Manufacturers.....	10, 328
Educational institutions.....	6, 784
Bureau of Standards.....	472
Miscellaneous.....	38, 785
Total distribution.....	70, 663

The above figures include the distribution of 20,867 Technical Reports, 15,076 Technical Notes, 19,136 Technical Memorandums, and 8,448 Aircraft Circulars of the National Advisory Committee for Aeronautics. Part IV of this report presents the titles of the publications issued during the past year the distribution of which is included in the foregoing figures. A total of 10,714 written requests for reports were received during the year in addition to innumerable telephone and personal requests, and 49,540 reports were distributed upon request.

## FINANCIAL REPORT

The appropriation for the National Advisory Committee for Aeronautics for the fiscal year 1928, as carried in the independent offices appropriation act approved May 16, 1928, was \$537,000, under which the committee reports expenditures and obligations during the year amounting to \$529,144.54, itemized as follows:

Personal services.....	\$387, 372. 16
Supplies and materials.....	29, 066. 58
Communication service.....	1, 008. 16
Travel expenses.....	12, 610. 09
Transportation of things.....	1, 244. 50
Furnishing of electricity.....	5, 636. 26
Rent of office (Paris).....	913. 43
Repairs and alterations.....	21, 225. 27
Special investigations and reports.....	39, 800. 00
Equipment.....	30, 268. 09
<hr/>	
Expenditures.....	529, 144. 54
Reserve, "Two Per Cent Club".....	7, 665. 33
Unobligated balance.....	190. 13
<hr/>	
Total.....	537, 000. 00

In addition to the above, the committee had a separate appropriation of \$13,000 for printing and binding, of which \$12,962.11 was expended.



## PART II

### GENERAL ACTIVITIES

---

#### METHOD OF ANALYSIS OF AIRCRAFT ACCIDENTS

In response to request of Assistant Secretary of the Navy Edward P. Warner, on behalf of the air coordination committee, which consists of the Assistant Secretaries for Aeronautics in the Departments of War, Navy, and Commerce, the National Advisory Committee for Aeronautics established on March 1, 1928, a special committee on the nomenclature, subdivision, and classification of aircraft accidents, for the purpose of preparing a basis for the classification and comparison of aircraft accidents, both civil and military. The request of the air coordination committee was the result of recognition of the difficulty of drawing correct conclusions from efforts to analyze and compare reports on aircraft accidents prepared by different organizations, owing to the different classifications and definitions used.

The membership of the special committee was as follows:

*Representatives of the National Advisory Committee for Aeronautics:*

Dr. George K. Burgess, chairman.

Mr. G. W. Lewis.

*Representatives of the Army Air Corps:*

Lieut. D. B. Phillips, United States Army.

Lieut. J. D. Barker, United States Army.

*Representatives of the Bureau of Aeronautics of the Navy:*

Lieut. Commander L. C. Stevens (C. C.), United States Navy.

Lieut. Charles R. Brown, United States Navy.

*Representatives of the Aeronautics Branch of the Department of Commerce:*

Mr. Daniel de R. Scarritt (later succeeded by Mr. Edward P. Howard).

Mr. Lester T. Bradbury.

In the work of the committee assistance was also rendered by Mr. E. M. Kintz, of the Aeronautics Branch of the Department of Commerce, and Mr. Starr Truscott, of the National Advisory Committee for Aeronautics, who attended most of the meetings, and, in the consideration of the physiological aspects of aviation, by Dr. L. H. Bauer, of the Aeronautics Branch, and Lieut. Commander John R. Poppen (M. C.), United States Navy.

Various methods of analyzing aircraft accidents, including study and classification by (a) the immediate causes, (b) the underlying causes, (c) the nature, and (d) the results of the accidents, were considered by the committee, and discussed in detail. A plan devised by Lieutenant Phillips and Lieutenant Brown for the division of the immediate causes of aircraft accidents into four major classes and for the further subdivision of these major classes as seemed desirable, together with proposed definitions of these classes and subdivisions, was submitted for consideration at the first meeting. This plan was carefully considered by the committee at a number of meetings, and modifications were made so as to provide for every type of aircraft accident in the light of the experience of the members in classifying and analyzing accidents in the Government services.

The meeting of May 22, 1928, was attended by Wing Commander T. G. Hetherington, air attaché, British Embassy; Lieut. Yoshitake Miwa, Imperial Japanese Navy, assistant naval attaché, Japanese Embassy; Commander Silvio Scaroni, air attaché, Italian Embassy; Maj. Georges Thenault, assistant military attaché for aeronautics, French Embassy. At this meeting the method of analyzing aircraft accidents according to immediate causes was explained and the



value of a uniform system for reporting accidents was discussed. It was suggested that the representatives of the foreign governments consult with the personnel in their governments who were responsible for analyzing and reporting aircraft accidents, regarding the possibility of adopting the proposed method and form. Great interest was expressed and it was the opinion of those present that the adoption of a uniform system would be advantageous. The representatives of the foreign governments were invited to submit comments and suggestions for changes, and it is hoped that this will result in the establishment of a procedure for the international exchange of information regarding aircraft accidents.

In working out the method of analysis, the committee tried to provide a plan which would permit of the careful analysis of aircraft accidents from the point of view of both personnel and matériel problems. The plan permits of the analysis of a particular accident into two or more distinct causes, and makes possible, by the use of percentages, the indication of the relative weight of each cause. The system provides also for the analysis of crashes according to the nature of the accident (take-off accidents, tail spins following engine failure, etc.), the degree of seriousness of personnel injuries, and amount of damage occurring to matériel, and, through the use of a cross-analysis method, allows for the analysis of pilot errors and matériel failures according to the underlying causes of these errors or failures. All these bases of analysis have been combined into a single chart, intended to be used in the study of each individual accident. In this way a method is provided for the analysis of aircraft accidents of different organizations on the same basis, so that the records will be comparable and the preparation of a composite report of all aircraft accidents will be possible. It is believed that if all aircraft accidents occurring in all agencies are classified in the manner recommended, a composite of all the accidents will offer a basis upon which a study may be made and correct conclusions drawn.

At its last meeting, held on July 17, 1928, the committee adopted its final report, presenting the analysis chart and describing in detail the method proposed. This report was approved by the executive committee of the National Advisory Committee for Aeronautics on October 3, 1928, and has been published as Technical Report No. 308 of the Advisory Committee. The method of analysis set forth therein has been adopted for use by the Army Air Corps, the Bureau of Aeronautics of the Navy, and the Aeronautics Branch of the Department of Commerce.

In accordance with recommendation of the special committee, the National Advisory Committee for Aeronautics has reorganized the personnel of the special committee on the nomenclature, subdivision, and classification of aircraft accidents into a standing committee on aircraft accidents for the consideration of questions as to the interpretation of the method of analysis, and for the study of information obtained as a result of this analysis.

#### COORDINATION OF STUDY OF AIR-NAVIGATION PROBLEMS

During the past year the attention of the committee has been invited to the need for the coordination of scientific research being conducted by a number of different agencies, both within and without the Government, on the problems of air navigation, particularly in the fields of navigation instruments, aerial communications, and meteorological problems. It is the function of the Department of Commerce to provide aids to air navigation, but the coordination of fundamental scientific research on the problems of air navigation falls within the scope of the functions of the National Advisory Committee for Aeronautics as stated in the act establishing the committee, which provides "That it shall be the duty of the Advisory Committee for Aeronautics to supervise and direct the scientific study of the problems of flight, with a view to their practical solution, and to determine the problems which should be experimentally attacked, and to discuss their solution and their application to practical questions."

In order to provide for the coordination of these activities, the committee organized, in August, 1928, a new standing committee on problems of air navigation, with members representing the principal agencies concerned with the development of aids to air navigation. The membership of this committee is as follows:

Dr. Joseph S. Ames, Johns Hopkins University, chairman.

Dr. L. J. Briggs, Bureau of Standards.



Dr. Edward B. Craft, American Telephone & Telegraph Co.  
Brig. Gen. B. D. Foulois, United States Army.  
Paul Henderson, National Air Transport (Inc.).  
Capt. S. C. Hooper, United States Navy.  
Dr. J. C. Hunsaker, Goodyear-Zeppelin Corporation.  
Capt. E. S. Land, the Daniel Guggenheim Fund for the Promotion of Aeronautics.  
George W. Lewis, National Advisory Committee for Aeronautics (ex officio member).  
Col. Charles A. Lindbergh.  
Prof. Charles F. Marvin, Weather Bureau.  
C. M. Young, Aeronautics Branch, Department of Commerce.

In order that the large and varied field of research on air-navigation problems may be effectively covered, three subcommittees have been organized under the committee on problems of air navigation, as follows:

*Subcommittee on problems of communication:*

Dr. Edward B. Craft, American Telephone & Telegraph Co., chairman.  
Maj. William R. Blair, Signal Corps, United States Army.  
Dr. J. H. Dellinger, Bureau of Standards.  
Dr. J. C. Hunsaker, Goodyear-Zeppelin Corporation.  
George W. Lewis, National Advisory Committee for Aeronautics (ex officio member).  
J. L. McQuarrie, International Telephone & Telegraph Co.  
C. J. Pannill, Radiomarine Corporation of America.  
Lieut. Commander W. J. Ruble, United States Navy.  
Eugene Sibley, Aeronautics Branch, Department of Commerce.

*Subcommittee on instruments:*

Dr. L. J. Briggs, Bureau of Standards, chairman.  
Marshall S. Boggs, Aeronautics Branch, Department of Commerce.  
Dr. W. G. Brombacher, Bureau of Standards.  
Dr. Samuel Burka, Dayton, Ohio.  
Charles H. Colvin, Society of Automotive Engineers.  
Lieut. A. F. Hegenberger, United States Army, Matériel Division, Air Corps, Wright Field.  
Dr. A. W. Hull, General Electric Co.  
Carl Keuffel, Keuffel & Esser Co.  
George W. Lewis, National Advisory Committee for Aeronautics (ex officio member).  
Lieut. T. C. Lonquest, United States Navy.  
Henry J. E. Reid, National Advisory Committee for Aeronautics.

*Subcommittee on meteorological problems:*

Prof. Charles F. Marvin, Weather Bureau, chairman.  
Thomas H. Chapman, Aeronautics Branch, Department of Commerce.  
Dr. W. R. Gregg, Weather Bureau.  
Dr. W. J. Humphreys, Weather Bureau.  
Dr. J. C. Hunsaker, Goodyear-Zeppelin Corporation.  
George W. Lewis, National Advisory Committee for Aeronautics (ex officio member).  
Lieut. F. W. Reichelderfer, United States Navy.  
Dr. C. G. Rossby, the Daniel Guggenheim Fund for the Promotion of Aeronautics.  
Capt. Bertram J. Sherry, Signal Corps, United States Army.

#### CONSIDERATION OF AERONAUTICAL INVENTIONS

By act of Congress approved July 2, 1926, a Patents and Design Board was created, and it was provided that upon recommendation of the National Advisory Committee for Aeronautics the board should determine questions as to the use and value to the Government of aeronautical inventions submitted to the Government. By act of Congress approved March 3, 1927, the act of July 2, 1926, was amended in such a manner as to limit the board to the con-



sideration of such cases as were favorably recommended to it by the National Advisory Committee for Aeronautics. This relieved the board of the burden of considering cases which were unfavorably recommended by the committee, but at the same time it made the National Advisory Committee for Aeronautics responsible for the final disapproval of the large majority of the devices submitted as applications for awards.

In order to discharge the duties devolving upon the committee under this legislation, a committee on aeronautical inventions and designs was created, with the following membership:

Dr. D. W. Taylor, chairman.

Dr. George K. Burgess, vice chairman.

Capt. E. S. Land, United States Navy.

Prof. Charles F. Marvin.

J. F. Victory, secretary.

The committee on aeronautical inventions and designs considers such inventions or designs as are deemed by the Director of Aeronautical Research to be worthy of favorable recommendation to the Aeronautical Patents and Design Board or as he desires to bring to the attention of the committee for its action. The Director of Aeronautical Research is authorized to submit any unfavorable recommendations direct to the Aeronautical Patents and Design Board, but any favorable recommendations must be considered and made by the committee on aeronautical inventions and designs.

Under the present procedure careful consideration is given to all inventions and designs submitted. The Aeronautical Patents and Design Board and the National Advisory Committee for Aeronautics are working in harmony and the burden of considering large numbers of inventions is placed so as to reduce the demands on the time of the members of the committee on aeronautical inventions and designs and of the members of the Aeronautical Patents and Design Board to the consideration of submissions which have received competent preliminary examination and are deemed worthy of further consideration.

In the second year of the operation of the Aeronautical Patents and Design Board the committee received about 2,200 letters relating to inventions. Of these, about 1,000 represented wholly new submissions. Of the number submitted for the consideration of the Aeronautical Patents and Design Board—approximately 200—the committee has submitted to the board reports and recommendations in 182 cases, which included favorable recommendation in one case only. The remaining cases were submitted for the direct consideration of the committee and consequently have been disposed of by direct correspondence with the submitters. One case, originally submitted only for the consideration of the committee, was considered to be worthy of consideration by the Aeronautical Patents and Design Board, and was so recommended to the board.

#### RELATIONS WITH THE AIRCRAFT INDUSTRY

In order to give the representatives of the aircraft industry an opportunity to become familiar with the facilities of the committee's laboratory and the type of investigations conducted there, and to encourage the representatives of the industry to present fundamental problems arising out of commercial aeronautics with a view to their possible incorporation in the committee's research program, the committee in 1926 inaugurated a policy of holding at its laboratory annual conferences between its representatives and the representatives of the industry.

In accordance with this policy, the Third Annual Aircraft Engineering Research Conference was held at the Langley Memorial Aeronautical Laboratory, Langley Field, Hampton, Va., on May 15, 1928. In addition to the aircraft manufacturers and operators, educational institutions engaged in aeronautical education and aeronautical trade journals were invited to send representatives. The committee was represented by eight of its members, its subcommittees on aerodynamics and power plants for aircraft, and members of its technical staff. Dr. Joseph S. Ames, chairman of the National Advisory Committee for Aeronautics, presided



At the morning session of the conference the functions and work of the committee were briefly explained, after which the representatives of the industry were conducted on a tour of inspection of the facilities of the laboratory and the investigations in progress. Among the more interesting developments explained or demonstrated were the investigation in flight of airplane maneuverability, the development of a nonspinning wing, the redesigned variable-density wind tunnel, the study in the propeller research tunnel of the cowling and cooling of air-cooled engines, the study of ice formation on aircraft in flight, the development of a 2-stroke cycle gasoline injection engine, the investigation of a 4-stroke cycle oil injection engine, and the development of the improved Roots type supercharger. A small water tunnel recently constructed for the testing of airfoil models at high Reynolds Number and a small demonstration model of a high-speed jet wind tunnel designed to operate on exhaust air from the variable-density wind tunnel were shown in operation.

The afternoon session was devoted to the discussion of the problems of commercial aeronautics, and 30 problems were presented, chiefly by representatives of the industry. Many of these problems were already being investigated by the committee, and the work in progress on these particular investigations was explained by members of the committee's staff. Among the problems discussed were control of airplanes at low speeds; study of wing slots; design factors of propellers; study of load factors for landing gears; effect on airplane performance of changes in tail surface areas and shapes; effect on drag of use of corrugated surface for fuselage and wings; study of downwash; application of study of maneuverability to commercial operation of airplanes; investigation of loads and pressure distribution in commercial flying, especially in rough air; silencing the airplane; heating and ventilation of closed cabin airplanes; comfortable seating of passengers and elimination of vibration; relation between maneuverability and control of an airplane and steadiness of flight in rough air; and landing characteristics as affected by heavy load. All the problems suggested have since been carefully considered by the committee on aerodynamics, and two of them—study of the mutual interference of airplane parts, including the effect of the use of fillets, and study of the effect of the position of the propeller with reference to the wings—have been incorporated in the committee's research program, while others are being given further consideration for investigation in the near future.

At the close of the afternoon session, in accordance with arrangements agreed upon between the Navy and the National Advisory Committee, a number of the members of the conference made flights in the Navy NY training type airplane equipped with Handley-Page automatic slots.

#### THE DANIEL GUGGENHEIM FUND FOR THE PROMOTION OF AERONAUTICS

The committee is pleased to note that Capt. Emory S. Land, Construction Corps, United States Navy, a member of the National Advisory Committee for Aeronautics, has become vice president and treasurer of the Daniel Guggenheim Fund for the Promotion of Aeronautics. The fund has continued its useful activities in the field of aeronautics during the past year, and has provided practical and substantial assistance to aviation in its commercial, industrial, and scientific aspects.

The fund has also continued its financial support of educational institutions offering courses in aeronautical engineering, with a view to making available in all sections of the country schools adequately equipped to give instruction along this line. This financial assistance has been rendered to the Massachusetts Institute of Technology, at Cambridge; New York University, in New York City; the University of Michigan, at Ann Arbor; Stanford University, California; and the California Institute of Technology, at Pasadena. The fund also sponsored a conference of representatives of these institutions in Washington on April 27, 1928, for the interchange of ideas relating to educational methods and research to be conducted.

The safe-aircraft competition inaugurated by the fund last year has been continued. This competition was initiated for the purpose of carrying out the primary aim of the fund, the promotion of safety in flying, and has led to efforts on the part of manufacturers and designers to make safer airplanes.



The fund has continued also its study of the problem of flying and landing in fog, and by means of a committee appointed for the purpose has accomplished much toward the coordination of activities along this line.

Another important activity of the fund during the past year was the joint sponsorship with the National Safety Council of a National Congress on Safety in Aviation, which was held in New York City on October 4 and 5, 1928. This conference was attended by representatives of most of the organizations in this country concerned with aeronautics, and problems relating to the promotion of safety in ground installations as well as in flight were discussed.

#### CONFERENCE OF REPRESENTATIVES OF EDUCATIONAL INSTITUTIONS ACTIVELY ENGAGED IN AERONAUTICAL EDUCATION

In continuation of a policy inaugurated more than a year ago, the Daniel Guggenheim Fund for the Promotion of Aeronautics held, on April 27, 1928, its second conference of representatives of educational institutions actively engaged in aeronautical education, for the purpose of interchanging ideas relative to educational methods, coordinating research work, and developing specialized courses in aeronautical education. The following educational institutions were represented:

- Massachusetts Institute of Technology.
- New York University.
- Stanford University.
- California Institute of Technology.
- University of Michigan.
- University of Toronto.

The Navy Department and the National Advisory Committee for Aeronautics were also represented.

Dr. William F. Durand, a member of the Daniel Guggenheim Fund for the Promotion of Aeronautics and a member and past chairman of the National Advisory Committee for Aeronautics, acted as chairman of the conference. Upon the request of Doctor Durand the committee gave the use of its conference room for the meeting.

The conference considered first the subject of an encyclopedia of aeronautics, and it was believed that there would be a field of usefulness for a work of an encyclopedic character dealing with aerodynamics in relation to the problems of aeronautics and including in particular a critical digest of the experimental and research data which are now available.

The members of the conference exchanged information regarding the equipment of their laboratories and the number of students enrolled in the courses in aeronautical engineering in their respective schools. There was also discussion of the probable ratio during the next few years of the number of aeronautical engineers available to the number demanded by the aeronautical activities of the country.

It was announced at the conference that that would be the last of such meetings under the auspices of the Guggenheim Fund, and that the coordination of aeronautical research in educational institutions would in the future be undertaken by a subcommittee on aeronautical research in universities, which was being organized by the National Advisory Committee for Aeronautics as a subcommittee of its committee on aerodynamics.

For the purpose of circulating research programs and other information among the institutions represented at the conference, Prof. E. P. Lesley, of Stanford University, was appointed secretary. The programs of research of the various schools were later submitted to the National Advisory Committee for Aeronautics and referred to the subcommittee on aeronautical research in universities, which has since been organized. These programs may be found under the report of that subcommittee in Part III of this report.

#### COORDINATION OF AERONAUTICAL RESEARCH IN UNIVERSITIES

In response to suggestion that the National Advisory Committee for Aeronautics undertake the coordination of the scientific research in aeronautics being conducted by a number of educational institutions in connection with their courses in aeronautical engineering, the committee



organized, in September, 1928, under the committee on aerodynamics, a standing subcommittee on aeronautical research in universities, with Prof. Charles F. Marvin as chairman. The purposes of this subcommittee are to coordinate the research work undertaken by the various institutions of learning and to aid in improving the courses in aeronautical engineering and in promoting the study of aeronautics and meteorology. This subcommittee will continue the work initiated two years ago by the Daniel Guggenheim Fund for the Promotion of Aeronautics and carried out by means of two conferences held under the auspices of the fund.

The subcommittee on aeronautical research in universities has been organized with a representative from each of the aeronautics departments of the California Institute of Technology, the Massachusetts Institute of Technology, the University of Michigan, New York University, and Stanford University. A complete statement of the organization and functions of this subcommittee will be found under the report of the committee on aerodynamics in Part III of this report.

#### COOPERATION WITH BRITISH AERONAUTICAL RESEARCH COMMITTEE

For the past several years the most cordial relations have been maintained between this committee and the Aeronautical Research Committee of Great Britain. These relations have been strengthened during the past year as a result of the visit to England in 1927 of Dr. Joseph S. Ames, chairman of the National Advisory Committee for Aeronautics, and by the visit in 1928 of Mr. George W. Lewis, the committee's director of aeronautical research. These visits have led to additional cooperation between the two committees in the study of several important problems of aeronautical research.

For a number of years the two committees have been engaged in the conduct of comparative tests of models in British and American wind tunnels with a view to the standardization of wind-tunnel results. Information obtained from these tests has been published from time to time by both this committee and the British committee.

In these comparative tests, the results obtained in the committee's variable-density wind tunnel at Langley Field were of particular value because they furnished important information regarding the effect of scale in model tests. As a result of these tests and of Doctor Ames's visit to England, the British committee decided to construct a variable-density wind tunnel at the National Physical Laboratory, and this committee has cooperated by supplying the British committee with information regarding the design of the variable-density wind tunnel at Langley Field and experience in its operation.

Comparative tests by the two committees have also been conducted on a metal propeller model, first in an open-jet wind tunnel at Stanford University and then in a closed-type wind tunnel at the National Physical Laboratory, and it is of interest to note that when correction was made in accordance with the Prandtl theory for the wall effect in the closed tunnel the results of the two series of tests showed excellent agreement.

An agreement has been reached for the exchange by the two committees of flight-test instruments, each committee conducting tests of instruments designed and built by the other. Definite arrangements for such an exchange are now being made, and it is hoped that these tests will prove mutually helpful to the two committees in the development of the best possible instruments for flight research.

#### COOPERATION OF ARMY AND NAVY

Through the personal contact of the heads of the Army and Navy air organizations serving on the main committee and the frequent personal contact on the subcommittees of their chief subordinates who have to do with technical matters in aeronautics there has been accomplished in fact not only a coordination of aeronautical research, which is the major function of the committee, but also a coordination of experimental engineering activities of the services and an exchange of first-hand information, comment, and suggestions that have had beneficial effects in both services. The needs of each service in the field of aeronautical research are discussed and agreements invariably reached that promote the public interests. The cordial relations that



usually follow from frequent personal contact are supplemented by the technical information service of the committee's Office of Aeronautical Intelligence, which makes available the latest scientific data and technical information secured from all parts of the world. Although there is a healthy rivalry between the Army and Navy air organizations, there is at the same time a spirit of cooperation and a mutual understanding of each other's problems that serve to prevent unnecessary duplication in technical developments in aeronautics.

Much of the fundamental research work of the committee has grown out of requests received from the Army and Navy for the study by the committee of particular problems encountered in the services, and in connection with this work the committee desires to give special recognition to the splendid spirit of cooperation of the two services with the committee. Each service has placed at the disposal of the committee airplanes and engines required for research purposes, and has otherwise aided in every practical way in the conduct of scientific investigations by the committee. Without this cooperation the committee could not have prosecuted successfully many of its investigations that have made for progress in aircraft development. The committee desires especially to acknowledge the many courtesies extended by the Army authorities at Langley Field, where the committee's laboratories are located, and by the naval authorities at the Hampton Roads Naval Air Station.

#### INVESTIGATIONS UNDERTAKEN FOR THE ARMY AND THE NAVY

As a rule research programs covering fundamental problems demanding solution are prepared by the technical subcommittees and recommended to the executive committee for approval. These programs supply the problems for investigation by the Langley Memorial Aeronautical Laboratory. When, however, the Army Air Corps or the Naval Bureau of Aeronautics desires special investigations to be undertaken by the committee, such investigations, upon approval by the executive committee, are added to the current research programs.

The investigations thus under conduct by the committee during the past year for the Army and the Navy may be outlined as follows:

##### FOR THE AIR CORPS OF THE ARMY

- Investigation of the flat spin of the Douglas O-2 airplane.
- Full-scale investigation of different wings on the Sperry messenger airplane.
- Investigation of the behavior of an airplane in landing and in taking off.
- Investigation of pressure distribution and accelerations in pursuit-type airplane.
- Acceleration readings on the PW-9 airplane.
- Wind-tunnel investigation of biplane cellules.
- Investigation of pressure distribution on observation-type airplane.
- Study of mutual interference of propeller and fuselage with geared engine.
- Study of comparative performance with various types of superchargers.
- Tests in special wind tunnel and in flight of atmospheric conditions causing ice formation.
- Determination of moment coefficients and hinge moment coefficients for different tail surfaces.
- Determination of aileron hinge moments versus rolling moments for various types of ailerons and wings.
- Investigation of wing flutter.

##### FOR THE BUREAU OF AERONAUTICS OF THE NAVY DEPARTMENT

- Investigation of pressure distribution on vertical tail surfaces fitted with balanced rudders.
- Investigation of methods of improving wing characteristics by control of the boundary layer.
- Development of a solid-injection type of aeronautical engine.
- Investigation of NY training airplane with Handley Page automatic slot.
- Determination of radii of gyration of O2U-1 airplane.



Investigation of windshields and fairings for protection from air currents.  
 Investigation of comparative aerodynamic resistance of riveted and bolted construction.  
 Investigation of parasite resistance and propeller efficiencies of PB-2.  
 Investigation of method of improvement in visibility in an airplane.  
 Investigation of maximum tail loads in dives.  
 Investigation of the forces on seaplane floats under landing conditions.  
 Investigation of water pressure distribution on seaplane hulls.  
 Study of design factors for metal propellers.  
 Investigation of application of compression ignition to air-cooled engine cylinders.  
 Investigation of flight path characteristics.  
 Effect of varying the aspect ratio and area of wings on performance of fighter airplane with supercharged air-cooled engine.  
 Investigation of aerodynamic loads on the U. S. S. *Los Angeles*.  
 Investigation of autorotation.  
 Investigation of spoiler aileron control.  
 Development of aircraft engine supercharger.  
 Effect of various forms of cowling on performance and engine operation of fighter airplane with supercharged air-cooled engine.  
 Prevention of ice formation in flight.  
 Comparative tests of rubber and Oleo type landing gears.  
 Investigation of the drag of a wing radiator.  
 Wind-tunnel tests of racing wing sections.

#### AMERICAN AIRSHIP DEVELOPMENT

In February, 1928, the question of the Nation's policy regarding the development of rigid airships and the creation of an American rigid-airship industry was pending before the Congress of the United States. There was a difference of opinion at the time as to whether appropriations should be made for the construction for the naval service of rigid airships. On February 16, 1928, Senator Hiram Bingham, of Connecticut, addressed a letter to the committee stating that he would appreciate having the committee answer from the information available the following questions regarding the development and operation of large rigid airships:

1. In the opinion of the National Advisory Committee for Aeronautics, does the present state of the art of constructing and operating large rigid airships justify the belief that such airships can be constructed and operated successfully?
2. What, in the opinion of the committee, are the most practical steps that can be taken at this time to encourage the development of an airship industry in the United States looking toward the promotion of commercial air navigation by rigid airships?

Under date of March 1, 1928, the committee replied to Senator Bingham as follows:

Hon. HIRAM BINGHAM,

*United States Senate, Washington, D. C.*

DEAR SENATOR BINGHAM: Your letter dated February 16, 1928, making certain inquiries as to the opinion of the National Advisory Committee for Aeronautics with reference to the construction and operation of rigid airships and the development of an airship industry in the United States, was considered at a meeting of the executive committee held March 1, 1928, and the following resolutions were adopted:

*Resolved*, That it is the opinion of the National Advisory Committee for Aeronautics that the present state of the art of constructing and operating large rigid airships has progressed to the point where we are justified in believing that large rigid airships can be constructed and operated successfully.

*Resolved further*, That it is the opinion of the National Advisory Committee for Aeronautics that the most practical step to be taken at the present time to encourage the development of an airship industry in the United States is to begin the construction of the airships authorized under the 5-year aircraft building program. The construction of these airships will foster the development of an airship industry, and this, with the knowledge to be acquired from experience in the operation of airships, will be necessary in order to enable the United States to meet the needs for commercial airship construction and operation when they arise.



The committee appends hereto a memorandum entitled "The Present Status of the Development of Rigid Airships in the United States," which states the facts on which its opinion is based.

Sincerely yours,

NATIONAL ADVISORY COMMITTEE FOR AERONAUTICS,  
JOSEPH S. AMES, *Chairman*.

The memorandum inclosed with the committee's letter follows:

#### THE PRESENT STATUS OF THE DEVELOPMENT OF RIGID AIRSHIPS IN THE UNITED STATES

##### CONSTRUCTION

No rigid airship has been built in this country since the *Shenandoah* was completed in 1923, but theoretical studies, research and practical tests have continued so that ultimately additional rigid airships might be designed and built in the United States. As a result, the United States is to-day as fully abreast of rigid airship development as could be expected without actual construction since 1923.

The *Shenandoah* was a remodeled copy of a 1916 German design and, when completed, was recognized as an admirable first American effort rather than as a modern rigid airship. The necessity for providing suitable materials for the *Shenandoah* led to the further development of aluminum alloys and brought to the United States expert talent who knew how to manufacture gas cells. Additional technical experts were brought to this country who were familiar with rigid airship fabrication, erection, and operation. Original thought and effort were expended along various lines connected with theoretical design, with the result that in spite of meager information as to the prototype the design of the *Shenandoah* was placed upon a sound basis. A special subcommittee of the National Advisory Committee for Aeronautics checked the design and found it reasonable. Recent information confirms this opinion.

The *Shenandoah* was operated successfully by the Navy for two years. Her operation proved the practicability of mooring masts ashore and afloat. She made a number of notable flights, including one of 9,000 miles to the west coast and return, during which she was based entirely on mooring masts for 21 days. A noteworthy flight resulted from a breakaway from the mooring mast. During this she weathered a gale in a badly damaged condition. The fact that she was finally caught in an unusually severe storm and succumbed to it is no reason to condemn her as an airship—much less to condemn airships in general. Engineering history is full of instances where final success has been reached only through lessons learned in early attempts.

The acquirement in 1924 of the *Los Angeles*, as an example of modern German airship construction, was an important step in airship development in the United States. With the *Los Angeles* there came much information about questions hitherto obscure. Shortly after the *Los Angeles* arrived there was brought to this country a group of the most experienced rigid airship engineers. They still remain and represent the quarter of a century of Germany's experience in airship design and construction.

The United States began its experience with rigid airships nearly 10 years ago, and the present "state of the art" may be summarized as follows: One rigid airship was built and operated successfully; another was acquired and is still being operated successfully; much thought and effort have been applied to engineering problems connected with airships; technical personnel familiar with airship matters are available, including those self-trained in the United States; the technical knowledge and experience available in the United States for the design and construction of rigid airships is ample; satisfactory materials are available, notable examples being aluminum alloys, steel wire, cotton cloths, gas-cell materials of various kinds, engines, and power plant equipment, including water-recovery apparatus; promising development of oil-burning engines is under way; and helium, available only in the United States, gives to American airships a unique measure of safety.

From a technical standpoint it is believed the United States is prepared to design and build rigid airships to any required degree of engineering exactitude. American ingenuity and production methods applied to airship construction will cheapen their cost and offset the present high cost differential between American and foreign airships.

##### OPERATION

The successful operation of rigid airships depends on two factors (a) trained personnel and (b) facilities available, which include weather information service. Operation is also a matter of experience. Although our experience is not as wide as that possessed by the Germans or English, it is more recent.

The American personnel engaged in rigid airship operation is the equal of any. They have been largely self-taught, but the foundation of the training was sound and embodied the best of German and British experiences, adapted to American conditions and to helium operation. As only one rigid airship has been in operation at a time, competitive effort has not been possible. Development would be faster if more rigid airships were available. The large cost of rigid airships and the fact that only one is now available forced a cautious, conservative scheme of operation which, though sound, has not as yet allowed the technique of rigid airship operation to develop to the full extent of its possibilities. This situation will correct itself when more airships and better facilities are available.



The facilities for the operation of rigid airships in the United States are not the best and additional facilities are needed. There are only two large sheds—at Lakelhurst and at Scott Field. The former in particular is poorly located from a meteorological standpoint. The shortage of helium and meager facilities for its transportation and storage have retarded the operation of rigid airships at intervals. Several mooring masts have been erected at strategic points, but the masts remote from the shed base have been used only once.

Arrangements and mechanical appliances for landing airships and handling them on the ground, and in or out of sheds, are being improved with experience. As a result we should be prepared to handle the larger airships now contemplated with no more difficulty, and perhaps with less difficulty, than airships of the *Los Angeles* size. There has been gratifying progress in developing the floating mast, the fixed stub mast, the mobile stub mast, mechanically operated docking trolleys, cars for supporting airships while moving in and out of sheds, artificial superheat device, remote control for hauling down winches and the deck landing platform.

The operation of airships, like airplanes, is influenced by weather conditions and will be facilitated by improved weather information service. A new system for the collection and distribution of weather reports has recently been worked out by the Weather Bureau in cooperation with the telegraph companies. This will much facilitate the prompt furnishing of aerological information so necessary for the safe navigation of the air.

#### FOREIGN DEVELOPMENT

No survey of rigid airship development would be complete without a résumé of what is being done by other nations.

Germany, the original home of the rigid airship, and where it finds most enthusiastic support, is just completing a 3,650,000 cubic foot airship, funds for which were raised largely by popular subscription. It is proposed that this airship, after making demonstration flights, including one to the United States, will be used to start a commercial line between Spain and South America. The design is a modern and enlarged copy of the *Los Angeles*. This airship will carry a large portion of its fuel in gaseous form. This permits an important increase in cruising range. This development is being watched with interest and a combination of helium and a fuel gas offers attractive possibilities without much greater risk than with helium alone and gasoline.

Great Britain, after abandoning airships for the sake of economy in 1919 and after being confirmed in her anti-airship convictions by the *R-38* disaster in 1921, executed an about face in 1923 and resumed the construction of rigid airships. Great Britain now believes airships will play an important rôle in linking up her outlying possessions.

Two rigid airships of 5,000,000 cubic foot volume and using hydrogen are nearly completed. One of these is being built by the Air Ministry, the other by the Airship Guarantee Co., a subsidiary of Vickers (Ltd.). From all information available the designs appear to be on a sound basis and there is no reason to doubt their success. The Airship Guarantee Co. uses a novel and ingenious type of girder which promises to simplify and cheapen the structural parts of an airship. The Air Ministry airship will use considerable alloy steel. Oil-burning engines are proposed for both airships, but they are not yet sufficiently developed to be pronounced satisfactory. Each airship is fitted with accommodations for about 100 passengers and both are intended for quasi subsidized commercial service to India.

Great Britain has five shed berths for large rigid airships. A new shed has been erected in India and one shed in England is being enlarged. Mooring masts have been built in England, India, and Egypt. Other masts are contemplated in Canada, Australia, and South Africa.

At least one of these British airships is expected to visit the United States during the summer of 1928.

France has several sheds suitable for large rigid airships, but probably for reasons of economy has not built such craft. Designs are available and she contents herself with trying to keep abreast of development without building or operation.

Italy still operates the small rigid airship *Esperia* delivered to her in 1922 by Germany. Italy's own airship efforts, however, are concentrated on developing the semirigid type, which satisfies her geographic requirements. An enlargement of the *Norge* type is under construction. In her chosen field of moderate sized airships Italy has developed a superior technique of design, construction, and operation.

The answer of the committee to Senator Bingham's inquiry was published in the Congressional Record of March 9, 1928. Subsequently the Congress made appropriation for the construction of two large rigid airships, and construction has actually begun on the contracts executed by the Navy Department with the Goodyear-Zeppelin Corporation, Akron, Ohio. This step marks the beginning of a rigid-airship industry in the United States, and without doubt will lead to material progress in the design, construction, and use of rigid airships.



## PART III

### REPORTS OF TECHNICAL COMMITTEES

---

#### REPORT OF COMMITTEE ON AERODYNAMICS

##### ORGANIZATION

The committee on aerodynamics is at present composed of the following members:

Dr. David W. Taylor, chairman.

Capt. H. C. Richardson (C. C.), United States Navy, vice chairman.

Dr. L. J. Briggs, Bureau of Standards.

Lieut. W. S. Diehl (C. C.), United States Navy.

Maj. C. W. Howard, United States Army, matériel division, Air Corps, Wright Field.

Prof. Alexander Kelmin, Department of Commerce.

George W. Lewis, National Advisory Committee for Aeronautics (ex officio member).

Maj. Leslie MacDill, United States Army, matériel division, Air Corps, Wright Field.

Prof. Charles F. Marvin, Weather Bureau.

Hon. Edward P. Warner, Assistant Secretary of the Navy for Aeronautics.

Dr. A. F. Zahm, construction department, Washington Navy Yard.

##### FUNCTIONS

The functions of the committee on aerodynamics are as follows:

1. To determine what problems in theoretical and experimental aerodynamics are the most important for investigation by governmental and private agencies.
2. To coordinate by counsel and suggestion the research work involved in the investigation of such problems.
3. To act as a medium for the interchange of information regarding aerodynamic investigations and developments, in progress or proposed.
4. To direct and conduct research in experimental aerodynamics in such laboratory or laboratories as may be placed either in whole or in part under its direction.
5. To meet from time to time on call of the chairman and report its actions and recommendations to the executive committee.

The committee on aerodynamics, by reason of the representation of the various organizations interested in aeronautics, is in close contact with all aerodynamical work being carried out in the United States. In this way the current work of each organization is made known to all, duplication of effort being thus prevented. Also all research work is stimulated by the prompt distribution of new ideas and new results, which add greatly to the efficient conduct of aerodynamic research. The committee keeps the research workers in this country supplied with information on European progress in aerodynamics by means of a foreign representative who is in close touch with aeronautical activities in Europe. This direct information is supplemented by the translation and circulation of copies of the more important foreign reports and articles.

The committee on aerodynamics has direct control of the aerodynamical research conducted at Langley Field and of a number of special investigations conducted at the Bureau of Standards. The aerodynamical investigations undertaken at the Washington Navy Yard, the matériel division of the Army Air Corps at Wright Field, and the Bureau of Standards are reported to the committee on aerodynamics.

## SUBCOMMITTEE ON AIRSHIPS

In order that the committee on aerodynamics may be kept in close touch with the latest developments in the field of airship design and construction, and that research on lighter-than-air craft may be fostered and encouraged, a subcommittee on airships has been organized under the committee on aerodynamics, the membership of which is as follows:

Hon. Edward P. Warner, Assistant Secretary of the Navy for Aeronautics, chairman.  
Starr Truscott, National Advisory Committee for Aeronautics, vice chairman.  
Dr. Karl Arnstein, Goodyear-Zeppelin Corporation.  
Commander Garland Fulton, United States Navy.  
George W. Lewis, National Advisory Committee for Aeronautics (ex officio member).  
Capt. William B. Mayer, United States Army, matériel division, Air Corps, Wright Field.

R. H. Upson, Aeromarine Klemm Corporation.

During the past year the results of investigations by the technical staff of the National Advisory Committee on the effect of length-diameter ratio on airship models of Goodyear-Zeppelin design, carried on in the variable-density wind tunnel and on the pressure distribution over the envelope and control surfaces of the U. S. S. *Los Angeles*, conducted at Lakehurst in cooperation with the Bureau of Aeronautics of the Navy, have been considered by the airships subcommittee. Reports on the *Los Angeles* tests will be published by the National Advisory Committee.

The airships subcommittee recommended for approval the study of airship forms, and especially of airship appendages, in the variable-density wind tunnel at Langley Field, and this problem was added to the committee's program. It is planned to include in this investigation the testing of two models with a number of different arrangements of power cars and fins.

A recent meeting of the subcommittee was to a large extent devoted to a discussion of the structure of the atmosphere and its effect on airship operation. Representatives of the Weather Bureau, the Signal Corps of the Army, and the Bureau of Aeronautics, who are in close touch with the study of wind gusts, were invited to the meeting. Some of the specific questions discussed were abrupt changes in wind velocity and the stresses set up in airships by such changes, instruments, and methods for the study of wind direction and velocity, and the importance of obtaining exact data on the variation and velocity of air flow. Consideration was given to the need of attacking these problems by the study of the atmosphere at ground level, at the greatest height at which a support can be placed, and at a great height by some means not yet fully defined. A careful study of the existing knowledge of the subject and of the work already done has been made for the subcommittee by a representative of the Weather Bureau under the direction of Doctor Gregg. With the organization of the recently established subcommittee on meteorological problems of the committee on problems of air navigation, it is hoped that these problems can be considered in cooperation with that subcommittee.

## SUBCOMMITTEE ON AERONAUTICAL RESEARCH IN UNIVERSITIES

In order to coordinate the aerodynamic research work undertaken by the various institutions of learning and to aid in improving the courses in aeronautical engineering and in promoting the study of aeronautics, a subcommittee on aeronautical research in universities was organized in September, 1928, with the following membership:

Prof. Charles F. Marvin, Weather Bureau, chairman.  
Prof. C. H. Chatfield, Massachusetts Institute of Technology.  
Prof. Alexander Klemin, New York University.  
Prof. E. P. Lesley, Stanford University.  
Mr. G. W. Lewis, National Advisory Committee for Aeronautics (ex officio member).  
Prof. Clark B. Millikan, California Institute of Technology.  
Prof. F. W. Pawlowski, University of Michigan.



The functions of the subcommittee on aeronautical research in universities are as follows.

1. To consider aeronautical problems with a view to the initiation and conduct of aeronautical research by educational institutions; and in connection therewith to prepare programs of suggested lines of research intended to supplement existing research programs and to develop and train personnel for the conduct of scientific research in aeronautics along original lines.

2. To seek through interchange of ideas to improve the courses in aeronautical engineering and to promote the study of aeronautics and aerology in educational institutions.

3. To meet from time to time on call of the chairman and to report its actions and recommendations to the committee on aerodynamics.

At a conference of representatives of educational institutions engaged in the teaching of aeronautical engineering held in Washington on April 27, 1928, under the auspices of the Daniel Guggenheim Fund for the Promotion of Aeronautics, at which conference the National Advisory Committee for Aeronautics, as well as the Navy Department, was represented, arrangements were made for the circulation by Prof. E. P. Lesley of research programs among the institutions represented at the conference, prior to the organization of the subcommittee on aeronautical research in universities. Through the courtesy of the Guggenheim Fund and of Professor Lesley copies of these programs have been forwarded to the National Advisory Committee for Aeronautics and referred to the subcommittee on aeronautical research in universities. The principal items of aerodynamic investigation included in the research programs received from the educational institutions in the United States are as follows:

*Massachusetts Institute of Technology.*—1. Construction and calibration of new 5-foot wind tunnel of the Venturi type, with closed experimental chamber.

2. Continuation of investigations of mutual interference effects of airplane propellers and other parts of the airplane. This is to include the effects of radical changes in fuselage form and location, the effect of radial engine cylinders with different types of cowling, the effect of different propellers on performance, and the effect of nacelles in multi-engine airplanes.

3. Measurements of flow around model airplane as influenced by the propeller, particularly in the region near the tail.

4. Possible experimental determination of actual air flow near the blades of the propeller as opposed to the mean air flow.

5. Pressure distribution on tail with slip stream.

6. Design and construction of a new type of rib testing machine.

7. Development of a unit instrument to facilitate airplane performance testing.

*New York University.*—1. Development of methods of measurement, calculation, and correction for tests in connection with the Guggenheim safe-aircraft competition.

2. Continuation of studies in the problem of longitudinal stability and control at the stall.

3. Continuation of work on the aerodynamic resistance of air-cooled engines with various types of cowling.

*Stanford University.*—1. An experimental investigation of the performance characteristics of a series of five metal model propellers in a free wind stream and in combination with a model of a VE-7 airplane.

2. An experimental investigation of the rotational velocity of the slip stream of air propellers. It is planned first to determine the rotation in the slip stream of a series of United States Navy standard model propellers and then to investigate the effect of straightening vanes upon the power absorbed and efficiency.

3. An experimental and theoretical investigation of the causes of discontinuous air flow. It is desired to formulate criteria which will enable the prediction of the departure of smooth flow from the surface of an airfoil or streamline body.

4. An experimental investigation of the induced drag of high aspect ratio airfoils. It is intended to test airfoils having aspect ratios from 6 to 15 and to compare the results with the predictions of the Lanchester-Prandtl theory.



5. An experimental investigation of the profile drag of certain airfoils. A special form of airfoil has been devised for which it appears that the induced drag should be zero and therefore that the profile drag may be measured directly by a balance. A metal airfoil (Clark Y section) has been constructed. If the results are as expected, the investigation will be extended to other forms.

*California Institute of Technology.*—1. Theoretical investigations in boundary layer, heat conduction, and other aerodynamical subjects.

2. Full-scale construction and free-flight testing of a new model of the Merrill type stagger-decalage biplane.

3. Installation and calibration of apparatus in the Daniel Guggenheim Laboratory.

*University of Michigan.*—1. Research into the economic and engineering aspects of air transportation.

2. Research in solution of St. Venant problem for typical propeller blade sections.

3. Design, construction, installation, and calibration of apparatus in the new wind tunnel.

UNIVERSITY OF TORONTO.—Through the courtesy of the Guggenheim Fund and of Prof. J. H. Parkin, of the University of Toronto, the committee has received the following information regarding aerodynamic research work at that university:

Researches completed and ready for printing.—1. Air flow over airfoils: Yawmeter study of air flow in neighborhood of wing tips for R. A. F. 15, U. S. A. 27, and Göttingen 387 airfoils.

2. Effects of mutual interference between wings and fuselage for three typical fuselages and their wing sections (R. A. F. 15, U. S. A. 27, and Göttingen 387) in typical monoplane and biplane combinations.

3. Report of international trials on airship models.

Researches in progress.—1. Stability characteristics of flying boat: Determination of aerodynamic characteristics and rotary derivatives of single-engine pusher biplane flying boat.

2. Undercarriage drag: Measurements of drag of wheel, ski, and float undercarriages on typical commercial monoplane and biplane.

#### LANGLEY MEMORIAL AERONAUTICAL LABORATORY

ATMOSPHERIC WIND TUNNEL—*Aerodynamic safety.*—The importance of safety in airplane flight is increasing with the present rapid growth of civil aviation. Airplane structures and engines are now highly reliable, but modern airplanes still possess certain aerodynamic characteristics to which many of the accidents occurring in flight must be attributed.

Recognizing the vital need of greater aerodynamic safety, the National Advisory Committee for Aeronautics for the past two years has been concentrating the efforts of its atmospheric wind-tunnel staff on an investigation of the aerodynamic factors that produce dangerous conditions in flight, with a view to remedying these conditions. As a guide in this work the requirements of the type of airplane which must be inherently safe to the greatest degree are being kept in mind. This is the type, as yet undeveloped in practice, which might be flown safely by the unskilled owner-pilot who now drives his own motor car. In general, the information obtained from the study of this extreme type will also make possible the solution of the less difficult safety problems of commercial and military airplanes.

The present investigation is concerned chiefly with the factors affecting the landing, stability, controllability, and spinning of airplanes. In addition, the aerodynamic aspects of dangerous ice formation on airplane parts when in flight are being studied.

*Landing.*—Bringing an airplane safely and comfortably to the ground is a precise operation requiring considerable skill, particularly when the landing is forced. Because of the necessary frequency of landings this problem is considered to be of first importance. In most airplanes the lift reaches a maximum quite sharply and then decreases rapidly when the control column is pulled back too far. The result of such a maneuver is a rapid drop of the airplane and frequently a crash. It is apparent that a wing having a maximum lift extending over several degrees of angle of attack would materially reduce this danger.



During the past year a new airfoil profile, the N. A. C. A. 84, has been developed by the committee, and wind-tunnel tests have shown that after reaching its maximum the lift remains practically constant over a range of  $9^\circ$ . However, this is but a first step toward reducing the skill required in landing, and further tests are to be made on tapered wings and biplane combinations, together with a study of the possibilities of landing automatically.

*Stability.*—An airplane for the private flyer should have a high degree of stability. Not only should it be able to fly itself in smooth air, but it should also be capable of returning, with controls released, to level flight when disturbed therefrom by an inadvertent act of the pilot or by a gust. It is, of course, imperative that under no conditions should a rapid loss of altitude occur against the desire of the pilot, for such a possibility places the airplane and its occupants in imminent danger when near the ground. A large number of present day accidents are due to just such a loss of altitude resulting from a sharp side slip or dive or both, following the stalling of the airplane. The side slip is due to the tendency of curved lifting surfaces to roll or autorotate when stalled, a characteristic that has been called "rotary instability." The diving tendency is due chiefly to the relatively rapid rearward travel of the center of pressure as the airplane becomes stalled.

The tests on the N. A. C. A. 84 airfoil have indicated that wings with flat-top lift curves may be expected to have but a small range of "rotary instability" and small diving tendencies when stalled. This part of the investigation will be continued in order to determine the factors affecting the stalled side slip and dive for the purpose of removing the causes.

*Controllability.*—The privately owned airplane should be capable of executing very gentle maneuvers only, and hence its controllability should be judiciously limited. However, the controls must be effective under all possible conditions of flight. The orthodox plain flap aileron becomes relatively ineffective beyond the angle of maximum lift, and lateral control is thereby seriously impaired. The British have within recent years developed the Frise and the Handley-Page ailerons, both of which are conceded to show marked improvement in lateral control in stalled flight.

However, it can not be emphasized too strongly that controllability is, at best, only a cure for the dangers of instability, whereas the proper degree of stability is positive prevention of these dangers.

During the past year, preliminary wind-tunnel tests have been made on six widely different types of lateral control devices, including the plain flap aileron for comparison. The results of these tests are now being prepared for publication.

*Spinning.*—The spinning of an airplane is largely dependent on the phenomenon of autorotation, previously mentioned, which may at present be considered the most important single factor affecting the safety of airplanes. It is therefore imperative that autorotation be investigated completely.

This task was undertaken two years ago by the committee, and a comprehensive test program is now in progress. The program includes force, pressure distribution, and autorotation torque tests on a wide variety of monoplane and biplane wing models covering practically all the wing systems in modern use. A large range of angles of attack is covered in each test. The force tests have been completed and two papers have been written presenting the results. The pressure distribution tests are now under way. The autorotation torque tests, which will be made on a specially designed and constructed dynamometer, will be started in the near future.

The primary object of this part of the investigation is to obtain information for the development of nonspinning wings or wing systems. In addition a large amount of detailed reference data will be made available for publication.

*Ice formation.*—During the past year or two many scheduled or long distance flights have been interrupted, sometimes disastrously, by the formation of a heavy layer of ice on the exposed parts of the airplane. The effect of this layer is to decrease the lift and increase the drag as well as to load the airplane heavily, and a dangerous condition results.

In order to study this phenomenon in the laboratory, a small wind tunnel having a 6-inch-diameter jet and equipped with apparatus for refrigerating the air has been built and is now in



operation. In preliminary tests ice formations which resemble those observed in flight have been obtained on round wires and on strut and airfoil sections.

These tests will be extended for the purpose of determining means for the prevention or the avoidance of ice formation. Several possible methods are under consideration.

*Aerodynamic efficiency.*—Airplane efficiency may be increased by decreasing the size of the wing or wings, provided the maximum lift coefficient can be increased. Two independent methods of obtaining this increase are the moving of trailing edge flaps downward, and boundary layer control by means of pressure or suction slots. For a large increase, the two methods may be used together. The Handley-Page slot-and-flag device is of the latter type.

Preliminary tests on boundary layer control were made last year and the results have been published this year. The method is still chiefly of academic interest on account of the practical difficulty of providing an independent source of pressure or suction in flight.

Tests have also been made on several types of trailing edge flaps, the results of which are being prepared for publication.

A test program has been planned, which includes tests on combinations of slots and flaps as well as a more detailed study of slot shapes, sizes, and positions.

*Wind tunnels and apparatus.*—Plans are under way for a rearrangement and expansion of the apparatus and facilities of the atmospheric wind-tunnel section. A larger wind tunnel is to replace the present 5-foot tunnel and a vertical tunnel designed primarily for the study of spinning will be added. The low-temperature tunnel, mentioned above, and another small tunnel previously used for miscellaneous experiments, have recently been added to the equipment of the section. The new arrangement will enable the space in the present wind tunnel building to be economically utilized, since, in addition to the housing of the four tunnels, about 2,000 square feet of office space will be made available.

In preparation for the design of the new tunnels, tests have been made in the small model tunnel on entrance and exit cones of a variety of shapes. Among other things, it has been found that the air vibration of an open-jet tunnel can be suppressed, that a honey-comb is unnecessary and even detrimental in a closed-return tunnel, and that a velocity increase of 4 to 1 in the entrance cone gives an excellent dynamic pressure distribution in the jet.

During the past year five new pieces of apparatus have been developed and put in operation. These are as follows: An attachment to the tunnel balances to enable measurement of roll and yaw due to ailerons; means of measuring directly the forces and pitching moments on an airfoil between end planes, together with provision for supplying air from a blower for slotted wing experiments; a multiple manometer for pressure distribution tests, with adjustable tubes to enable them to be spaced to suit the spacing of the orifices in the wing, making possible the fairing and integration of the pressure diagrams directly on the photostat record; a small dynamometer for measuring the rolling torques on wings in rotation; and the low-temperature wind tunnel previously referred to.

**VARIABLE DENSITY WIND TUNNEL.**—At the beginning of the past fiscal year, after the airship model testing program had been completed, a fire, probably having its origin in an electric spark from a broken light bulb, completely destroyed the interior of the tunnel. The heat and the additional pressure caused by it damaged approximately 2,000 rivets and most of the seams in the upper part of the tank. Consequently, most of the year was devoted to redesigning and rebuilding the tunnel and balance.

The rivets and seams were recalked. The tank was equipped with a safety valve and a larger blow-off valve and then tested to its normal working pressure.

In contrast to the situation when the tunnel was first built, there was a wealth of information available, collected through experience with the original tunnel, upon which to base the design of the new interior. Although the tunnel had proved capable of producing data which correctly represented full-scale results, it had been criticized at times on the ground that the air flow in the test section was excessively turbulent. In the new design this turbulence was reduced by using a Prandtl type entrance cone. In addition to making the structure simpler



and practically fireproof, several other improvements were incorporated in the new design. The most obvious difference is the change to an open-throat type of tunnel, experience with the previous tunnel and with the propeller research tunnel having shown the desirability of this change.

Although the new balance is not yet complete, the tunnel is again in operation. Preliminary tests showed that the energy ratio had been increased and the velocity distribution improved. Furthermore, drag tests on the Sperry messenger fuselage, using an auxiliary airship drag balance which was not in the tunnel at the time of the fire, gave results which were in good agreement with those from the original tunnel and from tests on the full-scale fuselage in the propeller research tunnel. It is expected that tests in the rebuilt tunnel will be conducted more rapidly and the full-scale results obtained with greater assurance than previously.

The new balance is, in general, similar to the old one, improvements being made in the details to increase the sensitivity of the drag and moment measurements and to make the balance mechanically more rigid. Other changes have been made in the balance to facilitate the reading and computing of the results of force tests.

*Preliminary pressure distribution tests.*—In the period between the completion of the tunnel and the installation of the balance, a series of pressure distribution tests is being conducted. These tests are of particular importance because they represent the first attempt to study directly scale effect on the pressure distribution over an airfoil. Previously the results of model tests have been compared with the results of flight tests, but the proportion of the discrepancy between them which should be attributed directly to scale effect on the airfoil has never been established. These tests will provide data at both a low and a high scale on the same airfoil mounted in the same way. Among the models which are being tested in this way is a symmetrical airfoil equipped with 10 per cent and 20 per cent chord flaps. The flaps will be set at angles ranging from  $50^\circ$  down to  $50^\circ$  up, so that scale effect on tail surfaces and ailerons as well as scale effect on their hinge moments may be studied.

*Open-throat wind-tunnel research.*—An investigation of the air flow in open-throat wind tunnels was carried out in the 6-inch wind tunnel to determine the best means of eliminating certain air vibrations which have been observed in some open-throat tunnels. The investigation was sufficiently extensive that the results should be very useful in designing tunnels of this type. A report covering this work has been prepared.

*Scale effect.*—Other methods of making high-scale model tests have been studied with a view to comparing the results of such methods when tests were made at the same Reynolds Number. Large objects at normal pressure and velocity may be tested in flight or in the propeller research tunnel. Small models may be tested at high density and usual velocity in the variable-density tunnel, or larger models may be tested at a lower velocity. Small models may also be tested at a moderate velocity in some fluid, other than air, having a lower kinematic viscosity; e. g., hot water. Another method, that of obtaining a high Reynolds Number by testing small models at normal pressure in air at very high velocities, has been given considerable thought, and as a result a high-speed wind tunnel has been built.

*High-speed tunnel.*—This piece of apparatus was designed to utilize the large amount of energy in the high-pressure air which had previously been discarded on the completion of each 20-atmosphere test in the variable-density tunnel. An air jet of extremely high velocity is produced by discharging the air from the variable-density tunnel tank through an annular nozzle in the high-speed tunnel. This jet induces a flow of air at a lower velocity through the throat of the tunnel, and in this induced air flow the models will be placed. Preliminary tests have not yet been completed, but results thus far indicate that it will be possible to obtain an air stream 1 foot in diameter having a velocity in the neighborhood of the velocity of sound.

*Prediction of airfoil characteristics.*—Data from airfoil tests in the variable-density tunnel have been carefully analyzed with a view to developing methods of predicting the characteristics of new airfoil sections. The results of tests on different airfoils at a high Reynolds Number are sufficiently consistent to make possible the development of combined empirical and theoretical equations which may be used to predict airfoil characteristics with an accuracy sufficient for most engineering work. A report on this subject has been prepared.



*Three British airplane models.*—The report covering the tests on the models of three British airplanes made in cooperation with the British Aeronautical Research Committee has been published. The results obtained from the tests on these models are compared with flight tests made on the airplanes at Farnborough. The fact that good agreement was obtained will do much to increase confidence in other results from the variable-density tunnel.

*PROPELLER RESEARCH TUNNEL—Tests of wooden propellers on VE-7 airplane.*—In order to develop the propeller-testing equipment of the new 20-foot propeller-research tunnel to the point where its operation and accuracy were satisfactory, and at the same time afford a comparison with flight tests and wind-tunnel tests on model propellers, several wooden propellers were tested on a VE-7 airplane. These identical propellers had previously been tested in flight, and similar models had been tested in a wind tunnel. The results of the flight and model tests were in fair agreement with those of the full-scale tests in the propeller research tunnel.

*Effect of wings and tail surfaces on propeller characteristics.*—Propeller tests were made on the VE-7 airplane with the tail surfaces removed, and with both the wings and tail surfaces removed. It was found that the effect of the tail surfaces on the propeller characteristics was negligible, but that the wings reduced the maximum propulsive efficiency and increased the power coefficient somewhat.

*Tests on a series of metal propellers.*—An adjustable-blade metal propeller was tested on the VE-7 airplane at five different angle settings, forming a series varying in pitch. The efficiencies were found to be from 4 to 7 per cent higher than those of standard wooden propellers operating under the same conditions. The results of these tests are given in a new form convenient for use in selecting propellers of similar shape for aircraft.

*Effect of tip speed.*—An investigation was made of the effect of tip speed on the aerodynamic characteristics of a thin-bladed metal propeller. The propeller was mounted on the VE-7 airplane and tested at tip speeds from 600 to 1,000 feet per second. It was found that the effect of tip speed on the propulsive efficiency was negligible throughout the range of the tests.

*Drag of a wing radiator.*—Tests were made on the left lower wing of the Williams racer in order to determine the effect of the wing radiator on the air-foil characteristics. It was found that the radiator, which had rather deep grooves, doubled the minimum drag of the portion of the wing which it covered, and also reduced the lift somewhat.

*Racing-type air foils.*—Tests were made on four racing-type air foils of 3-foot chord and 12-foot span in order to determine the high-speed characteristics. The air-foil sections tested were the N-9, N-38, C-62, and the N-46, which is a modified C-62 with rounded leading edge. The results indicate that the N-46 has about 12 per cent lower minimum drag than the regular C-62 section, and that both the N-38 and the N-46 have the exceptionally low minimum drag coefficient,  $C_{Dmin.} = 0.0073$ .

*Drag of radial air-cooled engines.*—The drag due to a Wright Whirlwind J-5 engine mounted on the nose of a cabin-type fuselage was measured with three different types of exhaust stacks: Short individual stacks, a circular cross-section collector ring, and stream-line cross-section collector ring. The drag due to the engine was found to be 85 pounds at 100 miles per hour with the individual stacks and 83 pounds at 100 miles per hour with each of the collector rings.

*Effect of fillets on drag.*—Tests were made to determine the effect of fillets between the wing and fuselage on the drag and propulsive efficiency of a high-wing cabin monoplane. It was found that at 100 miles per hour the drag was reduced 2 pounds by the use of fillets of 6-inch radius and 5.1 pounds by the use of fillets of 12-inch radius. The propulsive efficiency was very slightly increased by the use of 12-inch fillets.

Reports have been prepared on all of the above investigations.

*Cowling and cooling of air-cooled engines.*—The most extensive research yet undertaken in the propeller research tunnel—that on the cowling and cooling of air-cooled engines—is now under way and the testing is nearing completion. A Wright Whirlwind J-5 engine is being used in connection with both a cabin monoplane and an open-cockpit biplane. With the cabin fuselage the amount of cowling is varied in several steps from no cowling over the cylinders or crank case to complete cowling entirely inclosing the engine. Two forms are being tried, with



and without a spinner. With the open-cockpit fuselage only the smaller cowlings are used, since the fuselage is too small to make it practicable to inclose the engine entirely. The engine is fitted with thermocouples to measure the temperatures of the cylinders and each cowling is modified if necessary until the engine cools satisfactorily. Then the drag and propulsive efficiency are found for each satisfactory cowling. The tests indicate a decrease in drag with increase in cowling and a large decrease with that which completely incloses the engine. The effect of individual fairings behind each cylinder will also be investigated.

Using the set-ups for the cowling tests, which provide different shapes of bodies, propeller tests with series of propellers of varying pitch are being made in order to provide data on propeller characteristics and body interference. Surveys of the air flow in the propeller plane are also being made in connection with the drag test on each body in order to provide information on body interference.

FLIGHT RESEARCH—*Airships*.—The airship research work during the past year has been and concentrated chiefly upon the analysis of the data obtained in the flight researches of last year and upon preparing this material for publication. The preliminary reports which were submitted to the Navy Department covering the pressure distribution and aerodynamic loads experienced by the U. S. S. *Los Angeles* in flight have been revised and rewritten and combined into one paper, which is to be Part I of a published report. Part II of this report is to be prepared by the Navy Department and will cover the stresses which were imposed in various structural members of airship simultaneously with the loads of Part I.

The results of the speed and deceleration tests conducted last year on the U. S. S. *Los Angeles*, with and without water-recovery apparatus installed, have been completed and submitted in report form to the Navy Department. The water-recovery apparatus, which consists of banks of tubes suspended between the hull and power cars, was found to increase the drag of the airship approximately 20 per cent.

A preliminary study of the velocity of air in gusty or bumpy weather, in which a series of measurements of the velocity of the air were recorded over a period of time when the air was particularly gusty or bumpy, has been brought to a conclusion. These preliminary measurements showed accelerations of air ranging from one of 121 feet per second which lasted  $\frac{1}{4}$  second to one of 2 feet per second lasting  $15\frac{1}{4}$  seconds. This investigation gave no information on the size or extent of a gust, and the next step planned in this research is to conduct a similar investigation covering a large area with a number of recording instruments operated synchronously.

*Airplanes*.—A research is now in progress to determine the comparative maneuverability both at altitude and at sea level of a number of modern military airplanes of the pursuit and observation types. Particular attention is being directed toward the determination of the effect of water-cooled and air-cooled engine installations on maneuverability characteristics. Basically the comparison is being made upon the flight path attainable with each airplane in all conditions of flight, and for this purpose two methods of determining the airplane flight path in maneuvers have been developed. The first method makes use of data recorded in the airplane by the N. A. C. A. standard recording type instruments. The extreme accuracy of measurement required in this work has called for many refinements in the research instruments and in some cases has necessitated a redesign. The second method of flight path determination, which is used primarily as a check on the former, is made from the ground by means of a camera obscura simultaneously with the records obtained in the airplane. The camera obscura apparatus has been developed and constructed especially for this work and is so equipped that a series of photographs of a complete maneuver taken at  $\frac{1}{4}$ -second intervals are recorded on a sheet of film. Apparatus for use with the camera obscura for determining wind direction and velocity, and radio for control and synchronization of airplane and camera records have also been developed and used in this investigation. In addition to the specific data required for flight path determination, other measurements on each airplane are being obtained which will contribute to the general knowledge of airplane maneuverability and will assist in establishing an index of maneuverability that may be specified for new design. To date flight tests have been completed on one pursuit airplane and are now in progress on a second which is identical with the first with the exception of the engine installation.



As in previous years, a large portion of the flight research work has been conducted on the problems of determining the air loads experienced on airplanes in all conditions of flight, for the purpose of providing the necessary information for revising the loading specifications and methods of load computations now in use. A pressure distribution investigation has been completed on the entire supporting surfaces and control surfaces of a modern pursuit airplane. The results of this work are now being worked up and analyzed, and apparatus is being installed for an investigation of the pressure distribution on the fuselage of the same airplane. The results of a somewhat similar investigation on the air loads experienced on the tail surfaces of another type of pursuit airplane have been completed and a report has been prepared for publication. The results of this latter investigation confirm the advisability of revising present loading specifications, particularly those of pursuit airplanes, and the necessity of obtaining additional knowledge of the actual loads occurring in flight to provide a basis for such a revision, since it was found that the present specified load distribution was not exact, and that the specified total loads were too low to provide any safety factor in high-speed maneuvers. A program of pressure distribution research on airplanes has been prepared which includes complete investigations on cargo and observation type airplanes, and also includes the determination of the air loads on wing tips of various plan forms in steady and accelerated flight.

The research on the water-pressure distribution on the bottoms of various types of seaplanes at landing, take-off, and taxiing has been continued throughout the year. The results of the tests conducted last year on a single-float seaplane have been completed and reported on. A similar investigation has been conducted on a twin-float seaplane, the results of which are now being prepared for publication. In the latter investigation, in addition to the positive water pressures which were measured over the whole float bottom, measurements of the negative water pressures were made at several points abaft the step. The maximum negative pressures measured were approximately 1 pound per square inch, while the maximum positive pressures were about 10 pounds per square inch. In general, the loads measured were considerably less than those now specified for design purposes, indicating the possibility of decreasing the weight of seaplane floats.

The take-off characteristics of airplanes have been studied to determine whether it was possible to establish a formula for the ground run of airplanes during take-off. As a part of this work tests have been conducted on an airplane with three different loads and three different propellers. The ground run has been measured with each load and each propeller, in winds of different velocities. The results of these tests, together with those of tests previously conducted on a number of service airplanes, have been undergoing analysis, but as yet no satisfactory expression for ground run has been derived and the study is being continued.

The increasing use of airplane wheel brakes has made it desirable to determine the effectiveness of brakes in decreasing the landing run and improving the taxiing qualities of airplanes. For this purpose tests are being conducted on an airplane, both with and without brakes, with different loading and wind conditions. In the same tests a study is being made of the most suitable method for the pilot to apply the brakes.

With the adoption of the oleo type landing gear or its equivalent in place of rubber type it appears possible to decrease the structural weight of the landing chassis and the fuselage members which take the landing load, because of the smaller loads imposed with the oleo type gear. In this connection a research is now in progress to determine quantitative values, for use in the design of landing gear, of the energy absorbed in both oleo and rubber type landing gears. The investigation includes dropping tests with several designs of each type gear, and will be accompanied by flight tests with each in which the accelerations occurring in a number of different kinds of landings will also be measured.

The general study of the problem of the recovery of an airplane from a spin has been continued this year and has consisted mainly of a compilation of the data pertinent to the problem. Special attention has been directed toward the effect of mass distribution on spins and the policy has been established of measuring the moments of inertia of all airplanes undergoing test at the laboratory and such others as evidence any unusual spinning characteristics. As a



result, the moments and ellipsoids of inertia of several airplanes of normal spinning characteristics and of one in which recovery from spin is very difficult have been measured. In addition, incidental to the researches on pressure distribution and maneuverability mentioned above, considerable information has been obtained on the wing and tail surface loads and on the flight path, attitude, rate of rotation, axis of spin, etc., occurring in spins. A comparison of the ellipsoids of inertia of airplanes having normal and abnormal spinning characteristics, which is expected to indicate desirable dispositions of weight for new designs, is now in progress.

Preparations are being completed for a flight research to determine the effectiveness of various types of ailerons in producing lateral control. An airplane is to be rebuilt to use interchangeable ailerons and at the same time is to be equipped with flaps and spoiler gear. A stress analysis of the wing structure is at present in progress.

The formation of steam or the collection of rain, snow, or ice on windshields, particularly those of cabin type airplanes, very often seriously hampers the pilot's view and introduces an additional hazard of piloting. A research is now in progress to determine the possibility of eliminating this hazard under all atmospheric conditions. One possible solution is the use of a windshield containing an opening which is large enough for a reasonable amount of visibility but through which the entrance of rain, snow, etc., or an objectionable amount of air, is prevented by the air flow over the opening. Preliminary tests are now being conducted on a model cabin airplane in which an attempt is being made to accomplish the above by regulating the air flow either by means of the shape of the windshield or by cowling in front of the windshield.

#### WASHINGTON NAVY YARD

*Airplane models.*—During the past year the 8-foot wind tunnel at the Washington Navy Yard has been employed, as in the past, almost entirely in testing airplane models and airfoils. Twenty-nine complete tests in pitch and yaw were made on 17 models representing 15 designs. In addition to these tests, approximately 20 partial tests were made to investigate particular features such as control effectiveness, interference, etc. In so far as practicable the routine work is planned to include items of a research nature that arise in the course of design studies. This policy permits the carrying of research work along with the design testing without holding up the latter.

A number of the wind-tunnel tests made during the past year were on types for which flight-test data are now available. It is of interest to note that the predictions based on the model test data have been uniformly satisfactory. For example, the average agreement in maximum speed is well within 1 per cent, with an extreme deviation of less than 2 per cent. In the matters of stability and control the reliability of the wind tunnel has been demonstrated conclusively in the past, but data obtained during the past year in several cases of slight instability and slight deficiency of control are very convincing.

*Airfoils and wings.*—Routine tests have been made on 25 airfoil models, including the Navy series N-25 to N-46, the Göttingen sections 443, 444, and 445, and the N. A. C. A. M-6 and M-12. Several sections in the Navy series have sufficient merit to justify tests in the variable-density wind tunnel.

*Control surfaces.*—Measurements have been made for the control effectiveness of 5 rudders, 2 elevators, and 2 ailerons. These tests were made on various airplane models in connection with the problems of control-surface design. One aileron was tested for hinge moments, using a special model constructed for this purpose.

*Floats and fuselages.*—Tests of varying degrees of completeness have been made on eight seaplane floats. In all cases each model was tested for scale effect at 0° pitch and yaw and for lift and drag in pitch. Four additional models are now awaiting test.

Tests in pitch and yaw have been completed on four body models in continuation of a previous series and nine additional models are now awaiting test. This work is being carried out in the 4-foot wind tunnel.

*Radiators.*—A rather extensive research has been made on the cooling properties of wing radiators of various types, using sections of full-scale radiators where available.



*Handley-Page slotted wing.*—Two models of the Handley-Page slotted wing have been tested, one for the operation of the automatic slot and the other for air forces on the leading airfoil. The satisfactory direct measurement of air forces on the leading airfoil required unusual care, but the wind-tunnel staff is convinced that the method used is as reliable as the pressure-distribution method.

*Lighter-than-air craft.*—No tests on lighter-than-air craft have been made since the completion of the extensive research on the rigid airship designs last year. However, considerable work has been done in the design and construction of a new type of oscillator for measuring damping moments. This oscillator when completed will be used to measure damping moments on several models now awaiting such tests.

*Miscellaneous tests.*—An extensive research has been made in the 4-foot wind tunnel in studying the resistance of wire screens of varying wire and mesh sizes. The investigation is being completed by interference measurements on parallel rods and struts with variable spacing.

Tests have also been made in the 4-foot wind tunnel on a series of cylinders, disks, and other shapes. Additional tests of this nature are now contemplated.

A study is now being made to devise simple methods of measuring lateral stability derivatives with the view of adopting these tests as a part of the routine work on new designs.

#### BUREAU OF STANDARDS

*Wind-tunnel investigations.*—A final report has been prepared and submitted to the committee for publication as a technical report on the measurements of the characteristics of 24 airfoil sections at speeds of 0.5, 0.65, 0.8, 0.95, and 1.08 times the speed of sound. The airfoils were of 1-inch chord and extended entirely across the 2-inch air stream. The aspect ratio on these tests was rather small, and in order to determine the influence of aspect ratio at high speeds new equipment has been assembled to permit the use of aspect ratios of 6 or more. The equipment consists of three large tanks, each having a capacity of about 1,000 cubic feet, which may be filled with air under a pressure of 20 or 30 pounds per square inch. By means of a quick-opening valve the air in the three tanks may be released through a 6 or 8 inch nozzle, the speed dropping from the speed of sound to about one-half the speed of sound in about 20 seconds. An automatic balance is now being designed to give continuous records of the lift and drag on airfoils during the discharge period.

Apparatus has been assembled and used for the measurement of the time variations of air speed in wind tunnels. The speed variations produce changes in temperature and hence in the resistance of a fine platinum wire about 1 centimeter long and 0.0017 centimeter in diameter, which is heated electrically by a constant heating current. The variations in the voltage drop across the wire are amplified by means of a resistance-coupled direct-current amplifier. A theory has been worked out for the response of a hot wire as a function of the frequency and the theory has been checked experimentally and found to be substantially correct. It has been found possible to incorporate in the electrical circuits a device which compensates automatically for the effect of the lag for frequencies up to 150 cycles per second. A traverse across the working section of the wind tunnel shows that the stream consists of a core of approximately uniform speed in which the mean amplitude of the speed variation (turbulence) is small and uniform throughout the cross-section. This core is surrounded by a ring about 3 inches in thickness near the wall in which the speed decreases according to a power of the distance from the wall and the turbulence increases. Near the wall the percentage variation of local speed reaches a value of about  $\pm 15$  per cent.

The investigation of wind pressure on chimneys has been continued. The experimental chimney, 10 feet in diameter and 30 feet high, on the roof of one of the buildings of the Bureau of Standards has been mounted on siphons for the measurement of overturning moments. An installation for pressure-distribution measurements has also been made on the new power-plant stack at the Bureau of Standards. The observations obtained so far are not sufficiently numerous to justify a statement of conclusions at this time.



In cooperation with the aeronautics branch of the Department of Commerce and the National Advisory Committee for Aeronautics, measurements are being made of the rolling and yawing moments produced by ailerons of various chords and spans on 10 inch by 60 inch models of Clark Y and U. S. A. 27 wing sections. The results for an angle of attack of  $4^\circ$  have been submitted to the committee for publication as a Technical Report.

*Aeronautic instrument investigations.*—The work on aeronautic instruments has been conducted in cooperation with the Bureau of Aeronautics of the Navy Department and the National Advisory Committee for Aeronautics.

The purchase specifications for service aircraft instruments for the Bureau of Aeronautics require that a fraction of the number purchased be given type tests, which relate to the effect of temperature, vibration, elastic defects, and other factors. This testing increased greatly during the past fiscal year. In addition to the primary purpose of determining whether the instruments meet the specifications, the test data have been a valuable source of information in the preparation of new specifications.

The development program covered new and improved apparatus for testing aircraft instruments, improvements in service instruments, and the development of aircraft instruments for special purposes. Two vibration racks of new design were constructed which permit the independent control of frequency and amplitude of vibration. One of these racks is now being used to accumulate data on the effect of these factors on various types of service instruments as a basis for new specifications. An apparatus has been constructed which oscillates with simple harmonic motion comparable to the minor oscillations of an airplane. It is large enough to carry two observers and is for the purpose of studying the effect of small accelerations on the artificial horizons of sextants. An electric resistance thermometer was constructed for the Bureau of Aeronautics for use in flight testing. An earth inductor compass with the Heyl-Briggs method of indication was constructed for experimental purposes. Definite progress has been made in the development of a distant indicating tachometer of the direct-current magneto type for use in multi-engined airplanes. The completed instrument will probably consist of a small commercial magneto and a voltmeter with a pointer motion of  $270^\circ$ , both compensated for temperature. Development work on other types of distant indicating tachometers is also in progress.

Research has continued on the properties of elastic materials used in instrument design. A theoretical investigation of tuning forks of particular shape has been made, preliminary to the use of tuning forks of this design for the purpose of determining the elastic hysteresis modulus of various metals. The change in the modulus in torsion of diaphragm and spring metals in the temperature range  $+50^\circ\text{C.}$  to  $-20^\circ\text{C.}$  for various fiber stresses has been studied. A report has been submitted to the committee for publication on pressure elements of constant logarithmic stiffness for a temperature-compensated altimeter. A report has been prepared on the relations between time, fiber stress, and elastic afterworking, or drift, based largely on the experimental results given in the committee's Technical Note on tension experiments in diaphragm metals.

The results of the investigation of damping liquids for aircraft instruments have been submitted to the National Advisory Committee for Aeronautics for publication. The report includes data on the viscosity, change in viscosity, and lowest useful temperature of a number of selected liquids and mixtures in a temperature range from  $+30^\circ$  to  $-20^\circ\text{C.}$  The liquids include those commonly used in aircraft compasses, inclinometers, bubble horizons, and other instruments.

#### MATÉRIEL DIVISION, ARMY AIR CORPS

*General.*—The high-speed 14-inch wind tunnel has been dismantled throughout the past year, and the 5-foot wind tunnel has not been in operation since the middle of January, 1928, on account of the moving of the tunnels to the new Wright Field. Consequently the amount of wind-tunnel work carried on has been limited.

*Development of apparatus.*—An automatic air-speed control for the 5-foot wind tunnel has been developed and built, but not tested. This control depends for its operation upon the



cutting off of the light, by means of a colored manometer liquid, in front of a photo electric cell, which actuates a series of relays to vary the motor field resistance.

*Airplane model tests.*—Only one routine model test was made in the 5-foot wind tunnel. This test was made on a  $\frac{1}{24}$ -scale model of the Douglas O-2H observation airplane at 40 miles per hour on the N. P. L. balance.

*Wind-tunnel investigations.*—An intensive study was made to determine the characteristics of the horizontal tail surfaces of an airplane, particularly the relation between the elevator hinge moment and the total tail moment. The study was made in connection with the theoretical analysis of longitudinal stability made by the matériel division. Wind-tunnel tests were made upon a  $\frac{1}{5}$ -scale model of the Curtiss AT-4 fuselage and tail surfaces.

As a result of the directional instability observed on several of the new type airplanes, model tests were made in the wind tunnel to determine the remedy that would be the most effective in overcoming this difficulty. These tests consisted in the measuring of the effect upon the yawing moments caused by varying the size and type of vertical tail surfaces, by increasing the length of fuselage, and by the replacing of a single fin and rudder with double fins and rudders.

Tests were made to determine the merits of two methods suggested for obtaining lateral control of airplanes. The principle of the first method was based on the reduction of lift, by means of a device placed on the leading edge to destroy the air flow. The second method consisted in hinging the wing tips, thus causing the lift to vary because of the increase or decrease of effective area with the angle of the wing tips.

The path of a 25-pound demolition bomb for the first 5 feet after release from an airplane was determined by dropping dummy bombs in the wind tunnel at air speeds up to 250 miles per hour.

*Miscellaneous tests.*—The miscellaneous testing consisted of various calibration and comparative tests on wind-driven generators, earth-inductor compasses, Venturi tubes, and air-speed indicators.

## REPORT OF COMMITTEE ON POWER PLANTS FOR AIRCRAFT

### ORGANIZATION

The committee on power plants for aircraft is at present composed of the following members:

Dr. S. W. Stratton, Massachusetts Institute of Technology, chairman.

George W. Lewis, National Advisory Committee for Aeronautics, vice chairman.

Henry M. Crane, Society of Automotive Engineers.

Prof. Harvey N. Davis, Stevens Institute of Technology.

Dr. H. C. Dickinson, Bureau of Standards.

William F. Joachim, National Advisory Committee for Aeronautics.

Lieut. Commander James M. Shoemaker, United States Navy.

Prof. C. Fayette Taylor, Massachusetts Institute of Technology.

Capt. T. E. Tillinghast, United States Army, matériel division, Air Corps, Wright Field.

### FUNCTIONS

The functions of the committee on power plants for aircraft are as follows:

1. To determine which problems in the field of aeronautic power-plant research are the most important for investigation by governmental and private agencies.

2. To coordinate by counsel and suggestion the research work involved in the investigation of such problems.

3. To act as a medium for the interchange of information regarding aeronautic power-plant research in progress or proposed.

4. To direct and conduct research on aeronautic power-plant problems in such laboratories as may be placed either in whole or in part under its direction.

5. To meet from time to time on call of the chairman and report its actions and recommendations to the executive committee.



By reason of the representation of the Army, the Navy, the Bureau of Standards, and the industry upon this subcommittee, it is possible to maintain close contact with the research work being carried on in this country and to exert an influence toward the expenditure of energy on those problems whose solution appears to be of the greatest importance, as well as to avoid waste of effort due to unnecessary duplication of research.

The committee on power plants for aircraft has direct control of the power-plant research conducted at Langley Field and also of special investigations authorized by the committee and conducted at the Bureau of Standards. Other power-plant investigations undertaken by the Army Air Corps or the Bureau of Aeronautics are reported upon at the meetings of the committee on power plants for aircraft.

#### LANGLEY MEMORIAL AERONAUTICAL LABORATORY

ENGINE RESEARCH—*Aircraft oil engines*.—The outstanding improvement in the performance of the committee's single-cylinder oil engines during the past year has been the attainment of high power output and increased flexibility of the engines with low maximum cylinder pressures.

*Engine performance—High air turbulence*.—The investigation undertaken to determine the effect of high turbulence of the combustion air, as influenced by the design of cylinder head, on the performance characteristics of a high-speed oil engine have been continued with the No. 3 cylinder head having a pear-shaped precombustion chamber. The factors under investigation include the determination of the effects on engine performance of extending the fuel-valve nozzle into the bulb for distances of  $1\frac{1}{2}$ , 1, and  $\frac{1}{2}$  inch and directing the fuel charge toward the center of the  $\frac{9}{16}$ -inch diameter bulb-to-cylinder orifice. A series of orifices will be tested for each nozzle extension to determine the orifice diameter and length of nozzle extension which will give maximum engine performance.

Tests are in progress to determine the engine performance obtainable for a complete range of fuel quantities from zero load to full load with the  $1\frac{1}{2}$ -inch extension of fuel-valve nozzle. The orifices to be tested range from 0.020 inch to 0.035 inch in diameter. For these tests the start of injection, duration of injection, and spray start and cut-off characteristics of the fuel-injection system are being determined at an engine speed of 1,500 r. p. m. by observing the fuel sprays with an oscilloscope when injected into the atmosphere.

*Engine performance—Moderate air turbulence—Performance at low cylinder pressures*.—Investigations have been continued with the cylinder head having a vertical disk-type combustion chamber formed between the horizontally arranged inlet and exhaust valves. A moderate degree of air turbulence is produced in the combustion chamber of this cylinder head by displacing the air between the piston and the cylinder head through a large rectangular orifice into the combustion chamber. The effects on engine performance of various combinations of injection-valve orifices of small diameter located in one plane in the fuel-valve nozzle and designed to distribute the fuel charge throughout the combustion chamber are under investigation. The results obtained indicate that it is possible to lower the maximum cylinder pressures considerably in a high-speed oil engine and still obtain good engine performance by controlling the rate of fuel injection and proportioning the size and number of the orifices in the fuel-injection valve.

Fuel-injection valve nozzles having 3, 5, and 7 round orifices have been tested. Maximum engine performance to date has been obtained with an injection valve located in the center of the cylinder head at the top of the combustion chamber using a nozzle having seven orifices of small diameter. The diameters of the five orifices delivering fuel to the air in the upper portion of the vertical disk-shaped combustion chamber have been maintained constant and the diameters of the two main orifices delivering fuel to that portion of the air charge in the rectangular orifice directly above the piston crown have been varied from 0.010 to 0.021 inch. The engine performance has been determined for each fuel-injection-valve nozzle.

The maximum distance from the fuel-valve nozzle to the top of the piston is  $4\frac{1}{2}$  inches, with the piston at top center. The carbon formation on the piston showed that for main orifices of 0.012-inch diameter and larger the fuel sprays impinged on the piston.

The maximum engine performance with this cylinder head assembled on an N. A. C. A. single-cylinder test engine having a 5-inch bore and a 7-inch stroke, a compression ratio of 14



full-load fuel quantity (i. e., that fuel quantity giving 15 per cent excess air in the cylinder), and 1,500 r. p. m., was obtained with the nozzle having two main orifices of 0.018-inch diameter. The results showed that with 15 per cent excess air in the cylinder the indicated mean effective pressure increased from 99 to 122 pounds per square inch, with increase in orifice diameter from 0.010 inch to 0.018 inch. The corresponding fuel consumption decreased from 0.60 to 0.49 pound per indicated horsepower per hour. The maximum cylinder pressure, as indicated by a very light-weight disk-type maximum-cylinder, pressure indicator, did not exceed 500 pounds per square inch. An increase in main orifice diameter from 0.018 inch to 0.021 inch resulted in a slight decrease in indicated power.

At a fuel quantity giving approximately three-fourths full load torque, which corresponds to engine operation at cruising speeds, and maximum cylinder pressures below 500 pounds per square inch, the indicated mean effective pressure varied from 84.5 pounds per square inch with an orifice diameter of 0.010 inch to 90 pounds per square inch with an orifice diameter of 0.018 inch. The indicated fuel consumption for the nozzle with the two main orifices of 0.018-inch diameter was 0.39 pound per indicated horsepower per hour. The maximum brake mean effective pressure for cruising conditions, assuming a mechanical efficiency of 85 per cent, would be 76.5 pounds per square inch, and the corresponding fuel consumption 0.46 pounds per brake horsepower per hour.

*Engine performance—Moderate air turbulence—Performance at medium cylinder pressures.*—At 1,500 r. p. m., full-load fuel quantity, and a maximum recorded cylinder pressure of 665 pounds per square inch, the engine developed a maximum indicated mean effective pressure of 130 pounds per square inch with a corresponding fuel consumption of 0.45 pound per indicated horsepower per hour. Based on a mechanical efficiency of 85 per cent for multi-cylinder operation this performance gives a brake mean effective pressure of 113 pounds per square inch and a fuel consumption of 0.53 pound per brake horsepower per hour. The maximum brake mean effective pressure developed by the Liberty 12 engine is 123 pounds per square inch and the fuel consumption 0.53 pound per brake horsepower per hour. The performance obtained for the engine operating at cruising power with a maximum cylinder pressure of 650 pounds per square inch would be 76 pounds per square inch brake mean effective pressure and 0.44 pound per brake horsepower per hour fuel consumption. The single-cylinder engine can be idled at 150 r. p. m. and rapidly accelerated without knocking or missing to a rotative speed of 2,100 r. p. m.

*Cylinder-head design.*—The investigation to determine the effect on engine performance of various degrees of turbulence brought about by cylinder-head design will be continued with the cylinder head having a horizontal disk-type combustion chamber and a short large-diameter displacer on the piston. This cylinder head has been machined and the assembled cylinder head and valve gear are ready for installation and testing.

*Two-stroke cycle gasoline-injection engine investigation.*—The pursuit-type airplane having high speed, rapid climb, and the highest degree of maneuverability requires a power plant having a large power output with minimum weight. Because of the theoretical increase in power and decrease in engine weight when operating on the 2-stroke cycle, a radial air-cooled engine having gasoline injection and electric ignition is a type of power plant inherently suitable for this class of service. The fundamental factors affecting the operation of this type of engine will be investigated with a single-cylinder 2-stroke cycle air-cooled engine having a  $4\frac{5}{8}$ -inch bore and a 7-inch stroke. The engine will be designed to operate with a high compression ratio and a maximum rotative speed of 2,000 r. p. m.

*Cylinder assembly.*—The cylinder design for the 2-stroke cycle test engine will consist of a standard Liberty air-cooled engine cylinder altered for 2-stroke cycle operation and for assembling on the crank case of an N. A. C. A. universal engine. Ports will be machined in the lower portion of the cylinder barrel for admission of the scavenging and combustion air. The exhaust gases will be discharged through two standard poppet valves in the cylinder head. The design of the exhaust-valve operating mechanism and the combustion-chamber shape have been completed. The valve-operating mechanism consists of a cam mounted on the engine crank shaft, a spring-



loaded cam follower and tappet, and individual push rods for each exhaust valve. This type of valve-operating mechanism is readily adaptable to radial engines having push rods operated from a cam disk. The combustion chamber will be formed by the domed head of the standard Liberty air-cooled engine cylinder and a special aluminum-alloy piston having a concave head and moderately beveled edges. A detailed analysis has been made of the design of the combustion-chamber shape in order to meet definitely the fundamental requirements of the reliability of ignition, high-brake mean effective pressure, economy, and flexibility.

*Combustion air system.*—The combustion air for this engine will be supplied by an N. A. C. A. Roots type supercharger driven by an electric motor. The mounting of the supercharger outlet in relation to the air manifold closely simulates the type of mounting which would be required for a 2-stroke cycle multicylinder engine. Since the supercharger which will be used in this research has sufficient air capacity for operating a multicylinder, 2-stroke cycle engine, the excess air supplied by the supercharger will be by-passed under pressure conditions in the engine manifold, simulating those in a multicylinder engine manifold of a 2-cycle radial engine. In order to maintain practically constant air pressure in the inlet-air manifold of the experimental engine, an air by-pass valve consisting of a large number of rectangular spring-loaded steel strips and a housing integral with the manifold is being designed. Because of the low inertia of the moving parts of this type of by-pass valve, the pressure in the inlet air manifold will remain practically constant regardless of any tendency to surging of the air in the line due to the opening and closing of the inlet ports in the cylinder. The quantity of scavenging and combustion air required for the operation of the engine over a full range of engine speeds and loads will be determined by means of Venturi meters calibrated by a gasometer. The inlet-air manifold will consist of a 2-piece aluminum casting bolted directly to the steel cylinder.

*Fuel-injection system.*—The design of a fuel-injection system for the 2-stroke cycle engine which will give reliability and good fuel economy is complicated by the fact that the low air pressures into which the gasoline is injected permit considerable penetration of the sprays. Tests made with the N. A. C. A. spray photography apparatus showed that orifices 0.004 inch in diameter, even when used with low injection pressures, gave excessive penetration for this size of cylinder. It has been necessary, therefore, to design a new type of fuel-injection nozzle which will give a high degree of fuel atomization, but only sufficient penetration to permit the efficient distribution of the fuel-spray particles in the combustion air. The design of the fuel-injection valves has been started.

The fuel-injection pump for this engine will consist of a cam-operated fuel-injection pump driven from the engine crank shaft. The start and stop of injection will be controlled by the closing and opening of a fuel by-pass valve. The design of this fuel-injection pump has also been started.

*Cooling-air system.*—The cooling-air system for the 2-stroke cycle engine, consisting of a conoidal-type blower driven by electric motor and suitable air ducts, has been designed, constructed, and partially tested. The temperatures of the cylinder head, cylinder barrel, and fins will be recorded for all test conditions by fine wire thermocouples and recording pyrometers.

*Fuel-injection pumps and valves—Fuel valve extensions.*—In order to determine the effect of the position of the fuel valve nozzle and the turbulence of the cylinder air on the performance of a cylinder head having a precombustion chamber, it has been necessary to develop a method for preventing the rapid oxidation of the fuel-valve nozzle extensions when extended into the precombustion chamber for a maximum distance of  $1\frac{1}{2}$  inches. The extension must operate at such a temperature that any fuel blown onto it by the air movement in the cylinder is immediately vaporized and does not carbonize on the nozzle extension. Several designs of copper fins have been investigated, but the rapid oxidation of the copper fins resulted in a loss in the heat-transmission capacity of the copper and the consequent failure of the fins. In the present design, the finned surfaces have been replaced by three concentric insulating stainless-steel sleeves. The sleeves are machined so as to provide an insulating air gap 0.004 inch thick between each sleeve and the inner sleeve and the valve-nozzle extension. Preliminary engine tests made at 1,500 r. p. m. showed that the outer insulating sleeve attained a temperature of about



550° F. for one-half its length and was exceptionally clean and free from carbon. The colors on the tip of the fuel-valve stem and nozzle indicated a temperature of about 480 to 500° F., but the remainder of the stem maintained the original bright, polished surface.

*Fuel-injection pumps and valves—Dual-stem fuel-injection valve.*—The single-injection rate fuel-injection valve used with the No. 7 cam-operated fuel-injection pump in the investigation made to determine the effect on engine performance of various combinations and sizes of small-diameter orifices did not permit the attainment of the varying fuel-injection rates for which the cam-operated fuel-injection pump was designed. A dual-stem fuel-injection valve has therefore been designed, having spring-loaded lapped stems with opening pressures of 2,000 and 4,000 pounds per square inch. The orifice diameters of the fuel-valve nozzle have been proportioned to give uniform distribution of fuel sprays throughout the vertical disk-type combustion chamber of cylinder head No. 4. The injection valve is being constructed.

*Multi-cylinder fuel-injection systems.*—The previous work of the committee has been limited to the investigation of injection problems occurring in fuel-injection systems for single-cylinder aircraft-type oil engines. These investigations have not included data on the hydraulic distribution and injection problems encountered in the operation of fuel-injection systems for aircraft-type multi-cylinder oil engines. An investigation will therefore be made to determine the degree of application of the results obtained with fuel-injection systems for single-cylinder engines to multi-cylinder engine operation.

A six-plunger cam-operated fuel-injection pump having the start and duration of fuel injection controlled by the closing and opening of fuel by-pass valves has been designed for this investigation. The fuel-pump controls, which have been designed to simulate the throttle and spark controls of a carburetor-type engine, permit a variation in the start of injection of 65 crank degrees and a variation of 70° in the time at which the fuel by-pass valve may be opened to stop injection. The angular position of the cams may be varied 20 crank degrees in relation to the engine crank shaft while the engine is running. A method of compensating for irregularities in machining and wear which will insure accurate timing of injection for each pump plunger by the maintenance of the proper clearances in the by-pass valve operating mechanism has been incorporated in the design of the pump. The castings for this pump have been received and the machining of the pump is in progress.

*Aircraft-oil-engine pistons.*—Engine tests have been completed to determine the operating characteristics of the Y-alloy skeleton-type high-speed oil-engine pistons having the thrust faces of the piston lubricated by oil under pressure from the piston pin. This design of piston weighs only nine-tenths as much as the standard Army Liberty-type aluminum-alloy piston and is 30 per cent stronger. The factors studied have included the determination of the permissible rate of oil delivery to the thrust faces of the piston, the possible reduction in clearance between the piston and cylinder with satisfactory engine operation, and the piston friction and sealing ability of various combinations of narrow-compression and oil-scraper piston rings.

The results of the tests showed that it is possible to increase the quantity of oil delivered to the thrust faces of the piston at 1,500 r. p. m. to the point where a new film of oil 0.005 inch thick is delivered every stroke of the piston over the entire cylinder surface. This large quantity of oil cools the piston skirt so that the thrust faces operate at very low temperatures. The combination of compression and oil scraper rings which prevent the passing of the lubricating oil to the combustion chamber consists of two compression piston rings 0.100 inch wide and three oil scraper rings 0.100 inch wide. The oil consumption with this type of piston ring assembly with pressure lubrication to the piston is less than that of the standard Liberty aircraft engine. Satisfactory engine operation is being obtained over the complete range of engine loads from zero load to approximately 25 per cent overload with the piston to cylinder clearance, measured at the piston thrust faces, reduced to 0.010 inch on a 5-inch cylinder diameter. The use of these aluminum-alloy pistons in both the committee's single-cylinder oil engines has lowered the piston temperatures, decreased the wear of the pistons and liners, and resulted in quieter engine operation at all speeds and loads.



*Maximum cylinder-pressure indicators—Disk type.*—Tests have been continued with the balanced-pressure disk-type maximum cylinder-pressure indicator to determine the sensitivity of the disk in indicating high fast-rising cylinder pressures. Two disks having area-weight ratios of 0.475 and 0.0957 were tested at an engine speed of 1,500 r. p. m. A range of cylinder pressures having different rates of pressure rise and values of maximum intensity was obtained by varying the injection advance of the engine from  $4^\circ$  to  $12^\circ$  before top center. The disk having the area-weight ratio of 0.475 gave consistently higher pressure readings. The difference in the pressures indicated by the two disks varied from 10 pounds per square inch at an injection advance angle of  $4^\circ$  before top center to 310 pounds per square inch at an injection advance angle of  $12^\circ$ .

*Maximum cylinder-pressure indicators—Electrically operated type.*—A balanced-pressure diaphragm-type maximum cylinder-pressure indicator has been designed, constructed, and assembled for testing in an engine. The diaphragm element of this indicator is 0.004 inch thick, 0.5 inch in diameter, and is clamped between two surfaces so that its free diameter is 0.375 inch. The maximum movement of the center of the diaphragm is 0.005 inch in one direction from its unstressed position. Preliminary tests indicate that the accuracy of this instrument is limited only by the pressure gauges for measuring the balancing air pressures. The contact between the diaphragm and its support at equality of cylinder gas and balancing pressure is at present indicated by means of "clicks" in a head phone. A visual means for indicating this contact is being developed so that simultaneous observations may be taken of the maximum cylinder pressures of all cylinders in a multi-cylinder engine.

*Investigations completed—Performance of a 4-part automatic injection valve.*—As previously reported, the design, development, and testing on an engine of a new type fuel-injection valve having only four parts and suitable for disk or conical-shaped combustion chambers have been completed. The results of this investigation are being prepared for publication in two reports entitled "The Injection Characteristics of a Four-Part Automatic Injection Valve" and "High-Speed Oil Engine Performance with a Four-Part Automatic Injection Valve." The first of these reports will contain a description of the valve, a theoretical analysis of the injection characteristics of this type of valve, and the results of the engine development and bench tests. The second report will present the engine performance obtained with this type of fuel-injection valve when used with the standard N. A. C. A. universal test engine having a pent-roof-shaped combustion chamber. The factors investigated include the effect of speed, fuel quantity injected per cycle, injection-advance angle, valve-opening pressure, compression pressure, and preheating of the fuel oil on the performance of the engine at a speed of 1,500 r. p. m.

*Investigations completed—Heat losses from engine cylinders.*—A theoretical investigation has been made to determine the effect of bore-stroke ratio and shape of cylinder-head on the heat losses from an engine cylinder due to radiation and conduction. Relative heat losses have been calculated for four cylinder-head shapes; i. e., domed, two semidomed, and flat, and a range of bore stroke ratios from 0.6 to 1.4. A report entitled "The Effect of Bore-Stroke Ratio and Cylinder-Head Shape on the Radiation and Conduction Losses from an Engine Cylinder" is being prepared for publication.

*Investigations completed—Injection-system characteristics.*—A method has been developed for the determination of the start, duration, and cut-off characteristics of fuel-injection sprays when injected into the atmosphere from a fuel-injection system operated on an engine. Some test results obtained with an impact-type fuel-injection pump and a spring-loaded automatic fuel-injection valve have been published in a Technical Note entitled "The Determination of Several Spray Characteristics of a High-Speed Oil-Engine Injection System with an Oscilloscope."

*Investigations completed—Cylinder-pressure indicators.*—A part of the investigation to determine the methods and instruments for indicating the maximum gas pressures in high-speed internal-combustion engine cylinders has been completed and the results published in a report entitled "The Measurement of Maximum Cylinder Pressures." Five maximum cylinder-



pressure devices have been designed, developed, and tested, in addition to the testing of three commercial indicators. The results of the investigation at present indicate that the greatest degree of accuracy can be obtained with a gas balanced-pressure diaphragm or disk-type indicator.

**FUEL-INJECTION RESEARCH.**—The N. A. C. A. spray photography equipment has been used for further photographic investigation of the characteristics of injection systems and of fuel sprays produced by them. Injection pressures up to 12,000 pounds per square inch and chamber pressures up to 600 pounds per square inch, the air being either still or turbulent, are used in the investigation. Twenty-five pictures of each spray are obtained at rates of from 2,000 to 4,000 pictures per second on photographic film. The pictures are taken with an exposure of less than one-millionth second and show the start, development, cut-off, and distribution of the sprays.

*Injection time lags.*—The design of the injection system of a high-speed oil engine necessitates knowledge of the time lags involved in the operation of the system. An investigation of the velocity of pressure waves and the time lags of the spray photography injection system was completed during the previous year. The experimental data have been analyzed and formulæ have been derived for computing the velocity of pressure waves in the injection tubes and the lags due to the time required for the wave to travel the injection tube and cause the injection valve to open and inject oil. The effects of length of injection tube, injection pressure, initial tube pressure, and valve-opening pressure on the pressure-wave velocity and the injection lags are expressed by the formulæ. These formulæ are applicable to the computation of the lags of any injection system using pressure-wave injection. A report covering this investigation is being prepared for publication.

*Injection-valve operation.*—The operation of the spray photography injection system has been studied both by mathematical analysis and by taking records of the motion of the injection timing valve. The timing valve stem was held to its seat by a helical spring under light load, so adjusted that the hydraulic pressure on the stem actuated it immediately after it had been lifted mechanically from its seat. The motion of the stem was recorded photographically and the pressure variations at the stem seat were analyzed. The effect of the length of injection tube was also studied in this connection. The results of the analysis of the pressure variations and the equations of motion of the timing valve stem are applicable to a spring-loaded automatic injection valve. A report on this investigation is being prepared for publication.

*Effect of air turbulence on spray characteristics.*—Among the factors that affect the mixing of the particles of oil spray with the combustion air in the engine cylinder, air turbulence is usually considered to be important. An investigation was therefore carried out with the spray-photography apparatus in order to determine the effects of an air flow of known direction and velocity on oil sprays in dense air. The spray-photography chamber was arranged to simulate the shape of an engine combustion chamber of the flat disk-shaped type. Air was blown through the chamber against the spray at a maximum velocity of 60 feet per second, a static pressure of 200 pounds per square inch being maintained in the chamber. The oil was injected from a seven-orifice nozzle and from three single orifices of different sizes. It was found that air turbulence had very little effect on spray penetration, but it increased the width and probably the atomization of the sprays. The air flow did not materially affect the sprays until about 0.004 second after the start of injection. A report on the results of this investigation is being prepared for publication.

The characteristics of oil sprays from several multiorifice nozzles, each having a different combination of orifice sizes, have been studied. Increasing the size of the large orifices in the nozzles decreased the penetration of the sprays from the small orifices in the nozzles as much as 15 per cent. The penetration of the sprays as measured by means of spray photographs checked the penetration in the engine as indicated by the carbon deposit on the piston.

*Ignition lag of oil sprays.*—The determination of the ignition lag of oil sprays is of considerable importance in the design of high-speed oil engines. Pending the completion of the design and construction of the spray-photography-combustion equipment, which will closely



simulate engine conditions, tests have been made using an electrically heated sheet-metal chamber large enough to prevent the spray from coming in contact with the walls of the chamber. Because of the fact that atmospheric air pressure only was used in the chamber, the ignition lag was extremely long compared to that in an engine.

*Spray-combustion-photography equipment.*—The design of new apparatus to be used in connection with the present spray-photography equipment in order to make possible the study of the characteristics of combustion of atomized fuels for oil engines is well under way. Several preliminary designs have been completed, the final arrangement of the apparatus has been decided upon, and detail drawings have been started.

The apparatus as designed at present will consist of the spray-combustion chamber proper, the electric-heating chamber, the turbulence cylinder, and the motors, shafts, and clutches for operating the injection and turbulence apparatus. The spray chamber will have quartz-glass windows by means of which it will be possible to photograph the oil-spray combustion. Air will be circulated from the heater through the spray chamber by means of a 2-inch 2-bladed metal propeller operating at high speed. The turbulence apparatus will consist of a cylinder containing a piston operated by a connecting rod and crank so as to furnish air circulation with the desired velocity and in the desired direction during injection and combustion of the oil spray. The combustion chamber, heating chamber, and turbulence cylinder will be cast of nichrome in two parts and will be bolted together in one compact unit. The spray chamber, injection apparatus, and camera will be on top of a cast-iron table, the remainder of the apparatus being inclosed beneath the table top.

With this apparatus it will be possible to photograph oil sprays and their combustion when injected into air under conditions similar to those in an oil engine during injection. Temperatures up to 1,400° F. and pressures up to 600 pounds per square inch may be produced. The injection apparatus may be operated alone or in conjunction with the turbulence apparatus to give the desired turbulence. A complete temperature survey of the combustion chamber will be possible by means of special thermocouples, and the pressure rise during combustion will be recorded by means of a pressure indicator.

Various high-speed photographic films have been investigated in order to determine the best type of film for recording the combustion of oil sprays. High-speed panchromatic films from three manufacturers were found to record the combustion, and the best film was selected for future use.

*SUPERCHARGER AND COOLING RESEARCH—Supercharger analysis.*—Test data on the comparative performance of three sizes of N. A. C. A. Roots type superchargers, two-geared centrifugal supercharges, and one vane-type supercharger have been analyzed and compared. The minimum power required to compress air by hypothetical superchargers of the geared centrifugal, vane, and Roots types operating under the same conditions and at the same efficiencies as the superchargers actually tested, but of sufficient capacity to compress 1 pound of air per second, formed the basis for this comparison. The adiabatic efficiency for each supercharger was also computed. For pressure differences up to 15 inches of mercury, the range of pressures investigated, the results obtained show that the Roots type supercharger requires less power than either of the other two types. At higher pressure differences the trend of the curves indicates that the centrifugal supercharger may require less power. As the discharge rate at which certain superchargers operate at minimum power is very limited, considerable saving in power can be effected by selecting the size of supercharger that is best fitted for the service required. A report will be prepared in the near future presenting the results of this investigation.

*Supercharger modifications.*—The manufacturer of the welded steel impellers which are intended for use in the Roots type supercharger has been unable to make delivery to date because of unexpected constructional difficulties. A sample steel impeller delivered at the laboratory showed that electric welding was feasible, but that great care was necessary to obtain a good weld between the impeller shell and the ribs and at the same time obtain the correct impeller contour without the necessity of excessive grinding. A process of forming and grinding the



ribs before welding is now being investigated to overcome this difficulty. It is believed that these steel impellers in an aluminum case will give sufficient operating clearances at the temperatures obtained at high compression ratios to permit assembly and operation at low and medium compression ratios with small clearances. Should the clearances be excessive with steel impellers in an aluminum case at high operating temperatures the possibility of reducing the clearance by cooling the case will be considered.

*Cooling of superchargers.*—From both a thermodynamic and a mechanical point of view it is desirable that a supercharger operate in such a manner that the compression exponent  $n$  in the expression  $P_1 V_1^n = P_2 V_2^n$  shall have the minimum practical value. The thermodynamic reasons are that it requires less power to compress a given weight of air with a low compression exponent and the delivery air temperatures are lower, which will result in an increase in the weight of the air delivered to the engine and, therefore, in an increase in engine power. The mechanical reasons are that the supercharger operates at a lower temperature, as a result of which the heat, stresses are reduced and the friction, clearance, and lubrication difficulties are decreased. The theoretical power required to compress 1 pound of air per second from atmospheric pressure to 29.92 inches of mercury for altitudes from 0 to 50,000 feet, using compression exponents of 1, 1.1, 1.2, 1.3, 1.407, 1.5, 1.6, 1.7, 1.8, 1.9, and 2, has been computed. The temperatures of the discharge air for these conditions have also been computed. It was found that under standard atmospheric conditions a supercharger with a compression exponent of 1.24 would maintain a constant temperature in the air discharged up to about 36,000 feet, i. e., to the isothermal atmosphere. It was also found that a reduction of the compression exponent from the usual values to 1.24 would reduce the temperatures of the air discharged sufficiently to make possible a gain of approximately 50 horsepower on a supercharged Liberty engine at a critical altitude of 22,000 feet.

*Effect of supercharger capacity on performance.*—Tests to determine the effect of supercharger capacity on performance have been completed on a modified DH-4 airplane. During these tests measurements were obtained from which the high speed and climb performance of the airplane could be computed for the supercharged and unsupercharged flights. Four different rates of air delivery were obtained in these tests by driving an N. A. C. A. Model II Roots-type supercharger at 3, 2.4, 1.957, and 1.615 times engine speed. The power output of the engine was measured by a calibrated propeller. The quantity of air inducted was measured by the supercharger, which had previously been calibrated in the laboratory. The fuel consumption was measured by a Venturi type fuel-flow meter. In addition, the usual measurements for computing airplane performance were obtained. A report presenting the results of this investigation is now being prepared for publication.

*Hub dynamometer.*—A propeller hub dynamometer employing hydraulic pressures to transmit engine torque to a photographic recording apparatus is being designed. This type of dynamometer has been selected from several different types as the most suitable type for the measurement of power during flight. Considerable experimental and analytical work has been done on the component parts of the dynamometer. The torque transmitting and recording apparatus will be carried in a spinner. The hub dynamometer will be light in weight, compact, and easily adapted to performance testing of engines up to 400 horsepower in flight.

*Fuel flow meter.*—An experimental Venturi-type fuel-flow meter has been used on a number of supercharged and unsupercharged flights. Some difficulty has been experienced because of failure of the pressure-recording mechanism. Changes are now being made to eliminate this difficulty.

*Effect of cowling on cylinder-head temperatures.*—Measurements have been obtained of the temperatures of the cylinder heads, barrels, and fins of a Wright J-5 air-cooled engine without cowling and with three different amounts of cowling. These tests were conducted in conjunction with aerodynamic tests made in the propeller research tunnel on the same cowlings. Sixty-nine thermocouples were used for obtaining these temperatures. Forty-seven thermocouples were installed on cylinder No. 1, which gave a sufficient number of points to predict the approximate temperature of any other point on the cylinder. The remaining 22 thermo-



couples were attached to the other eight cylinders at the front and rear spark-plug bosses of each cylinder and below the top fin on several of these cylinders, thus giving sufficient information to check the engine performance under different conditions of cooling. During these tests measurements were also obtained of the power developed, manifold depression, oil-inlet and oil-outlet temperatures, carburetor air temperatures, atmospheric temperature, barometric pressure, air speed, and fuel consumption. For the first series of tests no cowling was used on any of the cylinders, for the second series of tests the cowling covered about one-third of each cylinder, and for the third series of tests the cowling covered about two-thirds of each cylinder. The fourth cowling tested was faired over the top of the cylinders and permitted the air to flow inside the cowling and around the cylinders and cylinder heads. The test data were taken at full throttle conditions at air speeds of 60, 80, and 100 miles per hour. The data for the four cowlings tested have been computed and plotted. A general examination of the test data collected to date shows that the cylinder-head temperatures were highest on the uncowed engine and lowest on the two-thirds-cowed engine. The temperatures on the lower parts of the cylinder barrel were lowest on the uncowed engine and highest on the two-thirds-cowed engine. The most uniform temperatures were obtained with the engine one-third cowed.

*Effect of fuel consumption on cylinder temperatures.*—Tests have been completed on a J-5 engine in the committee's propeller research tunnel in which the effect of fuel consumption on cylinder-head, barrel, and fin temperatures and on engine power were determined. The instruments and equipment used were the same as those used in the cowling tests. All measurements were taken at full-throttle conditions with air speeds of approximately 80 miles per hour. Six different mixture conditions were obtained by using jet sizes from No. 46 to No. 51, inclusive. A large reduction in cylinder temperatures was obtained by using rich mixtures. The data obtained in these tests will be analyzed and published.

*Cooling efficiency of air-cooled cylinders.*—An investigation has recently been started to determine the fundamental factors governing the cooling of finned surfaces. This investigation will consist primarily of determining the effects of pitch, length, and shape of fins on the cooling efficiency.

*Completed investigations.*—Two investigations reported as completed last year have been published this year under the titles "A Preliminary Investigation of Supercharging an Air-Cooled Engine in Flight" and "The Comparative Performance of Roots Type Aircraft Engine Superchargers as Affected by Change in Impeller Speed and Displacement."

A report has been prepared for publication on the results of tests previously conducted to determine the actual variation in power with altitude of an unsupercharged Liberty 12 engine. The engine torque in these tests was measured with a Bendemann hub dynamometer. The experimental results obtained were compared with those calculated by correcting the sea-level power of the engine for temperature and pressure at altitude. The results substantiate the theoretical relation of brake horsepower to altitude based on the correction of sea-level indicated horsepower for changes in atmospheric temperature and pressure with the subsequent deduction of friction horsepower corrected for altitude.

A theoretical investigation has been completed and the results prepared for publication on the possibility of using mechanically operated discharge valves in conjunction with a manually operated intake control for improving the performance of N. A. C. A. Roots type superchargers. Both oscillating and rotating valves were considered in this analysis, but the rotating valves were selected as the most desirable for high-speed superchargers. The intake control limits the quantity of air compressed to engine requirements by permitting the excess air to escape from the compression chamber before compression begins. The results of the analysis on these valves indicate that a power saving of approximately 26 per cent may be obtained at a critical altitude of 20,000 feet. The valves have the disadvantage of increasing the weight and of adding a high-speed mechanism to a supercharger of otherwise simple design.

*ENGINE ANALYSIS—Fuel-vapor pressure.*—The test data previously obtained for the effect of temperatures from 175° to 900° F. on the vapor pressures of several fuels have been analyzed.



Comparison of this data with the experimental data of Regnault, Ramsey, and Young indicates that the vapor pressures were lowered by the effect of catalytic or other action of the iron of the bomb and the nitrogen above the liquid. A pressure calibration curve has been established for these effects by means of the classical data available for the unmixed liquids. The experimental results show that the vapor pressures of the liquids tested increased rapidly with temperature, and that the rate of increase became greater as the fuel vapors approached their critical temperature. Beyond the critical temperature the rate of pressure increase was constant except at one or more temperatures for certain fuel vapors in which chemical changes took place. Permanent gases were generated in the case of some of the liquids to such an extent that the liquid removed from the bomb was materially different from that placed in it. Analysis indicates that the vapor pressure of a fuel is a quantitative measurement of the physical preparation of the fuel for autoignition in a fuel-injection engine. A report covering the analysis and the experimental data on gasoline, kerosene, Diesel fuel oil, ethyl alcohol, methyl alcohol, mixtures of methyl alcohol and gasoline, mixtures of benzol and gasoline, and an aircraft lubricating oil has been prepared for publication.

*Analysis of oil-engine cycle efficiencies.*—The performance of aircraft oil engines is dependent upon their over-all efficiency, which includes cycle, combustion, volumetric, mechanical, and cooling efficiencies. The cycle efficiency is of major importance because it determines the extent of the theoretical heat losses carried out by the exhaust gases. The engine cycle that should be used for aircraft oil engines is the dual cycle, a combination of constant-volume and constant-pressure combustion. This cycle, in comparison with the Otto cycle for the same power output, reduces the theoretical weight per horsepower and increases the reliability.

The theoretical investigation of a number of factors controlling the actual cycle efficiencies of oil engines has been continued. The effects on the efficiency of oil engines working on the dual cycle of compression ratio, maximum cylinder pressure, air available for combustion, temperature of the inducted air, temperature and pressure of the residual exhaust gases, and point of cut-off are being determined. A series of calculations leading to the determination of the pressures, temperatures, and volumes at various points on the theoretical indicator card for a wide range of compression ratios and maximum cylinder pressures is being made. These calculations require the determination of the specific heats of the several cylinder gases involved at constant volume and at constant pressure up to the highest temperature of combustion and their effects on the pressure, temperature, and volume. It is also necessary to determine the effects on the same quantities of the Joule-Thomson effect, volumetric efficiencies versus compression ratio, the chemical composition and weight of the working mixture at the various points of the cycle, the quantity of fuel required for constant-volume and constant-pressure combustion, and of other factors. The completed results of this work will determine the theoretical compression ratios and maximum cylinder pressures at which aircraft oil engines should operate to obtain maximum performance for different aircraft services, and will enable the rapid determination of the cycle and combustion efficiencies of an oil engine when the usual test data are known.

An analysis of the specific heats of the gases of combustion as determined by three methods—first, by consideration of the theoretical heat content of the molecule due to its translational, vibrational, and rotational energy; second, by experiment involving the velocity of sound method; and third, by experiment involving the explosion method—has been completed. This analysis included studies of the work of Holborn and Henning, Pier, Bjerrum, and Partington and Shilling, and the application of the Einstein and Nernst-Lindeman energy functions. The gases considered were  $\text{H}_2\text{O}$ ,  $\text{CO}_2$ ,  $\text{N}_2$ ,  $\text{O}_2$ ,  $\text{H}_2$ ,  $\text{CO}$ , and air. After extended analysis of the reliable data, curves have been prepared representing the variation of the specific heats of the above gases with temperature from  $0^\circ$  to  $3,000^\circ\text{C}$ . The equations for these curves have been derived, evaluated for each  $100^\circ\text{C}$ . from  $0^\circ$  to  $3,000^\circ\text{C}$ ., tabulated, and plotted for the instantaneous and mean specific heats at constant volume and constant pressure. The equations for instantaneous gamma, which is the ratio of the instantaneous specific heat at constant pressure to that at constant volume, have been derived, evaluated for each  $100^\circ\text{C}$ . from  $0^\circ$  to



3,000° C., tabulated, and plotted. The equations for mean gamma, where mean gamma between 0° C. and any temperature  $t^\circ$  C. is equal to the mean value of instantaneous gamma between the temperature limits of 0° and  $t^\circ$  C., have been derived, evaluated for each 100° C. from 0° to 3,000° C., tabulated, and plotted. A report covering this work is being prepared for publication.

The value of mean gamma between 32° F. and any temperature  $t^\circ$  F. up to 5,400° F. has been calculated and plotted for explosion mixtures for the case of complete combustion, using fuel quantities per cycle of 2, 2.5, and  $3.44 \times 10^{-4}$  pounds, which correspond to 72 per cent, 37.6 per cent, and 0 per cent excess air, respectively. Further calculations and graphs are being made so that the value of mean gamma for the case of complete combustion of oxygen with carbon and hydrogen between 32° F. and any temperature  $t^\circ$  F. up to 5,400° F. may be taken from a graph for any mixture of gases and for any excess air from 0 to 190 per cent. These graphs will greatly reduce the amount of work involved in calculating the value of mean gamma for any gas and fuel mixture between any two temperatures for the case of complete combustion.

Calculations of pressures, temperatures, and volumes at various points on the theoretical indicator card of oil engines working on the dual cycle, taking into account the actual constituents of the mixture and the variation of specific heat with temperature, have been made for the general case of no excess air, which has included to date a maximum cylinder pressure of 700 pounds per square inch, and compression ratios of 6.1, 8, 10, 12, 14, and 16.

Analysis of the results shows that a small change in the maximum temperature attained at the completion of constant-volume combustion causes a considerable change in the quantity of fuel burned at constant pressure, which changes the point of cut-off and therefore the cycle efficiency. More accurate calculations are being made to determine the exact quantity of fuel required for constant-volume combustion.

Calculations of pressures and temperatures have been made at 20 points on the expansion curve, first by using a constant value of the exponent, and second by using the varying value of the exponent for adiabatic changes of state to determine the extent of error involved by using the constant value. It was reported in the preceding annual report that the negative work found by using a constant value of the exponent in the calculations of the compression curve was less than that obtained by using a varying exponent, although the difference was small; i. e., the greatest variation in pressure being about 0.5 per cent. It was expected that this error would be greater on the expansion curve on account of the increase of the specific heats of gases with temperature. The error for the expansion stroke was found to be greater as expected, the greatest variation in the pressure being of the order of 1 per cent. Since the true pressures and temperatures for both the compression and expansion strokes are higher than those determined by using a constant value of the exponent, the difference in the network of the cycle as calculated by the two methods is small, being less than 0.5 per cent.

*Injection valves.*—One of the many problems involved in the successful operation of aircraft oil engines is that of the fuel-injection system. For hydraulic pressure systems the injection valves may be automatic or mechanically operated. The successful design of an efficient injection valve requires a study of the effects of weight, movement, and operating forces on all its parts. A practical and theoretical study of the effects of these factors on the injection lag, spray, cut-off, spray atomization and distribution, and fuel delivery rates is being made. The physical equation for the opening motion of an automatic injection valve with a stem which is held to its seat by a helical spring has been evaluated to show the effects of weight and operating forces on the lift of the valve stem for values of these factors generally met in practice. The rate of change of these effects has also been obtained and the results plotted. The investigation of the movement of a valve stem which is held to its seat by a diaphragm has been started.

*Maximum-cylinder-pressure indicator.*—The performance of aircraft oil engines depends to a large extent on the magnitude of the pressures and temperatures developed in the combustion chamber by the combustion of the fuel. Various instruments have been constructed to record the maximum cylinder pressures developed, but most of them are too complicated and expensive



for general use and the pressures recorded are usually considerably lower than the actual pressures. A simple and inexpensive maximum-cylinder-pressure indicator has been developed having only one moving part, a small diaphragm weighing 0.0004 pound, which has a movement of only 0.0025 inch. A report describing the operation and construction of this indicator is being prepared for publication.

#### BUREAU OF STANDARDS

*Supercharging of aircraft engines.*—During preliminary tests of a Curtiss D-12 engine equipped with a gear-driven centrifugal supercharger having a rated altitude of 20,000 feet, the supercharger impeller bearings failed and the impeller drive shaft was broken as a result. Since replacements were not available, the tests were discontinued pending the possible redesign of the supercharger.

In the tests made two years ago of a Curtiss D-12 engine and of a Liberty 12 engine under ideal supercharging conditions—that is, with air supplied to the carburetor at sea-level pressure while the pressure at the exhaust ports is reduced to the standard pressure corresponding to any desired altitude—the air-cooling box installed when the altitude chamber was originally built was found to have inadequate cooling capacity. It was therefore necessary to operate both engines at part throttle above an altitude of 10,000 feet. A new air-cooling box, having several times the capacity of the old box, has been designed and constructed. Other improvements have been made in the test equipment, and the test of the Curtiss D-12 engine under ideal supercharging conditions will be completed operating at full throttle up to at least 25,000 feet.

*Phenomena of combustion.*—Further studies of the gaseous explosive reaction at constant pressure using mixtures of carbon monoxide, oxygen, and argon confirm the conclusion, stated in Technical Report No. 280, that the effect of an inert gas on the reaction rate depends on its thermal properties. The similarity of the results obtained with helium and with argon suggests that the important factor is the molecular heat rather than the thermal conductivity, as previously believed. A report on the kinetics of composite fuels soon to be published by the National Advisory Committee for Aeronautics shows that it is possible, from the velocity coefficients of carbon monoxide and methane, to predict the flame velocity of any composite fuel made up of these ingredients for any mixture ratio of fuel and oxygen which will ignite. When hydrogen is a component of the fuel, analysis of the data becomes more difficult, although of unusual practical interest.

*Combustion in an engine cylinder.*—A single-cylinder engine has been provided with a special water-cooled cylinder head having a large number of quartz windows symmetrically distributed over the combustion space. Light from the explosion passes through these windows and, by means of a lens, is focussed on a stroboscope, consisting of two rotating disks driven by the engine crankshaft. Holes in the disks permit a momentary view of the windows at the same point in successive cycles. By making observations at different points in the cycle the progress of the flame may be charted and the effect of operating conditions and fuel composition on flame movement and velocity may be studied.

*Pressures and temperatures in an aircraft engine.*—A review of published work on this subject is being made in order to summarize the methods, results, and conclusions of previous investigations. Measurements of piston, cylinder, and valve temperatures in different types of engines and over a considerable range of operating conditions have been reported. A variety of indicators for determining cylinder pressures have been described, but very few aircraft engine indicator diagrams complete with data as to the conditions under which they were taken have been found in the literature. A single-cylinder Liberty test engine, provided with means for varying the compression ratio and adapted for operation under approximate altitude conditions, has been set up and will be used in obtaining indicator diagrams under a wide range of operating conditions.

*Automatic altitude control.*—At the request of the Navy an experimental multiplied-pressure pump of the sort proposed in Technical Note No. 108 of the National Advisory Committee was built and tested under approximate altitude conditions. This gave satisfactory performance, but a lighter and more compact pump was required for flight test. Two-cylinder models



suitable for installation on the Curtiss D-12 engine and on the Wasp engine have been designed. One of the latter will be constructed and fitted to operate the carburetor altitude control on a Navy pursuit airplane.

*Gaseous fuel carburetor.*—A report has been made to the Navy Department describing and giving design data for a simple type of gas-and-air mixing valve which was found to operate satisfactorily either in series or in parallel with a conventional gasoline carburetor. The report included a detailed comparison of the performance in an engine of city illuminating gas, aviation gasoline, and mixtures of the two fuels. The illuminating gas gave somewhat less power than the aviation gasoline, but later engine tests using gaseous fuels of higher heating value showed approximately the same power and economy with gas as with gasoline.

*Fuels for high-compression engines.*—For routine testing of fuels, the Bureau of Standards has continued to use as a criterion of relative antiknock value the maximum power which different fuels will develop in a single-cylinder Liberty test engine without excessive detonation as judged by ear. Ethyl benzene appears to be about 50 per cent more effective than motor benzol in reducing the tendency of gasoline to knock. It has the further advantage of a low freezing point.

In the work undertaken for the Navy on the development of a bomb method for comparing the antiknock characteristics of aviation gasolines, changing the shape of the bomb failed to give more reproducible results for knock intensity, and attention was centered on the tendency of fuels to autoignite. Autoignition in the bomb used takes place an appreciable time after liquid fuel is injected into the preheated air with which the bomb is filled. The results are conveniently expressed in the form of curves showing the time required for the charge to ignite at different bomb temperatures. Such curves, of course, do not give the temperature of the charge which ignites after a given time lag, but further data may permit some correlation between antiknock value and these ignition plots.

*Lubrication under starting conditions.*—From measurements on the rate of flow of about 40 commercial lubricating oils through the oil passages of a Wright J-4 engine there has been obtained a characteristic curve by means of which the oil flow under specified low-temperature starting conditions can be predicted from its viscosity as determined in the laboratory at the ice point, provided the oil is a simple viscous liquid. The flow of oils which are plastic at the temperature of test can not be predicted in advance. The earlier work on the flow of aircraft-engine oils at low temperatures is not yet available in report form.

*Type testing of commercial engines.*—The Bureau of Standards cooperated with representatives of the Army Air Corps and the Navy Department in formulating tentative requirements for the type testing of commercial aircraft engines. The present regulations of the Department of Commerce (Aeronautics Bulletin No. 14, pp. 40-42) state that engines which have passed the regular endurance tests of the Army Air Corps or the Navy Department will be approved and that other engines submitted for approval will be tested at the Bureau of Standards. Three engines have been tested at the bureau under the present regulations and two of these have been approved.

#### NEW ENGINE TYPES

The most notable development of the year was the production by the Packard Motor Car Co. of an air-cooled radial engine operating with fuel injection on the Diesel principle. This engine has been fitted in an airplane and used in several flights. It is the first lightweight Diesel engine to be used in the flight of an airplane. The builders have withheld practically all definite information regarding this engine, but it is reported that it develops about 200 horsepower and weighs about 3 pounds per horsepower.

A further feature of the development of the past year has been the many new types of air-cooled engines which were produced for use in civil airplanes. These have been mainly of the radial type. Even with these new types of engines in use by both the military and commercial activities the deliveries to the commercial concerns have exceeded those to the Army and Navy.

The Air Commerce Regulations require that the engines used in interstate air commerce shall be of types which have been approved after suitable tests. A large proportion of the new



types of engines have been submitted for the purpose of obtaining approved-type certificates. The Department of Commerce has issued approved-type certificates for 10 engines, and many other engines are awaiting tests which, of course, are delayed on account of the number on hand.

The stocks of engines of medium power (less than 150 horsepower) which were carried over from war-time production are nearly exhausted. The prices of new engines of the types which have recently been developed are usually many times the prices recently charged for the war-time surplus engines. This has led to attempts to produce cheaper engines by the modification of engines of types which exist in considerable numbers as war-time surplus but which are not suitable for use in their original form. However, there are many difficulties in design and construction introduced by the attempt to convert an existing engine into something quite different.

*Air-cooled engines.*—Both the Army Air Corps and the Bureau of Aeronautics of the Navy have been interested in the further development of air-cooled engines for service use. Many of these engines have been adopted for use in commercial airplanes.

The Curtiss Aeroplane & Motor Co. has produced the "Chieftain" (H-1640), which develops 600 horsepower at 2,200 r. p. m. This is the 12-cylinder 2-row radial engine referred to in last year's report as the "Hex" engine. The crank shaft has two throws, each working from six cylinders. By this arrangement the over-all diameter of the engine is reduced and the counterweight which would be required on a single-throw crank shaft is eliminated. This engine is still under development for use as a military engine, but has obtained an approved-type certificate for commercial use.

The Curtiss Co. has also introduced the Challenger (R-600) engine, which develops 170 horsepower at 1,800 r. p. m. This engine is a 2-row 6-cylinder air-cooled engine with a 2-throw crank shaft and three cylinders working on each throw. The advantages expected are the same as in the Chieftain. This engine also has received an approved-type certificate for commercial use.

The Pratt & Whitney "Wasp" 9-cylinder radial engine, rated at 410 horsepower at 1,900 r. p. m., which was made standard equipment for service airplanes of the Navy more than a year ago, has been used quite extensively in commercial service. The operators of commercial air lines found that a greater reserve of power was necessary to enable them to keep to schedules in flying passengers and mail. Consequently engines of considerably greater power than were originally fitted have been installed in many such airplanes. The Wasp engine has been quite largely adopted for this purpose.

The Pratt & Whitney Co. has now brought out a "Series B Wasp" engine which is rated at 450 horsepower at 2,100 r. p. m. By resorting to doped fuels this engine is reported to have developed 600 horsepower at 2,300 r. p. m.

The Pratt & Whitney "Hornet," rated at 525 horsepower at 1,900 r. p. m. has been standardized by the Bureau of Aeronautics of the Navy Department and by the Army Air Corps. It has also been adopted by the Boeing Air Mail. This engine is being built in production quantities.

The Wright Aeronautical Corporation "Cyclone" engine (R-1750), a 9-cylinder radial rated at 525 horsepower at 1,900 r. p. m., has been standardized by the Bureau of Aeronautics of the Navy Department and by the Army Air Corps and is being built in production quantities.

The Wright Aeronautical Corporation has brought out a new series of radial air-cooled engines, the J-6. These engines are made in three sizes—5 cylinders developing about 160 horsepower, 7 cylinders developing about 220 horsepower, and 9 cylinders developing about 300 horsepower, all at 2,000 r. p. m. In these engines the attempt has been made to have a maximum of parts interchangeable and the same cylinders are used. These engines are still under development as far as service use is concerned.

The Wright Corporation is still at work on the development of the 12-cylinder inverted "Vee" air-cooled engine of approximately 1,500-cubic-inch-piston displacement, which was mentioned in last year's report. This engine is intended to develop 600 horsepower at 2,500 r. p. m.

The 9-cylinder Wright Whirlwind engine continues in general favor in spite of the tendency to use higher powers in many airplanes. The reduction in cost resulting from a long series pro-



duction is also causing it to be used more widely where the medium-power engines would be expected.

The 24-cylinder "X" type air-cooled engine constructed by the Allison Engineering Co. for the Army Air Corps and intended to develop approximately 1,400 horsepower is still under development.

Service tests and development of the experimental inverted air-cooled Liberty engines built by the Allison Engineering Co. under the supervision of the Army Air Corps have not yet been completed.

*Water-cooled engines.*—Development work continues on the Curtiss V-1550 engines which are being sponsored by the Army Air Corps. These engines, which are of the 12-cylinder "Vee" type, have been given the name "Conqueror" and are being produced in both geared and direct drive forms. In the endeavor to obtain even more power from them than their present 600 horsepower at 2,400 r. p. m. superchargers are being resorted to. Both the gear-driven centrifugal and the gear-driven Roots-N. A. C. A. types of supercharger are being used. It is expected to obtain a substantial increase in power at all altitudes. The weight of the direct-drive Conqueror (V-1550) is about 740 pounds. The geared model (GV-1550) weighs about 835 pounds. This model has developed 625 horsepower at 2,500 r. p. m.

Both the geared and direct drive models of the Conqueror have been granted approved-type certificates by the Department of Commerce and rated at 600 horsepower at 2,400 r. p. m.

Development work continues on the series of Packard water-cooled engines bearing the designations A-1500 and A-2500 which have been given experimental and service tests by the Army Air Corps. The 3A-1500 is available in both inverted direct-drive model and in upright geared drive. It is rated at 600 horsepower at 2,500 r. p. m.

The 3A-2500 on one test was found to develop 770 horsepower at 2,000 r. p. m. A further development of this engine (4A-2500) using a supercharger develops approximately 950 horsepower at 2,200 r. p. m.

*Superchargers.*—In the endeavor to obtain a maximum of power and to maintain power to altitudes superchargers are being generally applied to existing and new models of engines. There is no longer hesitation in the application of a supercharger to either air-cooled or water-cooled engines. Both the Roots-N. A. C. A. and the centrifugal type of supercharger have been successfully applied to both types of engines, while the possible application of the vane type of blower as a supercharger is being investigated. The use of superchargers is being borrowed from the military services for commercial applications just as the military engines have been borrowed.

## REPORT OF COMMITTEE ON MATERIALS FOR AIRCRAFT

### ORGANIZATION

The present organization of the committee on materials for aircraft is as follows:

Dr. George K. Burgess, Bureau of Standards, chairman.

H. L. Whittemore, Bureau of Standards, vice chairman and acting secretary.

S. K. Colby, American Magnesium Corporation.

Warren E. Emley, Bureau of Standards.

Henry A. Gardner, Institute of Paint and Varnish Research.

Dr. H. W. Gillett, Bureau of Standards.

Lieut. C. B. Harper (C. C.), United States Navy.

Prof. George B. Haven, Massachusetts Institute of Technology.

C. H. Helms, National Advisory Committee for Aeronautics.

Zay Jeffries, Aluminum Co. of America.

J. B. Johnson, Matériel Division, Army Air Corps, Wright Field.

George W. Lewis, National Advisory Committee for Aeronautics (ex officio member).

C. L. Ofenstein, Aeronautics Branch, Department of Commerce.

Capt. H. C. Richardson, United States Navy.

E. C. Smith, Central Alloy Steel Corporation.



G. W. Trayer, Forest Products Laboratory, Forest Service.

Starr Truscott, National Advisory Committee for Aeronautics.

Hon. Edward P. Warner, Assistant Secretary of the Navy for Aeronautics.

In view of the increasing importance of steel and the welding of steel in aircraft structural design, it seemed desirable that a representative of the steel industry who would be familiar with the practical problems of steel construction be included in the membership of the materials committee. Mr. E. C. Smith was accordingly appointed a member with further assignment to the subcommittee on metals. During the past year Lieut. C. B. Harper has been appointed to membership to succeed Lieut. R. S. Barnaby, relieved, and Messrs. Emley, Helms, and Ofenstein have been appointed additional members.

#### FUNCTIONS

Following is a statement of the functions of the committee on materials for aircraft:

1. To aid in determining the problems relating to materials for aircraft to be solved experimentally by governmental and private agencies.
2. To endeavor to coordinate, by counsel and suggestion, the research and experimental work involved in the investigation of such problems.
3. To act as a medium for the interchange of information regarding investigation of materials for aircraft in progress or proposed.
4. To direct and conduct research and experiment on materials for aircraft in such laboratory or laboratories, either in whole or in part, as may be placed under its direction.
5. To meet from time to time on call of the chairman and report its actions and recommendations to the executive committee.

The committee on materials for aircraft, through its personnel acting as a medium for the interchange of information regarding investigations on materials for aircraft, is enabled to keep in close touch with research in this field of aircraft development. Much of the research, especially in the development of light alloys, must necessarily be conducted by the manufacturers interested in the particular problems, and both the Aluminum Co. of America and the American Magnesium Corporation are represented on the committee. In order to cover effectively the large and varied field of research for aircraft, four subcommittees have been formed, as follows:

##### *Subcommittee on metals:*

Dr. H. W. Gillett, Bureau of Standards, chairman.

Zay Jeffries, Aluminum Co. of America.

J. B. Johnson, matériel division, Army Air Corps, Wright Field.

George W. Lewis, National Advisory Committee for Aeronautics (ex officio member).

E. C. Smith, Central Alloy Steel Corporation.

Starr Truscott, National Advisory Committee for Aeronautics.

H. L. Whittemore, Bureau of Standards.

##### *Subcommittee on woods and glues:*

G. W. Trayer, Forest Products Laboratory, Forest Service, chairman.

H. S. Betts, Forest Service.

George W. Lewis (ex officio member).

H. L. Whittemore, Bureau of Standards.

##### *Subcommittee on coverings, dopes, and protective coatings:*

Henry A. Gardner, Institute of Paint and Varnish research, chairman.

Dr. W. Blum, Bureau of Standards.

Warren E. Emley, Bureau of Standards.

Prof. George B. Haven, Massachusetts Institute of Technology.

Isadore M. Jacobsohn, Bureau of Standards.

C. H. Helms, National Advisory Committee for Aeronautics.

George W. Lewis (ex officio member).

P. H. Walker, Bureau of Standards.

E. R. Weaver, Bureau of Standards.



*Subcommittee on aircraft structures:*

Starr Truscott, National Advisory Committee for Aeronautics, chairman.

Charles Ward Hall, Hall-Aluminum Aircraft Corporation.

Lieut. Lloyd Harrison, United States Navy.

G. W. Lewis (ex officio member).

Charles J. McCarthy, Chance Vought Corporation.

C. L. Ofenstein, Aeronautics Branch, Department of Commerce.

L. B. Tuckerman, Bureau of Standards.

John E. Younger, Matériel Division, Army Air Corps, Wright Field.

Most of the research in connection with the development of materials for aircraft is financed directly by the Bureau of Aeronautics of the Navy Department, the matériel division of the Army Air Corps, and the National Advisory Committee for Aeronautics.

The Bureau of Aeronautics and the matériel division of the Air Corps, in connection with the operation of tests in their own laboratories, apportion and finance research problems on materials for aircraft to the Bureau of Standards, the Forest Products Laboratory, and the industrial research laboratories.

## MEETINGS OF THE COMMITTEE

Meetings of the committee were held several times during the year to consider reports on the work being conducted by the subcommittees. Particular attention was given the continuation of work on the development of methods for protecting light alloys, particularly duralumin, from corrosion. This work was begun some years ago and has always formed a major subject for investigation.

## SUBCOMMITTEE ON METALS

The Bureau of Standards conducts practically all the investigations on the properties of metals and their application to aircraft construction. These investigations are undertaken at the request of the Bureau of Aeronautics of the Navy Department, the matériel division of the Army Air Corps, or the National Advisory Committee for Aeronautics. In some instances the manufacturers of materials which appear to have promise for use in aircraft cooperate with the Bureau of Standards in the investigation of these materials and occasionally a manufacturer presents the results of his own research work directly to the committee. Some of the more important investigations completed during the past year or now in progress are outlined below.

*Intercrystalline embrittlement of sheet duralumin.*—The results of earlier phases of the study of the behavior of sheet duralumin with respect to the tendency toward embrittlement under corrosive conditions have been summarized and issued during the year in the form of four Technical Notes of the National Advisory Committee, Nos. 282–285. These notes deal with (a) the practical aspects of the problem, (b) accelerated corrosion tests and the behavior of high-strength aluminum-alloy sheet of different compositions, (c) the effect of the treatment of duralumin on its susceptibility to embrittlement, and (d) the use of protective coatings.

Further work on the effect of heat treatment on the propensity of sheet duralumin to embrittlement by corrosion has confirmed the previous conclusion that heat treatment by quenching in cold water, rather than hot water or oil, and aging at room temperature imparts higher corrosion resistance to the material. With very thin material, however—for example 0.008 inch sheet—the corrosion resistance does not appear to be influenced very much by varying the heat treatment. “Alclad” duralumin, which according to laboratory corrosion and exposure tests is the most dependable of the materials of the duralumin type, should also be heat-treated in the manner just described in order to develop the highest degree of corrosion resistance. “Alclad” duralumin sheet which had been heat-treated by hot-water quenching has been found to show evidence of corrosive attack on cut edges.

A detailed study of the microstructure of duralumin after different types of heat treatment failed to show any definite relation between the degrees of susceptibility to intercrystalline corrosive attack and the visible microstructure. Evidently the tendency of the material in this regard is determined by the ultramicroscopic features. X-ray studies by the Laue method



have been made of sheet duralumin in various conditions and after various degrees of corrosive attack. The conclusion was reached that this method of test can not be depended upon as a sure means for evaluating the propensity of this material toward intercrystalline embrittlement. This is contrary to the conclusion reached by some other workers in this field, such conclusions being based, however, on a very limited number of specimens.

The weather-exposure tests of sheet duralumin have been in progress for a little more than one year in Washington, D. C., and Hampton Roads, Va., and for about nine months at Coco Solo, Canal Zone. Tension specimens exposed to the weather are tested periodically and compared with similar specimens which have been stored in a *dry* atmosphere within sealed containers in the laboratory. After testing, all bars are examined microscopically for evidence of intercrystalline corrosive attack.

While the tests have not yet advanced sufficiently to permit final conclusions, comparison of the results brings out some interesting points. Fourteen-gauge sheet duralumin, heat-treated by cold-water quenching and aging at room temperature, when exposed in the bare state was unharmed after one year's exposure in Washington. Similar material lost about a quarter to a fifth of its ductility in one year at Hampton Roads and about the same in 4½ months at Coco Solo. Material of similar gauge, heat-treated by quenching in hot water or oil, is just starting to lose ductility after one year's exposure in Washington. Similar material has lost half its ductility and fallen considerably in tensile strength after one year's exposure at Hampton Roads or 4½ months' at Coco Solo.

Although visual examination of coated specimens at Washington and Hampton Roads indicates that many coatings are in excellent shape, tensile tests from the Hampton Roads and Coco Solo exposure tests of hot-water quenched and variously coated specimens show that only the Alclad coating and aluminum-sprayed coatings fully protect the metal under the conditions prevailing at these locations (sea air). Aluminum pigmented varnish and grease covered with aluminum powder stood up well for a while, but after 7½ months at Coco Solo and a year at Hampton Roads they, too, showed evidence of failure. No tensile results are yet available on the linseed oil-carbon black coating on hot-water quenched duralumin, which coating, according to the tests carried out by the subcommittee on protective coatings, is the most promising one of this type. The aluminized rubber-cement coatings have not shown up quite so well in exposure as they did in laboratory tests. Final conclusions must await longer exposure, however, and in any event they would seem to deserve consideration as priming coats.

The exposure tests indicate in general that for purely inland service cold-water-quenched room-temperature-aged duralumin with any nonmetallic coating that shows fair life by visual inspection, or even the bare material, should have satisfactory life. Salt mist on a broken-down coating or on bare material can, however, do much damage.

For seacoast work no nonmetallic coating has as yet proved reliable indefinitely. Cleaning and recoating as often as every six months would probably be required. For the combination of ease of cleaning and degree of protection grease with aluminum powder coating would appear to stand well toward the head of the coatings other than Alclad.

The indications of the exposure tests may be summed up as:

(1) Favoring Alclad or sprayed aluminum coatings for general use; and, for still further protection,

(2) Favoring *flexible* coatings such as the replaceable aluminized grease or perhaps carbon black in linseed oil (on the basis of the old Junkers airplane at Hampton Roads).

The exposure tests will be continued during the coming year.

Very thin sheet duralumin (0.008 inch) has shown a relatively very low corrosion resistance in exposure tests carried out in Washington. Varying the heat treatment does not very materially improve the corrosion-resistance of this material. Anodic surface oxidation and a greasing treatment (lanolin) protected this material for only a relatively short time. Frequent regreasing, at least every two months and probably once a month, would be required for perfect protection of this material in Washington. At Hampton Roads the attack was even more severe. Thin (0.010 inch) Alclad duralumin sheet exposed under the same conditions at Washington



showed a very high degree of resistance during six months' exposure. The same material reheated, however, showed noticeably lower resistance than did the commercial sheet.

The scope of the laboratory corrosion tests during the year has been extended to include the effect of stress acting on the material simultaneously with corrosive attack. There is some reason to believe that duralumin under the stress conditions which obtain in service is more subject to the embrittling attack than unstressed material is. The effect of both static tensile stress and repeated flexural stress has been studied. For the latter, two machines of special design whereby the tension bar could be corroded by immersion at stated intervals while it was being repeatedly bent back and forth were built.

Static tensile stress increases the rate of intercrystalline attack. Repeated bending stress increases it still more, 10,000 pounds fiber stress in repeated bending accelerating the attack as much as 20,000 pounds in static tension. The acceleration of the attack is much more marked on hot-water-quenched than on cold-water-quenched duralumin. This behavior is consistent with the superior behavior of cold-water-quenched material in all other laboratory and exposure tests. Accelerated corrosion tests on the repeated flexure machine appear to give the bare material the most searching corrosion test yet possible in the laboratory. Alclad duralumin tested in this way has shown the highest resistance of all materials tested. Other types of coated specimens have not as yet been tested.

As a supplement to the exposure tests, a determination of the permeability to atmospheric moisture of spar varnish, both plain and aluminum-pigmented, has been made. The results confirm in all respects the results of exposure tests as to the advantage to be gained by incorporating aluminum powder into a varnish to be used for out-of-doors exposure.

In the search for light alloys suitable for aircraft, considerable attention has been given to beryllium, which is not at present available commercially. If the modulus of elasticity of this metal is as high as some of the values reported, it should be particularly suitable for long columns. Although this metal is very expensive, it might be advisable to use it in aircraft if, for example, the cruising radius could thereby be increased 50 per cent.

In addition to the other publications reported by this subcommittee attention is invited to the recent circular of the Bureau of Standards, No. 346, Light Metals and Alloys—Aluminum and Magnesium. This publication assembles much information of value to aircraft designers and builders.

*High-speed fatigue testing.*—Work with the high-speed fatigue testing machine has continued. As was reported last year, the method of supporting the specimen in the machine has been changed from a pivot support to an air-jet support, thus freeing the specimen wholly from any possible longitudinal restraint due to the pivots which might introduce adventitious stresses.

The change from pivot support to air-jet support of the specimen has resulted in greater uniformity of the test results and has practically eliminated machine trouble. A consistent series of tests on duralumin to 300,000,000 alternations of stress has been completed. It is felt that with the changes which have been made in the machine the design is now satisfactory for the frequencies used (approximately 200 to 600 cycles per second). Three new machines have been built and the battery of four are now in continuous operation.

The discrepancy between results obtained in the high-speed machine and those previously obtained in the low-speed (1,000 to 2,000 revolutions per minute) crank-driven machines has not yet been explained. The design of a machine to close the gap in frequencies (200 per second to 20 per second) between the two types of machines has been investigated but has not been satisfactorily worked out. Although the discrepancy is still unexplained, the consistency of the results on the high-speed machines justifies their use for comparative tests of different materials. The results of these comparative tests may help to explain the discrepancy.

Material has been obtained and tests have been started to compare the endurance of 14 different light alloys of both aluminum and magnesium bases.

*Low-frequency flexural fatigue of Alclad duralumin and duralumin.*—Alclad duralumin has been studied in the low-frequency machines up to a life of 100,000,000 cycles, at which it withstands an indicated stress of over 10,000 pounds per square inch, or more than four times the



so-called yield point, far above the proportional limit of the pure aluminum coating and not far below its tensile strength. At very high stresses, far above the tensile strength of the coating, the coating becomes dulled and contains tiny checks or cracks, which, however, do not at once propagate through the specimen as similar surface cracks would in an all-duralumin specimen. This behavior gives reason to expect that when the surface is dented or scratched the relative endurance properties of Alclad duralumin will show a quite favorable comparison to duralumin, and experiments along this line, which are scheduled, are awaited with interest.

The machines being used are not suitable for stress-corrosion studies and for that angle of the problem the special machines mentioned above under the subject of intercrystalline embrittlement of sheet duralumin will have to be used.

#### SUBCOMMITTEE ON WOODS AND GLUES

The Forest Products Laboratory of the Department of Agriculture conducts practically all the investigations on the application of woods and glues to aircraft construction. These investigations are undertaken at the request of the Bureau of Aeronautics of the Navy Department, the matériel division of the Army Air Corps, or the National Advisory Committee for Aeronautics.

The steady increase in the use of metal in the parts of airplanes previously made of wood and the tendency toward all-metal construction is leading to a lessening in the need for additional data on woods and glues. However, wood will undoubtedly be used for some time to come. Attention is therefore being directed rather to the completion of work which has been under way than to the initiation of new projects.

The more important investigations in progress during the last year are described below.

*The lateral buckling and twisting of deep beams.*—The investigation of this subject was undertaken at the request of the Bureau of Aeronautics of the Navy Department in order to obtain information as to the maximum loads which could be carried by wing beams under varying conditions of loading and fixity. For some years a series of studies on the strength of beams has been in progress. These have included researches into the behavior of continuous beams and into the design of detailed parts of various types of beams.

Over 100 beams have been tested and the results have been compared with all the available formulas for rigidity and strength. The values computed by the formulas developed by Griffith and Taylor agree fairly well with the experimental values obtained with some cross sections.

Among the objects of the investigation has been the determination of the influence of form of cross section on the torsional stiffness of the beams. The computation of the torsional properties of bars having irregular sections is very complicated and presents many difficulties. A method using soap bubbles has been applied to this work and empirical formulas have been developed which have been used satisfactorily for some sections.

*The bearing strength of wood under bolts, washers, and fittings.*—The purpose of this investigation was to determine the allowable bearing strength of wood under bolts subjected to loads acting at various angles to the grain, the allowable distance between bolts, the influence of crossbolts, and the combined action of bolts of different diameters, the allowable bearing stresses under washers, fittings, etc. A series of progressive investigations was carried out in which the various phases of the problem were covered in detail. A report summarizing the work was made to the Navy Department and has been published by the National Advisory Committee for Aeronautics as Technical Note No. 296.

*The water resistance of glues.*—One of the subjects which has engaged considerable attention has been the resistance of the glues used in the manufacture of plywood to deterioration as a result of the absorbing of moisture. In order to determine the properties of the glues, films of glue alone were produced and were studied to determine the effect of various compositions and treatments on their permanance. This work is now being extended to tests of wood panels consisting of plywood and larger pieces.



## SUBCOMMITTEE ON COVERINGS, DOPES, AND PROTECTIVE COATINGS

Much of the work on the development of coverings, dopes, and protective coatings is carried out at the Bureau of Standards, since in many cases it involves cooperation with the work of the subcommittee on metals. Investigations are also carried out by the exposure of test panels at the United States naval air stations at Hampton Roads, Va., and Coco Solo, Canal Zone. Exposure tests were also made on the roof of the laboratory of Mr. H. A. Gardner.

Some of the more important investigations in progress during the last year are outlined below.

*Gas-cell fabrics.*—This investigation appears to be nearing a successful conclusion. A substitute for goldbeater's skin gas-cell fabric has been made in large quantities. About 1,700 square yards were made on one order and fabricated into a gas cell for the *Los Angeles* at the Naval Aircraft Factory. The weight of this fabric unvarnished was 4 ounces per square yard and varnished, 4.3 ounces per square yard. This is slightly less than the weight of corresponding fabrics made with goldbeater's skin. The permeability obtained is about one-tenth liter per square meter in 24 hours, and some specimens showed practically no permeability. Laboratory tests showed that the endurance of this fabric is very great and that it retained its flexibility and permeability over an extended period. However, only service tests will tell how it really compares with goldbeater's-skin fabric. This fabric consists of a light and strong cotton cloth to which there is applied a thin coat of rubber and then successive coats of a mixture of viscose and latex. After drying the coatings the complete fabric is treated to revert the viscose.

A gas cell has been made from a fabric consisting of the usual light cotton cloth with spread rubber to which there has been cemented a layer of cellophane, which has greater flexibility and elasticity than the usual product. This cell will be installed in the *Los Angeles* for service test.

*Coatings for duralumin to prevent corrosion.*—The exposure tests at the naval air station at Hampton Roads, which have continued for about two years, show that the protection given to duralumin by linseed oil paints of the iron oxide, zinc chromate, or carbon black types are practically perfect. These coatings show no flaking or cracking such as is often observed with varnish or lacquer. Aluminum pigmented paints are also satisfactory, but the best coating of all seems to be carbon black or lampblack in linseed oil. Unfortunately paints of this type are naturally slow in drying. It has been found that the drying can be very much accelerated by the use of ultraviolet lights in the painting room or in the baking oven. In the latter case drying can be accomplished in about one hour. Apparently this method of accelerating the drying does not affect the durability of the paint. The application of such paints in "flat" surface films allows the use of aluminum finishing coats where the latter is desired.

Many new quick drying coatings based on synthetic resins are now being developed. These are being studied, as they appear to offer great promise as materials for aircraft finishes.

The anodic treatment of duralumin continues to be used and apparently has demonstrated a definite effect in improving the corrosion-resisting properties of material to which it has been applied. The process is also being used to provide a better surface for paints or further coatings. The use of a grease over the anodic coating gives very much better results than the plain coating. However, it has been found that the use of lanolin for this purpose can not be recommended as it takes up moisture from the air and rather assists than protects against corrosion. A very good grease coating can be made from vaseline by grinding in 5 per cent of zinc chromate. This coating has a yellow color and when the color disappears from the surface it gives a clear indication that the coating should be renewed.

A report on Representative Coatings for Duralumin and Other Aircraft Alloys, by Mr. H. A. Gardner, was issued as Circular No. 330, June, 1928, Scientific Section, American Paint and Varnish Association.

The method of protecting duralumin against corrosion by the application of a thin coat of pure aluminum has now been given thorough tests both experimentally and in service. The duralumin sheets protected on both sides by this method and supplied by the Aluminum



Co. of America as "Alclad" duralumin have been remarkably successful in resisting corrosion in service. Apparently this material has demonstrated its suitability for the purpose and may be accepted as a standard protective coating. The increase in the use of duralumin due to the introduction of this coating which was predicted last year appears to have taken place.

The success of the pure aluminum coating in preventing corrosion of duralumin has led to its application to other of the aluminum alloys with equally successful results. Tubing has not yet been produced using this method of protection, but the possibilities of this application are being investigated.

The exposure tests on protective coatings for duralumin are being continued. Only by carrying out a lengthy series of these tests in various localities will it be possible to determine the suitability of the various coatings for use in different services and localities. It has already been found that exposure at Coco Solo, Canal Zone, is a much more severe test of a protective coating than an exposure of the same time at Hampton Roads, Va.

*Airplane dopes.*—Experiments on airplane dopes are being continued and include the older forms and the newer semipigmented dopes. Heretofore the determination of the durability of an airplane dope has required the exposure of test panels for periods of from two to six months. A method of accelerating the testing of these panels has been developed which appears to give results comparable to three months' exposure on the roof within a period of 100 hours.

*Substitute for silk parachute cloth.*—American manufacturers of silk cloth have become interested in the possibility of supplying domestic-woven material for use in the manufacture of parachutes. Many samples of domestic-woven silk cloths which might be suitable for this purpose have been submitted. These have been tested and criticized. The manufacturers are now working in cooperation with the Bureau of Standards and other governmental agencies in the endeavor to develop a specification for silk parachute cloth which will be satisfactory to both War and Navy Departments. Such a cloth will also be suitable for use in parachutes for commercial work.

Work on the development of a substitute for silk cloth has been continued, but, as was related in the report of the committee last year, it has been found that domestic yarns with the necessary properties are difficult to obtain. It finally became necessary to make the yarn at the Bureau of Standards. Although the manufacture of the yarn is not yet complete, preparations for its treatment are being made. Further experiments have been made on the mercerization in the piece of lightweight cotton cloth. These experiments are not yet completed but it has been concluded that the cloth woven from yarns mercerized according to the methods which have been developed should approximate the required qualities.

#### SUBCOMMITTEE ON AIRCRAFT STRUCTURES

The Bureau of Standards conducts practically all the investigations under the cognizance of this subcommittee. These are undertaken at the request of the Bureau of Aeronautics of the Navy Department, the matériel division of the Army Air Corps, or the National Advisory Committee for Aeronautics. Some of the more important investigations in progress or completed during the past year are outlined below.

*Welded joints.*—In view of the increasing interest in metal construction, the committee has endeavored to obtain information on the properties of welds, particularly the metallurgical and fatigue properties. Tests on butt welds made in sheets of duralumin, carbon steel, and chrome-vanadium steel, in four different thicknesses and by three different processes (atomic hydrogen, oxyacetylene, and electric arc) have been completed. The results show that sound welds by any of the three processes have tensile properties somewhat lower than the unwelded material. In the case of duralumin the strength is materially increased by heat treatment followed by cold working consisting of a reduction in thickness of approximately 10 per cent by hammering.

The properties of the adjacent sheet material were altered least by atomic hydrogen welding and altered most by oxyacetylene welding.



Alternating-stress tests in the flexural-fatigue machines were carried to approximately 5,000,000 alternations of stress. The comparison with unwelded sheet was made by testing both specimens with the same throw of the crank arm. Because of the greater thickness of the material in the weld this gave a higher nominal but a lower actual stress in the weld material. The tests indicated that the fatigue resistance of the welds as structures was not much lower than that of the unwelded sheet.

*Strength of flat plates.*—This investigation of the column strength of flat plates of nickel, duralumin, stainless steel, and Monel metal was undertaken because of the increasing use of structures in which the shell plating is required to act as a compression member carrying all or part of the load. Very little information existed as to the manner in which such loads were carried, and as a preliminary step toward the obtaining of such information the column strengths of flat plates of the different materials were determined. The effect of variations in width alone was considered. The plates were always flat, and, while the edges were fixed in position, they were not fixed in direction.

The value given by the theoretical equation for the buckling stress corresponds to the stress at which experimentally the plate begins to buckle. In the plates tested the maximum deflections at the theoretical buckling stresses varied from about 0.04 inch for the narrower specimens to about 0.07 inch for the wider specimens.

The maximum loads were generally higher than the theoretical buckling loads. This was especially true of the wider and thinner specimens, for which the theoretical buckling stresses are small compared to the proportional limits of the materials. Both the maximum loads and loads producing permanent deformation seem to depend on the proportional limits of the materials as well as on the elastic constants. In other words, after buckling begins the loads and deflections of the plate can be further increased until permanent deformation takes place.

The average maximum stress was calculated for each plate by dividing the maximum load by the area of the section. Curves based on these maximum stresses were drawn for plates varying in width from 4 to 24 inches and in thickness from 0.015 inch to 0.100 inch. One set of curves may be used for duralumin with a modulus of elasticity of about 10,000,000 pounds per square inch and proportional limit between 35,000 and 40,000 pounds per square inch. Another set of curves is for iron, Monel metal, or nickel, with modulus of elasticity between 24,000,000 and 28,000,000 pounds per square inch and proportional limit between 20,000 and 30,000 pounds per square inch.

The form of the buckled plates was generally as predicted by the theory; i. e., the number of half waves in the length of the buckled plate was in most cases equal to the nearest whole number to the ratio of the length to the width.

*Form factors for tubing of duralumin and steel under combined column and beam loads.*—This research was undertaken to increase the amount of information available as to the loads which could be sustained by steel and duralumin tubing when used either in the fuselage or other structure of an airplane. So far the tests on one size of duralumin tubing and three sizes of chrome-molybdenum tubing have been completed, and curves for the use of the designer have been prepared for one size of each material.

A characteristic difference has been noted between duralumin and chrome-molybdenum tubing. For duralumin tubing the modulus of rupture is practically equal to the tensile strength, and nearly independent of the ratio of the diameter of the tube to the thickness,  $d/t$  ratio, while for the chrome-molybdenum tubing tested the modulus of rupture averages 20 per cent higher than the tensile strength and is markedly dependent on the  $d/t$  ratio. The cause of this difference has not been investigated, but it is thought to be related to the difference in shape of the stress-strain curves of the two materials.

*Structures for airships.*—Tests on airship girders and their chord members have been continued, the greater portion of the time being spent on box girders similar in general design to those used in some parts of the *Los Angeles*. In these, lattices are not used, but the chord members and webs of one side of the girder are stamped in one piece and four (or sometimes three) of these riveted together to form the girder. These have shown about the same chord-



member stresses as the tubular type of lattice girder, giving no evidence of twisting failure of the chord members. Their strength-weight ratio is higher, however, because the material in the lightened webs is relatively lighter than the lattices in the latticed tubular girders.

The studies designed to relate the occurrence of twisting instability in chord members to the three (or possibly four) constants of the chord member and the rigidity of the lattice or web support have so far not resulted in any quantitative relationships being found, although the general character of the effects seems clear.

*Electrically welded steel tubing.*—The possibility of producing tubing more cheaply and with thinner and more uniform walls by automatic welding of flat strip which has been rolled up into a tube than is at present possible with seamless tubing has led to a comprehensive investigation of electrically welded steel tubing. So far the tests have included tension, torsion, bursting, crushing, and flattening tests on 100 different low-carbon-steel tubes ranging in outside diameter from five-eighths inch to 3 inches and in thickness from 0.028 to 0.095 inch.

In these tests the welded tubes have compared favorably with seamless tubing of the same composition. It is planned to extend the tests to axial compression and combined compression and bending with tubes of higher carbon content so as to furnish a direct comparison with the duralumin and chrome-molybdenum tubing now being tested.

*Welded joints in tubing.*—The Department of Commerce in administering the inspection and airworthiness provisions of the air commerce act of 1926, found great diversity in commercial practice in the design of joints and fittings, and no comprehensive test data by which to compare their relative value. On the advice of the structures subcommittee the design of welded joints in tubing was selected as the first problem to be investigated.

In consultation with airplane manufacturers, the Army Air Corps, the Bureau of Aeronautics of the Navy, and the American Bureau of Welding a thorough preliminary study of joint types, welding procedure, and test methods has been made.

Test fixtures have been constructed and tried out on the different types of welded joints. The program of tests includes about 135 types of 2 and 3 piece joints in seamless chrome-molybdenum and carbon-steel tubing. The welding will be done under procedure specifications prepared in cooperation with the American Bureau of Welding.

*Technique of testing flat plates under normal pressure.*—The data on which the design of flat plates under normal pressure is based are almost wholly taken from tests on relatively thick plates such as ship plating. Even for thick plating practically no tests have been made except on single panels with normally fixed (clamped) edges. The increasing use in aircraft of thin plates supported by ribbing is sufficiently important to make it desirable to have methods for convenient testing of varied designs under different conditions of edge constraint. A small testing apparatus has been built and methods are being developed for sealing against hydrostatic pressure under different types of edge constraints (fixed, supported, etc.) which permit of easy change of specimens.

*Welding of corrosion-resisting steels.*—The difficulties which have been encountered with corrosion of metallic aircraft structures has led to a search for measures to protect the usual materials and for materials which will resist the corrosion by virtue of their own constitution. Corrosion-resisting high-chromium steels have been introduced into the industry for many purposes and would appear to afford very satisfactory solutions for many of the difficulties encountered with corrosion if their adaptability for the processes and constructions used in the manufacture of aircraft were demonstrated. Since practically all fuselages made in this country are of steel tubing welded together, the use of corrosion-resisting steel for this purpose would be dependent upon the ability to produce satisfactory welds. Similarly, the use of corrosion-resisting steels in fittings depends upon the same ability to produce welds. At the instance of the committee a paper was prepared by Mr. W. B. Miller on welding high-chromium steels. This was issued by the National Advisory Committee for Aeronautics as Technical Note No. 290.



## PART IV

### TECHNICAL PUBLICATIONS OF THE COMMITTEE

The National Advisory Committee for Aeronautics has issued technical publications during the past year covering a wide range of subjects. There are four series of publications, namely, Technical Reports, Technical Notes, Technical Memorandums, and Aircraft Circulars.

The Technical Reports present the results of fundamental research in aeronautics carried on in different laboratories in this country, including the Langley Memorial Aeronautical Laboratory, the aerodynamical laboratory at the Washington Navy Yard, the Bureau of Standards, the Weather Bureau, Stanford University, and the Massachusetts Institute of Technology. In all cases the reports were recommended for publication by the technical subcommittees having cognizance of the investigations. During the past year 26 Technical Reports were submitted for publication.

Technical Notes present the results of small research investigations and the results of studies of specific detail problems which form parts of long investigations. The committee has issued during the past year, in mimeographed form, 31 Technical Notes.

Technical Memorandums contain translations and reproductions of important aeronautical articles of a miscellaneous character. A total of 51 Technical Memorandums were issued during the past year.

Aircraft Circulars contain translations or reproductions of articles descriptive of new types of aircraft. During the past year 26 Aircraft Circulars were issued.

Summaries of the 26 Technical Reports and lists of the Technical Notes, Technical Memorandums, and Aircraft Circulars follow:

#### SUMMARIES OF TECHNICAL REPORTS

The first annual report of the National Advisory Committee for Aeronautics for the fiscal year 1915 contained Technical Reports Nos. 1 to 7; the second annual report, Nos. 8 to 12; the third annual report, Nos. 13 to 23; the fourth annual report, Nos. 24 to 50; the fifth annual report, Nos. 51 to 82; the sixth annual report, Nos. 83 to 110; the seventh annual report, Nos. 111 to 132; the eighth annual report, Nos. 133 to 158; the ninth annual report, Nos. 159 to 185; the tenth annual report, Nos. 186 to 209; the eleventh annual report, Nos. 210 to 232; the twelfth annual report, Nos. 233 to 256; the thirteenth annual report, Nos. 257 to 282; and since the preparation of the thirteenth annual report for the year 1927 the committee has authorized the publication of the following Technical Reports, Nos. 283 to 308:

*Report No. 283*, entitled "A Preliminary Investigation of Supercharging an Air-Cooled Engine in Flight," by Marsden Ware and Osear W. Sehey, National Advisory Committee for Aeronautics.

This report presents the results of tests made in a preliminary investigation of the effects of supercharging an air-cooled engine under airplane flight conditions.

This investigation comprises the first of its kind that has been conducted and for which results have been published.

Service training airplanes were used in the investigation equipped with production types of Wright J engines. An N. A. C. A. Roots type supercharger was driven from the rear of the engine.

In addition to measuring those quantities that would enable the determination of the climb performance, measurements were made of the cylinder-head temperatures and the carburetor pressures and temperatures. The supercharging equipment was not removed from the airplane



when making flights without supercharging, but a by-pass valve, which controlled the amount of supercharging by returning to the atmosphere the surplus air delivered by the supercharger, was left full open.

With the supercharger so geared that ground-level pressure could be maintained to 18,500 feet, it was found that the absolute ceiling was increased from 19,400 to 32,600 feet, that the time to climb to 16,000 feet was decreased from 32 to 16 minutes, and that this amount of supercharging apparently did not injure the engine.

*Report No. 284*, entitled "The Comparative Performance of Roots Type Aircraft Engine Superchargers as Affected by Change in Impeller Speed and Displacement," by Marsden Ware and Ernest E. Wilson, National Advisory Committee for Aeronautics.

This report presents the results of tests made on three sizes of Roots type aircraft engine superchargers. The impeller contours and diameters of these machines were the same, but the lengths were 11,  $8\frac{1}{4}$ , and 4 inches, giving displacements of 0.509, 0.382, and 0.185 cubic foot per impeller revolution. The information obtained serves as a basis for the examination of the individual effects of impeller speed and displacement on performance and of the comparative performance when speed and displacement are altered simultaneously to meet definite service requirements.

According to simple theory, when assuming no losses, the air weight handled and the power required for a given pressure difference are directly proportional to the speed and the displacement. These simple relations are altered considerably by the losses.

In estimating the effect of speed on performance it is of interest to note that—

(1) The difference between the actual power and the theoretical power was found to vary with the speed raised to the 2.5 power. The theoretical power was obtained by multiplying the pressure difference by the displacement and speed and dividing by the horsepower constant.

(2) The volumetric efficiency of the actual machine remains nearly constant over a large part of the interesting speed range, the decrease in volumetric efficiency at a speed of 6,000 r. p. m. being less than 2 per cent.

(3) The ratio of the discharge air temperature to the inlet temperature was found to depend on speed. This effect of speed is represented by the coefficient  $C$  in the relation

$$\frac{T_2}{T_1} = C \left( \frac{P_2}{P_1} \right)^{\frac{n-1}{n}},$$

which has a value of 1 at zero r. p. m., increasing to 1.04 at 6,500 r. p. m.

With regard to the effect of displacement on performance, the following points are of interest:

(1) The power loss was found to increase with displacement.

(2) The maximum volumetric efficiency increased somewhat with increase in displacement.

(3) The relation between the inlet and discharge temperatures and pressures as represented by the exponent  $n$  in the above equation was found to increase from 1.36 to 1.53, with increase in impeller length from 4 to 11 inches.

When comparing the performance of different sizes of machines whose impeller speeds are so related that the same service requirements are met, it is found that the individual effects of speed and displacement are canceled to a large extent, and the only considerable difference is the difference in the power losses which decrease with increase in the displacement and the accompanying decrease in speed. This difference is small in relation to the net power of the engine supercharger unit, so that a supercharger with short impellers may be used in those applications where the space available is very limited without any considerable sacrifice in performance.

*Report No. 285*, entitled "A Study of Wing Flutter," by A. F. Zahm and R. M. Bear, construction department, Washington Navy Yard.

Part I describes vibration tests, in a wind tunnel, of simple airfoils and of the tail plane of an MO-1 airplane model; it also describes the air flow about this model. From these tests are drawn inferences as to the cause and cure of aerodynamic wing vibrations. Part II derives



stability criteria for wing vibrations in pitch and roll, and gives design rules to obviate instability. Part III shows how to design spars to flex equally under a given wing loading and thereby economically minimize the twisting in pitch that permits cumulative flutter.

Resonant flutter is not likely to ensue from turbulence of air flow alone past wings and tail planes in usual flying conditions. To be flutter proof a wing must be void of reversible autorotation and not have its centroid far aft of its pitching axis; i. e., axis of pitching motion. Danger of flutter is minimized by so proportioning the wing's torsional resisting moment to the air pitching moment at high-speed angles that the torsional flexure is always small.

*Report No. 286*, entitled "Aerodynamic Characteristics of Airfoils—V," by the National Advisory Committee for Aeronautics.

This collection of data on airfoils has been made from the published reports of a number of the leading aerodynamic laboratories of this country and Europe. The information which was originally expressed according to the different customs of the several laboratories is here presented in a uniform series of charts and tables suitable for the use of designing engineers and for purposes of general reference.

It is a well-known fact that the results obtained in different laboratories, because of their individual methods of testing are not strictly comparable even if proper scale corrections for size of model and speed of test are supplied. It is, therefore, unwise to compare too closely the coefficients of two wing sections tested in different laboratories. Tests of different wing sections from the same source, however, may be relied on to give true relative values.

The absolute system of coefficients has been used, since it is thought by the National Advisory Committee for Aeronautics that this system is the one most suited for international use and yet it is one from which a desired transformation can be easily made. For this purpose a set of transformation constants is given.

Each airfoil section is given a reference number, and the test data are presented in the form of curves from which the coefficients can be read with sufficient accuracy for designing purposes. The dimensions of the profile of each section are given at various stations along the chord in per cent of the chord length, the latter also serving as the datum line. When two sets of ordinates are necessary, on account of taper in chord or ordinate, those for the maximum section (at center of span) are given on the individual characteristic sheets, while those for the tip (dotted) section are given in separate tables (p. 375). The shape of the section is also shown with reasonable accuracy to enable one to more clearly visualize the section under consideration, the outside of the heavy line representing the profile.

The authority for the results here presented is given as the name of the laboratory at which the experiments were conducted, as explained under abbreviations, with the size of model, wind velocity, and year of test.

*Report No. 287*, entitled "Theories of Flow Similitude," by A. F. Zahm, construction department, Washington Navy Yard.

The laws of comparison of dynamically similar fluid motions are derived by three different methods based on the same principle and yielding the same or equivalent formulas. In this report are outlined the three current methods of comparing dynamically similar motions, more especially of fluids, initiated respectively by Newton, Stokes (or Helmholtz), and Rayleigh. These three methods—viz, the integral, the differential, and the dimensional—are enough alike to be studied profitably together.

*Report No. 288*, entitled "Pressure Distribution Over a Rectangular Monoplane Wing Model Up to  $90^\circ$  Angle of Attack," by Montgomery Knight and Oscar Loeser, jr., National Advisory Committee for Aeronautics.

The pressure distribution tests herein described, covering angles of attack up to  $90^\circ$ , were made on a rectangular monoplane wing model in the atmospheric wind tunnel of the Langley Memorial Aeronautical Laboratory.

These tests indicate that a rectangular wing, by reason of its large tip loads, is uneconomical aerodynamically and structurally, has pronounced lateral instability above maximum lift, and is not adaptable to accurate calculation based on the classical wing theory.



*Report No. 289*, entitled "Forces on Elliptic Cylinder in Uniform Air Stream," by A. F. Zahm, R. H. Smith, and F. A. Loudon, construction department, Washington Navy Yard.

This report presents the results of wind tunnel tests on four elliptic cylinders with various fineness ratios, conducted in the Navy Aerodynamic Laboratory, Washington. The object of the tests was to investigate the characteristics of sections suitable for streamline wire which normally has an elliptic section with a fineness ratio of 4; also to learn whether a reduction in fineness ratio would result in improvement; also to determine the pressure distribution on the model of fineness ratio 4.

Four elliptic cylinders with fineness ratios of 2.5, 3, 3.5, and 4 were made and then tested in the 8 by 8 foot tunnel—first, for cross-wind force, drag, and yawing moment at 30 miles an hour and various angles of yaw; next for drag at  $0^\circ$  pitch and  $0^\circ$  yaw and various wind speeds; then for end effect on the smallest and largest models; and lastly for pressure distribution over the surface of the largest model at  $0^\circ$  pitch and  $0^\circ$  yaw and various wind speeds. In all tests, the length of the model was transverse to the current. The results are given for standard air density,  $\rho = 0.002378$  slug per cubic foot.

*Report No. 290*, entitled "Water-Pressure Distribution on a Seaplane Float," by F. L. Thompson, National Advisory Committee for Aeronautics.

The investigation reported herein was conducted by the National Advisory Committee for Aeronautics at the request of the Bureau of Aeronautics, Navy Department, for the purpose of determining the distribution and magnitude of water pressures likely to be experienced on seaplane hulls in service. It consisted of the development and construction of apparatus for recording water pressures lasting one one-hundredth second or longer and of flight tests to determine the water pressures on a UO-1 seaplane float under various conditions of taxiing, taking off, and landing.

The apparatus developed was found to operate with satisfactory accuracy and is suitable for flight tests on other seaplanes.

The tests on the UO-1 showed that maximum pressures of about 6.5 pounds per square inch occur at the step for the full width of the float bottom. Proceeding forward from the step the maximum pressures decrease in magnitude uniformly toward the bow, and the region of highest pressures narrows toward the keel. Immediately abaft the step the maximum pressures are very small, but increase in magnitude toward the stern and there once reached a value of about 5 pounds per square inch.

*Report No. 291*, entitled "Drag of C-Class Airship Hulls of Various Fineness Ratios," by A. F. Zahm, R. H. Smith, and F. A. Loudon, construction department, Washington Navy Yard.

This report presents the results of wind-tunnel tests on eight C-class airship hulls with various fineness ratios, conducted in the Navy Aerodynamic Laboratory, Washington. The purpose of the tests was to determine the variation of resistance with fineness ratio, and also to find the pressure and friction elements of the total drag for the model having the least shape coefficient.

Seven C-class airship hulls with fineness ratios of 1, 1.5, 2, 3, 6, 8, and 10 were made and verified. These models and also the previously constructed original C-class hull, whose fineness ratio is 4.62, were then tested in the 8 by 8 foot tunnel for drag at  $0^\circ$  pitch and yaw, at various wind speeds. The original hull, which was found to have the least shape coefficient, was then tested for pressure distribution over the surface at various wind speeds.

*Report No. 292*, entitled "Characteristics of Five Propellers in Flight," by J. W. Crowley, jr., and R. E. Mixson, National Advisory Committee for Aeronautics.

This investigation was made for the purpose of determining the characteristics of five full-scale propellers in flight. The equipment consisted of five propellers in conjunction with a VE-7 airplane and a Wright E-2 engine. The propellers were of the same diameter and aspect ratio. Four of them differed uniformly in thickness and pitch and the fifth propeller was identical with one of the other four with the exception of a change of the airfoil section. The propeller



efficiencies measured in flight are found to be consistently lower than those obtained in model tests. It is probable that this is mainly a result of the higher tip speeds used in the full-scale tests. The results show also that because of differences in propeller deflections it is difficult to obtain accurate comparisons of propeller characteristics. From this it is concluded that for accurate comparisons it is necessary to know the propeller pitch angles under actual operating conditions.

*Report No. 293*, entitled "Two Practical Methods for the Calculation of the Horizontal Tail Area Necessary for a Statically Stable Airplane," by Walter S. Diehl, Bureau of Aeronautics, Navy Department.

This report is concerned with the problem of calculation of the horizontal tail area necessary to give a statically stable airplane. Two entirely different methods are developed, and reduced to simple formulas easily applied to any design combination. Detailed instructions are given for use of the formulas, and all calculations are illustrated by examples. The relative importance of the factors influencing stability is also shown.

*Report No. 294*, entitled "The Measurement of Maximum Cylinder Pressures," by Chester W. Hicks, National Advisory Committee for Aeronautics.

The work presented in this report was undertaken to determine a suitable method for measuring the maximum pressures occurring in aircraft engine cylinders. The study and development of instruments for the measurement of maximum cylinder pressures has been conducted in connection with carburetor and oil-engine investigations on a single cylinder aircraft-type engine. Five maximum cylinder-pressure devices have been designed, constructed, and tested, in addition to the testing of three commercial indicators.

Values of maximum cylinder pressures are given as obtained with various indicators for the same pressures and for various kinds and values of maximum cylinder pressures, produced chiefly by variation of the injection advance angle in a high-speed oil engine. It is the high pressure of short duration that is most difficult to measure, because the time of its duration is so short that little work can be done to operate an indicator.

The investigations conducted thus far indicate that the greatest accuracy in determining maximum cylinder pressures can be obtained with an electric, balanced-pressure diaphragm or disk-type indicator so constructed as to have a diaphragm or disk of relatively large area and minimum seat width and mass.

*Report No. 295*, entitled "The Variation in Engine Power with Altitude Determined from Measurements in Flight with a Hub Dynamometer," by W. D. Gove, National Advisory Committee for Aeronautics.

The rate of change in power of aircraft engines with altitude has been the subject of considerable discussion. Only a small amount of data from direct measurements of the power delivered by airplane engines during flight, however, have been published. This report presents the results of direct measurements of the power delivered by a Liberty 12 airplane engine taken with a hub dynamometer at standard altitudes from zero to 13,000 feet. Six flights were made with the engine installed in a modified DH-4 airplane. The tests were conducted at the Langley Memorial Aeronautical Laboratory.

The experimental relation of brake horsepower to altitude is compared with two theoretical relations and with the experimental results, for a second Liberty 12 engine, given in N. A. C. A. Technical Report No. 252. The rate of change in power with altitude of a third Liberty engine, measured with a calibrated propeller, is also given for comparison.

The data presented substantiate the theoretical relation of brake horsepower to altitude based on the correction of ground level indicated horsepower for changes in atmospheric temperature and pressure with the subsequent deduction of friction horsepower corrected by altitude. The equation for this relation is

$$B.HP_a = B.HP^o \left[ \left( \frac{P_a}{P_o} \right) \left( \frac{T_o}{T_a} \right)^{1/2} \left( 1 + \frac{\lambda - \lambda n}{n} \right) - \left( \frac{\lambda - \lambda n}{n} \right) \right]$$



where  $P$  is the absolute atmospheric pressure,  $T$  is the absolute temperature,  $\eta$  is the mechanical efficiency of the engine at sea level, and  $\lambda$  is the ratio of mechanical friction to friction horsepower at sea level. The subscripts  $_0$  and  $_a$  denote sea level and altitude conditions, respectively.

*Report No. 296*, entitled "Pressure Distribution Tests on PW-9 Wing Models from  $-18^\circ$  through  $90^\circ$  Angle of Attack," by Oscar E. Loeser, jr., National Advisory Committee for Aeronautics.

At the request of the Army Air Corps, an investigation of the pressure distribution over PW-9 wing models was conducted in the atmospheric wind tunnel of the National Advisory Committee for Aeronautics. The primary purpose of these tests was to obtain wind-tunnel data on the load distribution on this cellule to be correlated with similar information obtained in flight tests, both to be used for design purposes. Because of the importance of the conditions beyond the stall as affecting control and stability, this investigation was extended through  $90^\circ$  angle of attack. The results for the range of normal flight have been given in N. A. C. A. Technical Report No. 271. The present paper presents the same results in a different form and includes, in addition, those over the greater range of angle of attack,  $-18^\circ$  through  $90^\circ$ .

The results show that—

At angles of attack above maximum lift, the biplane upper wing pressures are decreased by the shielding action of the lower wing.

The burble of the biplane lower wing, with respect to the angle of attack, is delayed, due to the influence of the upper wing.

The center of pressure of the biplane upper wing (semispan) is, in general, displaced forward and outward with reference to that of the wing as a monoplane, while for the lower wing there is but slight difference for both conditions.

The overhanging portion of the upper wing is little affected by the presence of the lower wing.

*Report No. 297*, entitled "The Reduction of Observed Airplane Performance to Standard Conditions," by Walter S. Diehl, Bureau of Aeronautics, Navy Department.

This report shows how the actual performance of an airplane varies with air temperature when the pressure is held constant. This leads to comparatively simple methods of reducing observed data to standard conditions. The new methods which may be considered exact for all practical purposes, have been used by the Navy Department for about a year, with very satisfactory results.

The report also contains a brief historical review of the important papers which have been published on the subject of performance reduction, and traces the development of the standard atmosphere.

*Report No. 298*, entitled "Effect of Chord and Span of Ailerons on Rolling and Yawing Moments in Level Flight," by R. H. Heald and D. H. Strother, Bureau of Standards.

This report presents the results of an investigation of the rolling and yawing moments due to ailerons of various chords and spans on two airfoils having the Clark Y and U. S. A. 27 wing sections. Some attention is devoted to a study of the effect of scale on rolling and yawing moments and to the effect of slightly rounding the wing tips.

The results apply to level flight with the wing chord set at an angle of attack of  $+4^\circ$  and to conditions of zero pitch, zero yaw, and zero roll of the airplane. It is planned later to extend the investigation to other attitudes for monoplane and biplane combinations.

The work was conducted in the 10-foot wind tunnel of the Bureau of Standards on models of 60-inch span and 10-inch chord.

*Report No. 299*, entitled "Investigation of Damping Liquids for Aircraft Instruments," by G. H. Keulegan, Bureau of Standards.

This report covers the results of an investigation carried on at the Bureau of Standards under a research authorization from, and with the financial assistance of, the National Advisory Committee for Aeronautics.



The choice of a damping liquid for aircraft instruments is difficult owing to the range of temperature at which aircraft operate. Temperature changes affect the viscosity tremendously. The investigation was undertaken with the object of finding liquids of various viscosities otherwise suitable which had a minimum change in viscosity with temperature. The new data relate largely to solutions.

The effect of temperature on the kinematic viscosity of the following liquids and solutions was determined in the temperature interval  $-18^{\circ}$  to  $+30^{\circ}$  C.

(1) Solutions of animal and vegetable oils in xylene. These were poppy-seed oil, two samples of neat's-foot oil, castor oil, and linseed oil.

(2) Solutions of mineral oil in xylene. These were Squibb's petrolatum of naphthene base and transformer oil.

(3) Glycerine solutions in ethyl alcohol and in mixture of 50-50 ethyl alcohol and water.

(4) Mixtures of normal butyl alcohol with methyl alcohol.

(5) Individual liquids, kerosene, mineral spirits, xylene, recoil oil.

The apparatus consisted of four capillary-tube viscometers, which were immersed in a liquid bath in order to secure temperature control. The method of calibration and the related experimental data are presented in detail.

The viscosity data for the liquids are given in curves in which  $\log_{10} \frac{t_{\theta}}{t_{30}}$  is plotted against temperature, where  $t_{30}$  and  $t_{\theta}$  are, respectively, the times of discharge through the viscometer at  $30^{\circ}$  C. and  $\theta^{\circ}$  C. Except for a correction which is usually small, the following relation holds:

$$\log_{10} \frac{t_{\theta}}{t_{30}} = \log_{10} \frac{\nu_{\theta}}{\nu_{30}}$$

in which  $\nu_{30}$  and  $\nu_{\theta}$  are, respectively, the kinematic viscosities at  $30^{\circ}$  C. and  $\theta^{\circ}$  C. The density at  $30^{\circ}$  C. the coefficient of cubical thermal expansion for each solution, and  $\nu_{30}$  are given, together with other data, so that the absolute viscosity may be computed. The accuracy is within 1 per cent.

*Report No. 300*, entitled "The Twenty-Foot Propeller Research Tunnel of the National Advisory Committee for Aeronautics," by Fred E. Weick and Donald H. Wood, National Advisory Committee for Aeronautics.

This report describes in detail the new propeller research tunnel at Langley Field, Va. This tunnel has an open jet air stream 20 feet in diameter in which velocities up to 110 miles per hour are obtained. Although the tunnel was built primarily to make possible accurate full-scale tests on aircraft propellers, it may also be used for making aerodynamic tests on full-size fuselages, landing gears, tail surfaces, and other aircraft parts, and on model wings of large size.

*Report No. 301*, entitled "Full Scale Tests of Wood Propellers on a VE-7 Airplane in the Propeller Research Tunnel," by Fred E. Weick, National Advisory Committee for Aeronautics.

The investigation described in this report was made primarily to afford a comparison between propeller tests in the new Propeller Research Tunnel and flight tests and small model tests on propellers. Three wood propellers which had been previously tested in flight on a VE-7 airplane, and of which models had also been tested in a wind tunnel, were tested again on a VE-7 airplane in the Propeller Research Tunnel. The results of these tests are in fair agreement with those of the flight and model tests.

Tests were also made with the tail surfaces removed, and with both the wings and tail surfaces removed. It was found that the effect of the tail surfaces on the propeller characteristics was negligible, but that the wings reduced the maximum propulsive efficiency about 5 per cent.



*Report No. 302*, entitled "Full Scale Tests on a Thin Metal Propeller at Various Tip Speeds," by Fred E. Weick, National Advisory Committee for Aeronautics.

This report describes an investigation made in order to determine the effect of tip speed on the characteristics of a thin-bladed metal propeller. The propeller was mounted on a VE-7 airplane with a 180-horsepower E-2 engine and tested in the 20-foot propeller research tunnel of the National Advisory Committee for Aeronautics. It was found that the effect of tip speed on the propulsive efficiency was negligible within the range of the tests, which was from 600 to 1,000 feet per second (about 0.5 to 0.9 the velocity of sound in air).

*Report No. 303*, entitled "An Investigation of the Use of Discharge Valves and an Intake Control for Improving the Performance of N. A. C. A. Roots Type Superchargers," by Oscar W. Schey and Ernest E. Wilson, National Advisory Committee for Aeronautics.

This report presents the results of an analytical investigation on the practicability of using mechanically operated discharge valves in conjunction with a manually operated intake control for improving the performance of N. A. C. A. Roots type superchargers. The investigation was conducted by the staff of the National Advisory Committee for Aeronautics at Langley Field, Va.

These valves, which may be either of the oscillating or rotating type, are placed in the discharge opening of the supercharger and are so shaped and synchronized with the supercharger impellers that they do not open until the air has been compressed to the delivery pressure. The intake control limits the quantity of air compressed to engine requirements by permitting the excess air to escape from the compression chamber before compression begins.

The percentage power saving and the actual horsepower saved were computed for altitudes from 0 to 20,000 feet. These computations are based on the pressure-volume cards for the conventional and the modified Roots type superchargers and on the results of laboratory tests of the conventional type.

The use of discharge valves shows a power saving of approximately 26 per cent at a critical altitude of 20,000 feet. In addition, these valves reduce the amplitude of the discharge pulsations and increase the volumetric efficiency. With slow-speed Roots blowers operating at high-pressure differences even better results would be expected. For aircraft engine superchargers operating at high speeds these discharge valves increase the performance as above, but have the disadvantages of increasing the weight and of adding a high-speed mechanism to a simple machine.

*Report No. 304*, entitled "An Investigation of the Aerodynamic Characteristics of an Airplane Equipped with Several Different Sets of Wings," by J. W. Crowley, jr., and M. W. Green, National Advisory Committee for Aeronautics.

This investigation was conducted by the National Advisory Committee for Aeronautics at Langley Field, Va., at the request of the Army Air Corps, for the purpose of comparing the full scale lift and drag characteristics of an airplane equipped with several sets of wings of commonly used airfoil sections. A Sperry Messenger airplane with wings of R. A. F.-15, U. S. A.-5, U. S. A.-27, and Göttingen 387 airfoil sections was used and the lift and drag characteristics of the airplane with each set of wings were determined by means of glide tests.

The results are presented in tabular and curve form.

*Report No. 305*, entitled "The Gaseous Explosive Reaction—A Study of the Kinetics of Composite Fuels," by F. W. Stevens, Bureau of Standards.

This report deals with the results of a series of studies of the kinetics of gaseous explosive reactions where the fuel under observation, instead of being a simple gas, is a known mixture of simple gases. In the practical application of the gaseous explosive reaction as a source of power in the gas engine, the fuels employed are composite, with characteristics that are apt to be due to the characteristics of their components and hence may be somewhat complex. The simplest problem that could be proposed in an investigation either of the thermodynamics or kinetics of the gaseous explosive reaction of a composite fuel would seem to be a separate study



of the reaction characteristics of each component of the fuel and then a study of the reaction characteristics of the various known mixtures of those components forming composite fusel more and more complex. This is the order followed in the simple studies described.

*Report No. 306*, entitled "Full Scale Wind Tunnel Tests of a Series of Metal Propellers on a VE-7 Airplane," by Fred E. Weick, National Advisory Committee for Aeronautics.

An adjustable blade metal propeller was tested at five different angle settings, forming a series varying in pitch. The propeller was mounted on a VE-7 airplane in the 20-foot propeller research tunnel of the National Advisory Committee for Aeronautics. The efficiencies were found to be from 4 to 7 per cent higher than those of standard wood propellers operating under the same conditions. The results are given in convenient form for use in selecting propellers for aircraft.

*Report No. 307*, entitled "The Pressure Distribution Over the Horizontal and Vertical Tail Surfaces of the F6C-4 Pursuit Airplane in Violent Maneuvers," by R. V. Rhode, National Advisory Committee for Aeronautics.

This investigation of the pressure distribution on the tail surfaces of a pursuit airplane in violent maneuvers was conducted by the National Advisory Committee for Aeronautics at the request of the Navy Bureau of Aeronautics for the purpose of determining the maximum loads likely to be encountered on these surfaces in flight. The information is a part of that needed for a revision of existing loading specifications to bring these into closer agreement with actual flight conditions. A standard F6C-4 airplane was used and the pressure distribution over the right horizontal and complete vertical tail surfaces was recorded throughout violent maneuvers. The results show that the existing loading specifications do not conform satisfactorily to the loadings existent in critical conditions, and in some cases were exceeded by the loads obtained.

An acceleration of 10.5 *g* was recorded in one maneuver in which the pilot suffered severely. It is therefore indicated that the limits of the physical resistance of the pilot to violent maneuvers are being approached.

Navy specifications for the structural design of tail surfaces are included as an appendix.

*Report No. 308*, entitled "Aircraft Accidents: Method of Analysis," prepared by special committee on the nomenclature, subdivision, and classification of aircraft accidents, National Advisory Committee for Aeronautics.

This report on a method of analysis of aircraft accidents has been prepared by a special committee on the nomenclature, subdivision, and classification of aircraft accidents organized by the National Advisory Committee for Aeronautics in response to a request dated February 18, 1928, from the air coordination committee consisting of the Assistant Secretaries for Aeronautics in the Departments of War, Navy, and Commerce. The work was undertaken in recognition of the difficulty of drawing correct conclusions from efforts to analyze and compare reports of aircraft accidents prepared by different organizations using different classifications and definitions. The air coordination committee's request was made "in order that practices used may henceforth conform to a standard and be universally comparable." The purpose of the special committee therefore was to prepare a basis for the classification and comparison of aircraft accidents, both civil and military.

#### LIST OF TECHNICAL NOTES ISSUED DURING THE PAST YEAR

- |      |   |
|------|---|
| No.  |   |
| 267. | Pressure Distribution on Wing Ribs of the VE-7 and TS Airplanes in Flight. By R. V. Rhode. Part I: Level Flight.  |
| 268. | Mass Distribution and Performance of Free Flight Models. By Max Scherberg and R. V. Rhode.  |
| 269. | The Distribution of Loads Between the Wings of a Biplane Having Decalage. By Richard M. Mock.   |
| 270. | The Characteristics of the N. A. C. A. 97, Clark Y, and N. A. C. A.-M6 Airfoils with Particular Reference to the Angle of Attack. By George J. Higgins. |



- No.
271. Full Scale Drag Tests on Various Parts of Sperry Messenger Airplane. By Fred E. Weick.
  272. Special Propeller Protractor. By A. L. Heim.
  273. The Effect on Performance of a Cutaway Center Section. By Thomas Carroll.
  274. The Effect of the Sperry Messenger Fuselage on the Air Flow at the Propeller Plane. By Fred E. Weick.
  275. Determination of Propeller Deflection by Means of Static Load Tests on Models. By Fred E. Weick.
  276. Helium Tables. By Lieut. Commander Clinton H. Havill, U. S. N.
  277. Pressure Distribution on Wing Ribs of the VE-7 and TS Airplanes in Flight. Part II: Pull-Ups. By R. V. Rhode.
  278. An Automatic Speed Control for Wind Tunnels. By A. F. Zahm.
  279. Resistance of Streamline Wires. By George L. DeFoe.
  280. Drag of Exposed Fittings and Surface Irregularities on Airplane Fuselages. By Donald H. Wood.
  281. A Comparison of Propeller and Centrifugal Fans for Circulating the Air in a Wind Tunnel. By Fred E. Weick.
  282. Corrosion Embrittlement of Duralumin. I. Practical Aspects of the Problem. By Henry S. Rawdon.
  283. Corrosion Embrittlement of Duralumin. II. Accelerated Corrosion Tests and the Behavior of High-Strength Aluminum Alloys of Different Compositions. By Henry S. Rawdon.
  284. Corrosion Embrittlement of Duralumin. III. Effect of the Previous Treatment of Sheet Material on the Susceptibility to this Type of Corrosion. By Henry S. Rawdon.
  285. Corrosion Embrittlement of Duralumin. IV. The Use of Protective Coatings. By Henry S. Rawdon.
  286. Preliminary Investigation on Boundary Layer Control by Means of Suction and Pressure with the U. S. A. 27 Airfoil. By E. G. Reid and M. J. Bamber.
  287. A Dangerous Seaplane Landing Condition. By Thomas Carroll.
  288. The Reaction on a Float Bottom When Making Contact with Water at High Speeds. By H. C. Richardson.
  289. Preliminary Biplane Tests in the Variable Density Wind Tunnel. By James M. Shoemaker.
  290. Welding High Chromium Steels. By W. B. Miller.
  291. Gluing Practice at Aircraft Manufacturing Plants and Repair Stations. By T. R. Truax.
  292. The Drag of a J-5 Radial Air-Cooled Engine. By Fred E. Weick.
  293. The Formation of Ice Upon Exposed Parts of an Airplane in Flight. By Thomas Carroll and William H. McAvoy.
  294. Wind Tunnel Force Tests in Wing Systems Through Large Angles of Attack. By Carl J. Wenzinger and Thomas A. Harris.
  295. The Effect of Tip Shields on a Horizontal Tail Surface. By Paul V. Dronin, Earl I. Ramsden, and George J. Higgins.
  297. Preliminary Report on the Flar-Top Lift Curve as a Factor in Control at Low Speed. By Montgomery Knight and Millard J. Bamber.
  298. The Determination of Several Spray Characteristics of a High-Speed Oil Engine Injection System with an Oscilloscope. By Chester W. Hicks and Charles S. Moore.

#### LIST OF TECHNICAL MEMORANDUMS ISSUED DURING THE PAST YEAR

- No.
432. Slotted-Wing Airplanes. By E. Everling. Translation from "Zeitschrift des Vereines deutscher Ingenieure," May 7, 1927.
  433. Some German Gliders of 1920-1923. By Alfred Gymnich. Translation from "Der Gleit- und Segelflugzeugbau" (ch. 3). Published by Richard Carl Schmidt & Co., Berlin, 1925.
  434. Glider Construction and Design. By Alfred Gymnich. Translation from "Der Gleit- und Segelflugzeugbau" (ch. 4, secs. 1-3), 1925.



No.

435. Turbulent Flow. By L. Prandtl. Lecture delivered before the International Congress for Applied Mechanics, Zurich, September, 1926.
436. Approximation Method for Determining the Static Stability of a Monoplane Glider. By A. Lippisch. Translation from "Zeitschrift für Flugtechnik und Motorluftschiffahrt," June 14, 1927.
437. Experiments on Airfoils with Aileron and Slot. By A. Betz. Translation from Report III, "Ergebnisse der Aerodynamischen Versuchsanstalt zu Göttingen" (Aerodynamic Institute).
438. Safety in Airplane Flight. By H. Brunat. Communication by H. Brunat, of the "Service de la Navigation Aérienne," to the "Société Française de Navigation Aérienne," November 10, 1927.
439. Structural Details of German Gliders. By Alfred Gymnich. Translation from "Der Gleit- und Segelflugzeugbau" (ch. 4, secs. 6-9), 1925.
440. Metal Aircraft Construction at Vickers. Some Interesting New Forms Developed. From Flight, September 15, 1927.
441. Increasing Lift by Releasing Compressed Air on Suction Side of Airfoil. By F. Seewald. Translation from "Zeitschrift für Flugtechnik und Motorluftschiffahrt," August 16, 1927.
442. "Gloster" High-Lift Biplane Wings. By H. E. Preston. From The Gloster, Volume II, No. 5, January-February, 1927.
443. Duralumin—Defects and Failures. By Lieut. Commander William Nelson (C. C.), United States Navy. From Aviation, August 29, 1927.
444. Calculating Thrust Distribution and Efficiency of Air Propellers. By Theodor Bienen. Translation from "Zeitschrift für Flugtechnik und Motorluftschiffahrt," November 27, 1926.
445. Tensile Strength of Welded Steel Tubes. First Series of Experiments. By A. Rechtlich. Translation from "Zeitschrift für Flugtechnik und Motorluftschiffahrt," September 14, 1927.
446. Crank Case Scavenging of a Two-Stroke-Cycle Engine. By Otto Holm. Translation from "Zeitschrift des Vereines deutscher Ingenieure," June 11, 1927.
447. Stressed Coverings in Naval and Aeronautic Constuction. By L. L. Kahn. Translation from "Association Technique Maritime et Aéronautique," May-June, 1927.
448. Mechanical Properties of Some Materials Used in Airplane Construction. By E. B. Wolff and L. J. G. Van Ewijk. Translation from Report M 219 of the "Rijks-Studiedienst voor de Luchtvaart," reprinted from "De Ingenieur," August 7, 1926.
449. Results of Aerodynamic Tests on Slotted Airfoils in the Aerotechnical Laboratory (S. T. Aé.) of Rhode St. Genese, Brussels. By Paul Puvrez. Translation from Bulletins Nos. 1 and 4, April and July, 1927, of the "Service Technique de L'Aéronautique Belge."
450. Parachutes for Aircraft. By Waldemar Müller. Translation from "Zeitschrift für Flugtechnik und Motorluftschiffahrt," October 28, 1927.
451. Aviation Fuels (with Special Reference to "White Spirit"). By P. Dumanois. Translation from "La Technique Aeronautique," April 15, 1927.
452. Motion of Fluids with Very Little Viscosity. By L. Prandtl. Translation from "Vier Abhandlungen zur Hydrodynamik und Aerodynamik," Göttingen, 1927.
453. Welding in Airplane Construction. By A. Rechtlich and M. Schrenk. Translation from the 1927 Yearbook of the "Deutsche Versuchsanstalt für Luftfahrt."
454. The 1926 German Seaplane Contest. Part I: Lessons Taught. By F. Seewald. Part II: Method of Rating. By H. Blenk and F. Liebers. Translation from the 1927 Yearbook of the "Deutsche Versuchsanstalt für Luftfahrt."
455. Note on Research Work by Helmholtz and Wein Relating to the Form of Waves Propagated Along the Surface of Separation of Two Liquids. By J. M. Burgers. Translation from a reprint from "Rendiconti della R. Accademia Nazionale dei Lincei," Volume V, No. 5.



- No.
456. Calculation of Airplane Performances without the Aid of Polar Diagrams. By Martin Schrenk. Translation from the 1927 Yearbook of the "Deutsche Versuchsanstalt für Luftfahrt."
457. A Few More Mechanical-Flight Formulas without the Aid of Polar Diagrams. By Martin Schrenk. Translation from the 1927 Yearbook of the "Deutsche Versuchsanstalt für Luftfahrt." (Supplement to Technical Memorandum No. 456.)
458. Steel Spars. By Brian L. Martin. From *The Gloster*, September–December, 1927.
459. Variable Pitch Propellers. By H. L. Milner. From *The Gloster*, September–December, 1927.
460. Take-Off of Heavily Loaded Airplanes. By A. Pröll. Translation from "Zeitschrift für Flugtechnik und Motorluftschiffahrt," January 28, 1928.
461. Contribution to the Systematic Investigation of Joukowsky Profiles. By Göttfried Loew. Translation from "Zeitschrift für Flugtechnik und Motorluftschiffahrt," November 28, 1927.
462. Comments on Crankless Engine Types. Translation from "Der Motorwagen," November 20, 1927.
463. Prospective Development of Giant Airplanes. By B. Von Romer. Translation from "Luftfahrt," October 22, 1927.
464. Discussion of Problems Relating to the Safety of Aviation. By J. Sabatier. Part I. Translation from "Bulletin Technique" No. 42, of the "Service Technique et Industriel de l'Aeronautique," June 18, 1927.
465. Discussion of Problems Relating to the Safety of Aviation. By J. Sabatier. Part II. Translation from "Bulletin Technique" No. 42, of the "Service Technique et Industriel de l'Aeronautique," June 18, 1927.
466. Wheel Brakes and Their Application to Aircraft. By G. H. Dowty. From *Flight*, November 24 and December 29, 1927, and January 26, 1928.
467. The Diesel as a Vehicle Engine. By Kurt Neumann. Translation from "Zeitschrift des Vereines deutscher Ingenieure," May 28, 1927.
468. Choice of Profile for the Wings of an Airplane. Part I. By A. Toussaint and E. Carafoli. Translation from "L'Aeronautique," December, 1927.
469. Choice of Profile for the Wings of an Airplane. Part II. By A. Toussaint and E. Carafoli. Translation from "L'Aeronautique," January, 1928.
470. On Improvement of Air Flow in Wind Tunnels. By C. Wieselsberger. From *Journal, Society of Mechanical Engineers (of Japan)*, June, 1925, volume 29, No. 98.
471. Technical Progress Shown in the 1927 Rhön Soaring-Flight Contest. By W. Hübner. Translation from "Zeitschrift des Vereines deutscher Ingenieure," December 3, 1927.
472. Experiments with a Wing from Which the Boundary Layer Is Removed by Pressure or Suction. By K. Wieland. Translation from "Zeitschrift für Flugtechnik und Motorluftschiffahrt," August 16, 1927.
473. The Problem of Noise in Civil Aircraft and the Possibilities of Its Elimination. By W. S. (I) Tucker. From *Journal of the Royal Aeronautical Society*, March, 1928, volume 32, No. 207.
473. The Problem of Noise in Civil Aircraft and the Possibilities of Its Elimination. By W. S. (II) Tucker. From *Journal of the Royal Aeronautical Society*, March, 1928, volume 32, No. 207.
474. Windmills in the Light of Modern Research. By A. Betz. Translation from "Die Naturwissenschaften," November 18, 1927, volume 15, No. 46.
475. Recent Researches on the Air Resistance of Spheres. By O. Flachsbart. Translation from "Physikalische Zeitschrift," volume 28, 1927.
476. Synopsis of French Aeronautic Equipment—Aeronautic Instruments. Translation from "L'Aeronautique," September, 1927, No. 100.



- No.  
 477. Contribution to the Design and Calculation of Fuel Cams and Fuel Valves for Diesel Engines. By Jatindra Nath Basu. Translation from "Der Motorwagen," May 10 and July 31, 1927.  
 478. The Cells of Giant Airplanes. By E. Offermann. From Offermann's "Riesenflugzeuge," 1927.  
 479. The Span as a Fundamental Factor in Airplane Design. By G. Lachmann. Translation from "Zeitschrift für Flugtechnik und Motorluftschiffahrt," May 14, 1928.  
 480. Airplane Strength Calculations and Static Tests in Russia. (An Attempt at Standardization.) Translation from "L'Aeronautique," February, 1928.  
 481. Considerations on Propeller Efficiency. By A. Betz. Translation from "Zeitschrift für Flugtechnik und Motorluftschiffahrt," April 28, 1928.

## LIST OF AIRCRAFT CIRCULARS ISSUED DURING THE PAST YEAR

- No.  
 57. The De Haviland *Tiger Moth*—A Low-Wing Monoplane. From Flight, September 22, 1927.  
 58. The Fairchild *All-Purpose* Cabin Monoplane. From a circular issued by the Fairchild Airplane Manufacturing Corporation.  
 59. The Focke-Wulf F. 19 *Ente* Tail-First Airplane. From Flight, September 29, 1927.  
 60. Stinson Commercial Airplane, type SM-1—A Semicantilever Monoplane. Prepared by the Stinson Aircraft Corporation.  
 61. Lockheed *Vega* Airplane—A Commercial Cabin Monoplane. Prepared by the Lockheed Aircraft Co.  
 62. The Pitcairn *Mailwing* PA-5—A Single-Seat Commercial Biplane. Prepared by Pitcairn Aviation (Inc.).  
 63. *Avimeta*—Three-Engine Commercial Monoplane, type A. V. M. 132. From a circular issued by the Avimeta Co.  
 64. The Heinkel Commercial Airplane *H. D. 40* From a circular issued by the Ernst Heinkel Airplane Co.  
 65. The De Haviland 61 *Canberra* (British)—A Six to Eight Passenger Airplane. From Flight, December 29, 1927.  
 66. Focke-Wulf A. 17 Commercial Airplane *Moewe* (German). From a circular issued by the Focke-Wulf Airplane Construction Co.  
 67. Supermarine *S-5* Seaplane (British)—Winner of the 1927 Schneider Cup Race. From Flight, February 16, 1928.  
 68. The Short *Calcutta*—First British All-Metal Commercial Seaplane. From Flight, February 23, 1928.  
 69. The *Gloster IV* Seaplane (British). From Flight, March 1, 1928.  
 70. The Avro *Avian III* Airplane (British). From Flight, March 8, 1928.  
 71. The Boulton and Paul *Sidestrander I* Bomber Airplane (British). From Flight, March 29, 1928.  
 72. The Parnall *Imp*—A New British Light Airplane. From Flight, April 12, 1928.  
 73. The Fokker *Universal* Commercial Airplane. From a circular issued by the Atlantic Aircraft Corporation.  
 74. The Bleriot *Spad 91* Airplane—Pursuit Single-Seater "Jockey" type. Translation from Les Ailes, April 19, 1928.  
 75. Morane-Saulnier 121 Single-Seat Pursuit Airplane (French). By J. Serryer. Translation from Les Ailes, October 20, 1927.  
 76. The Fokker *Trimotor F VII* Commercial Transport Monoplane. From a circular issued by the Atlantic Aircraft Corporation.  
 77. René Couzinet Monoplane (French). By J. Serryer. Translation from Les Ailes, March 29, 1928.  
 78. Savoia Marchetti *S 64* Airplane. By Maurice Victor. Translation from Les Ailes, June 14, 1928.



No.

79. The Sikorsky Twin-Engined Amphibian, type S-38, Model 1928. Prepared by Sikorsky Manufacturing Corporation.
80. C. A. M. S. 54 G. R. Transatlantic Seaplane (French). Prepared by Paris Office, N. A. C. A.
81. Westland *Wapiti* (British). Prepared by the Westland Aircraft Works, England.
82. The Armstrong Whitworth *Starling* (British)—Single-Seat Fighter. From Flight, August 2, 1928.

## BIBLIOGRAPHY OF AERONAUTICS

During the past year the committee issued a bibliography of aeronautics for the year 1925. It had previously issued bibliographies for the years 1909 to 1916, 1917 to 1919, 1920 to 1921, 1922, 1923, and 1924. A bibliography for the year 1926 is now in the hands of the printer, and should be ready for distribution during the coming year. A bibliography is now being published annually by the committee.

Citations of the publications of all nations are included in the language in which the publications originally appeared. The arrangement is in dictionary form, with author and subject entry, and one alphabetical arrangement. Detail in the matter of subject reference has been omitted on account of cost of presentation, but an attempt has been made to give sufficient cross reference to make possible the finding of items in special lines of research.



## PART V

### THE PRESENT STATE OF AERONAUTICAL DEVELOPMENT

---

#### PROGRESS IN TECHNICAL DEVELOPMENT

##### AERODYNAMICS

As in past years a majority of the aerodynamic problems investigated have been closely related either to particular design requirements or to the study of unusual phenomena. Their study has been made necessary by the immediate technical requirements of air commerce and the military and naval services. These problems usually demand prompt attention, and it has always been the policy of the committee to undertake as much of this type of work as practicable without unbalancing the research programs. Fundamental research along lines having no immediate prospect of practical use is as a rule limited to problems of general interest, but whenever possible the test programs are so laid out as to have a bearing on some fundamental problem.

**WIND TUNNELS—Additional equipment.**—There have been several additions to the wind-tunnel equipment at the Langley Memorial Aeronautical Laboratory and others are planned. A small wind tunnel having a 6-inch jet has been constructed and fitted with refrigerating apparatus to enable the study of ice formation. A small water tunnel has also been constructed for use in the study of scale effect. A high-speed tunnel has been added to the equipment of the variable-density tunnel. This new tunnel gives an air stream about 1 foot in diameter with a velocity in the neighborhood of that of sound. Steps are also being taken to replace the present 5-foot atmospheric wind tunnel by two new tunnels. One will be a somewhat larger closed-circuit open-throat tunnel and the other a smaller tunnel having a vertical air flow in the testing section. This latter tunnel is for use in the study of spinning. The additional equipment will be of great value in expediting important tests now on the program.

**Aerodynamic safety.**—Considerable work has been done in the atmospheric wind tunnel in connection with the problems of safety. Attention has been focused on the possibility of the development of an airfoil having a flat-top lift curve as a means of preventing accidental stalls in landing or taking off. This work is being continued in an attempt to improve the aerodynamic characteristics of the N. A. C. A. 84 airfoil section and to develop a suitable section for full-flight testing. This research is considered highly important and it will be made in conjunction with the investigation of lateral control and autorotation.

**Autorotation.**—The research on autorotation has been continued and during the past year force tests have been made through a large range of angles of attack for a systematic series of monoplane and biplane combinations. This research is being supplemented by pressure-distribution tests now under way, upon completion of which it is proposed to make a series of autorotational torque tests on a specially designed dynamometer. The primary object of these investigations is to supply information for the development of nonspinning wings or wing systems. Several reports have already been issued.

**Ice formation.**—This problem, as apart of the general safety program, has been studied in the laboratory with a special 6-inch wind tunnel equipped with refrigerating apparatus. Preliminary tests have been very satisfactory in that ice formations have been obtained on model air foils and struts similar to those observed on airplanes in flight. The investigation will be extended to determine practical means for the prevention or the avoidance of ice formations.

**Slots and flaps.**—Several types of trailing-edge flaps have been tested and this work is to be extended to cover the effects of slots, singly and in combination with various flaps. This investigation is made as a part of the research on control and stability at low speeds.



*Variable-density wind tunnel.*—Following the fire in 1927, which completely destroyed the interior fittings, this tunnel has been rebuilt and improved. It has been converted to an open-throat type and preliminary tests indicate a marked improvement in the energy ratio, with a better velocity distribution. The new balance is expected to be installed and the tunnel again in full operation at an early date.

**FREE FLIGHT TESTS—*Flight-path determination.***—Two independent methods have been used for measuring the flight path of airplanes in a very important research on this subject. The integrated indications of special recording instruments developed for this purpose are checked by simultaneous ground records made with a camera obscura. The test runs are controlled from the ground by radiotelephone communication with the pilot. The results of this investigation will supply information regarding the comparative maneuverability of various airplanes, the loadings encountered, and similar information of value in the design and operation of airplanes. Flight tests have been completed on one airplane and have been partially completed on a second differing from the first in the engine installation only.

*Ice formation.*—A number of flight tests have been made to study the conditions under which ice forms on the wings, struts, wires, etc., of an airplane. In these flights records are made of cloud formations, altitude, temperature, etc. Various methods of preventing or avoiding ice formation will be studied and the data obtained will be correlated with that from the wind-tunnel tests.

*Landing-gear loads.*—Dropping tests, followed by flight tests, are under way on airplane landing gear equipped with several types of oleo and rubber shock absorbers in order to obtain quantitative values of the energy absorbed and the accelerations resulting from different kinds of landings. This investigation will supply data for the more accurate design of landing gears fitted with the various types of shock absorbers.

*Loading on float bottoms.*—The research on water pressure distribution on float bottoms has been continued on a twin-float seaplane with very satisfactory results. The maximum pressures measured were considerably less than those given in the design specifications. It would appear that by designing for the lighter loads the weight of airplane floats could be reduced.

*Pressure distribution.*—Pressure-distribution tests have been completed on the entire control and supporting surfaces of a modern pursuit airplane and the investigation is being extended to cover the pressure distribution on the fuselage. Pressure-distribution tests on the tail surfaces of another pursuit-type airplane have also been completed and the results will soon be published. These investigations indicate that the present specifications for the loads on control surfaces should be revised and recommendations to this effect have been made to the Army and the Navy. The present pressure-distribution program includes cargo and observation types. The information obtained from this work is invaluable to the designer.

*Spinning.*—In connection with the study of recovery from spins the moments of inertia of all available airplanes have been measured. These data are now being analyzed with reference to normal and abnormal spinning characteristics. This information is expected to supplement the wind-tunnel autorotation study in supplying the designer with fairly definite restrictions on weight distribution.

*Take-off and landing runs.*—The investigation of take-off runs has been continued and tests have been made on one airplane with three loads and three different propellers. The test data now available are being analyzed in order to establish if practicable a simple empirical formula for take-off runs. Landing runs have also been measured with and without brakes under various conditions. The information so far obtained is of considerable interest and value to commercial pilots operating from small fields.

**PROPELLER RESEARCH TUNNEL.**—During the past year this tunnel has made a number of tests on propellers, propeller interference, full-scale drag, and cowling and cooling of air-cooled engines. The information obtained is of the highest value.

*Cowling and cooling of air-cooled engines.*—This investigation is one of the most important studies yet made by the committee and the results have been highly gratifying. The full-scale



information now made available for the first time is of fundamental importance in design. The data include full-scale drag measurements on radial air-cooled engines with installations ranging from no cowling to complete cowling, the cooling characteristics and the propulsive characteristics being measured for each installation. Incidental to the main investigation a number of important tests were also made such as the drag of various types of exhaust stacks and collector rings and the drag of various types of bodies and fairings. Obviously, this information is of the greatest value to the designer of commercial and military airplanes.

*Effect of tip speed.*—Tests have been made on a thin metal propeller mounted on a VE-7 fuselage, at tip speeds from 600 to 1,000 feet per second. Within this range the effect of tip speed on propulsive efficiency was negligible, but the investigation will be extended to include higher tip speeds and other blade shapes.

*Miscellaneous drag measurements.*—A number of very important full-scale drag measurements have been made during the propeller testing program. One of the most important of these was the drag analysis of the Sperry messenger airplane. A full-scale airplane was mounted on the balance, and the drag measured as successive parts were removed until there remained only the bare fuselage. The results were highly satisfactory and indicate the great possibilities of the propeller research tunnel. Another test of considerable interest was the determination of the effect of wing fillets on drag. Using one of the "cowling" investigation models, it was found that fillets of 6-inch and 12-inch radii between the lower wing surface and the fuselage reduced the drag 2 pounds and 5.1 pounds, respectively, at 100 miles per hour.

A special gear has been devised and used for the testing of models of wings up to 3-foot chord by 12-foot span, at a speed of 100 miles per hour. Full-scale tests were made with this equipment on four airfoils and a full-scale racing wing fitted with wing radiators.

*Propeller interference.*—Considerable information on this subject has now been accumulated. In the VE-7 tests, readings were obtained with the tail surfaces removed and then with wings and tail removed. The tail surfaces were found to have no appreciable effect on the propeller, but the wings reduced the propulsive efficiency and increased the power coefficient. In the cowling and cooling investigation, the data on propeller interference will form a considerable item. These tests are now nearing completion and the data will soon be available for design purposes.

*VE-7 airplane with various propellers.*—A full-scale VE-7 fuselage has been tested with two series of propellers, one wood and one metal. The wooden series had previously been tested in flight and in model form in a wind tunnel. The metal-propeller series was obtained from five blade-angle settings for a service propeller. The data so obtained are very important in propeller design and further work is to be done.

*LIGHTER-THAN-AIR CRAFT.*—A preliminary study of wind velocities and accelerations in bumpy air has been concluded with satisfactory results. Accelerations were found ranging from 121 feet per second, per second lasting  $\frac{1}{4}$  second, to 2 feet per second, per second lasting  $15\frac{1}{4}$  seconds, but the preliminary study was made for the purpose of trying out instruments and finding the magnitude of the accelerations to be expected. The next step is to determine the size or extent of the gusts, and it is planned to cover a large area with recording instruments for this purpose.

The results of the pressure-distribution, speed, and acceleration tests on the *Los Angeles* have been worked up and will soon be ready for publication.

*FIELDS FOR FUTURE RESEARCH.*—It has been pointed out in previous summaries that the greatest progress in aerodynamics may be expected along the line of refinement in design and increase in safety. The refinement will result from improved knowledge regarding air loads and load distribution, the phenomena which affect control and control effectiveness particularly at low speeds, full-scale wing characteristics, and methods of reducing drag or improving propulsive efficiencies. The increasing of safety is obviously very closely connected with the problems encountered in general design refinement. The present research programs are based on these considerations.



The immediate design needs are for more information on loads and load distributions in commercial types of airplanes and for additional data on mutual interference between propellers and structure, particularly in multi-engined installations. The questions regarding safety are considered to be by far the most important facing the committee and the aircraft industry. These questions relate chiefly to stability, control, and operation, rather than structural strength.

The propeller research wind tunnel has been of great value in the investigation of design problems that can not be studied in smaller wind tunnels or in free flight. The information so far obtained has indicated that the future development of aeronautics can be greatly accelerated by the provision of a wind tunnel large enough for testing full-scale airplanes up to, say, 35-foot span. The need for this equipment is so great that the design of such a tunnel has been started and tests on small-scale models are now being made.

#### AIRPLANE STRUCTURES

**TREND OF DESIGN—*Standardization of types.***—No notable changes from the tendencies noted in last year's report have appeared. The monoplane appears firmly established for regular scheduled commercial service carrying passengers and express. These airplanes practically invariably have two or more engines. An increasing appreciation of the importance of reducing parasite resistance has led to improved performances from airplanes of this type. The monoplane is also beginning to appear in the smaller classes of airplanes where its better aerodynamic efficiency usually enables either a reduction in engine power for the same performance as the generally equivalent biplane, or a better performance for the same power.

The biplane, however, continues to hold a large place in production and is profiting by the appreciation of the necessity for reducing parasite resistance. By far the larger number of the airplanes sold for use by individual owners and pilots are of this type.

Inclosed or cabin-type bodies are being fitted in increasing numbers and in airplanes of all types and sizes. Apparently the old feeling that the pilot could not handle his craft properly unless he were in an open cockpit is rapidly fading. This also reflects the demand of the new owners of airplanes for increased comfort.

The influence of the production department on the designer of airplanes is beginning to be apparent. This is leading to the construction of airplanes which, without sacrifice of quality in design, materials, or performance, are less costly to produce than many earlier designs.

Monoplane bombers have not been as successful as was hoped, and bombers of this type are still strictly experimental.

The military biplanes for any particular service continue to grow more alike. Experience under service conditions quickly weeds out the airplanes having undesirable characteristics and shows that in order to obtain desirable ones the arrangement of parts must be along fairly restricted lines.

***Number and location of engines.***—As the engines available increase in power the tendency to use several engines in military aircraft is reduced. Most multi-engined military aircraft can not fly loaded with one engine out of commission. A single engine of the same total horsepower is usually lighter and the airplane has less structure in the wind to produce resistance.

In civil aircraft the effort is distinctly to enable flight to continue if one engine is out of commission. For such aircraft several engines offer a real increase in safety. However, the use of several engines continues to be uneconomic in the smaller types carrying either mail or only a few passengers.

The tendency to locate the engines well above the wing, which has been a conspicuous feature in large foreign monoplanes, has not yet appeared in American designs, where the lines of thrust of all propellers are usually approximately in the same plane which passes very close to the fore-and-aft center line of the body. The effect of overlapping propeller circles in producing vibration and reducing efficiencies has been appreciated, and in most of the recent designs of multi-engined airplanes the distance apart of the engines has been made sufficient to prevent overlap of propellers. Advantage is usually taken of the construction which is made necessary by the greater distance apart to fit the landing wheels directly under the outer engines, thus widening the track and reducing the structure in the wind.



*Amphibian airplanes.*—The amphibian type of airplane has grown in favor and several manufacturers now offer production models. Most of the earlier models were of the boat type and these still continue. Float type seaplanes incorporating amphibian gear were developed during the past year.

*Landing gear.*—Many airplane manufacturers are now prepared to supply their product as either landplane or seaplane. The arrangement is such that the change from one landing gear to the other is relatively easy and quick. Although not amphibian these interchangeable gears make the airplane much more adaptable for service in a variety of locations. By arranging for the fitting of skis also the same airplane can be used in a wide range of services.

*Shock absorbers.*—The old rubber-cord shock absorber is being fitted on few new airplanes. The general use of the hydraulic shock absorber with the resulting lighter landing gear loads, has led to the raising of the question whether the structure of the airplane might not be reduced accordingly.

*Wheel tail skids.*—These are being introduced in both large and small airplanes and are being applied to increasing numbers. They are, of course, invariably associated with wheel brakes on at least the main landing wheels.

*Brakes.*—The general application of brakes has reduced the amount of manhandling of airplanes on the field. With increased knowledge of how to use the brakes new methods of handling have appeared. Many pilots land and bring their airplanes to the line or point for discharge of passengers and cargo without assistance from ground crews. Frequently the pilot "drives" right into a hangar and in some cases maneuvers inside on his own power.

New types of brakes and combinations of brakes and wheels and brakes and shock absorbers with the wheels are being tried. Airplane wheels of the disk type in which metal disks form the sides of the wheel are coming into use. These wheels are unusually well adapted for the fitting of internal brakes and are usually so fitted.

*Difference between military and commercial types.*—The demand for increased safety in civil airplanes, which has been supported by the requirements of the Department of Commerce, is causing the general introduction of higher grade materials and better workmanship. It is now felt that the materials and general workmanship in the better grade of civil airplanes compare very favorably with those in military airplanes and may be just as good. With the increasing use of engines of larger power, and of several engines, in civil airplanes the value of the product becomes so great, and the demands on it in service so heavy, that the use of the best of materials and workmanship is a true economy.

In spite of the increase in quality of materials and workmanship the civil airplane has been still further differentiated from the military airplane. The chances of successful application of civil types to military uses are correspondingly reduced.

**STRUCTURAL MATERIALS—Metal construction.**—Interest in metal construction has increased markedly. As long as only a few airplanes, usually with individual changes, were being produced by an airplane factory, the use of metal construction was restricted to the simpler parts of the structure where elaborate jigs and fittings were not required. With increasing production of repetition models the expense of special tools becomes justified and the all-metal, or nearly all-metal, airplane may ultimately be cheaper than the part-metal part-wood one.

Specialization in the supply of metal parts, such as wing spars and ribs, is appearing. With the ability to purchase such parts from a parts maker at a less cost than they can be made by the individual airplane builder, an increase in the number of full-metal framed airplanes is sure.

Original designs notable for the ingenuity of the designers continue to appear. The introduction of the Alclad method of protecting duralumin from corrosion has prompted the use of this material in such designs. With reports of practical immunity to corrosion for long periods the drift to other materials has slowed down.

*Steel tubing.*—Progress has been made in the welding of the corrosion-resisting steels, but as yet tubing of this type is not generally available. There appears no reason to doubt that eventually it will be. In the meantime much attention is being paid to the protection of the inside of steel tubing against corrosion.



*Duralumin tubing.*—Progress has been made on the application of the Alclad process to duralumin tubing. Until this is accomplished many designers will look with suspicion on duralumin tubing and continue the use of open sections in which the entire surface is accessible.

*Floats.*—The metal float is rapidly driving the wooden float from the field. Here again the use of duralumin protected by a coat of pure aluminum has removed one of the main troubles with corrosion. However, floats have been built of nickel, Monel metal, and of stainless steel. A float of the latter material was only slightly heavier than a duralumin float, and the designers believe it can be made as lightly. The recent work of the committee on the loads experienced by the bottoms of airplane floats promises to enable more accurate design of floats.

*Rubber protective coatings.*—Work on these coatings has continued but progress has been slow. The use of more corrosion-resisting materials which require no coating has drawn attention away from this method of protection.

#### AIRSHIPS

*Technical development and present situation.*—With the promise that two large rigid airships will be built in the United States the development of this type of airship has again become active in this country. A second design competition looking toward the procurement of two 6,500,000-cubic foot airships for the Navy Department was held. A contract for the building of two of these airships has been signed and the United States has taken the first steps to resume its one-time position with the leaders in this field.

Experimental investigation and research on the development of improved materials and methods of construction for the new airships have continued. Further methods for the protection of duralumin against corrosion have been developed. A substitute for goldbeater's-skin fabric has been tested in service in the form of a cell in the *Los Angeles*. The results are satisfactory although not perfect. However, succeeding cells will probably be much superior.

In connection with the research on the corrosion of duralumin a large number of samples of girders taken from the *Shenandoah*, either as test members or from the wreckage, have been under observation to determine the rate of progress of corrosion. Recent tests on this material, now more than five years old, have revealed the surprising fact that the strength of the material has remained practically unchanged since the time when the airship was wrecked.

*Work with the "Los Angeles".*—The continued operation of the *Los Angeles* has demonstrated the skill which has been acquired by the personnel engaged in this work. The airship has made several notable flights, of which the one to Panama and return deserves special mention. On this flight the airship moored to a stub mast at Panama and to the *Patoka* at Guacanayabo Bay, Cuba. Both of these operations were maneuvers largely developed by the personnel connected with the operation of the airship.

In the course of the operation of the *Los Angeles* much information has been gained which has been applied in the design of the new airships for the Navy. Improvements have been made in the water-recovery system to increase its efficiency and methods of producing artificial superheat in the gas have been tried.

Work on the development of improved methods of mooring and handling has continued, and the indications are that these methods can be developed to allow a large reduction in the number of men required.

*Metal-clad airship.*—The rapid development of intercrystalline corrosion in the duralumin used for the shell plating of this airship led to the substitution of Alclad duralumin 0.010 inch thick in place of the plain duralumin 0.008 inch thick. The hull has been constructed in two sections and is ready to be joined into one. Methods for inflating using carbon dioxide to displace the original air inside the shell and then passing in helium on top of the carbon dioxide as it is drawn out have been tried experimentally with success.

*New mooring masts.*—No large mooring masts have been built in the United States during the past year. The "stub mast" has been developed to a very successful stage at the naval air station at Lakehurst, N. J. It is now common practice to "take off" directly from this mast, but a flying mooring has not yet been attempted. While the *Los Angeles* has not ridden



out any severe weather at this mast, wind shifts of sufficient force to cause the after car to move at a speed of about 5 miles per hour have been experienced.

A mobile stub mast is being erected at Lakehurst and is expected to still further improve the methods of handling airships on the ground.

*Helium.*—An additional helium tank car using a number of smaller cylinders has been obtained by the Navy Department. The helium storage at Lakehurst has been increased by about 2,500,000 cubic feet by permanently manifolding about 14,000 small cylinders. This use of semiobsolete material has provided an urgently needed increase in storage capacity at a relatively low cost.

Arrangements have been made for the development of a large field of helium-bearing gas near Amarillo, Tex. Pipe lines and a helium production plant are being constructed. It is hoped to demonstrate by this operation what can be done in the way of conservation when practically a whole field is controlled.

The privately owned helium plant is finding no difficulty in disposing of the production beyond that taken by the Government. It has fixed a price for this gas which is only about three times that of hydrogen.

*Progress in Great Britain.*—The completion of the two large airships building in Great Britain has been delayed and they are not expected to be ready for flight until 1929. Preparations for mooring and handling them on their route to the East are practically complete.

*Progress in Germany.*—The rigid airship which was under construction in Germany was given the appropriate name of *Graf Zeppelin*. Her recent trip to the United States and return has given renewed impetus to the proposals to apply rigid airships to transoceanic transportation. The voyage was notable for the illustration it gave of the possibility of effecting repairs on an airship while in flight.

This airship is the largest which can be built in the sheds at Friedrichshafen. It is reported that Doctor Eckener believes that larger airships must be used if trans-Atlantic traffic by airship is to be successful. Either larger sheds must be built at Friedrichshafen or any such larger airships must be built elsewhere.

*Progress in Spain.*—For some time it has been reported that the Spanish Government desired to see an airship line to South America. A company was formed for this purpose and it is now reported that sheds for the construction and docking of the airships of the proposed line are building near Seville.

#### AIRCRAFT ENGINES

The most notable event in connection with the development of aircraft engines during the past year was undoubtedly the first successful use in repeated flights of an engine using fuel injection and burning heavy oil instead of gasoline. This engine was constructed by the Packard Motor Car Co. It is an air-cooled static radial engine of about 200 horsepower and is reported to weigh about 3 pounds per horsepower.

Aside from the Packard fuel-injection engine no radical developments in the form of unconventional engines have appeared. Air-cooled engines which are suitable for use in military aircraft and which have proved their value, are now available in sizes of 200, 300, 425, 500, and 600 horsepower. The demands for increased performance have led to the provision of higher powers, while the refusal of the military services to accept anything which did not have a maximum of reliability has resulted in the development of remarkable stamina without sacrifice of lightness.

The conspicuous success of the air-cooled radial engine has led many manufacturers to attempt the production of medium-powered engines of that type for commercial use. Although they were faced with new design requirements and in some cases the necessity for long periods of development work in order to produce a conspicuous success was not appreciated, several engines have been produced which have passed the requirements for an approved-type certificate of the Department of Commerce.

The search for a relatively inexpensive substitute for the cheap engines which were available from the war-time stock of engines, which is now nearly exhausted, has led to the rebuilding and adaptation of types which in their original form were not suited for commercial use. The



conversion of a water-cooled in-line engine into an air-cooled one or of a rotary radial into a static radial involves serious problems of design and construction, which may be even greater than those involved in a new design. It is not surprising that suitable engines of this character have not appeared in this country.

Operators of aircraft which must keep to fixed schedules, either on mail lines or passenger and mail lines, are fitting engines of higher power than would have been considered necessary a few years ago. The demand that an airplane shall keep to a schedule makes necessary a reserve of power, with its possible additional speed. As a result, many of the higher powered engines originally developed for military airplanes are going into commercial service.

Commercial operators of regular services are also beginning to use fuels of higher qualities, in some cases even superior to the fuels ordinarily used in the military services. This is a further example of how experience in operation leads to and enforces demands for improved measures and better materials to avoid difficulties which have been encountered.

No new types of water-cooled engines were brought out during the past year. Development and improvement in the existing engines have continued. By resorting to higher rotative speeds, higher compressions, and the use of reduction gears, the water-cooled engines have been brought to nearly the same weights per horsepower as air-cooled engines.

Air-cooled radial engines intended for use in both military and commercial aircraft are being developed with reduction gears. The use of reduction gears promises to become general in large multi-engined airplanes, especially in flying boats. These require high propeller thrusts in taking off but can afterward fly at greatly reduced power.

The tendency toward improved aerodynamic form and reduction of parasite resistance in airplanes will probably be strengthened by the results of recent work by the committee on the cowling and cooling of radial air-cooled engines. By the application of one form of cowling a notable increase in performance at the same power has been obtained.

#### SUMMARY

The year 1928 marked the twenty-fifth anniversary of the first successful flight of an airplane, namely, that made by Orville Wright at Kitty Hawk, N. C., December 17, 1903, in a machine designed and built by Wilbur Wright and Orville Wright. The Government of the United States is formally commemorating this twenty-fifth anniversary of the triumph of the Wright brothers by inviting the nations of the world to attend an international civil aeronautics conference in the city of Washington. On the twenty-fifth anniversary of the first flight there will be a pilgrimage of the delegates and guests of the conference to the scene of the early experiments and of the first flight of the Wright brothers at Kitty Hawk. On this occasion the cornerstone of the national memorial authorized by act of Congress will be laid on the top of Kill Devil Hill, which for four years was used by the Wright brothers in their early flying experiments. On the same occasion there will be unveiled a memorial erected by the National Aeronautic Association to mark the spot near Kill Devil Hill from which the first successful flight of an airplane was made.

Among the demonstrated evidences of the notable progress made during the year 1928 may be mentioned the following: The inauguration in the United States of regular air transport passenger services; the entrance of express companies into the field of aerial express service; the announcement of plans by the Pennsylvania and Santa Fe railroads for a combined air and rail passenger service between the east and west coasts of the United States; an increase of over 100 per cent in the production of airplanes for private ownership and operation; the extension of national airways by the Department of Commerce; the extension of the air mail service; the reduction of air mail postage rates by more than 50 per cent; and the general noticeable improvement in the performance, efficiency, and safety of airplanes. All of these have combined to enable aeronautics to assume an increasingly important rôle in the economic life of the Nation.

The development of the civil and commercial uses of airplanes in the United States has been without the direct subsidies that have characterized European developments, but the Federal Government has nevertheless contributed materially to the development of American aeronautics. The 5-year aircraft building programs of the Army and Navy have served to stabilize the



industry. The effective administration of the air commerce act by the Department of Commerce, particularly in the regulation and licensing of aircraft and airmen and in the establishment of lighted airways, including the furnishing of meteorological information by the Weather Bureau, have been important factors. The coordination and prosecution of scientific research on the fundamental problems of flight by the National Advisory Committee for Aeronautics have led to material improvement in the safety and efficiency of airplanes.

The latest important contribution from the committee's laboratories at Langley Field, Va., resulted from a study in the propeller research tunnel of drag and cooling with various forms of cowling for an air-cooled radial engine in a cabin fuselage. By the application of the results of this study to a Curtiss AT-5A Army pursuit training airplane, the maximum speed was increased from 118 to 137 miles per hour. This is equivalent to providing approximately 83 additional horsepower without additional weight or cost of engine, fuel consumption, or weight of structure. This single contribution will repay the cost of the propeller research tunnel many times and fully justifies the committee, not only in having built such a tunnel, but also in recommending as it does that additional funds be provided next year for the construction of a full-scale wind tunnel. Never before in the committee's history or in the history of the development of aeronautics has the value of a new piece of scientific equipment been so well demonstrated.

The development of aviation in America during the past year has been amazing, and emphasizes the necessity for the continued study on a large scale of the basic problems of increase in safety and reduction in cost of construction, maintenance, and operation of aircraft. The research programs of the committee have been enlarged during the past year to serve the increasing needs of a growing industry. Three important new subcommittees have been established—namely, committee on problems of air navigation, committee on aircraft accidents, and committee on aeronautical research in universities. All of the committee's activities are conducted in cooperation with existing agencies, public and private, to the end that the maximum return may be obtained from their use without duplication of effort or loss of time.

The greatest stimulation to the development of aeronautics will come from the education of the public by the private use of airplanes and by the safe operation of commercial air lines. These will come with the solution of the serious and difficult problems of navigating and landing in fog. The development of instruments which will indicate the true position of the aircraft when flying without the assistance of ground vision, and the development of adequate communication systems, are problems now pressing for solution in order that air transport services may be operated with assurance of safety and reliability.

The National Advisory Committee for Aeronautics, as the coordinating agency of the Federal Government for the scientific study of fundamental problems in aeronautics, endeavors to maintain a broad view and wide contact over the whole field of aeronautics without losing sight of the immediate problems of the governmental services. The committee is actively prosecuting investigations which will promote the safety and efficiency of military and civil aircraft. Continuous progress can be assured only by continuous research and experimentation.

#### CONCLUSION

The manner in which aeronautical progress in the United States has exceeded expectations has been most gratifying. This progress has derived its inspiration and support from many sources. In the main, it is the cumulative result of years of study, research, and experimentation, and the direct relation between notable developments and the preceding scientific studies is clear. Further substantial progress may be expected from the continued prosecution of scientific research. Accordingly, the committee recommends the continuance of the liberal support which has in the past been accorded its work in the fields of pure and applied research on the fundamental problems of flight.

Respectfully submitted.

NATIONAL ADVISORY COMMITTEE FOR AERONAUTICS,  
JOSEPH S. AMES, *Chairman*.



---

---

**REPORT No. 283**

---

**A PRELIMINARY INVESTIGATION  
OF SUPERCHARGING AN AIR-COOLED ENGINE  
IN FLIGHT**

**By MARSDEN WARE and OSCAR W. SCHEY  
Langley Memorial Aeronautical Laboratory**







## REPORT No. 283

---

### A PRELIMINARY INVESTIGATION OF SUPERCHARGING AN AIR-COOLED ENGINE IN FLIGHT

By MARSDEN WARE and OSCAR W. SCHEY

---

#### SUMMARY

*This report presents the results of tests made by the National Advisory Committee for Aeronautics in a preliminary investigation of the effects of supercharging an air-cooled engine under airplane flight conditions.*

*This investigation comprises the first of its kind that has been conducted and for which results have been published.*

*Service training airplanes were used in the investigation equipped with production types of Wright J engines. An N. A. C. A. Roots type supercharger was driven from the rear of the engine.*

*In addition to measuring those quantities that would enable the determination of the climb performance, measurements were made of the cylinder-head temperatures and the carburetor pressures and temperatures. The supercharging equipment was not removed from the airplane when making flights without supercharging, but a by-pass valve, which controlled the amount of supercharging by returning to the atmosphere the surplus air delivered by the supercharger, was left full open.*

*With the supercharger so geared that ground-level pressure could be maintained to 18,500 feet, it was found that the absolute ceiling was increased from 19,400 to 32,600 feet, that the time to climb to 16,000 feet was decreased from 32 to 16 minutes, and that this amount of supercharging apparently did not injure the engine.*

#### INTRODUCTION

The air-cooled engine has reached such a stage of development in recent years that investigation of its application to all kinds of service conditions becomes of great interest. In this respect, the investigation of the effects of supercharging air-cooled engines is of considerable importance.

While supercharging consists merely of the delivery to the engine of an air-fuel charge of greater density than it could induce normally, its influence upon the engine depends on the nature of the application. For instance, the application may require that an engine be supercharged at ground level in order to increase the power per unit volume of displacement. On the other hand, the amount of supercharging may be zero at ground level and may be increased in amount as the altitude of operation is increased for the purpose of compensating for the decrease in power due to the reduction in density of the atmosphere. In the former case, supercharging causes an increase in both heat and mechanical stresses, while in the latter, the mechanical problems are comparatively inconsequential. Aircraft engine supercharging is concerned primarily with the latter case, especially when any considerable amount of supercharging is involved. It is this phase of supercharging that will be considered in this report.

In the case of water-cooled engines the alteration of cooling conditions can be readily provided for by changing the amount of radiation. Regulation of the cooling as operating conditions require may be made in a given installation by means of shutters.



Obviously this same condition does not apply to the present day air-cooled engine, where the amount of the cooling surface is fixed by the design of the engine and control of the amount of air passing over the surface in the usual installation is not as simple as in the water-cooled engine. If the air-cooled engine were to be designed with sufficient cooling surface to meet the extremes of cooling requirements encountered and with provision for controlling the amount of air passing over the surface, the problems of the two types of engines would be practically the same. At present, however, the problem of supercharging an air-cooled engine is not as simple as that of supercharging a water-cooled, and depends primarily on the cylinder design.

The purpose of the work reported herein was to make a preliminary investigation of the general problem of supercharging an air-cooled engine, using an engine that had proven successful in service under conditions of normal operation. The work was done at Langley Field, Va., by the staff of the National Advisory Committee for Aeronautics.

#### DESCRIPTION OF APPARATUS

Standard service airplanes and engines were used in this work. Two airplanes of the training type were used: The first was a single-seater (Navy symbol—TS); the second was a two-seater of more refined design (Navy symbol—UO-1), which is shown in Figure 1. The engines were production types of the Wright J series. Details of construction for this series of

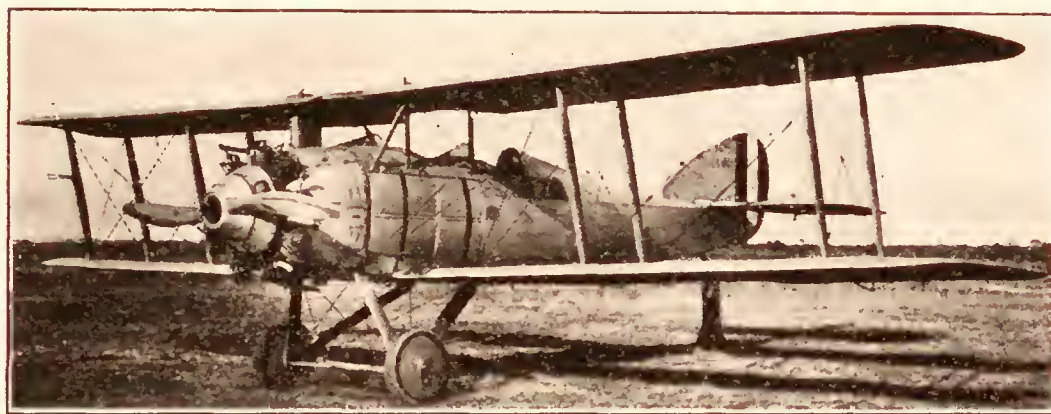


FIG. 1.—UO-1 airplane with Wright J-4 engine and experimental installation of N. A. C. A. Roots type supercharger

engines are given in a paper entitled "The Development of the Wright Whirlwind Type J-5 Aircraft Engine," by E. T. Jones. (Reference 1.)

An N. A. C. A. Roots type supercharger was installed at the rear of the engine and was connected directly to the end of the engine crank shaft. The supercharger was essentially the same as described in Technical Report No. 230. (Reference 2.)

Since this supercharger was designed for use with the Liberty engine, which has a displacement of 1,649 cubic inches, while the displacement of the Wright J engine is only 787 cubic inches, this supercharger is considerably oversize for the latter engine. For most of the tests the capacity of the supercharger was reduced so that ground-level pressure could be maintained to about 18,000 feet by driving the supercharger impellers at crank-shaft speed.

A large size duct of streamline form was provided on the intake side of the supercharger. This duct extended well above the fuselage to minimize the induction of hot air from the engine cylinder. The discharge side of the supercharger was connected directly to the engine carburetor by a pipe 5 inches in diameter, in a branch of which was located a valve for the control of the amount of supercharging. The control was effected by returning excess air to the atmosphere. The branch pipe carrying the control or by-pass valve may be seen in Figure 1 extending a short distance below the bottom of the fuselage.

When the work was started with the TS airplane, a receiver having a volume of 1.8 cubic feet was inserted in the air duct between the supercharger and the carburetor to dampen the pulsating pressure created by the supercharger and thus to prevent impairment of engine performance. Since later tests with a direct connection gave equal engine performance, no receiver was used for work herein reported.

In the usual engine installation, the fuel pressure is maintained somewhat in excess of the atmospheric pressure. Fuel would not flow into the carburetor if the system were tried in the supercharged engine installation with the carburetor located between the supercharger and the engine, due to the fact that the carburetor air pressure is considerably greater than the atmospheric pressure. Modifications were made to the fuel system to maintain the fuel pressure



a definite amount above the carburetor pressure and automatically dependent on the amount of supercharging pressure, in the same manner as made in previous work at this laboratory with water-cooled engines as described in Technical Report No. 263. (Reference 3.)

Cylinder-head temperatures were measured by iron-constantan thermocouples and an indicating pyrometer. The couples were inserted in each cylinder at a point immediately in the rear of the spark plug located on the top and near the front of each cylinder, as may be seen in Figure 2. The pyrometer and instruments for measuring the carburetor air temperature, the free air temperature, the carburetor air pressure, and the engine speed were installed in a light-tight box and pictures of the instrument dials were taken automatically at regular intervals with a small motor-driven camera using moving-picture film. Since space permitted the use of only one pyrometer for the cylinder temperatures, and the temperatures of all nine cylinders were desired, the various thermocouples were connected consecutively to the pyrometer by means of a motor-driven switch.

The diameter of the propeller was 8 feet 9 inches and the pitch was 6 feet 2.3 inches. The weight of the airplane ready to fly was 1,980 pounds.

### TEST RESULTS

Due to the preliminary nature of this investigation the work was confined primarily to the determination of the performance with and without supercharging. Cylinder-head temperatures were measured in all flights as an indication of the thermal stress created by supercharging. In addition, measurements were made of flight performance as given in Tables I to VI.

Figures 3, 4, and 5 show the results obtained with the UO-1 airplane in those tests where the supercharger impeller speed was equal to the engine crankshaft speed. These results are plotted from average data obtained in three supercharged and three unsupercharged flights. The fuel was a 30-70 blend of benzol and aviation gasoline.

Some work was done with the supercharger impellers operating at 1.5 times crankshaft speed. This change permitted ground-level pressure to be maintained to much higher altitudes, at which considerable trouble was experienced from detonation. This work was therefore discontinued.

The equipment was not changed in making the flights without supercharging, but the supercharger by-pass valve was kept full open. The power required to drive the supercharger under the condition of free inlet and discharge resulting from this method of operation is less than 5 HP., so that the power of the engine was essentially the same as that of the normal engine. Since the same propeller was used for all tests, higher engine speeds were obtained when supercharging.

A series of climbs to an altitude of 15,000 feet was made with the TS airplane and with some variation in the amounts of supercharging. While some differences in performance and temperature were noted, they were not definite enough to show the influence of the different amounts of supercharging. The work demonstrated, however, that little trouble would be encountered in maintaining full supercharging to moderate altitudes. In continuing with the work on the UO-1 airplane, practically all flights were made with the carburetor pressure maintained at approximately 29 inches of mercury.

A comparison was made of the effect of oil cooling with the TS airplane by making comparative flights with and without an oil radiator. At 20,000 feet the cylinder temperature was 505° F. with the oil radiator and 550° F. without the radiator. While these data are hardly

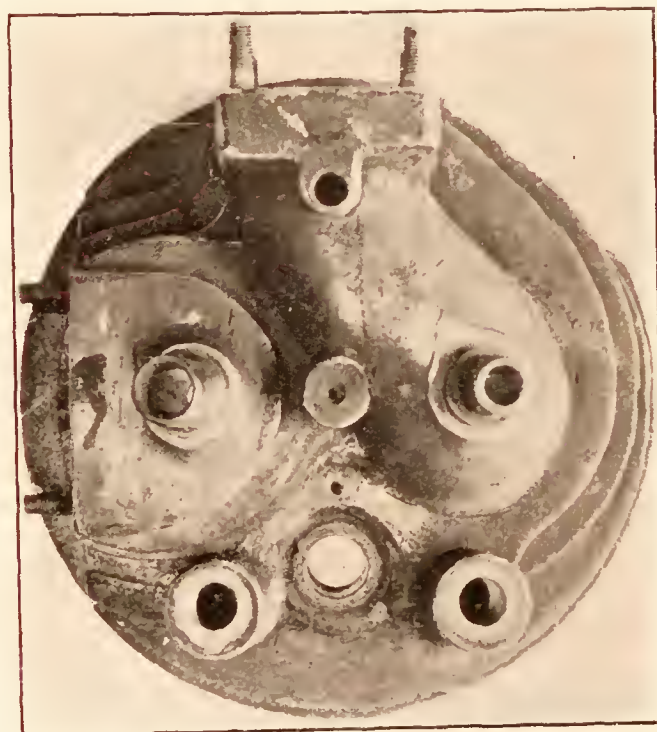


FIG. 2.—Top view of cylinder head, showing location of hole for thermocouple plug between spark plug and center of cylinder



sufficient to justify making a definite conclusion, they indicate that the lubricating oil has an appreciable effect on cooling and it may be an important consideration in the application of supercharging an air-cooled engine when the cylinder temperature approaches a dangerous limit.

### DISCUSSION OF RESULTS

Figures 3, 4, and 5 show that a material improvement in performance is obtained as the result of supercharging; the absolute ceiling is increased from 19,400 to 32,600 feet, and the time required to climb to 16,000 feet is reduced from 32 to 16 minutes. The supercharged engine performances were obtained without any impairment of the engine structure, and it seemed evident from the experiences of the entire work that the engine could endure satisfactorily this amount of supercharging.

While it would be necessary to have temperature measurements of other parts of the cylinder to form any very satisfactory conclusions of the effect of supercharging on the heat flow through

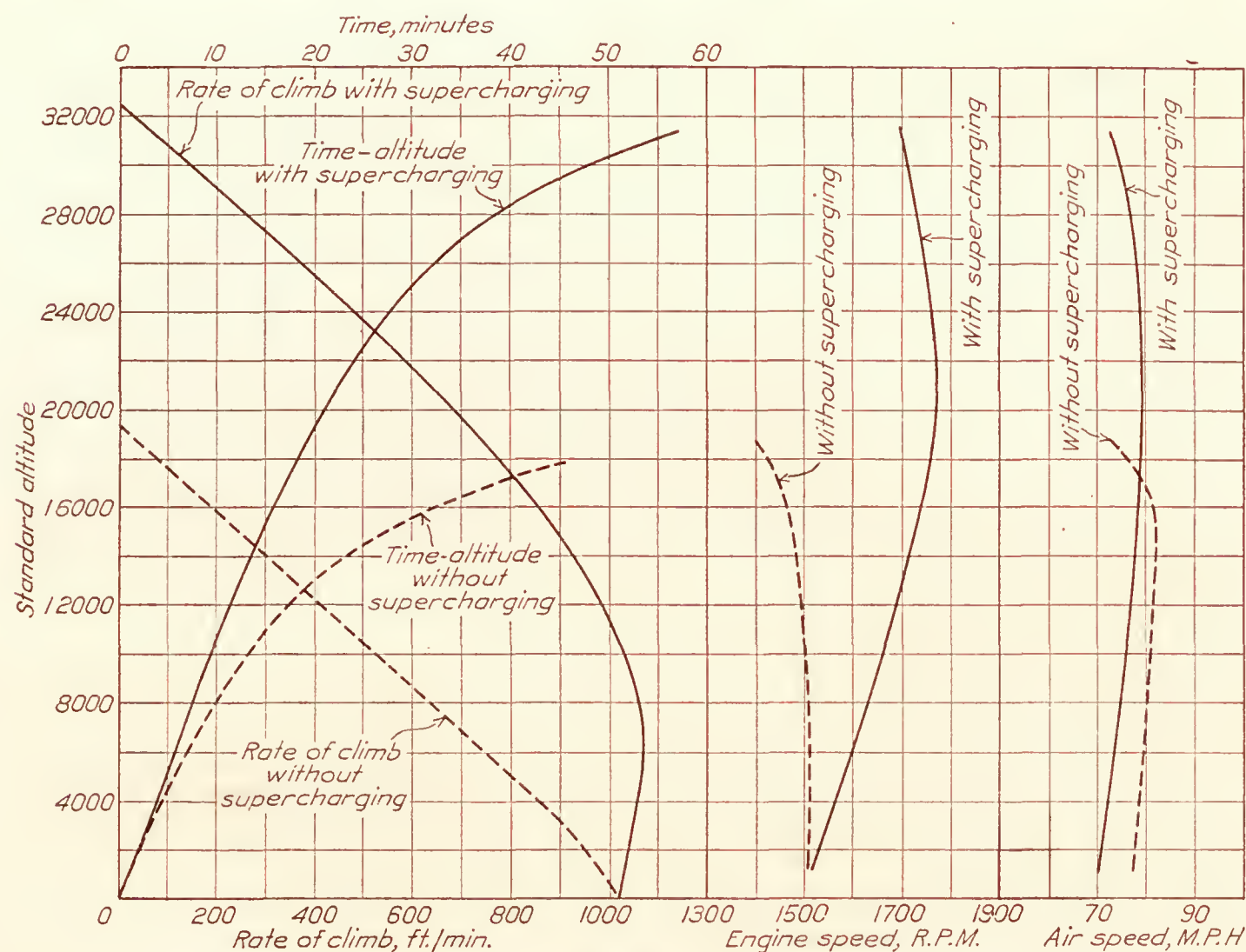


FIG. 3.—UO-1 performance with and without supercharging

the cylinder, these tests indicate the temperature increase that may be expected to result from supercharging. According to the maximum permissible temperature of  $550^{\circ}\text{F}$ . for satisfactory operation given by Heron (Reference 4), the temperatures recorded under the supercharged condition can not be said to be excessive. Although no maximum permissible operating temperature has been published for this engine, its excellent performance may be taken as an indication that this temperature approaches that set by Heron. It is of interest to note that the maximum cylinder temperature is reached at an altitude slightly above that at which the carburetor pressure begins to drop or the altitude where the increase in engine power resulting from supercharging is a maximum.

There are a number of important specific problems entering into the question of supercharging that were left for further investigation. Among these, the influence of air-fuel ratio is one of the most important. Heron (Reference 4) has shown the relation between cylinder



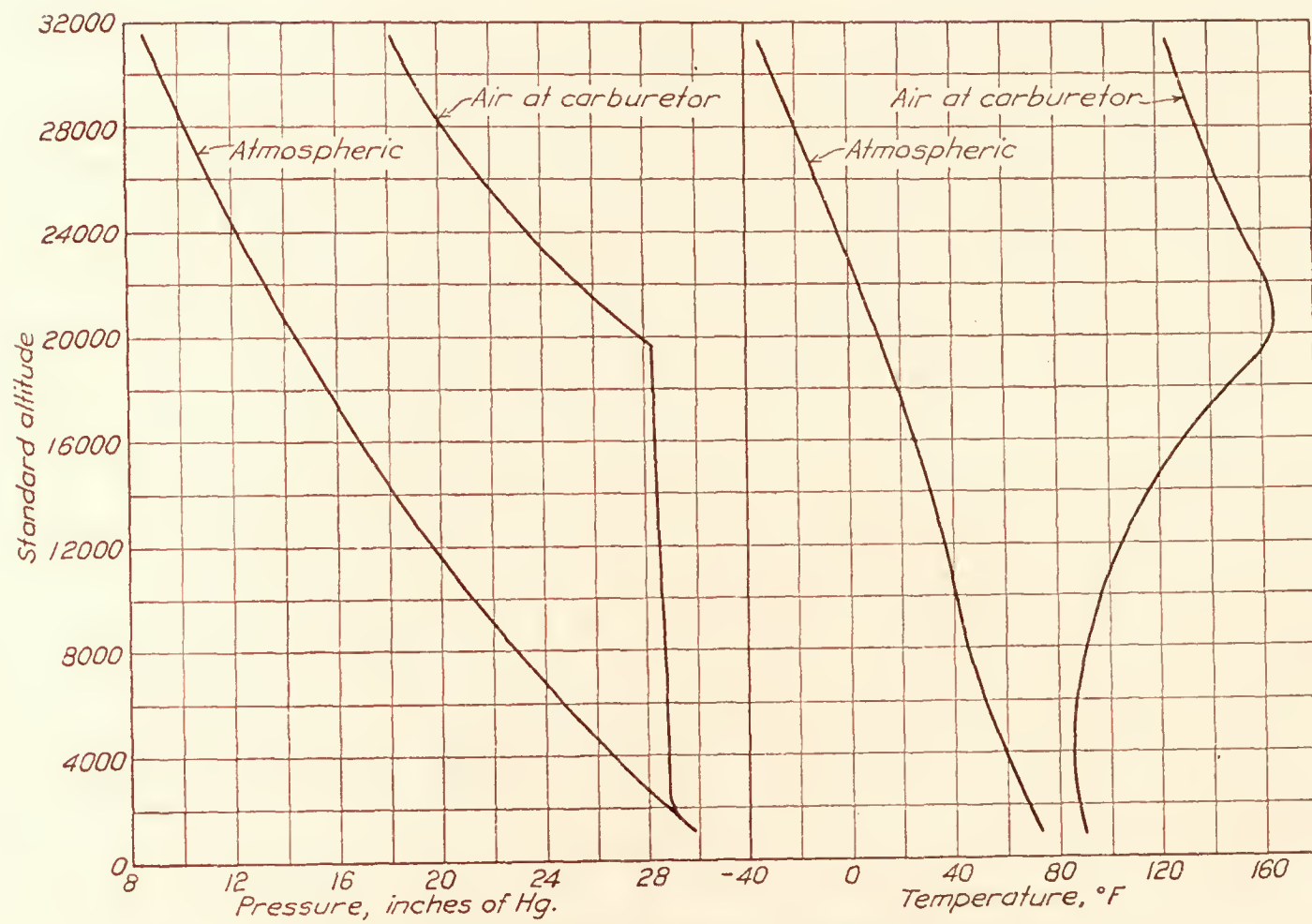


FIG. 4.—Effect of supercharging on carburetor air temperature and pressure

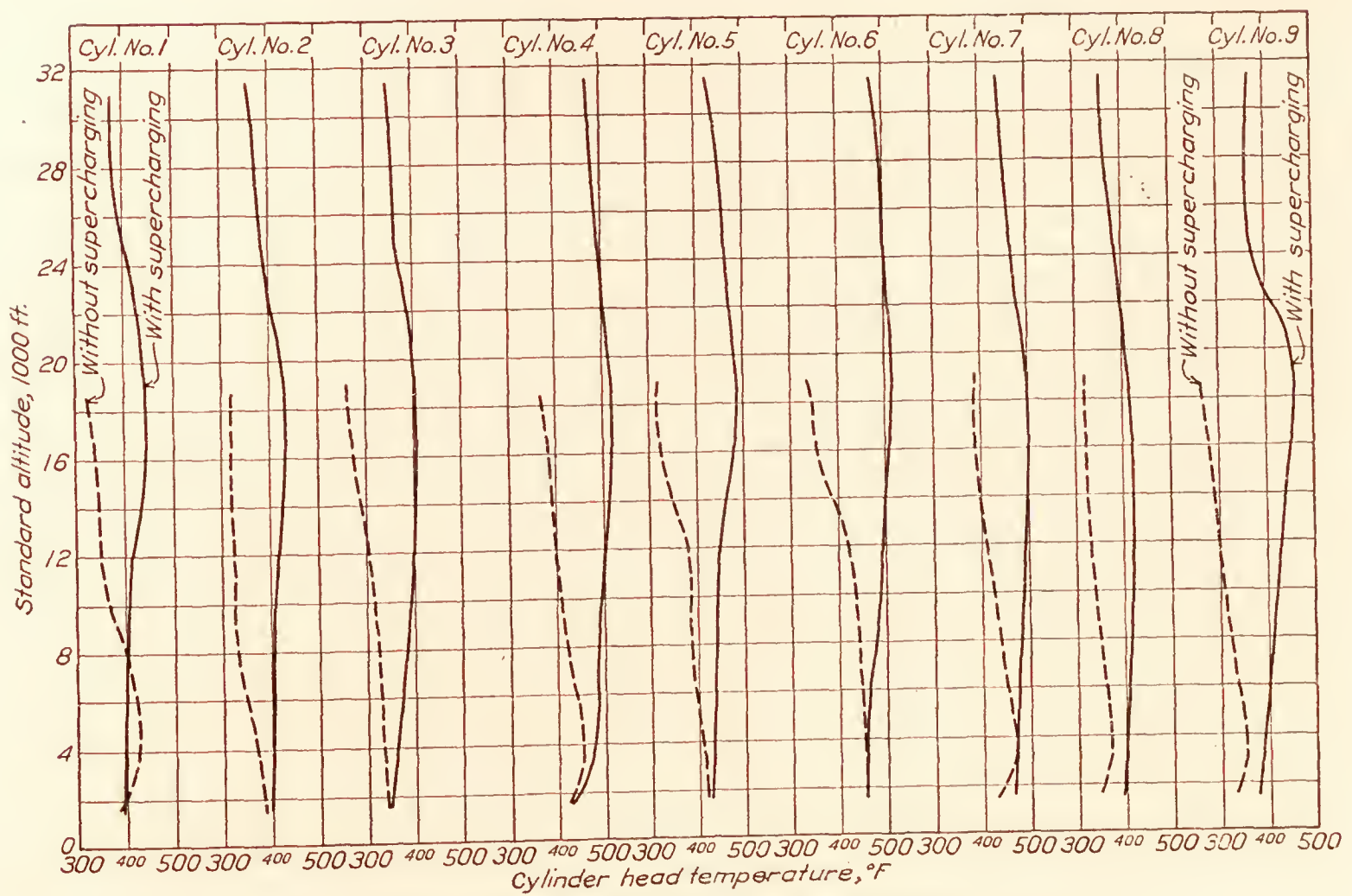


FIG. 5.—Effect of supercharging on cylinder-head temperatures



temperature and air-fuel ratio. A portion of the data given in the reference is reproduced in Figure 6. As no reliable fuel flow meter was available at the time these tests were made, it was impossible to determine the air-fuel ratios. In order to obtain a rough estimate of the influence of mixture ratio in this work, a computation of the probable ratios based on carburetor characteristics was made. Similar computations made in connection with some later work with a supercharged water-cooled engine and after a suitable flow meter had been developed showed that the method probably would give a fair estimate of the order of the change in ratio. This computation indicated that the charge was enriched quite appreciably as the altitude was increased, and there is little doubt that the maximum temperatures shown are somewhat lower than they would be if the charge was not enriched. The cylinder temperatures were probably lower at high altitudes in the unsupercharged flights, due also to some enrichment of

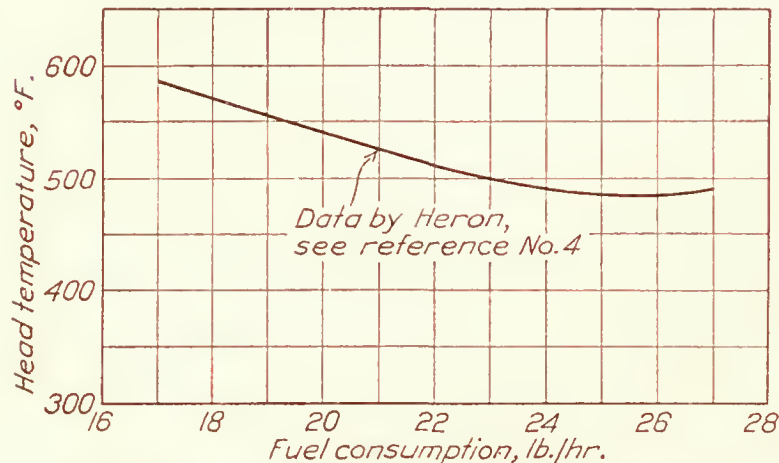


FIG. 6.—Effect of fuel consumption on cylinder-head temperatures

the mixture, but in this case the enrichment serves no useful purpose, in that the temperatures are already well below the maximum which occurred at ground level.

### CONCLUSIONS

The work reported herein has shown the possibility of obtaining a material improvement in airplane performance by supercharging a modern air-cooled engine. The absolute ceiling was raised from 19,400 to 32,600 feet, and the time of climb to 16,000 feet was reduced from 32 to 16 minutes. While no limit of supercharging was established, it is evident that ground-level pressure may be maintained up to an altitude of 18,500 feet without imposing excessive stresses upon the engine.

LANGLEY MEMORIAL AERONAUTICAL LABORATORY,  
NATIONAL ADVISORY COMMITTEE FOR AERONAUTICS,  
LANGLEY FIELD, VA., July 30, 1927.

### REFERENCES AND BIBLIOGRAPHY

1. JONES, E. T. The Development of the Wright Whirlwind Type J-5 Aircraft Engine. *Journal of the Society of Automotive Engineers*, 1926, XIX, 303-308.
2. WARE, MARSDEN. Description and Laboratory Tests of a Roots Type Aircraft Engine Supercharger. N. A. C. A. Technical Report No. 230, 1926.
3. GARDINER, ARTHUR W., and REID, E. G. Preliminary Flight Tests of the N. A. C. A. Roots Type Aircraft Engine Supercharger. N. A. C. A. Technical Report No. 263, 1927.
4. HERON, S. D. Air-cooled Cylinder Design and Development. *Transactions of the Society of Automotive Engineers*, 1922, XVII, Part 1, 347-430.
5. LANCHESTER, F. W. The Cylinder Cooling of Internal Combustion Engines. *Proceedings of The Institution of Automobile Engineers*, 1915-16, X, 59-158.



TABLE I.—*Flight data for UO-1 airplane (supercharged)*

Standard altitude (feet)	Time (minutes)	Engine speed (R. P. M.)	Air speed (M. P. H.)	Atmospheric pressure (in. Hg.)	Carburetor pressure (in. Hg.)	Atmospheric temperature (°F.)	Carburetor temperature (°F.)
700	0. 64	1, 600	73	30. 35	30. 40	77	97
2, 650	2. 42	1, 555	71	28. 25	28. 95	69	90
4, 300	4. 18	1, 572	73	26. 65	28. 45	65	86
6, 000	5. 90	1, 605	74	24. 95	28. 30	59	93
7, 700	7. 65	1, 635	75	23. 35	28. 95	51	95
9, 250	9. 41	1, 625	76	21. 98	28. 00	45	98
10, 900	11. 18	1, 690	79	20. 60	28. 60	39	102
12, 900	13. 29	1, 710	80	19. 27	28. 40	37	115
14, 800	15. 21	1, 720	81	17. 97	28. 35	33	126
16, 650	17. 16	1, 730	81	16. 80	28. 25	30	137
18, 100	18. 76	1, 760	81	15. 74	27. 95	21	148
19, 800	20. 64	1, 775	83	14. 75	27. 95	17	163
21, 350	22. 59	1, 760	82	13. 90	26. 60	14	165
22, 600	24. 44	1, 760	82	13. 22	25. 20	9	163
23, 550	26. 03	1, 730	81	12. 64	24. 10	5	157
24, 250	27. 52	1, 725	79	12. 20	23. 20	0	151
24, 950	28. 94	1, 725	82	11. 75	22. 45	-5	145
25, 650	30. 73	1, 722	81	11. 40	21. 70	-8	140
26, 200	32. 32	1, 705	80	11. 10	21. 10	-11	134
26, 600	33. 70	1, 700	78	10. 85	20. 65	-15	130
27, 000	35. 39	1, 677	72	10. 65	20. 30	-16	126
27, 350	36. 85	1, 670	72	10. 45	19. 90	-19	124
27, 650	38. 49	1, 665	72	10. 30	19. 60	-20	122
28, 100	40. 93	1, 685	74	10. 15	19. 50	-20	122
28, 550	43. 33	-----	73	10. 00	-----	-20	95

TABLE II.—*Flight data for UO-1 airplane (supercharged)*

Standard altitude (feet)	Time (minutes)	Engine speed (R. P. M.)	Air speed (M. P. H.)	Atmospheric pressure (in. Hg.)	Carburetor pressure (in. Hg.)	Atmospheric temperature (°F.)	Carburetor temperature (°F.)
400	0. 53	-----	-----	30. 65	-----	78	90
550	. 72	1, 480	70	30. 35	30. 65	74	90
2, 150	2. 30	1, 510	70	28. 38	28. 60	64	86
3, 900	4. 20	1, 570	73	26. 70	28. 73	60	86
5, 650	5. 95	1, 600	73	24. 95	28. 73	53	88
7, 600	7. 89	1, 600	74	23. 30	28. 60	48	90
9, 200	9. 57	1, 640	75	21. 80	28. 73	40	91
11, 100	11. 54	1, 680	77	20. 25	28. 32	36	99
13, 000	13. 55	1, 700	75	18. 90	28. 93	33	108
14, 600	15. 23	1, 700	77	17. 80	28. 20	26	115
16, 550	17. 25	1, 720	73	16. 60	27. 93	22	126
17, 750	18. 92	1, 740	77	15. 75	28. 52	16	138
19, 300	20. 75	1, 780	83	14. 80	28. 73	11	151
20, 650	22. 68	1, 760	81	14. 05	27. 25	6	164
21, 600	24. 27	1, 760	76	13. 43	25. 86	1	160
22, 600	25. 95	1, 750	82	12. 84	24. 65	-4	151
23, 800	27. 75	1, 740	81	12. 20	23. 61	-8	147
24, 550	29. 49	1, 740	79	11. 80	22. 70	-10	142
25, 400	31. 19	1, 730	77	11. 35	22. 10	-14	138
26, 250	33. 21	1, 730	72	10. 98	21. 48	-15	138
26, 950	35. 37	1, 730	77	10. 70	21. 10	-16	138
27, 650	37. 13	1, 740	77	10. 37	20. 80	-18	138
28, 000	38. 81	1, 740	77	10. 20	20. 40	-20	136
28, 600	40. 52	1, 740	76	9. 92	20. 10	-23	135
29, 000	42. 68	1, 735	74	9. 73	19. 92	-25	135
29, 300	44. 47	1, 730	74	9. 60	19. 70	-26	133
29, 700	46. 01	1, 730	77	9. 40	19. 55	-29	133
30, 000	48. 28	1, 730	76	9. 30	19. 35	-29	131
30, 400	50. 27	1, 725	73	9. 15	19. 15	-30	131
30, 750	51. 98	1, 725	74	9. 00	18. 94	-31	127
30, 800	52. 72	1, 720	74	8. 95	18. 75	-32	126
31, 200	54. 94	1, 720	73	8. 82	18. 56	-33	126
31, 350	56. 48	1, 715	73	8. 75	18. 50	-34	126
31, 450	57. 92	1, 715	-----	8. 70	-----	-35	-----



TABLE III.—*Flight data for UO-1 airplane (supercharged)*

Standard altitude (feet)	Time (minutes)	Engine speed (R. P. M.)	Air speed (M. P. H.)	Atmospheric pressure (in. Hg.)	Carburetor pressure (in. Hg.)	Atmospheric temperature (°F.)	Carburetor temperature (°F.)
500	0. 60	-----	-----	30. 36	-----	74	-----
700	. 84	-----	71	30. 20	-----	74	-----
2, 450	2. 61	1, 545	71	28. 30	29. 00	67	88
3, 800	4. 17	1, 530	69	26. 70	28. 95	58	84
5, 400	5. 75	1, 600	71	24. 93	28. 80	49	84
7, 200	7. 59	1, 630	73	23. 30	28. 95	42	88
9, 600	9. 62	1, 630	76	21. 45	29. 20	38	93
11, 900	11. 58	1, 680	77	19. 78	28. 10	34	102
13, 900	13. 56	1, 670	80	18. 41	28. 10	31	115
15, 300	15. 34	1, 730	81	17. 40	28. 30	24	124
16, 900	17. 11	1, 750	82	16. 30	27. 95	19	137
18, 650	18. 94	1, 800	84	15. 20	28. 70	14	158
20, 050	20. 87	1, 800	88	14. 40	27. 15	9	165
21, 400	22. 68	1, 800	86	13. 62	25. 75	5	162
22, 700	24. 50	1, 770	85	12. 90	24. 40	0	158
23, 550	26. 05	1, 770	84	12. 37	23. 60	-4	157
24, 350	28. 08	1, 790	87	12. 00	23. 20	-6	157
25, 300	29. 80	1, 770	86	11. 50	22. 40	-9	157
25, 950	31. 71	1, 740	85	11. 20	21. 80	-12	149
26, 500	33. 15	1, 740	85	10. 87	21. 20	-16	146
27, 150	35. 35	1, 750	85	10. 62	20. 80	-16	146
27, 700	36. 77	1, 720	81	10. 30	20. 40	-20	145
28, 200	38. 80	1, 740	81	10. 10	20. 10	-21	141
28, 700	40. 79	1, 740	80	9. 90	19. 80	-22	138
28, 850	41. 97	1, 720	76	9. 80	19. 60	-24	136
29, 300	43. 73	1, 700	77	9. 60	19. 50	-26	134
29, 500	45. 28	-----	78	9. 50	-----	-26	130

TABLE IV.—*Flight data for UO-1 airplane (without supercharging)*

Standard altitude (feet)	Time (minutes)	Engine speed (R. P. M.)	Air speed (M. P. H.) ( <sup>1</sup> )	Atmospheric pressure (in. Hg.)	Carburetor pressure (in. Hg.)	Atmospheric temperature (°F.)	Carburetor temperature (°F.)
700	0. 75	1, 520	-----	30. 10	30. 20	70	88
1, 600	1. 72	1, 500	-----	28. 65	28. 80	61	84
3, 100	3. 67	1, 500	-----	27. 20	27. 25	56	79
4, 500	5. 50	1, 510	-----	25. 82	26. 00	52	72
5, 950	7. 65	1, 530	-----	24. 66	24. 90	51	70
7, 100	9. 42	1, 520	-----	23. 58	23. 80	46	68
8, 050	11. 09	1, 500	-----	22. 67	22. 75	41	64
9, 200	13. 15	1, 500	-----	21. 80	21. 95	39	62
10, 150	15. 05	1, 510	-----	21. 05	21. 15	37	58
10, 800	16. 72	1, 490	-----	20. 48	20. 65	35	55
11, 450	18. 66	1, 500	-----	20. 00	20. 00	33	54
12, 200	20. 51	1, 480	-----	19. 43	19. 55	30	52
12, 850	22. 58	1, 490	-----	19. 00	19. 15	28	50
13, 200	23. 94	1, 480	-----	18. 65	18. 75	25	48
13, 700	25. 60	1, 470	-----	18. 25	18. 40	23	46
14, 000	26. 92	1, 470	-----	17. 95	18. 05	20	45
14, 450	28. 59	1, 460	-----	17. 60	17. 60	17	42
14, 700	29. 87	1, 470	-----	17. 35	17. 50	14	42
15, 000	32. 12	1, 460	-----	17. 18	17. 25	14	42
15, 500	34. 36	1, 460	-----	16. 90	16. 95	14	42
15, 900	36. 61	1, 450	-----	16. 68	16. 80	14	41
16, 100	37. 97	1, 450	-----	16. 50	16. 65	13	40
16, 450	41. 51	1, 450	-----	16. 38	16. 55	13	39
16, 600	42. 52	1, 430	-----	16. 20	16. 30	12	38
16, 600	42. 52	1, 430	-----	16. 20	16. 25	12	37
17, 000	46. 51	1, 410	-----	16. 08	16. 20	13	37
17, 100	47. 98	1, 390	-----	16. 00	16. 20	13	40

<sup>1</sup> No air speed because of failure of recording instrument.



TABLE V.—Flight data for UO-1 airplane (without supercharging)

Standard altitude (feet)	Time (minutes)	Engine speed (R. P. M.)	Air speed (M. P. H.)	Atmospheric pressure (in. Hg.)	Carburetor pressure (in. Hg.)	Atmospheric temperature (°F.)	Carburetor temperature (°F.)
500	0. 57	1, 500	84	30. 20	-----	71	-----
2, 100	2. 40	1, 500	83	28. 50	28. 70	65	88
3, 750	4. 31	1, 500	84	26. 90	27. 25	61	84
5, 200	6. 11	1, 520	83	25. 48	25. 95	56	80
6, 500	7. 90	1, 520	84	24. 25	24. 75	51	73
7, 750	9. 67	1, 500	85	23. 10	23. 60	45	68
8, 800	11. 47	1, 480	87	22. 18	22. 70	41	62
9, 950	13. 25	1, 500	89	21. 20	21. 90	38	60
10, 800	14. 91	1, 470	87	20. 45	21. 10	34	55
11, 700	16. 83	1, 480	87	19. 78	20. 50	32	52
12, 400	18. 66	1, 460	87	19. 25	19. 90	29	50
13, 200	20. 72	1, 470	87	18. 72	19. 35	28	50
13, 750	22. 69	1, 460	87	18. 35	18. 90	27	50
14, 350	24. 69	1, 480	88	17. 95	18. 55	25	50
14, 950	26. 84	1, 490	90	17. 60	18. 30	24	48
15, 300	28. 22	1, 470	89	17. 28	18. 00	22	46
15, 650	30. 65	1, 470	88	17. 10	17. 70	22	43
16, 000	32. 18	1, 460	88	16. 82	17. 50	20	42

TABLE VI.—Flight data for UO-1 airplane (without supercharging)

Standard altitude (feet)	Time (minutes)	Engine speed (R. P. M.)	Air speed (M. P. H.)	Atmospheric pressure (in. Hg.)	Carburetor pressure (in. Hg.)	Atmospheric temperature (°F.)	Carburetor temperature (°F.)
500	0. 42	-----	-----	30. 40	-----	75	90
2, 300	1. 92	1, 560	78	28. 30	28. 50	65	88
4, 050	3. 71	1, 540	78	26. 50	26. 90	58	81
5, 700	5. 62	1, 530	79	25. 00	25. 50	55	73
7, 250	7. 59	1, 530	79	23. 70	24. 20	51	70
8, 400	9. 17	1, 530	79	22. 50	23. 10	43	63
9, 700	11. 31	1, 520	80	21. 57	22. 40	44	63
10, 950	13. 43	1, 520	81	20. 70	21. 33	42	59
11, 850	15. 50	1, 510	81	20. 08	20. 65	40	59
12, 600	17. 28	1, 500	81	19. 50	20. 05	39	57
13, 350	19. 12	1, 500	82	18. 95	19. 60	35	55
14, 000	20. 87	1, 500	82	18. 46	19. 13	33	54
14, 550	22. 61	1, 500	82	18. 05	18. 68	31	52
15, 250	24. 59	1, 490	83	17. 60	18. 38	30	52
15, 950	26. 76	1, 480	82	17. 20	17. 92	29	52
16, 300	28. 19	1, 470	80	16. 90	17. 57	26	48
16, 600	29. 64	1, 470	80	16. 65	17. 30	25	46
16, 800	31. 24	1, 470	79	16. 50	17. 18	23	46
17, 100	33. 02	1, 460	77	16. 30	16. 96	22	45
17, 350	34. 48	1, 440	76	16. 10	16. 72	20	43
17, 700	36. 56	1, 440	75	15. 90	16. 53	20	43
17, 950	38. 48	1, 450	78	15. 75	16. 40	20	43
18, 050	39. 63	1, 440	77	15. 65	16. 30	18	39
18, 350	41. 91	1, 430	76	15. 50	16. 18	18	39
18, 500	44. 03	1, 420	74	15. 42	16. 10	18	39
18, 650	45. 43	1, 410	72	15. 30	16. 00	16	39







---

**REPORT No. 284**

---

**THE COMPARATIVE PERFORMANCE  
OF ROOTS TYPE AIRCRAFT ENGINE SUPERCHARGERS  
AS AFFECTED BY CHANGE IN IMPELLER SPEED  
AND DISPLACEMENT**

**By MARSDEN WARE and ERNEST E. WILSON  
Langley Memorial Aeronautical Laboratory**







## REPORT No. 284

### THE COMPARATIVE PERFORMANCE OF ROOTS TYPE AIRCRAFT ENGINE SUPERCHARGERS AS AFFECTED BY CHANGE IN IMPELLER SPEED AND DISPLACEMENT

By MARSDEN WARE and ERNEST E. WILSON

#### SUMMARY

This report presents the results of tests made by the National Advisory Committee for Aeronautics on three sizes of Roots type aircraft engine superchargers. The impeller contours and diameters of these machines were the same, but the lengths were 11, 8¼, and 4 inches, giving displacements of 0.509, 0.382, and 0.185 cubic foot per impeller revolution. The information obtained serves as a basis for the examination of the individual effects of impeller speed and displacement on performance and of the comparative performance when speed and displacement are altered simultaneously to meet definite service requirements.

According to simple theory, when assuming no losses, the air weight handled and the power required for a given pressure difference are directly proportional to the speed and the displacement. These simple relations are altered considerably by the losses.

In estimating the effect of speed on performance it is of interest to note that:

(1) The difference between the actual power and the theoretical power was found to vary with the speed raised to the 2.5 power. The theoretical power was obtained by multiplying the pressure difference by the displacement and speed and dividing by the horsepower constant.

(2) The volumetric efficiency of the actual machine remains nearly constant over a large part of the interesting speed range, the decrease in volumetric efficiency at a speed of 6,000 R. P. M. being less than 2 per cent.

(3) The ratio of the discharge air temperature to the inlet temperature was found to depend on speed. This effect of speed is represented by the coefficient "C" in the relation

$$\frac{T_2}{T_1} = C \left( \frac{P_2}{P_1} \right)^{\frac{n-1}{n}},$$

which has a value of 1 at zero R. P. M. increasing to 1.04 at 6,500 R. P. M.

With regard to the effect of displacement on performance, the following points are of interest:

(1) The power loss was found to increase with displacement.

(2) The maximum volumetric efficiency increased somewhat with increase in displacement.

(3) The relation between the inlet and discharge temperatures and pressures as represented by the exponent "n" in the above equation was found to increase from 1.36 to 1.53 with increase in impeller length from 4 to 11 inches.

When comparing the performance of different sizes of machines whose impeller speeds are so related that the same service requirements are met, it is found that the individual effects of speed and displacement are canceled to a large extent and the only considerable difference is the difference in the power losses which decrease with increase in the displacement and the accompanying decrease in speed. This difference is small in relation to the net power of the engine supercharger unit, so that a supercharger with short impellers may be used in those applications where the space available is very limited without any considerable sacrifice in performance.



## INTRODUCTION

The general performance of the Roots type aircraft engine supercharger has been discussed in Technical Report No. 230 (Reference 1) and a brief comparison made with some of the important characteristics of other types of compressors that are used as superchargers. This comparison showed that the Roots type compressor has several features which make attractive its use as an aircraft engine supercharger. Of these features, its adaptability to a simple method of control involving a minimum of power loss and its good efficiency are especially noteworthy.

In determining the proportions of a Roots supercharger for a particular application there are two variables that are primarily concerned, namely, the displacement per revolution and the rotative speed of the impellers. The action of a Roots supercharger is to transfer a fixed volume of air at intake density from the inlet side to the discharge side where it is compressed to the discharge pressure by the back flow of high pressure air (Reference 1). The theoretical delivery in weight per unit time, assuming no clearance and no losses, is, then, the product of the displacement in unit time and the density of the inlet air. Since the displacement in unit time is directly proportional to the product of displacement per revolution and revolutions per unit time, and the size and weight are to a large extent proportional to the displacement per revolution, it is evident that a great saving in space occupied and weight can be made by operating a small machine at high impeller speeds. The theoretical power required with no losses is given by the equation

$$HP = \frac{DN(P_2 - P_1)}{33000}$$

where

$D$  = Displacement per revolution

$N$  = R. P. M.

$P_2 - P_1$  = Pressure difference.

The theoretical power is, therefore, directly proportional to the speed, and the power per unit of air delivered in unit time, assuming no losses, is the same regardless of speed or size.

Certain losses enter, however, to alter these simple relations and a knowledge of the effects of speed and displacement per revolution becomes important in the application of this type of supercharger.

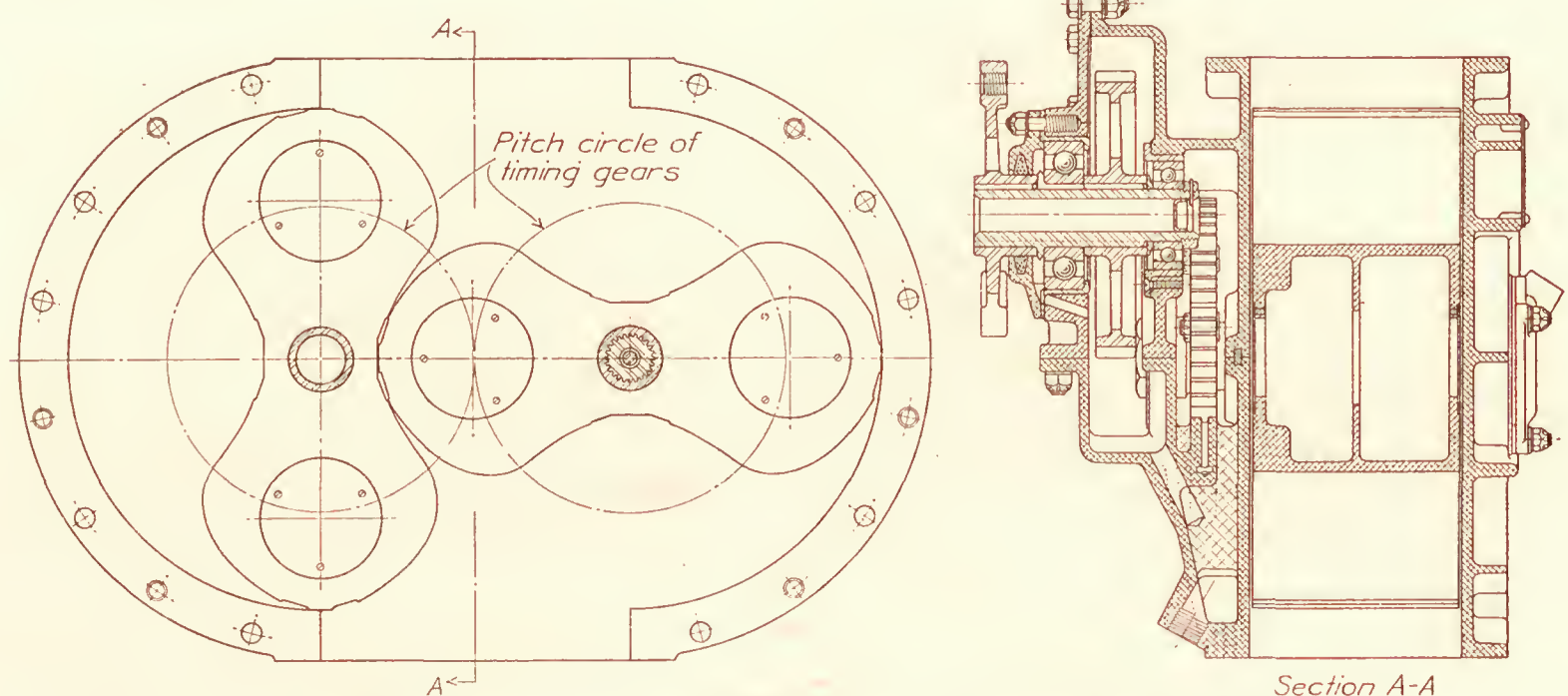


FIG. 1.—N. A. C. A. Roots type supercharger with gear end plate removed and supercharger cross section showing 4-inch impellers

Tests covering a large range of impeller speeds have been made at the Langley Memorial Aeronautical Laboratory on three sizes of Roots type superchargers. These three machines have the same impeller contour and diameter so that change in displacement and delivery with no losses is proportional to the change in impeller length. The displacements per revolution are 0.509, 0.382, and 0.185 cubic foot and the impeller lengths are 11,  $8\frac{1}{4}$ , and 4 inches.



The machine with the 11-inch impellers has been described in detail in Technical Report No. 230 and, except for changes tending for better mechanical conditions, the type of construction of all three machines is essentially that given therein. Figure 1 shows the constructional details of the machine with 4-inch impellers.

The purpose of this report is to present the performances of these three machines on a comparative basis and point out the effects of speed and displacement on performance.

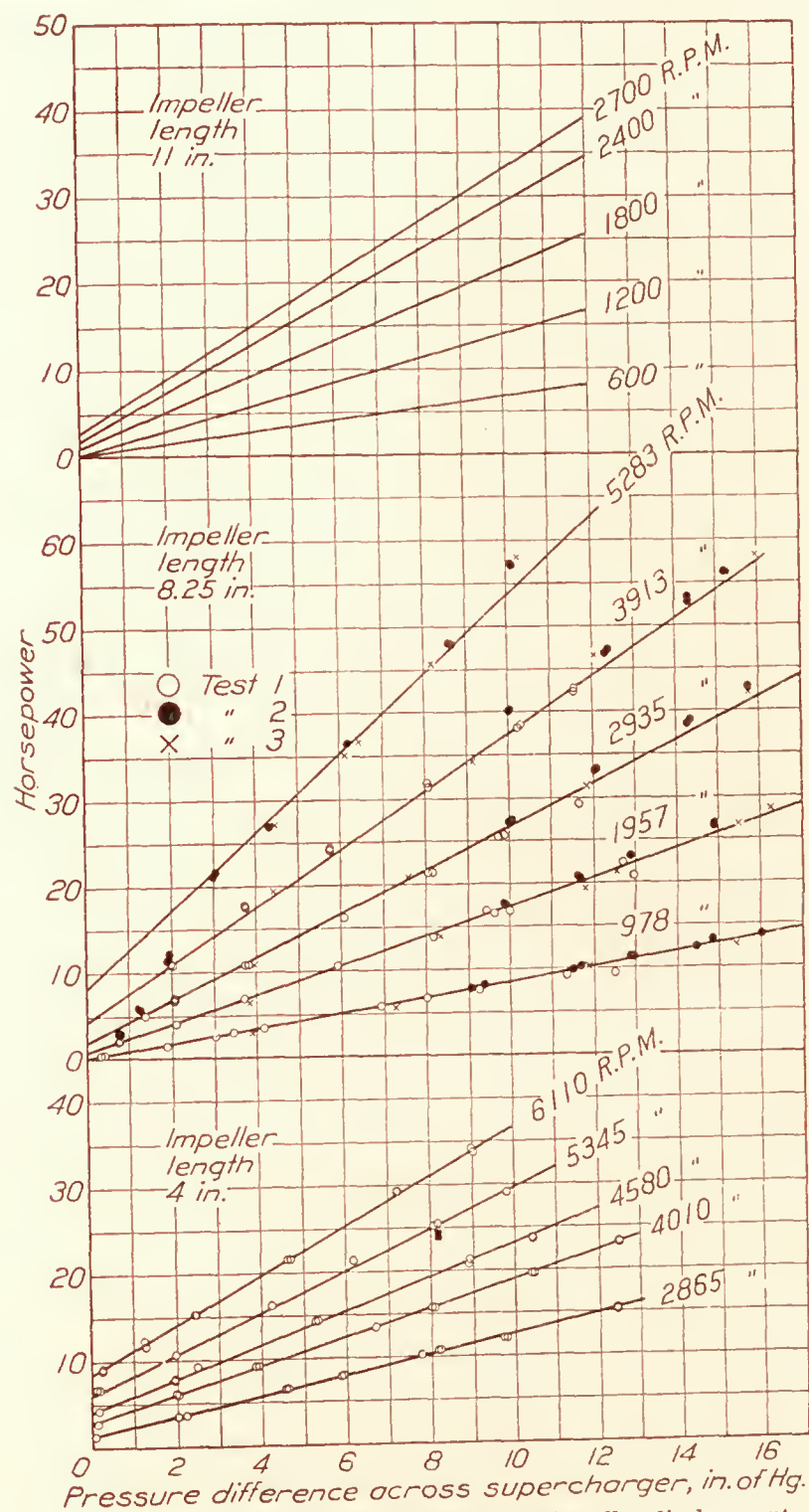


FIG. 2.—Power requirements as affected by impeller displacement, speed, and pressure difference

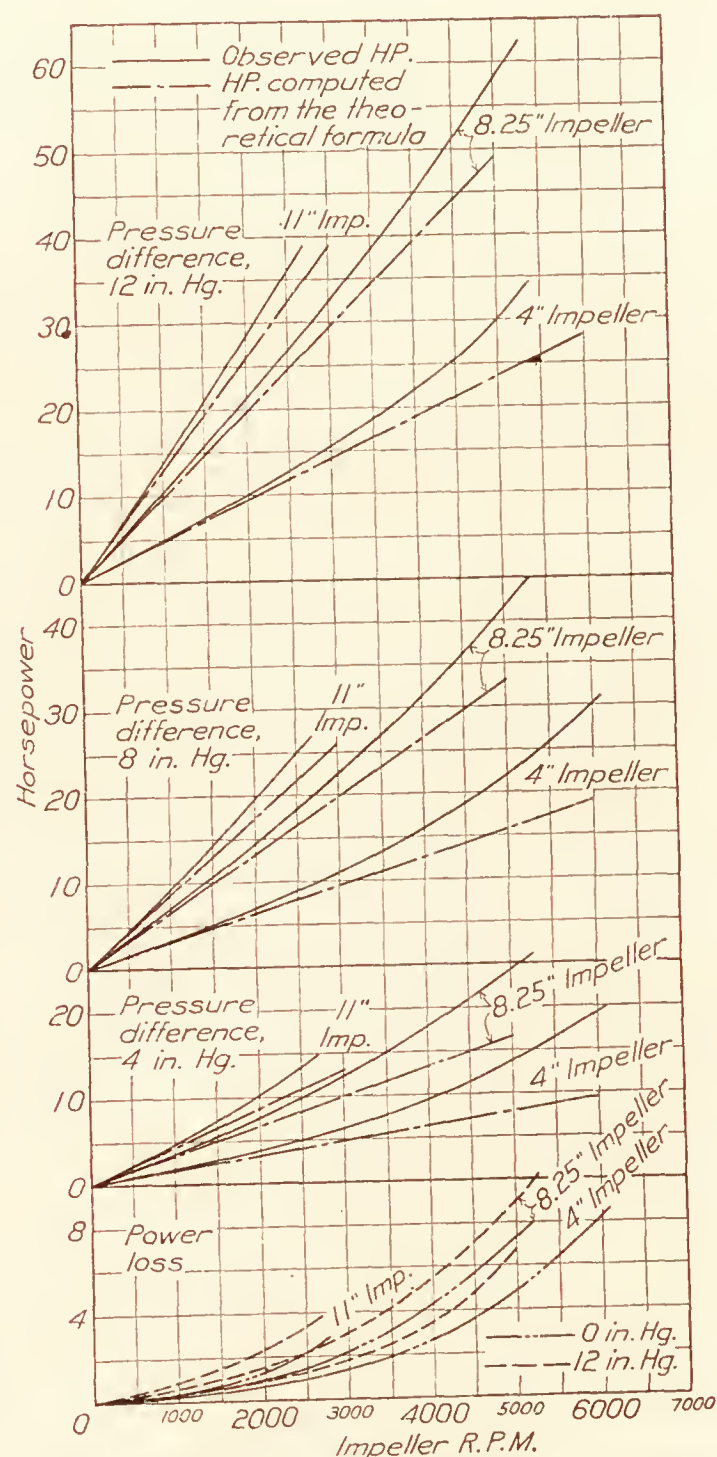


FIG. 3.—Power and power losses as affected by impeller displacement, speed, and pressure difference

### TEST RESULTS

The performances of the superchargers were obtained from tests made by throttling their inlet ports and driving them at speeds up to 2,700 R. P. M. for the 11-inch machine, 5,283 R. P. M. for the 8 $\frac{1}{4}$ -inch machine, and 6,110 R. P. M. for the 4-inch machine. The air was discharged at atmospheric pressure. The quantity of air delivered was measured by a Durley Orifice Box, the power required to drive the superchargers was measured by an electric dynamometer and the inlet and discharge temperatures and pressures were measured by mercury thermometers and manometers. Experimental data for the tests of the 8 $\frac{1}{4}$ -inch supercharger are shown in Tables I to V, inclusive. Since the temperatures of the air varied somewhat



while the tests were in progress, the delivered air weights were corrected to a temperature of 59° F. in order to provide comparable data. The apparatus used and the methods of computation were, in general, the same as given in Technical Report No. 230.

Figure 2 shows the brake power for the three superchargers. The data for the 8¼ and 4 inch superchargers were obtained by operating them at fixed speeds, but those for the 11-inch supercharger were obtained by maintaining the delivered air weight constant over a range of pressure differences. It was necessary, therefore, to cross plot the original data for the 11-inch supercharger to find the relation shown in this figure; hence, data points are not shown for this machine.

Three distinct series of tests were made to obtain the data shown for the 8¼-inch supercharger. The range of pressure differences used in the first series was extended in the second and third series, although these latter included data within the range of the first series. There appeared to be some contacting between the rotors at the higher pressure differences in the second series which probably accounts for the fact that the power was highest for this series.

A brief analysis of power is shown in Figure 3. The brake power shown in this figure was obtained by cross plotting from Figure 2. The theoretical power was obtained from the theoretical equations given in the introduction and explained in Technical Report No. 230. The differences between these two powers represent the power losses.

Figure 4 shows the weight of air delivered; the curves are cross plots of the original data, which gave definite relations.

The ratios of the discharge air temperature to the inlet air temperature plotted against the ratios of the discharge pressure to the inlet air pressure on a logarithmic basis are shown in Figure 5. It may be noted that, for the 8¼ and 4 inch superchargers the intercept of straight lines representing the data with the temperature ratio axis increases with increase in speed. The tests of the 11-inch supercharger were not carried to those speeds where a definite speed effect is apparent. The data for the 8¼-inch supercharger appears to give two straight lines of different slopes, intersecting at a pressure ratio of about 1.5. Although some of the points were obtained in the second series of tests where some contacting had been noted, the few points obtained in the third series show the same effect.

Measurements were also made of slip speed, i. e., that speed required to maintain definite pressure differences with no air delivery. These tests were made by blocking off the inlet to the supercharger. The results of these measurements are given in Figure 6. The lower part of this figure shows the effect of a change in impeller end clearance from 0.015 to 0.020 inch. The dotted lines shown in this part of the figure indicate the manner in which the slip speed changes with temperatures.

#### ANALYSIS OF THE PERFORMANCES OF THE THREE SUPERCHARGERS

In making a comparison of the performances of these superchargers the test results used should apply to that condition of each supercharger necessary for the most efficient operation under ordinary service conditions. Since the performance of a Roots supercharger is affected by the clearances between the two impellers and between the impellers and the parts composing the compression chamber, the comparison must be made for comparative clearances. The clearances that should obtain for a fair comparison depend on the tolerances used and on the materials and details of construction. The tolerances and freedom in the bearings and the method of locating them prohibit the use of clearances proportional to the impeller length, although such a proportion might have been possible from a consideration of the relative amount of expansion with increased temperature. A definite comparison was obtained by reducing all performances for the three machines to the same clearances that obtained in the tests of the 4-inch supercharger — 0.007 inch between the impellers and between the tips of the impellers and the curved sides of the compression chamber, and 0.010 inch between the ends of the impellers and the ends of the compression chamber.



A change in clearance does not affect the air handled which is the sum of the air delivered and that which slips back through the impeller-case clearances, but it does affect the ratio of these two components. The amount of air delivered decreases with increased clearance, as is shown in Figure 4. The amount of air that is lost in slip increases with the clearance since the slip speed increases with clearance, as shown by Figure 6.

The method used herein for correcting the air delivered assumes that it is proportional to the difference between the impeller speed and the slip speed. It is realized, however, that the

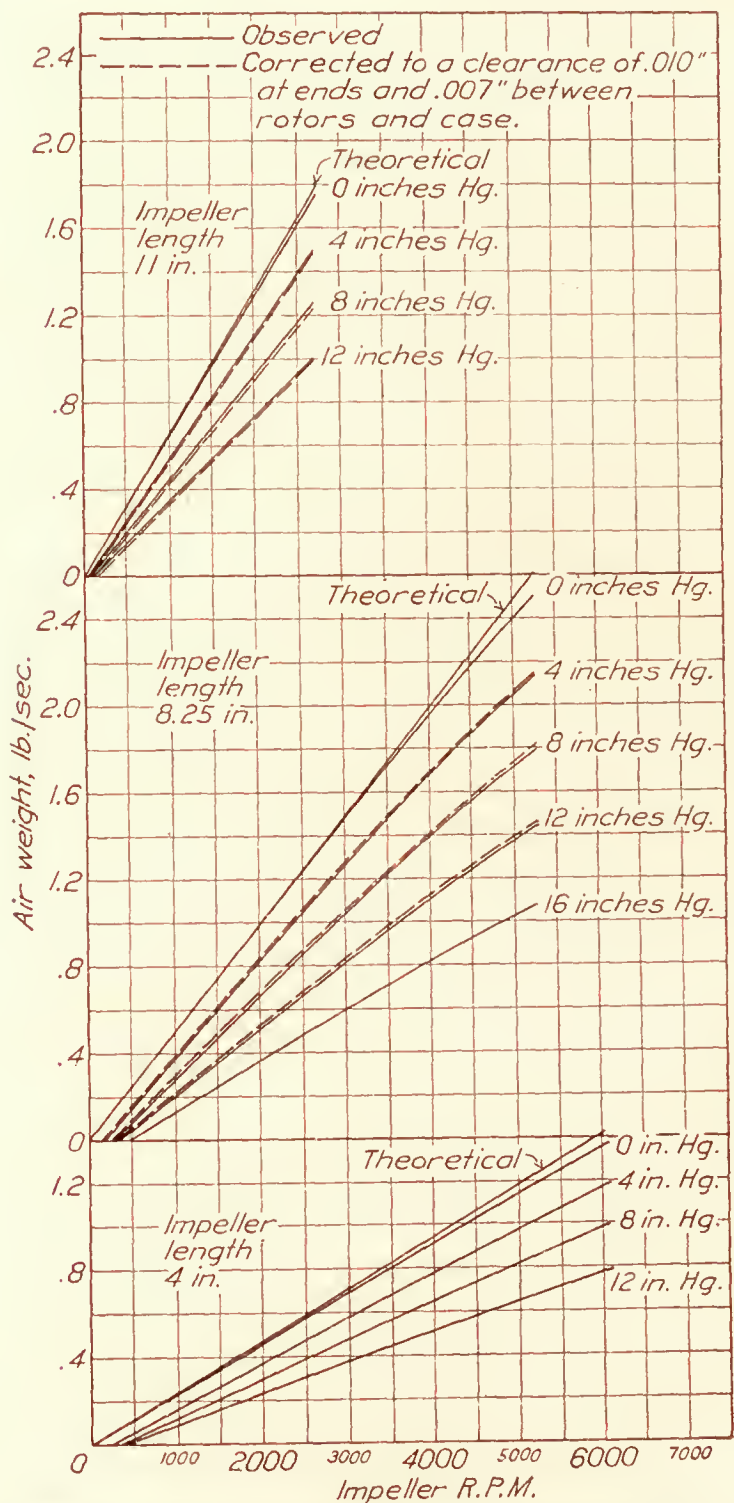


FIG. 4.—Rate of air delivery as affected by impeller displacement, speed, pressure difference, and clearance

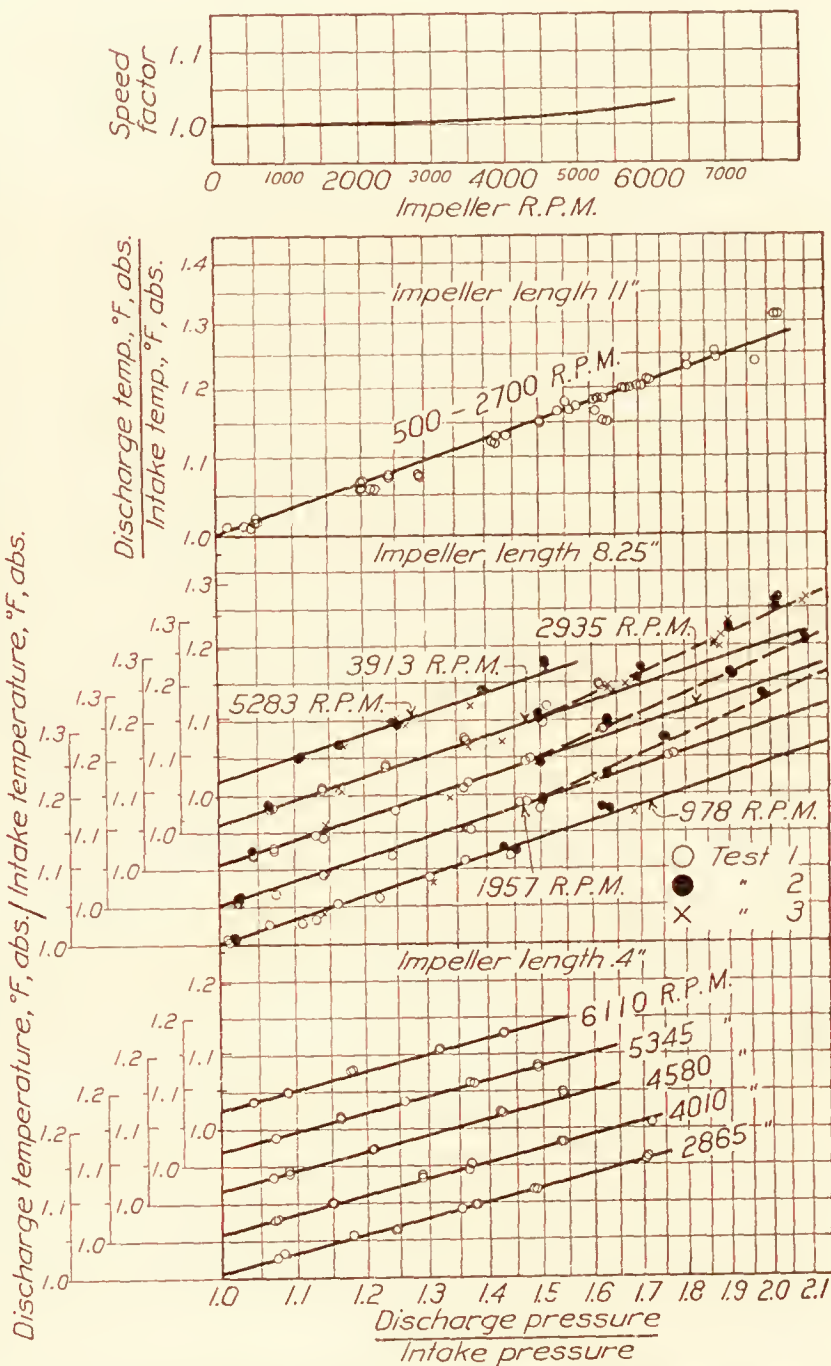


FIG. 5.—Temperature-pressure relations as affected by impeller displacement and speed. Plotted on a logarithmic scale

slip, i. e., that air which slips back through the impeller-case clearances, measured at a given pressure difference with no delivery, as obtained by blocking off the inlet, may be in error when used at the same pressure difference for high impeller speeds during air delivery. Since the corrections made are for the same impeller speeds, the relative errors resulting from the use of slip at no delivery are small. Slip speeds for the three machines reduced to the same clearances by rational processes are shown on Figure 6. Plots of air delivered corrected by this method are shown as dotted lines in Figure 4. Volumetric efficiencies as computed from these air weights are shown by Figure 7. The power required to drive the supercharger, being mainly a function of speed and pressure difference, is not affected very much by change in clearance.



The test results and the comparative volumetric efficiencies form the basis for an estimation of the comparative performance for definite service requirements. This will be preceded by consideration of the independent effects of speed and displacement, without regard to service requirements, in order that the comparison may be more readily appreciated.

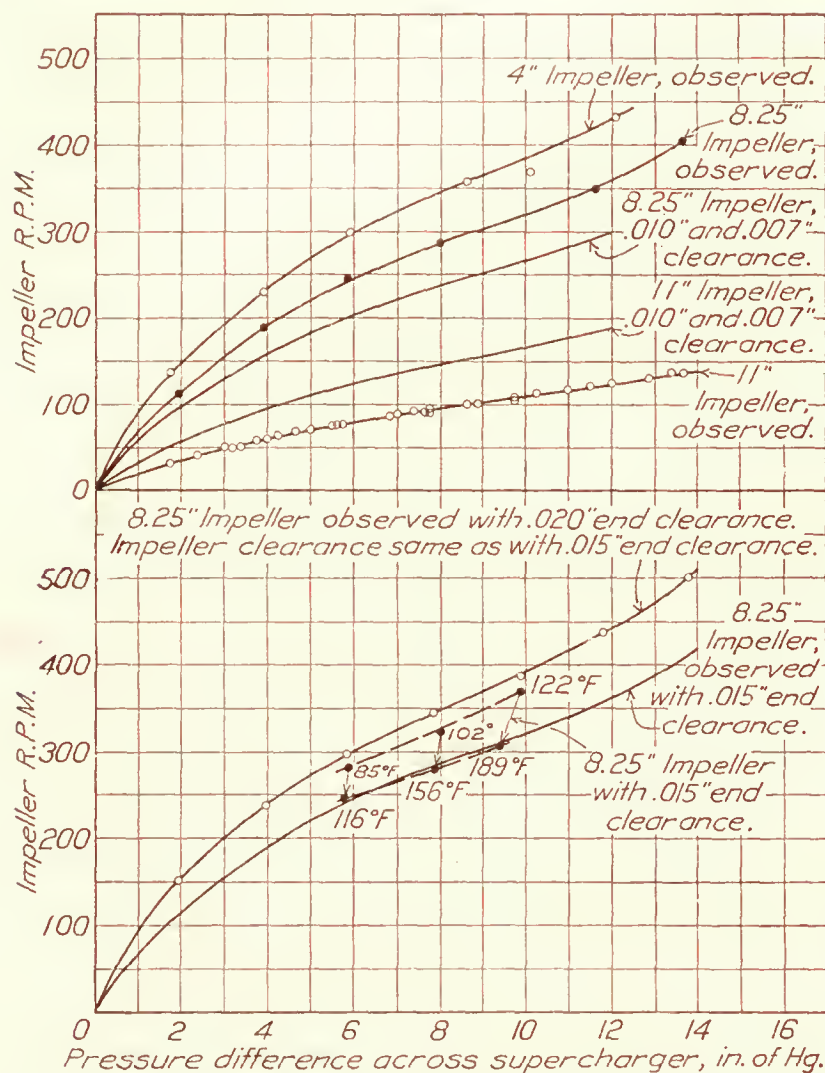


FIG. 6.—Slip speed as affected by impeller displacement, pressure difference, clearance, and temperature

increasing the power required to drive the supercharger and decreasing the air delivered beyond that computed from observed pressures.

The effect of these losses on the relations of air delivered and volumetric efficiency to speed will be considered first. On Figure 4 the theoretical air delivery, assuming no losses, is plotted together with the measured deliveries. The difference between the air weight delivered at zero pressure difference and the theoretical value shows the effect of speed which is made up of the effect of pressure loss and the effect of the loss due to air friction. The displacement of the other curves is due partially to the reduced inlet density and partially to the slip. For the condition of no losses the volumetric efficiency is 100 per cent regardless of speed. At the lower impeller speeds, loss of air through the impeller-case clearances reduces the volumetric efficiency below 100 per cent, having less effect as the speed increases. If this loss were the only loss, volumetric efficiency would approach 100 per cent at infinite speed. Actual tests, however, show that the pressure loss serves to reduce the volumetric efficiency within a practical speed range, but the reduction is quite gradual with increase in speed.

#### THE EFFECT OF SPEED ON PERFORMANCE:

Since simple theory, when assuming no losses, shows that the air delivered depends only on the displacement per revolution and the revolutions per minute while the power required depends on the air delivered and the pressure difference, consideration of the effect of speed on performance in the actual machine depends on consideration of the losses occurring in the supercharger, their kind and effect on performance, and the effect of speed on their magnitude. The one item of loss that causes the greatest departure from the no-loss performance is that due to the air leaking from the delivery side to the inlet side through the clearance spaces. Other losses entering are the power lost in gears and bearings, the power due to air friction, and an apparent loss in power and air delivery that will be termed pressure loss. This apparent loss is due to the fact that at the high speeds encountered the pressure within the displacement volume before compression will be less than that measured at the inlet to the machine, and after compression it will be greater than that measured at the discharge side, thus

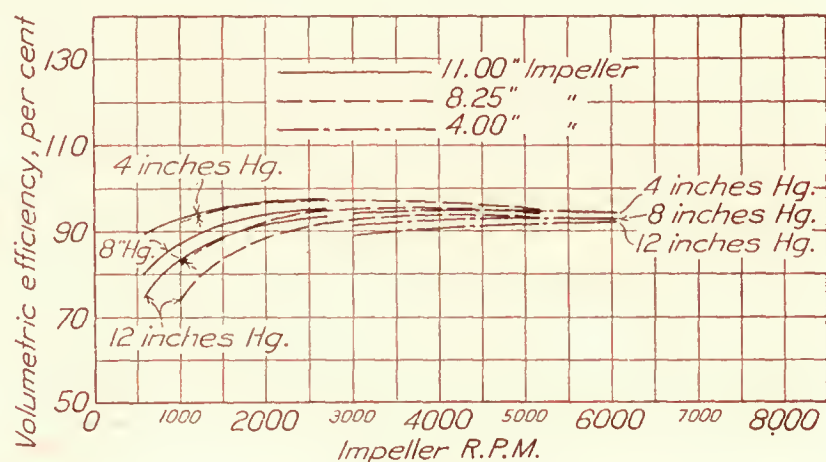


FIG. 7.—Volumetric efficiency as affected by impeller displacement, pressure difference, and speed



The effect of speed on power losses is shown graphically by Figure 3, from which it may be seen that the departure of the measured power from theoretical power increases with speed. The power losses, at zero pressure difference, as given by differences of the theoretical and actual power, are exponential functions of the speed, showing a variation with speed raised to the 2.5 power. The increases in the power losses with pressure difference, as shown on Figure 3, are largely caused by the increased gear and bearing friction.

The power losses given by these differences are composed of gear and bearing friction, pressure losses, and air friction. Since the power depends on the geometrical displacement and not on the air delivered, the effect of slip does not enter.

Speed will also have an effect on the temperature-pressure relations, tending to increase the temperature ratio for a given pressure ratio because of the fact that the radiating surface remains constant while the total amount of heat generated in the compression of an increased amount of air increases with speed. Counteracting this effect is the loss of air through the clearance spaces. Assuming that the amount of air that returns from the pressure side of the supercharger to the inlet side depends primarily on the pressure difference, then the proportion of heated air that is returned and recompressed with further increase in temperature decreases as the speed is increased, thus resulting in a lower temperature for the delivered air. The fact that the temperature-pressure relation plotted on a log basis, Figure 5, shows a definite temperature increase with increase in speed for a discharge-inlet air-pressure ratio equal to 1 indicates that the radiation condition controls. This speed effect may be represented by inserting a coefficient "C" in the usual relation between temperature and pressure, giving

$$\frac{T_2}{T_1} = C \left( \frac{P_2}{P_1} \right)^{\frac{n-1}{n}}$$

The value of "C" is taken from the speed-curve intercepts on the temperature axis, and is plotted against speed at the top of Figure 5. The increase in temperature ratio due to increase in speed is seen to be less than 5 per cent for speeds up to 6,500 R. P. M.

It was noted previously that the data for the 8¼-inch supercharger shows a definite change in slope in the temperature-pressure relation at a pressure ratio of approximately 1.5. It appears from rational processes of reasoning that this effect is independent of speed.

#### THE EFFECT OF DISPLACEMENT ON PERFORMANCE:

In view of the fact that the theoretical equation, omitting the influence of losses, shows that the power required and air weight delivered are directly proportional to displacement, an analysis of the effect of displacement on performance is reduced to analyses of the effects of the losses on the simple relations as in the discussion of the effects of speed on performance. Slip has the greatest influence on the difference between the simple theoretical and the actual performances. Since slip speed at a given pressure difference is directly proportional to the clearance area and inversely proportional to the displacement, it is necessary to know the relative change in displacement and clearance area with a change in dimension. The displacement varies with the length of the supercharger, but since there are fixed clearance areas at the ends of the impellers which are not changed by an increase in length the total clearance will not vary as rapidly as the length. For example, doubling the length of the impellers doubles the displacement but does not double the clearance area. The slip, therefore, will be less for the machine with greater displacement, as is evident from Figure 6.

The influence of slip on the air delivery can be seen from Figure 7. If all three superchargers had the same slip, volumetric efficiency curves for the three superchargers would be approximately superimposed when the pressure difference is the same. The displacement of the curves which show higher volumetric efficiencies for the longer superchargers indicates the extent to which slip enters into the consideration of the effect of displacement and air weight delivered.

Since the power required depends upon the work done on the air handled by the supercharger and this work is the same regardless of the proportion of the air handled that returns to



the intake side, slip has no effect on the relation between displacement and power unless the power for a given weight of air is considered.

The magnitude of the effect of displacement on the other losses—namely, the pressure, mechanical and air friction losses—is shown at the bottom of Figure 3.

A pronounced effect of change in displacement is its influence on the temperature-pressure relations. The heat radiation surface of a Roots supercharger is composed of the two ends and two sides of the compression chamber. When a change in size is obtained by a change in length the heat generated in unit time will increase in proportion with the increase in length for a given pressure difference and speed. The increase in radiating surface with an increase in length, however, is less than the proportional increase in length; consequently, the compression exponent will increase with increase in displacement. It may be noted that for the two larger superchargers the compression exponent is greater than the theoretical adiabatic exponent of 1.41. This is due to the magnitude of the power losses, which are such that the additional heat generated by these losses is not completely radiated by the supercharger case. Under the conditions of the laboratory tests, the compression exponent " $n$ " in the equation

$$\frac{T_2}{T_1} = C \left( \frac{P_2}{P_1} \right)^{\frac{n-1}{n}}$$

varies with the size in the following manner:

- 11 in. supercharger;  $n = 1.53$
- $8\frac{1}{4}$  in. supercharger;  $n = 1.48$
- 4 in. supercharger;  $n = 1.36$

#### COMPARATIVE PERFORMANCE FOR GIVEN REQUIREMENTS:

While the individual effects of speed and displacement have been discussed in the preceding paragraphs, speed and displacement must be considered simultaneously in the usual case of selection of a supercharger for a specific purpose, entailing, as it does, a definite weight of air delivered.

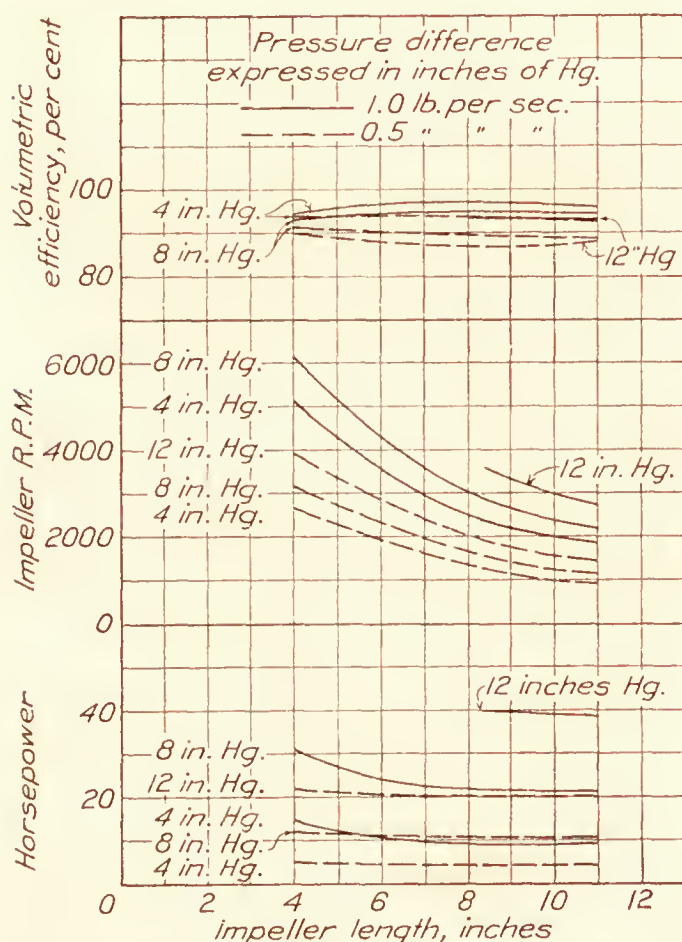


FIG. 8.—Comparative performances of three superchargers for definite rates of air delivery and variable impeller length

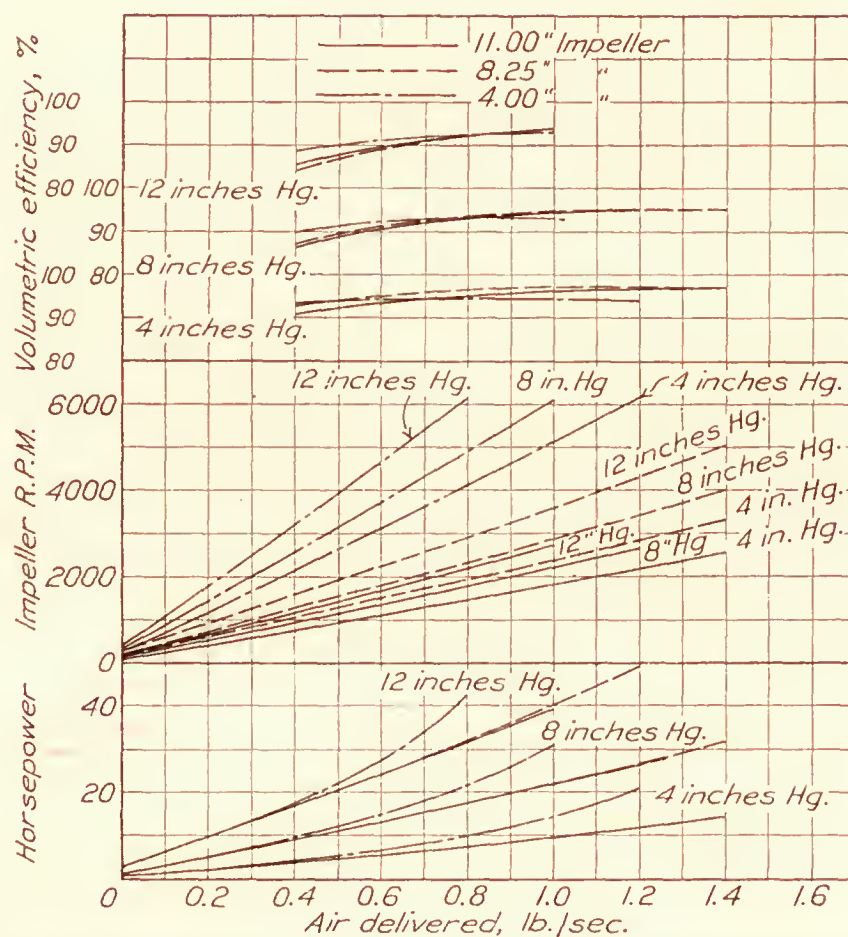


FIG. 9.—Comparative performances for three superchargers for definite impeller length and variable rate of air delivery



In Figure 8 several performance factors are plotted against impeller length for constant rates of air delivery of 1 and 0.5 pound per second. These values were selected because they approximate the air requirements of the two most popular sizes of engines in use to-day—engines of 400 to 450 and 200 to 220 H.P., respectively.

It will be noted that the volumetric efficiency remains at a satisfactorily high value, regardless of length; hence, there is very little choice between different lengths from this viewpoint. This is accounted for by the fact that the tendency for reduced volumetric efficiency caused by higher slip for the smaller machines is counteracted by the tendency for increased volumetric efficiency caused by the increased speed at which the smaller machine must be operated. The rapid increase in impeller speed with reduction in length results in an increase in power required for the shortest supercharger, as discussed heretofore. While the percentage increase may seem considerable in a reduction of length from 11 to 4 inches, the actual difference may not be considered prohibitive, since at a pressure difference of 8 inches of mercury and a delivery rate of 1 pound per second the difference of 9 H.P. is small in relation to the net power of the engine-supercharger unit. It is well to point out, however, that very high speeds may cause a considerable increase in power due to the exponential nature of the power losses. Figure 9 shows the same information plotted against air delivered.

With regard to the temperature-pressure relations which were shown to be influenced by a change in displacement and speed, it should be noted that the independent effects of each are practically canceled at speeds that are of interest in the supercharger application when considering simultaneous changes in speed and displacement to meet a specific requirement.

With this information as a basis, the actual selection may be made more intelligently, but, since the performance is, in general, improved somewhat by increasing the size of the machine, the selection will be governed to a large extent by the space requirements of the particular application.

#### THE REDUCTION OF LABORATORY PERFORMANCE TO ALTITUDE PERFORMANCE

The pressure conditions in these tests are comparable to actual service conditions where the supercharger is used to maintain sea-level pressure at the carburetor as the altitude of operation is increased because they were created by throttling the inlet to the supercharger with free discharge into the atmosphere. The intake temperature was nearly constant for all pressure differences while in service the temperature decreases considerably with increase in pressure difference caused by increase in altitude of operation. In using the test data in this report for the estimation of altitude performance of the supercharger it is necessary, therefore, to take into account this difference in temperature conditions.

The chief effect of the difference in temperature is to change the density of the inlet air and, therefore, the weight of air handled in unit time. A simple method of finding the air weight that would be handled at altitude consists in multiplying the air weight given herein for the pressure corresponding to the altitude under consideration by the ratio of the absolute temperature of these tests (519° F.) to the absolute temperature of the altitude. The power required will be sensibly that given herein, since power for a given machine is dependent on the pressure difference and the speed.

No attempt is made to consider here the agreement of flight results with laboratory results; it is intended merely to point out the importance of the difference in laboratory and flight intake air temperatures. While the different temperature conditions give some difference in clearance and consequently some difference in the volumetric efficiency, the results that have been obtained by the use of this method in connection with actual flight work makes this effect appear inconsequential for most purposes.

#### CONCLUSION

It is evident from these tests that impeller speed and displacement have an appreciable effect on the performance characteristics of Roots superchargers aside from their effect as a result of a direct proportional relation. It may be concluded, however, that the speed of impeller



operation may be increased to at least 6,000 R. P. M. without imposing any serious performance limitation—the volumetric efficiency is not seriously reduced and the power required per pound of air delivered is not increased excessively at this speed. The results obtained with the 4-inch supercharger indicate that good performance characteristics may be obtained with this relatively small machine, which lends itself to a compact type of construction so much desired in aircraft practice.

When the three sizes of machines are compared on a basis of the same rate of air delivery it is seen that the performance characteristics are the same in general, except that the power loss introduced by high speeds of operation result in somewhat greater power requirements for the smallest supercharger.

LANGLEY MEMORIAL AERONAUTICAL LABORATORY,  
NATIONAL ADVISORY COMMITTEE FOR AERONAUTICS,  
LANGLEY FIELD, VA., *December 23, 1927.*

### BIBLIOGRAPHY

1. Ware, Marsden: Description and Laboratory Tests of a Roots Type Aircraft Engine Supercharger. N. A. C. A. Technical Report No: 230, 1926.
- Gardiner, Arthur W.: A Roots-type Aircraft-engine Supercharger. Journal of the Society of Automotive Engineers, 1926, XIX, 253-264.

TABLE I

EXPERIMENTAL DATA USED TO DETERMINE THE EFFECTS OF IMPELLER SPEED AND DISPLACEMENT  
[8.25-inch supercharger]

Run No.	Speed (impeller) (R. P. M.)	Horse-power	Air weight (lb. per sec.)	Pressure difference (In. Hg.)	Pressure ratio	Temperature ratio
<i>Test 1</i>						
4	978	1.48	0.4165	1.86	1.067	1.024
5	978	3.39	.3615	4.14	1.162	1.050
6	978	5.81	.2970	6.93	1.304	1.085
7	978	9.46	.1890	12.51	1.728	<sup>1</sup> 1.177
8	978	.36	.5100	.35	1.010	1.002
9	978	2.91	.3465	3.43	1.131	1.030
10	978	2.48	.3955	3.00	1.111	1.025
11	978	3.32	.3334	5.56	1.227	1.059
12	978	7.60	.2555	9.26	1.446	1.115
13	978	6.65	.2775	8.00	1.363	1.108
14	978	9.26	.2255	11.35	1.607	1.167
15	978	.39	.4855	.36	1.012	1.006
<i>Test 2</i>						
64	978	.19	.4935	.32	1.011	1.001
65	978	.17	.4950	.32	1.011	1.000
66	978	8.00	.2647	9.38	1.453	1.121
67	978	7.83	.2658	9.07	1.431	1.125
68	978	10.07	.2186	11.70	1.636	1.182
69	978	9.88	.2212	11.50	1.618	1.184
70	978	11.24	.1750	12.92	1.750	<sup>1</sup> 1.180
71	978	11.24	.1740	12.88	1.746	<sup>1</sup> 1.185
72	978	13.82	.1222	16.03	2.135	<sup>1</sup> 1.196
73	978	12.91	.1452	14.85	1.970	<sup>1</sup> 1.216
74	978	12.47	.1454	14.45	1.921	<sup>1</sup> 1.237
<i>Test 3</i>						
208	978	3.16	.3570	3.75	1.143	1.040
209	978	5.90	.2680	7.06	1.307	1.078
210	978	10.31	.1712	12.18	1.684	<sup>1</sup> 1.127
211	978	12.68	.1276	14.81	1.974	<sup>1</sup> 1.183

<sup>1</sup> These points were not used in determining the temperature-pressure relations because the discharge temperatures had not reached a sufficiently constant condition.



TABLE II  
EXPERIMENTAL DATA USED TO DETERMINE THE EFFECTS OF IMPELLER SPEED AND DISPLACEMENT  
[8.25-inch supercharger]

Run No.	Speed (impeller) (R. P. M.)	Horse-power	Air weight (lb. per sec.)	Pressure difference (In. Hg.)	Pressure ratio	Temperature ratio
Test 1						
16	1,957	1.95	0.9450	0.78	1.027	1.010
17	1,957	4.00	.8825	2.09	1.074	1.015
18	1,957	6.85	.8160	3.73	1.142	1.039
19	1,957	10.50	.7240	5.90	1.244	1.065
20	1,957	13.93	.6410	8.18	1.374	1.099
21	1,957	16.68	.5765	10.00	1.498	1.128
22	1,957	1.75	.9385	.74	1.025	1.009
23	1,957	1.73	.9330	.74	1.025	1.006
24	1,957	16.80	.5810	9.44	1.459	1.136
25	1,957	16.55	.5820	9.64	1.473	1.136
26	1,957	22.25	.4570	12.70	1.775	1.205
27	1,957	20.62	.4650	12.97	1.761	1.203
Test 2						
75	1,957	3.00	.9275	.71	1.024	1.010
76	1,957	2.98	.9250	.74	1.025	1.010
77	1,957	17.85	.5775	9.87	1.489	1.138
78	1,957	17.63	.5800	9.87	1.488	1.143
79	1,957	20.75	.5088	11.63	1.631	1.176
80	1,957	20.58	.5090	11.63	1.631	1.180
81	1,958	23.05	.4585	12.90	1.750	1.230
82	1,957	23.02	.4620	12.90	1.750	1.230
83	1,957	26.68	.3955	14.92	1.986	1.296
84	1,957	26.50	.3952	14.90	1.981	1.298
Test 3						
206	1,957	19.55	.5040	11.31	1.606	1.168
207	1,957	28.55	.3310	16.28	2.188	<sup>1</sup> 1.254
212	1,957	21.25	.4202	12.38	1.703	<sup>1</sup> 1.146
213	1,957	26.85	.3735	15.45	2.063	<sup>1</sup> 1.237
214	1,957	6.55	.7910	3.75	1.143	1.044
215	1,957	14.00	.6190	8.12	1.367	1.100

<sup>1</sup> These points were not used in determining the temperature-pressure relations because the discharge temperatures had not reached a sufficiently constant condition.

TABLE III  
EXPERIMENTAL DATA USED TO DETERMINE THE EFFECTS OF IMPELLER SPEED AND DISPLACEMENT  
[8.25-inch supercharger]

Run No.	Speed (impeller) (R. P. M.)	Horse-power	Air weight (lb. per sec.)	Pressure difference (In. Hg.)	Pressure ratio	Temperature ratio
Test 1						
28	2,935	4.94	1.360	1.35	1.047	1.018
29	2,935	4.94	1.352	1.35	1.047	1.018
30	2,935	6.81	1.327	2.05	1.073	1.023
31	2,935	6.66	1.319	2.05	1.073	1.026
32	2,935	10.76	1.215	3.75	1.141	1.043
33	2,935	10.71	1.236	3.79	1.143	1.039
34	2,935	16.13	1.105	6.07	1.251	1.076
35	2,935	16.13	1.102	6.07	1.251	1.076
36	2,935	21.26	1.006	8.07	1.363	1.105
37	2,935	21.46	1.002	8.16	1.368	1.112
38	2,935	25.51	.918	9.74	1.472	1.142
39	2,935	25.61	.915	9.85	1.481	1.148
40	2,935	29.14	.820	11.62	1.621	1.187
41	2,935	29.16	.817	11.65	1.625	1.191
Test 2						
85	2,935	5.67	1.354	1.25	1.043	1.022
86	2,935	5.55	1.358	1.25	1.043	1.021
87	2,935	27.44	.886	10.05	1.500	1.138
88	2,935	27.14	.890	10.00	1.500	1.147
89	2,935	33.18	.784	12.10	1.668	1.197
90	2,935	33.30	.782	12.06	1.671	1.203
91	2,935	38.74	.669	14.34	1.908	1.268
92	2,935	38.67	.669	14.30	1.903	1.273
93	2,935	42.70	.593	15.75	2.095	1.324
94	2,935	42.70	.593	15.72	2.090	1.333
Test 3						
202	2,935	10.87	1.212	3.86	1.148	1.052
203	2,935	20.82	1.032	7.56	1.337	1.093
204	2,935	31.50	.793	11.74	1.642	1.177
205	2,935	42.25	.590	15.65	2.090	<sup>1</sup> 1.288

<sup>1</sup> These points were not used in determining the temperature-pressure relations because the discharge temperatures had not reached a sufficiently constant condition.



TABLE IV  
EXPERIMENTAL DATA USED TO DETERMINE THE EFFECTS OF IMPELLER SPEED AND DISPLACEMENT  
[8.25-inch supercharger]

Run No.	Speed (impeller) (R. P. M.)	Horse-power	Air weight (lb. per sec.)	Pressure difference (In. Hg.)	Pressure ratio	Temperature ratio
Test 1						
42	3,913	11.15	1.783	1.94	1.068	1.030
43	3,913	11.10	1.791	1.99	1.070	1.032
44	3,913	17.50	1.662	3.76	1.141	1.053
45	3,913	17.55	1.655	3.76	1.141	1.055
46	3,913	24.00	1.527	5.75	1.234	1.083
47	3,913	24.25	1.520	5.75	1.233	1.086
48	3,913	31.35	1.359	8.10	1.365	1.120
49	3,913	31.55	1.365	8.06	1.362	1.122
50	3,913	38.05	1.215	10.22	1.507	1.145
51	3,913	38.45	1.212	10.28	1.513	1.168
52	3,913	42.15	1.125	11.58	1.616	1.196
53	3,913	42.40	1.129	11.59	1.616	1.199
Test 2						
95	3,913	12.05	1.782	1.98	1.068	1.032
96	3,913	11.40	1.778	1.88	1.066	1.032
97	3,913	40.05	1.209	10.06	1.498	1.149
98	3,913	40.00	1.212	10.03	1.496	1.158
99	3,913	46.93	1.038	12.37	1.696	1.209
100	3,913	47.25	1.041	12.42	1.701	1.225
101	3,913	52.75	.909	14.32	1.904	1.283
102	3,913	53.05	.902	14.32	1.904	1.288
103	3,913	56.20	.853	15.21	2.016	1.318
104	3,913	-----	.840	15.21	2.016	1.329
105	3,913	56.05	.833	15.25	2.021	1.333
Test 3						
164	3,913	(1)	(1)	13.98	1.865	1.261
165	3,913	(1)	(1)	13.98	1.865	1.262
166	3,913	(1)	(1)	14.00	1.877	1.257
167	3,913	(1)	(1)	14.05	1.880	1.276
168	3,913	(1)	(1)	14.20	1.898	1.294
192	3,913	(1)	(1)	1.91	1.080	1.050
193	3,913	(1)	(1)	4.17	1.172	1.057
194	3,913	(1)	(1)	7.79	1.365	1.116
195	3,913	(1)	(1)	11.71	1.657	1.192
196	3,913	(1)	(1)	11.66	1.646	1.194
197	3,913	(1)	(1)	11.70	1.651	1.198
198	3,913	(1)	(1)	15.72	2.110	1.328
199	3,913	(1)	(1)	15.76	2.115	1.338
200	3,913	46.60	1.074	12.07	1.670	1.200
201	3,913	58.00	.827	15.85	2.170	1.299
216	3,913	19.50	1.620	4.32	1.168	1.053
217	3,913	34.20	1.286	9.08	1.429	1.119

<sup>1</sup> These values were not computed since these runs were made for purposes other than the determination of power and air delivery.

TABLE V  
EXPERIMENTAL DATA USED FOR DETERMINING THE EFFECTS OF IMPELLER SPEED AND DISPLACEMENT  
[8.25-inch supercharger]

Run No.	Speed (impeller) (R. P. M.)	Horse-power	Air weight (lb. per sec.)	Pressure difference (In. Hg.)	Pressure ratio	Temperature ratio
Test 1						
No runs made at 5,283 impeller R.P.M.						
Test 2						
115	5,283	21.06	2.225	2.96	1.109	1.047
116	5,283	21.60	2.220	3.00	1.110	1.050
117	5,283	26.87	2.133	4.30	1.164	1.063
118	5,283	26.87	2.125	4.30	1.164	1.063
119	5,283	36.45	1.953	6.17	1.255	1.090
120	5,283	36.38	1.933	6.17	1.245	1.094
121	5,283	48.05	1.738	8.60	1.394	1.136
122	5,283	48.00	1.751	8.64	1.397	1.137
123	5,283	57.48	1.596	10.20	1.508	1.177
124	5,283	57.24	1.595	10.20	1.508	1.178
Test 3						
222	5,283	27.15	2.106	4.42	1.169	1.066
223	5,283	36.70	1.837	6.43	1.267	1.091
224	5,283	45.37	1.797	8.24	1.372	1.116
225	5,283	58.20	1.648	10.23	1.510	1.167
226	5,283	35.45	1.973	6.10	1.251	1.100



---

# REPORT No. 285

---

## A STUDY OF WING FLUTTER

IN THREE PARTS

By A. F. ZAHM and R. M. BEAR

Aerodynamical Laboratory, Bureau of Construction and Repair,  
U. S. Navy







# REPORT No. 285

---

## A STUDY OF WING FLUTTER

IN THREE PARTS

By A. F. ZAHM and R. M. BEAR

---

### SUMMARY

*Part I describes vibration tests, in a wind tunnel, of simple airfoils and of the tail plane of an MO-1 airplane model; it also describes the air flow about this model. From these tests are drawn inferences as to the cause and cure of aerodynamic wing vibrations. Part II derives stability criteria for wing vibrations in pitch and roll, and gives design rules to obviate instability. Part III shows how to design spars to flex equally under a given wing loading and thereby economically minimize the twisting in pitch that permits cumulative flutter.*

*Resonant flutter is not likely to ensue from turbulence of air flow alone past wings and tail planes in usual flying conditions. To be flutterproof a wing must be void of reversible autorotation and not have its centroid far aft of its pitching axis, i. e., axis of pitching motion. Danger of flutter is minimized by so proportioning the wing's torsional resisting moment to the air pitching moment at high-speed angles that the torsional flexure is always small.*

### INTRODUCTION

Under wind forces a wing or tail plane may vibrate partly in torsion about its length, partly in flexure about its chord direction, and jointly about both. For clearness the motions are studied first separately, then together.

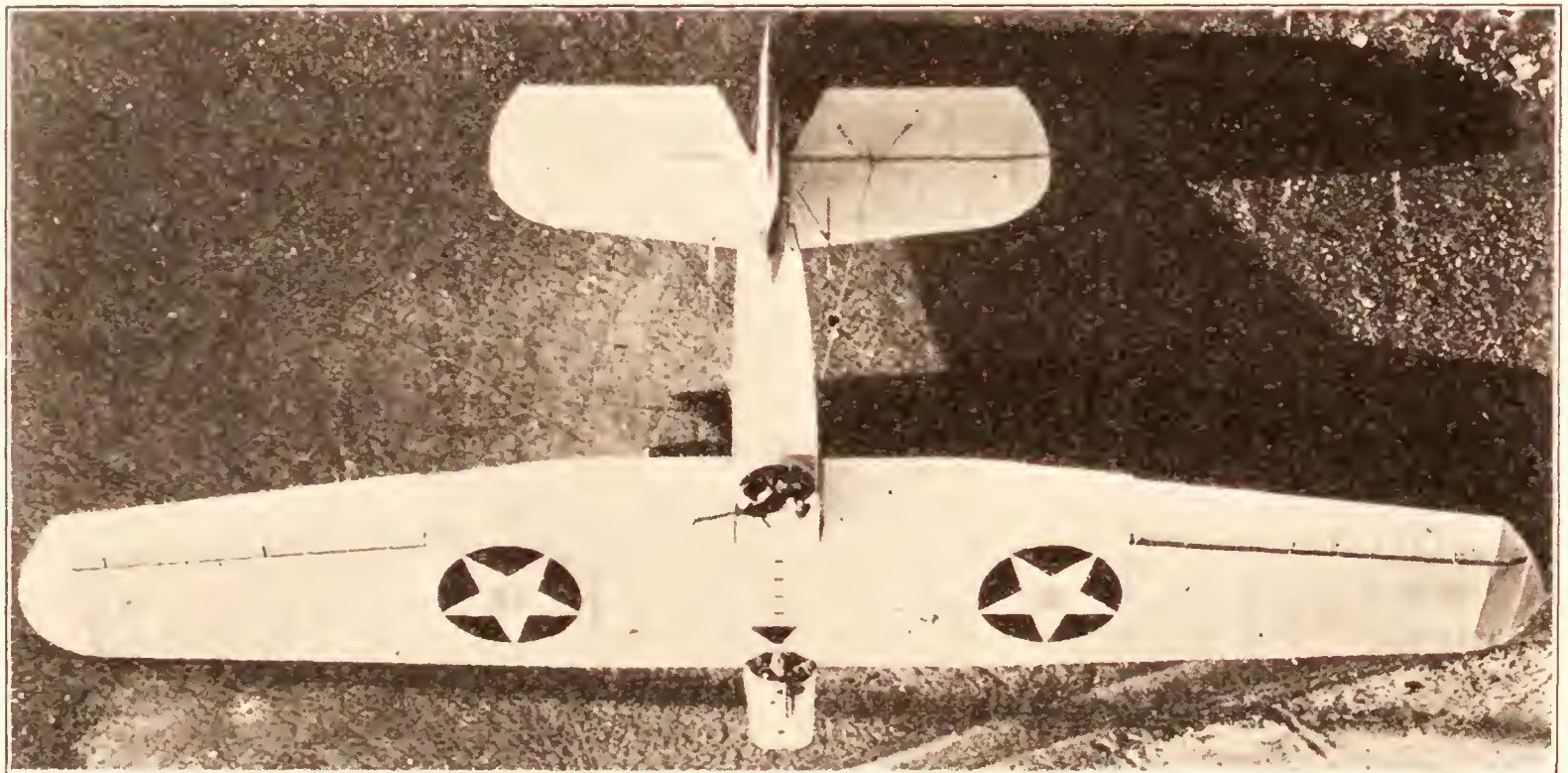
When an airfoil in a uniform stream executes only torsional vibration, its angle of attack with respect to both the relative stream and the fixed stream direction varies periodically; while in flexural vibration alone its angle of attack to the relative stream direction only, varies. In a study of the phenomena the problem then is, to determine the combinations of factors causing these vibrations to be damped, sustained, or reinforced, and the complete nature of the resulting structural oscillation for each case. Naturally the airplane designer is most interested in the practical application of the conditions which tend to preclude oscillation.

A comparatively recent instance of aerodynamic structural vibration was that exhibited by the horizontal tail surfaces on the MO-1 monoplane at normal flying angles, endangering the safety of the craft and lowering its performance efficiency. It was particularly to investigate this defect that the experiments and analyses described in this report were made.

While it is thought that the fundamental factors of aerodynamic structural oscillations have been sufficiently disclosed by the qualitative and theoretical considerations of the report, for favorable practical application, it is nevertheless realized that much remains to be done in the way of a quantitative study of the phenomenon before laws regarding it can be definitely formulated, and theoretical deductions concerning it completely verified.

The following text of the report is a slightly revised form of Report No. 306 prepared for the Bureau of Aeronautics, March 13, 1926, and by it submitted for publication to the National Advisory Committee for Aeronautics.





MO-1 MONOPLANE



# REPORT No. 285

## A STUDY OF WING FLUTTER

IN THREE PARTS

---

### PART I

#### VIBRATION OF MO-1 TAIL PLANE AND OTHER AIRFOILS

By R. M. BEAR

---

#### PREFACE

This part of the report is chiefly a description of tests made in February, 1925, and later, for the Bureau of Aeronautics, in the 4 by 4 foot wind tunnel of the C. & R. Aerodynamical Laboratory, Washington Navy Yard, on a model of the MO-1 airplane and several simple models of airfoil structures, in an attempt to determine the reason and remedy for the rolling vibrations of the MO-1 tail surfaces, occurring on the full-size craft in flight. These vibrations were described as being unaffected by the action of the motor and having a variable amplitude and a constant frequency of about 6 cycles per second.

Experiments previously conducted at Langley Field on the full-size airplane, for showing the nature of the airflow over that portion of the wing surfaces next to the fuselage by means of a smoke jet, indicated an undulatory wake from the wing roots passing back over the tail surfaces, and this disturbed airflow was thought to be a very probable source of the tail vibration.

It was therefore the primary object of the wind-tunnel tests to verify the presence of the disturbed airflow about the model, and to determine its effectiveness in producing vibrations of the tail unit, flexibly hinged to the fuselage about a fore and aft axis. (Fig. 1.) If this disturbed flow and vibration were present, additional tests were to be made in an attempt to find a practical means of improving the flow or a possible location for the tail unit outside of its influence.

The somewhat indefinite and partially negative results of these preliminary tests, however, led to a consideration of the flexibility only of the tail surface structure as a possible source of vibrations, and it is the outcome of a few simple experiments and calculations in this field that apparently furnishes the most promising clue to the solution of tail plane and other similar aerodynamic oscillations.

In this report of the tests no attempt has been made to enter into the complex mathematical theory of aerodynamic structural oscillations, and the mere qualitative nature and limited scope of the experiments and results described are evident. The factors entering into this type of oscillation are many, and before their effects can be completely determined other more carefully planned and mathematically outlined investigations are necessary. The effects of some of the most important of these factors for several simple types of airfoil structure are theoretically treated in Part II, however, and certain fundamental requirements of design for an economic spar structure to prevent airfoil flutter are considered in Part III.

#### TEST APPARATUS

In order to make conveniently the desired tests for tail vibration on the model airplane, the detachable tail unit was mounted on an elastic knife-edge structure of special design (fig. 1), facilitating variation in flexibility and vertical adjustment. One side of the elastic knife-edge was soldered fast in the stem of a brass T whose flange was screwed to the base of the tail unit, and the opposite side was set in a similar slit in the end of a rectangular brass web,



which fitted into a vertical saw slot cut for the purpose at the rear of the fuselage. The elastic knife-edge and the slitted end of the brass web holding it were cut into several coinciding sections, each of which was provided with a small clamping screw. By sliding the brass web in the fuselage slot, the tail unit could be adjusted easily to various heights above its normal position, and by varying the number of elastic knife-edge sections clamped, several different values of restoring moment for a given roll of the tail unit could be obtained.

For exploring the airflow about the model, short lengths of silk and wool<sup>1</sup> threads were used. To show the flow in the vicinity of the tail surfaces, the threads were tied at inch intervals along several fine wires stretched vertically an inch apart on a stiff wire frame, mounted across the wind in the position of the removed tail unit. To explore the flow about the wings and other parts of the model in detail, a strand of wool thread about 3 inches long fastened to a fine needle on the end of a long  $\frac{1}{8}$ -inch drill rod was employed.

### VIBRATION TESTS

Before mounting the complete model of the airplane in the tunnel, a brief test was made on the horizontal part of the tail unit alone, with elevators neutral, for reversible autorotation<sup>2</sup> about the  $X$  axis, since theory and experiment indicate that surfaces exhibiting this phenomena

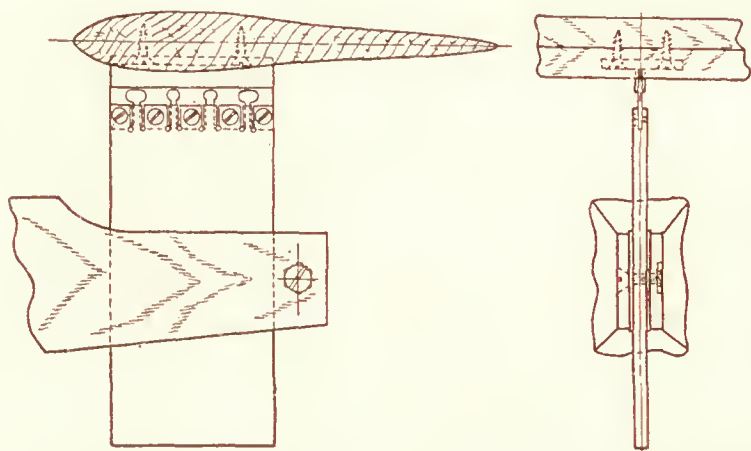


FIG. 1.—MO-1 horizontal tail plane on elastic knife-edge mounting

at any fixed attitude to an air stream are susceptible of sustained rolling oscillations when flexibly hinged in this attitude about an axis along the stream.

With the elevators of the tail surface model aligned and set at  $0^\circ$  to the stabilizer, and the stabilizer mounted for balanced free rotation about an axle along its  $X$  axis pointing upstream, no autorotation occurred for axle settings to the wind from  $0^\circ$  to  $20^\circ$  and beyond.

A true test for autorotation of this surface at other angles than  $0^\circ$  to the air stream would necessitate changing its attitude to the central axle by rotating the surface about an axis through its center of gravity at right angles to the  $X$  axis, while maintaining the central axle exactly in line with the wind and preserving the dynamic balance of the model. Such a test would have shown autorotation near the burble angle of the surface, but was thought unnecessary because the lift curve of the tail plane section indicated no autorotation of the surface at lower angles. (Fig. 7, Part III.)

With the model of the MO-1 airplane in the wind tunnel, and the tail unit, with elevators fixed at  $0^\circ$ , mounted on the elastic knife-edge previously described (fig. 1), no violent rhythmic oscillations of the tail surfaces were observed at any natural angle of attack, even though the stiffness of the elastic knife-edge was reduced to a very small value and a final test made with the tail unit freely hinged about the rolling axis.

However, on allowing one or both elevators of the tail plane to swing freely from attached hinges, very violent rolling oscillations of the tail unit developed with the precipitation of pitching oscillations of the one free elevator, or of the two separate free elevators in opposite directions. In this vibratory rolling motion of the tail unit, the inertia of the free elevators always caused them to lag behind their neutral positions relative to the stabilizer throughout a portion of its path, thus causing the air pressure to be in the direction of the motion, and thereby amplifying and sustaining the vibration.

<sup>1</sup> On account of their greater fluffiness and flexibility, wool threads were found to be superior to silk threads as airflow indicators.

<sup>2</sup> The phenomenon of reversible autorotation about an axis along the wind is known to occur for airplane wings at attitudes near their burble points, and an illustration of its effect in producing sustained aerodynamic oscillations of a wing is frequently observed in the rolling flutter of an airfoil near its burble angle of attack, when mounted in the wind tunnel on an end or a central holder. Also certain thick struts of faired twin-cambered section, besides struts having sections of simple geometrical form, as square, triangular or semicircular, have been shown by wind tunnel tests to autorotate in either direction about a centrally located transverse axis for certain attitudes of the surface at or near its symmetrical position to the wind.



When the freely hinged elevators were interconnected to prevent them from pitching in opposite directions no sustained rolling oscillations of the tail unit occurred.

When the model airplane was fitted with a drill-rod spindle, whose axis coincided with the design  $Y$  axis of the full-size craft, and was mounted in the tunnel with the wings vertical and the supporting spindle clamped in the balance-shaft chuck, a slight natural pitching of the freely hinged interconnected elevators or of a single free elevator started a pitching oscillation of the model about its torsionally elastic support, and produced a reciprocating interaction of air and inertia forces that developed and sustained violent pitching oscillations of the model and free elevator in lag phase. But, on allowing the model thus mounted to pitch freely about the supporting spindle axis without elastic restraint, no pitching oscillations of the freely hinged interconnected elevators could build up, and any forced oscillations of the model or its elevator were rapidly damped out.

On substituting for the cambered model tail surface, flat surfaces of heavy paper or thin wood, free to pitch or roll without elastic restraint, and adapted by their light weight to respond readily to any general fluctuations in airflow, no marked disturbance of the airflow about any of these surfaces was indicated by their motion until the wings of the model airplane attained the burble angle of around  $15^\circ$ , as the model nosed up; and the turbulent flow then started was observed to persist until the wings passed the  $11^\circ$  angle of attack, as the model nosed down. These observations were made at an air speed of around 10 miles an hour. With higher speeds it was noted, as has been observed before in quantitative tests on models, that the burble angles for the wings advanced slightly.

When the model tail unit was mounted in the tunnel alone on its elastic knife-edge with rudder neutral and the elevator set at several natural flying angles, it acquired slight irregular rolling oscillations of small amplitude at an air speed near 20 miles an hour. Similar slight vibrations were noted also when the tail unit was elastically mounted on the model airplane. It is believed, however, that these irregular oscillations are due to slight natural fluctuations of airflow to be expected around any surface, and are hence of no consequence in predicting unsteady airflow conducive to dangerous aerodynamic vibrations of the full-size structure.

#### AIRFLOW OVER MODEL

The exploration of the airflow over the wings and in the vicinity of the tail surfaces of the model with threads showed at the usual flying angles an unsteady oscillating wake from the region of the wing roots passing along either side of the fuselage and extending laterally about 2 inches with diminishing vibratory intensity. The tail surface appeared to lie in the midst of this wavering wake when the wings made an angle of about  $8^\circ$  to the tunnel air stream. The middle of the wing wake was defined by an imaginary line lying midway between the half lengths of a long wool thread extending around the wing and streaming back past the tail plane. As the model nosed up from a wing angle of  $0^\circ$ , the tier of threads on the wire frame mounted in place of the tail plane showed slight pitching oscillations as it descended through the wing wake, but no great disturbance of the threads occurred until the wings approached their burble angle of about  $15^\circ$ . A very turbulent flow was then indicated by a violent pitching and swirling of the threads, which appeared to increase in intensity with heights above the fuselage within the wing wake, and persisted to the  $11^\circ$  wing angle as the model nosed down, in agreement with a test previously described. For a wing angle of  $0^\circ$  the slight quivering of the threads above the tail plane showed a very steady flow, but a slight pitching oscillation of the threads below the tail plane indicated the presence of the upper boundary of the wing wake in this vicinity. For a wing angle of about  $10^\circ$  the upper boundary of the wing wake was observed to lie about  $1\frac{1}{2}$  inches above the position of the horizontal tail surface on the model, corresponding to about 3 feet on the full-sized craft.

A more detailed exploration of the flow over the model airplane with a single wool thread about 3 inches long on the end of the exploring rod previously mentioned showed the beginning of an unsteady discontinuous flow about the rear portion of the upper surface of the wing opposite its juncture with the fuselage, when a wing angle of  $4^\circ$  was passed as the model nosed up. As a wing angle of  $8^\circ$  was attained this flow became quite turbulent, as was shown by the jerky



curling motion of the exploring thread, which at some points along the afterpart of the upper surface of the wing near the fuselage pointed upstream away from the trailing edge. In the angle between the fuselage and afterpart of the upper surface of the wing the exploring thread showed a slight swirling motion for wing angles above  $4^\circ$ . Similar swirls were also noted all along the upper edges of the fuselage, even for wing angles below  $4^\circ$ . These swirls were caused by the air spilling over the sharp edges of the fuselage, and the direction of their rotary motion was the same as that for the corresponding wing tip vortex.

All efforts to improve the flow about the wing roots by better fairing with plasticine at their fore and aft intersections with the fuselage were apparently ineffective. Also the rounding of the sharp edges of the fuselage did not prevent the minute air swirls about them.

In order to obtain some notion of the degree of turbulence in the air flow about airplane models which may be considered to indicate an undesirable flow about the full-size craft, conducive to structural oscillations of its parts or otherwise impairing its efficient performance, it was thought advisable to explore the flow about a model airplane similar to the MO-1 type, whose full-size performance was known to be satisfactory, and compare it with that about the MO-1, whose full-size performance has been poor. For this purpose a model of the Fokker FT airplane was chosen as one more nearly resembling the MO-1 than any of the existing types, in superficial design and assembly of wing and body.

An exploration of the air flow about the Fokker model showed a vibratory and turbulent flow from the roots and in the wake of the wings very similar to if not worse than that observed on the MO-1.

#### STRUCTURAL CONSIDERATIONS AND TESTS

Therefore, since the Fokker airplane was known to have given satisfactory service without any serious structural vibrations, and the slightly disturbed flow noted on its model and that of the MO-1 in the vicinity of the tail surfaces seemed insufficient alone to produce any material vibration of these members when rigidly constructed, it was finally supposed, as originally suspected, that the rolling tail plane vibration on the MO-1 airplane was due, not so much to a disturbed air flow from the wings as to a relative weakness in spar structure which permitted a lateral distortion of the surface under its normal air pressures or inertia forces.

This supposition was primarily based on a study of the data for the elastic coefficients of the spars of various typical tail surfaces, determined from spar tip deflection tests made at Langley Field on the tail planes of 12 full-size airplanes, including the MO-1. From these data the ratio of the figures for the rear and forward spar elastic coefficients for the horizontal tail surface of the MO-1 airplane was seen to be 17 as compared to a maximum value of 4 for the tail surfaces of the other planes. In other words, the flexural stiffness of the MO-1 tail surface at the rear spar is  $1/17$  of its value at the forward spar, while on the other airplanes the rear spar is never less than  $1/4$  the stiffness of the forward spar.

As emphasizing the necessity for a stiff rear spar as well as a stiff forward spar to resist the distortion of thick tail surfaces of the MO-1 type, attention is here called to N. A. C. A. Report No. 118 describing tests for the pressure distribution over full-size tail surfaces in flight, which show thick-sectioned tail planes to be subjected to exceedingly large twisting moments about their  $Y$  axes and to receive their greatest air loading at the leading edge and tips. These conditions are graphically portrayed in Figures 34 and 243 to 264 of that report.

As pertaining especially to the MO-1 tail plane vibration, it was thought that the relatively weak rear spar present permitted a material distortion of the surface under its large aerodynamic torsional moment, the fluctuations of which, due to unsteady air flow, started torsional pitching oscillations of the surface about the forward spar, which was in turn set into a transverse vibration in lag phase by the interaction of the air and inertia loads of the system, thus precipitating a reinforced rolling oscillation of the entire tail unit.

In order to investigate some of the structural conditions conducive to tail surface vibrations, wind tunnel tests were made on several simple airfoil models reproducing in an elementary way some of the essentials of tail-plane structure.



The simplest and perhaps most instructive of these models consisted of a flexurally elastic drill rod  $\frac{1}{8}$  inch in diameter with either a model cambered tail surface or flat rectangular surface swinging about it. (Figs. 2 and 3.) A special spring was provided for producing on the surface a readily variable pitching restoring moment about the rod to correspond to the torsional reaction of a forward spar. This model therefore represented roughly a tail surface structure without a rear spar to aid in resisting the torsional moment about the supporting forward spar. From

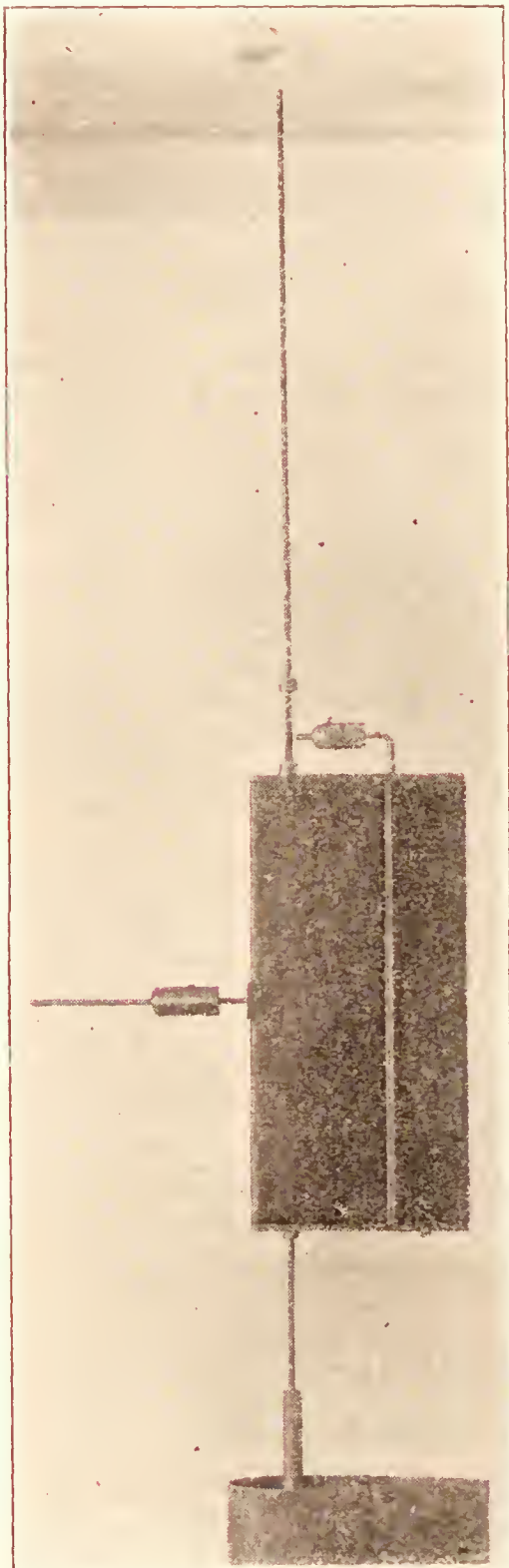


FIG. 2.—Rigid plane surface free to pitch and roll

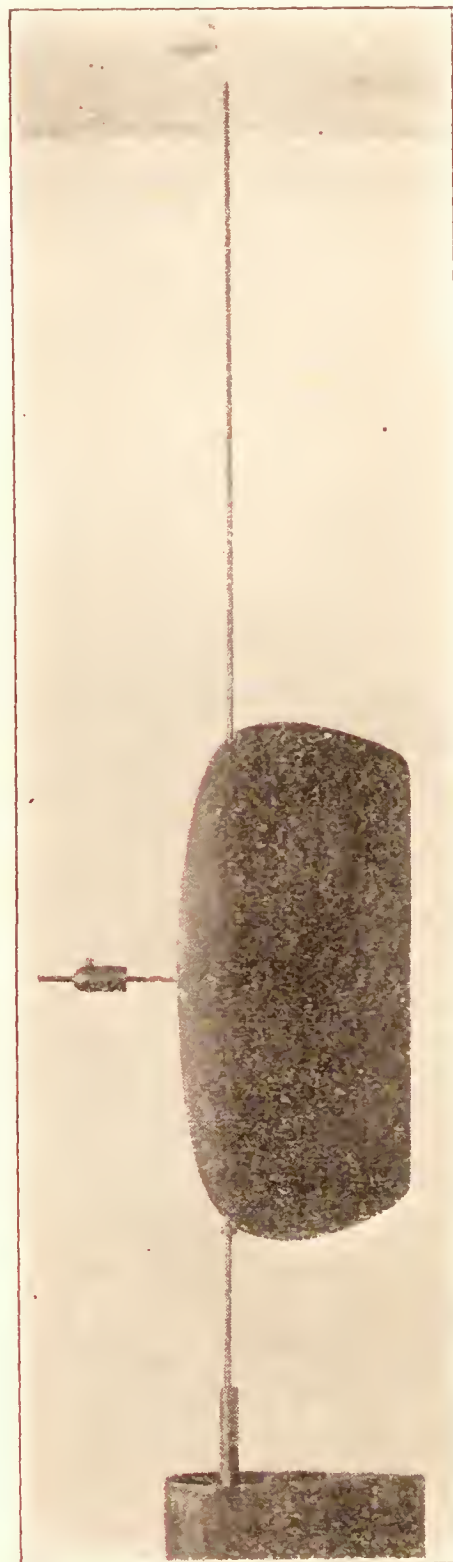


FIG. 3.—Rigid cambered surface free to pitch and roll

the middle of the leading edge of the surface a slender rod projected along the  $X$  axis, having a sliding weight on it for varying the position of the center of mass of the system. In the flat-surface model of this type ( $8\frac{3}{8}$  by 4 by  $\frac{1}{4}$  inches), the interior was spanned by ducts at various distances from the leading edge, fitting the flexible drill rod, so as to vary the position of the torsional axis of the surface relative to its center of pressure. The drill rod stood vertically in the tunnel with its lower end set in a short  $\frac{3}{8}$ -inch spindle clamped in the balance chuck, and the remainder left free to flex to and fro with the hinged surface.



Tests on this model surface elastically hinged about its flexible cantilever support (fig. 2) showed it to be susceptible of reinforced oscillations for center of pressure positions on either side of the hinge axis when the center of mass of the surface lay back of the axis; but to resist such oscillations when the center of pressure lay back of the axis with the center of mass in or forward of the axis.

The type of oscillation developed for the unstable positions of these centers was a combination of pitching and rolling in which the surface vibrated in pitch about the supporting rod and at the same time in roll with the transverse flexure of the rod. The interaction of the air and inertia forces thus produced was such as to reinforce the oscillations and give them a resonant violence, even at very low air speeds.

For all dispositions of center of mass and center of pressure the reinforced oscillations of the surface could be stopped by preventing the free flexure of the supporting rod, thus making the hinged surface rigid in roll only; or by an arm along one end of the surface, clamped to it and the supporting flexible rod, thus making the surface rigid in pitch only.

Similar tests with the model surface freely hinged as a weather vane about its flexible cantilever support showed the same positions of center of mass and center of pressure and other conditions for no oscillations as when it was elastically hinged about this support.

In Figure 2 it is seen that the flat-surface model was provided with an elevator having a special sliding counterweight for center of mass adjustment. When this model was hinged about its flexible rod, as in former tests, but with the elevator swinging freely about a rigid axis near its leading edge with its center of pressure and center of mass back of this axis, violent rolling and pitching oscillations of the whole surface developed even when the centers of mass and of pressure of the system were in their stable locations. But when these centers were stably located for the elevator, by moving its counterweight until the center of mass of its system was in its rigid axis, no oscillations of the surfaces occurred for the original stable conditions, and any forced oscillations were rapidly clamped out.

A test made with a rectangular wooden model of the MO-1 horizontal tail plane profile freely hinged about the flexible rod,  $\frac{3}{4}$  of an inch from its leading edge (C. M. & C. P. back of rod) with provision for limiting its amplitude of pitch, showed a development of pitching and rolling oscillations at low air speeds when the rigid model surface was allowed to pitch freely as little as  $1^\circ$  about its flexible cantilever support. When the surface was held rigid in pitch at  $0^\circ$  by clamping it to the supporting flexible rod, no oscillations developed and any forced oscillations were damped out. But it was observed that the very turbulent wake from the body of a person in the tunnel in front of the model gave it irregular rolling oscillations even though the surface was rigid in pitch. However, when the model of the MO-1 airplane was held fixed at various attitudes in front of this surface rigid in pitch but flexible in roll, no marked oscillations occurred.

Excepting surfaces exhibiting reversible autorotation and perhaps any exposed to unusually turbulent airflow, the foregoing tests seem to indicate that a surface supported on a single cantilever spar, irrespective of the center of mass or center of pressure positions, will not be susceptible of reinforced aerodynamic oscillations, even though free to pitch about the spar, if the transverse flexure of the spar is resisted; or, even though free to roll with transverse flexure of the spar, if a material distortion or displacement of the surface in pitch is prevented.

Since the relations of the centers of mass and of pressure to the main cantilever support of a wing, found in these tests to resist sustained oscillations of a rolling and pitching surface, do not normally occur in ordinary plane and cambered surfaces at usual flying attitudes, and their alteration for stability might not often be convenient or economical, it seemed that structural design for the prevention of surface distortion would be the simpler and more practical method of precluding the aerodynamic flutter of cantilever wings or airfoils.

So, further wind tunnel tests were next made on a somewhat crude reproduction of a two-spar tail plane structure (fig. 4) consisting of a wooden vise in which were clamped by their ends two wooden strips of rectangular section, 18 inches long, set parallel to each other about 6 inches



apart, and having a heavy cloth sack stretched taut over them, forming a flat rectangular surface. The base of the vise was fitted with a short  $\frac{3}{8}$ -inch spindle at its center for clamping in the chuck of the balance shaft, thus mounting the model in the tunnel with the surface vertical, and permitting ready changes in angle of attack, by rotating the balance-shaft.

A variation in spar stiffness was obtained by using wooden strips of different breadths and depths. These strips varied in breadth from 2 inches to  $\frac{1}{2}$  inch, and in depth from  $\frac{1}{2}$  inch to  $\frac{1}{8}$  inch. They were cut from the same block of white pine, and their relative stiffness was figured, according to the usual engineering formula, to vary directly as the breadth and the cube of the depth.

In trying different methods for keeping the cloth taut over the ends of the spars in the tests on this model, it was found that any bracing of the spar ends or reinforcement of their cloth covering with heavy paper or cardboard interfered with their independent flexure and tended to prevent oscillations of the structure, while any slack in the cloth covering caused it to flutter and precipitated violent oscillations of the structure for all spar stiffness ratios. On account of these and other indefinite circumstances the performance of the model could not be always satisfactorily controlled, but it nevertheless illustrated well the type of oscillation which may occur in a tail surface that materially distorts or warps under its air or inertia loads. The model, however, can not be regarded as a true duplicate of a tail surface structure, on account of the unusual location of the spars at the extreme fore and aft portions of the surface and the lack of interconnecting ribs.

All of the surface oscillations observed in the tests on this model developed between the air speeds of 25 and 40 miles an hour at or within  $1^\circ$  or  $2^\circ$  of the null or no-lift attitude of the surface, with the two supporting spars always vibrating in lag phase. In general, the observations indicated that the stiffer the spars for a given relative stiffness, the higher the speed required

to precipitate the resonant vibration. The relative stiffness of the two spars, however, did not seem to influence materially the wind speed required to start oscillations, as resonant vibrations of the surface were obtained at nearly the same speeds for the same forward spar, when the rear spar stiffness was less than, equal to, and greater than the stiffness of the forward spar. It was noted that the entire vibration could in most cases be stopped by steadying either spar at its tip, or by pitching the surface to angles beyond  $2^\circ$  or  $3^\circ$  of the zero-lift attitude. But, in some cases when the rear spar was extremely flexible, the rear portion of the surface continued to oscillate about the zero-lift setting, even when the forward spar was stopped; and on reinforcing the surface of this structure with cardboard, slight vibrations of the weak rear spar of very small amplitude were observed for several angles beyond the vicinity of the zero-lift position, at which the violent resonant oscillations of the free structure always occurred. When the vise, grasping the spars, was removed from the balance-shaft and more rigidly supported by screwing it fast to the tunnel floor, the oscillations of the structure appeared to be precipitated at slightly lower air speed than on the more flexible shaft support.

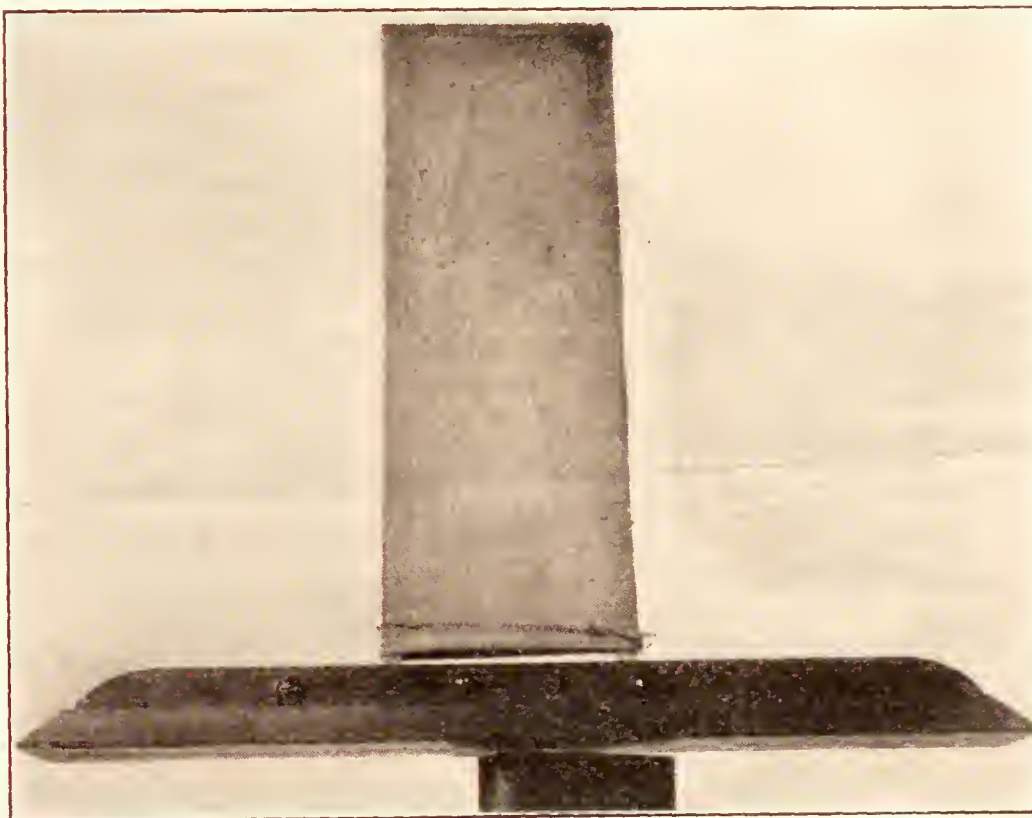


FIG. 4.—Warpable two-spar surface



Irrespective of any incidental observations, however, the important points noted in these tests were, that in every case the oscillations of the cantilever surface structure were precipitated and reinforced by the occurrence of a warpage in the surface due to the unequal or opposite deflection of the supporting spars under the interaction of the air and inertia forces of the system, and that any reinforcement of the surface covering or rigid interconnection of the spars at their tips which precluded their independent flexure and vibration tended to prevent sustained oscillation of the structure. Also, another important observation, previously intimated, and here emphasized on account of its special bearing on structural design to prevent airfoil flutter, discussed later, is that distortable cantilever surfaces are susceptible of dangerous oscillations only at attitudes in the vicinity of the no-lift setting, and comparatively free from such oscillations at higher angles.

It would therefore seem that, if the spars of full-size tail surfaces and other cantilever airfoil structures were designed with sufficient flexural stiffness to resist their stresses with small deflections, and with such a relative stiffness that their tips would deflect about equally under their stresses at small-angle flying attitudes, there would be no possibility, providing the elevators were rigidly interconnected, of the occurrence of a distortion of the surface in pitch, which would start any violent oscillations in roll.

In an attempt to obtain some idea of the relative stiffness of spars necessary in the MO-1 tail plane to give equal deflection with no surface distortion under the normal air loading at small angles, calculations to this effect were made, using center of pressure data from a special wind tunnel test at 40 miles an hour on a rectangular wooden model of the MO-1 tail plane profile (fig. 7, Part III) and taking into account the oblique leading edge of the surface on the full-size plane and the consequent inclination of the center of pressure line to the spars. The tail plane dimensions and location of the spars were obtained from blueprints of the full-size member.

The relation of the maximum bending moments for the two spars (fig. 8, Part III) obtained from these calculations, indicates that the ratio of the rear and forward spar elastic coefficients for this surface should be between 3 and 4 for minimum distortion under the normal air loading, instead of 17 as actually present. This means that the rear spar should be between  $\frac{1}{4}$  and  $\frac{1}{3}$  as stiff as the forward spar for small relative spar deflection and minimum surface warpage. These values are for the maximum forward location of the center of pressure and neutral elevators. When the elevators are turned from the neutral position the center of pressure of the surface travels farther backward, and hence a relatively stiffer rear spar than is specified above would then be required for no surface warpage. But by giving the stronger spar sufficient stiffness to resist its maximum stress with small deflection for the rearmost center of pressure position, the former spar stiffness ratios may be used and the surface still confined within small allowable distortion limits for all normal attitudes.

The principal formulas used in stress calculations for the design of cantilever wing spars for equal or minimum relative deflections, and the data for their application to the MO-1 tail plane with the final results, are presented in Part III of this report. In this case only the air loading of the surface has been considered, as in most cases when the center of pressure line lies off of the forward spar and the spar stiffness ratio for no surface warpage is small, the strength and stiffness of structure required to safely carry the air loading with small relative spar deflections and minimum surface distortion will provide sufficient stiffness to prevent any material distortion of the surface under the inertia loading. However, when the center of pressure line lies along the forward spar, or is so related to it as to give a large spar stiffness ratio for no surface warpage, and thus require a relatively weak rear spar to balance the surface air loading, it is likely that a stronger rear spar will be required to provide sufficient stiffness to confine the surface within small distortion limits under a possible inertia load; and if the original spar stiffness ratio were still maintained a stronger and stiffer forward spar than is really necessary to carry the air load would be demanded. In other words, the relative spar stiffness required for no surface distortion under the air loads and the inertia loads taken separately, may often be quite different on account of the different positions of application of these loads relative to



the spars, and structural economy necessitates that a compromise be effected between them in arriving at the minimum spar stiffness required to confine the surface within its small allowable distortion limits under either load.

Also, on account of the shift of the center of pressure of an airfoil along the chord with changing angle of attack each attitude of the surface would require a different spar stiffness ratio for no warpage. This fact, however, should cause no perplexity, since the preceding tests indicate that surface warpage is conducive to dangerous flutter only at surface attitudes in the vicinity of the zero-lift position, and for this reason is not particularly objectionable at higher angles. The spar stiffness ratio used to prevent airfoil warpage and consequent flutter should therefore be derived from the center of pressure location for small angle attitudes around the zero-lift setting.

In consideration of the conflicting requirements connected with the separate center of mass and center of pressure positions, it may be stated in general that, for economic design of spars to prevent flutter in cantilever airfoil structures, the weaker spar should always be stiff enough to resist possible inertia loads with small deflections, and the stronger spar stiff enough to resist possible air loads with perhaps somewhat larger deflections, while at the same time the relative spar stiffness required for minimum surface warpage under normal air loads at small flying angles is maintained at or near its estimated value whenever the air load stresses on the weaker spar exceed the inertia load stresses on this spar, but altered for reverse conditions, as the maximum inertia stress and permissible deflection of the weaker spar demands.

By thus roughly proportioning the stiffness of wing and tail plane spars to their received stresses, with special attention to airfoils having tapering plan forms and consequent diagonal loading, it is believed a minimum value of spar stiffness to prevent any dangerous surface warpage will be obtained, which will result in a more economic and lighter spar structure than could otherwise be effected, while at the same time eliminating the possibility of airfoil flutter. For, with the additional torsional rigidity furnished by the ribs and surface covering of a wing or tail plane structure, if the spars are given the proper relative stiffness to deflect as nearly equally as possible under their received loads, their actual stiffness need not be great, since flexure of the surface without twisting is not conducive to flutter.

### CONCLUSIONS

1. The airflow over the MO-1 model airplane, especially in the vicinity of the tail plane, is apparently not sufficiently disturbed to produce any marked rhythmic oscillations of the rigid tail unit flexibly hinged to the fuselage about its fore and aft axis. The type of airflow about this model is very similar to, if not better than, that about an analogous model of the Fokker FT airplane, whose wings or tail plane have never been reported to flutter in flight.

2. Excepting surfaces having forms or attitudes which exhibit the phenomena of reversible autorotation, a surface that deflects under its received loads about an axis along the wind without otherwise turning or distorting will not be susceptible of sustained oscillations unless it be exposed to exceptionally turbulent, undulatory, or gusty airflow. (Pt. II.)

3. A cantilever surface, such as an ordinary wing or tail plane, which, under its received loads at small, high-speed angles of attack experiences a differential deflection of its supporting spars, may, in perfectly smooth airflow, become susceptible of sustained oscillations, which may attain dangerous amplitudes as the surface approaches its no-lift attitude. The torsional deformation of surface entailed by a differential spar deflection is not so dangerous, however, at large, low-speed angles of attack.

4. The aerodynamic flutter of cantilever airfoil structures may be obviated by locating the center of mass of the system in or forward of the main supporting spar with the center of pressure aft of this member (Pt. II); or, more practically, by providing for sufficient structural rigidity to prevent any material torsional deformation of the surface under its received loads at high speed flying angles. Formulas for estimating the most economic relative spar stiffness for the latter design are given in Part III.



5. The vibration of the MO-1 tail plane results mostly from the large inequality of the ratios of stiffness to bending moment for the two supporting spars; wherefore these spars deflect unequally and entail sufficient surface deformation to precipitate sustained oscillations of the cantilever structure.

6. The vibration of the MO-1 tail plane may be economically minimized by giving its spars the proper relative stiffness required by their bending moment ratios to cause them to deflect about equally under their received loads in normal high speed flight. Calculations (Pt. III) for the spar stresses of this surface show that the rear spar should have somewhere around  $\frac{1}{3}$  or  $\frac{1}{4}$  the stiffness of the forward spar for minimum differential spar deflection, instead of  $\frac{1}{17}$ , as found present by spar deflection tests on the full-size MO-1 tail plane.

With the stiffness of the spars correctly proportioned to their received moments it is possible that the torsional rigidity of the surface supplied by the connecting ribs and covering will permit the use of a less stiff forward spar than now present, thus lowering the weight of the structure, while still preventing any objectionable surface deformation that might be conducive to vibrations.



# REPORT No. 285

## A STUDY OF WING FLUTTER

### PART II

### THEORY OF OSCILLATIONS OF AN AIRFOIL IN PITCH AND ROLL

By A. F. ZAHM

#### PREFACE

Apropos of Part I the possible types of small oscillation, in a uniform wind, of a rigid airfoil about a longitudinal or transverse axis, round which it elastically pivots, are here analyzed. The more general cases when warpage and flexure occur are left for further consideration.

Figure 5 illustrates the assumed conditions for the airfoil. Subject to moments of wind and elastic torsion it can be assumed to oscillate in roll, pitch, or both at once. We treat the three motions successively for cases of small displacement from equilibrium.

#### MOTION ABOUT X AXIS

The oscillation in roll is given by

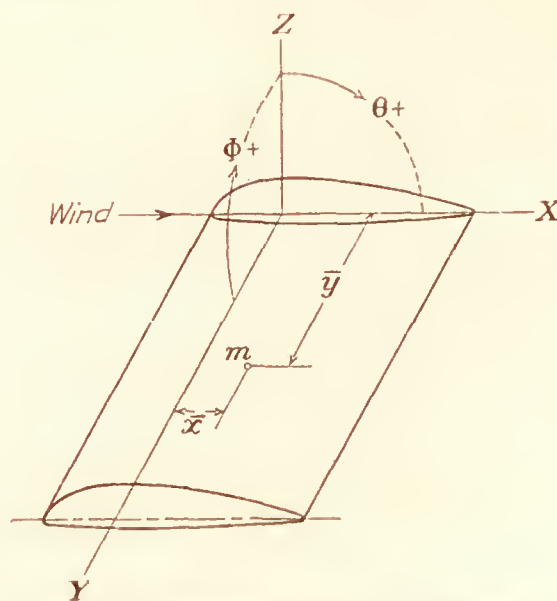


FIG. 5. Assumed conditions for the airfoil

- $m$  = mass of wing, with centroid at  $\bar{x}, \bar{y}$ .
- $A, B$  = moments of inertia about  $X, Y$  axes.
- $\Phi, \dot{\Phi}, \ddot{\Phi}$  = angle, speed, acceleration of wing about  $X$ .
- $\Theta, \dot{\Theta}, \ddot{\Theta}$  = angle, speed, acceleration of wing about  $Y$ .
- $\ddot{y} \pm \ddot{x}\dot{\Theta}$  = acceleration of  $m$ ;  $m(\ddot{y}^2 \pm \ddot{x}\dot{\Theta})$  = moment of  $m$  about  $X$ .
- $L, M$  = moments about  $X, Y$ , due to uniform wind.
- $L_\theta, L_p = \partial L / \partial \Theta, \partial L / \partial p$ , where  $p = \dot{\Phi} = d\Phi/dt$ .
- $M_\theta, M_q = \partial M / \partial \Theta, \partial M / \partial q$ , where  $q = \dot{\Theta} = d\Theta/dt$ .

$$A\ddot{\Phi} = L_p\dot{\Phi} - k_\Phi\Theta \quad (1)$$

where  $L_p = \partial L / \partial p$  \* is the damping derivative,  $k_\Phi = -\partial L / \partial \Phi$  the elastic restoring moment per radian of  $\Phi$ . The damping coefficient,  $L_p/A$  is positive for autorotative surfaces, zero or negative for others;  $k_\Phi/A$  is always negative and finite.

\* In his Stability in Aviation, Bryan writes  $L_p = -\partial L / \partial p$ , a convention not so much used by his followers. Here we use the standard symbols adopted by the National Advisory Committee for Aeronautics.



From textbooks we derive the following properties of (1): for  $L_p = 0$  the motion is simple harmonic; for  $L_p < 0$  it is either damped harmonic or subsiding aperiodic; for  $L_p > 0$  it is divergent either oscillatingly or continuously. Hence to secure decay of vibration the airfoil should at all wind speeds, have  $L_p < 0$ , viz, antirotative.

#### MOTION ABOUT Y AXIS

The oscillation in pitch is

$$B\ddot{\Theta} = M_q\dot{\Theta} - (k_\Theta - M_\Theta)\Theta \quad (2)$$

where  $k_\Theta$  is the elastic moment per unit of  $\Theta$ . The damping derivative  $M_q$  is usually negative or antirotative; the coefficient of  $\Theta$  is negative except when  $k_\Theta < M_\Theta$ .

From textbooks we derive the following properties of (2): For  $k_\Theta - M_\Theta = 0$  the motion continuously asymptotes a finite limit; for  $k_\Theta - M_\Theta > 0$  it is either damped harmonic or subsiding aperiodic; for  $k_\Theta - M_\Theta < 0$  it diverges continuously. Hence to insure decay of vibration in pitch the airfoil should, at all wind speeds have  $k_\Theta - M_\Theta > 0$ .

#### MOTIONS ABOUT X, Y

If the  $\Phi$ ,  $\Theta$  motions are simultaneous they add to (1) the moments  $m\bar{x}\bar{y}\ddot{\Theta} - L_\Theta\Theta$ ; to (2) the moment  $m\bar{x}\bar{y}\ddot{\Phi}$ .† Thus,

$$A\ddot{\Phi} - L_p\dot{\Phi} + k_\Phi\Phi + m\bar{x}\bar{y}\ddot{\Theta} - L_\Theta\Theta = 0 \quad (3)$$

$$B\ddot{\Theta} - M_q\dot{\Theta} + (k_\Theta - M_\Theta)\Theta + m\bar{x}\bar{y}\ddot{\Phi} = 0$$

where all the coefficients are positive, save possibly  $L_p$ ,  $L_\Theta$ ,  $M_q$ ,  $M_\Theta$ .

To solve (3) first put therein  $D = d/dt$ : thus

$$(AD^2 - L_pD + k_\Phi)\Phi + (m\bar{x}\bar{y}D^2 - L_\Theta)\Theta = 0 \quad (3)$$

$$m\bar{x}\bar{y}D^2\Phi + [BD^2 - M_qD + (k_\Theta - M_\Theta)]\Theta = 0$$

whence eliminating  $\Theta$  gives

$$\{(AD^2 - L_pD + k_\Phi)[BD^2 - M_qD + (k_\Theta - M_\Theta)] - (m\bar{x}\bar{y})^2D^4 + L_\Theta m\bar{x}\bar{y}D^2\}\Phi = 0 \quad (4)$$

which is a linear differential equation in  $\Phi$  with constant coefficients, expressing the airfoil motion about  $X$ . Putting  $\Theta$  for  $\Phi$  in (4) gives the motion about  $Y$ . We now can solve (4) for the amplitude; but to ascertain merely whether the motion is stable or not it suffices to examine the coefficients of (4), as in the next three paragraphs.

#### CRITERIA FOR STABILITY ABOUT X, Y

If  $\bar{x}$  or  $m\bar{x}\bar{y}D^2 - L_\Theta$  is zero, the last two terms of (4) vanish, leaving in form the simple product of (1), (2). If for this case, (1), (2) both are stable their resultant (4) must be so. Now  $\bar{x} = 0$  if the airfoil centroid is on the pitch axis  $Y$ ; and  $L_\Theta = \partial L / \partial \Theta = 0$  for the burble incidence. Frequently  $m\bar{x}\bar{y}\ddot{\Theta}$  is small and negligible. In this case we conclude that if the centroid is on the  $Y$  axis, or if the equilibrium incidence is burble, the simultaneous small motions (3) about  $X$  and  $Y$  are stable if the uniaxial motions (1), (2) are so.

If  $\bar{x}$  or  $m\bar{x}\bar{y}D^2 - L_\Theta$  is not zero, we examine the auxiliary equation of (4), viz

$$aD^4 + bD^3 + cD^2 + dD + e = 0 \quad (5)$$

where  $a = AB - (m\bar{x}\bar{y})^2$ ;  $b = -AM_q - BL_p$ ;  $c = A(k_\Theta - M_\Theta) + L_pM_q + m\bar{x}\bar{y}L_\Theta$ ;  $d = -L_p(k_\Theta - M_\Theta) - k_\Phi M_q$ ;  $e = k_\Phi(k_\Theta - M_\Theta)$ . By Routh's rule (4) is stable if  $a$ ,  $b$ ,  $c$ ,  $d$ ,  $e$  and Routh's discriminant  $bcd - ad^2 - eb^2$  all are positive.

† For closer estimate  $-M_p\dot{\Phi}$  can be added here. It vanishes for well-known conditions.



For usual conditions  $a, b, c, d, e$  are positive. Putting the given values of these in the discriminant one finds<sup>1</sup> it positive if

$$-L_p M_q / L_0 > m \bar{x} \bar{y} \quad (6)$$

which therefore is a criterion of stability for the motion (4). One device for realizing (6) is to make the centroidal distance  $\bar{x} \leq 0$ , or small positive; another is to magnify  $-L_p M_q / L_0$ .

#### SUMMARY

The present analysis suggests the following rules of design to obviate airfoil flutter.

1. Use an airfoil having  $L_p$  negative, to avoid autorotative tendency; choose one with  $-L_p M_q / L_0 > m \bar{x} \bar{y}$ .
2. Make  $\bar{x} \leq 0$ , or small if positive; viz., avoid placing the airfoil centroid far aft of the axis of pitch rotation.
3. Make  $k_\theta > M_\theta$ ; viz., make the coefficient of elastic pitching moment exceed that of wind disturbing moment at all speeds.

In practice these stability devices may have to be compromised with other design provisions.

#### ROTATIONAL AMPLITUDE, SPEED, PERIOD

For the oscillations (1), (2) about a single axis the amplitude, speed, and period can be found directly by well-known procedure. For the double motion (3) one finds by solution of (4).

$$\Phi = C_1 \Theta^{\lambda_1 t} + C_2 \Theta^{\lambda_2 t} + C_3 \Theta^{\lambda_3 t} + C_4 \Theta^{\lambda_4 t} \quad (7)$$

where  $\lambda_1, \lambda_2, \lambda_3, \lambda_4$  are the four roots of (5), and the  $C$ 's are integration constants determined by the initial conditions. Putting  $\Theta$  for  $\Phi$  in (4) and solving gives  $\Theta$  in the form (7) except for different integration constants. The plot of  $\Phi$  or  $\Theta$  against  $t$  is in general the resultant of four exponential or sine curves which represent the four component terms of (7). Examples of such component curves are given in works on aircraft stability.

#### CASE OF THE NONRIGID AIRFOIL

In practice a fluttering airfoil pitches and rolls by structural deformation, say by flap motion or spar flexure. In this latter case the rotation angles  $\Phi, \Theta$  are roughly those of the median airfoil section, and the damping coefficients in (1), (2) may be written  $h_p + L_p, h_q + M_q$ , where the  $h$ 's are viscous moments per unit of  $p, q$ , due to internal friction of the airfoil structure. The magnitude of  $k_\phi, k_\theta, h_p, h_q$ , could be determined in a full-scale craft, but not so well predicted from a model test, except perhaps when both model and full-scale were of uniform material besides being structurally similar. The case for a wing and aileron vibrating jointly or independently is treated in the cited N. A. C. A. Mem. No. 223, "On the Stability of Oscillations of an Airplane Wing," by A. C. Von Baumhauer and C. Koning. See also "Wing Flutter," by R. A. Frazer, Reports and Memoranda No. 1042, British Aeronautical Research Committee.

#### PRACTICAL DETERMINATION OF $L_p, M_q$

The damping derivatives,  $L_p, M_q$ , can best be found experimentally, say by testing a wing model with an oscillator in a uniform air stream. They can also be estimated as explained in textbooks, e. g. Wilson's Aeronautics, article 40; ready formulas for  $L_p, M_q$ , to suit various practical shapes and loadings, may thus be derived.

For example, assuming the load uniform along  $Y$ , one finds  $L = 4/3 \cdot s \bar{y}^3 / V$ , where  $V$  is the flight speed, and  $s = dL/d\theta$  is the slope of the lift curve for the particular wing. Again assuming an elliptic loading along  $Y$  one finds  $L_p = s \bar{y}^3 / V$ .

In the general equations (1), (2) therefore, the damping derivatives are symbolized broadly by  $L_p, M_q$  rather than by more specific quantities applicable to but one wing type. Tables giving experimental values of  $L_p, M_q$  along with the usual wing characteristics for a few typical wing types, would be serviceable to aeronautical engineers.

<sup>1</sup> For a more detailed treatment, illustrated by experiment, the reader is referred to Tech. Mem. No. 223 of the National Advisory Committee for Aeronautics.







# REPORT No. 285

## A STUDY OF WING FLUTTER

---

### PART III

### DESIGN OF SPARS FOR EQUAL FLEXURE

By R. M. BEAR

---

#### PREFACE

The foregoing text shows that a cantilever airfoil, not reversibly autorotative, is void of flutter of its spars flex equally in the same direction under their received loads; e. g., if their ensuing curvatures are the same at corresponding sections. A method of designing the spars for such equal flexure when given the wing plan and profile is outlined in the ensuing text. By its use the minimum torsional rigidity of structure required to prevent flutter may be obtained with a maximum economy in material.

#### CURVATURE RATIO

By mechanics the elastic curvature at any beam section is  $1/R = M/EI$ , where  $R$  is the radius of curvature of the neutral surface,  $M$  the bending moment,  $E$  the modulus of elasticity,  $I$  the moment of inertia of the section area about its neutral axis. Hence for corresponding sections of two parallel spars,

$$\frac{\text{Curvature}_2}{\text{Curvature}_1} = \frac{R_1}{R_2} = \frac{M_2 E_1 I_1}{M_1 E_2 I_2} \quad (1)$$

Usually  $E_1 = E_2$ ; hence for equal flexure ( $R_1 = R_2$ ) the spars must be designed so that

$$I_1/I_2 = M_1/M_2 \quad (2)$$

#### STIFFNESS RATIO

The stiffnesses of the two spars at corresponding sections are as the bending moments there causing equal flexure; that is

$$\frac{\text{Stiffness}_1}{\text{Stiffness}_2} = \frac{M_1}{M_2} = \frac{I_1}{I_2} \quad (2a)$$

Since the deflection of a beam is a direct function of the curvature, the stiffnesses of beams are compared by comparing the loads they can carry with a given deflection, or the deflections at corresponding sections for a given loading.

#### STRESS RATIO

By mechanics the maximum unit fiber stress at any beam section is  $s = Me/I$ ,  $e$  being the distance of the outermost fiber from the neutral axis of the section. Hence for corresponding sections of the two spars,

$$\frac{\text{Stress}_1}{\text{Stress}_2} = \frac{s_1}{s_2} = \frac{M_1 e_1 I_2}{M_2 e_2 I_1} \quad (3)$$

and for equal flexure, from (2)

$$s_1/s_2 = e_1/e_2 \quad (4)$$



From this relation it is seen that if the spar of greater  $e$  is first designed for the maximum allowable unit stress,  $s_{\max.}$ , the other will have  $s < s_{\max.}$ , and hence a greater factor of safety and ample strength; but if the spar of lesser  $e$  is first designed for  $s_{\max.}$ , the other will have  $s > s_{\max.}$ , and be unsafe.

Therefore, to provide conveniently for structural safety, it is best, first to design the deeper spar for sufficient strength, and then the shallower spar for equal flexure.

#### STRENGTH RATIO

The strengths of the two spars at corresponding sections are inversely as the maximum unit fiber stresses there produced by a given bending moment. Hence, making  $M_1 = M_2$  in (3),

$$\frac{\text{Strength}_1}{\text{Strength}_2} = \frac{s_2}{s_1} = \frac{I_1 e_2}{I_2 e_1} \quad (5)$$

The strengths of beams are compared by comparing the loads they can carry with an assigned maximum unit fiber stress, or by comparing the maximum fiber stresses produced by an assigned loading.

#### RELATIONS OF STRENGTH AND STIFFNESS

If in (5)  $e_1 = e_2$ , the strength ratio equals the stiffness ratio in (2). For this condition the two beams have equal safety factors, and for the same permissible maximum depths, less weight than for  $e_1, e_2$  unequal. But, since the maximum depths of spars and hence also their least weights are determined by the airfoil profile depths, the relation of strength and stiffness ratios will vary with different airfoils and hence has no special significance.

#### GENERAL DESIGN PROCEDURE

In obtaining actual values for  $I_1, I_2$  in (2), the deeper spar is considered first, and its value of  $e_1$  selected, equal to or less than half the maximum wing depth. Then

$$I_1 = M_1 e_1 / s_{\max.} \quad (6)$$

whence, from (2)

$$I_2 = r_M M_1 e_1 / s_{\max.} = M_2 e_1 / s_{\max.} \quad (7)$$

where  $r_M = M_2 / M_1$ .

A suitable value of  $e_2 < e_1$ , corresponding to the wing depth is then chosen for the shallower spar.

As mentioned previously, this order of procedure will keep  $s_2 < s_{\max.}$  and the safety factor always above the assigned value, but not conversely.

#### SPAR STRESS EQUATIONS

To obtain  $M_1$  and  $M_2$  of the preceding formulas, the separate loadings of the two spars must be determined. In the ensuing text the fundamental equations and derived general formulas for loading intensity  $W$ , vertical shear  $Z$ , and bending moment  $M$ , for the two parallel spars of a cantilever airfoil with oblique leading edge and consequent diagonal loading, are presented, and their use illustrated in designing the MO-1 tail plane for minimum distortion at small angles of attack to prevent flutter.

Figure 6 is a diagram of an airfoil of the above-mentioned type, resembling the MO-1 tail plane in plan form. Referring to it and the indicated symbols the following equations are readily understood.



The equations for the condition of static equilibrium, assuming equal deflection of the two spars, are,

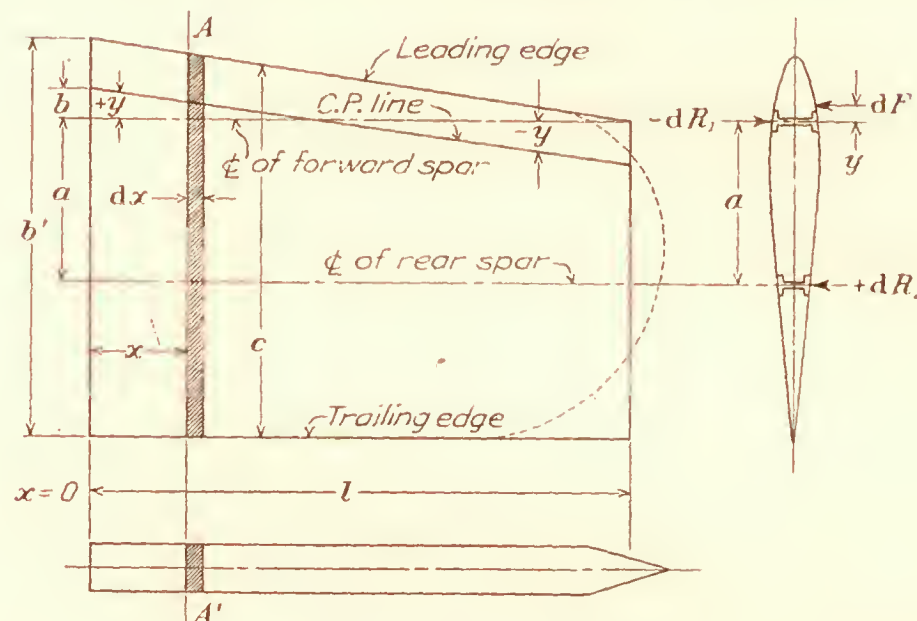


FIG. 6.—Diagram of airfoil

$A A' dx$  = any elementary transverse section of a tail plane or wing.  
 $dF$  = air force acting on the surface of this section at its center of pressure.  
 $dR_1$  = elementary reaction of forward spar at this section.  
 $dR_2$  = elementary reaction of rear spar at this section.

$$-dR_1 \cdot a = dF \cdot (a + y) \quad (8)$$

$$dR_2 \cdot a = dF \cdot y \quad (9)$$

The intensity of loading,  $W$  at any spar section is of opposite sign to the elementary reaction at this section. The equation for  $W$  is

$$W = -\frac{dR}{dx} \quad (10)$$

The equation for vertical shear  $Z$  at any spar section is

$$Z = \int_x^l W dx = - \int_x^l dR \quad (11)$$

The equation for bending moment,  $M$  at any spar section is

$$M = \int_x^l Z dx \quad (12)$$

The equation of the center of pressure line or load line for  $X$  axis along the forward spar axis is

$$y = sx + b \quad (13)$$

The equation of the airfoil leading edge line for  $X$  axis along the trailing edge line parallel to the spars is

$$c^* = s'x + b' \quad (14)$$

Also,

$$dF = C c dx \quad (15)$$

where  $C = 1/2 C_{NF} \rho V^2$ , and

$C_{NF}$  = coefficient of normal force,  $NF$  perpendicular to wing chord.

$\rho$  = air density in slugs per cubic feet.

$V$  = air speed in feet per second.

#### \* GENERAL FORMULAS FOR TAPERED WINGS

$c$  is the wing chord at any section. If the trailing edge of the wing is inclined at a slope  $s''$  to the spars, equation (14) becomes

$$c = (s' - s'')x + b' \quad (14)$$

By substituting in the deduced formulas for  $W$ ,  $Z$ , and  $M$ ,  $(s' - s'')$  for  $s'$ , these formulas become more general and apply to wings with leading edge and trailing edge both tapered.



## FORWARD SPAR STRESSES

Fundamental equations—

$$-dR_1.a = dF. (a + y) \quad (8)$$

$$dR_1.a = Ccdx. (a + sx + b) \quad (16)$$

$$dR_1.a = Cdx. (s'x + b') (a + sx + b) \quad (17)$$

$$dR_1 = \frac{C}{a} (asx. dx + ss'x^2. dx + bs'x. dx + b'a. dx + b'sx. dx + bb'. dx) \quad (17)$$

Loading intensity,  $W$ —

$$W_1 = -\frac{dR_1}{dx} \quad (10)$$

$$W_1 = \frac{C}{a} \{ ss'x^2 + x [s' (a + b) + sb'] + b' (a + b) \} \quad (18)$$

Vertical shear,  $Z$ —

$$Z_1 = -\int_x^l dR_1 = \int_x^l W_1 dx \quad (11)$$

$$Z_1 = \frac{C}{a} \left[ \frac{ss'}{3} (l^3 - x^3) + \frac{s'(a + b) + b's}{2} (l^2 - x^2) + b'(a + b) (l - x) \right] \quad (19)$$

Bending moment,  $M$ —

$$M_1 = \int_x^l Z_1 dx \quad (12)$$

$$M = \frac{C}{a} \left[ \frac{ss'}{12} (3l^4 - 4l^3x + x^4) + \frac{s'(a + b) + b's}{6} (2l^3 - 3l^2x + x^3) + \frac{b'(a + b)}{2} (l - x)^2 \right] \quad (20)$$

## REAR SPAR STRESSES

Fundamental equations—

$$dR_2.a = dF.y \quad (9)$$

$$dR_2.a = Ccdx. (sx + b) \quad (21)$$

$$dR_2.a = Cdx. (s'x + b') (sx + b) \quad (22)$$

$$dR_2 = \frac{C}{a} (ss'x^2. dx + b'sx. dx + bs'x. dx + bb'. dx) \quad (22)$$

Loading intensity,  $W$ —

$$W_2 = -\frac{dR_2}{dx} \quad (10)$$

$$W_2 = -\frac{C}{a} [ss'x^2 + x (sb' + s'b) + bb'] \quad (23)$$

Vertical shear,  $Z$ —

$$Z_2 = -\int_x^l dR_2 \quad (11)$$

$$Z_2 = -\frac{C}{a} \left[ \frac{ss'}{3} (l^3 - x^3) + \frac{b's + bs'}{2} (l^2 - x^2) + bb' (l - x) \right] \quad (24)$$

Bending moment,  $M$ —

$$M_2 = \int_x^l Z_2 dx \quad (12)$$

$$M_2 = -\frac{C}{a} \left[ \frac{ss'}{12} (3l^4 - 4l^3x + x^4) + \frac{b's + bs'}{6} (2l^3 - 3l^2x + x^3) + \frac{bb'}{2} (l - x)^2 \right] \quad (25)$$



SPAR STRESSES FOR SLOPES,  $s, s' = 0$ 

For a tail plane or wing with leading edge parallel to the spars,  $s$  and  $s'$  in the previous equations become 0, and the equations for the spar stresses are simplified as follows:

## FORWARD SPAR

$$W_1 = \frac{C}{a} b' (a + b) \quad (26)$$

$$Z_1 = \frac{C}{a} [b' (a + b) (l - x)] \quad (27)$$

$$M_1 = \frac{C}{a} \left[ \frac{b' (a + b)}{2} (l - x)^2 \right] \quad (28)$$

## REAR SPAR

$$W_2 = -\frac{C}{a} b b' \quad (29)$$

$$Z_2 = -\frac{C}{a} [b b' (l - x)] \quad (30)$$

$$M_2 = -\frac{C}{a} \left[ \frac{b b'}{2} (l - x)^2 \right] \quad (31)$$

SPAR STIFFNESS RATIO,  $r_M$ 

The ratio of the bending moments or the relative stiffness required for equal spar flexure then becomes from (28), (31), (2)

$$\frac{M_1}{M_2} = \frac{I_1}{I_2} = r_M = -\frac{a + b}{b} = -\left(\frac{a}{b} + 1\right) \quad (32)$$

THE  $\pm$  SIGNS

In the foregoing equations, the distance between the spars,  $a$  is always positive, and  $b$  positive or negative, depending on whether the center of pressure for  $x=0$  is forward or aft of the front spar axis.

## CONDITIONS FOR NO SURFACE WARPAGE

For equal flexure of the spars in the same direction, and hence no surface warpage,  $r_M$  must always be  $+$ ; i. e.,  $M_1, M_2$  must have like signs. This condition is most always fulfilled in the usual location of spars and is effected by so placing them that all or the greater part of the airfoil center of pressure line, or load line, lies between them.

In order that  $r_M$  always be  $+$  in (32),  $b$  must always be  $-$ , and numerically less than  $a$ . This condition fixes the center of pressure line between the spars, and for this special case of parallelism the spar loadings, shears, and bending moments all have like signs.

See Figure 9 in which  $a$  and  $b$  of the preceding equations are replaced by  $n$  and  $-x$ , and  $r_M = \eta = R_1/R_2$ .

## EQUATIONS FOR MO-1 TAIL PLANE

Substituting in the previous equations the following values obtained from aerodynamic data and design drawings for the MO-1 tail plane, (Table I; figs. 7, 8.)

$$\begin{array}{lll} s = -0.1290 & b = 0.0575 & a = 2.417 \\ s' = -0.1721 & b' = 6.448 & l = 6.33 \end{array}$$

the following equations are obtained.

## FORWARD SPAR

$$W_1 = C(0.0092x^2 - 0.5204x + 6.601)$$

$$Z_1 = C(0.2602x^2 - 0.0031x^3 - 6.601x + 32.14)$$

$$M_1 = C(0.00077x^4 - 0.0868x^3 + 3.301x^2 - 32.14x + 91.94)$$

## REAR SPAR

$$W_2 = C(0.3483x - 0.0092x^2 - 0.1534)$$

$$Z_2 = C(0.0031x^3 - 0.1741x^2 + 0.1534x + 5.231)$$

$$M_2 = C(0.0580x^3 - 0.00077x^4 - 0.0767x^2 - 5.231x + 22.69)$$

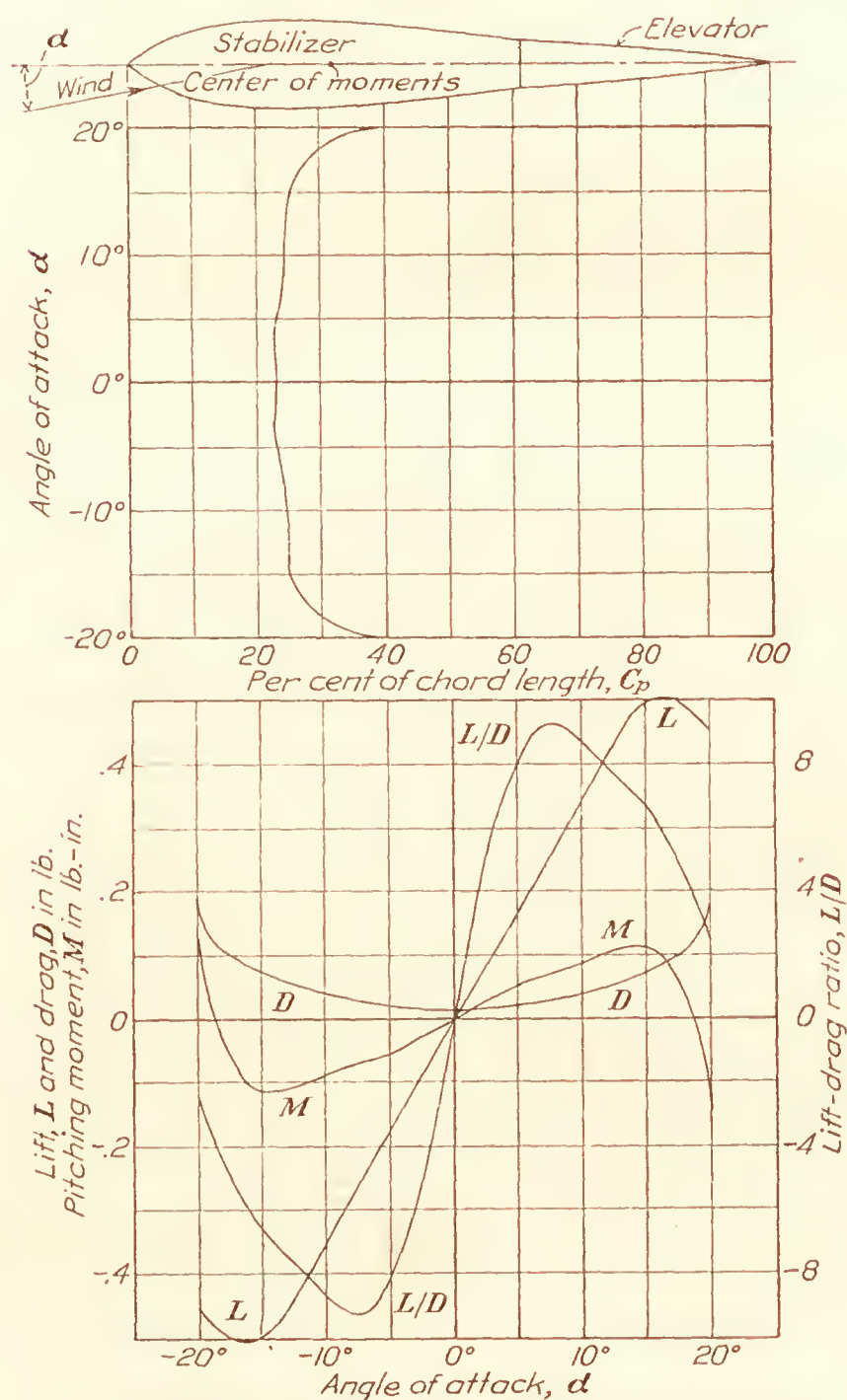


FIG. 7.—Profile characteristics. Air speed 40 miles per hour. Original data corrected for model asymmetry

The maximum bending moments occur at  $x=0$ , and by (2a) the spar stiffness ratio here required for equal flexure and no flutter is

$$r_M = \frac{M_1}{M_2} = \frac{I_1}{I_2} = \frac{91.94}{22.69} = 4.05$$

This ratio decreases as  $x$  increases, as shown in Figure 8.

For  $l=7.00$  instead of 6.33 the above equations becom



## FORWARD SPAR

$W_1$  = same as before

$$Z_1 = C(0.2602x^2 - 0.0031x^5 - 6.601x + 34.51)$$

$$M_1 = C(0.00077x^4 - 0.0868x^5 + 3.301x^2 - 34.51x + 107.7)$$

## REAR SPAR

$W_2$  = same as before

$$Z_2 = C(0.0031x^3 - 0.1741x^2 + 0.1534x + 6.410)$$

$$M_2 = C(0.0580x^3 - 0.00077x^4 - 0.0767x^2 - 6.410x + 30.55)$$

and

$$r_M = \frac{M_1}{M_2} = \frac{I_1}{I_2} = \frac{107.7}{30.55} = 3.53.$$

For several corresponding spar sections, the variable factors in parentheses in the above equations for  $l=6.33$  were evaluated and are given with their ratios in Table II. These data are plotted in Figure 8.

TABLE I.—Air forces, moments and center of pressure for MO-1 horizontal tail plane section at 40 miles per hour

Twin camber section.

Elevator neutral.

Angle of attack $\alpha$	Lift $L$	Drag $D$	Lift/drag, $L/D$	Pitching moment about $M$ axis <sup>†</sup>	Center of pressure, per cent chord length, $C_p$
°	Pounds	Pounds		Lb.-in.	
0	0.0	0.019	0.0	0.0	22.7
1	.038	.019	2.06	+.011	22.8
2	.079	.019	4.25	.021	22.8
3	.117	.020	5.94	.032	22.5
4	.155	.022	7.00	.044	22.1
6	.238	.027	8.92	.062	23.2
8	.323	.035	9.26	.074	23.9
10	.407	.046	8.75	.090	24.1
12	.488	.062	7.92	.102	24.4
14	.557	.078	7.15	.112	24.7
16	.589	.098	6.04	.104	25.5
18	.574	.125	4.57	+.037	28.7
20	.527	.215	2.45	−.141	38.5

<sup>†</sup>  $M$  axis of model holder is on chord center line, 31.1 per cent of chord length aft of the leading edge.

Dimensions of model, 8.18 by 3.218 inches.

$$C_L = 1.337 L$$

$$C_D = 1.337 D$$

$$K_y = 0.00342 L$$

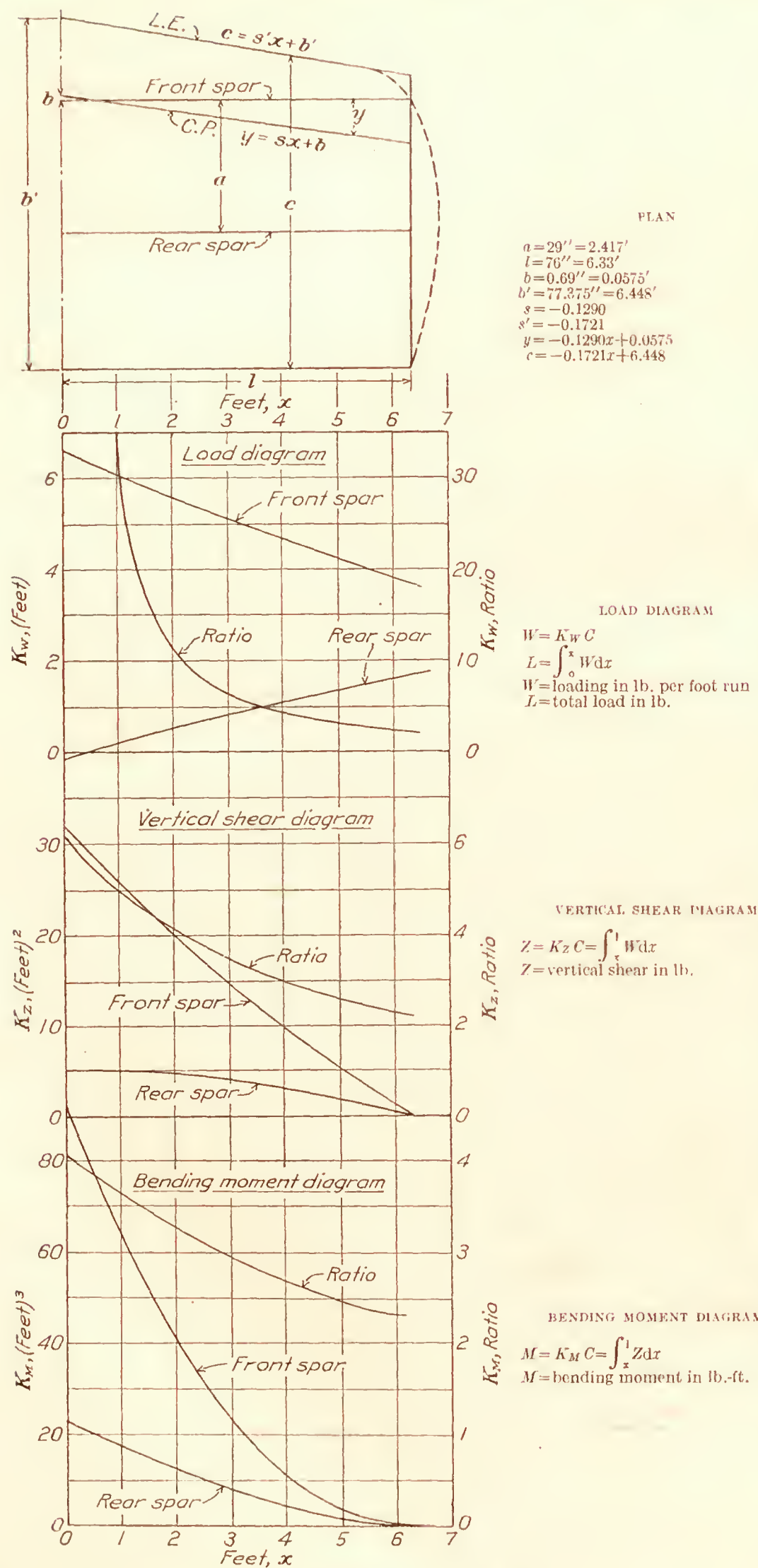
$$K_x = 0.00342 D$$

$$C_R = \sqrt{C_L^2 + C_D^2}$$

$$\tan \theta = C_L / C_D$$

$$C_{NF} = C_R \sin (\alpha + \theta)$$

$$C_{NF} = \text{coefficient of normal air force } NF \perp \text{ to wing chord.}$$





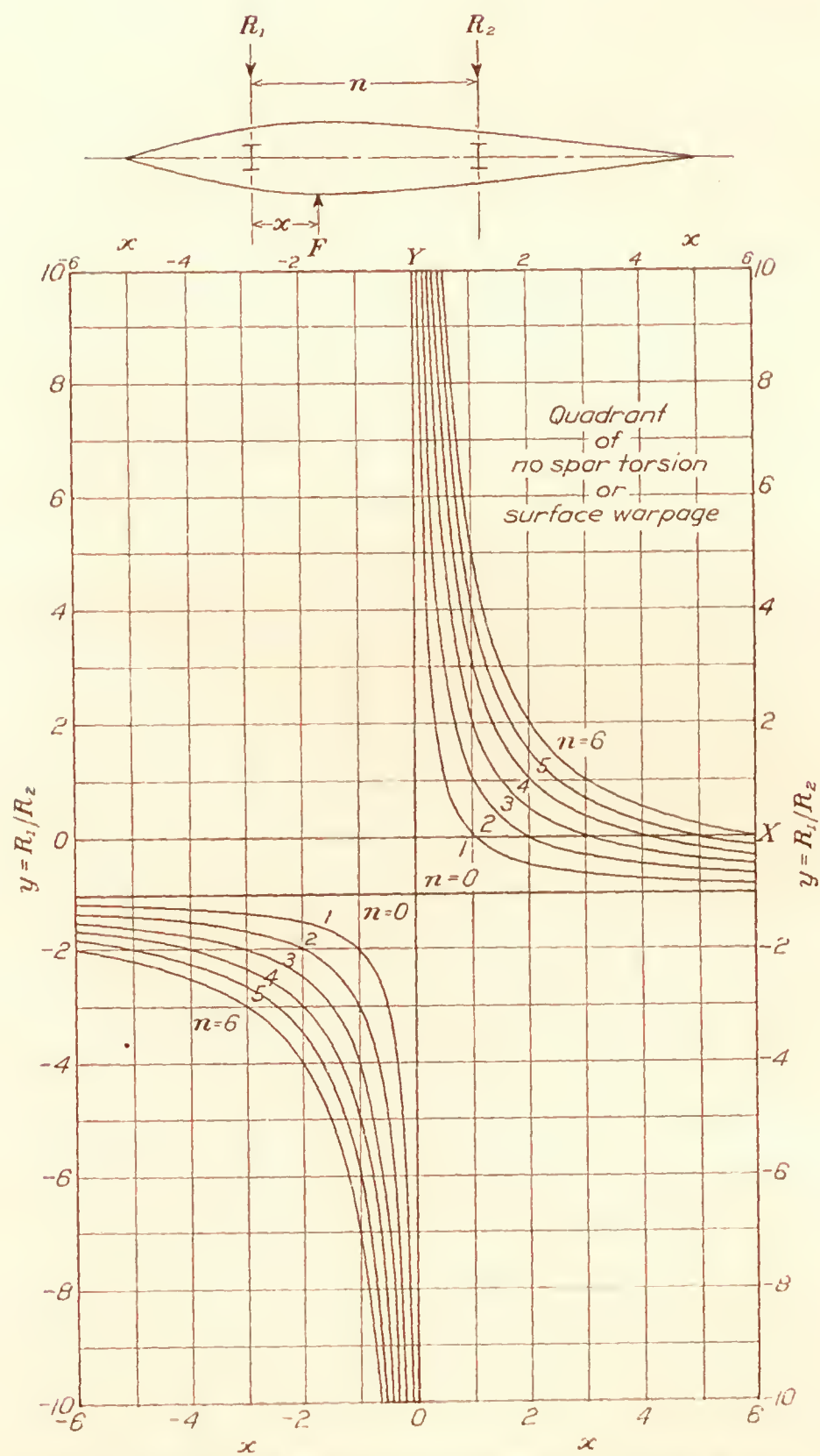


FIG. 9.—Rectangular two-spar airfoil spar-stiffness ratios for equal flexure  
For equal spar deflection under load  $F$ ,

$$R_1/R_2 = y = \frac{n-x}{x}$$

For  $+x < n$ ,  $y$  is always  $+$  and the spars flex equally in the same direction without torsion or surface warpage.

For  $+x = n$ , and any  $-x$ ,  $y$  is always  $-$  and the spars flex equally in opposite direction with torsion and surface warpage.

TABLE II.—*Spar stress factors and ratios for design of MO-1 tail plane for equal spar flexure under surface air loading*<sup>1</sup>

Distance along span $x$	Forward spar			Rear spar			Ratios		
	$K_W$	$K_M$	$K_Z$	$K_W$	$K_M$	$K_Z$	$r_W$	$r_M$	$r_Z$
<i>Feet</i>									
0	+6.60	+91.94	+32.14	-0.15	+22.69	+5.23	-43.05	+4.05	+6.14
1	6.09	63.02	25.79	+0.19	17.44	5.21	+32.76	3.61	4.95
2	5.60	40.19	19.95	0.51	12.37	4.87	11.05	3.25	4.10
3	5.12	22.96	14.59	0.81	7.81	4.21	6.32	2.94	3.47
4	4.67	10.85	9.70	1.09	4.06	3.25	4.28	2.67	2.98
5	4.23	3.41	5.25	1.36	1.39	2.03	3.11	2.45	2.59
6	3.81	0.20	+1.24	1.60	0.09	+0.54	2.38	2.30	2.27
6.33	3.68	0.00	0.00	1.68	0.00	0.00	2.19	2.30	2.20
6.5	+3.61	+0.05	-0.62	+1.72	+0.02	-0.29	+2.10	+2.37	+2.14

<sup>1</sup> For surface span, 6.33 feet and center of pressure 22.7 per cent of chord from leading edge. See Figure 8.

$$W = K_W C \quad Z = K_Z C \quad M = K_M C \quad C = \frac{1}{2} C_{NF} \rho V^2$$

## FORWARD SPAR

$$K_W = 0.00918x^2 - 0.5204x + 6.6014$$

$$K_M = 0.00077x^4 - 0.0868x^3 + 3.3007x^2 - 32.1364x + 91.9446$$

$$K_Z = 0.2602x^2 - 0.0031x^3 - 6.6014x + 32.1364$$

## REAR SPAR

$$K_W = 0.3483x - 0.00918x^2 - 0.1534$$

$$K_M = 0.0580x^3 - 0.00077x^4 - 0.0767x^2 - 5.2309x + 22.6890$$

$$K_Z = 0.0031x^3 - 0.1741x^2 + 0.1534x + 5.2309$$

$W$  = loading in pounds per foot run

$M$  = bending moment in foot-pounds

$Z$  = vertical shear in pounds

AERODYNAMICAL LABORATORY,

BUREAU OF CONSTRUCTION AND REPAIR, UNITED STATES NAVY,

WASHINGTON, D. C., May 11, 1927.



---

# REPORT No. 286

---

## AERODYNAMIC CHARACTERISTICS OF AIRFOILS—V

### CONTINUATION OF REPORTS

Nos. 93, 124, 182, AND 244

By

NATIONAL ADVISORY COMMITTEE  
FOR AERONAUTICS

---

REPRINT OF REPORT No. 286, ORIGINALLY PUBLISHED APRIL, 1928

---





## TABLE OF CONTENTS

---

	Page
Introduction.....	139
Transformation constants.....	139
Chart index.....	141
Index of abbreviations.....	141
Group index.....	142-143
Alphabetical index.....	144
Airfoil sections.....	145-178
United States sections.....	145-147
British sections.....	147-148
German sections.....	149-164
French sections.....	164-171
Belgium sections.....	171-172
Italian sections.....	172-178
Tables of ordinates not given on the individual characteristic sheets.....	179
Charts numbers 17, 18, 19, 20.....	180-183





# REPORT No. 286

## AERODYNAMIC CHARACTERISTICS OF AIRFOILS—V

CONTINUATION OF REPORTS Nos. 93, 124, 182, and 244

By THE NATIONAL ADVISORY COMMITTEE FOR AERONAUTICS

REPRINT OF REPORT No. 286, ORIGINALLY PUBLISHED APRIL, 1928

### INTRODUCTION

This collection of data on airfoils has been made from the published reports of a number of the leading aerodynamic laboratories of this country and Europe.<sup>1</sup> The information which was originally expressed according to the different customs of the several laboratories is here presented in a uniform series of charts and tables suitable for the use of designing engineers and for purposes of general reference.

It is a well-known fact that the results obtained in different laboratories, because of their individual methods of testing, are not strictly comparable even if proper scale corrections for size of model and speed of test are supplied. It is, therefore, unwise to compare too closely the coefficients of two wing sections tested in different laboratories. Tests of different wing sections from the same source, however, may be relied on to give true relative values.

The absolute system of coefficients has been used, since it is thought by the National Advisory Committee for Aeronautics that this system is the one most suited for international use and yet it is one from which a desired transformation can be easily made. For this purpose a set of transformation constants is given.

Each airfoil section is given a reference number, and the test data are presented in the form of curves from which the coefficients can be read with sufficient accuracy for designing purposes. The dimensions of the profile of each section are given at various stations along the chord in per cent of the chord length, the latter also serving as the datum line. When two sets of ordinates are necessary, on account of taper in chord or ordinate, those for the maximum section (at center of span) are given on the individual characteristic sheets, while those for the tip (dotted) section are given in separate tables, page 375. The shape of the section is also shown with reasonable accuracy to enable one to more clearly visualize the section under consideration, the outside of the heavy line representing the profile.

The authority for the results here presented is given as the name of the laboratory at which the experiments were conducted, as explained under abbreviations, with the size of model, wind velocity, and year of test.

### TRANSFORMATION CONSTANTS

For the convenience of those who prefer to use a system of units other than the absolute system, there is given below a table of transformation constants based on the standard condition adopted by the National Advisory Committee for Aeronautics of—

Temperature	=15° C.	=59° F.
Pressure	=760 mm Hg.	=29.92 in. Hg.
Humidity	=0.	
Gravity	=9.80665 m/s <sup>2</sup>	=32.1740 ft./sec. <sup>2</sup>

<sup>1</sup> A previous collection of airfoil sections numbered 1 to 623 and Charts 1 to 16 may be found in N. A. C. A. Reports Nos. 93, 124, 182, and 244

thus giving values of specific weight of air

$$W = 1.2255 \text{ kg/m}^3 = 0.07651 \text{ lb./ft.}^3$$

and of density

$$\rho = 0.12497 \text{ in the French engineering or kilogram, meter, second system.}$$

Or  $\rho = 0.002378 \text{ in the English or pound, foot, second system.}$

In absolute units.....	$P = CV^2\rho/2$
In kg/m <sup>2</sup> (m/s).....	$P = .0625 CV^2$
In kg/m <sup>2</sup> (km/h).....	$P = .004822 CV^2$
In lb./sq. ft. (ft./sec.).....	$P = .001189 CV^2$
In lb./sq. ft. (mi./hr.).....	$P = .002558 CV^2$

(Note that these constants are half as large as those used in Reports Nos. 93 and 124 and that the absolute coefficients used in this report are twice as large as the old coefficients. See Report No. 240 regarding change in absolute coefficients.)

### INDEX

Three separate types of index are given—chart indexes which make it possible for a designer to select the wing section most suitable for the particular design in which he is interested; a group index which is arranged by countries and laboratories at which tests were conducted, each section also being designated by a reference number; and an alphabetical index.

### CHART INDEX

In order that the designer may easily pick out a wing section which is suited to the type of airplane on which he is working, four index charts are given which classify the wings according to their aerodynamic and structural properties. In the charts of this report a lower-case letter is placed adjacent to the reference number giving  $Vl$  values, so that a comparison can be made without referring to the individual drawings. In this value  $V$  represents the wind velocity in feet per second and  $l$  a linear dimension, the chord length in feet.

In chart No. 17 the minimum drag,  $C_D$  is plotted against the  $L/D$  at one-fourth the maximum lift,  $C_L$ . This chart should be used in choosing a wing section for a high-speed airplane, the wing sections being more suited for this use the farther they are from the lower left-hand corner.

In chart No. 18 the mean spar depth is plotted against the maximum lift,  $C_L$ , in order to show the possible strength and lightness of the wing structure. The higher the maximum lift coefficient is the smaller will be the wing area and the lighter the structural weight, and in the same way the greater the depth of the spars the lighter will be their weight, so that the sections the greatest distance from the lower left-hand corner will give the lightest and strongest wings. The "mean spar depth" is obtained by assuming the spars to be located, respectively, at 15 and 60 per cent of the chord, and by dividing the sum of their thicknesses, in per cent of chord length at these points, by 2. In the case of sections tapered in ordinate or chord, or both, the mean spar depth of the maximum section (section at center of span) is taken in per cent of the constant chord for the ordinate taper, and of the mean chord for the chord taper, although accompanied, in certain airfoils, with an ordinate taper.

In chart No. 19 the maximum  $L/D$  is plotted against the maximum lift,  $C_L$ , which is of use in choosing the wing section for a slow and efficient airplane. In the same way as before the sections farthest from the lower left-hand corner are the best for this purpose.

In chart No. 20 the  $L/D$  at two-thirds the maximum lift,  $C_L$  is plotted against the maximum lift,  $C_L$ . This chart can be used for choosing a section that will give an efficient climb or a long range at cruising speed. The best sections for this purpose will be farthest from the lower left-hand corner of the chart.



## CHART INDEX

	Page
Chart No. 17. Minimum drag, $C_D$ , plotted against $L/D$ at one-fourth the maximum lift, $C_L$ -----	180
Chart No. 18. Mean spar depth plotted against the maximum lift, $C_L$ -----	181
Chart No. 19. Maximum $L/D$ plotted against maximum lift, $C_L$ -----	182
Chart No. 20. $L/D$ at two-thirds the maximum lift, $C_L$ , plotted against the maximum lift, $C_L$ -----	183

## INDEX OF ABBREVIATIONS

Name of laboratory at which tests were made	Abbreviations used on figures
Langley Memorial Aeronautical Laboratory (N. A. C. A.), U. S. A.-----	L. M. A. L.
Washington Navy Yard, U. S. A.-----	W. N. Y.
Engineering Division, McCook Field, U. S. A.-----	McC. F.
Royal Aircraft Establishment, Great Britain-----	R. A. E.
Service Technique de l'Aeronautique, France-----	S. T. Aé
Ergebnisse der Aerodynamischen Versuchsanstalt zu Göttingen, Germany-----	Göttingen.
Istituto Sperimentale Aeronautico, Italy-----	I. S. A.
Laboratorio della Direzione del Genio Aeronautico, Italy-----	D. G. A.
Laboratoire Aerotechnique de Rhode St. Genese-Bruxelles, Belgium-----	Rhode St. Genese.

# GROUP INDEX

Airfoil	Wind tunnel where tested	Report reference number	Airfoil	Wind tunnel where tested	Report reference number
UNITED STATES			GERMANY—continued		
N. A. C. A. 81J	L. M. A. L.	624	Göttingen 532	Göttingen	681
N. A. C. A.-CYH	do	625	Göttingen 533	do	682
B-2 (Modified M-80)	W. N. Y.	626	Göttingen 534	do	683
C-2 (Modified M-80)	do	627	Göttingen 535	do	684
Boeing 103	do	628	Göttingen 546	do	685
N-22	do	629	Göttingen 547	do	686
N-23	do	630	Göttingen 548	do	687
N-24	do	631	Göttingen 549	do	688
Clark Y-15	McC. F.	632	Göttingen 559	do	689
Clark Y-18	do	633	Göttingen 561	do	690
Clark Y-21	do	634	Göttingen 562	do	691
GREAT BRITAIN			Göttingen 570	do	692
R. A. F. 25	R. A. E.	635	Göttingen 571	do	693
R. A. F. 26	do	636	Göttingen 572	do	694
R. A. F. 27	do	637	Göttingen 573	do	695
R. A. F. 28	do	638	Göttingen 574	do	696
R. A. F. 34	do	639	Göttingen 575	do	697
GERMANY			Göttingen 587	do	698
Göttingen 417a	Göttingen	640	Göttingen 590	do	699
Göttingen 456	do	641	Göttingen 592	do	700
Göttingen 458	do	642	Göttingen 593	do	701
Göttingen 461	do	643	Göttingen 595	do	702
Göttingen 462	do	644	FRANCE		
Göttingen 464	do	645	Eiffel 400 (Pescara)	S. T. Aé. Lab.	703
Göttingen 481	do	646	Eiffel 401 (Pescara)	do	704
Göttingen 481a	do	647	Eiffel 403 (Pescara)	do	705
Göttingen 482	do	648	Eiffel 428 (Blériot)	do	706
Göttingen 483	do	649	Eiffel 430 (Lachassagne)	do	707
Göttingen 484	do	650	Eiffel 431 (Lachassagne)	do	708
Göttingen 490	do	651	St. Cyr 150 (Royer)	do	709
Göttingen 491	do	652	St. Cyr 151 (Royer)	do	710
Göttingen 492	do	653	St. Cyr 154 (Royer)	do	711
Göttingen 493	do	654	St. Cyr 155 (Royer)	do	712
Göttingen 494	do	655	St. Cyr 158 (Royer)	do	713
Göttingen 495	do	656	St. Cyr 159 (Royer)	do	714
Göttingen 496	do	657	St. Cyr 160 (Royer)	do	715
Göttingen 497	do	658	St. Cyr 161 (Royer)	do	716
Göttingen 498	do	659	St. Cyr 171 (Royer)	do	717
Göttingen 499	do	660	St. Cyr 172 (Royer)	do	718
Göttingen 500	do	661	St. Cyr 173 (Royer)	do	719
Göttingen 501	do	662	St. Cyr 175 (Royer)	do	720
Göttingen 502	do	663	St. Cyr 176 (Royer)	do	721
Göttingen 503	do	664	St. Cyr 177 (Royer)	do	722
Göttingen 504	do	665	St. Cyr 178 (Royer)	do	723
Göttingen 505	do	666	St. Cyr 185 (Monge)	do	724
Göttingen 506	do	667	St. Cyr 234 (Bartel 17-IC)	do	725
Göttingen 509	do	668	St. Cyr 236 (Bartel 26-IC)	do	726
Göttingen 510	do	669	St. Cyr 238 (Bartel 4-IC)	do	727
Göttingen 511	do	670	St. Cyr 241 (Bartel 37-IIC)	do	728
Göttingen 512	do	671	St. Cyr 244 (Bartel 35-IIIC)	do	729
Göttingen 513	do	672	BELGIUM		
Göttingen 514	do	673	Rhode St. Genese 28	Rhode St. Genese	730
Göttingen 518	do	674	Rhode St. Genese 30	do	731
Göttingen 522	do	675	Rhode St. Genese 32	do	732
Göttingen 523	do	676	Rhode St. Genese 34	do	733
Göttingen 527	do	677	Rhode St. Genese 36	do	734
Göttingen 528	do	678			
Göttingen 529	do	679			
Göttingen 530	do	680			
Göttingen 531	do				

<sup>1</sup> Göttingen 461 of this series published in Report No. 182.



Airfoil	Wind tunnel where tested	Report reference number	Airfoil	Wind tunnel where tested	Report reference number
ITALY			ITALY—continued		
I. S. A. 571	I. S. A.	735	I. S. A. 923b	I. S. A.	748
I. S. A. 573	do	736	I. S. A. 960	do	749
I. S. A. 607	do	737	I. S. A. 961	do	750
I. S. A. 608	do	738	I. S. A. 962	do	751
I. S. A. 666	do	739	I. S. A. 993	do	752
I. S. A. 691	do	740	I. S. A. 994a	do	753
I. S. A. 692	do	741	I. S. A. 994c	do	754
I. S. A. 802	do	742	Bambino 5	D. G. A.	755
I. S. A. 808	do	743	Bambino 6	do	756
I. S. A. 843	do	744	Bambino, E: 7	do	757
I. S. A. 906	do	745	D. G. A. 1138	do	758
I. S. A. 909	do	746	D. G. A. 1182	do	759
I. S. A. 923a	do	747			

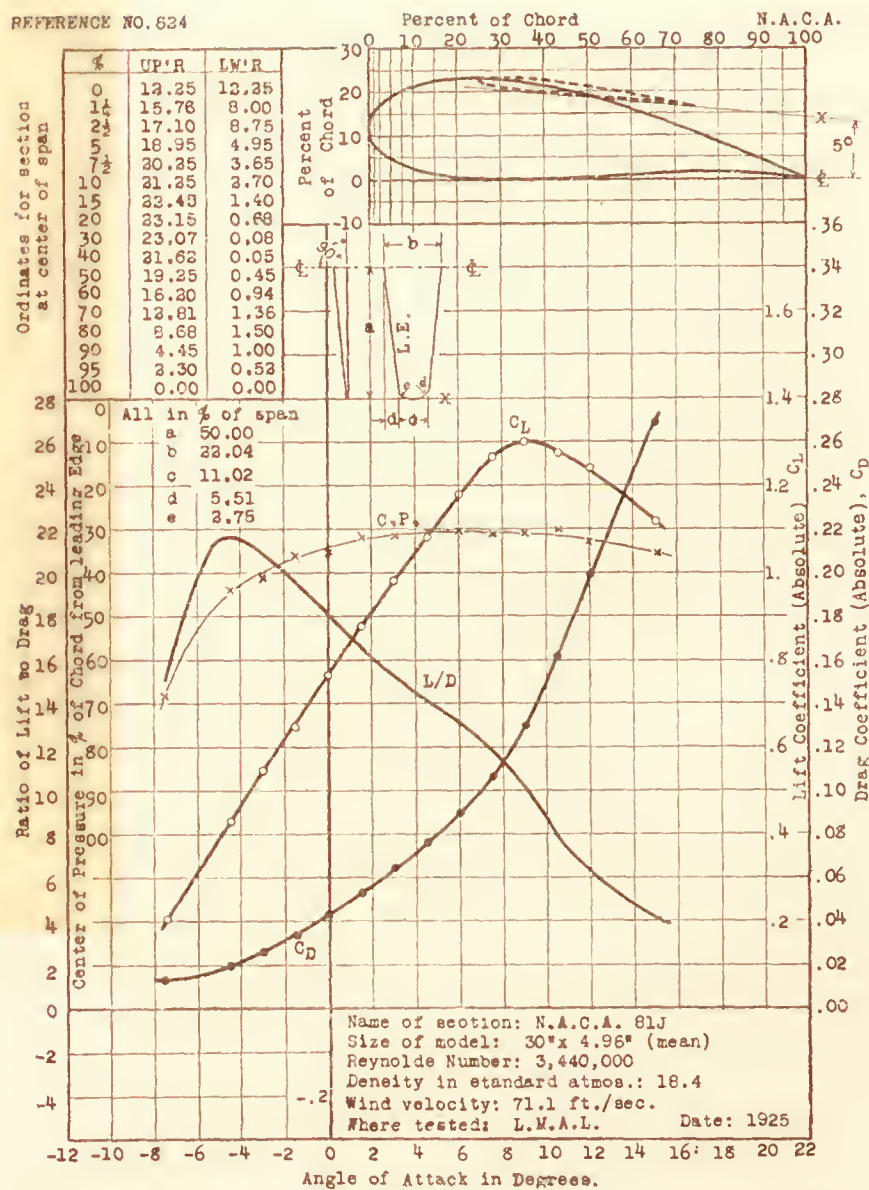
# ALPHABETICAL INDEX

Airfoil	Report reference number	Airfoil	Report reference number
B-2 (Modified M-80)	626	Göttingen 562	691
Bambino 5	755	Göttingen 570	692
Bambino 6	756	Göttingen 571	693
Bambino, E: 7	757	Göttingen 572	694
Boeing 103	628	Göttingen 573	695
C-2 (Modified M-80)	627	Göttingen 574	696
Clark Y-15	632	Göttingen 575	697
Clark Y-18	633	Göttingen 587	698
Clark Y-21	634	Göttingen 590	699
D. G. A. 1138	758	Göttingen 592	700
D. G. A. 1182	759	Göttingen 593	701
Eiffel 400 (Pescara)	703	Göttingen 595	702
Eiffel 401 (Pescara)	704	I. S. A. 571	735
Eiffel 403 (Pescara)	705	I. S. A. 573	736
Eiffel 428 (Blériot)	706	I. S. A. 607	737
Eiffel 430 (Lachassagne)	707	I. S. A. 608	738
Eiffel 431 (Lachassagne)	708	I. S. A. 666	739
Göttingen 417a	640	I. S. A. 691	740
Göttingen 456	641	I. S. A. 692	741
Göttingen 458	642	I. S. A. 802	742
Göttingen 461	<sup>1</sup> 430	I. S. A. 808	743
Göttingen 462	643	I. S. A. 843	744
Göttingen 464	644	I. S. A. 906	745
Göttingen 481	645	I. S. A. 909	746
Göttingen 481a	646	I. S. A. 923a	747
Göttingen 482	647	I. S. A. 923b	748
Göttingen 483	648	I. S. A. 960	749
Göttingen 484	649	I. S. A. 961	750
Göttingen 490	650	I. S. A. 962	751
Göttingen 491	651	I. S. A. 993	752
Göttingen 492	652	I. S. A. 994a	753
Göttingen 493	653	I. S. A. 994c	754
Göttingen 494	654	N-22	629
Göttingen 495	655	N-23	630
Göttingen 496	656	N-24	631
Göttingen 497	657	N. A. C. A. 81J	624
Göttingen 498	658	N. A. C. A.—CYH	625
Göttingen 499	659	R. A. F. 25	635
Göttingen 500	660	R. A. F. 26	636
Göttingen 501	661	R. A. F. 27	637
Göttingen 502	662	R. A. F. 28	638
Göttingen 503	663	R. A. F. 34	639
Göttingen 504	664	Rhode St. Genese 28	730
Göttingen 505	665	Rhode St. Genese 30	731
Göttingen 506	666	Rhode St. Genese 32	732
Göttingen 509	667	Rhode St. Genese 34	733
Göttingen 510	668	Rhode St. Genese 36	734
Göttingen 511	669	St. Cyr 150 (Royer)	709
Göttingen 512	670	St. Cyr 151 (Royer)	710
Göttingen 513	671	St. Cyr 154 (Royer)	711
Göttingen 514	672	St. Cyr 155 (Royer)	712
Göttingen 518	673	St. Cyr 158 (Royer)	713
Göttingen 522	674	St. Cyr 159 (Royer)	714
Göttingen 523	675	St. Cyr 160 (Royer)	715
Göttingen 527	676	St. Cyr 161 (Royer)	716
Göttingen 528	677	St. Cyr 171 (Royer)	717
Göttingen 529	678	St. Cyr 172 (Royer)	718
Göttingen 530	679	St. Cyr 173 (Royer)	719
Göttingen 531	680	St. Cyr 175 (Royer)	720
Göttingen 532	681	St. Cyr 176 (Royer)	721
Göttingen 533	682	St. Cyr 177 (Royer)	722
Göttingen 534	683	St. Cyr 178 (Royer)	723
Göttingen 535	684	St. Cyr 185 (Monge)	724
Göttingen 546	685	St. Cyr 234 (Bartel 17-IC)	725
Göttingen 547	686	St. Cyr 236 (Bartel 26-IC)	726
Göttingen 548	687	St. Cyr 238 (Bartel 4-IC)	727
Göttingen 549	688	St. Cyr 241 (Bartel 37-IIIC)	728
Göttingen 559	689	St. Cyr 244 (Bartel 35-IIIC)	729
Göttingen 561	690		

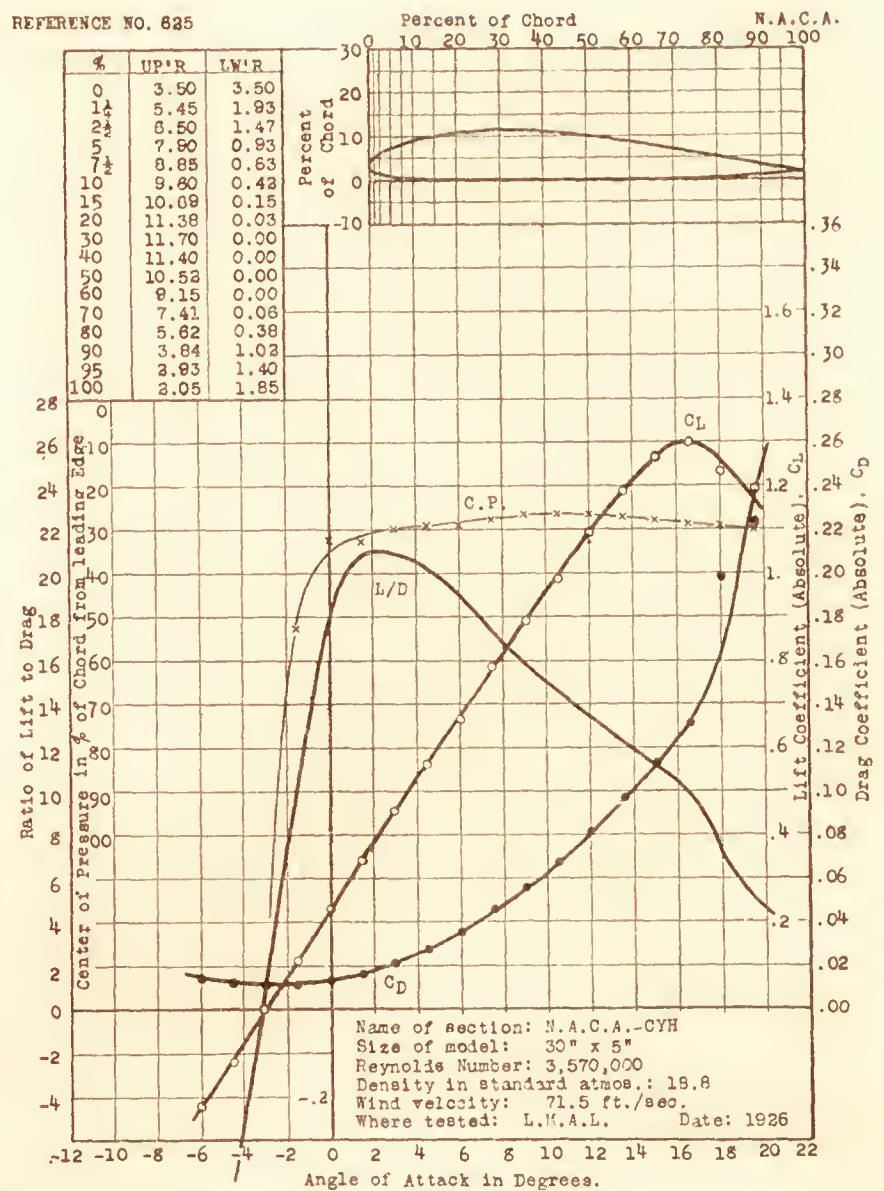
<sup>1</sup> Göttingen 461 of this series published in Report No. 182.



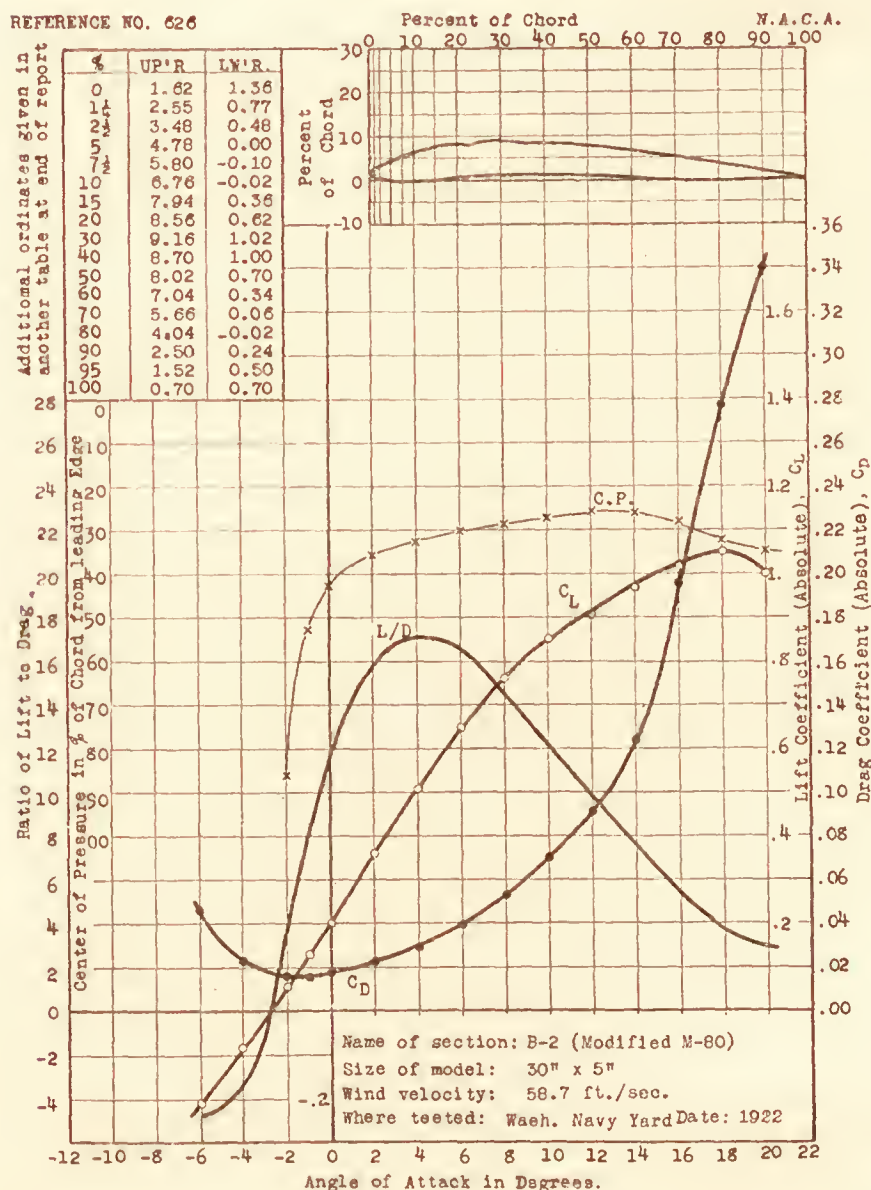
REFERENCE NO. 624



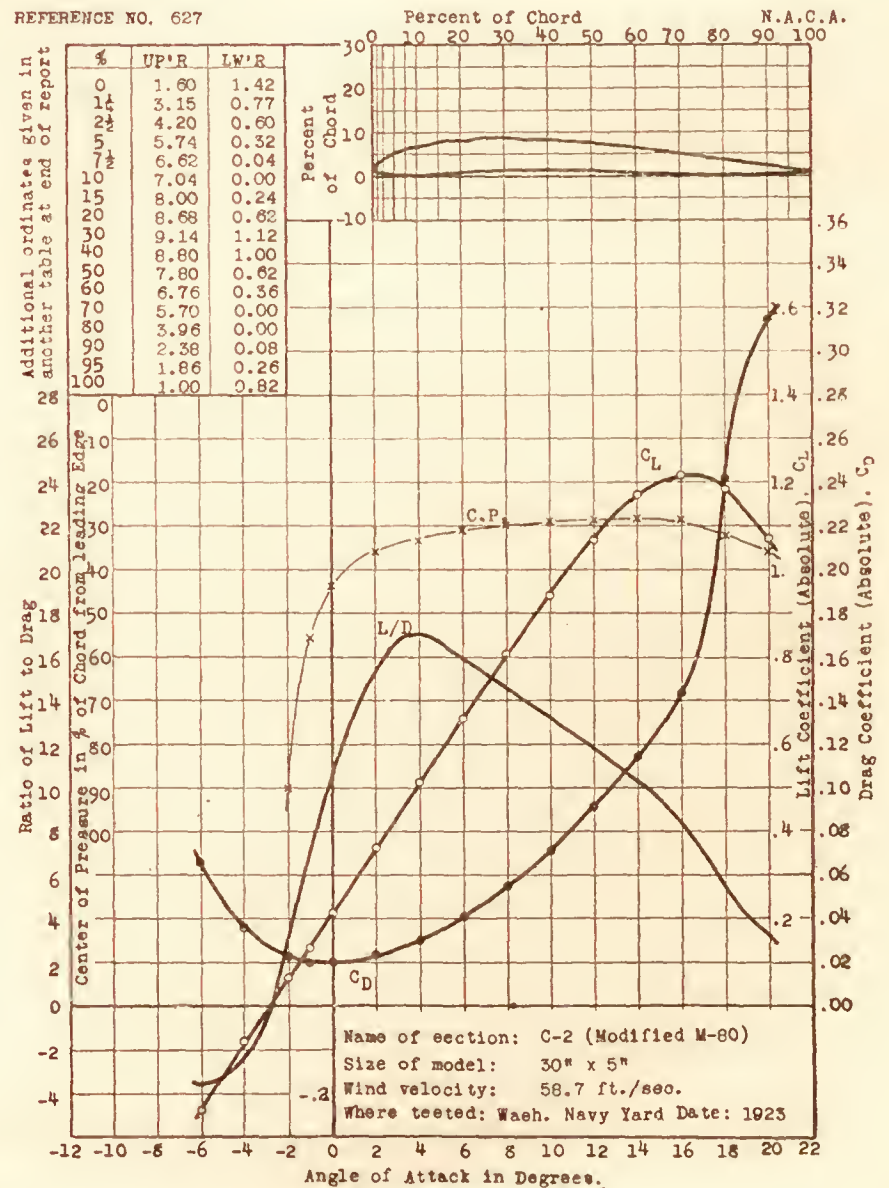
REFERENCE NO. 625



REFERENCE NO. 626

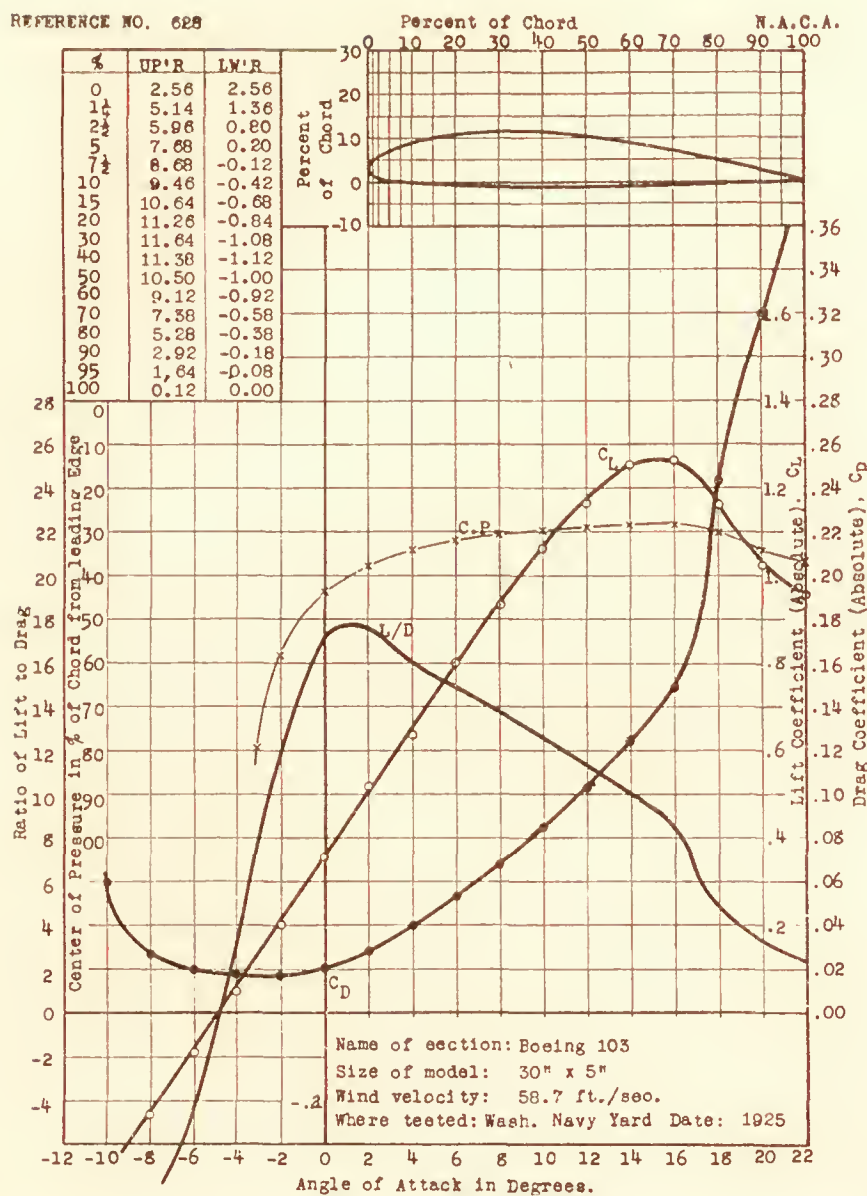


REFERENCE NO. 627

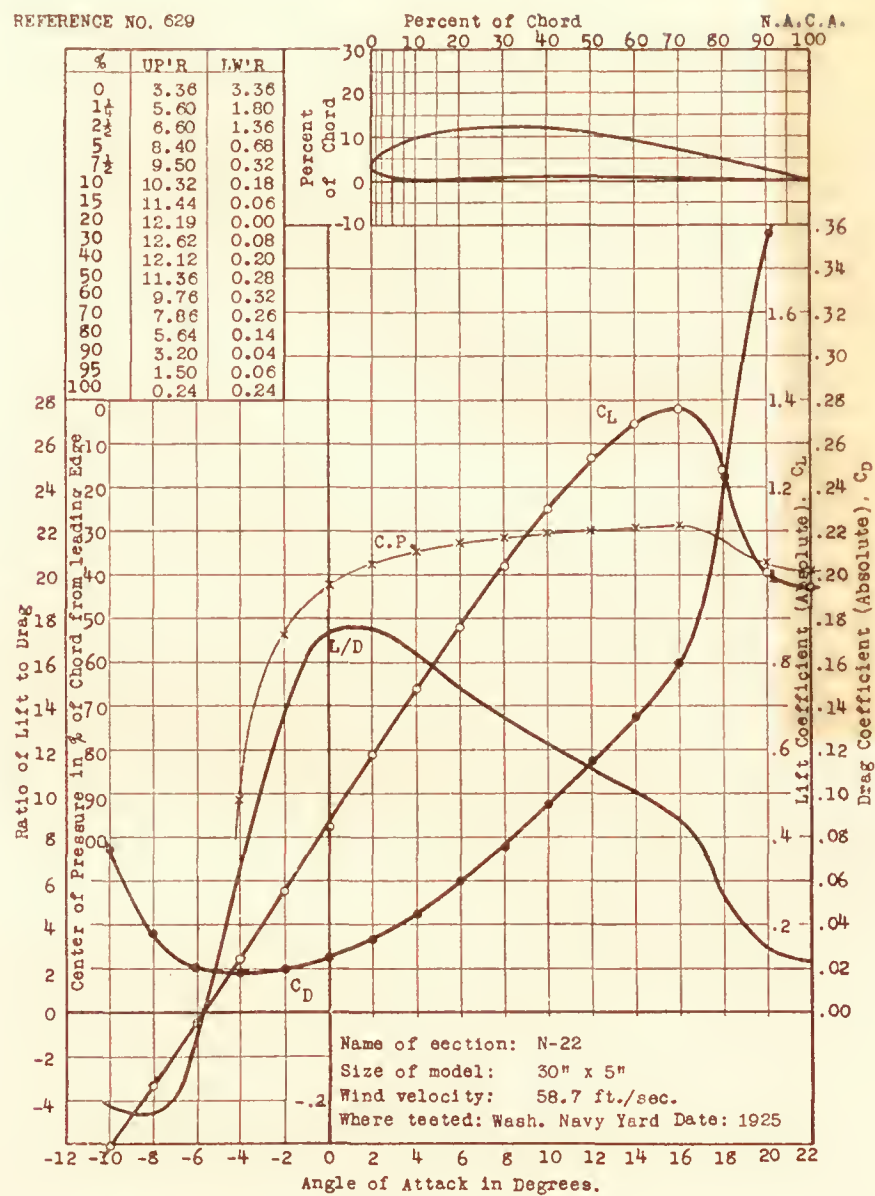




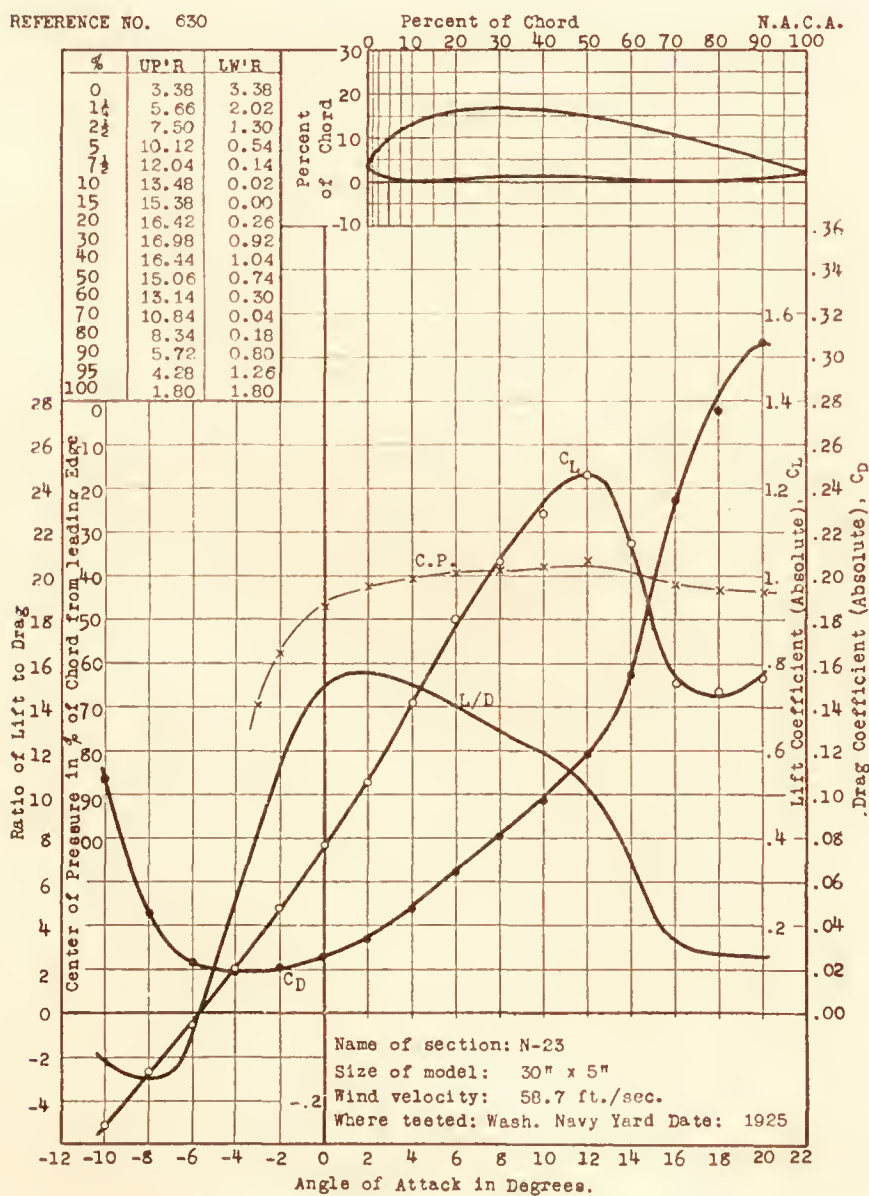
REFERENCE NO. 628



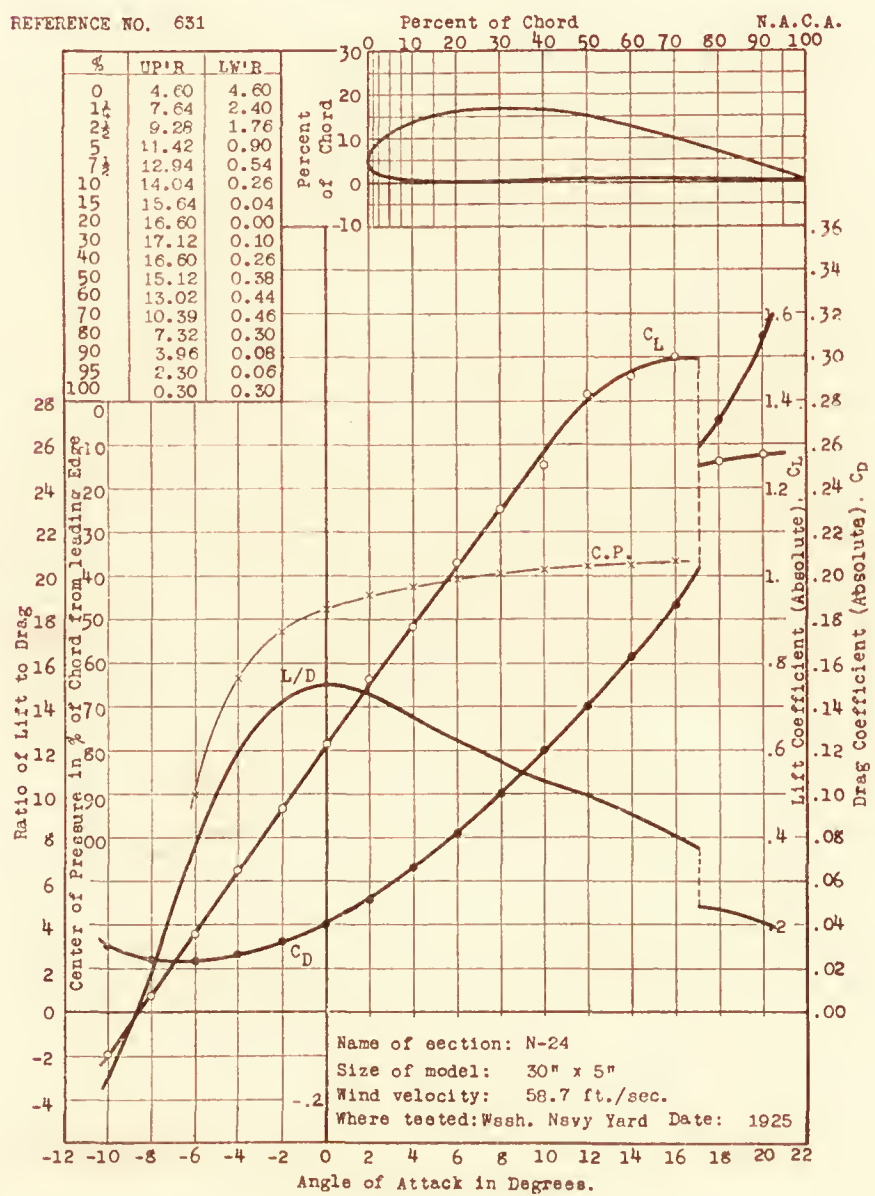
REFERENCE NO. 629



REFERENCE NO. 630

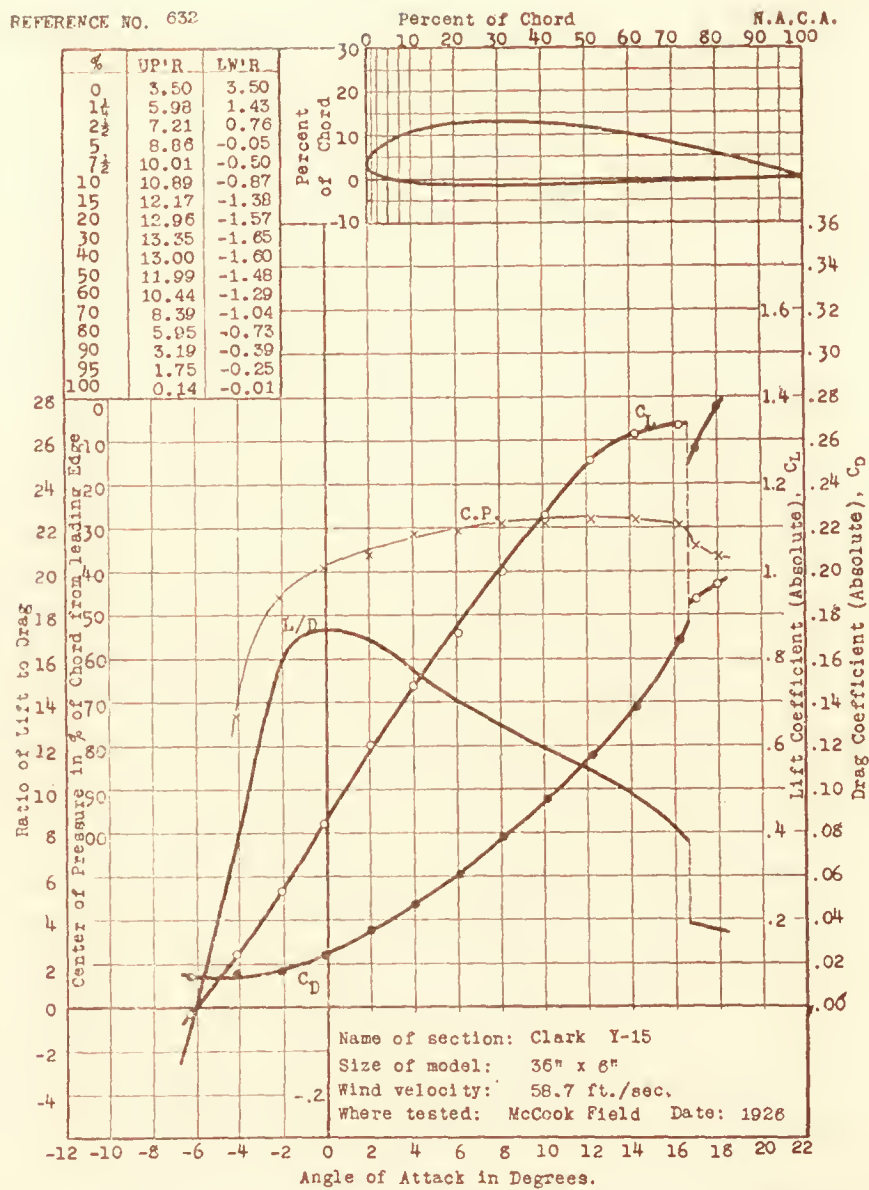


REFERENCE NO. 631

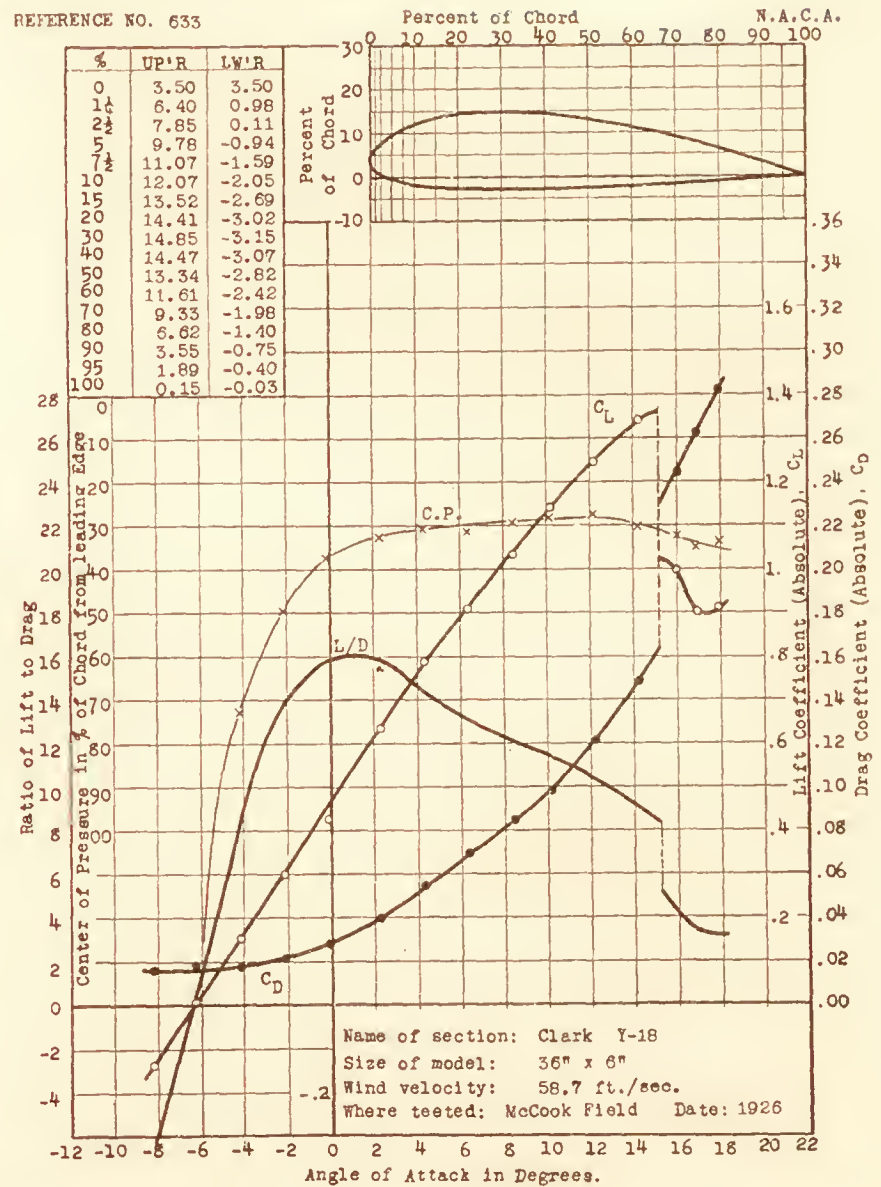




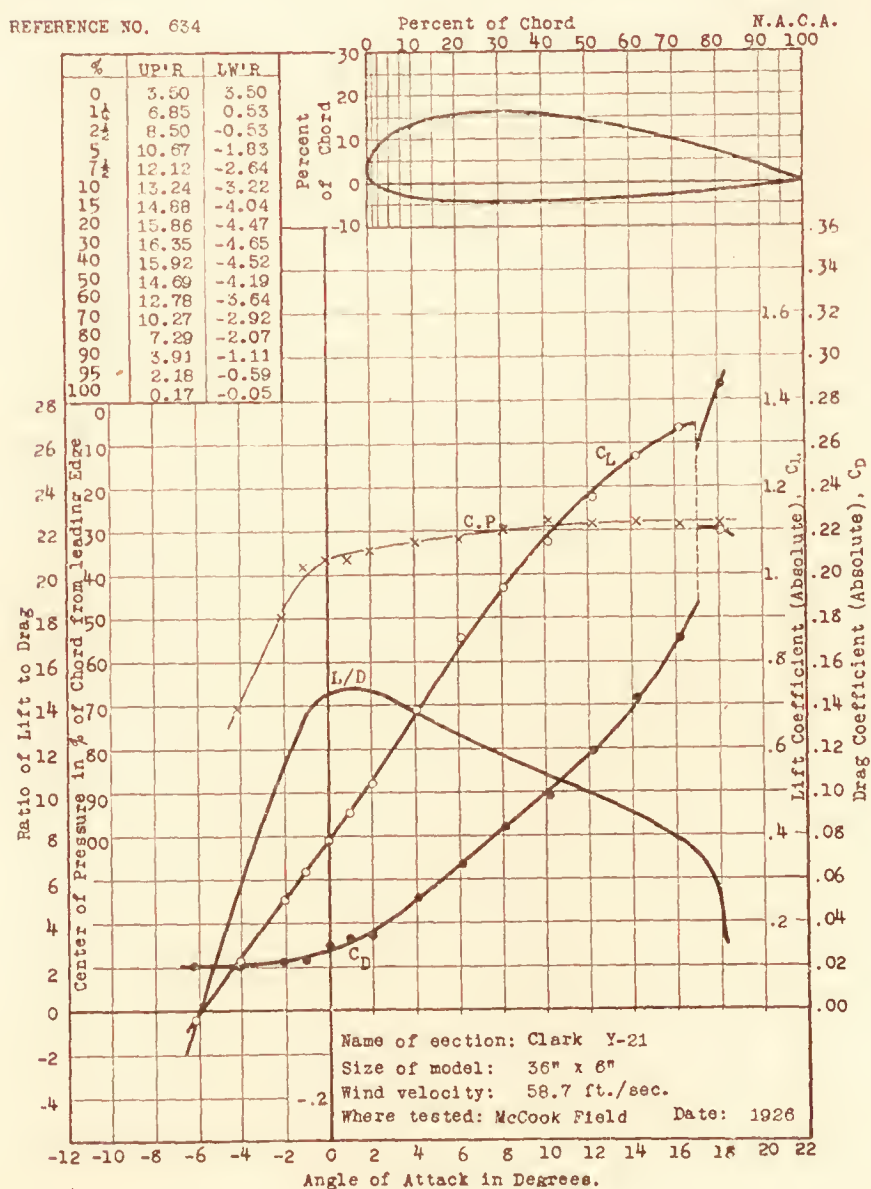
REFERENCE NO. 632



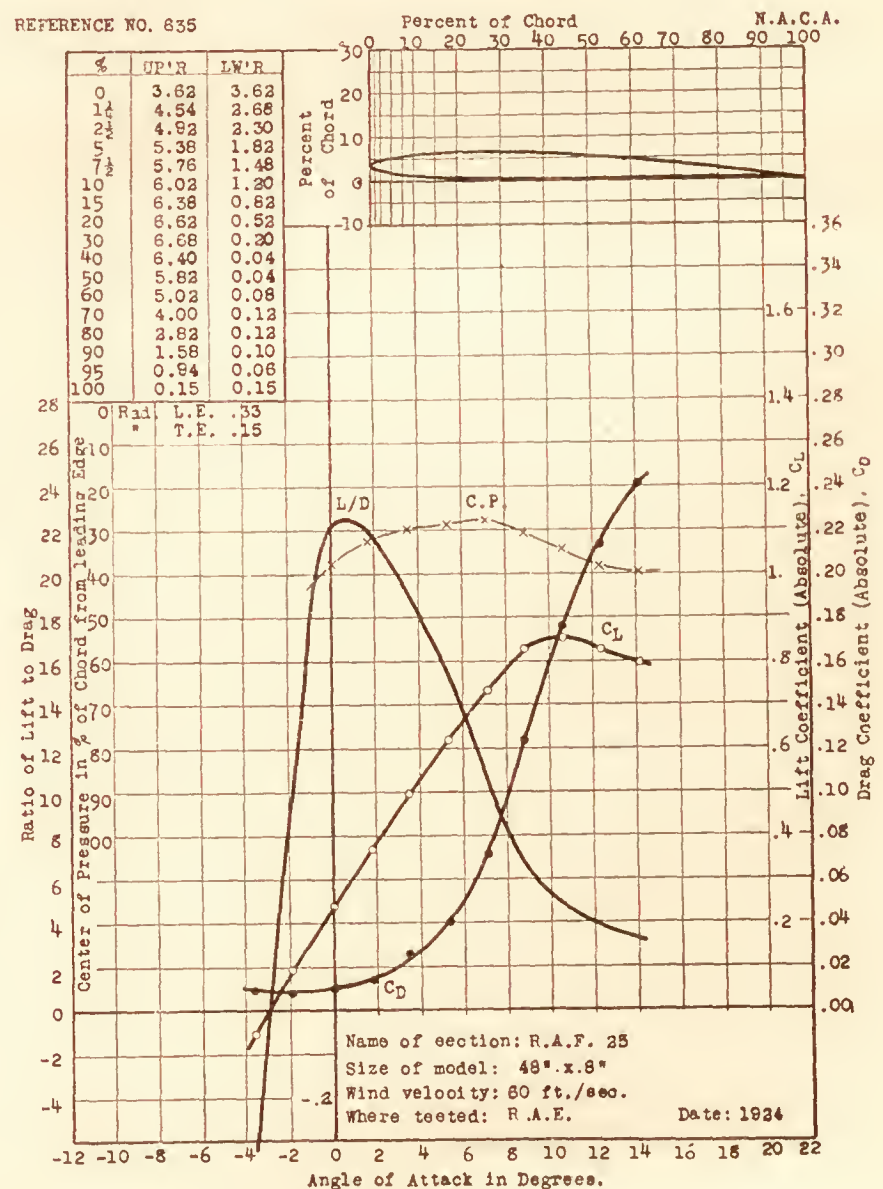
REFERENCE NO. 633



REFERENCE NO. 634

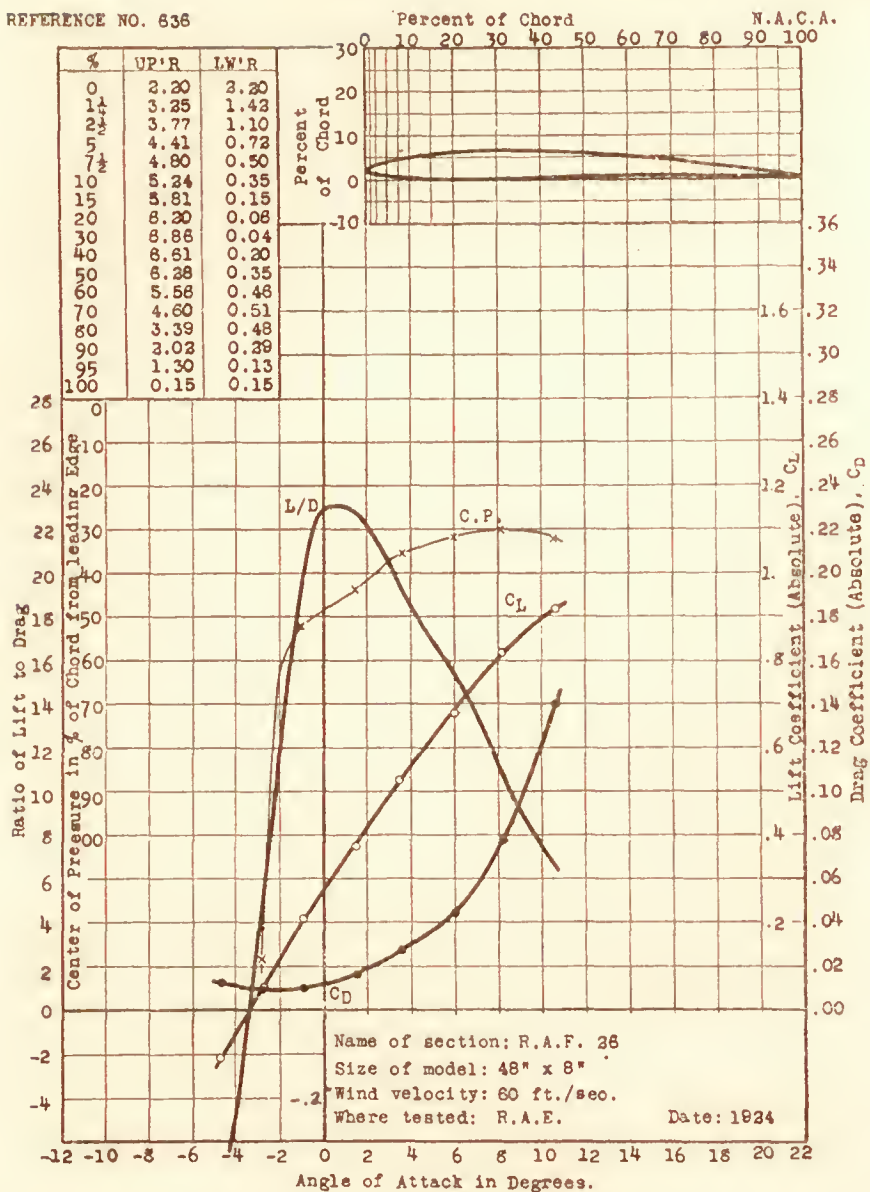


REFERENCE NO. 635

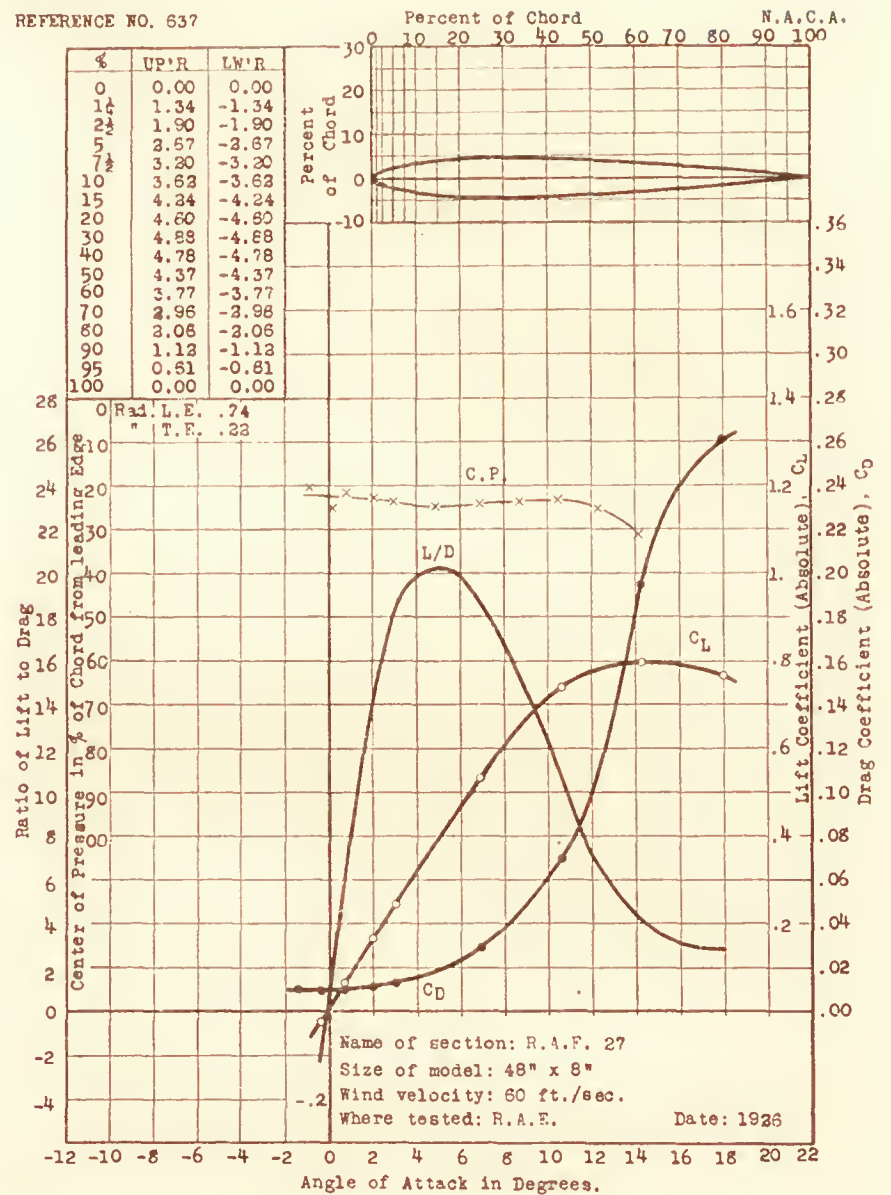




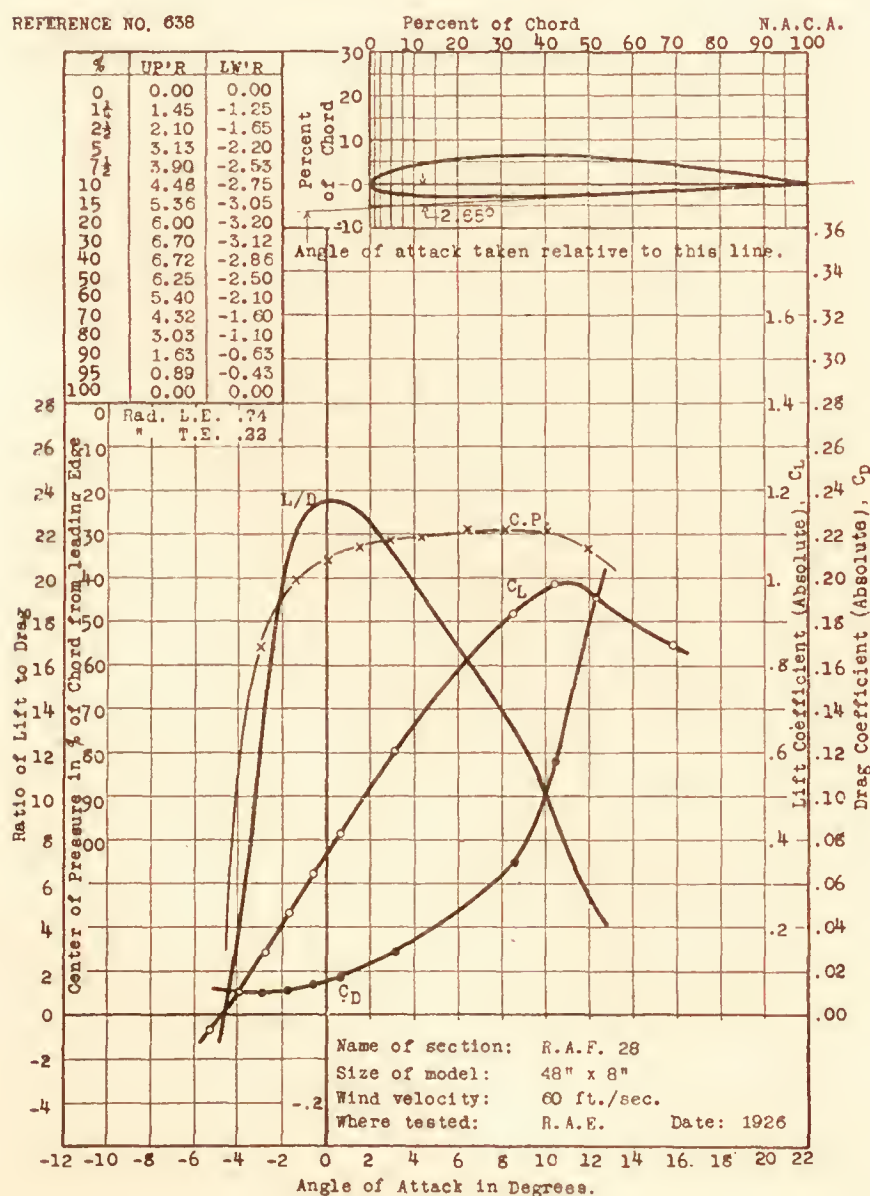
REFERENCE NO. 636



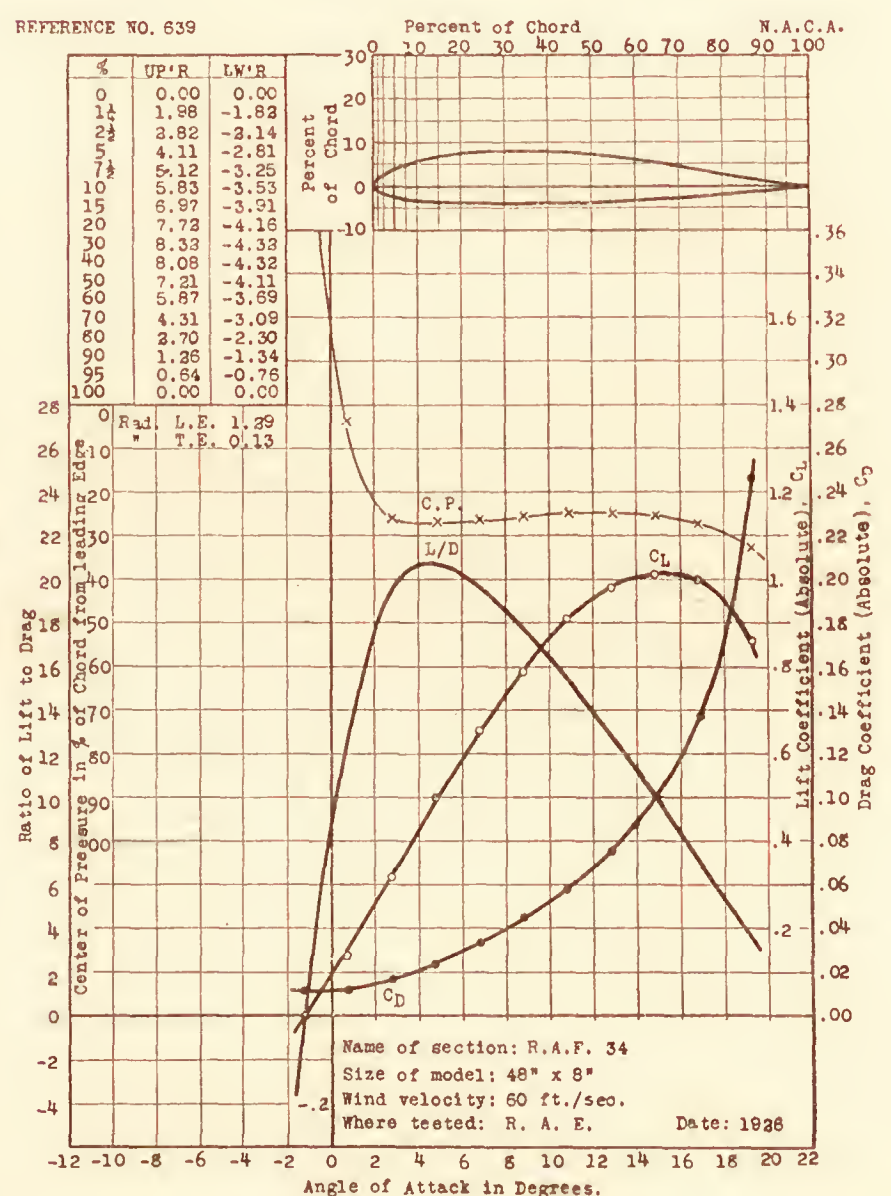
REFERENCE NO. 637



REFERENCE NO. 638

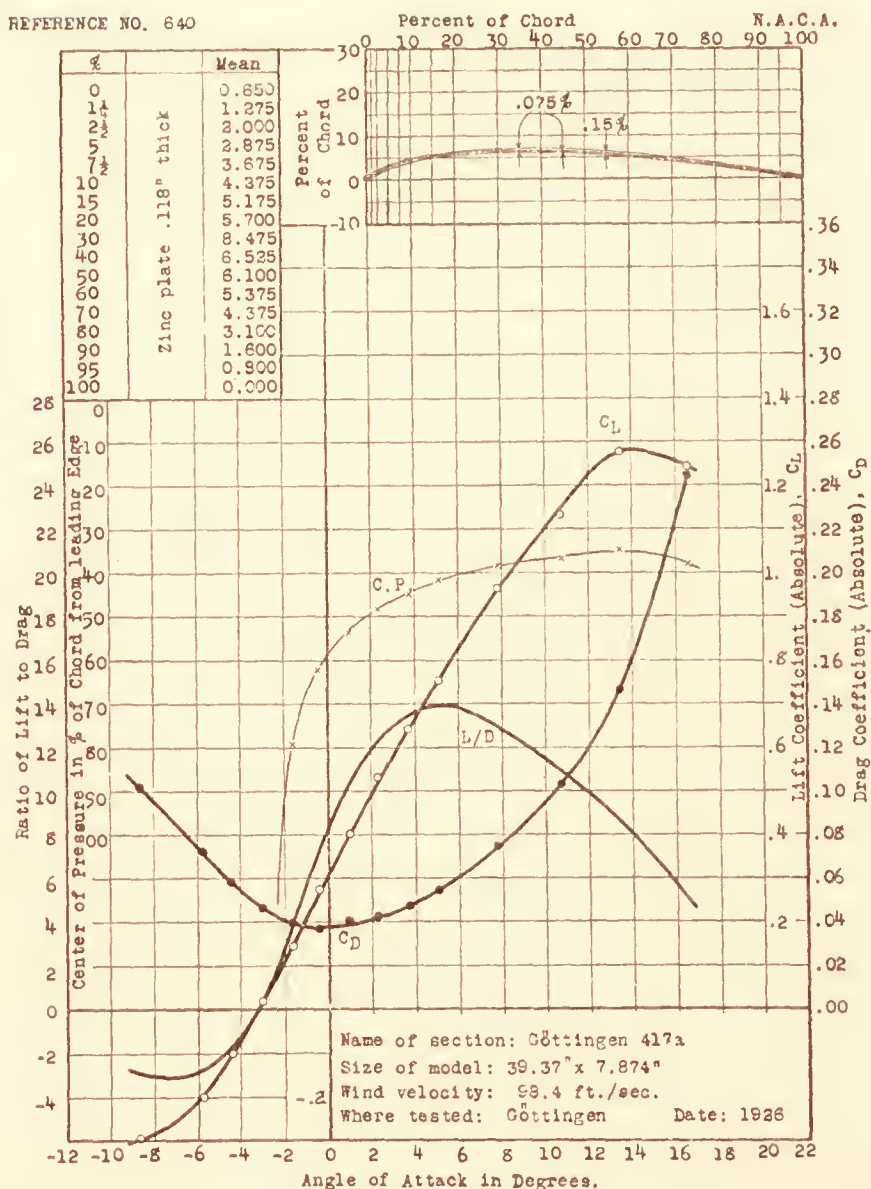


REFERENCE NO. 639

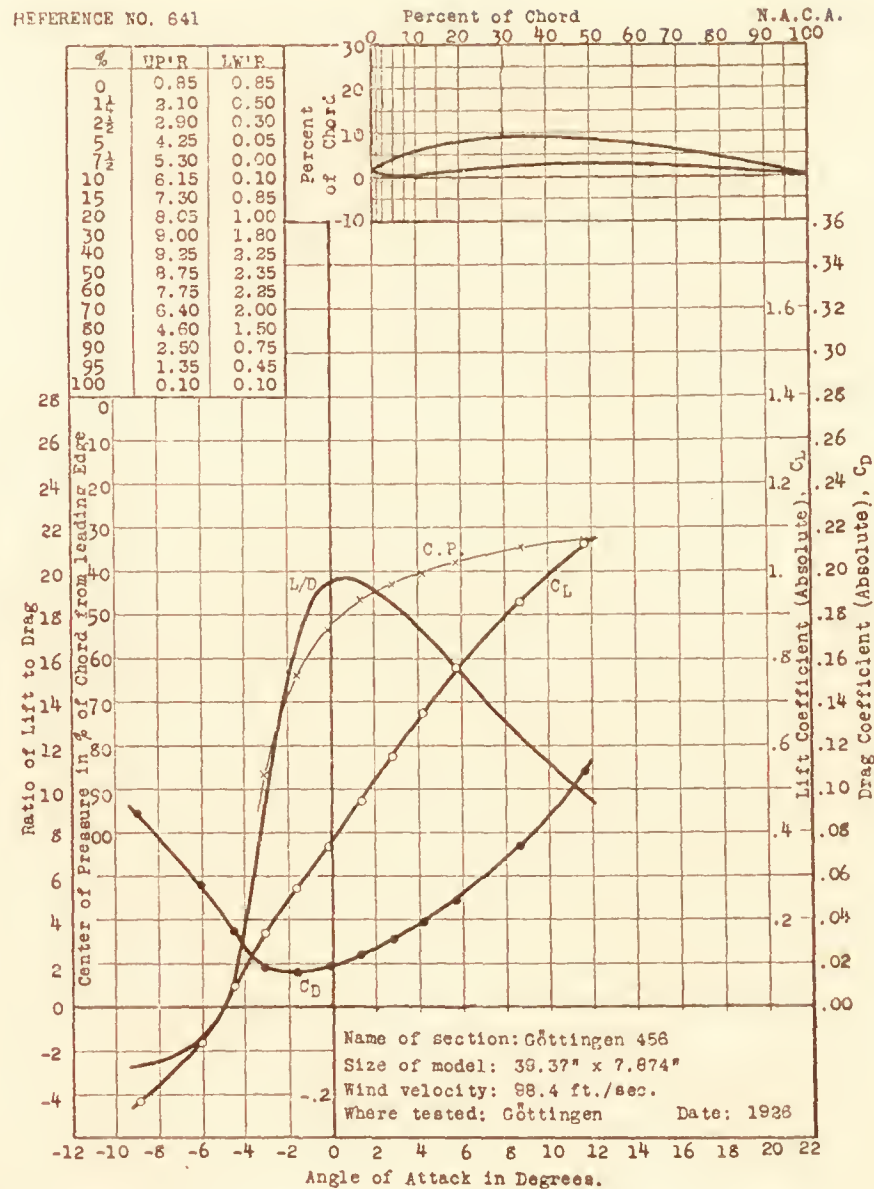




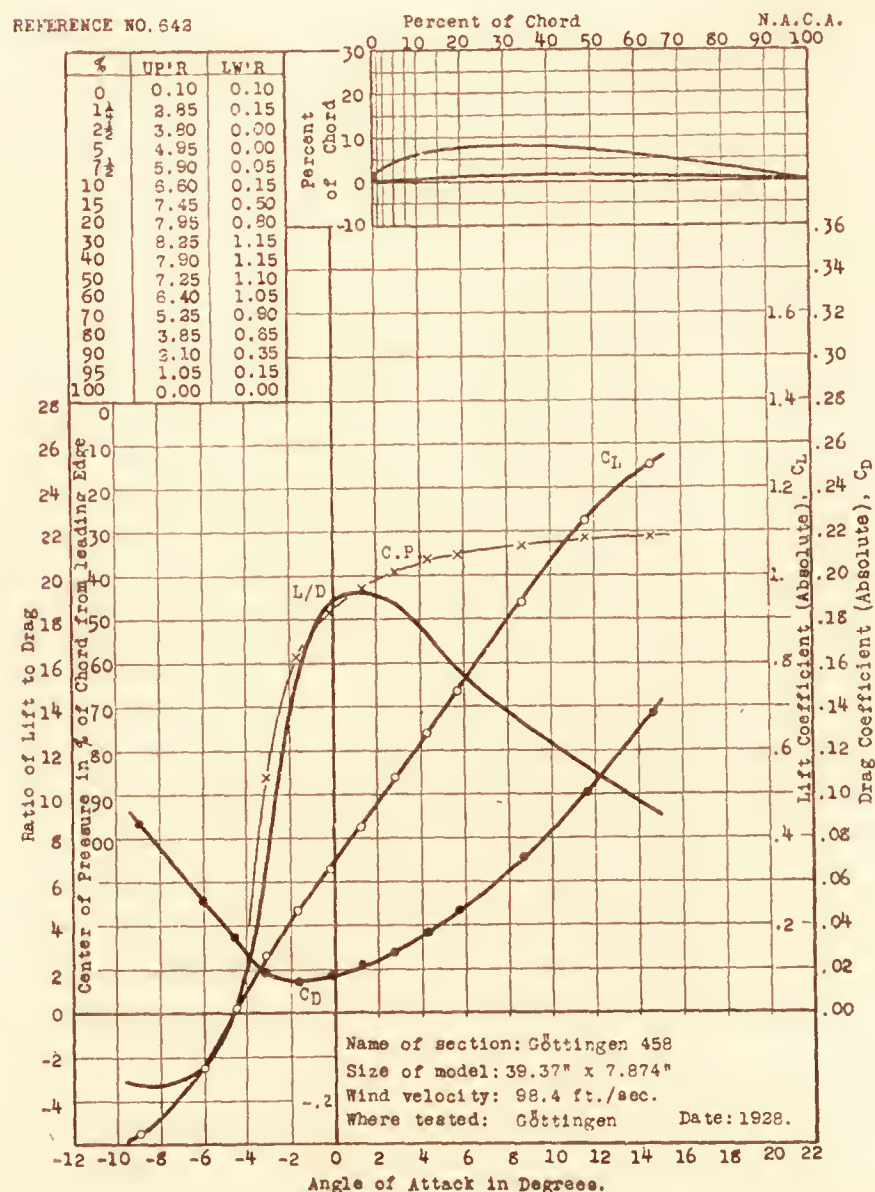
REFERENCE NO. 640



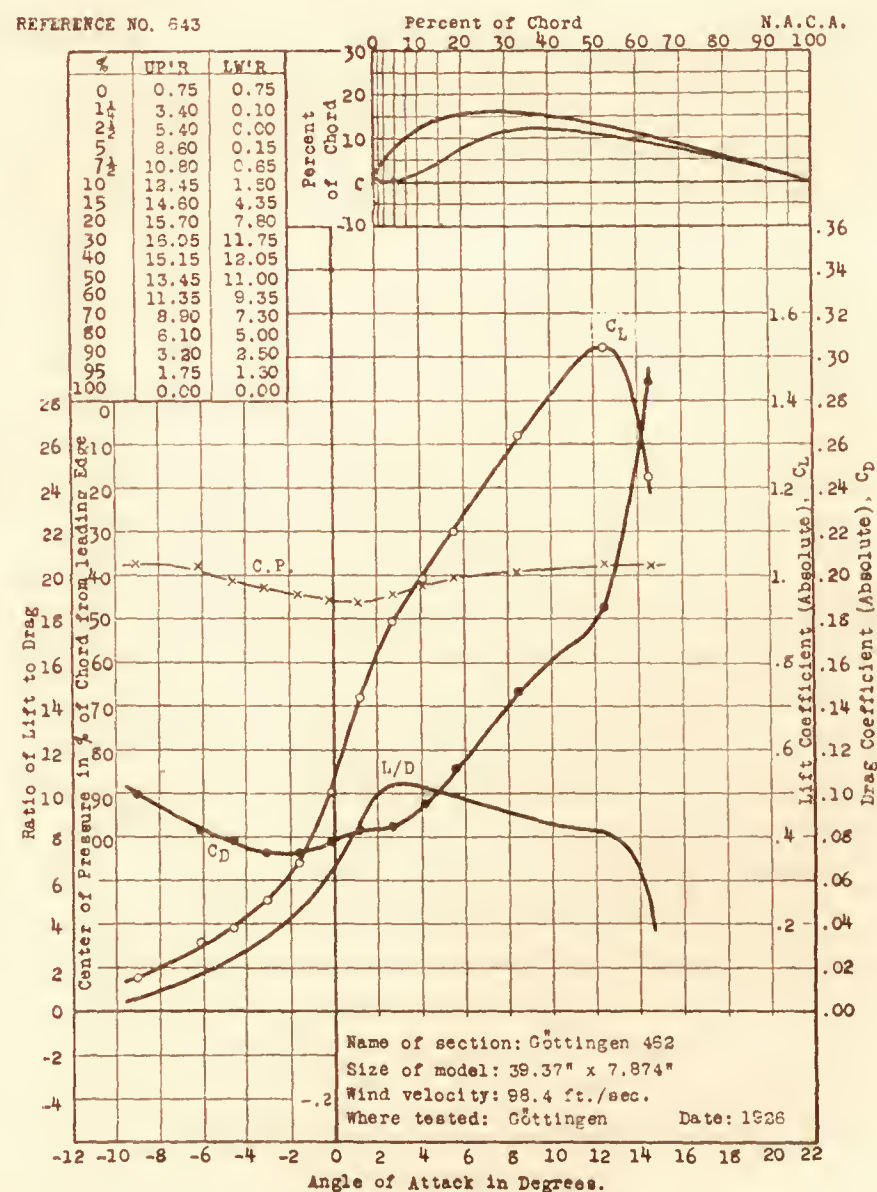
REFERENCE NO. 641



REFERENCE NO. 642

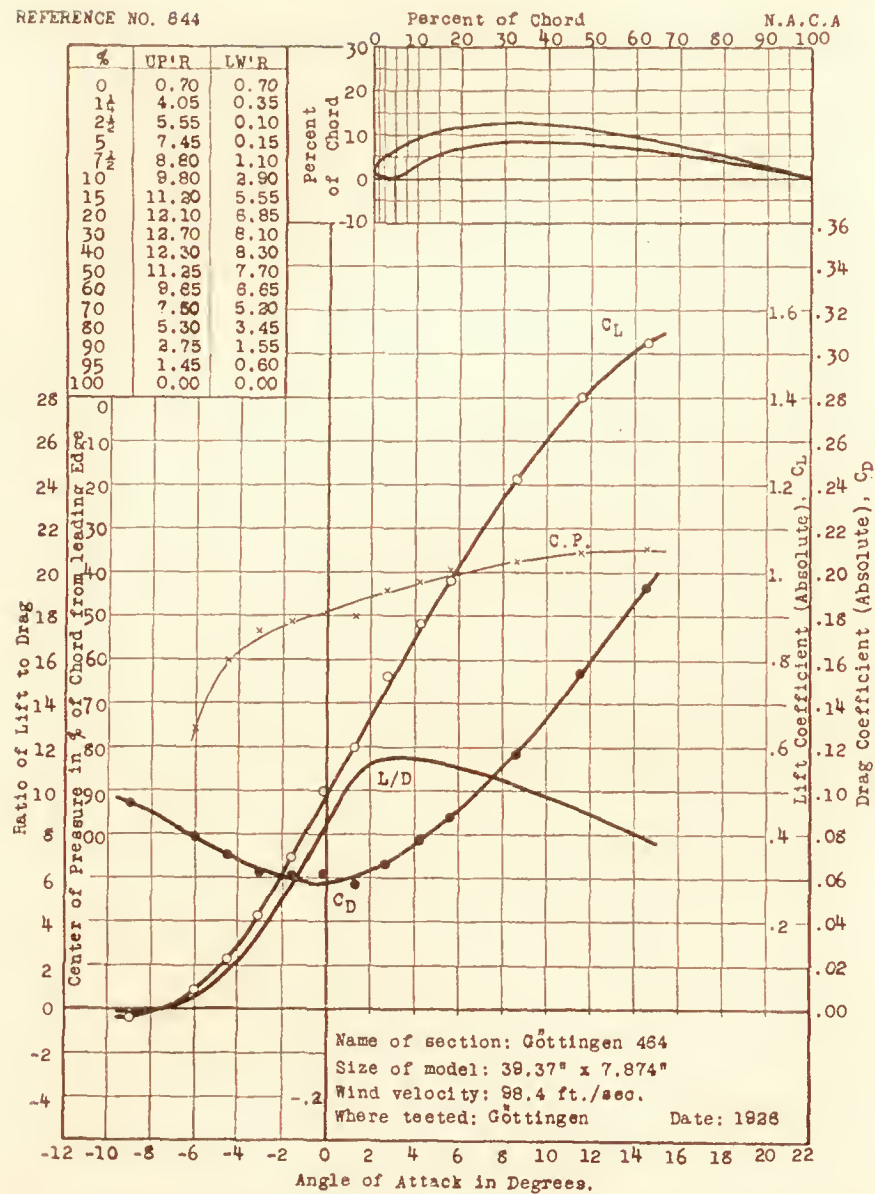


REFERENCE NO. 643

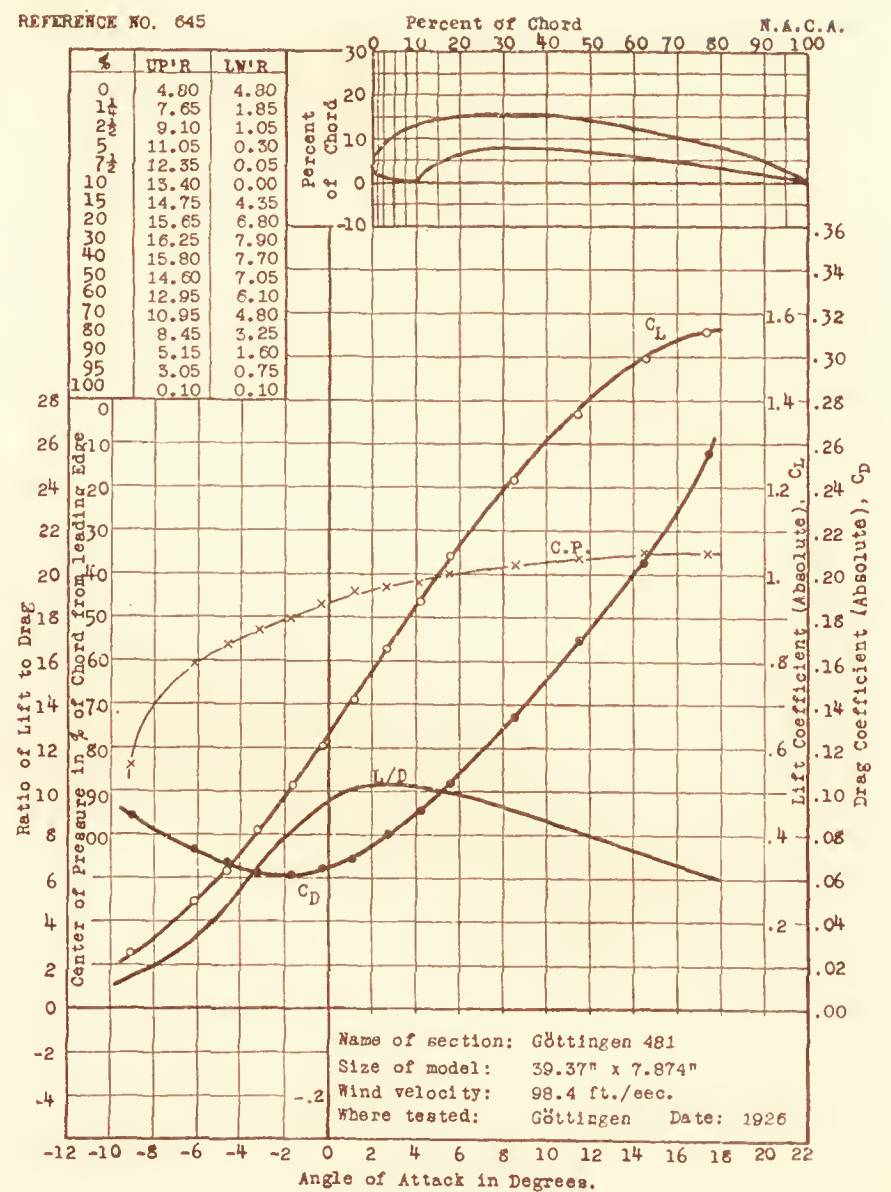




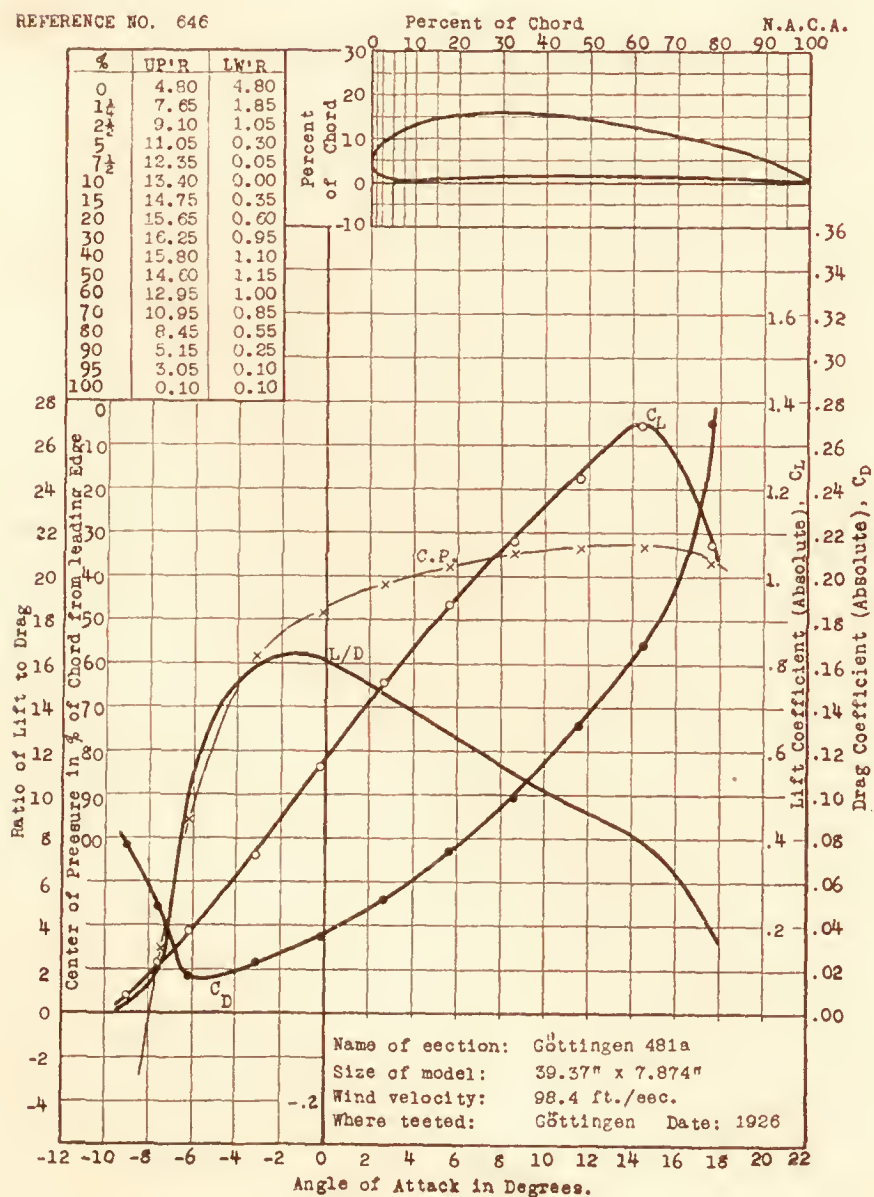
REFERENCE NO. 844



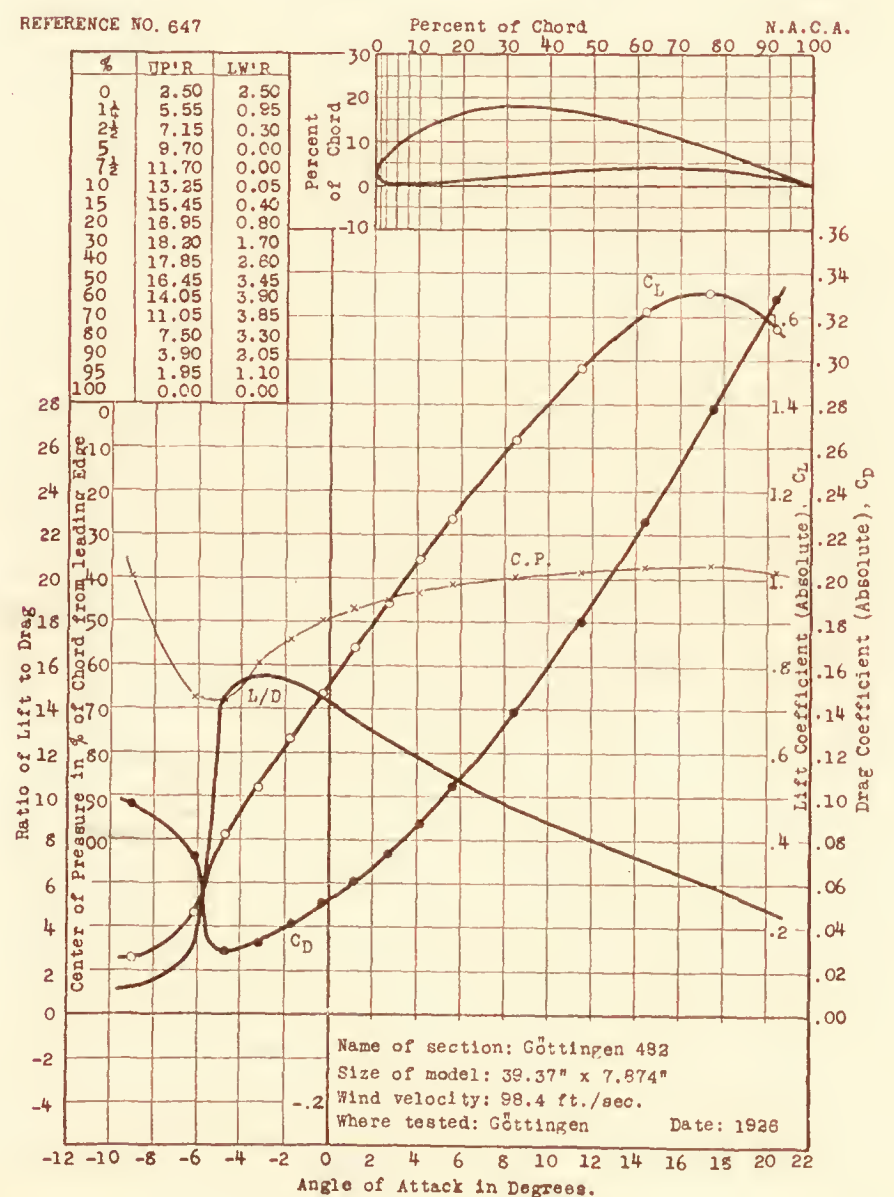
REFERENCE NO. 845



REFERENCE NO. 846

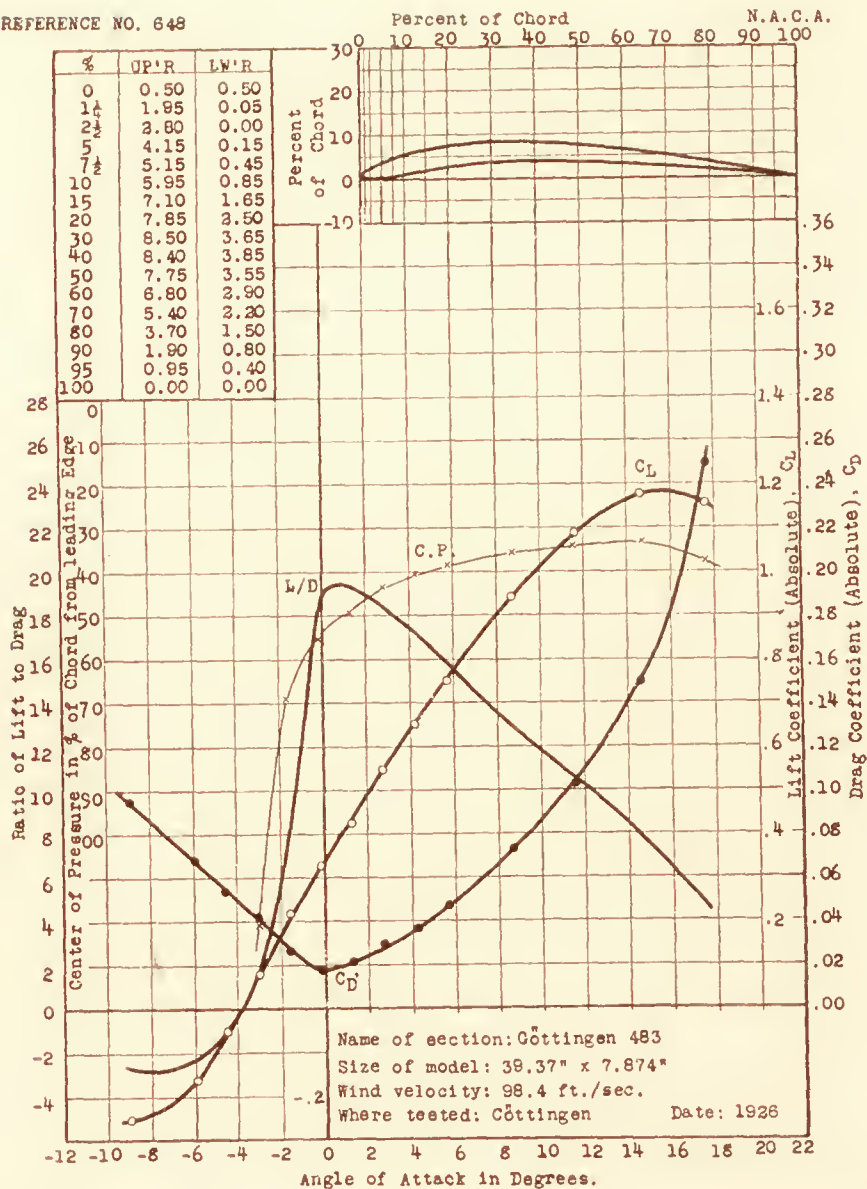


REFERENCE NO. 847

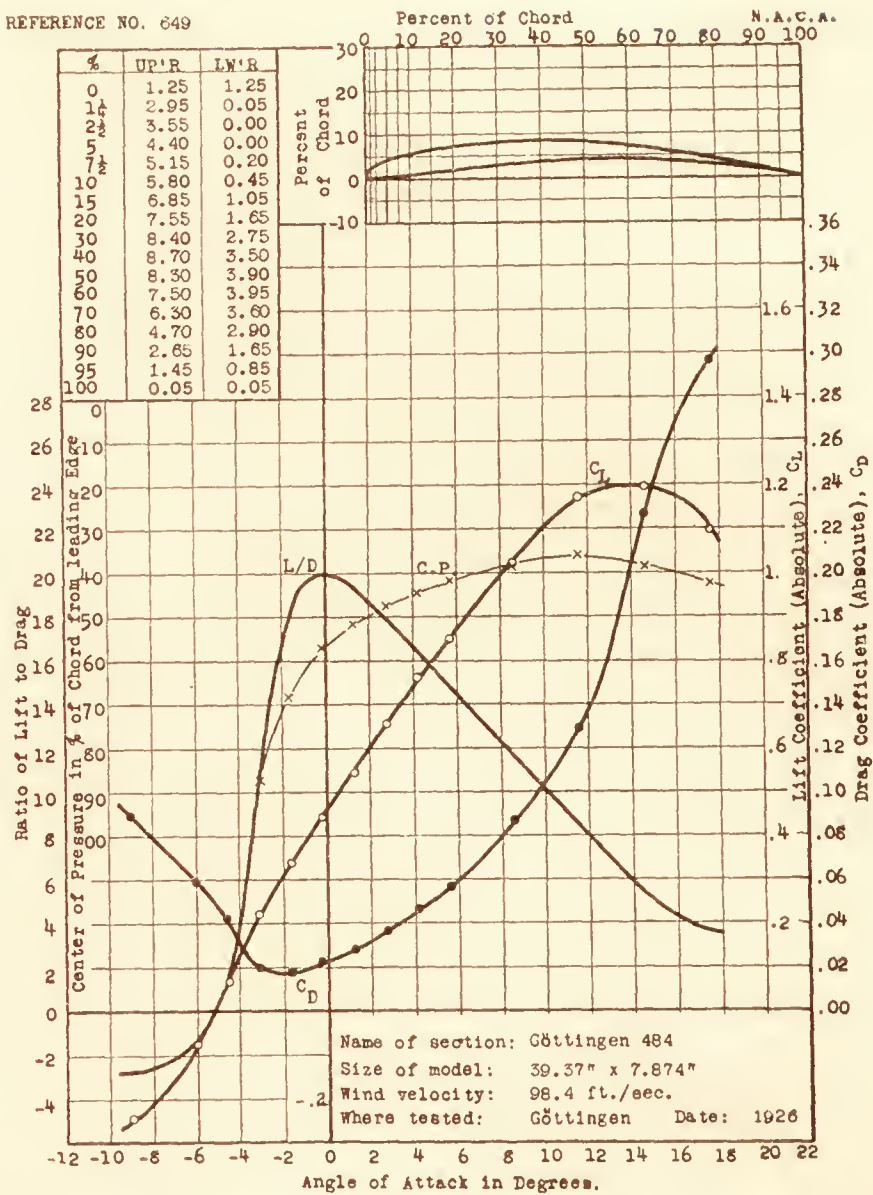




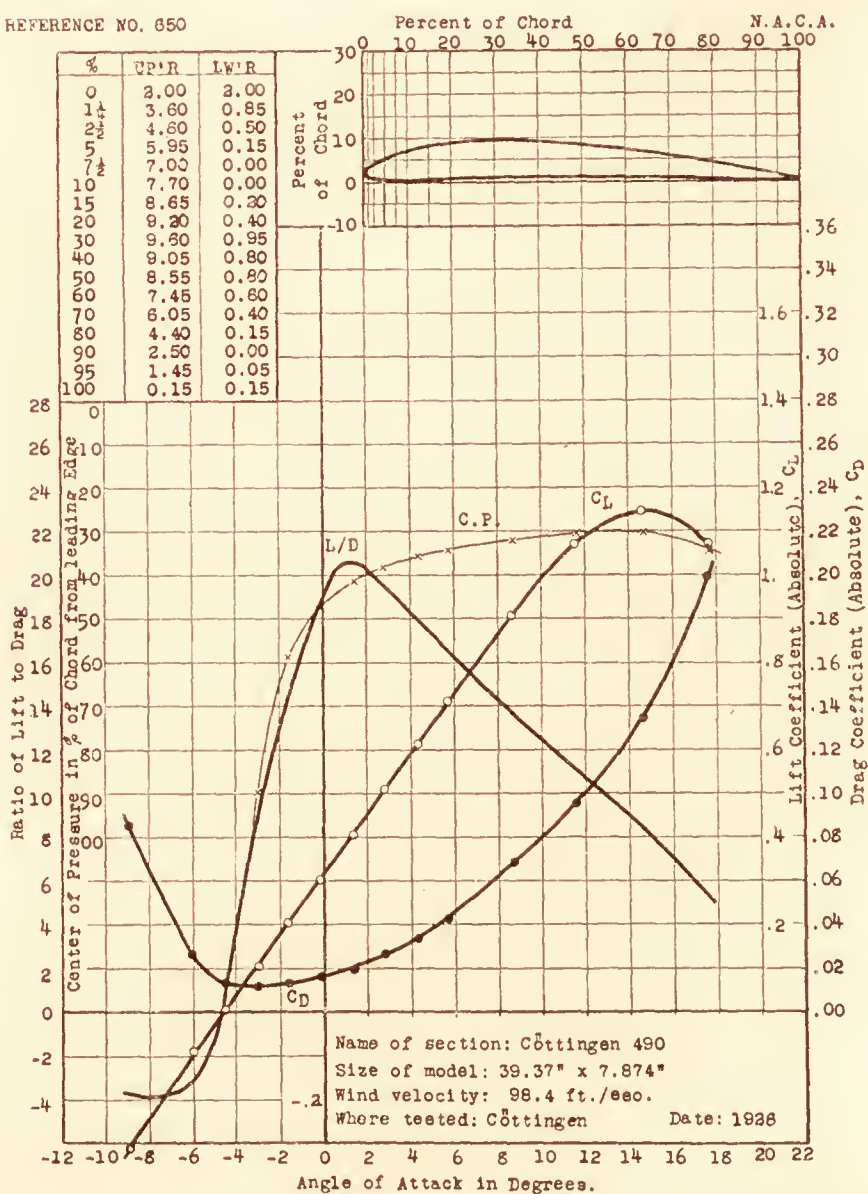
REFERENCE NO. 648



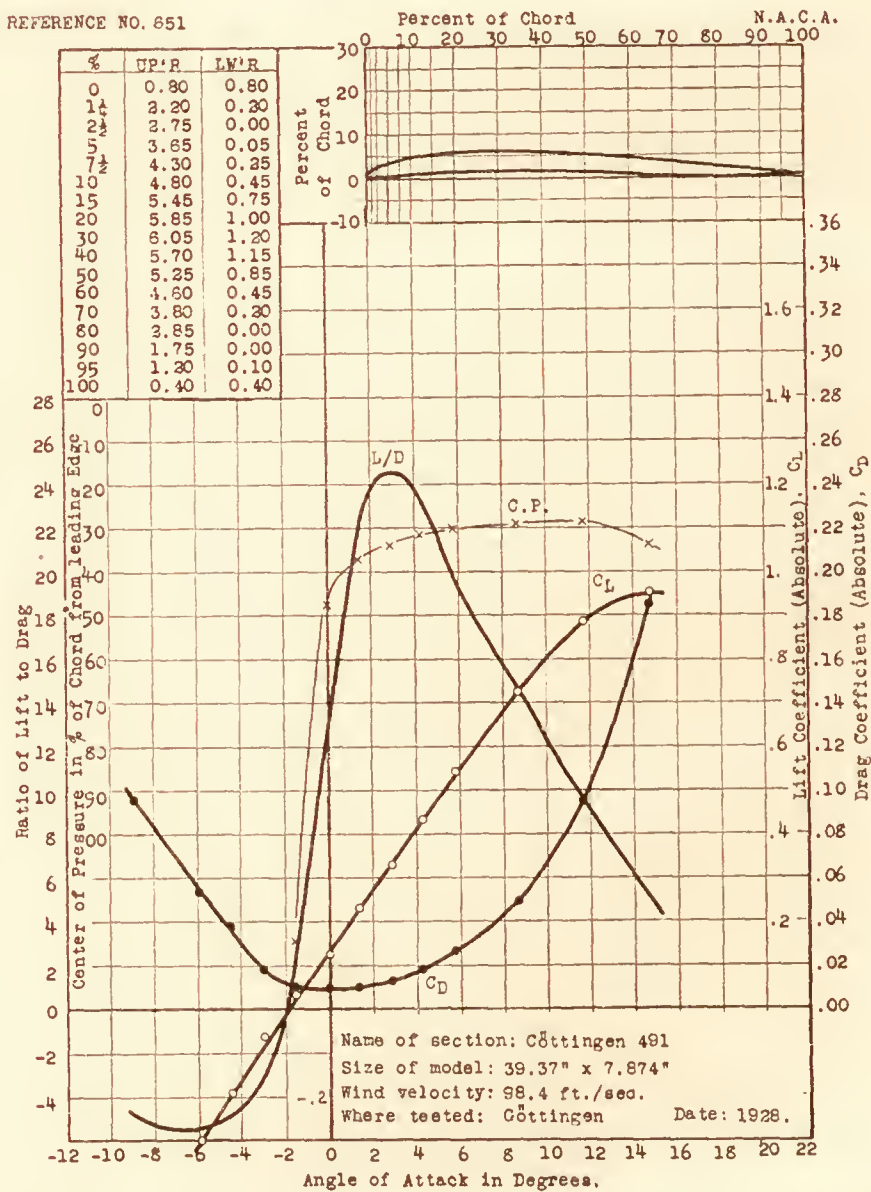
REFERENCE NO. 649



REFERENCE NO. 650

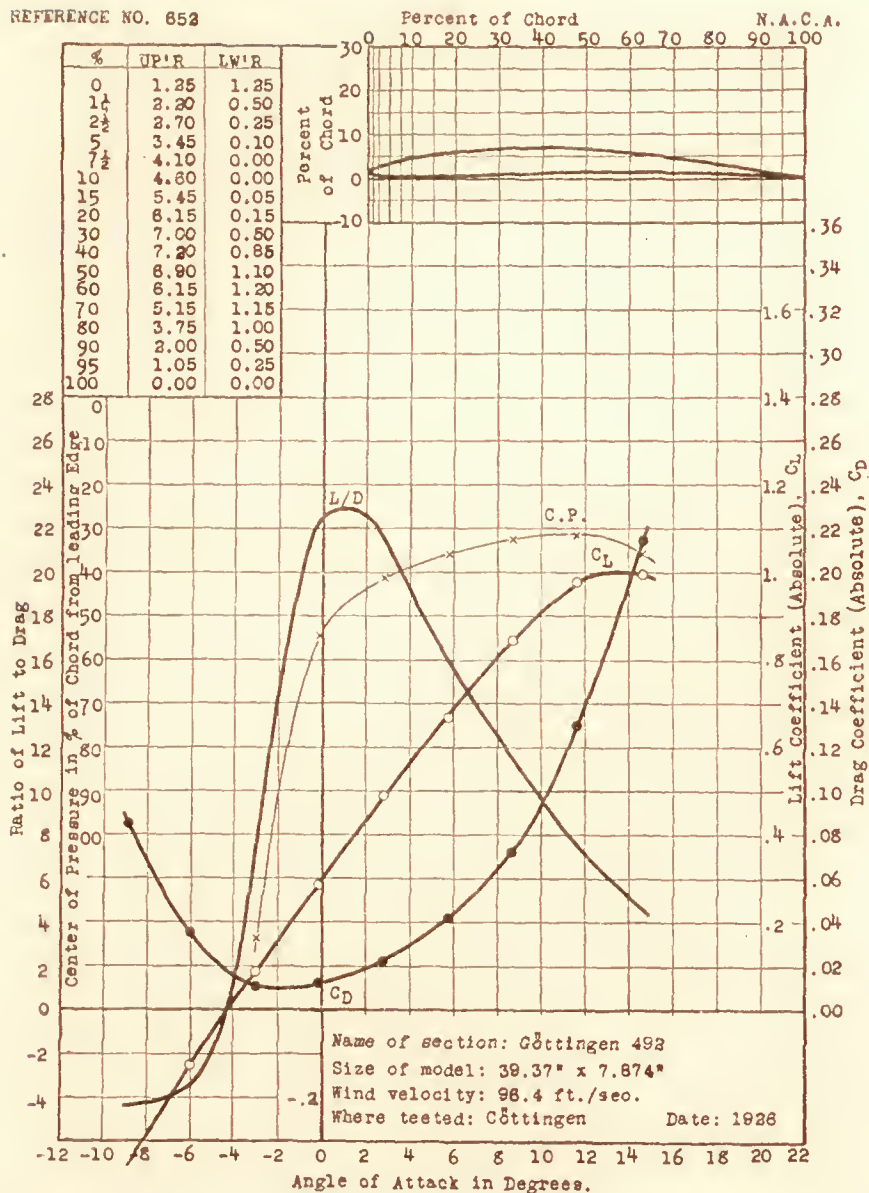


REFERENCE NO. 651

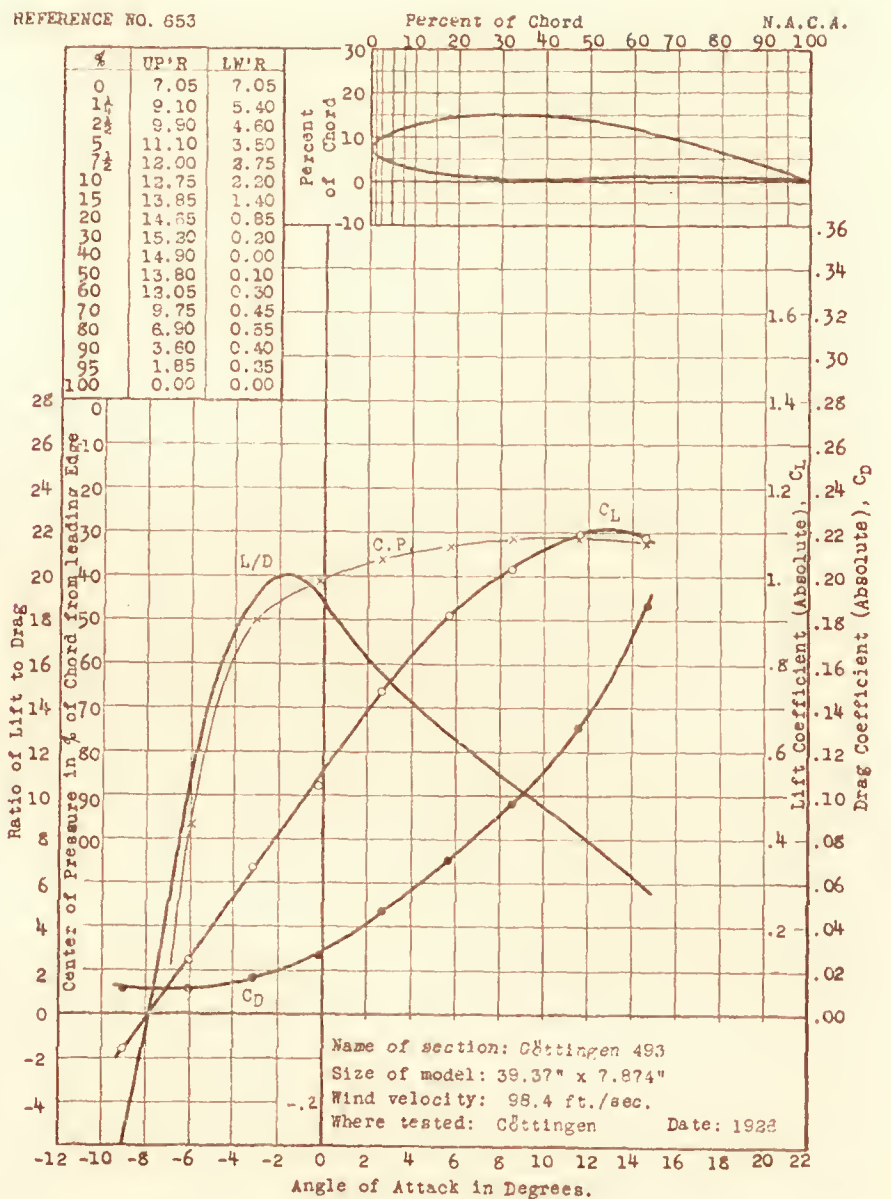




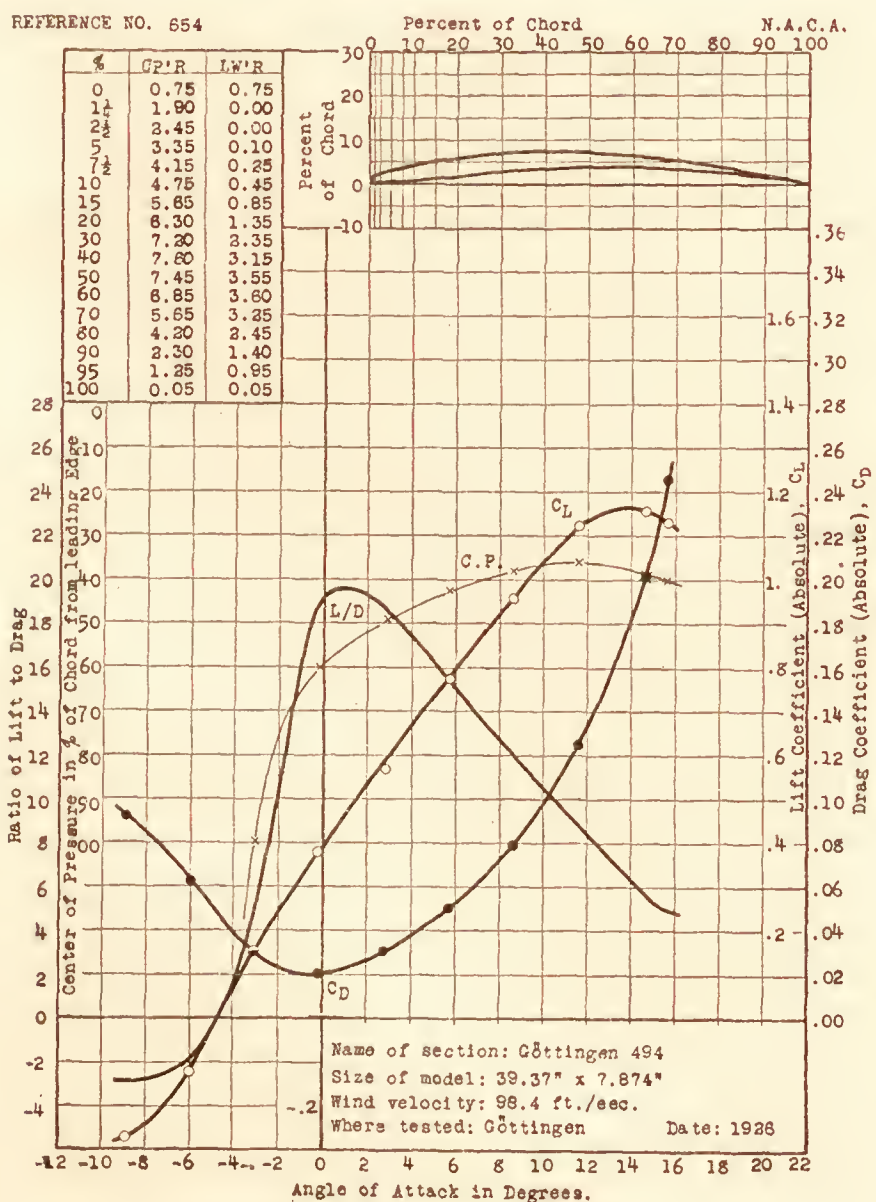
REFERENCE NO. 652



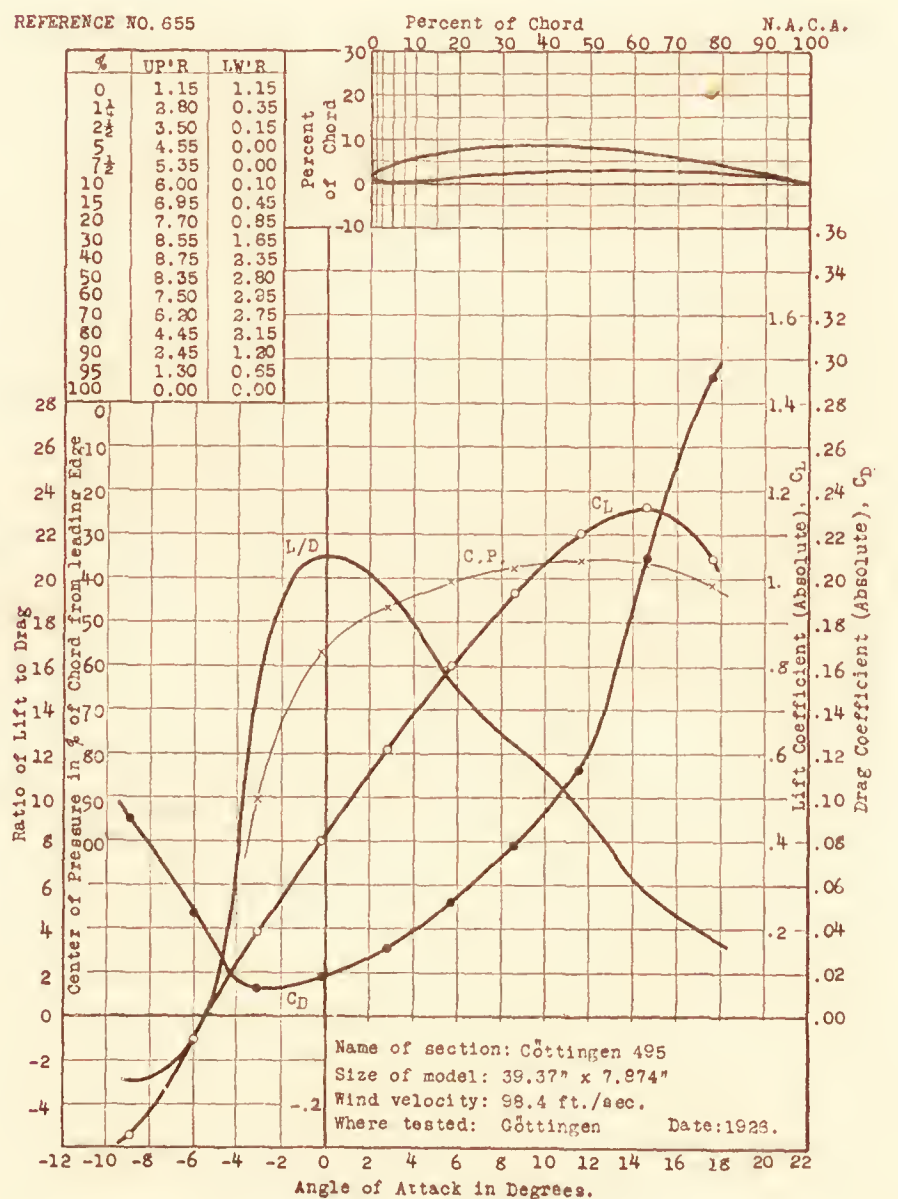
REFERENCE NO. 653



REFERENCE NO. 654



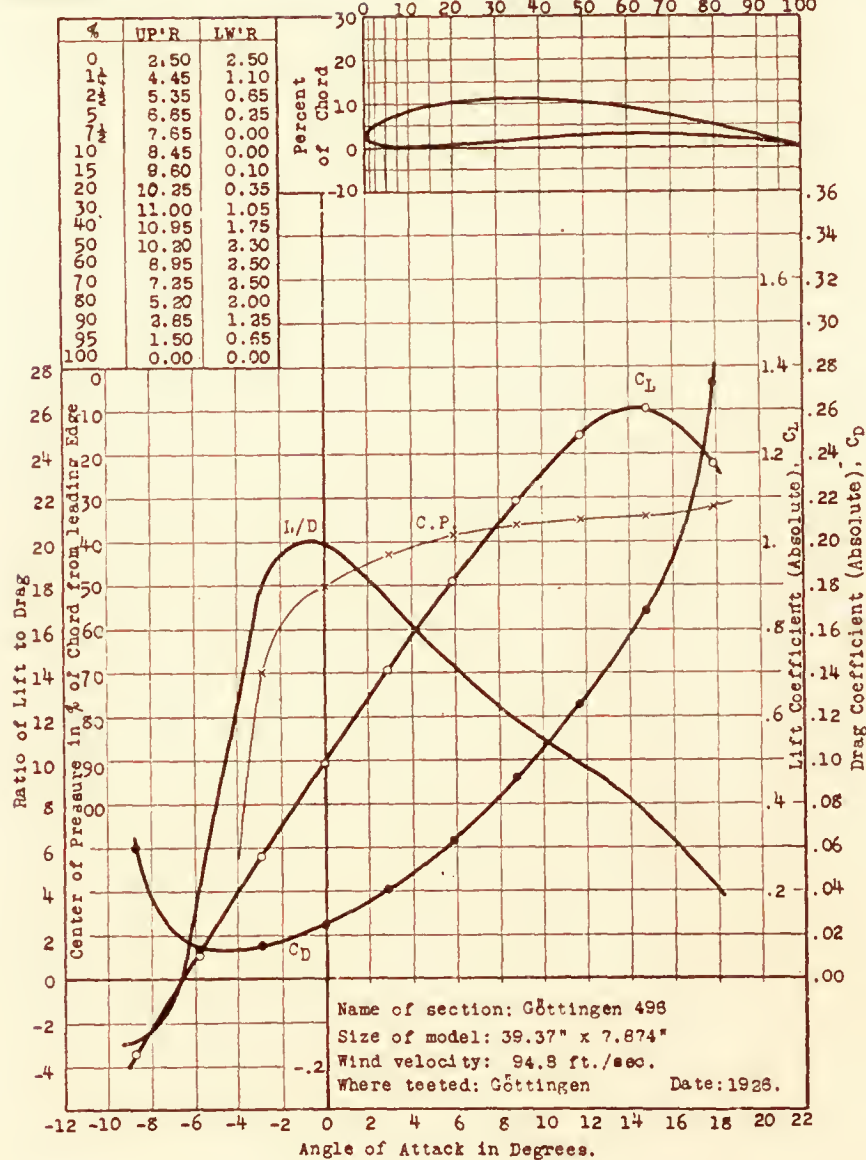
REFERENCE NO. 655





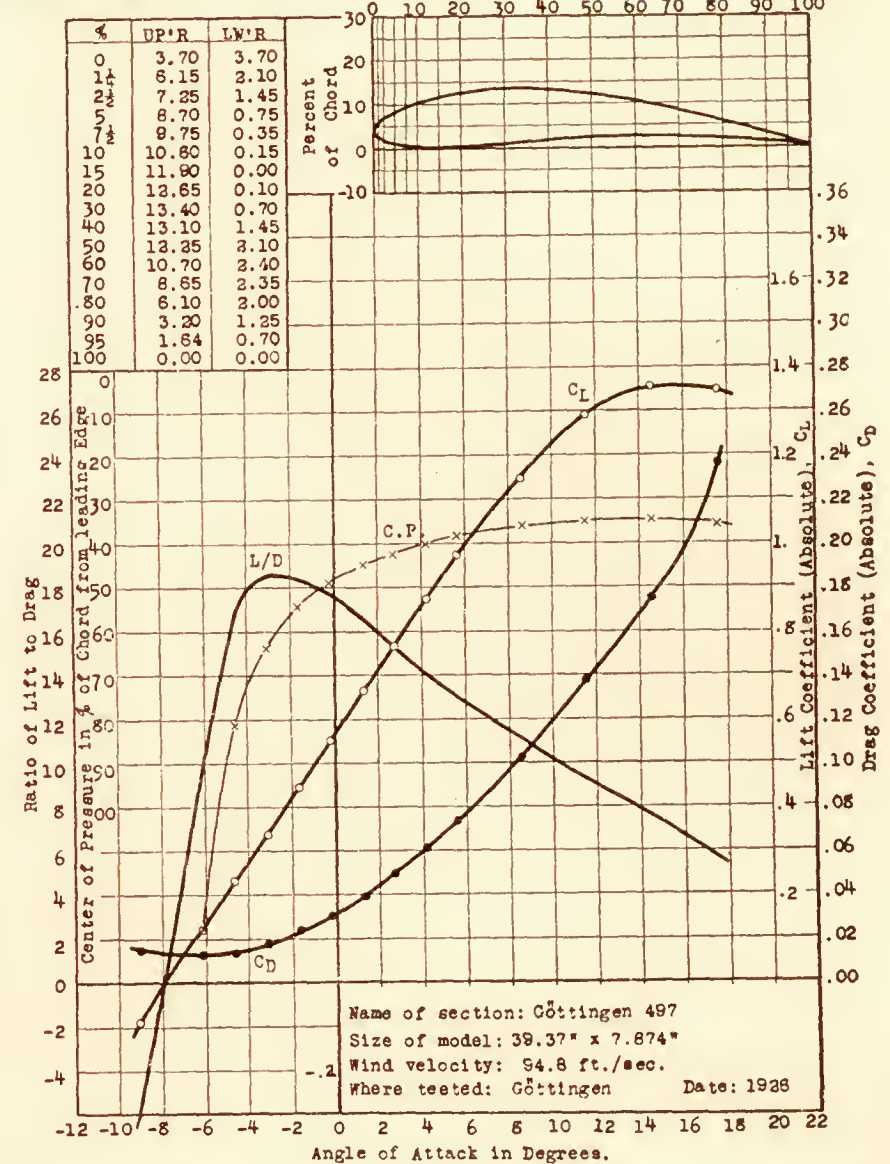
REFERENCE NO. 856

Percent of Chord N.A.C.A.



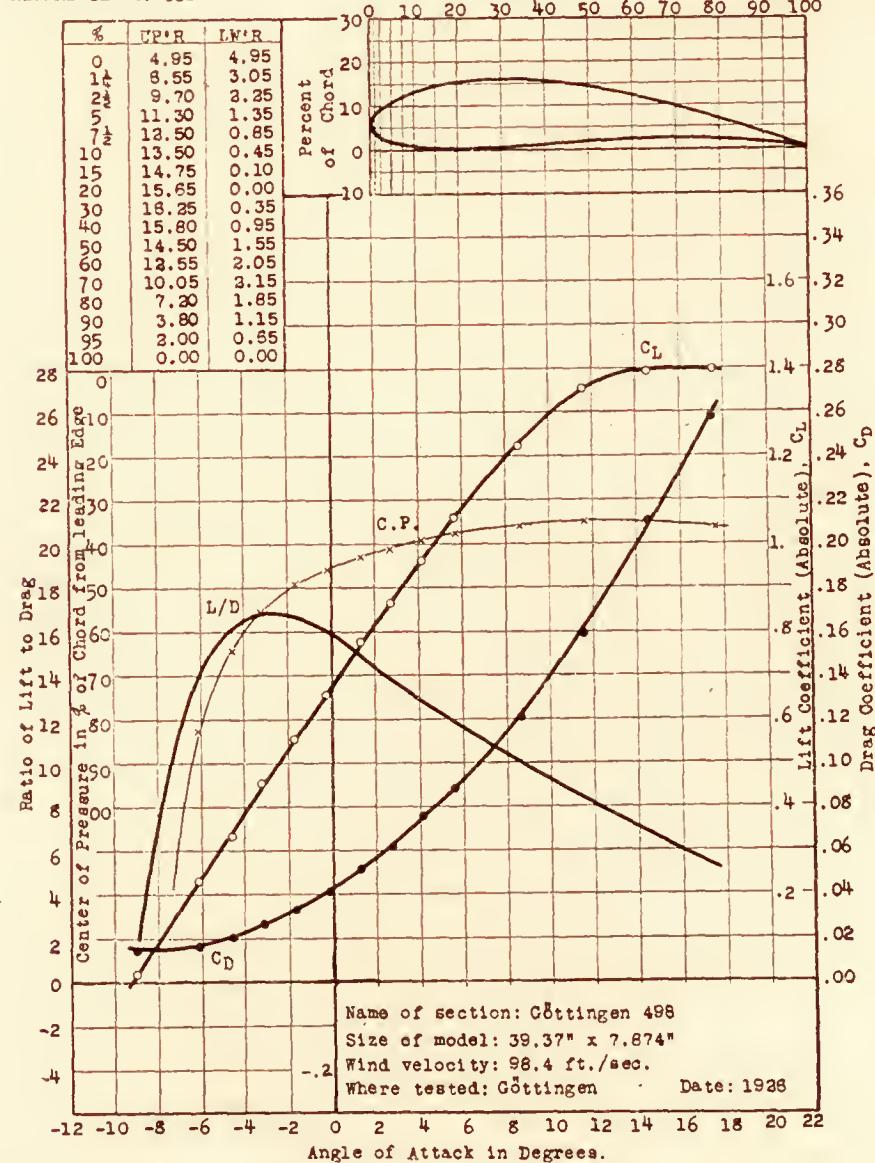
REFERENCE NO. 857

Percent of Chord N.A.C.A.



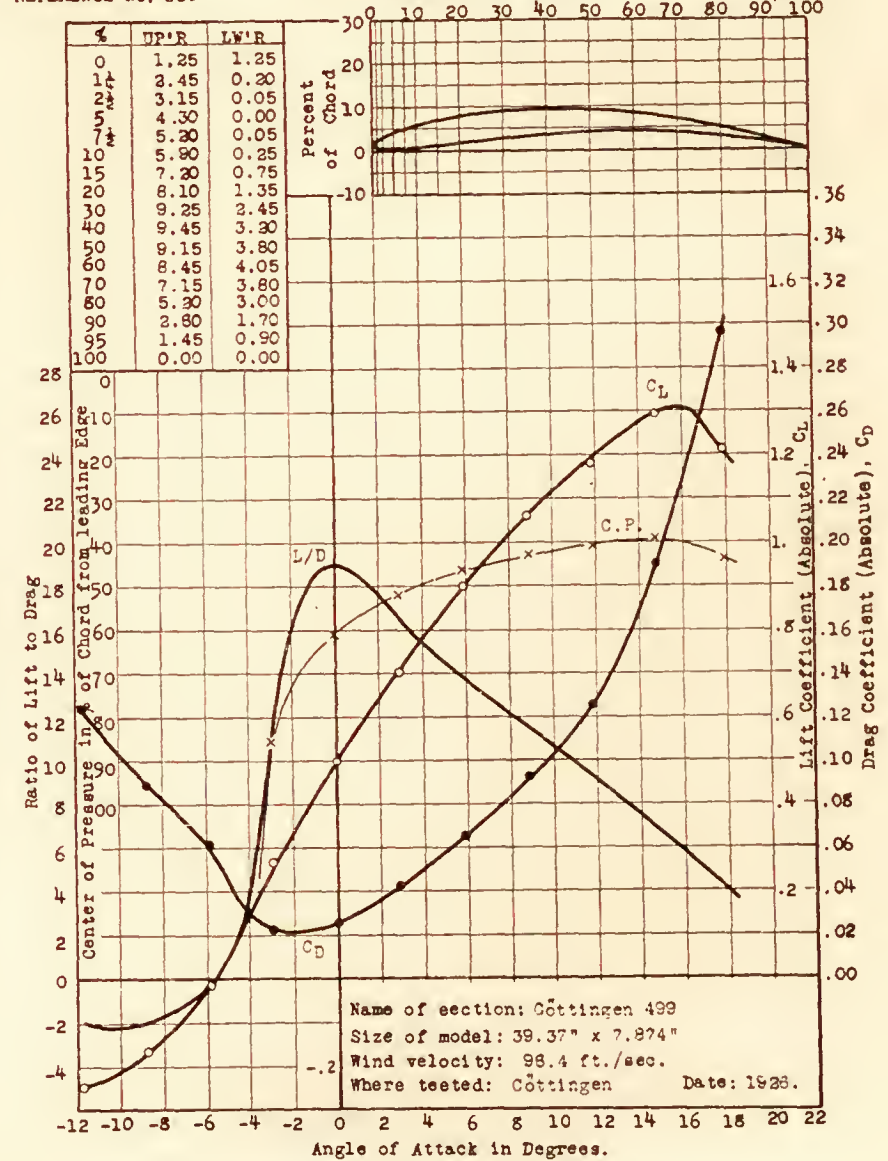
REFERENCE NO. 858

Percent of Chord N.A.C.A.



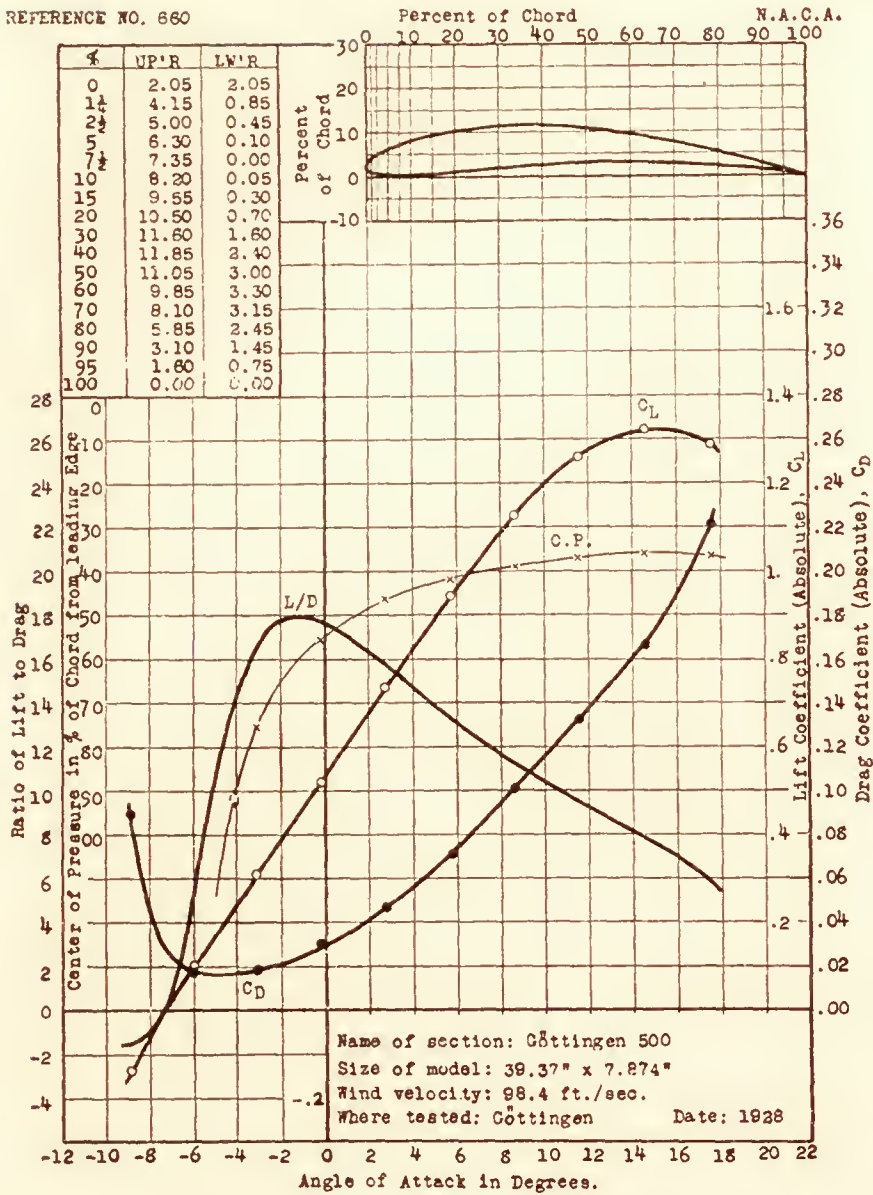
REFERENCE NO. 859

Percent of Chord N.A.C.A.

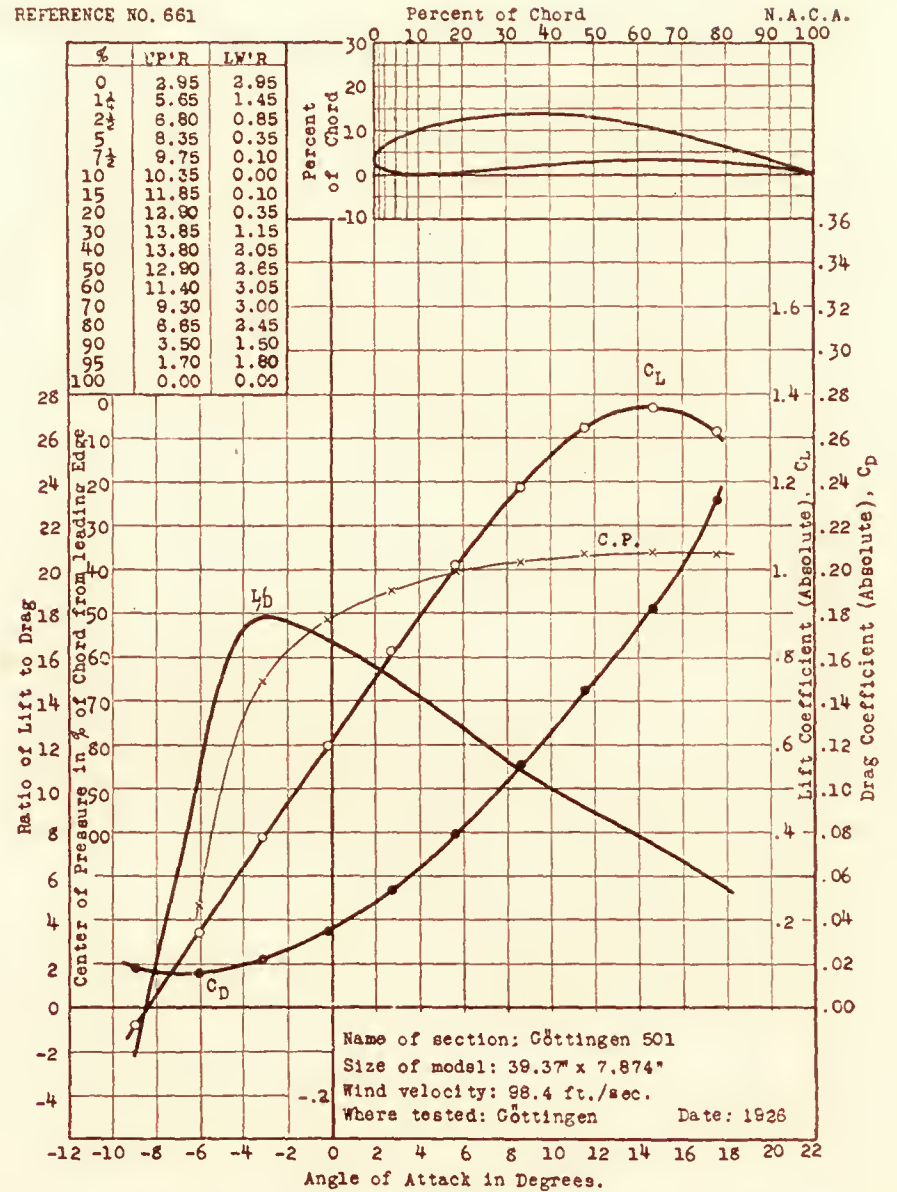




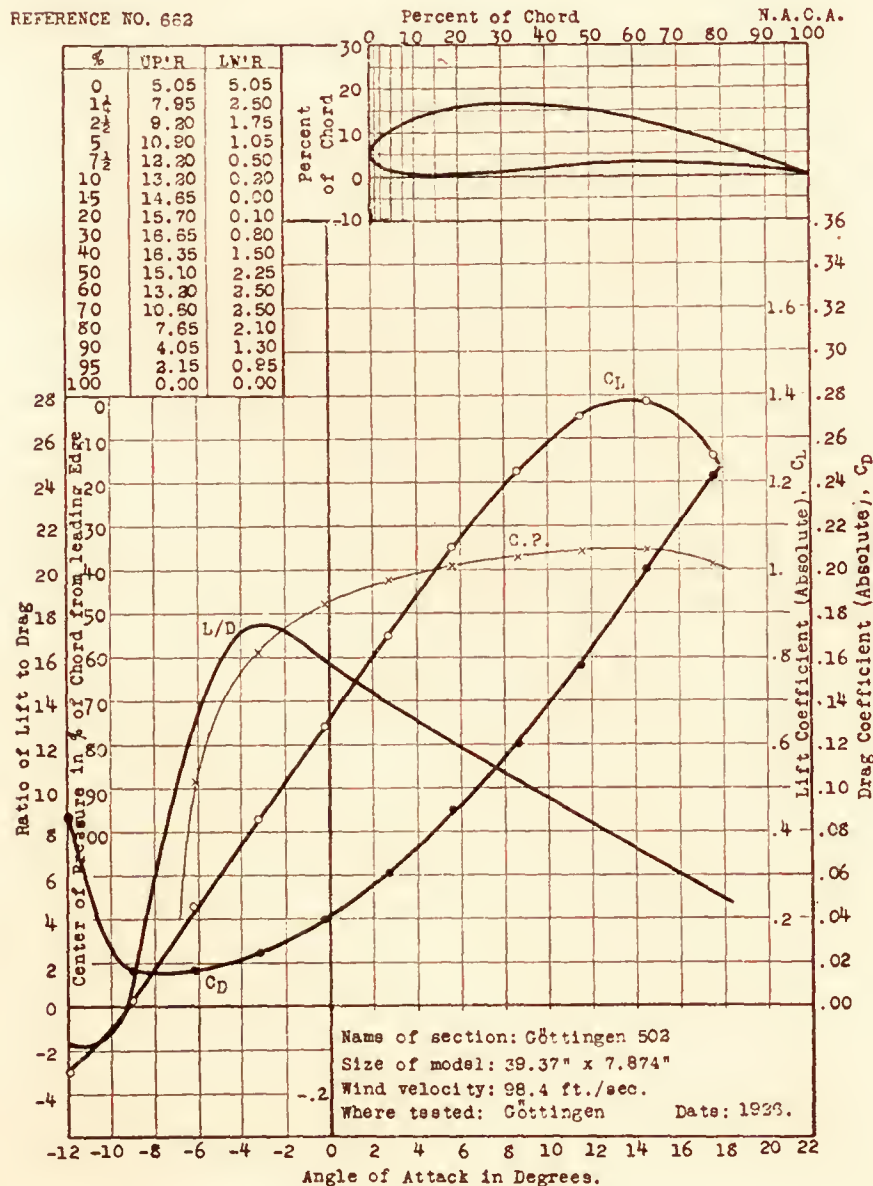
REFERENCE NO. 660



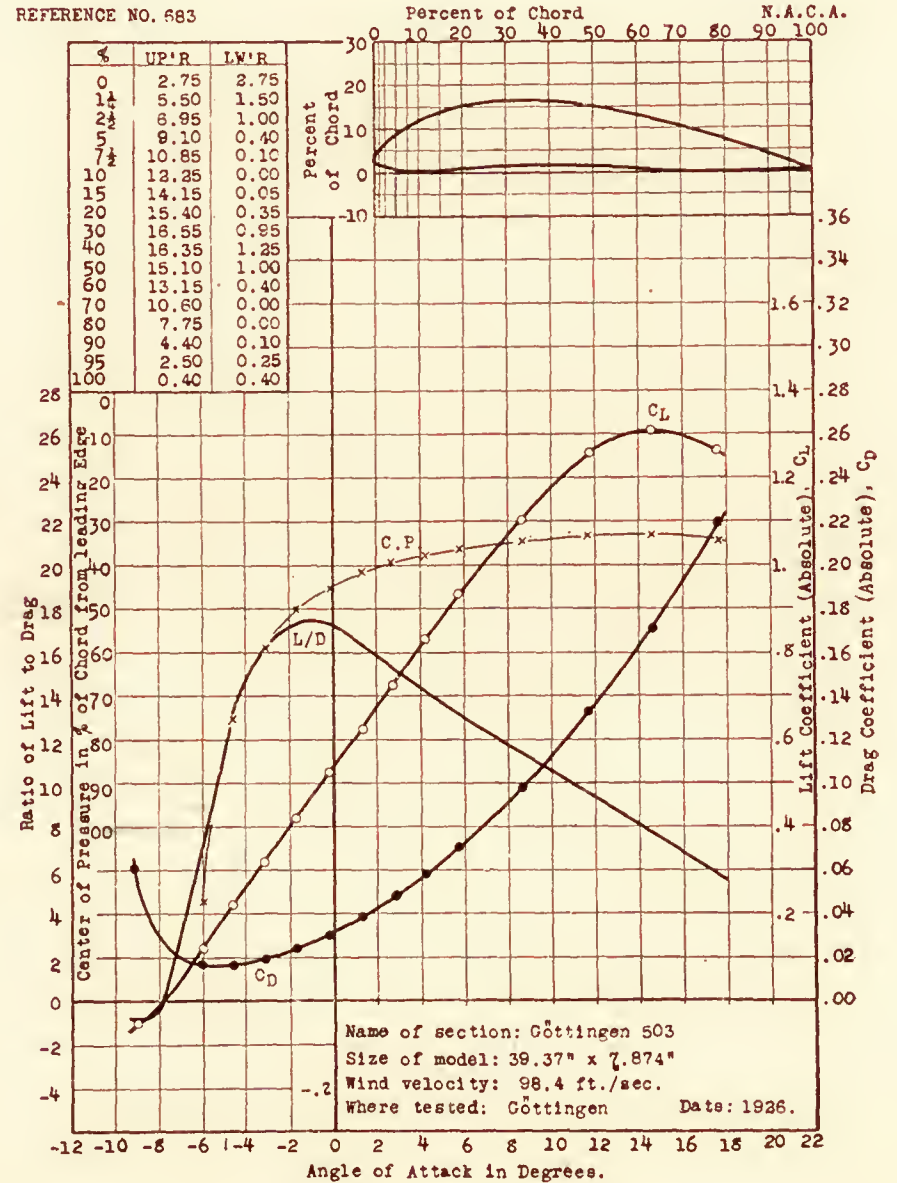
REFERENCE NO. 661



REFERENCE NO. 662

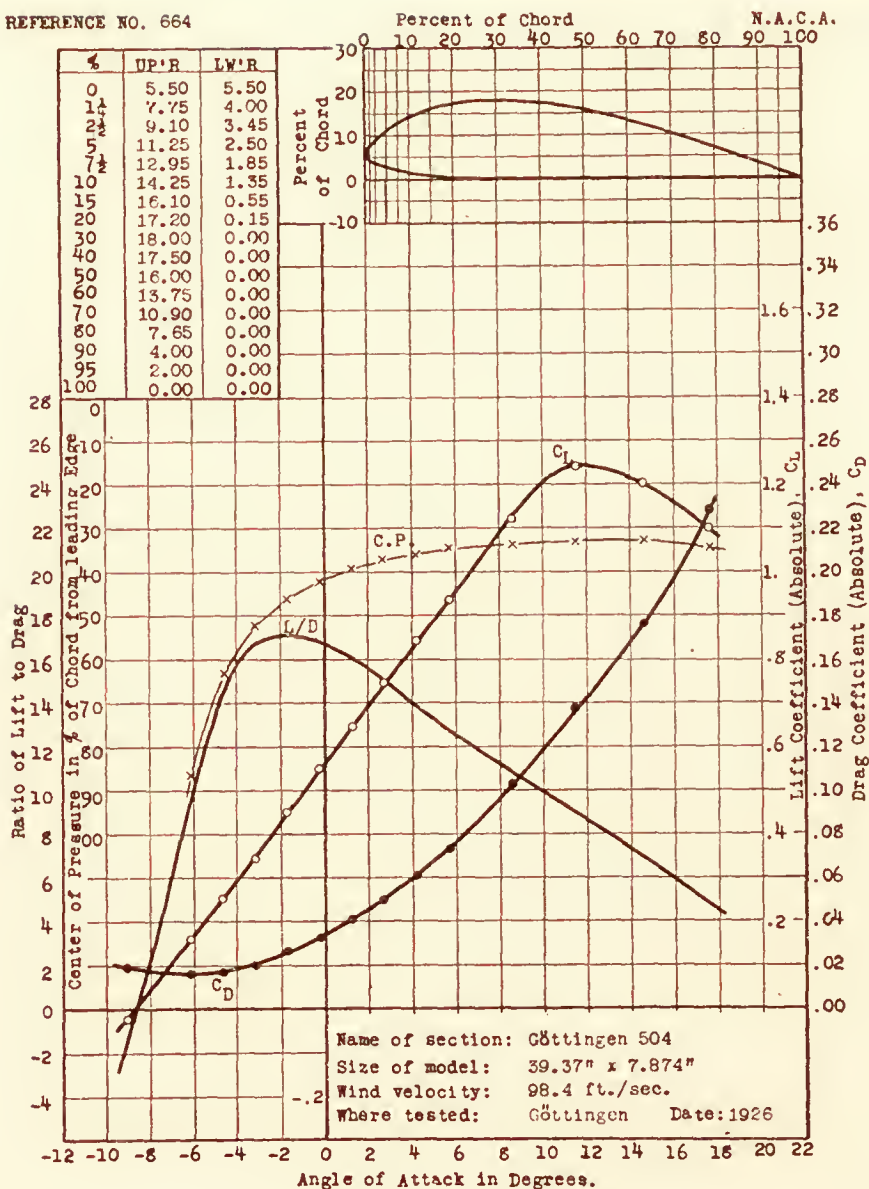


REFERENCE NO. 683

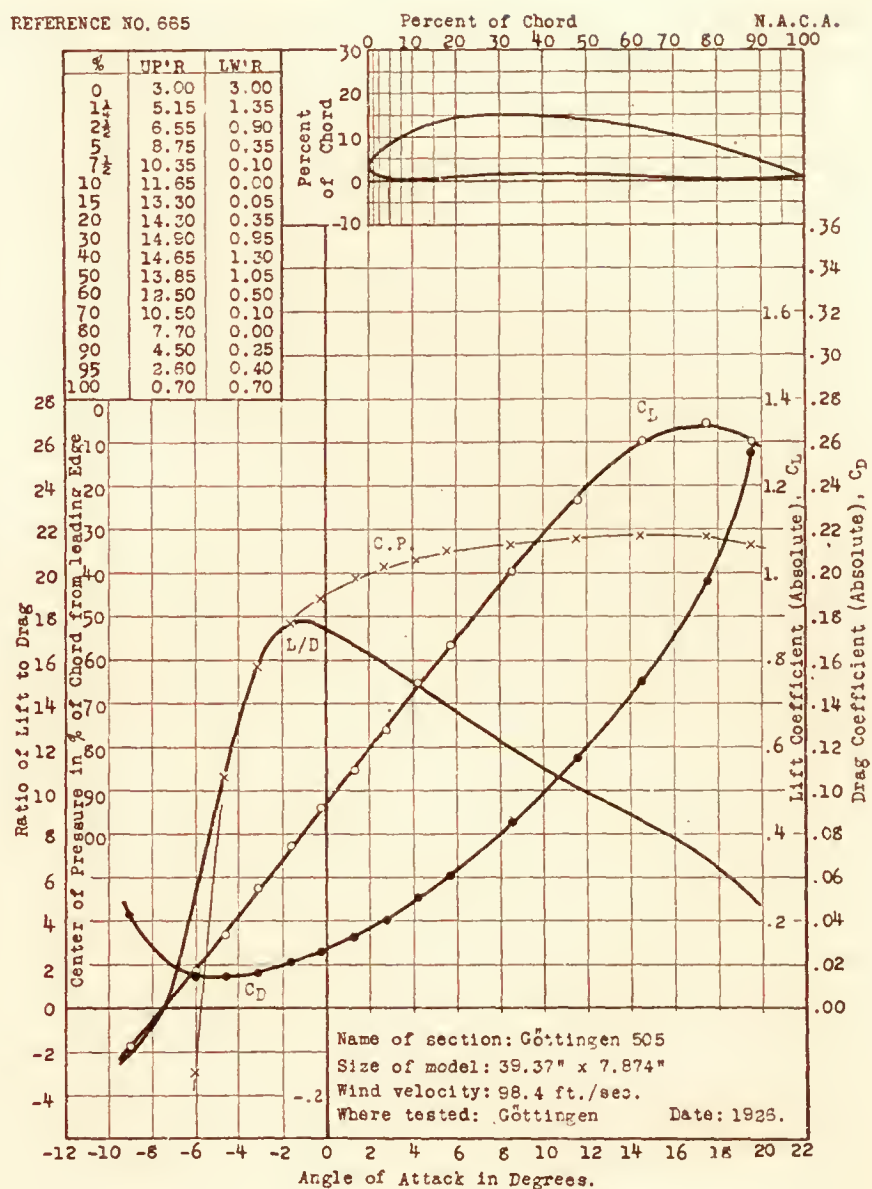




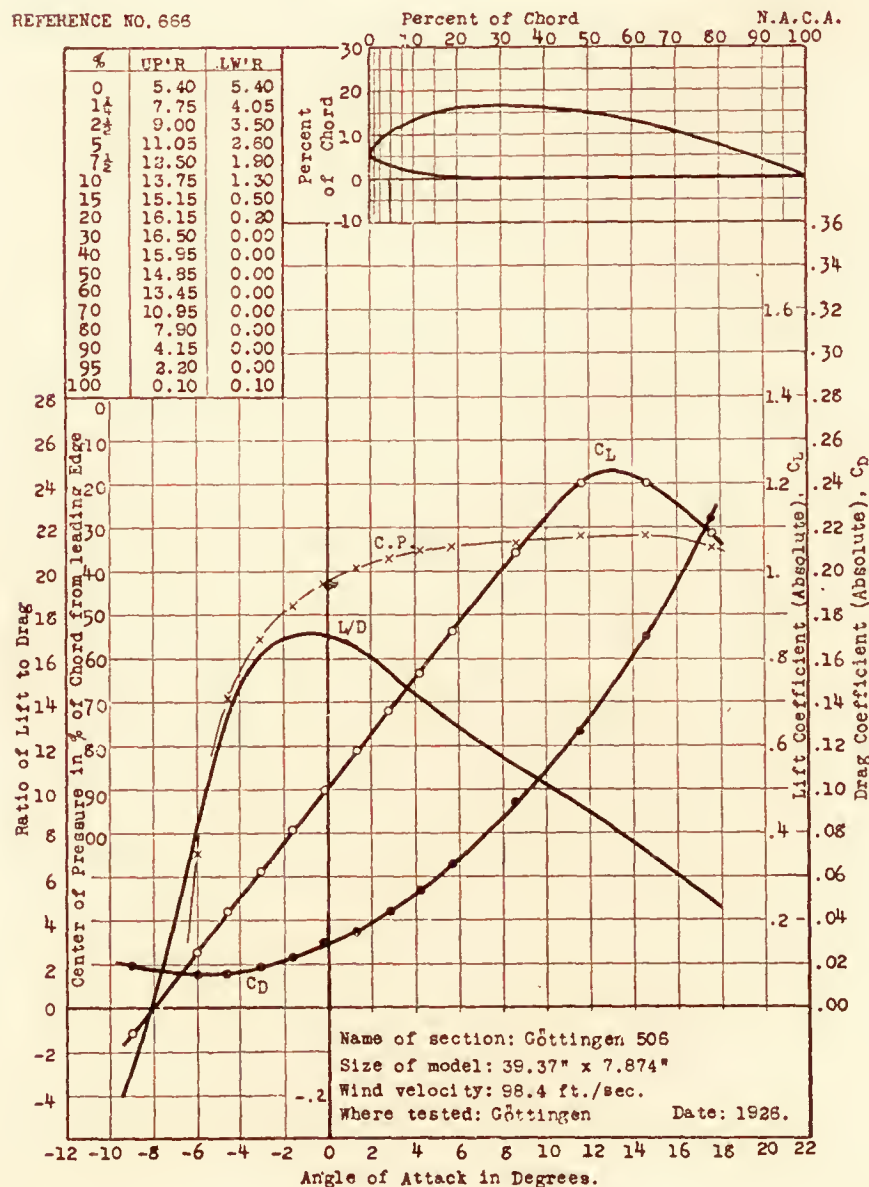
REFERENCE NO. 664



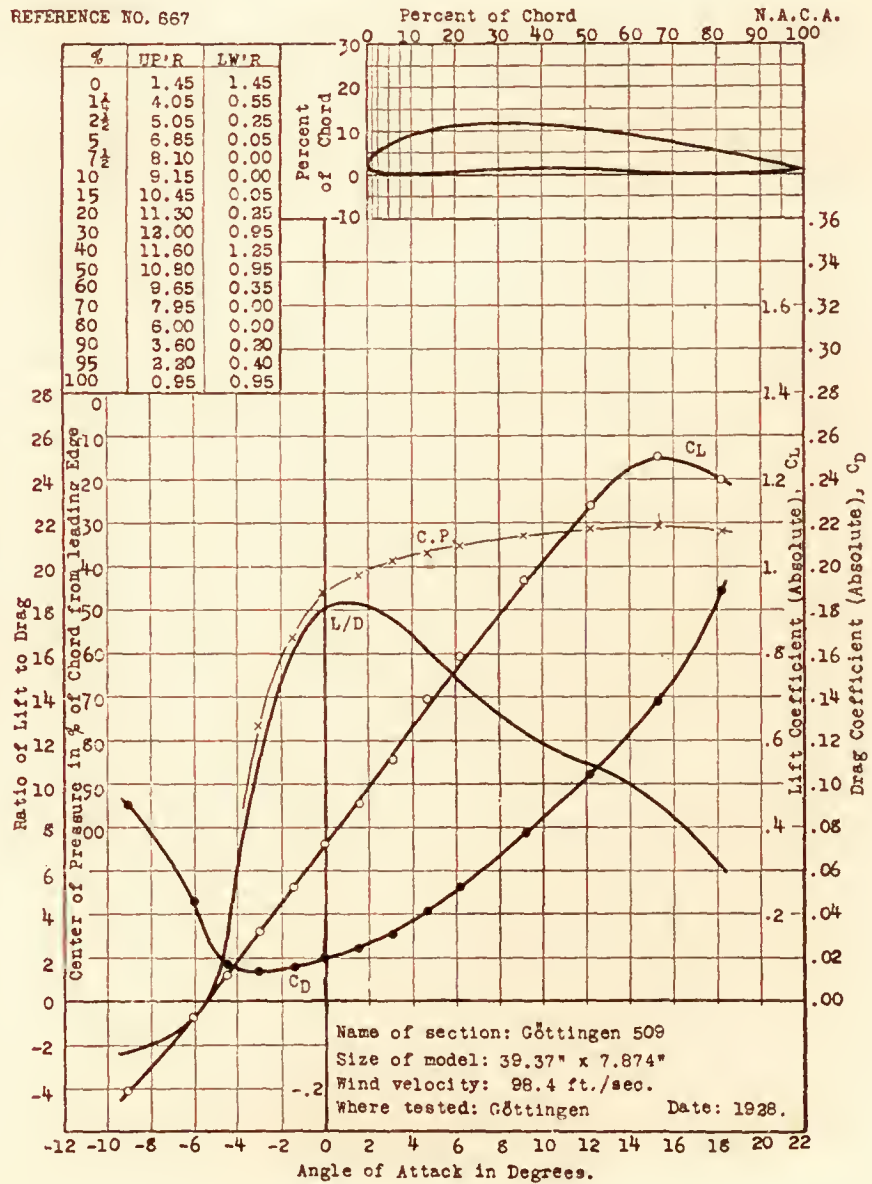
REFERENCE NO. 665



REFERENCE NO. 666

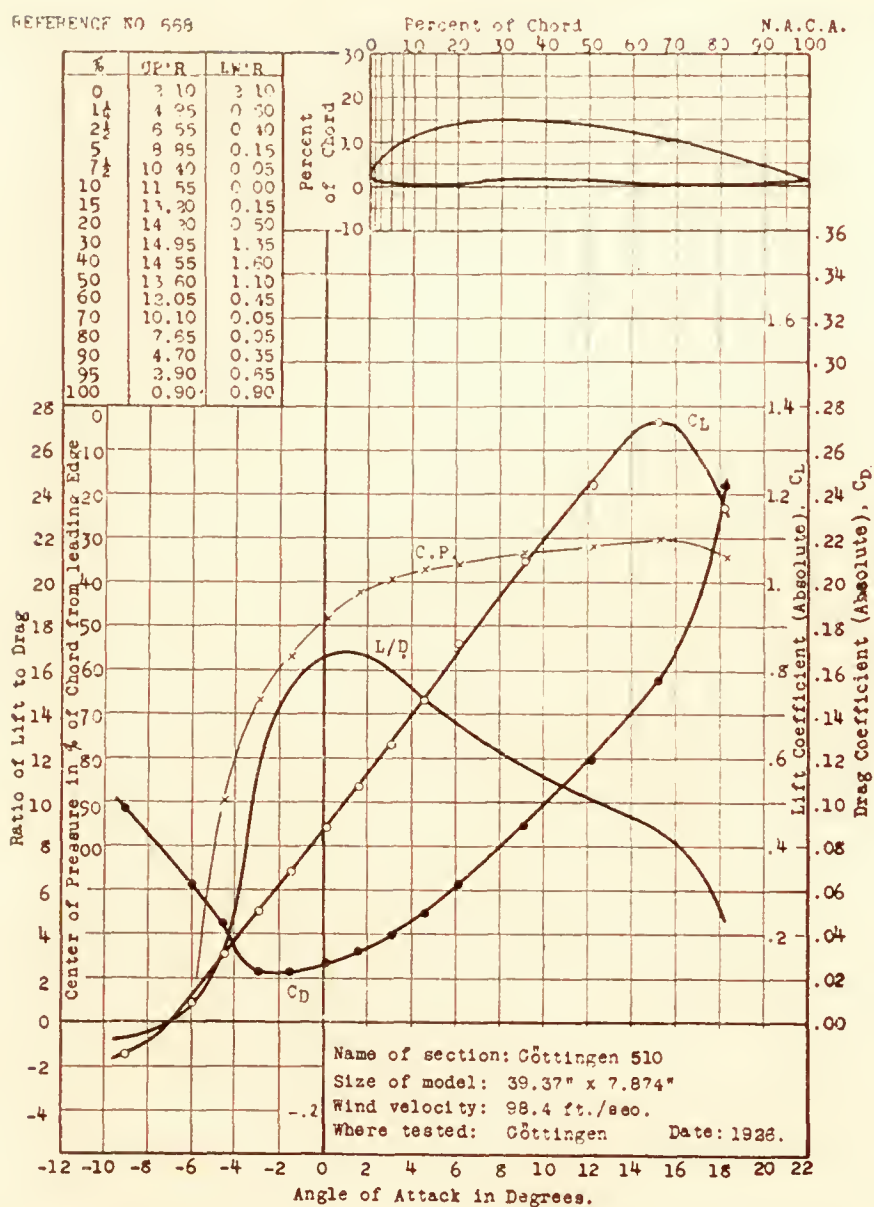


REFERENCE NO. 667

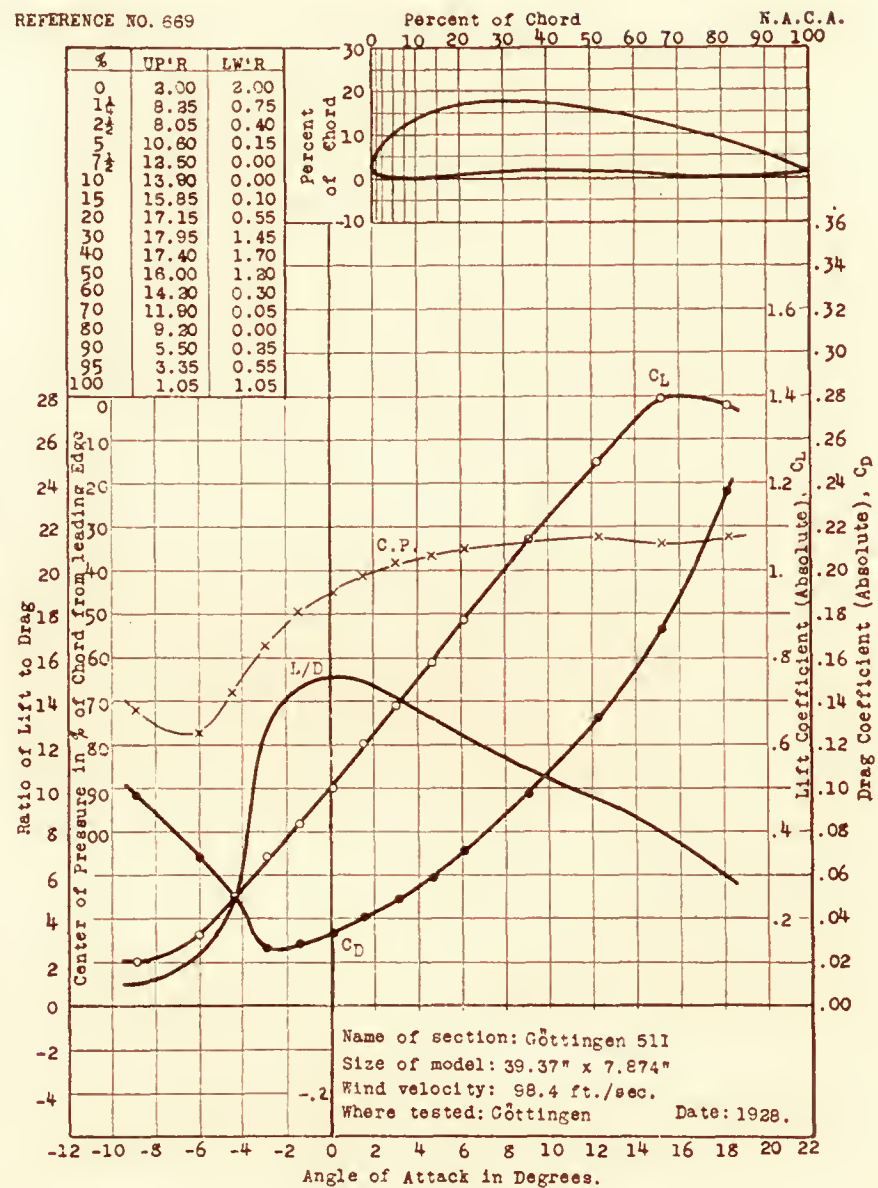




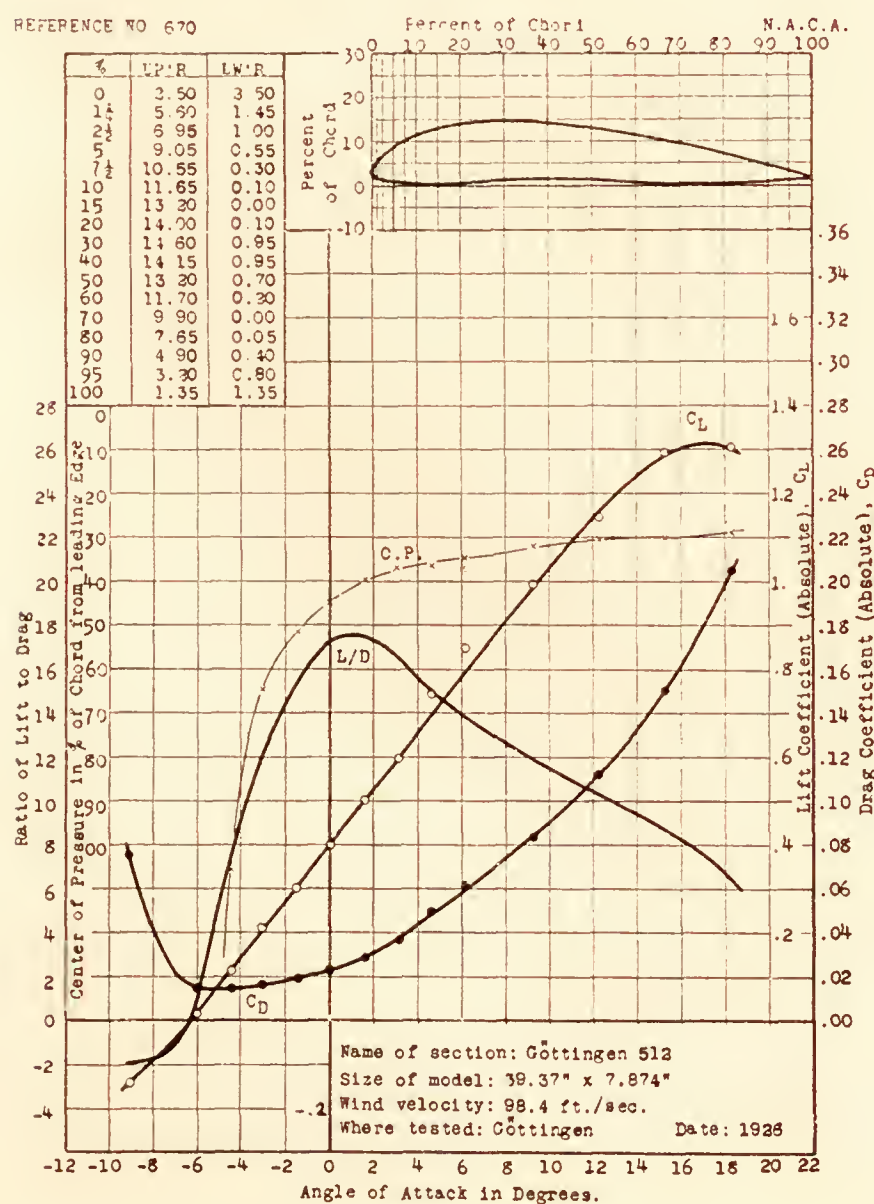
REFERENCE NO. 668



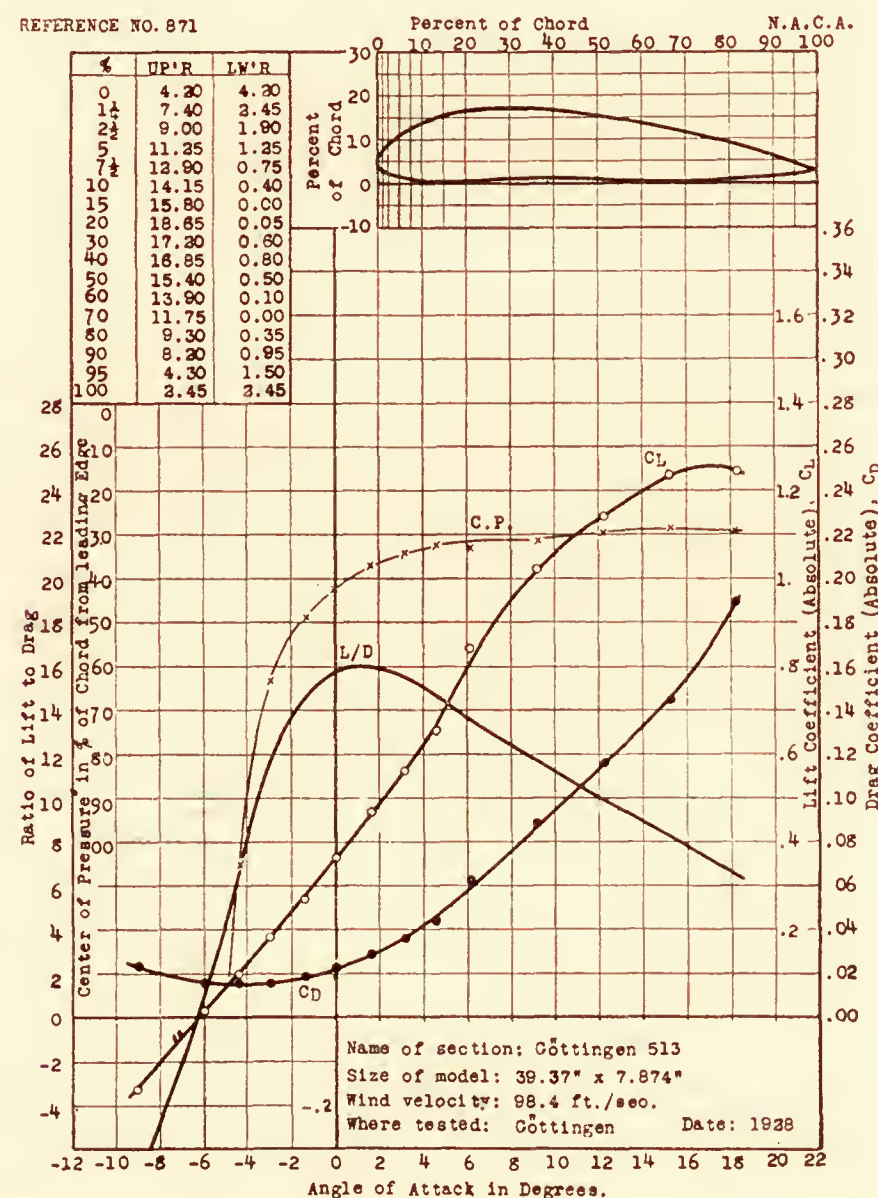
REFERENCE NO. 669



REFERENCE NO. 670

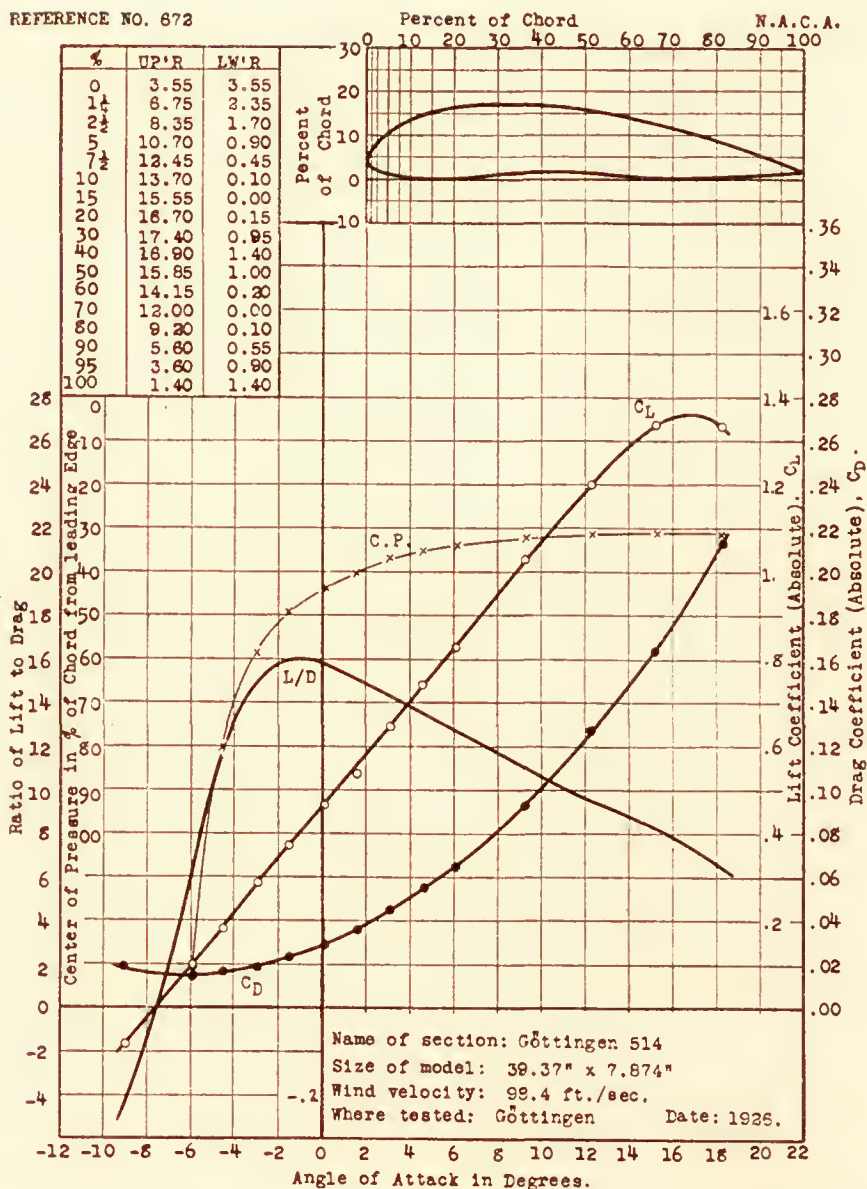


REFERENCE NO. 871

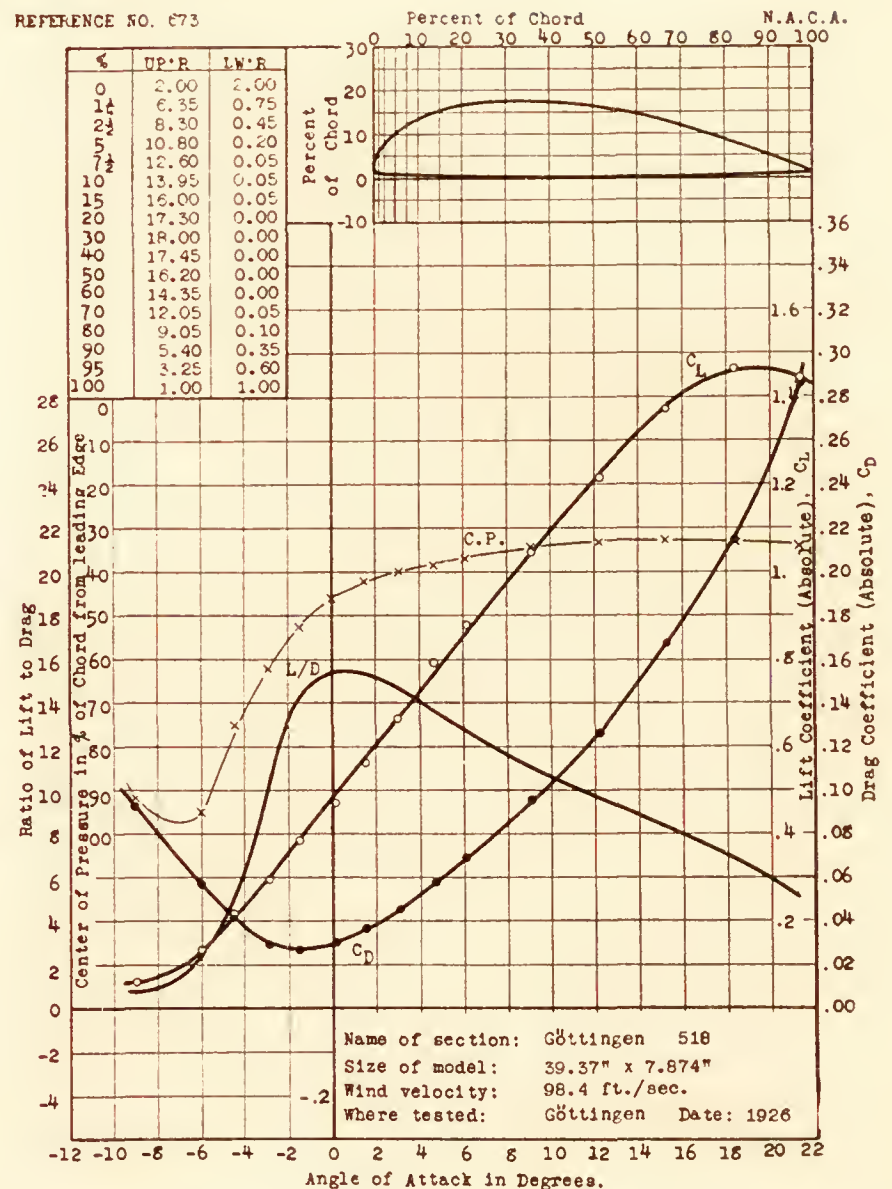




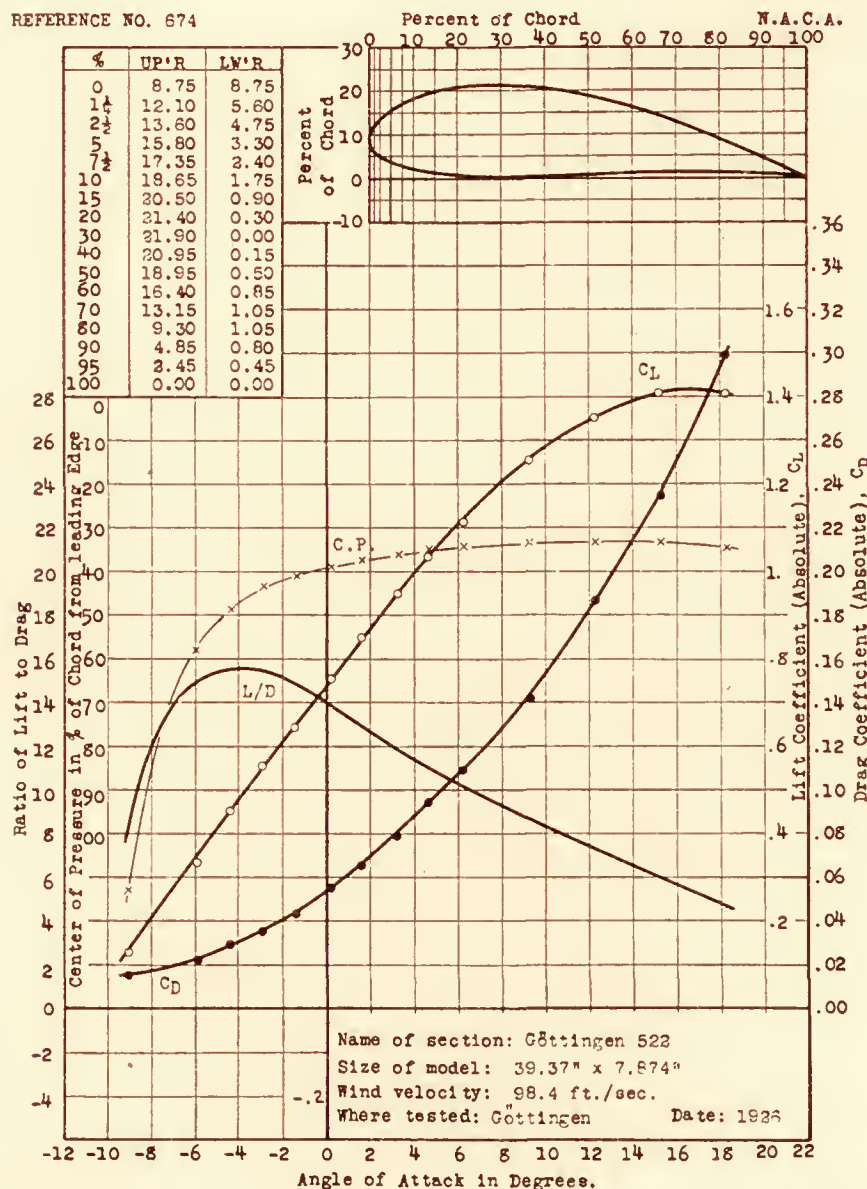
REFERENCE NO. 672



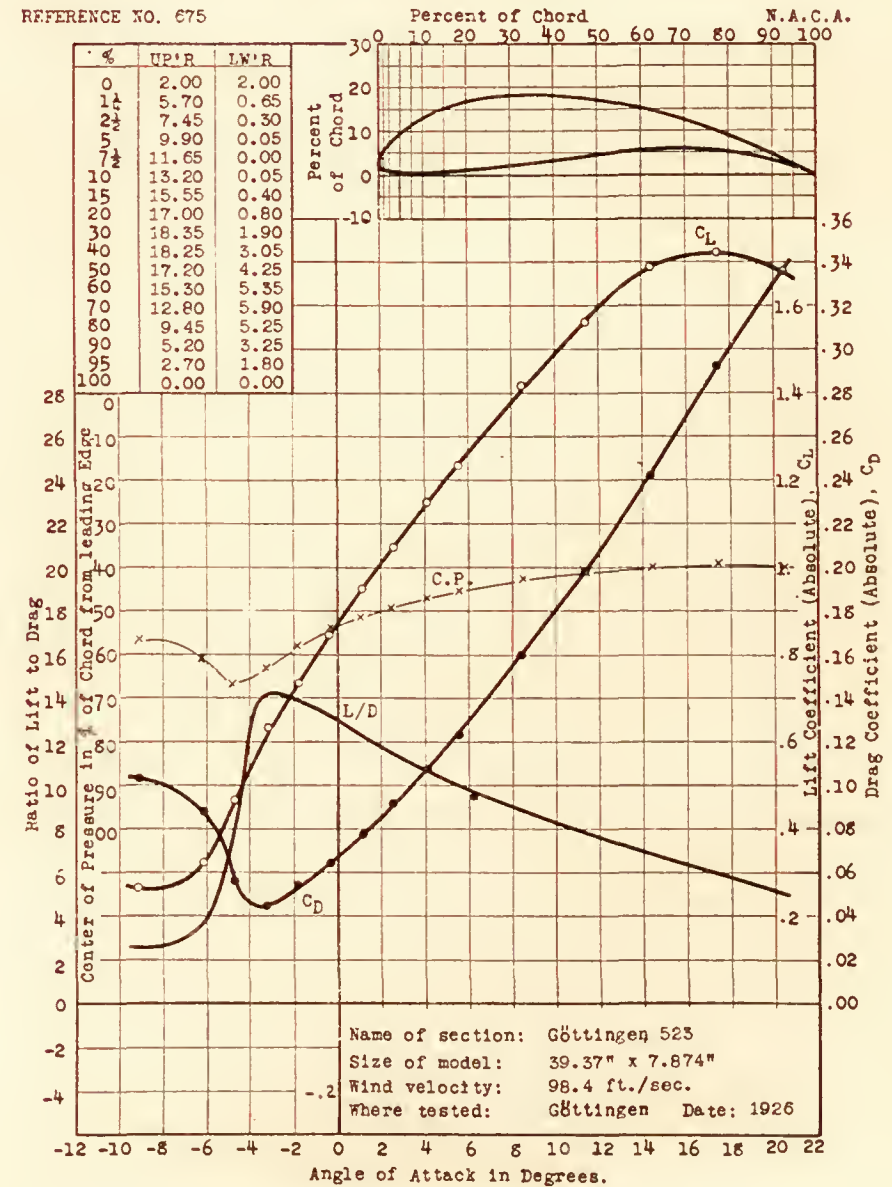
REFERENCE NO. 673



REFERENCE NO. 674

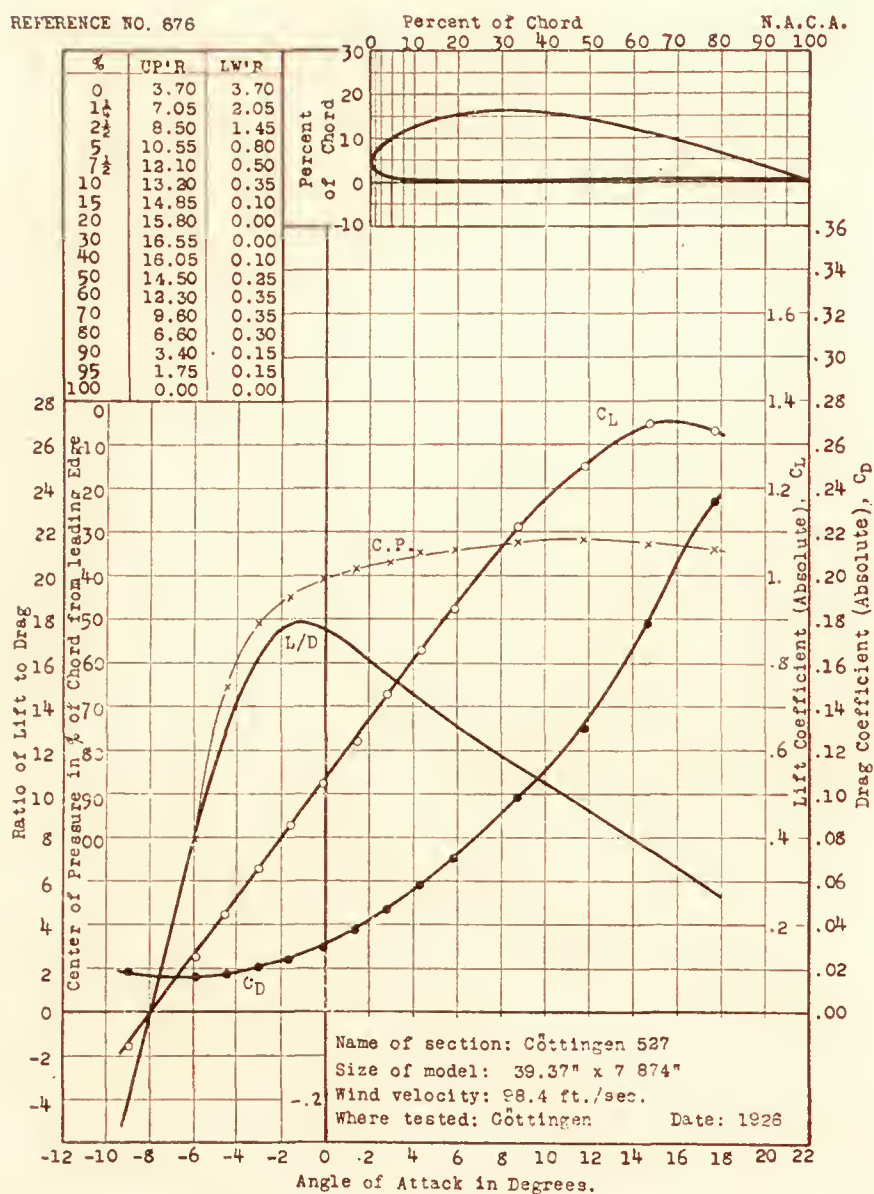


REFERENCE NO. 675

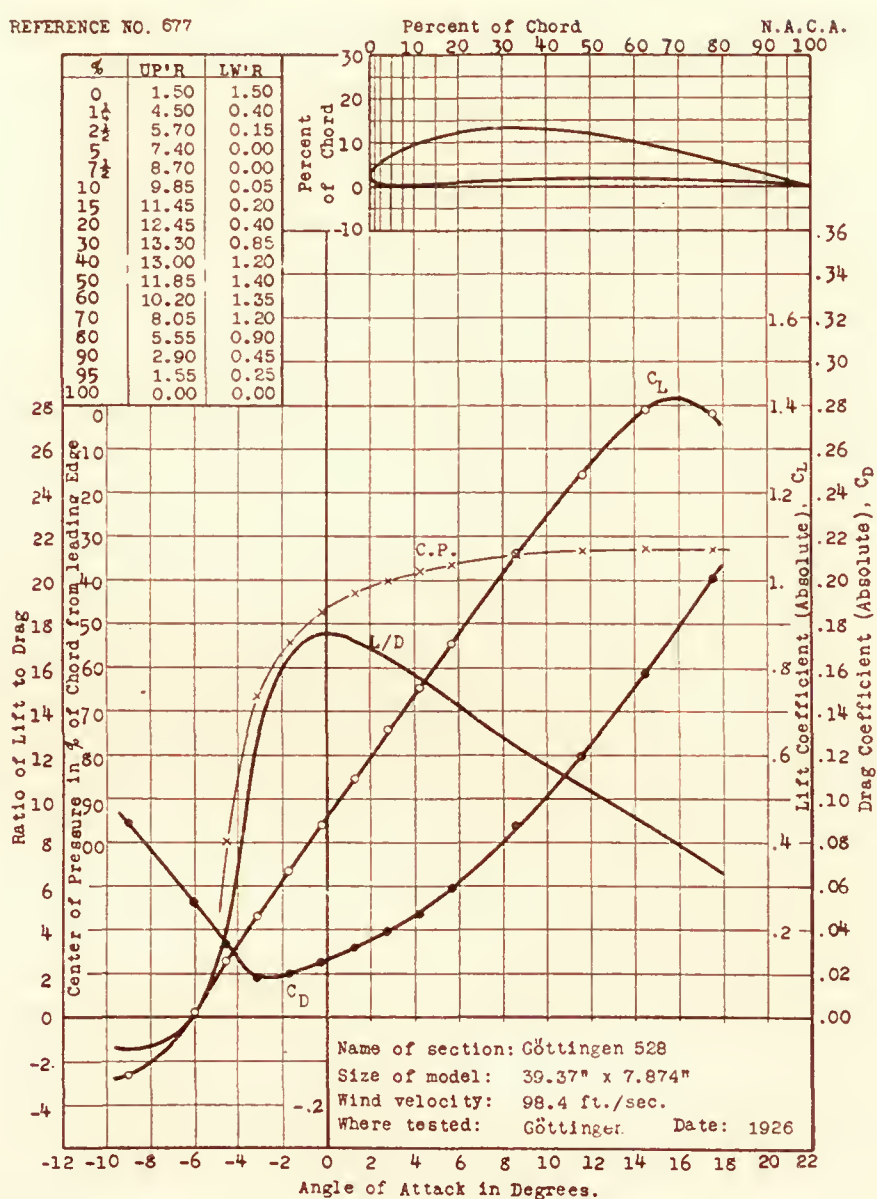




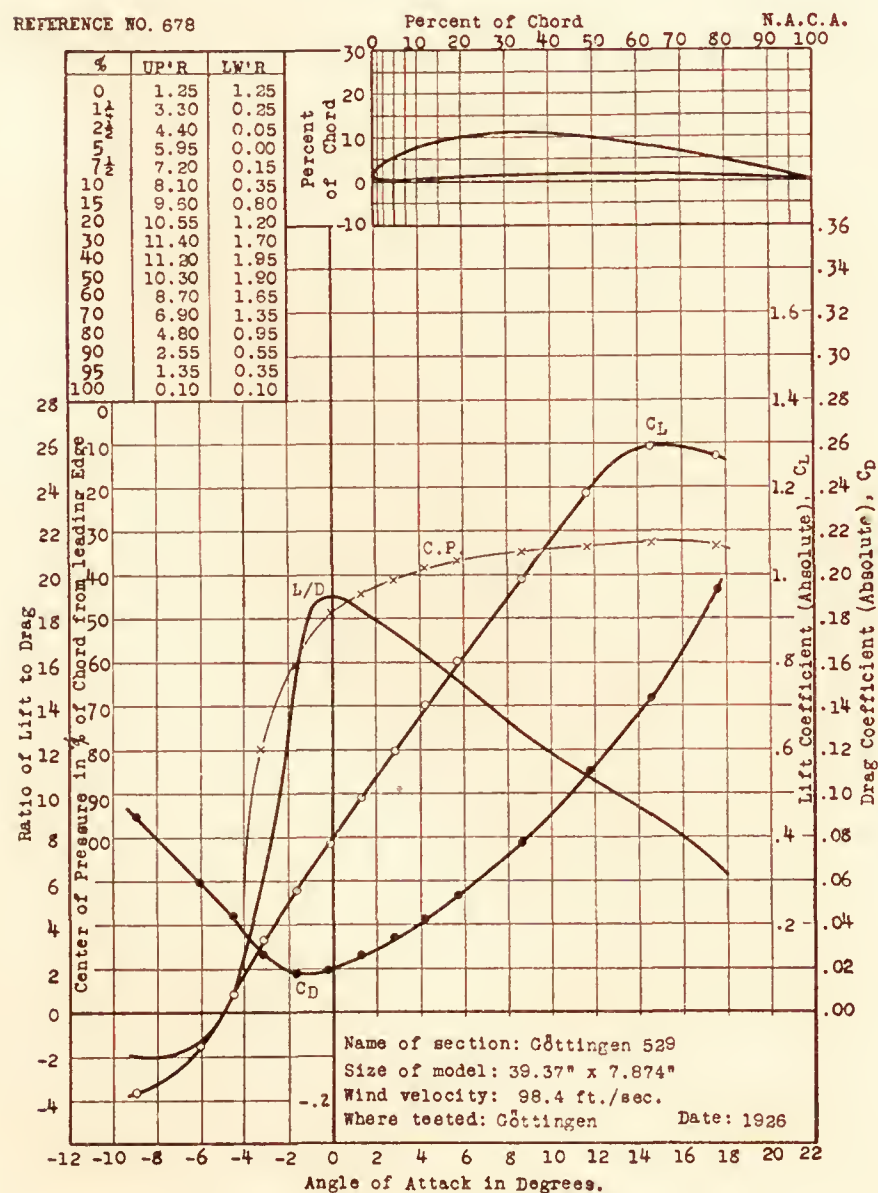
REFERENCE NO. 676



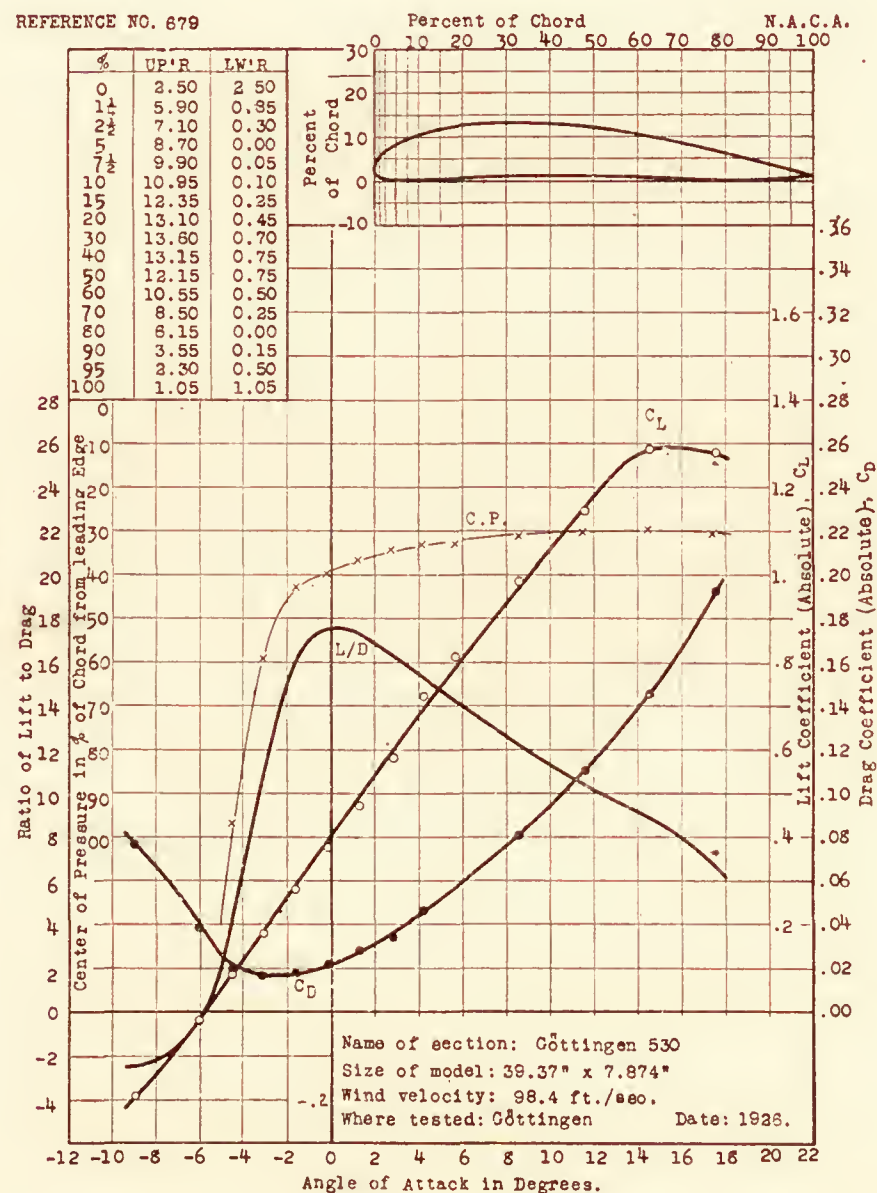
REFERENCE NO. 677



REFERENCE NO. 678

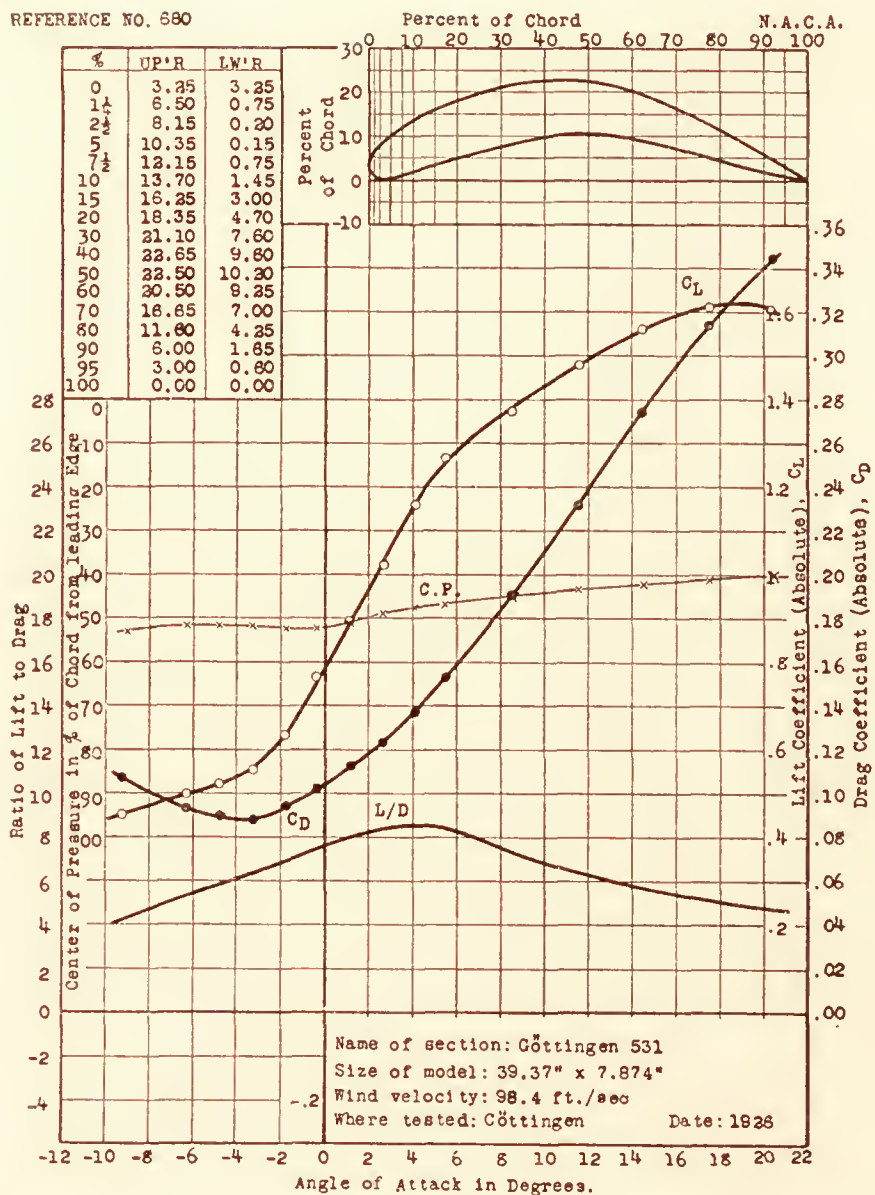


REFERENCE NO. 679

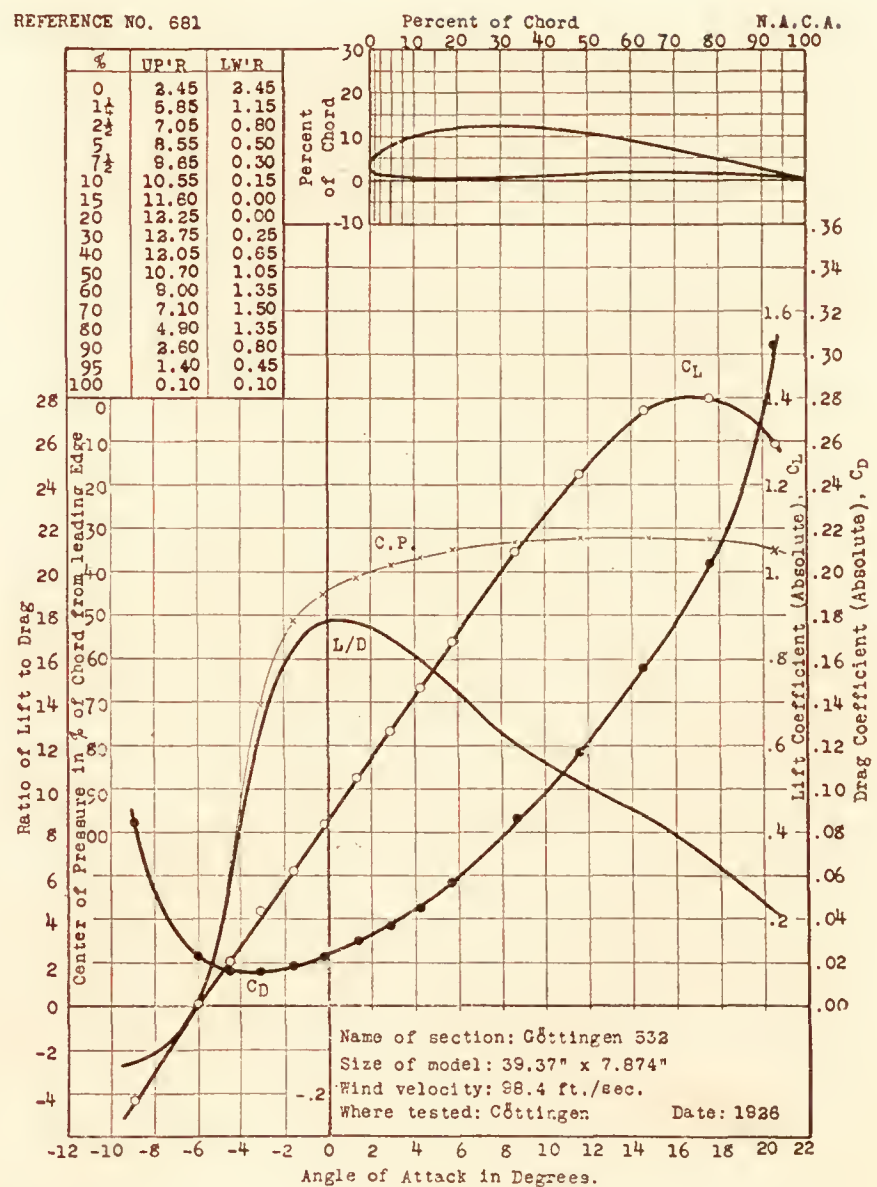




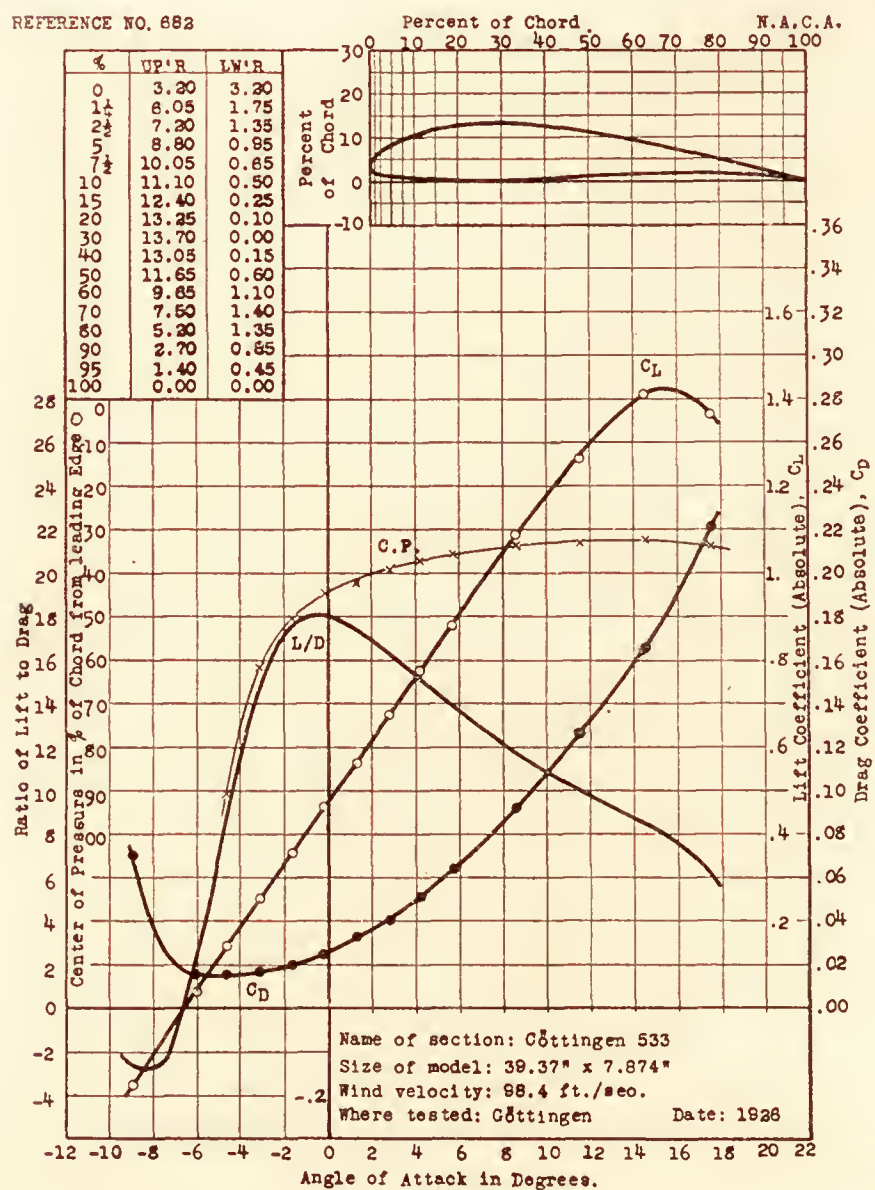
REFERENCE NO. 680



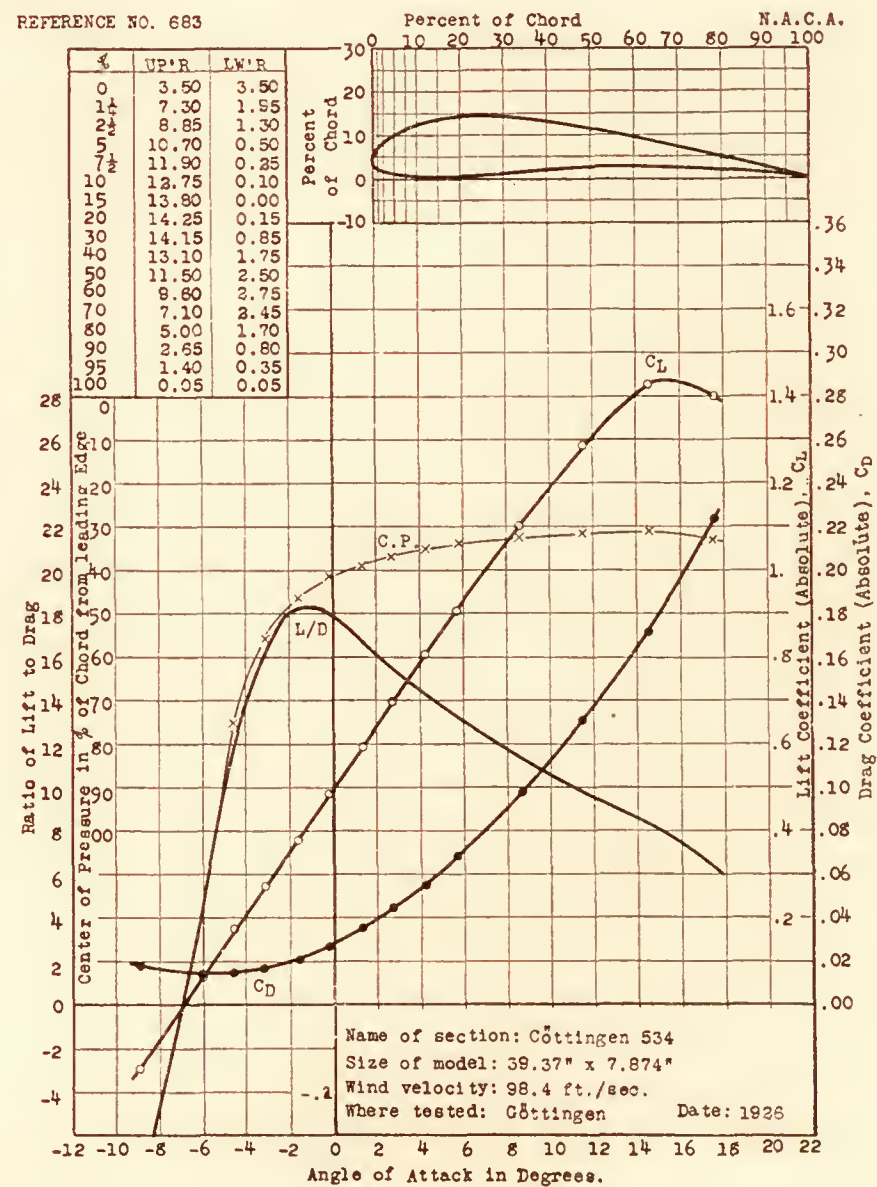
REFERENCE NO. 681



REFERENCE NO. 682

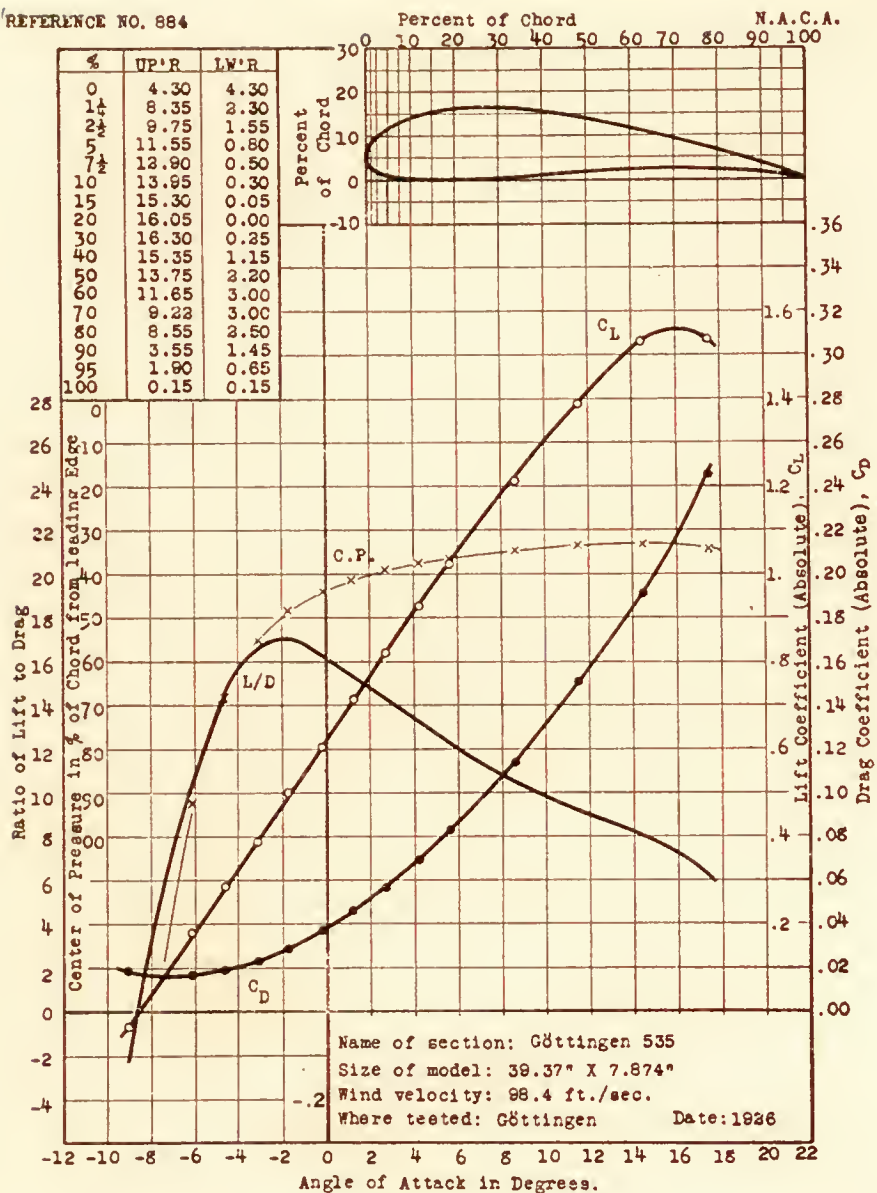


REFERENCE NO. 683

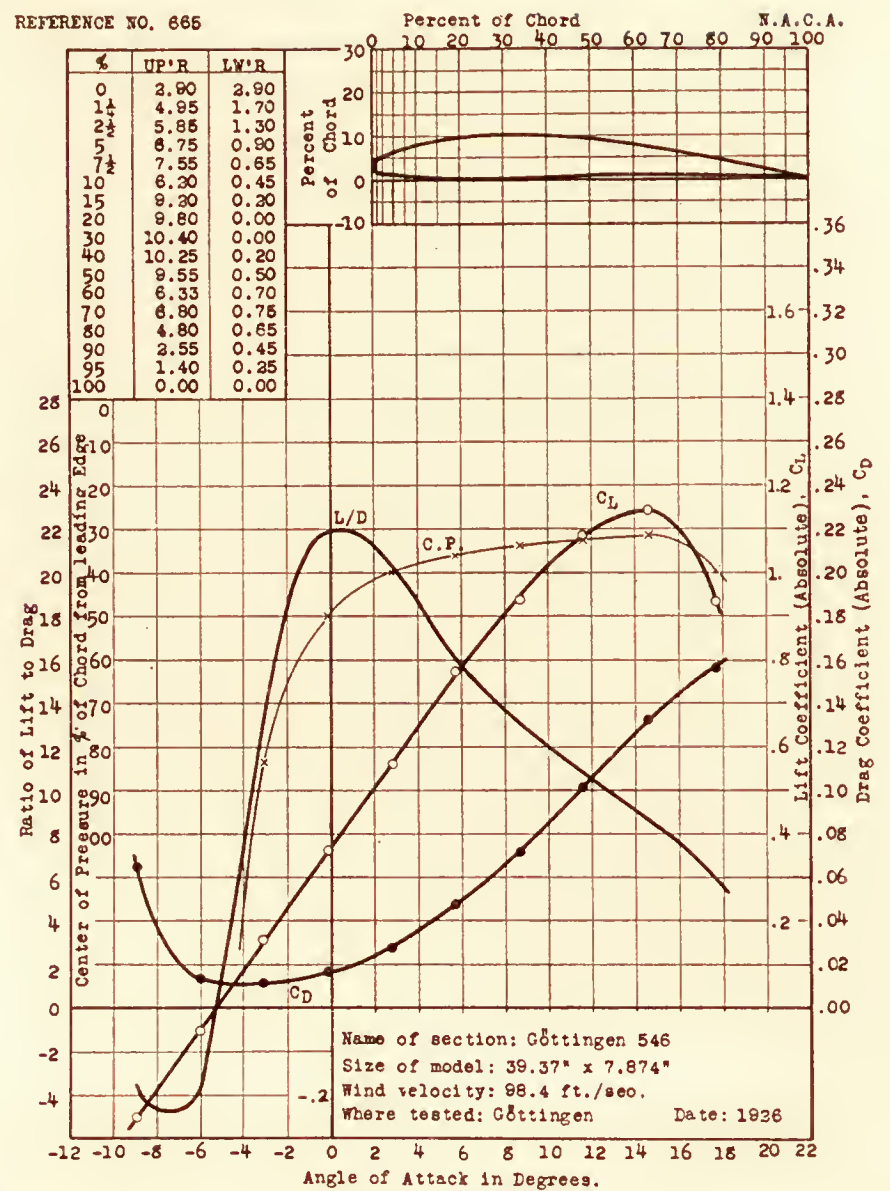




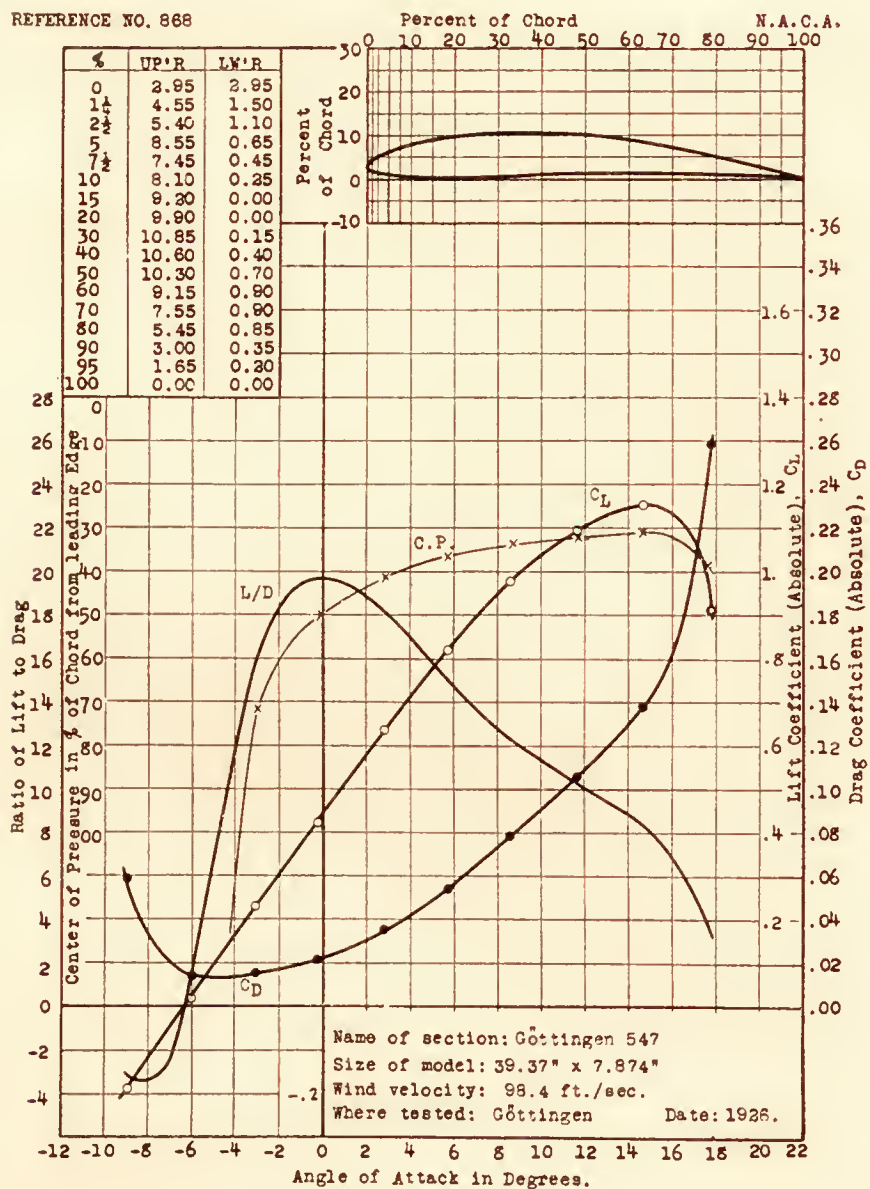
REFERENCE NO. 884



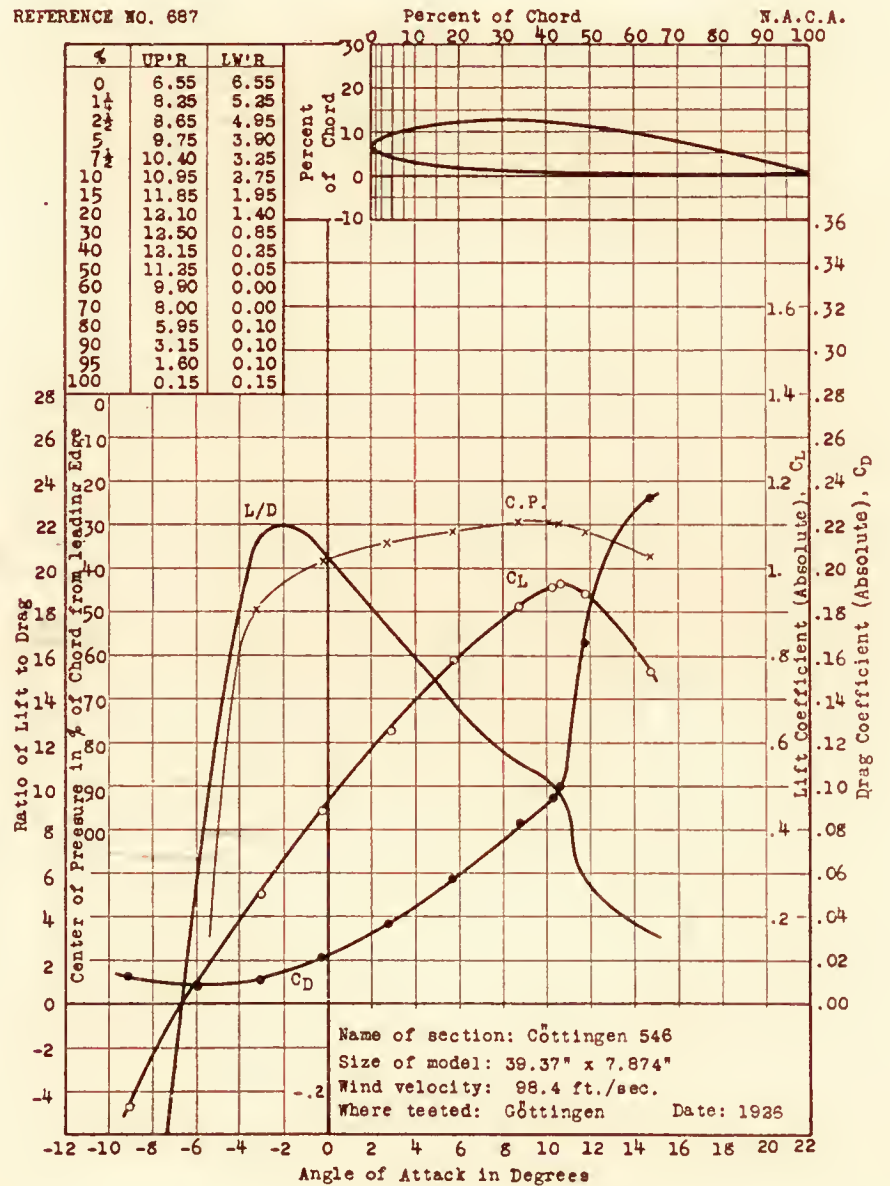
REFERENCE NO. 885



REFERENCE NO. 886

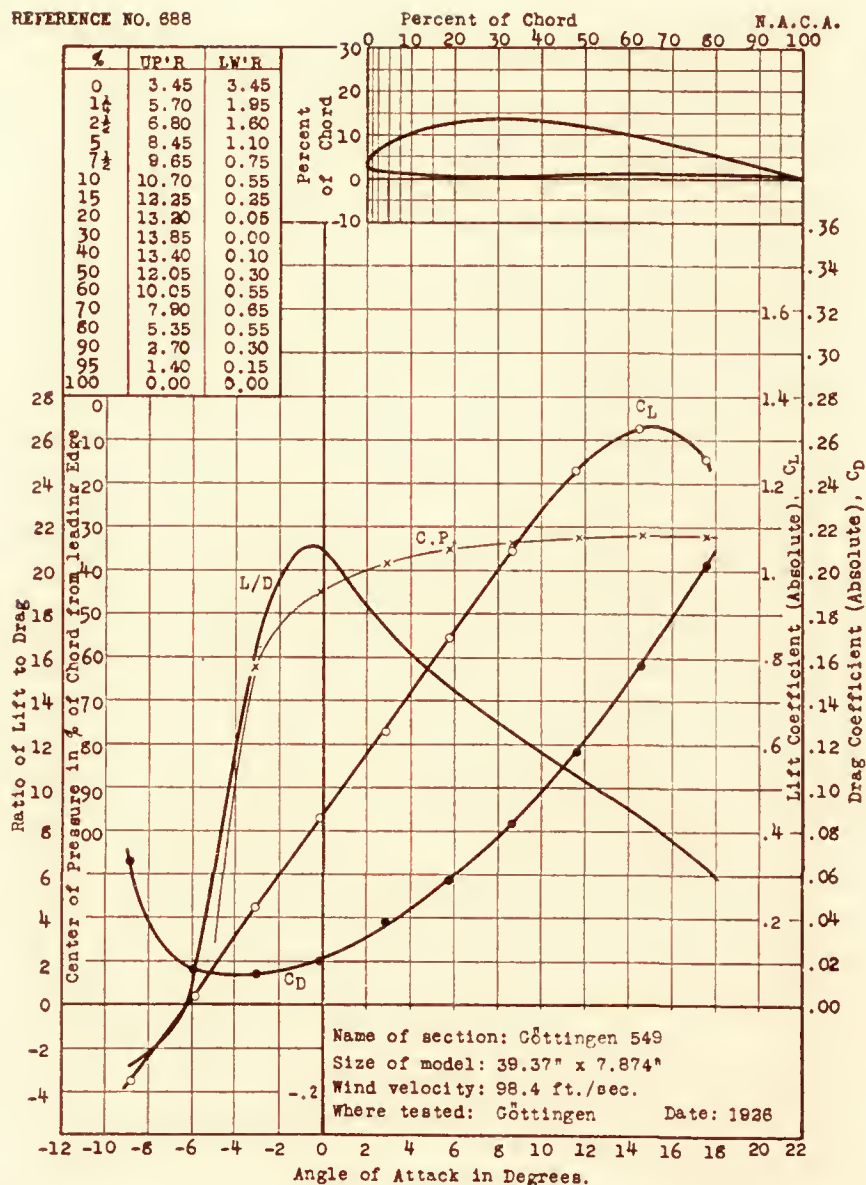


REFERENCE NO. 887

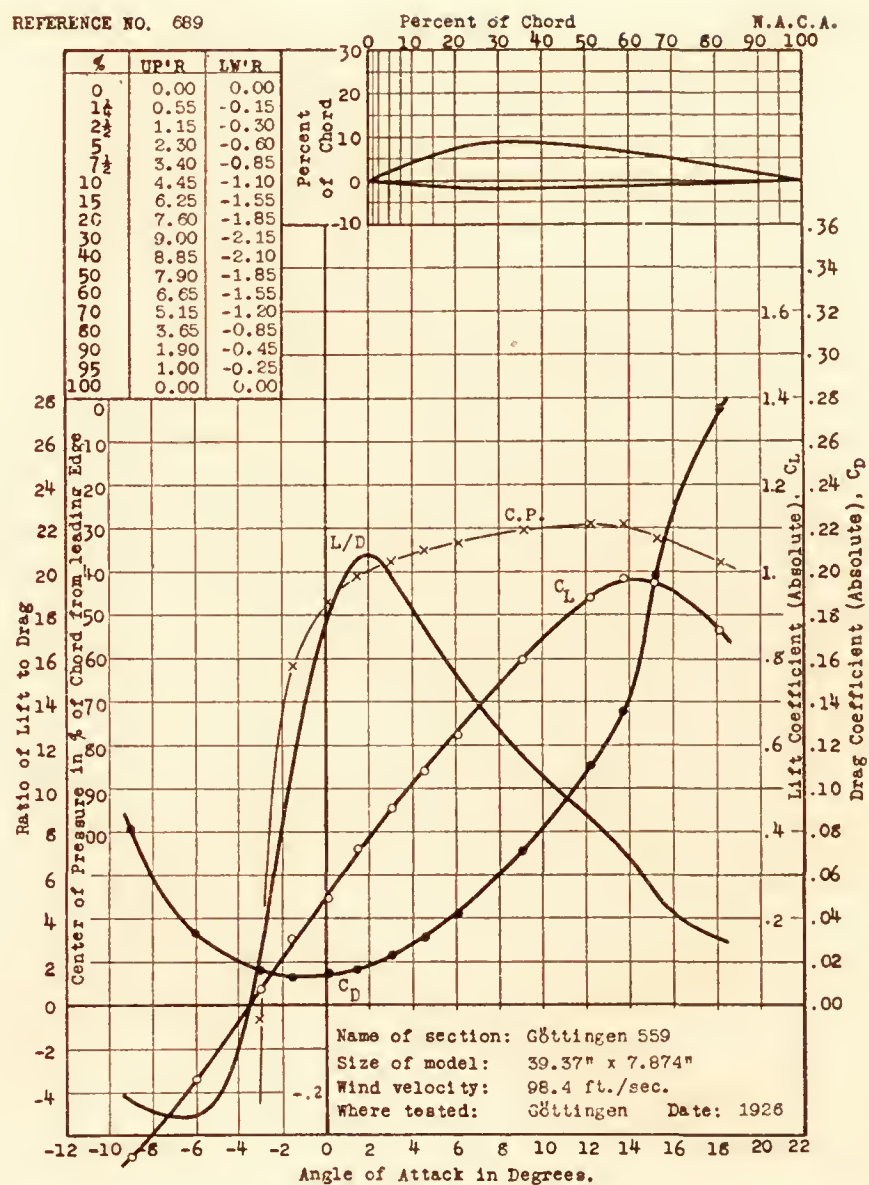




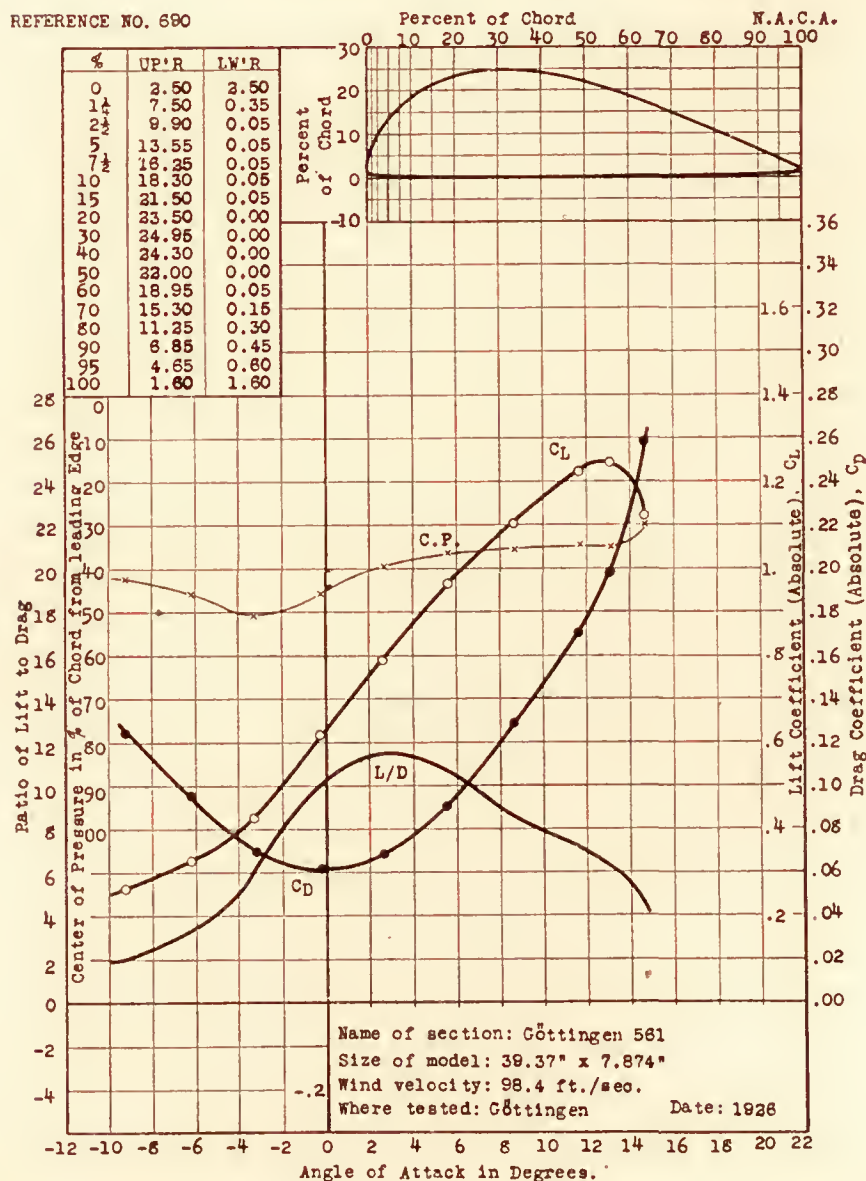
REFERENCE NO. 688



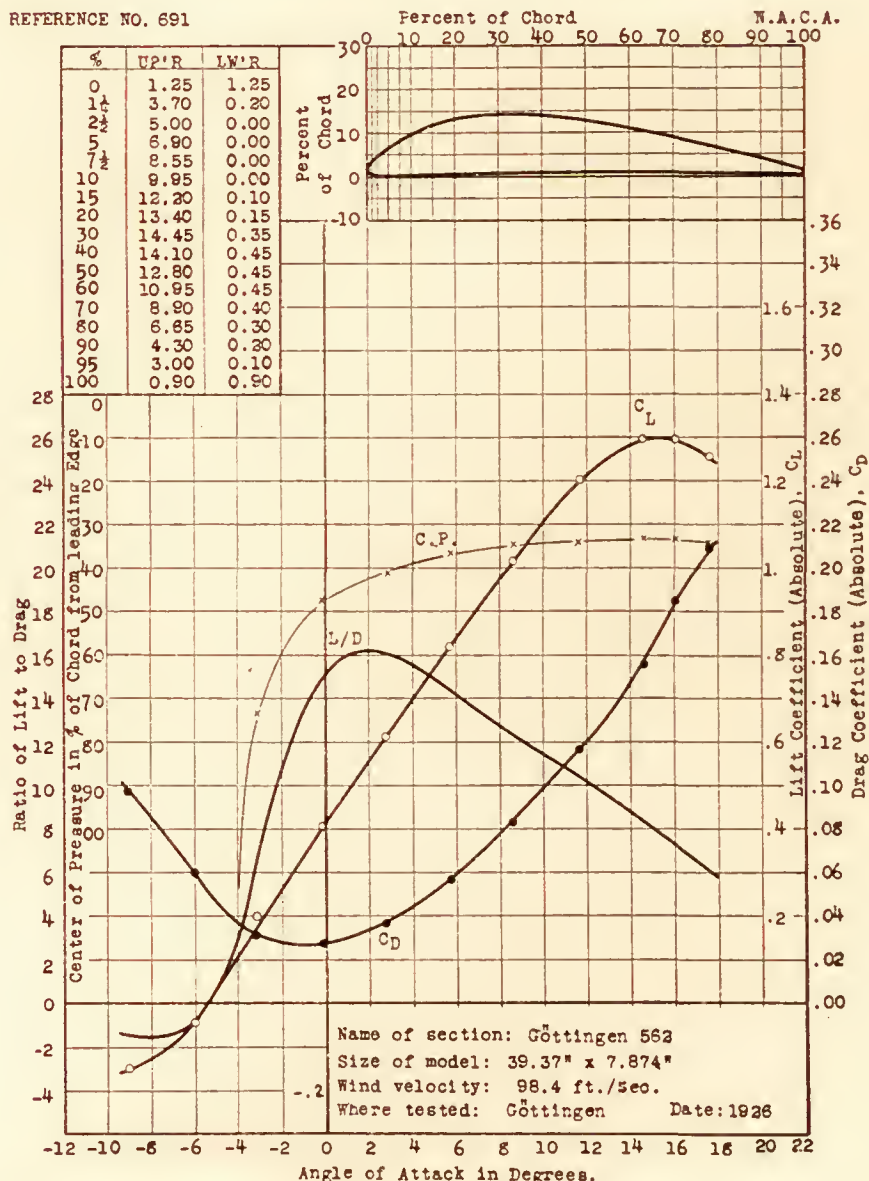
REFERENCE NO. 689



REFERENCE NO. 690

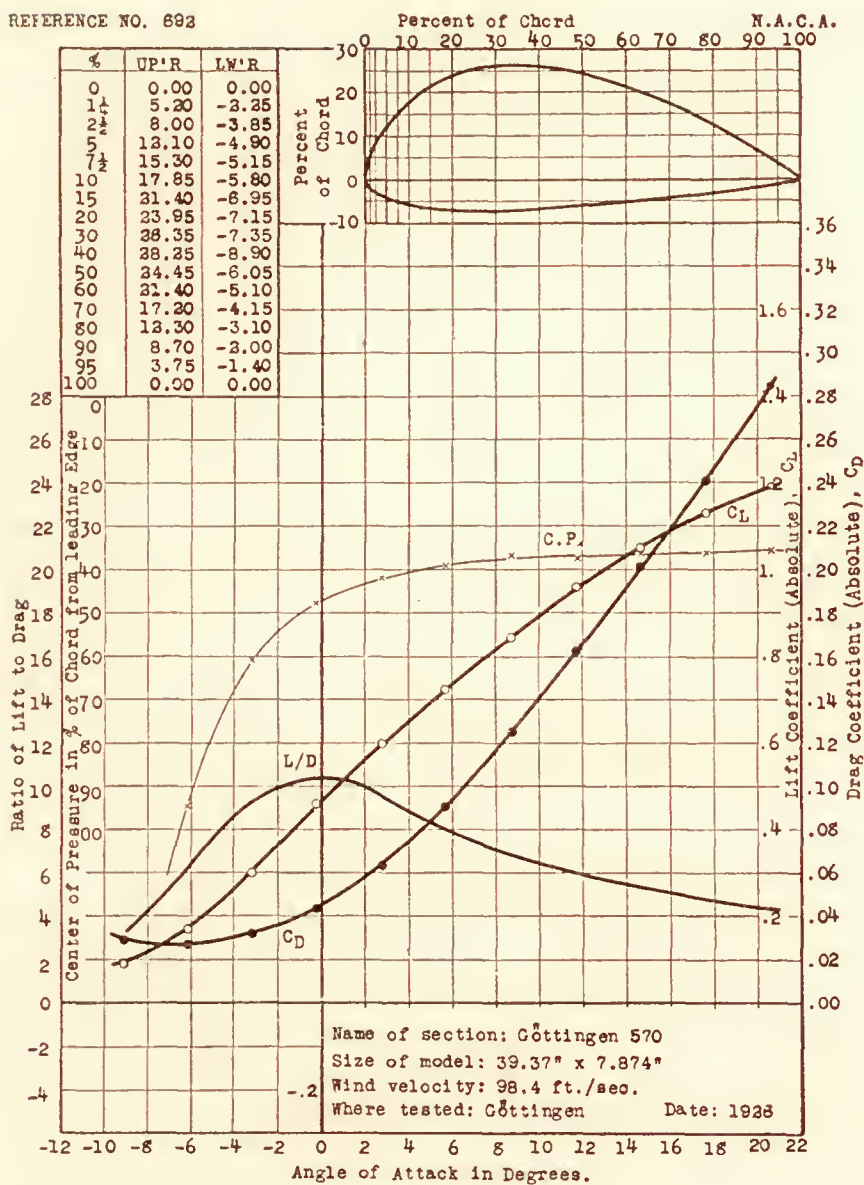


REFERENCE NO. 691

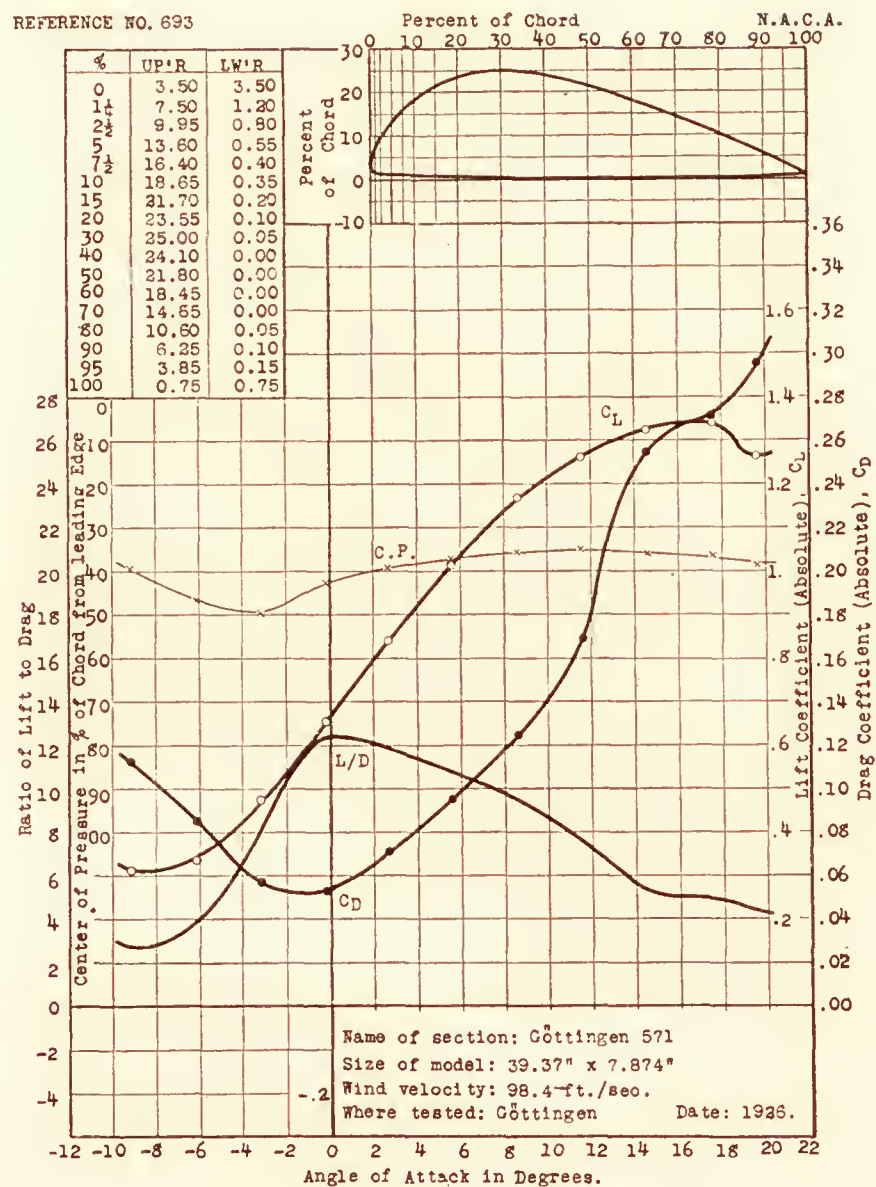




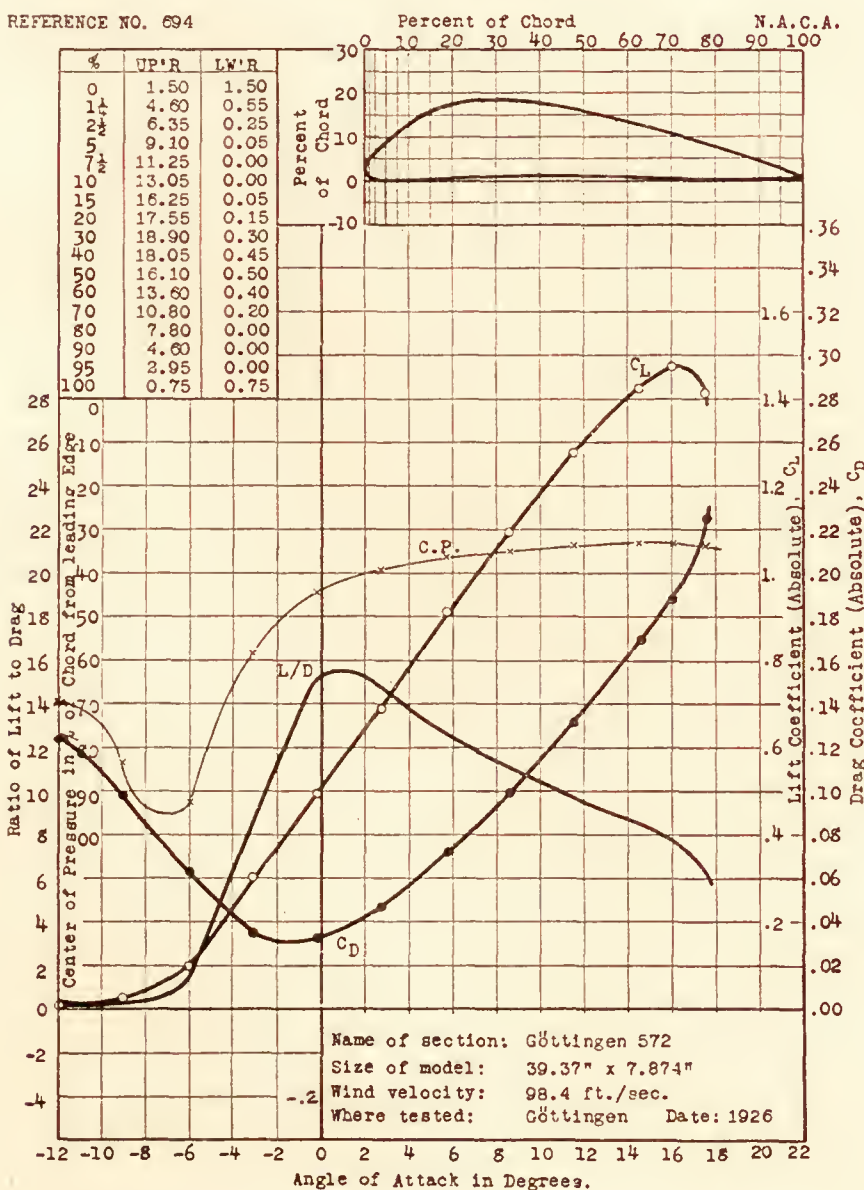
REFERENCE NO. 692



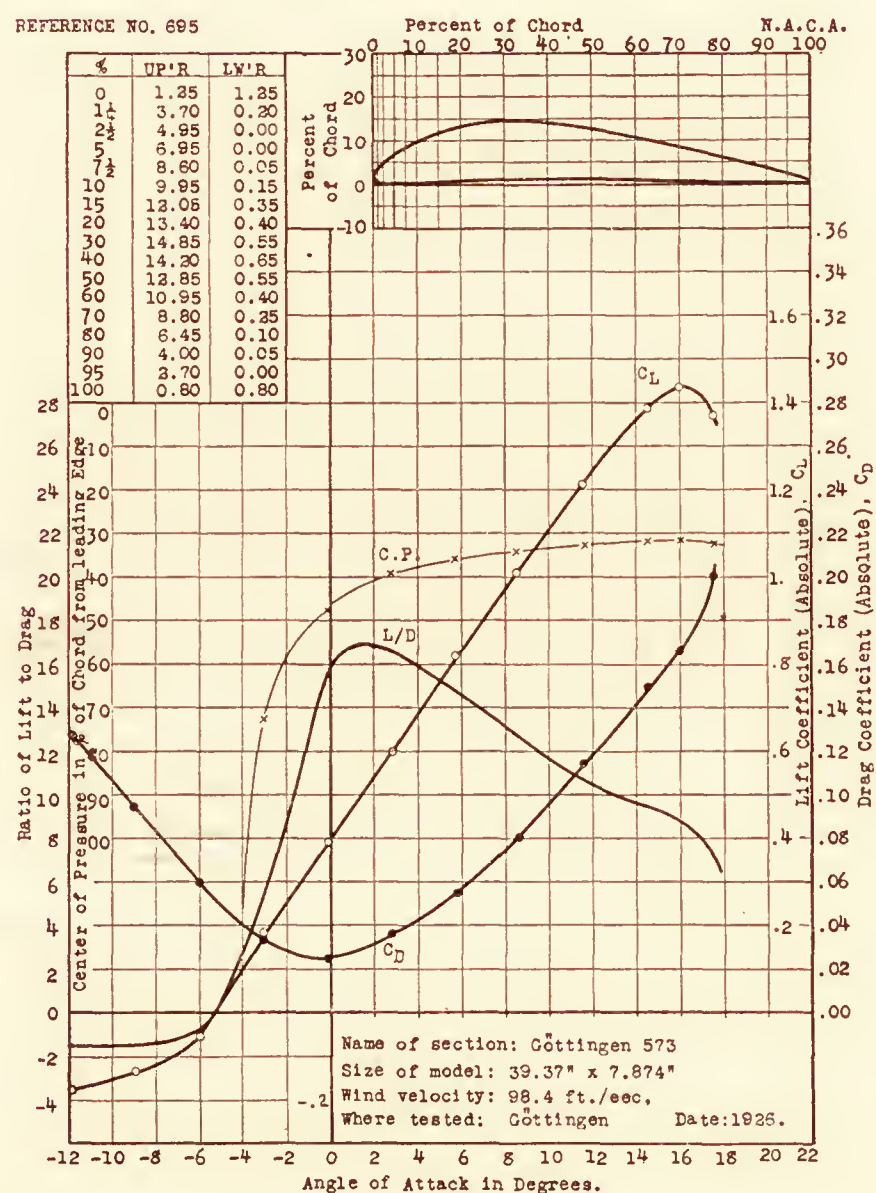
REFERENCE NO. 693



REFERENCE NO. 694

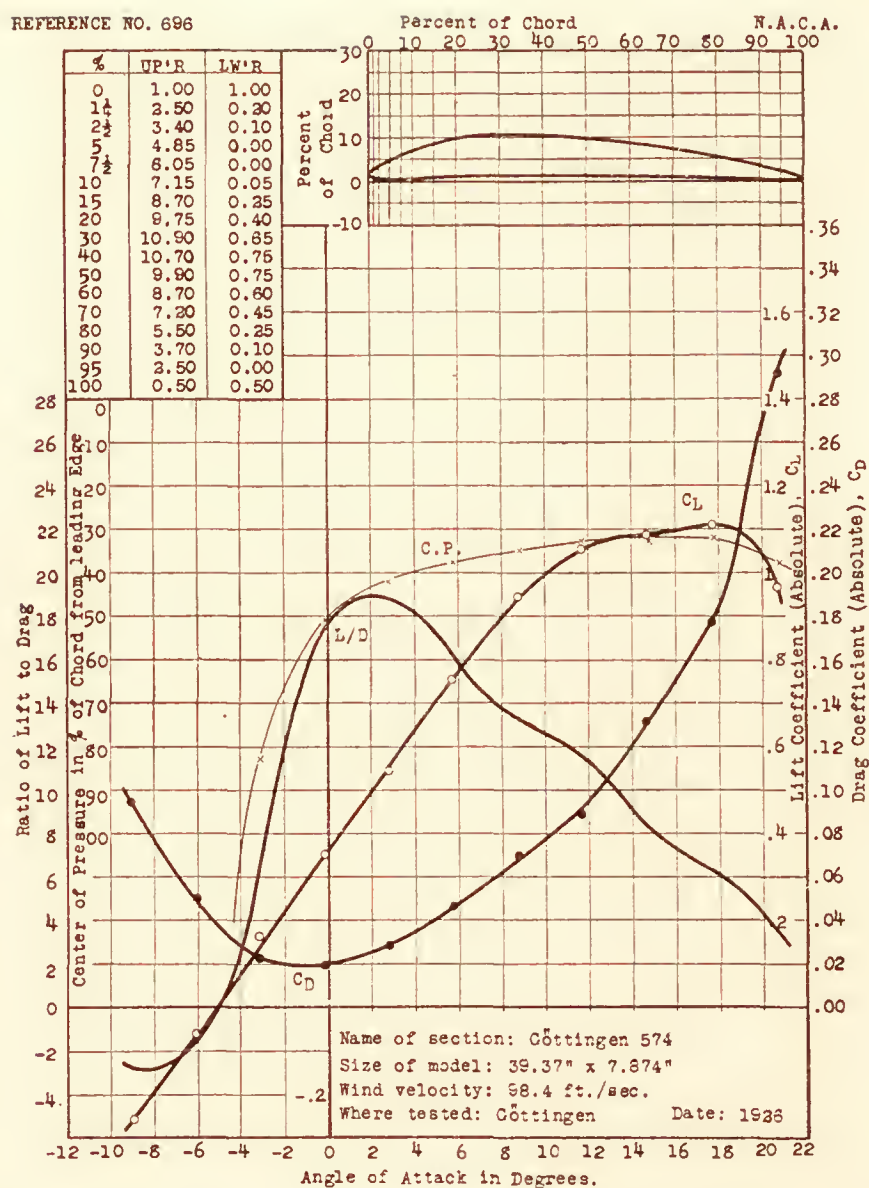


REFERENCE NO. 695

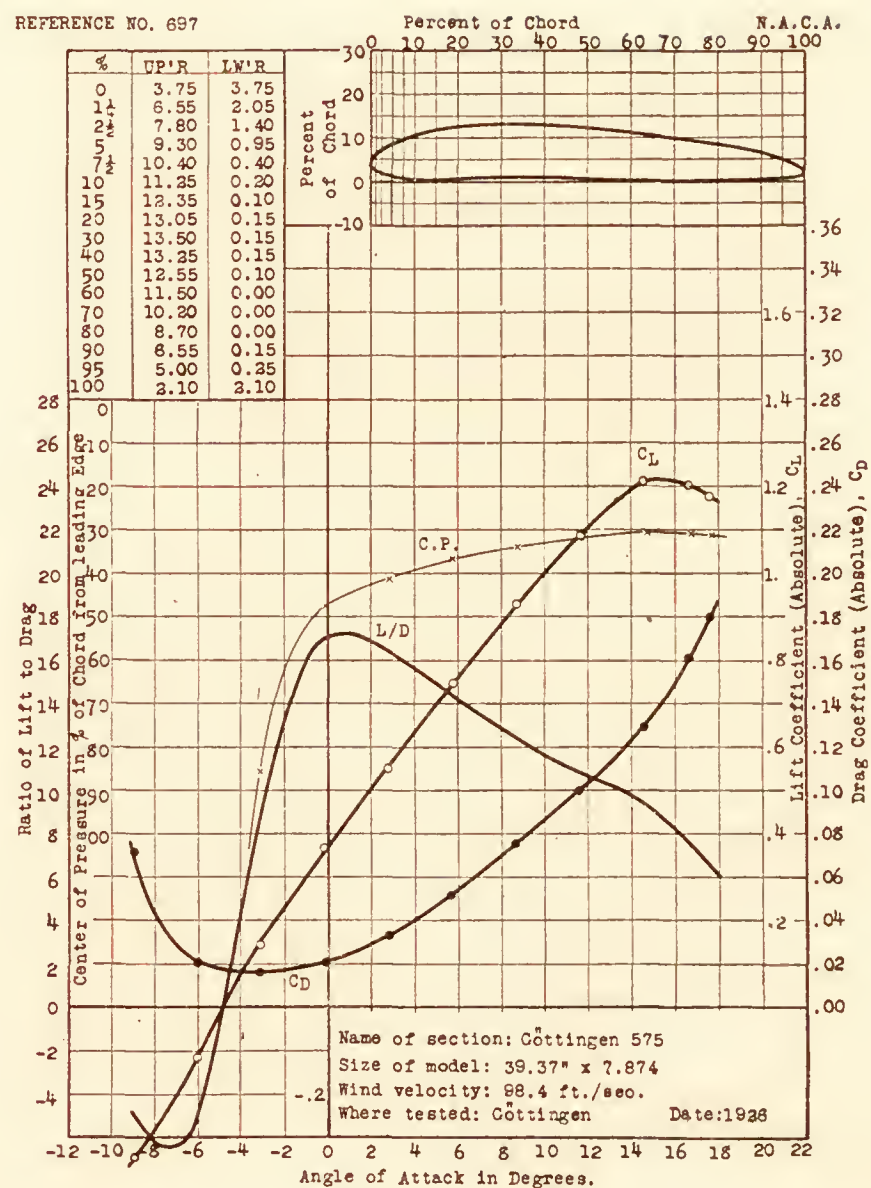




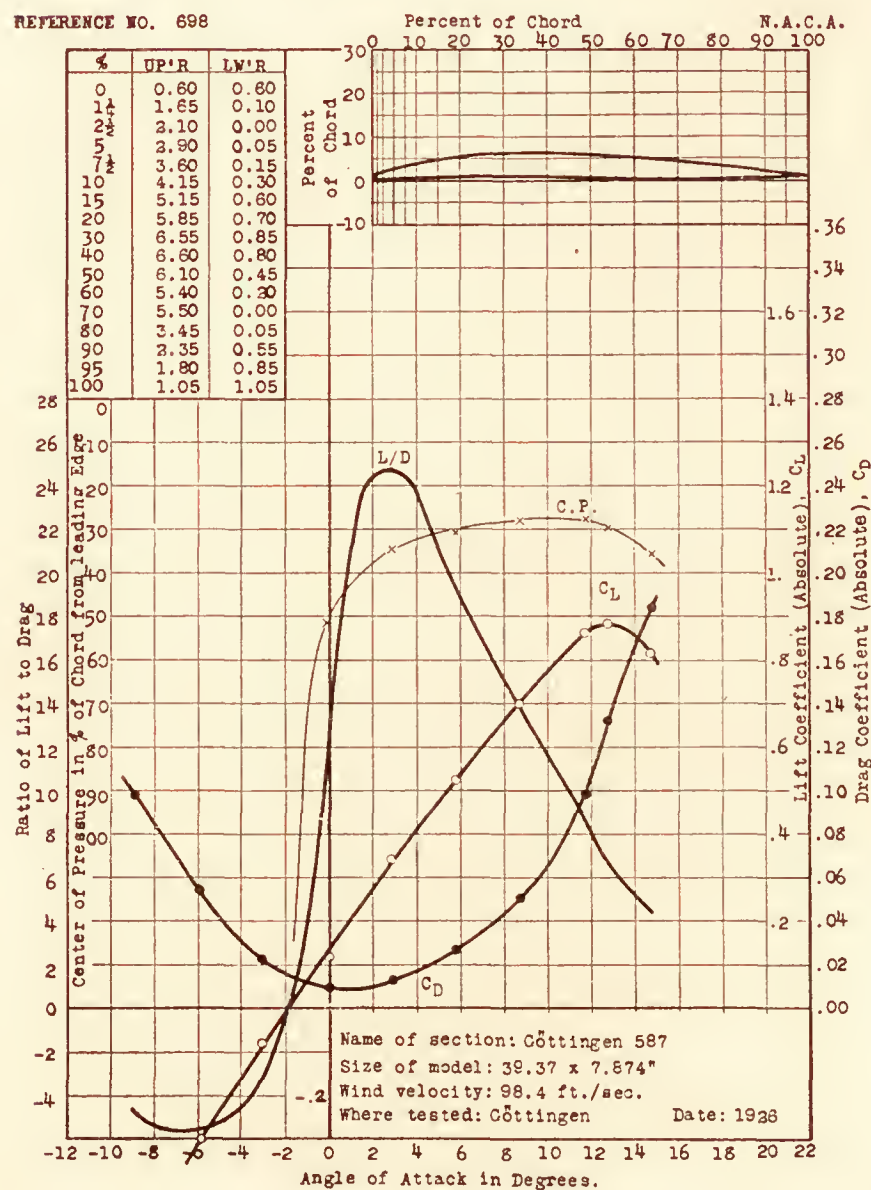
REFERENCE NO. 696



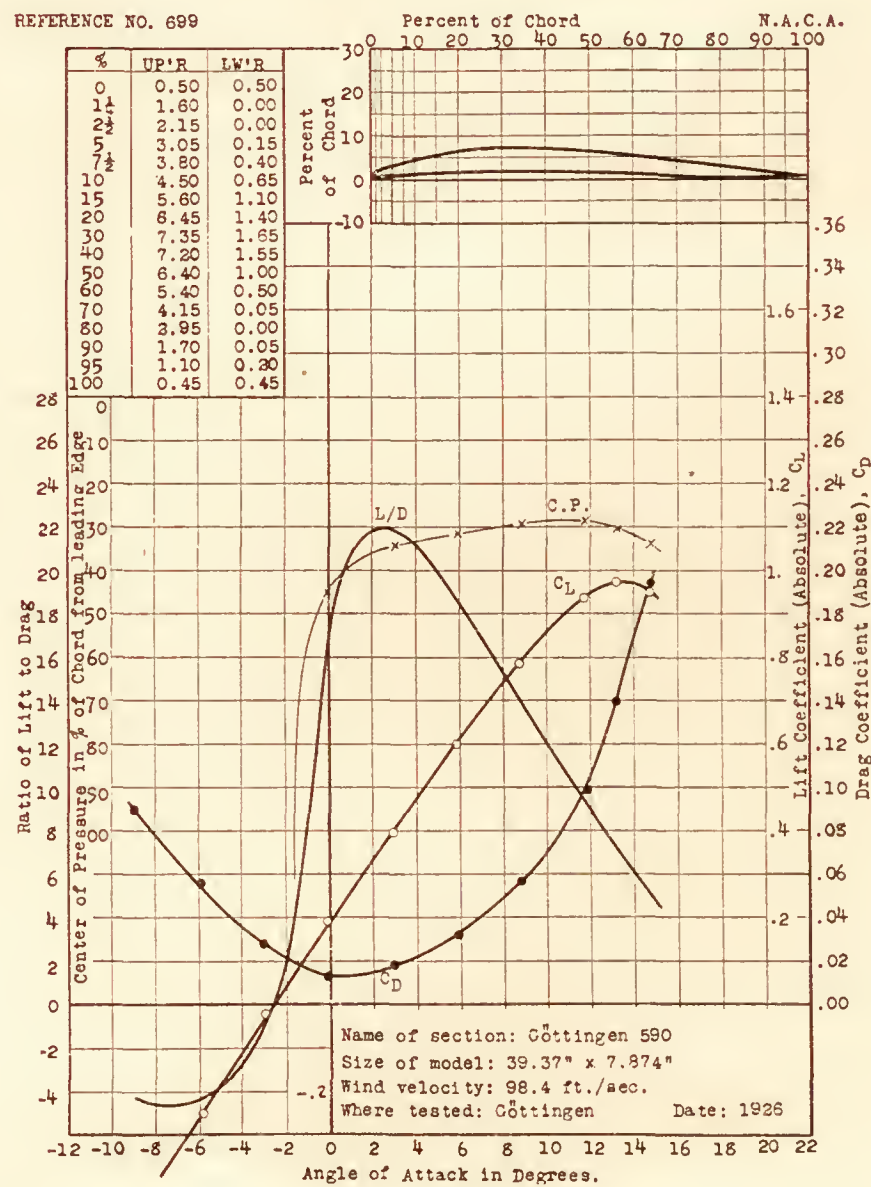
REFERENCE NO. 697



REFERENCE NO. 698

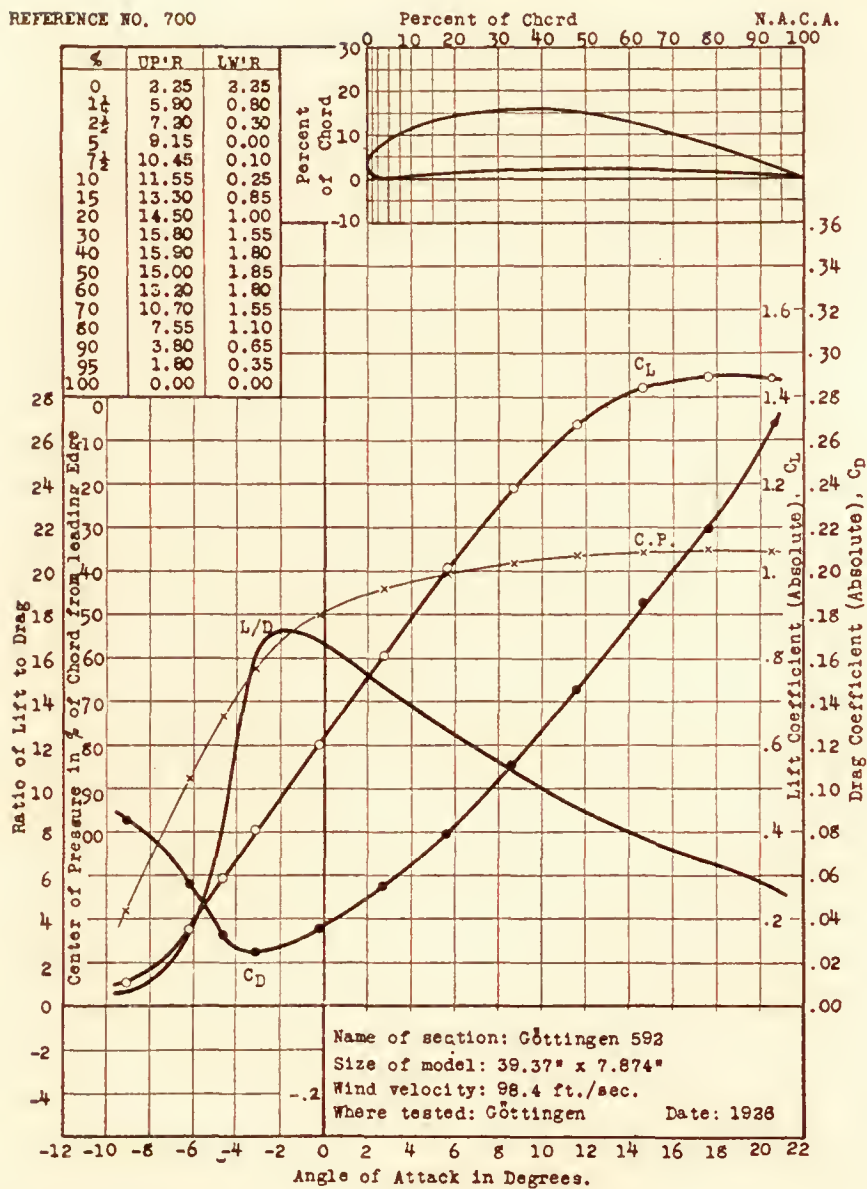


REFERENCE NO. 699

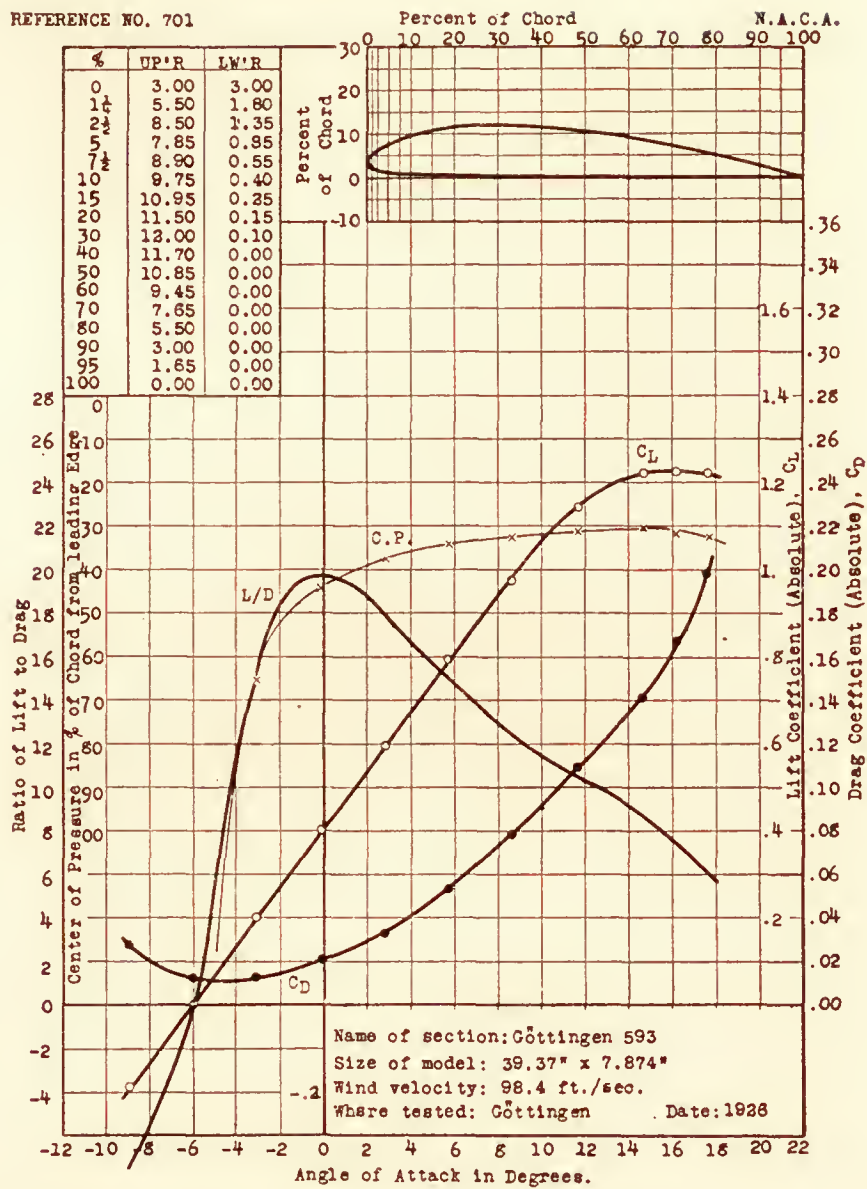




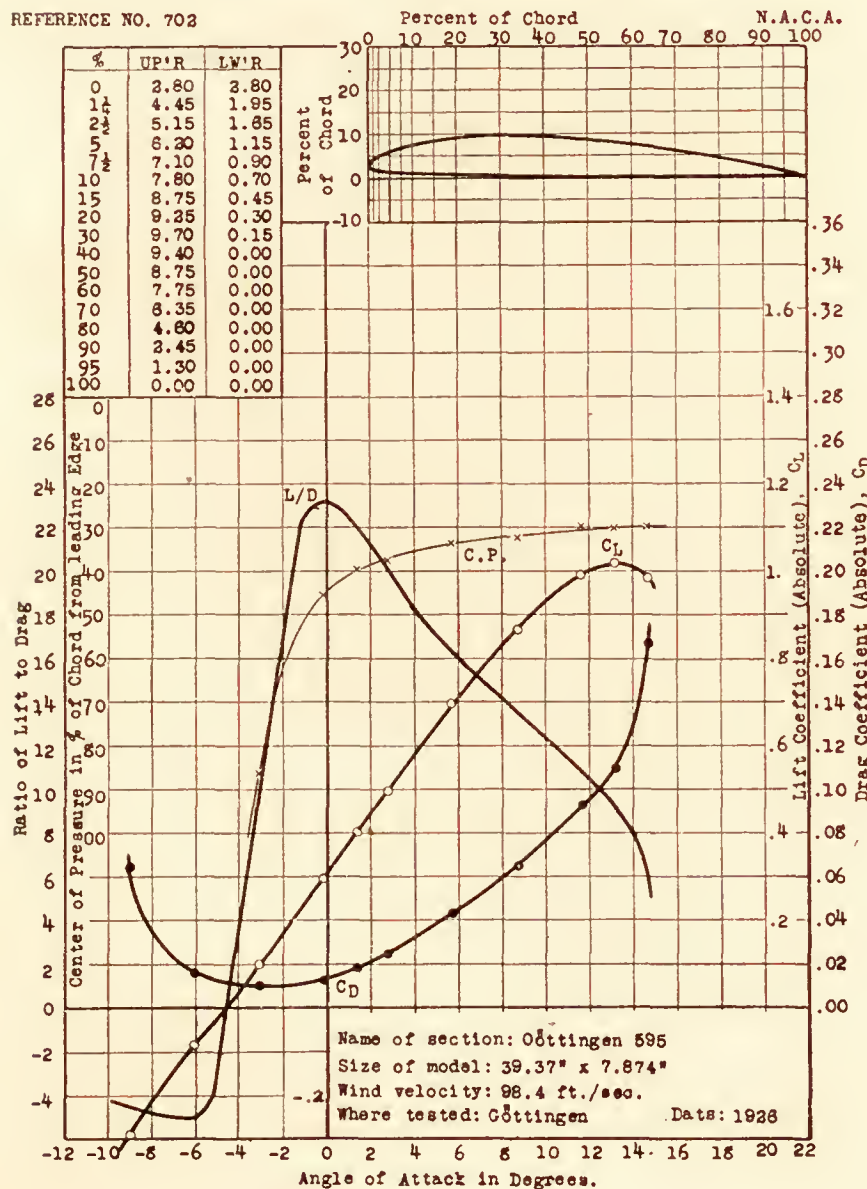
REFERENCE NO. 700



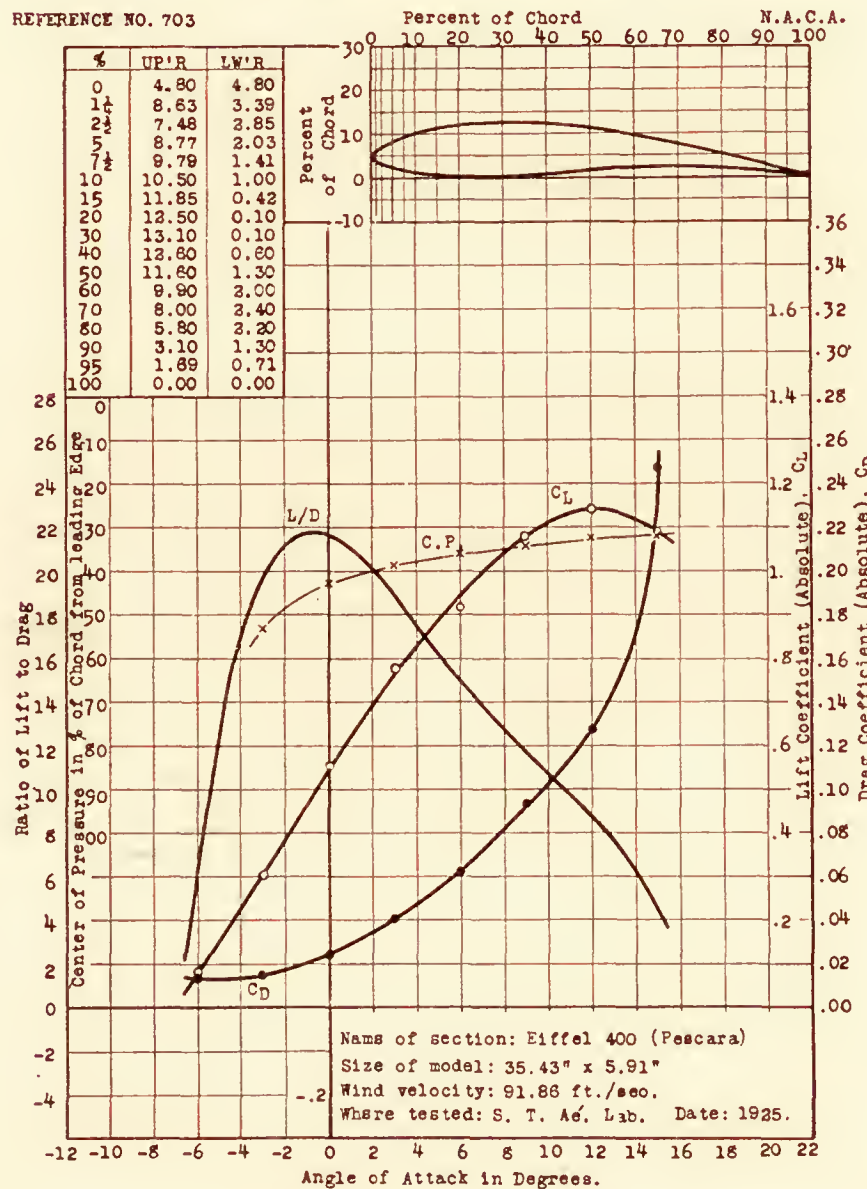
REFERENCE NO. 701



REFERENCE NO. 702

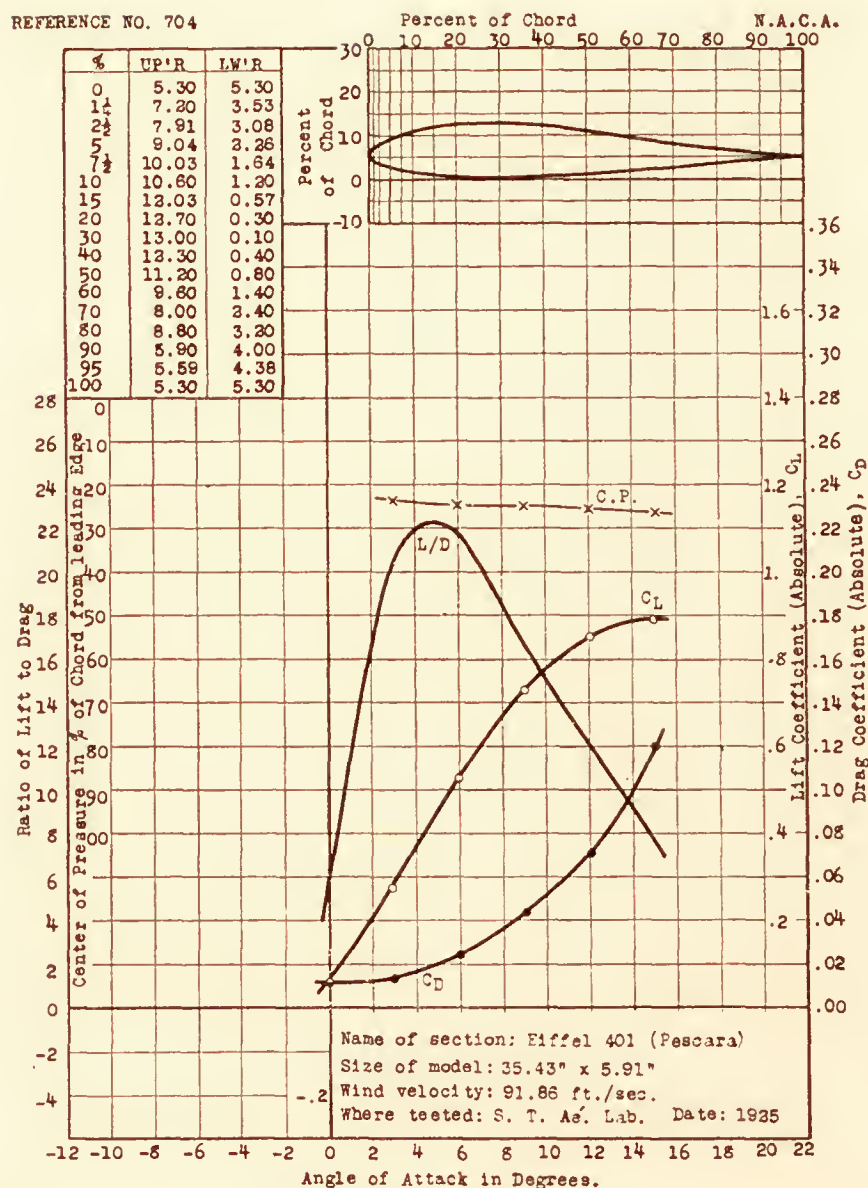


REFERENCE NO. 703

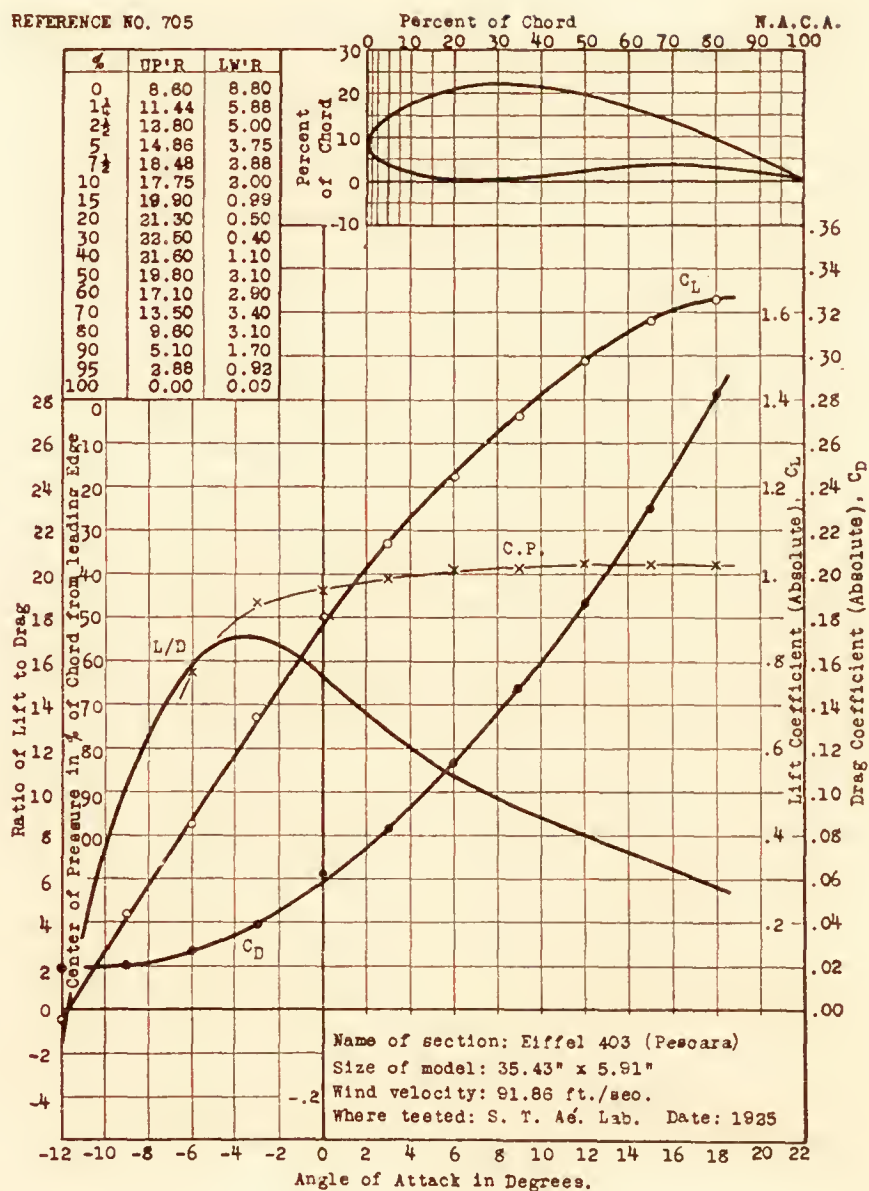




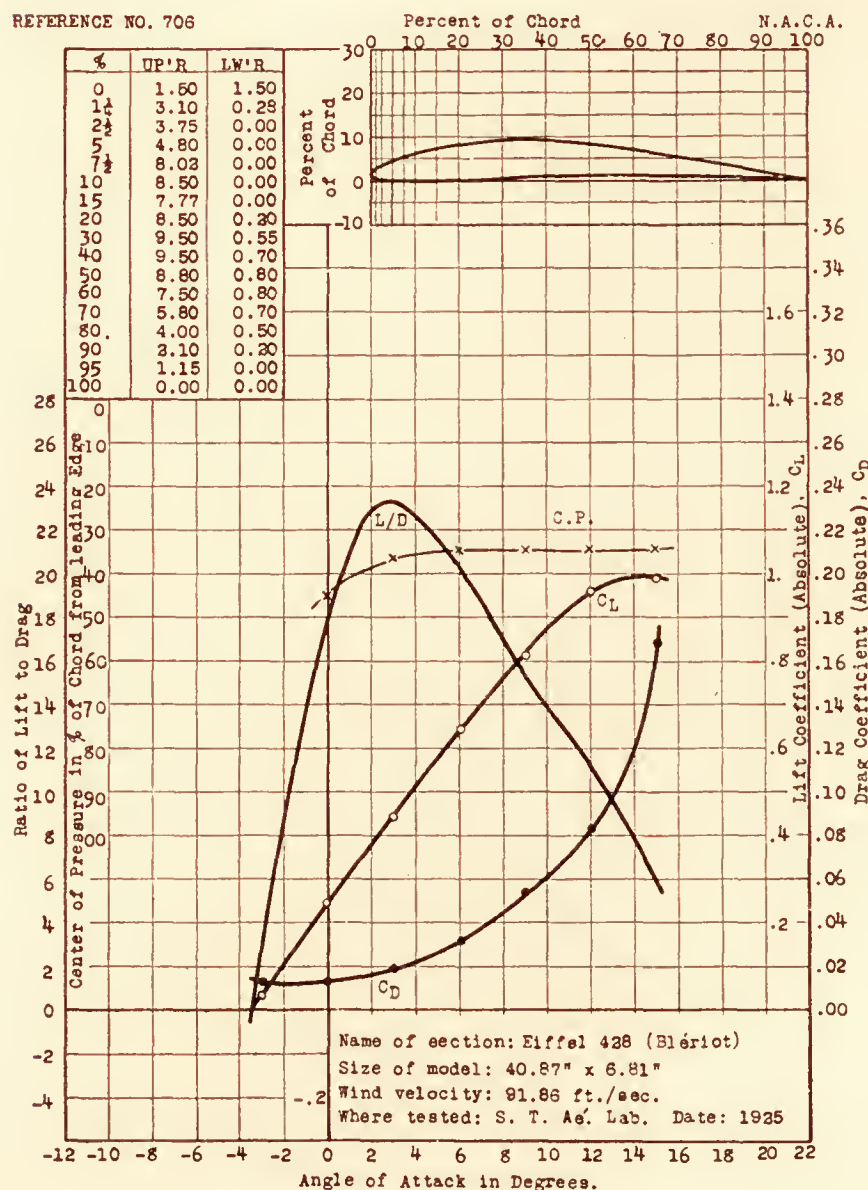
REFERENCE NO. 704



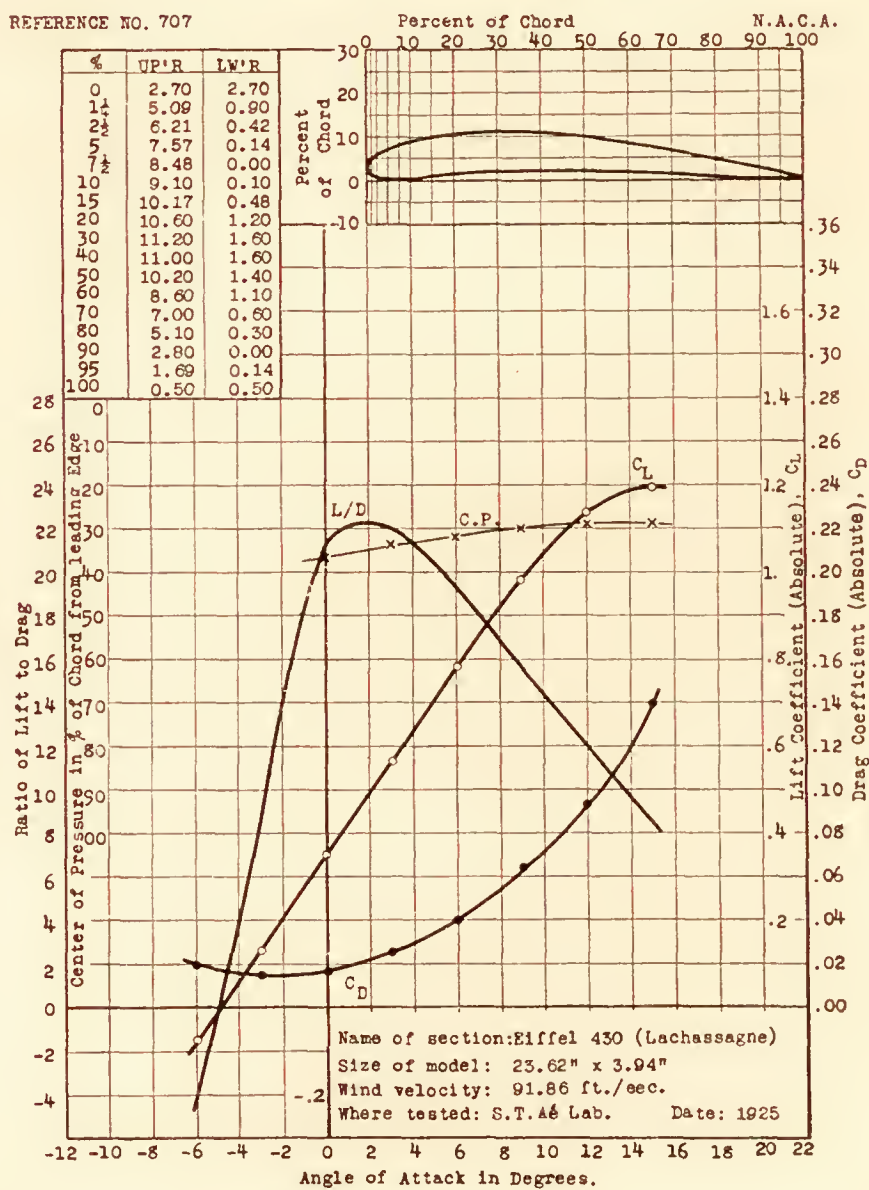
REFERENCE NO. 705



REFERENCE NO. 706

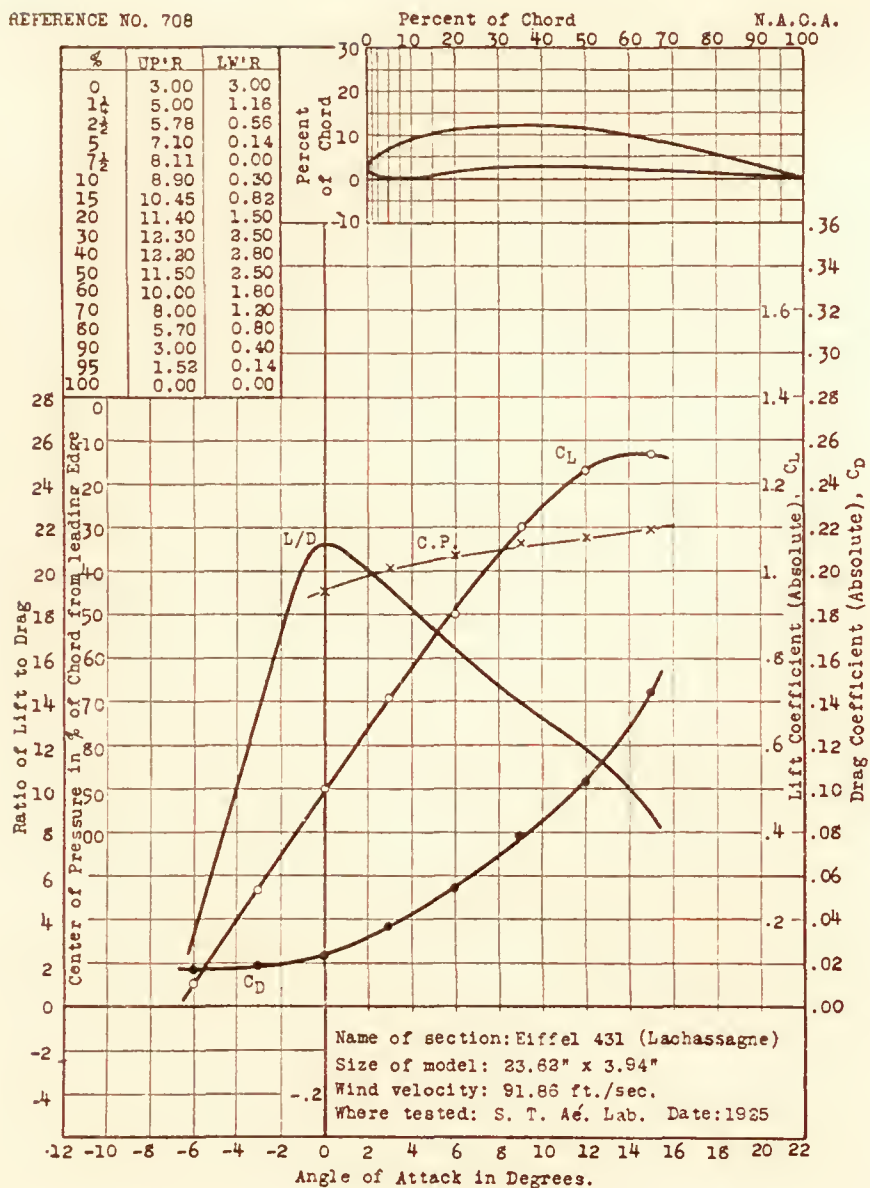


REFERENCE NO. 707

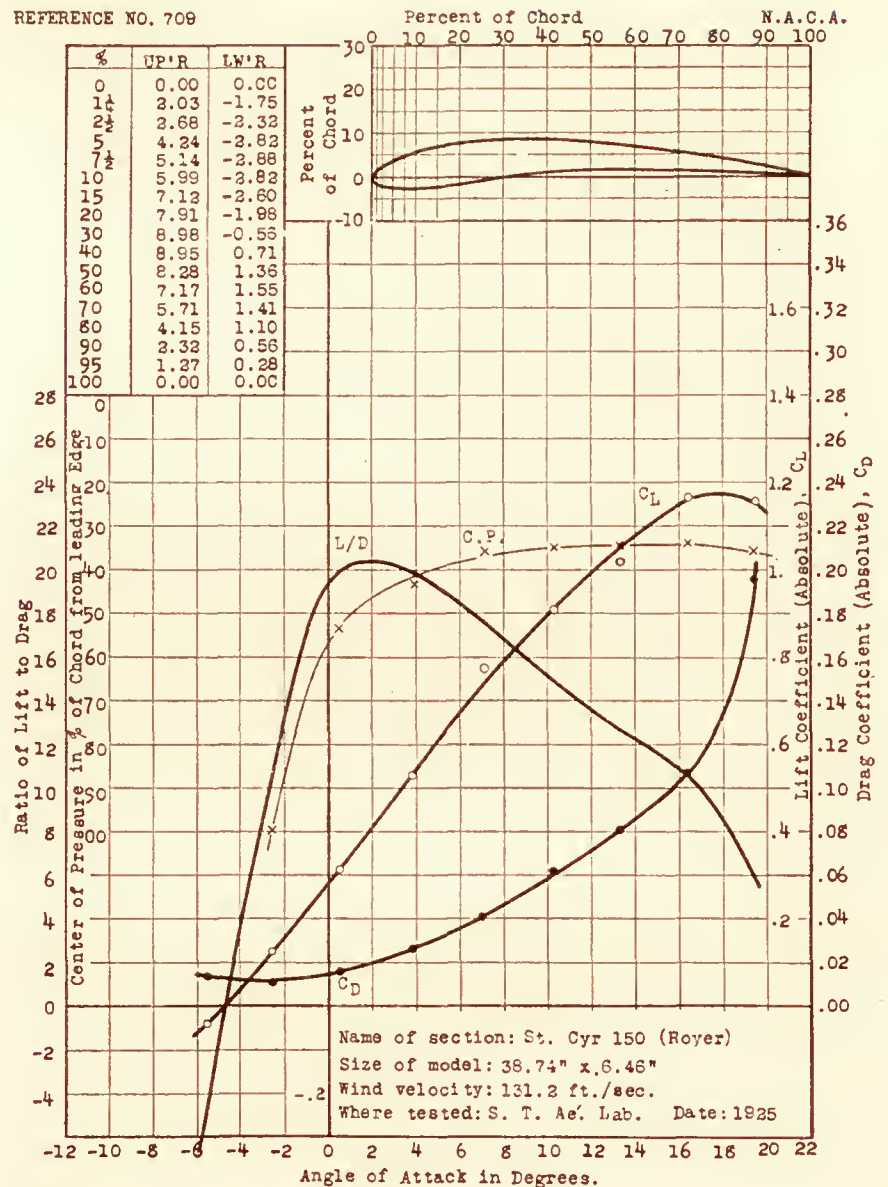




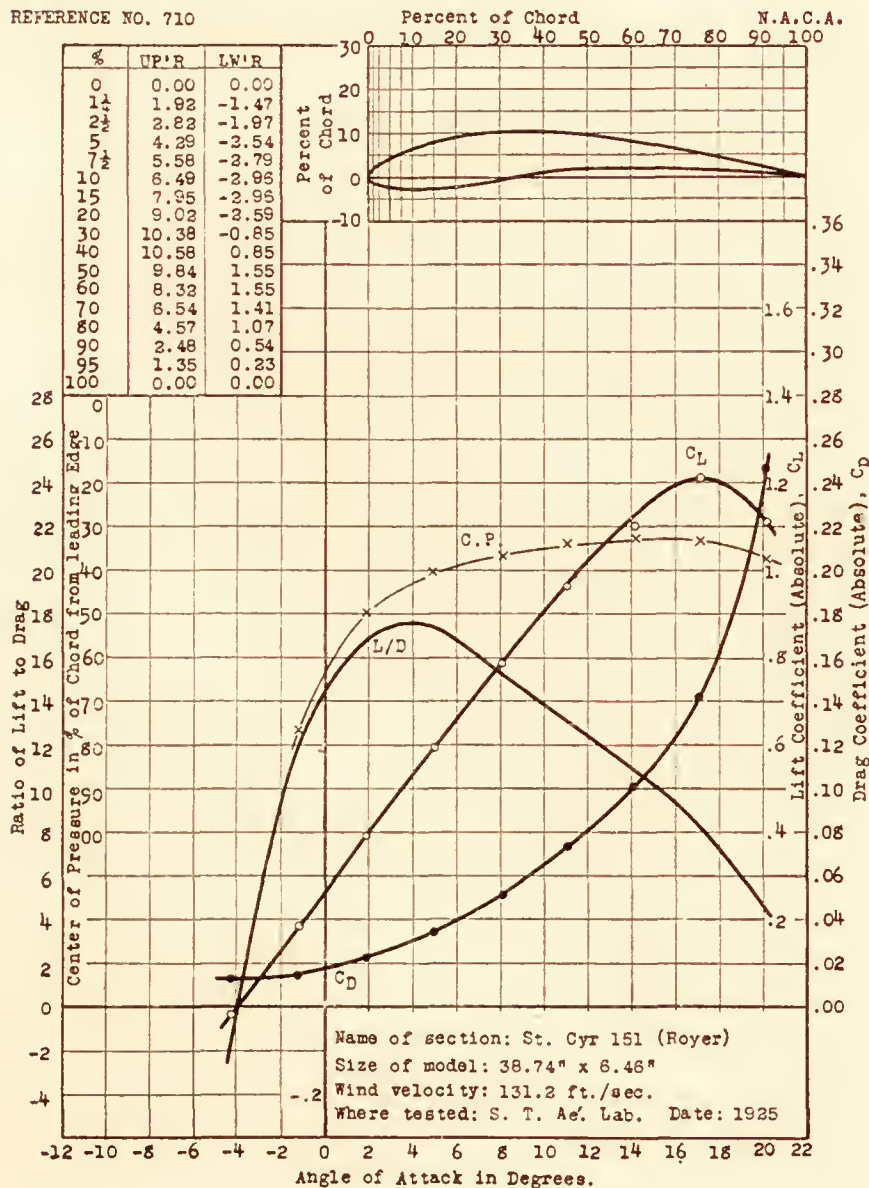
REFERENCE NO. 708



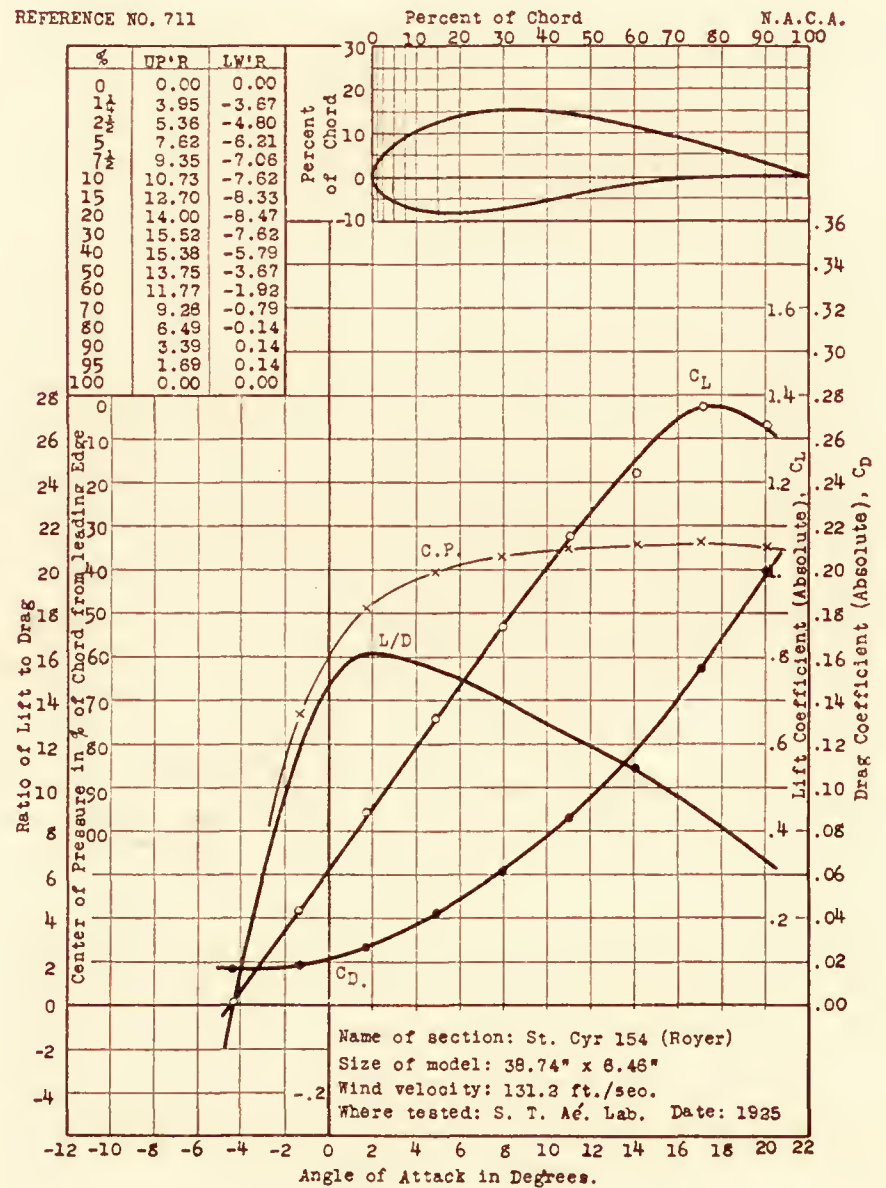
REFERENCE NO. 709



REFERENCE NO. 710

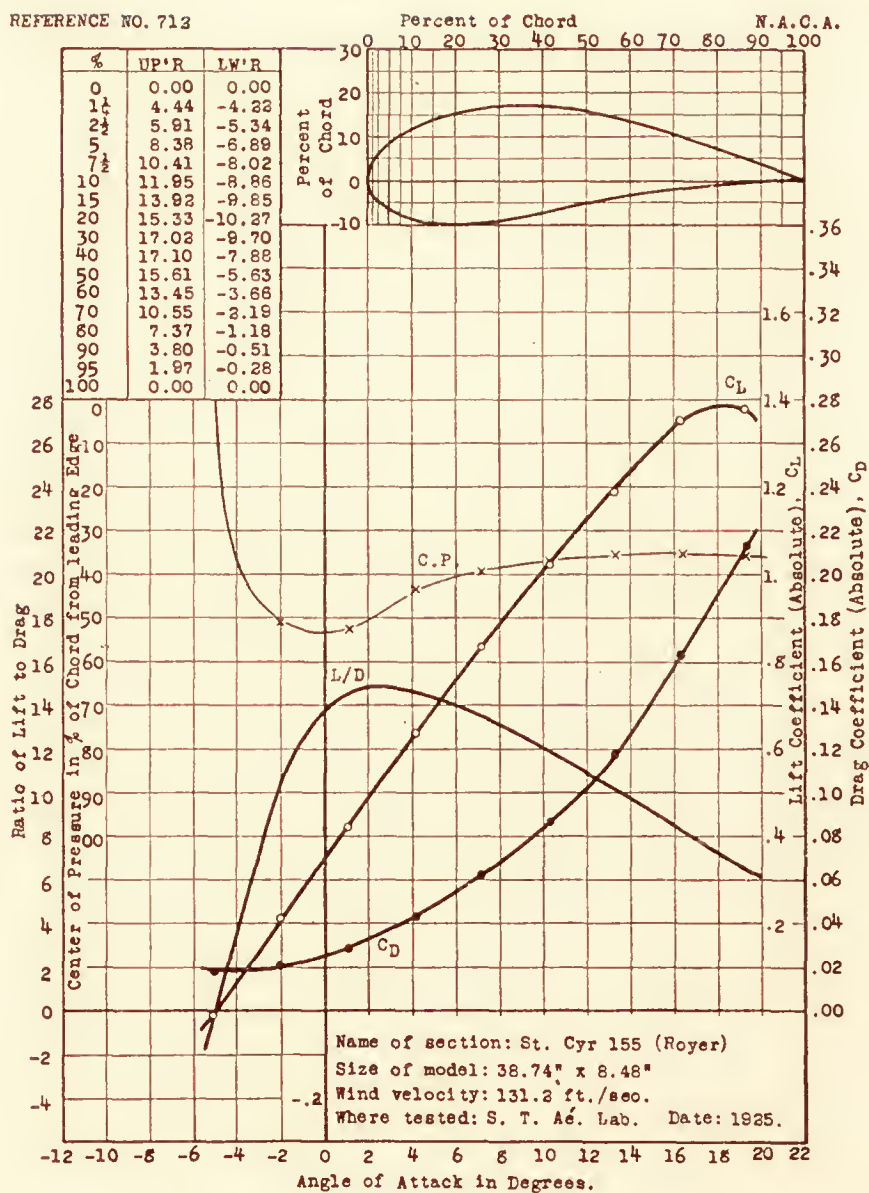


REFERENCE NO. 711

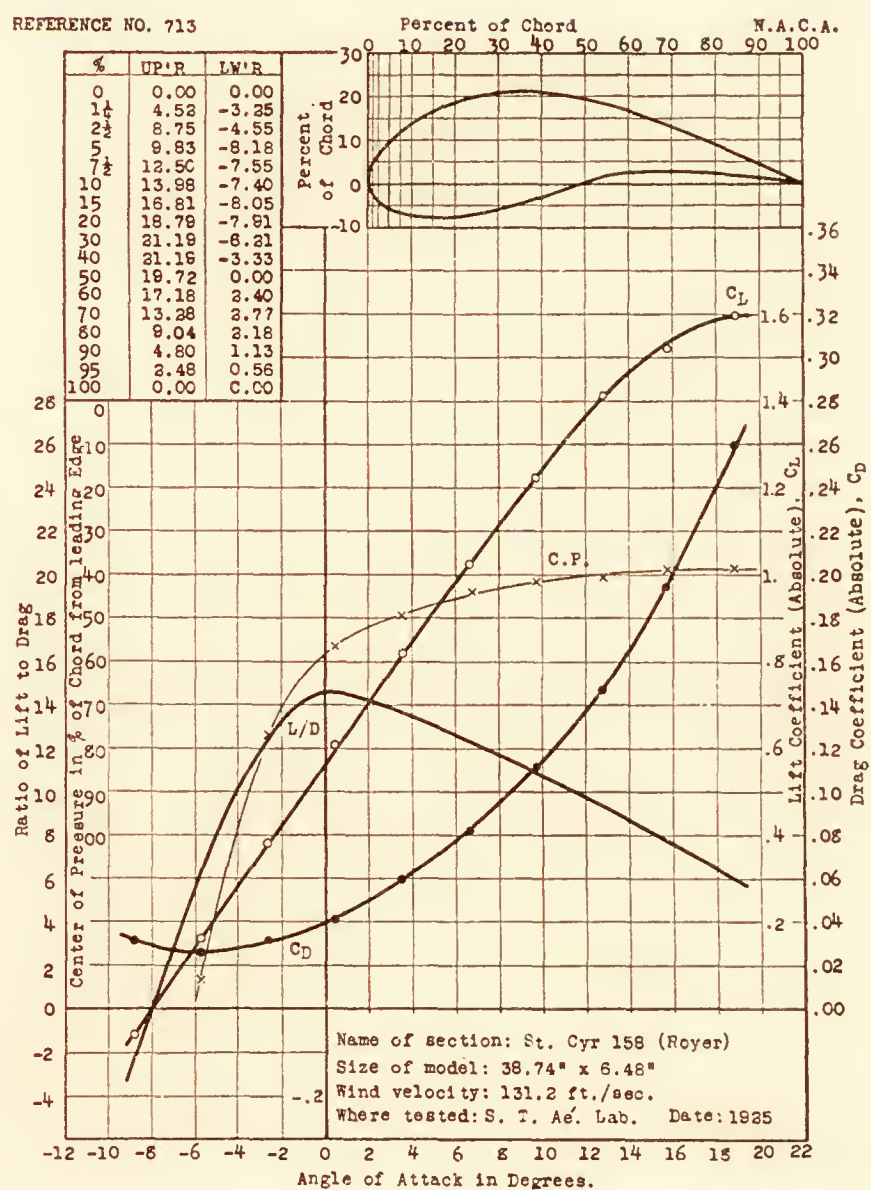




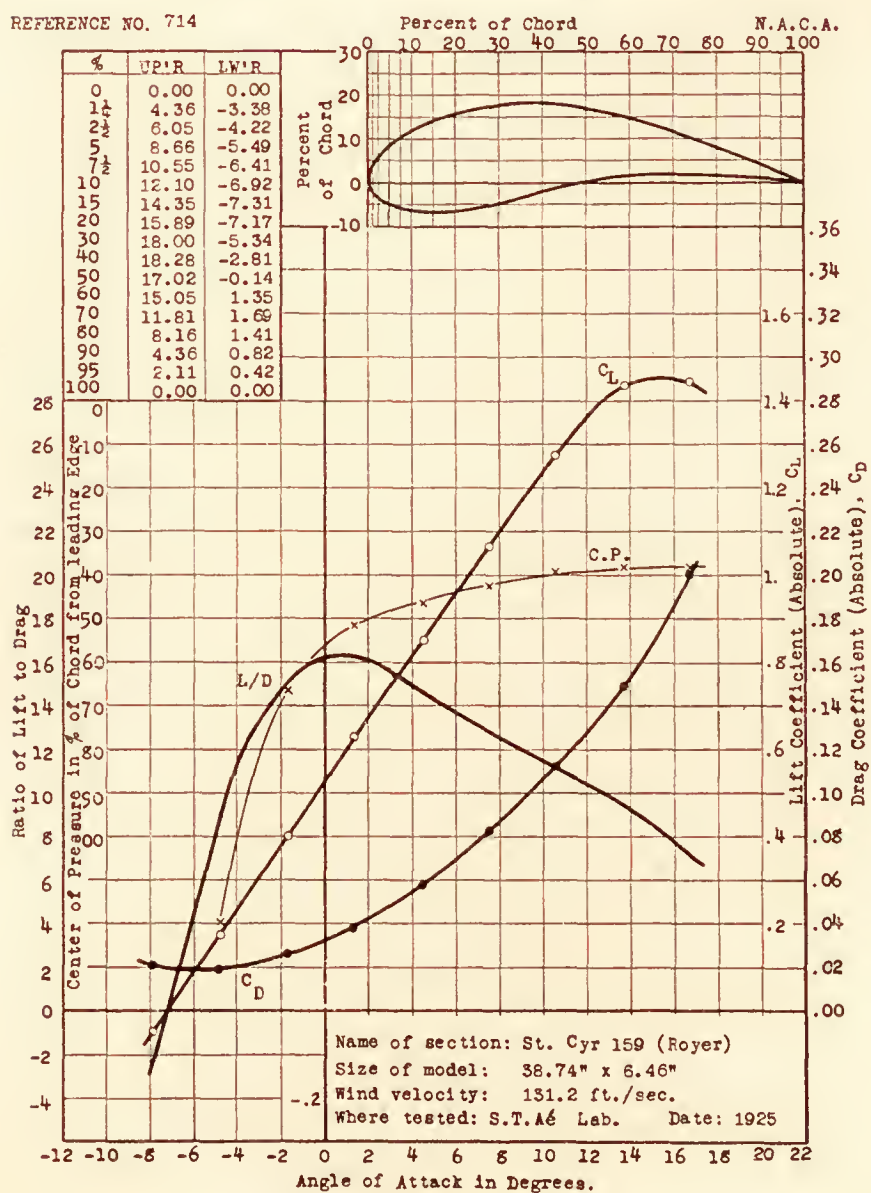
REFERENCE NO. 712



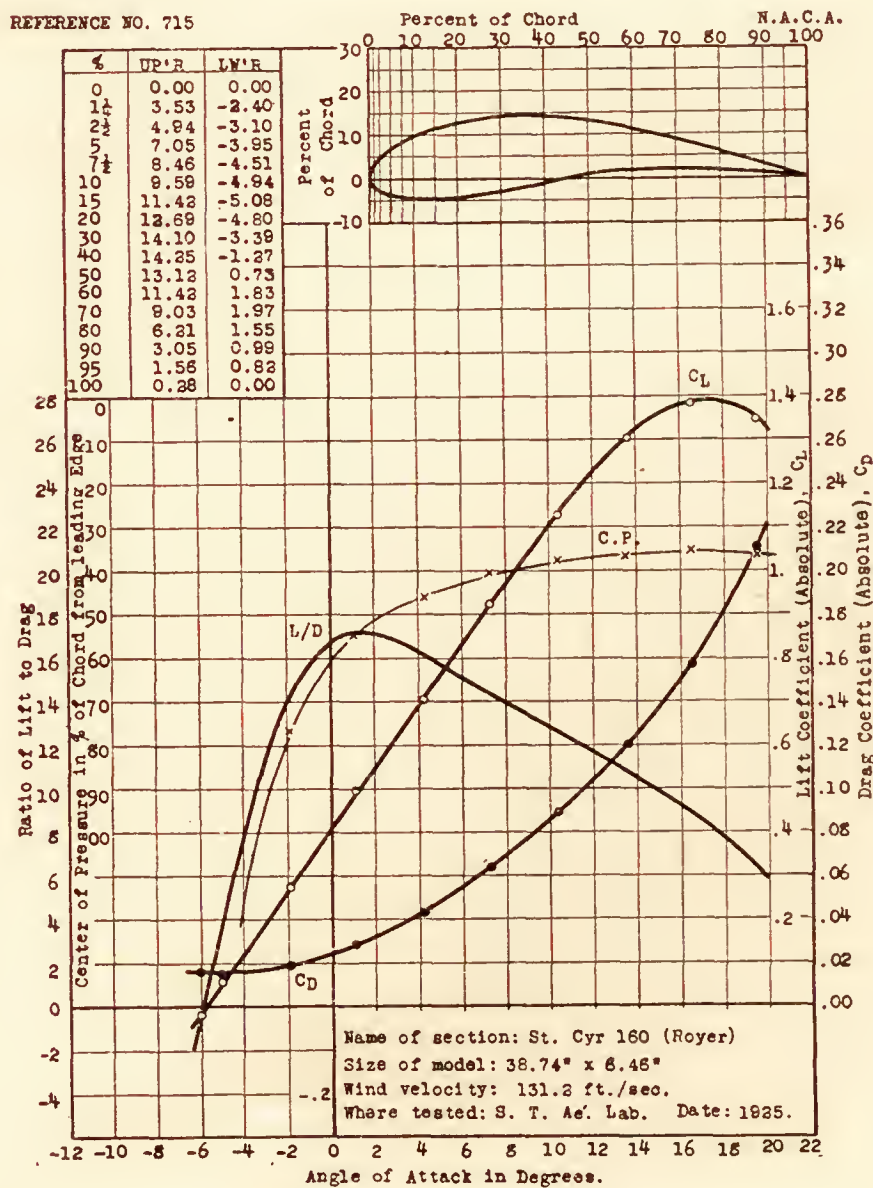
REFERENCE NO. 713



REFERENCE NO. 714

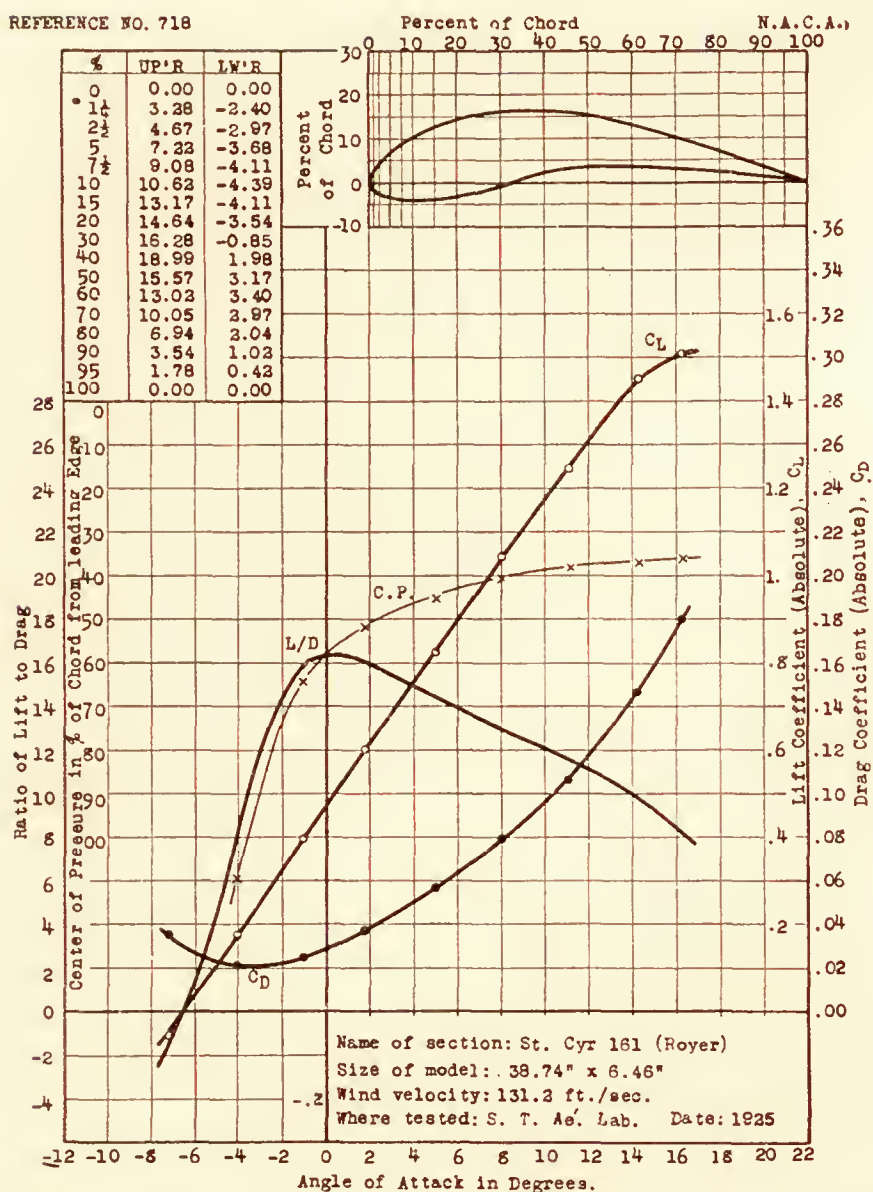


REFERENCE NO. 715

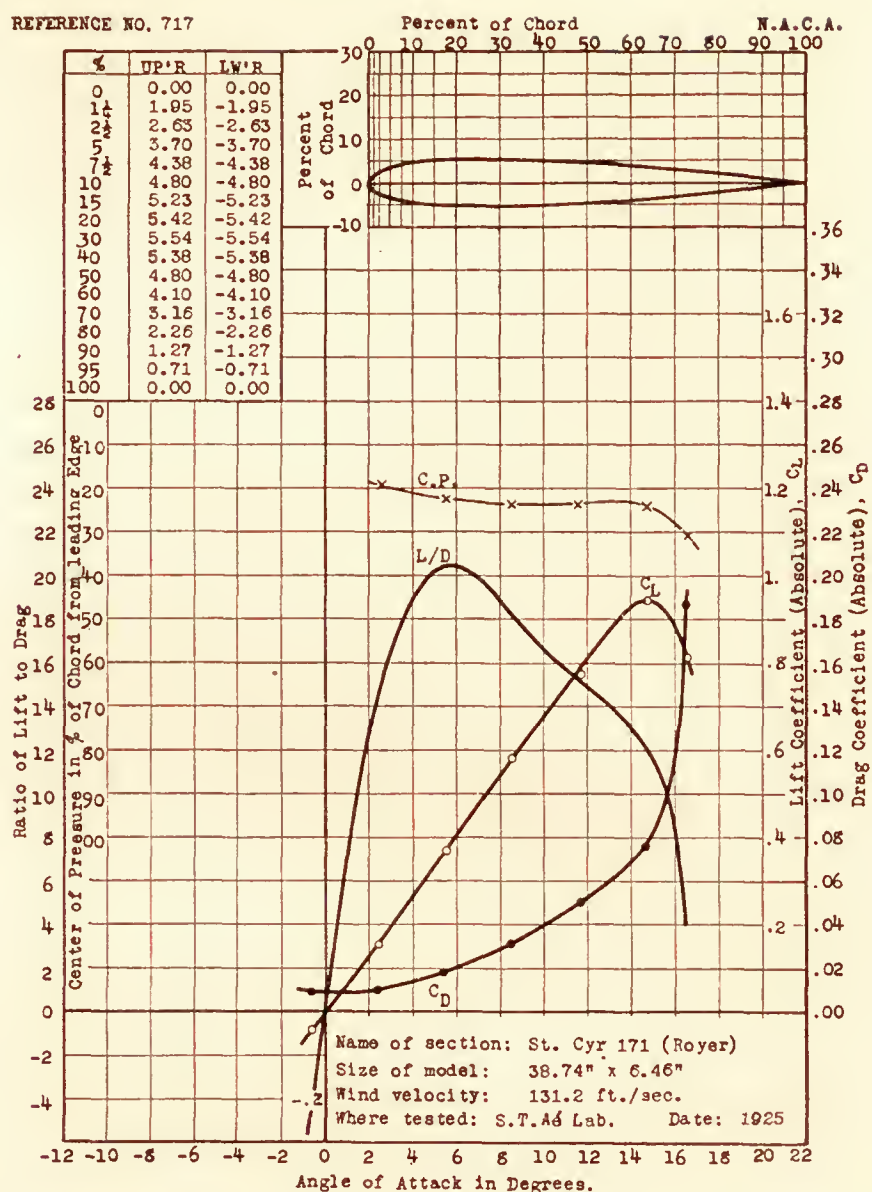




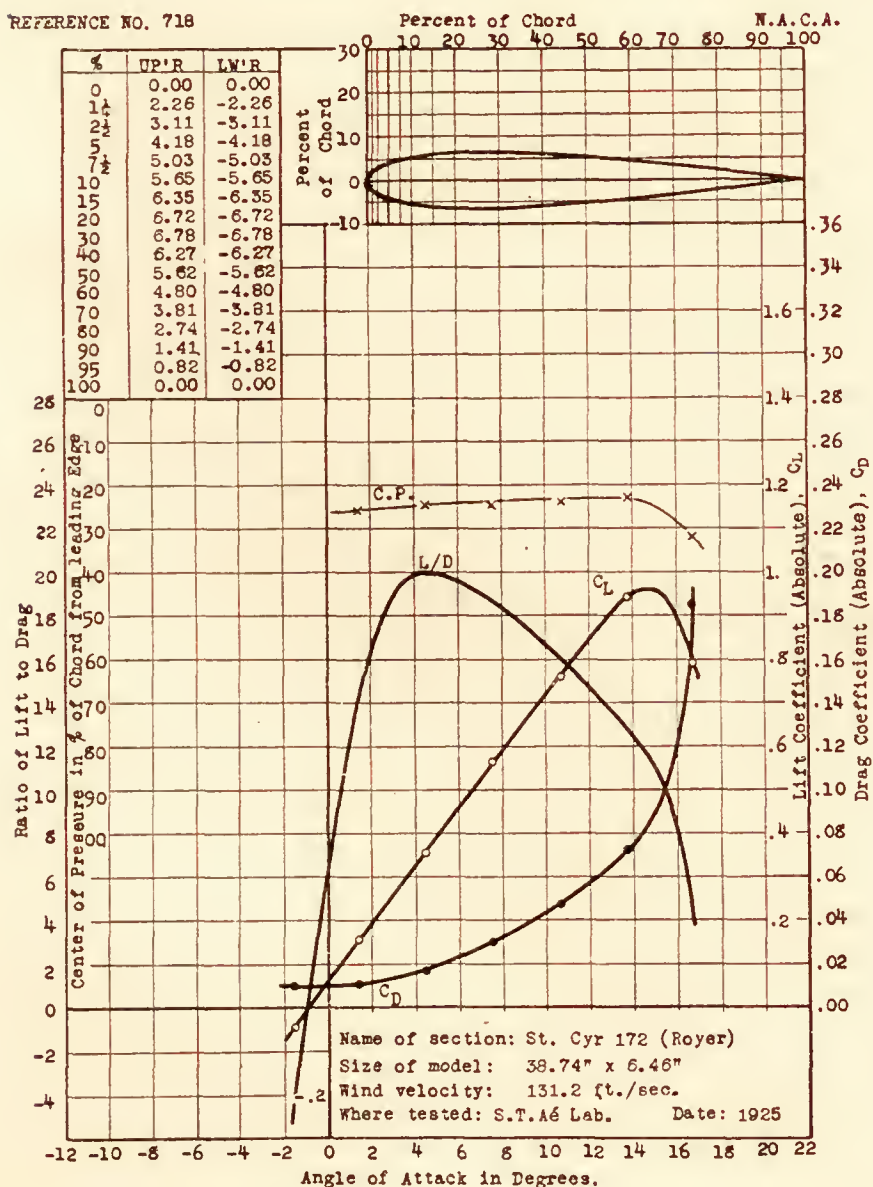
REFERENCE NO. 718



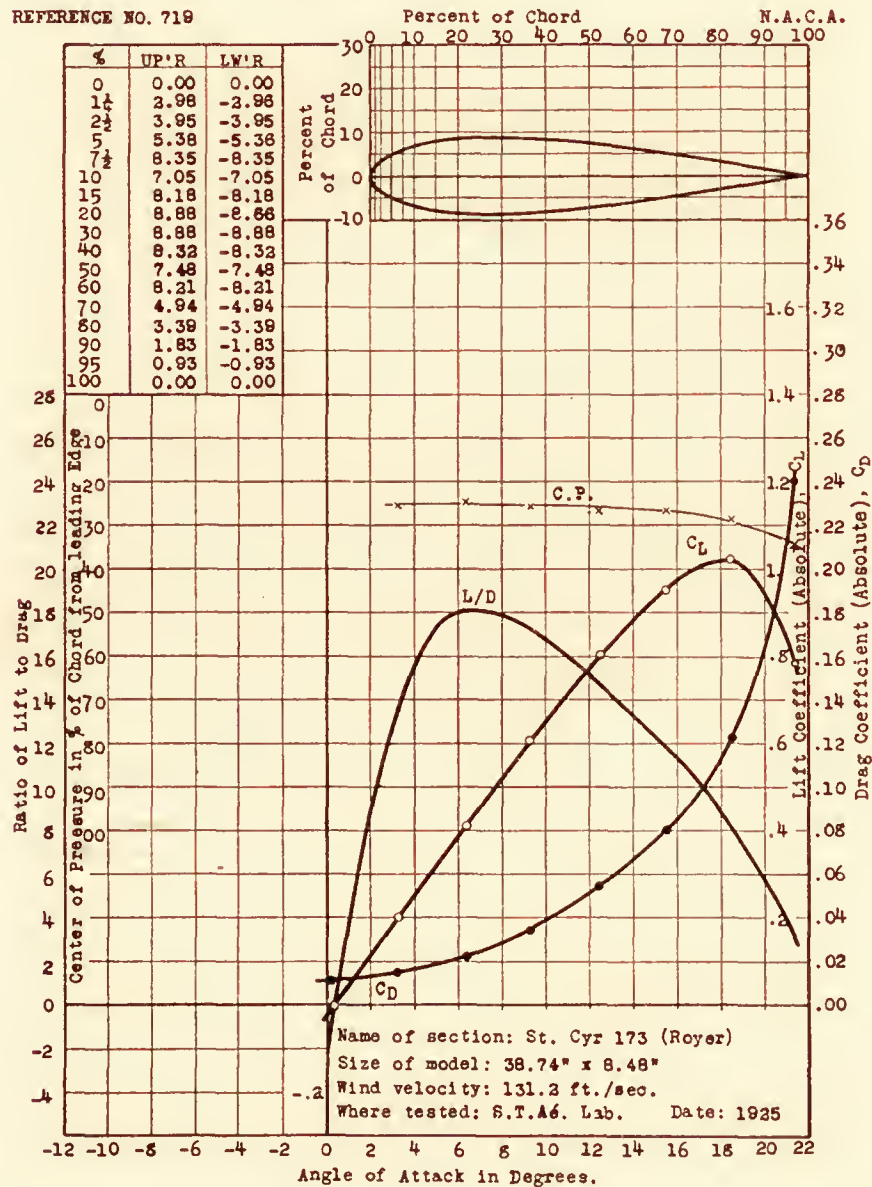
REFERENCE NO. 717



REFERENCE NO. 718

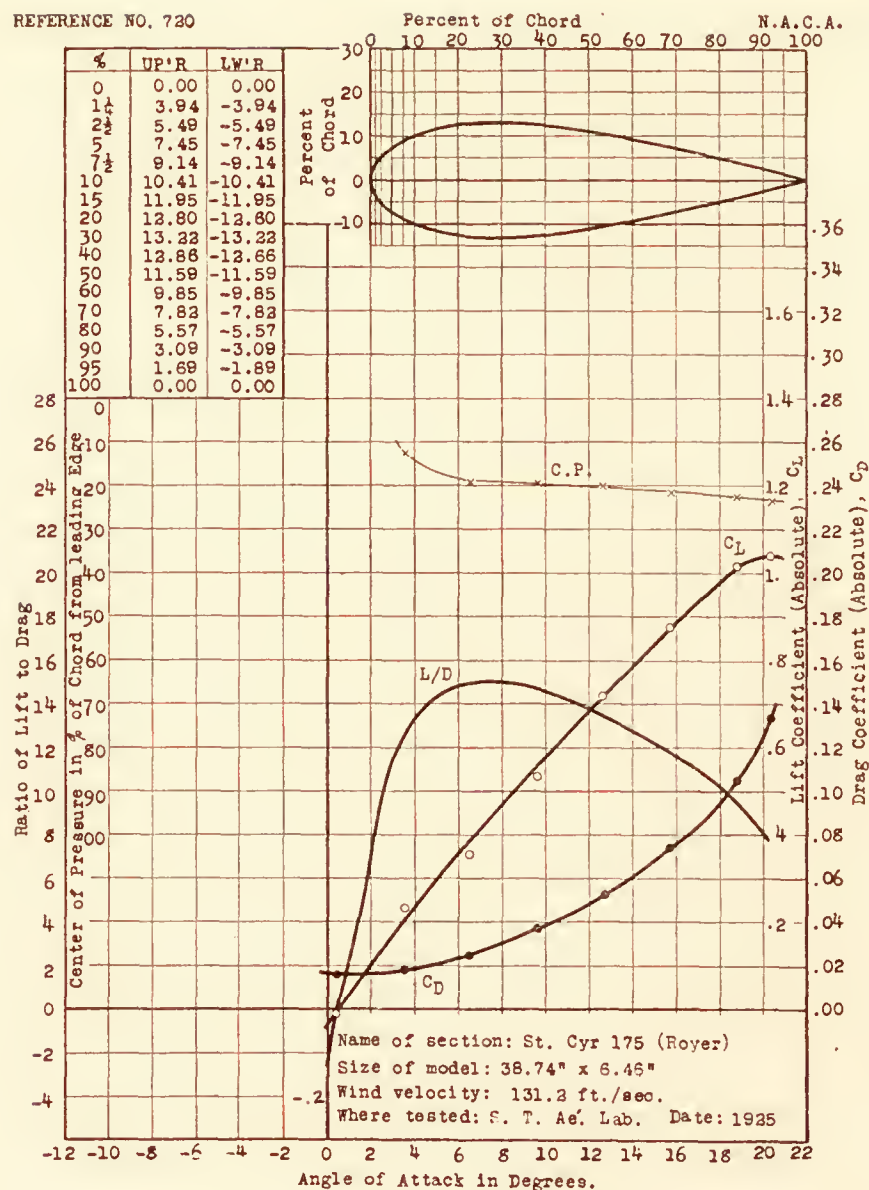


REFERENCE NO. 719

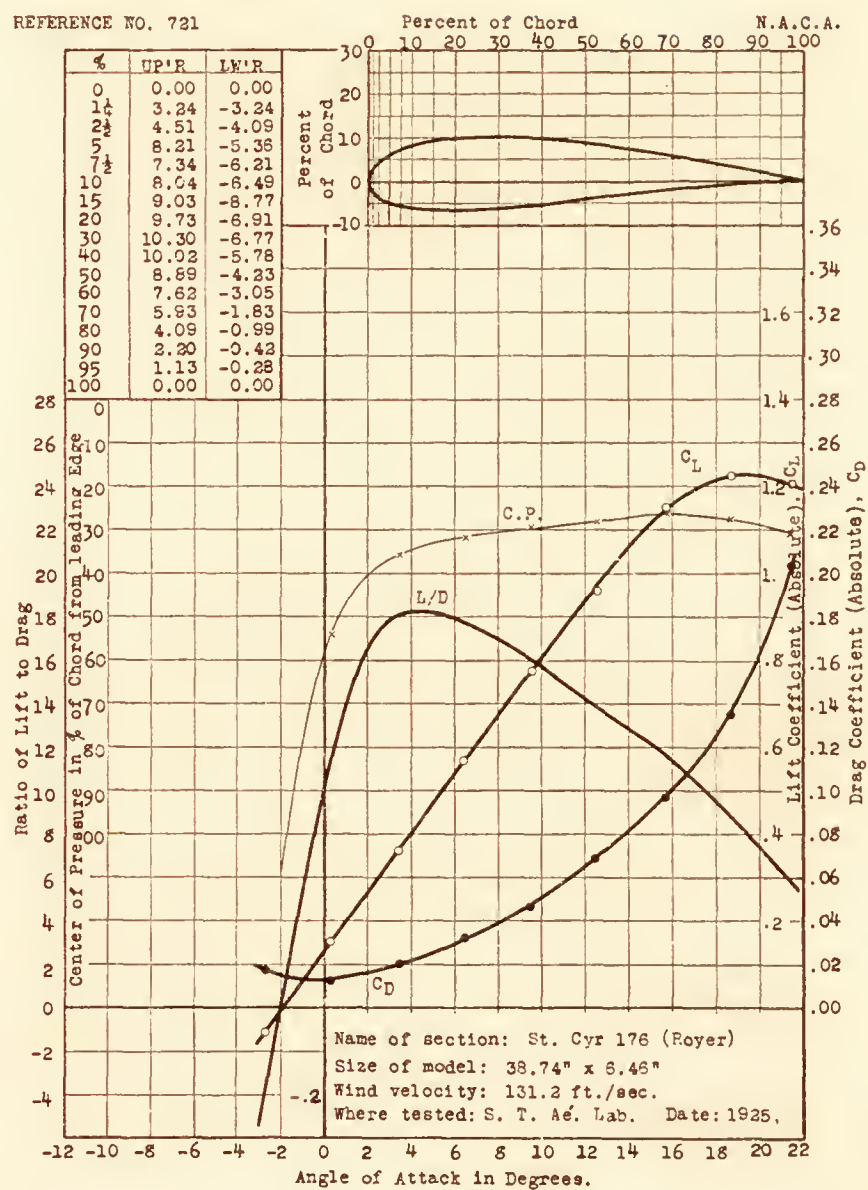




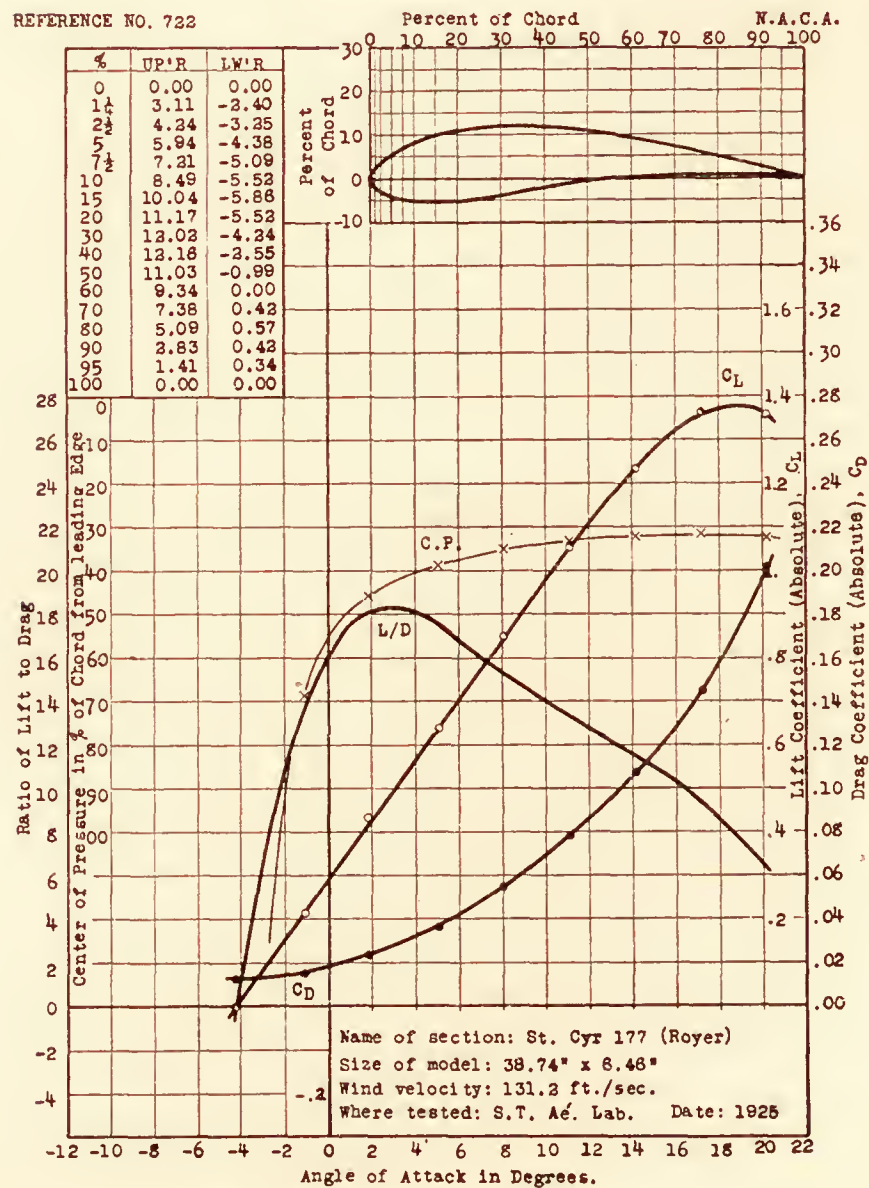
REFERENCE NO. 720



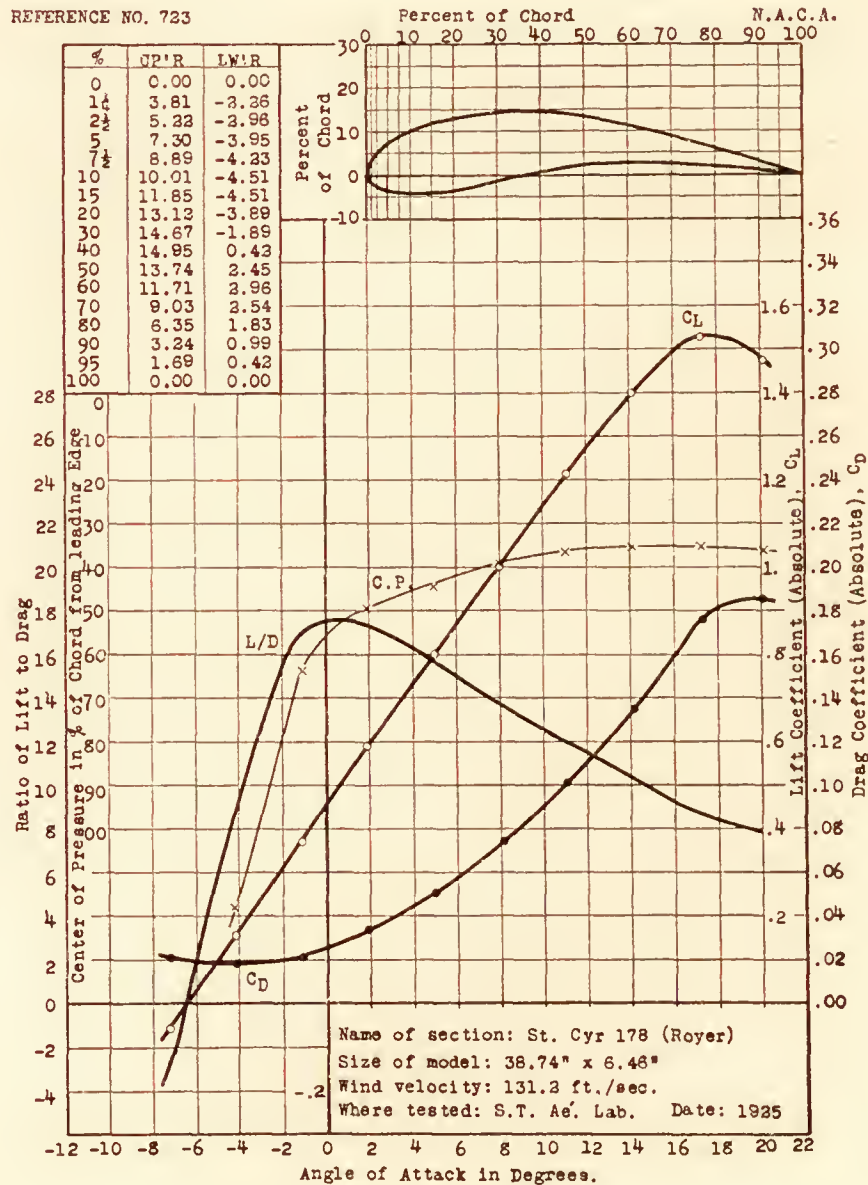
REFERENCE NO. 721



REFERENCE NO. 722

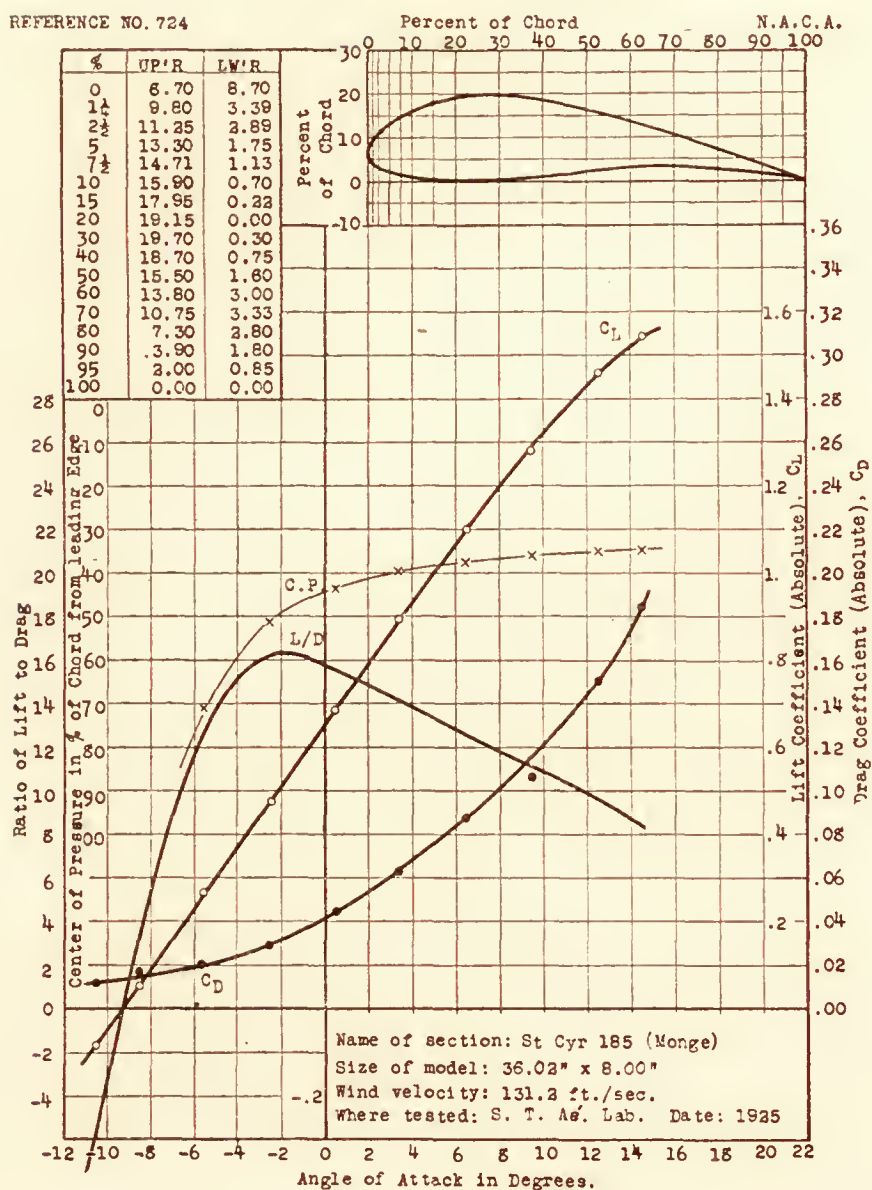


REFERENCE NO. 723

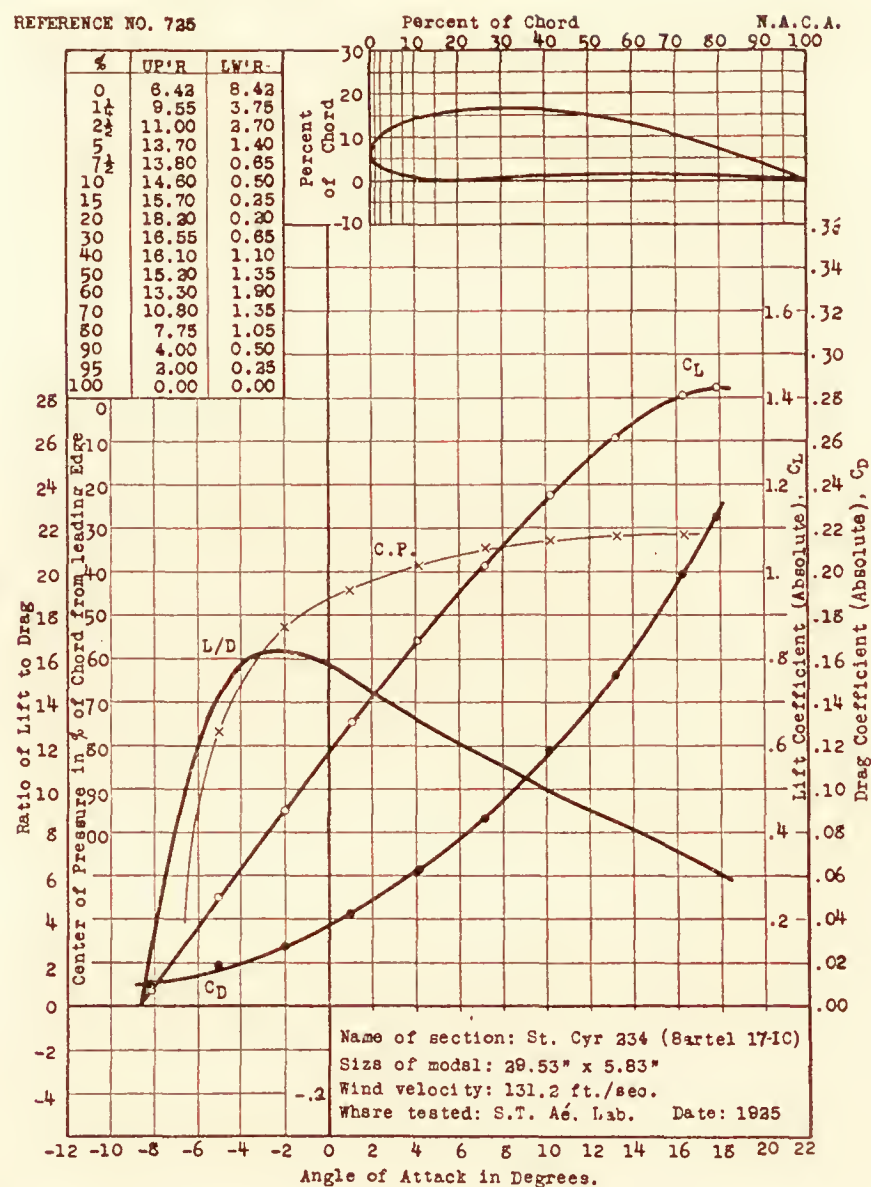




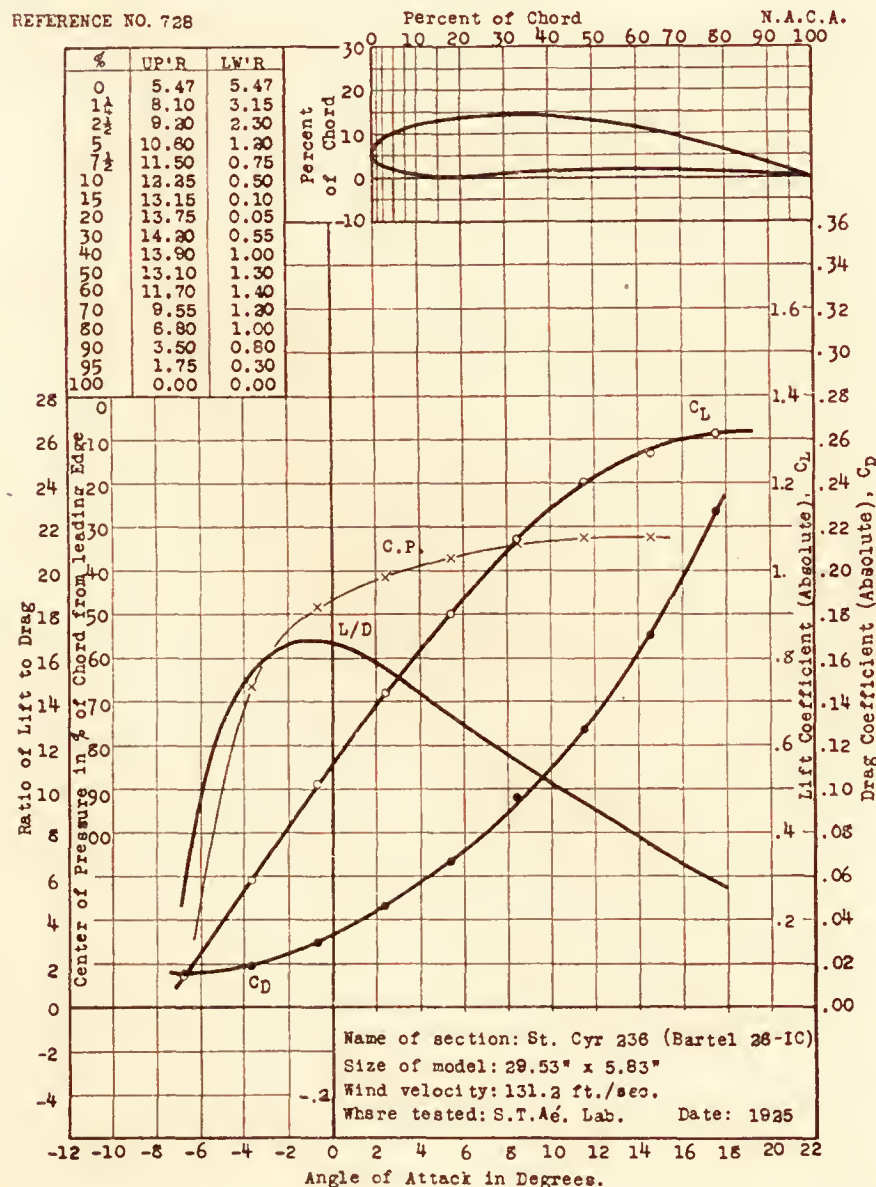
REFERENCE NO. 724



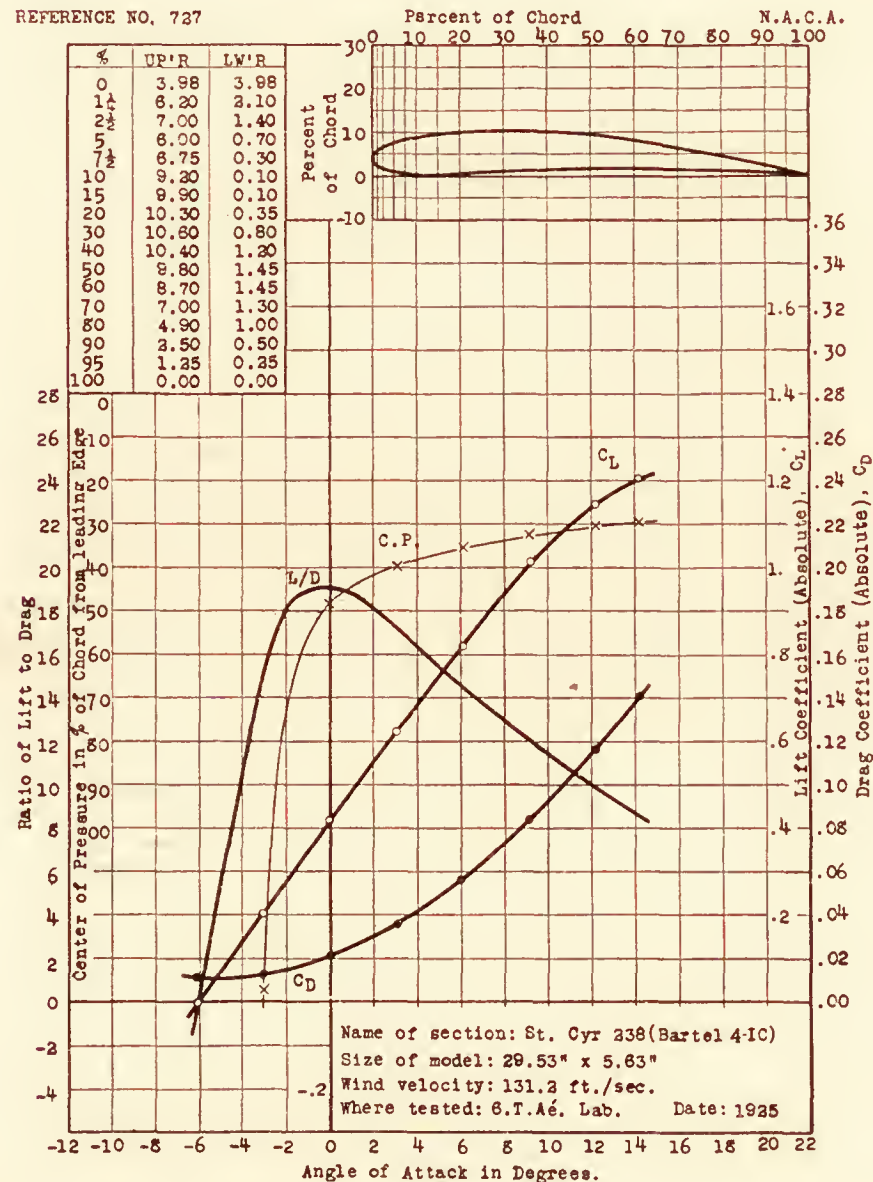
REFERENCE NO. 725



REFERENCE NO. 728

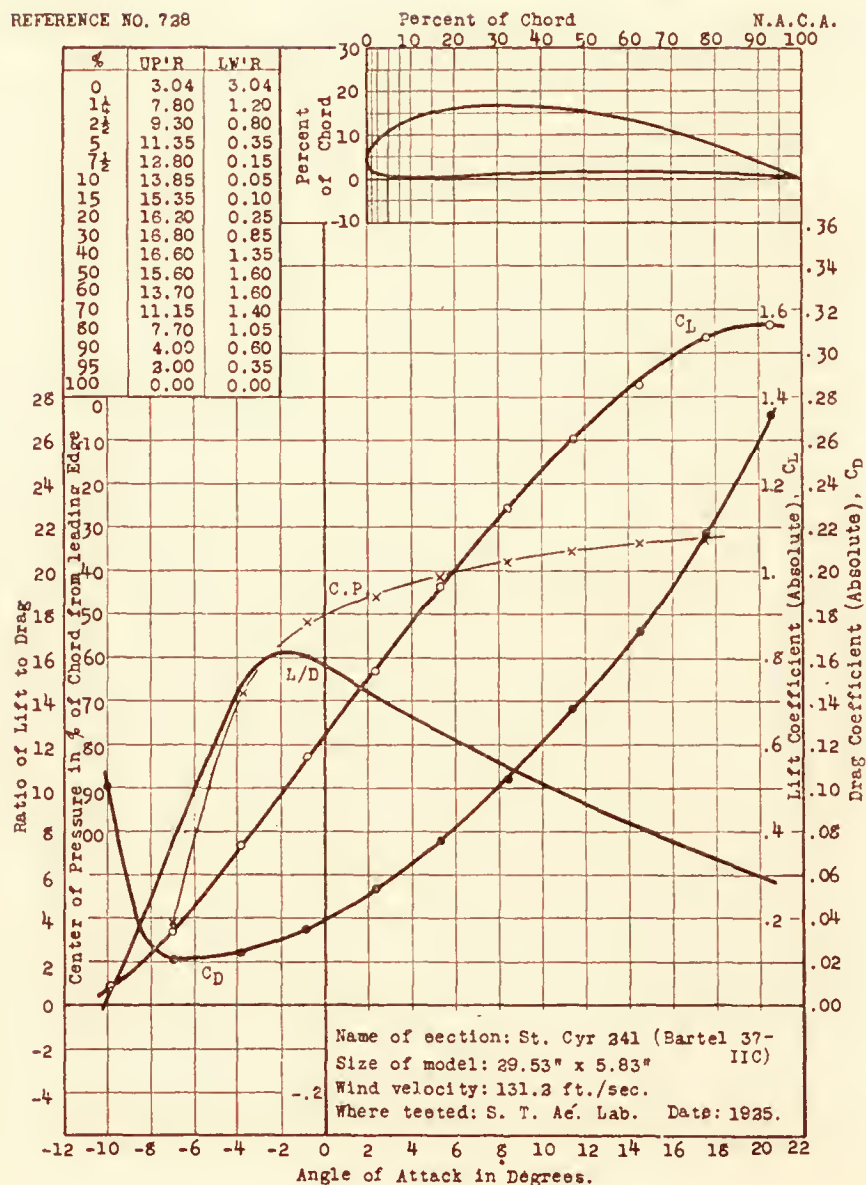


REFERENCE NO. 727

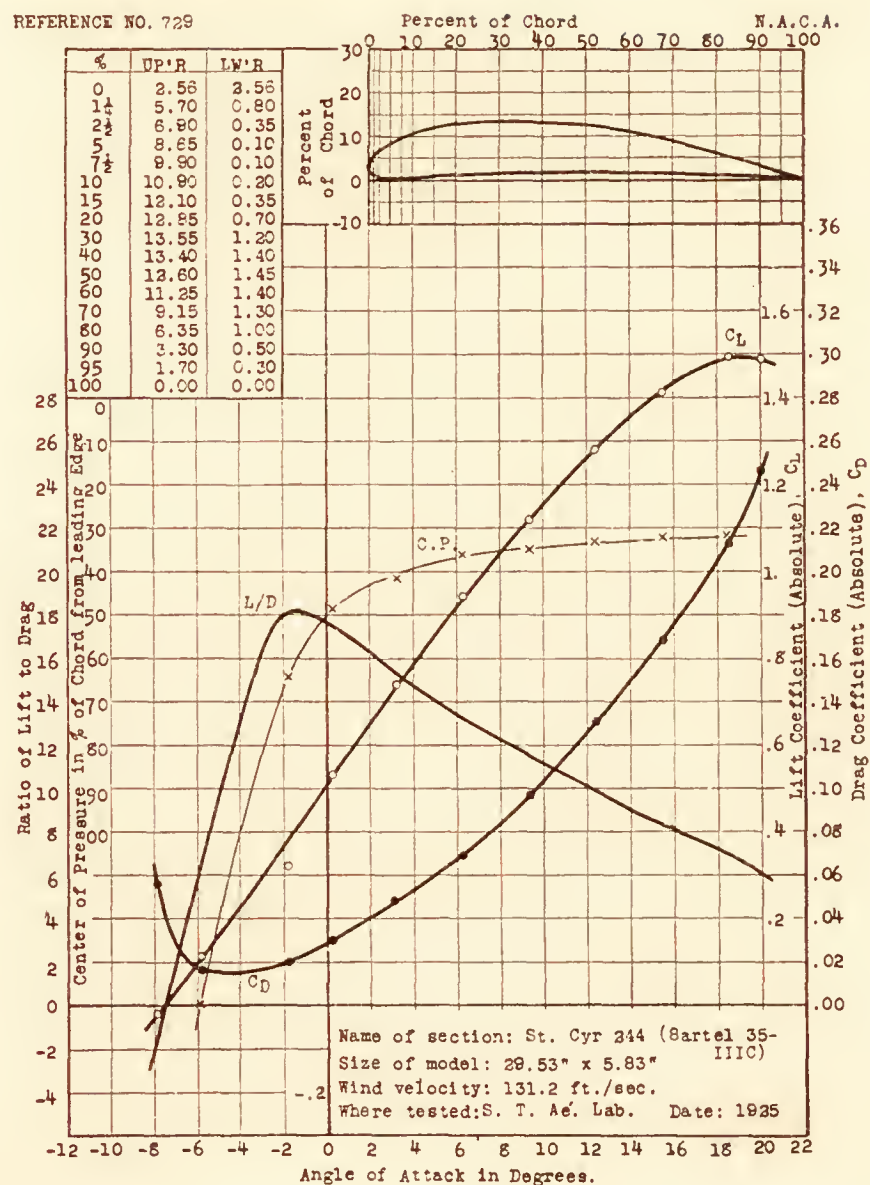




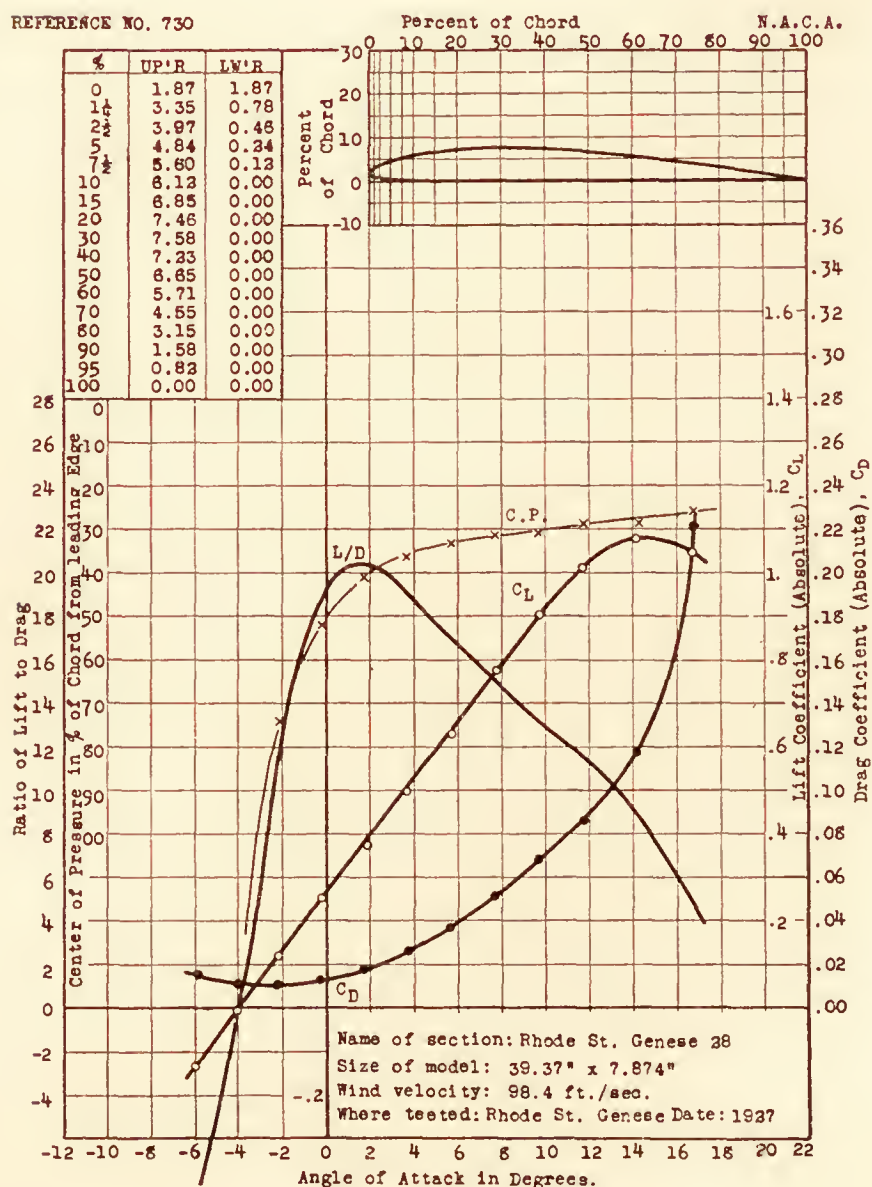
REFERENCE NO. 728



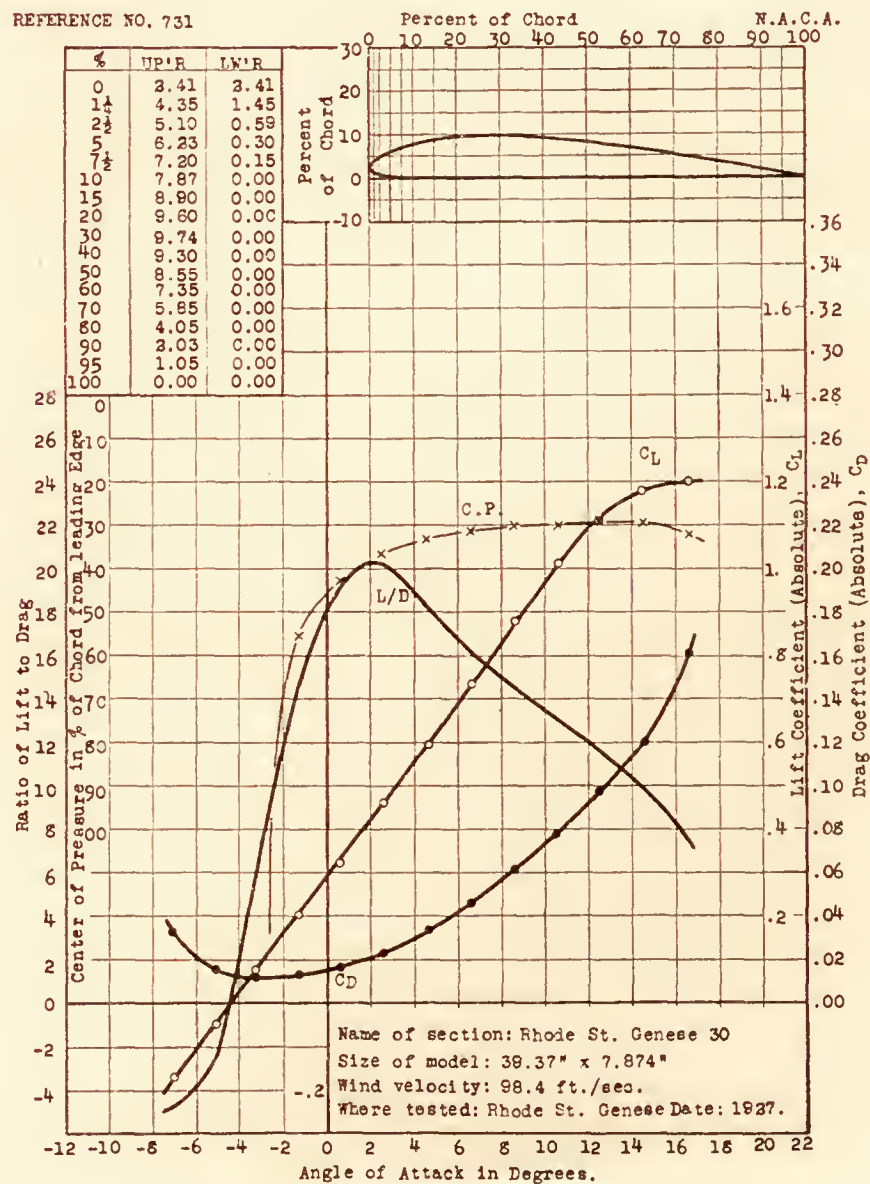
REFERENCE NO. 729



REFERENCE NO. 730

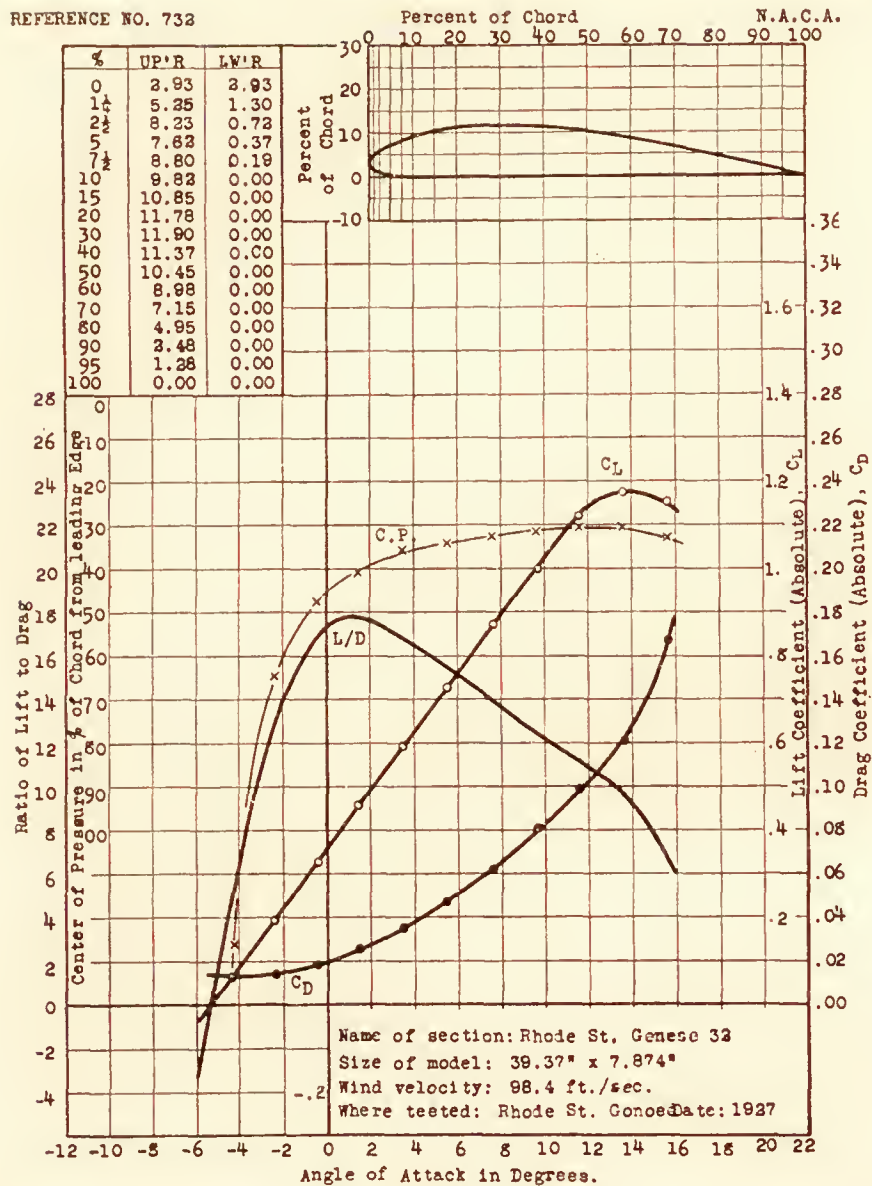


REFERENCE NO. 731

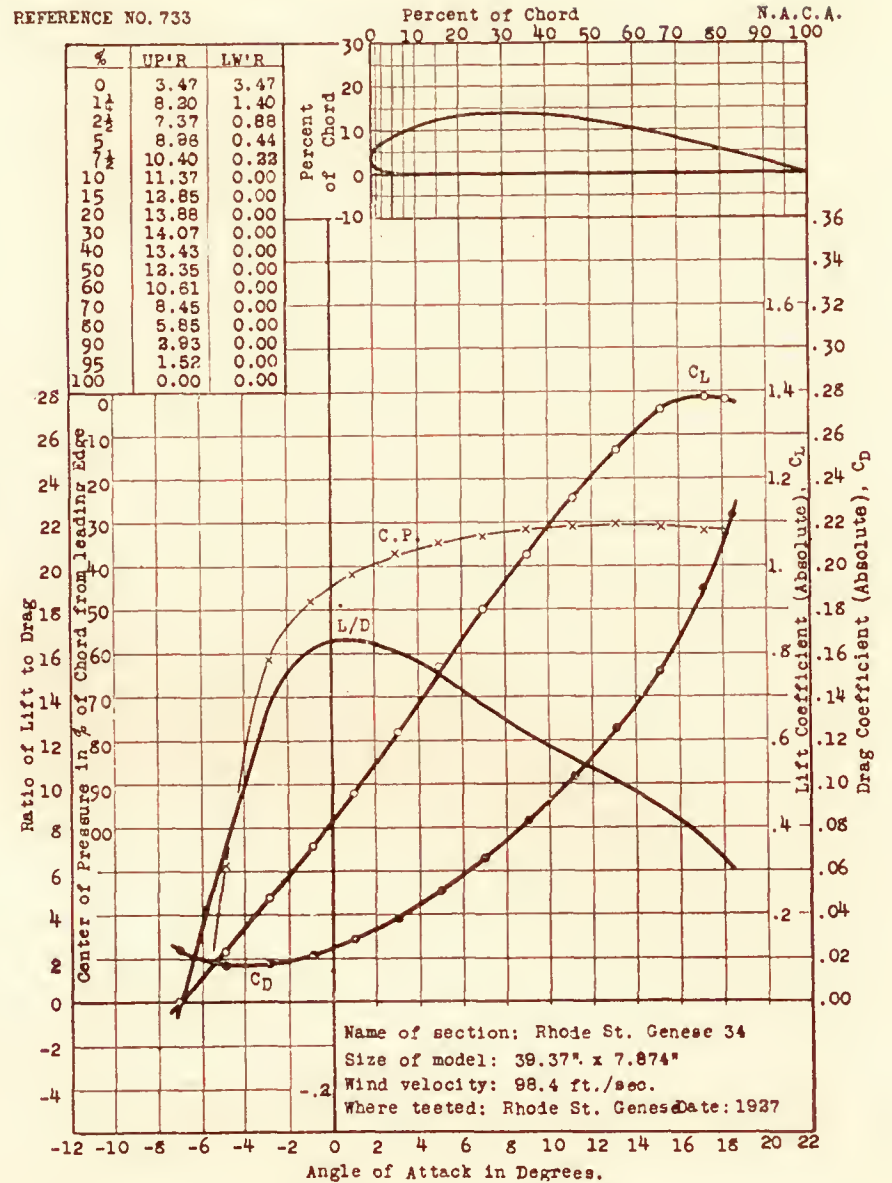




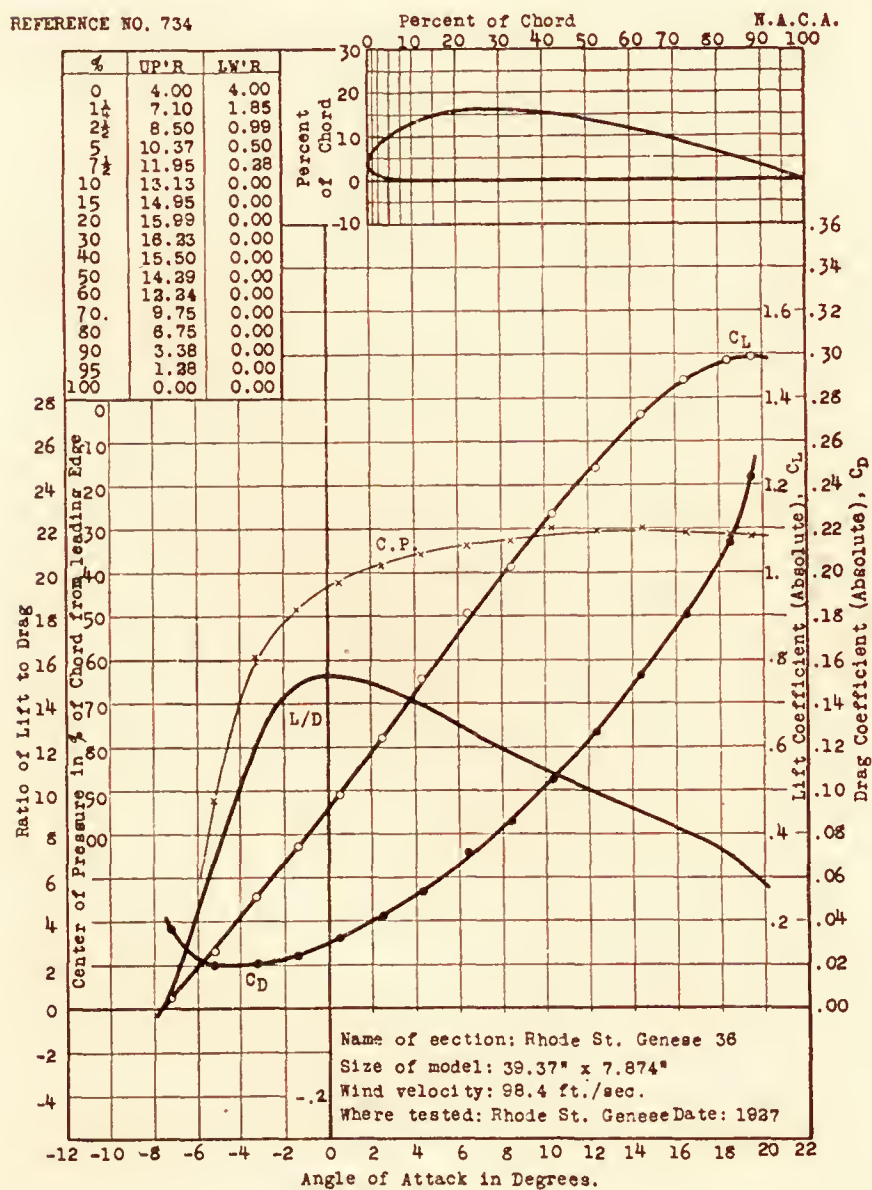
REFERENCE NO. 732



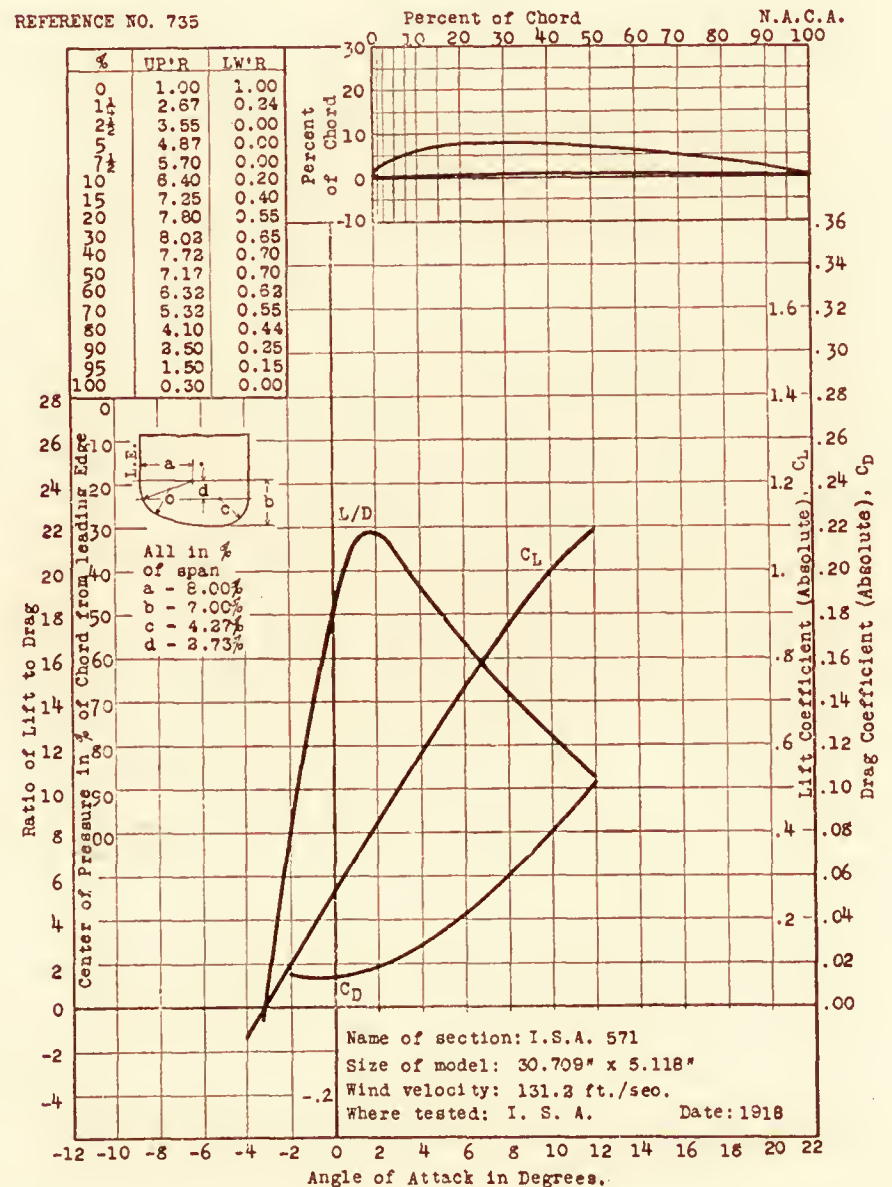
REFERENCE NO. 733



REFERENCE NO. 734

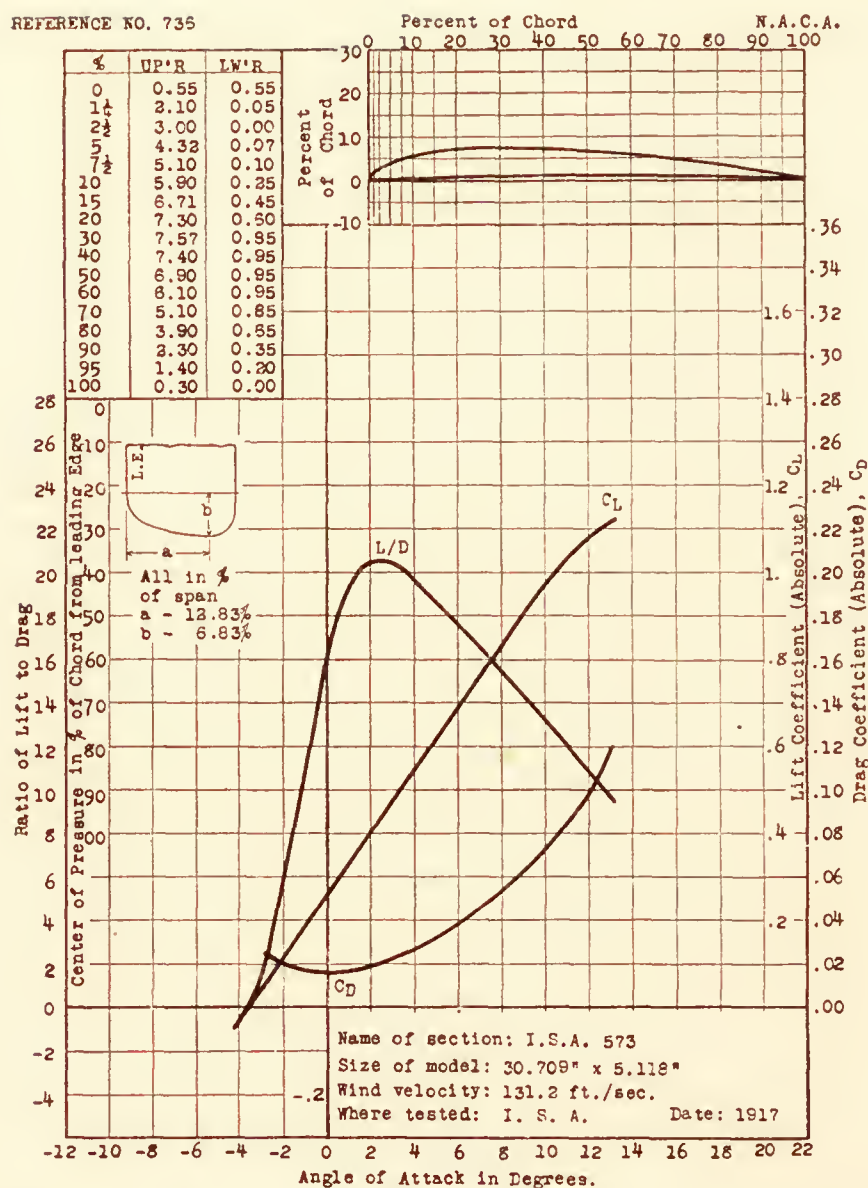


REFERENCE NO. 735

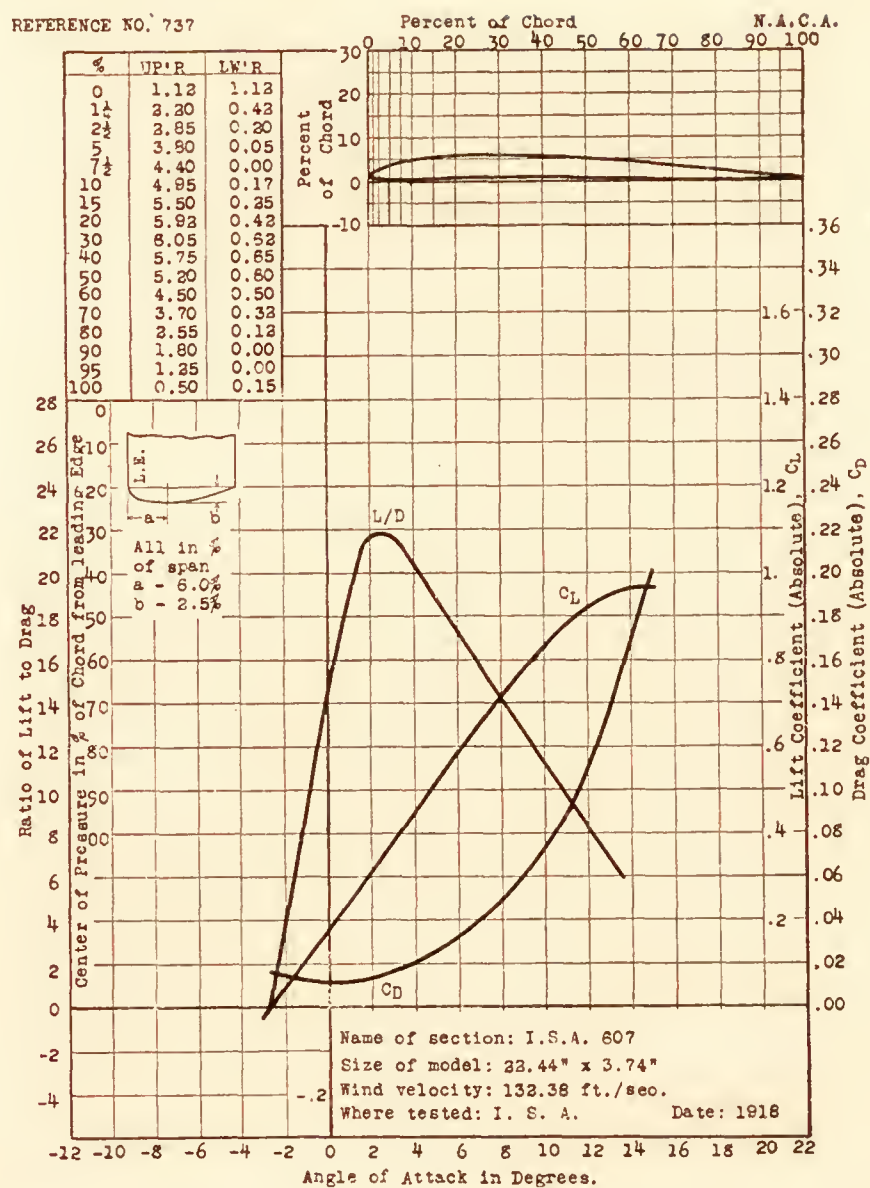




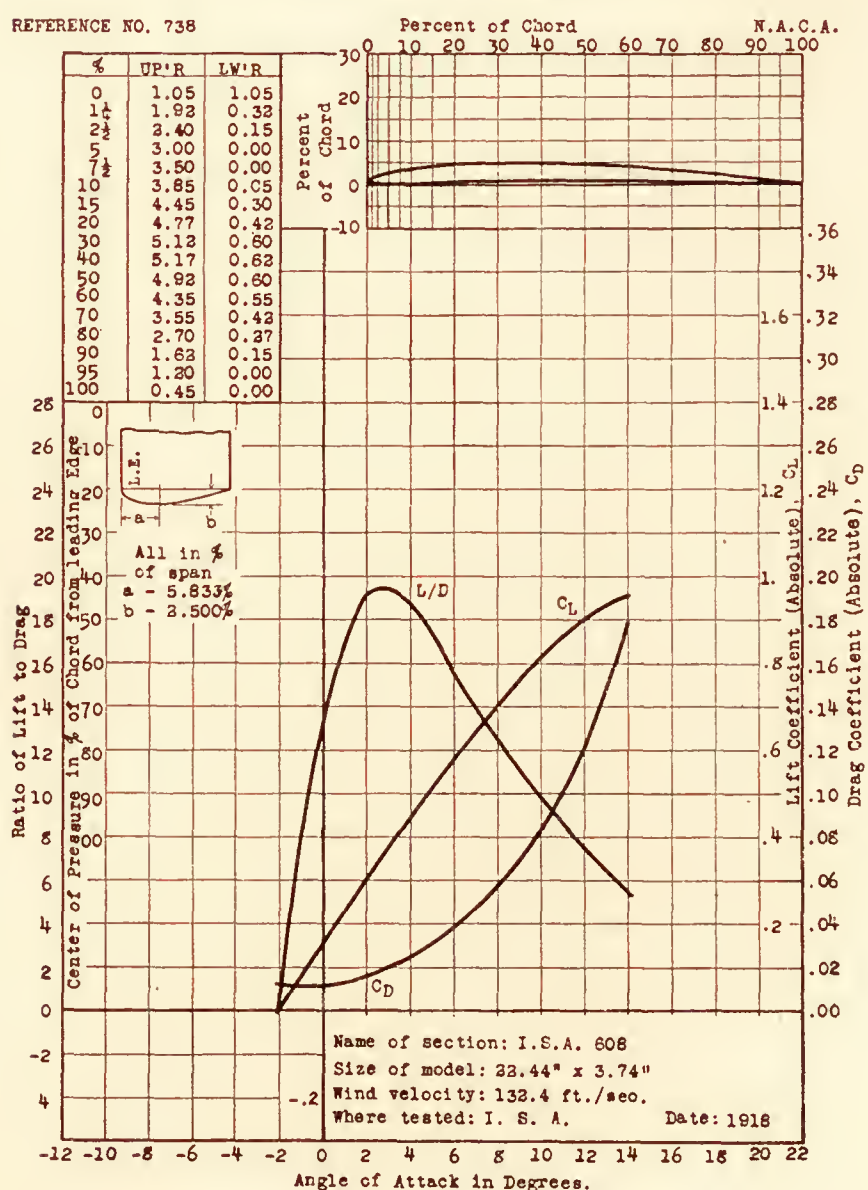
REFERENCE NO. 735



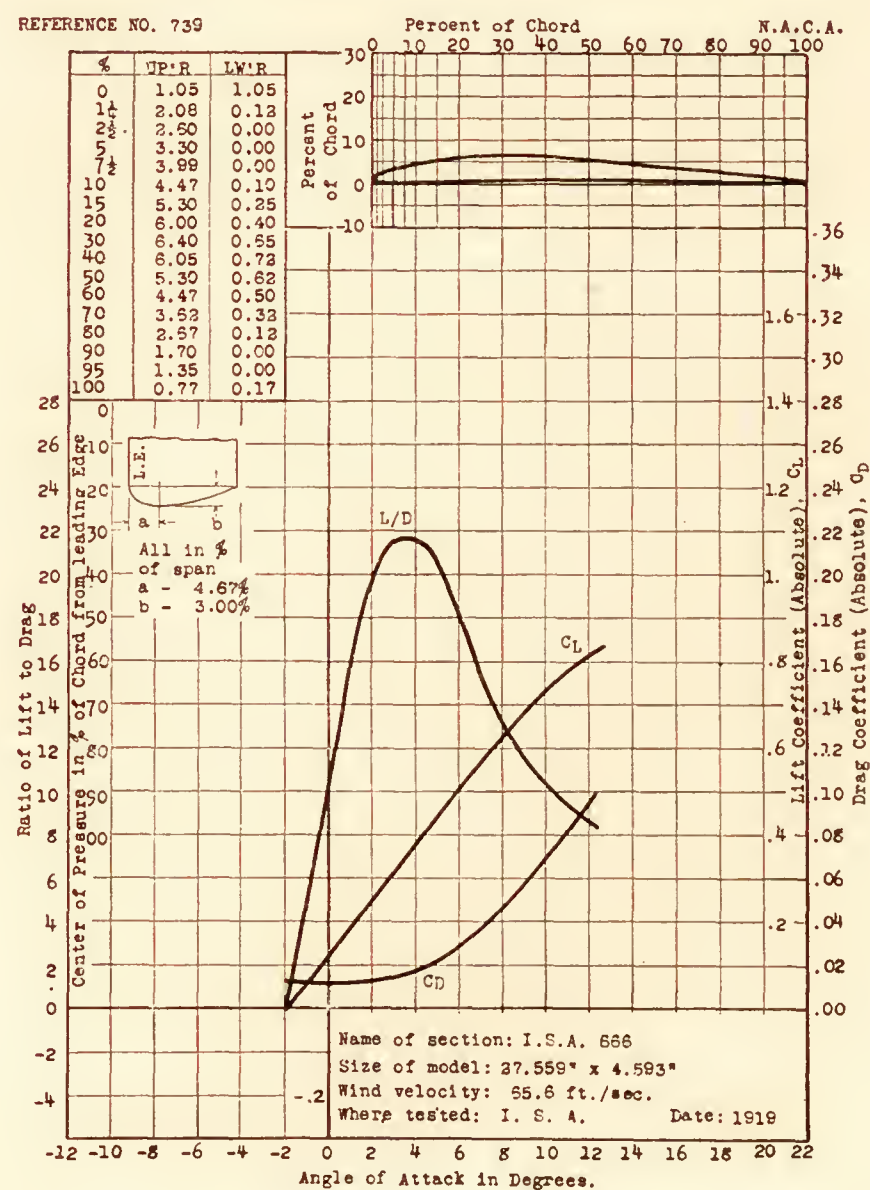
REFERENCE NO. 737



REFERENCE NO. 738

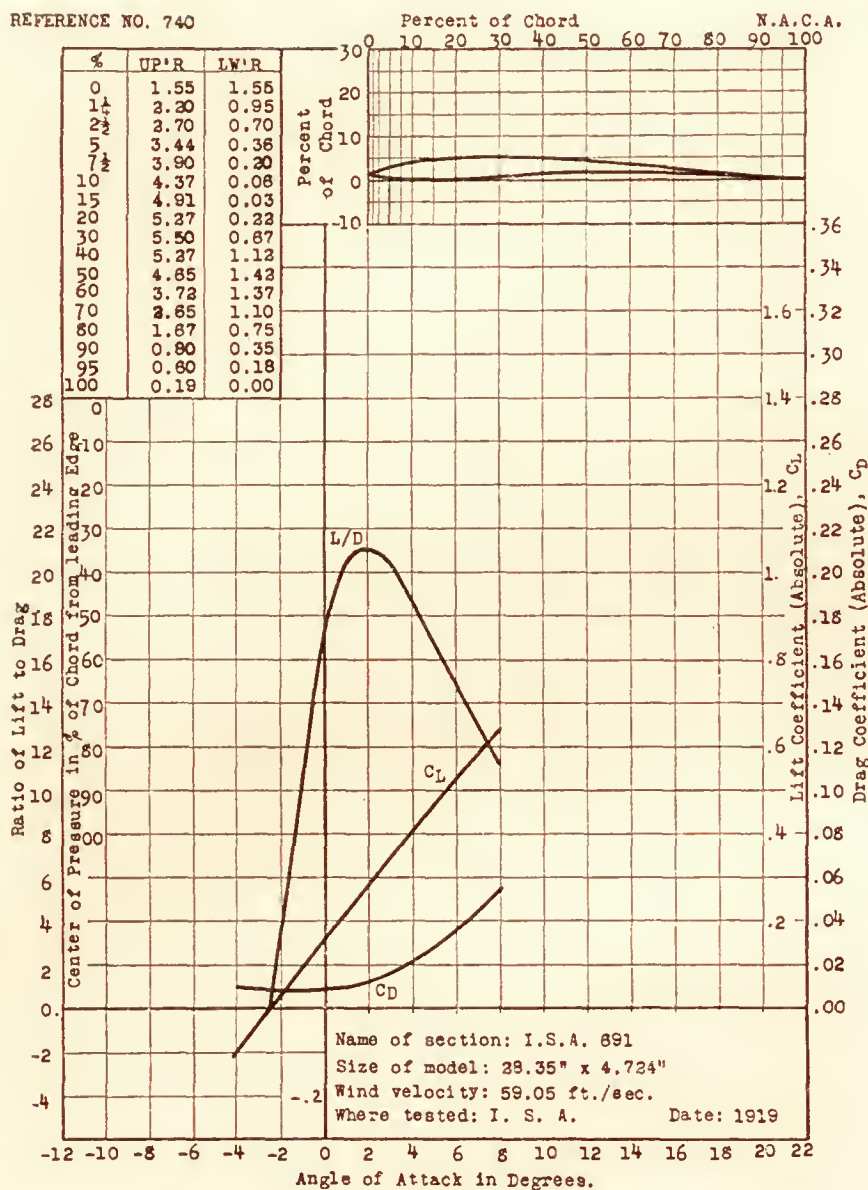


REFERENCE NO. 739

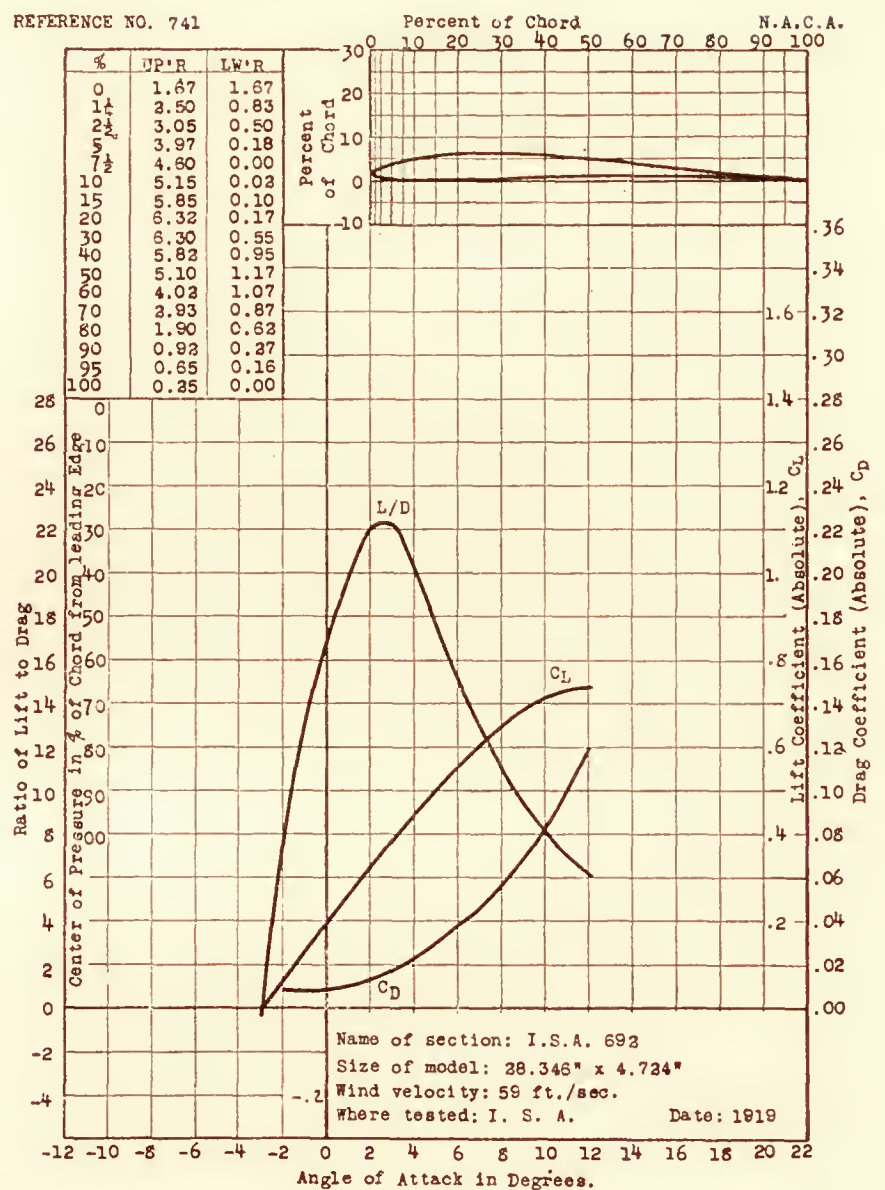




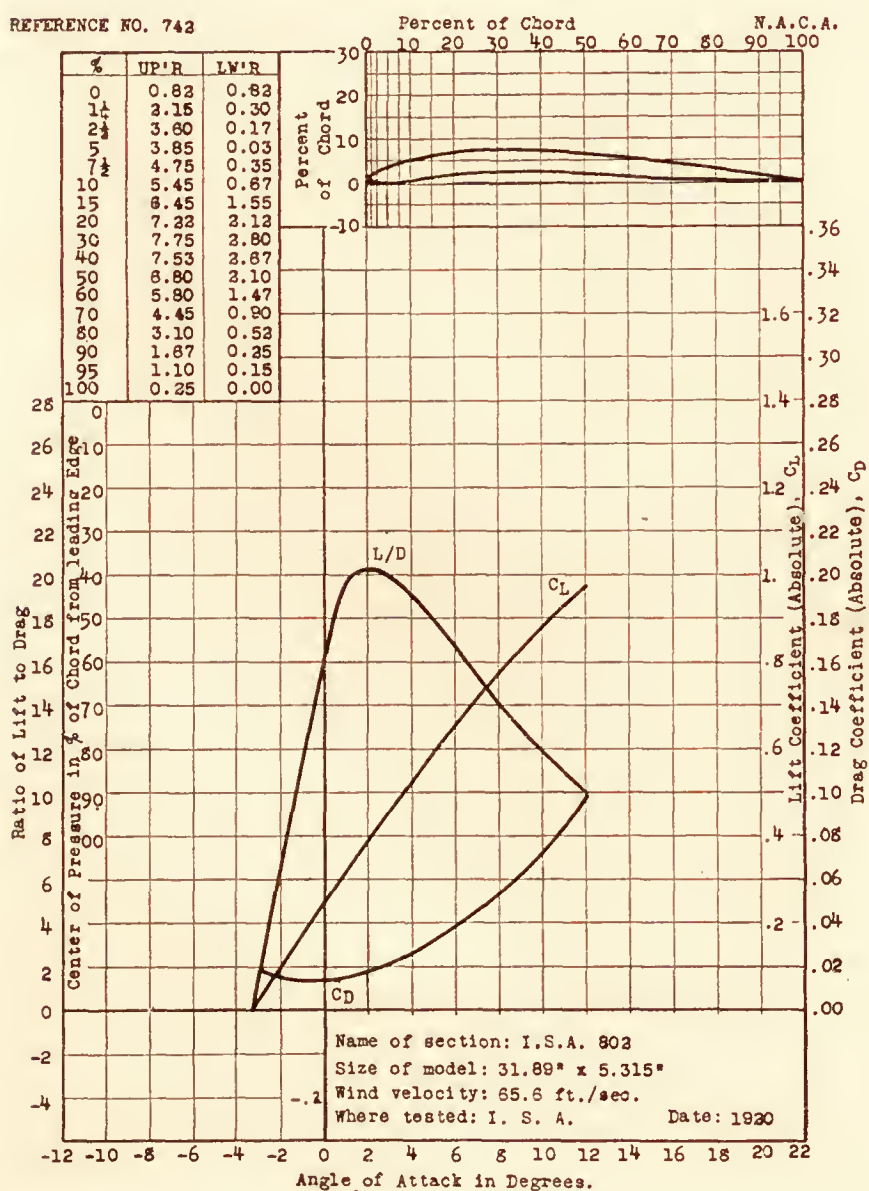
REFERENCE NO. 740



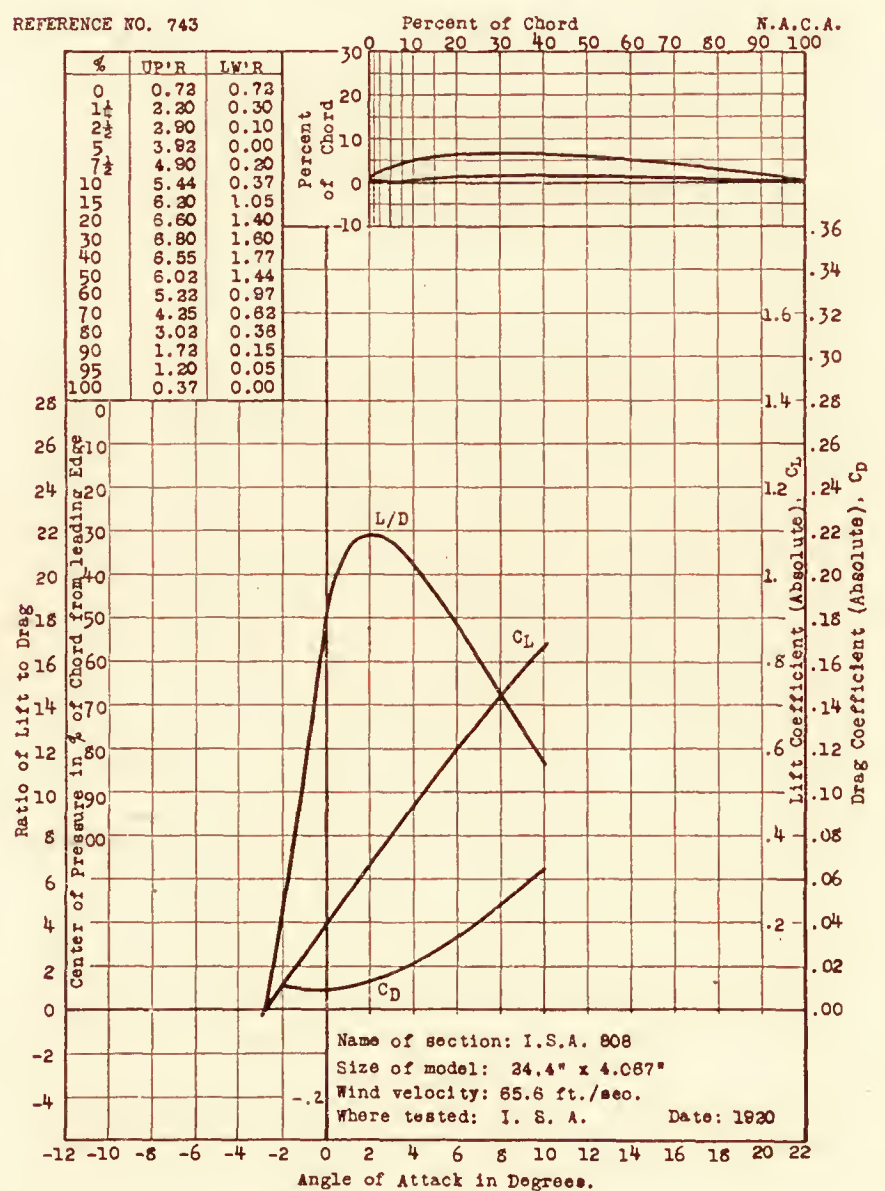
REFERENCE NO. 741



REFERENCE NO. 742

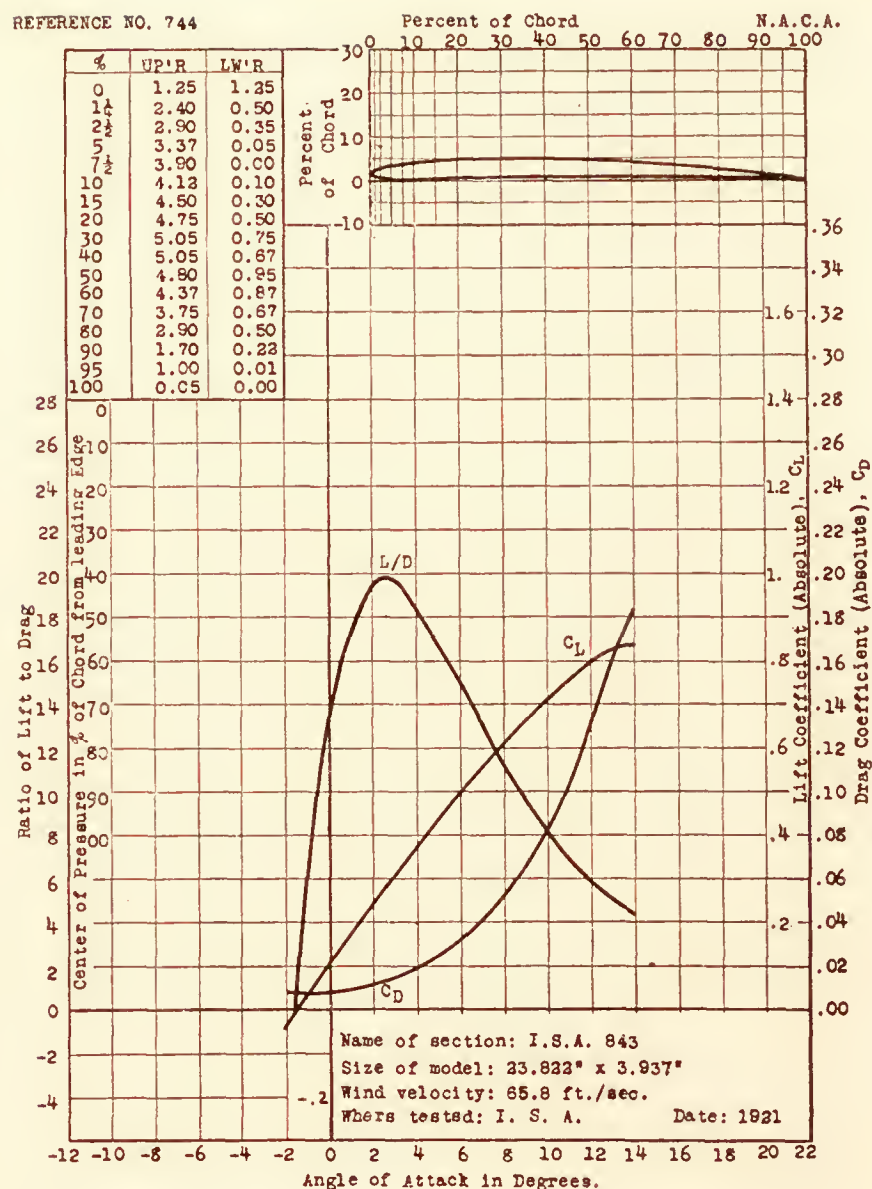


REFERENCE NO. 743

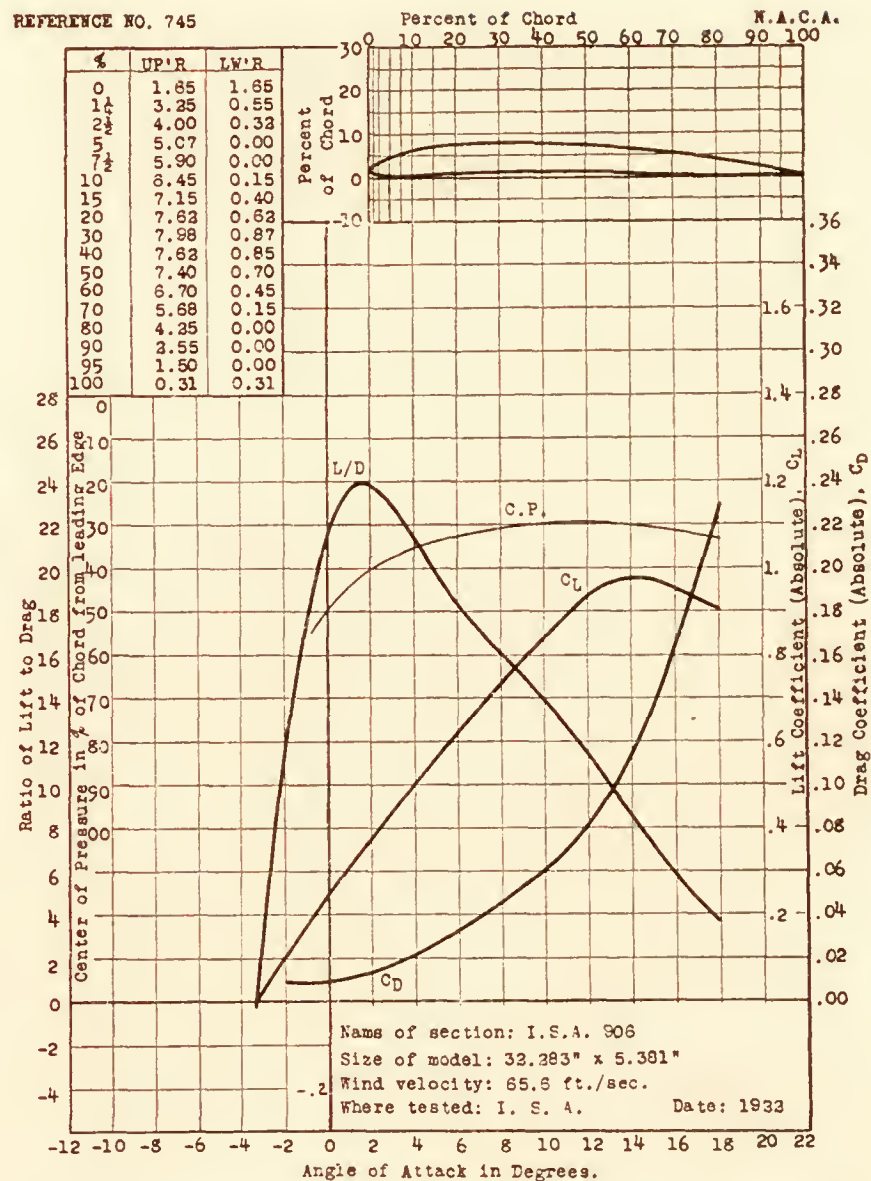




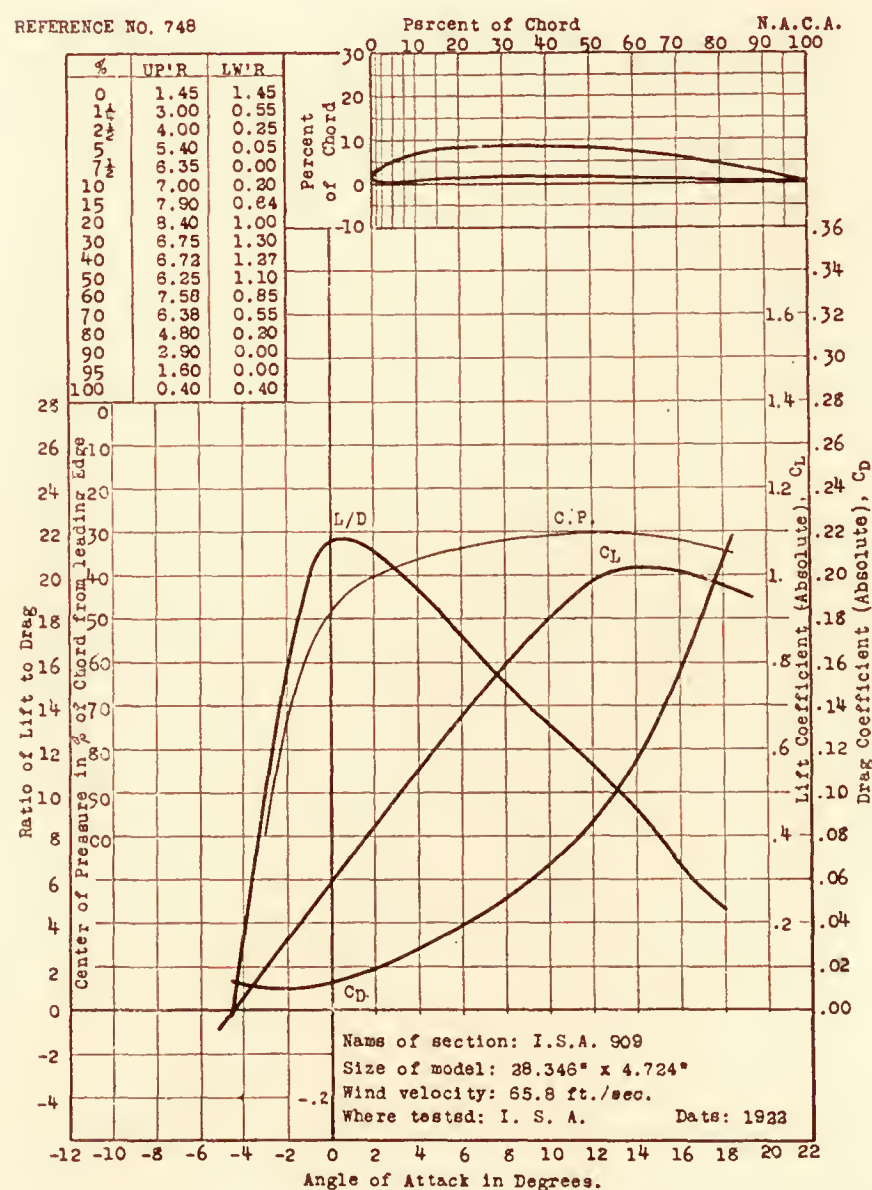
REFERENCE NO. 744



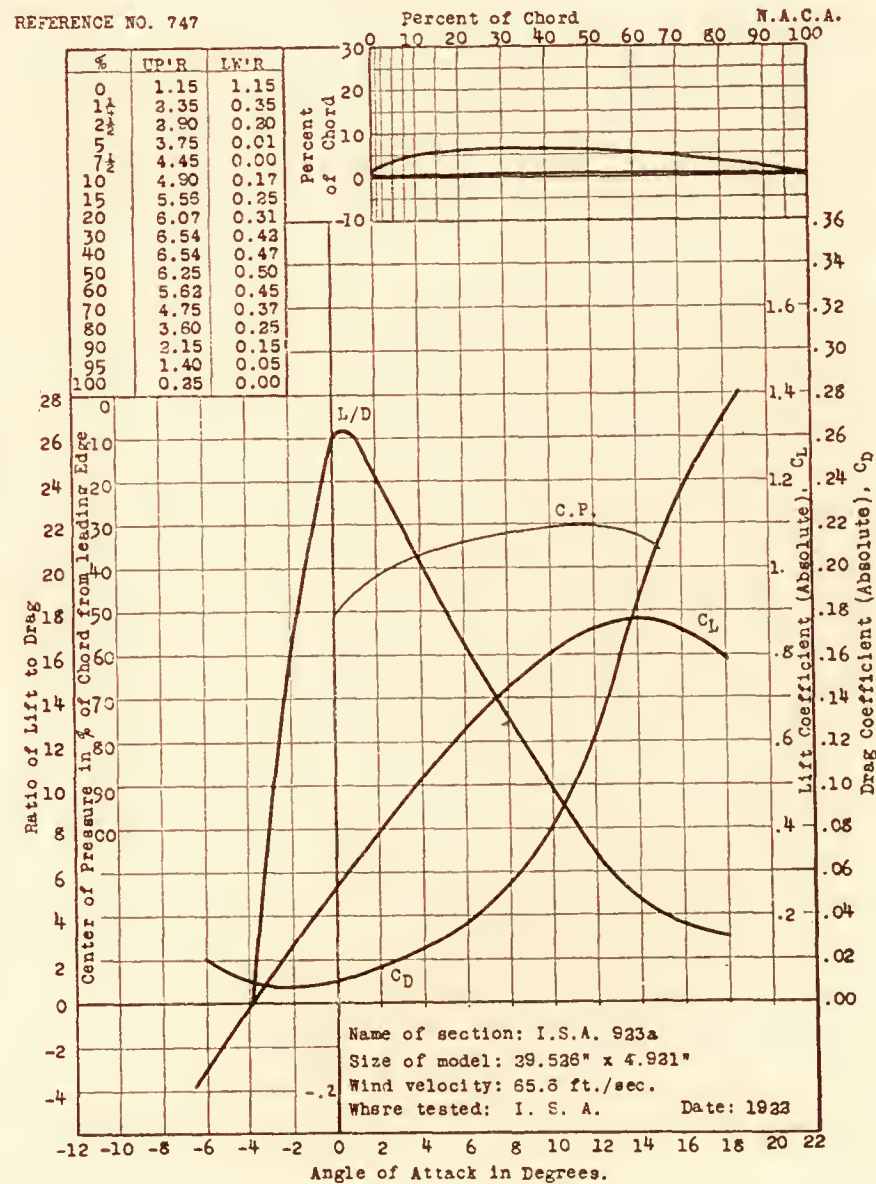
REFERENCE NO. 745



REFERENCE NO. 748

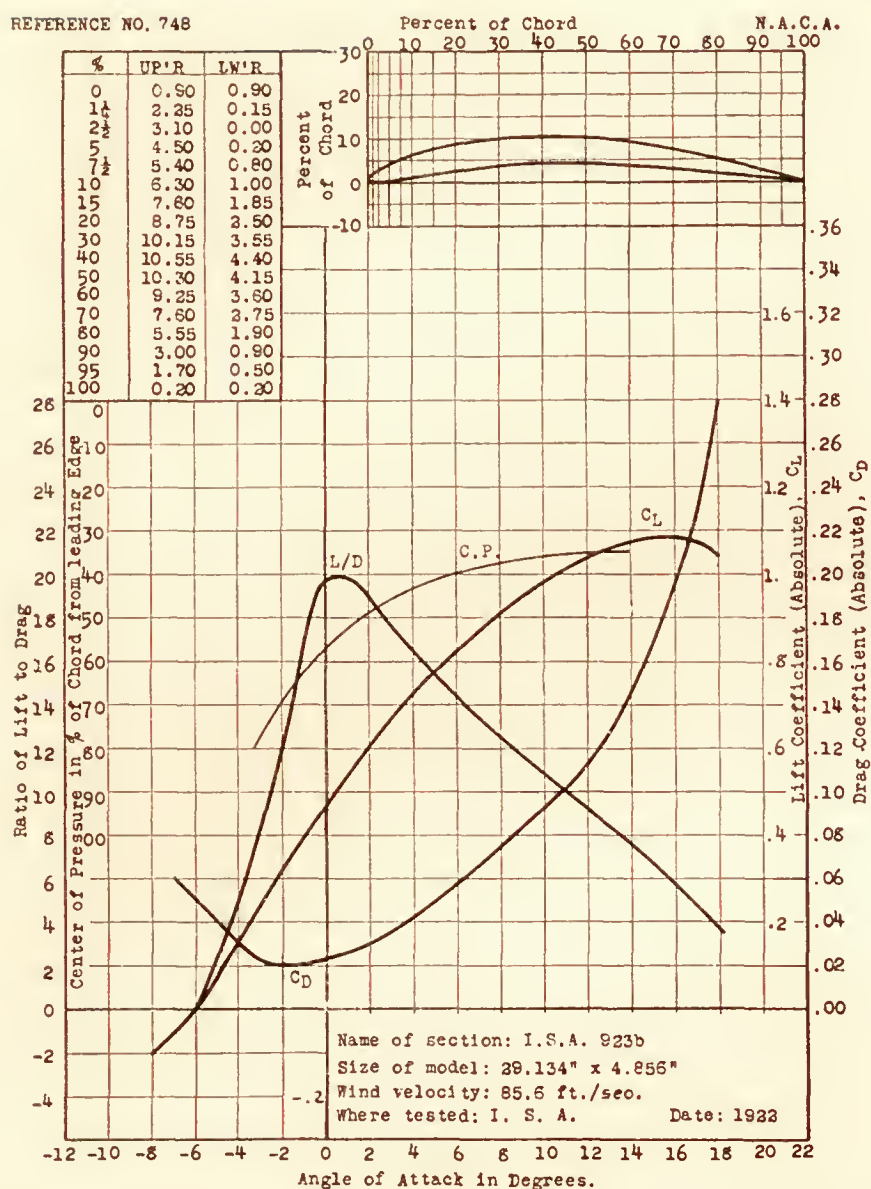


REFERENCE NO. 747

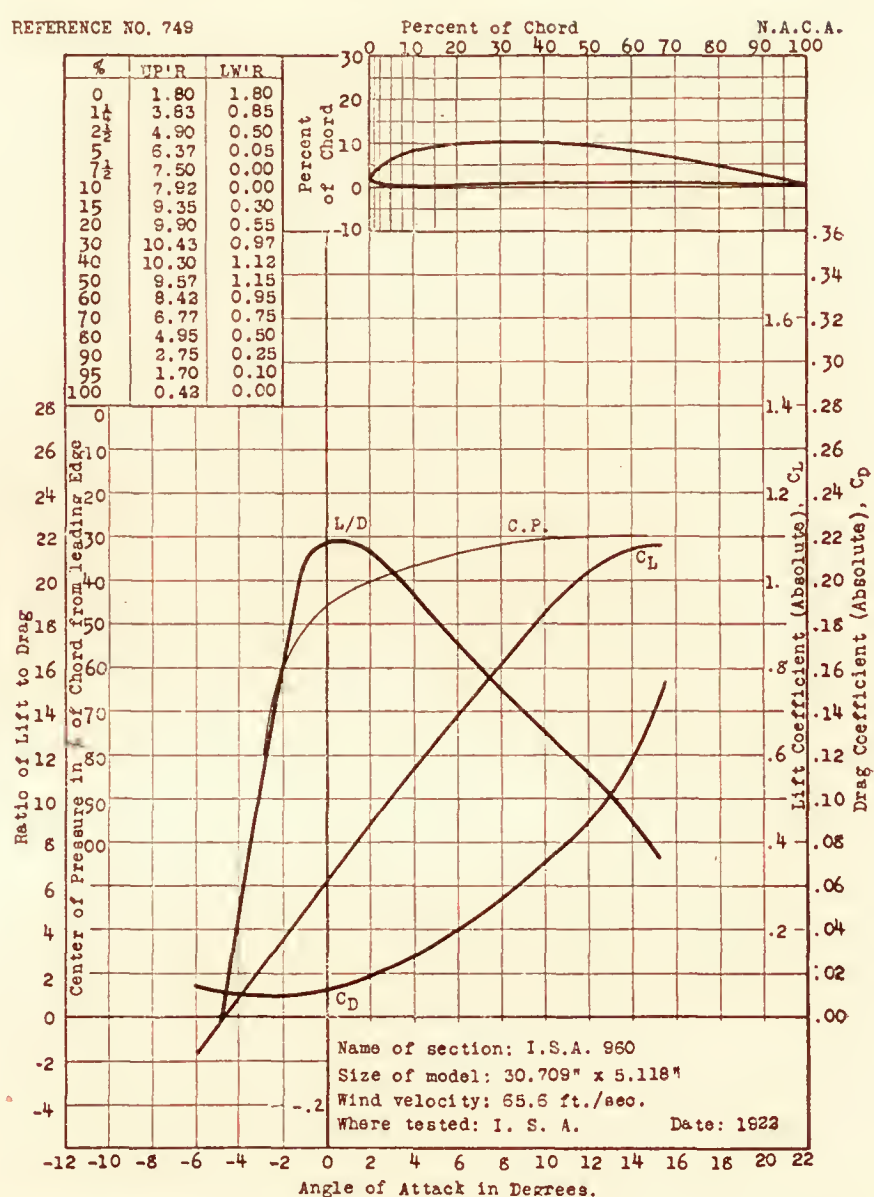




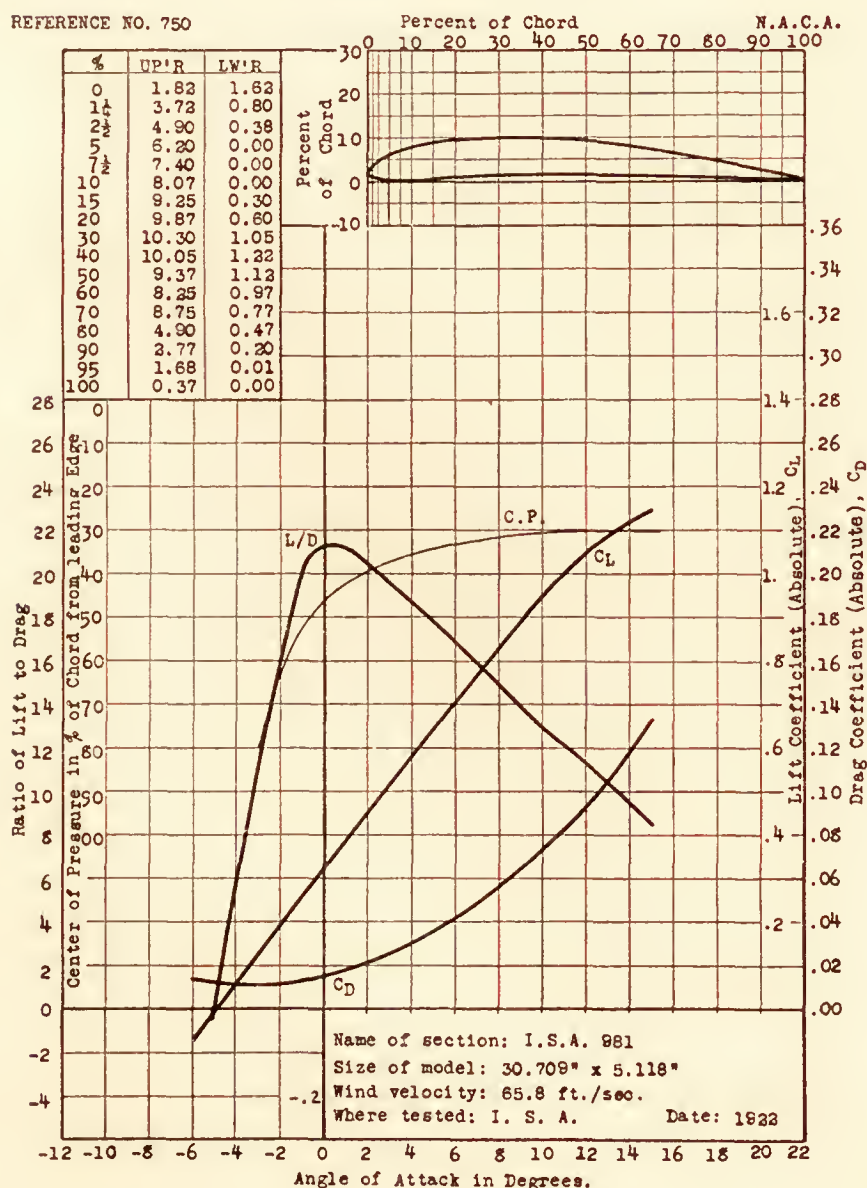
REFERENCE NO. 748



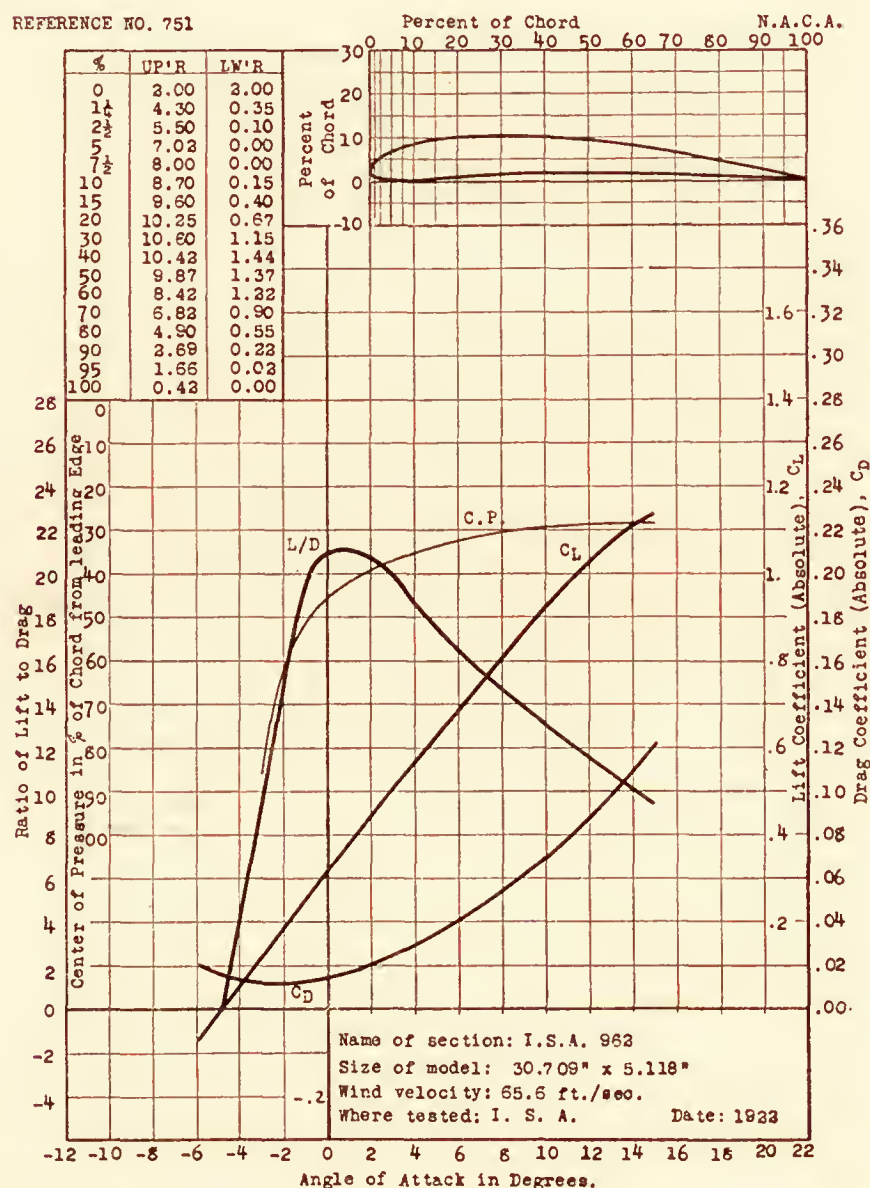
REFERENCE NO. 749



REFERENCE NO. 750

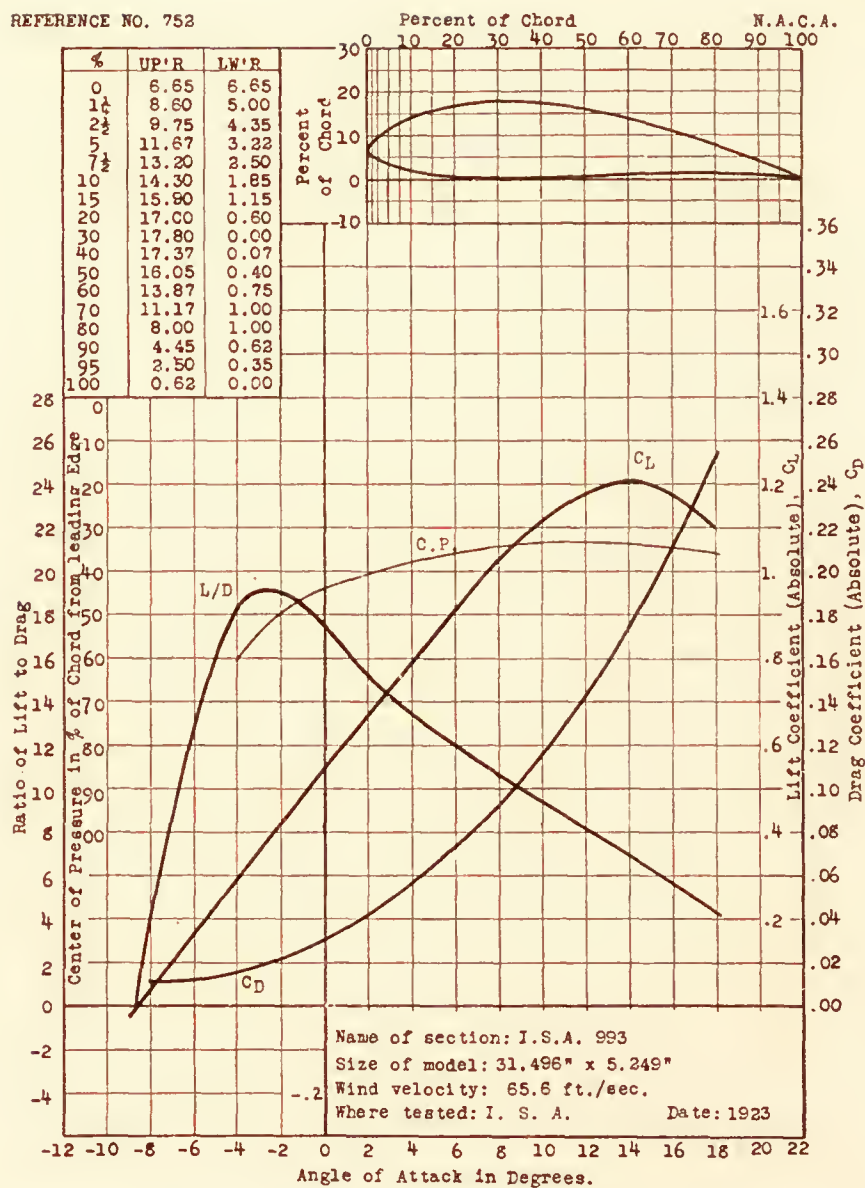


REFERENCE NO. 751

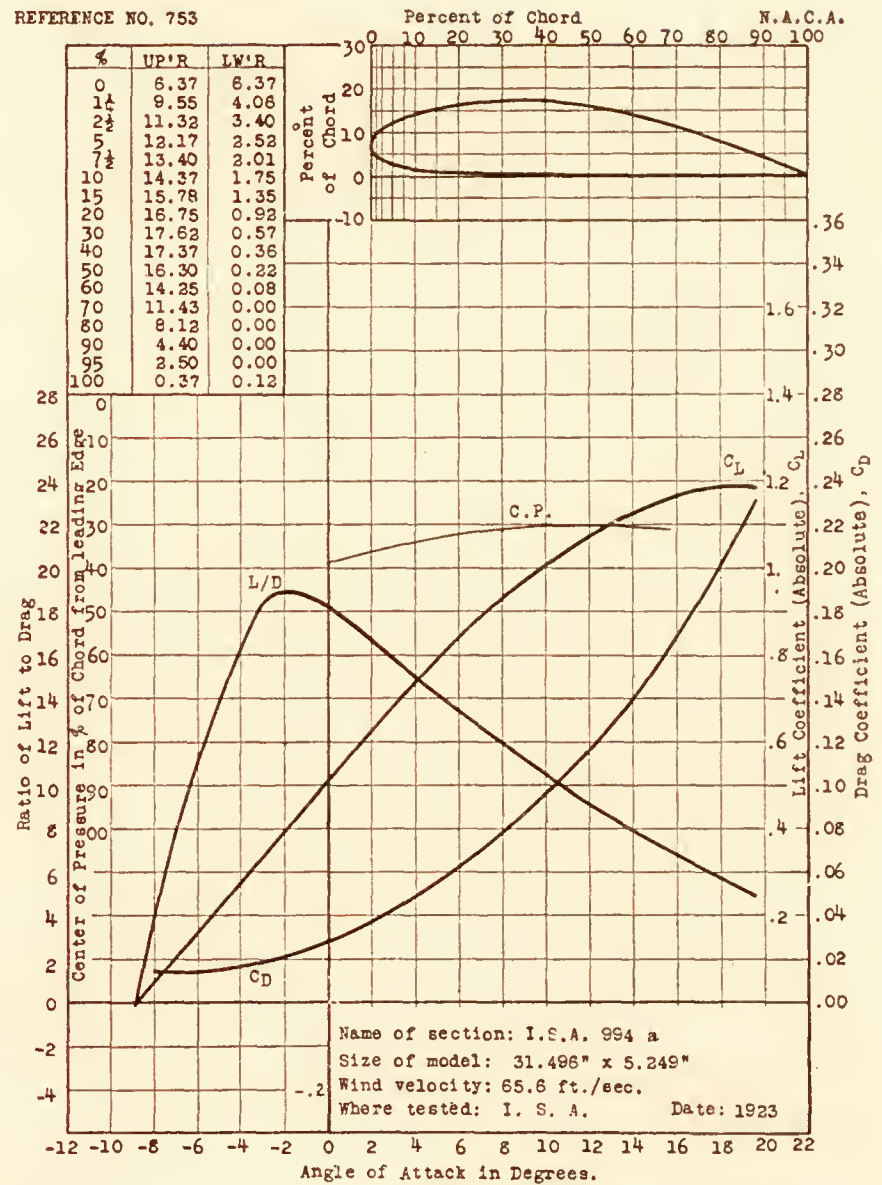




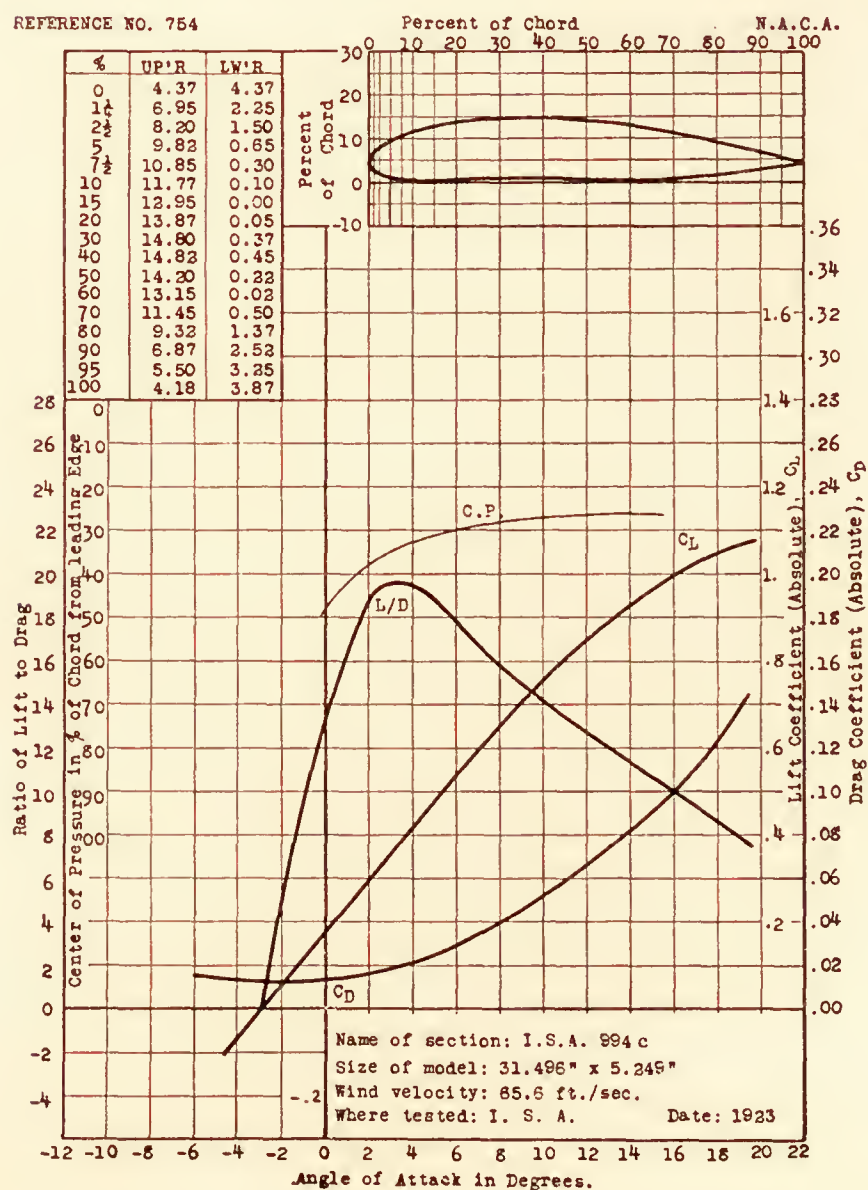
REFERENCE NO. 752



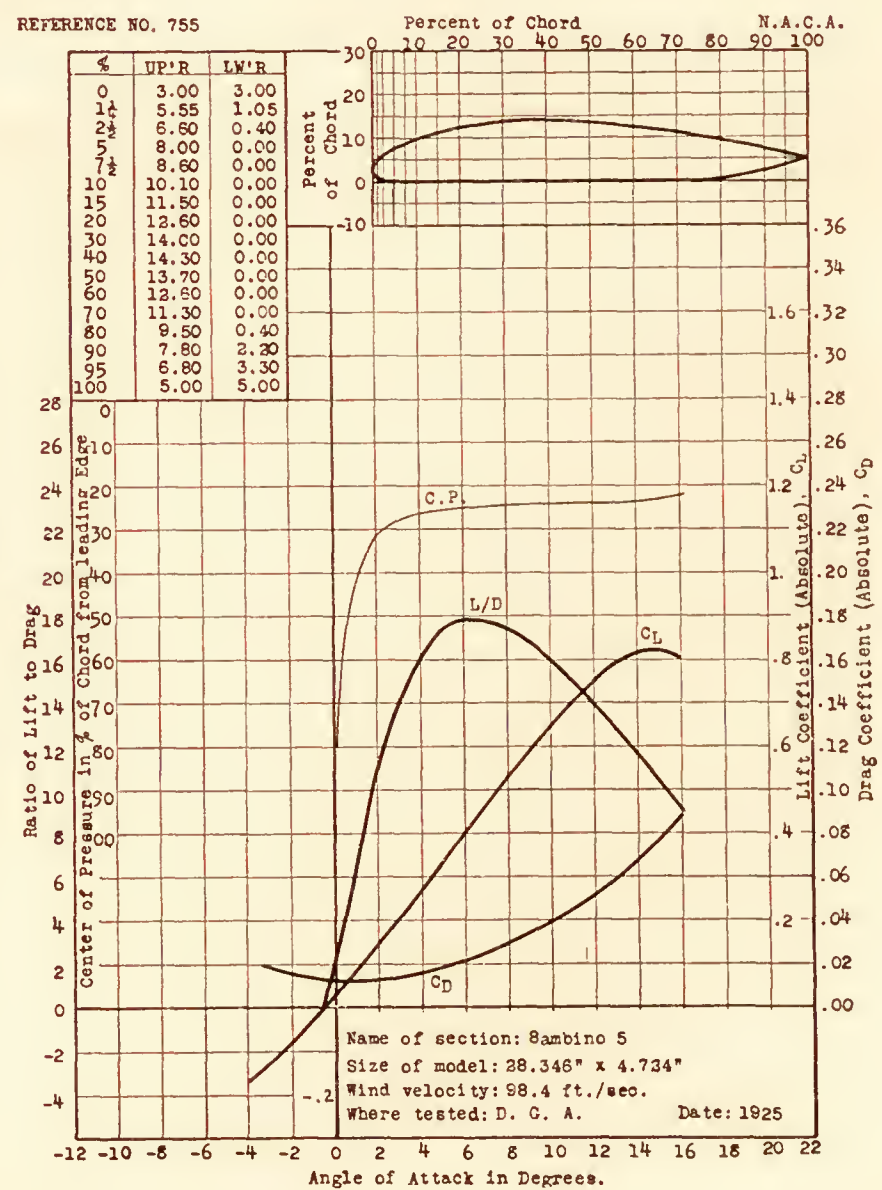
REFERENCE NO. 753



REFERENCE NO. 754

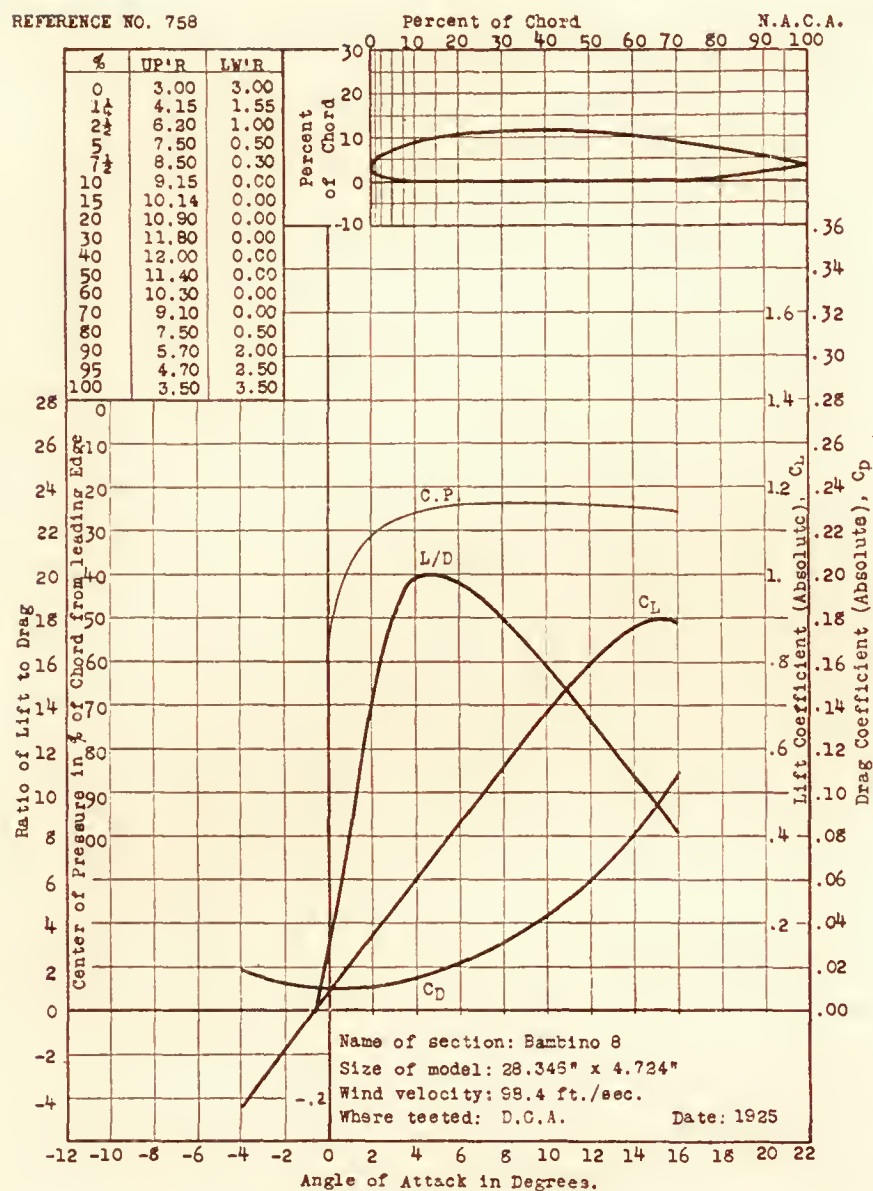


REFERENCE NO. 755

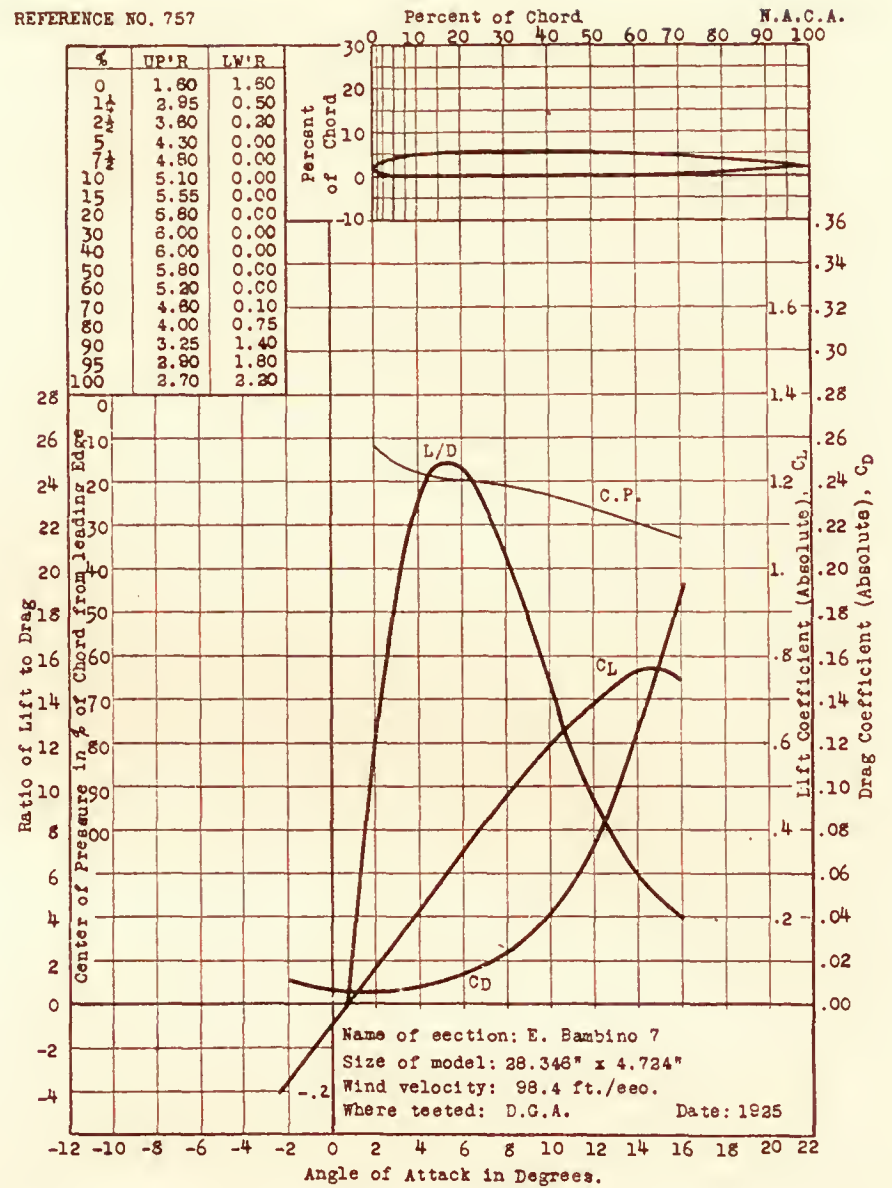




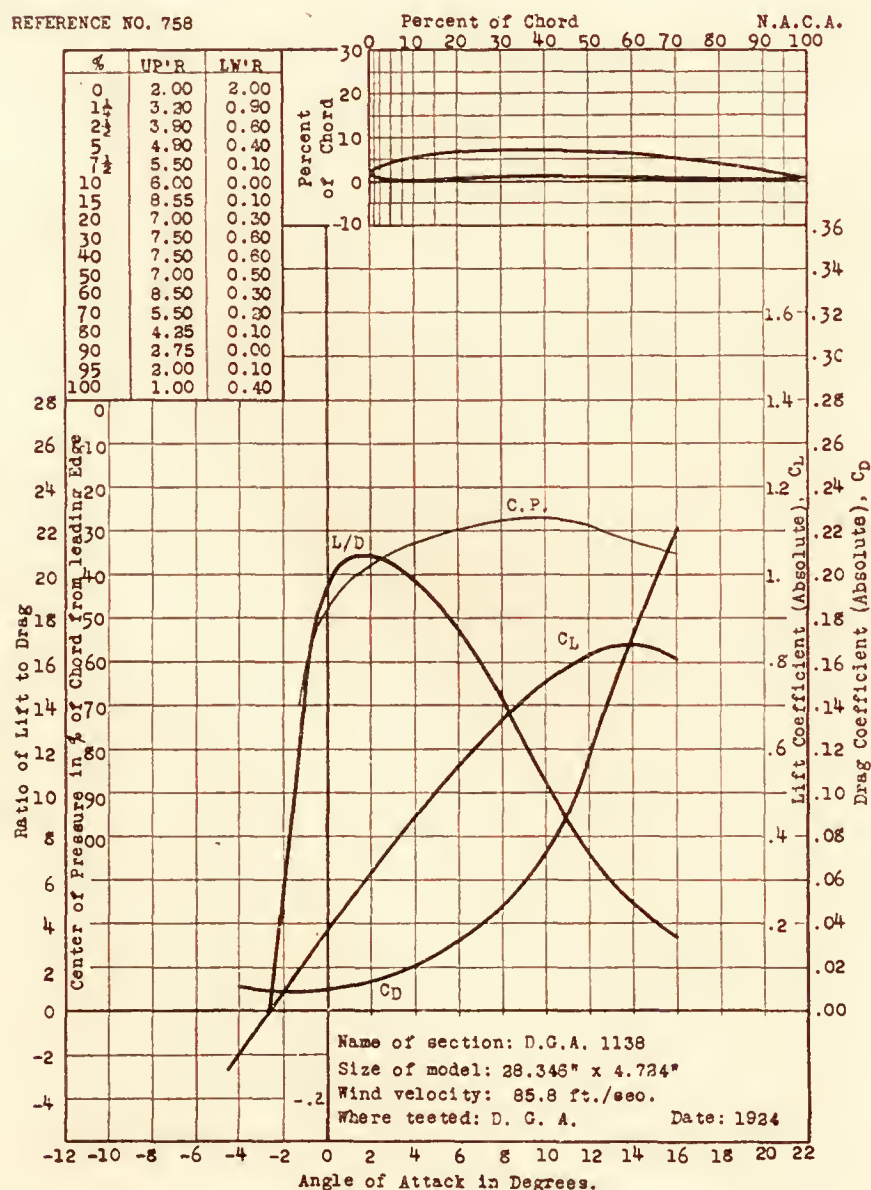
REFERENCE NO. 758



REFERENCE NO. 757



REFERENCE NO. 758



REFERENCE NO. 759

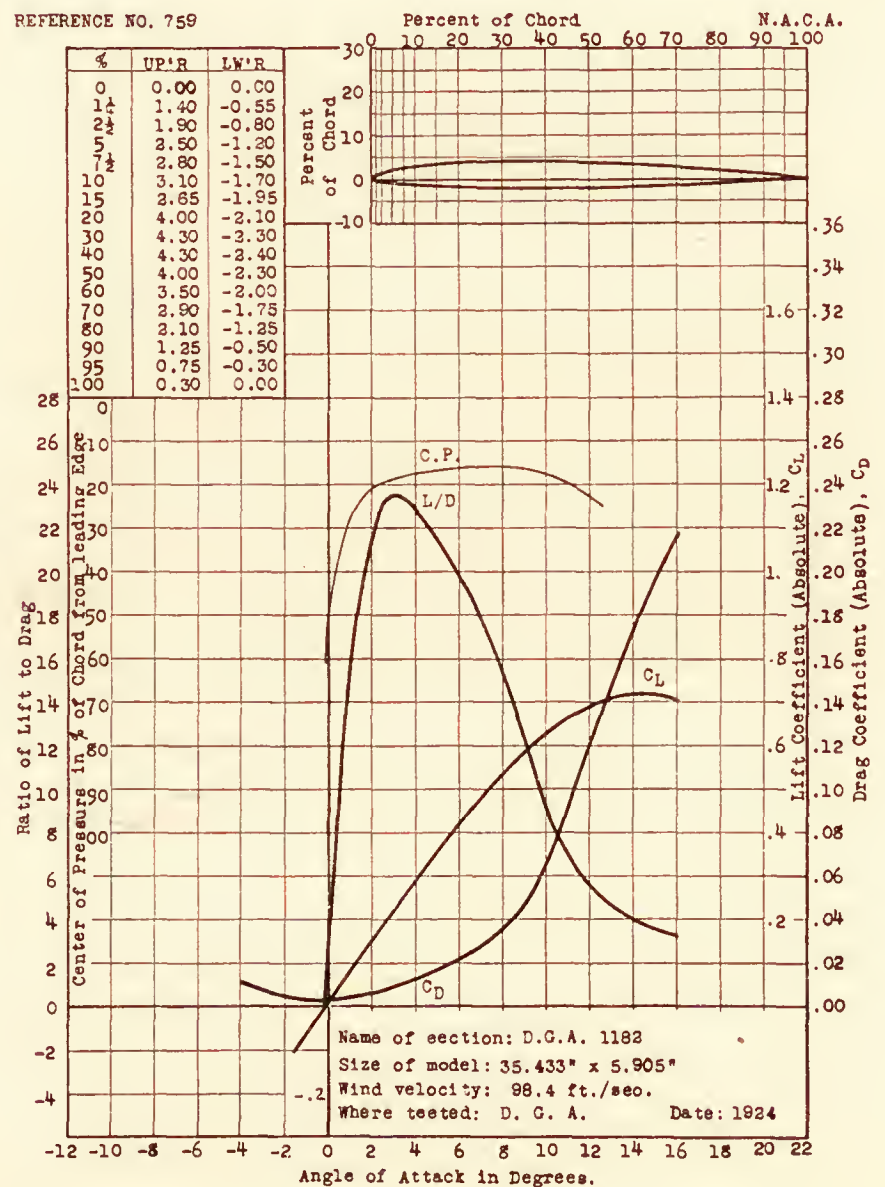
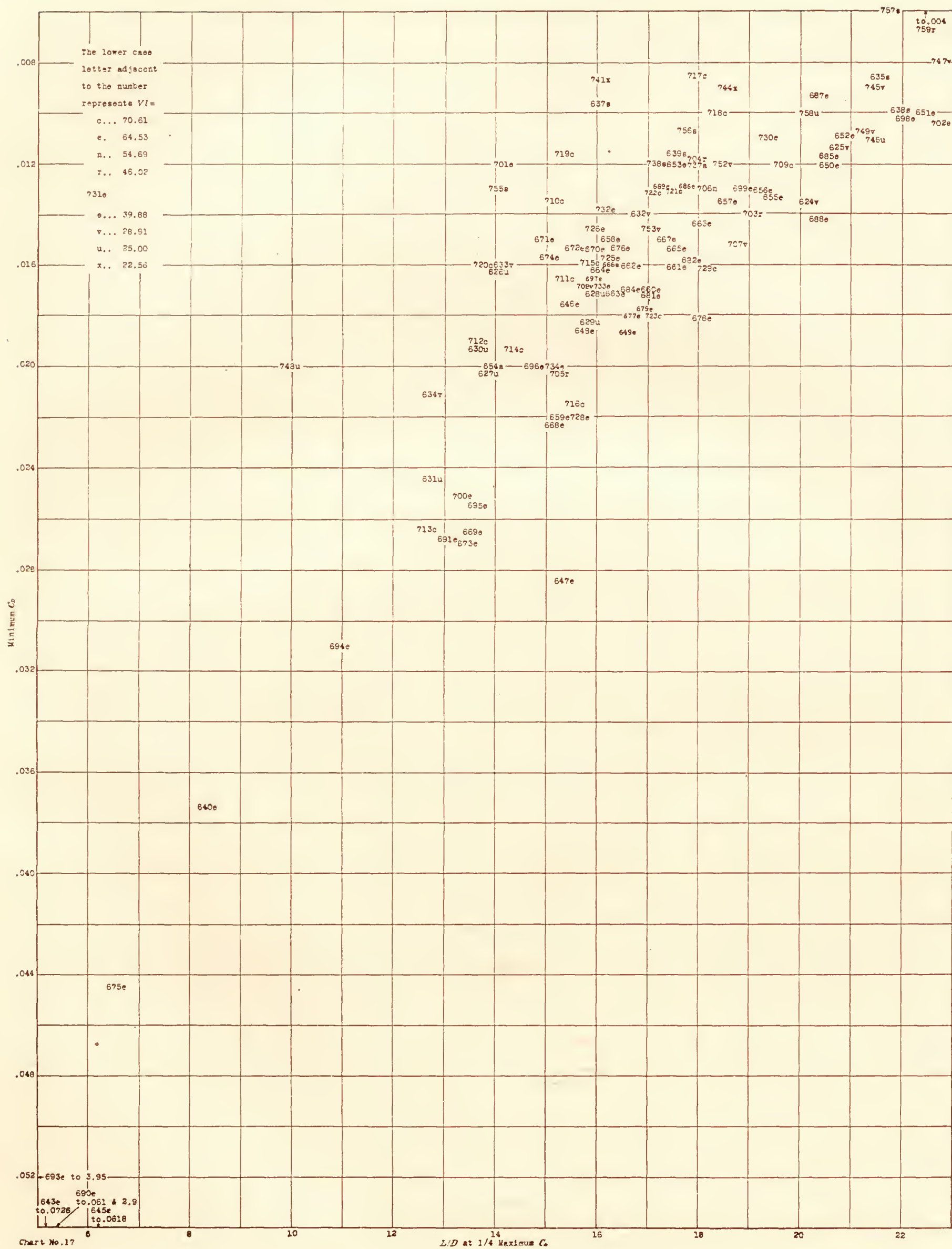




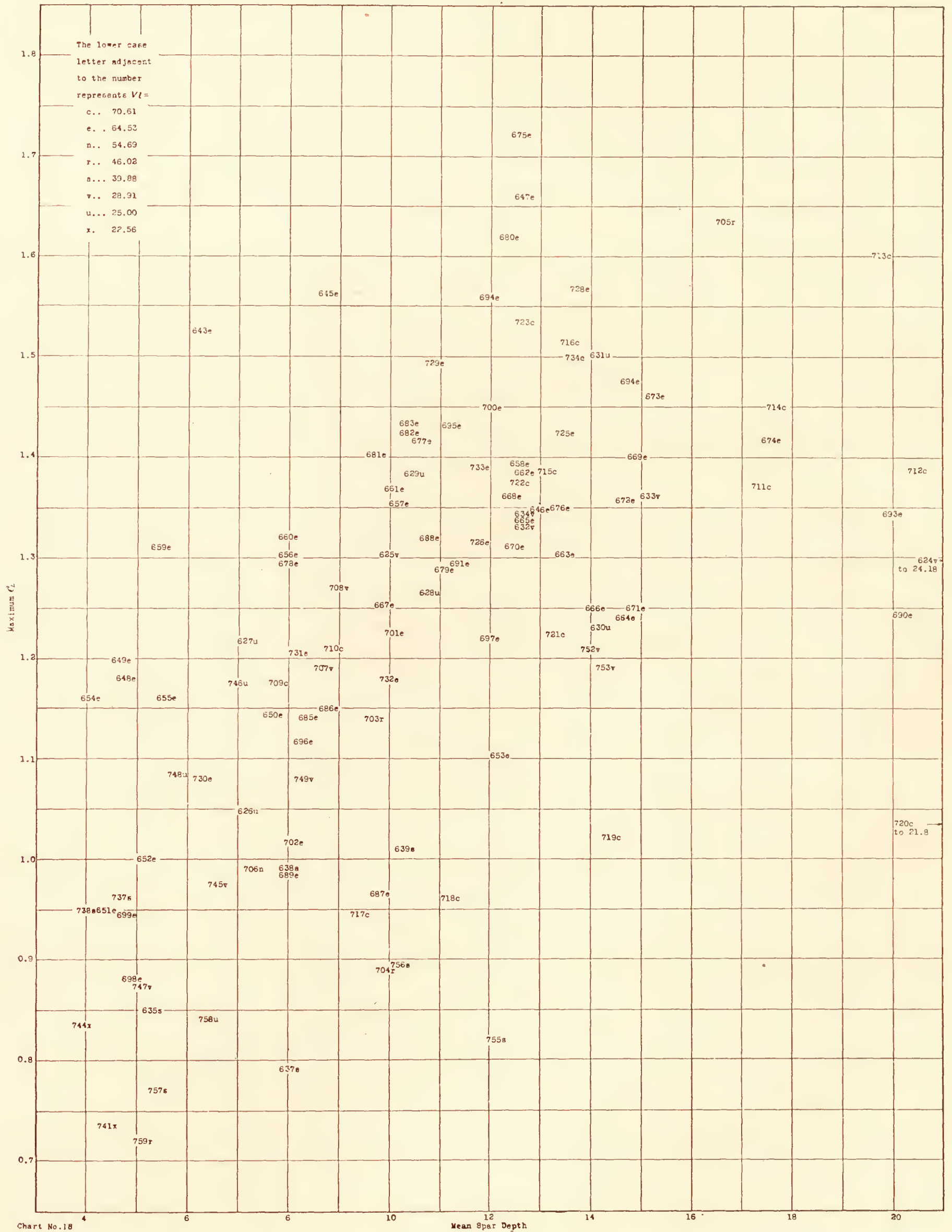
TABLE OF ORDINATES NOT GIVEN ON INDIVIDUAL CHARACTERISTIC SHEETS

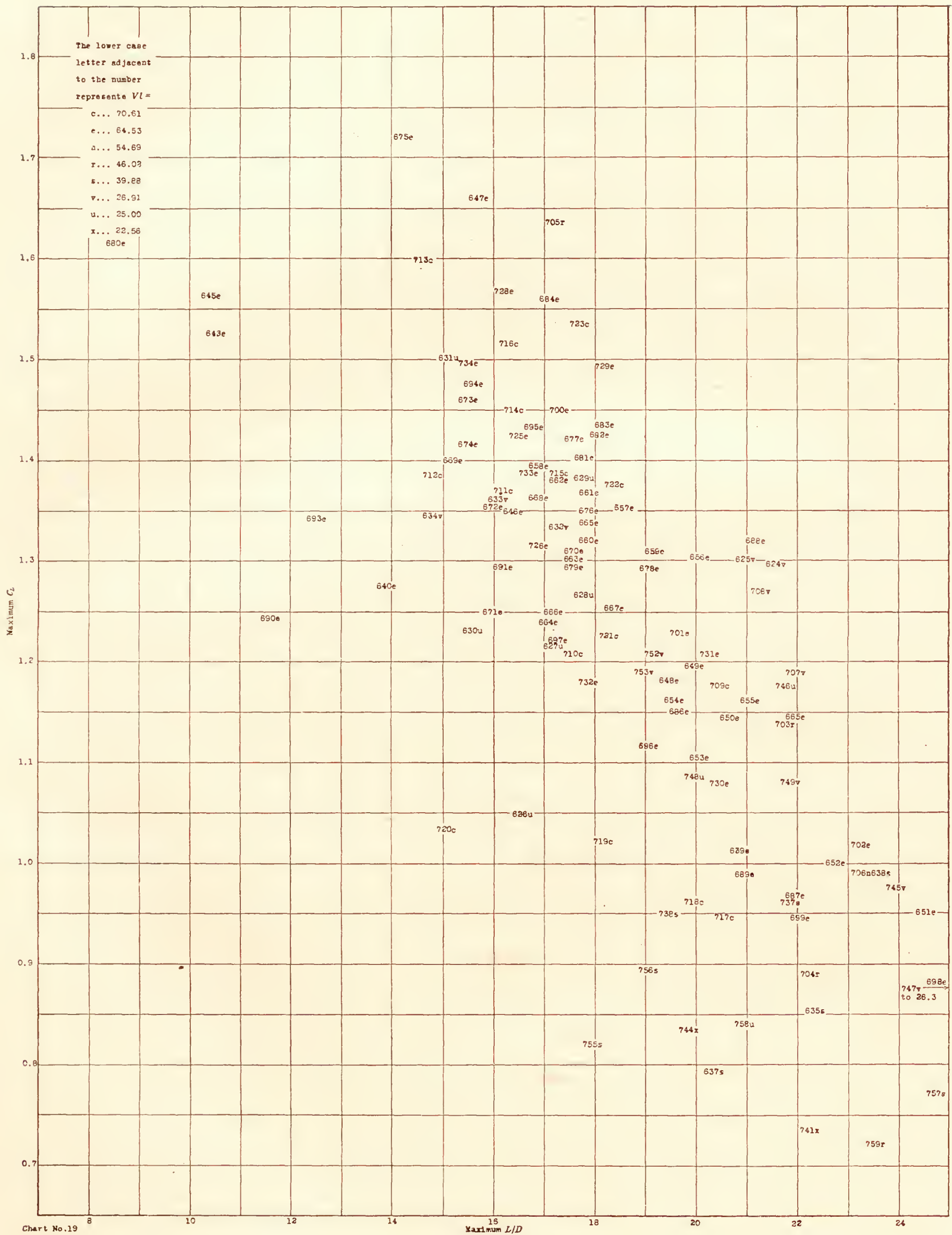
*Ordinates for dotted section, at tip, where ratio of ordinate to chord differs from that of section at center of span*      *Additional ordinates required to give camber at stations, not given on individual characteristic sheets*

Stations in per cent of chord	Reference 624 N. A. C. A. 81J (tapered)		Stations in per cent of chord	Reference 626 B-2 (Modified M-80)		Stations in per cent of chord	Reference 627 C-2 (Modified M-80)	
	Upper	Lower		Upper	Lower		Upper	Lower
0-----	3. 06	3. 06	8.95-----		0. 00			0. 00
1.25-----	3. 94	2. 00	12.70-----	7. 36			7. 38	
2.50-----	4. 28	1. 66	22.50-----	8. 28			8. 58	0. 78
5.00-----	4. 74	1. 24	25.00-----	8. 96	0. 78		8. 92	0. 98
7.50-----	5. 06	0. 91	35.00-----	8. 70	1. 06		8. 82	1. 12
10-----	5. 31	0. 68	45.00-----	8. 40			8. 20	
15-----	5. 61	0. 35	74.50-----		0. 02			0. 00
20-----	5. 79	0. 17	98.00-----				1. 30	0. 40
30-----	5. 76	0. 02	99.00-----				1. 10	0. 60
40-----	5. 41	0. 01						
50-----	4. 81	0. 11						
60-----	4. 05	0. 23						
70-----	3. 15	0. 34						
80-----	2. 17	0. 37						
90-----	1. 11	0. 25						
95-----	0. 58	0. 13						
100-----	0. 00	0. 00						

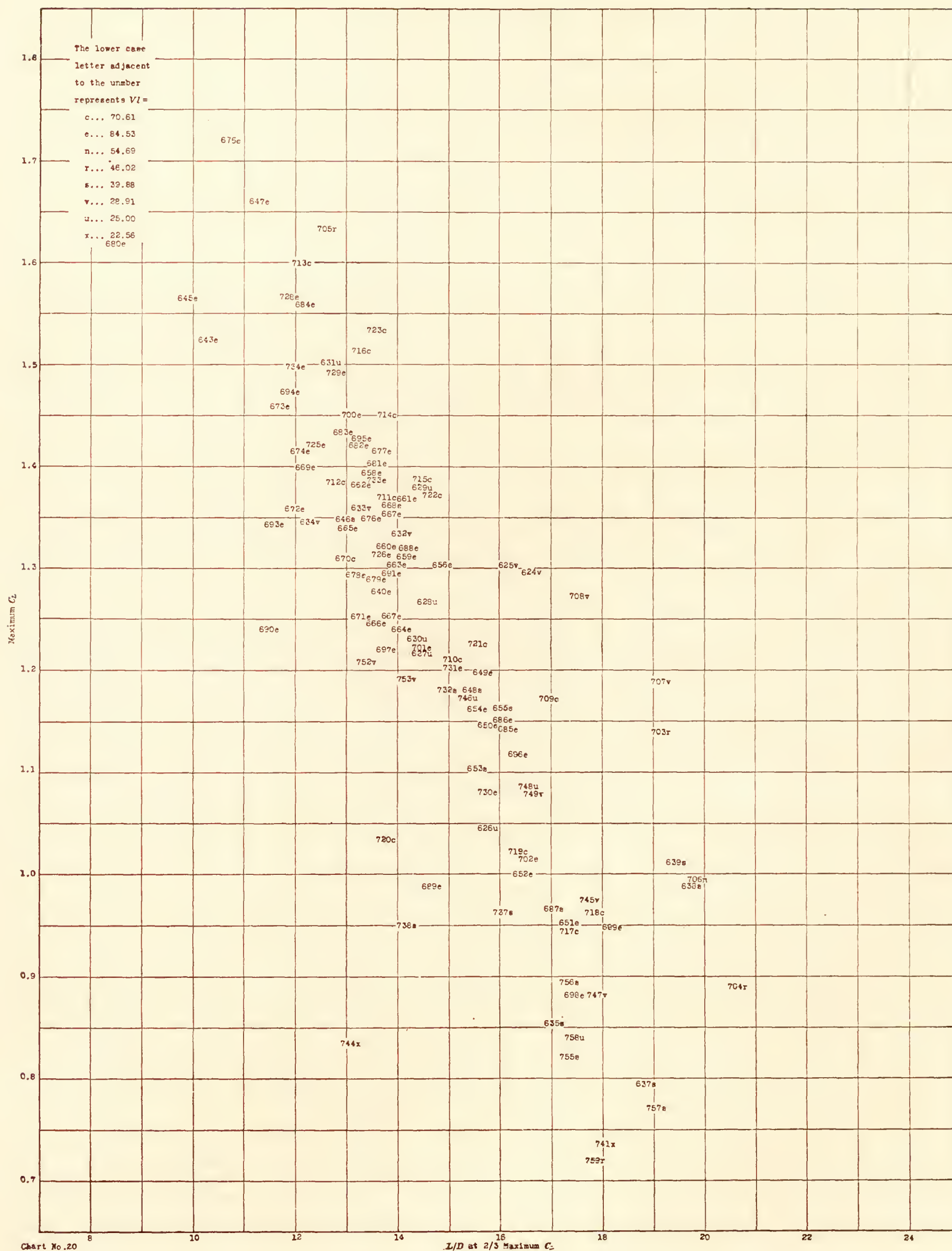
















---

# REPORT No. 287

---

## THEORIES OF FLOW SIMILITUDE

By A. F. ZAHM  
Aerodynamical Laboratory, Bureau of Construction  
and Repair, U. S. Navy





# REPORT No. 287

## THEORIES OF FLOW SIMILITUDE

By A. F. ZAHM

### SUMMARY

The laws of comparison of dynamically similar fluid motions are derived by three different methods based on the same principle and yielding the same or equivalent formulas. In this report prepared for publication by the National Advisory Committee for Aeronautics, in June, 1927, are outlined the three current methods of comparing dynamically similar motions, more especially of fluids, initiated respectively by Newton, Stokes (or Helmholtz), and Rayleigh. These three methods, viz., the integral, the differential, and the dimensional, are enough alike to be studied profitably together. They will presently be treated in succession then compared.

### INTRODUCTION

*Geometrically similar figures.*—If two figures are geometrically similar, they have a constant scale ratio

$$l/l_1 = a \text{-----} (1)$$

where  $l, l_1$  are any two homologous lengths. If  $x, x_1$  etc., are homologous point coordinates for the figures,  $x/x_1 = y/y_1 = z/z_1 = a$ .

*Geometrically similar motions.*—Two similar configurations perform geometrically similar motions when their homologous points trace similar paths in proportional times; that is, in times  $t, t_1$  having any arbitrary ratio  $b$ , the same for all homologous path segments. Thus  $v, v_1$  being corresponding path speeds,

$$t/t_1 = b \quad v/v_1 = lt_1/l_1t = a/b \quad \dot{v}/\dot{v}_1 = lt_1^2/l_1t^2 = l_1v^2/lv_1^2 = a/b^2 \text{-----} (2)$$

where  $l/l_1$  is the scale ratio of homologous moving parts, path segments, radii of curvature, etc. Since by (2) the ratio  $l_1v^2/lv_1^2$  of accelerations normal to the path elements equals  $\dot{v}/\dot{v}_1$  along them, the resultant accelerations,  $j, j_1$  bear the same ratio and are alike directed. The constant ratios  $l/l_1, t/t_1, v/v_1, \dot{v}/\dot{v}_1$  all may be different; only two can be independent, as (2) shows.<sup>1</sup>

*Dynamically similar systems.*—Let the homologous elements of two similar configurations in similar motion be masses  $m, m_1$  having the constant ratio

$$m/m_1 = c = \rho l^3/\rho_1 l_1^3 \text{-----} (3)$$

$\rho, \rho_1$  being their densities; then, to keep their motions similar, all corresponding impressed forces must be in constant ratio and like direction.<sup>2</sup> For since these elements have resultant accelerations  $j, j_1 \propto v^2/l, v_1^2/l_1$ , their resultant impressed forces  $R, R_1$  have the ratio

$$R/R_1 = mj/m_1j_1 = \rho l^2v^2/\rho_1 l_1^2v_1^2 \text{-----} (4)$$

which is constant throughout, since  $\rho/\rho_1, l/l_1, v/v_1$  are so. Further, the accelerations  $j, j_1$  are alike directed; so then must be  $R, R_1$ . So, too, the corresponding forces on large homologous

<sup>1</sup> Were the paths similar irrespective of describing time, the motions still would be geometrically similar, but not as defined here and in usual writings on similitude. The geometrically similar motions here treated are kinematically similar because they trace similar paths in proportional times.

<sup>2</sup> That is, their magnitudes are in constant ratio and their lines of action similarly located in the two systems, though the systems themselves may be neither simultaneous nor alike oriented in space.

parts must be in constant ratio and like direction, as appears on compounding those on their constituent elements.<sup>3</sup> Also by the argument for (4) the constituents  $P$ ,  $Q$ ,  $P_1$ ,  $Q_1$ , etc., of  $R$ ,  $R_1$ , such as weight, pressure, friction, etc., must be in constant ratio and like direction, viz,  $P$  to  $P_1$ ,  $Q$  to  $Q_1$ , etc. In fact for homologous elements they are concurrent and have similar force polygons. Hence

$$R/R_1 = \rho l^2 v^2 / \rho_1 l_1^2 v_1^2 = P/P_1 = Q/Q_1 = \text{etc.} \quad (4_1)$$

Such systems are dynamically similar and have (1), (2), (4) as their conditions or criteria of similarity.

By (4) when  $\rho/\rho_1$ ,  $l/l_1$ ,  $v/v_1$  are assumed constant  $R/R_1$  is found constant. So, too, if  $\rho/\rho_1$ ,  $l/l_1$ ,  $R/R_1$  are constant,  $v/v_1$  is constant, and the motions are similar. Fixing either three of these ratios determines the fourth. Thus, premised initial similarity, similar mass systems in similar motion are similarly forced; conversely similar mobile mass systems similarly forced similarly move. In either case the systems are dynamically similar.

*Summation of impressed forces.*—The resultant forces  $R$ ,  $R_1$  at homologous elements have the components

$$\left. \begin{aligned} m j_x &= P_x + Q_x + \text{etc.} \\ m_1 j_{1x} &= P_{1x} + Q_{1x} + \text{etc.} \end{aligned} \right\} \quad (5)$$

with like values for the  $y$ ,  $z$  directions. These equations may be compared with (17), where the magnitudes of  $P$ ,  $Q$ , etc., not merely their ratios, have definite expression; also with (13), where the magnitudes have only proportionate expression.

## DYNAMICALLY SIMILAR FLOWS

### A) NEWTONIAN OR INTEGRAL METHOD

*Definition.*—Fluid streams that everywhere satisfy (1), (2), (4) are dynamically similar systems, with similar flow fields and boundaries; hence are comparable in their corresponding characteristics.

*Classification of chief force ratios.*—As before, the ratio of the acceleration forces on homologous parts of such systems must be the same throughout and must equal severally the ratios of the corresponding impressed forces. The following table exhibits the chief ratios of present interest. Their proof follows the table. For all homologous elements the ratios  $g/g_1$ ,  $\rho/\rho_1$ ,  $\mu/\mu_1$  are assumed constant,  $\mu$  denoting viscosity.

TABLE I  
RATIO OF CORRESPONDING FORCES ON HOMOLOGOUS FLUID ELEMENTS

Ratio of acceleration forces $m j / m_1 j_1$	Ratio of impressed forces		
	Gravitational $mg/m_1 g_1$	Pressural, $l^3 \frac{\partial p}{\partial l} / l_1^3 \frac{\partial p_1}{\partial l_1}$	Viscous $\mu \partial v / \partial l = \mu_1 \partial v_1 / \partial l_1$
$\rho l^2 v^2 / \rho_1 l_1^2 v_1^2$	$g \rho l^3 / g_1 \rho_1 l_1^3$	$\left\{ \begin{aligned} &\rho l^2 v^2 / \rho_1 l_1^2 v_1^2, \text{ for incompressible fluid} \\ &\kappa l^2 / \kappa_1 l_1^2, \text{ for elastic fluid} \end{aligned} \right.$	$\mu l v / \mu_1 l_1 v_1$

*Proof of force ratios.*—The ratio in column 1 has been proved; that in column 2 is obviously true.

To prove column 3, the pressure force on any small volume of frictionless fluid, being proportional to volume times along-stream pressure gradient, varies as  $l^3 \cdot \partial p / \partial l$ , as is well known, where  $\partial p / \partial l \propto \partial(\rho v^2) / \partial l$ . Hence for  $\rho$  constant the resultant pressure force varies as  $\rho l^2 v^2$ ; and for  $\rho$  variable  $\partial p / \partial l = \kappa / \rho \cdot \partial \rho / \partial l$ , by hydrostatics; that is, the pressure force varies as  $\kappa l^2$ , where  $\kappa$  is the bulk modulus. One recalls that  $\kappa / \kappa_1 = \rho c^2 / \rho_1 c_1^2$  where  $c$ ,  $c_1$  are the speeds of sound in the fluids under the actual working conditions.

<sup>3</sup> Newton, reference 1, proves this theorem verbally without using symbols. A different symbolic treatment is given by Sir Richard Glazebrook in reference 2.



If  $\partial v/\partial l$  is the rate of distortion in any fluid element, the entailed force on it varies as  $l^2 \cdot \mu \partial v/\partial l \propto \mu l v$ ; hence the ratio in column 4.

*Examples of similar flow conditions.*—Granted kinematic similarity, when the impressed forces are as in Table I the general conditions (4<sub>1</sub>) for dynamic similarity are

$$\frac{\rho l^2 v^2}{\rho_1 l_1^2 v_1^2} = \frac{g \rho l^3}{g_1 \rho_1 l_1^3} = \frac{\mu l v}{\mu_1 l_1 v_1} = \begin{cases} \rho l^2 v^2 / \rho_1 l_1^2 v_1^2, & \text{for incompressible fluids} \\ \kappa l^2 / \kappa_1 l_1^2, & \text{for elastic fluids} \end{cases} \quad (6)$$

where only the ratios of predominant forces are to be retained. A few examples will illustrate.

(α) Thus, if weight is the only dominant impressed force, the motions are dynamically similar when the first ratio in (6) equals the second, viz, when

$$g l / v^2 = g_1 l_1 / v_1^2 \quad (7)$$

which is the well-known Reech and Froude “law of corresponding speeds.”

(β) If weight and elasticity are negligible, the first ratio in (6) is equated to the third, giving

$$\frac{v}{l v} = \frac{v_1}{l_1 v_1} \quad (8)$$

which is the familiar Reynolds’s condition for similarity of motion of fluids. It applies to the motion of airships, submarines, skin friction planes, fluids in pipes, etc.

(γ) If there is considerable compression, while gravity and friction are negligible, the first term is equated to the lower fourth, giving

$$\frac{c}{v} = \frac{c_1}{v_1} \quad (9)$$

which is Booth and Bairstow’s condition for similarity.

(δ) If  $g$ ,  $\mu$ ,  $c$  all are important, conditions (7), (8), (9) must coexist; if all are negligible, (6) gives  $\rho l^2 v^2 / \rho_1 l_1^2 v_1^2 = \rho l^2 v^2 / \rho_1 l_1^2 v_1^2$ , that is, all flows with similar boundaries are similar, whatever the densities and velocities.<sup>4</sup>

*Reactions in similar flows.*—If  $P$ ,  $P_1$  are corresponding reactions of a craft and its model under conditions (7),  $P/P_1 = g \rho l^3 / g_1 \rho_1 l_1^3$ , whence

$$P = N_1 g \rho l^3 \quad (10)$$

where  $N_1 = P_1 / g_1 \rho_1 l_1^3$  is a dimensionless coefficient, say, given by model tests.

If  $g$ ,  $\kappa$  are negligible, conditions (8) obtain, and  $P/P_1 = \mu l v / \mu_1 l_1 v_1$ , or  $P/P_1 = \rho l^2 v^2 / \rho_1 l_1^2 v_1^2$ , whence

$$P = N_2 \mu l v, \text{ or } P = C \rho l^2 v^2 \quad (11)$$

where  $N_2 = P_1 / \mu_1 l_1 v_1$ ,  $C = P_1 / \rho_1 l_1^2 v_1^2$ , both dimensionless coefficients.

If  $g$ ,  $\mu$  are negligible, and compression important,  $P/P_1 = \kappa l^2 / \kappa_1 l_1^2$ ; hence

$$P = N_3 \kappa l \quad (12)$$

where  $N_3 = P_1 / \kappa_1 l_1^2$ , and conditions (9) prevail.

Let the  $P$ s be all lifts or all drags or other like directed forces. Then, if  $g$ ,  $\mu$ ,  $\kappa$  all are important together, the total of such reactions on the craft is

$$R = N_1 g \rho l^3 + N_2 \mu l v + N_3 \rho c^2 l^2 = \rho l^2 v^2 f(g l / v^2, v / l v, c / v) \equiv N \rho l^2 v^2 \quad (13)$$

got by summing (10), (11), (12), using  $\kappa = \rho c^2$ , then factoring off  $\rho l^2 v^2$ . One notes that (13) can be written: Total reaction = gravitational + frictional + pressural.

The validity of (13) was premised on dynamic similarity of motion of the craft and its model, as defined by the simultaneous conditions (7), (8), (9). That is,

$$N_1 g l / v^2 + N_2 v / l v + N_3 c^2 / v^2 = f(g l / v^2, v / l v, c / v) = f(g_1 l_1 / v_1^2, v_1 / l_1 v_1, c_1 / v_1) = N \quad (14)$$

<sup>4</sup> (7) has the alternative form  $g/j = g_1/j_1$ ; (8) the alternative  $f/p = f_1/p_1$ , where  $f$ ,  $p$ ,  $p_1$  are corresponding frictions and pressures per unit area of homologous surface elements  $\delta S$ ,  $\delta S_1$ . With  $f$ ,  $f_1 \perp$  to  $p$ ,  $p_1$  the resultant stresses have slopes  $f/p$ ,  $f_1/p_1$  to the normals at  $\delta S$ ,  $\delta S_1$ . The “laws” (7), (8) (9) are but corollaries of (6) or (4<sub>1</sub>).

<sup>5</sup> More conventionally one writes  $R = \rho l^2 v^2 f_1(v^2/g l, v/l v, v/c)$ .

Alternatively (13) can be written

$$R = \mu l v f'(gl/v^2, \nu/lv, c/v) = N' \mu l v \text{-----} (13_1)$$

found by factoring off  $\mu l v$  and rearranging the result.

Writers sometimes say (13) shows that  $R$  varies as  $\rho l^2 v^2$ ; they can as well say  $R \propto \mu l v$  by (13<sub>1</sub>). The first statement is true for conditions making  $f$  constant; the second for  $f'$  constant. (Fig. 1.)

*Dynamic scale and scale effect.*—If  $N_1 (= P_1/g_1 \rho_1 l_1^3)$ , found from a model test; is plotted against  $g_1 l_1/v_1^2 (= gl/v^2)$  the graph is directly applicable to computing the full-scale reaction (10); similarly for the graph of  $N_2$  against  $\nu/lv$  and  $N_3$  against  $c/v$ .

In such plots the dimensionless argument, say,  $\nu/lv$ , is treated as a single independent variable. The graph is the same whether  $\nu$  varies alone or  $l$  alone or  $v$  alone, or if two or three vary together. If  $N_2$  varies as  $(lv/\nu)^n$ , it varies as  $l^n$ ,  $v^n$ ,  $\nu^{-n}$ . The effect, for instance, of varying  $l$  can be learned by varying  $v$  or  $\nu$  in the model test, and so for  $N_1$ ,  $N_3$ .

One calls the independent dimensionless argument  $gl/v^2$  the dynamic scale for the motion ( $\alpha$ ), and the variation of  $N_1$  with scale the scale effect. Similarly  $\nu/lv$  is the dynamic scale for

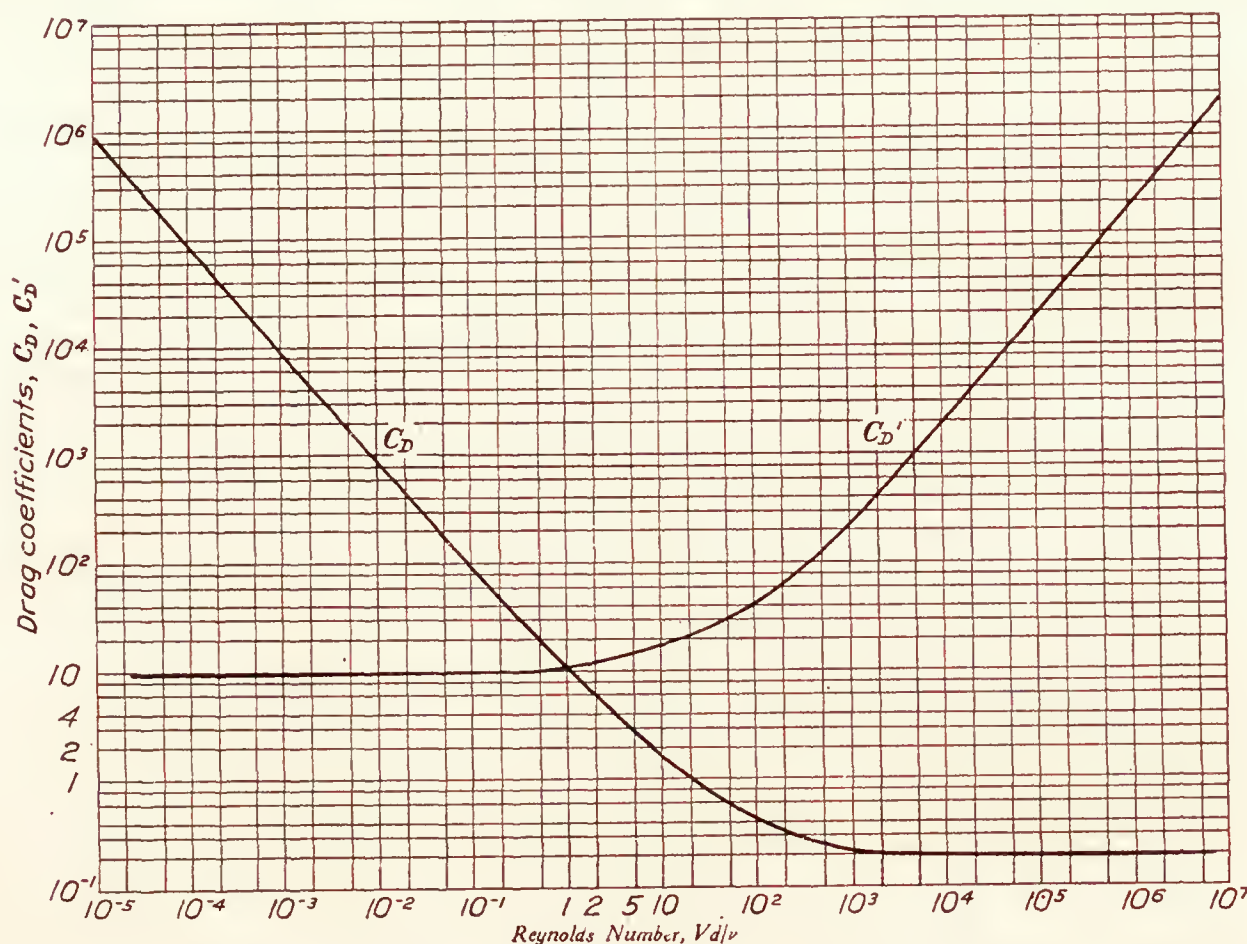


FIG. 1.—Drag coefficients  $C_D = D/\rho V^2 d^2$ ,  $C_D' = D/\mu V d$ , plotted against  $Vd/\nu$  for a sphere in uniform translation through a viscous fluid. Data given in N. A. C. A. Report No. 253. Either graph can be plotted from the other, since  $C_D'/C_D = Vd/\nu$ .

motion ( $\beta$ ), and  $l/c$  for ( $\gamma$ ). No doubt the term “scale effect” originally meant the effect of changing the linear scale ratio  $l/l_1$ , then was extended to mean the effect of changing some more complex argument, such as  $gl/v^2$ ,  $\nu/lv$ ,  $c/v$ , etc., now called the dynamic scale. The simpler scale ratios  $l/l_1$ ,  $t/t_1$ ,  $p/p_1$ , etc., are called scales of length, time, pressure, etc.

The more complex reaction (13) is a function of three dynamic scales, shown in parentheses. The scale effect here is the variation of  $N$  or  $R$  with one or more of the dynamic scales, or independent arguments  $gl/v^2$ ,  $\nu/lv$ ,  $c/v$ . But for the particular case  $g, \nu, c = 0$ , as for a perfect liquid unaffected by gravity,  $N_1$ ,  $N_2$ ,  $N_3$  are constant and have straight-line graphs when plotted against their scales. Then (13) gives  $R = \text{const. times } \rho l^2 v^2$ .

Generally, therefore, for dynamically similar fluid motions a dynamic scale is any one of the independent dimensionless arguments in the formula for the fluid reaction; the scale effect is the variation of such reaction due to variation of the arguments.

*Arbitrary and derived scale ratios.*—As seen in the introduction, geometric similarity requires one constant scale ratio, say,  $l/l_1$ , for length; kinematic similarity two scales, say,  $l/l_1$ ,  $t/t_1$ , for length and time; dynamic similarity three, say,  $l/l_1$ ,  $t/t_1$ ,  $\rho/\rho_1$ . From these many others may be



derived, say,  $v/v_1$ ,  $\dot{v}/\dot{v}_1$ ,  $p/p_1$ ,  $\nu/\nu_1$ , etc., in case of fluids. Any three can be taken as determinative, then combined to form derived ratios, as exemplified in (2). For dynamic similarity we arbitrarily chose, at the outset,  $l/l_1$ ,  $t/t_1$ ,  $m/m_1$ , because length, time, and mass usually appear as basic. For the same service with fluid systems Helmholtz (reference 3) takes  $\rho/\rho_1$ ,  $\nu/\nu_1$ ,  $v/v_1$ , while other writers choose still other scales as fundamental.

Thus for geometrically similar fluid motions Helmholtz, assuming

$$\rho_1/\rho = r \quad \nu_1/\nu = q \quad u_1/u = v_1/v = w_1/w = n \text{-----} (15)$$

as given constants, thence derives the further ratios

$$x_1/x = y_1/y = z_1/z = q/n \quad t_1/t = q/n^2 \quad p_1/p = n^2 r p + \text{const} \text{-----} (16)$$

for use in comparing the differential equations of motion of the two fluids.

#### (B) DIFFERENTIAL METHOD

The conditions (6) for dynamically similar motion of two fluids can also be derived from the standard differential equations of motion of such fluids, viz, from

$$\left. \begin{aligned} \rho \dot{u} &= \rho g_x - c^2 \frac{\partial \rho}{\partial x} + \mu \Delta^2 u + \frac{1}{3} \mu \frac{\partial \theta}{\partial x} \\ \rho_1 \dot{u}_1 &= \rho_1 g_{1x} - c_1^2 \frac{\partial \rho_1}{\partial x_1} + \mu_1 \Delta^2 u_1 + \frac{1}{3} \mu_1 \frac{\partial \theta_1}{\partial x_1} \end{aligned} \right\} \text{-----} (17)$$

with like expressions for the  $y$ ,  $z$  and  $y_1$ ,  $z_1$  directions.<sup>6</sup> For if the motions are dynamically similar corresponding terms, all being forces, must have the same ratio,

$$\frac{\rho \dot{u}}{\rho_1 \dot{u}_1} = \frac{\rho g_x}{\rho_1 g_{1x}} = \frac{c^2}{c_1^2} \frac{\partial \rho / \partial x}{\partial \rho_1 / \partial x_1} = \frac{\mu \Delta^2 u}{\mu_1 \Delta^2 u_1} = \frac{\mu \partial \theta / \partial x}{\mu_1 \partial \theta_1 / \partial x_1}$$

Expressing these ratios in finite dimensions gives

$$\frac{\rho x_1 u^2}{\rho_1 x u_1^2} = \frac{\rho g_x}{\rho_1 g_{1x}} = \frac{\rho x_1 c^2}{\rho_1 x c_1^2} = \frac{\mu x_1^2 u}{\mu_1 x^2 u_1}$$

which multiplied by  $x^3/x_1^3$  become the relations (6) for the  $x$  direction, viz,

$$\frac{\rho x^2 u^2}{\rho_1 x_1^2 u_1^2} = \frac{g \rho x^3}{g_1 \rho_1 x_1^3} = \frac{\rho x^2 c^2}{\rho_1 x_1^2 c_1^2} = \frac{\mu x u}{\mu_1 x_1 u_1}$$

Thus the differential method yields the same result as the Newtonian. It is Newton's method in Stokes's shorthand, except that Stokes would first write the forces, then their ratio; Newton would write their ratio directly. But to write their ratio one must know approximately their nature and analytic expression.

Helmholtz reverses the above argument. Assuming the relations (15), (16), he says they transform the first of (17) into the second, omitting the  $g$  terms. Hence he infers that model data serve to predict the hydrodynamic behavior of full-scale craft when the relations (15), (16) are maintained.

Diverse and sundry treatments of this topic are found in references 8, 9, 10.

#### (C) DIMENSIONAL METHOD

*Mechanical units.*—In mechanics three measuring units, say, of length, mass, time  $\equiv L$ ,  $M$ ,  $T$ , arbitrarily taken as fundamental, are combined in various powers to form other kinds called derived units, such as  $U = AL^x M^y T^z$ ,  $A$  being constant, and  $x$ ,  $y$ ,  $z > 1$ . Table II illustrates. These two classes of units, viz, fundamental and derived, serve to measure mechanical quantities of every kind, such as length, speed, torque, etc. Thus any mechanical quantity  $R$ , if a function of  $n$  others, all differing in kind, can be written

$$R = \Sigma M Q_1^a Q_2^b \text{-----} Q_n^m \text{-----} (18)$$

where  $M$ ,  $a$ ,  $b$ ----- $m$  are pure numbers, and  $Q$  may involve either fundamental or derived units. Table II gives examples.

<sup>6</sup> Here  $\Delta^2 u = \frac{\partial^2 u}{\partial x^2} + \frac{\partial^2 u}{\partial y^2} + \frac{\partial^2 u}{\partial z^2}$ ;  $\theta = \frac{\partial u}{\partial x} + \frac{\partial v}{\partial y} + \frac{\partial w}{\partial z}$ ; etc., for  $\Delta^2 u_1$ ,  $\theta_1$ .

*Basic formula.*—To be valid for all unit systems (18) must be dimensionally homogeneous.<sup>7</sup> Then it can be written, if  $[R] = [Q_1^a Q_2^b \dots Q_n^m] = [P]$ ,

$$R = \Sigma NP \text{-----} (19)$$

where  $N$  is a pure number. This is the basic formula of dimensional theory, and is most general when the  $P$ s are all the separate independent  $Q$  products that can be formed having the dimensions of  $R$ .<sup>8</sup>

*Homogeneous products.*—To find these  $P$  products, we first multiply any  $Q$  triad, say  $Q^x Q^y Q^z$ , by each remaining  $Q$  successively, and equate to  $[R]$  the dimensions of each resulting product. The ensuing  $n-3$  equations, with tentative exponents  $a, b, c$ , are

$$[P_1] = [Q_1^a Q_2^b Q_3^c Q_4] = [R] \quad [P_2] = [Q_1^d Q_2^e Q_3^f Q_5] = [R], \text{ etc.} \text{-----} (20)$$

Now replacing  $[R]$  and  $[Q]$  by their values in  $L, M, T$  and solving (20) for  $a, b, c, \dots$ , gives  $P_1, P_2, \dots$ . The following example illustrates. For a rigorous analysis special works on dimensional theory may be consulted (references 4, 5).

*Reactions in similar flows.*—If the reaction  $R$  of a body in a fluid stream depends solely on  $\rho, l, v, g, \mu, c$ , or density, size, speed, weight, viscosity, elasticity, all the separate independent products having the dimensions of  $R$  possible to make with them amount to 6-3, say,  $P_1, P_2, P_3$ . To form these, we take any triad  $\rho^x l^y v^z$  of the six independent quantities and multiply it successively by the remaining ones  $g, \mu, c$ , giving

$$P_1 = \rho^a l^b v^c \cdot g \quad P_2 = \rho^d l^e v^f \cdot \mu \quad P_3 = \rho^g l^h v^i \cdot c$$

and equate the dimensions of each product to  $[R] = [ML/T^2]$ . The first yields, by Table II,

$$(M/L^3)^a \cdot L^b \cdot (L/T)^c \cdot L/T^2 = ML/T^2$$

each unit having the same aggregate exponent in both terms. On equating the indices of  $L, M, T$  successively this gives

$$-3a + b + c + 1 = 1 \quad a = 1 \quad -c - 2 = -2$$

Thus  $a = 1, b = 3, c = 0$ , whence  $P_1 = \rho l^3 g$ . A like procedure gives  $d = 0, e = 1 = f$ , whence  $P_2 = lv\mu$ . Similarly  $g = 1, h = 2, i = 1$ , whence  $P_3 = \rho l^2 v c$ .

By (19) the reaction now is

$$R = N_1 \rho l^3 g + N_2 \mu l v + N_3 \rho l^2 v c = \rho l^2 v^2 f(gl/v^2, v/lv, c/v) \text{-----} (13)$$

which is a general resistance equation for the specified dynamical conditions, viz, that  $R$  is a function solely of  $\rho, l, v, g, \mu, c$ . From this (13<sub>1</sub>) also is found as before.

By (13), if the arguments in parentheses are given any specific values the same for model and full scale,  $f$  is the same for both; hence

$$R = N \rho l^2 v^2$$

where  $N = f(g_1 l_1 / v_1^2, v_1 / l_1 v_1, c_1 / v_1)$ , the same as by Newton's method.

#### COMPARISON OF THE THREE METHODS

In the foregoing text the same criteria for dynamical similarity in two flow systems were found by three different methods of analysis—the Newtonian, the differential, and the dimensional. In each the physical quantities governing the flow were premised from experience. Thence were found the ratios of corresponding impressed forces of each kind on homologous parts of the fluid, viz, weight ratio, pressure ratio, etc. These ratios, by definition of dynamic similarity, must each equal the ratio of the resultant acceleration forces on those parts; viz, the ratio  $m_j / m_1 j_1$ .

By Newton's method we directly equated the ratio of these acceleration forces to the several ratios of corresponding impressed forces, thus obtaining specific conditions for dynamical

<sup>7</sup> That is, all terms of (18) must comprise the same fundamental units, each having a constant aggregate exponent throughout the equation.

<sup>8</sup> Dividing (19) by  $R$  gives  $\psi(\pi_1, \pi_2, \dots, \pi_i) = 0$ , the  $\pi$ s being dimensionless products. This is Buckingham's  $\pi$  theorem (reference 4).



similarity, and formulas for the reactions of any fluid system in terms of those of its model. By the second method we first wrote the differential equations for the two fluid motions assumed dynamically similar, then equated the ratios of corresponding terms, thus obtaining the same result as before. By the third method we first equated the unknown reaction  $R$  on one fluid element to the sum of all the terms we could form from the flow-governing quantities arranged in power products each having the dimensions of  $R$ . Doing the same for the homologous element, then taking the ratio of the  $R$  forces, gave the same reaction formula as found by the other methods.

At first sight the dimensional process seems to be a routine algebraic operation requiring less knowledge than is needed for the two other methods. In reality all three demand adequate judgment of the kind of physical quantities governing the motion, and their comparative importance. In all three cases the assumed physical agencies are the same, the terms in the dynamic equations are analogous, and the final working formulas are the same or equivalent. In all, the derived working formula contains a dimensionless coefficient that is not deduced theoretically, but is to be found from model tests, then applied to full-scale apparatus operating under dynamically similar conditions. In all, the "laws of comparison" are merely-expressions of equality of like dynamic scales, viz, equality of the ratio of the acceleration forces to the corresponding ratios of the dominant impressed forces.

TABLE II

QUANTITIES EXPRESSED IN BASIC UNITS OF LENGTH, TIME, AND MASS,  $L$ ,  $T$ ,  $M$ 

The "dimensions" of a physical quantity are the degrees of the fundamental units in its formula. Thus the dimensions of an acceleration, which are symbolized by  $[L T^{-2}]$ , are 1 in length and  $-2$  in time. Commonly the brackets are omitted from such simple  $L$ ,  $T$ ,  $M$  expressions not containing other symbols. The dimensions of a force are  $MLT^{-2}$ , viz, 1 in mass, 1 in length,  $-2$  in time; the dimension of an angle, a sine, cosine, tangent, etc., is  $L L^{-1}$ , that is zero. Logarithms in physical equations operate only on dimensionless quantities, such as pure numbers or ratios of like physical quantities; hence are dimensionless.

A derived unit, being formed of powers of fundamental units, has the form  $U = AL^x M^y T^z$ , with dimensions  $L^x M^y T^z$ . Thus a force  $F = ms/t^2 = AL^x M^y T^z$ , where  $m$ ,  $s$ ,  $t$  are mass, length, time in any convenient units. Its dimensions are written  $[F] = [ms/t^2] = [AL^x M^y T^z] = MLT^{-2}$ .

In homogeneous equations all terms have the same dimensions, that is, the same aggregate exponent for each basic unit. Thus in the last equation of Table II each term has the dimensions  $ML^{-1} T^{-2}$ : for  $[\rho v^2] = ML^{-3} L^2 T^{-2} = ML^{-1} T^{-2}$ , and  $[\mu v/a] = ML^{-1} T^{-1} L T^{-1}/L = ML^{-1} T^{-2}$ . In the familiar projectile formula  $c = gt + c$ ,  $[gt] = L T^{-2}$ ,  $T = L T^{-1} = [v] = [c]$ , where  $c$  ( $=v_0$ ) is a velocity.

Kind of quantity	Symbol. Formula	Dimensions of each term
Derived units, $U = AL^x M^y T^z$		
Area, surface	$S = l^2$	$L^2$ .
Volume	$\tau = l^3$	$L^3$ .
Angle	$e = s/r = \text{arc} \div \text{radius}$	$L^0$ .
Linear velocity	$u = x/t = dx/dt = \dot{x}$	$LT^{-1}$ .
Linear acceleration	$j = u/t = du/dt = d^2x/dt^2$	$LT^{-2}$ .
Angular velocity	$\omega = \theta/t = d\theta/dt = du/dy$	$T^{-1}$ .
Angular acceleration	$\alpha = \omega/t = d\omega/dt = \theta/t^2$	$T^{-2}$ .
Density	$\rho = m/\tau = m/l^3$	$ML^{-3}$ .
Force, thrust	$F = mj = ms/t^2$	$MLT^{-2}$ .
Torque, moment	$\mathcal{Q} = Fl$	$ML^2T^{-2}$ .
Pressure, friction	$p = F/S$ , $f = F/S$	$ML^{-1}T^{-2}$ .
Work, energy, potential	$W = Fs$	$ML^2T^{-2}$ .
Power, activity	$P = Fu$	$ML^2T^{-3}$ .
Viscosity	$\mu = f \div du/dy = f/\omega$	$ML^{-1}T^{-1}$ .
Kinematic viscosity	$\nu = \mu/\rho$	$L^2T^{-1}$ .
Flux of fluid	$\psi = \int q_n dS$	$L^3T^{-1}$ .
Velocity potential	$\phi = -\int q_t ds$	$L^2T^{-1}$ .
Geometrical and mechanical equations, $R = \Sigma NP$		
Length of catenary	$s = \frac{c}{2} (e^{x/c} - e^{-x/c}) = c \sinh \left( \frac{x}{c} \right)$	$L$ , $= L L^0$ .
Area of ellipse	$S = \pi ab$	$L^2$ ,
Volume of frustum of cone	$\tau = \frac{1}{3} \pi h (r^2 + rr' + r'^2)$	$L^3$ , $= [L(L^2 + LL + L^2)]$ .
Period of simple pendulum	$t = 2\pi \sqrt{l/g}$	$T$ , $= \sqrt{L/LT^{-2}}$ .
Mutual attrac. of two particles	$F = \kappa mm^1/r^2$ , where $[\kappa] = L^3/MT^2$	$LMT^{-2}$ , $= L^3M^{-1}T^{-2} M^2L^{-2}$ .
Strength of line source	$m = 2\pi a q_n$	$L^2T^{-1}$ , $= L.LT^{-1}$ .
$\phi$ for source-sink in plane stream	$\phi = ux + \sigma \log \frac{r_2}{r_1}$ , where $[\sigma] = L^2/T$	$L^2T^{-1}$ , $= [LT^{-1}.L + L^2T^{-1} \log L^0]$ .
Acceleration of viscous particle	$\dot{u} = -\partial p/\rho \partial x + \nu \Delta^2 u$	$LT^{-2}$ $= [p/\rho.x + \nu u/x^2]$ .
Nose pressure on falling droplet	$p_n = \rho v^2/2 + 1.5\mu v/a$	$ML^{-1}T^{-2} = [\rho v^2 + \mu v/a]$ .

## SYMBOLS USED IN TEXT

$l, l_1$ -----	Homologous lengths in similar figures.
$x, x_1$ , etc-----	Homologous coordinates.
$t, t_1$ -----	Times of tracing homologous paths.
$v, v_1$ -----	Corresponding path velocities.
$\dot{v}, \dot{v}_1$ -----	Corresponding path accelerations.
$j, j_1$ -----	Corresponding total accelerations.
$m, m_1$ -----	Homologous masses.
$a, b, c$ -----	Arbitrary numerical ratios $l/l_1, t/t_1, m/m_1$ ; also tentative exponents.
$\rho, \mu, \nu, \kappa$ -----	Density, viscosity, kinematic viscosity, bulk modulus; ditto for $\rho_1, \mu_1, \nu_1, \kappa_1$ .
$c = \sqrt{\kappa/\rho}$ -----	Speed of sound in elastic fluid; ditto for $c_1$ .
$R, R_1$ -----	Resultant forces on mass elements $m, m_1$ .
$P, Q$ , etc-----	Components of $R$ ; $P_1, Q_1$ , etc., components of $R_1$ .
$p, f$ -----	Pressure and friction, per unit area; ditto for $p_1, f_1$ .

## REFERENCES

1. Sir Isaac Newton----- Principia, Book II, Propositions 32, 33.
2. T. E. Stanton and J. H. Pannell----- Similarity of Motion in Relation to the Surface Friction of Fluids. Phil. Trans. Roy. Soc. Lond., ser. A, vol. 24.
3. Hermann von Helmholtz----- On a Theorem Relative to Movements that are Geometrically Similar in Fluid Bodies, etc. Smith, Misc. Col. 843. Also given in his collected papers.
4. Edgar Buckingham----- On Physically Similar Systems; Illustrations of the Use of Dimensional Equations. Phys. Rev., October, 1914.
5. P. W. Bridgman----- Dimensional Analysis. Yale University Press, 1922.
6. A. H. Gibson----- Principle of Dynamical Similarity, etc. Engineering, March, 1924.
7. Lord Rayleigh----- Phil. Trans. Roy. Soc., 1883. Phil. Mag., 1892, 1899, 1904.
8. Stokes----- Mathematical and Physical Papers, Vol. III, p. 17.
9. N. Joukowski----- Aerodynamique. Gauthier-Villars.
10. Escande & Ricaud----- Rapport sur les Lois de la Similitude Aerodynamique. Inst. Electrique Toulouse.
11. E. Jouguet----- Indications Historiques sur l'Application des Lois de la Similitude Mechanique au Mouvement des Fluides. La Technique Aeronautique, March 15, 1924.
12. D. Riabouchinsky----- Methode des Variables de Dimensions Zero. L'Aerophile, September 1, 1911.
13. Osborne Reynolds----- Phil. Trans. March 15, 1883.
14. L. Bairstow and H. Booth----- Principle of Dynamical Similarity, etc. R. & M. No. 38, Adv. Com. Aeron.

AERODYNAMICAL LABORATORY,  
 BUREAU OF CONSTRUCTION AND REPAIR,  
 NAVY YARD, WASHINGTON, D. C., May 7, 1928.



---

---

**REPORT No. 288**

---

**PRESSURE DISTRIBUTION  
OVER A RECTANGULAR MONOPLANE WING MODEL  
UP TO 90° ANGLE OF ATTACK**

**By MONTGOMERY KNIGHT and OSCAR LOESER, Jr.  
Langley Memorial Aeronautical Laboratory**





## REPORT No. 288

### PRESSURE DISTRIBUTION OVER A RECTANGULAR MONOPLANE WING MODEL UP TO 90° ANGLE OF ATTACK

By MONTGOMERY KNIGHT and OSCAR LOESER, Jr.

#### SUMMARY

*The pressure distribution tests herein described, covering angles of attack up to 90°, were made on a rectangular monoplane wing model in the atmospheric wind tunnel of the Langley Memorial Aeronautical Laboratory.*

*These tests indicate that a rectangular wing, by reason of its large tip loads, is uneconomical aerodynamically and structurally, has pronounced lateral instability above maximum lift, and is not adaptable to accurate calculation based on the classical wing theory.*

#### INTRODUCTION

The pressure distribution tests described in this report were made at the Langley Memorial Aeronautical Laboratory primarily to obtain information relative to the autorotational characteristics of a particular rectangular monoplane wing model. However, the results obtained are indicative of the distribution over square-tipped monoplane wings in general, and are presented herewith at the suggestion of Lieut. W. S. Diehl, United States Navy, to add to the meager supply of information on the aerodynamic characteristics of wings at large angles of attack. Such information is of value in studies of the spinning airplane and of stability and controllability at large angles of attack.

#### METHODS AND APPARATUS

The tests, covering angles of attack ( $\alpha$ ) from  $-8^\circ$  (approximately zero lift) to  $90^\circ$ , were made in the 5-foot atmospheric wind tunnel, which has a circular closed throat. (Reference 1.) The method of half-span wing and reflecting plane (references 2, 3, 4, 5) was used. In Figure 1 is shown the arrangement of wing and plane in the tunnel. Retardation of the flow close to the plane is compensated for by dipping the leading edge of the plane slightly, the correct amount of dip being determined from a series of velocity surveys taken normal to the plane.

The rectangular mahogany wing which had a Göttingen 387-FB (flat bottom) profile, had been tested previously in autorotation experiments as a 5-inch by 30-inch full-span wing. For pressure distribution purposes, 12 small brass tubes were inlaid in slots cut in the surface of the wing parallel to the span. The pressure orifices consisted of holes drilled at intervals in these tubes. The tube locations around the profile, and the spacing of orifice groups or sections along the span, are given in Figure 2. Figure 3 shows the model with tubes, connections, and mounting block.

Pressures were recorded photographically on photostat paper placed against the tubes in the multiple liquid manometer illustrated in Figure 4. In this figure are also shown the rubber pressure tubes from the wing, and the handles attached to the lower end of the wing supporting bracket for changing the angle of attack.



In order to simplify the drawing of the pressure distribution diagrams, the positions of the orifice tubes in the wing surface were so chosen that when projected on the chord they corresponded to certain selected tubes on the manometer, the distance between the end manometer tubes representing the wing chord. This arrangement made it possible to draw the pressure diagrams directly on the manometer record as shown in Figure 5, which is a photograph of a specimen record. Only the manometer tubes labeled at the top of this record were used in the tests, the others being left open to the air in the experimental chamber.

The testing procedure consisted first in sealing all orifices with wax, checking each tube for leaks, and then opening with a needle the orifices of the desired section. This section was then tested through the complete angle of attack range.

Throughout the tests the dynamic pressure ( $q = \frac{1}{2} \rho V^2$ , where  $\rho$  = air density and  $V$  = velocity) in the vicinity of the model was held constant at 4.09 pounds per square foot, using as

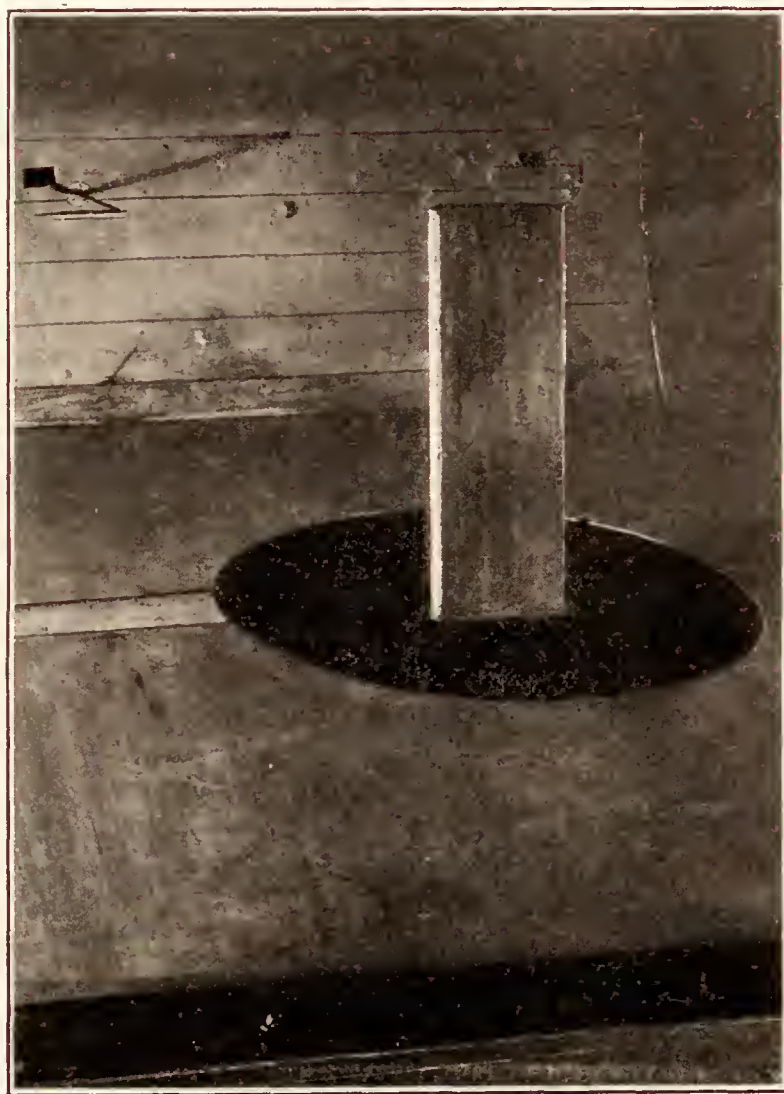


FIG. 1.—Half-span wing model and reflecting plane mounted in tunnel

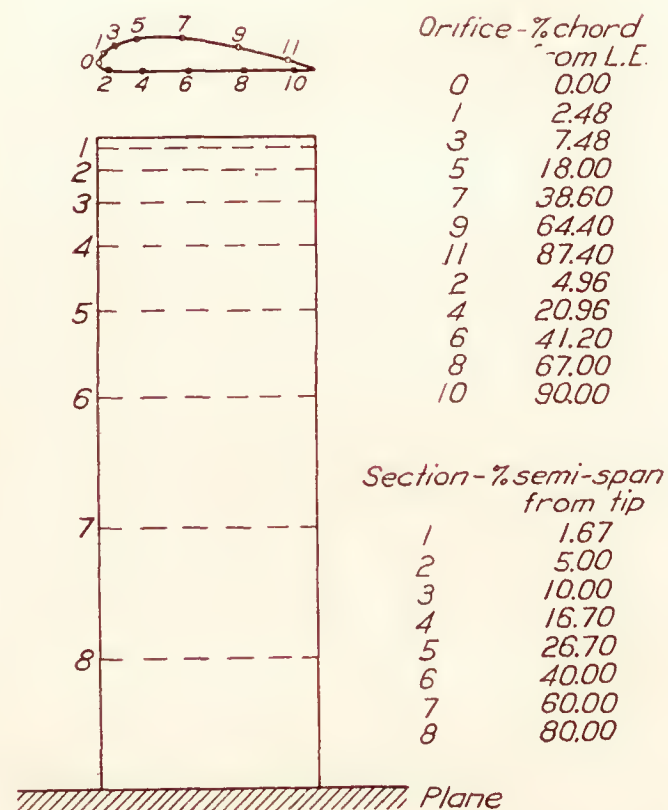


FIG. 2.—Location of pressure distribution orifices in Göttingen 387-FB wing

a reference the Pitot-static tube shown at the left of Figure 1. This instrument was connected to a vernier manometer outside the tunnel. The static pressure side of this Pitot tube was also connected to two of the multiple manometer tubes for the purpose of locating the static pressure line on the manometer record. The mean velocity corresponding to the above dynamic pressure was 59.5 feet per second. The mean Reynolds Number was 147,000, with the wing chord as the characteristic length.

A comparison of the integrated areas of original and check manometer records indicated over-all errors of about 1 per cent, covering the tests and the drawing and integration of the pressure diagrams. This error, together with the error in the values of  $q$  used in computing the coefficient of normal force ( $C_{NF}$ ) for each section, resulted in a probable error of about 3 per cent in the final results.





FIG. 3.—Model wing showing pressure connections and mounting block

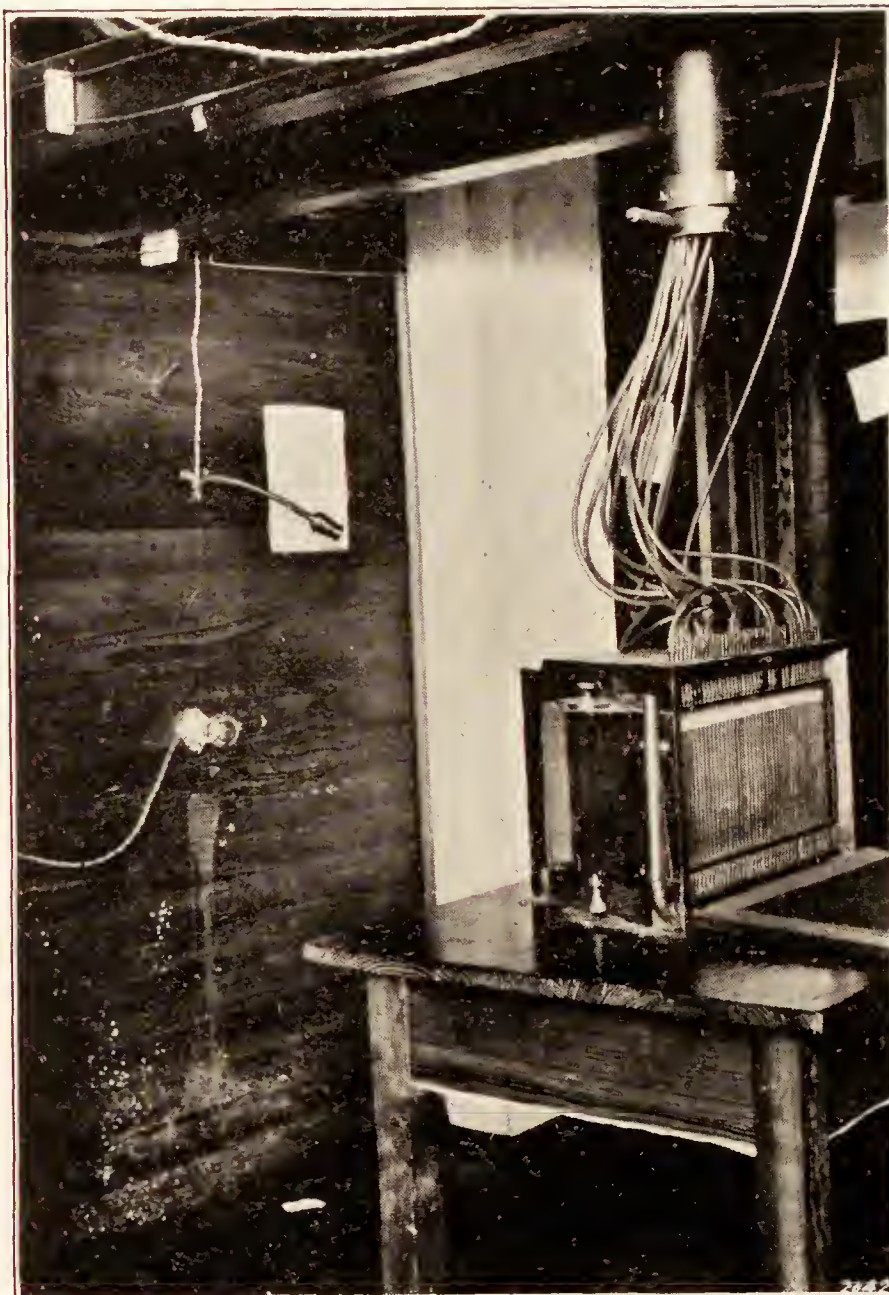


FIG. 4.—Multiple photographic manometer in place beneath tunnel

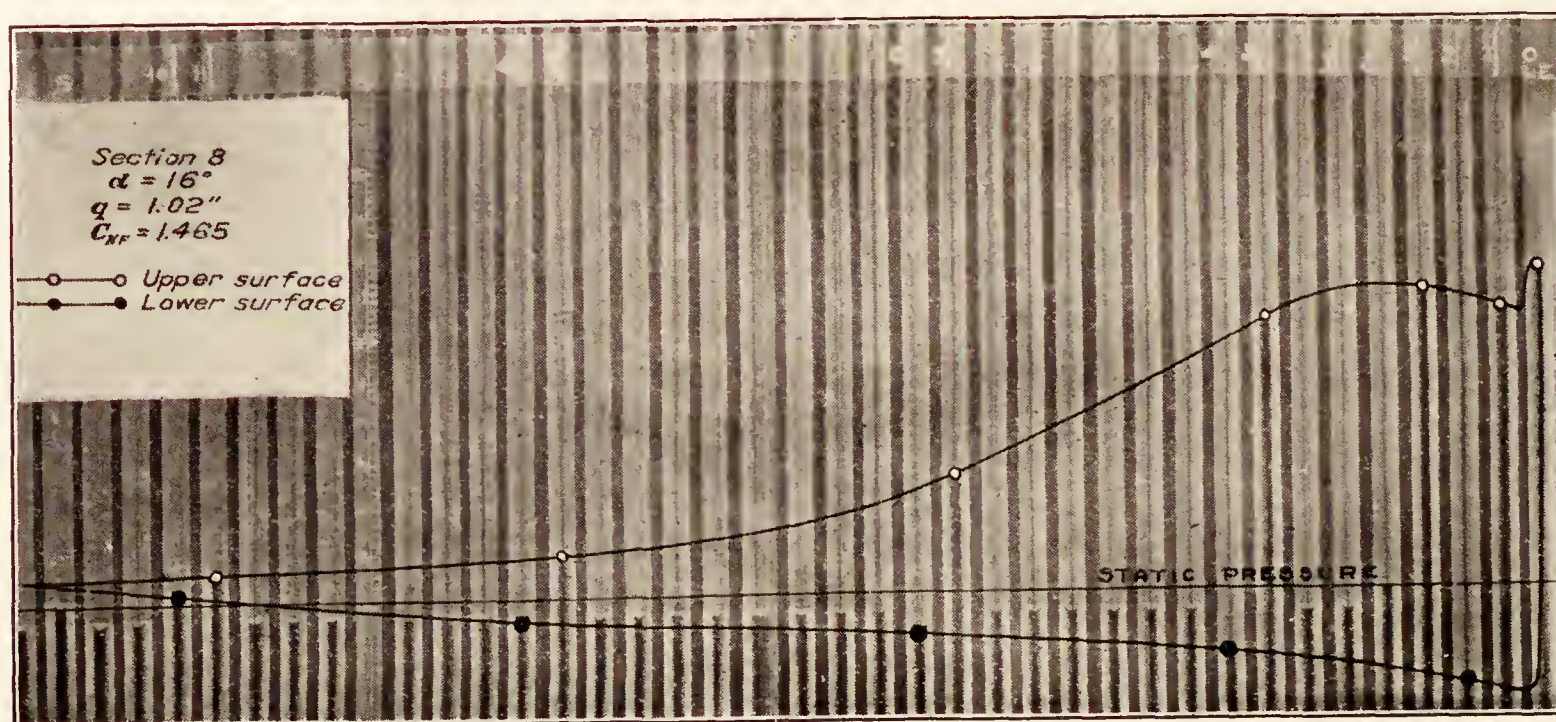
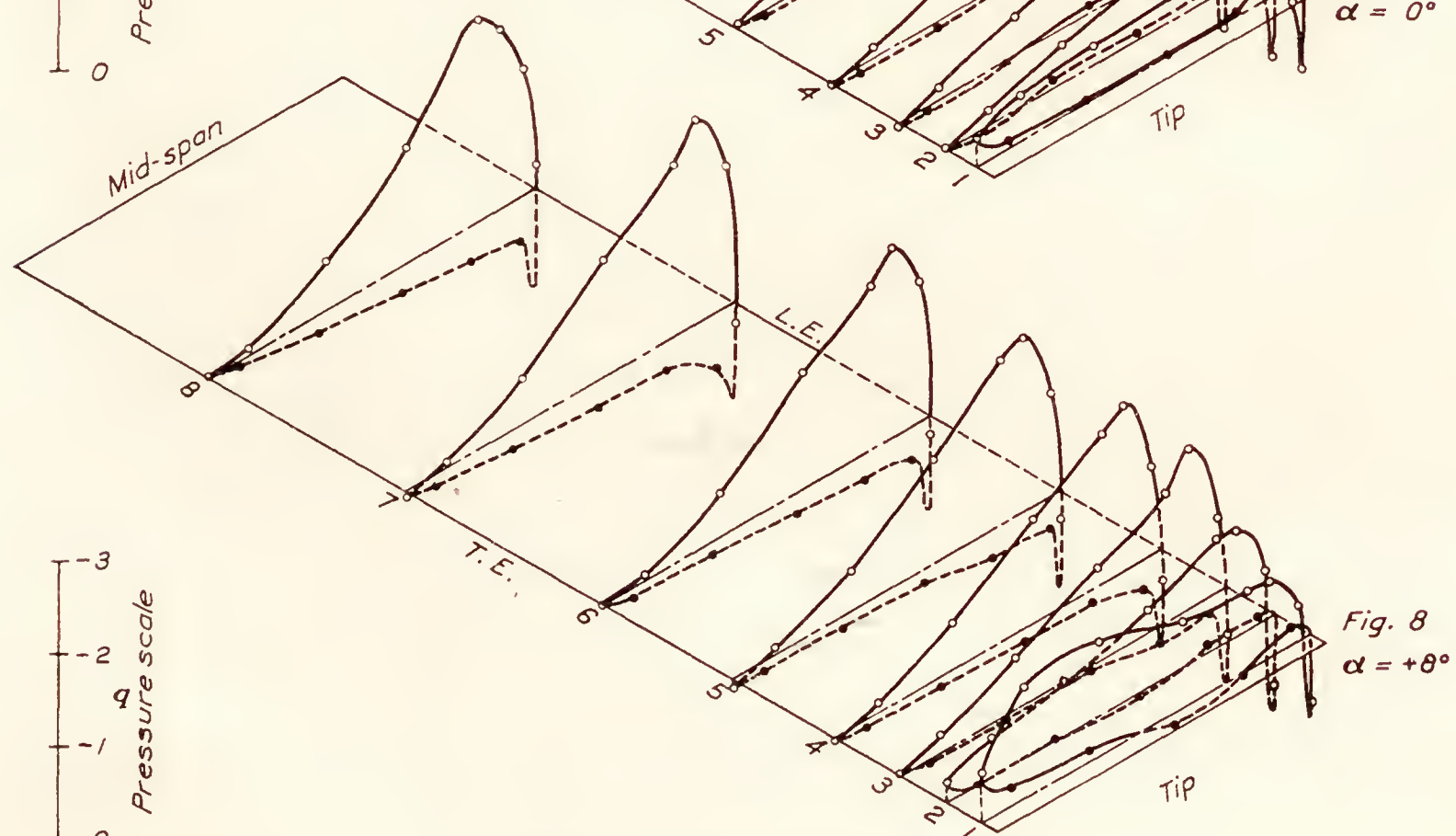
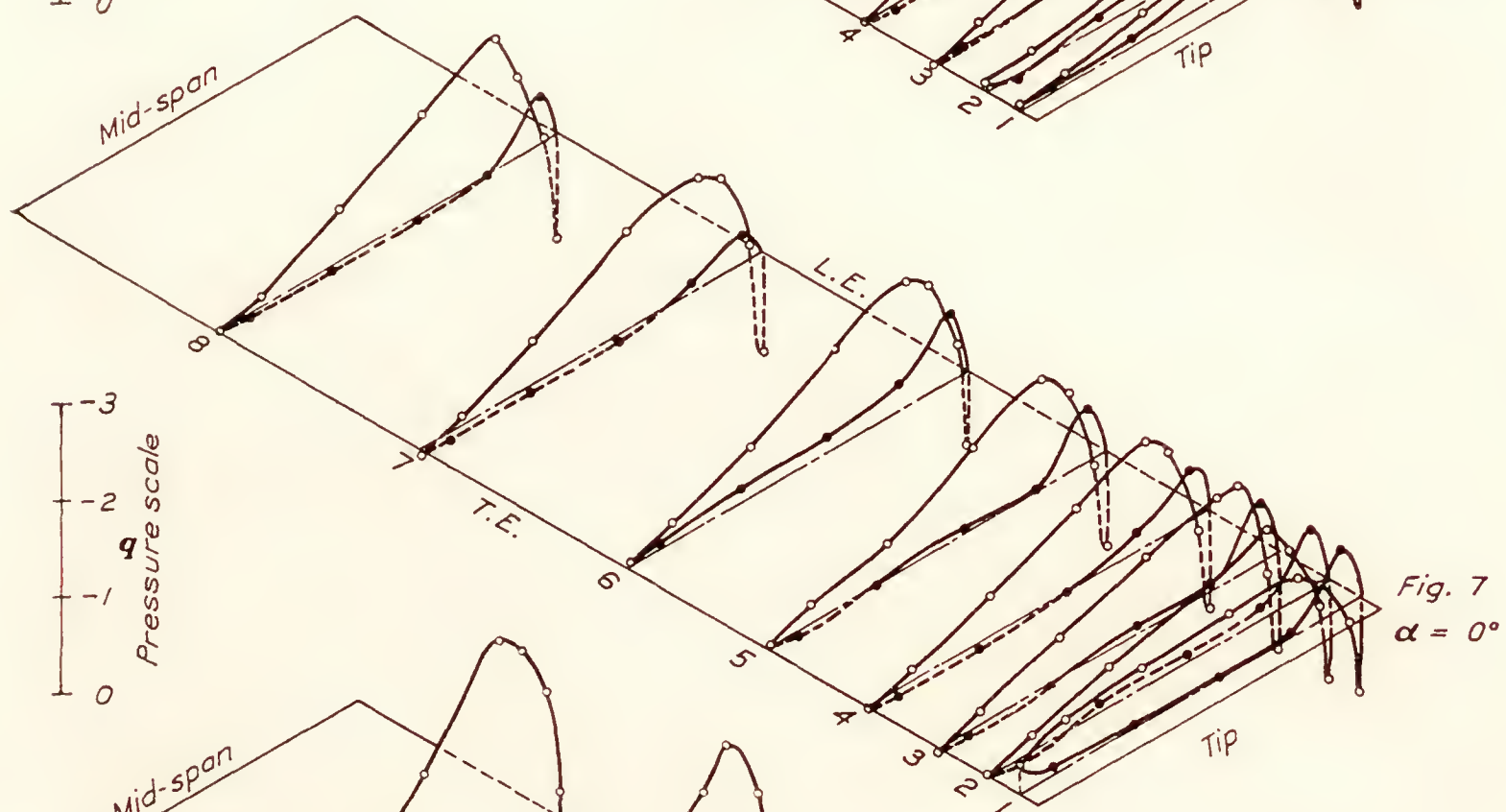
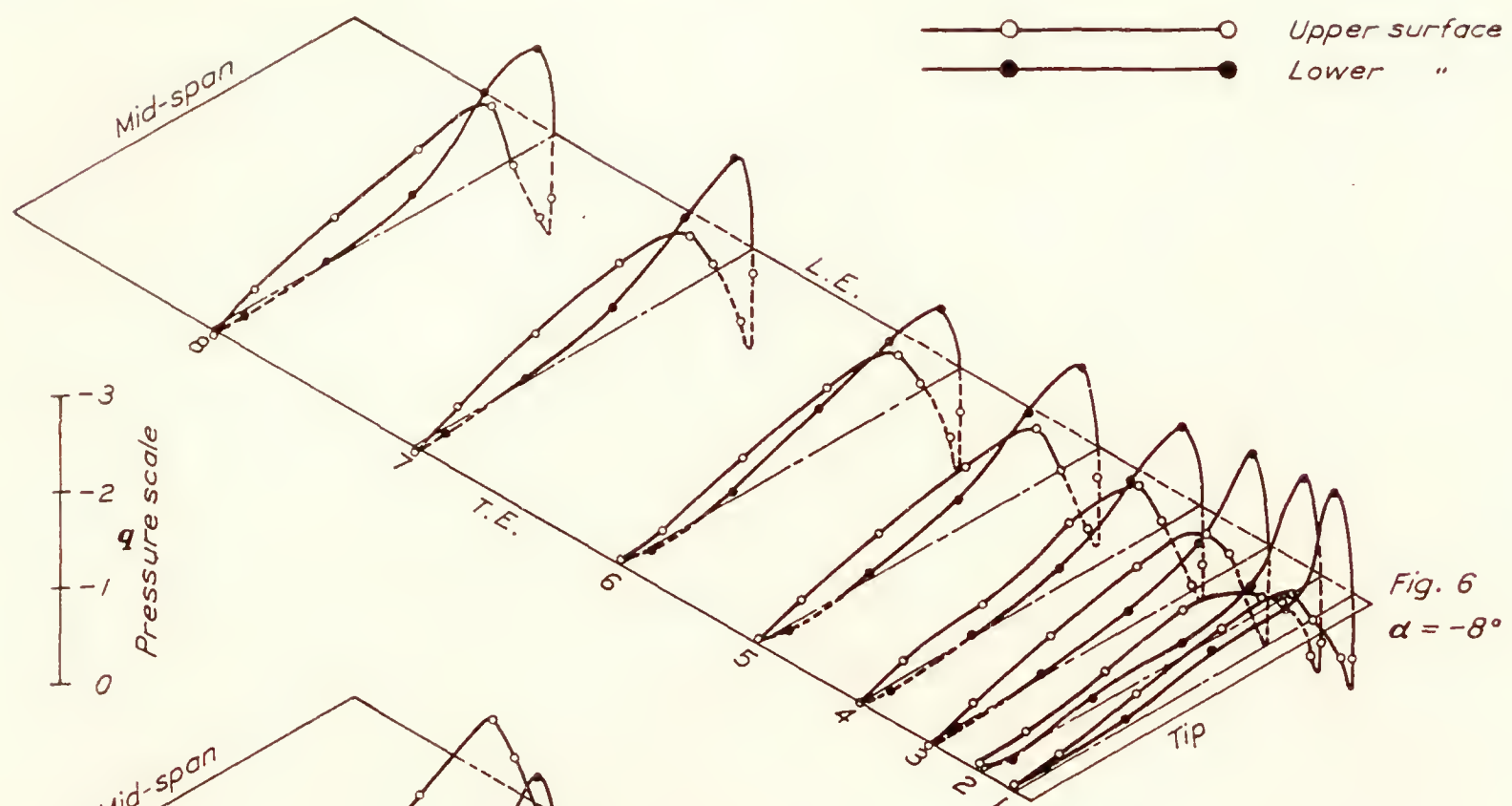


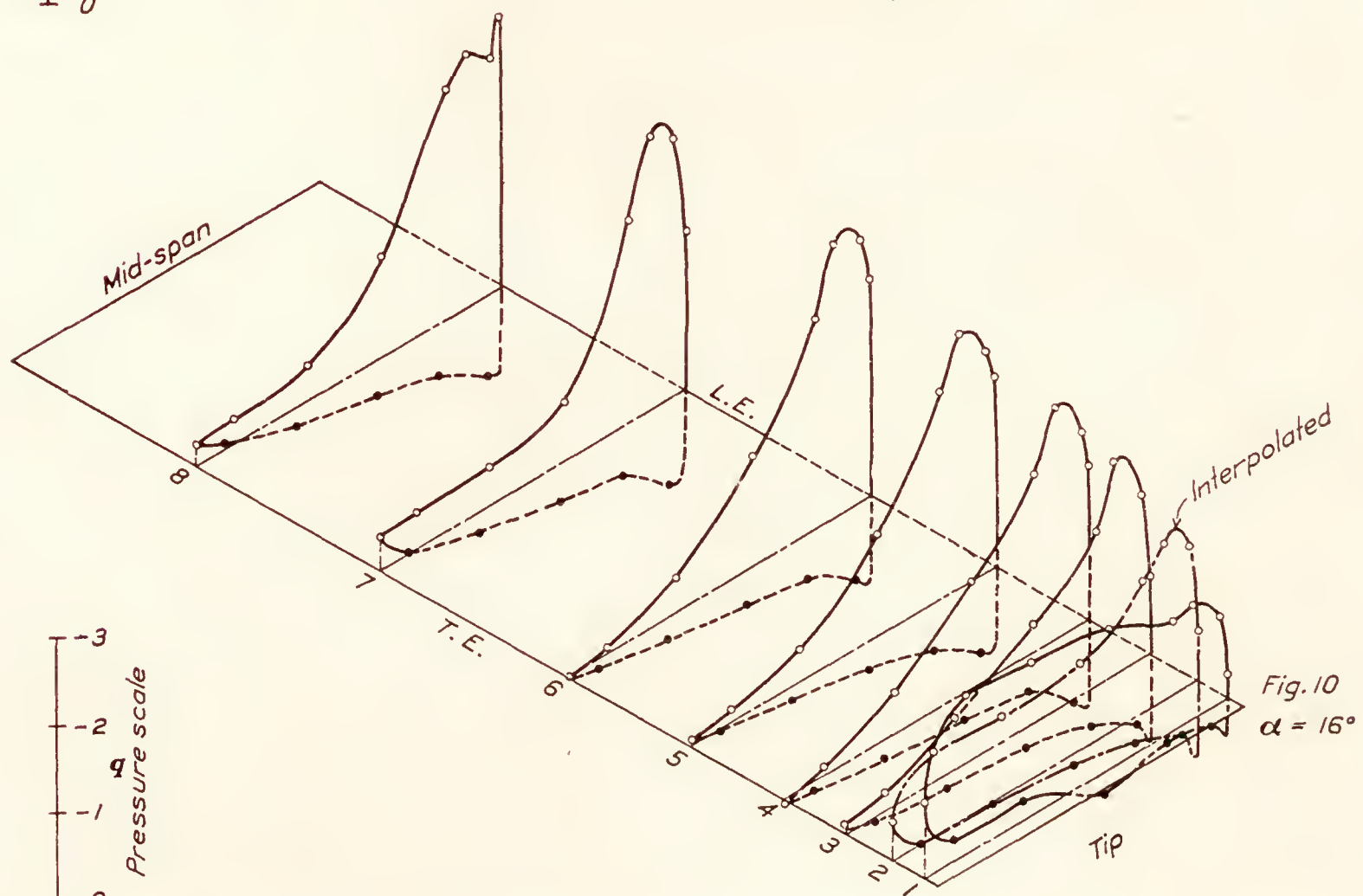
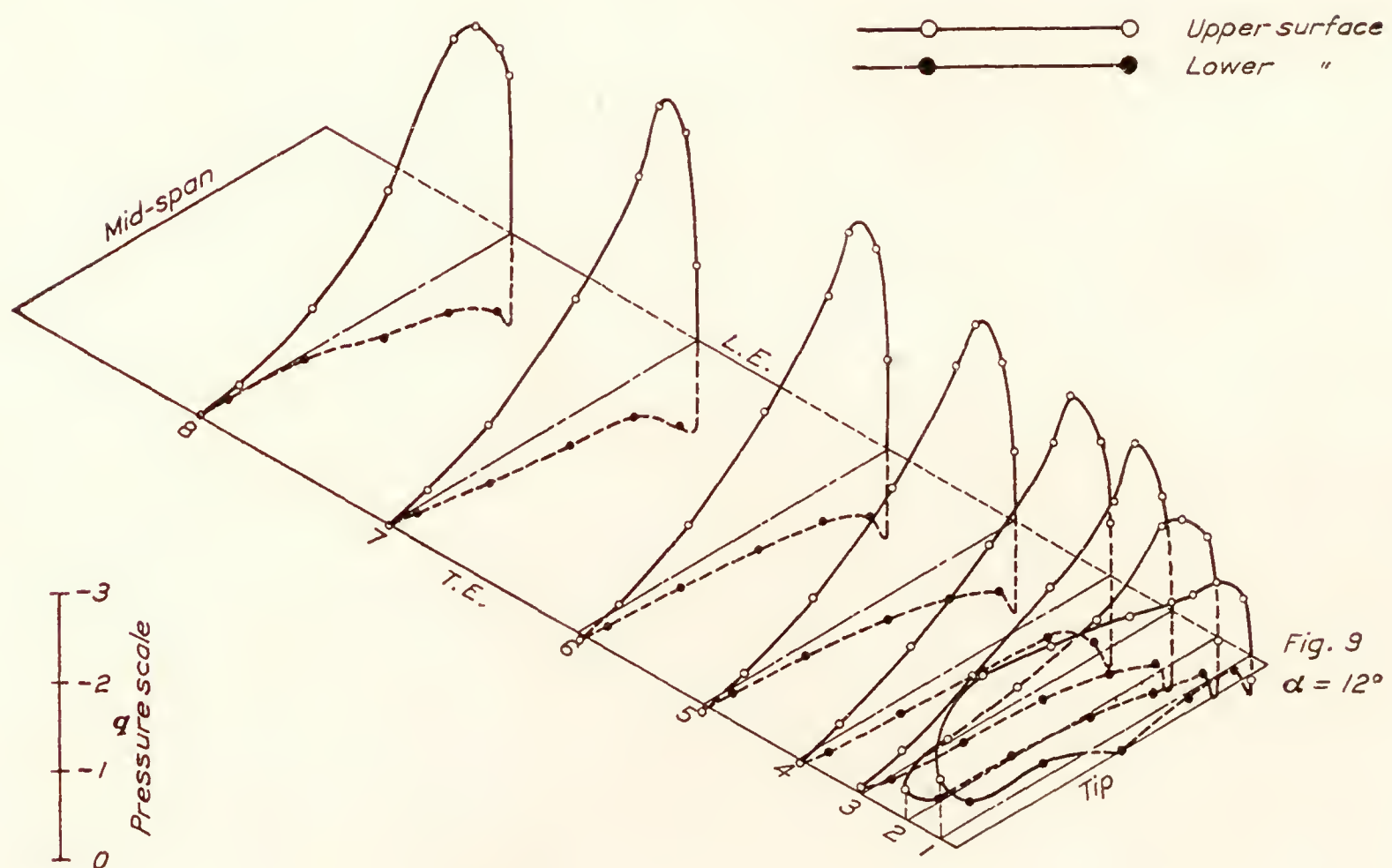
FIG. 5.—Specimen manometer record with pressure diagram



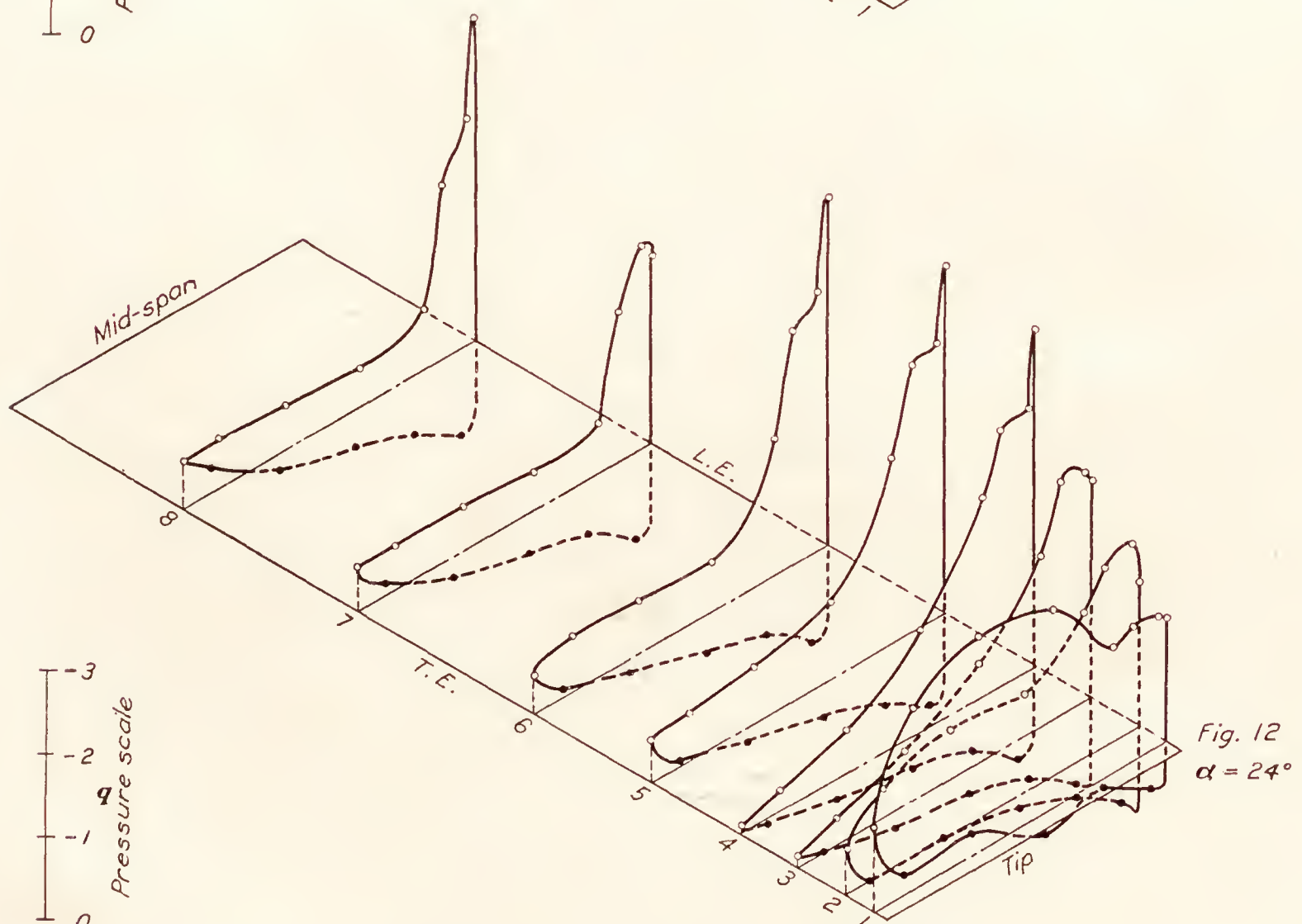
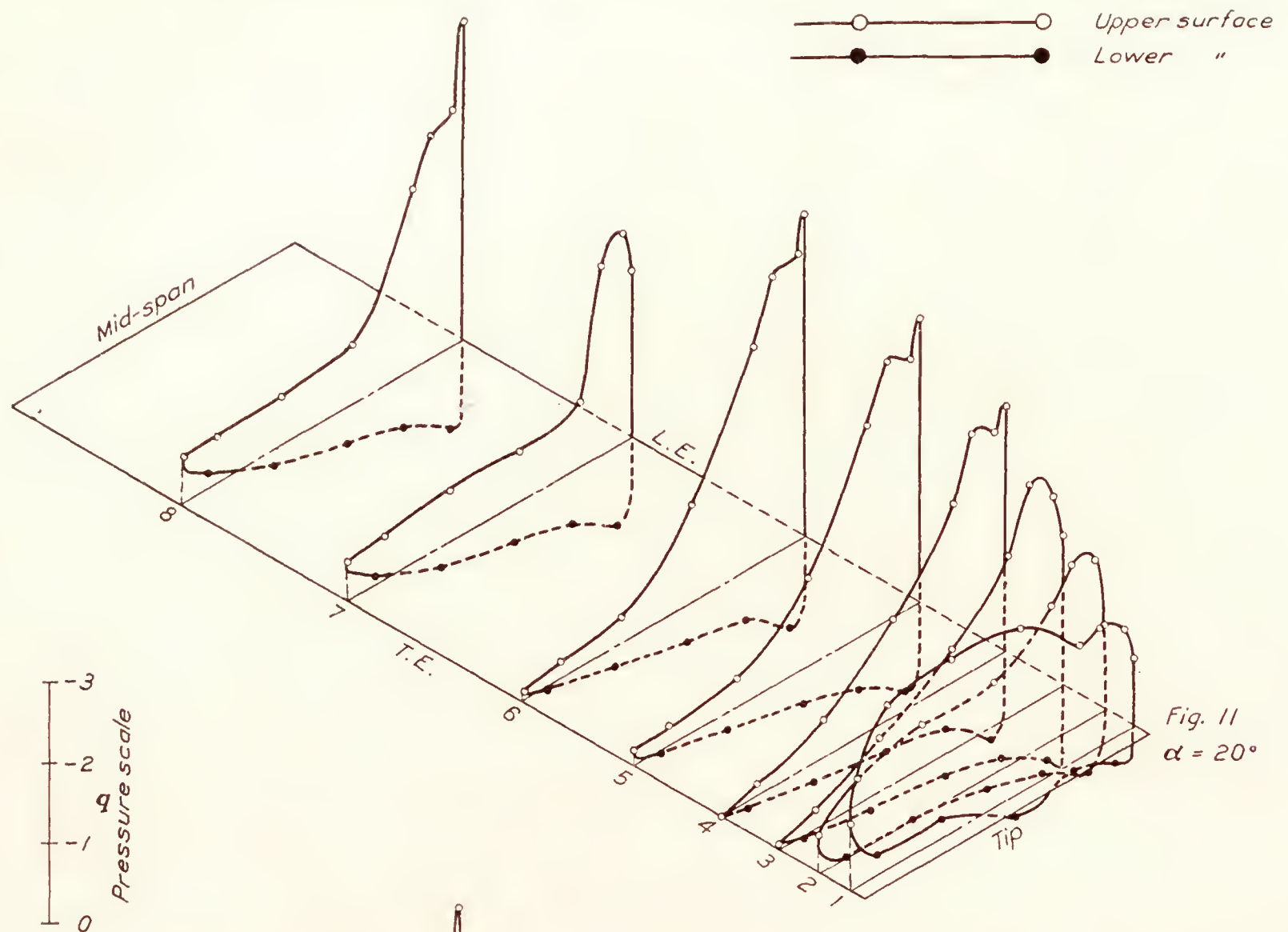


FIGS. 6, 7, and 8.—Surface normal pressure distribution



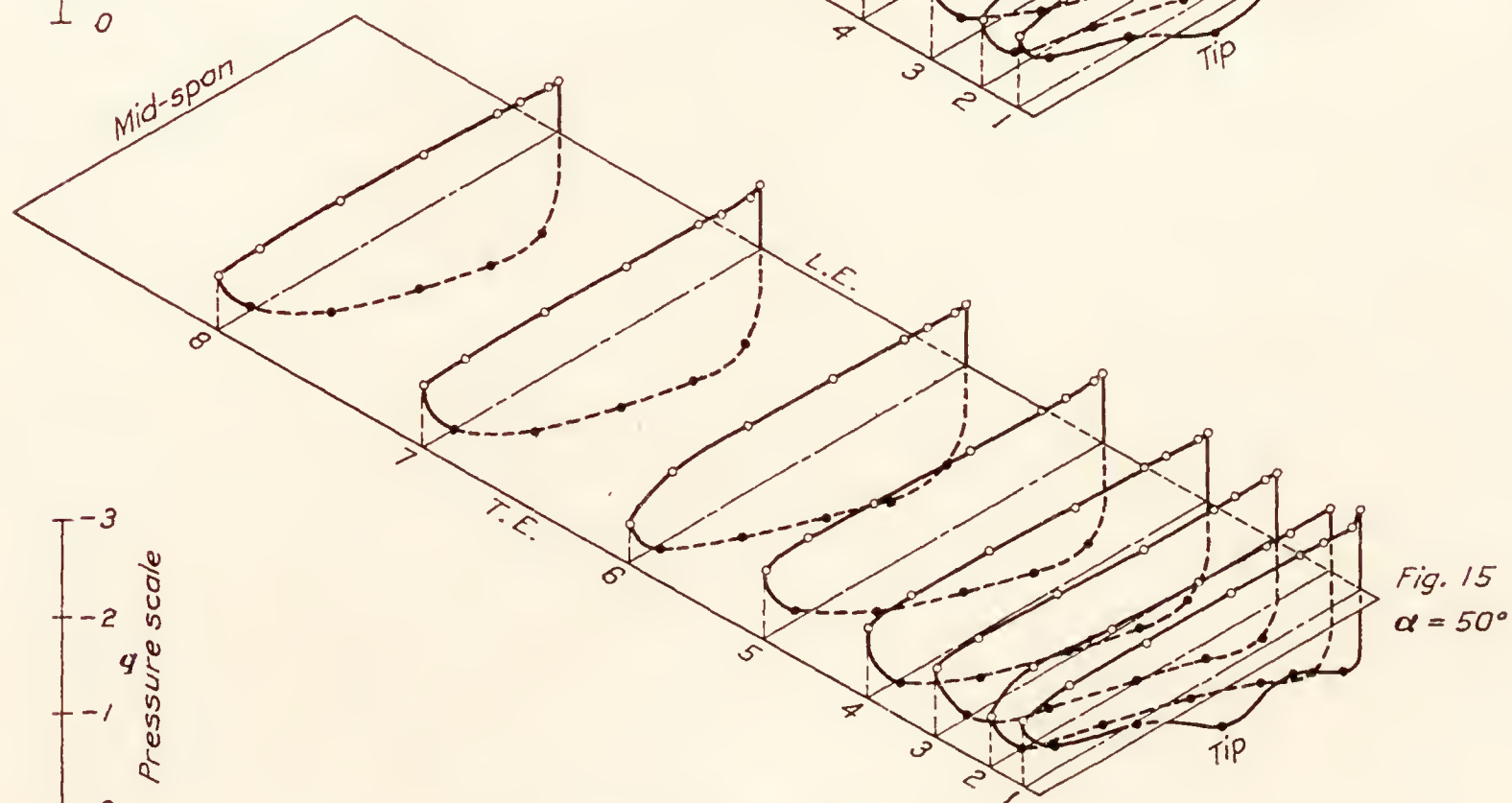
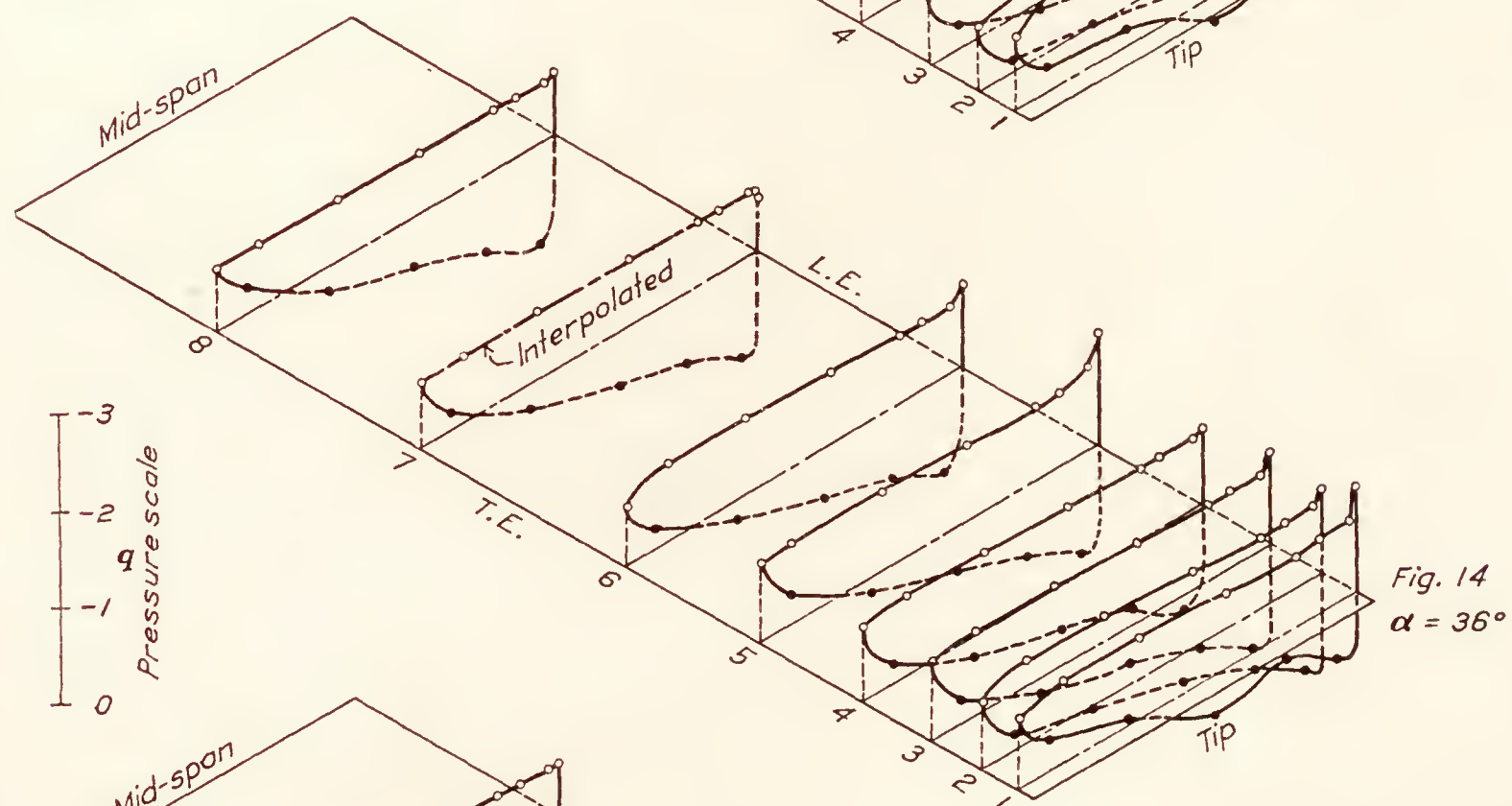
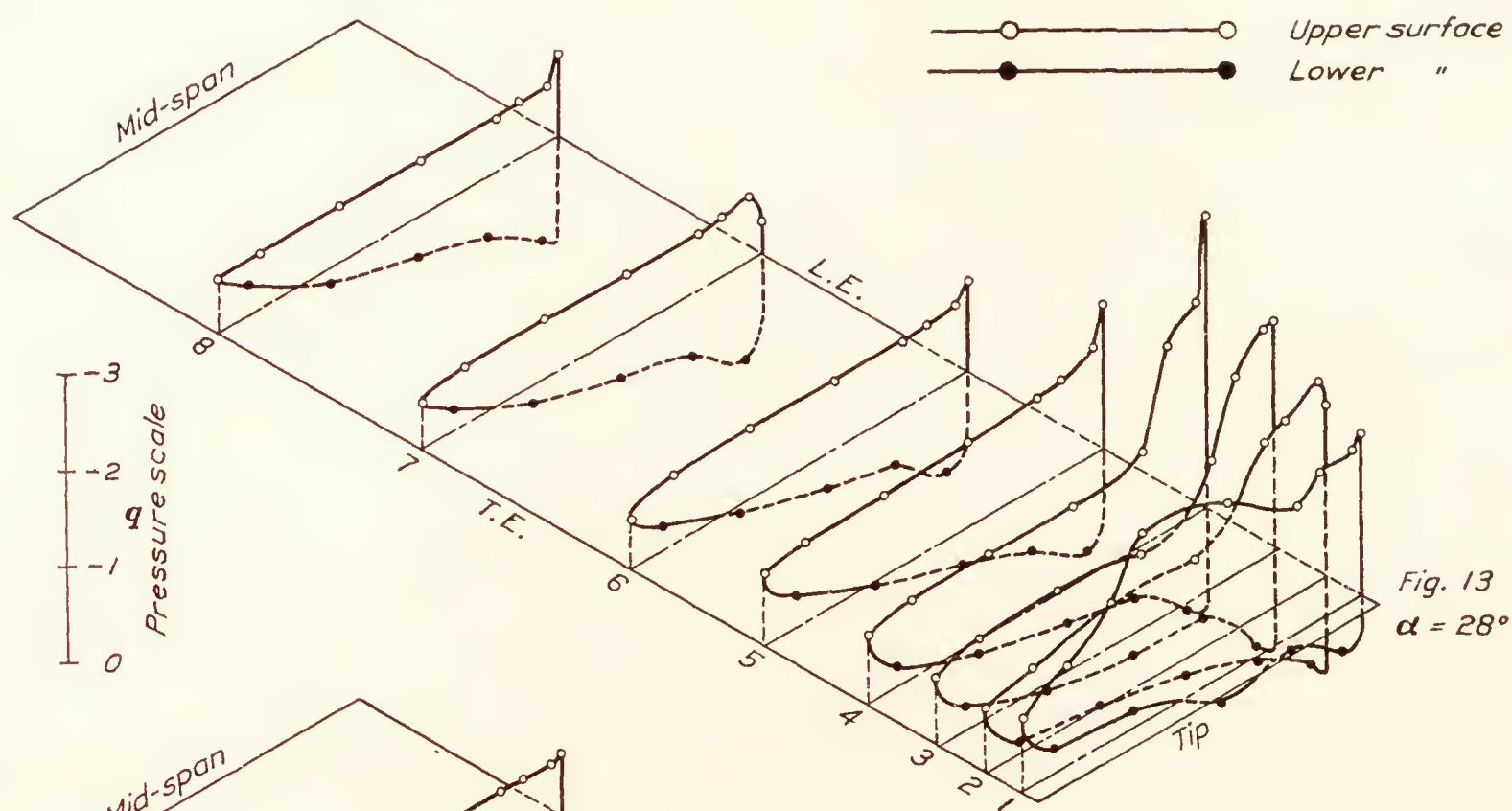


Figs. 9 and 10.—Surface normal pressure distribution

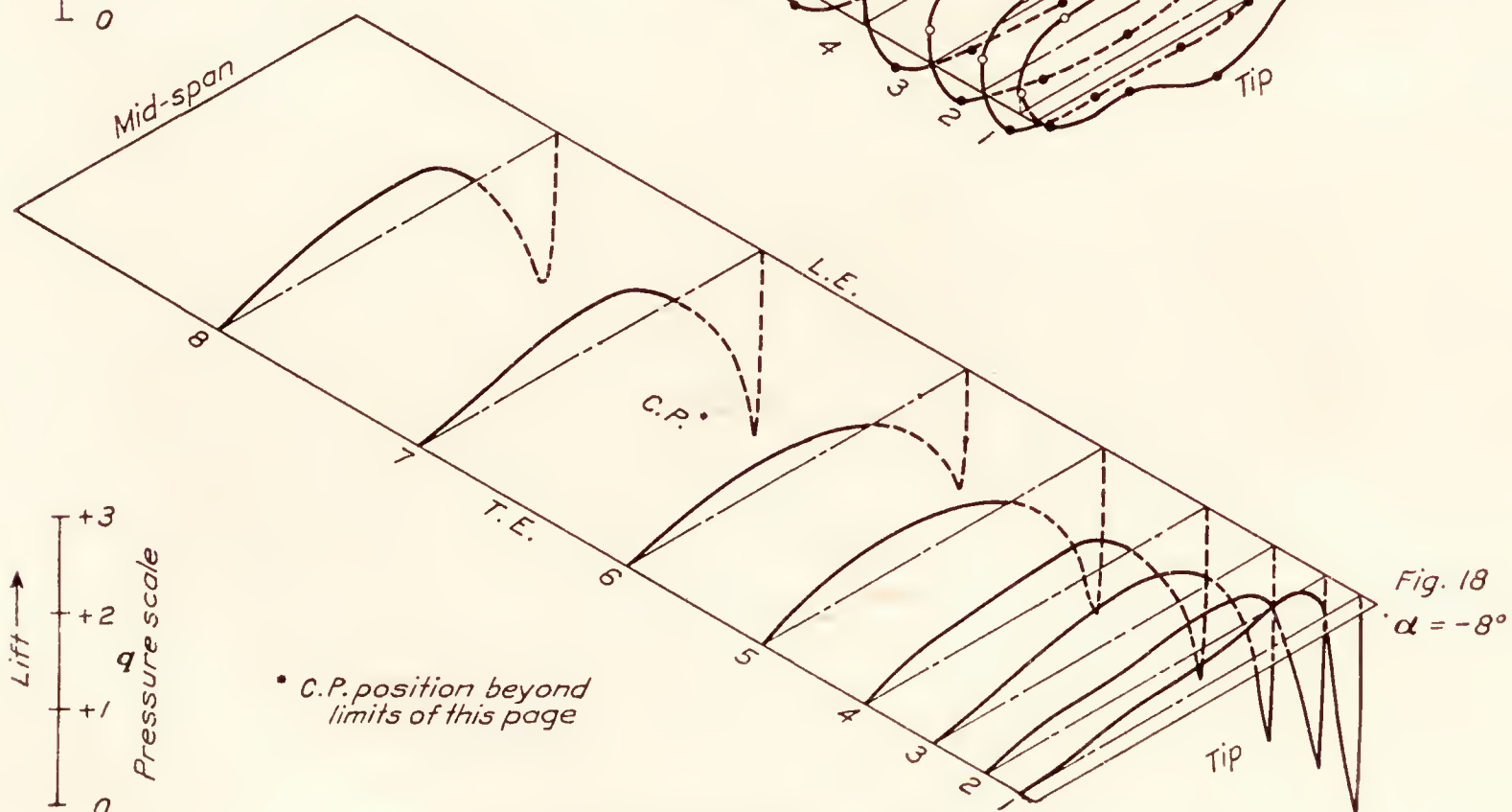
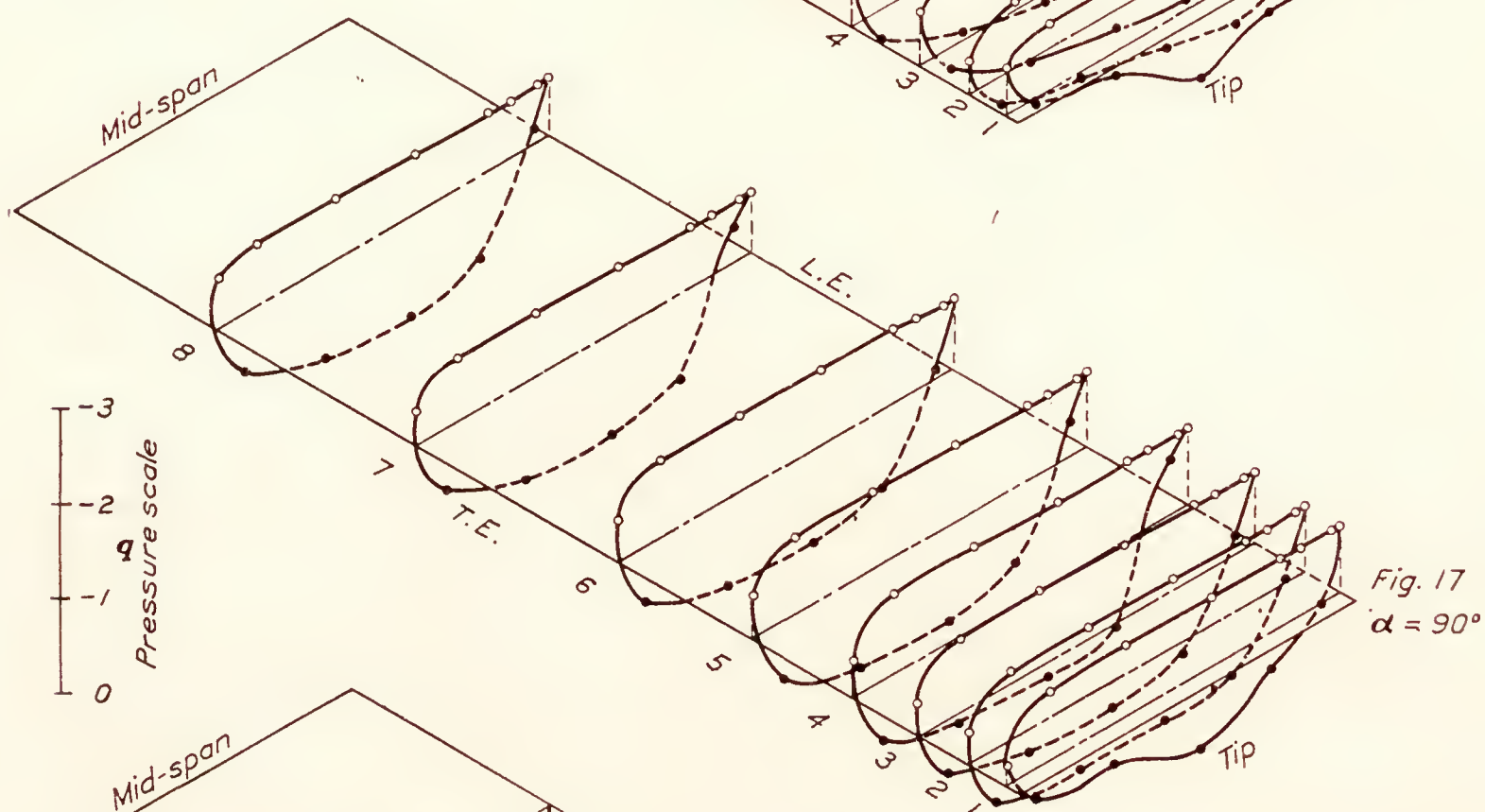
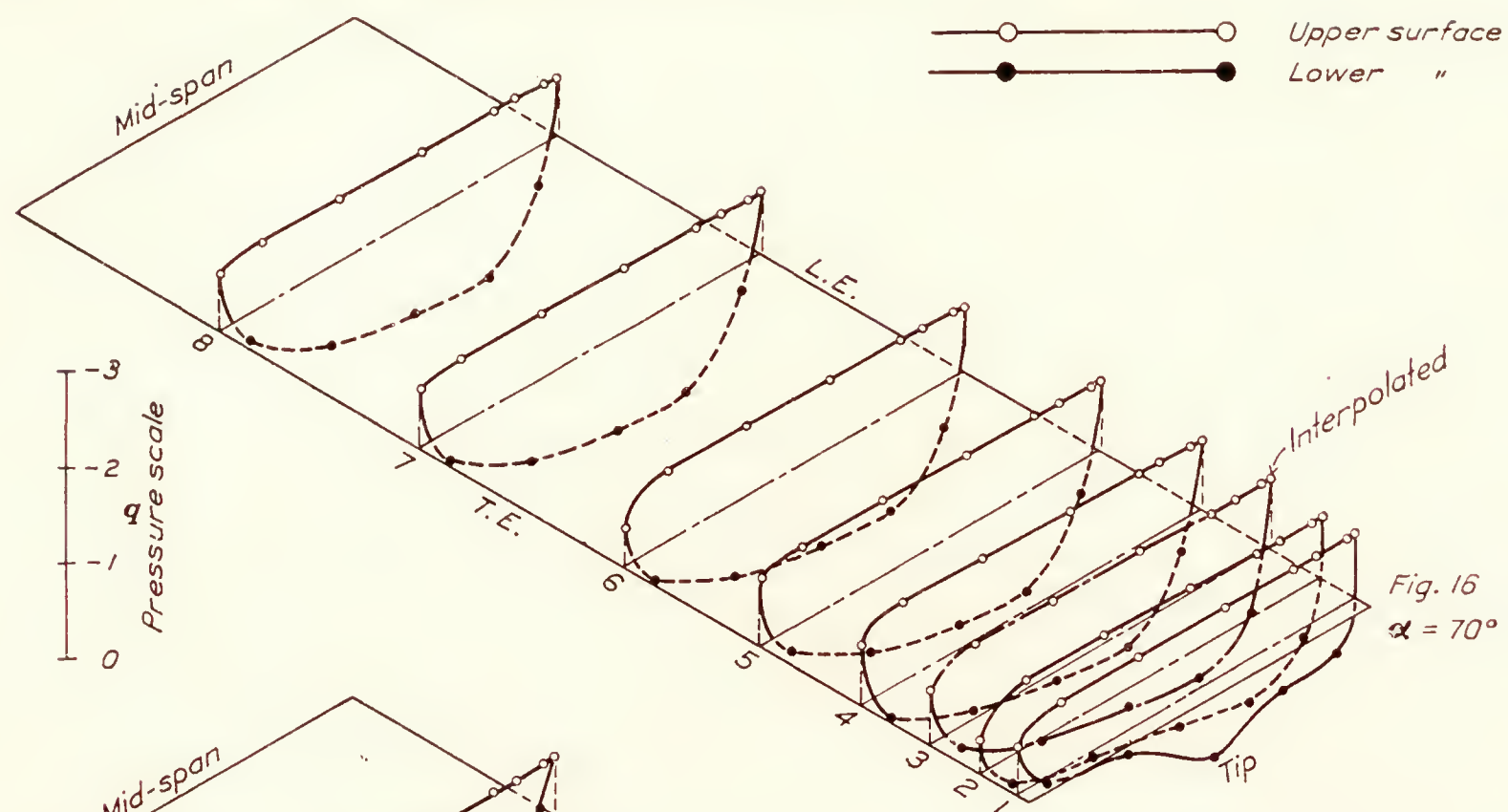


FIGS. 11 and 12.—Surface normal pressure distribution





FIGS. 13, 14, and 15.—Surface normal pressure distribution



FIGS. 16 and 17.—Surface normal pressure distribution  
FIG. 18.—Resultant normal pressure distribution



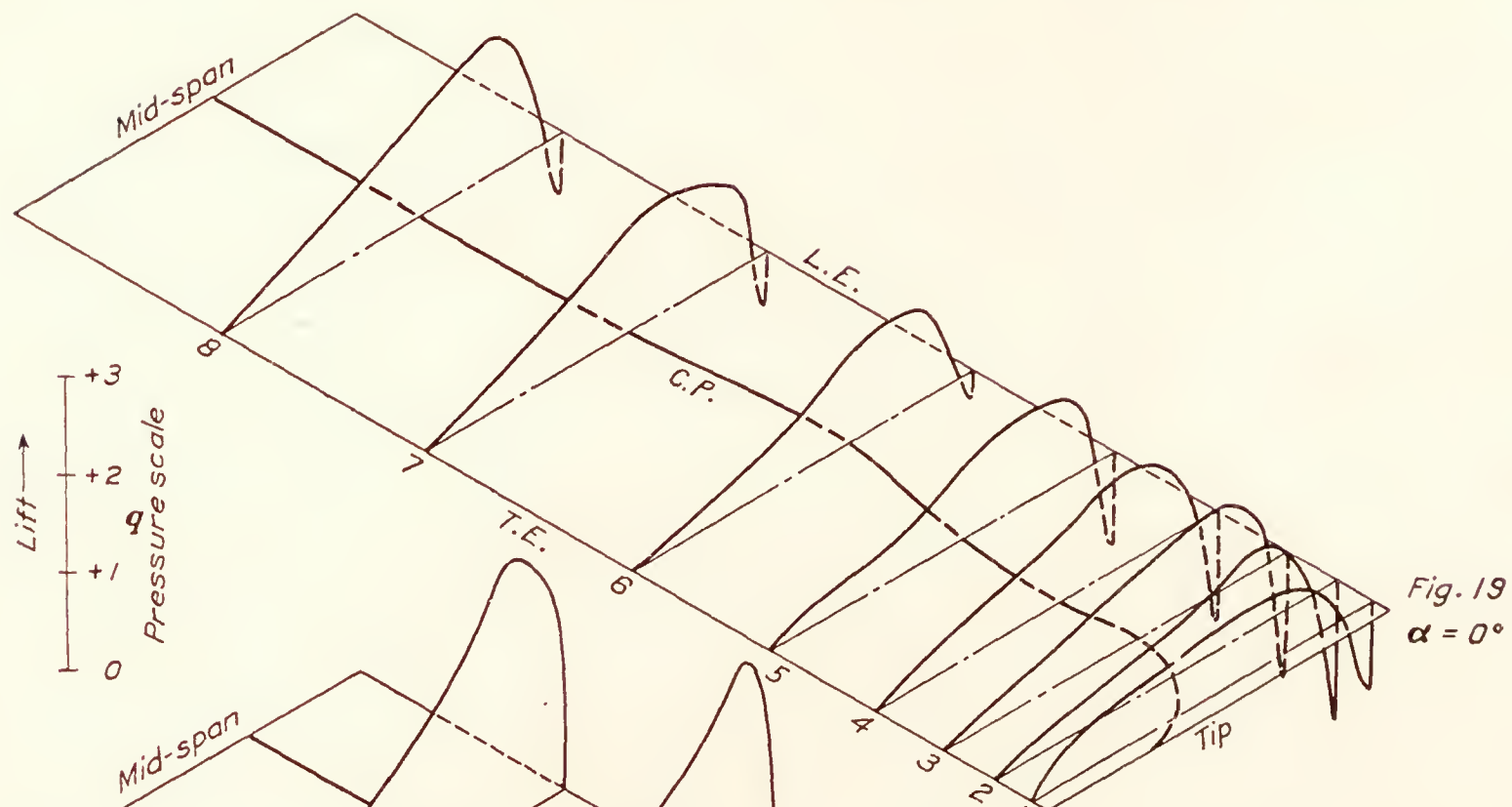


Fig. 19  
 $\alpha = 0^\circ$

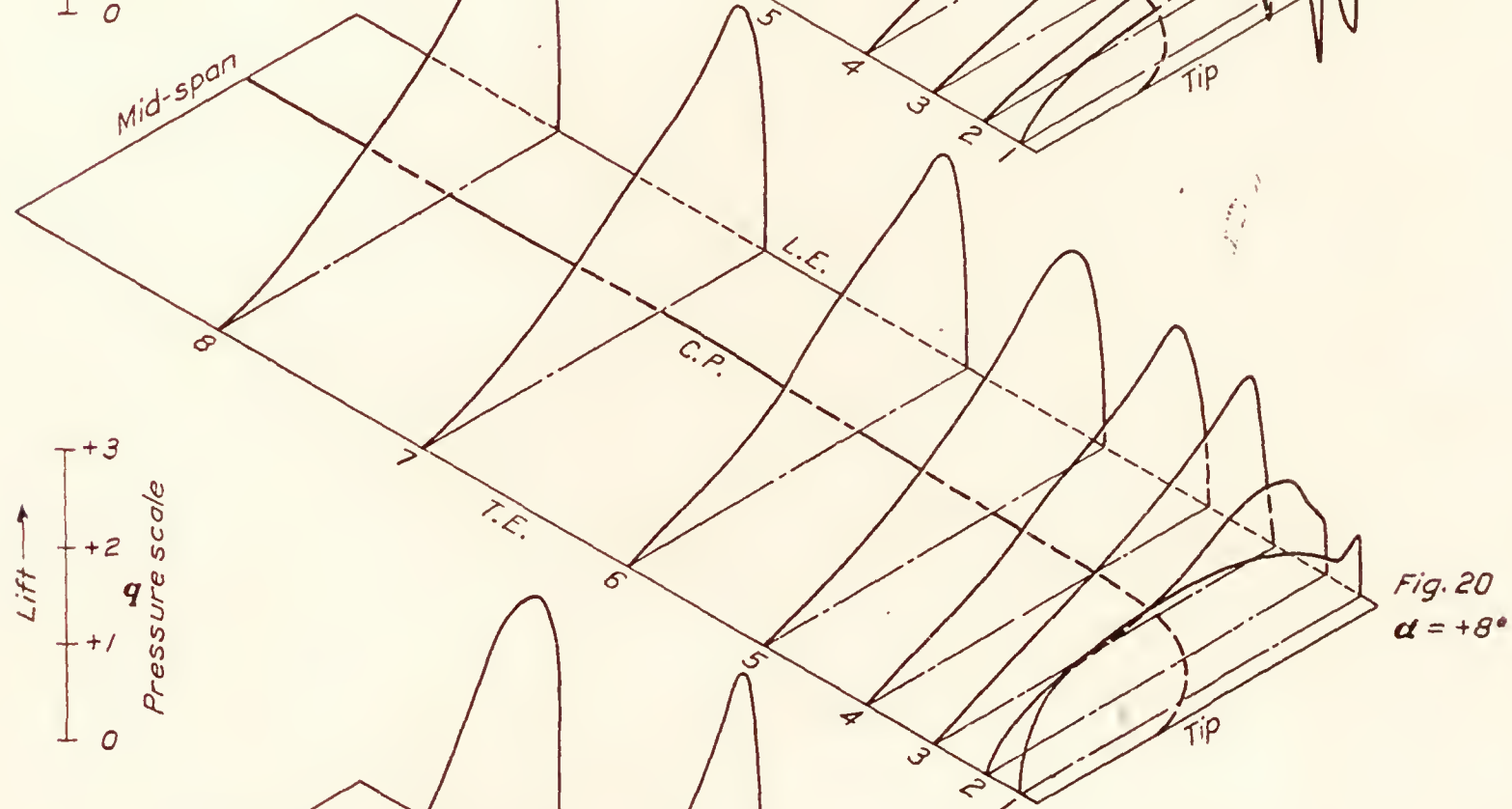


Fig. 20  
 $\alpha = +8^\circ$

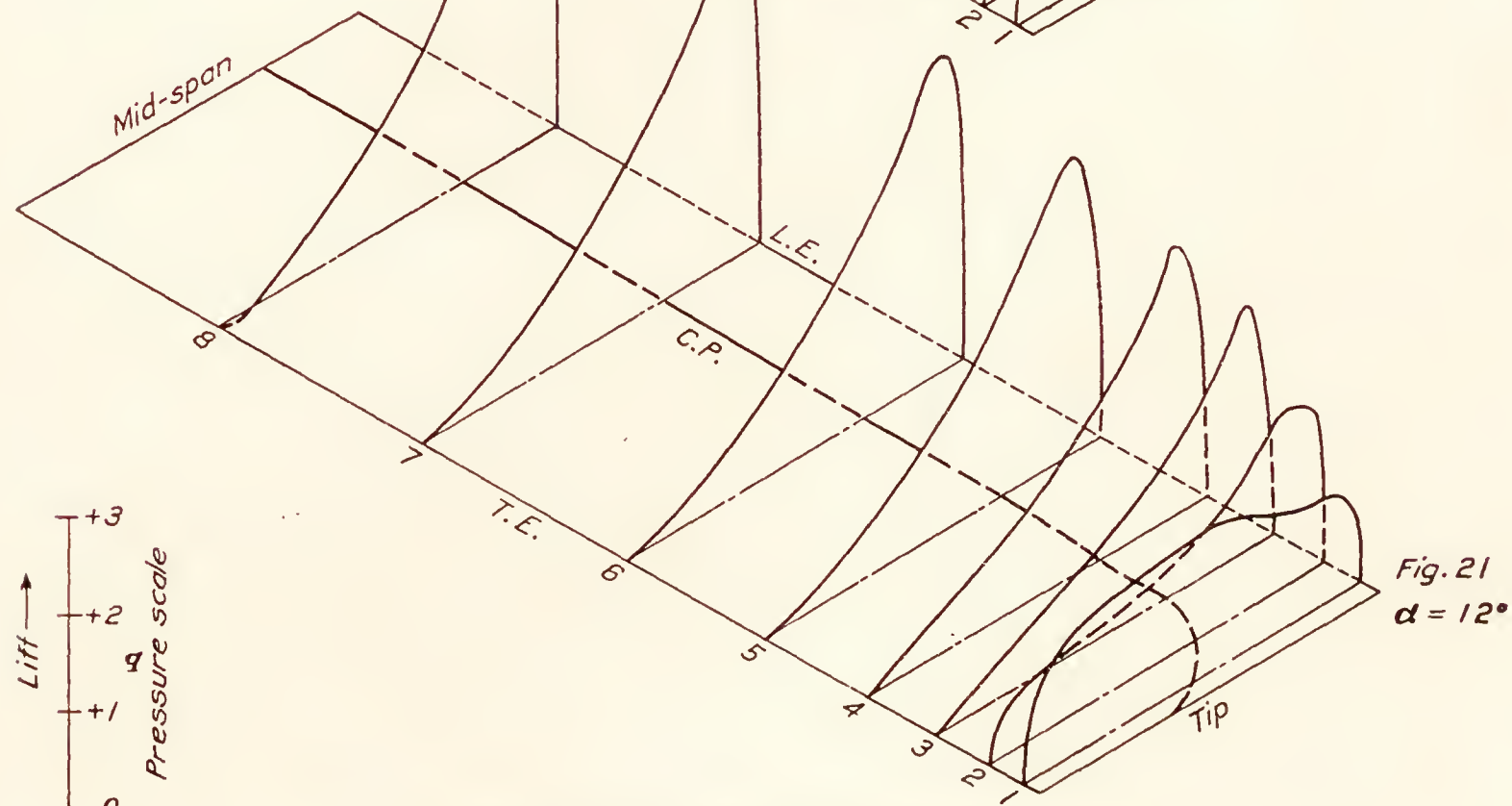
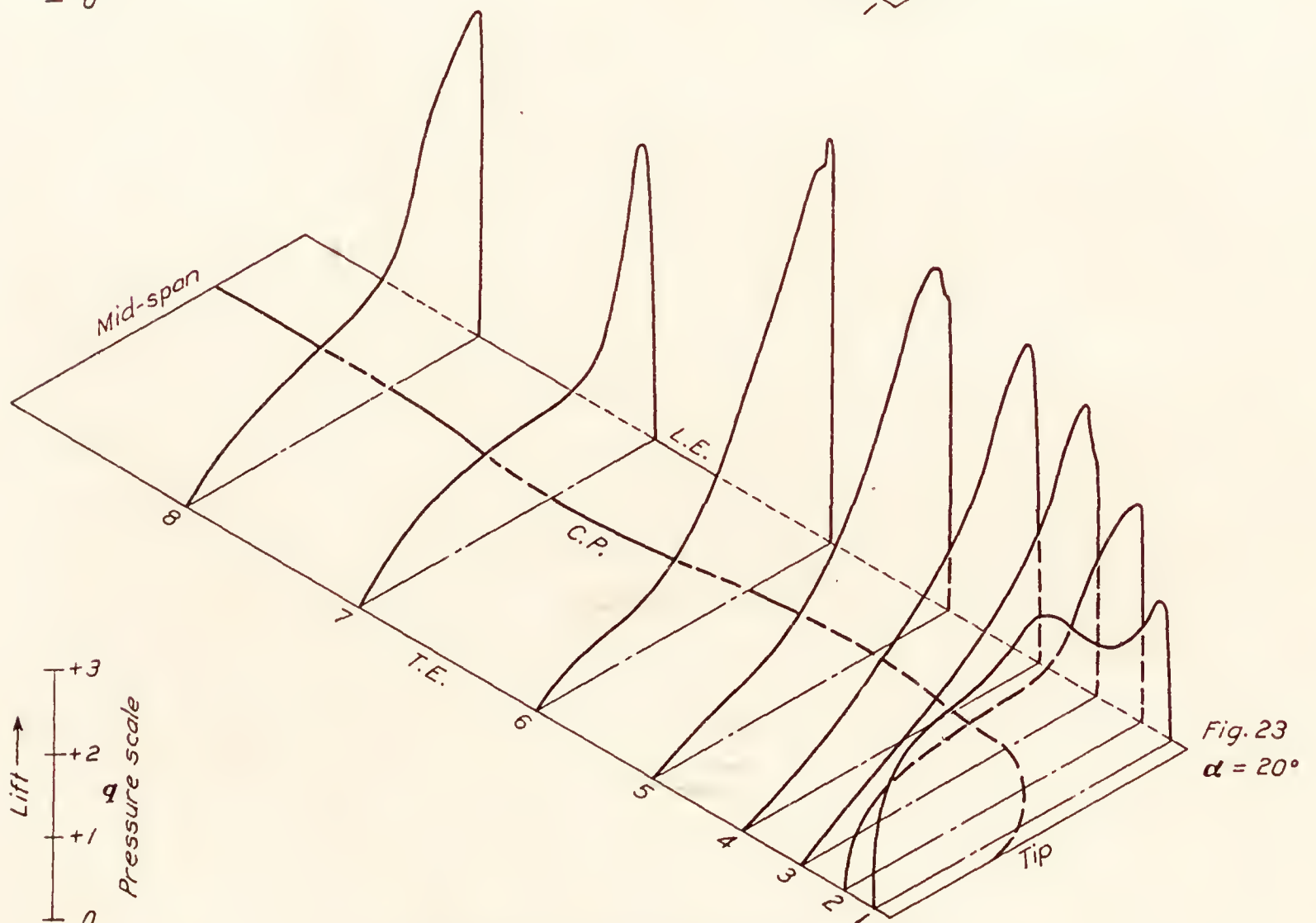
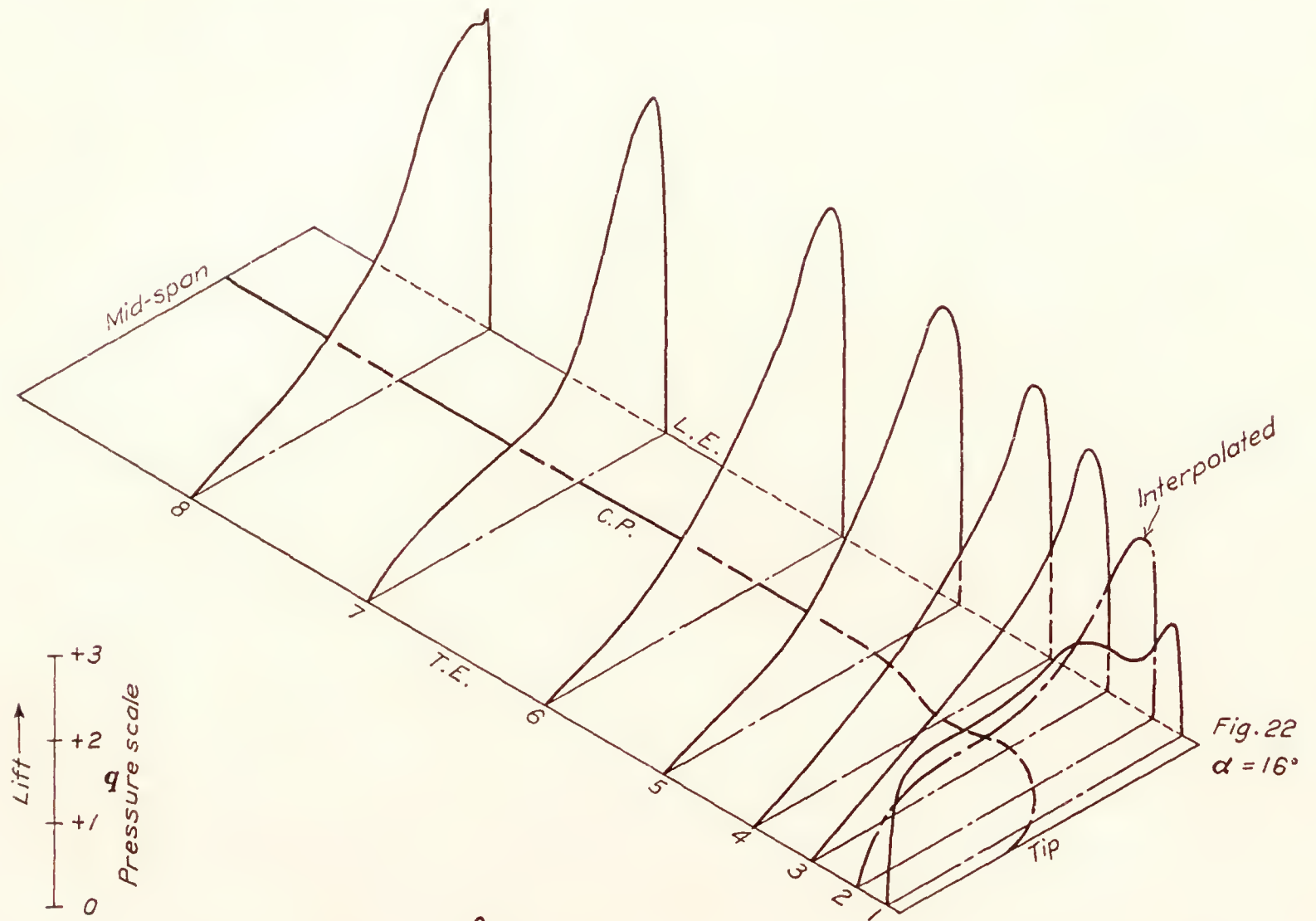


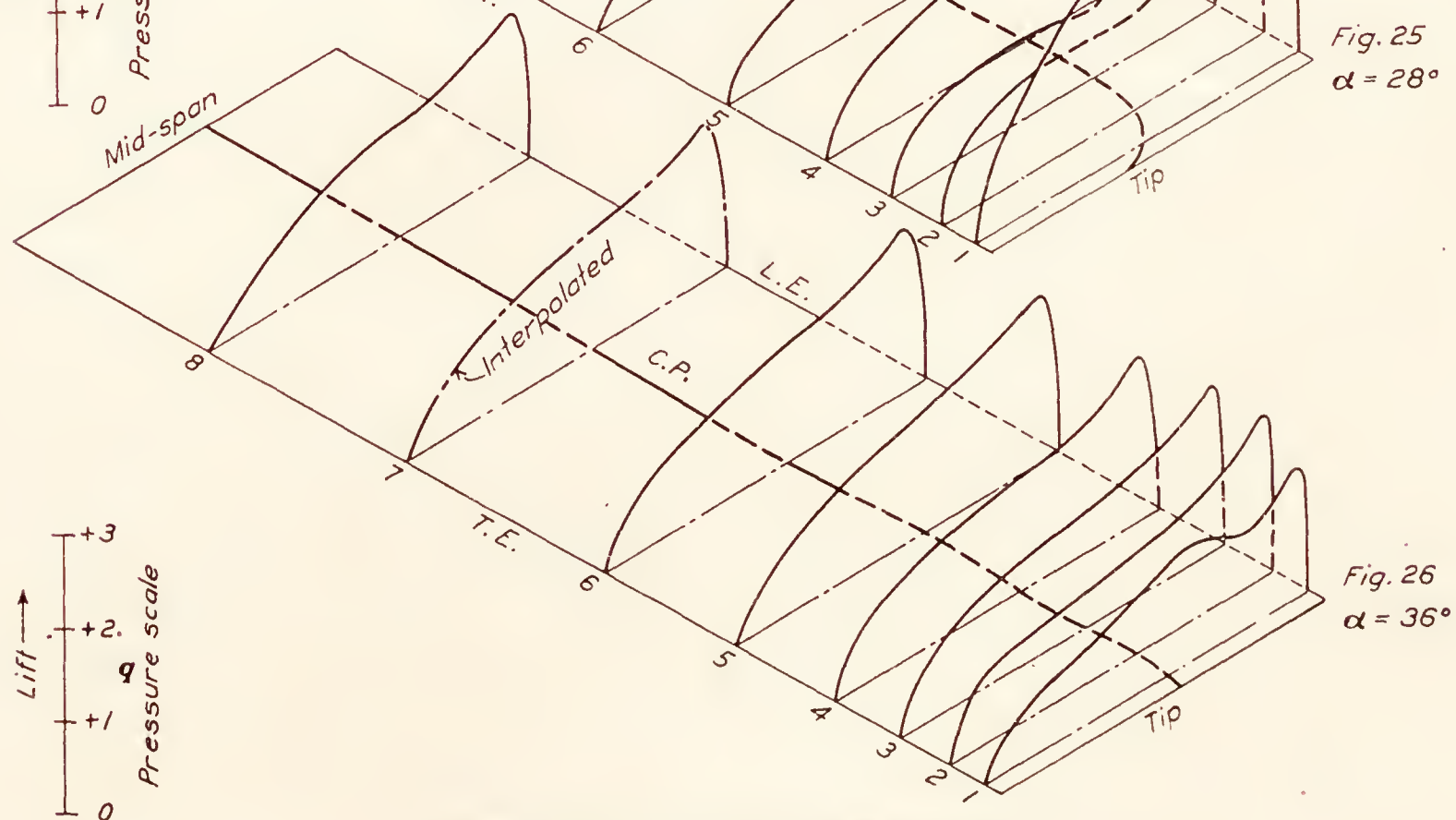
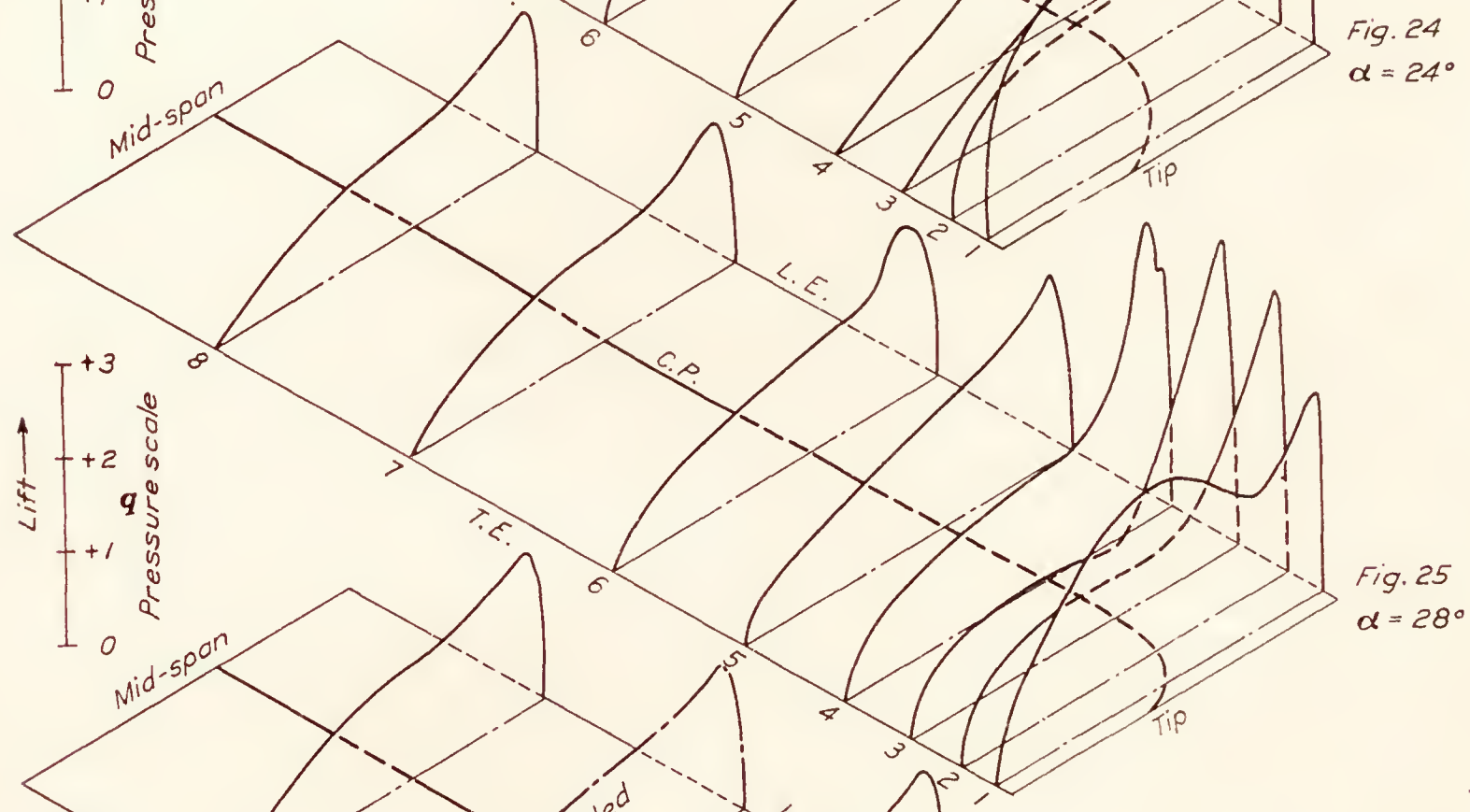
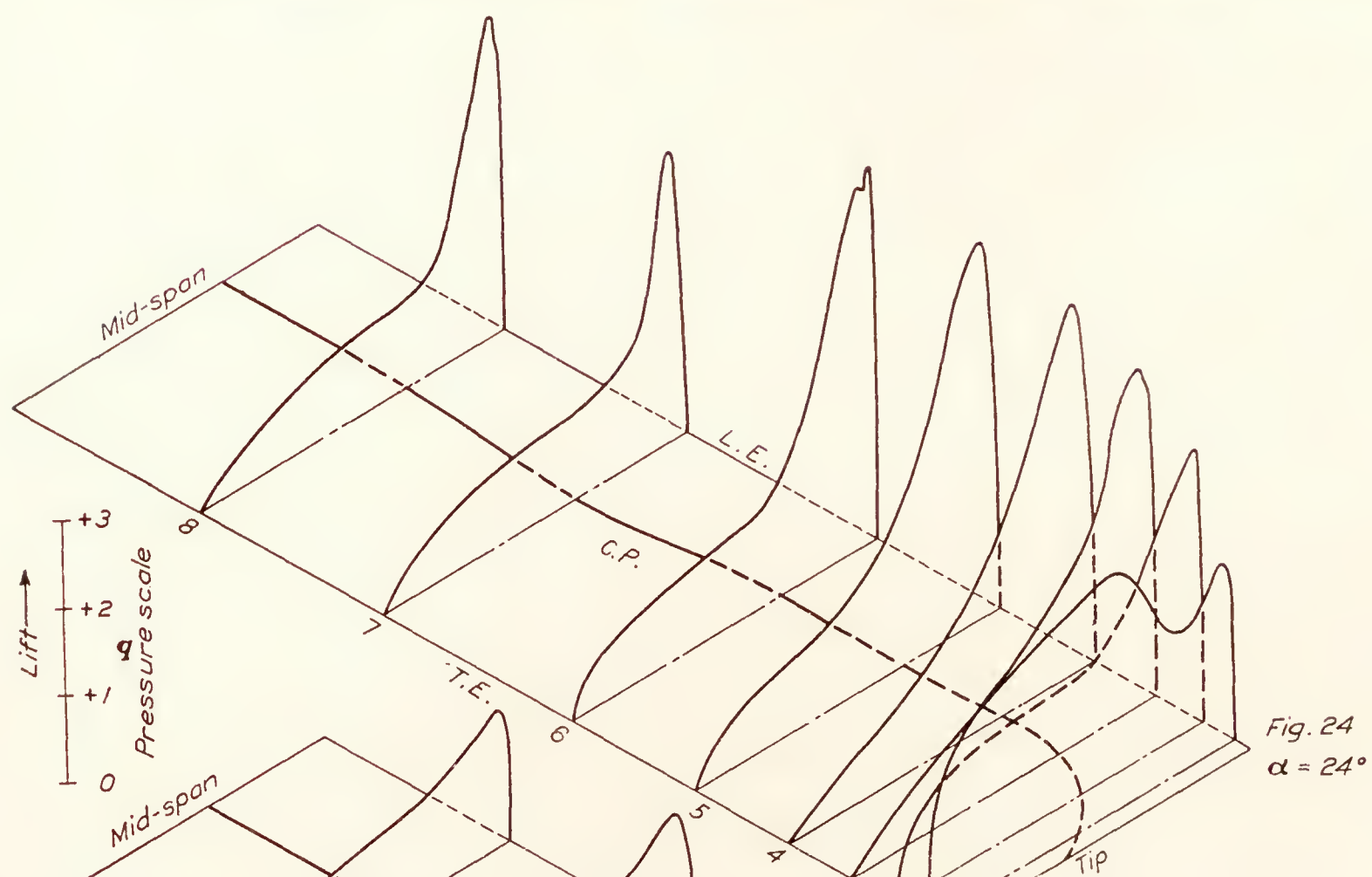
Fig. 21  
 $\alpha = 12^\circ$

FIGS. 19, 20, and 21.—Resultant normal pressure distribution

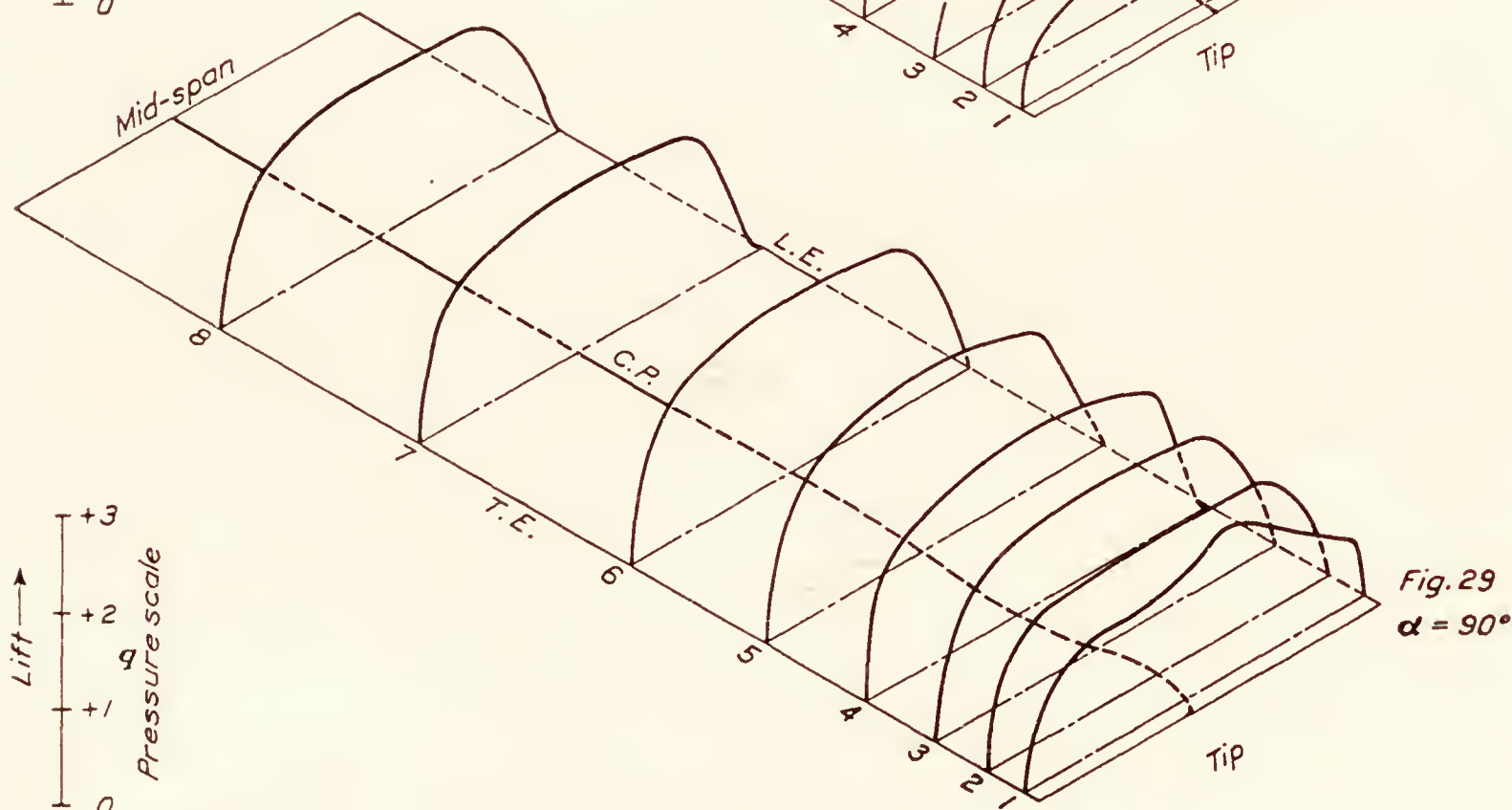
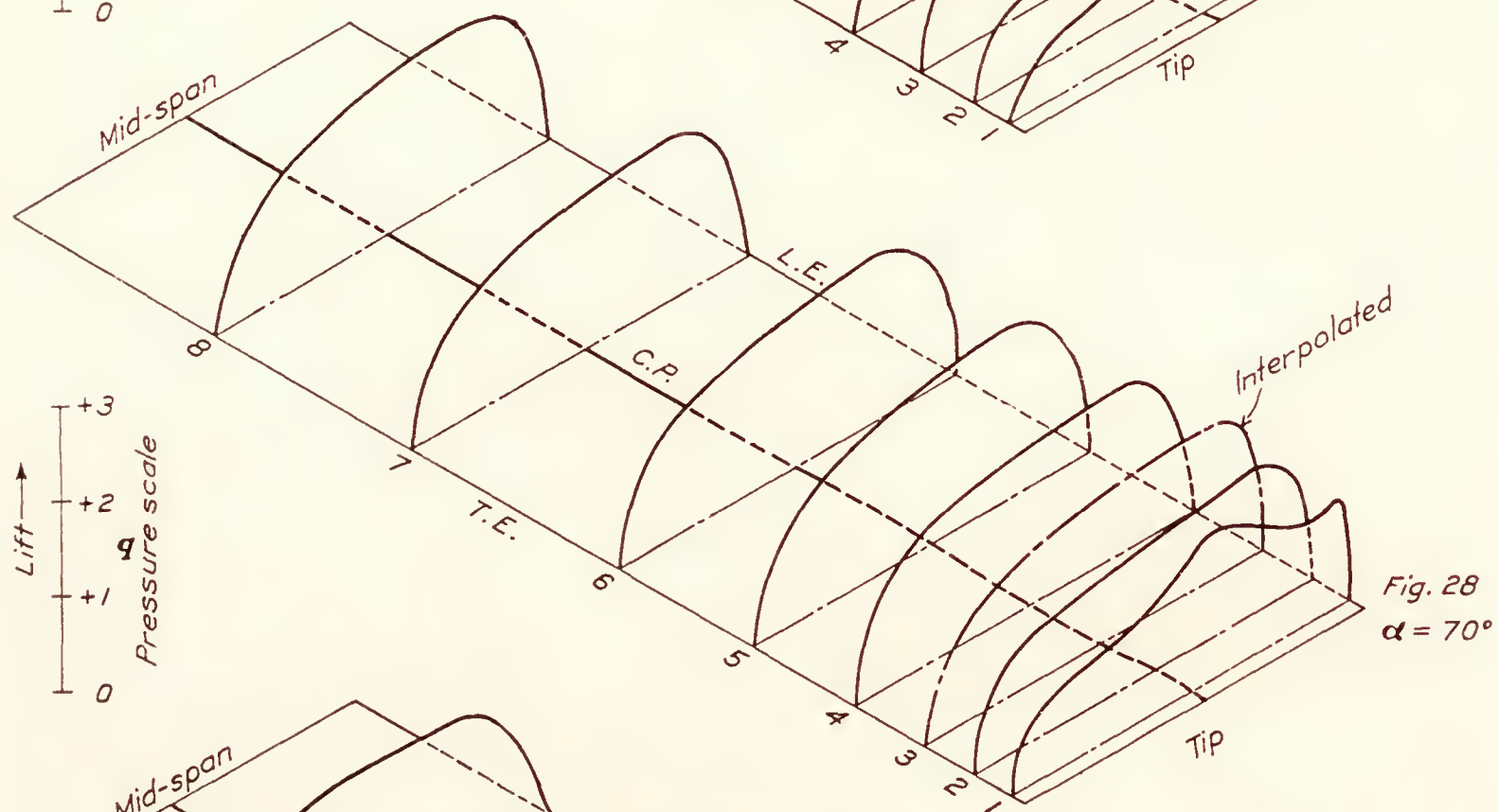
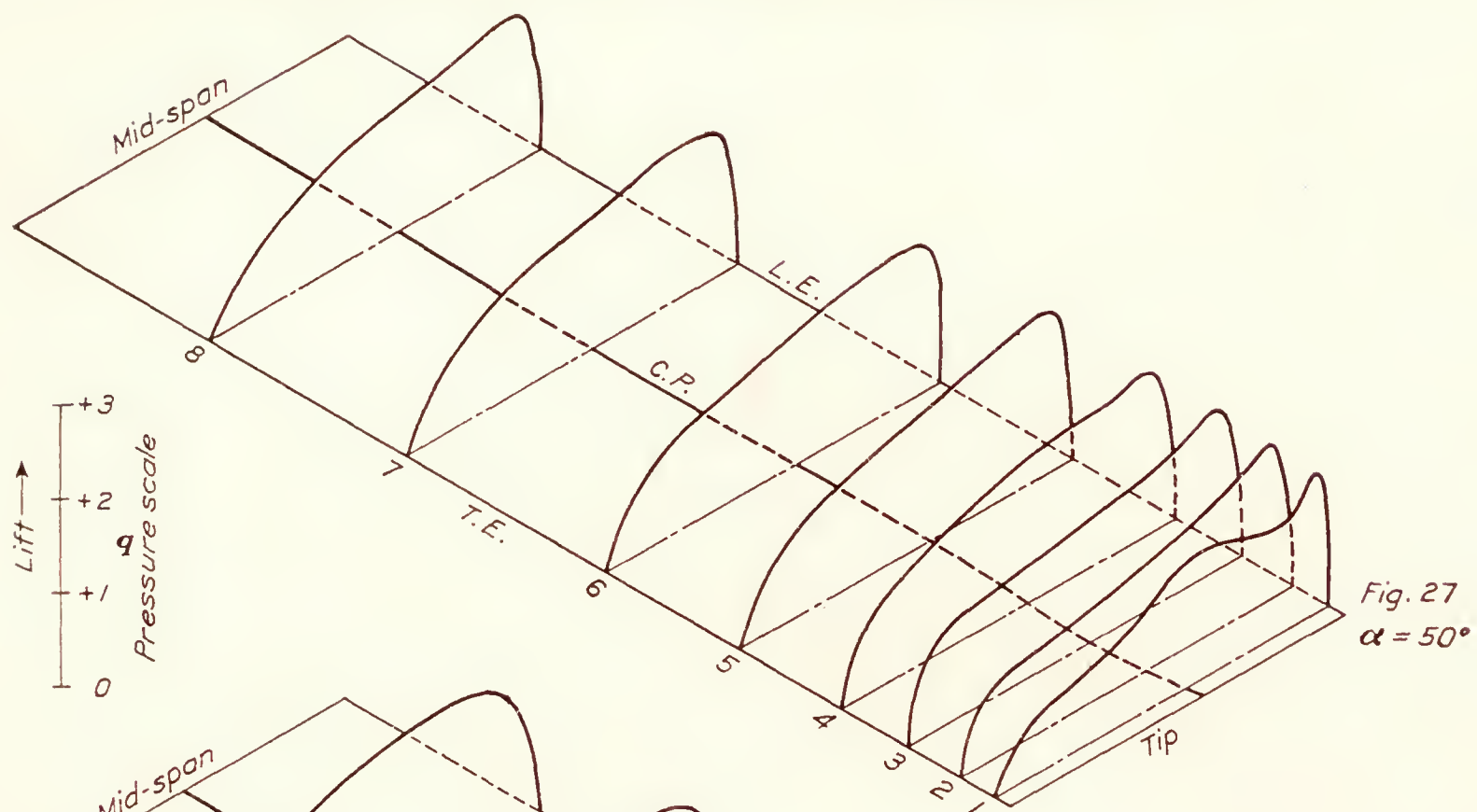


FIGS. 22 and 23.—Resultant normal pressure distribution





FIGS. 24, 25, and 26.—Resultant normal pressure distribution

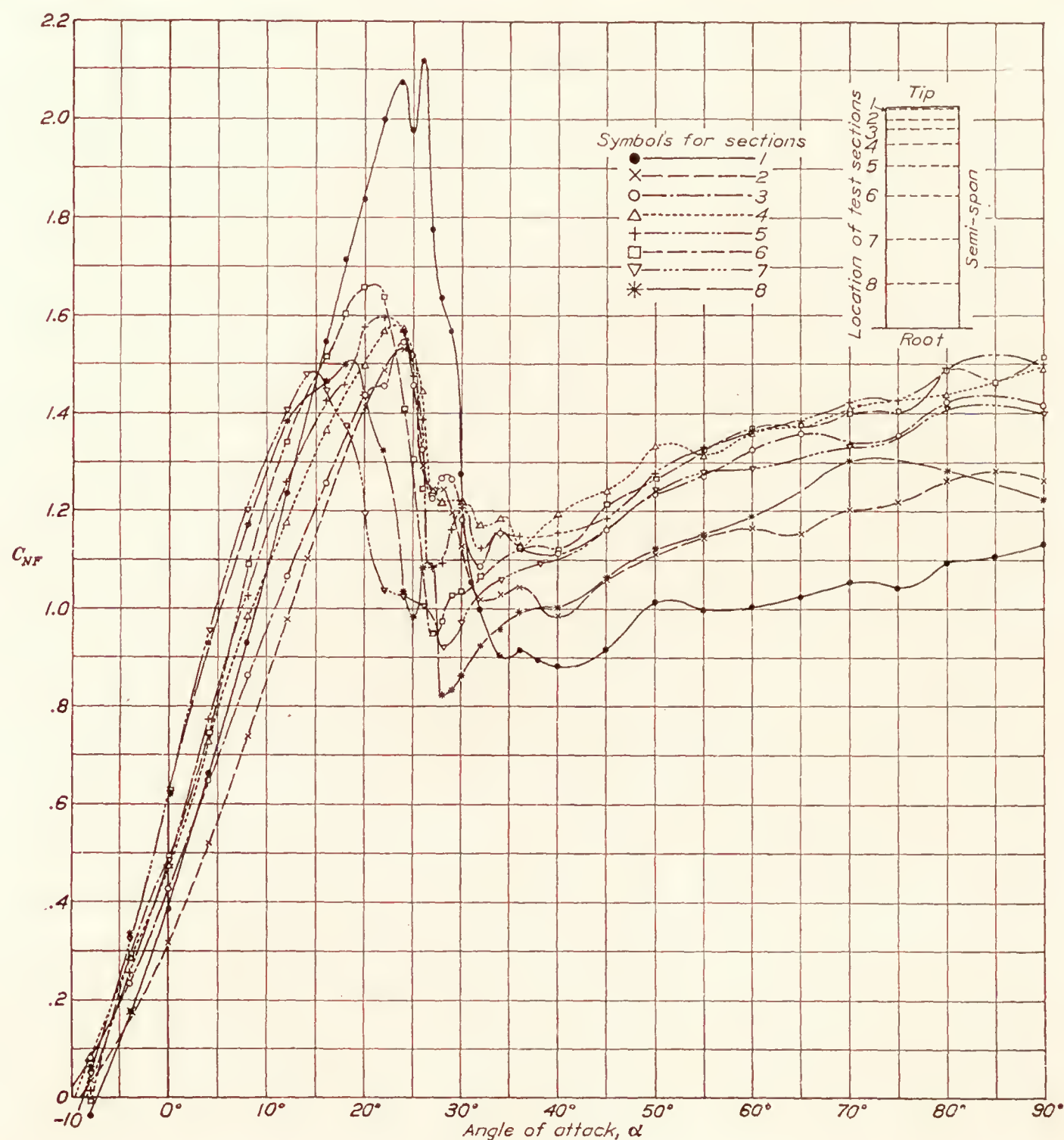


FIGS. 27, 28, and 29.—Resultant normal pressure distribution



## RESULTS

In order to give a three-dimensional impression of the distribution of pressure over the wing model, the pressure diagrams for each section at a given angle of attack are plotted in their respective positions along the span of an isometric plan view of the half wing. The pressures on the upper and lower wing surfaces are presented in this manner in Figures 6-17. Negative

FIG. 30.—Section curves of  $C_{NF}$ 

pressures are plotted upward and positive pressures downward with respect to the chord plane. Figures 18-29 are corresponding diagrams of resultant or total pressures. Lifting pressures are plotted upward. The latter diagrams also contain curves of centers of pressure (C. P.) along the span. A pressure scale in terms of  $q$  is included at the left of each figure. Each of the two sets of diagrams is for angles of attack of  $-8^\circ$ ,  $0^\circ$ ,  $8^\circ$ ,  $12^\circ$ ,  $16^\circ$ ,  $20^\circ$ ,  $24^\circ$ ,  $28^\circ$ ,  $36^\circ$ ,  $50^\circ$ ,  $70^\circ$ , and  $90^\circ$ , the angles being so chosen that interpolations may be made with fair accuracy.

In Figure 30 are given the curves of  $C_{NF}$  vs.  $\alpha$  for each section. The values of  $C_{NF}$  were obtained directly from the manometer records by integrating the pressure diagrams—

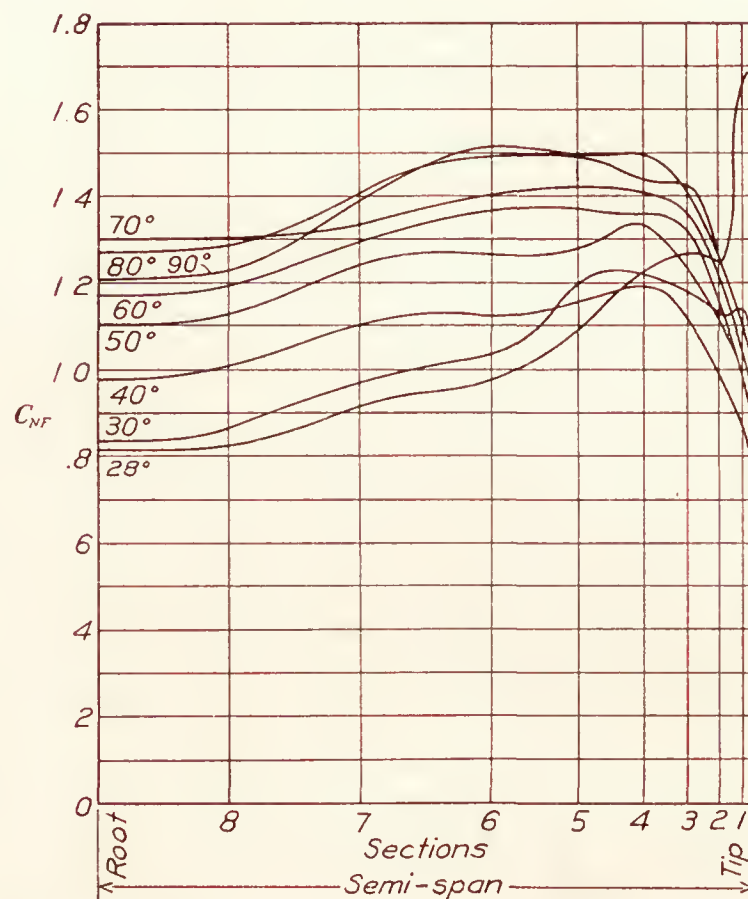
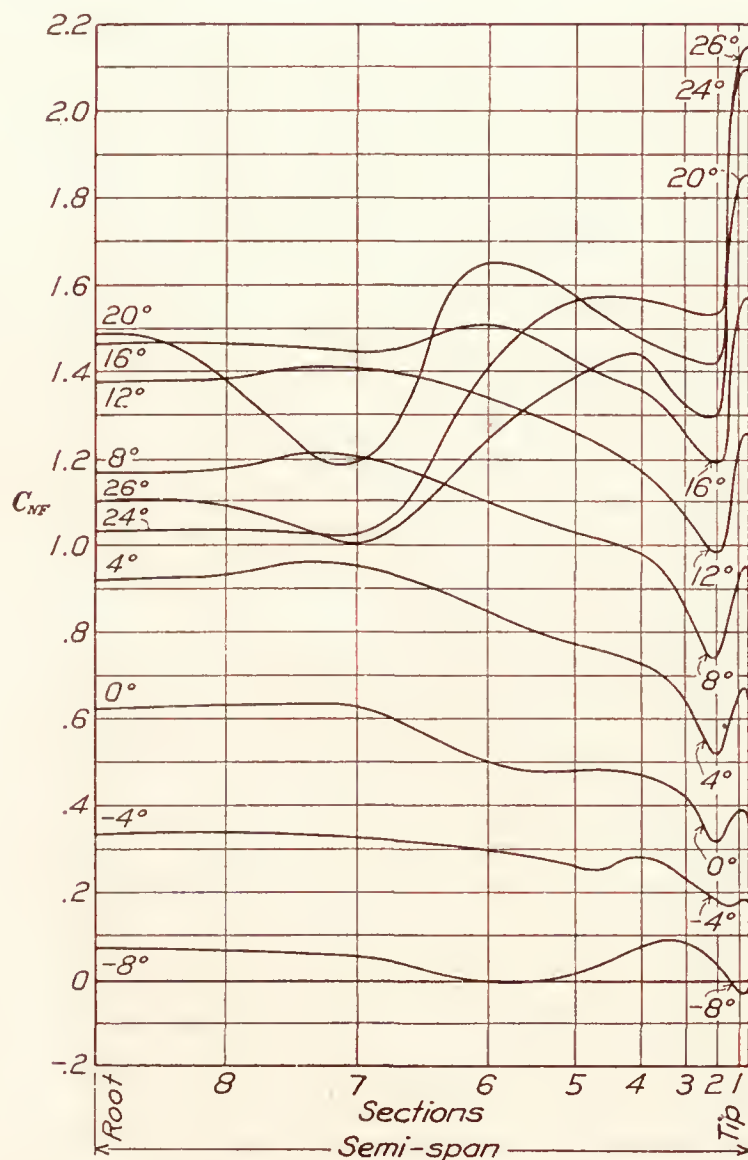
$$C_{NF} = \frac{A}{ql}$$

where  $A$  = integrated area of diagram,

$q$  = dynamic pressure expressed as pressure head determined from stagnation point,

$l$  = length of diagram.

The determination of  $q$  at large angles of attack proved to be a difficult matter. From a careful study of the stagnation points of the pressure diagrams a curve of  $q$  vs.  $\alpha$  was finally obtained for each section. The values of  $q$  taken from these curves were used in the above equation for  $C_{NF}$ .



FIGS. 31a and 31b.—Semispan loads

Considering the wing as a "lifting line,"  $C_{NF}$  is merely the pressure in terms of  $q$  at any point on that line. Figures 31a and 31b show  $C_{NF}$  plotted along the lifting line for various angles of attack. These diagrams not only represent the variation in  $C_{NF}$  along the span, but are also a measure of the load distribution since the wing chord is a constant.

By integrating each of the curves in Figures 31a and 31b and dividing by the length of the diagram the value of  $C_{NF}$  may be obtained for the entire wing for each angle of attack represented. These values are plotted together with the force test results for this wing in Figure 32.

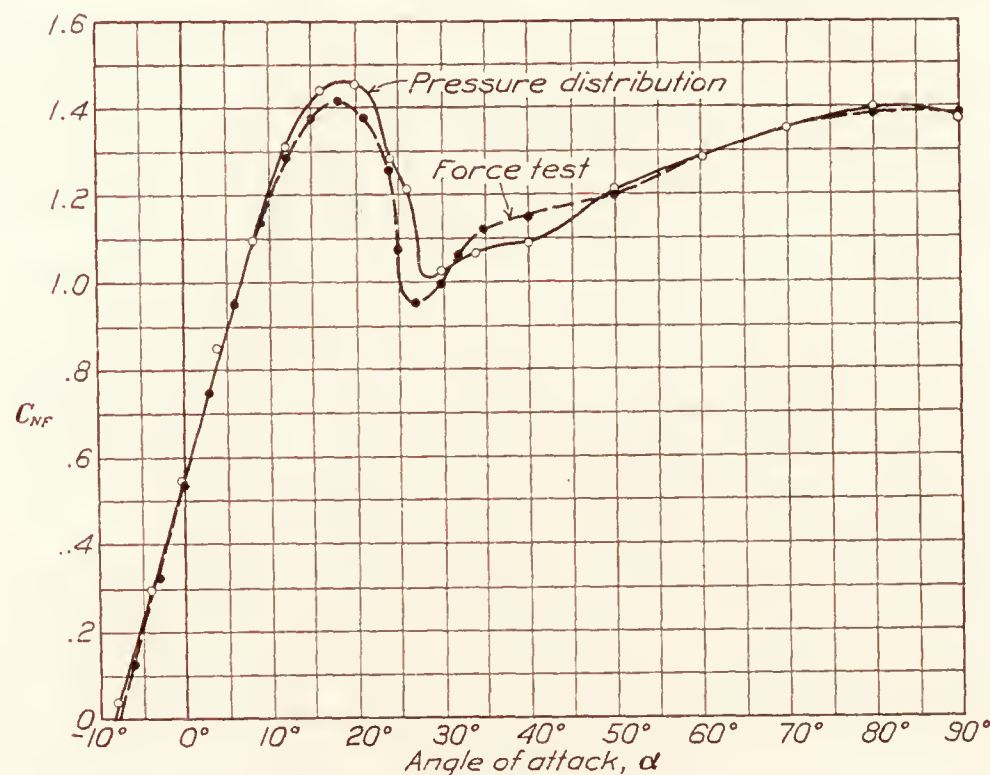
Figure 33 gives the longitudinal center of pressure travel versus  $\alpha$  for the entire wing. This curve is determined from moment integrations of the C. P. curves in Figures 18–29.

A similar curve for the lateral C. P. travel along the semispan is given in Figure 34. This curve is obtained from moment integrations of the semispan load curves of Figures 31a and 31b.



## DISCUSSION

The isometric diagrams of Figures 6-17 furnish a graphic representation of the growth and final collapse of wing surface pressures as the angle of attack is increased. The forward movement of the upper surface boundary layer is shown, beginning with a slight thickening at the

FIG. 32.—Curves of total  $C_{NP}$ 

trailing edge of the diagram of section 7 at  $16^\circ$  (fig. 10), and culminating in complete flow breakdown for all sections at some angle between  $28^\circ$  and  $36^\circ$ , as shown by the flattening of the upper surface diagrams of Figures 13 and 14. These diagrams indicate the nature of the stresses imposed upon the coverings of rectangular airplane wings in steady flight. Figures 10-13 also

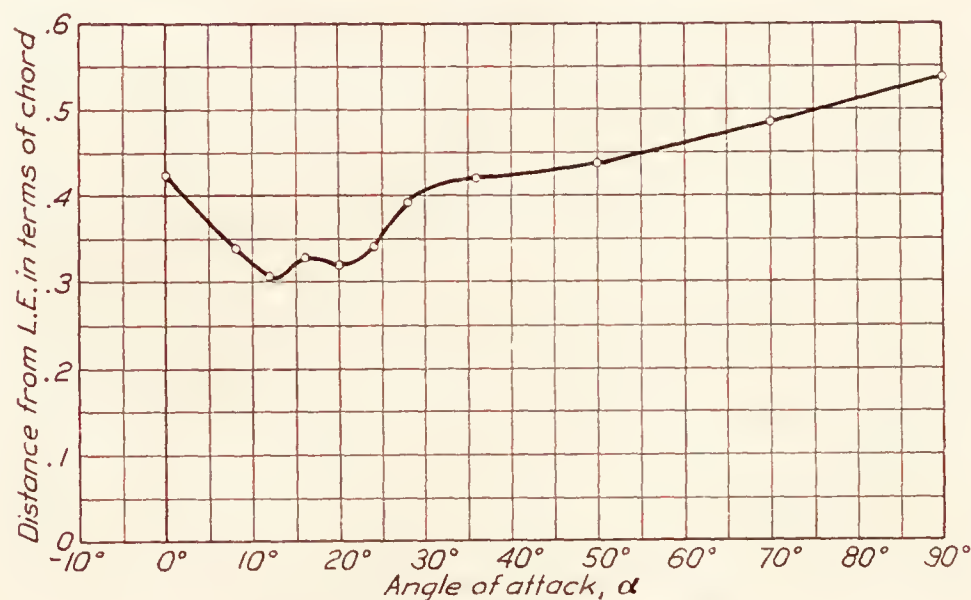


FIG. 33.—Longitudinal center of pressure

show the presence of high nose pressures, signifying that the nose of the Göttingen 387 profile is somewhat too sharp for best results in the vicinity of maximum lift.

The isometric diagrams of Figures 18-29 show the growth and collapse of resultant pressures acting normal to the chord. There is a noteworthy difference both as to shape and size of the pressure diagrams of section 1 as compared with those of other sections. This difference is due to the action of the trailing vortices at the wing tip and practically disappears at  $36^\circ$ . (Fig. 26.)

The curves of longitudinal center of pressure included in Figures 19–29 show that, due to the large tip loads and rearward centers of pressure, undesirable twisting moments are present at the wing tip.

In Figure 30, which contains the curves of  $C_{NF}$  for each section, the high loading of the tip section (No. 1) is evident, reaching a maximum value of 2.12 at  $26^\circ$ . The sharp drop from this value to .90 at  $34^\circ$  is indicative of the strong autorotational tendencies of the rectangular wing tip.

In Figures 31a and 31b the excessive tip loads are once more evident. The load distribution departs considerably from the desired elliptical shape which is the theoretical condition for minimum drag. This fact indicates that inaccurate results will be obtained when the theoretical corrections for aspect ratio, biplane interference, and tunnel wall effect are applied to rectangular wings.

In Figure 32, the comparison between pressure distribution and force test values of  $C_{NF}$  shows good agreement between  $-8^\circ$  and  $+10^\circ$  and between  $50^\circ$  and  $90^\circ$ . Between  $10^\circ$  and  $50^\circ$  the discrepancies are variable, reversing in sign at  $31^\circ$ . The results of force tests at large angles

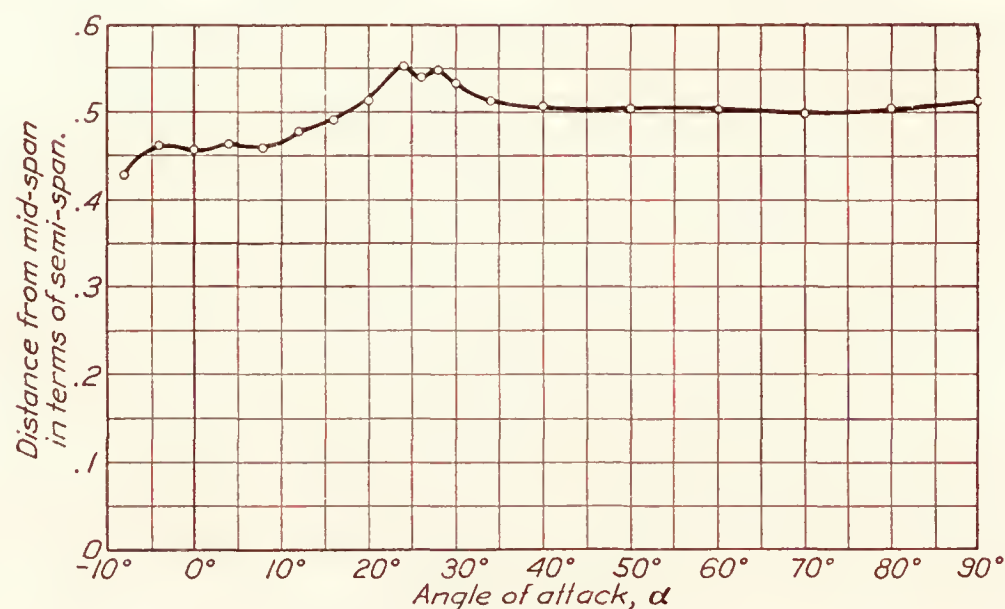


FIG. 34.—Lateral center of pressure

of attack now in progress in the atmospheric tunnel lead to the belief that tunnel wall interference may be the chief cause of these differences. The distance from the wing tip to the tunnel wall was 15 inches for the force tests and about 29 inches for the pressure distribution experiments.

### CONCLUSIONS

Although these tests were run at a low Reynolds Number, it is safe to state that a full scale rectangular wing possesses the following disadvantages:

1. The excessively high tip loads up to large angles of attack ( $C_{NF}=2.12$  at  $\alpha=26^\circ$  for a section 2.48 per cent of semispan from tip) produce large lateral bending moments and longitudinal twisting moments in the wing structure.
2. Above maximum lift such a wing has a high degree of lateral instability.
3. The considerable deviation from elliptical span loading results in increased drag, and also introduces appreciable errors in calculations based on this type of loading.

LANGLEY MEMORIAL AERONAUTICAL LABORATORY,  
NATIONAL ADVISORY COMMITTEE FOR AERONAUTICS,  
LANGLEY FIELD, VA., October 27, 1927.



## REFERENCES AND BIBLIOGRAPHY

- Reference 1. Reid, Elliott G.: Standardization Tests of N. A. C. A. No. 1 Wind Tunnel. N. A. C. A. Technical Report No. 195 (1924).
2. Norton, F. H., and Bacon, David L.: Pressure Distribution Over Thick Airfoils—Model Tests. N. A. C. A. Technical Report No. 150 (1922).
3. Bacon, David L.: The Distribution of Lift Over Wing Tips and Ailerons. N. A. C. A. Technical Report No. 161 (1923).
4. Reid, Elliott G.: Pressure Distribution Over Thick Tapered Airfoils: N. A. C. A. 81, U. S. A. 27 C Modified, and U. S. A. 35. N. A. C. A. Technical Report No. 229 (1926).
5. Fairbanks, A. J.: Distribution of Pressure Over Model of the Upper Wing and Aileron of a Fokker D-VII Airplane. N. A. C. A. Technical Report No. 254 (1927).
6. Fairbanks, A. J.: Pressure Distribution Tests on PW-9 Wing Models Showing the Effects of Biplane Interference. N. A. C. A. Technical Report No. 271 (1927).





---

**REPORT No. 289**

---

**FORCES ON ELLIPTIC CYLINDERS IN UNIFORM  
AIR STREAM**

**By A. F. ZAHM, R. H. SMITH, and F. A. LOUDEN**

**Aerodynamical Laboratory, Bureau of Construction and Repair  
United States Navy**





# REPORT No. 289

## FORCES ON ELLIPTIC CYLINDER IN UNIFORM AIR STREAM

By A. F. ZAHM, R. H. SMITH, and F. A. LOUDEN

### INTRODUCTION

This report presents the results of wind tunnel tests on four elliptic cylinders with various fineness ratios, conducted in the Navy Aerodynamic Laboratory, Washington. The object of the tests was to investigate the characteristics of sections suitable for streamline wire which normally has an elliptic section with a fineness ratio of 4.0; also to learn whether a reduction in fineness ratio would result in improvement; also to determine the pressure distribution on the model of fineness ratio 4.

Four elliptic cylinders with fineness ratios of 2.5, 3.0, 3.5, and 4.0 were made and then tested in the 8 by 8 foot tunnel; first, for cross-wind force, drag, and yawing moment at 30 miles an hour and various angles of yaw; next for drag at 0° pitch and 0° yaw and various wind speeds; then for end effect on the smallest and largest models; and lastly for pressure distribution over the surface of the largest model at 0° pitch and 0° yaw and various wind speeds. In all tests, the length of the model was transverse to the current. The results are given for standard air density,  $\rho = .002378$  slug per cubic foot.

This account is a slightly revised form of Report No. 315, prepared for the Bureau of Aeronautics, July 13, 1926, and by it submitted for publication to the National Advisory Committee for Aeronautics. A summary of conclusions is given at the end of the text.

### DESCRIPTION OF MODELS

The four elliptic cylinders, the smallest of which is shown in Figure 1, and profiles of which are shown in Figure 10, were each 62 inches long and 2 inches thick; their widths were 5, 6, 7, and 8 inches. The specified offsets are given in Table 1 and for each case can be derived from the equation of an ellipse. All of the cylinders were of laminated pine, varnished, and then verified by application of their construction templates. After the tests, however, a few measurements of offsets taken on the plane table indicated that the models were slightly unsymmetrical. The 2 by 8 inch cylinder had detachable end segments to fill up the space between the floor and ceiling of the tunnel during the pressure distribution test.

In a second test series adjoining end plates, Figure 1, were used to determine the end effect on two of the cylinders. They were made from fairly plane galvanized-iron plate and measured 24 by 24 inches.

In Figure 2 the pressure collector is shown inserted as a center segment in the 2 by 8 inch model. It was made of bronze accurate to 0.001 inch in the offsets. Its dimensions and the location of its 16 holes are given in Figure 3. The pressure leads, one running from a hole in the nose and the other successively from each surface hole, were each connected with  $\frac{1}{4}$ -inch tubing which ran lengthwise through the strut to a manometer outside the tunnel.

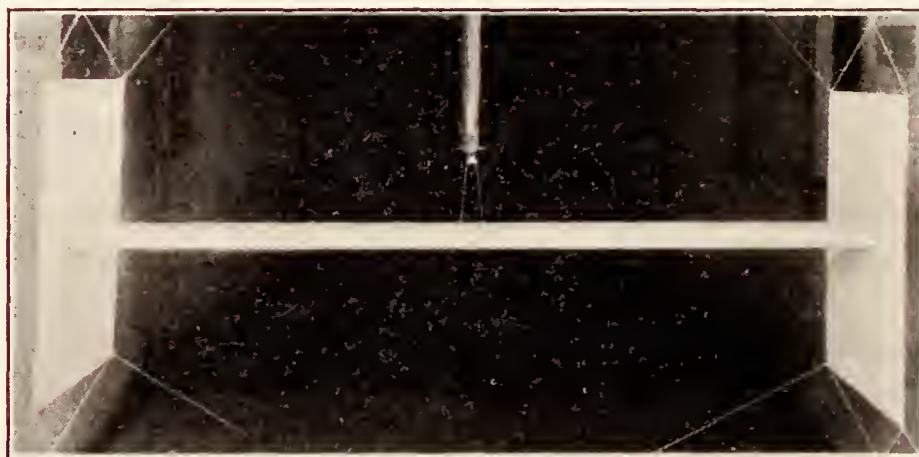


FIG. 1.—Elliptic cylinder 2 by 5 inches mounted with end plates



## METHOD OF TESTING

To measure the forces and yawing moment, each cylinder was mounted, without end plates, at its center on the two-prong fork, Figure 1, extending from the shank of the tri-dimensional balance described in reference 1. The angle of yaw was varied from  $-6^\circ$  to  $20^\circ$  by  $2^\circ$  intervals, the wind speed was held at 30 miles an hour, and the cross-wind force, drag, and yawing

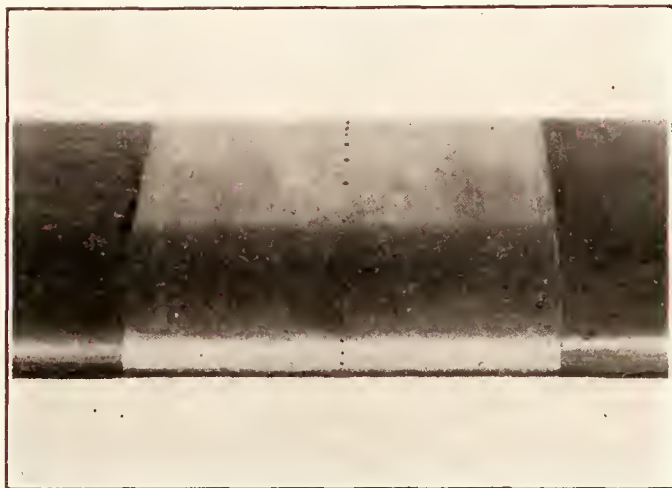


FIG. 2.—Pressure collector inserted in 2 by 8 inch elliptic cylinder

moment were simultaneously measured on the cylinder and exposed portion of the holder; then on the holder alone with the cylinder detached but not removed. The difference was taken as the true force or moment component. The precision of such measurements is given in Reference 2. The drag measurements with the cylinders at  $0^\circ$  pitch and  $0^\circ$  yaw were taken in the same way; the wind speed being varied from 20 to 60 miles an hour by 10 mile intervals.

To determine the end effect of the smallest and largest cylinders, the plates were mounted at the ends of the model as shown in Figure 1, and the cross-wind force and drag were measured at intervals of  $4^\circ$  yaw. The measurements were repeated without the plates.

The percentage difference applied to the original force data gave values for the infinite cylinder.

The pressure distribution measurements were made on the 2 by 8 inch cylinder, which was mounted vertically in the tunnel with extension end segments accurately in line and with the pressure collector inserted in the middle of its span. The difference of pressure between the nose and each of the holes aft of the nose was determined successively. To do this all the surface holes were plugged except one which was joined to one pressure lead, while the nose hole was joined to the other lead. The wind speed was then varied from 20 to 70 miles an hour, by 10 mile intervals, and the differential pressure was measured on an alcohol manometer having a 1 to 10 slope. These measurements could be read in all cases to within 0.005 inch vertical of alcohol. Thus the point pressure could be determined to about one-half of 1 per cent for speeds above 40 miles an hour; to within less than 2 per cent for the lower speeds. The air speed was held constant to within one-half of 1 per cent.

## RESULTS OF FORCE AND MOMENT MEASUREMENTS

The cross-wind force and drag on the 62-inch cylinders at various angles of yaw are given in Tables II and III together with

their coefficients which are the respective forces divided by  $\frac{1}{2} \rho V_1^2$  times the frontal area  $S$ ,  $V_1$  being feet per second. The coefficients are plotted in Figures 4 and 6.

The cross-wind coefficient <sup>1</sup> increases positively at negative yaw and negatively at positive yaw as the fineness ratio is increased from 2.5 to 4.0. The fact that the force is not zero at zero yaw is probably due to the models being slightly unsymmetrical. The maximum coefficient is  $-4.28$  for the 2 by 8 inch cylinder.

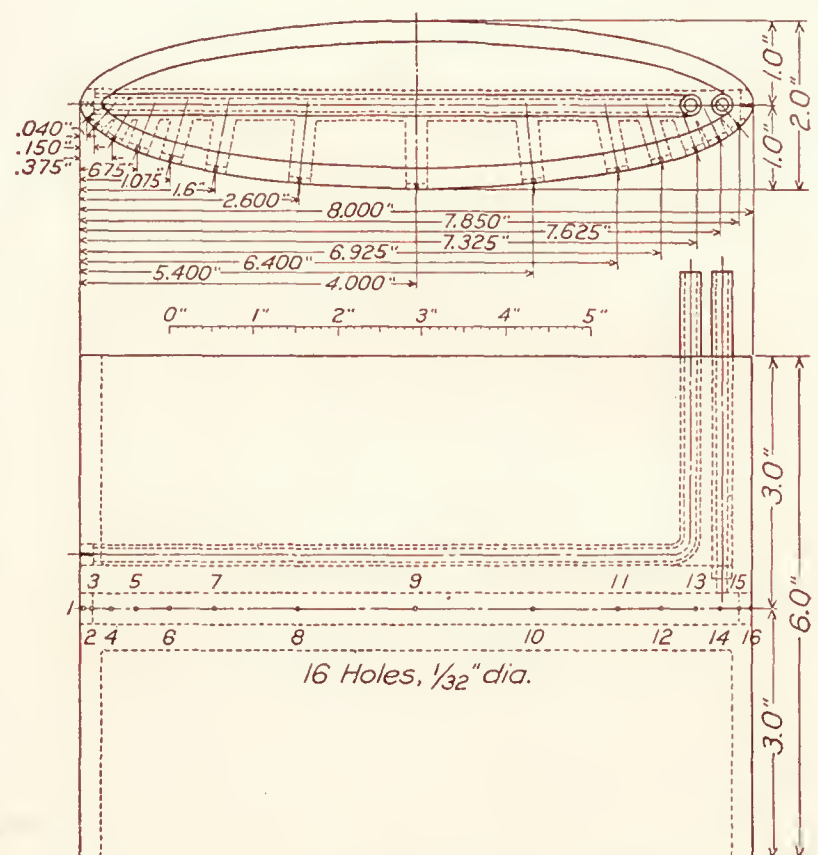


FIG. 3.—Bronze pressure collector for elliptic cylinder 2 by 8 inches, fineness ratio 4

<sup>1</sup> To express these cross-wind coefficients as lift coefficients, multiply them by frontal area/chord-plane area



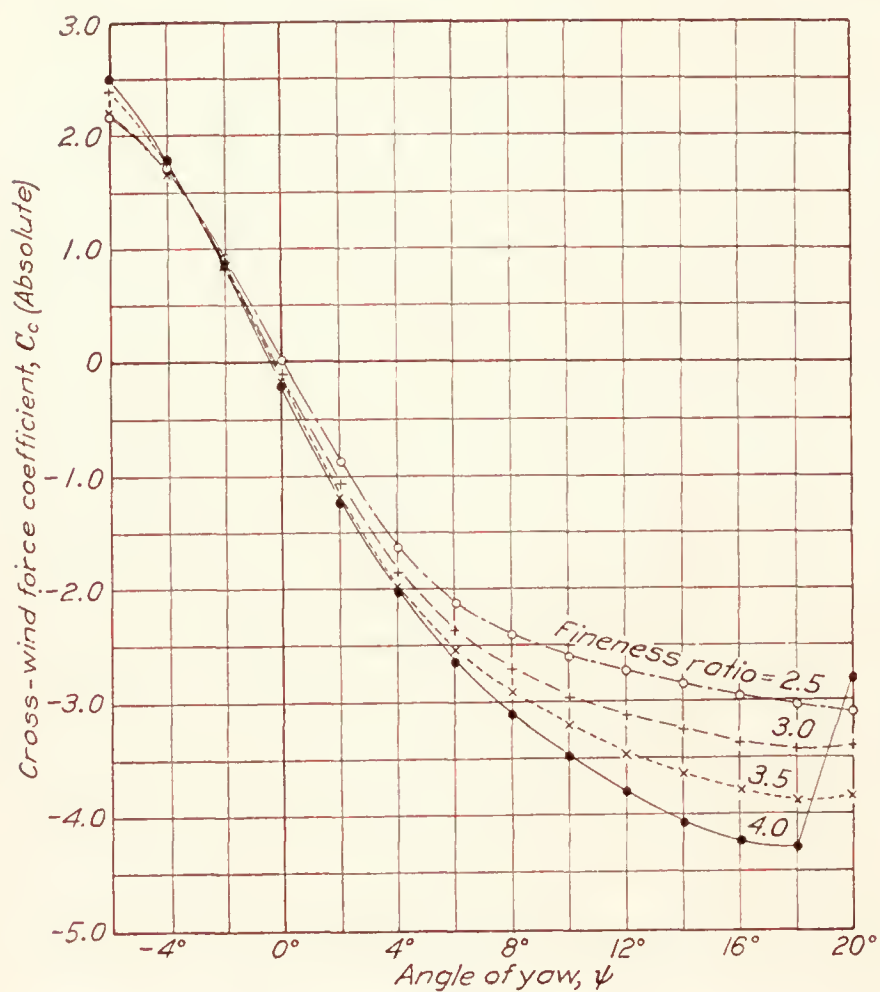


FIG. 4.—Elliptic cylinders of various fineness ratios. Length of cylinder 62 inches, models at 0° pitch, air speed 30 M. P. H.

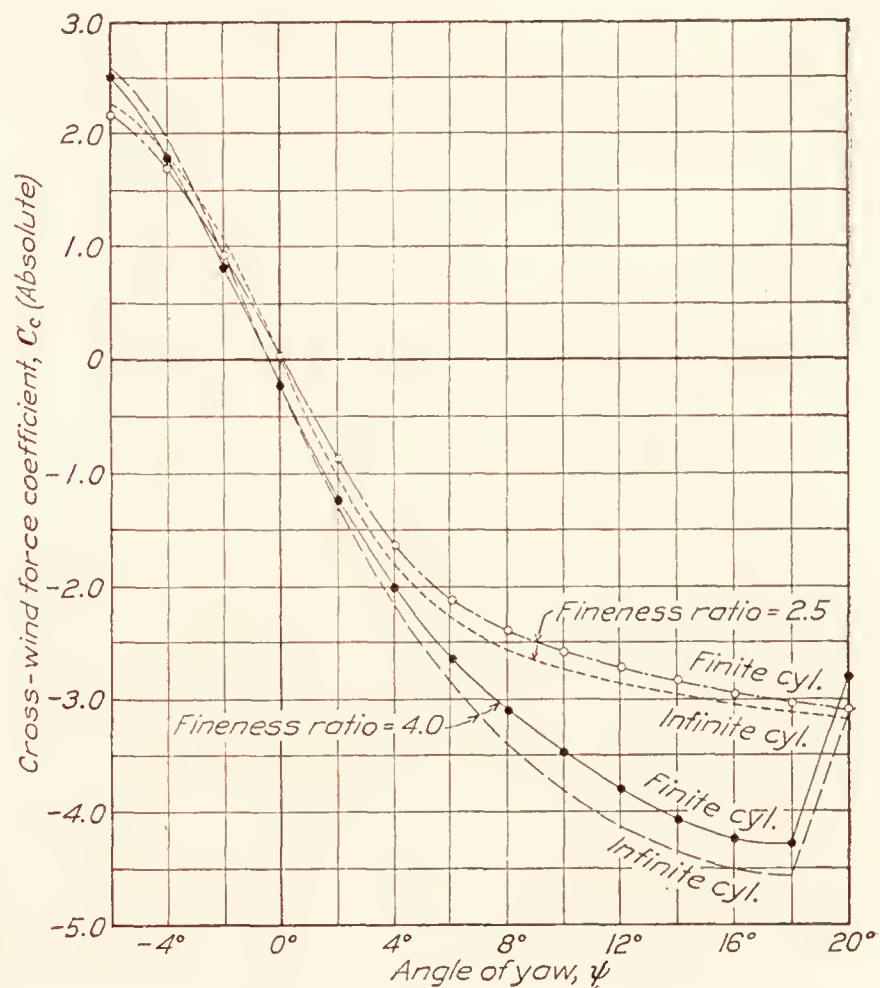


FIG. 5.—Elliptic cylinders of fineness ratios 2.5 and 4. Length of cylinder 62 inches, models at 0° pitch, air speed 30 M. P. H.

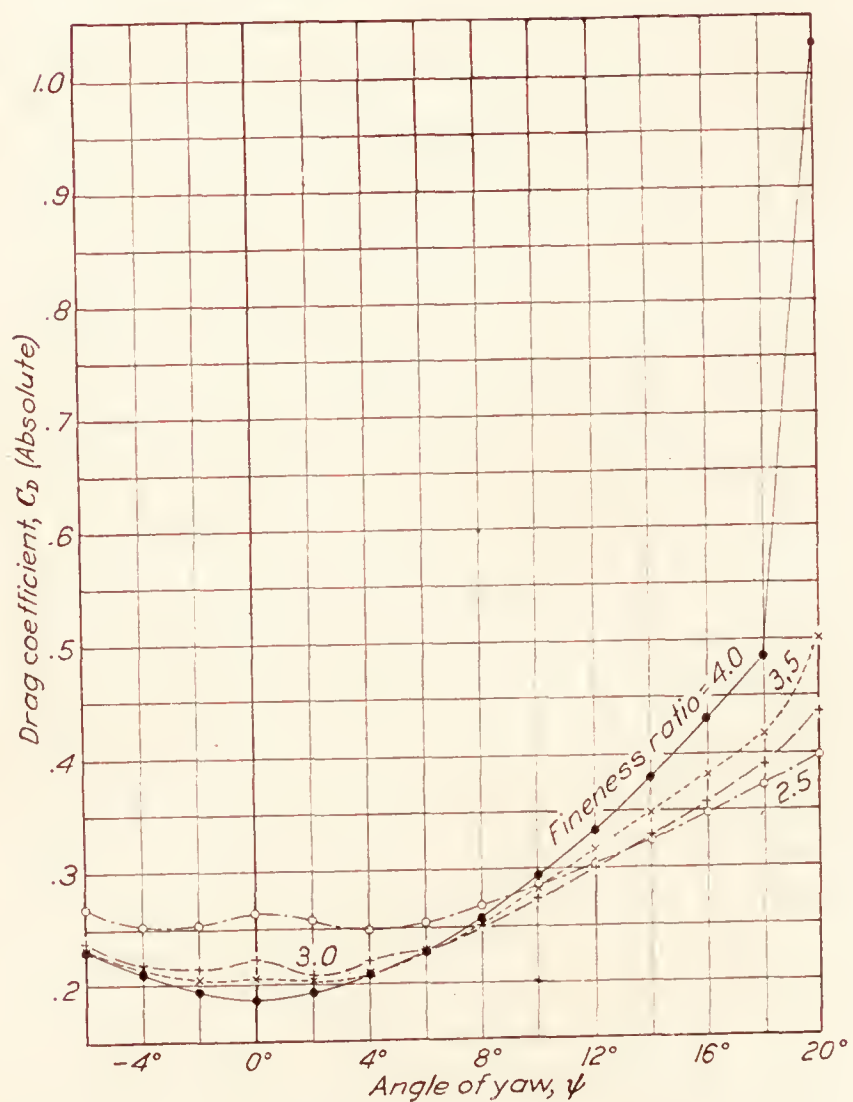


FIG. 6.—Elliptic cylinders of various fineness ratios. Length of cylinder 62 inches, models at 0° pitch, air speed 30 M. P. H.

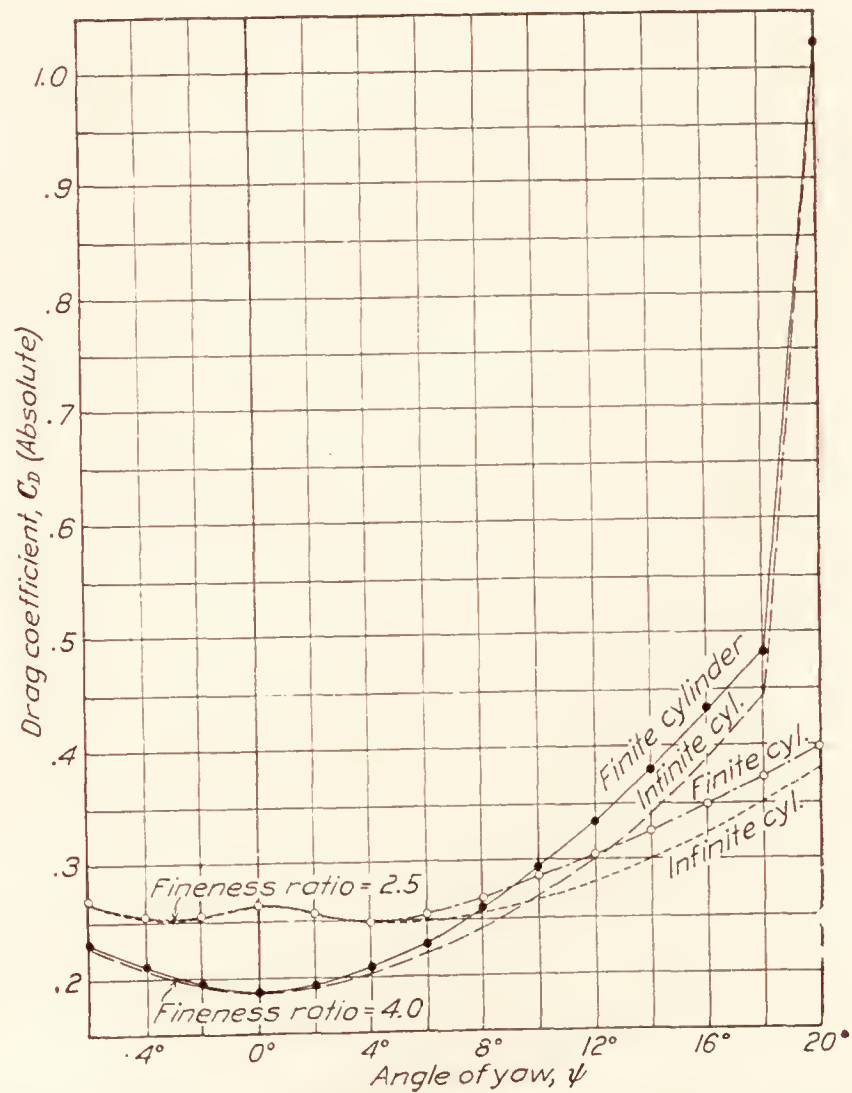


FIG. 7.—Elliptic cylinders of fineness ratios 2.5 and 4. Length of cylinder 62 inches, models at 0° pitch, air speed 30 M. P. H.

The drag coefficient is decreased by increasing the fineness ratio at zero yaw, but the difference is less as the yaw increases and between  $4^\circ$  and  $6^\circ$  the cylinder of fineness ratio 3.5 has a drag coefficient equally as low as the 2 by 8 inch cylinder. From  $6^\circ$  to  $13^\circ$ , the 2 by 6 inch cylinder has the least drag coefficient; beyond  $13^\circ$  yaw, the greater the fineness ratio the greater the drag coefficient.

The yawing moment about the N-axis is presented in Table IV; the resulting lines of force and the center of pressure travel are shown in Figures 9 and 10. As the fineness ratio of the cylinder increases, the center of pressure moves slightly aft.

The ratio of the forces  $C/D$ , is given in Table 5 and the graphs are given in Figure 8. The 2 by 8 inch cylinder is superior for angles of yaw up to  $16^\circ$ .  $C/D$  max. for this cylinder is  $-12$  at  $8^\circ$  yaw.

Tables VI and VII give the force measurements on the smallest and largest model with and without end plates, the percentage difference and the coefficients for the infinite cylinder; Figures 5 and 7 compare the coefficients of the finite and infinite cylinders. The cross-wind force coefficient is increased positively at negative yaw and negatively at positive yaw when the cylinder becomes endless. The drag coefficient for the infinite cylinder is less than for the finite.

With the cylinders at  $0^\circ$  pitch and yaw, the resistance and corresponding coefficients for various speeds are given in Table VIII and plotted in Figure 11. Here the resistance of the 62-inch cylinder was taken to be substantially the same as for a 62-inch segment of an infinite cylinder, as the increment due to end effect was small and could not be measured. On comparing the four struts, it is seen that at high speeds the drag coefficient is not lowered by increase of fineness ratio; at speeds of 50 and 60 miles an hour, the models with fineness ratios of 3.0 and 3.5 have a lower coefficient than the 2 by 8 inch model.

#### RESULTS OF PRESSURE DISTRIBUTION MEASUREMENTS

The differential pressure measurements made on the 2 by 8 inch cylinder are presented in Table IX, and their conversion from inches of alcohol on a 1 to 10 slope to vertical inches of water is also given. Table X gives the point pressure at the several holes found by subtracting the differential pressure from the nose pressure. These data are plotted in Figures 12 and 13. Table XI gives the point pressure in terms of the nose pressure.

One sees from Figure 12 that for this strut shape the point pressure at all used speeds decreases from full impact  $\frac{1}{2} \rho V^2$  at the nose to zero at a distance of 2.1 per cent of the cylinder width from the nose; the maximum suction occurs at about three-eighths of the width from the leading edge and is equal to about .6 the nose pressure. For speeds of 40 to 70 miles an hour there is another point of zero pressure near the trailing edge and a positive pressure aft of that; for the lower speeds, a slight suction is still evident at the trailing edge. Figure 13 shows that the pressure at each hole varies nearly as the square of the velocity.

The graphs of the faired values of the point pressure, multiplied by  $(70/V)^2$  to make them comparable are shown in Figure 14. The integrals of each pressure graph, giving the elements of the pressure drag and the summation of these or the resultant pressure-drag, are given in Table 12 and plotted in Figure 15. With them are shown the total drag and the resultant friction. The order of graphic integration here used to find the force  $\int p dy$  over the various portions of the surface of the 1-foot-long center segment of the cylinder is detailed in the diagrams of Figure 17.

It is seen that the downstream push and the upstream suction vary as  $V^n$ . The upstream push is zero at low speeds since the pressure did not become positive near the trailing edge of the model at these speeds. The difference between the total downstream and upstream pressure forces, which is the pressure drag, is seen to increase up to a speed of 35 miles an hour and then decrease. The difference between the curves of total drag and pressure drag, giving the frictional drag, varies as  $V^n$  where  $n = 1.97$ .



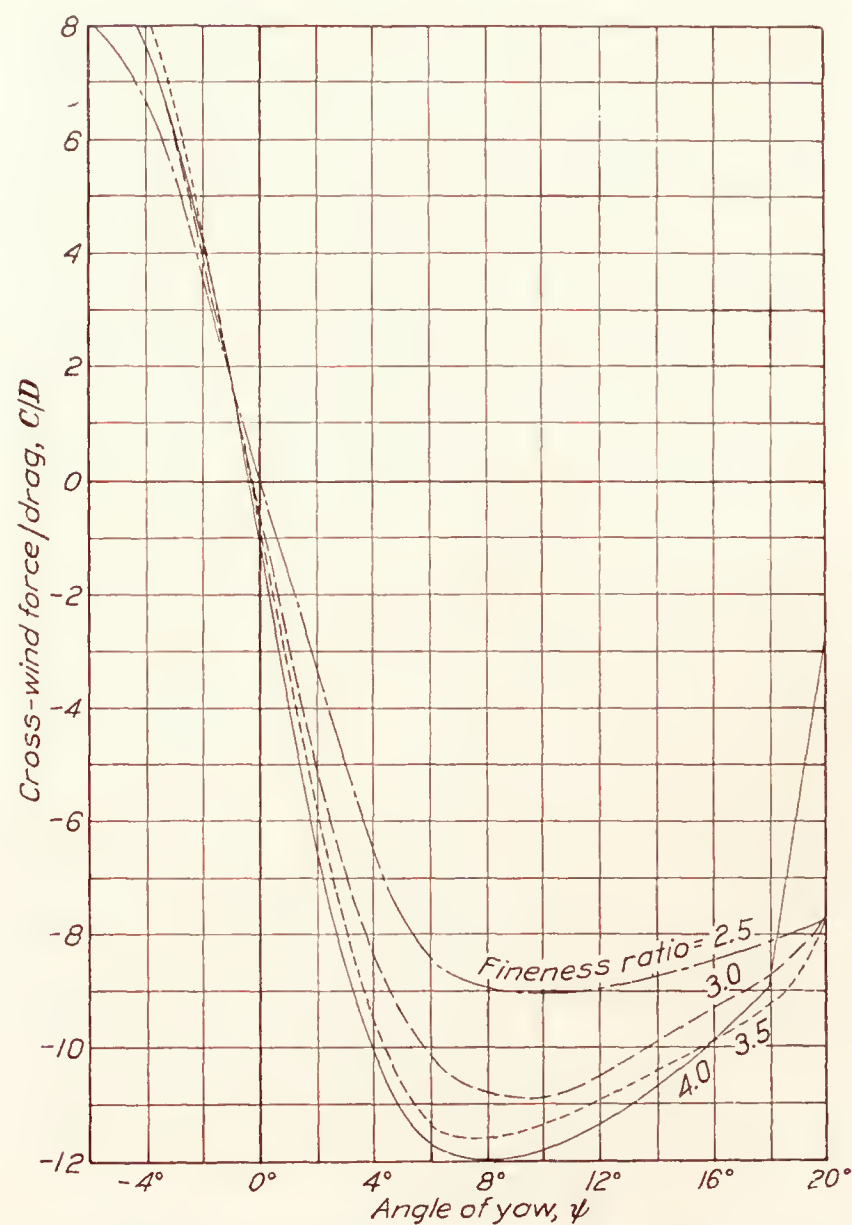


FIG. 8.—Elliptic cylinders of various fineness ratios. Length of cylinder 62 inches, models at 0° pitch, air speed 30 M. P. H.

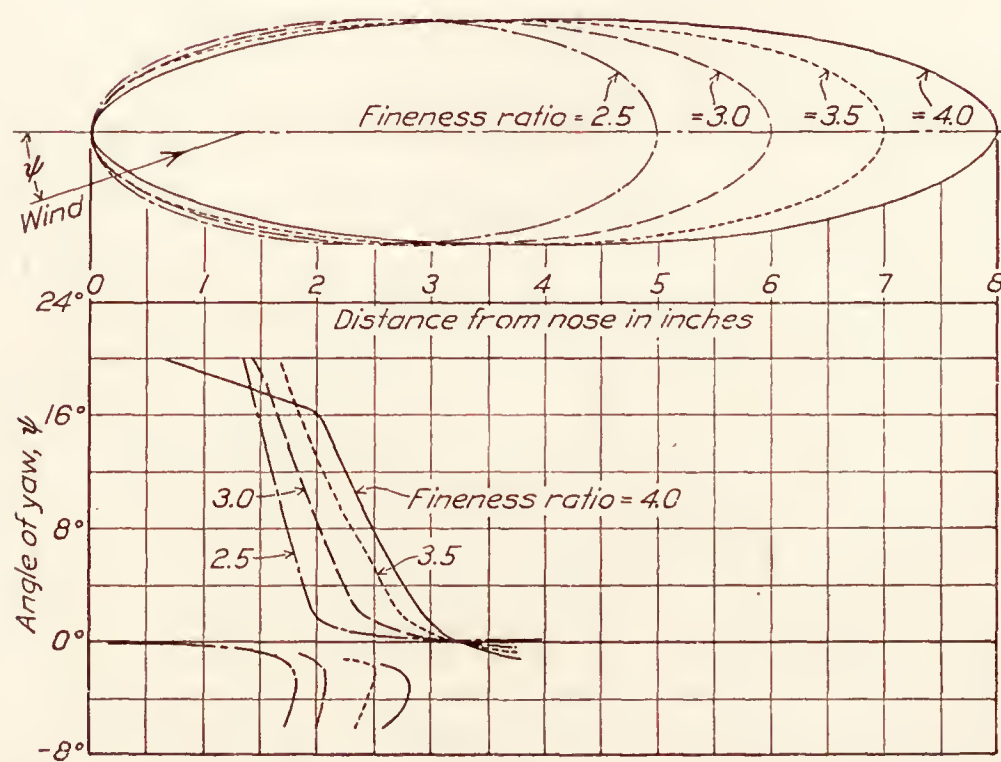


FIG. 10.—Center of pressure at various angles of yaw, of elliptic cylinders of various fineness ratios. Length of cylinder 62 inches, models at 0° pitch, air speed 30 M. P. H.

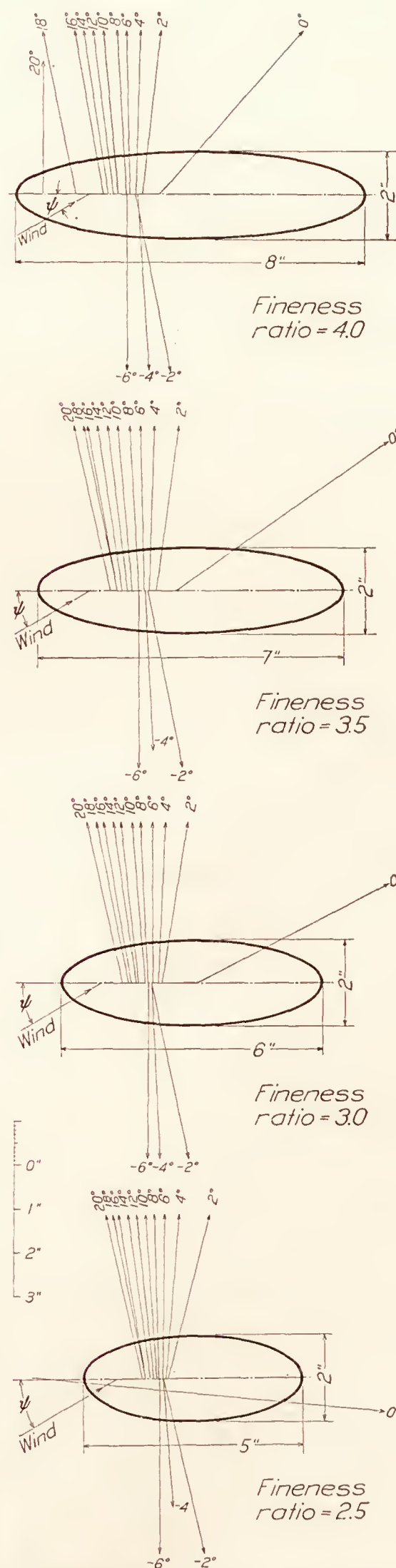


FIG. 9.—Lines of resultant air force at 30 M. P. H. of elliptic cylinders of various fineness ratios. Length of cylinder 62 inches, models yawed at 0° pitch

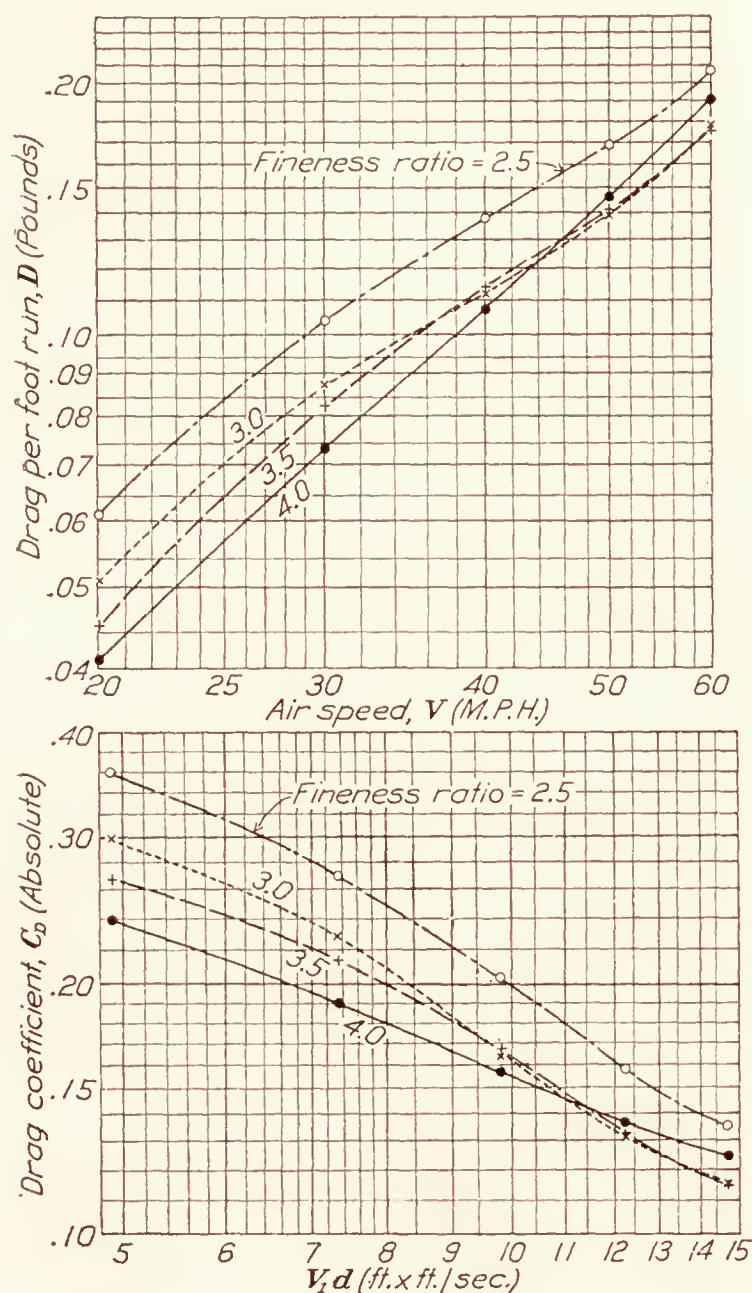


FIG. 11.—Elliptic cylinders at various fineness ratios. Models at  $0^\circ$  pitch and  $0^\circ$  yaw

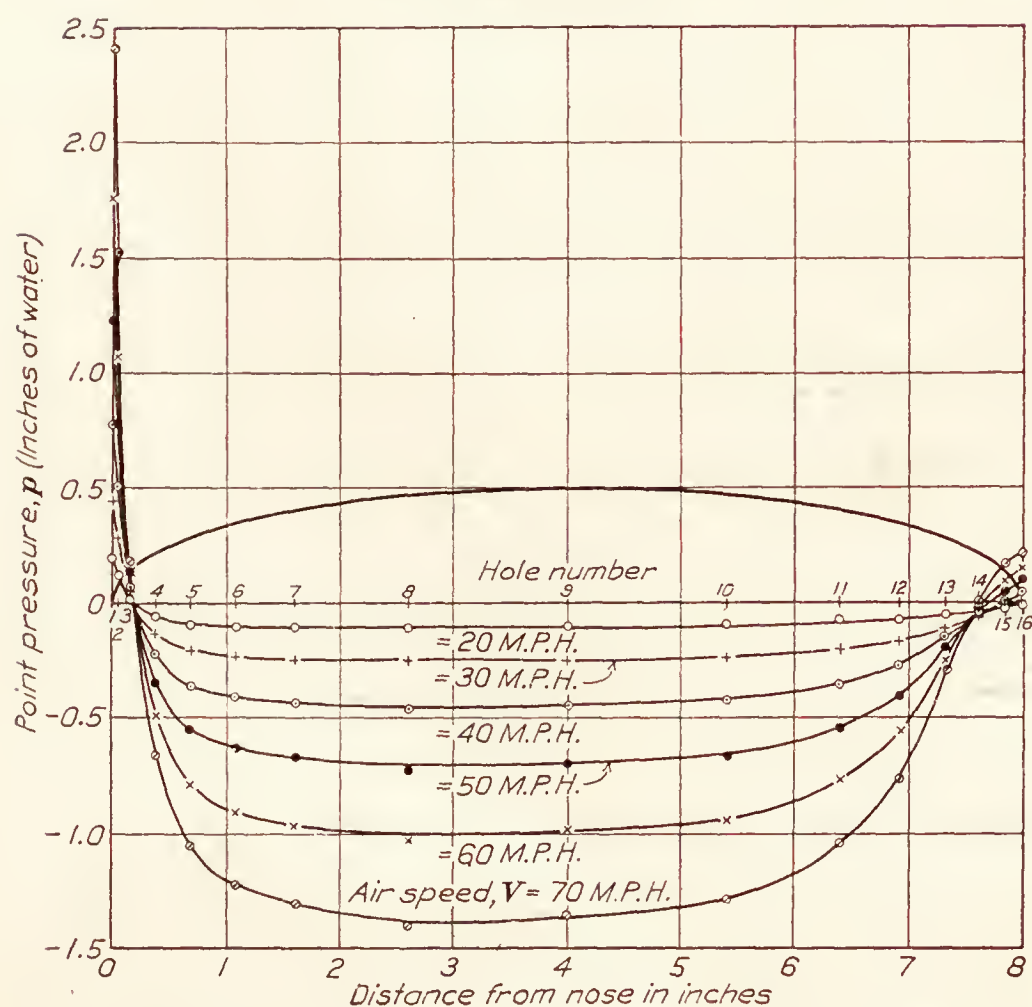


FIG. 12.—Elliptic cylinder 2 by 8 inches at various air speeds. Model at  $0^\circ$  pitch and  $0^\circ$  yaw

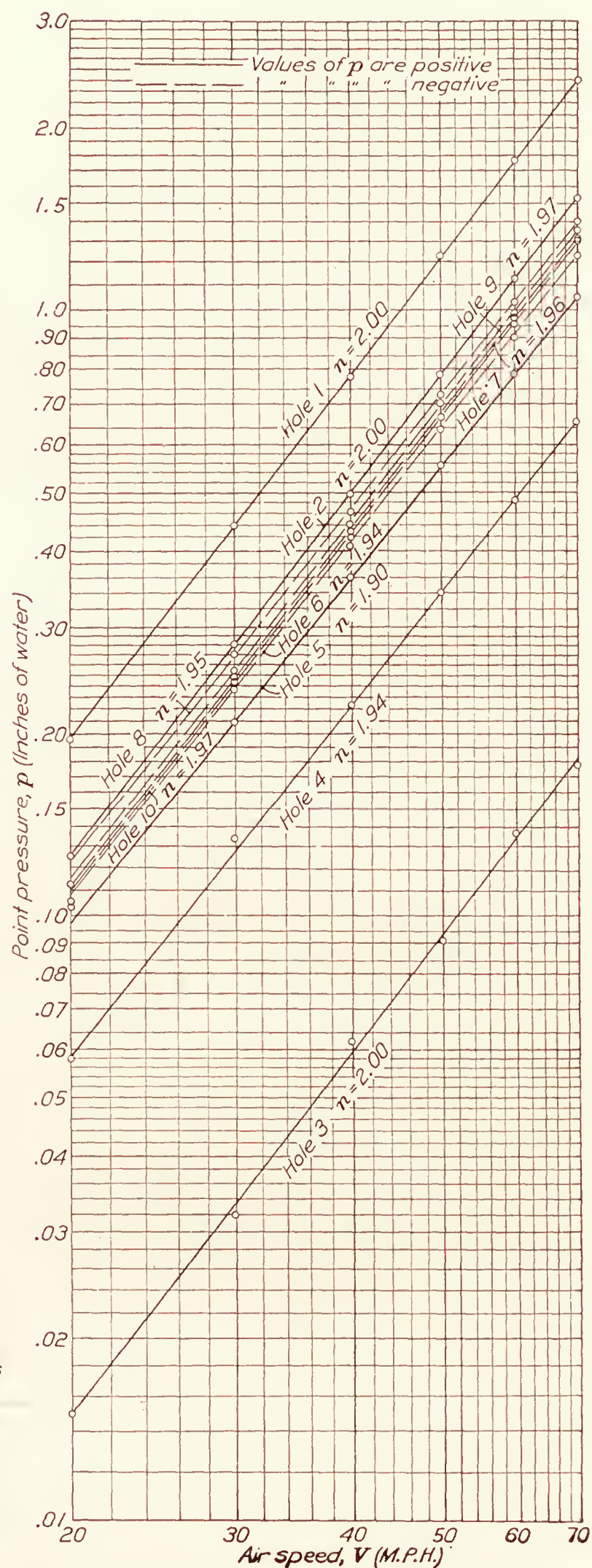


FIG. 13.—Elliptic cylinder with fineness ratio of 4. Model at  $0^\circ$  pitch and  $0^\circ$  yaw



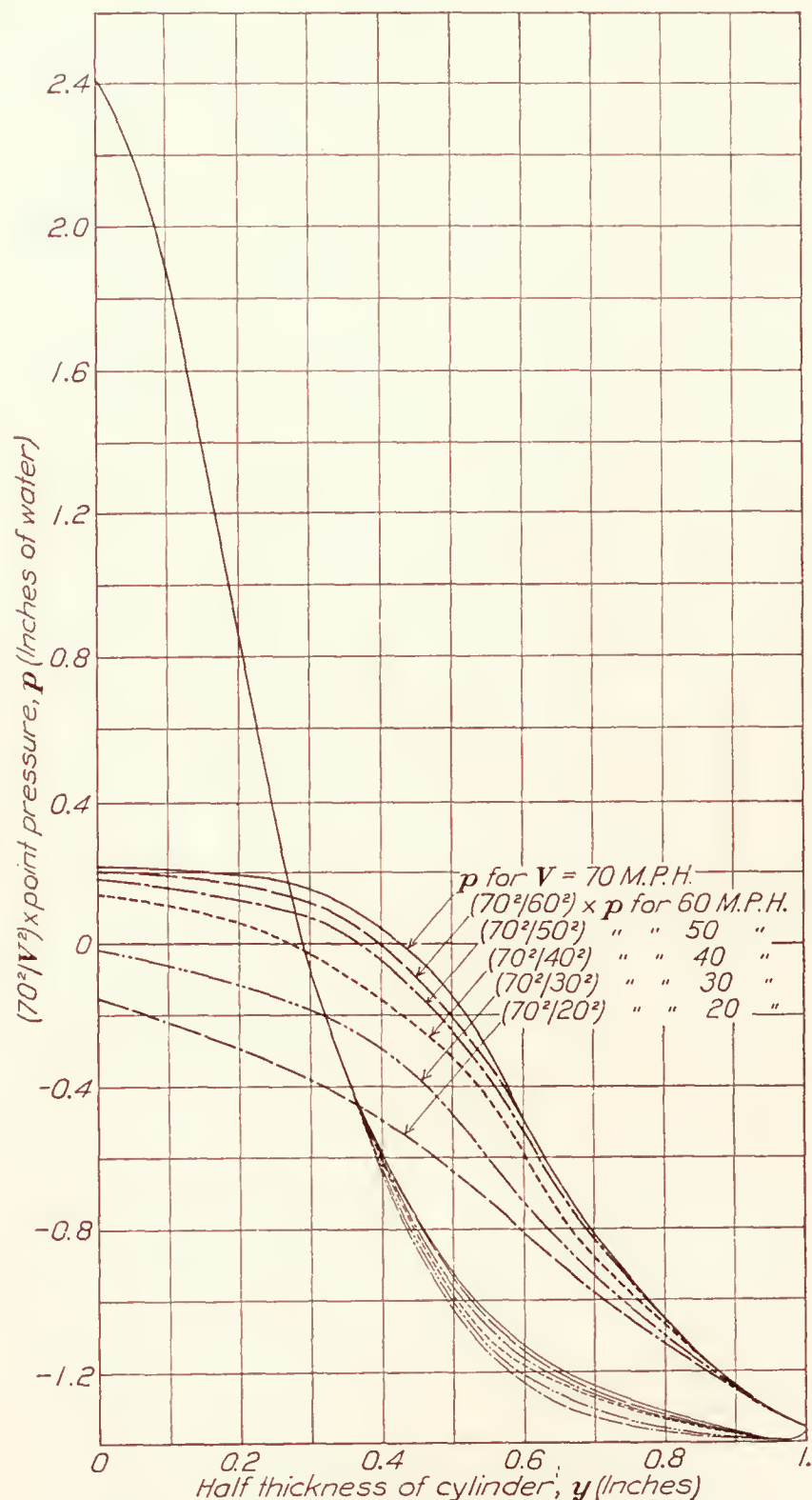


FIG. 14.—Elliptic cylinder 2 by 8 inches, model at 0° pitch and 0° yaw

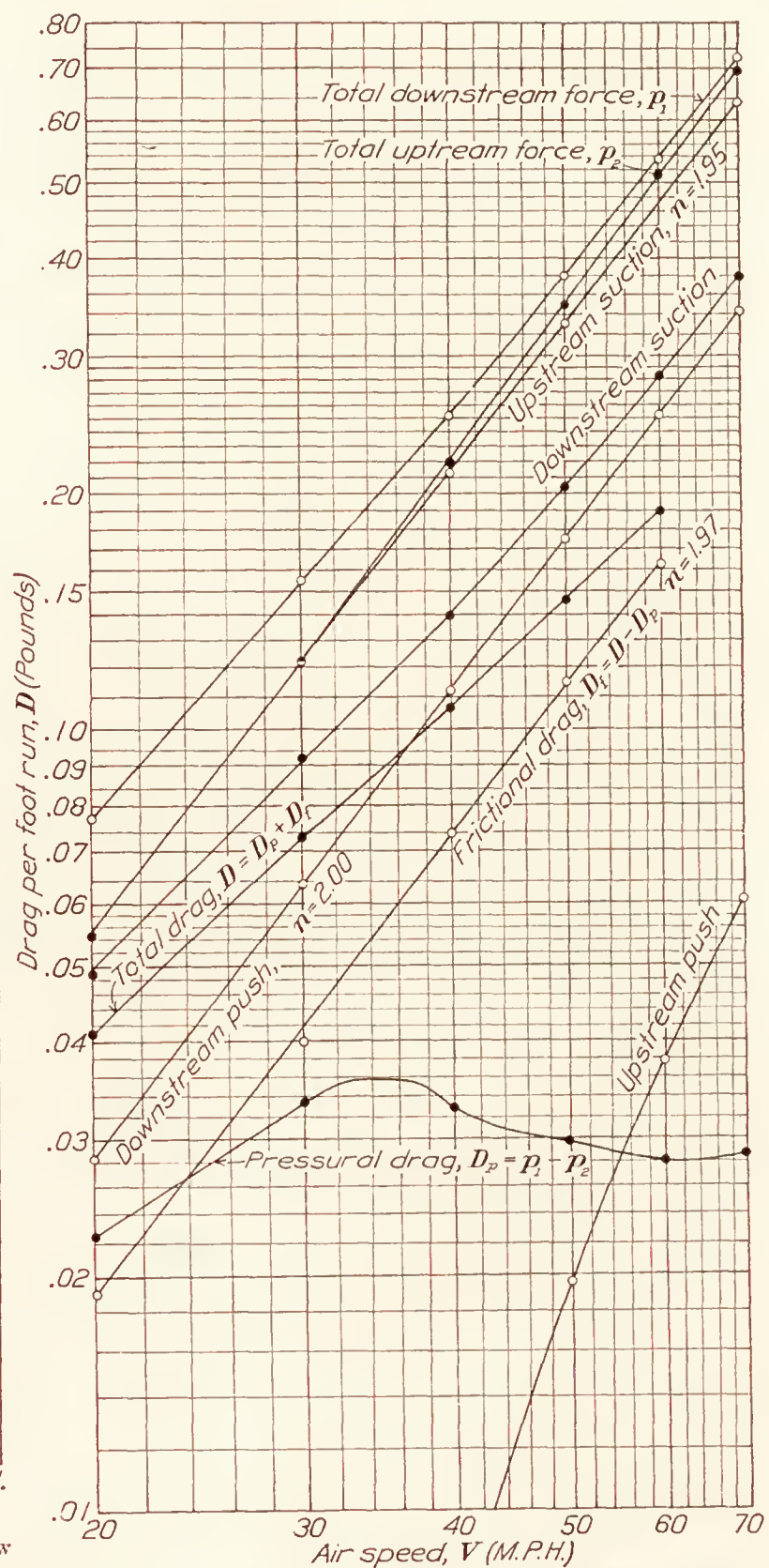


FIG. 15.—Elliptic cylinder 2 by 8 inches, model at 0° pitch and 0° yaw

Figure 16 portrays theoretical curves of point pressure and zonal pressure drag together with the measured pressure, all at 40 miles an hour, and the pressure drag computed from these measurements. Formulas for the theoretical curves are given in reference 3.

The measured pressures agree well with the theoretical except at the rear where the flow is turbulent. The pressure drag is a maximum where  $p = 0$  and a minimum amidships. The whole pressure drag on the front half of the model is negative. Theoretically this is balanced by the rear drag, but actually there is a downstream resultant which here is one-third the whole measured drag or one-half the friction drag.

### CONCLUSIONS

From Figures 4, 6, 8, it is seen that for  $V_1 d = 7.33$  (ft.  $\times$  ft./sec.) the best characteristics occur when the elliptic cylinder has a fineness ratio of 4.0. Figure 11 indicates that the above conclusion would hold for small Reynolds Numbers, but for large Reynolds Numbers,  $V_1 d > 11$ , the drag is less for a cylinder fineness ratio of 3.0 or 3.5, and this would probably result in an improved

$C/D$  curve which would mean that improved characteristics could be obtained with a fineness ratio smaller than 4.0.

If we assume a speed of 150 miles an hour and streamline wire with a thickness of one-fourth inch,  $V_1 d = 4.6$  (ft.  $\times$  ft./sec.), at such a Reynolds Number an elliptic section with a fineness ratio of 4.0 would have better characteristics than a section with a smaller fineness ratio.

Comparing the point pressure over the surface of the elliptic cylinder with that over the surface of the Navy No. 1 modified strut given in Reference 4, it is seen that the maximum suction is further aft for the elliptic section, and the streamlined trailing edge of the strut results in the pressure being zero at the same point near the trailing edge for any speed, while for the elliptic cylinder as the speed decreases the pressure is zero further aft, and for the low-test speeds there is still a suction at the trailing edge. Thus the character of the air flow at the after part of the elliptic cylinder is different for different speeds.

For an elliptic cylinder or any simple quadric, fixed at any attitude in a uniform infinite stream of inviscid liquid, it can be shown, Reference 3, that the zonal pressure drag is upstream on the fore part; downstream on the rear part; zero on the whole. The model in Figure 16 exhibits these properties except that the resultant pressure drag, owing to viscosity, is not quite zero.

At 40 miles an hour the drag coefficient of the 2 by 8 inch elliptic strut, at zero yaw and with free ends, is about 2.5 times that previously found for the best Navy strut, as given in Reference 4.

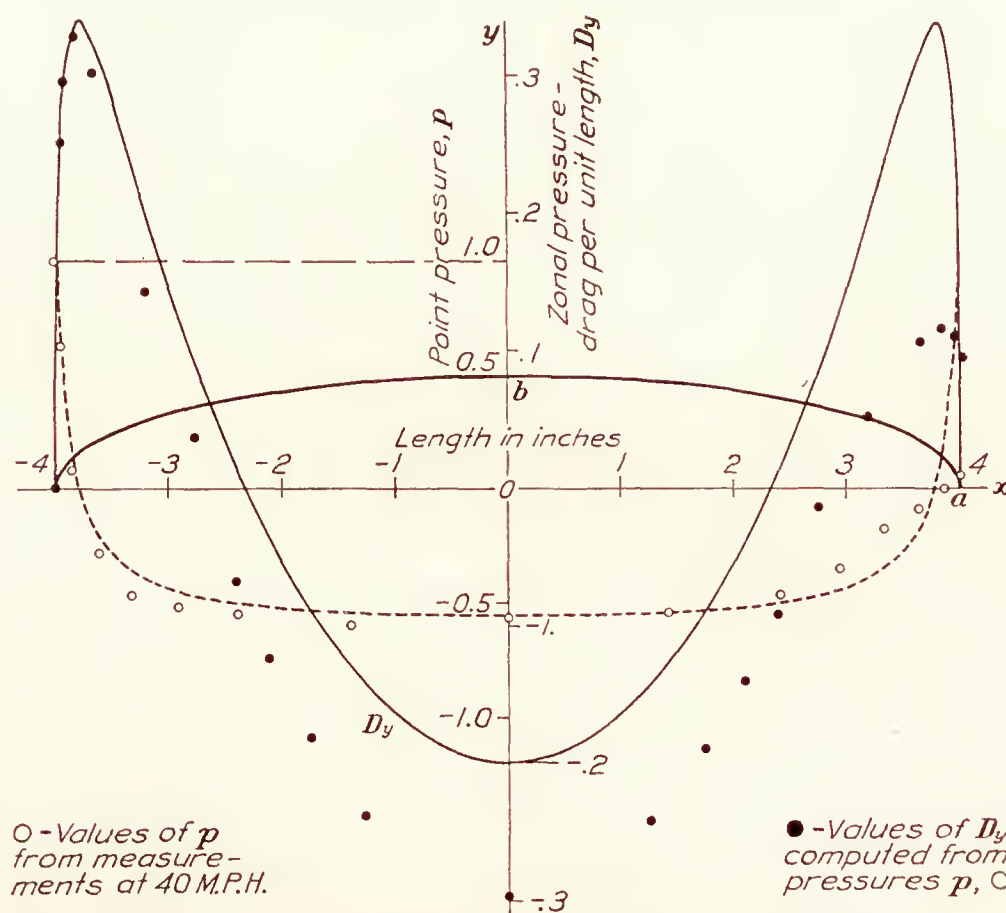


FIG. 16.—Elliptic cylinder 2 by 8 inches. Graphs indicate theoretical values.  $p = 1 - \frac{(a+b)^2 y^2}{[b^4 + (a^2 - b^2)y^2]}$  where unit pressure  $= \rho V^2/2$ .  $D_y = 2 \int_0^y p dy$

#### REFERENCES

- Reference 1.—A. F. Zahm, "The Six-Component Wind Balance." N. A. C. A. Technical Report No. 146, 1922.
- Reference 2.—Aeronautics Staff, "Air Force and Center of Pressure of M-80 Airfoil." C. & R. Aeronautical Report No. 175, March 31, 1921.
- Reference 3.—A. F. Zahm, "Flow and Drag Formulas for Simple Quadrics." N. A. C. A. Technical Report No. 253, 1926.
- Reference 4.—A. F. Zahm, R. H. Smith, and G. C. Hill, "Point Drag and Total Drag of Navy Struts No. 1 Modified." N. A. C. A. Technical Report No. 137, 1922.



[Elliptic cylinder. Various fineness ratio]

TABLE I  
SPECIFIED OFFSETS

Distance from leading edge (inches)				Thickness (inches)
2 by 5 inch cylinder	2 by 6 inch cylinder	2 by 7 inch cylinder	2 by 8 inch cylinder	
0.	0.	0.	0.	0.
.050	.060	.070	.080	.399
.125	.150	.175	.200	.624
.250	.300	.350	.400	.872
.275	.450	.525	.600	1.054
.500	.600	.700	.800	1.200
.750	.900	1.050	1.200	1.428
1.000	1.200	1.400	1.600	1.600
1.500	1.800	2.100	2.400	1.833
2.000	2.400	2.800	3.200	1.960
2.500	3.000	3.500	4.000	2.000
3.000	3.600	4.200	4.800	1.960
3.500	4.200	4.900	5.600	1.833
4.000	4.800	5.600	6.400	1.600
4.250	5.100	5.950	6.800	1.428
4.500	5.400	6.300	7.200	1.200
4.625	5.550	6.475	7.400	1.054
4.750	5.700	6.650	7.600	.872
4.875	5.850	6.825	7.800	.624
4.950	5.940	6.930	7.920	.399
5.000	6.000	7.000	8.000	0.

[Elliptic cylinder. Various fineness ratio]

TABLE II  
NET MEASURED CROSS-WIND FORCE AT 30 M. P. H. AND CROSS-WIND FORCE COEFFICIENTS

Model at 0° pitch

Angle of yaw (degrees)	Cross-wind force on 62-inch cylinder $C$ (pounds)				Cross-wind force coefficient $C_c=2C/\rho V_1^2S$ (absolute)			
	Fineness ratio							
	2.5	3.0	3.5	4.0	2.5	3.0	3.5	4.0
-6-----	+4.308	+4.366	+4.761	+4.969	+2.1733	+2.2026	+2.4019	+2.5068
-4-----	3.383	3.326	3.526	3.550	1.7067	1.6779	1.7788	1.7909
-2-----	1.828	+1.676	+1.741	+1.662	.9222	+.8455	+.8783	+.8385
0-----	+.058	-.234	-.284	-.420	+.0293	-.1181	-.1433	-.2119
+2-----	-1.722	-2.116	-2.344	-2.448	-.8687	-1.0675	-1.1825	-1.2350
4-----	-3.241	-3.698	-3.945	-4.005	-1.6350	-1.8656	-1.9902	-2.0205
6-----	-4.203	-4.640	-5.005	-5.247	-2.1204	-2.3408	-2.5250	-2.6470
8-----	-4.738	-5.353	-5.774	-6.152	-2.3903	-2.7005	-2.9129	-3.1036
10-----	-5.124	-5.896	-6.336	-6.886	-2.5850	-2.9745	-3.1964	-3.4739
12-----	-5.384	-6.146	-6.856	-7.526	-2.7162	-3.1006	-3.4588	-3.7968
14-----	-5.633	-6.415	-7.195	-8.037	-2.8418	-3.2363	-3.6298	-4.0546
16-----	-5.851	-6.645	-7.475	-8.394	-2.9518	-3.3523	-3.7710	-4.2347
18-----	-6.000	-6.769	-7.664	-8.489	-3.0269	-3.4149	-3.8664	-4.2826
+20-----	-6.109	-6.721	-7.574	-5.534	-3.0819	-3.3907	-3.8210	-2.7918

$C_c$  = Cross-wind force coefficient =  $2C/\rho V_1^2 S$ .  
 $C$  = Net (model without holder) cross-wind force in pounds.  
 $S$  = Frontal area of cylinder = 0.8611 sq. ft.  
 $V_1$  = Air speed = 44 ft./sec.  
 $\rho$  = Air density = 0.002378 slug/cu. ft.

[Elliptic cylinder. Various fineness ratio]

TABLE III  
NET MEASURED DRAG AT 30 M. P. H. AND DRAG COEFFICIENTS  
Model at 0° pitch

Angle of yaw (degrees)	Drag of 62-inch cylinder $D$ (pounds)				Drag coefficient $C_D=2D/\rho V_1^2 S$ (absolute)			
	Fineness ratio							
	2.5	3.0	3.5	4.0	2.5	3.0	3.5	4.0
−6-----	0. 531	0. 471	0. 464	0. 456	0. 2679	0. 2376	0. 2341	0. 2300
−4-----	. 501	. 431	. 424	. 416	. 2527	. 2174	. 2139	. 2099
−2-----	. 503	. 424	. 404	. 385	. 2538	. 2139	. 2038	. 1942
0-----	. 521	. 441	. 406	. 369	. 2628	. 2225	. 2048	. 1862
+2-----	. 507	. 411	. 401	. 383	. 2558	. 2073	. 2023	. 1932
4-----	. 491	. 437	. 411	. 411	. 2477	. 2205	. 2073	. 2073
6-----	. 501	. 454	. 449	. 449	. 2527	. 2290	. 2265	. 2265
8-----	. 530	. 494	. 498	. 511	. 2674	. 2492	. 2512	. 2578
10-----	. 566	. 542	. 560	. 583	. 2855	. 2734	. 2825	. 2941
12-----	. 602	. 594	. 628	. 660	. 3037	. 2997	. 3168	. 3330
14-----	. 643	. 649	. 693	. 751	. 3244	. 3274	. 3496	. 3789
16-----	. 690	. 706	. 756	. 858	. 3481	. 3562	. 3814	. 4329
18-----	. 736	. 774	. 830	. 954	. 3713	. 3905	. 4187	. 4813
+20-----	. 791	. 868	. 991	2. 029	. 3991	. 4379	. 4999	1. 0236

$C_D$ = Drag coefficient= $2D/\rho V_1^2 S$ .  
 $D$ = Net (model without holder) drag in pounds.  
 $S$ = Frontal area of cylinder=0.8611 sq. ft.  
 $V_1$ = Air speed=44 ft./sec.  
 $\rho$ = Air density=0.002378 slug/cu. ft.

[Elliptic cylinder. Various fineness ratio]

TABLE IV  
NET MEASURED YAWING MOMENT ABOUT N=AXIS<sup>1</sup> OF MODEL HOLDER IN POUND-INCHES AT 30 M. P. H.  
Model at 0° pitch

Angle of yaw (degrees)	Fineness ratio			
	2.5	3.0	3.5	4.0
−6-----	−2. 738	−3. 109	−4. 587	−5. 807
−4-----	−3. 295	−3. 329	−4. 433	−5. 135
−2-----	−3. 821	−3. 519	−3. 857	−4. 029
0-----	−3. 794	−3. 161	−2. 727	−2. 346
+2-----	−2. 546	−1. 601	−. 634	+ . 288
4-----	−. 640	+ . 522	+2. 356	3. 514
6-----	+1. 404	2. 856	5. 444	7. 092
8-----	3. 383	5. 381	8. 337	10. 311
10-----	5. 244	7. 860	11. 528	14. 406
12-----	7. 190	10. 306	14. 772	18. 246
14-----	9. 218	12. 376	17. 856	21. 828
16-----	11. 336	14. 882	20. 728	25. 212
18-----	12. 963	16. 837	22. 633	32. 251
+20-----	+14. 696	+18. 590	+24. 215	+18. 732

<sup>1</sup> N=axis is 6.91 inches above chord of cylinder for all fineness ratios, and 2.26 inches aft of nose for fineness ratio=2.0; 2.72 inches aft of nose for fineness ratio=3.0; 3.35 inches aft of nose for fineness ratio=3.5; 3.84 inches aft of nose for fineness ratio=4.0.



[Elliptic cylinder. Various fineness ratio]

TABLE V  
C/D AT 30 M. P. H. FOR 62 INCH LONG CYLINDERS  
Model at 0° pitch

Angle of yaw (degrees)	Fineness ratio			
	2.5	3.0	3.5	4.0
-6-----	+8.12	+9.28	+10.3	+10.4
-4-----	6.76	7.72	8.32	7.56
-2-----	3.63	+3.95	+4.31	+4.32
0-----	+.111	-.531	-.700	-1.14
+2-----	-3.40	-5.15	-5.85	-6.62
4-----	-6.61	-8.46	-9.60	-10.1
6-----	-8.40	-10.2	-11.4	-11.7
8-----	-8.94	-10.8	-11.6	-12.0
10-----	-9.06	-10.9	-11.3	-11.8
12-----	-8.95	-10.3	-10.9	-11.4
14-----	-8.77	-9.89	-10.4	-10.7
16-----	-8.48	-9.42	-9.89	-9.79
18-----	-8.15	-8.75	-9.23	-8.90
+20-----	-7.72	-7.75	-7.65	-2.73

[Elliptic cylinder. Fineness ratio=2.5 and 4.0]

TABLE VI  
CROSS-WIND FORCE WITH AND WITHOUT END PLATES AT 30 M. P. H., PERCENTAGE  
DIFFERENCE, AND COEFFICIENT FOR INFINITE CYLINDER  
Model at 0° pitch

Angle of yaw (degrees)	Cross-wind force on 62-inch cylinder (pounds)		Percentage difference $\frac{100 (C' - C)}{C}$	Cross-wind force coefficient (absolute)	
	Without end plates $C$	With end plates $C'$		Finite cylinder $C_c=2 \frac{C}{\rho V_1^2 S}$ . (See Table 2)	Infinite cylinder $C_c + C_c \times \frac{C' - C}{C}$
Fineness ratio=2.5					
-4-----	+3. 332	+3. 560	+6. 8	+1. 7067	+1. 8228
0-----	-. 108	-. 133	23. 1	+. 0293	+. 0361
+4-----	-3. 226	-3. 576	10. 9	-1. 6350	-1. 8132
8-----	-4. 801	-5. 178	7. 9	-2. 3903	-2. 5791
12-----	-5. 591	-5. 878	5. 1	-2. 7162	-2. 8547
16-----	-6. 155	-6. 393	3. 9	-2. 9518	-3. 0669
+20-----	-6. 517	-6. 707	+2. 9	-3. 0819	-3. 1713
Fineness ratio=4.0					
-4-----	+3. 376	+3. 745	+10. 9	+1. 7909	+1. 9861
0-----	-. 070	-. 078	11. 4	-. 2119	-. 2361
+4-----	-3. 632	-3. 923	8. 0	-2. 0205	-2. 1821
8-----	-6. 016	-6. 590	9. 5	-3. 1036	-3. 3984
12-----	-7. 624	-8. 289	8. 7	-3. 7968	-4. 1271
16-----	-8. 594	-9. 151	6. 5	-4. 2347	-4. 5100
+20-----	-6. 949	-7. 796	+12. 2	-2. 7918	-3. 1324

[Elliptic cylinder. Fineness ratio=2.5 and 4.0]

TABLE VII  
DRAG WITH AND WITHOUT END PLATES AT 30 M. P. H., PERCENTAGE DIFFERENCE,  
AND COEFFICIENT FOR INFINITE CYLINDER

Model at 0° pitch

Angle of yaw (degrees)	Drag of 62-inch cylinder (pounds)		Percentage difference $\frac{100 (D' - D)}{D}$	Drag coefficient (absolute)	
	Without end plates $D$	With end plates $D'$		Finite cylinder $C_D = 2D/\rho V_1^2 S$ . (See Table 3)	Infinite cylinder $C_D + C_D \times \frac{D' - D}{D}$
Fineness ratio = 2.5					
-4-----	0 492	0. 484	-1. 63	0. 2527	0. 2511
0-----	. 515	. 517	+ . 39	. 2628	. 2638
+4-----	. 498	. 494	- . 80	. 2477	. 2457
8-----	. 541	. 513	-5. 18	. 2674	. 2535
12-----	. 595	. 549	-7. 74	. 3037	. 2802
16-----	. 680	. 629	-7. 50	. 3481	. 3220
+20-----	. 798	. 758	-5. 02	. 3991	. 3791
Fineness ratio = 4.0					
-4-----	0. 397	0. 388	-2. 27	0. 2099	0. 2051
0-----	. 349	. 352	+ . 86	. 1862	. 1878
+4-----	. 389	. 379	-2. 57	. 2073	. 2020
8-----	. 488	. 455	-6. 77	. 2578	. 2403
12-----	. 641	. 577	-9. 99	. 3330	. 2997
16-----	. 839	. 751	-10. 49	. 4329	. 3875
+20-----	1. 668	1. 640	-1. 68	1. 0236	1. 0064



[Elliptic cylinder. Various fineness ratio]

TABLE VIII  
 DRAG AND DRAG COEFFICIENTS AT VARIOUS SPEEDS  
 Model at 0° pitch and 0° yaw

Air speed (M. P. H.)	Net <sup>1</sup> measured drag of 62-inch cylinder or 62-inch segment of infinite cylinder (pounds)	Net drag per foot run, $D$ (pounds)	$V_1 d$ (ft.×ft./sec.)	Drag coefficient $C_D = \frac{2 D}{\rho V_1^2 S}$
Fineness ratio=2.5				
20-----	0. 316	0. 061	4. 88	0. 3587
30-----	. 535	. 194	7. 33	. 2699
40-----	. 715	. 138	9. 78	. 2029
50-----	. 866	. 168	12. 22	. 1573
60-----	1. 072	. 207	14. 67	. 1352
Fineness ratio=3.0				
20-----	0. 262	0. 051	4. 88	0. 2974
30-----	. 452	. 087	7. 33	. 2280
40-----	. 581	. 112	9. 78	. 1649
50-----	. 720	. 139	12. 22	. 1308
60-----	. 916	. 177	14. 67	. 1155
Fineness ratio=3.5				
20-----	0. 235	0. 045	4. 88	0. 2667
30-----	. 424	. 082	7. 33	. 2139
40-----	. 591	. 114	9. 78	. 1677
50-----	. 728	. 141	12. 22	. 1322
60-----	. 908	. 176	14. 67	. 1145
Fineness ratio=4.0				
20-----	0. 210	0. 041	4. 88	0. 2384
30-----	. 377	. 073	7. 33	. 1902
40-----	. 551	. 107	9. 78	. 1564
50-----	. 752	. 146	12. 22	. 1366
60-----	. 986	. 191	14. 67	. 1244

 $V_1$ =Air speed in ft./sec. $d$ =Thickness of cylinder=0.16667 ft. $S$ =Frontal area per foot run of cylinder=0.16667 sq. ft. $\rho$ =Air density=0.002378 slug/cu. ft.<sup>1</sup> Net indicates model without holder. At 0° the increment due to end effect was negligible.

[Elliptic cylinder 2 by 8 inches]

TABLE IX

OBSERVED DIFFERENCE IN PRESSURE BETWEEN NOSE AND HOLES AFT OF NOSE,  $dp$

$$dp = \frac{1}{2} \rho V^2 - p$$

Model at 0° pitch and 0° yaw

Number of hole	Air speed in miles per hour					
	20	30	40	50	60	70
$dp$ in inches of alcohol on 1 to 10 slope and 0.832 specific gravity						
1-----	0	0	0	0	0	0
2-----	. 85	1. 93	3. 42	5. 33	7. 67	10. 57
3-----	2. 17	4. 95	8. 70	13. 70	19. 65	26. 85
4-----	3. 05	6. 95	12. 15	18. 92	27. 15	36. 90
5-----	3. 50	7. 87	13. 85	21. 45	30. 72	41. 67
6-----	3. 60	8. 20	14. 40	22. 45	32. 17	43. 78
7-----	3. 63	8. 32	14. 67	22. 80	32. 96	44. 75
8-----	3. 70	8. 60	15. 10	23. 52	33. 70	45. 88
9-----	3. 63	8. 40	14. 83	23. 23	33. 18	45. 33
10-----	3. 50	8. 30	14. 58	22. 85	32. 71	44. 68
11-----	3. 27	7. 75	13. 80	21. 35	30. 55	41. 64
12-----	3. 23	7. 30	12. 77	19. 64	28. 08	38. 25
13-----	3. 08	6. 68	11. 15	17. 10	24. 25	32. 53
14-----	2. 80	6. 05	10. 21	15. 40	21. 63	28. 90
15-----	2. 70	5. 70	9. 44	14. 22	20. 10	26. 93
16-----	2. 50	5. 38	8. 90	13. 65	19. 50	26. 38
$dp$ converted to inches of water						
1-----	0	0	0	0	0	0
2-----	. 071	. 161	. 284	. 443	. 638	. 879
3-----	. 181	. 412	. 724	1. 139	1. 634	2. 233
4-----	. 254	. 578	1. 010	1. 573	2. 258	3. 069
5-----	. 291	. 654	1. 152	1. 784	2. 556	3. 464
6-----	. 299	. 682	1. 197	1. 866	2. 674	3. 640
7-----	. 302	. 692	1. 220	1. 895	2. 741	3. 721
8-----	. 308	. 716	1. 255	1. 955	2. 803	3. 815
9-----	. 302	. 698	1. 233	1. 932	2. 759	3. 770
10-----	. 291	. 690	1. 212	1. 900	2. 720	3. 715
11-----	. 272	. 645	1. 148	1. 775	2. 540	3. 462
12-----	. 269	. 616	1. 062	1. 632	2. 335	3. 181
13-----	. 256	. 556	. 928	1. 422	2. 017	2. 708
14-----	. 233	. 503	. 850	1. 281	1. 800	2. 403
15-----	. 225	. 474	. 785	1. 183	1. 671	2. 240
16-----	. 208	. 447	. 740	1. 135	1. 621	2. 194



[Elliptic cylinder 2 by 8 inches]

TABLE X

POINT PRESSURE,  $p$ , IN INCHES OF WATER AT THE 16 HOLES

$$p = \frac{1}{2} \rho V^2 - dp$$

Model at 0° pitch and 0° yaw

Number of hole	Air speed in miles per hour					
	20	30	40	50	60	70
1-----	+0. 196	+0. 444	+0. 786	+1. 230	+1. 771	+2. 411
2-----	. 125	. 283	. 502	. 787	1. 133	1. 532
3-----	+ . 015	+ . 032	+ . 062	+ . 091	+ . 137	+ . 178
4-----	− . 058	− . 134	− . 224	− . 343	− . 487	− . 658
5-----	− . 095	− . 210	− . 366	− . 554	− . 785	−1. 053
6-----	− . 103	− . 238	− . 411	− . 636	− . 903	−1. 229
7-----	− . 106	− . 248	− . 434	− . 665	− . 970	−1. 310
8-----	− . 112	− . 272	− . 469	− . 725	−1. 032	−1. 404
9-----	− . 106	− . 254	− . 447	− . 702	− . 988	−1. 359
10-----	− . 095	− . 246	− . 426	− . 670	− . 949	−1. 304
11-----	− . 076	− . 201	− . 362	− . 545	− . 769	−1. 051
12-----	− . 073	− . 172	− . 276	− . 402	− . 564	− . 770
13-----	− . 060	− . 112	− . 142	− . 192	− . 246	− . 297
14-----	− . 037	− . 059	− . 064	− . 051	− . 029	+ . 008
15-----	− . 029	− . 030	+ . 001	+ . 047	+ . 100	. 171
16-----	− . 012	− . 003	+ . 046	+ . 095	+ . 150	+ . 217

[Elliptic cylinder 2 by 8 inches]

TABLE XI

POINT PRESSURE IN TERMS OF NOSE PRESSURE  $p/\frac{1}{2} \rho V^2$ , AT VARIOUS AIR SPEEDS

Model at 0° pitch and 0° yaw

Number of hole	Air speed in miles per hour					
	20	30	40	50	60	70
1-----	+1. 000	+1. 000	+1. 000	+1. 000	+1. 000	+1. 000
2-----	. 638	. 638	. 639	. 640	. 640	. 637
3-----	+ . 077	+ . 072	+ . 079	+ . 074	+ . 077	+ . 074
4-----	− . 296	− . 302	− . 285	− . 279	− . 275	− . 273
5-----	− . 485	− . 473	− . 465	− . 450	− . 443	− . 437
6-----	− . 525	− . 535	− . 522	− . 517	− . 509	− . 509
7-----	− . 544	− . 559	− . 550	− . 541	− . 547	− . 543
8-----	− . 574	− . 612	− . 596	− . 589	− . 582	− . 583
9-----	− . 544	− . 572	− . 569	− . 571	− . 557	− . 564
10-----	− . 485	− . 554	− . 542	− . 545	− . 535	− . 542
11-----	− . 388	− . 454	− . 460	− . 443	− . 434	− . 436
12-----	− . 372	− . 388	− . 351	− . 327	− . 318	− . 319
13-----	− . 306	− . 252	− . 180	− . 156	− . 139	− . 123
14-----	− . 189	− . 133	− . 081	− . 041	− . 016	+ . 003
15-----	− . 148	− . 068	+ . 001	+ . 038	+ . 056	. 071
16-----	− . 061	− . 007	+ . 059	+ . 077	+ . 085	+ . 090

[Elliptic cylinder 2 by 8 inches]

TABLE XII

ALONG-STREAM FORCES PER FOOT RUN OF CYLINDER EXPRESSED IN POUNDS AND IN TERMS OF TOTAL MEASURED DRAG

Model at 0° pitch and 0° yaw

Air speed (M. P. H.)	Downstream			Upstream			Pressural drag $D_p = p_i - p_s$	Frictional drag $D_f$	Total drag $D = D_p + D_f$
	Push	Suction	Total $p_i$	Push	Suction	Total $p_s$			
	Pounds per foot run								
20-----	0. 0282	0. 0490	0. 0772	0	0. 0548	0. 0548	0. 0224	0. 019	0. 041
30-----	. 0633	. 0921	. 1554	0	. 1222	. 1222	. 0332	. 040	. 073
40-----	. 1125	. 1406	. 2531	. 0068	. 2134	. 2202	. 0329	. 074	. 107
50-----	. 1761	. 2044	. 3805	. 0196	. 3311	. 3507	. 0298	. 116	. 146
60-----	. 2536	. 2855	. 5391	. 0378	. 4734	. 5112	. 0279	. 163	. 191
70-----	. 3450	. 3807	. 7257	. 0608	. 6363	. 6971	. 0286	-----	-----
	Per cent of total measured drag								
20-----	69	120	189	0	134	134	55	45	100
30-----	87	126	213	0	167	167	46	54	100
40-----	105	131	236	6	199	205	31	69	100
50-----	121	140	261	13	227	240	21	79	100
60-----	133	149	282	20	248	268	14	86	100
70-----	-----	-----	-----	-----	-----	-----	-----	-----	-----

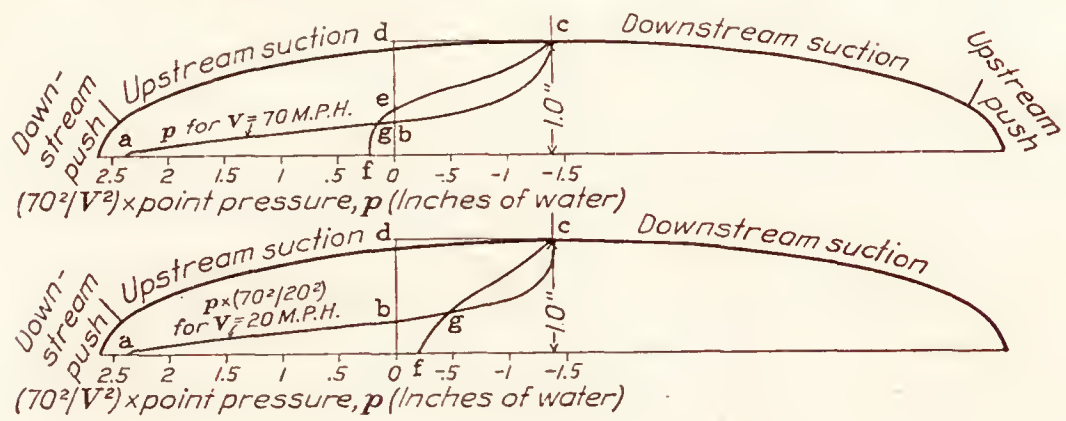


FIG. 17.—For  $V=40, 50, 60$ , or  $70$  M. P. H.  
Downstream push  $\propto$   $abo$   
Downstream suction  $\propto$   $ced$   
Upstream push  $\propto$   $eof$   
Upstream suction  $\propto$   $bed$   
Total area =  $(abo + ced) - (eof + bed)$   
 $= agf - gecg$   
For  $V=20$  or  $30$  M. P. H.  
Downstream push  $\propto$   $abo$   
Downstream suction  $\propto$   $cfod$   
Upstream push =  $0$   
Upstream suction  $\propto$   $bged$   
Total area =  $(abo + cfod) - (0 + bged)$   
 $= abgf - gecg$



---

# **REPORT No. 290**

---

## **WATER-PRESSURE DISTRIBUTION ON A SEAPLANE FLOAT**

**By F. L. THOMPSON**  
**Langley Memorial Aeronautical Laboratory**





## REPORT No. 290

---

### WATER-PRESSURE DISTRIBUTION ON A SEAPLANE FLOAT

By F. L. THOMPSON

---

#### SUMMARY

*The investigation reported herein was conducted by the National Advisory Committee for Aeronautics at the request of the Bureau of Aeronautics, Navy Department, for the purpose of determining the distribution and magnitude of water pressures likely to be experienced on seaplane hulls in service. It consisted of the development and construction of apparatus for recording water pressures lasting one one-hundredth second or longer and of flight tests to determine the water pressures on a UO-1 seaplane float under various conditions of taxiing, taking off, and landing.*

*The apparatus developed was found to operate with satisfactory accuracy and is suitable for flight tests on other seaplanes.*

*The tests on the UO-1 showed that maximum pressures of about 6.5 pounds per square inch occur at the step for the full width of the float bottom. Proceeding forward from the step the maximum pressures decrease in magnitude uniformly toward the bow, and the region of highest pressures narrows toward the keel. Immediately abaft the step the maximum pressures are very small, but increase in magnitude toward the stern and there once reached a value of about 5 pounds per square inch.*

#### INTRODUCTION

The design of seaplane floats and hulls for strength has in the past been largely determined by experience because of the lack of data regarding the loads to which they are subjected. A float that suffers no damage under the conditions it is expected to withstand is satisfactorily strong, but, on the other hand, it may have excess strength and therefore excess weight, which is objectionable. In safely reducing float and hull weights to a minimum it is necessary to know the magnitude and distribution of water pressures to which they are subjected.

To supply data for application in the design of lighter float gear, the Bureau of Aeronautics, Navy Department, requested this investigation of the water-pressure distribution on a seaplane float. It is intended that it will later be extended to include both the twin-float and boat type seaplanes.

The major portion of a two-year period over which this investigation extended was devoted to the development and construction of apparatus. After numerous trials and laboratory tests an instrument was developed to satisfactorily record water-pressure impulses of one one-hundredth second or longer duration.

A UO-1 single float seaplane was used for the tests, it being particularly suitable for an initial trial of the apparatus and method, as it is easily handled, is of proven ruggedness, and has a float of modern design. The test work was made to include taxiing, taking off, and landing runs under various conditions, with particular emphasis on bad conditions. On each run records were obtained of the water pressures at 15 stations on one side of the float bottom, of the longitudinal float angle, and of the air speed. The average wind velocity was also determined for use in finding the water speed of the seaplane.

This report includes a full description of the instrument developed to record water pressures, a description of the apparatus and methods used in the tests, a table of the water pressures found at all stations on each run, a graphical and tabular representation of the maximum pressures



at each station regardless of the run; and the conclusions arrived at as a result of the investigation. In the complete table of results each maneuver is described as to air speed, water speed, longitudinal float angle, and condition of the water surface. The pressures recorded are maximum pressures that occurred during each run and are not necessarily simultaneous values since the runs had an average duration of two to three seconds.

## APPARATUS AND METHOD

### APPARATUS

A Vought UO-1 seaplane (fig. 1) was used for these tests. It was equipped with a Wright J4-A engine and a wooden float. The specified stalling speed of this seaplane is 55.5 M. P. H.

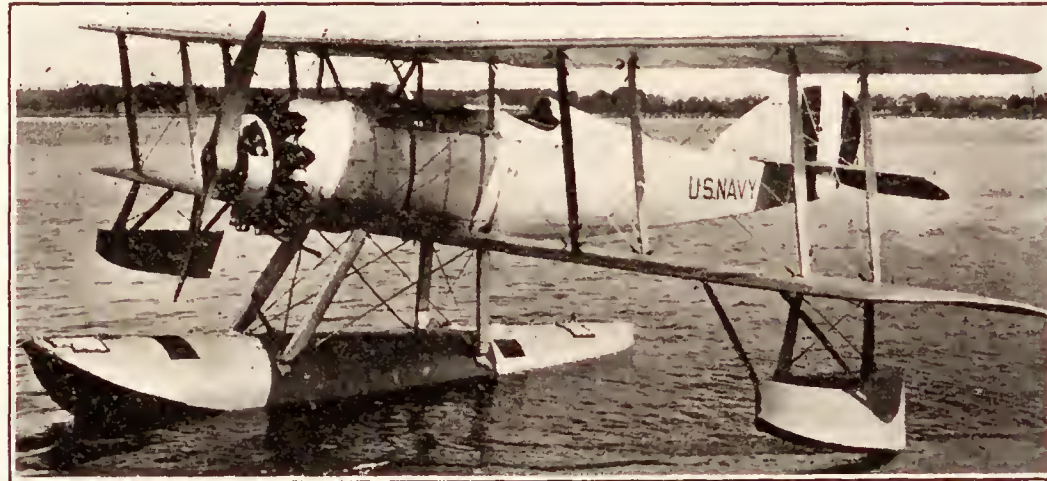


FIG. 1.—UO-1 seaplane

The gross weight with instruments installed was 2,764 pounds, which is but 19 pounds less than the maximum specified gross weight for service conditions.

The lines of the UO-1 float are shown in Figure 2. It has an angle of  $V$  of  $20^\circ$  at the step and aft. Forward of the step the angle of  $V$  gradually increases toward the bow. The step is  $2\frac{1}{2}$  inches high, and the angle of the after keel is  $5^\circ$ . This combination is such that an inclina-

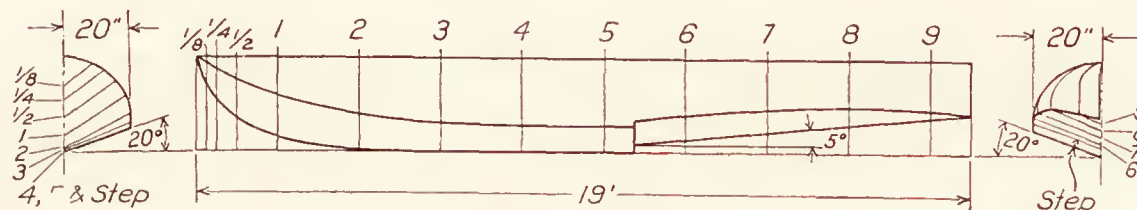


FIG. 2.—UO-1 float

tion of  $6\frac{1}{2}^\circ$  or more in landing causes the stern of the float to make first contact with the water. The float deck line is rigged parallel to the thrust axis of the seaplane, thereby making angles of  $1\frac{3}{4}^\circ$  and  $2\frac{1}{4}^\circ$ , respectively, with the upper and lower wing chords.

The instrument installation included the following:

1. Float-angle observer.
2. Two recording manometers—two pressure cells each.
3. Air-speed swiveling Pitot-static head.
4. Motor-type timer.
5. Water-pressure apparatus.

1. A small motion-picture camera driven by a constant-speed electric motor was used to photograph the shore line parallel to the path of the seaplane, thereby recording the longitudinal angle of the float. The camera was driven at a speed of five pictures per second.

2. The two recording manometers were of the type described in Reference 1 as the N. A. C. A. recording air-speed meter with the exception of having two pressure cells each instead of one. One of the four pressure cells thus provided was used to record air speed. The other three had heavy diaphragms and were used to record pneumatic pressures in connection with the water-pressure apparatus described later.



3. The swiveling Pitot-static head was located on the right front outboard wing strut and connected to the air-speed recording pressure cell.

4. An N. A. C. A. motor-type timer was used to synchronize records by means of timing lines at one-second intervals. In reference 2 the N. A. C. A. chronometric timer and the method of synchronizing records are described. The motor-type timer is used in exactly the same manner as the chronometric timer, but it depends for its periodic electrical contacts on a rotating switch driven by a constant-speed electric motor. The two manometer records and the float-angle record were synchronized by this means.

5. The water-pressure apparatus was used for the first time in this investigation and is therefore described in detail.

#### WATER-PRESSURE APPARATUS

For the determination of water pressures, 15 water-pressure units of the type shown in Figures 3 and 4 were used. Each unit has four brass pistons fitted in a brass case with 0.001 inch clearance. The water pressures on the external ends of these pistons are balanced by a hand-controlled internal pneumatic pressure.

The external areas of the four pistons are unequal, thereby causing unequal forces to be imposed on the pistons at any given intensity of water pressure. The internal areas are equal, and the pneumatic load resisting the water pressure load is therefore the same for each piston. The external piston areas range from 0.196 square inch for the smallest to 0.276 square inch for the largest piston; thus the range of water pressure necessary

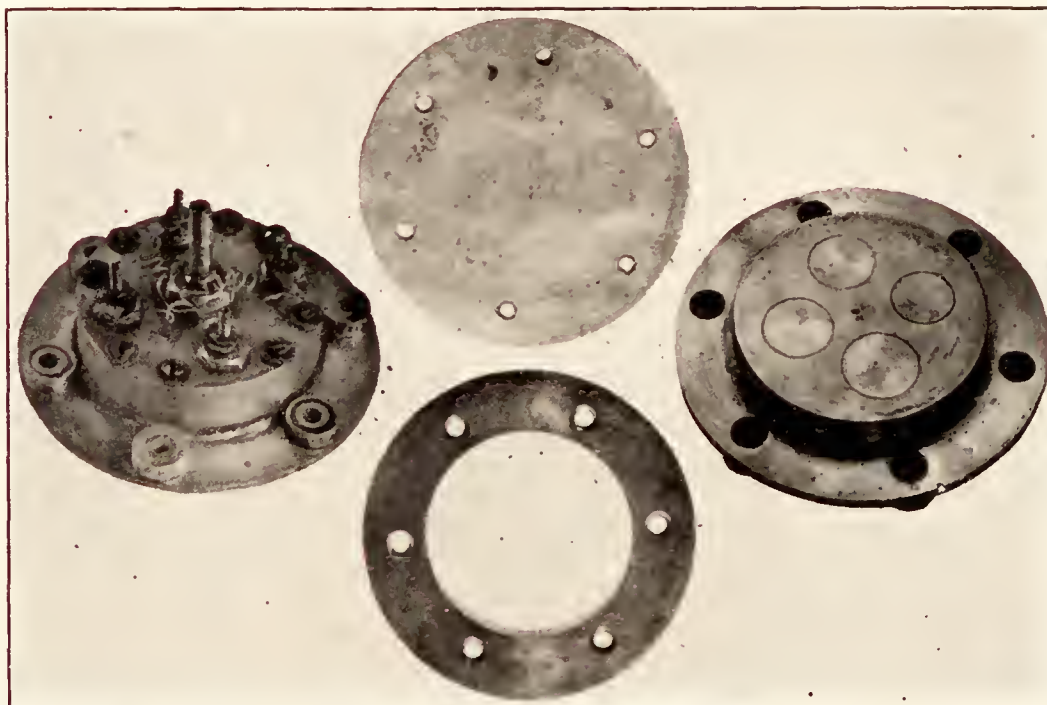


FIG. 3.—Water-pressure unit top and bottom views and its external diaphragm and retainer ring

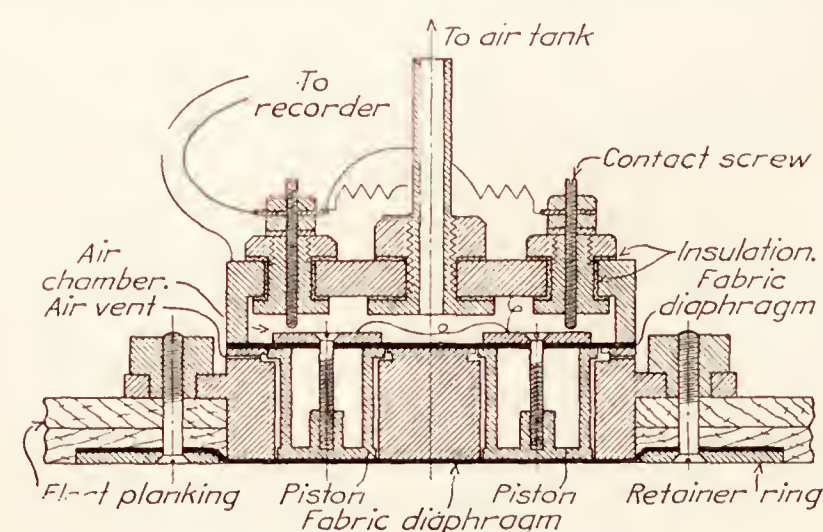


FIG. 4.—Cross section of water-pressure unit

to operate the four pistons at a given pneumatic pressure is proportionately the same. In test work the pneumatic pressure is adjusted to such a value that the expected range of water pressures as determined by preliminary trials will operate at least the largest piston but not the smallest. This determines the magnitude of the water pressure between limits. If none of the pistons operate, only a pressure not exceeded is known, and if all operate only a pressure exceeded is known.

Figure 4 is a cross-section drawing of a water-pressure unit. The pistons are hollow for lightness. Their inner ends are secured to an air-tight fabric diaphragm, and a similar diaphragm over the external ends excludes water from the instrument. These diaphragms are sufficiently flexible to permit the longitudinal piston displacement of about 0.002 inch that is required to bring each piston against its respective contact screw. The contact screws of the three largest pistons are connected to the fourth screw through parallel resistances. Figure 5 shows a diagram of the resulting circuit. Successive operation of the pistons results in step-by-step increase of the current to the recorder until a maximum is reached when the smallest piston operates.



When installed in the float bottom, the pressure units present a smooth surface flush with the float-bottom planking. Figure 6 shows the float bottom with the pressure units in place. Twenty-two units were installed, but the recorder could accommodate only 15 at a time. It was intended that a series of runs would be made with 15 units connected and the runs repeated with 7 of the units replaced by the remaining 7. The first 15 units connected included representative points well distributed over the float bottom, and in order to shorten the program the remaining 7 units were not connected.

Referring again to Figure 5, the essential parts of the recording unit are shown to be a plunger-type solenoid, a mirror, a light source, and a revolving film drum. The light beam remains in a zero position until one or more pistons in the pressure unit operate, when it is deflected in steps. The measured deflection then indicates the number of pistons operating. A multiple recording instrument with 15 such units was used. It was a modification of an N. A. C. A. recording manometer with a centrally located, electrically driven, film drum (Reference 3). The original diaphragms of the recording units were actuated by the solenoid plungers. Laboratory tests with this mechanism showed that it would record satisfactorily in less than one one-hundredth of a second. The film was driven at an approximate speed of 2 inches per second, thereby obtaining records showing even the very short pressure impulses.

The pneumatic system used in applying internal pressure to the water-pressure units consisted of a hand pump, three 125 cubic inch capacity air tanks, a sight gauge and a pressure-recording manometer for each tank, and aluminum tubing connections. Air was supplied to the three air tanks by the hand pump at pressures that could be controlled individually. Each tank supplied a particular group of water-pressure units. Group 1 included all units abaft the step; group 2, those units immediately forward of the step; and group 3, the remainder. By this arrangement it was possible to record a different range of water pressures simultaneously in each of the three portions of the float bottom.

Calibrations of the water-pressure units, either in or out of the float, were made at frequent intervals by applying pneumatic pressures externally on the units. With external pressure as ordinate and internal pressure abscissa the calibration curve for each piston of a pressure unit was found to be a straight line; and the slopes of the four curves varied from a minimum for the largest piston to a maximum for the smallest piston. Due to the effect of the two diaphragms, one at each end of the pistons, the calibrations were dependent to some extent on the piston displacement necessary to make contact. To obtain suitable calibrations, it was therefore necessary to make very careful adjustments of the contact screws.

Figure 7 is a photograph of the observer's cockpit. In the immediate foreground is the control board on which all switches and gauges were mounted. In the lower right corner is the water-pressure recorder with the film drum removed. The three shut-off cocks in the upper right corner were used for individual control of the three tank pressures of the pneumatic system, and the three gauges on the control board indicated the pressures on the tanks. The 15 knife switches were in circuits connecting the water-pressure and recording units and could be closed at any convenient time before a run. The small toggle switch marked "Motors" controlled the recording of all instruments except the water-pressure recorder, in which it only controlled

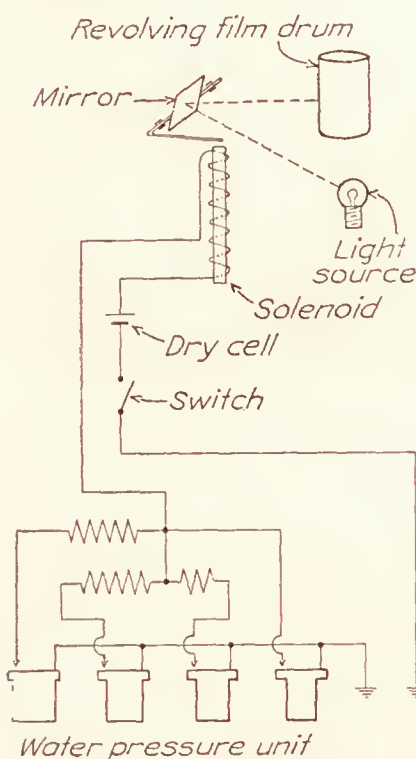


FIG. 5.—Diagram of the electrical circuit of a water-pressure unit and a recording unit



FIG. 6.—UO-1 float bottom with pressure units installed



movement of the film drum. The source light in the water-pressure recorder was in the circuit of another toggle switch marked "Timing lights." Closing and opening of that switch also caused start and stop timing lines to appear on the other records.

With the above instruments and apparatus on each run, continuous records of about five or six seconds' duration were obtained of the air speed, the float angle, and the three tank pressures; and shorter records about two to three seconds in duration were obtained simultaneously of the water pressures at 15 stations on one side of the float bottom. Air-speed, float-angle, and tank-pressure records were synchronized by timing lines at one-second intervals, and by the arrangement described above two additional timing lines on these records

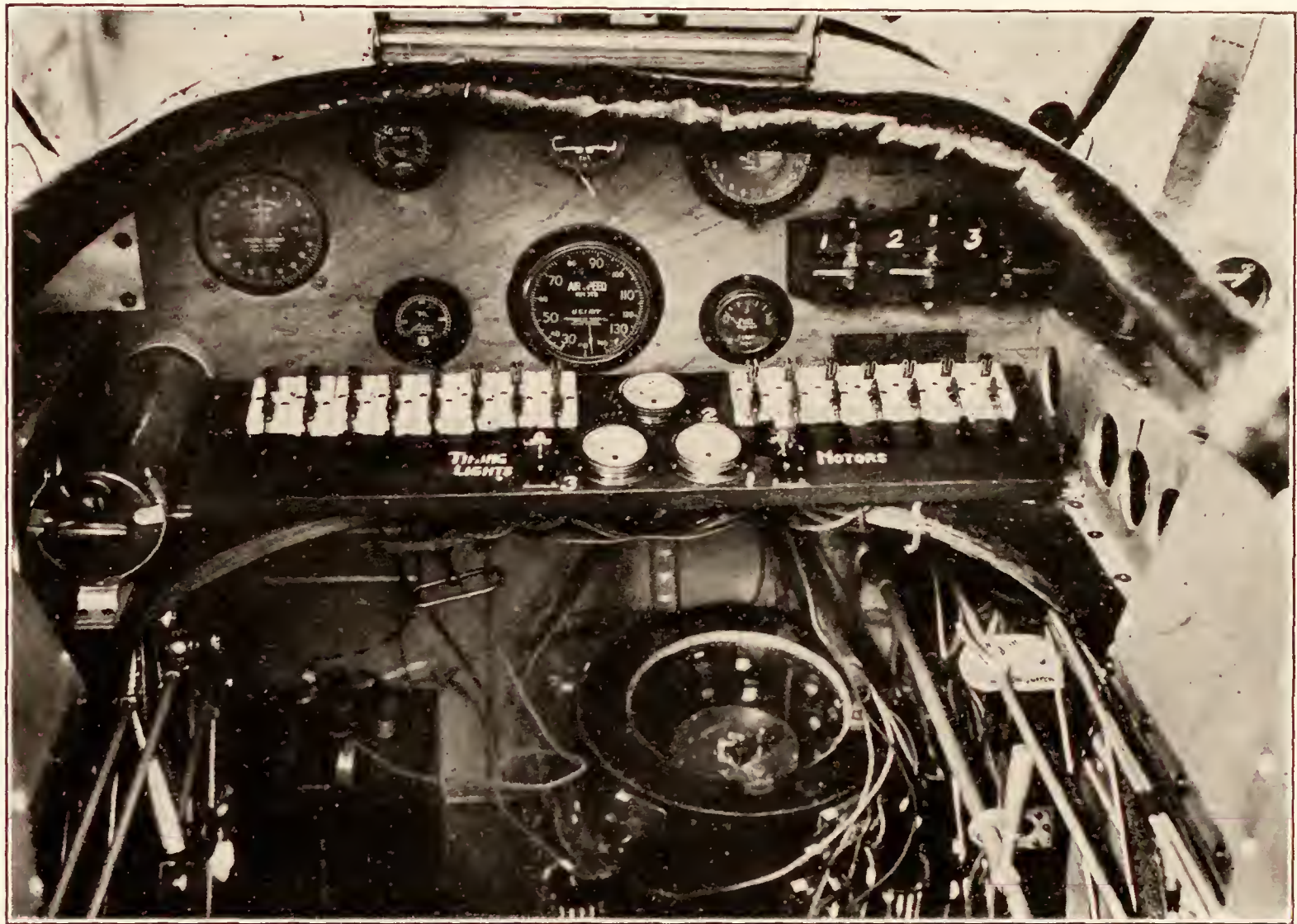


FIG. 7.—Interior of the observer's cockpit

indicated the start and stop times of the water-pressure record. The shortness of the runs made it necessary for the observer to time the operation of the switches very carefully, particularly in landing runs.

#### METHOD OF TESTS

The program of test work was made to include the following maneuvers:

- Taking off in smooth and rough water.
- Taxying in smooth and rough water.
- Landing—power off.
- Landing—power on.
- Landing—pancake.
- Landing—fast.
- Landing—cross wind; wind on right.
- Landing—cross wind; wind on left.

This program was planned to include every type of water run likely to be encountered in safe operation of a seaplane, and more particularly the maneuvers causing highest pressures on the float. With the latter point in mind, the pilot often made maneuvers as roughly as possible with discretion.



Taxying maneuvers are further divided to distinguish between the two taxying stages mentioned in References 4 and 5, and named "plowing" and "planing" in Reference 5. The same classification is used here. "Plowing" is taxying in the low-speed range before rising to the step, in which condition the float angle is largely independent of the controls. "Planing" is taxying on the step and follows naturally after "plowing" in accelerated taxying. In this condition the longitudinal angle is much more controllable in a widening range as take-off speed is approached.

The test work was done on the sheltered waters bounding Langley Field, with the exception of four rough-water take-offs made in choppy tide-disturbed water in Chesapeake Bay at the mouth of Back River at a time when the wind was not of sufficient velocity to roughen the more sheltered water.

Each time that runs were made an observer determined the average wind velocity in the vicinity of the test with a vane-type anemometer. The average velocity computed from three two-minute readings was used in determining the approximate water speed of the seaplane from the air-speed record.

Two maneuvers—low-angle plowing and low-angle planing—were attempts to bring high-water pressures to their maximum forward position. In the low-angle plowing maneuver the seaplane was rocked and a record was taken to include a nose-down attitude, but this did not give the small angles desired. Low-angle planing was more successful and float angles of  $0^\circ$  were obtained. It was accomplished by a "trick" maneuver invented by the pilot for the purpose and is described briefly in the following paragraph. Of special interest in this connection is run 85, in which both the low-angle planing and the subsequent pancake landing were recorded. The description follows:

Immediately following a fast landing, with the float at an angle of from  $3^\circ$  to  $6^\circ$ , and without much loss in speed, the control column was given a sharp push forward. The seaplane immediately went to an approximate horizontal attitude for an instant (not more than one-fifth of a second) and then bounced several feet into the air. Skillful maneuvering was then required to make the subsequent pancake landing safely.

The above maneuver is interesting as an example of what can happen when making water runs at speeds above the stalling speed. With a float less deep at the bow it would be a dangerous maneuver, and with a pilot not sufficiently skillful it might be disastrous in any case.

The seaplane was subjected to some very severe conditions, but suffered no more serious damage than the knocking loose of the copper seam covering on one wing-tip float. The two cross-wind landings made in a 16 M. P. H. wind were too severe for repetition. The rough-water take-offs and some of the pancake landings were also very severe. A seaplane could not reasonably be expected to withstand without damage conditions more severe than some of those imposed.

### PRECISION OF RESULTS

There are four sources of error that affect the accuracy of the results obtained with the water pressure unit. They are (1) accelerated motion of the float bottom at the instant that pressures are recorded; (2) displacement of the pistons finite distances in very short time intervals; (3) changes in calibration; (4) the method of recording pressures indirectly by "bracketing" them between high and low limits.

#### 1. EFFECT OF ACCELERATIONS

When calibrated, the external pressure required to operate each piston against any internal pressure includes the weight per unit area of the piston. Under operating conditions when the float is decelerated by contact with the water or given an upward acceleration by a wave the pressure required to move the piston is increased by the amount,  $w\left(\frac{a}{g} - 1\right)$ , where  $w$  is the weight per unit area of the piston and  $a$  is the acceleration. If the weight per unit area of the piston were the same as the float planking, the value recorded by the pressure unit would be the resultant pressure imposing stresses upon the float structure. This is the pressure that it



is desired to measure for use in the design of float structures. Actually the pistons are 13 to 17 times heavier than the float planking and a correction to the measured pressures is necessary. With due consideration for flexibility of the structure it is believed that  $8g$  represents an acceleration seldom, if ever, exceeded in these tests, while  $4g$  represents a probable average condition. The corrections necessary for  $4g$  and  $8g$  are tabulated below.

Piston No.	Piston weight (lb./sq. in.)	Planking weight (lb./sq. in.)	Correction (lb./sq. in.)	
			$a = 4g$	$a = 8g$
1-----	0.078	0.006	0.216	0.504
2-----	.084	.006	.234	.546
3-----	.094	.006	.264	.616
4-----	.105	.006	.297	.693
Average-----	-----	-----	.25	.59

## 2. PISTON DISPLACEMENT

Because each piston must move a finite distance to make electric contact, some of the external force on the piston is expended in producing this movement. This additional force represents an error that may be computed providing the time required to move the piston and its weight and travel are known. The period of the water-pressure impulses which are to be measured is something greater than  $1/100$  second. Therefore pistons will not be required to operate in less time than that. The piston travel is 0.002 inch and the weight of the heaviest piston is 0.105 pound per square inch. By making the pistons light and the travel small the error has been made negligible even for the assumed minimum time of  $1/100$  second. The magnitude of the error is shown in the following computations:

We have

$$s = \frac{1}{2} at^2 \text{ or } a = \frac{2s}{t^2}.$$

and

$$f = ma.$$

Then

$$f = m \frac{2s}{t^2}.$$

where

$s$  = displacement.

$a$  = acceleration.

$t$  = time.

$m$  = mass.

and

$f$  = force.

Using the values of weight, displacement, and time given above

$$f = \frac{.105 \times 2 \times .002 \times 10000}{32.2 \times 12} = .011 \text{ lb./sq. in.}$$

## 3. CALIBRATION CHANGES

Changes in calibration were found to occur probably because of changes in the piston-wall friction and changes of flexibility of the diaphragms. Errors from this cause were minimized by frequent calibrations.

## 4. "BRACKETING" METHOD

The accuracy with which exact values may be determined is limited by the method of "bracketing" between limits of a pressure exceeded and one not exceeded. If the differences in piston areas were made very small, the limits would be correspondingly close, but the range of pressures that could be included would also be small when the number of pistons is limited. A compromise must be made between the closeness of limits and the included pressure range so that both will be satisfactory. When limiting pressures are found by this method, an assumed true value which is the mean of the limits has the least probable error.

Due to differences in the calibration curves of the various pressure units, the range between limits varies somewhat for different pressure units, as may be noted from the results given in Table I. The following table, however, was taken from a typical calibration and shows the pressure range at two values of the internal pressure and the maximum errors, assuming the true pressure to be the mean of the limits. The probable error is, of course, less than these maxima.

Internal pressure (lb./sq. in.)	Piston number	Water pressure (lb./sq. in.)	Mean (lb./sq. in.)	Maximum error	
				Lb./sq. in.	Per cent
3.0	1	4.8	5.2	$\pm 0.4$	$\pm 7.7$
3.0	2	5.6	6.05	.45	7.4
3.0	3	6.5	7.05	.55	7.8
3.0	4	7.6			
1.5	1	2.6	3.0	.2	6.7
1.5	2	3.0	3.25	.25	7.7
1.5	3	3.5	3.9	.4	10.2
1.5	4	4.3			

From the above discussion of errors it is concluded that the accuracy of the limiting pressures is affected considerably by acceleration, and the limits probably should be corrected to read 0.25 pound per square inch higher than the recorded values. This is the average correction for an acceleration of  $4g$  and should therefore be correct within a small plus or minus error. It is further brought to attention that when definite values are desired they should be taken as the mean of the limits. When this is done the maximum error may be computed, and the probable error is something less than the maximum.

Errors in the pneumatic pressure records would affect the accuracy with which records could be interpreted. Such errors, however, were so small that they may be entirely neglected.

Air-speed records have an estimated precision of  $\pm 1$  per cent.

Float-angle check readings indicated a possible error in reading of  $\pm \frac{1^\circ}{2}$ .

For wind velocities up to 20 M. P. H. the velocity of unsteady air is not likely to change more than 5 M. P. H. in a short time. Average wind velocity as determined with the anemometer would then be correct within  $\pm 2.5$  M. P. H.

Water speed is the difference between air speed and wind velocity for a head wind, and is therefore subject to the same error as the wind velocity—i. e.,  $\pm 2.5$  M. P. H.

## RESULTS

The magnitudes of the maximum pressures occurring at all pressure stations during each run are recorded in Table I, and the locations of the stations are shown in Figure 8. These values are not necessarily simultaneous values, but are the maximum pressures that occurred during each run, which was usually two to three seconds in duration. Table II is a summary of the complete data of Table I giving the five highest pressures at all points. Curves showing the distribution of maximum pressures are given in Figure 9. Figure 10 represents graphically the distribution of maximum pressures on the float bottom. The values for Figures 9 and 10 are the highest pressures of Table II. In plotting, pressures exceeded are assumed to be exceeded by the average value of 0.5 pound per square inch.



Referring again to Figure 8 and Table II, it is seen that the highest pressures occurred immediately forward of the step for the full width of the float bottom. Going forward from the step the region of high pressures gradually narrows toward the keel and the magnitudes of the maximum pressures decrease. Pressure units (1), (2), and (3) located near the step recorded maximum pressures in excess of 6 pounds per square inch, while the maximum pressure exceeded at (15), which was farthest forward along the keel, was 2.5 pounds per square inch. Pressures at (15) were seldom of sufficient magnitude to be recorded by the pressure unit, and when they were they were obviously caused by waves. At (12), (8), and (5) there occurred pressures of increasing magnitude and of more and more frequent occurrence in the order named. Station (14), which was as far forward as (15), but near the chine, never operated; (11) operated but four times, the maximum pressure exceeded being 2.3 pounds per square inch; (10) operated more frequently than (11) and recorded higher pressures; and (6) operated frequently, often recording pressures as great as those at (1), (2), and (3). The highest pressure recorded at (6) was between 5 and 6.8 pounds per square inch.

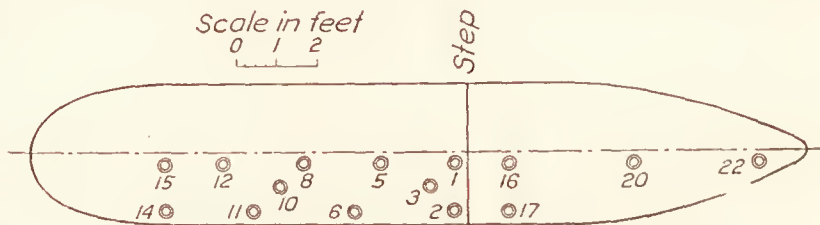


FIG. 8.—Water-pressure unit locations in the UO-1 float bottom

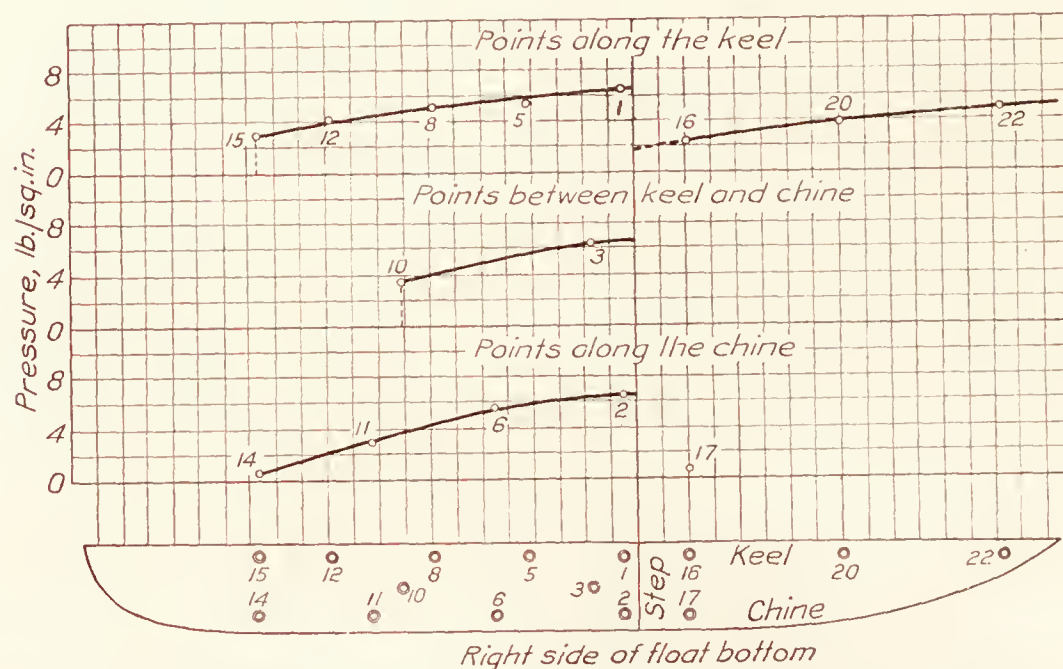


FIG. 9.—Distribution of maximum water pressures on the UO-1 seaplane float bottom

square inch; (20) operated five times during the entire series of runs and once recorded a pressure in excess of 3.4 pounds per square inch; (22) operated frequently and once in a very severe pancake landing on glassy water it recorded a pressure of between 4.5 and 5.5 pounds per square inch.

The time interval of water-pressure impulses and the frequency with which they occur are not shown in the table of results. In general, it may be said that high pressures were of longer duration and more frequent occurrence at stations (1), (2), (3), (5), and (8) than elsewhere. The high maximum pressures that occurred were not more than one-twentieth second in duration and often were much less, but the pressures were likely to be maintained near the maximum values for longer periods ranging approximately from one-tenth to one-half second. Maximum pressures at these stations were likely to recur several times during a run.

It has been mentioned that high pressures as great as those at (1), (2), and (3) often occurred at (6), but such pressures at (6) were of shorter duration (about one-fortieth second) and seldom appeared more than two or three times during a run. Between these maxima the pressure invariably dropped back to small values, usually within about one-tenth second.

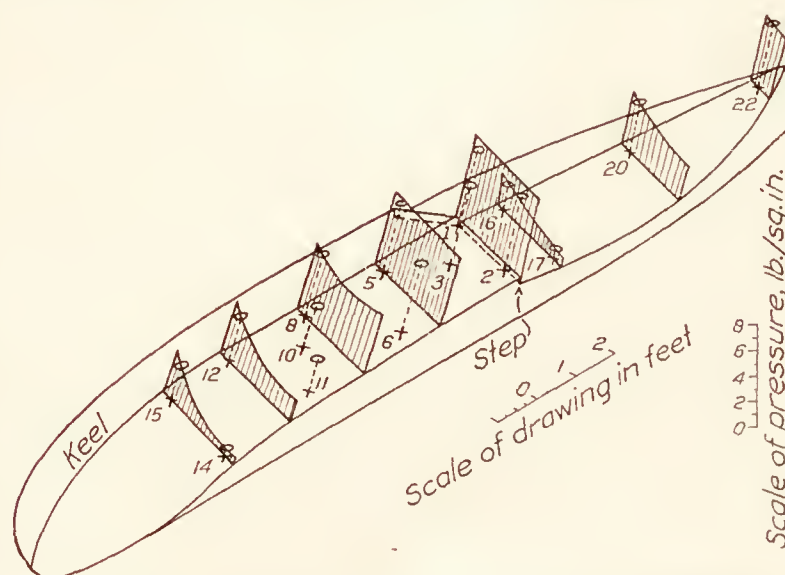


FIG. 10.—UO-1 seaplane float bottom showing the distribution of maximum water pressures over one side of the bottom



The other units forward of the step—viz, (10), (11), (12), and (15)—also recorded maximum pressures of short duration (one-thirtieth to one-fiftieth second or less). At (12) there was sometimes evidence of pressures maintained near the maximum values for much longer periods, but (10) and (11) gave records quite similar to those obtained at (6).

Aft the step the one pressure recorded at (16) and those at (20) were of very short duration (one-fiftieth to one one-hundredth second approximately). At (22) maximum pressures were of an approximate duration of one-fortieth second and were likely to recur several times in rapid succession.

The results suggest that a right triangular area bounded by the step, the keel, and a line drawn from the outermost part of the step to the point on the keel nearest (15) as the hypotenuse would include an area of high and more or less sustained pressures decreasing in magnitude toward the bow. Along the hypotenuse and outside the triangle would lie stations (6), (10), and (15), at which occurred pressures of shorter duration and decreasing magnitude toward the bow.

The highest pressures were obtained in rough-water take-offs and pancake landings, although the maxima for some points were obtained in other maneuvers. The rough-water take-offs were very severe, due to their being made in choppy tide-disturbed water with little wind. All other rough-water maneuvers were made in a much stronger wind on more sheltered water.

The results indicate that high pressures are most likely to occur generally over the float bottom in rough water, but that pressures just as great may result from bad handling in perfectly smooth water. The truth of the latter part of the above statement is borne out in run 85 (*b*). In that run the pressures were not only very high at the step, but the high pressure of 4.5 to 5.5 pounds per square inch was recorded at (22) in the stern. Such a pressure so far from the center of gravity must impose very severe stresses in the float structure.

The only available comparative data are those contained in the British reports of Reference 6, which were obtained on flying-boat hulls. On the F. 3 and H. 16 hulls (R. and M. 683) the highest pressures exceeded were, respectively, 8.2 and 8.7 pounds per square inch, and pressures greater than 6 pounds per square inch were exceeded several times. These pressures are roughly 2 pounds per square inch greater than those recorded on the UO-1 float. The F. 3 and H. 16 hulls have approximately the same bottom V angle as the UO-1 float. It is of interest to note that these seaplanes are heavier per beam length in approximately the same ratio as the difference in maximum pressures.

### CONCLUSIONS

In the following conclusions regarding the method and results those concerning the results should be construed as strictly applicable only to the UO-1 float as used in these tests:

The method employed is feasible, although subject to mechanical difficulties that are indicated by a lack of pressure records at various stations on different runs, but which may be largely eliminated in future test work.

The highest water pressures on the UO-1 float occur at the step for the full width of the float bottom.

Extending forward from the step the region of high water pressures narrows toward the keel and the magnitudes of the pressures decrease gradually toward the bow.

Local water pressures of considerable magnitude are likely to occur at the stern of the float.

There are large portions of the float bottom, both aft and forward of the step, on which the water pressures are never likely to be greater than 2 to 3 pounds per square inch.

LANGLEY MEMORIAL AERONAUTICAL LABORATORY,  
NATIONAL ADVISORY COMMITTEE FOR AERONAUTICS.  
LANGLEY FIELD, VA., *December 22, 1927.*



## REFERENCES AND BIBLIOGRAPHY

- REFERENCE 1. Norton, F. H.: N. A. C. A. Recording Air-Speed Meter; N. A. C. A. Technical Note No. 64. (1921.)
- REFERENCE 2. Brown, W. G.: The Synchronization of N. A. C. A. Flight Records. N. A. C. A. Technical Note No. 117. (1922.)
- REFERENCE 3. Norton, F. H., and Brown, W. G.: The Pressure Distribution Over the Horizontal Tail Surfaces of an Airplane, III. N. A. C. A. Technical Report No. 148. (1922.)
- REFERENCE 4. Crowley, jr., J. W., and Ronan, K. M.: Characteristics of a Single Float Seaplane During Take-Off. N. A. C. A. Technical Report No. 209. (1925.)
- REFERENCE 5. Crowley, jr., J. W., and Ronan, K. M.: Characteristics of a Twin-Float Seaplane During Take-Off. N. A. C. A. Technical Report No. 242. (1926.)
- REFERENCE 6. Baker, G. S., and Keary, E. M.:  
Experiments with Full-Sized Machines. (Second Series.) Local Water Pressures on Flying-Boat Hulls. British Aeronautical Research Committee Reports and Memoranda No. 683. (September, 1920.)  
P. 5 Flying Boat N. 86, Impact Tests (Experiments with Full-Sized Machines, Third Series). British Aeronautical Research Committee Reports and Memoranda No. 926. (April, 1924.)
- Bottomley, G. H.: The Impact of a Model Seaplane Float on Water. British Advisory Committee for Aeronautics Reports and Memoranda No. 583. (March, 1919.)
- Herrmann, H.: Seaplane Floats and Hulls. Part I. N. A. C. A. Technical Memorandum No. 426. (1927.) Part II. N. A. C. A. Technical Memorandum No. 427. (1927.)
- Richardson, H. C.: Airplane and Seaplane Engineering. Bureau of Aeronautics, Navy Department Technical Note No. 59. (1923.)





TABLE I.—WATER-PRESSURE DISTRIBUTION ON A SEAPLANE FLOAT

Run No.	Maneuver	Condition of water	Air speed in M. P. H.	Average wind in M. P. H.	Water speed in M. P. H.	Longitudinal float angle in degrees	Water pressures in pounds per square inch																						Remarks								
							Station number																														
							1		2		3		5		6		8		10		11		12		14		15			16		17		20		22	
							a	b	a	b	a	b	a	b	a	b	a	b	a	b	a	b	a	b	a	b	a	b		a	b	a	b	a	b	a	b
55	Plowing	Smooth	33	8.5	24.5	10							4.7			2.7		2.0		2.2		2.1		2.0		2.4		2.5		2.3		2.8					
56	do	do	36	8.5	27.5	10							2.6			1.4		1.0		1.1		1.0		1.0		1.1				1.2		1.5					
59	do	Fairly smooth	31	11	20	10½							4.4	4.7		3.0		2.0		2.3		2.1		2.0		2.4				2.7		2.9	2.5	2.6			
60	do	do	44	11	33	4-8	2.9		2.7	2.9	2.1	2.6	2.1	2.9	2.4	3.1	2.5		1.6	2.2		1.5		1.5		1.7				1.9		2.2		1.8			
75	do	do	27	11	16	9-12		3.0		3.2		2.8		3.2		3.0	2.4	3.0		2.6		2.5		2.3		2.8				3.1		3.3		2.9			
76	do	do	26	11	15	10-12		1.5		1.9		1.4		1.8	2.7	2.0	2.2		1.3		1.2		1.1		1.3				1.0		1.3		1.7	1.3			
46	do	15 to 18 inch waves with whitecaps.	30	17	13	11								2.5	3.8		1.9	2.1		1.7		1.5		1.6		1.8		2.0		1.7		2.3					
47	do	do	27	17	10	11							2.3		2.2		1.3			1.0		.8		1.0		1.0		1.3		.7		1.2					
48	do	do	33	17	16	10							2.7		2.7		1.1			1.2		1.1		1.1		1.2		1.5		1.0		1.6					
49	do	do	44	17	27	8-11							3.2	3.7		2.4		1.8		1.9		1.7		1.7		2.0		2.2		1.9							
62	Low-angle plowing	Fairly smooth	41	11	30	3-7	1.5		2.1	2.4	2.1	2.5	2.5	2.8	2.6	2.0	2.2				1.2	1.7		1.7		1.3				1.0		1.3		1.3			
85(a)	Low-angle planing	Glassy	58.5	3	55.5	0-4	5.2	5.5			4.0	4.7		4.4	4.2	5.2		6.7		4.5		4.1		4.8		4.8				5.0		5.7		6.6			
64	do	12 to 15 inch waves	54.5	13	41.5	½-9	3.3		3.4		3.0	3.5	2.4	3.3	3.6		3.3	3.7	3.0		2.1		2.0		2.5				2.6		2.9		3.1	2.8	3.4		
86	Taking-off	Smooth	41	10	31	5		4.1			4.1		4.4		4.1		6.8		4.6		4.2		4.9		4.9				5.1		5.8		6.8		4.5		
61	do	Fairly smooth	54	11	43	4-9	3.2		4.1	4.4	3.1		5.0		3.2		2.1			2.2		2.2		2.1		2.0				2.5		2.8		3.0	2.6		
28	do	12 to 15 inch waves	43.5	15	28.5	6-9	3.3		3.2	3.7	3.1		2.8	4.3		1.0	1.2	1.0			1.2	1.1	1.3		1.2		1.2		1.5		1.6		2.2				
57	do	do	52	15	37	4-6	3.1	3.5	3.8	4.2	3.8	4.6	4.1	4.4		2.7	2.1		2.4		2.2		2.0		2.5				2.4		2.7		3.0	2.5			
58	do	do	49	15	34	4-6	1.4	1.6		2.1	2.2		2.6		1.3	1.9			1.1				1.0		1.1				.8		1.2			1.2			
77	do	Choppy; 18 to 24 inch waves.	43.5	11	32.5	5-10	5.4		5.5	6.2	3.5		4.0	5.3		3.6	2.8	3.5		3.2		3.0		2.8	3.3				3.4		3.6		3.8	3.1			
78	do	do	49	11	38	5-18	2.0	2.4	2.7		2.5		2.5	2.8	2.6		2.3			1.3		1.3		1.2		1.4				1.1		1.5		1.8	2.0		
79	do	do	49.5	11	38.5	5-10	5.9		6.0	7.0	6.3		4.3		5.0	6.8	4.8	5.9		4.4		4.0		3.8	4.5				4.7		5.2		5.1	4.4			
80	do	do	50	11	39	4-9	2.0		2.8		2.8	3.2	3.2	3.5	3.5		3.5				2.1		2.0		2.4				2.2		2.5	2.8		3.1			
11	Landing—power off	Smooth	62	9	53	12½	1.5						2.4			1.3	1.4		1.4			.9		1.9		.7		.9		2.0		2.3					
36	do	do	56	10	46	12½			2.4	2.7			2.6				1.4			1.5		1.1		2.0		1.2			1.6		1.0		1.2				
37	do	do	55	10	45	9				2.3				1.9			1.4			1.4		1.4		1.4		1.5			1.8		1.5		1.8	1.5			
38	do	do	57	10	47	8							2.1			1.1	1.1		1.0			.8		.8		1.2			.6		1.1		1.3				
39	do	do	49	10	49	9	1.9		3.1				3.1			1.7	1.5		1.5		1.2		1.3		1.4		1.7		1.3		1.6		1.9				
82	do	do	58	8	50	12	5.3	5.6	5.5	6.3	4.1	4.9	4.5	6.0		4.1		6.9			4.2		5.0		4.9				5.1		5.5		6.8	4.5			
71	do	Fairly smooth	59	11	48	9	4.3		3.2	3.8	2.8	3.4	3.1	4.3	3.1	3.7	2.8	3.5		2.5		2.3		2.2		2.7			2.6		2.9		3.1	3.5			
72	do	do	55	11	44		2.3		2.6	2.8	2.5	2.8	3.2		2.3	3.0	2.0	2.2			1.2		1.6		1.2				.9		1.2		1.6				
73	Landing—power on	do	59	11	48	7½	4.3		3.7	4.1	2.7	3.3	3.1	4.2		2.9	2.1	2.7		2.5		2.2		2.2		2.6			2.5		2.9		3.1	2.7			
74	do	do	63	11	52	7	2.4		2.3	2.5			2.8		2.0	2.7	1.8	2.0		1.1		1.1		1.0		1.1			.7		1.1		1.4	1.3			
24	do	12 to 15 inch waves	49.5	15	34.5	11½		2.7					2.7		2.8		1.1		1.4		1.4		2.5			1.5		1.5		1.6		1.7		2.3	1.7		
25	do	15 to 18 inch waves with whitecaps.	52	17	35	10	2.5	3.5					2.3	3.0	3.3	1.2			1.9		1.2		2.6			1.3	1.3			1.4		1.5	3.4				
26	do	do	49	17	32	10		2.6					2.6	3.9		1.5	2.0	2.1		1.3		2.8			1.4	2.4			1.5		1.6		2.2				
27	do	do	50	17	33	10½		2.7					2.6	3.5		3.9	1.3	1.6	2.2		2.3		3.0			1.5	2.5			1.6		2.3	2.6				
51	Landing—fast	Smooth	67	7	60	6							2.4			1.3	1.5				.9		.9		1.0		1.3			.7		1.2		1.4			
52	do	do	63.5	7	56.5								4.5			2.7	1.9				1.9		1.8		2.1		2.3			2.1		2.3		2.7			
53	do	do	61																																		







TABLE II.—SUMMARY OF FIVE HIGHEST WATER PRESSURES AT ALL STATIONS

Station number																							
1			2			3			5			6			8			10			11		
Run No.	Pressure (lb./sq. in.)		Run No.	Pressure (lb./sq. in.)		Run No.	Pressure (lb./sq. in.)		Run No.	Pressure (lb./sq. in.)		Run No.	Pressure (lb./sq. in.)		Run No.	Pressure (lb./sq. in.)		Run No.	Pressure (lb./sq. in.)		Run No.	Pressure (lb./sq. in.)	
	a	b		a	b		a	b		a	b		a	b		a	b		a	b		a	b
79	5.9	-----	79	6.0	7.0	79	6.3	-----	61	5.0	-----	79	5.0	6.8	79	4.8	5.9	64	3.0	-----	27	2.3	-----
77	5.4	-----	77	5.5	6.2	85b	6.1	-----	52	4.5	-----	28	4.3	-----	80	3.5	-----	45	2.7	-----	64	2.1	-----
82	5.3	5.6	82	5.5	6.3	87	5.5	6.5	82	4.5	6.0	85a	4.2	5.2	64	3.3	3.7	44	2.3	-----	20	1.3	-----
85a	5.2	5.5	67	4.5	4.9	67	4.1	4.7	59	4.4	4.7	26	3.9	-----	65	3.3	3.6	68	2.3	-----	17	1.0	-----
85b	5.0	-----	61	4.1	4.4	82	4.1	4.9	79	4.3	-----	46	3.8	-----	77	2.8	3.5	27	2.2	-----			-----

Station number																						
12			14			15			16			17			20			22				
Run No.	Pressure (lb./sq. in.)		Run No.	Pressure (lb./sq. in.)		Run No.	Pressure (lb./sq. in.)		Run No.	Pressure (lb./sq. in.)		Run No.	Pressure (lb./sq. in.)		Run No.	Pressure (lb./sq. in.)		Run No.	Pressure (lb./sq. in.)			
	a	b		a	b		a	b		a	b		a	b		a	b		a	b		
79	3.8	4.5	-----	-----	27	2.5	-----	20	1.8	-----	-----	25	3.4	-----	85b	4.5	5.5					
27	3.0	-----	-----	-----	26	2.4	-----	-----	-----	-----	-----	20	3.3	-----	71	3.5	-----					
77	2.8	3.3	-----	-----	14	1.8	-----	-----	-----	-----	-----	80	2.8	-----	80	3.1	-----					
26	2.8	-----	-----	-----	20	1.7	-----	-----	-----	-----	-----	27	2.3	-----	69	2.8	-----					
25	2.6	-----	-----	-----	25	1.3	-----	-----	-----	-----	-----	68	1.5	1.8	64	2.8	3.4					

a=pressure exceeded; b=pressure not exceeded.

NOTE.—The lack of agreement between run numbers and highest pressures at adjacent points (particularly 1, 2, and 3) is likely due to lack of records at some points on various runs. (See Table I.) Units 14 and 17 never operated, 16 operated but once, and 11 four times.





---

## REPORT No. 291

---

### DRAG OF C-CLASS AIRSHIP HULLS OF VARIOUS FINENESS RATIOS

By A. F. ZAHM, R. H. SMITH, and F. A. LOUDEN  
Aerodynamical Laboratory, Bureau of Construction and Repair  
United States Navy





# REPORT No. 291

## DRAG OF C-CLASS AIRSHIP HULLS OF VARIOUS FINENESS RATIOS

By A. F. ZAHM, R. H. SMITH, and F. A. LOUDEN

### PREFACE

This report presents the results of wind-tunnel tests on eight C-class airship hulls with various fineness ratios, conducted in the Navy Aerodynamic Laboratory, Washington. The purpose of the tests was to determine the variation of resistance with fineness ratio, and also to find the pressure and friction elements of the total drag for the model having the least shape coefficient.

Seven C-class airship hulls with fineness ratios of 1.0, 1.5, 2.0, 3.0, 6.0, 8.0, and 10.0 were made and verified. These models and also the previously constructed original C-class hull, whose fineness ratio is 4.62, were then tested in the 8 by 8 foot tunnel for drag at  $0^\circ$  pitch and yaw, at various wind speeds. The original hull, which was found to have the least shape coefficient, was then tested for pressure distribution over the surface at various wind speeds.

This account is a slightly revised form of Report No. 335, prepared in the Bureau of Construction and Repair for the Bureau of Aeronautics, May 14, 1927, and by it submitted for publication to the National Advisory Committee for Aeronautics. A summary of conclusions and a comparison with previous data are given at the end of the text.

### DESCRIPTION OF MODELS

The eight models, the smallest of which is shown in Figure 1, and hull outlines of which are shown in the sketches of Figures 5 to 12, were all 7.7 inches in their specified maximum diameter. The specified and measured offsets and the length and volume of the various models are given in Table I. The models were made of laminated pine and varnished.

The original C-class hull, previously described in References 1 and 2, was fitted with 17 pressure-collecting holes as shown in Figure 3. The pressure leads, one running from a hole in the nose and the other successively from each surface hole, were connected to an inclined-tube manometer outside the tunnel.

### METHOD OF TESTING

The drag of the hulls was measured with the bifilar balance, which is shown in Figure 2. The models with a fineness ratio of 4.62 and greater were mounted as indicated in Figure 2;



FIG. 1.—Model of C-class airship, fineness ratio 1, mounted on bifilar balance



the models with fineness ratios of 1.0, 1.5, 2.0, and 3.0 were mounted as shown in Figure 1. The provisions, method, and precision of such tests are discussed in Reference 3.

The pressure distribution measurements were made on the original C-class hull which was mounted in the tunnel at  $0^\circ$  pitch and  $0^\circ$  yaw as shown in Figure 4. The difference of pressure

between the nose and each of the holes aft of the nose was determined successively. To do this all the surface holes were plugged except one which was joined to one pressure lead, while the nose hole was joined to the other lead. The wind speed was then varied from 20 to 60 miles an hour, by 10-mile intervals, and the differential pressure was measured on an alcohol manometer having a 1 to 10 slope. These pressure differences could be read in all cases to within 0.005" vertical of alcohol.

### RESULTS OF DRAG MEASUREMENTS

Table II gives the gross and net drags for all the models, as found for the various conditions; Table III gives the derived shape coefficients and values of  $V_1 D$  where  $V_1$  is the air speed in feet per second and  $D$  the maximum model diameter in feet; Table IV

gives values of the disk ratio for the various models at 40 miles an hour. The drag of a normally exposed thin disk with a diameter equal to that of the hull's major circle was found to be  $0.00298 S V^2$  pounds at  $V$  miles an hour, where  $S$  is the area of the disk in square feet. The ratio of this force to the actual head-on drag of the hull is called the "disk ratio."

In Figures 5 to 12 the gross and net drags are plotted against air speed in individual graphs, to illustrate the various experimental corrections; the shape coefficient is plotted against  $V_1 D$ . Figure 13 gives plots at 40 miles an hour, of the drag, shape coefficient, and disk ratio versus

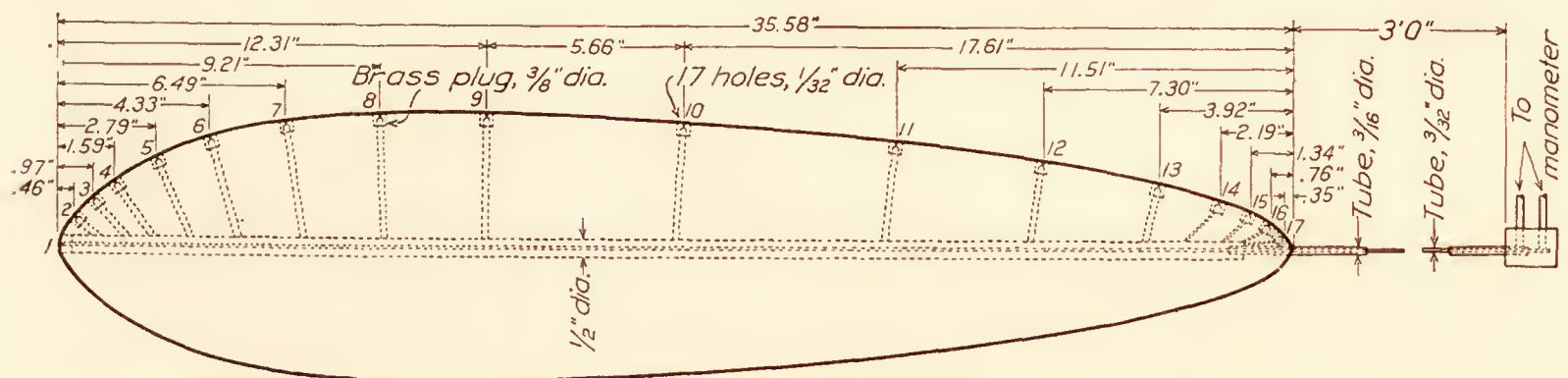


FIG. 3.—Pressure collector on C-class airship model with fineness ratio of 4.62

fineness ratio; the resistance of a sphere and of a disk each with a diameter equal to the maximum diameter of the various hulls is also shown.

One sees from Figures 5 to 12 that, for the present speed range, the net resistance of all the models is of the form  $R = a V^n$ , where  $a$  and  $n$  are numerical constants. Substituting this empirical value of  $R$  in the equation of the shape coefficient  $C_s = 2R/\rho (\text{Vol.})^{2/3} V^2$  gives  $C_s = 2a V^{n-2}/\rho (\text{Vol.})^{2/3}$  which on logarithmic paper is a straight line since the air density  $\rho$  is constant. Values of  $n$  for all the models are slightly less than 2 except that for the smallest model with a fineness ratio of 1.0,  $n = 2.04$ .

Figure 13 indicates that, at 40 miles an hour, the model of least resistance and greatest disk ratio, 25.31, has a fineness ratio of 2.0; the model with a fineness ratio of 4.62 has the smallest shape coefficient,  $C_s = .028$ . The resistance of a sphere with a diameter equal to the maximum model diameter is almost three times as great, at 40 miles an hour, as that of the model with a fineness ratio of 1.0.



## RESULTS OF PRESSURE DISTRIBUTION MEASUREMENTS

The differential pressure measurements made on the model of best shape coefficient, viz, fineness ratio = 4.62, are presented in Table V. Table VI gives the point pressure at the several holes, found by subtracting the differential pressure from the nose pressure. These data are plotted in Figures 14 and 15. Table VII gives the point pressure in terms of the nose pressure. The graphs of the faired values of point pressure multiplied by  $(60/V)^2$  to make them comparable are shown in Figure 16. The integrals of each pressure graph, giving the elements of pressure drag, and the summation of these, or the resultant pressure-drag, are given in Table VIII and plotted in Figure 17. With them are shown the total drag and the resultant friction. The order of graphic integration here used to find the force  $\pi \int p \cdot d(r)^2$ , where  $r$  is the radius of the model at any point along its axis, over the various portions of the surface of the model, is detailed in Figure 19.

One sees from Figure 14 that the point pressure at all speeds decreases from full impact  $\frac{1}{2}\rho V^2$  at the nose of the model to zero at a distance of 5.4 per cent of the model length from the nose; the maximum suction occurs at about one-seventh of said length, and is equal to about 43 per cent of the nose pressure. There is another point of zero pressure at 4.4 per cent of the model length from the stern; aft of this point the pressure is positive. Figure 15 shows that the pressure at each hole varies nearly as the square of the velocity.  $n$  indicates exponent in equation,  $P = KV^n$ .

From Figure 17 it is seen that the total drag and its elements vary as  $V^n$  for the range of speeds used. The difference between the curves of total drag and pressure drag, giving the frictional drag, varies as  $V^{1.79}$ .  $n$  indicates exponent in equation,  $R = KV^n$ .

Figure 18 gives, for the present perforated model and a Parseval model tested in England, the point pressure and zonal pressure-drag for various zone<sup>1</sup> lengths. The point pressure is in terms of the nose pressure; the zonal drag is in terms of the whole measured model drag, comprising pressure and friction. The whole drag of the Navy model is seen to be 26 per cent pressural, hence 74 per cent frictional; the drag of the other is 20 per cent pressural and 80 per cent frictional. The pressure graphs for the British model were plotted from the tabulated data of Reference 4.

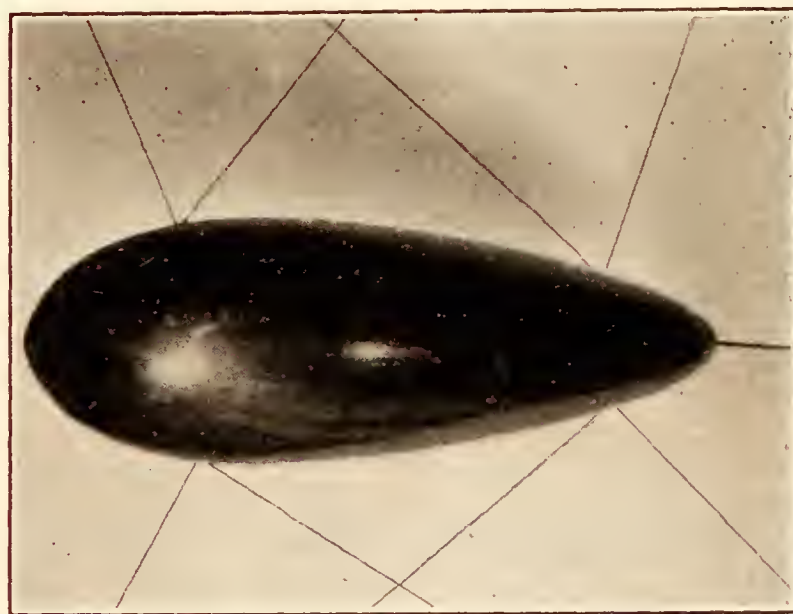


FIG. 4.—Model of C-class airship, fineness ratio 4.62, mounted for pressure distribution test

## CONCLUSIONS

Figures 5 to 12 indicate that the drag of each of the C-class models of various fineness ratio varies as  $V^n$ , where  $n$  is less than 2.0, except for the smallest model with a fineness ratio of 1.0, for which  $n = 2.04$ .

Figure 13 shows that at 40 miles an hour the model with a fineness ratio of 2.0 has the least drag and the greatest disk ratio, 25.31; the model whose fineness ratio is 4.62 has the smallest shape coefficient,  $C_s = 2R/\rho(\text{Vol.})^{2/3} V_1^2 = .028$ .

Figure 17 indicates that, at 20 to 60 M. P. H., all the elements of the total drag of the model whose fineness ratio equals 4.62 vary as  $V^n$ . At 40 miles an hour, the total downstream pressure is 408 per cent of the total measured drag; the total upstream pressure, 382 per cent; the resultant pressural drag, 26 per cent; the frictional drag, 74 per cent.

The graph of total drag versus model length, Figure 13, is a smooth continuous curve for all lengths from 0 upward, indefinitely.

<sup>1</sup> A zone is a part of the surface bounded by two planes normal to  $V$ . Usually one plane is assumed tangent to the surface at its upstream end



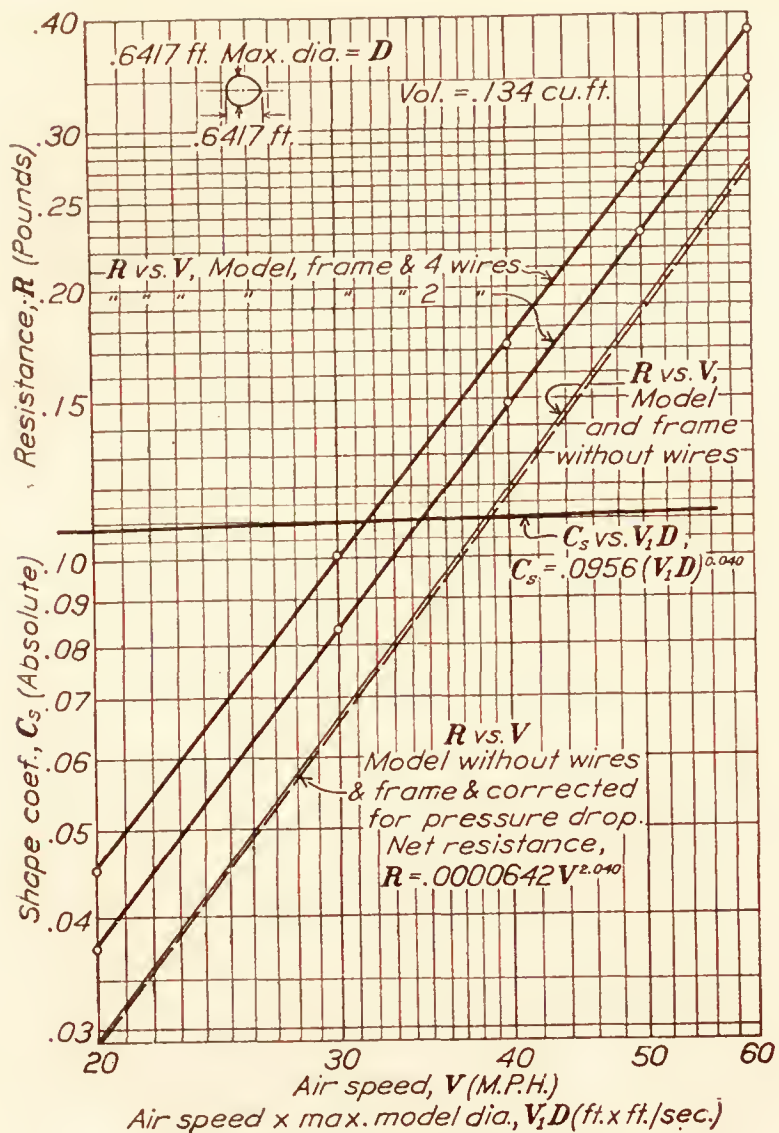


FIG. 5.—Fineness ratio=1

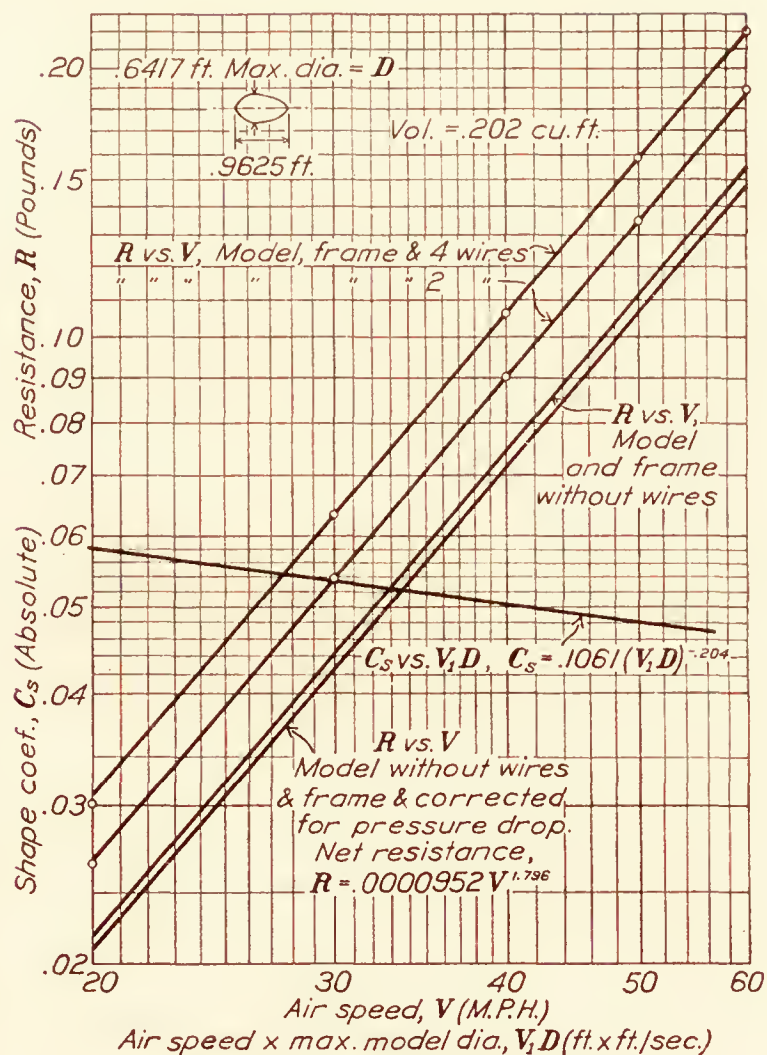


FIG. 6.—Fineness ratio=1.5

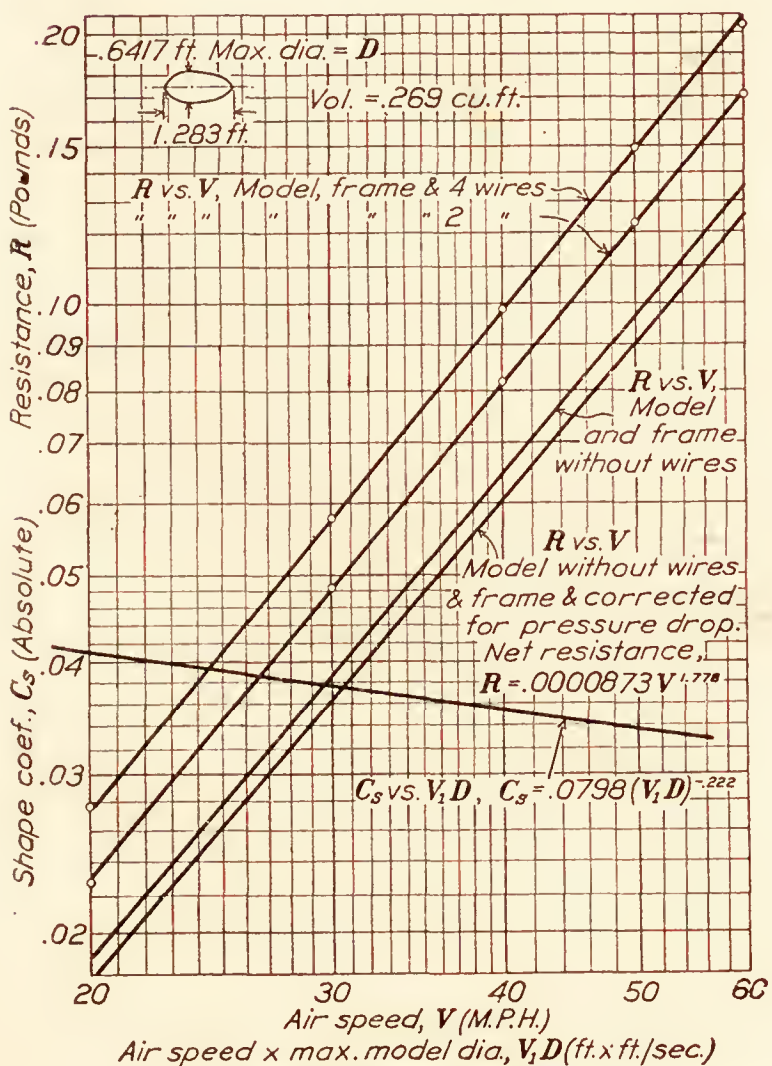


FIG. 7.—Fineness ratio=2

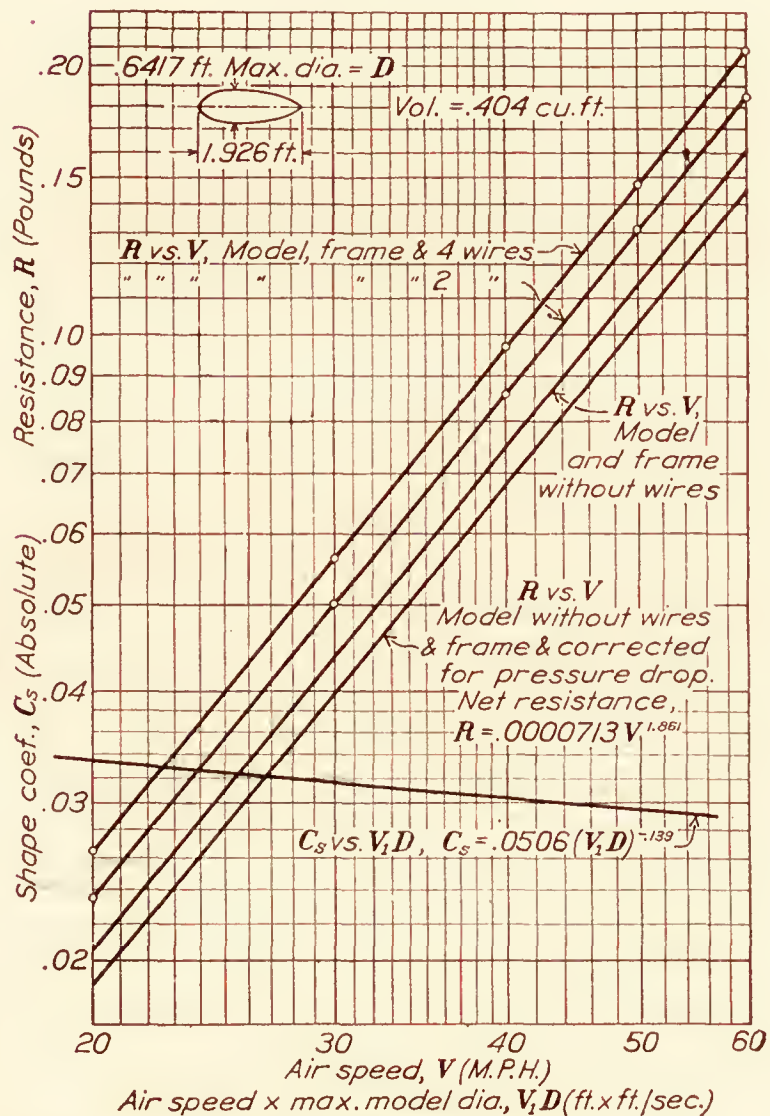


FIG. 8.—Fineness ratio=3

C-class airship. Model at  $0^\circ$  pitch and  $0^\circ$  yaw



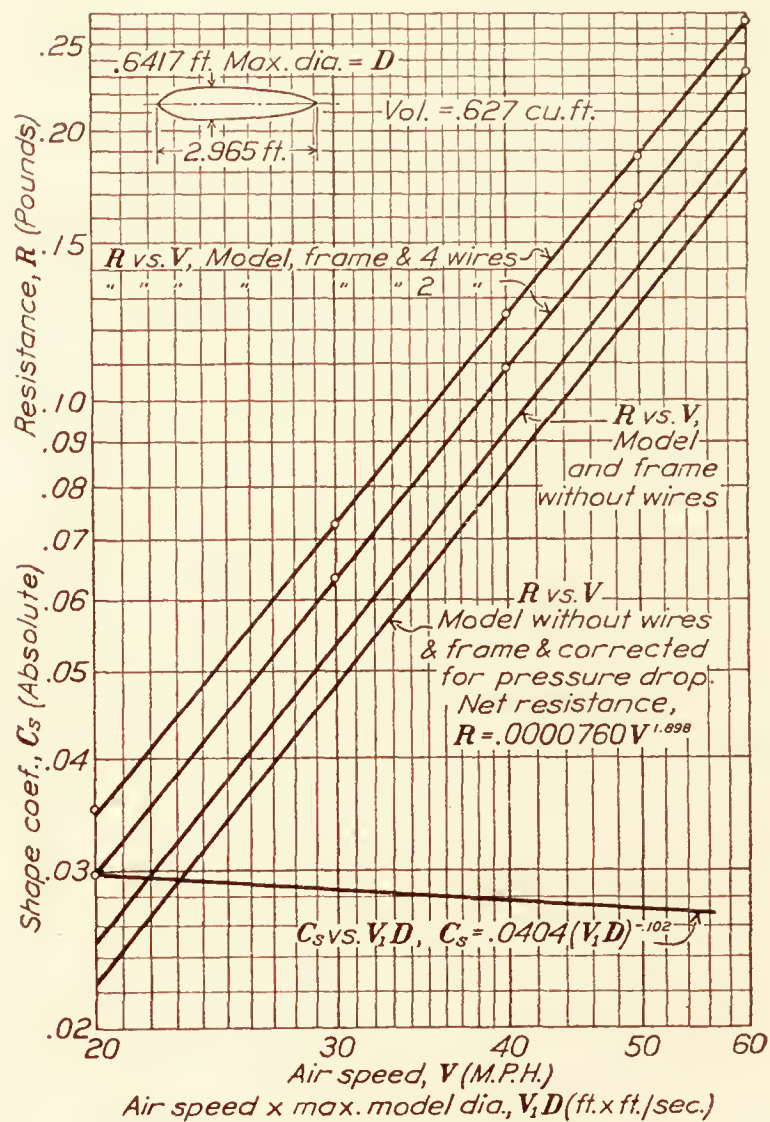


FIG. 9.—Fineness ratio=4.62

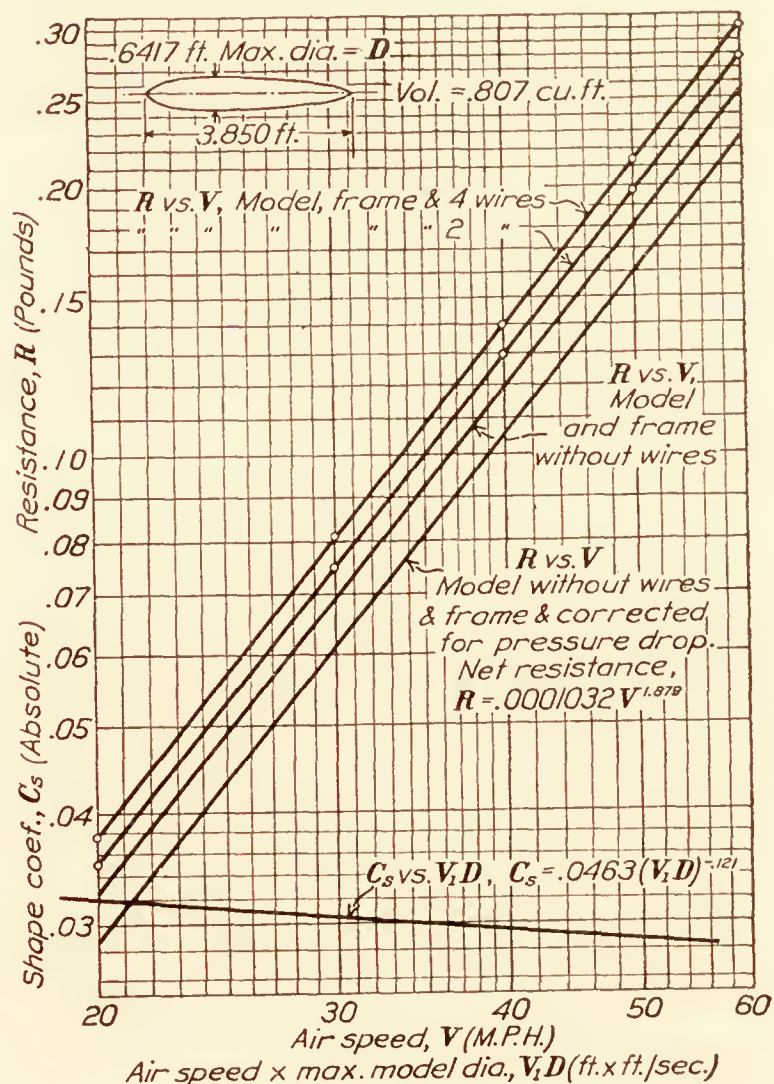


FIG. 10.—Fineness ratio=6

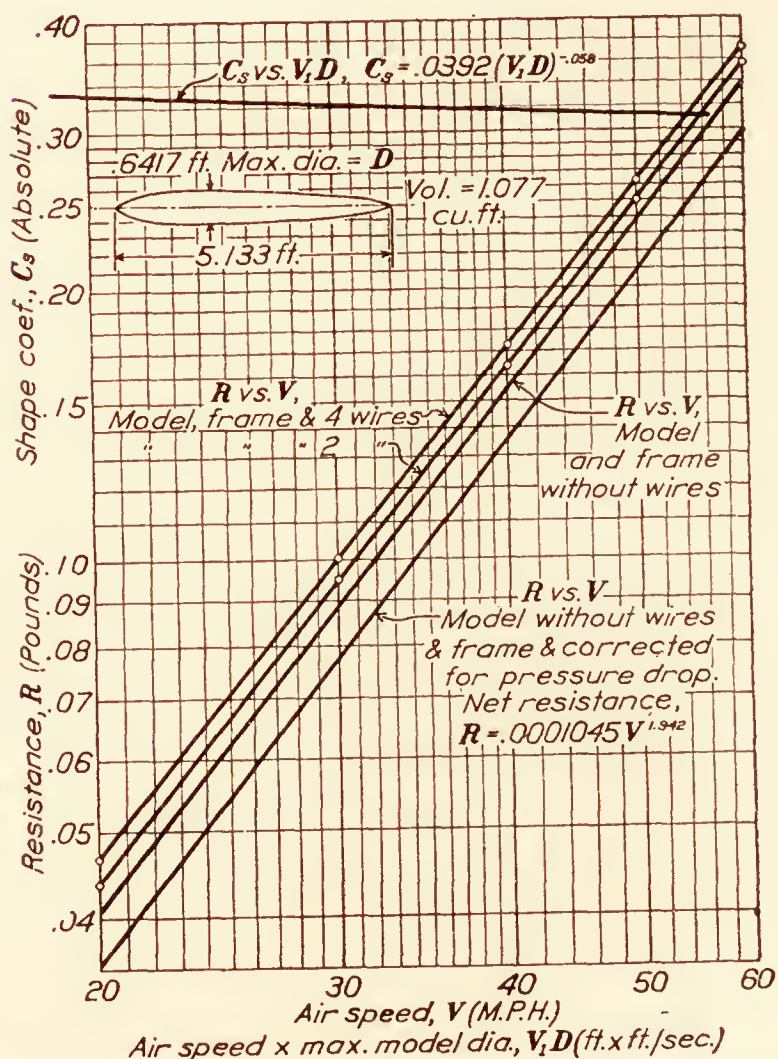


FIG. 11.—Fineness ratio=8

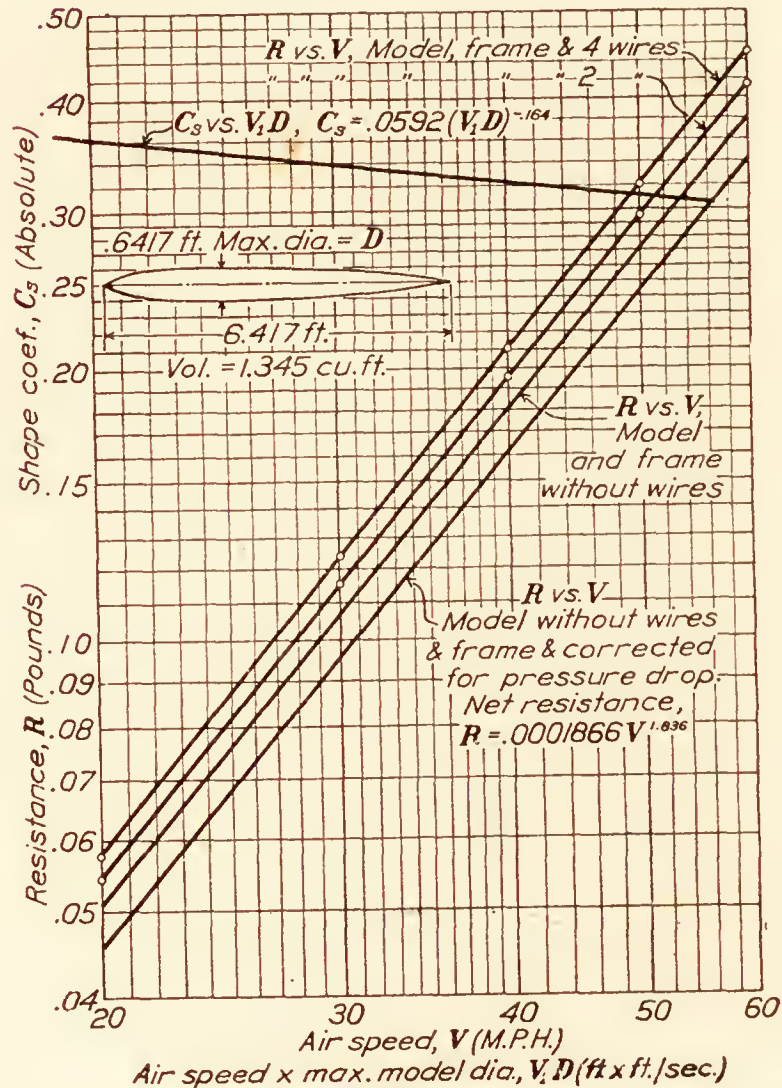


FIG. 12.—Fineness ratio=10

 C-class airship. Model at  $0^\circ$  pitch and  $0^\circ$  yaw

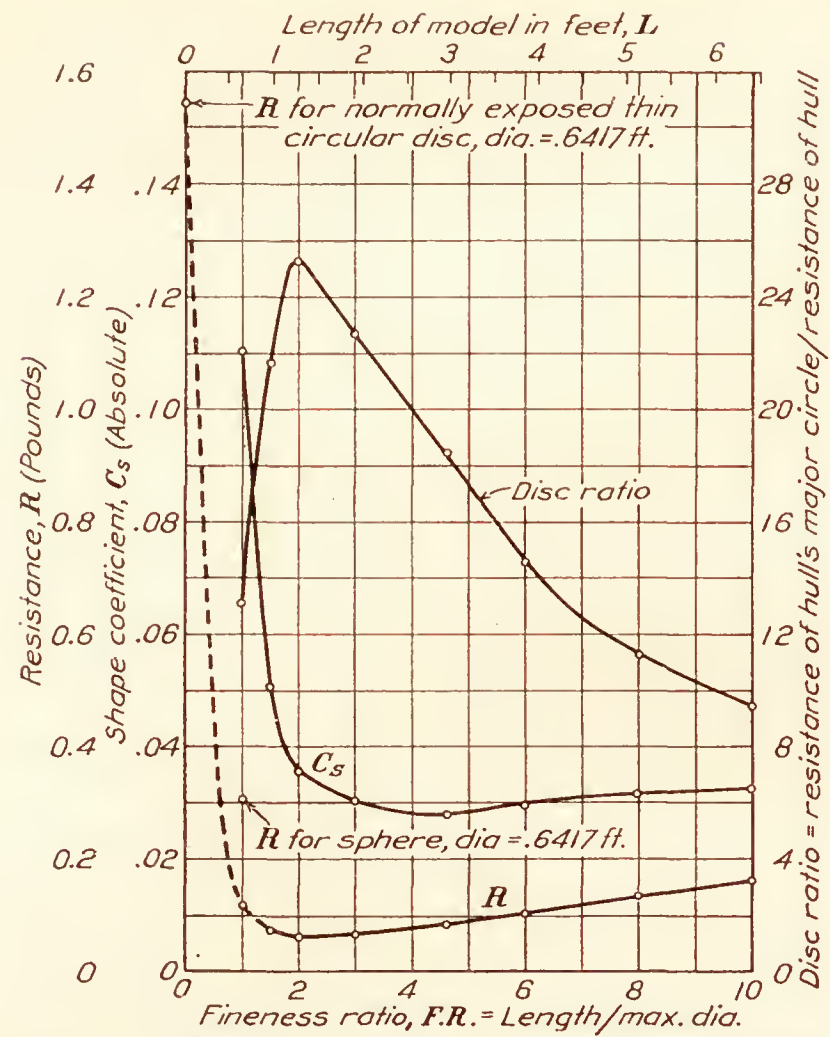


FIG. 13.—C-class airship. Models with various fineness ratios. Air speed 40 M. P. H. Model at  $0^\circ$  pitch and  $0^\circ$  yaw

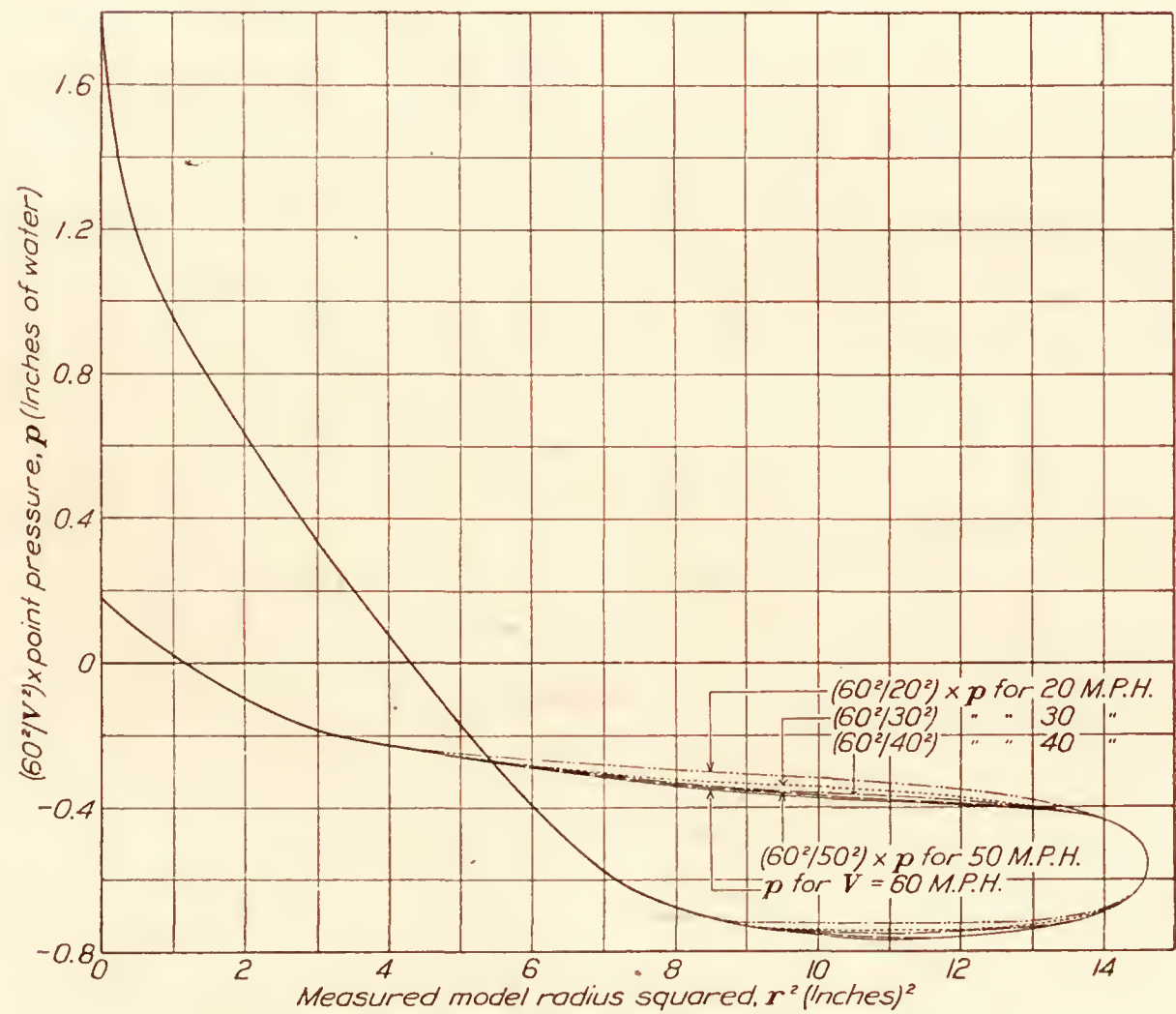
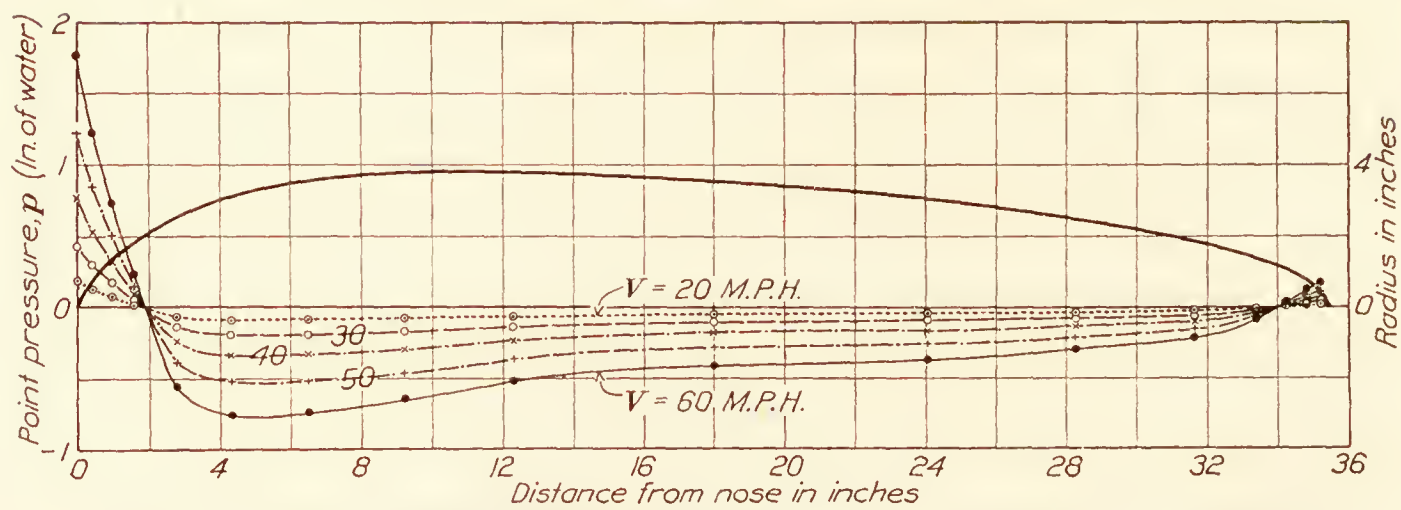
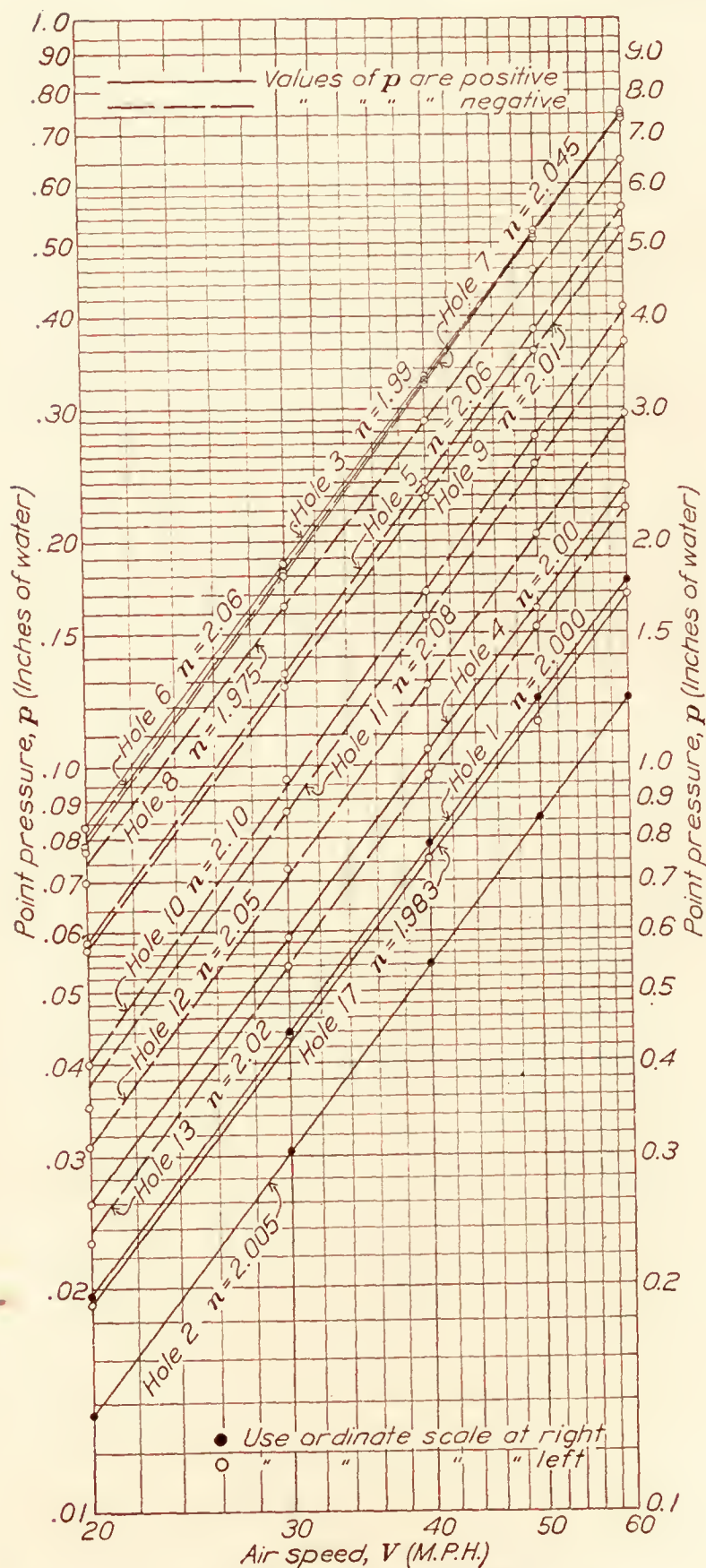
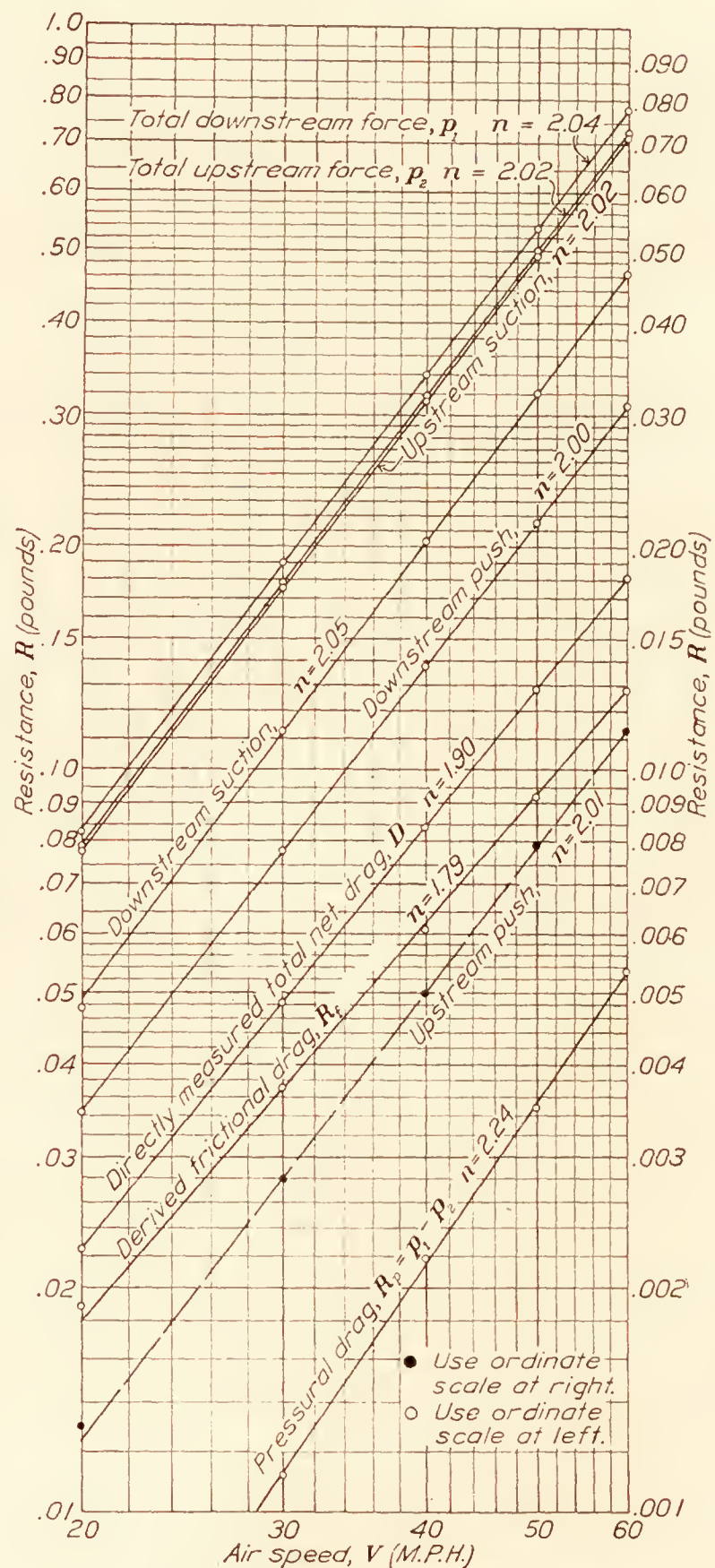


FIG. 16.—C-class airship. Fineness ratio=4.62 Model at  $0^\circ$  pitch and  $0^\circ$  yaw




 FIG. 14.—C-class airship. Fineness ratio=4.62. Model at  $0^\circ$  pitch and  $0^\circ$  yaw. Air speeds,  $V=20$  to 60 M. P. H.

 FIG. 15.—C-class airship. Fineness ratio=4.62. Model at  $0^\circ$  pitch and  $0^\circ$  yaw

 FIG. 17.—C-class airship. Fineness ratio=4.62. Model at  $0^\circ$  pitch and  $0^\circ$  yaw

## COMPARISON WITH PREVIOUS DATA

For any ellipsoid or simple quadric, fixed at any attitude in a uniform infinite stream of inviscid liquid, it can be shown, Reference 5, that the zonal pressure-drag is upstream on the fore part; downstream on the rear part; zero on the whole. The models in Figure 18 exhibit these properties except that the resultant pressure-drag, owing to viscosity, is not quite zero.

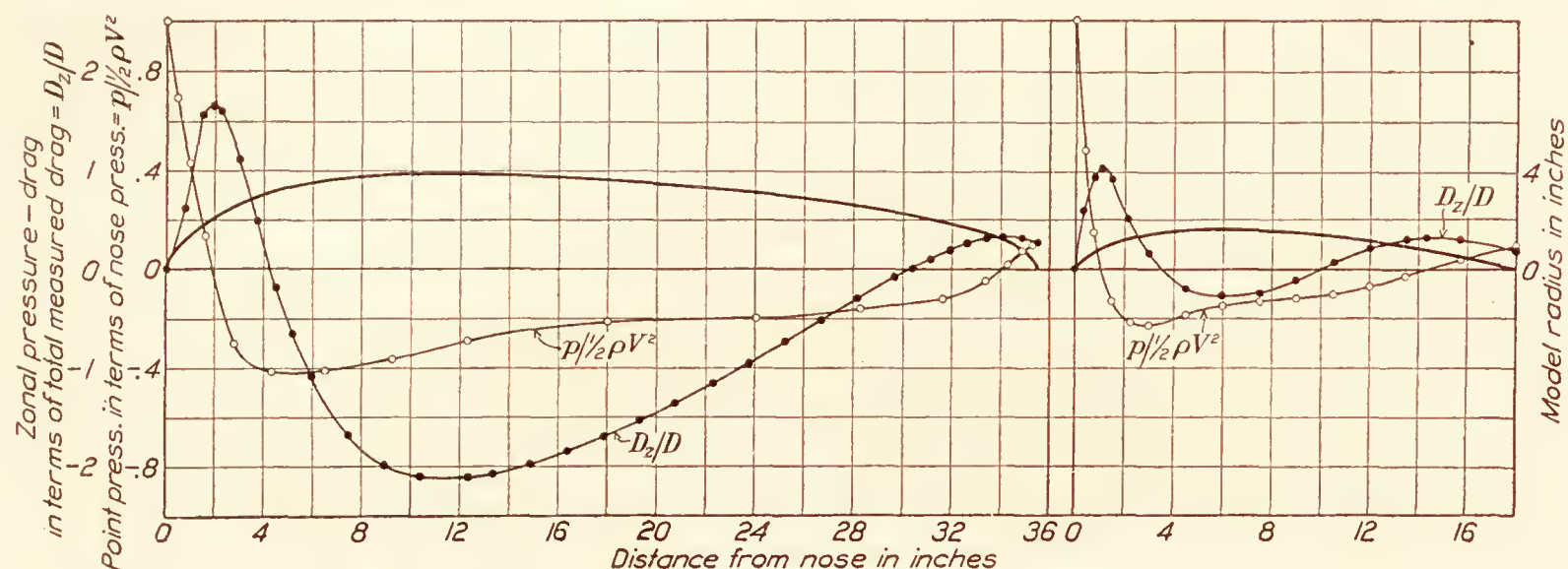


FIG. 18.—At left C-class airship. Fineness ratio=4.62. Air speed 40 M. P. H.  
At right Parseval type airship, British test, see R. & M. No. 107. Air speed 40.91 M. P. H.

The pressure-drag and friction-drag for the C-class are compared in the following table with those of the Parseval model, tested by the British, and Fuhrmann's best model, No. IV, in Reference 6.

## DRAG ELEMENTS OF FUHRMANN, PARSEVAL, AND C-CLASS MODELS

	Length, inches	Major diameter, inches	Fineness ratio	Test speed M. P. H.	Pressural drag, per cent	Frictional drag, per cent
Navy C-class-----	35. 58	7. 7	4. 62	40. 00	26	74
Parseval-----	18. 00	3. 17	5. 68	40. 91	20	80
Fuhrmann No. IV-----	45. 43	7. 4	6. 14	22. 37	63	37

The disk ratio and shape coefficient, as found at 40 miles an hour, are given for the present C-class model of fineness ratio=4.62 and for some other hulls, in the following table:

## COEFFICIENTS FOR VARIOUS BARE HULLS

Model	Disk ratio	Shape coefficient, $C_s = 2R/\rho(\text{Vol})^{2/3}V_1^2$
Long ZR-1-----	10. 71	0. 03077
Short ZR-1-----	11. 07	. 03122
Goodrich B-----	16. 22	. 03090
F-class-----	16. 48	. 02984
I. E-----	17. 16	. 03098
E. P-----	18. 28	. 02932
C-class-----	18. 47	. 02795



## C-CLASS AIRSHIP, VARIOUS FINENESS RATIOS

TABLE I

## PRINCIPAL DIMENSIONS

Station number <sup>1</sup>	Specified radius (inches)	Measured radius in inches for fineness ratio of—							
		1.00	1.50	2.00	3.00	4.62	6.00	8.00	10.00
0-----	0	0	0	0	0	0	0	0	0
1-----	1. 001			1. 000	1. 01	1. 05	1. 01	1. 05	1. 003
2-----	1. 747			1. 750	1. 75	1. 75	1. 76	1. 75	1. 747
3-----	2. 286		2. 272	2. 300	2. 29	2. 28	2. 32	2. 28	2. 278
4-----	2. 688		2. 688	2. 688	2. 71	2. 66	2. 71	2. 67	2. 682
5-----	2. 982	2. 989	2. 982	2. 973	3. 01	2. 95	3. 00	2. 98	2. 989
6-----	3. 204	3. 200	3. 205	3. 189	3. 24	3. 18	3. 23	3. 21	3. 207
7-----	3. 379	3. 379	3. 380	3. 350	3. 40	3. 35	3. 40	3. 38	3. 379
8-----	3. 511	3. 505	3. 512	3. 495	3. 54	3. 49	3. 52	3. 51	3. 513
10-----	3. 683	3. 680	3. 691	3. 660	3. 71	3. 69	3. 69	3. 68	3. 693
12-----	3. 779	3. 780	3. 792	3. 760	3. 81	3. 79	3. 80	3. 77	3. 791
14-----	3. 830	3. 831	3. 845	3. 801	3. 86	3. 82	3. 84	3. 81	3. 833
16-----	3. 849	3. 853	3. 860	3. 820	3. 87	3. 83	3. 87	3. 82	3. 847
16. 6-----	3. 850	3. 856	3. 864	3. 822	3. 87	3. 85			3. 851
18-----	3. 840	3. 844	3. 854	3. 810	3. 86	3. 81	3. 86	3. 80	3. 854
20-----	3. 797	3. 802	3. 810	3. 780	3. 83	3. 77	3. 82	3. 77	3. 826
22-----	3. 738	3. 740	3. 745	3. 720	3. 76	3. 70	3. 76	3. 73	3. 761
24-----	3. 659	3. 659	3. 660	3. 650	3. 67	3. 62	3. 69	3. 65	3. 674
26-----	3. 558	3. 570	3. 563	3. 550	3. 58	3. 52	3. 53	3. 55	3. 581
28-----	3. 443	3. 465	3. 453	3. 440	3. 47	3. 41	3. 48	3. 44	3. 456
30-----	3. 318	3. 343	3. 322	3. 312	3. 34	3. 29	3. 34	3. 31	3. 328
32-----	3. 170	3. 196	3. 186	3. 170	3. 19	3. 13	3. 18	3. 16	3. 195
34-----	3. 005	3. 024	3. 020	3. 006	3. 02	2. 97	3. 01	3. 01	3. 024
36-----	2. 817	2. 853	2. 827	2. 819	2. 84	2. 78	2. 82	2. 82	2. 835
38-----	2. 608	2. 628	2. 611	2. 615	2. 62	2. 56	2. 61	2. 60	2. 624
40-----	2. 369	2. 386	2. 376	2. 370	2. 38	2. 32	2. 36	2. 36	2. 379
41-----	2. 236	2. 264	2. 241	2. 240	2. 24	2. 19	2. 25	2. 22	2. 244
42-----	2. 098	2. 116	2. 101	2. 100	2. 10	2. 04	2. 10	2. 09	2. 098
43-----	1. 945	1. 961	1. 952	1. 956	1. 94	1. 86	1. 95	1. 93	1. 938
44-----	1. 766	1. 782	1. 772	1. 782	1. 77	1. 66	1. 77	1. 75	1. 758
45-----	1. 554	1. 560	1. 564	1. 561	1. 56	1. 44	1. 55	1. 54	1. 542
46-----	1. 281	1. 291	1. 286	1. 290	1. 31	1. 18	1. 26	1. 27	1. 292
47-----	. 912	. 919	. 900	. 991	. 96	. 85	. 87	. 90	. 878
48-----	0	0	0	0	0	0	0	0	0

<sup>1</sup> Station 0 is at nose of model, Station 48 is at stern

Fineness ratio	Interval along model axis be- tween stations (inches)	Length of model (inches)	Volume of model (cubic feet)
1. 00	0. 16042	7. 700	0. 134
1. 50	. 24063	11. 550	. 202
2. 00	. 32083	15. 400	. 269
3. 00	. 48125	23. 100	. 404
4. 62	. 74125	35. 580	. 627
6. 00	. 96250	46. 200	. 807
8. 00	1. 28333	61. 600	1. 077
10. 00	1. 60417	77. 000	1. 345

## C-CLASS AIRSHIP, VARIOUS FINENESS RATIO

TABLE II

## RESISTANCE OF C-CLASS AIRSHIP MODELS

[Models at 0° pitch and 0° yaw]

Air speed (M. P. H.)	Displace- ment due to model and 4 wires (inches)	Corre- sponding resistance (pounds)	Displace- ment due to model and 2 wires (inches)	Corre- sponding resistance (pounds)	Resist- ance of model without wires (from curves) (pounds)	Resist- ance due to frame (pounds)	Resist- ance due to pres- sure drop (pounds)	Net total resist- ance $R$ (pounds)
Fineness ratio=1.0								
20-----	0. 500	0. 0451	0. 410	0. 0369	0. 0292	-0. 0001	0. 0005	0. 0288
30-----	1. 120	. 1009	. 925	. 0833	. 0664	0	. 0011	. 0653
40-----	1. 910	. 1721	1. 650	. 1486	. 1205	+. 0005	. 0018	. 1182
50-----	3. 000	. 2703	2. 540	. 2289	. 1895	. 0010	. 0027	. 1858
60-----	4. 250	. 3829	3. 750	. 3379	. 2760	+. 0018	. 0037	. 2705
Fineness ratio=1.5								
20-----	0. 436	0. 0301	0. 374	0. 0258	0. 0213	-0. 0001	0. 0008	0. 0206
30-----	. 921	. 0635	. 782	. 0540	. 0444	0	. 0017	. 0427
40-----	1. 542	. 1064	1. 308	. 0903	. 0746	+. 0005	. 0027	. 0714
50-----	2. 296	. 1584	1. 956	. 1350	. 1116	. 0010	. 0040	. 1066
60-----	3. 200	. 2208	2. 746	. 1895	. 1552	+. 0018	. 0055	. 1479
Fineness ratio=2.0								
20-----	0. 550	0. 0277	0. 453	0. 0228	0. 0187	-0. 0001	0. 0011	0. 0177
30-----	1. 150	. 0578	. 961	. 0483	. 0387	0	. 0022	. 0365
40-----	1. 954	. 0983	1. 629	. 0819	. 0653	+. 0005	. 0037	. 0610
50-----	2. 965	. 1491	2. 452	. 1233	. 0972	. 0010	. 0054	. 0908
60-----	4. 073	. 2049	3. 390	. 1705	. 1349	+. 0018	. 0074	. 1257
Fineness ratio=3.0								
20-----	0. 320	0. 0266	0. 283	0. 0235	0. 0206	-0. 0001	0. 0019	0. 0188
30-----	. 679	. 0564	. 604	. 0501	. 0438	0	. 0040	. 0398
40-----	1. 173	. 0974	1. 035	. 0859	. 0752	+. 0005	. 0066	. 0681
50-----	1. 780	. 1477	1. 590	. 1320	. 1144	. 0010	. 0099	. 1035
60-----	2. 510	. 2083	2. 223	. 1845	. 1607	+. 0018	. 0135	. 1454
Fineness ratio=4.62								
20-----	0. 378	0. 0351	0. 321	0. 0298	0. 0249	-0. 0001	0. 0026	0. 0224
30-----	. 785	. 0729	. 681	. 0633	. 0536	0	. 0052	. 0484
40-----	1. 343	. 1248	1. 167	. 1084	. 0926	+. 0005	. 0085	. 0836
50-----	2. 014	. 1871	1. 775	. 1649	. 1415	. 0010	. 0125	. 1286
60-----	2. 850	. 2648	2. 513	. 2335	. 2005	+. 0018	. 0172	. 1815
Fineness ratio=6.0								
20-----	0. 275	0. 0376	0. 256	0. 0350	0. 0324	-0. 0001	0. 0038	0. 0287
30-----	. 598	. 0817	. 551	. 0753	. 0695	0	. 0081	. 0614
40-----	1. 024	. 1399	. 950	. 1298	. 1196	+. 0005	. 0133	. 1058
50-----	1. 569	. 2143	1. 445	. 1974	. 1810	. 0010	. 0197	. 1603
60-----	2. 210	. 3019	2. 038	. 2784	. 2549	+. 0018	. 0271	. 2260



C-CLASS AIRSHIP, VARIOUS FINENESS RATIO—Continued

TABLE II--Continued

RESISTANCE OF C-CLASS AIRSHIP MODELS—Continued

Air speed (M. P. H.)	Displace- ment due to model and 4 wires (inches)	Corre- sponding resistance (pounds)	Displace- ment due to model and 2 wires (inches)	Corre- sponding resistance (pounds)	Resist- ance of model without wires (from curves) (pounds)	Resist- ance due to frame (pounds)	Resist- ance due to pres- sure drop (pounds)	Net total resist- ance $R$ (pounds)
-------------------------	---	--	---	--	--	---	--	--

Fineness ratio=8.0

20-----	0. 279	0. 0465	0. 261	0. 0435	0. 0405	−0. 0001	0. 0051	0. 0355
30-----	. 604	. 1006	. 575	. 0957	. 0885	0	. 0108	. 0777
40-----	1. 040	. 1732	. 985	. 1640	. 1545	+ . 0005	. 0177	. 1363
50-----	1. 581	. 2632	1. 503	. 2502	. 2373	. 0010	. 0263	. 2100
60-----	2. 234	. 3720	2. 149	. 3578	. 3361	+ . 0018	. 0361	. 3000

Fineness ratio=10.0

20-----	0. 313	0. 0576	0. 296	0. 0544	0. 0508	−0. 0001	0. 0055	0. 0454
30-----	. 675	. 1241	. 631	. 1160	. 1066	0	. 0111	. 0955
40-----	1. 145	. 2106	1. 065	. 1959	. 1810	+ . 0005	. 0181	. 1624
50-----	1. 746	. 3211	1. 609	. 2959	. 2720	. 0010	. 0267	. 2443
60-----	2. 440	. 4487	2. 251	. 4140	. 3800	+ . 0018	. 0367	. 3415

C-CLASS AIRSHIP, VARIOUS FINENESS RATIOS

TABLE III

SHAPE COEFFICIENT AND CORRESPONDING VALUES OF  $V_1 D$

[Symbols defined below]

Air speed $V$ (M. P. H.)	$V_1 D$ (ft × ft/sec.)	Shape coefficient $C_s = 2R/\rho(\text{Vol.})^{2/3} V_1^2$ (absolute)							
		$F. R. = 1$	$F. R. = 1.5$	$F. R. = 2$	$F. R. = 3$	$F. R. = 4.62$	$F. R. = 6$	$F. R. = 8$	$F. R. = 10$
20-----	18. 80	0. 10804	0. 05867	0. 04161	0. 03390	0. 02996	0. 03243	0. 03323	0. 03661
30-----	28. 23	. 10863	. 05393	. 03805	. 03182	. 02870	. 03076	. 03225	. 03415
40-----	37. 67	. 11047	. 05066	. 03573	. 03059	. 02795	. 02978	. 03179	. 03263
50-----	47. 04	. 11137	. 04851	. 03411	. 02982	. 02735	. 02894	. 03141	. 03148
60-----	56. 47	. 11250	. 04670	. 03277	. 02906	. 02691	. 02831	. 03113	. 03053

$R$  = Resistance of model in pounds.

$\rho$  = Air density=0.00237 slugs per cubic foot.

Vol. = Volume of model in cubic feet.

$V$  = Air speed in miles per hour.

$V_1$  = Air speed in feet per second.

$D$  = Maximum model diameter in feet=0.6417.

$F. R.$  = Fineness ratio=Length of model/ $D$ .

C-CLASS AIRSHIP, VARIOUS FINENESS RATIOS

TABLE IV

DISK RATIO AT 40 M. P. H.

Fineness ratio of model	Net resistance of model <i>R</i> (pounds)	Disk ratio <i>R</i> <sub>Disk</sub> <sup>*</sup> / <i>R</i>
1. 00	0. 1182	13. 06
1. 50	. 0714	21. 62
2. 00	. 0610	25. 31
3. 00	. 0681	22. 67
4. 62	. 0836	18. 47
6. 00	. 1058	14. 59
8. 00	. 1363	11. 33
10. 00	. 1624	9. 51

<sup>\*</sup>*R*<sub>Disk</sub>=Resistance of a normally exposed thin circular disk whose diameter is equal to the diameter of the hull's major circle (0.6417 ft.)=*K*<sub>D</sub>*S**V*<sup>2</sup>=1.544 lb. at *V*=40 M. P. H.  
*K*<sub>D</sub>=0.00298 lb. /ft.<sup>2</sup>/mi.<sup>2</sup>/hr.<sup>2</sup>

C-CLASS AIRSHIP. FINENESS RATIO=4.62

TABLE V

OBSERVED DIFFERENCE IN PRESSURE BETWEEN NOSE AND HOLES AFT OF NOSE, *dp*

$$dp=\frac{1}{2}\rho V^2-p$$

[Model at 0° pitch and 0° yaw]

Number of hole	Air speed in miles per hour				
	20	30	40	50	60
<i>dp</i> in inches of alcohol on 1 to 10 slope and 0.819 specific gravity					
1-----	0	0	0	0	0
2-----	. 73	1. 65	2. 95	4. 59	6. 65
3-----	1. 36	3. 09	5. 53	8. 67	12. 58
4-----	2. 04	4. 68	8. 21	12. 95	18. 56
5-----	3. 09	7. 05	12. 50	19. 57	28. 27
6-----	3. 33	7. 65	13. 55	21. 14	30. 60
7-----	3. 32	7. 63	13. 51	21. 07	30. 49
8-----	3. 23	7. 45	13. 08	20. 50	29. 34
9-----	3. 07	6. 98	12. 28	19. 26	27. 78
10-----	2. 82	6. 60	11. 66	18. 25	26. 46
11-----	2. 80	6. 48	11. 52	18. 02	25. 95
12-----	2. 75	6. 33	11. 15	17. 40	25. 05
13-----	2. 65	6. 08	10. 76	16. 77	24. 15
14-----	2. 45	5. 70	10. 06	15. 66	22. 60
15-----	2. 38	5. 41	9. 44	14. 70	21. 17
16-----	2. 20	5. 06	8. 92	13. 93	19. 97
17-----	2. 14	4. 88	8. 68	13. 54	19. 40
<i>dp</i> converted to inches of water <sup>1</sup>					
1-----	0	0	0	0	0
2-----	. 061	. 137	. 244	. 377	. 543
3-----	. 113	. 255	. 452	. 708	1. 032
4-----	. 170	. 383	. 680	1. 064	1. 530
5-----	. 254	. 575	1. 025	1. 610	2. 326
6-----	. 274	. 624	1. 113	1. 740	2. 518
7-----	. 273	. 622	1. 109	1. 735	2. 508
8-----	. 266	. 606	1. 074	1. 688	2. 414
9-----	. 253	. 570	1. 014	1. 585	2. 287
10-----	. 233	. 538	. 956	1. 501	2. 177
11-----	. 231	. 529	. 944	1. 479	2. 135
12-----	. 227	. 515	. 913	1. 430	2. 061
13-----	. 219	. 496	. 882	1. 379	1. 987
14-----	. 203	. 464	. 824	1. 287	1. 860
15-----	. 197	. 435	. 773	1. 207	1. 741
16-----	. 182	. 413	. 731	1. 143	1. 643
17-----	. 177	. 398	. 710	1. 112	1. 597

<sup>1</sup> *dp* was changed to inches of water by employing the manometer's calibration curve.



C-CLASS AIRSHIP. FINENESS RATIO=4.62

TABLE VI

POINT PRESSURE,  $p$ , IN INCHES OF WATER AT THE 17 HOLES  $p=\frac{1}{2}\rho V^2-dp$ 

[Model at 0° pitch and 0° yaw]

Number of hole	Air speed in miles per hour				
	20	30	40	50	60
1-----	+0.196	+0.442	+0.785	+1.226	+1.766
2-----	.135	.305	.541	.849	1.223
3-----	.083	.187	.333	.518	.734
4-----	+.026	+.059	+.105	+.162	+.236
5-----	-.058	-.133	-.240	-.384	-.560
6-----	-.078	-.182	-.328	-.514	-.752
7-----	-.077	-.180	-.324	-.509	-.742
8-----	-.070	-.164	-.289	-.462	-.648
9-----	-.057	-.128	-.229	-.359	-.521
10-----	-.040	-.096	-.171	-.275	-.411
11-----	-.035	-.087	-.159	-.253	-.369
12-----	-.031	-.073	-.128	-.204	-.295
13-----	-.023	-.054	-.097	-.153	-.211
14-----	-.007	-.022	-.039	-.061	-.094
15-----	+.002	+.007	+.012	+.019	+.025
16-----	.014	.029	.054	.083	.123
17-----	+.019	+.044	+.075	+.114	+.169

C-CLASS AIRSHIP. FINENESS RATIO=4.62

TABLE VII

POINT PRESSURE IN TERMS OF NOSE PRESSURE,  $p/\frac{1}{2}\rho V^2$ 

[Model at 0° pitch and 0° yaw]

Number of hole	Air speed in miles an hour				
	20	30	40	50	60
1-----	+1.000	+1.000	+1.000	+1.000	+1.000
2-----	.689	.690	.689	.692	.693
3-----	.423	.423	.424	.423	.416
4-----	+.133	+.133	+.134	+.132	+.134
5-----	-.296	-.301	-.306	-.313	-.317
6-----	-.398	-.412	-.418	-.419	-.426
7-----	-.393	-.407	-.413	-.415	-.420
8-----	-.357	-.371	-.368	-.377	-.367
9-----	-.291	-.290	-.292	-.293	-.295
10-----	-.204	-.217	-.218	-.224	-.233
11-----	-.179	-.197	-.203	-.206	-.209
12-----	-.158	-.165	-.163	-.166	-.167
13-----	-.117	-.122	-.124	-.125	-.119
14-----	-.036	-.050	-.050	-.050	-.053
15-----	+.010	+.016	+.015	+.015	+.014
16-----	.071	.066	.069	.068	.070
17-----	+.097	+.100	+.096	+.093	+.096

C-CLASS AIRSHIP. FINENESS RATIO=4.62

TABLE VIII

ALONG-STREAM FORCES EXPRESSED IN POUNDS AND IN TERMS OF TOTAL DRAG

[Model at 0° pitch and 0° yaw]

Air speed M. P. H.	Downstream			Upstream			Pressural drag $R_p=P_1-P_2$	Fric- tional drag $R_f$	Total drag $R=R_p+R_f$
	Push	Suction	Total $P_1$	Push	Suction	Total $P_2$			
	Pounds								
20-----	0. 0344	0. 0476	0. 0820	0. 0013	0. 0771	0. 0784	0. 0936	0. 0188	0. 0224
30-----	. 0775	. 1123	. 1898	. 0028	. 1758	. 1786	. 0112	. 0372	. 0484
40-----	. 1377	. 2033	. 3410	. 0050	. 3141	. 3191	. 0219	. 0617	. 0836
50-----	. 2151	. 3216	. 5367	. 0079	. 4938	. 5017	. 0350	. 0930	. 1280
60-----	. 3098	. 4681	. 7779	. 0113	. 7131	. 7244	. 0535	. 1280	. 1815
	Per cent of total drag								
20-----	154	212	366	6	344	350	16	84	100
30-----	160	232	393	6	364	370	23	77	100
40-----	165	243	408	6	376	382	26	74	100
50-----	168	251	419	6	386	392	27	73	100
60-----	171	258	429	6	393	399	30	70	100

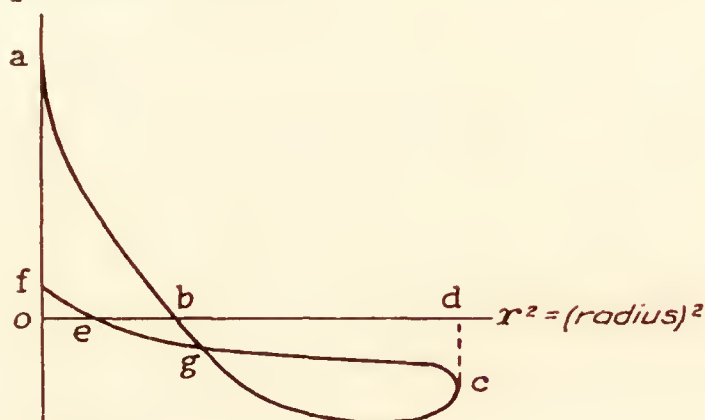
*p*, Point pressure

FIG. 19.—

Downstream push  $\propto$  abo  
 Downstream suction  $\propto$  ced  
 Upstream push  $\propto$  eof  
 Upstream suction  $\propto$  bcd  
 Total area = (abo + ced) - (eof + bcd) = (agf - ggc)  $\propto$   $R_p$

## REFERENCES

- Reference 1.—Aeronautics Staff, "Resistance of Airship Hulls C-Class and S. S. T. Enlarged," C. & R. Aeronautical Report No. 128, April, 1919.  
 Reference 2.—Aeronautics Staff, "Lift, Drag,  $N\psi$  and  $N_r$  for C-Class Airship Hull," C. & R. Aeronautical Report No. 162, November, 1920.  
 Reference 3.—A. F. Zahm and R. H. Smith, "Drag of Two NPL Airship Models," C. & R. Aeronautical Report No. 206, November, 1922.  
 Reference 4.—A. Fage and W. J. Stern, Advisory Committee for Aeronautics, Reports and Memoranda No. 107, May, 1914. (British.)  
 Reference 5.—A. F. Zahm, "Flow and Drag Formulas for Simple Quadrics," N. A. C. A. Technical Report No. 253, 1926.  
 Reference 6.—G. Fuhmann, "Theoretische und experimentelle Untersuchungen an Ballon-Modellen," Jahrbuch der Motorluftschiff-Studiengesellschaft, Fünfter Band, 1911-12.

AERODYNAMICAL LABORATORY,

BUREAU OF CONSTRUCTION AND REPAIR,

NAVY YARD, WASHINGTON, D. C., May 7, 1927.



---

## REPORT No. 292

---

# CHARACTERISTICS OF FIVE PROPELLERS IN FLIGHT

By J. W. CROWLEY, Jr., and R. E. MIXSON  
Langley Memorial Aeronautical Laboratory





# REPORT No. 292

## CHARACTERISTICS OF FIVE PROPELLERS IN FLIGHT

By J. W. CROWLEY, Jr., and R. E. MIXSON

### SUMMARY

*This investigation was made by the National Advisory Committee for Aeronautics at Langley Field for the purpose of determining the characteristics of five full-scale propellers in flight. The equipment consisted of five propellers in conjunction with a VE-7 airplane and a Wright E-2 engine. The propellers were of the same diameter and aspect ratio. Four of them differed uniformly in thickness and pitch and the fifth propeller was identical with one of the other four with the exception of a change of the airfoil section. The propeller efficiencies measured in flight are found to be consistently lower than those obtained in model tests. It is probable that this is mainly a result of the higher tip speeds used in the full-scale tests. The results show also that because of differences in propeller deflections it is difficult to obtain accurate comparisons of propeller characteristics. From this it is concluded that for accurate comparisons it is necessary to know the propeller pitch angles under actual operating conditions.*

### INTRODUCTION

While there are considerable propeller data available from tests of model propellers, there is comparatively little available from tests of full-scale propellers under flight conditions, and consequently there is insufficient information from which the scale effect of model propeller tests can be determined. One comparison between the results of model and full-scale propeller tests is given in N. A. C. A. Technical Report No. 220 (Reference 1), and the British Advisory Committee for Aeronautics has published the results of full-scale propeller tests in a number of reports. The present research was conducted to provide additional data on the characteristics of full-scale propellers in flight.

The method used in this investigation was similar to that described in N. A. C. A. Technical Report No. 220, and consisted essentially of two parts: (1) The measurement of the lift and drag characteristics of a VE-7 airplane by means of glide tests, and (2) the determination of the propeller characteristics by means of full-throttle power flights with a calibrated engine. The propellers tested were all of wood, were of the standard Navy plan form, and were of the same diameter and blade width. Four differed uniformly in thickness and pitch and the fifth, while similar to one of the four, differed in that the airfoil sections were altered. One of the propellers was the exact duplicate of a propeller of the series reported on in N. A. C. A. Technical Report No. 220.

### APPARATUS

*Test propellers.*—Drawings of the propellers tested are shown in Figures 1–5, and the main dimensions are tabulated in Table I. They were all of the standard Navy plan form, 8 feet 2 inches in diameter, and with an aspect ratio of 6. They were made of birch in the

usual laminated construction and were covered with cotton fabric. No metal tipping was used. The blade angles were measured before and after the tests and in each case were found to be within the tolerance allowed by the Navy specifications with only a very slight change

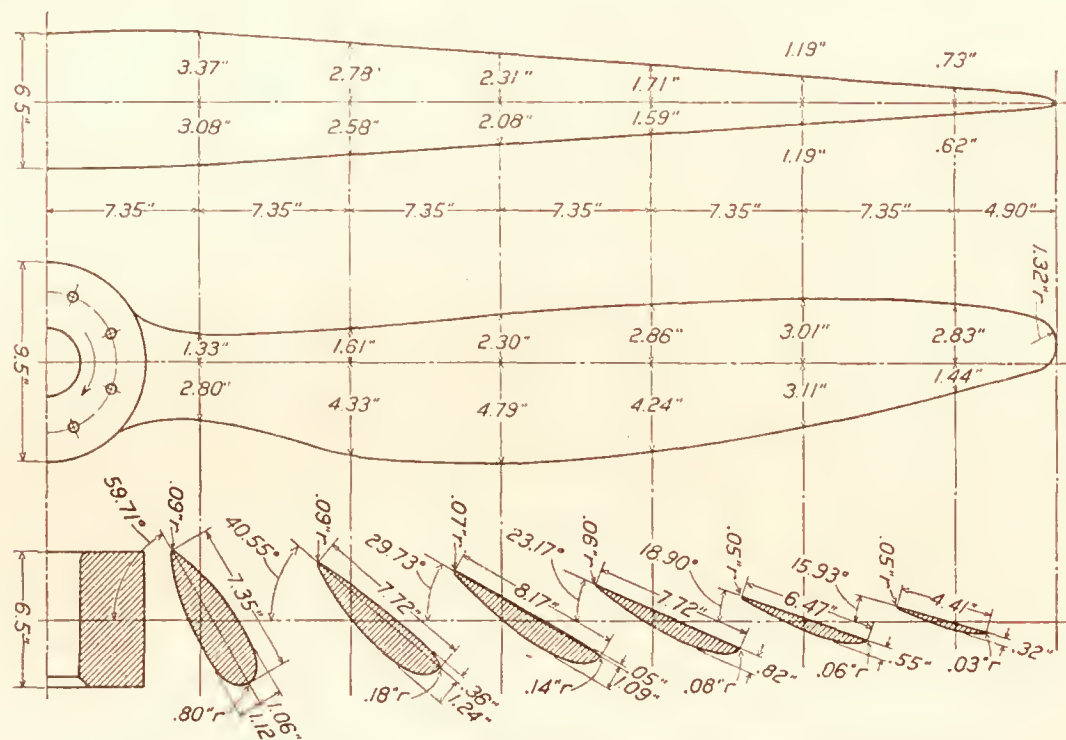


FIG. 1.—Propeller 3712. Diameter, 8' 2"; pitch, 6' 7"; aspect ratio, 6; camber, 8

between the measurements before and after. The measured pitches and thickness ratios of the propellers are given below. Thickness ratio as used herein is the ratio of the thickness of the propeller used to the thickness of the standard Navy propeller:

Propeller	T. R.	Mean geometrical pitch	
		ft.	in.
3712	0.8	6	7.1
3713	1.0	6	2.0
3714	1.2	5	8.8
3715	1.4	5	3.3
3872	1.2	5	8.7

Propeller 3714 is a duplicate of propeller I of the series of propellers reported on in N. A. C. A. Technical Report No. 220. Propeller 3872 is similar to 3714 except that an experimental airfoil section based on the Göttingen 398 was used in place of the standard Navy section.



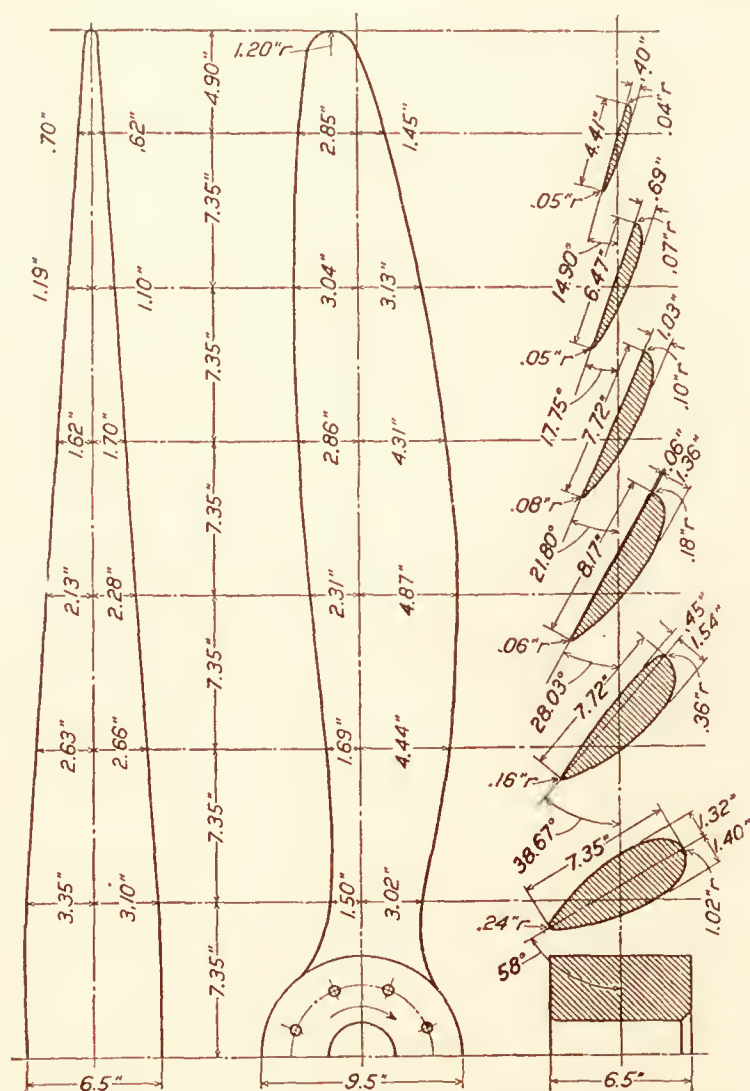


FIG. 2.—Propeller 3713. Diameter, 8' 2"; pitch 6' 1.8"; aspect ratio, 6; camber, 1.0

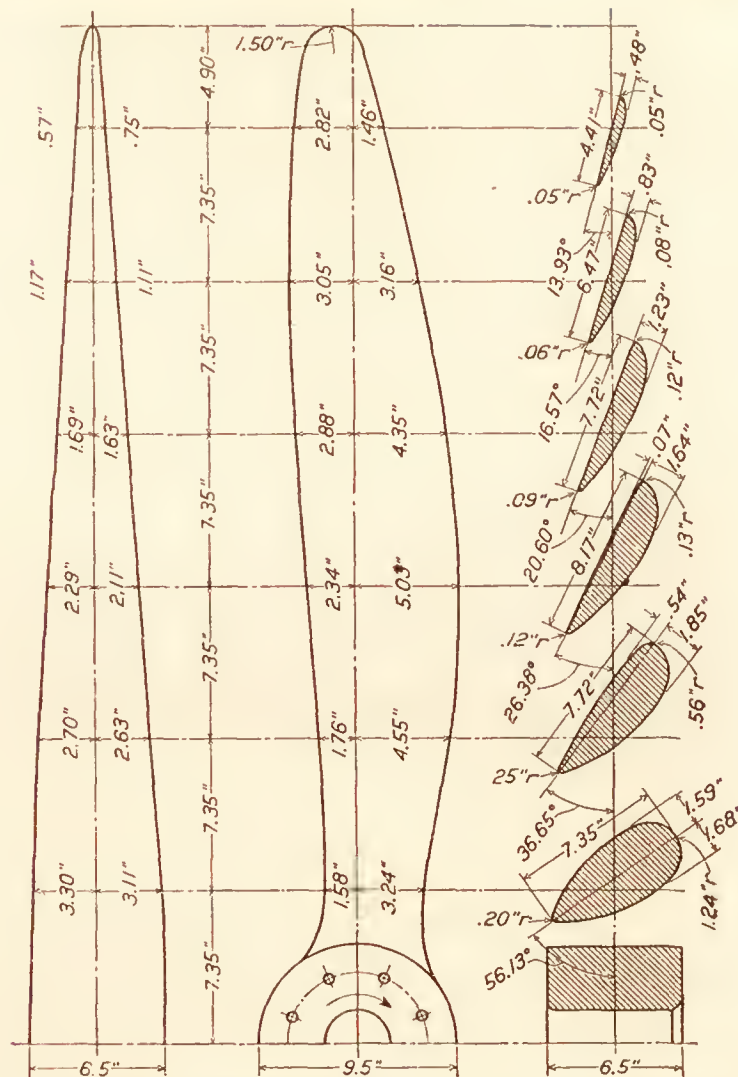


FIG. 3.—Propeller 3714. Diameter, 8' 2"; pitch, 5' 8.6"; aspect ratio, 6; camber, 1.2

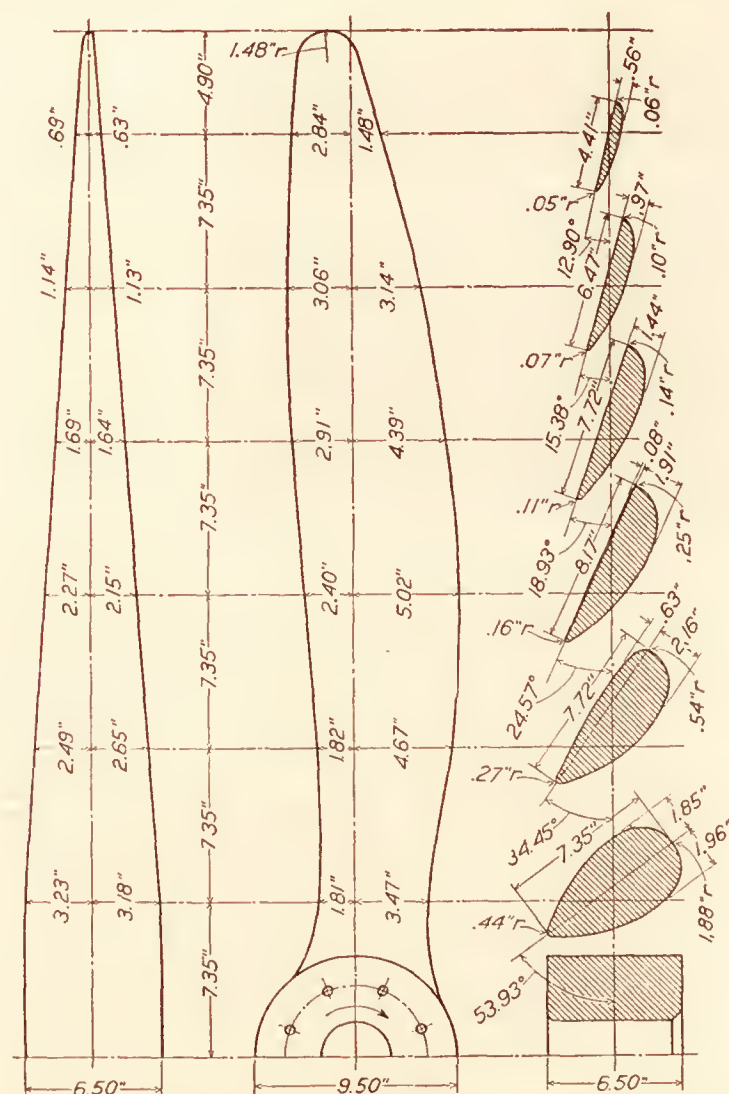


FIG. 4.—Propeller 3715. Diameter, 8' 2"; pitch 5' 3.4"; aspect ratio, 6; camber, 1.4

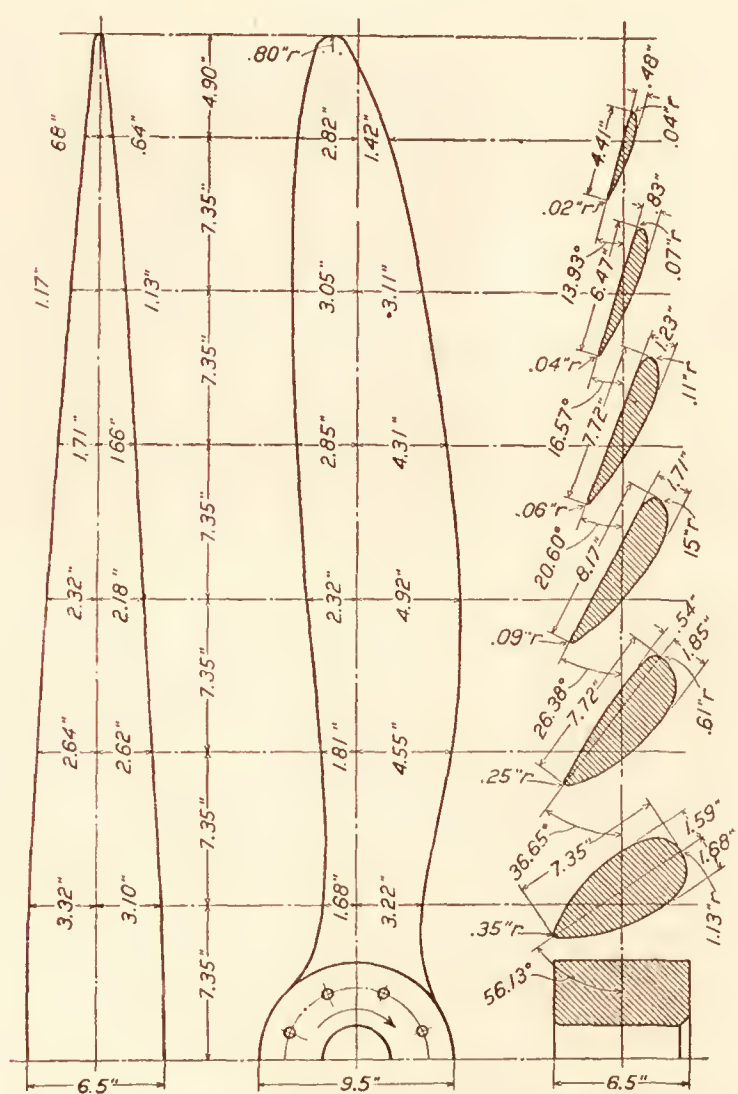


FIG. 5.—Propeller 3872. Diameter, 8' 2"; pitch, 5' 8.6"; aspect ratio, 6; camber, 1.2



*Instruments.*—The following special-test instruments were used:

(1) N. A. C. A. Flight Path Angle and Air-Speed Recorder. This instrument was developed especially for these tests for measuring continuously for a period of time, the angle of the flight path relative to the horizontal and the air speed along the flight path. Briefly, it consists of a streamlined case with stabilizing tail surfaces and a Pitot static tube in the nose. (Fig. 6.) In the case is inclosed an oil-damped pendulum, a diaphragm type air-speed measuring unit, and a film drum rotated by an electric motor. In operation the instrument is lowered approximately 50 feet below the airplane, where it takes up a path through the air parallel to that of the airplane. The inclination of the instrument, due to an inclined flight path, is recorded by



FIG. 6.—The N. A. C. A. flight path angle and air-speed recorder

means of the pendulum and the air speed is recorded by the differential pressure given by the Pitot static tube. A complete description of the instrument is given in Reference 2. A record taken of a series of glides is shown in Figure 6 (a).

(2) N. A. C. A. Recording Altimeter and Pendulum Inclinometer. This instrument, mounted in the airplane, was used for measuring the change of altitude with time and the attitude of the airplane. It consists of an aneroid mechanism and an oil-damped pendulum incorporated in the standard photographic recording type of instrument used by the National

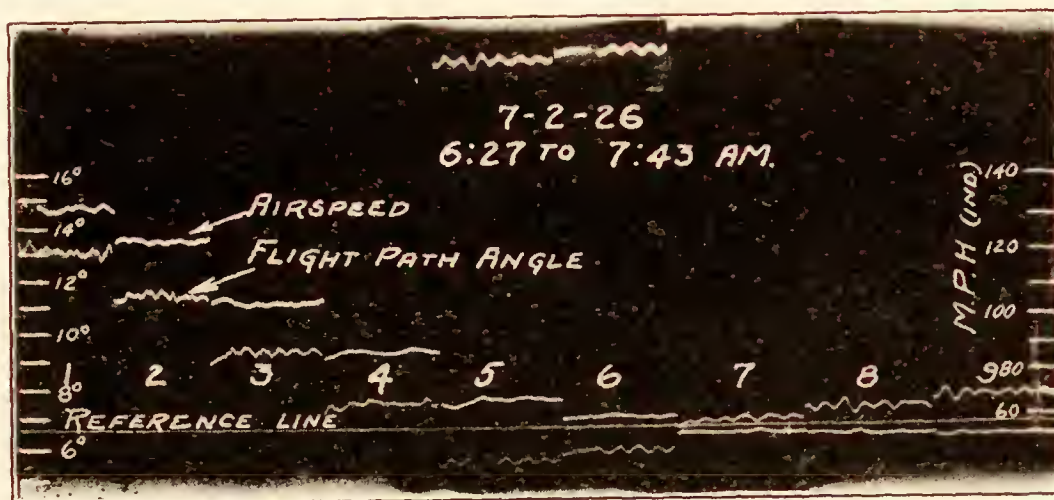


FIG. 6a.—Typical record of the N. A. C. A. flight path angle and air-speed recorder

Advisory Committee for Aeronautics. The altimeter readings together with air speed were used as a check upon the flight path angle measured by the flight path angle recorder. The inclinometer readings were used in conjunction with the flight path angle for determining the angle of attack of the airplane.

(3) Revolution Counter. A revolution counter, connected to the cam shaft by a mechanical clutch was used in conjunction with a stop watch to determine the engine speed. The readings were taken by an observer.

(4) Thermometers. Indicating distance thermometers were used to measure the strut and carburetor air intake temperatures. These readings were taken throughout each test by an observer.



## ENGINE CALIBRATION

The engine was calibrated on an electric cradle dynamometer before and after the power flight tests. The results of these calibrations are shown in Figure 7. To prevent detonation during the calibration a fuel of 20 per cent benzol and 80 per cent gasoline (by volume) was used. As the flight tests were all made at altitudes above 1,000 feet, it was assumed that no detonation would occur during the tests and consequently straight gasoline used in the flight tests would be comparable, for the power developed, to the fuel mixture used in calibration. This assumption has been verified by laboratory and flight tests. In addition to the calibrations before and after the tests the power was checked at intervals during the tests by using the standing R. P. M. at full throttle with propeller 3714 as an index of the condition of the engine. This was never different by more than 20 R. P. M., which was the limit of accuracy of the tachometer used. It will be noted that the maximum difference between the calibrations before and after the tests is approximately 3 per cent. This difference is probably negligible, but to make certain of the power developed in flight the engine was assumed to have deteriorated

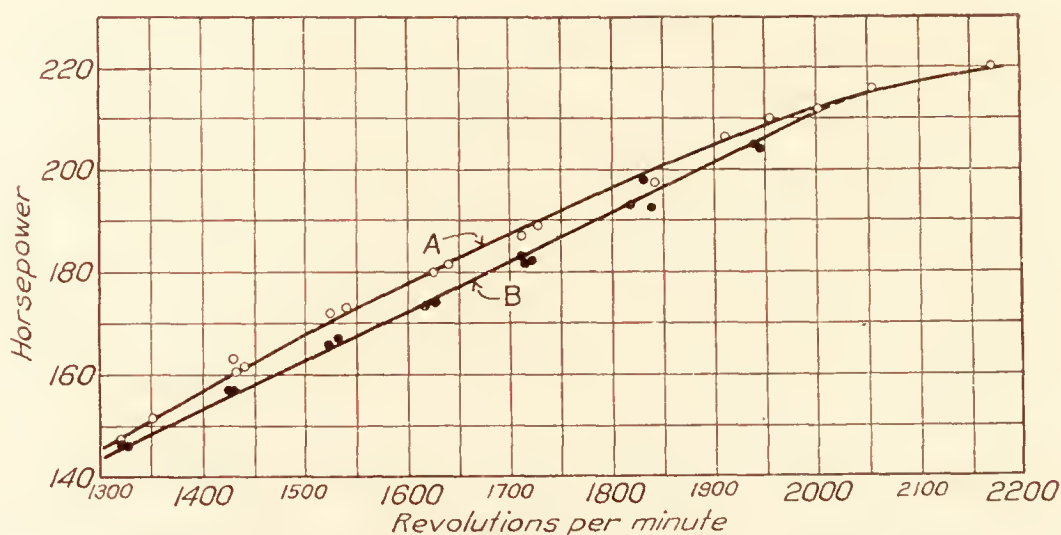


FIG. 7.—Calibration of Wright E-2 engine, reduced to standard air. Fuel: 20 per cent benzol, 80 per cent gasoline. Curve A, July 13, 1926. Curve B, September 21, 1926

progressively during the flight tests, and the power used for calculations of any particular flight was taken from the calibrations at a point between the two curves corresponding to the time the engine had been in operation.

## FLIGHT TESTS

The flight tests were conducted in two parts: (1) Glide tests to determine the lift and drag of the airplane; and (2) full throttle power flights with a calibrated engine to determine the propeller characteristics.

The glide tests were conducted with propeller 3714 operating at approximately the  $V/nD$  for zero thrust. This value of  $V/nD$  was previously determined from model tests of a 3-foot propeller mounted on a model of the VE-7 airplane. (Reference 1.) Glides were started at about 3,000 feet and the records were taken for a period of three-fourths minute after the airplane had reached a steady condition in glide. The range of speed covered was from 50 to 140 M. P. H. In the glide tests the following data were obtained from the instrument records: Flight path angle, true air speed, angle of attack, and engine R. P. M.

The power flights consisted of full throttle runs at air speeds of 50 to 135 M. P. H. with each propeller. The flights were climbing, level, or diving, as determined by the air speed. Corresponding data were obtained as in the glide tests with the addition of the carburetor air intake temperature.

## REDUCTION OF DATA

*Glide tests.*—From the flight data obtained in the glide tests the lift and drag characteristics were determined. The essential observed and computed data for this determination

are given in Table II. Lift is taken as  $W \cos \gamma$ , where  $\gamma$  is the angle of the flight path, and the apparent drag is equal and opposite in sign to  $W \sin \gamma$ . True drag is apparent drag plus thrust, and the thrust is determined from the thrust coefficient of a model propeller for the value of  $V/nD$  attained in the flight tests. While the glide tests were supposedly conducted with the propeller operating at the  $V/nD$  for zero thrust (0.972), this  $V/nD$  was seldom exactly realized. It was, therefore, necessary to correct the apparent drag for thrust as mentioned above.

The final coefficients  $C_L$  and  $C_D$ , plotted as a polar diagram, are given in Figure 8, and  $C_L$  versus angle of attack is shown in Figure 9.  $C_L$  and  $C_D$  are  $\frac{L}{\frac{1}{2}\rho V^2 S}$  and  $\frac{D}{\frac{1}{2}\rho V^2 S}$  respectively, where  $S$  is 284.5 square feet.

*Power flights.*—From the data obtained in the power flights the propeller characteristics were determined. The essential data for this determination are given in Table II. Lift,

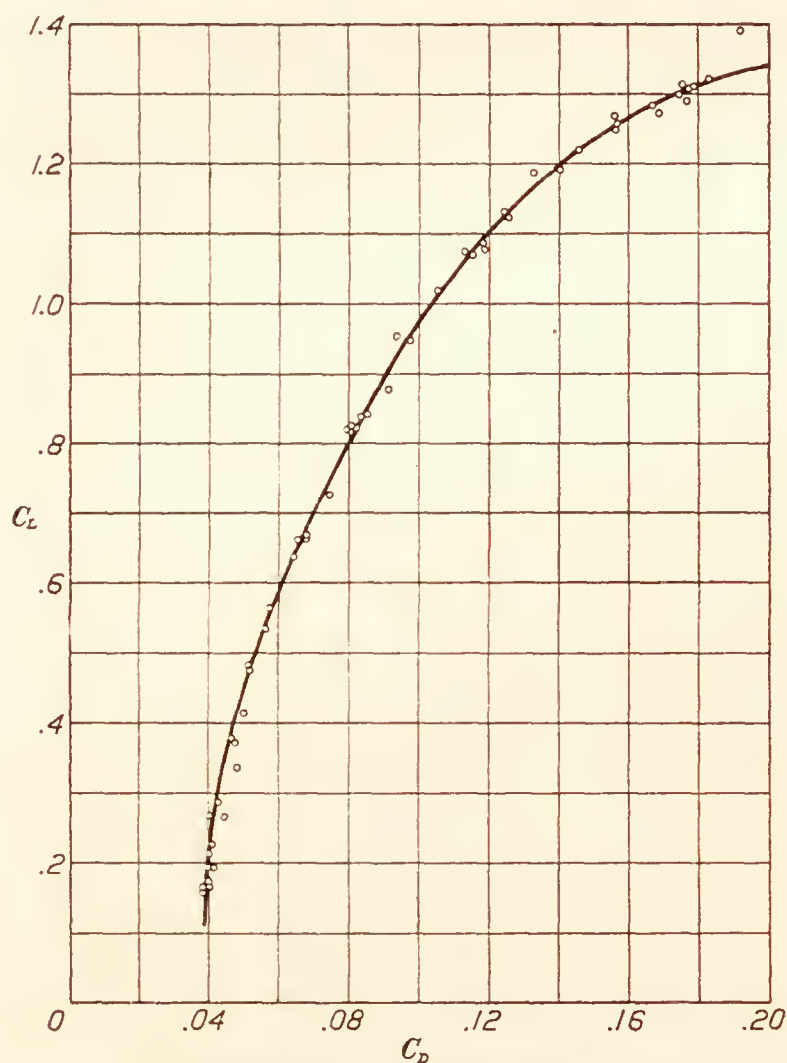


FIG. 8.—Polar diagram of Vought E-7 airplane

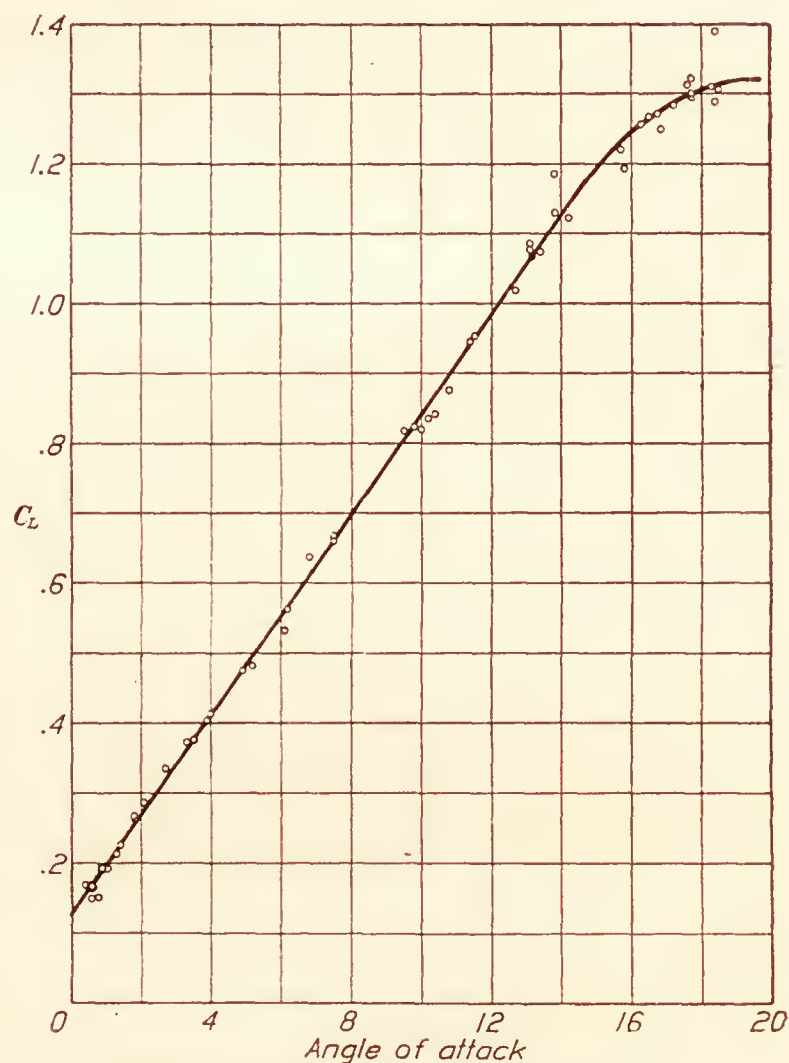


FIG. 9.—Lift characteristics of Vought E-7 airplane

drag, and thrust were determined as follows: A tentative lift,  $L' = W \cos \gamma$ , was assumed, thus neglecting the lift component of propeller thrust. A tentative lift coefficient  $C_L'$  was computed from  $L'$ . A corresponding  $C_D'$  was read from Figure 8 and a tentative angle of attack from Figure 9. A tentative drag  $D'$  was computed from  $C_D'$ . A tentative thrust  $T'$ , equal to  $D' + W \sin \gamma$  was then deduced. A second approximation of lift was then determined by deducting  $T' \sin \epsilon$ , the lift component of tentative thrust, from the tentative lift (where  $\epsilon$  is the angle the propeller axis makes with the flight path). From this second approximation of lift a new lift coefficient, angle of attack, drag coefficient, and drag were derived. A second approximation of thrust was determined, as before, by adding  $W \sin \gamma$  to the drag. A third approximation was found to be unnecessary since it differed only slightly from the second. The lift and drag of Table II are, therefore, the second approximations, the angle of attack is that read from Figure 9 for the lift coefficient derived from the second approximation of lift,



and the thrust is the second approximation of drag plus  $W \sin \gamma$ . This method was used rather than working directly from the angle of attack measured in flight since the inclinometer records, from which the angle of attack is determined, were not satisfactory in the power flights.

Horsepower was determined from the calibration curves of Figure 7. As previously mentioned, it was assumed that the engine deteriorated progressively with time of operation and that for any flight between the dates of engine calibrations the engine power would be represented by a calibration curve between curves A and B of Figure 7, its distance from A depending on the time of engine operation. The horsepower for standard conditions was thus determined. The horsepower developed under the conditions of flight was derived from this through the relation,  $HP = C \frac{p}{\sqrt{T}}$ , where  $p$  is the barometric pressure,  $T$  is the absolute carburetor air intake temperature, and  $C$  is a constant.

The coefficients  $C_T$ ,  $C_P$ , and  $\eta$  were plotted against  $V/nD$ , where

$$C_T = \frac{\text{Thrust}}{\rho n^2 D^4}$$

$$C_P = \frac{\text{Power}}{\rho n^3 D^5}$$

$$\eta = \frac{\text{thrust} \times \text{velocity}}{\text{power}}$$

$$\eta = \frac{C_T}{C_P} \frac{V}{nD}$$

In general the probable error of  $C_P$  is likely to be greater than that of  $C_T$ . This is because the power measurements are all based on the assumption that the engine consistently developed the same power in flight as on the calibrating stand, and, while previous tests have shown this assumption to be justified, it was not possible to verify it in these tests by actual measurement of the power in flight. Any future tests of this character should include direct measurement of power as a part of the flight tests.

### RESULTS

The results of the propeller tests are given in curve and tabular form in Figures 10 to 14 and Tables III and IV, respectively. The experimental points from which Figures 10 to 14 were plotted, are given in Table III. Table IV gives the values of  $C_T$ ,  $C_P$ , and  $\eta$  taken from the faired curves of Figures 10 to 14.

The performance of the Vought VE-7 airplane with the different propellers tested is shown in Figures 18 to 22. These figures are derived from the power flight tests by means of the polar diagram (fig. 8), the engine calibration (fig. 7), and the propeller characteristics (figs. 10 to 14).

### DISCUSSION

The lift and drag characteristics of the VE-7 determined in these tests differed considerably from those obtained on the same airplane in the tests reported in N. A. C. A. Report No. 220. (Reference 1.) It was expected that a difference would exist since the airplane was newly covered for the present tests while the condition of the fabric was poor in the previous ones. However, the difference obtained was larger than expected and this led to a very careful rechecking of the lift and drag determinations. Suspecting a possible error in the flight path angle measurements due to effect of down wash on the flight path angle recorder, an investigation was made with the recorder suspended 100 feet below the airplane and consequently quite definitely away from down wash effects. No measureable difference was found between the 50 and 100 feet suspension. As a further check the flight path was determined independently by use of the altimeter and air-speed readings and an excellent agreement was obtained with the flight path

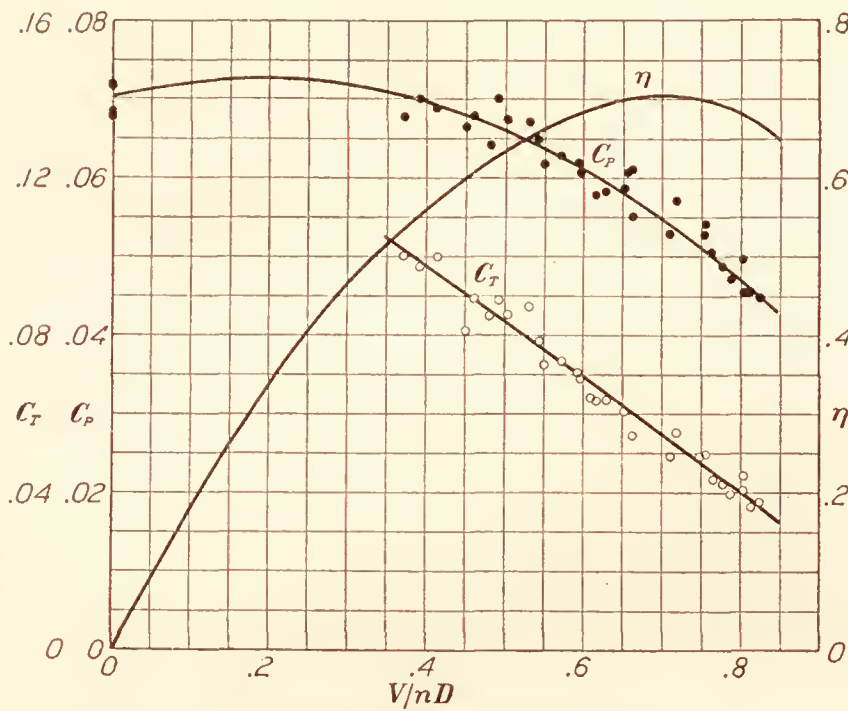


FIG. 10.—Characteristics of propeller 3712

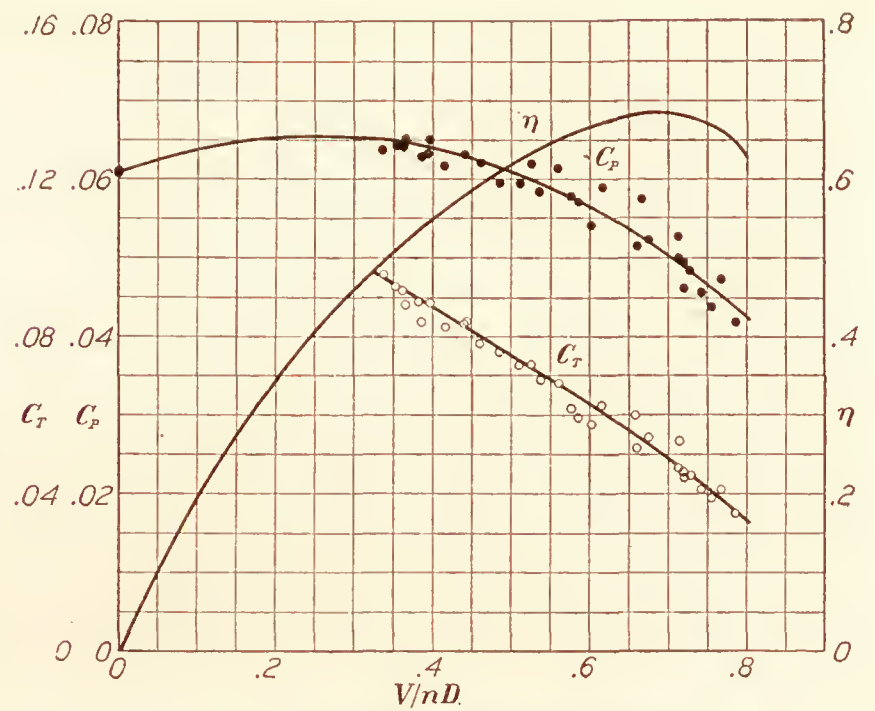


FIG. 11.—Characteristics of propeller 3713

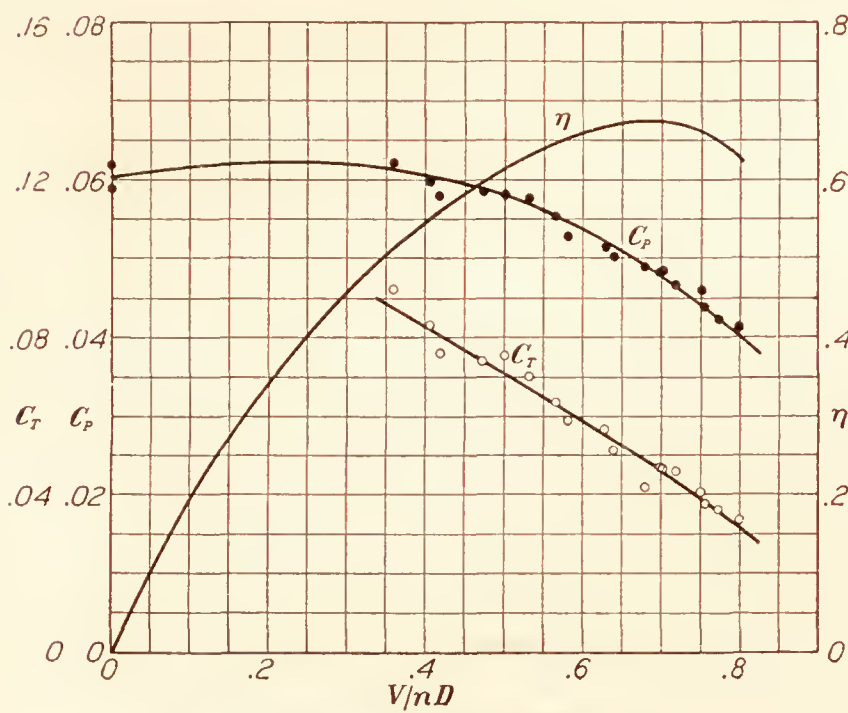


FIG. 12.—Characteristics of propeller 3714

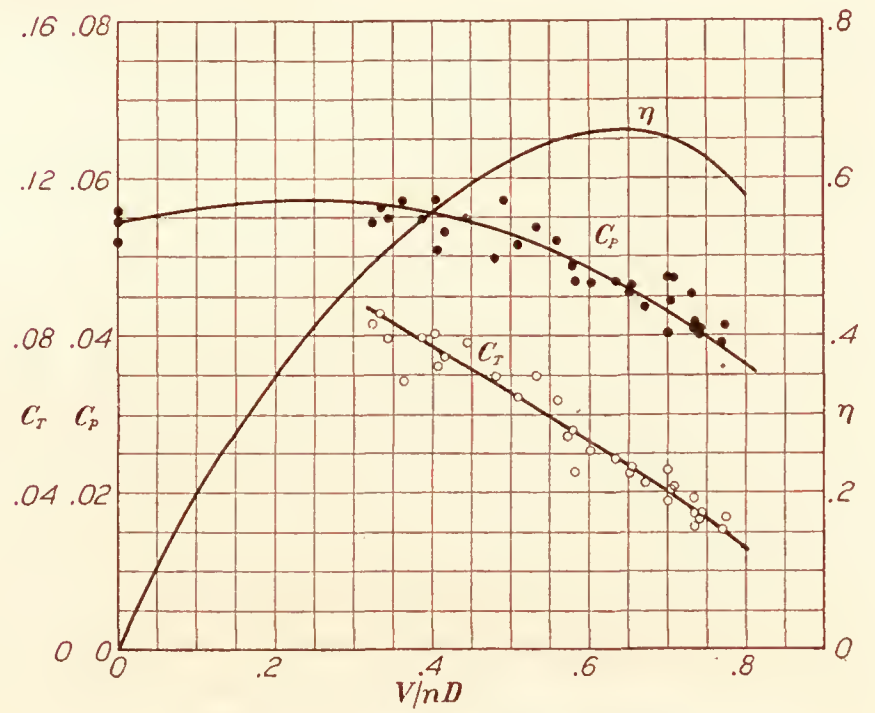


FIG. 13.—Characteristics of propeller 3715

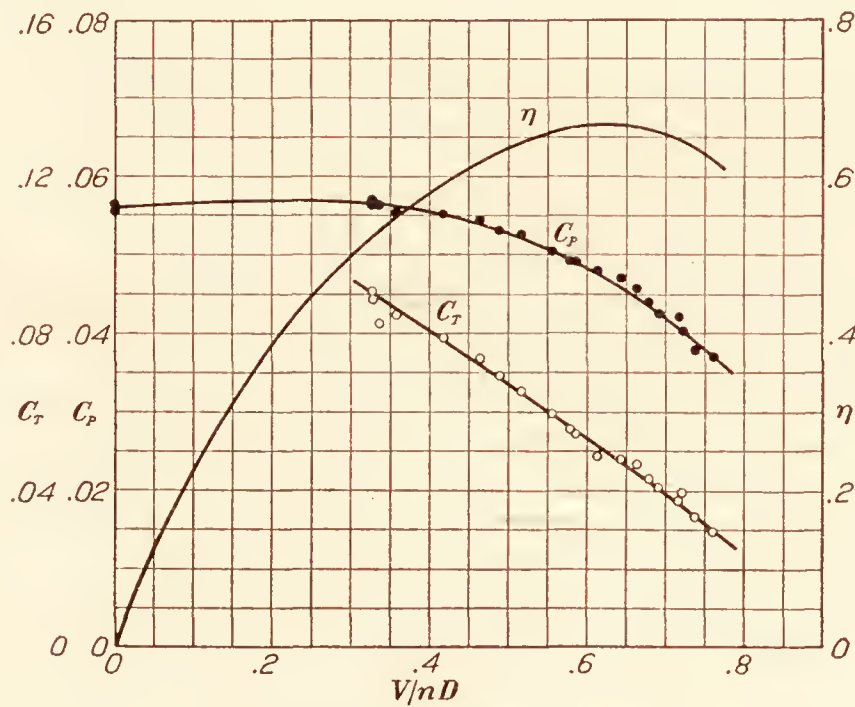


FIG. 14.—Characteristics of propeller 3872



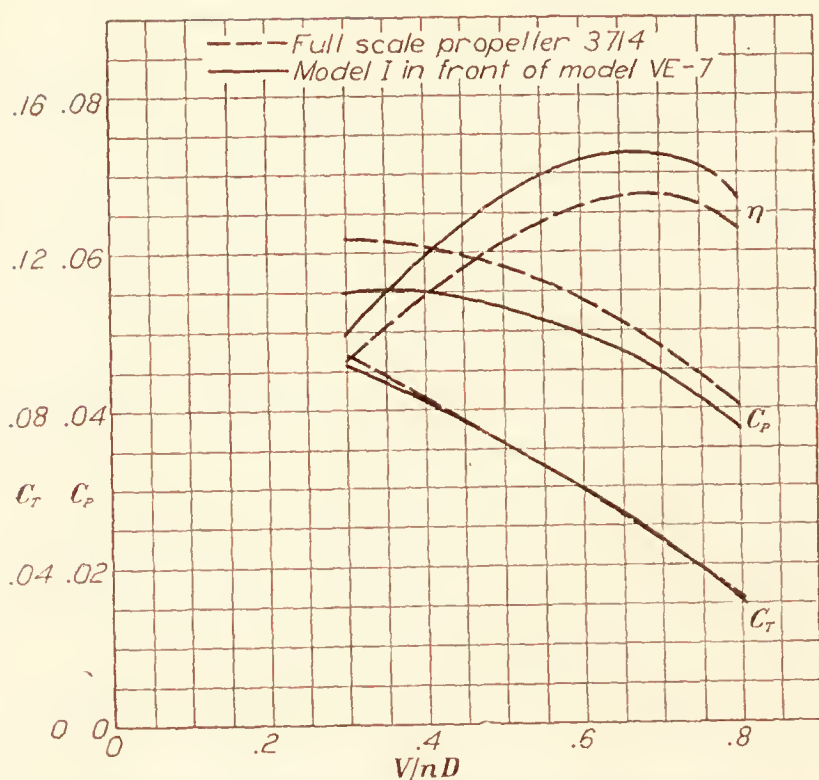


FIG. 15.—A comparison of Model I with full-scale propeller 3714

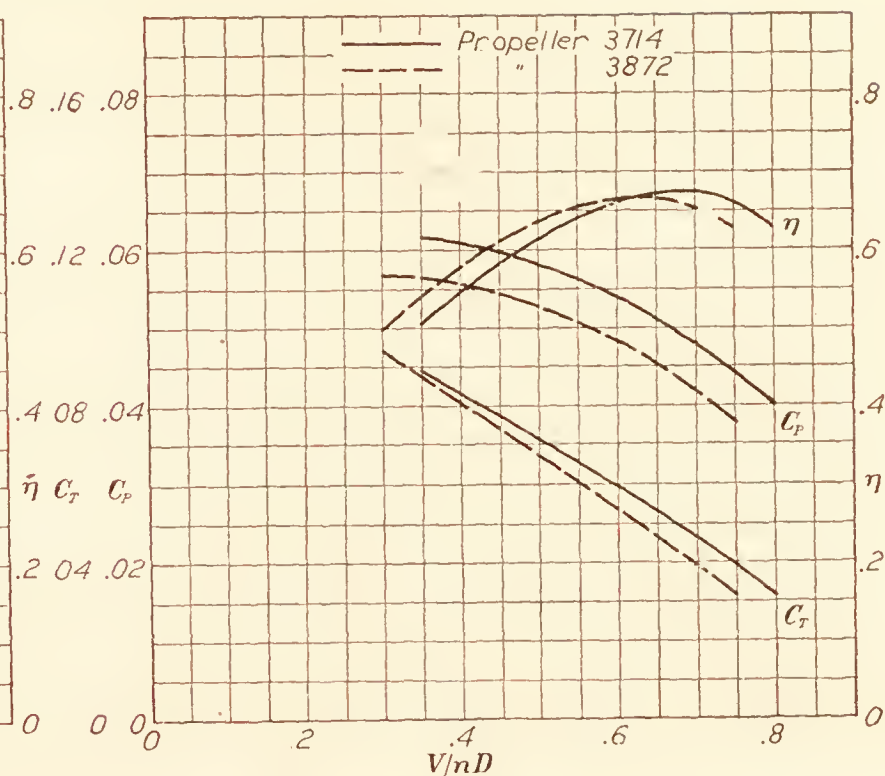


FIG. 17.—A comparison of propellers 3714 and 3872

Average  $\frac{\pi n D}{a}$  for tests on propeller 3714,  
Model, & Full scale.

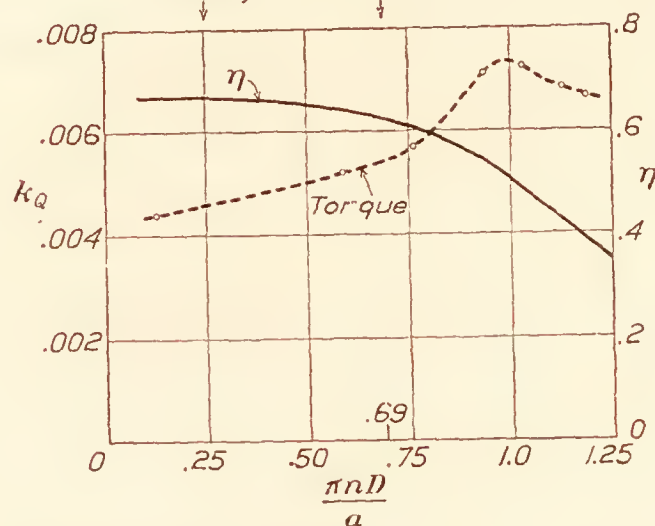


FIG. 16.—The effect of tip speed on efficiency and torque

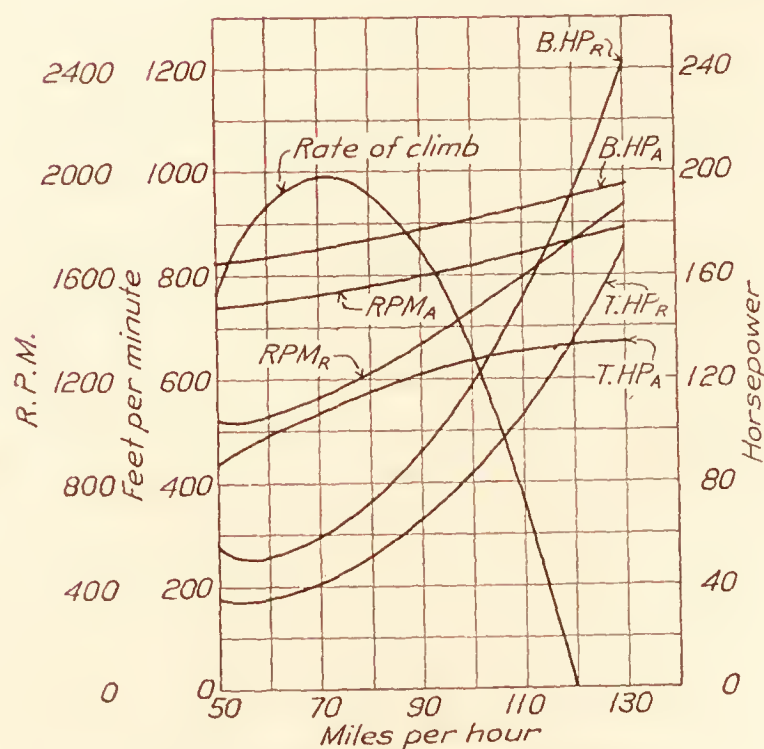


FIG. 18.—Curves for propeller 3712. Standard air

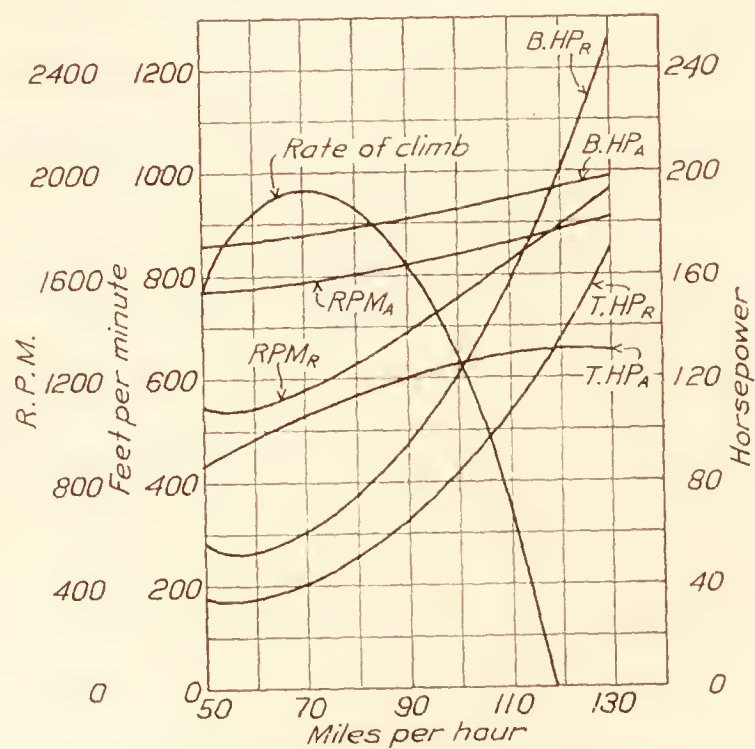


FIG. 19.—Curves for propeller 3713. Standard air

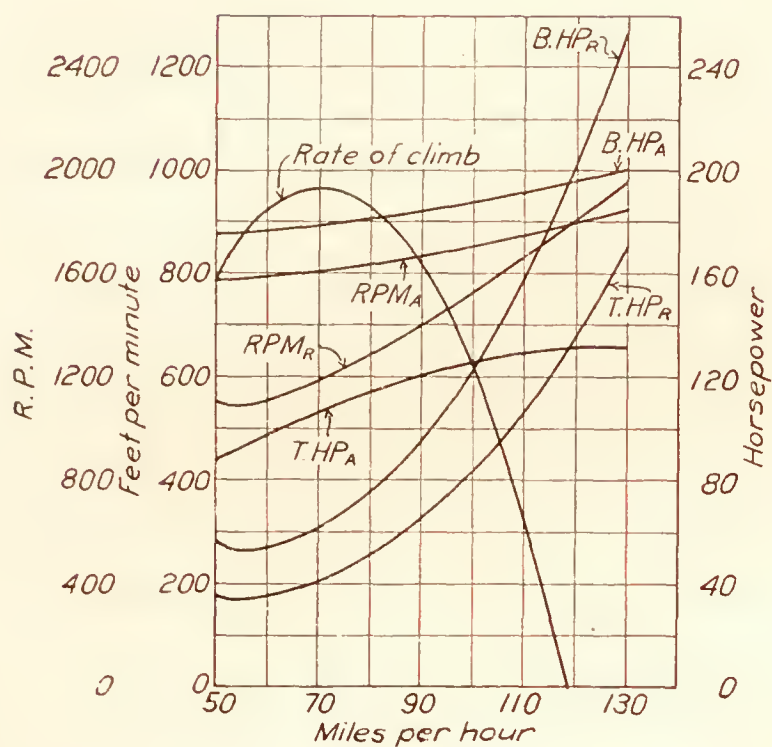


FIG. 20.—Curves for propeller 3714. Standard air

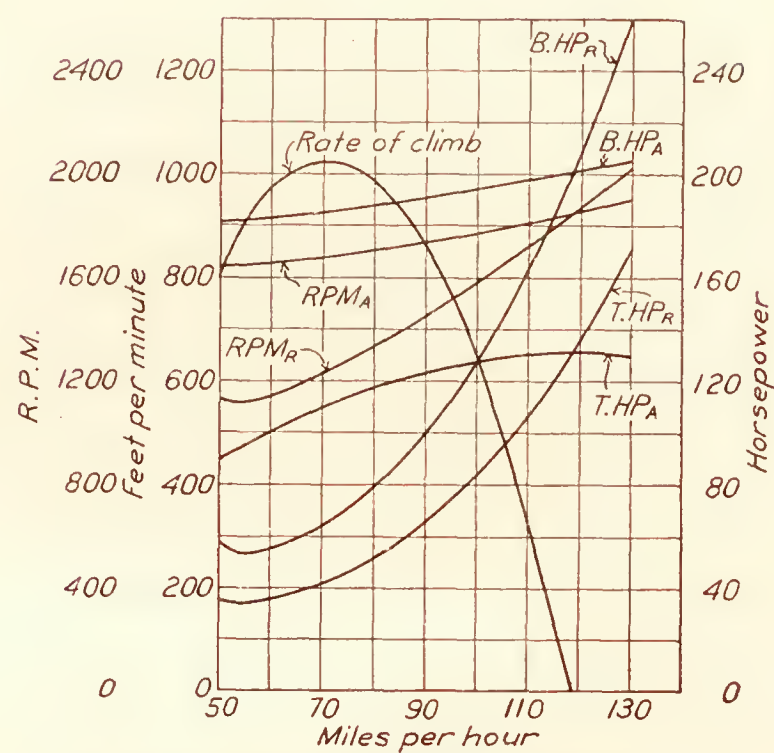


FIG. 21.—Curves for propeller 3715. Standard air

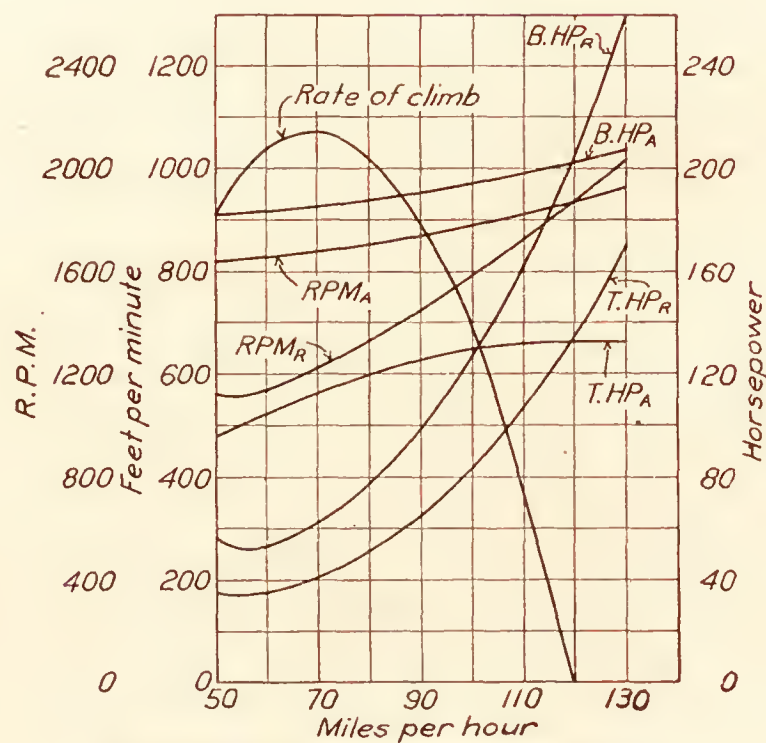


FIG. 22.—Curves for propeller 3S72. Standard air



measured by the flight path angle recorder. Nearly all the gliding flights were made in the early morning hours in extremely smooth and steady air conditions. As a consequence of the care and the number of measurements made it is reasonably certain that the faired lift and drag curves are accurate to within  $\pm 1\frac{1}{2}$  per cent.

The most striking results of the propeller tests were the low efficiencies obtained. As will be noted in Figures 10 to 14, the efficiency in no case exceeded 71 per cent, while estimates based on model results would have been at least 4 or 5 per cent larger. A wind-tunnel test of a 3-foot model of propeller 3714 was made previously at Leland Stanford University (Reference 1) and the results of this test are shown in Figure 15, together with the full-scale flight results. These curves show a change of approximately 5 per cent in efficiency between the flight and model results that is due to a greater power absorbed in the former. This difference is believed to be attributable mainly to the different tip velocities used in the two experiments. It is known that an increase of tip speed, within the limits reached in these flight tests, produces a considerable increase in the power absorbed and a small increase in the thrust developed, with a consequent decrease in efficiency. To illustrate this quantitatively, a curve taken from R. & M. No. 884 (Reference 3) is reproduced (fig. 16) on which are shown the average values of  $\frac{\pi n D}{a}$  (where  $a$  is the velocity of sound) for both the flight and model tests of propeller 3714. This figure shows a decrease of efficiency of the same order as shown in Figure 15. There is a difference between the two, however, that is at present unaccounted for in that the results of Figure 16 indicate a definite although small change of thrust with tip speed while Figure 15 shows no change of thrust.

In addition to different tip speeds, the flight tests differ from the model tests in that the propellers in flight are always operating at some degree of yaw while the model propellers are operating at zero yaw. There is comparatively little known of the effect of yaw on propeller characteristics, but such data as are available indicate that very little effect should occur within the usual operating range of angles.

Propellers 3714 and 3872 are similar except for the change in airfoil sections and are plotted together for comparison in Figure 17. The section used in propeller 3872, having a better  $L/D$  ratio, was expected to increase the propeller efficiency for the same power absorbed. Actually, as will be noted, the efficiency was improved at the higher slips but the power absorbed was decreased. This was probably occasioned by a difference in deflection between the two propellers, which is entirely possible, particularly inasmuch as propeller 3872 was constructed at a later date than 3714 and could differ considerably in the material used. The data indicate that in operation the pitch of propeller 3872 was less than that of propeller 3714, since the maximum efficiency was lower, the efficiency at high slips was greater, and the power absorbed was less. From this it appears that an accurate comparison of propeller characteristics is not possible unless the pitch angles under operating conditions are known.

Figures 18 to 22 have been included to illustrate the effect of the various propellers tested on the performance of the VE-7 airplane. There is no great difference in the rate of climb with any of the propellers. The largest maximum rate of climb, obtained with propeller 3872, was only 110 feet per minute greater than the smallest maximum rate of climb, with propellers 3713 and 3714.

### CONCLUSIONS

It appears probable that propellers in flight operate at lower efficiencies than the usual model tests indicate, mainly because of the higher tip speeds encountered in flight. It is concluded that accurate comparison of propeller characteristics is not feasible unless the pitch angles under operating conditions are known, which makes the measurement of blade twist necessary. Additional research should be conducted on the effect of tip velocity on propeller characteristics and also on the effects of yaw on the same. Future propeller tests in flight should include direct measurement of power absorbed.



REFERENCES AND BIBLIOGRAPHY

Reference 1. Durand, W. F., and Lesley, E. P. Comparison of Tests on Air Propellers in Flight with Wind Tunnel Tests on Similar Models. N. A. C. A. Technical Report No. 220. 1926.

Reference 2. Coleman, D. G. N. A. C. A. Flight Path Angle and Air-Speed Recorder. N. A. C. A. Technical Note No. 223. 1926.

Reference 3. Douglas, G. P., and Wood, R. McKinnon. The Effects of Tip Speed on Airscrew Performance. R. & M. No. 884. 1923.

Aerodynamics Staff of the R. A. E. Report on Various Airscrews Designed for SE-5, with 150 H. P. Ung geared Hispano-Suiza Engine. R. & M. 586. 1921.

Stevens, H. L., and Layman, E. J. H. Comparative Performance of Various Airscrews for SE-5, with Woleseley Viper Engine. R. & M. 704. 1920.

Meredith, F. W. Full-Scale Determination of the Characteristics of a Variable Pitch Airscrew. R. & M. 870. 1923.

LANGLEY MEMORIAL AERONAUTICAL LABORATORY,  
NATIONAL ADVISORY COMMITTEE FOR AERONAUTICS,  
LANGLEY FIELD, VA., *November 8, 1927.*

TABLE I  
SECTION ORDINATES FOR PROPELLER 3712  
[All ordinates in inches. Stations in per cent of chord]

Radius.....	7. 35''		14. 70''		22. 05''		29. 40''	36. 75''	44. 10''
Chord.....	7. 35''		7. 72''		8. 17''		7. 72''	6. 47''	4. 41''
	Upper	Lower	Upper	Lower	Upper	Lower	Upper	Upper	Upper
Leading-edge radius...	0. 80		0. 28		0. 14		0. 08	0. 06	0. 03
2. 5.....	. 46	. 43	. 51	. 15	. 45	. 02	. 34	. 23	. 13
5.....	. 66	. 63	. 73	. 21	. 64	. 03	. 48	. 32	. 19
10.....	. 89	. 84	. 98	. 28	. 86	. 04	. 65	. 43	. 25
20.....	1. 06	1. 01	1. 18	. 34	1. 04	. 05	. 78	. 52	. 30
30.....	1. 12	1. 06	1. 24	. 36	1. 09	. 05	. 82	. 55	. 32
40.....	1. 11	1. 05	1. 23	. 36	1. 08	. 05	. 81	. 54	. 32
50.....	1. 06	1. 01	1. 18	. 34	1. 04	. 05	. 78	. 52	. 30
60.....	. 97	. 92	1. 08	. 31	. 95	. 04	. 77	. 48	. 28
70.....	. 83	. 78	. 92	. 27	. 81	. 04	. 61	. 41	. 24
80.....	. 62	. 59	. 69	. 20	. 61	. 03	. 46	. 31	. 20
90.....	. 39	. 37	. 43	. 13	. 38	. 02	. 29	. 21	. 16
Trailing-edge radius...	. 09		. 09		. 07		. 06	. 05	. 05

SECTION ORDINATES FOR PROPELLER 3713

Leading-edge radius...	1. 02		0. 36		0. 18		0. 10	0. 07	0. 04
2.5.....	. 57	. 54	. 63	. 18	. 56	. 02	. 42	. 28	. 16
5.....	. 83	. 78	. 91	. 27	. 80	. 04	. 61	. 41	. 24
10.....	1. 11	1. 04	1. 22	. 36	1. 07	. 05	. 81	. 55	. 32
20.....	1. 33	1. 25	1. 46	. 43	1. 29	. 06	. 98	. 66	. 38
30.....	1. 40	1. 32	1. 54	. 45	1. 36	. 06	1. 03	. 69	. 40
40.....	1. 39	1. 31	1. 53	. 45	1. 35	. 06	1. 02	. 68	. 40
50.....	1. 33	1. 25	1. 46	. 43	1. 29	. 06	. 98	. 66	. 38
60.....	1. 22	1. 15	1. 34	. 39	1. 18	. 05	. 90	. 60	. 35
70.....	1. 04	. 98	1. 14	. 33	1. 01	. 04	. 76	. 51	. 30
80.....	. 78	. 74	. 86	. 25	. 76	. 03	. 58	. 39	. 24
90.....	. 49	. 46	. 54	. 16	. 48	. 02	. 36	. 25	. 17
Trailing-edge radius...	. 24		. 16		. 08		. 08	. 05	. 05



TABLE I—Continued

## SECTION ORDINATES FOR PROPELLER 3714

Radius-----	7. 35''		14. 70''		22. 05''		29. 40''	36. 75''	44. 10''
Chord-----	7. 35''		7. 72''		8. 17''		7. 72''	6. 47''	4. 41''
	Upper	Lower	Upper	Lower	Upper	Lower	Upper	Upper	Upper
Leading edge radius--	1. 44		0. 68		0. 28		0. 12	0. 08	0. 05
2.5-----	. 69	. 65	. 76	. 22	. 67	. 03	. 50	. 34	. 20
5-----	. 99	. 94	1. 09	. 32	. 97	. 04	. 73	. 49	. 28
10-----	1. 33	1. 26	1. 46	. 43	1. 30	. 06	. 97	. 66	. 38
20-----	1. 60	1. 51	1. 76	. 51	1. 56	. 07	1. 17	. 79	. 46
30-----	1. 68	1. 59	1. 85	. 54	1. 64	. 07	1. 23	. 83	. 48
40-----	1. 66	1. 57	1. 83	. 53	1. 62	. 07	1. 22	. 82	. 48
50-----	1. 60	1. 51	1. 76	. 51	1. 56	. 07	1. 17	. 79	. 46
60-----	1. 46	1. 38	1. 61	. 47	1. 43	. 06	1. 07	. 72	. 42
70-----	1. 24	1. 18	1. 37	. 40	1. 21	. 05	. 91	. 61	. 36
80-----	. 94	. 89	1. 04	. 30	. 92	. 04	. 69	. 46	. 28
90-----	. 59	. 56	. 65	. 19	. 57	. 02	. 43	. 29	. 20
Trailing edge radius--	. 20		. 16		. 12		. 09	. 06	. 05

## SECTION ORDINATES FOR PROPELLER 3715

Leading edge radius--	1. 78		0. 64		0. 20		0. 14	0. 10	0. 06
2.5-----	. 80	. 76	. 89	. 26	. 78	. 03	. 59	. 40	. 23
5-----	1. 16	1. 07	1. 28	. 37	1. 13	. 05	. 85	. 57	. 33
10-----	1. 55	1. 46	1. 71	. 50	1. 51	. 06	1. 14	. 77	. 41
20-----	1. 86	1. 76	2. 05	. 60	1. 81	. 08	1. 37	. 92	. 53
30-----	1. 96	1. 85	2. 16	. 63	1. 91	. 08	1. 44	. 97	. 56
40-----	1. 94	1. 83	2. 14	. 62	1. 89	. 08	1. 43	. 96	. 55
50-----	1. 86	1. 76	2. 05	. 60	1. 81	. 08	1. 37	. 92	. 53
60-----	1. 71	1. 61	1. 88	. 55	1. 66	. 07	1. 25	. 84	. 49
70-----	1. 45	1. 37	1. 60	. 47	1. 41	. 06	1. 07	. 72	. 41
80-----	1. 10	1. 04	1. 21	. 35	1. 07	. 04	. 81	. 54	. 31
90-----	. 69	. 65	. 76	. 22	. 67	. 03	. 50	. 34	. 20
Trailing edge radius--	. 28		. 22		. 16		. 11	. 07	. 05

## SECTION ORDINATES FOR PROPELLER 3872

Radius-----	7. 35''		14. 70''		22. 05''		29. 40''		36. 75''		44. 10''	
Chord-----	7. 35''		7. 72''		8. 17''		7. 72''		6. 47''		4. 41''	
	Upper	Lower	Upper	Lower	Upper	Lower	Upper	Lower	Upper	Lower	Upper	Lower
Leading edge radius--	1. 48		0. 58		0. 15		0. 11		0. 07		0. 04	
2.5-----	. 69	. 65	. 76	. 22	. 92	. 15	. 66	. 11	. 45	. 07	. 26	. 04
5-----	. 99	. 94	1. 09	. 32	1. 15	. 09	. 82	. 06	. 56	. 04	. 32	. 02
10-----	1. 33	1. 26	1. 46	. 43	1. 40	. 02	1. 01	. 01	. 68	. 01	. 39	-----
20-----	1. 60	1. 51	1. 76	. 51	1. 66	-----	1. 19	-----	. 81	-----	. 47	-----
30-----	1. 68	1. 59	1. 85	. 54	1. 71	-----	1. 23	-----	. 83	-----	. 48	-----
40-----	1. 66	1. 57	1. 83	. 53	1. 66	-----	1. 19	-----	. 81	-----	. 47	-----
50-----	1. 60	1. 51	1. 76	. 51	1. 54	-----	1. 11	-----	. 75	-----	. 43	-----
60-----	1. 46	1. 38	1. 61	. 47	1. 33	-----	. 96	-----	. 65	-----	. 37	-----
70-----	1. 24	1. 18	1. 37	. 40	1. 09	-----	. 79	-----	. 53	-----	. 31	-----
80-----	. 94	. 89	1. 04	. 30	. 82	-----	. 59	-----	. 40	-----	. 23	-----
90-----	. 59	. 56	. 65	. 19	. 51	-----	. 37	-----	. 25	-----	. 14	-----
Trailing edge radius--	. 20		. 14		. 09		. 06		. 04		. 02	

TABLE II  
GLIDE TEST DATA

Flight and run No.	Angle of flight path $\gamma$	Angle of wing	Angle of attack $\alpha$	Weight	Lift	Apparent drag	$1/2 \rho V^2$	Specific weight  <i>Lb./cu. ft.</i>	Velocity  <i>Ft./sec.</i>	R. P. M.	$\frac{V}{nD}$	Thrust	True drag	$C_L$	$C_D$
1-2	-6.1	-1.2	4.9	2,208	2,196	234.3	16.22	0.0680	124.0	950	0.959	5.8	240.1	0.475	0.0520
1-3	-5.8	1.4	7.2	2,203	2,192	222.5	13.67	.0677	114.0	857	.970	.9	223.6	.564	.0575
1-5	-5.7	4.3	10.0	2,193	2,184	217.9	9.36	.0670	94.8	693	.998	-6.2	211.7	.820	.0795
1-6	-6.1	-----	-----	2,188	2,176	232.1	8.07	.0675	87.6	640	1.005	-6.7	225.1	.948	.0983
1-8	-5.2	-----	-----	2,178	2,169	197.3	11.51	.0676	104.7	851	.904	16.1	213.4	.662	.0652
1-9	-5.9	-----	-----	2,173	2,161	223.1	8.43	.0674	89.6	676	.973	0	223.1	.726	.0749
4-1	-6.4	7.4	13.8	2,213	2,198	246.5	6.50	.0668	79.2	594	.979	-8	245.7	1.187	.1327
4-2	-6.5	6.6	13.1	2,208	2,191	249.9	7.08	.0671	82.3	580	1.041	-11.3	230.6	1.088	.1184
4-3	-6.2	5.3	11.5	2,203	2,190	238.0	8.07	.0671	87.9	618	1.042	-13.3	214.7	.954	.0935
4-4	-6.0	3.8	9.8	2,198	2,186	229.7	9.32	.0672	94.4	662	1.046	-15.7	214.0	.824	.0807
4-5	-6.5	7.3	13.8	2,193	2,178	248.2	6.76	.0680	80.1	573	1.026	-8.8	239.4	1.131	.1244
4-6	-6.3	6.8	13.1	2,188	2,173	240.0	7.08	.0684	81.6	614	.976	-7	239.3	1.078	.1187
4-7	-5.9	5.5	11.4	2,183	2,171	224.4	8.07	.0672	87.9	652	.989	-3.4	221.0	.946	.0963
4-8	-6.5	7.7	14.2	2,178	2,163	246.4	6.76	.0672	80.4	583	1.002	-5.1	241.3	1.124	.1254
4-9	-6.1	6.6	12.7	2,173	2,160	230.8	7.44	.0677	84.3	612	1.011	-7.1	223.7	1.020	.1056
5-1	-14.3	-13.7	.6	2,213	2,145	547.0	47.40	.0703	208.6	1,539	.995	-27.6	519.4	.158	.0385
5-3	-11.0	-9.6	1.4	2,203	2,161	420.5	33.54	.0691	176.7	1,295	1.003	-27.4	393.1	.226	.0412
5-4	-8.5	-6.4	2.1	2,198	2,172	324.9	26.61	.0685	158.2	1,196	.972	0	324.9	.287	.0430
5-5	-7.3	-4.0	3.3	2,193	2,174	278.5	20.53	.0665	141.0	1,059	.970	-1.4	277.1	.372	.0475
5-6	-6.4	-1.2	5.2	2,188	2,173	243.9	15.86	.0660	124.3	916	.996	-9.5	234.4	.482	.0519
5-7	-6.1	1.4	7.5	2,183	2,170	232.7	11.44	.0660	105.6	766	1.013	-11.5	221.2	.667	.0680
5-8	-5.8	5.0	10.8	2,178	2,167	225.4	8.69	.0663	91.8	710	.950	5.4	214.6	.877	.0912
6-1	-13.2	-12.8	.4	2,213	2,160	506.0	44.40	.0692	203.0	1,536	.968	4.1	510.1	.171	.0403
6-2	-11.8	-10.8	1.0	2,208	2,155	452.0	39.00	.0692	190.5	1,448	.967	3.9	455.9	.194	.0411
6-3	-10.8	-9.5	1.3	2,203	2,160	413.0	35.60	.0680	183.5	1,376	.980	-7.1	405.9	.213	.0400
6-4	-8.3	-6.5	1.8	2,198	2,170	317.0	28.70	.0676	165.0	1,282	.958	11.3	328.3	.266	.0402
6-5	-7.7	-5.0	2.7	2,193	2,175	294.0	23.50	.0682	149.0	1,172	.932	27.2	321.2	.336	.0481
6-6	-6.8	-2.8	4.0	2,188	2,170	259.0	18.45	.0670	133.0	1,014	.962	4.8	263.8	.414	.0504
6-7	-5.6	.5	6.1	2,183	2,170	213.0	14.30	.0660	118.0	936	.930	17.1	230.1	.533	.0565
6-8	-4.9	2.6	7.5	2,178	2,170	185.5	11.45	.0660	105.8	888	.873	36.6	222.1	.665	.0680
6-9	-7.7	10.7	18.4	2,173	2,160	291.0	5.46	.0675	72.2	562	.932	6.3	297.3	1.390	.1920
7-3	-11.4	-10.4	1.0	2,203	2,159	435.2	39.10	.0678	192.8	1,478	.958	15.6	450.8	.194	.0405
7-4	-7.9	10.5	18.4	2,198	2,178	302.0	5.93	.0661	76.0	559	.998	-3.9	298.1	1.290	.1767
7-5	-7.3	10.3	17.6	2,193	2,176	278.5	5.82	.0701	73.1	594	.904	12.0	290.5	1.314	.1755
7-6	-6.4	9.4	15.8	2,188	2,175	243.8	6.40	.0688	77.4	642	.885	17.6	255.8	1.194	.1404
7-7	-6.0	7.2	13.2	2,183	2,171	227.9	7.13	.0661	83.3	652	.948	7.1	235.0	1.070	.1158
7-8	-5.8	4.6	10.4	2,178	2,168	220.0	9.05	.0656	94.2	710	.974	-5	219.5	.842	.0852
7-9	-6.6	9.9	16.5	2,173	2,159	249.5	5.98	.0663	76.2	638	.888	15.9	265.4	1.269	.1560
8-1	-13.1	-12.5	.6	2,213	2,150	502.0	45.10	.0698	204.0	1,564	.958	18.1	520.1	.167	.0406
8-2	-11.4	-10.5	.9	2,208	2,165	436.5	39.15	.0692	190.8	1,452	.964	7.8	444.3	.194	.0399
8-3	-9.4	-7.6	1.8	2,203	2,170	360.0	28.62	.0686	163.7	1,230	.975	2.9	362.9	.266	.0447
8-4	-7.5	-4.0	3.5	2,198	2,175	287.0	20.30	.0684	138.2	1,010	1.006	-14.9	272.1	.376	.0488
8-5	-5.6	1.2	6.8	2,193	2,182	213.4	12.07	.0658	108.8	840	.950	7.2	220.6	.637	.0644
8-6	-5.8	4.4	10.2	2,188	2,170	221.2	9.12	.0658	94.3	696	.994	-5.1	216.1	.838	.834



8-7	-6.8	8.9	15.7	2,183	2,165	258.6	6.25	.0656	78.2	592	.970	-.4	258.2	1.212	.1455
8-8	-7.2	9.6	16.8	2,178	2,160	275.0	6.09	.0666	76.6	564	.996	-3.6	271.4	1.249	.1569
8-9	-7.6	10.7	18.3	2,173	2,155	287.7	5.83	.0689	73.8	584	.928	7.4	295.1	1.301	.1783
9-1	-7.7	10.7	18.4	2,213	2,193	296.7	5.83	.0678	74.4	588	.930	7.2	303.9	1.321	.1830
9-2	-7.6	10.1	17.7	2,208	2,189	292.0	5.93	.0678	75.1	576	.958	2.4	294.4	1.296	.1744
9-3	-7.3	9.4	16.7	2,203	2,184	279.8	6.04	.0683	76.0	608	.918	9.6	289.4	1.271	.1684
9-4	-6.0	7.4	13.4	2,198	2,184	229.8	7.13	.0673	82.6	656	.925	9.9	239.7	1.076	.1131
9-5	-5.8	3.7	9.5	2,193	2,182	221.6	9.31	.0680	93.9	696	.990	-4.3	217.3	.824	.0821
9-6	-7.3	11.2	18.5	2,188	2,170	278.0	5.83	.0701	73.2	608	.884	16.3	294.3	1.307	.1773
9-7	-6.9	10.3	17.2	2,183	2,169	262.3	5.93	.0680	74.9	630	.873	19.1	281.4	1.285	.1666
9-8	-7.0	9.3	16.3	2,178	2,162	265.3	6.04	.0678	75.7	588	.946	4.4	269.7	1.259	.1569
9-9	-7.7	10.0	17.7	2,173	2,153	291.2	5.83	.0685	74.0	554	.981	-1.3	289.9	1.298	.1745

TABLE III  
POWER FLIGHT DATA  
PROPELLER 3712

Flight and run No.	Specific weight	Velocity	R. P. M.	Angle of Flight path $\gamma$	Angle of attack $\alpha$	$W$	$L$	$D$	$T$	HP	$\frac{V}{nD}$	$C_T$	$C_P$	$\eta$
	<i>Lb./cu. ft.</i>	<i>Ft./sec.</i>												
1-1	0.0698	100.4	1,500	8.3	8.1	2,213	2,132	214.5	534.3	155.7	0.492	0.0890	0.0701	0.626
1-3	.0700	192.2	1,756	-2.3	.9	2,203	2,207	455.0	367.4	178.1	.804	.0444	.0497	.720
1-4	.0693	85.2	1,510	10.4	12.0	2,198	2,056	208.0	605.0	155.6	.414	.1000	.0690	.601
1-5	.0688	114.7	1,552	7.2	5.8	2,193	2,120	222.8	498.3	158.0	.543	.0784	.0649	.656
1-6	.0694	206.8	1,842	-4.7	.5	2,188	2,189	517.5	338.3	183.1	.825	.0374	.0447	.692
1-7	.0707	175.5	1,710	0.0	1.4	2,183	2,187	389.4	389.4	176.1	.754	.0491	.0527	.703
1-8	.0692	129.2	1,594	5.7	4.2	2,178	2,150	249.3	465.4	162.5	.596	.0690	.0606	.678
1-9	.0690	144.5	1,630	3.8	3.0	2,173	2,161	282.9	426.9	165.3	.652	.0608	.0586	.676
2-1	.0700	94.1	1,535	7.8	9.4	2,213	2,125	212.2	512.2	159.2	.450	.0812	.0665	.550
2-2	.0690	104.5	1,524	8.0	7.4	2,208	2,138	216.3	523.5	155.6	.504	.0851	.0674	.636
2-3	.0692	76.8	1,520	10.2	15.2	2,203	2,023	224.1	614.5	156.0	.372	.1001	.0678	.547
2-7	.0695	122.6	1,577	6.5	4.8	2,183	2,146	238.0	485.1	161.7	.572	.0730	.0628	.664
2-8	.0699	139.6	1,632	4.8	3.4	2,178	2,160	272.1	454.5	167.6	.629	.0637	.0583	.686
2-9	.0704	199.8	1,828	-3.5	.7	2,173	2,176	498.0	365.4	184.6	.804	.0407	.0455	.720
2-10	.0765	0	1,504							164.7	0		.0718	
14-3	.0702	179.1	1,724	-1.4	1.3	2,203	2,204	402.2	348.4	171.3	.764	.0437	.0505	.661
14-4	.0701	149.4	1,656	2.6	2.7	2,198	2,190	301.2	400.9	165.5	.663	.0545	.0551	.656
14-5	.0681	100.6	1,536	8.2	8.1	2,193	2,114	211.6	524.5	150.3	.481	.0850	.0642	.637
14-6	.0677	135.1	1,612	4.4	3.8	2,188	2,168	258.8	426.6	155.3	.616	.0632	.0579	.674
14-7	.0693	190.7	1,780	-2.9	.9	2,183	2,186	444.4	334.0	173.2	.788	.0399	.0471	.668
14-8	.0691	117.1	1,564	6.4	5.5	2,178	2,135	227.8	470.4	154.4	.550	.0726	.0618	.647
14-9	.0691	163.3	1,688	1.0	1.9	2,173	2,173	332.5	370.4	166.3	.711	.0491	.0529	.660
14-10	.0703	130.6	1,580	4.7	3.9	2,168	2,147	254.0	431.7	158.9	.608	.0643	.0607	.643
14-11	.0765	0	1,480							158.9	0		.0678	
15-1	.0682	94.3	1,504	8.2	9.6	2,213	2,119	212.0	527.8	148.8	.461	.0893	.0679	.606
15-2	.0688	171.5	1,668	-0.1	1.7	2,208	2,210	367.8	364.0	162.9	.756	.0497	.0541	.695
15-3	.0675	79.1	1,489	8.8	14.5	2,203	2,012	216.6	553.6	145.8	.392	.0972	.0701	.543
15-4	.0689	185.3	1,748	-2.0	1.2	2,198	2,204	417.0	340.2	169.5	.778	.0421	.0487	.673
15-5	.0682	108.6	1,504	7.2	6.8	2,193	2,135	217.1	492.1	146.8	.531	.0873	.0671	.660
15-6	.0683	200.0	1,808	-4.5	.7	2,188	2,188	481.0	309.4	173.3	.813	.0362	.0455	.647
15-7	.0682	126.5	1,564	5.5	4.5	2,183	2,152	242.1	451.3	152.7	.594	.0706	.0620	.677
15-8	.0679	158.9	1,624	1.5	2.2	2,178	2,177	320.7	377.7	157.1	.719	.0552	.0571	.696
15-10	.0670	142.4	1,581	3.4	3.3	2,168	2,155	272.4	401.0	153.0	.662	.0626	.0612	.677
15-11	.0765	0	1,482							158.9	0		.0683	



PROPELLER 3713

3-1	0. 0693	94. 5	1, 564	8. 6	9. 4	2, 213	2, 114	210. 5	541. 5	158. 8	0. 444	0. 0834	0. 0632	0. 586
3-2	. 0694	157. 0	1, 704	2. 5	2. 3	2, 208	2, 204	324. 6	420. 8	169. 8	. 676	. 0544	. 0522	. 705
3-3	. 0705	186. 0	1, 772	-2. 0	1. 1	2, 203	2, 208	431. 5	354. 6	177. 2	. 769	. 0411	. 0472	. 670
3-5	. 0692	172. 5	1, 752	0	1. 3	2, 193	2, 198	370. 0	370. 0	173. 7	. 721	. 0456	. 0494	. 666
3-6	. 0695	80. 6	1, 545	8. 8	13. 3	2, 188	2, 154	231. 6	566. 1	156. 8	. 383	. 0888	. 0645	. 527
3-8	. 0727	120. 5	1, 578	6. 2	4. 7	2, 178	2, 143	238. 1	473. 0	166. 0	. 561	. 0682	. 0614	. 623
3-9	. 0725	135. 0	1, 605	4. 8	3. 4	2, 173	2, 154	269. 0	450. 5	167. 7	. 617	. 0627	. 0589	. 657
4-1	. 0711	99. 0	1, 576	8. 2	8. 1	2, 213	2, 132	213. 8	529. 6	162. 6	. 461	. 0782	. 0621	. 581
4-2	. 0712	82. 3	1, 564	9. 0	12. 5	2, 208	2, 076	213. 2	558. 4	161. 6	. 387	. 0838	. 0628	. 516
4-3	. 0714	174. 9	1, 764	- . 4	1. 4	2, 203	2, 207	392. 5	377. 3	178. 9	. 729	. 0443	. 0484	. 669
4-4	. 0702	76. 6	1, 550	9. 7	14. 8	2, 198	2, 028	222. 5	593. 0	158. 3	. 363	. 0916	. 0641	. 519
4-6	. 0725	113. 0	1, 576	7. 3	5. 7	2, 188	2, 137	225. 4	503. 4	166. 2	. 527	. 0729	. 0621	. 619
4-7	. 0714	146. 4	1, 632	3. 7	2. 7	2, 183	2, 174	296. 2	437. 0	168. 5	. 659	. 0600	. 0575	. 688
4-8	. 0708	165. 3	1, 700	1. 7	1. 8	2, 178	2, 175	353. 0	417. 6	172. 8	. 715	. 0534	. 0527	. 725
4-9	. 0717	127. 8	1, 628	5. 3	4. 1	2, 173	2, 146	250. 2	451. 1	169. 3	. 577	. 0619	. 0578	. 616
4-10	. 0702	76. 6	1, 536	9. 0	14. 7	2, 168	2, 013	220. 5	559. 5	157. 0	. 366	. 0881	. 0652	. 495
4-11	. 0765	0	1, 582							173. 8	0		. 0607	
5-1	. 0710	90. 1	1, 588	9. 2	10. 2	2, 213	2, 104	211. 4	565. 4	165. 6	. 417	. 0824	. 0617	. 557
5-2	. 0702	169. 8	1, 748	. 4	1. 7	2, 208	2, 206	367. 0	382. 2	176. 8	. 714	. 0465	. 0498	. 665
5-3	. 0705	137. 9	1, 680	4. 4	3. 4	2, 203	2, 185	272. 0	441. 0	171. 1	. 603	. 0578	. 0541	. 644
5-4	. 0714	184. 0	1, 820	-1. 4	1. 1	2, 198	2, 202	425. 0	371. 4	184. 7	. 743	. 0410	. 0455	. 669
5-5	. 0715	106. 1	1, 604	8. 4	6. 8	2, 193	2, 125	216. 4	537. 0	167. 2	. 486	. 0761	. 0595	. 622
5-7	. 0724	119. 1	1, 628	7. 1	4. 9	2, 183	2, 135	236. 4	506. 4	172. 2	. 538	. 0690	. 0585	. 634
5-9	. 0682	75. 5	1, 569	9. 7	16. 0	2, 173	2, 010	229. 0	595. 1	159. 5	. 354	. 0928	. 0643	. 511
5-10	. 0673	155. 8	1, 733	2. 4	2. 4	2, 168	2, 163	310. 0	400. 8	170. 7	. 661	. 0518	. 0515	. 665
5-11	. 0765	0	1, 576							173. 4	0		. 0610	
6-1	. 0716	94. 2	1, 568	9. 1	9. 1	2, 213	2, 104	210. 6	560. 6	164. 7	. 442	. 0831	. 0632	. 581
6-3	. 0714	190. 7	1, 852	-2. 4	. 9	2, 203	2, 195	457. 0	365. 0	187. 8	. 757	. 0389	. 0438	. 672
6-4	. 0709	131. 0	1, 644	4. 6	3. 9	2, 198	2, 176	257. 8	435. 5	169. 5	. 586	. 0593	. 0571	. 598
6-5	. 0727	203. 0	1, 896	-4. 5	. 4	2, 193	2, 177	523. 0	351. 0	194. 1	. 787	. 0350	. 0418	. 666
6-6	. 0713	112. 8	1, 620	7. 8	5. 8	2, 188	2, 134	224. 3	521. 3	169. 6	. 512	. 0729	. 0594	. 627
6-7	. 0712	177. 7	1, 812	- . 4	1. 3	2, 183	2, 178	402. 0	386. 8	184. 5	. 721	. 0431	. 0461	. 675
6-8	. 0703	83. 8	1, 548	9. 6	12. 0	2, 178	2, 046	208. 2	571. 2	159. 8	. 398	. 0887	. 0651	. 542
6-9	. 0696	71. 5	1, 552	10. 2	20. 0	2, 173	1, 923	230. 2	615. 2	158. 9	. 338	. 0956	. 0638	. 506

CHARACTERISTICS OF FIVE PROPELLERS IN FLIGHT

TABLE III—Continued  
POWER FLIGHT DATA—Continued  
PROPELLER 3714

Flight and run No.	Specific weight	Velocity	R. P. M.	Angle of Flight path $\gamma$	Angle of attack $\alpha$	$W$	$L$	$D$	$T$	HP	$\frac{V}{nD}$	$C_T$	$C_P$	$\eta$
	<i>Lb./cu. ft.</i>	<i>Ft./sec.</i>												
8- 1	0.0710	104.7	1,624	8.1	7.2	2,213	2,143	218.0	530.0	168.0	0.474	0.0740	0.0586	0.599
8- 3	.0698	185.4	1,812	-1.7	1.1	2,203	2,207	421.0	356.0	180.2	.752	.0406	.0460	.664
8- 4	.0692	88.6	1,604	9.4	11.0	2,198	2,079	209.4	568.0	161.1	.406	.0833	.0598	.565
8- 5	.0707	197.2	1,872	-3.7	.7	2,193	2,181	483.5	342.0	185.5	.774	.0360	.0432	.659
8- 6	.0709	168.5	1,772	.9	1.7	2,188	2,190	365.0	399.4	179.7	.699	.0469	.0483	.679
8- 7	.0705	134.7	1,700	5.2	3.6	2,183	2,161	263.3	461.1	172.8	.582	.0590	.0528	.651
8- 8	.0702	150.4	1,728	2.9	2.5	2,178	2,168	306.5	416.6	174.2	.640	.0511	.0502	.652
8- 9	.0688	118.3	1,632	6.9	4.4	2,173	2,177	231.8	492.8	163.4	.532	.0702	.0578	.647
8-10	.0690	168.7	1,768	.7	1.7	2,168	2,170	356.0	382.5	174.2	.702	.0465	.0485	.673
8-11	.0765	0	1,564							169.2	0		.0620	
9- 1	.0715	92.1	1,620	8.7	9.6	2,213	2,115	211.8	546.5	166.7	.418	.0761	.0580	.548
9- 2	.0700	190.6	1,852	-2.8	.9	2,208	2,211	450.4	342.7	184.4	.756	.0377	.0437	.651
9- 3	.0696	110.0	1,616	7.9	6.4	2,203	2,142	220.0	522.9	160.8	.501	.0753	.0582	.648
9- 4	.0699	176.0	1,800	-1.5	1.4	2,198	2,202	390.3	371.1	179.9	.719	.0428	.0467	.660
9- 5	.0696	145.3	1,696	3.9	2.9	2,193	2,180	287.5	436.6	168.4	.629	.0568	.0515	.693
9- 7	.0689	206.8	1,900	-5.1	.5	2,183	2,182	512.0	318.0	183.9	.800	.0335	.0414	.648
9- 8	.0690	127.8	1,652	5.8	4.3	2,178	2,149	246.0	466.0	164.7	.566	.0638	.0554	.652
9- 9	.0684	79.1	1,612	10.0	15.0	2,173	2,000	219.6	596.9	160.2	.360	.0923	.0623	.457
9-10	.0681	163.4	1,767	1.4	2.0	2,168	2,168	335.4	340.7	173.8	.680	.0419	.0490	.581
9-11	.0765	0	1,604							172.8	0		.0590	



PROPELLER 3715

10- 1	0. 0706	89. 6	1, 624	9. 5	10. 4	2, 213	2, 100	210. 9	576. 2	165. 0	0. 405	0. 0804	0. 0574	0. 567
10- 2	. 0704	169. 5	1, 784	. 6	1. 7	2, 208	2, 206	367. 2	390. 6	178. 5	. 700	. 0455	. 0474	. 673
10- 3	. 0690	75. 0	1, 648	10. 0	16. 5	2, 203	2, 005	230. 2	612. 8	163. 9	. 335	. 0857	. 0562	. 511
10- 4	. 0688	101. 0	1, 664	9. 3	8. 1	2, 198	2, 109	211. 8	567. 3	163. 3	. 446	. 0782	. 0549	. 635
10- 5	. 0682	121. 0	1, 668	7. 3	5. 1	2, 193	2, 147	233. 2	512. 0	162. 3	. 533	. 0699	. 0538	. 693
10- 6	. 0698	184. 0	1, 844	-1. 7	1. 1	2, 188	2, 191	416. 4	351. 1	187. 5	. 733	. 0385	. 0452	. 623
10- 7	. 0702	136. 0	1, 748	4. 9	3. 6	2, 183	2, 162	262. 9	449. 2	173. 9	. 572	. 0546	. 0491	. 636
10- 8	. 0703	200. 0	1, 896	-4. 4	. 7	2, 178	2, 177	497. 1	329. 8	187. 4	. 775	. 0338	. 0412	. 637
10- 9	. 0708	140. 0	1, 764	2. 9	3. 0	2, 173	2, 167	282. 5	392. 0	176. 4	. 583	. 0452	. 0468	. 564
10-10	. 0765	0	1, 640							177. 4	0		. 0561	
11- 1	. 0709	94. 2	1, 696	9. 2	9. 2	2, 213	2, 111	211. 3	564. 9	166. 4	. 408	. 0723	. 0509	. 580
11- 2	. 0709	189. 7	1, 896	-3. 8	. 9	2, 208	2, 205	454. 0	307. 7	188. 7	. 735	. 0312	. 0409	. 561
11- 3	. 0712	109. 8	1, 676	8. 2	6. 3	2, 203	2, 139	220. 7	534. 8	157. 5	. 481	. 0698	. 0498	. 675
11- 4	. 0712	175. 2	1, 828	- . 6	1. 4	2, 198	2, 202	394. 0	371. 0	182. 3	. 705	. 0408	. 0444	. 648
11- 5	. 0706	81. 5	1, 648	10. 2	12. 8	2, 193	2, 063	213. 8	502. 2	167. 8	. 364	. 0685	. 0571	. 443
11- 7	. 0682	130. 1	1, 708	6. 2	4. 2	2, 183	2, 152	249. 7	485. 5	166. 7	. 560	. 0638	. 0520	. 687
11- 8	. 0697	160. 4	1, 800	1. 8	2. 1	2, 178	2, 177	332. 5	400. 9	177. 8	. 655	. 0463	. 0464	. 653
11- 9	. 0695	192. 5	1, 904	-3. 1	. 9	2, 173	2, 176	453. 0	335. 5	185. 7	. 743	. 0348	. 0410	. 630
11-10	. 0765	0	1, 668							179. 2	0		. 0545	
12- 1	. 0708	88. 4	1, 676	10. 2	10. 7	2, 213	2, 087	210. 1	603. 3	172. 1	. 388	. 0795	. 0548	. 563
12- 2	. 0710	170. 1	1, 860	. 7	1. 7	2, 208	2, 210	369. 8	397. 2	188. 0	. 672	. 0423	. 0437	. 651
12- 3	. 0705	74. 2	1, 680	10. 6	16. 5	2, 203	2, 000	227. 0	631. 8	171. 8	. 325	. 0830	. 0544	. 496
12-4	. 0712	183. 2	1, 916	-1. 1	1. 1	2, 198	2, 204	422. 3	380. 0	191. 0	. 702	. 0378	. 0403	. 658
12-6	. 0716	193. 8	1, 920	-3. 5	. 8	2, 193	2, 197	475. 0	341. 2	192. 1	. 742	. 0336	. 0401	. 622
12-7	. 0709	119. 2	1, 712	7. 4	5. 1	2, 188	2, 140	235. 1	517. 5	174. 3	. 510	. 0648	. 0515	. 642
12-9	. 0687	154. 0	1, 784	2. 5	2. 4	2, 178	2, 167	310. 9	405. 8	173. 1	. 635	. 0484	. 0468	. 656
12-10	. 0682	138. 0	1, 752	4. 8	3. 5	2, 173	2, 153	265. 7	447. 0	169. 0	. 579	. 0560	. 0489	. 663
12-11	. 0765	0	1, 648							178. 4	0		. 0559	
13-1	. 0695	95. 2	1, 676	9. 0	9. 2	2, 213	2, 115	211. 7	557. 8	168. 6	. 417	. 0746	. 0532	. 572
13-2	. 0696	176. 1	1, 828	- . 6	1. 4	2, 208	2, 204	391. 8	368. 7	191. 4	. 708	. 0413	. 0474	. 616
13-4	. 0712	203. 3	1, 940	-5. 3	. 5	2, 198	2, 180	514. 0	311. 0	192. 5	. 770	. 0302	. 0391	. 596
13-6	. 0710	161. 2	1, 816	1. 5	2. 0	2, 188	2, 187	340. 5	397. 8	182. 0	. 652	. 0448	. 0453	. 641
13-7	. 0690	147. 0	1, 792	3. 6	2. 8	2, 183	2, 173	294. 2	431. 2	175. 3	. 603	. 0508	. 0467	. 656
13-9	. 0695	191. 5	1, 912	-3. 0	. 9	2, 173	2, 164	450. 0	336. 3	192. 1	. 736	. 0345	. 0418	. 607
13-10	. 0682	78. 4	1, 668	9. 5	14. 4	2, 168	2, 011	217. 1	574. 9	163. 8	. 345	. 0792	. 0549	. 491
13-11	. 0765	0	1, 700							182. 1	0		. 0519	

CHARACTERISTICS OF FIVE PROPELLERS IN FLIGHT

TABLE III—Continued  
POWER FLIGHT DATA—Continued  
PROPELLER 3872

Flight and run No.	Specific weight	Velocity	R. P. M.	Angle of Flight path $\gamma$	Angle of attack $\alpha$	$W$	$L$	$D$	$T$	H P	$\frac{V}{nD}$	$C_T$	$C_P$	$\eta$
	<i>Lb./cu. ft.</i>	<i>Ft./sec.</i>												
16-1	0.0685	75.4	1,640	9.2	16.6	2,213	2,007	228.5	582.0	161.1	0.337	0.0825	0.0563	0.494
16-2	.0683	183.5	1,880	-1.4	1.2	2,208	2,211	409.0	345.1	179.9	.717	.0374	.0421	.637
16-3	.0677	72.5	1,624	9.6	20.4	2,203	2,022	259.7	627.0	157.5	.328	.0909	.0570	.523
16-4	.0678	170.5	1,844	.5	1.8	2,198	2,198	359.7	379.0	176.5	.679	.0429	.0439	.663
16-5	.0673	105.7	1,668	8.2	7.2	2,193	2,122	214.9	527.7	160.8	.465	.0736	.0545	.629
16-6	.0694	197.6	1,968	-3.6	.6	2,188	2,192	477.5	340.1	188.4	.738	.0331	.0377	.646
16-7	.0687	118.8	1,688	6.8	5.3	2,183	2,140	230.2	488.6	164.2	.517	.0651	.0526	.640
16-8	.0669	137.1	1,740	4.5	2.7	2,178	2,166	261.7	432.7	164.0	.579	.0557	.0492	.655
16-9	.0664	155.7	1,780	2.1	2.5	2,173	2,169	306.2	386.0	166.1	.643	.0479	.0471	.654
16-10	.0653	138.7	1,740	4.0	2.7	2,168	2,156	261.0	412.2	159.7	.586	.0544	.0491	.650
16-11	.0765	0	1,624							172.5	0		.0564	
17-1	.0695	93.5	1,644	9.3	9.6	2,213	2,107	209.8	567.5	161.0	.418	.0790	.0553	.597
17-2	.0695	174.7	1,856	-1.3	1.5	2,208	2,211	384.0	372.5	177.9	.692	.0407	.0425	.663
17-3	.0681	80.6	1,652	10.0	13.8	2,203	2,044	216.7	599.4	160.0	.359	.0845	.0553	.549
17-4	.0690	188.2	1,916	-2.2	1.1	2,198	2,204	429.0	383.0	184.1	.722	.0394	.0401	.709
17-5	.0676	112.0	1,684	7.5	6.4	2,193	2,133	220.2	506.4	161.0	.489	.0693	.0531	.638
17-6	.0677	162.8	1,800	1.5	2.1	2,188	2,187	333.0	390.3	170.7	.664	.0465	.0475	.675
17-7	.0669	130.0	1,720	5.4	4.3	2,183	2,154	246.1	451.5	161.8	.555	.0595	.0503	.655
17-8	.0674	205.8	1,988	-5.3	.6	2,178	2,181	501.0	300.0	184.8	.761	.0295	.0369	.607
17-9	.0676	147.3	1,764	2.8	2.9	2,173	2,165	286.1	329.3	167.6	.614	.0488	.0479	.625
17-10	.0674	72.9	1,626	10.0	19.6	2,168	1,926	229.1	605.6	155.3	.329	.0884	.0565	.515
17-11	.0765	0	1,636							171.9	0		.0554	



TABLE IV  
VALUES FROM THE FAIRED CURVES OF FIGURES 10 TO 14

PROPELLER 3712				PROPELLER 3713			
$\frac{V}{nD}$	$C_T$	$C_P$	$\eta$	$\frac{V}{nD}$	$C_T$	$C_P$	$\eta$
0.35	0.1047	0.0711	0.516	0.35	0.0936	0.0648	0.507
.40	.0980	.0698	.559	.40	.0876	.0639	.548
.45	.0910	.0682	.599	.45	.0817	.0627	.586
.50	.0839	.0662	.632	.50	.0754	.0610	.619
.55	.0768	.0638	.662	.55	.0692	.0590	.646
.60	.0696	.0611	.684	.60	.0637	.0565	.667
.65	.0623	.0583	.698	.65	.0561	.0536	.680
.70	.0551	.0547	.705	.70	.0490	.0503	.684
.75	.0478	.0510	.700	.75	.0418	.0467	.671
.80	.0402	.0420	.683	.80	.0335	.0425	.632

PROPELLER 3714				PROPELLER 3715			
$\frac{V}{nD}$	$C_T$	$C_P$	$\eta$	$\frac{V}{nD}$	$C_T$	$C_P$	$\eta$
0.35	0.0889	0.0615	0.506	0.35	0.0836	0.0564	0.516
.40	.0829	.0607	.546	.40	.0777	.0556	.556
.45	.0771	.0597	.583	.45	.0716	.0543	.592
.50	.0710	.0582	.613	.50	.0657	.0528	.622
.55	.0652	.0561	.639	.55	.0596	.0509	.644
.60	.0590	.0538	.660	.60	.0534	.0487	.657
.65	.0528	.0511	.671	.65	.0472	.0466	.661
.70	.0459	.0478	.674	.70	.0403	.0431	.652
.75	.0391	.0442	.662	.75	.0332	.0398	.625
.80	.0316	.0402	.627	.80	.0258	.0363	.578

PROPELLER 3872			
$\frac{V}{nD}$	$C_T$	$C_P$	$\eta$
0.30	0.0940	0.0567	0.497
.35	.0872	.0563	.541
.40	.0806	.0555	.578
.45	.0739	.0543	.609
.50	.0670	.0527	.636
.55	.0601	.0507	.654
.60	.0532	.0483	.664
.65	.0462	.0453	.665
.70	.0391	.0418	.653
.75	.0315	.0379	.627





---

---

**REPORT No. 293**

---

**TWO PRACTICAL METHODS FOR THE CALCULATION  
OF THE HORIZONTAL TAIL AREA NECESSARY  
FOR A STATICALLY STABLE AIRPLANE**

**By WALTER S. DIEHL  
Bureau of Aeronautics**





## REPORT No. 293

### TWO PRACTICAL METHODS FOR THE CALCULATION OF THE HORIZONTAL TAIL AREA NECESSARY FOR A STATICALLY STABLE AIRPLANE

By WALTER S. DIEHL

#### SUMMARY

*This report is concerned with the problem of calculation of the horizontal tail area necessary to give a statically stable airplane. Two entirely different methods are developed, and reduced to simple formulas easily applied to any design combination. Detailed instructions are given for use of the formulas, and all calculations are illustrated by examples. The relative importance of the factors influencing stability is also shown.*

#### INTRODUCTION

In 1925 the author began a study of the problem of horizontal tail-surface design. A preliminary survey disclosed that several of the published methods appeared to give good results but were too complicated for general use. No method was found to combine the qualities of simplicity and accuracy, necessary to give it wide use. Many designers were using empirical methods based largely on average values of a coefficient such as Hunsaker's "th."<sup>1</sup> These methods were obviously incorrect and leading to serious deficiency of tail area in some cases. There was an evident need for a logical design method which could be reduced to a practical form easily and quickly applied to any design combination. With these requirements in view, two methods were finally developed and thoroughly tested by application to a number of designs for which wind-tunnel data were then available. The very encouraging results which were obtained have been fully verified by subsequent use over a period of about two years. It is believed that these methods will prove of considerable interest and value to all airplane designers.

#### THE FIRST EQUATION FOR HORIZONTAL TAIL AREA

A general equation for horizontal tail area may be derived by writing the equation for pitching moment either about the leading edge of the mean wing chord or about the center of gravity. From a theoretical standpoint the leading edge of the mean wing chord has certain advantages, but these appear to be offset by the fact that most of the available data are referred to the center of gravity. In either case the final results are substantially the same. The following derivation will therefore be based on moments about the center of gravity, with the degree instead of the radian as the unit for angular measure.

Assuming that the resultant force vector is normal to the wing chord and equal to the lift, the equation for wing pitching moment about the *c. g.* is

$$M_w = q S_w c \left[ C_L \left( \frac{a-x}{c} \right) \right] \text{-----} (1)$$

where  $q$  is the dynamic pressure  $\frac{1}{2} \rho V^2$ ,  $S_w$  the total wing area,  $c$  the mean aerodynamic wing chord,  $C_L$  the absolute lift coefficient,  $x$  the center of pressure location, and  $a$  the fore and aft *c. g.* location on the mean wing chord.

---

<sup>1</sup> th =  $\frac{\text{horizontal tail area}}{\text{total wing area}} \times \frac{\text{tail length}}{\text{mean chord}} = \frac{S_t l}{S_w c}$

Differentiating  $M_w$  with respect to  $\alpha$  gives

$$\begin{aligned}\frac{dM_w}{d\alpha} &= qS_w c \left[ \frac{dC_L}{d\alpha} \left( \frac{a}{c} - \frac{x}{c} \right) - C_L \frac{d\left(\frac{x}{c}\right)}{d\alpha} \right] \\ &= qS_w c \frac{dC_L}{d\alpha} \left[ \frac{a}{c} - \left( C_P + \alpha_a \frac{dC_P}{d\alpha} \right) \right] \dots\dots\dots (2)\end{aligned}$$

since

$$\frac{x}{c} = C_P \text{ and } C_L = \alpha_a \frac{dC_L}{d\alpha}$$

The pitching moment due to the lift on the horizontal tail surface is

$$M_t = -qC_{Lt} \cdot S_t \cdot l \dots\dots\dots (3)$$

Where  $C_{Lt}$  is the absolute lift coefficient for the tail surfaces,  $S_t$  the total horizontal tail area, and  $l$  the distance from the center of pressure of tail lift to the center of gravity. Without appreciable error,  $l$  may be taken as the distance from the center of gravity to the elevator hinge axis, and considered constant. The negative sign is required since a positive lift causes a diving, or negative moment.

The slope of the curve of tail pitching moment against angle of attack is

$$\frac{dM_t}{d\alpha} = \frac{dM_t}{d\alpha_t} \frac{d\alpha_t}{d\alpha} = -\frac{dC_{Lt}}{d\alpha_t} \frac{d\alpha_t}{d\alpha} qS_t l \dots\dots\dots (4)$$

$\alpha_t$  being the effective angle of attack of the tail surfaces.

The resultant moment on the entire airplane may be divided into three components due, respectively, to the wings, the tail surfaces, and the remaining parts such as fuselage, landing gear, etc. Denoting the residual moment by  $M_r$ , the total moment is

$$M = M_w + M_t + M_r \dots\dots\dots (5)$$

The variation of  $M_r$  with  $\alpha$  is usually small in comparison with that of  $M_w$  and  $M_t$ , so that

$$\frac{dM}{d\alpha} = \frac{dM_w}{d\alpha} + \frac{dM_t}{d\alpha} \dots\dots\dots (5a)$$

It has been customary to base the horizontal tail area on the geometrical proportions of the airplane. This results in a restoring moment proportional to the product of the wing area by the mean wing chord, while for constant effectiveness the restoring moment should vary as the product of the weight by the mean chord. Wind-tunnel tests on models of airplanes having satisfactory static stability show that the slope of the curve of pitching moment against angle of attack is substantially constant over a considerable angular range. Changing the stabilizer setting merely shifts the curve without changing the slope, as shown by Figure 1. Since the wind-tunnel tests are made at a constant dynamic pressure  $q$ , the equation for the slope of the moment curve is either

$$\frac{dM}{d\alpha} = KqWc \dots\dots\dots (6)$$

or

$$\frac{dM}{d\alpha} = K_1 q S c \dots\dots\dots (6a)$$

Table I contains values of  $K$  and  $K_1$  obtained from wind-tunnel test data on various airplanes. It will be noted that  $K_1$  is more nearly constant than  $K$ , owing to the former arbitrary design methods. An inspection of the values of  $K$ , however, shows definitely that it should be greater than  $-0.0005$  to insure stability at all speeds, while values greater than  $-0.0010$ , probably indicate excessive stability.



The complete equation for stability can now be written. Substituting equations (2), (4), and (6) into (5a) gives

$$KqWc = qS_w c \cdot \frac{dC_L}{d\alpha} \left[ \frac{a}{c} - \left( C_p + \alpha_a \frac{dC_p}{d\alpha} \right) \right] + \frac{dC_{Lt}}{d\alpha_t} \cdot \frac{d\alpha_t}{d\alpha} qSl \quad (7)$$

Dividing by  $\left( qS_w c \frac{dC_{Lt}}{d\alpha_t} \cdot \frac{d\alpha_t}{d\alpha} \right)$  and arranging terms, one obtains

$$\frac{S_t}{S_w} \cdot \frac{l}{c} = \frac{1}{\frac{dC_{Lt}}{d\alpha_t} \cdot \frac{d\alpha_t}{d\alpha}} \left[ -K \left( \frac{W}{S_w} \right) + \left[ \frac{a}{c} - \left( C_p + \alpha_a \frac{dC_p}{d\alpha} \right) \right] \frac{dC_L}{d\alpha} \right] \quad (8)$$

Letting

$$\frac{dC_{Lt}}{d\alpha_t} = F_1, \quad \frac{d\alpha_t}{d\alpha} = F_2, \quad \left( C_p + \alpha_a \frac{dC_p}{d\alpha} \right) = F_3$$

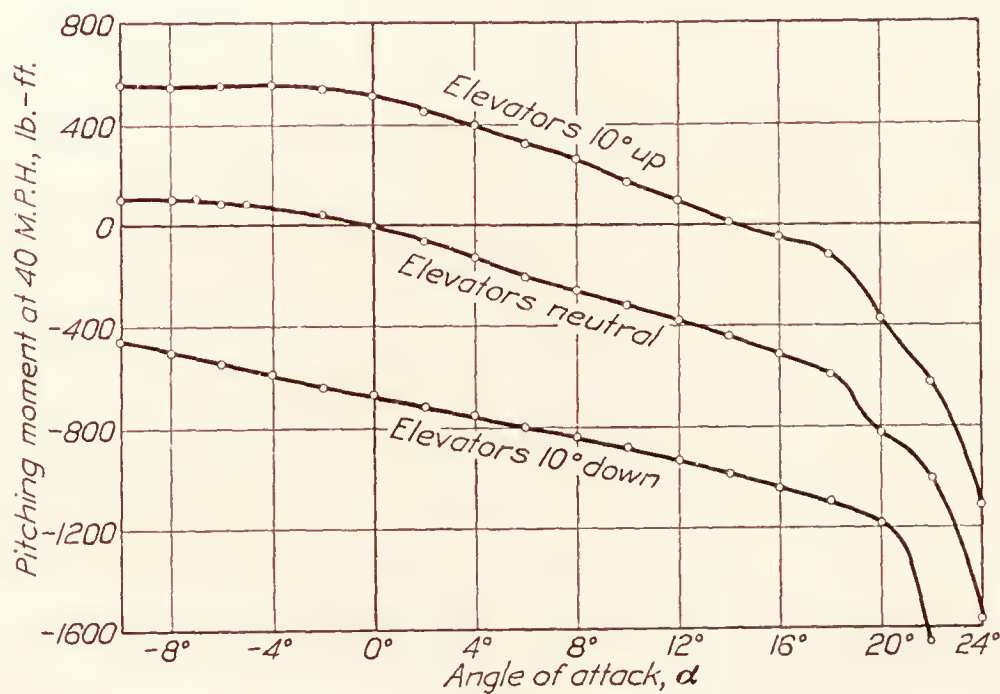


FIG. 1.—Pitching moments for a typical airplane. Wind tunnel test data, model scale 1:12

and

$$\frac{dC_L}{d\alpha} = F_4, \text{ equation (8) becomes}$$

$$\frac{S_t}{S_w} \cdot \frac{l}{c} = \frac{1}{F_1 F_2} \left[ -K \left( \frac{W}{S_w} \right) + \left( \frac{a}{c} - F_3 \right) F_4 \right] \quad (9)$$

An analysis of this equation shows that it is easily applied to the design of horizontal tail surfaces. The left-hand side is the well-known horizontal surface coefficient "th" used by Hunsaker.<sup>1</sup>  $F_1$  is the slope of the lift curve of the tail surfaces,  $F_2$  is a downwash factor,  $F_3$  is a wing section stability factor, and  $F_4$  is the slope of the lift curve of the wings. These factors can readily be determined for any particular design. Their derivation will be given briefly before the equation is analyzed further.

#### FACTORS $F_1$ AND $F_4$ —SLOPE OF LIFT CURVES

The slope of the lift curve against angle of attack depends on the airfoil section and the effective aspect ratio. For any given section it will depend only on the aspect ratio. The variation with section must be determined experimentally, but the variation with aspect ratio

<sup>1</sup> See footnote, p. 291.

may be calculated by the method used in N. A. C. A. Technical Note No. 79 (Reference 2). Briefly, this method is as follows:

The difference between the induced angles of attack for two aspect ratios is

$$\Delta\alpha = (\alpha_1 - \alpha_2) = \frac{57.3C_L}{\pi} \left[ \frac{S_1}{(k_1b_1)^2} - \frac{S_2}{(k_2b_2)^2} \right] \quad (10)$$

Where  $S_1$  and  $S_2$  are the total areas of the wings having respective maximum spans  $b_1$  and  $b_2$ , and  $k_1$  and  $k_2$  are Munk's factors for equivalent monoplane span. Since  $\Delta\alpha$  is the difference in angle of attack for the same lift coefficient at the two aspect ratios, the relation between the two slopes is

$$\frac{dC_L}{d\alpha_2} = \frac{\Delta C_L}{\left[ \frac{\Delta C_L}{\left( \frac{dC_L}{d\alpha_1} \right)} + \Delta\alpha \right]} \quad (11)$$

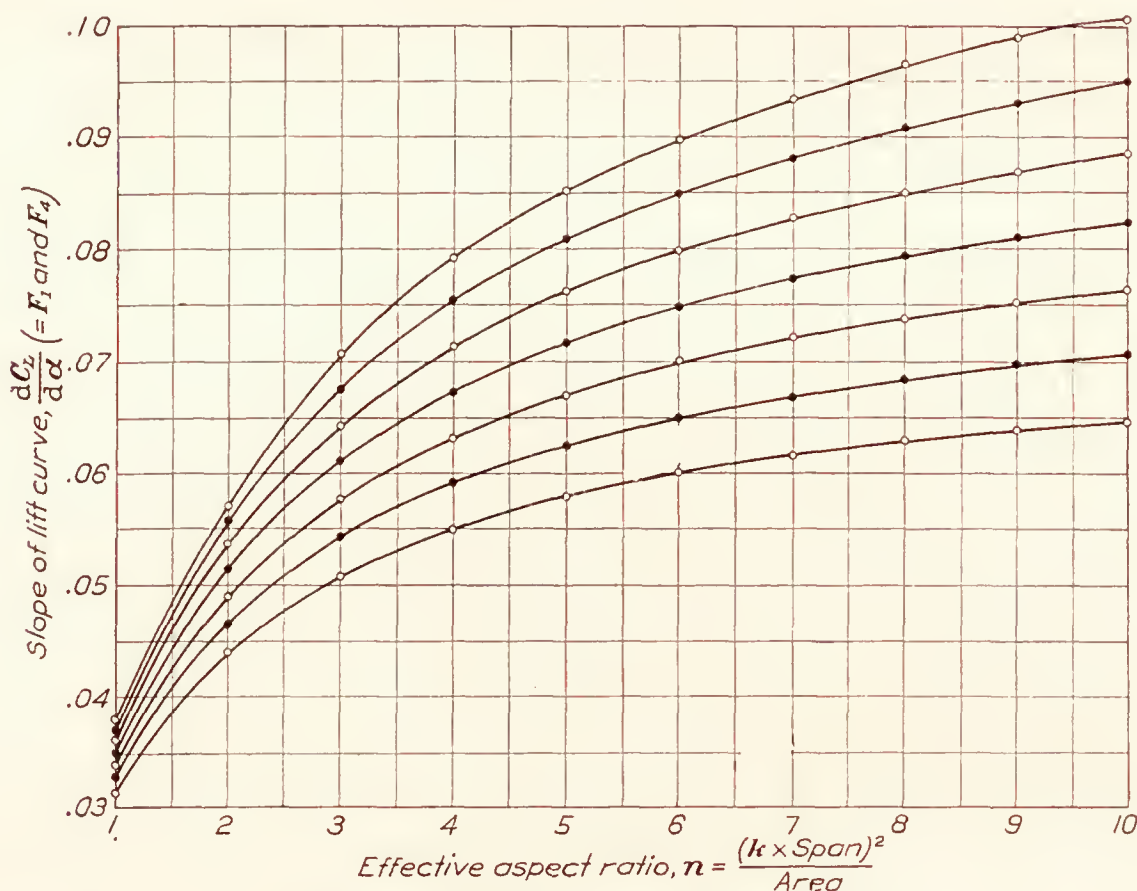


FIG. 2.—Slope of lift curve, variation with aspect ratio

$\Delta C_L$  being any convenient increment of lift. Equation (10) shows that  $\Delta\alpha$  is positive or negative according as the effective aspect ratio is decreased or increased.  $\frac{dC_L}{d\alpha}$  therefore increases with aspect ratio.

Figure 2 is a family of curves of  $\frac{dC_L}{d\alpha}$  against effective aspect ratio, as calculated by equations (10) and (11). In order to use Figure 2, the value of  $\frac{dC_L}{d\alpha}$  must be known at some given effective aspect ratio. Table II contains the values of  $\frac{dC_L}{d\alpha}$  at aspect ratio 6 for a number of standard wing sections.

The first step in finding  $F_1$  and  $F_4$  is to find the effective aspect ratio of the horizontal tail surfaces and the wings. The effective aspect ratio  $n$  of any wing arrangement is

$$n = \frac{(kb)^2}{S} \quad (12)$$



where  $S$  is the total area,  $b$  the maximum span, and  $k$  Munk's factor for equivalent monoplane span. For a monoplane  $k=1.00$ , but for a biplane  $k$  varies with the ratios of gap to maximum span  $\frac{G}{b_1}$  and shorter span to longer span  $\frac{b_2}{b_1}$ , and also with the area distribution. The value of  $k$  for any normal biplane may be obtained from either Figure 3 or Figure 4, representing

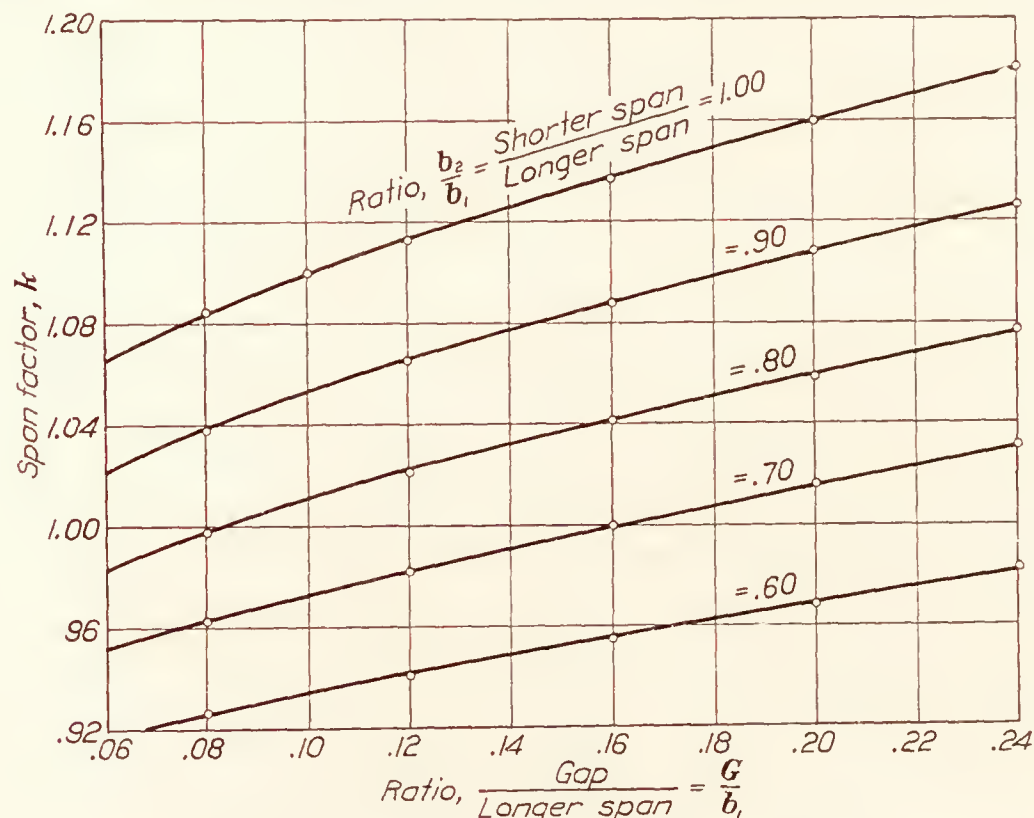


FIG. 3.—Span factors for biplanes with wings of equal chord

equal chords and equal aspect ratios, respectively. These data are based on the theoretical interference values given by Prandtl in N. A. C. A. Technical Report No. 116 (Reference 2). For a wing having raked tips the span should be taken slightly less than the extreme spread. This reduction is largely a matter of judgment and is usually unimportant.

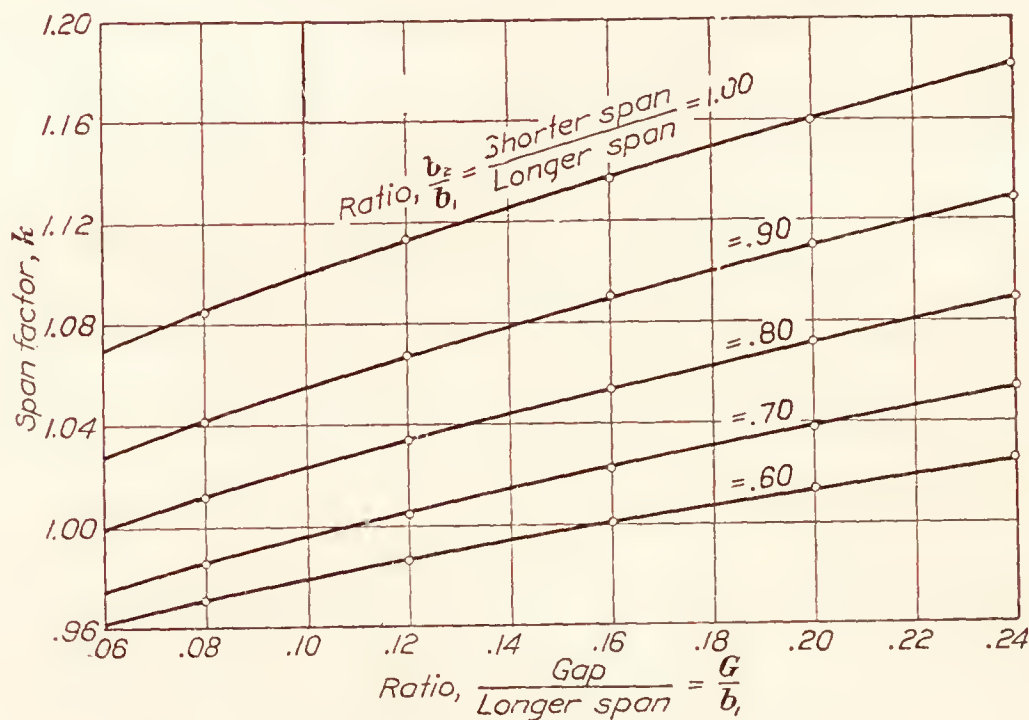


FIG. 4.—Span factors for biplanes with wings of equal aspect ratio

The effective aspect ratios of the wings and tail having been determined, the next step is to find the value of  $\frac{dC_L}{d\alpha}$  at some given aspect ratio for the wing and tail sections. This value, if not given in Table II, may be obtained from wind-tunnel test data or it may be estimated. The average slope for the normal wing section is about 0.072 at aspect ratio 6. The average

slope for the symmetrical cambered sections, commonly used in tail surfaces, runs slightly higher and may be taken as 0.075 at aspect ratio 6. At any other aspect ratio the value will lie on the curve in Figure 2 which passes through the given value of  $F_1$  or  $F_4$  at aspect ratio 6. For example, if  $F_1=0.075$  at aspect ratio 6, Figure 2 shows that  $F_1=0.061$  at aspect ratio 3; or if  $F_1=0.072$  at aspect ratio 6, then  $F_1=0.059$  at aspect ratio 3.

#### DOWNWASH FACTOR $F_2$

The angle of downwash at any given point depends on the lift coefficient, the effective aspect ratio of the wings and the location of the given point with respect to the wings. In N. A. C. A. Technical Note No. 42 (Reference 3) the writer has shown that the angle of downwash is given by

$$\begin{aligned}\epsilon &= \frac{K}{n} F_x F_y C_L \\ &= \frac{K}{n} F_x F_y \alpha_a \frac{dC_L}{d\alpha} \text{-----(13)}\end{aligned}$$

where  $F_x$  and  $F_y$  are empirical factors for the subsidence of the downwash angle in the horizontal and vertical planes respectively,  $n$  the effective aspect ratio, and  $K$  a constant. The value of  $K$

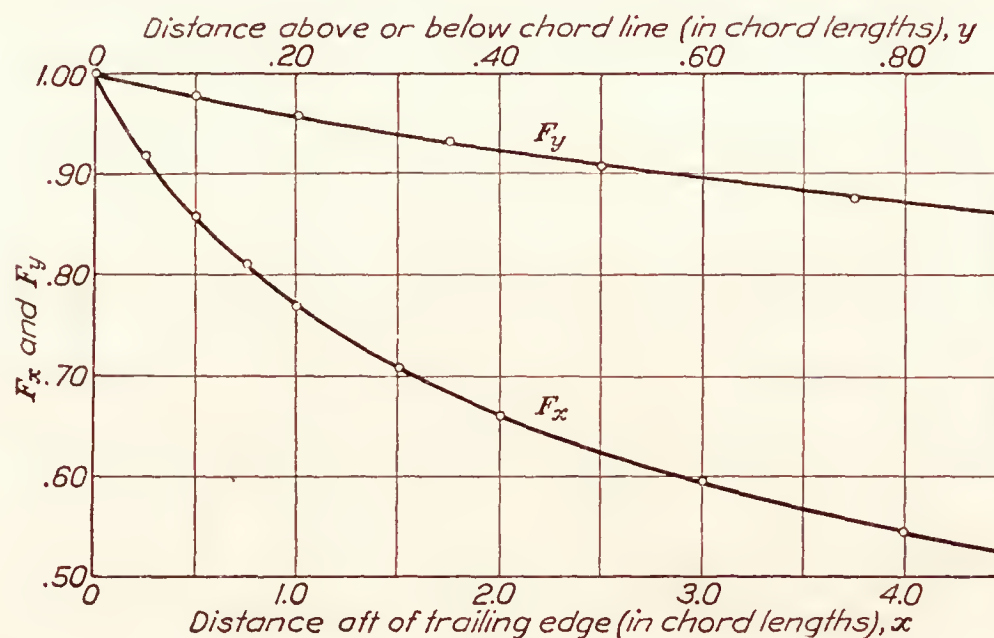


FIG. 5

has been calculated from a group of 10 tests on biplanes and monoplanes in which it varies from 45 to 54.6 with an average value of 52.

If the stabilizer is set at an angle  $\beta$  to the wing chord, the angle of attack of the tail surfaces is

$$\begin{aligned}\alpha_t &= (\alpha_w + \beta) - \epsilon \\ &= \alpha_w + \beta - \frac{52}{n} F_x F_y \alpha_a \frac{dC_L}{d\alpha} \text{-----(14)}\end{aligned}$$

Therefore

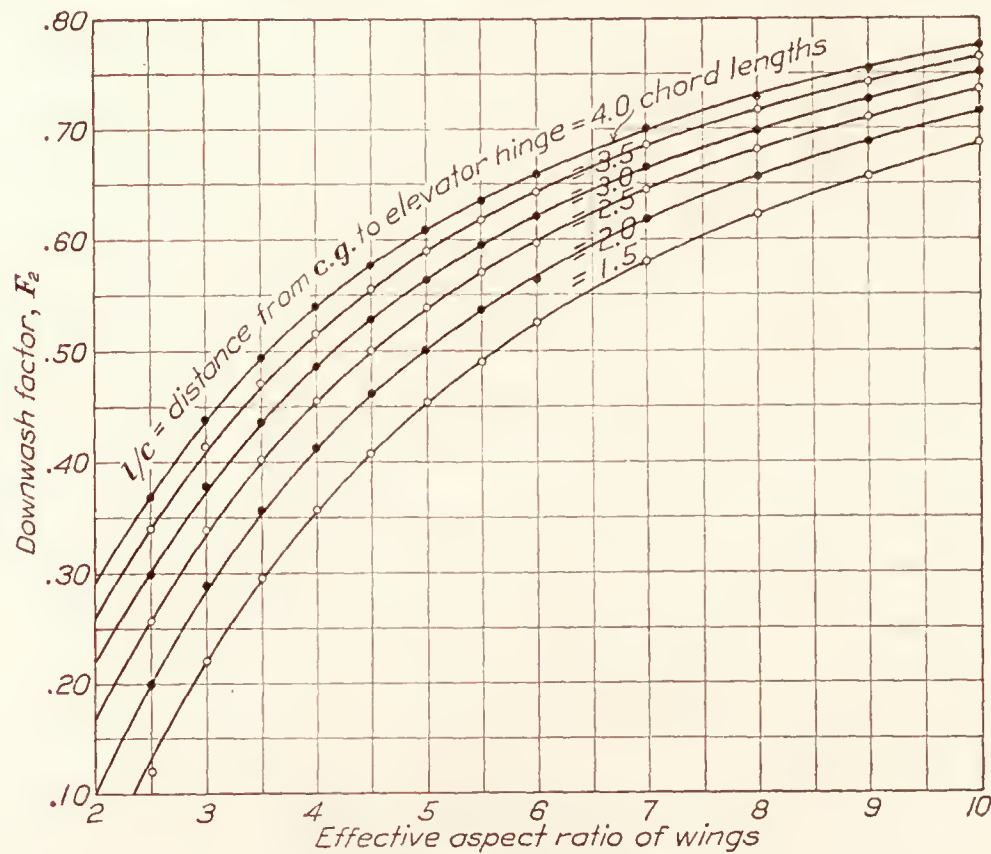
$$\frac{d\alpha_t}{d\alpha_w} = \left( 1 - \frac{52}{n} F_x F_y \frac{dC_L}{d\alpha} \right) = F_2 \text{-----(15)}$$

since

$$\alpha_a = (\alpha_w + \alpha_0) \text{ and } \frac{d^2 C_L}{d\alpha^2} = 0.$$

$F_2$  is readily determined from equation (15), by the use of Figures 2 and 5, which give the values of  $\frac{dC_L}{d\alpha}$ ,  $F_x$  and  $F_y$ . For the average case in which  $\frac{dC_L}{d\alpha_w}=0.072$  and the tail plane is substantially in the plane of the wing of monoplane or midway between the wings of a biplane ( $F_y$  greater than 0.95) the value of  $F_2$  may be read directly from Figure 6.



FIG. 6.—Downwash factor,  $F_2$ 

NOTE.—This chart is based on  $F=1.00$  (see eq. 15). If the tail location is either high or low a correction must be applied (see Fig. 5).

WING SECTION STABILITY FACTOR  $F_3$ 

The wing section stability factor  $F_3 = \left( C_p + \alpha_a \frac{dC_p}{d\alpha} \right)$  is obtained by plotting  $C_p$  against  $\alpha$  to a large scale so that the slope  $\frac{dC_p}{d\alpha}$  may be determined with reasonable accuracy. Table III illustrates the method employed and Table IV contains values of  $F_3$  obtained in a similar manner for a number of well-known wing sections. These values of  $F_3$  are plotted against  $\frac{V}{V_s} \left( = \sqrt{\frac{C_{Lmax}}{C_L}} \right)$  in Figure 7.

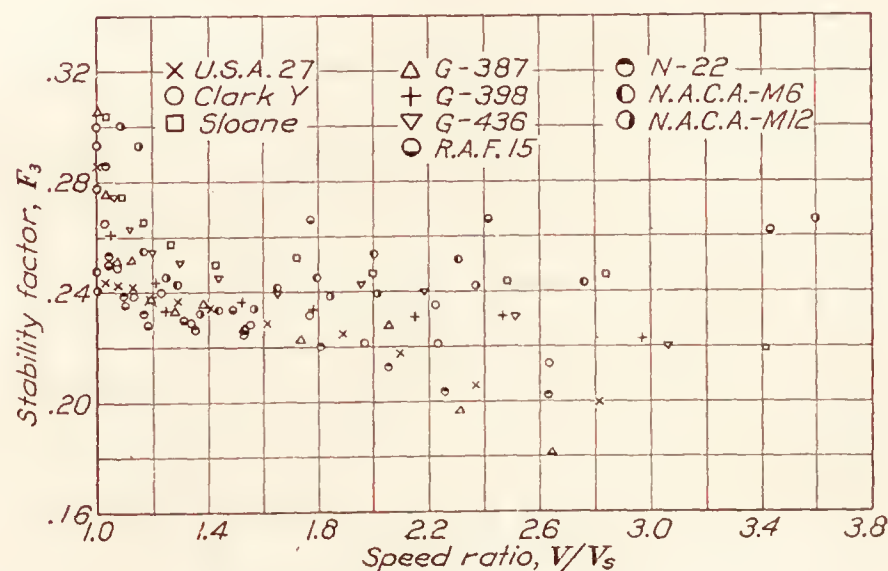


FIG. 7.—Wing section stability factor

$$F_3 = \left( C_p + \alpha_a \frac{dC_p}{d\alpha} \right).$$

It will be noted (Table III) that  $\frac{dC_p}{d\alpha}$  is negative under normal conditions where the center of pressure moves aft as  $\alpha$  is decreased. However, the value of  $C_p$  is positive and greater than  $\alpha_a \frac{dC_p}{d\alpha}$  so that the factor  $F_3$  is positive although normally less than the usual values of the

center of gravity location,  $\frac{a}{c} \cdot \left( \frac{a}{c} - F_3 \right)$  is positive under average conditions, and therefore the effect of moving the *c. g.* aft, i. e., increasing  $\frac{a}{c}$ , is to increase the horizontal tail area required. It is of considerable interest to note that a stable center of pressure movement does not necessarily mean a marked reduction in horizontal tail area required since the values of  $F_3$  for the N. A. C. A.-M6 section do not differ greatly from those for the R. A. F. 15, owing to the change in sign of  $\frac{dC_p}{d\alpha}$ .

#### SECOND EQUATION FOR TAIL AREA

A very simple equation for horizontal tail area may be derived from a consideration of the conditions at zero lift. Neglecting the effects of slip stream and fuselage interference the pitching moment due to the horizontal tail surfaces is

$$M_t = C_{L_t} q S_t l = \alpha_v \frac{dC_{L_t}}{d\alpha_t} q S_t l \text{-----} (16)$$

where  $\alpha_v$  is the effective longitudinal dihedral measured between the zero lift lines of the wings and tail surfaces  $\frac{dC_{L_t}}{d\alpha_t}$  the slope of the lift curve for the tail surfaces,  $q$  the dynamic pressure,  $S_t$  the tail area, and  $l$  the distance from the center of gravity to the center of pressure of the tail surfaces.

When the wing lift is zero the downwash is zero and  $\alpha_v$  is the aerodynamic angle of attack of the tail surfaces. Under these conditions the wing pitching moment about any lateral axis is

$$M_w = C_{M_0} q S_w c \text{-----} (17)$$

where  $C_{M_0}$  is the absolute moment coefficient about the leading edge of the wing chord, taken at zero lift,  $S_w$  the total wing area, and  $c$  the aerodynamic mean chord.

It has previously been shown (equation (6) and Table I) that the slope of the resultant pitching moment is

$$\frac{dM}{d\alpha} = K q W c \text{-----} (6)$$

If the airplane be balanced at an absolute angle of attack  $\alpha_a'$ , the resultant moment at zero lift should be

$$M_0 = \alpha_a' \frac{dM}{d\alpha} = K_0 q W c \text{-----} (18)$$

equating the moments

$$M_t + M_w = M$$

or

$$\alpha_v \cdot \frac{dC_{L_t}}{d\alpha_t} q S_t l + C_{M_0} q S_w c = K_0 q W c \text{-----} (19)$$

from which

$$\frac{S_t l}{S_w c} = \frac{1}{\alpha_v \frac{dC_{L_t}}{d\alpha_t}} \left[ K_0 \left( \frac{W}{S} \right) - C_{M_0} \right] \text{-----} (20)$$

$$= \frac{1}{\alpha_v F_1} \left[ K_0 \left( \frac{W}{S} \right) - C_{M_0} \right] \text{-----} (21)$$

Values of  $K_0$  are determined for various airplanes in Table V, and these values are plotted against  $\alpha_a'$  in Figure 8. An inspection of Figure 8 shows  $K_0$  to vary linearly with  $\alpha_a'$ , that is,

$$K_0 = k \alpha_a' \text{-----} (22)$$

where  $k$  varies from 0.00040 to 0.0010, according to the stability.



If the tail setting  $\alpha_v$  be plotted against the absolute angle of attack for balance  $\alpha_a'$ , as in Figure 9 where data from Table V are used, a linear relation is found. For the average airplane

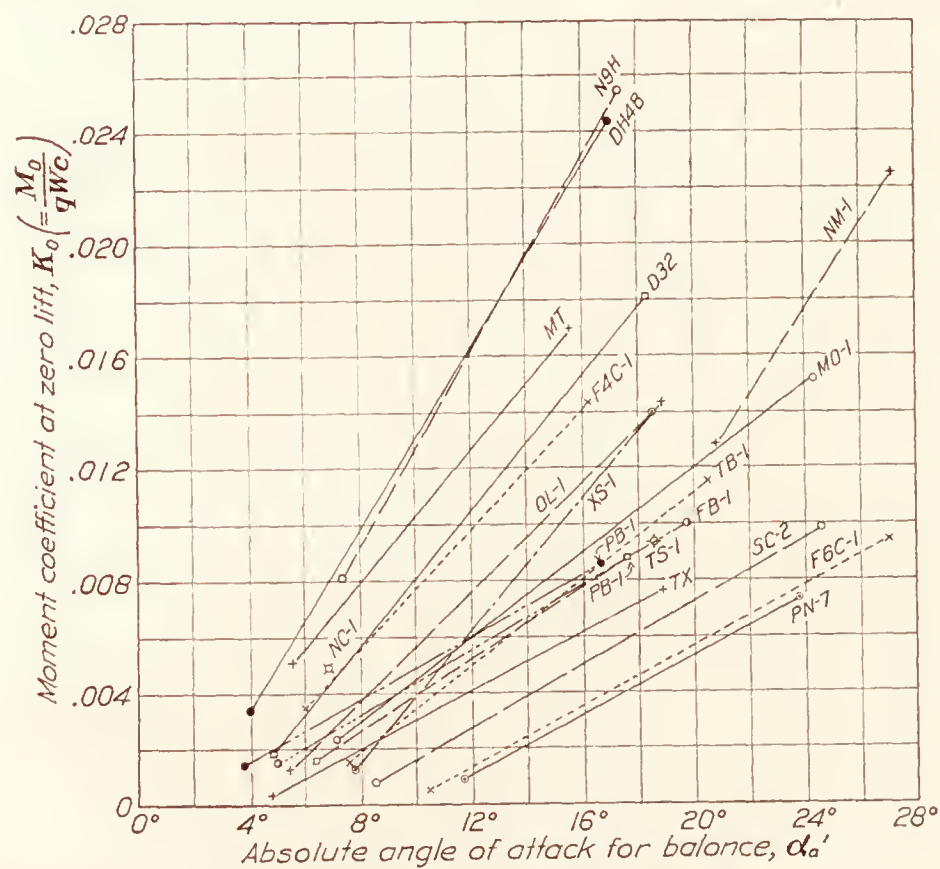


FIG. 8.—Pitching moment coefficient at zero lift

taking into consideration the stability characteristics desired, it appears that

$$\alpha_v = (3.0^\circ + 0.25 \alpha_a') \text{-----} (23)$$

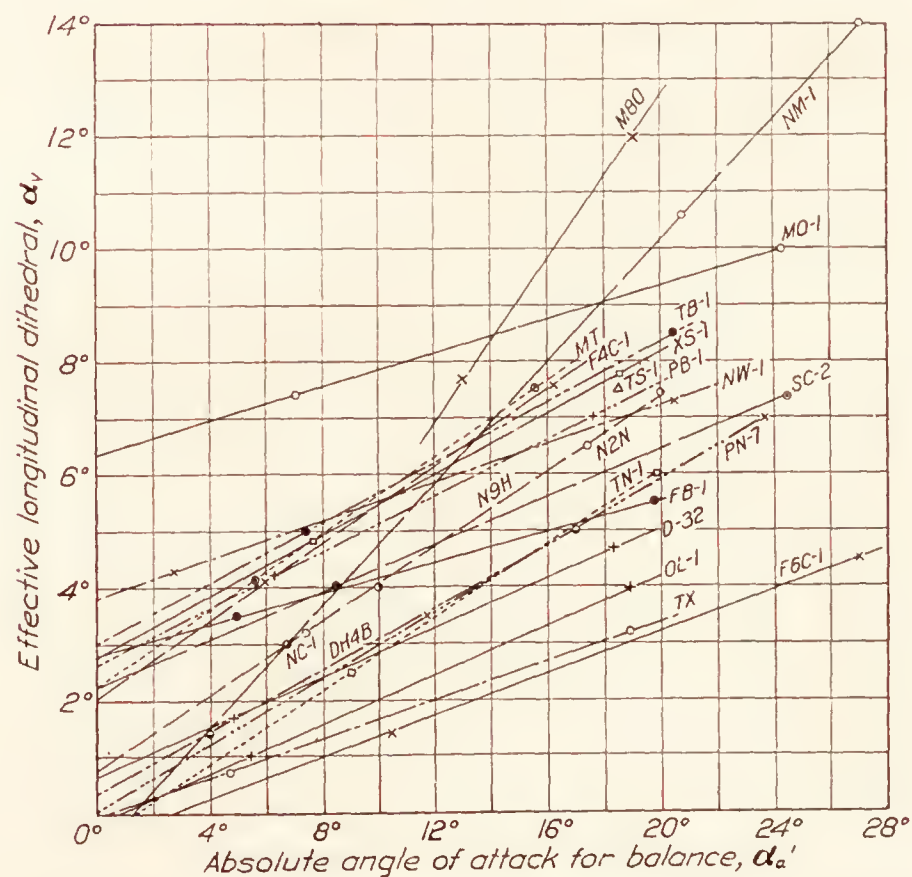


FIG. 9.—Relation between effective longitudinal dihedral and absolute angle of attack for balance

Substituting equations (22) and (23) into (21) gives

$$\frac{S_t}{S_w} \frac{l}{c} = \frac{1}{F_1 (3 + 0.25 \alpha_a')} \left[ k \alpha_a' \left( \frac{W}{S} \right) - C_{M0} \right] \text{-----} (24)$$

As noted before  $k$  varies from 0.0004 to 0.0010 according to the stability desired. The average values of  $k$  for various types of airplanes are

Pursuit, racers.....	$k=0.0004$ to $0.0006$
Observation, light bombers.....	$k=0.0005$ to $0.0008$
Training, heavy bombers, boats.....	$k=0.0006$ to $0.0010$

The value of  $\alpha_a'$  is determined from the angular range between zero lift and maximum lift for the wing section used, and from the speed at which balance is desired. For example, a heavy bomber, or a flying boat might be balanced at its normal cruising speed which is about 1.5 times the stalling speed. Since  $\frac{dC_L}{d\alpha}$  is substantially constant the corresponding absolute angle of attack is

$$\alpha_a' = \frac{\alpha_r}{\left(\frac{V}{V_s}\right)^2} = \frac{\alpha_r}{(1.5)^2} \quad (25)$$

where  $\alpha_r$  is the angular range between zero and maximum lifts. The effect of  $\alpha_a'$  on area required is very small and any convenient angle, say  $\alpha_a' = 6^\circ$  may be used.

In order to simplify the application of equation (24), values of  $C_{M0}$  for various standard airfoils are given in Table VI.

#### DISCUSSION OF EQUATIONS

The first equation

$$\frac{S_t}{S_w} \frac{l}{c} = \frac{1}{F_1 F_2} \left[ -K \left( \frac{W}{S_w} \right) + \left( \frac{a}{c} - F_3 \right) F_4 \right] \quad (9)$$

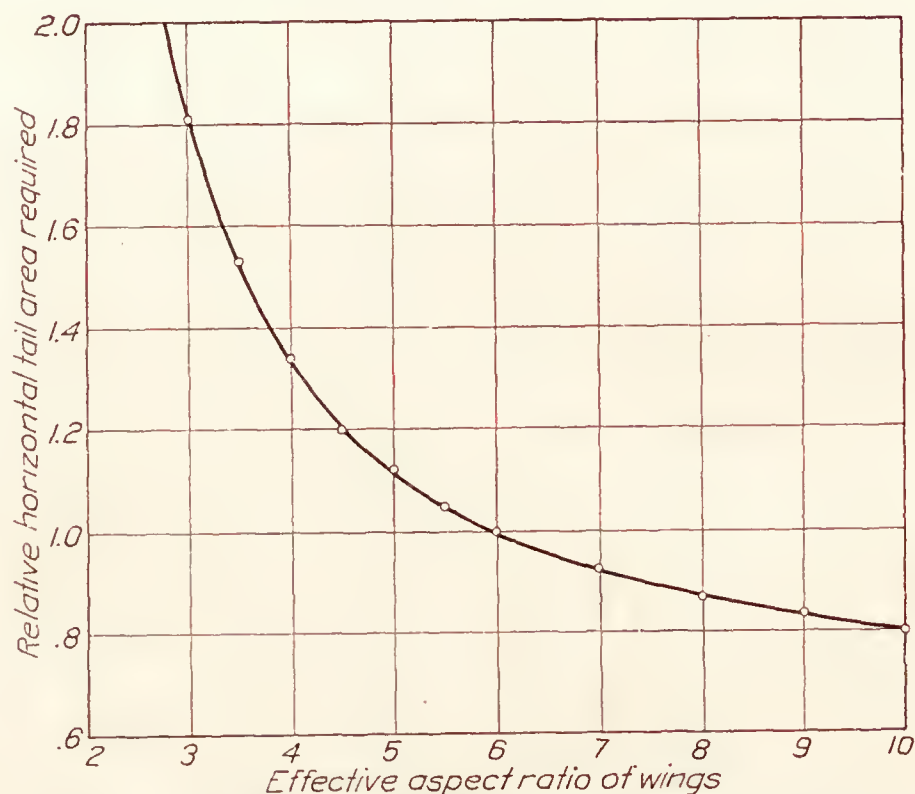


FIG. 10.—Effect of wing horizontal tail area required for constant static stability

is based on considerations affecting the slopes of the moment curves. It accounts for the effect of wing section, wing aspect ratio, tail aspect ratio, tail length, downwash, and fore and aft *c. g.* location. It is an approximation in so far as (1) the resultant force is not normal to the wing chord, (2) the residual moment (due to parts other than wing or tail) is not negligible, and (3) certain effects of vertical *c. g.* location are concerned. If the resultant force were always normal to the wing chord, then the vertical *c. g.* location would not affect the stability. The values of the constant  $K$  are based on normal *c. g.* locations between  $0.20c$  and  $0.40c$  below the mean chord. Lowering the *c. g.* improves stability; raising the *c. g.* decreases stability.



The second equation

$$\frac{S_t l}{S_w c} = \frac{1}{F_1(3 + 0.25 \alpha_a')} \left[ k \alpha_a' \left( \frac{W}{S_w} \right) - C_{M0} \right] \quad (24)$$

is based on considerations at zero lift, and it merely insures an adequate positive moment for

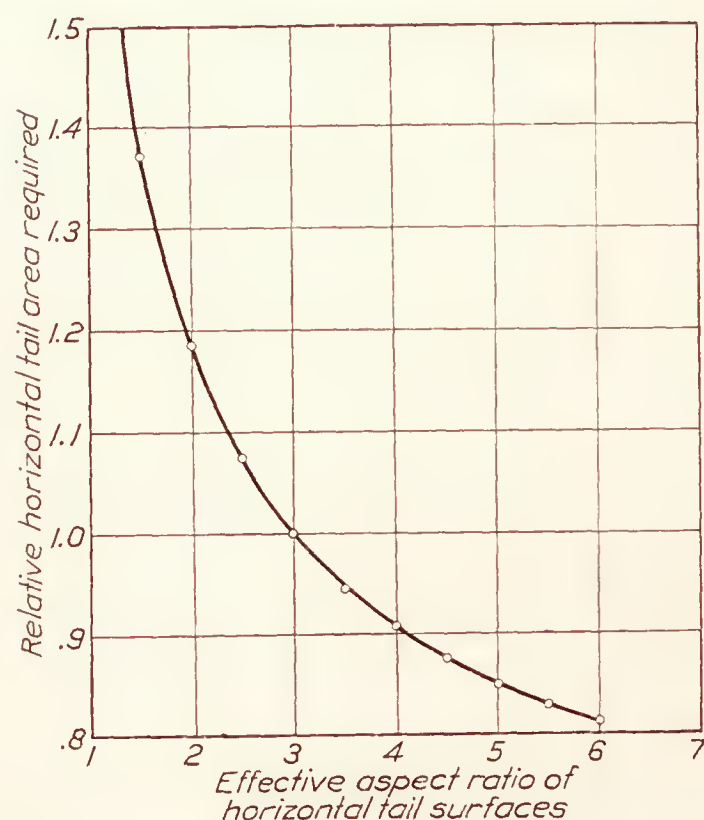


FIG. 11.—Effect of tail aspect ratio on horizontal tail area required for constant static stability

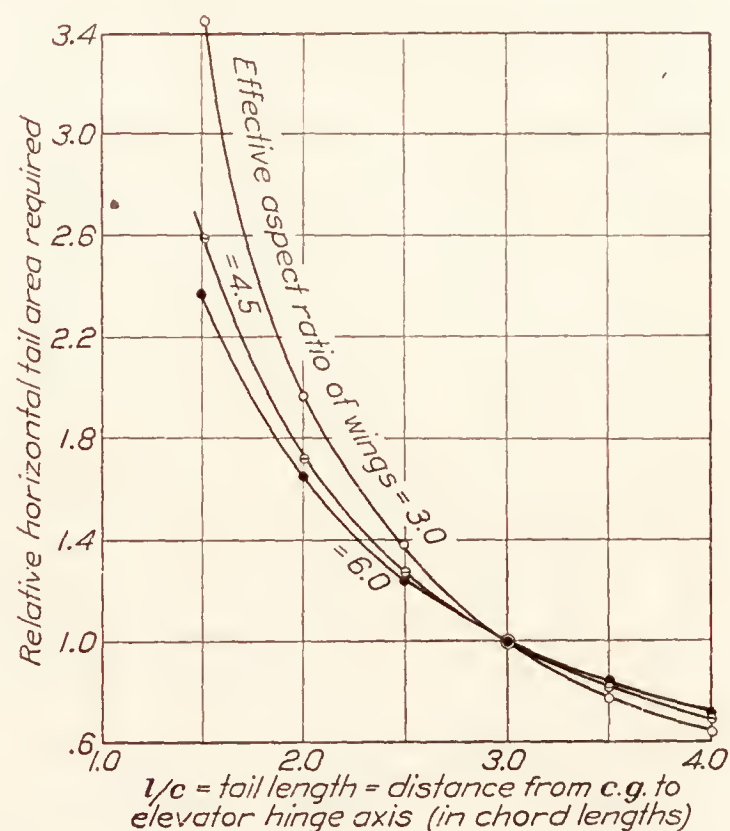


FIG. 12.—Effect of tail length on horizontal tail area required for constant static stability

this condition. Experience indicates, however, that when this adequate restoring moment at zero lift is obtained with a normal *c. g.* location the moments at other lifts will be satisfactory.

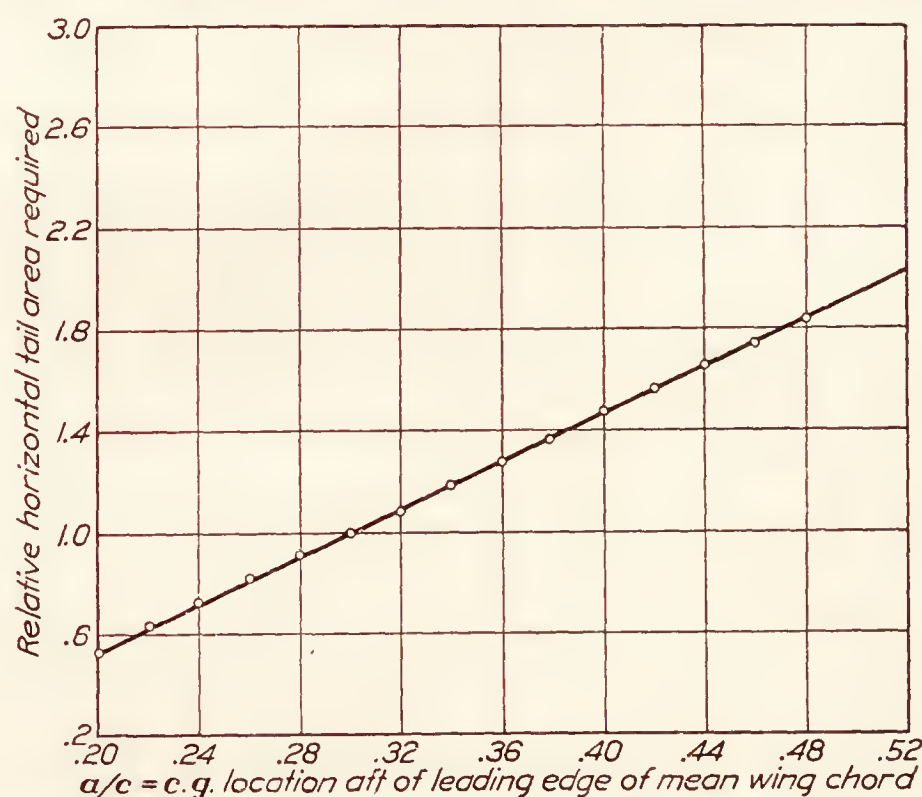


FIG. 13.—Effect of fore and aft *c. g.* location on horizontal tail area required for constant static stability

For a *c. g.* location at about 30 per cent of the mean chord the two equations give almost identical results, but the second method does not include the effect of fore and aft *c. g.* location. For this reason the first method should be used whenever the *c. g.* is forward of say, 0.28 *c.*, or aft of 0.33 *c.*

From data now at hand it appears that in general a horizontal tail area less than about 90 per cent of the value indicated by the first method, will result in static instability. Three cases have been found in wind tunnel tests where the area indicated by the first method gave satisfactory static stability, while a 5 per cent reduction in area resulted in an unsatisfactory condition. In no case yet studied has the area indicated by the first method been found to give unsatisfactory stability.

It is of considerable interest to find the effect of varying the different factors in equation (9). Figures 10 to 13 show the effect of varying wing aspect ratio, tail aspect ratio, tail length and fore and aft *c. g.* location. The magnitude of some of these effects may appear surprising at first glance, but there seems to be little question as to the general correctness of these indications when they are compared with test data. There is one point, however, which demands qualification. For constant static stability the effect of fore and aft center of gravity location is as shown on Figure 13, but this does not consider the questions of control and loading on the tail surfaces. The effect of these factors is to offset to a great extent, the reduction in tail which would be possible with constant static stability for *c. g.* locations well forward.

#### INSTRUCTIONS FOR USING EQUATIONS

For the benefit of the aeronautical engineer who does not have the time to follow through the complete derivation of the equations and also to avoid any possible misunderstanding, an outline will be given of the steps necessary to calculate the "th" coefficient by the two methods.

I. *First method.*—Equation (9). This method may be used with any fore and aft *c. g.* location. The following steps are necessary:

1. Find effective aspect ratio  $n = \frac{(kb)^2}{S}$  for wings and for tail surfaces.  $k$  may be obtained from Figure 3 or 4.
2. Find slope of lift curve at some aspect ratio for wing section and tail surface section and obtain slopes of lift curves at actual aspect ratios for wings and for tail,  $F_4$  and  $F_1$ , from Figure 2. For average wing section  $F_4 = 0.072$  at aspect ratio 6. For average tail section  $F_1 = 0.075$  at aspect ratio 6.
3. Read downwash factor  $F_2$  from Figure 6. For example, for effective wing aspect ratio of 5, tail length  $\frac{l}{c} = 3.0$ , the value of  $F_2$  is 0.564.
4. Find value of  $F_3 = \left( C_p + \alpha_a \frac{dC_p}{d\alpha} \right)$  for the wing section used; Tables III or IV, or Figure 7. Take value of  $F_3$  at a high value of  $\frac{V}{V_s}$ , i. e.,  $\frac{V}{V_s} > 2.0$ .
5. Select value of stability constant  $K$ , according to type of airplane. The following limits may be used:

Type	$-K$
Pursuit.....	0.0005 to 0.0007
Observation, light bombers.....	0.0006 to 0.0008
Training, heavy bombers, boats.....	0.0007 to 0.0010

II. *Second method.*—Equation (24). This method should not be used unless the *c. g.* is between 0.28 and 0.34*c.* The following steps are necessary:

1. Find or assume effective aspect ratio of horizontal tail surfaces.
2. Find slope of lift curve of tail surfaces  $F_1$ , using Figure 2.
3. Assume value of absolute angle of attack for balance, say  $\alpha_a' = 6^\circ$ .
4. Find value of absolute moment coefficient at zero lift for wing section used. Table VI.
5. Select value of stability constant  $k$ , according to type of airplane. The following limits may be used:

Type	$k$
Pursuit.....	0.0004 to 0.0006
Observation, light bombers.....	0.0005 to 0.0008
Training, heavy bombers, boats.....	0.0006 to 0.0010



The calculations will be illustrated by the tabulation of data for a typical pursuit type airplane:

	First method	Second method
Gross weight $W$ lb.	2, 800	2, 800
Wing area $S$ sq. ft.	250	250
Wing loading $\frac{W}{S}$	11. 20	11. 20
Wing section	Clark Y.	Clark Y.
Span { Upper $b_1$	31. 5	
Lower $b_2$	26. 0	
Span ratio $\frac{b_2}{b_1}$	. 83	
Average gap $G$	5. 44	
Gap $G$	. 173	
Max. span $b_1$	1. 075	
Span factor (equal aspect ratios fig. 4) $k$	4. 60	
Effective wing aspect ratio $\frac{(kb_1)^2}{S}$	13. 73'	13. 73'
Tail length $l$	4. 83'	4. 83'
Mean chord $c$	3. 35	3. 35
Tail aspect ratio	. 071	
$\frac{dC_L}{d\alpha}$ for wings { at aspect ratio 6	. 0665	
$F_4$	. 075	. 075
$\frac{dC_L}{d\alpha_t}$ for tail { at aspect ratio 6	. 0635	. 0635
$F_1$		
Downwash factor $\left\{ \begin{array}{l} n=4.60 \\ \frac{l}{c}=2.84 \end{array} \right\} F_2$	. 528	
Wing section stability factor $F_3$	. 22	
Moment coefficient at zero lift $C_{M0}$	— . 0006	— . 080
Stability coefficient $K$ and $k$		+ . 0005
$c. g.$ location $\frac{a}{c}$	. 32	

Applying these data,

$$\begin{aligned} \text{I. } \frac{S_t}{S_w} \frac{l}{c} &= \frac{1}{F_1 F_2} \left[ -K \left( \frac{W}{S_w} \right) + \left( \frac{a}{c} - F_3 \right) F_4 \right] \\ &= \frac{1}{0.0635 \times 0.528} [0.0006 \times 11.20 + (0.32 - 0.22) \times 0.0665] \\ &= 0.400 \end{aligned}$$

$$S_t = 0.400 \frac{S_w}{\left(\frac{l}{c}\right)} = 0.400 \left(\frac{250}{2.84}\right) = 35.2 \text{ sq. ft.}$$

$$\begin{aligned} \text{II.} \quad \frac{S_t}{S_w} \frac{l}{c} &= \frac{1}{F_1 (3 + 0.25 \alpha_a')} \left[ k \alpha_a' \left( \frac{W}{S_w} \right) - C_{M0} \right] \\ &= \frac{1}{0.0635 (3 + 0.25 \times 6)} [0.0005 \times 6 \times 11.20 - (-0.08)] \\ &= 0.397 \end{aligned}$$

from which,  $S_t = 35.0$  sq. ft.

The agreement obtained in this example is exceptional, but for normal *c. g.* locations it is usually within 5 per cent.

## REFERENCES

- Reference 1. Hunsaker, J. C.: Naval Architecture in Aeronautics. Royal Aeronautical Journal, July, 1920.
- Reference 2. Diehl, W. S.: Effect of Airfoil Aspect Ratio on the Slope of the Lift Curve. N. A. C. A. Technical Note No. 79 (1922).
- Reference 3. Prandtl, L.: Applications of Modern Hydrodynamics to Aeronautics. N. A. C. A. Technical Report No. 116 (1921).
- Reference 4. Diehl, W. S.: The Determination of Downwash. N. A. C. A. Technical Note No. 42 (1921).
- Reference 5. Warner, E. P.: Statical Longitudinal Stability of Airplanes. N. A. C. A. Technical Report No. 96 (1920).
- Reference 6. Hamburger, H.: Practical Method for Balancing Airplane Moments. N. A. C. A. Technical Note No. 179 (1924).
- Reference 7. Bienen, Theodor: Approximate Calculation of the Static Longitudinal Stability of Airplanes. N. A. C. A. Technical Memorandum No. 387 (1926).



TABLE I

SLOPE OF STABLE PITCHING MOMENT CURVES FROM WASHINGTON NAVY YARD WIND-TUNNEL TEST DATA

Airplane	Class	Weight $W$ (pounds)	Wing area $S$ (square feet)	Mean wing chord $c$ (feet)	Slope of pitching moment curve $\frac{dM}{d\alpha}$	$K$ $\frac{dM}{d\alpha} = \frac{qWc}{qSc}$	$K_1$ $\frac{dM}{d\alpha} = \frac{qSc}{qSc}$	Remarks
N9H---	Training---	2,765	467	4.92	-100	-0.00180	-0.0107	Very stable.
N2N---	do-----	2,405	285	4.63	-38	-0.00835	-0.00705	Do.
NY-1---	do-----	2,818	320	4.50	-61	-0.0118	-0.0104	Do.
NB-1---	do-----	2,570	344	5.00	-15	-0.00286	-0.00214	Unstable at high speed.
F4C-1---	Pursuit---	1,700	185	3.67	-21	-0.00825	-0.00759	Excellent.
F6C-1---	do-----	2,808	250	4.60	-18	-0.00340	-0.00382	Slightly unstable at high speed.
FB-1---	do-----	2,945	242	4.68	-32	0.00568	0.00696	Satisfactory.
D-38---	do-----	2,450	245	4.83	-23.5	-0.00488	-0.00488	Stable at all speeds.
TS-1---	do-----	2,025	227	4.75	-18	-0.00460	-0.00410	Unstable at high speeds.
XS-1---	Single scater---	1,000	99	3.00	-7	-0.00490	-0.00495	Stable at all speeds.
NW-1---	Racer-----	3,000	180	4.92	-20	-0.00333	-0.00553	Just stable at high speeds.
DH4B---	Observation---	3,876	440	5.50	-82	-0.00943	-0.00832	Very stable.
D-32---	do-----	3,876	400	6.00	-50	-0.00530	-0.00514	Excellent.
OL-1---	do-----	4,800	504	6.00	-50	-0.00426	-0.00405	Neutral at high speeds.
UO-1---	do-----	2,230	289	4.63	-30	-0.00712	-0.00552	Very satisfactory.
VE-7---	do-----	2,125	289	4.63	-40	-0.0100	-0.00736	Very stable.
MO-1---	do-----	4,885	488	9.57	-97	-0.00510	-0.00510	Stable at all speeds.
T3M-1---	Torpedo-----	9,863	856	8.25	-120	-0.00362	-0.00416	Just stable at high speed.
TN-1---	do-----	10,535	882	8.5	-100	-0.00274	-0.00328	Neutral at high speeds.
TB-1---	do-----	10,550	882	8.5	-220	-0.0060	-0.00718	Stable at all speeds.
PN-7---	Boat-----	14,236	1,220	9.0	-220	-0.00425	-0.00496	Just stable at high speeds.
PB-1---	do-----	25,000	1,810	11.0	-590	-0.00520	-0.00727	Excellent.
F5L---	do-----	14,000	1,387	8.0	-160	-0.00350	-0.00353	Neutral at high speeds.

TABLE II  
SLOPE OF LIFT CURVE FOR WELL-KNOWN AIRFOIL SECTIONS—ASPECT RATIO=6

Section	$\frac{dC_L}{d\alpha}$	Section	$\frac{dC_L}{d\alpha}$
RAF-6	0.075	Navy N-9	0.072
RAF-15	.077	Navy N-10	.080
RAF-19	.094	Navy N-14	.081
USA-5	.082	Navy N-22	.074
USA-16	.082	Göttingen 387	.072
USA-27	.071	Göttingen 398	.072
USA-35A	.073	Göttingen 413	.078
USA-35B	.075	Göttingen 429	.072
USA-45	.076	Göttingen 430	.077
USA-TS-5	.075	Göttingen 436	.072
Sloane	.080	Eiffel 32	.075
Albatross	.075	Eiffel 36	.076
Clark Y	.071	NACA-81	.070
Loening M-80	.073	NACA M-6	.072

TABLE III  
WING SECTION STABILITY FACTOR  $F_3$  FOR USA-27

$$F_3 = \left[ C_p + \alpha_a \frac{dC_p}{d\alpha} \right]$$

Angle of attack from chord line $\alpha$	Absolute angle of attack $\alpha_a$	$C_L$	$\sqrt{\frac{C_{Lmax}}{C_L}}$ $\frac{V}{V_s}$	Center of pressure $C_p$	$\frac{dC_p}{d\alpha}$	$\alpha_a \frac{dC_p}{d\alpha}$	$F_3$
°	°						
-4	1.4	0.102	3.669				
-3	2.4	.174	2.817	0.728	-0.22	-0.528	+0.200
-2	3.4	.245	2.371	.580	-.11	-.374	.206
-1	4.4	.316	2.088	.500	-.064	-.282	.218
0	5.4	.387	1.887	.452	-.042	-.227	.225
2	7.4	.531	1.610	.388	-.0215	-.159	.229
4	9.4	.688	1.415	.360	-.0133	-.125	.235
6	11.4	.825	1.293	.336	-.0087	-.099	.237
8	13.4	.966	1.194	.320	-.0061	-.082	.238
10	15.4	1.086	1.125	.310	-.0044	-.068	.242
12	17.4	1.211	1.067	.304	-.0035	-.061	.243
14	19.4	1.289	1.031	.298	-.0028	-.054	.244
16	21.4	1.356	1.008	.288	-.0020	-.043	.245
18	23.4	1.378	1.000	.286	0	0	.286

TABLE IV  
VALUES OF STABILITY FACTOR  $F_3$  FOR WELL-KNOWN WING SECTIONS

Clark Y		Sloane		RAF-15		G-387°		G-398	
$\frac{V}{V_s}$	$F_3$	$\frac{V}{V_s}$	$F_3$	$\frac{V}{V_s}$	$F_3$	$\frac{V}{V_s}$	$F_3$	$\frac{V}{V_s}$	$F_3$
1.00	0.294	1.000	0.310	1.000	0.280	1.000	0.306	1.000	0.300
1.028	.265	1.031	.304	1.041	.250	1.033	.276	1.052	.261
1.072	.249	1.093	.275	1.104	.235	1.066	.251	1.105	.244
1.137	.239	1.164	.266	1.184	.228	1.117	.252	1.175	.239
1.223	.240	1.262	.258	1.309	.230	1.186	.241	1.255	.233
1.336	.229	1.421	.250	1.487	.244	1.270	.241	1.372	.234
1.551	.228	1.719	.253	1.775	.266	1.377	.236	1.529	.237
1.774	.232	2.000	.247	2.413	.266	1.526	.227	1.780	.234
1.965	.221	2.498	.244	3.432	.262	1.736	.223	2.15	.231
2.226	.221	3.409	.219			2.057	.229	2.47	.232
2.635	.214					2.310	.197	2.963	.223
						2.64	.182		



TABLE IV—Continued

VALUES OF STABILITY FACTOR  $F_3$  FOR WELL-KNOWN WING SECTIONS

G-436		N-22		M-6		M-12	
$\frac{V}{V_s}$	$F_3$	$\frac{V}{V_s}$	$F_3$	$\frac{V}{V_s}$	$F_3$	$\frac{V}{V_s}$	$F_3$
1.000	0.296	1.000	0.286	1.000	0.248	1.000	0.241
1.061	.276	1.047	.252	1.068	.256	1.083	.301
1.120	.264	1.098	.239	1.167	.255	1.150	.293
1.198	.255	1.164	.232	1.282	.243	1.250	.245
1.297	.251	1.255	.232	1.426	.234	1.375	.235
1.441	.246	1.367	.226	1.646	.241	1.565	.234
1.648	.241	1.532	.225	1.790	.246	1.835	.238
1.953	.244	1.803	.220	2.000	.254	2.010	.239
2.178	.241	2.050	.213	2.300	.252	2.370	.242
2.509	.233	2.243	.203	2.760	.243	2.84	.246
3.058	.220	2.630	.202	-----	-----	3.60	.266

TABLE V

MOMENT COEFFICIENT AT ZERO LIFT AND EFFECTIVE LONGITUDINAL DIHEDRAL

Airplane	Weight $W$ (pounds)	Mean chord $c$ (feet)	Balance at $\alpha_a'$	Pitching moment at $C_L=0$ $M_o$ (lb./ft. at 40 M. P. H.)	Coefficient $K_o = \frac{M_o}{qWc}$	Effective longitudi- dinal dihedral $\alpha_v$
FB-1-----	2,945	4.68	{ 5.0	85	0.00151	-3.5
			{ 19.8	560	.0100	-5.5
F4C-1-----	1,700	3.68	{ 6.0	90	.00353	-4.1
			{ 16.2	365	.0143	-7.6
F6C-1-----	3,186	4.6	{ 10.4	30	.00050	-1.4
			{ 27.0	560	.0094	-4.5
MSO-----	2,780	8.0	{ 12.5	280	.00308	-7.7
			{ 19.0	1,060	.0117	-12.0
NW-----	3,000	4.92	{ 2.8	60	.00099	-4.3
			{ 20.5	730	.0121	-7.3
TX-----	2,900	4.33	{ 4.7	18	.000352	-0.7
			{ 18.9	390	.00762	-3.2
N9H-----	2,765	5.0	{ 7.4	460	.00816	-3.2
			{ 17.4	1,440	.0255	-6.5
N2N-----	2,405	4.62	{ 10	310	.00682	-4.0
			{ 20	1,040	.0228	-7.5
DH4B-----	3,876	5.5	{ 4.0	300	.00344	-1.4
			{ 17.0	2,130	.0244	-5.0
D-32-----	3,876	6.0	{ 4.8	180	.00189	-1.7
			{ 18.3	1,720	.0182	-4.7
OL-1-----	5,000	6.0	{ 5.4	150	.00124	-1.0
			{ 18.9	1,740	.0143	-4.0
MO-1-----	4,885	9.57	{ 7.1	440	.00231	-7.4
			{ 24.3	2,880	.0151	-10.0
XS-1-----	1,000	3.0	{ 7.7	16	.00130	-4.8
			{ 18.5	172	.0140	-7.8

TABLE V—Continued

MOMENT COEFFICIENT AT ZERO LIFT AND EFFECTIVE LONGITUDINAL DIHEDRAL

Airplane	Weight $W$ (pounds)	Mean chord $c$ (feet)	Balance at $\alpha_a'$	Pitching moment at $C_L=0$ $M_0$ (lb./ft. at 40 M. P. H.)	Coefficient $K_0 = \frac{M_0}{qWc}$	Effective longitudi- nal dihedral $\alpha_e$
NM-1-----	4, 190	6. 5	{ 20. 8	1, 400	0. 0128	-10. 6
			{ 27. 1	2, 500	. 0225	-14. 0
MT-----	12, 098	7. 98	{ 5. 6	2, 000	. 00506	-4. 1
			{ 15. 6	6, 700	. 0170	-7. 5
PN-7-----	14, 250	9. 00	{ 11. 7	500	. 00096	-3. 5
			{ 23. 7	3, 800	. 00728	-7. 0
PB-1-----	25, 000	11. 00	{ 6. 3	1, 850	. 00165	-4. 2
			{ 17. 6	9, 900	. 00883	-7. 0
SC-2-----	9, 434	8. 24	{ 8. 5	250	. 000793	-4. 0
			{ 24. 5	3, 100	. 0098	-7. 3
TB-1-----	10, 550	8. 5	{ 7. 5	550	. 00150	-5. 0
			{ 20. 5	4, 200	. 0115	-8. 5
TN-1-----	10, 535	8. 5	{ 8. 5	200	. 000547	-2. 5
			{ 19. 9	3, 300	. 00904	-6. 0

TABLE VI

MOMENT COEFFICIENT AT ZERO LIFT FOR STANDARD WING SECTIONS

(Reference axis is at leading edge of wing chord)

Section	Moment coefficient at zero lift  $C_{M0}$	Reference
G-398-----	-0. 079	McCook Field tests.
G-436-----	-. 078	Do.
G-387-----	-. 095	N. A. C. A. Technical Note No. 219.
RAF-15-----	-. 050	Do.
USA-27-----	-. 086	Do.
USA-35A-----	-. 120	Do.
USA-35B-----	-. 075	Do.
Clark Y-----	-. 080	Do.
NACA-M6-----	+. 010	Do.
NACA-M12-----	-. 005	Do.

BUREAU OF AERONAUTICS,  
NAVY DEPARTMENT,  
*April 6, 1928.*



---

## **REPORT No. 294**

---

# **THE MEASUREMENT OF MAXIMUM CYLINDER PRESSURES**

**By CHESTER W. HICKS**  
**Langley Memorial Aeronautical Laboratory**





# REPORT No. 294

## THE MEASUREMENT OF MAXIMUM CYLINDER PRESSURES

By CHESTER W. HICKS

### SUMMARY

*The work presented in this report was undertaken at the Langley Memorial Aeronautical Laboratory of the National Advisory Committee for Aeronautics to determine a suitable method for measuring the maximum pressures occurring in aircraft engine cylinders. The study and development of instruments for the measurement of maximum cylinder pressures has been conducted in connection with carburetor and oil engine investigations on a single cylinder aircraft-type engine. Five maximum cylinder-pressure devices have been designed, constructed, and tested, in addition to the testing of three commercial indicators.*

*Values of maximum cylinder pressures are given as obtained with various indicators for the same pressures and for various kinds and values of maximum cylinder pressures, produced chiefly by variation of the injection advance angle in a high-speed oil engine. It is the high pressure of short duration that is most difficult to measure, because the time of its duration is so short that little work can be done to operate an indicator.*

*The investigations conducted thus far indicate that the greatest accuracy in determining maximum cylinder pressures can be obtained with an electric, balanced-pressure, diaphragm or disk-type indicator so constructed as to have a diaphragm or disk of relatively large area and minimum seat width and mass.*

### INTRODUCTION

The problem of designing and developing instruments for measuring and recording the maximum pressures within the cylinders of high-speed internal-combustion engines requires a considerable amount of research work. There is little accurate information available, at present, on the rate of rise, intensity, and duration of cylinder pressures. Knowledge of the intensity and character of cylinder pressures is important for two reasons. First, it is necessary in engine research to establish a limiting pressure beyond which it is not desired to operate an engine. Second, it is desirable to know the character of those pressures that affect engine life.

The types of combustion to be considered in the measurement of engine cylinder pressures are constant volume combustion, constant pressure combustion, and combinations of these two. It is possible to have a large part of the fuel charge burn at practically constant volume in either the carburetor engine or the high-speed oil engine. With suitable conditions, as in slow-speed oil-engine operation, there can be a combination of both constant volume and constant pressure combustion with a large percentage of the fuel burning at constant pressure. There may be enough constant volume combustion, however, in high-speed oil engines to require serious consideration, since it is the constant volume combustion that may give rise to excessive cylinder pressures and subsequent destruction of engine parts. As the conditions affecting combustion in the high-speed oil engine are altered, there is a change in the rate of rise and duration of the maximum cylinder pressure which brings out the limitations of the available instruments for measuring maximum pressures.

The maximum cylinder pressure indicators now available may be classified under two types. One type makes use of the cylinder pressure in recording directly—that is, all the work of recording is done by the gas in the cylinder. The other type uses the cylinder pressure to operate only an auxiliary part of the recording apparatus.



The material for this report has been obtained in connection with various carburetor and oil-engine investigations (References 1 and 2) made with a N. A. C. A. Universal test engine (Reference 3) at the Langley Memorial Aeronautical Laboratory of the National Advisory Committee for Aeronautics. The study and development of instruments for the measurement of cylinder pressures has been conducted in connection with engine tests in an effort to obtain accurate cylinder-pressure data, and was not carried on as a separate research. Five instruments for indicating maximum cylinder pressures have been designed, constructed, and tested at this laboratory in addition to the testing of three commercial indicators.

### METHODS AND APPARATUS

The maximum cylinder-pressure indicator shown in Figure 1 is of the type that receives all the energy for its operation from the cylinder gases. The working parts of this indicator consist of a spring-loaded piston exposed to the cylinder pressure and a pointer operated by the piston and indicating its movement. The procedure in taking a reading is to allow the piston to move

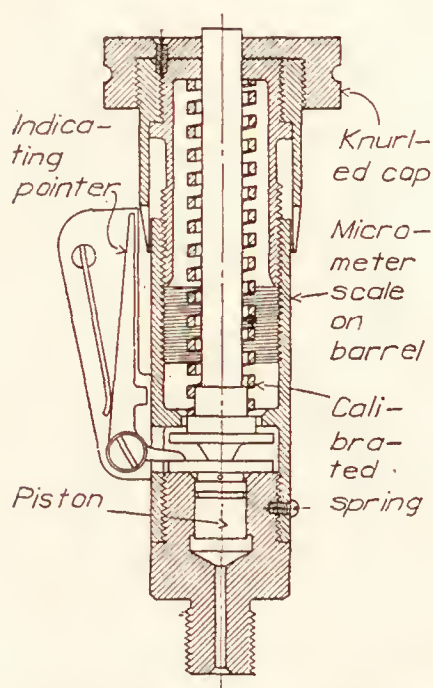


FIG. 1.—Piston type maximum pressure indicator

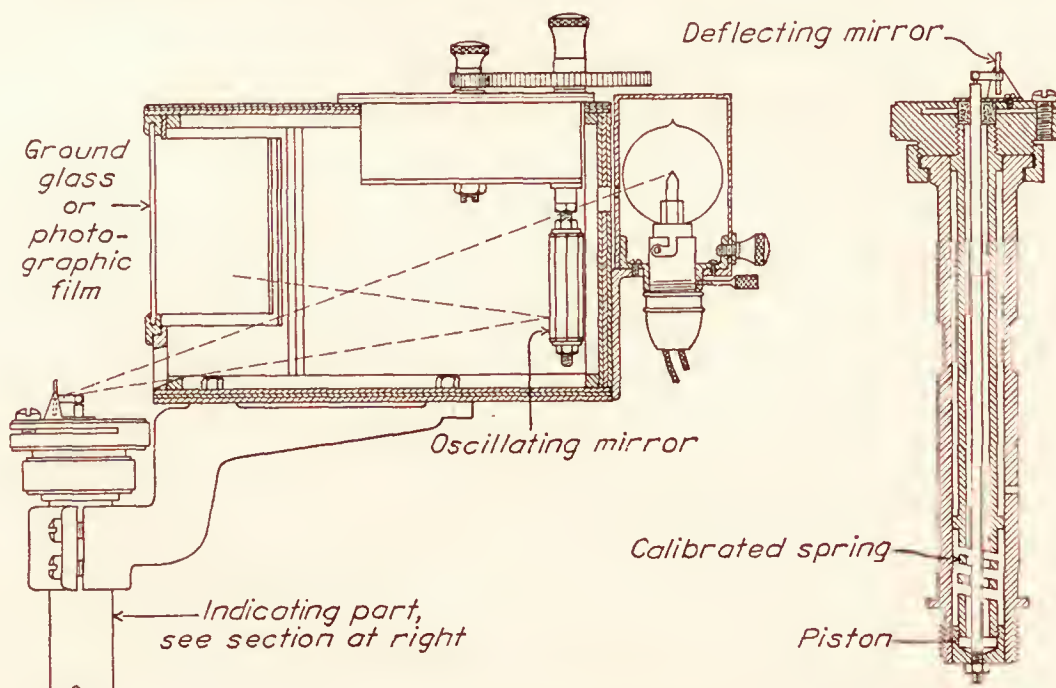


FIG. 2.—Optical type indicator

with each explosion and then screw down the knurled cap until the spring tension is just sufficient to stop any piston movement. At this point the spring tension, friction, and the inertia of the moving parts just balance the force of the maximum cylinder pressure.

The indicator shown in Figure 2 is of the same type as that shown in Figure 1. This instrument is designed to operate with a small piston movement which is magnified by means of a reflected light beam. Cylinder pressures are recorded throughout the engine cycle by reflecting a beam of light onto a ground glass or photographic film by means of a mirror directly connected to the operating piston by a tie rod and pivoted arm. A driving mechanism which operates an oscillating mirror in synchronism with the engine may, at the discretion of the operator, cause the light beam to trace either a pressure-volume or a pressure-time card.

The instrument shown in Figure 3 was designed to aid in detecting detonation by means of a diaphragm exposed directly to the rapidly varying cylinder pressure and communicating the resultant pressure wave through water to a telephone diaphragm. The carbon pile indicator, shown in Figure 4, was also designed to aid in detecting detonation. In this instrument the diaphragm was exposed to the water in the cylinder-head jacket and a direct mechanical connection was made with a carbon pile. The assumption was that the detonation pressures would transmit a shock wave to the water around the cylinder head with sufficient force to move the diaphragm and compress the carbon pile. The carbon pile was later connected in series with an external electric circuit that included head phones.



The "bouncing pin" method of measuring detonation was tried under conditions of variable compression ratio and combustion characteristics. This instrument, as shown in Figure 5, has a pin resting freely on a piston element. Contact points are held in position in an electrical circuit by springs, in such a way as to be closed when the bouncing pin is thrown free of the

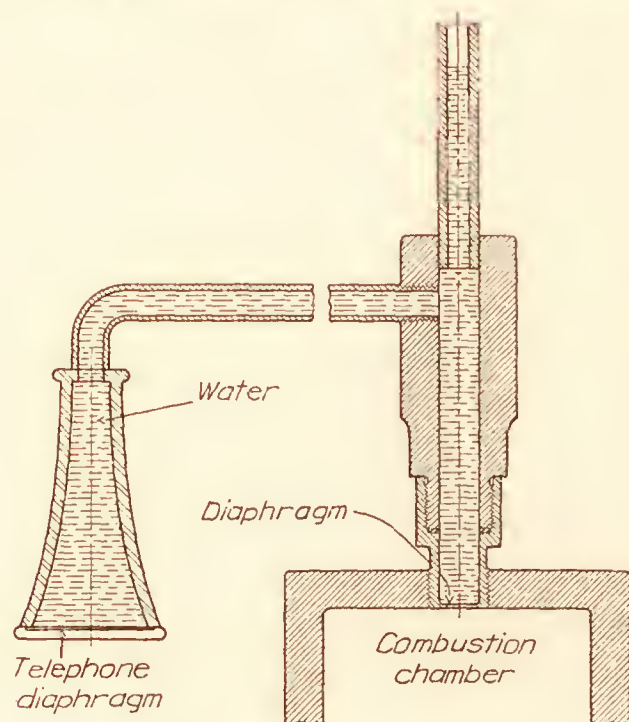


FIG. 3.—Detonation detector

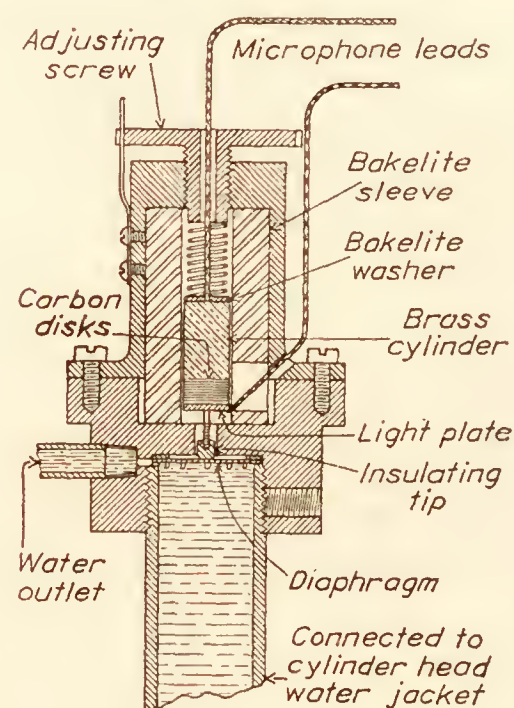


FIG. 4.—Carbon-pile pressure indicator

piston. It is assumed that the amount of throw is proportional to the intensity of the detonation pressure, and the total length of time the contact points are closed, during a test period, is obtained by measuring the volume of gases generated from the electrolysis of a quantity of acidulated water placed in series with the contact points.

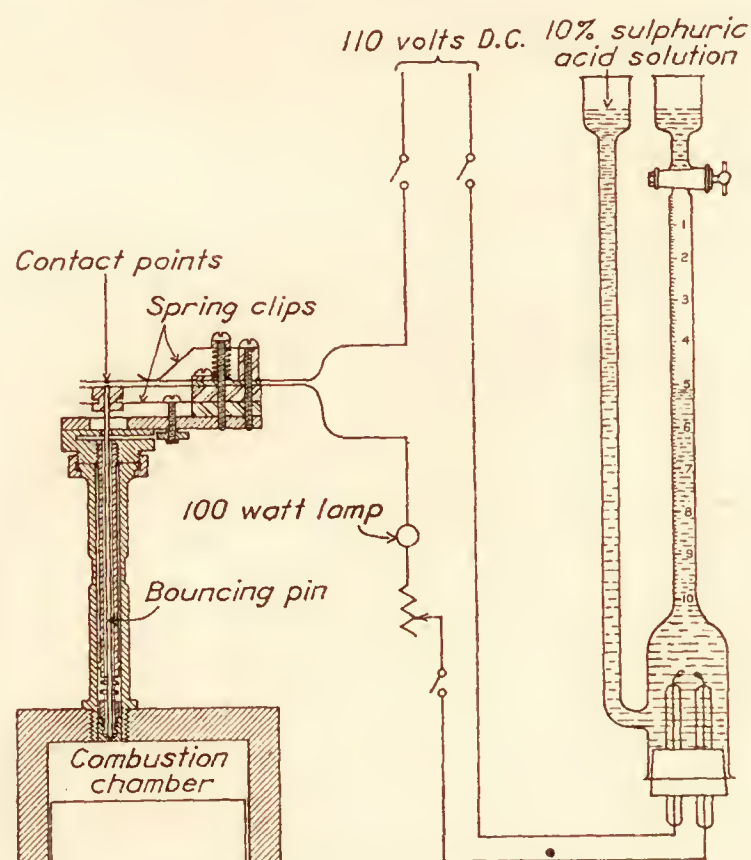


FIG. 5.—Bouncing-pin detonation meter

The indicator shown in Figure 6 was designed for the recording of maximum cylinder pressures by the balanced pressure method. The ball check valve was later replaced by a more sensitive disk-valve as shown in Figure 7. Both "balanced" and "trapped" pressures were recorded with this disk-type indicator. In recording by the balanced pressure method an



auxiliary air-pressure tank is used to insure pressure in excess of the cylinder pressure to be measured. This air pressure is admitted to the outer side of the disk and so regulated that the maximum cylinder pressures are balanced as indicated by a pressure gauge needle. The gauge needle will fluctuate when the external pressure is less than the maximum cylinder pressure,

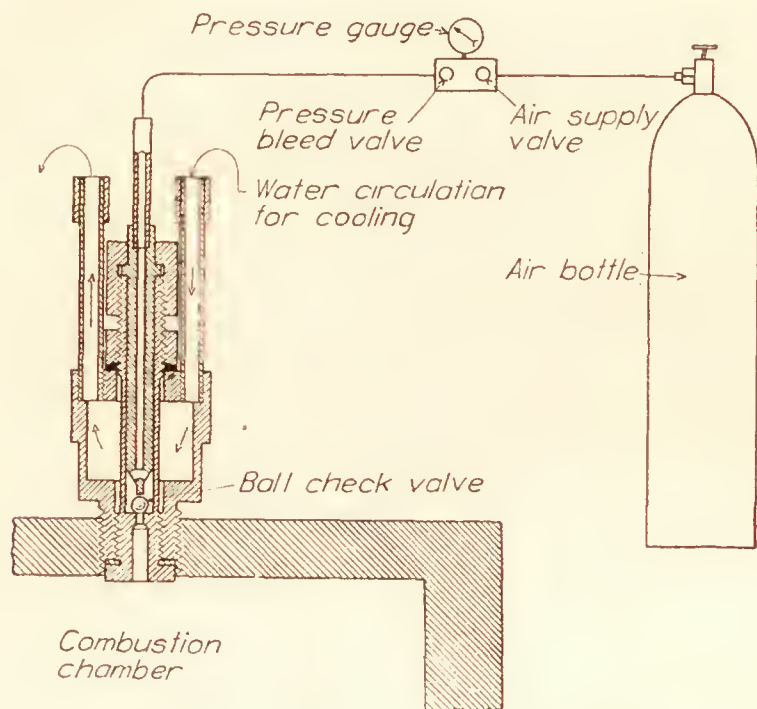


FIG. 6.—Ball check maximum pressure indicator

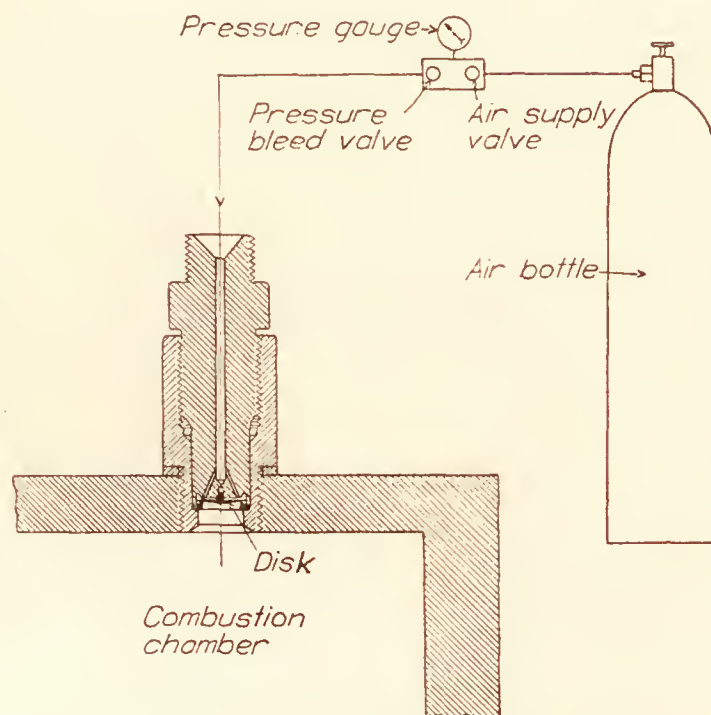


FIG. 7.—Disk-valve maximum pressure indicator

for there will be a pressure wave produced in the line when the disk is just lifted from its seat. In the trapped pressure method the gas in the engine cylinder is allowed to lift the disk and some of the gas that passes through the seat is trapped above the disk when it reseats. The principle of operation is that of a one-way, automatic, by-pass valve. There is, therefore, a pressure built up in the external line in communication with the pressure gauge which is lower than but indicates the maximum cylinder pressure.

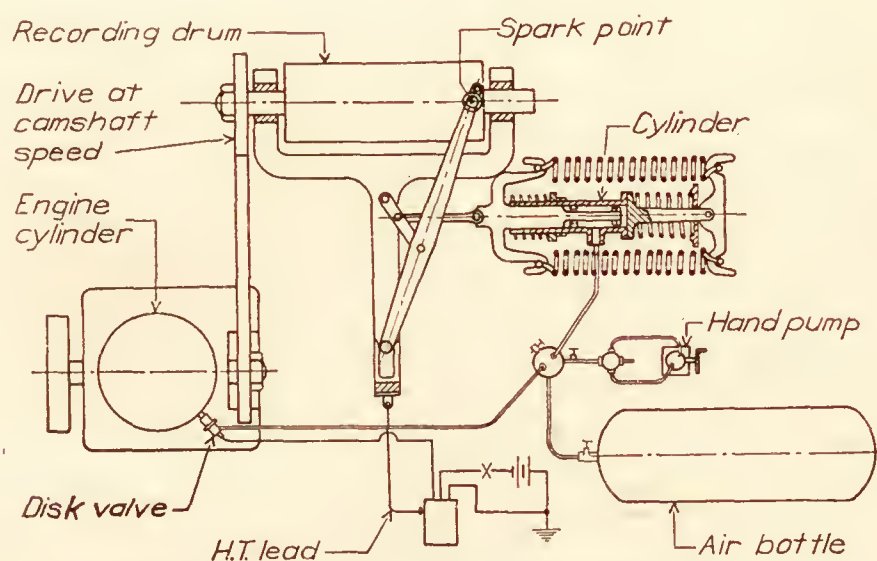


FIG. 8.—Electrical balanced pressure disk type indicator

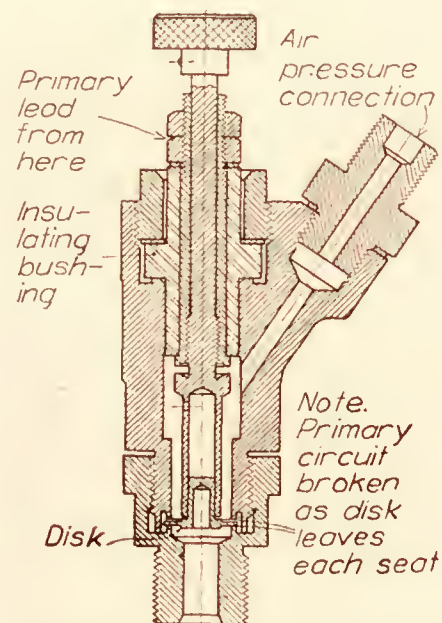


FIG. 9.—Electrical balanced pressure disk valve

An electric type pressure indicator is shown in the diagrammatic drawing in Figure 8, and the balanced disk valve used with this indicator is shown in cross section in Figure 9. This instrument is an example of the type that uses the energy of the cylinder gases to operate only a small part of the recording mechanism. Air under pressure is admitted to the disk valve and also to the recording drum mechanism. A spring-constrained piston in the latter moves a sparking point in straight-line motion along the recording drum. This drum carries a record paper and is driven by the engine at cam-shaft speed. The disk of the valve is exposed on the



underside to the engine cylinder pressure and moves from one seat to the other as the cylinder pressure and the external pressure alternately become greater. This disk acts as a breaker point for an electrical induction system, and as it leaves each seat a spark is caused to jump from the spark point to the recording drum and perforate the paper. When the controlled external pressure is varied over the complete range of engine cylinder pressures a pressure-time card is recorded representing the average of many cycles.

The audible manifestations of high cylinder pressures, such as those produced by detonation give a means of comparing pressure values directly by the ear. It is possible, with training, to separate the detonation sound from other engine noises, but the personal rating of the intensity of the sound is far from being accurate.

#### DISCUSSION AND ANALYSIS OF RESULTS

The main source of error found in the use of the maximum pressure indicator shown in Figure 1 are the inertia of moving parts, piston friction, and temperature effect on the load spring. Although there is no movement of the piston at the time of recording with this indicator, the inertia and friction forces are present to prevent movement and cause inaccurate settings to be made. The same sources of error are present with the optical indicator of Figure 2, but the errors may be reduced because of continuous movement of the piston throughout the cycle and the small amount of piston displacement required to produce a large scale indicator card.

The detonation detector shown in Figure 3 did not transmit a sound that could be distinguished from other engine noises. Mechanical vibrations and temperature effect on the indicator parts prevented any consistent checking of the results with the indicator shown in Figure 4. In addition to the attempt to record the current fluctuations in the external line, a set of head phones was connected in series with the carbon pile in an effort to obtain an audible "click." The "clicks" heard in the head phones were independent of the cylinder pressures, and any audible sounds produced by the head phones during detonation were also present when the engine was not detonating.

The "bouncing pin" detonation meter shown in Figure 5 did not give consistent results over a range of variable compression ratios. While this method of detecting detonation may give comparative results at a low compression ratio, it does not give a true indication of the cylinder pressure involved. It was possible, at engine speeds of 1,500 R. P. M., to make the pin bounce and record by compression alone when the compression ratio was raised above 7.3.

The indicators operating with check valves have given consistent readings when used for recording by both the balanced and trapped pressure methods. The ball check valve shown in Figure 6 required a seat width that introduced errors due to the difference in the area exposed to the cylinder pressure and the balancing pressure. Balanced pressures have been recorded quite accurately with the disk valve shown in Figure 7. The disk of this valve has a large area exposed to the cylinder pressures for its mass, and has a seat width of less than 0.005 inch. The greatest error introduced with this instrument is in observing or obtaining similar small fluctuations of the Bourbon gauge needle in all tests just before they are damped out.

The commercial, electric, balanced-pressure indicator (fig. 9) has a disk-seat width of 0.034 inch, which gives incorrect readings, because of the different areas exposed to the cylinder and balancing gas pressures. With an air pressure of 700 pounds per square inch holding the disk on its seat, a cylinder pressure of 935 pounds per square inch is required to equalize the force on the disk and cause it to record. Even though the disk of this indicator has excessive seat width and mass the recording of maximum cylinder pressures has been consistent and corrections and alterations may be made to improve its performance, such as replacing the disk with a thin diaphragm clamped at its outer edge between two perforated supports to limit its displacement. (Reference 4.) This method of operating the electric circuit-breaker mechanism will greatly reduce the inertia of the indicator parts.

Curves of brake mean effective pressure and the corresponding maximum cylinder pressure as recorded by the balanced-pressure method and the trapped pressure method with the disk



valve shown in Figure 7 are given in Figure 10. The compression pressures were 350 pounds per square inch and 560 pounds per square inch and the engine speed was 1,500 R. P. M. The difference in compression pressure caused a difference in combustion and provided a means for comparing the two methods of measuring maximum cylinder pressures. It may be noted that the pressures recorded are not in accordance with the brake mean effective pressure. At 350 pounds compression pressure there was less heat for the preparation of the fuel, and therefore more fuel was burned at constant volume with a resultant high maximum cylinder pressure as evidenced by the high B. M. E. P. and sound of the combustion knock. Because of the poor penetration of the fuel at the high-compression pressure, all injection conditions being maintained constant, the brake mean effective pressure is low, but there is more constant pressure combustion and a slower pressure rise which gives a higher maximum pressure reading.

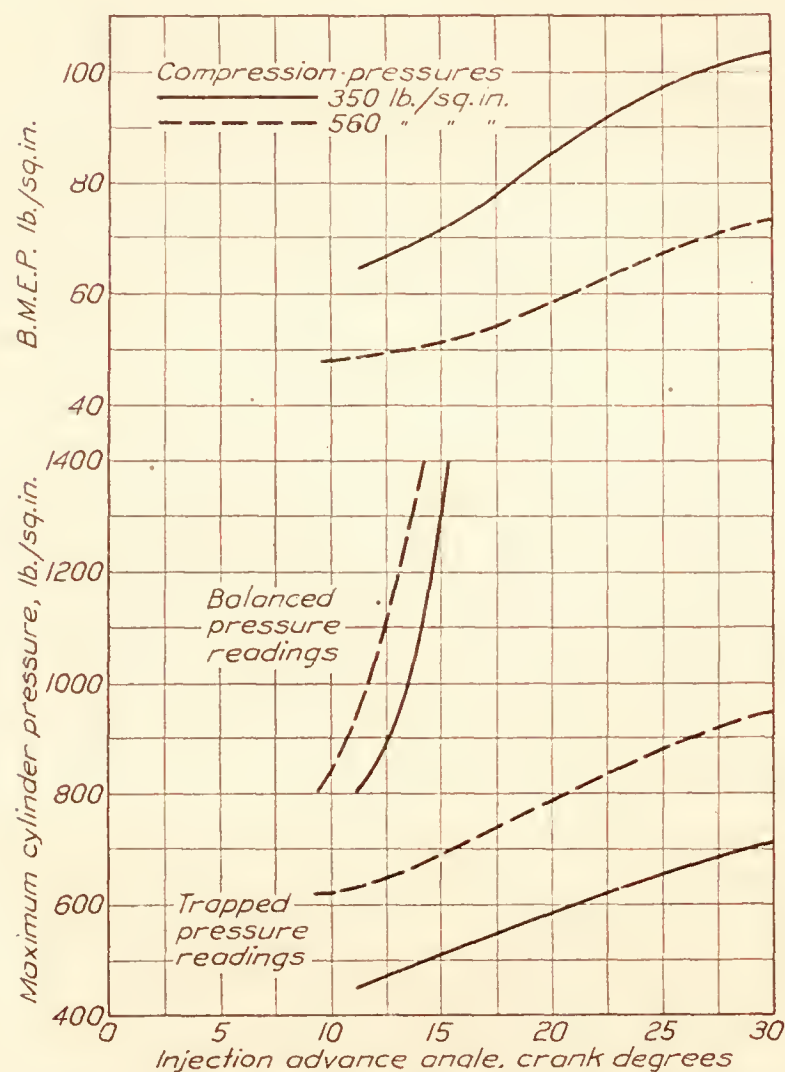


FIG. 10.—Comparison of the cylinder pressures recorded by the disk-valve of Fig. 7. Universal test engine, oil engine operation, 1,500 R. P. M., with fuel quantity and operating temperatures maintained at constant values

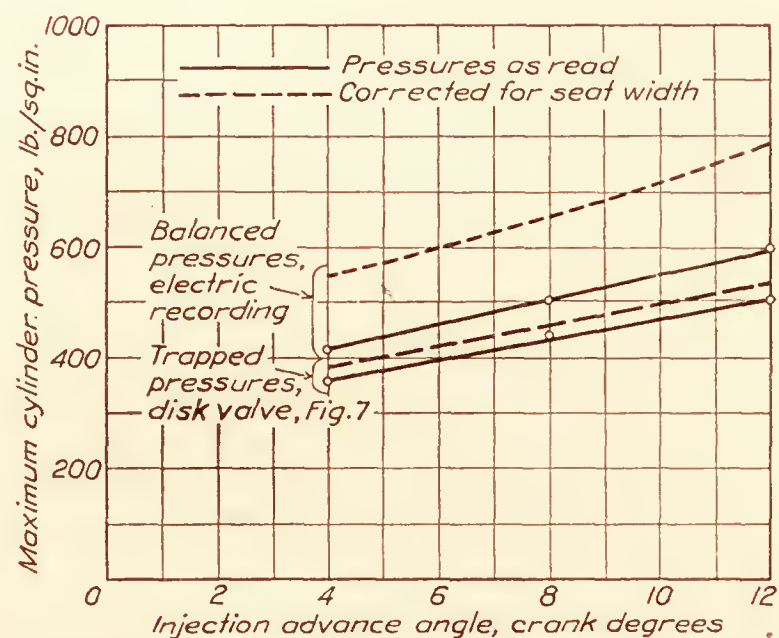


FIG. 11.—Effect of disk seat width on the recording of cylinder pressures by the disk-valves of Figs. 7 and 9. Universal test engine, oil engine operation, 1,500 R. P. M., with fuel quantity, compression ratio, and operating temperatures maintained at constant values

A fast rising pressure with a high maximum value of short duration does not have time to do the necessary work on the disk to record, whereas a slow pressure rise with a low maximum pressure will record a relatively high pressure. The trapped pressure readings are too low, because the cylinder gas must lift the disk and enter the valve against the existing trapped pressure. The balanced-pressure readings are probably a better indication of the true pressures, for only the inertia of the light disk and sensitivity of the gauge must be accounted for in the actual movement of the indicating mechanism.

The effect of seat width on pressure recording by a balanced-pressure disk valve is shown in Figure 11. For these tests the conditions of engine operation were maintained constant, which should give approximately the same maximum cylinder pressures to record. The trapped pressures were recorded by the disk-valve indicator of Figure 7, and the electric recording was done by the electrical, balanced-pressure indicator of Figure 9. The dotted curves give cylinder



pressures corrected for the effect of differential disk-pressure area produced by the seat widths. The electric recording gives higher values than those recorded by the trapped-pressure method, because it is only necessary that the disk leave its seat to record.

The effect of the mass of the disk on the recording of cylinder pressures, as represented by the area-weight ratio, is shown in the curves of Figure 12. As in the tests shown in Figure 11, the engine-test conditions were maintained at constant values. The readings were made by the balanced-pressure method with the valves of Figures 7 and 9, the disks of which had area-weight ratios of 0.475 and 0.0957, respectively. Corrections were made for the seat widths in each instrument so that the pressure differences between the two curves in Figure 12 indicate the effect of the inertias of the disks.

The type of maximum pressure indicator using the pressure itself to do all of the work of recording, has an inherent disadvantage, because it can not respond to rapid variations of

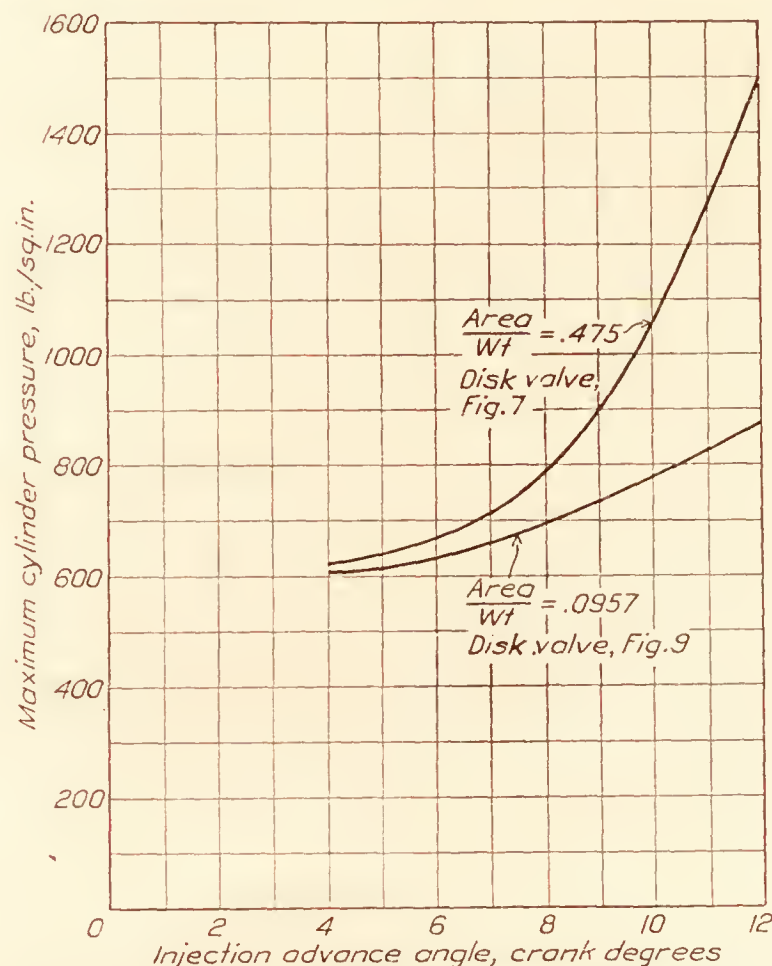


FIG. 12.—Effect of the mass and area of the valve disk on the recording of cylinder pressures by the valves of Figs. 7 and 9. Universal test engine, oil engine operation, 1,500 R. P. M., with fuel quantity compression ratio, and operating temperatures maintained at constant values

pressure. It must absorb a definite amount of energy from the cylinder pressure to overcome large inertia forces, and, since the time rate of pressure rise is variable, it is difficult to attempt a correction for this loss.

In some instruments the inertia of the moving parts or the movement of these parts is reduced to a small value, but this only reduces the error and does not give accurate results or an accurate method for making a correction. With the type of instruments using the cylinder pressure to operate only a small part of the recording mechanism, the error is reduced and may lead to the elimination of enough variables so that more accurate corrections can be made.

The human ear has been used for indicating the approximate intensity of maximum cylinder pressures. Although the personal rating of sound intensity is not considered reliable, the point at which detonation becomes audible may be checked with a fair degree of accuracy. The high-pressure "pink" of detonation has a sound frequency much different from the noise of valve gears, tappets, rocker arms, and other moving engine parts. An observer, accustomed

to listening to detonation, may have his ear trained so that he can distinguish a high-pressure knock even though it be of less intensity than other engine noises.

In analyzing the destructive power of cylinder pressures there are three characteristics which must be considered—the cylinder pressure attains a certain force value, it attains this value in a definite time, and the pressure is maintained a definite length of time. The ability of the cylinder gas to do work on the indicator is a function of force and time. The work done by the cylinder pressure may be separated into the useful work done on the piston as mean effective pressure and the destructive work. If the maximum cylinder pressure is of too short duration it can do little useful work. The pressure may be of sufficient duration, however, to cause a deflection of the cylinder and cylinder head with enough movement to set up a sound wave. This deflection need not be much when it is realized that the amplitude of sound waves in air, audible to the human ear, range from  $5.0 \times 10^{-8}$  to  $4.0 \times 10^{-3}$  inch. (Reference 5.) The detonation "pink" of the carburetor engine is the manifestation of an extremely high and fast-rising pressure of short duration. This type of pressure rise delivers a blow to the piston and cylinder head; and, if its force is sufficient to stress the metal beyond its fatigue limit, repeated stressing will cause failure. The detonation pressure is also accompanied by a high temperature that may cause trouble in engine operation.

It was noted during certain tests that the sound-wave frequency of the knock changed with a change of compression ratio and subsequent change of combustion characteristics. An adjustable tuning fork was used for comparing the sound of the engine knock with a known frequency. With a compression ratio of 14.4 and oil injection, the sound frequency of the knock was checked as being approximately 200 vibrations per second. It was noted that as the compression ratio was lowered to 10.2 the frequency of the sound wave increased. At a still lower compression ratio—i. e., 6.0—a check on the carburetor engine "pink" gave a frequency of approximately 2,000 vibrations per second. During the change in compression ratio from 14.4 to 10.2 there was a change in the combustion characteristics and subsequent rate of pressure rise. The high compression ratio and the standard conditions of engine operation gave a maximum amount of constant pressure combustion accompanied by a slow rate of pressure rise. With the low compression ratio there was a maximum amount of constant volume combustion. In the case of the carburetor engine the combustion is practically constant volume during detonation. The foregoing brief discussion on sound frequencies indicates the variable rate of pressure rise under which a cylinder pressure indicator must operate.

### CONCLUSIONS

This investigation on the measurement of maximum cylinder pressures has served mainly to bring out some of the limitations of the available instruments for measuring these pressures. The main factors affecting the accuracy of the maximum cylinder pressure indicators tested are the friction and inertia of moving parts, the differential areas exposed in balanced-gas type indicators, and the short duration of the maximum cylinder pressures.

The investigations conducted thus far indicate that the greatest accuracy in determining maximum cylinder pressures can be obtained with an electric, balanced-pressure, diaphragm or disk-type indicator so constructed as to have a diaphragm or disk of relatively large area and minimum seat width and mass.

LANGLEY MEMORIAL AERONAUTICAL LABORATORY,  
NATIONAL ADVISORY COMMITTEE FOR AERONAUTICS,  
LANGLEY FIELD., VA., *March 30, 1928.*



## BIBLIOGRAPHY

- Reference 1. Joachim, Wm. F., and Kemper, Carlton: The Performance of Several Combustion Chambers Designed for Aircraft Oil Engines. N. A. C. A. Technical Report No. 282, 1928.
- Reference 2. Gardiner, Arthur W., and Whedon, Wm. E.: The Relative Performance Obtained with Several Methods of Control of an Overcompressed Engine Using Gasoline. N. A. C. A. Technical Report No. 272, 1927.
- Reference 3. Ware, Marsden: Description of the Universal Test Engine and Some Test Results. N. A. C. A. Technical Report No. 250, 1927.
- Reference 4. Dickinson, H. C., and Newell, F. B.: A High-Speed Engine Pressure Indicator of the Balanced Diaphragm Type. N. A. C. A. Technical Report No. 107, 1921.
- Reference 5. Shaw, P. E.: The Amplitude of Minimum Audible Impulsive Sounds. Proceedings of the Royal Society of London, vol. 76A, p. 360, 1905.
- Dumanois, P.: Fatigue of Internal Combustion Engines. N. A. C. A. Technical Memorandum No. 259, 1924.
- Sparrow, Stanwood W., and Lee, Stephen M.: Comparing Maximum Pressures in Internal Combustion Engines. N. A. C. A. Technical Note No. 101, 1922.
- Midgley, Thomas, jr., and Boyd, T. A.: Methods of Measuring Detonation in Engines. S. A. E. Journal, January, 1922.
- Whatmough, W. A.: Some Practical Considerations of Detonation. The Automobile Engineer, January, 1927.
- Morgan, Prof. W., and Rubbra, A. A.: The Optical Indicator as a Means of Examining Combustion in Explosion Engines. The Automobile Engineer, January, 1927.
- Midgley, Thomas, jr., Delbridge, T. J., Sparrow, S. W., and Wilson, R. E.: What are Detonation Facts? Report of Research Subcommittee, S. A. E. Journal, March, 1927.





---

**REPORT No. 295**

---

**THE VARIATION IN ENGINE POWER WITH ALTITUDE  
DETERMINED FROM MEASUREMENTS IN FLIGHT  
WITH A HUB DYNAMOMETER**

**By W. D. GOVE**

**Langley Memorial Aeronautical Laboratory**





## REPORT No. 295

### THE VARIATION IN ENGINE POWER WITH ALTITUDE DETERMINED FROM MEASUREMENTS IN FLIGHT WITH A HUB DYNAMOMETER

By W. D. GOVE

#### SUMMARY

*The rate of change in power of aircraft engines with altitude has been the subject of considerable discussion. Only a small amount of data from direct measurements of the power delivered by airplane engines during flight, however, has been published. This report presents the results of direct measurements of the power delivered by a Liberty 12 airplane engine taken with a hub dynamometer at standard altitudes from zero to 13,000 feet. Six flights were made with the engine installed in a modified DH-4 airplane. The tests were conducted at the Langley Memorial Aeronautical Laboratory of the National Advisory Committee for Aeronautics.*

*The experimental relation of brake horsepower to altitude is compared with two theoretical relations and with the experimental results, for a second Liberty 12 engine, given in N. A. C. A. Technical Report No. 252. The rate of change in power with altitude of a third Liberty engine, measured with a calibrated propeller, is also given for comparison.*

*The data presented substantiate the theoretical relation of brake horsepower to altitude based on the correction of ground level indicated horsepower for changes in atmospheric temperature and pressure with the subsequent deduction of friction horsepower corrected for altitude. The equation for this relation is*

$$B.HP_a = B.HP_o \left[ \left( \frac{P_a}{P_o} \right) \left( \frac{T_o}{T_a} \right)^{1/2} \left( 1 + \frac{\lambda - \lambda n}{n} \right) - \left( \frac{\lambda - \lambda n}{n} \right) \right]$$

*where  $P$  is the absolute atmospheric pressure,  $T$  is the absolute temperature,  $n$  is the mechanical efficiency of the engine at sea level and  $\lambda$  is the ratio of mechanical friction to friction horsepower at sea level. The subscripts  $_o$  and  $_a$  denote sea level and altitude conditions respectively.*

#### INTRODUCTION

The effects of altitude conditions on the power delivered by airplane engines have been the subject of considerable discussion. However, there has been in the past very little information available for analysis and publication from the direct power measurements on airplane engines during flight. Further information has been obtained on the decrease in power delivered by a Liberty 12 engine with altitude during several flight tests made for the purpose of calibrating propellers. These tests were conducted at the Langley Memorial Aeronautical Laboratory of the National Advisory Committee for Aeronautics, the engine power having been measured directly by means of a Bendemann type hub dynamometer. (Reference 1.) Six full throttle flights were made to approximately 13,000 feet altitude on which the engine speed was maintained practically constant by varying the altitude of the airplane. The relation of power to altitude, determined experimentally from these six flights, is compared with two theoretical relations in which sea level indicated horsepower is corrected for changes in atmospheric temperature and pressure at altitude. Further experimental evidence of the rate of change in power of a Liberty engine with altitude, taken from the data given in N. A. C. A. Technical Report No. 252 (reference 1), and from power measurements on a third Liberty engine made with a calibrated propeller, is also given for comparison.



## METHODS AND APPARATUS

The flight tests were made as full throttle climbs to approximately 13,000 feet altitude on which measurements were taken of engine torque, engine speed, air speed, atmospheric pressure, atmospheric temperature, and carburetor air temperature. Engine speed was maintained as nearly constant as possible during these tests to avoid large speed corrections to power at altitudes where torque-engine speed relations were not known. For the small speed variations encountered, the engine power was corrected to a constant speed by ratio of the constant to the observed engine speeds.

Before an experimental relation of brake horsepower to altitude could be derived, it was necessary to correct the brake horsepower from existing flight conditions to the temperatures and pressures of the standard altitude at which the engine was considered to be operating. This standard altitude was taken as that corresponding to the density determined from the observed atmospheric pressure and temperature. (Reference 2.) A given air density may be obtained with a high temperature and pressure or with a low temperature and pressure while the power delivered by an engine under the two conditions would not be the same, density being a function of  $\frac{P}{T}$ , while indicated horsepower is a function of  $\frac{P}{\sqrt{T}}$  ( $P$  denoting absolute pressure and  $T$  denoting absolute temperature). The observed power measurements were corrected for the differences between observed and standard altitude atmospheric conditions, by the direct ratio of standard altitude pressure to observed atmospheric pressure. A similar correction for temperature was also applied, using the inverse square-root relation. These corrections were applied directly to brake horsepower, rather than to indicated horsepower, for the reason that the pressure and temperature differences were small.

These flight tests were conducted with a modified DH-4 airplane powered with a Liberty 12 engine equipped with Zenith carburetors. Measurements of engine torque were obtained with a Bendemann type hub dynamometer which consists of a system of hydraulic pistons and cylinders interposed between the engine shaft and the propeller in such a manner that the hydraulic pressure generated in the cylinders is proportional to the torque. This pressure is transmitted through small tubes and recorded by an instrument in the cockpit. A more complete description of the Bendemann hub dynamometer is given in reference 1. All other measurements were recorded by means of an "automatic observer," developed by this committee, consisting essentially of a motor-driven motion-picture camera focused on the dials of indicating instruments mounted on a panel. These instruments consisted of an altimeter for the measurement of atmospheric pressure, an electric resistance thermometer for the measurement of atmospheric temperature, a distance type vapor pressure thermometer for the measurement of carburetor air temperature, an air-speed meter, and a chronometric tachometer.

## RESULTS

Data from a representative climb are shown graphically in Figure 1 where brake horsepower, atmospheric pressure, atmospheric and carburetor air temperatures, engine speed and air speed are plotted against standard altitude. The data for the six flights analyzed in this report are given in Tables I to VI. Carburetor air temperatures are not given in the tables for the first five flights, because the thermometer used for this measurement was found from later calibrations to be unreliable.

The experimental relations of brake horsepower to altitude for all three engines are shown in Figure 2. The ratios of corrected brake horsepower at altitude to brake horsepower at zero altitude for each engine are plotted against standard altitude. Curve **A** of this figure represents the data taken from the engine used on the six flights at constant engine speed, curve **B** represents the relation for the engine used in the tests given in the report on the Bendemann hub dynamometer (reference 1), and curve **C** represents the power relation for the third engine where power was measured with a calibrated propeller.

Two theoretical relations of power to altitude, explained later in the report, are shown in Figure 3 as curves **D** and **E**. The experimental curve **A** of Figure 2 is also reproduced without



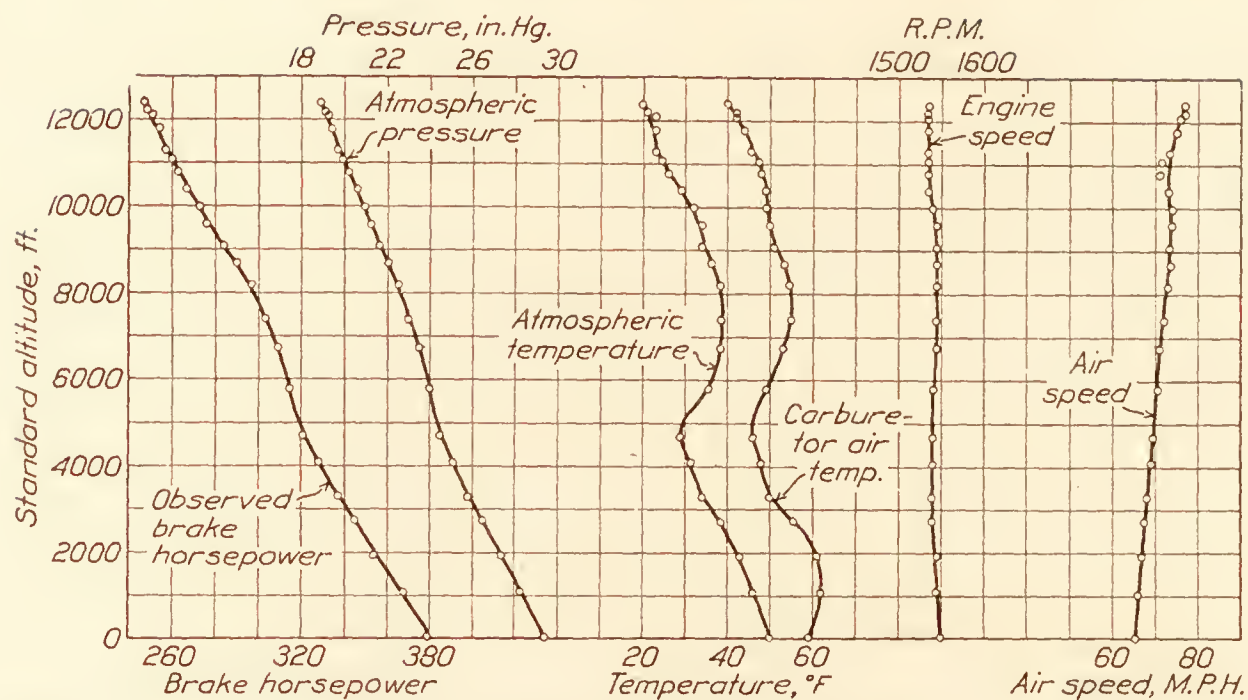


FIG. 1.—Data from a representative climb. Flight No. 6 of the modified DH-4 airplane with a Liberty 12 engine and a standard Martin bomber propeller

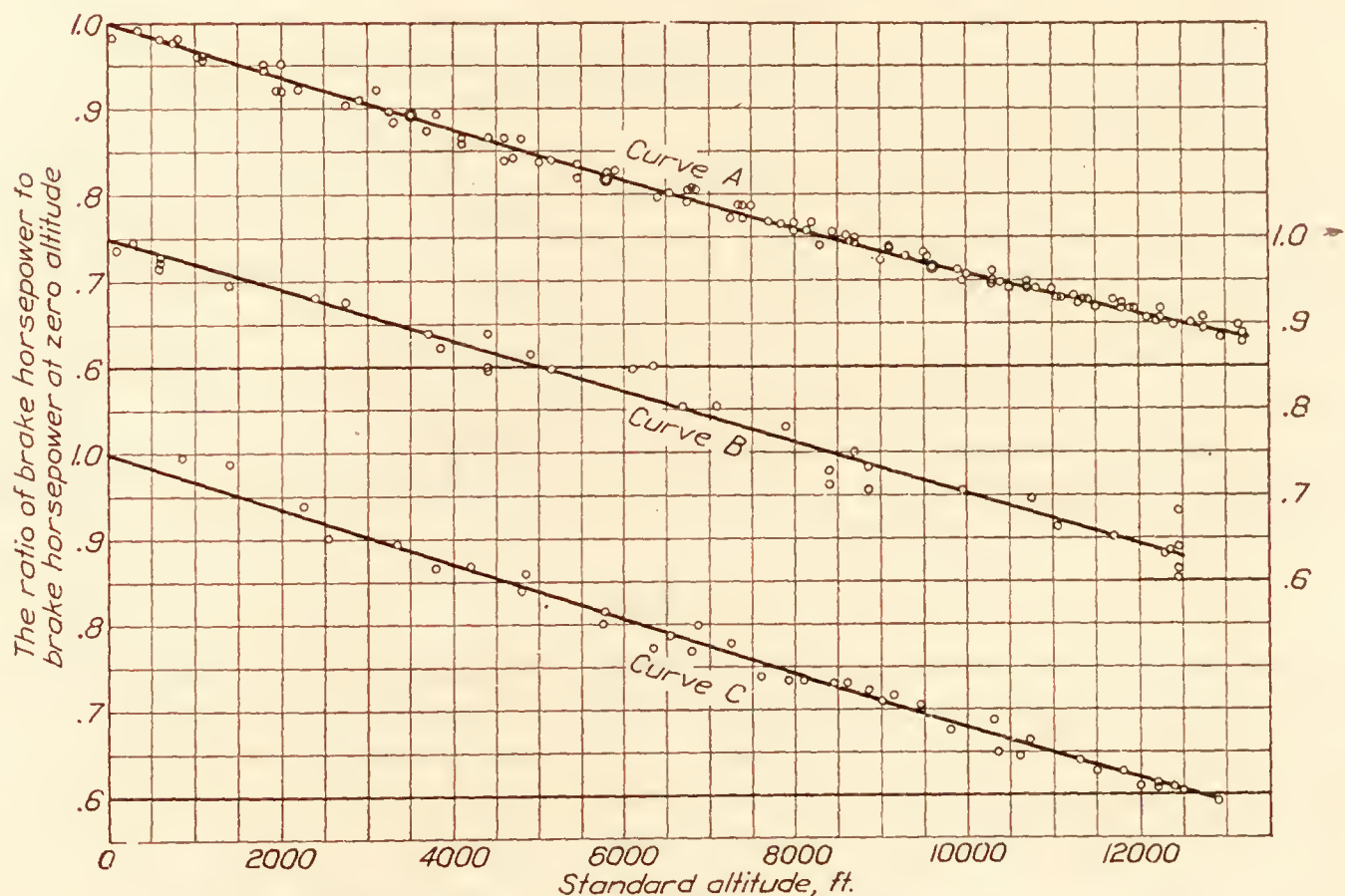


FIG. 2.—The percentage relation of brake horsepower to altitude for three Liberty 12 engines

data points to give a comparison of the two theoretical relations with the most reliable experimental relation.

Figure 4 illustrates the variation in the power delivered by the three engines with altitude. The more accurate theoretical relation of power to altitude, curve E, is also reproduced on this chart to show its agreement with all of the experimental data.

#### DISCUSSION OF RESULTS

Two theoretical relations of engine power to altitude are given for comparison with the relations determined experimentally from the three engines. The agreement of these theoretical relations with the experimental relations as represented by curves is taken as a criterion of the accuracy with which engine power at altitude can be computed from sea level engine performance.

The first relation is based on the assumption that indicated horsepower varies directly with pressure and inversely with the square root of the absolute temperature (reference 3),

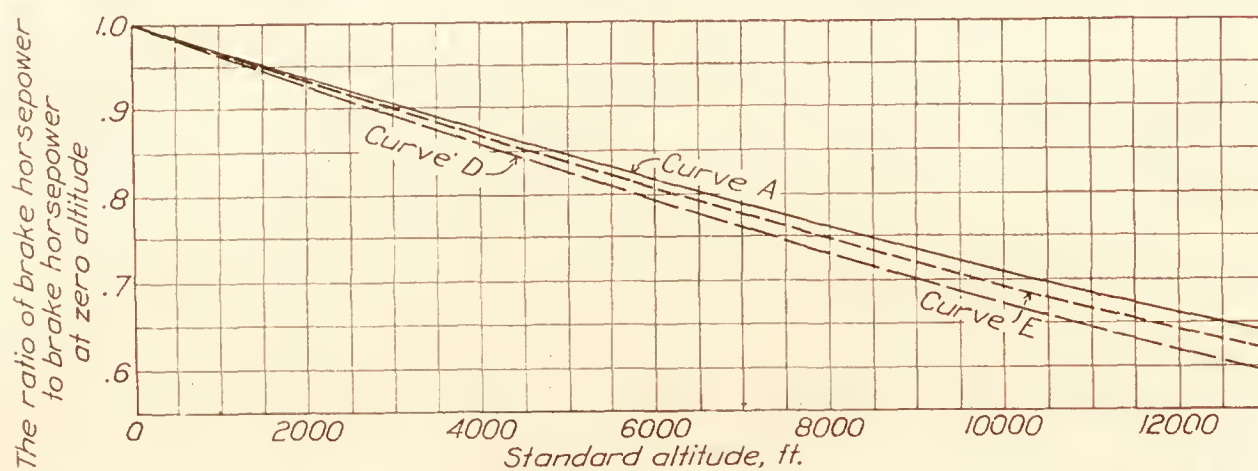


FIG. 3.—Comparison of the experimental percentage relation of power to altitude, determined from the six flights analyzed in this report, with two theoretical relations

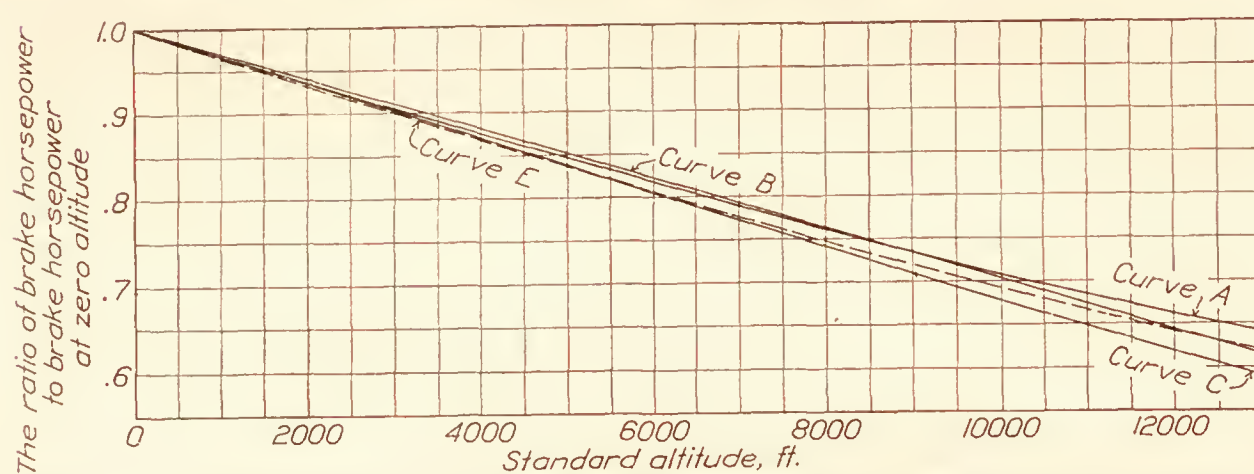


FIG. 4.—Comparison of the theoretical percentage relation of brake horsepower to altitude with curves determined experimentally from three Liberty 12 engines

and that the friction horsepower at constant engine speed is the same at all altitudes. This relation, based on brake horsepower at sea level and mechanical efficiency  $n$ , can be expressed as

$$\text{B.H.P.}_a = \text{B.H.P.}_o \left[ \left( \frac{P_a}{P_o} \right) \left( \frac{T_o}{T_a} \right)^{1/2} \left( \frac{1}{n} \right) - \frac{(1-n)}{n} \right]. \quad (1)$$

Curve D of Figure 3 is based on the above equation, using values of pressure and temperature from the standard altitude chart and a value of 88 per cent for mechanical efficiency at sea level. (Reference 4.) This relation gives 7 per cent less power at 12,000 feet altitude than that determined experimentally from the six flights.

The second method corrects indicated horsepower for temperature and pressure in the usual manner, and the friction horsepower for decreased pumping losses at altitude. The pumping losses were considered to vary directly with atmospheric pressure (reference 5) and inversely with the square root of the absolute temperature. Experimental justification of the latter assumption is found in the curves of friction horsepower versus temperature given in reference 6. The friction horsepower given in this report was divided into pumping losses and mechanical friction according to the ratio of pumping losses to friction horsepower given by Gage. (Reference 7.) From these data it was determined that the pumping losses varied with the square root of the absolute temperature ratio.

The second method, expressed in the form of an equation in terms of brake horsepower at sea level, mechanical efficiency at sea level, and the ratio of mechanical friction to sea level friction horsepower  $\lambda$ , becomes:

$$\text{B.H.P.}_a = \text{B.H.P.}_o \left[ \left( \frac{P_a}{P_o} \right) \left( \frac{T_o}{T_a} \right)^{1/2} \left( 1 + \frac{\lambda - \lambda n}{n} \right) - \left( \frac{\lambda - \lambda n}{n} \right) \right]. \quad (2)$$

Curve E of Figure 3 shows this relation as computed for the Liberty engine using a value of



$\lambda$  equal to 0.5, as given in reference 7. This equation gives a closer estimation of power at altitude than equation (1), the discrepancy at 12,000 feet being only 3.5 per cent. A derivation of these two equations is given in the appendix.

The curves for the two theoretical relations have the same general form as the experimental relation determined from the six flights, although in both cases there is a gradual divergence with altitude. No attempt has been made to evolve a method of computing power at altitudes which would give closer agreement with this experimental relation than equation (2), because the power of different engines of the same model operating at the same altitude may vary as much as the percentage variation shown for the three engines in Figure 4. It may be seen that the theoretical curve given in this figure is in fair agreement with the experimental data from all three engines for the range of altitudes shown.

Of the three experimental relations given in Figures 2 and 4, curve A was the most accurately determined, both in the number of observations and in the refinement of methods with which they were taken. The variation of the test points from the average power curve for the data taken on these six flights was within plus or minus 2 per cent.

A comparison of the power developed at zero altitude for the engine, represented by curve A, with a calibration of the same engine, made in the laboratory with an electric dynamometer shows that less power was recorded with the engine installed in the airplane. The cause of this was not determined. However, since the laboratory calibration was made first, the decrease in power could be attributed to changes in condition of the engine with length of service. Were the power at zero altitude taken from the laboratory calibration, the ratios of power at altitude to power at zero altitude given in curve A, Figures 2 and 4 would be slightly lower, and the curve would agree more closely with the theoretical curve computed from equation (2).

Carburetor air temperatures measured in the inlet to the carburetor, on the flight for which the data is shown in Table VI, were found to be from 10° to 20° F. higher than the atmospheric temperatures. However, only a small error is incurred in using atmospheric rather than carburetor air temperatures in computing power at altitude from sea level engine power, for the reason that the temperature drop with altitude is very nearly the same for the atmospheric as for the carburetor air temperature as shown in Figure 1. All temperature corrections applied to both the theoretical and experimental power of engines in this report were based on the temperature of the air surrounding the engine rather than on the temperatures measured in the carburetor air-inlet passage.

#### CONCLUSIONS

The experimental results from the three Liberty 12 engines tested substantiate the second theoretical relation given in this report, the departure of any one of the experimental relations from the theoretical curve being less than plus or minus 3.5 per cent at 12,000 feet altitude. This theoretical relation is based on the correction of sea level indicated horsepower for changes in atmospheric temperature and pressure with the subsequent deduction of friction horsepower corrected for altitude and is expressed in the following equation:

$$\text{B.H.P.}_a = \text{B.H.P.}_o \left[ \left( \frac{P_a}{P_o} \right) \left( \frac{T_o}{T_a} \right)^{1/2} \left( 1 + \frac{\lambda - \lambda n}{n} \right) - \left( \frac{\lambda - \lambda n}{n} \right) \right]$$

LANGLEY MEMORIAL AERONAUTICAL LABORATORY,  
NATIONAL ADVISORY COMMITTEE FOR AERONAUTICS,  
LANGLEY FIELD, VA., May 7, 1928.

## BIBLIOGRAPHY

- Reference 1. Gove, W. D., and Green, M. W.: The Direct Measurement of Engine Power on an Airplane in Flight with a Hub Dynamometer. N. A. C. A. Technical Report No. 252 (1927).
- Reference 2. Diehl, Walter S.: Standard Atmosphere—Tables and Data. N. A. C. A. Technical Report No. 218 (1925).
- Reference 3. Sparrow, Stanwood W.: Correcting Horsepower Measurements to a Standard Temperature. N. A. C. A. Technical Report No. 190 (1924).
- Reference 4. Sparrow, S. W., and White, H. S.: Performance of a Liberty 12 Airplane Engine. N. A. C. A. Technical Report No. 102 (1921).
- Reference 5. Sparrow, S. W., and Thorne, M. A.: Friction of Aviation Engines. N. A. C. A. Technical Report No. 262 (1927).
- Reference 6. Gardiner, Arthur W., and Schey, Oscar W.: The Comparative Performance of an Aviation Engine at Normal and High Inlet Air Temperatures. N. A. C. A. Technical Report No. 277 (1927).
- Reference 7. Gage, Victor R.: Some Factors of Airplane Engine Performance. N. A. C. A. Technical Report No. 108 (1921).
- Pinsent, D. H., and Renwick, H. A.: The Variation of Engine Power with Height. British Reports and Memoranda No. 462 (March, 1918).
- Stevens, H. L.: Variation of Engine Power with Height. British Reports and Memoranda No. 960 (August, 1924).
- Glauert, H.: A Discussion of the Variation of Engine Power with Height. British Reports and Memoranda No. 1099 (March, 1927).



## APPENDIX

Derivation of equation (1) (neglecting the decrease in pumping losses with altitude).  
Assumptions:

$$(I) \quad \text{B.HP}_a = \text{I.HP}_o \left( \frac{P_a}{P_o} \right) \left( \frac{T_o}{T_a} \right)^{1/2} - \text{F.HP}_o$$

Let  $n$  = mechanical efficiency at sea level. Then

$$(II) \quad \text{I.HP}_o = \frac{\text{B.HP}_o}{n} \text{ and } \text{F.HP}_o = \frac{(1-n) \text{B.HP}_o}{n},$$

Substituting (II) in (I)

$$(III) \quad \text{B.HP}_a = \frac{\text{B.HP}_o}{n} \left( \frac{P_a}{P_o} \right) \left( \frac{T_o}{T_a} \right)^{1/2} - \frac{(1-n) \text{B.HP}_o}{n},$$

or,

$$\text{Equation (1). } \text{B.HP}_a = \text{B.HP}_o \left[ \left( \frac{P_a}{P_o} \right) \left( \frac{T_o}{T_a} \right)^{1/2} \left( \frac{1}{n} \right) - \left( \frac{1-n}{n} \right) \right].$$

Derivation of equation (2) (taking account of the decrease in pumping losses with altitude).  
Assumptions:

$$(I) \quad \text{B.HP}_a = \text{I.HP}_o \left( \frac{P_a}{P_o} \right) \left( \frac{T_o}{T_a} \right)^{1/2} - \text{F.HP}_a$$

where  $\text{F.HP}_a$  = mechanical friction at sea level plus pumping losses at sea level corrected to the temperature and pressure at altitude.

Let  $\lambda$  the ratio of mechanical friction to friction horsepower at sea level and  $n$  = mechanical efficiency at sea level.

Then

$$(II) \quad \text{I.HP}_o = \frac{\text{B.HP}_o}{n},$$

and

$$(III) \quad \text{F.HP}_a = \lambda \text{F.HP}_o + (1-\lambda) \text{F.HP}_o \left( \frac{P_a}{P_o} \right) \left( \frac{T_o}{T_a} \right)^{1/2}$$

but

$$(IV) \quad \text{F.HP}_o = \frac{(1-n) \text{B.HP}_o}{n},$$

hence

$$(V) \quad \text{F.HP}_a = \frac{\lambda (1-n) \text{B.HP}_o}{n} + \frac{(1-\lambda) (1-n) \text{B.HP}_o}{n} \left( \frac{P_a}{P_o} \right) \left( \frac{T_o}{T_a} \right)^{1/2}$$

Substituting values from (II) and (V) in (I).

$$(VI) \quad \text{B.HP}_a = \frac{\text{B.HP}_o}{n} \left( \frac{P_a}{P_o} \right) \left( \frac{T_o}{T_a} \right)^{1/2} - \frac{\lambda (1-n) \text{B.HP}_o}{n} - \frac{(1-\lambda) (1-n) \text{B.HP}_o}{n} \left( \frac{P_a}{P_o} \right) \left( \frac{T_o}{T_a} \right)^{1/2},$$

simplifying

$$\text{Equation (2). } \text{B.HP}_a = \text{B.HP}_o \left[ \left( \frac{P_a}{P_o} \right) \left( \frac{T_o}{T_a} \right)^{1/2} \left( 1 + \frac{\lambda - \lambda n}{n} \right) - \left( \frac{\lambda - \lambda n}{n} \right) \right].$$

TABLE 1

Reading No.	Atmospheric pressure (inches Hg.)	Atmospheric temperature (°F. Abs.)	Standard altitude (feet)	R. P. M.	Airspeed (M. P. H.)	Observed B. HP.	Standard altitude pressure (inches Hg.)	Pressure correction factor	Standard altitude temperature (°F. Abs.)	Temperature correction factor	B. HP. corrected for T. and P. at observed R. P. M.	Corrected B. HP. at 1,400 R. P. M.	Ratio corrected B. HP. to B. HP. <sub>0</sub> = 356
1	27.50	482	350	1,400	73.0	341	29.55	1.074	517	0.965	353	353	0.992
2	26.65	478	1,100	1,400	74.0	329	28.75	1.078	514	.964	352	342	.961
3	25.80	475	2,000	1,405	75.0	317	27.82	1.078	511	.964	329	328	.921
4	24.85	481	3,700	1,410	77.0	305	26.13	1.052	505	.975	313	311	.874
5	24.15	481	4,600	1,405	77.5	293	25.27	1.047	502	.978	300	299	.840
6	23.55	481	5,450	1,405	78.0	287	24.47	1.038	499	.981	293	292	.820
7	22.85	480	6,400	1,405	78.5	280	23.62	1.034	496	.984	285	284	.798
8	22.20	480	7,250	1,405	79.0	272	22.86	1.029	493	.985	276	275	.773
9	21.80	480	7,850	1,405	79.0	270	22.35	1.026	490	.989	274	273	.767
10	21.35	478	8,450	1,405	79.5	268	21.84	1.023	488	.989	271	270	.758
11	20.90	478	9,100	1,400	79.5	260	21.30	1.018	486	.992	263	263	.739
12	20.55	476	9,550	1,400	79.5	256	20.94	1.018	484	.992	259	259	.728
13	20.25	475	9,950	1,400	79.5	247	20.62	1.018	483	.992	249	249	.700
14	19.90	475	10,500	1,400	80.0	244	20.18	1.013	481	.994	246	246	.691
15	19.55	475	11,050	1,400	80.0	240	19.75	1.011	479	.996	242	242	.680
16	19.30	475	11,500	1,400	80.0	237	19.41	1.006	477	.998	238	238	.669

Data from flight No. 1 of a modified DH-4 airplane with a Liberty 12 engine and a Martin bomber supercharger propeller.

TABLE 2

Reading No.	Atmospheric pressure (inches Hg.)	Atmospheric temperature (°F. Abs.)	Standard altitude (feet)	R. P. M.	Airspeed (M. P. H.)	Observed B. HP.	Standard altitude pressure (inches Hg.)	Pressure correction factor	Standard altitude temperature (°F. Abs.)	Temperature correction factor	B. HP. corrected for T. and P. at observed R. P. M.	Corrected B. HP. at 1,550 R. P. M.	Ratio corrected B. HP. to B. HP. <sub>0</sub> = 384
1	28.15	497	600	1,540	75.0	368	29.28	1.040	516	0.980	375	377	0.982
2	26.95	493	1,800	1,550	76.5	358	28.02	1.040	512	.982	366	366	.953
3	25.95	500	3,500	1,555	78.0	345	26.32	1.014	506	.984	344	343	.893
4	25.05	500	4,600	1,570	79.0	335	25.27	1.008	502	.998	337	333	.867
5	24.30	497	5,450	1,550	79.5	320	24.47	1.006	499	.997	321	321	.836
6	23.35	497	6,850	1,550	80.0	311	23.21	.995	494	1.002	310	310	.807
7	22.85	495	7,350	1,550	80.5	302	22.78	.997	492	1.002	302	302	.787
8	22.30	492	8,000	1,550	81.5	294	22.22	.997	490	1.002	294	294	.766
9	21.70	489	8,600	1,545	82.0	287	21.72	1.000	488	1.000	287	288	.753
10	21.25	485	9,000	1,550	83.0	277	21.39	1.007	486	.999	278	278	.724
11	20.85	484	9,600	1,535	84.0	272	20.90	1.002	484	1.000	272	275	.716
12	20.50	484	10,300	1,540	84.5	270	20.34	.992	482	1.002	268	269	.700
13	20.00	481	10,700	1,545	85.0	266	20.03	.998	480	1.000	265	266	.693
14	19.60	481	11,400	1,545	85.5	259	19.48	.994	478	1.002	258	259	.677
15	19.25	481	11,900	1,545	86.0	256	19.11	.993	476	1.005	255	256	.667
16	18.95	484	12,600	1,545	87.0	251	18.58	.981	473	1.011	249	250	.651
17	18.60	484	13,200	1,545	88.0	247	18.14	.975	471	1.013	244	245	.638

Data from flight No. 2 of a modified DH-4 airplane with a Liberty 12 engine and a standard Martin bomber propeller.



TABLE 3

Reading No.	Atmospheric pressure (inches Hg.)	Atmospheric temperature (°F. Abs.)	Standard altitude (feet)	R. P. M.	Airspeed (M. P. H.)	Observed B. HP.	Standard altitude pressure (inches Hg.)	Pressure correction factor	Standard altitude temperature (°F. Abs.)	Temperature correction factor	B. HP. corrected for T. and P. at observed R. P. M.	Corrected B. HP. at 1,550 R. P. M.	Ratio corrected B. HP. to B. HP. = 384
1	28.60	507	750	1,555	75.0	372	29.22	1.022	516	0.991	377	376	0.979
2	27.55	504	1,800	1,555	76.0	361	28.02	1.017	512	.992	364	363	.946
3	26.55	501	2,900	1,550	76.5	348	26.91	1.013	508	.992	350	350	.911
4	25.80	496	3,500	1,550	77.0	339	26.32	1.021	506	.990	343	343	.893
5	24.95	493	4,400	1,550	77.5	330	25.46	1.021	503	.990	333	333	.867
6	24.25	490	5,150	1,550	78.0	320	24.75	1.021	500	.990	323	323	.841
7	23.65	487	5,800	1,550	78.5	311	24.16	1.021	498	.988	314	314	.818
8	23.00	485	6,550	1,550	79.0	305	23.48	1.021	495	.990	308	308	.802
9	22.40	489	7,700	1,550	80.0	295	22.48	1.002	491	.998	295	295	.768
10	21.85	492	8,650	1,550	81.0	287	21.76	.996	488	1.003	287	287	.747
11	21.40	492	9,300	1,545	82.0	879	21.14	.988	485	1.007	279	280	.729
12	21.60	492	9,900	1,545	82.5	275	20.66	.984	483	1.008	273	274	.713
13	20.75	490	10,300	1,545	83.0	270	20.34	.980	482	1.009	267	268	.698
14	20.40	489	10,700	1,545	83.0	267	20.03	.983	480	1.009	264	265	.690
15	20.10	487	11,000	1,545	83.5	266	19.79	.984	479	1.008	264	265	.690
16	19.75	484	11,350	1,545	84.0	260	19.56	.990	478	1.006	259	260	.677
17	19.40	482	11,800	1,545	84.5	259	19.18	.990	475	1.007	258	259	.674
18	19.05	481	12,250	1,545	85.0	256	18.84	.988	474	1.007	255	256	.667
19	18.75	481	12,750	1,545	85.5	253	18.46	.985	473	1.008	251	252	.656
20	18.50	481	13,150	1,545	86.0	250	18.17	.982	471	1.010	248	249	.648

Data from flight No. 3 of a modified DH-4 airplane with a Liberty 12 engine and a standard Martin bomber propeller.

TABLE 4

Reading No.	Atmospheric pressure (inches Hg.)	Atmospheric temperature (°F. Abs.)	Standard altitude (feet)	R. P. M.	Airspeed (M. P. H.)	Observed B. HP.	Standard altitude pressure (inches Hg.)	Pressure correction factor	Standard altitude temperature (°F. Abs.)	Temperature correction factor	B. HP. corrected for T. and P. at observed R. P. M.	Corrected B. HP. at 1,550 R. P. M.	Ratio corrected B. HP. to B. HP. = 384
1	28.70	509	800	1,560	75.5	379	29.07	1.008	516	0.993	379	377	0.982
2	27.60	508	2,000	1,560	76.5	367	27.82	1.008	511	.997	368	366	.953
3	26.50	503	3,100	1,560	77.5	355	26.72	1.008	507	.994	356	354	.922
4	25.70	500	3,800	1,555	78.0	342	26.03	1.013	505	.995	344	343	.893
5	24.75	497	4,800	1,555	79.0	330	25.08	1.013	501	.996	333	332	.865
6	24.00	497	5,900	1,555	80.0	318	24.07	1.003	497	1.000	319	318	.828
7	23.35	497	6,800	1,555	80.5	311	23.26	.997	494	1.002	311	310	.807
8	22.70	493	7,500	1,555	81.0	303	22.65	.998	492	1.000	303	302	.787
9	22.15	490	8,150	1,555	82.0	293	22.09	.997	489	1.000	292	291	.758
10	21.60	487	8,700	1,550	83.0	286	21.64	1.002	487	1.000	286	286	.745
11	21.10	489	9,500	1,550	84.0	282	20.98	.995	485	1.004	282	282	.734
12	20.70	489	10,300	1,550	84.5	275	20.34	.984	482	1.008	273	273	.711
13	20.30	487	10,700	1,550	85.0	270	20.03	.987	480	1.007	268	268	.698
14	19.90	486	11,250	1,550	85.5	266	19.60	.995	478	1.007	266	266	.682
15	19.55	484	11,700	1,550	86.0	260	19.26	.995	477	1.008	260	260	.677
16	19.30	482	11,950	1,545	86.5	256	19.07	.988	476	1.006	255	256	.667
17	19.05	481	12,250	1,545	87.0	253	18.84	.989	475	1.006	252	253	.657
18	18.75	481	12,750	1,545	88.0	248	18.47	.985	473	1.008	246	247	.643
19	18.60	481	12,950	1,545	89.0	244	18.32	.984	472	1.008	242	243	.633
20	18.40	480	13,200	1,545	90.0	241	18.14	.986	471	1.011	240	241	.627

Data from flight No. 4 of a modified DH-4 airplane with a Liberty 12 engine and a standard Martin bomber propeller.



TABLE 5

Reading No.	Atmospheric pressure (inches Hg.)	Atmospheric temperature (°F. Abs.)	Standard altitude (feet)	R. P. M.	Airspeed (M. P. H.)	Observed B. HP.	Standard altitude pressure (inches Hg.)	Pressure correction factor	Standard altitude temperature (°F. Abs.)	Temperature correction factor	B. HP. corrected for T and P. at observed R. P. M.	Corrected B. HP. at 1,550 R. P. M.	Ratio corrected B. HP. to B. HP. <sub>0</sub> =384
1	27.85	497	1,050	1,545	66.0	363	28.80	1.033	515	0.982	368	369	0.961
2	26.90	497	2,200	1,545	67.5	350	27.62	1.027	511	.986	354	355	.924
3	26.00	496	3,250	1,545	68.0	340	26.57	1.022	507	.990	344	345	.898
4	25.25	494	4,100	1,545	69.0	329	25.74	1.018	504	.991	332	333	.867
5	24.40	490	5,000	1,545	70.0	319	24.89	1.019	501	.989	321	322	.839
6	23.75	490	5,800	1,540	70.0	309	24.16	1.017	498	.992	312	314	.818
7	23.15	490	6,750	1,535	71.0	301	23.30	1.007	494	.995	301	304	.792
8	22.65	490	7,400	1,535	71.5	294	22.74	1.004	492	.998	294	297	.773
9	22.25	490	8,000	1,540	72.0	289	22.22	1.000	490	1.000	289	291	.758
10	21.90	487	8,300	1,545	72.0	284	21.97	1.002	489	.998	284	285	.742

Data from flight No. 5 of a modified DH-4 airplane with a Liberty 12 engine and a standard Martin bomber propeller.

TABLE 6

Reading No.	Atmospheric pressure (inches Hg.)	Atmospheric temperature (°F. Abs.)	Standard altitude (feet)	Carburetor air temperature (°F. Abs.)	R. P. M.	Airspeed (M. P. H.)	Observed B. HP.	Standard altitude pressure (inches Hg.)	Pressure correction factor	Standard altitude temperature (°F. Abs.)	Temperature correction factor	B. HP. corrected for T. and P. at observed R. P. M.	Corrected B. HP. at 1,550 R. P. M.	Ratio corrected B. HP. to B. HP. <sub>0</sub> =384
1	29.40	509	50	518	1,550	65.5	379	29.86	1.016	518	0.991	378	378	0.984
2	28.25	505	1,100	521	1,545	66.0	368	28.75	1.017	515	.991	367	368	.958
3	27.40	502	1,950	520	1,545	67.0	354	27.87	1.017	511	.991	353	354	.922
4	26.50	498	2,750	515	1,540	67.5	345	27.06	1.021	509	.990	345	347	.904
5	25.80	493	3,300	509	1,540	68.0	337	26.52	1.028	507	.987	338	340	.885
6	25.10	491	4,100	507	1,540	69.0	328	25.74	1.025	504	.987	328	330	.860
7	24.50	488	4,700	505	1,540	69.5	321	25.17	1.027	502	.986	322	324	.844
8	24.00	495	5,800	508	1,540	70.5	315	24.16	1.007	498	.996	316	317	.826
9	23.50	498	6,750	512	1,545	71.0	309	23.31	.992	494	1.004	308	309	.805
10	23.00	498	7,400	514	1,545	72.0	303	22.74	.988	492	1.007	301	302	.786
11	22.50	498	8,200	514	1,545	73.0	297	22.05	.980	489	1.010	294	295	.768
12	22.05	496	8,700	513	1,545	73.5	290	21.64	.981	487	1.008	287	288	.750
13	21.65	493	9,100	510	1,545	73.5	284	21.30	.984	486	1.008	282	283	.737
14	21.25	493	9,600	509	1,545	74.0	276	20.90	.983	484	1.011	274	275	.716
15	20.95	491	10,000	508	1,540	74.0	273	20.58	.982	483	1.008	270	272	.708
16	20.60	488	10,400	508	1,535	73.0	267	20.26	.984	481	1.008	265	268	.698
17	20.20	485	10,800	507	1,535	71.0	263	19.95	.988	480	1.006	262	265	.690
18	19.90	484	11,100	507	1,535	71.5	260	19.72	.991	479	1.006	259	262	.682
19	19.70	482	11,300	505	1,535	73.5	257	19.56	.994	479	1.002	256	259	.674
20	19.40	482	11,800	503	1,535	75.0	254	19.18	.988	476	1.006	253	256	.667
21	19.25	482	12,100	501	1,535	76.0	251	18.96	.985	475	1.007	249	252	.656
22	19.10	480	12,200	501	1,535	77.0	248	18.88	.988	475	1.007	247	250	.651
23	18.90	479	12,400	499	1,535	77.0	247	18.73	.991	474	1.006	246	249	.648

Data from flight No. 6 of a modified DH-4 airplane with a Liberty 12 engine and a standard Martin bomber propeller.



---

---

## REPORT No. 296

---

### PRESSURE DISTRIBUTION TESTS ON PW-9 WING MODELS FROM $-18^\circ$ THROUGH $90^\circ$ ANGLE OF ATTACK

By OSCAR E. LOESER, Jr.  
Langley Memorial Aeronautical Laboratory





## REPORT No. 296

### PRESSURE DISTRIBUTION TESTS ON PW-9 WING MODELS FROM $-18^\circ$ THROUGH $90^\circ$ ANGLE OF ATTACK

By OSCAR E. LOESER, Jr.

#### SUMMARY

*At the request of the Army Air Corps, an investigation of the pressure distribution over PW-9 wing models was conducted in the atmospheric wind tunnel of the National Advisory Committee for Aeronautics. The primary purpose of these tests was to obtain wind-tunnel data on the load distribution on this cellule to be correlated with similar information obtained in flight tests, both to be used for design purposes. Because of the importance of the conditions beyond the stall as affecting control and stability, this investigation was extended through  $90^\circ$  angle of attack. The results for the range of normal flight have been given in N. A. C. A. Technical Report No. 271. The present paper presents the same results in a different form and includes, in addition, those over the greater range of angle of attack,  $-18^\circ$  through  $90^\circ$ .*

*The results show that—*

*At angles of attack above maximum lift, the biplane upper wing pressures are decreased by the shielding action of the lower wing.*

*The burble of the biplane lower wing, with respect to the angle of attack, is delayed, due to the influence of the upper wing.*

*The center of pressure of the biplane upper wing (semispan) is, in general, displaced forward and outward with reference to that of the wing as a monoplane, while for the lower wing there is but slight difference for both conditions.*

*The overhanging portion of the upper wing is little affected by the presence of the lower wing.*

#### INTRODUCTION

The increased speeds and maneuverability of modern pursuit airplanes call for careful consideration of design and of wing loads over a large range of angle of attack. Similarly, the consideration being given to stability and control above the stall requires an extension of the usual range of pressure distribution investigations. To this end, at the request of the Army Air Corps, the distribution of pressure over the wing models of a modern pursuit airplane, PW-9, has been investigated in the atmospheric wind tunnel of the National Advisory Committee for Aeronautics (Reference 1). The test results were given in part in N. A. C. A. Technical Report No. 271 (Reference 2). In the present paper the pressures are plotted (normal to the chord) as resultant or total pressures from  $-18^\circ$  through  $90^\circ$  angle of attack, while in the former report they were plotted as individual upper and lower surface pressures in the conventional manner over the range of normal flight.

#### APPARATUS AND METHODS

Half-span, laminated wooden models accurate to  $\pm 0.003$ -inch, with inlaid pressure tubes of 0.032-inch bore, were used in this investigation. (Fig. 1.) These models were 1:9.6 scale of the PW-9 airplane cellule and of Göttingen 436 airfoil section throughout. (Fig. 2.) The most unusual features of this biplane cellule are the difference in plan form of the wings and the increased angle of incidence of the center section. Three-foot to four-foot lengths of  $\frac{3}{16}$ -inch, inside diameter, rubber tubing served to connect the pressure tubes of the manometer.

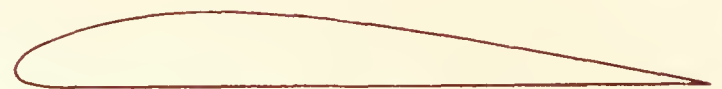


Compensation was made for the missing half span by means of a reflecting plane. (Figs. 3 and 4.) Static and dynamic pressure surveys were made normal to this plane two chord lengths ahead of the models, and, as expected, the velocity close to the plane was found lower than that in the free stream above it. This condition was remedied by slightly bending the leading edge of the reflecting plane downward.

The integrated mean pressures of the final surveys were used to calibrate a Pitot static tube, located 3 feet ahead of the honeycomb, forward of the test section. This tube was then used to maintain an air speed of approximately 30 meters per second.



FIG. 1.—PW-9 Pressure-distribution wing models



*Göttingen 436 airfoil*

Station per cent chord	Upper per cent chord	Lower per cent chord
0	2.85	2.85
1¼	4.59	1.21
2½	5.54	0.69
5	6.86	0.37
7½	8.02	0.21
10	8.92	0.05
15	10.03	0.00
20	10.82	0.00
30	11.08	0.00
40	10.55	0.00
50	9.60	0.00
60	8.28	0.00
70	6.60	0.00
80	4.70	0.00
90	2.59	0.00
95	1.43	0.00
100	0.26	0.00

In calculating the results, no allowance was made for the change in dynamic and static pressure with increasing angle of attack due to the blocking of the air stream by the models, since an evaluation of this effect would have required a separate investigation. Consequently, above maximum lift the accuracy of the results may be expected to decrease slightly.

To obtain a pressure distribution record as shown in Figure 5, the model was set at the desired angle of attack and an exposure made upon a sheet of photostat paper held against the manometer tubes, after a constant condition of pressures had been obtained. The recorded pressures were then scaled off accurately, tabulated, and plotted to obtain the individual test section pressure distribution curves. A comprehensive discussion of airfoil pressure distribution principles is given in Reference 3.



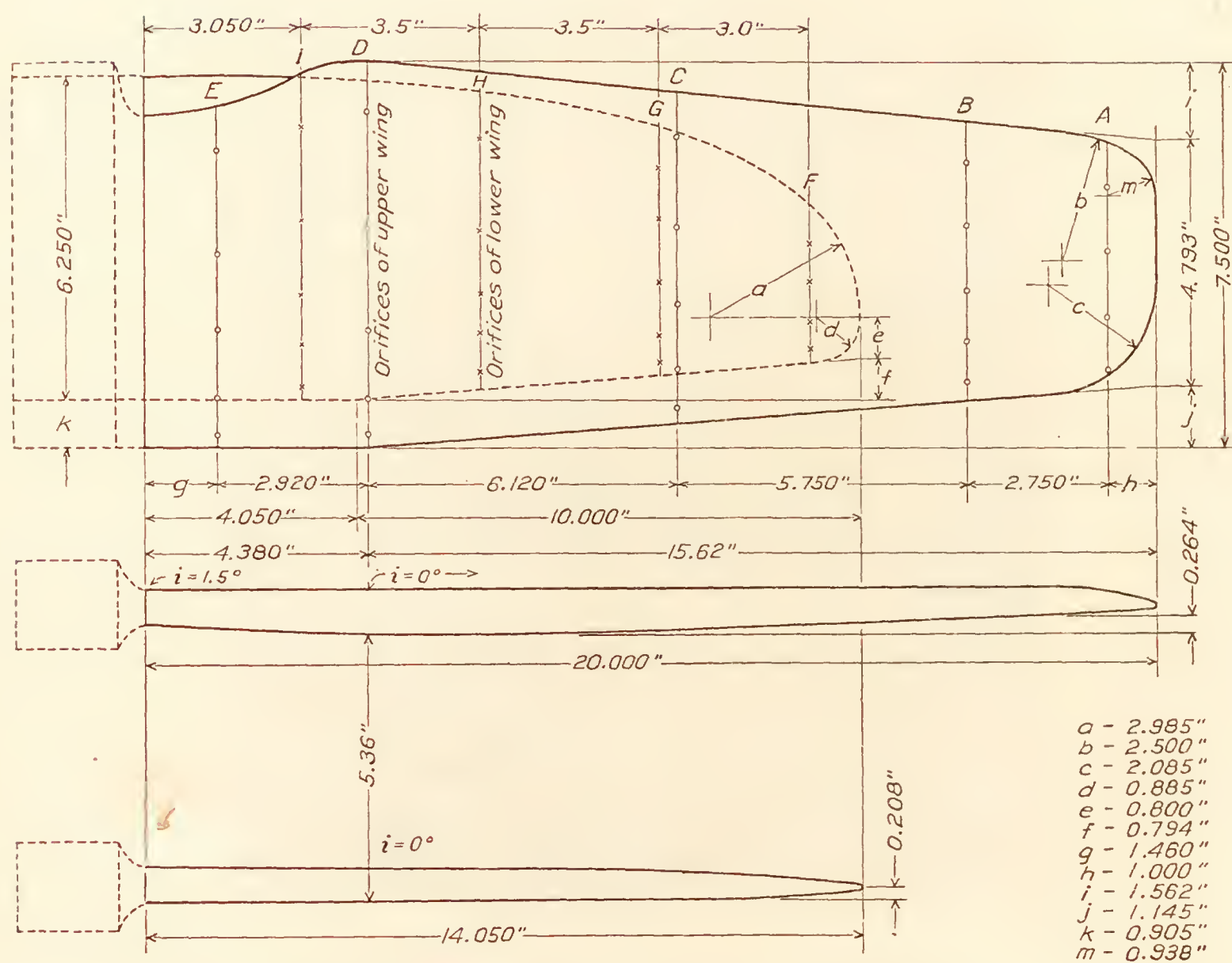


FIG. 2.—Plan and front elevation of PW-9 wing models. Göttingen 436 airfoil

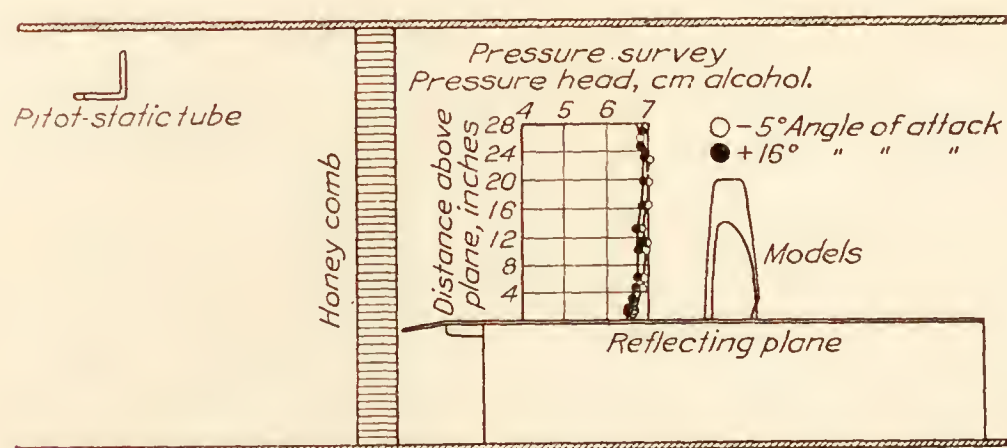


FIG. 3.—Longitudinal section of wind tunnel



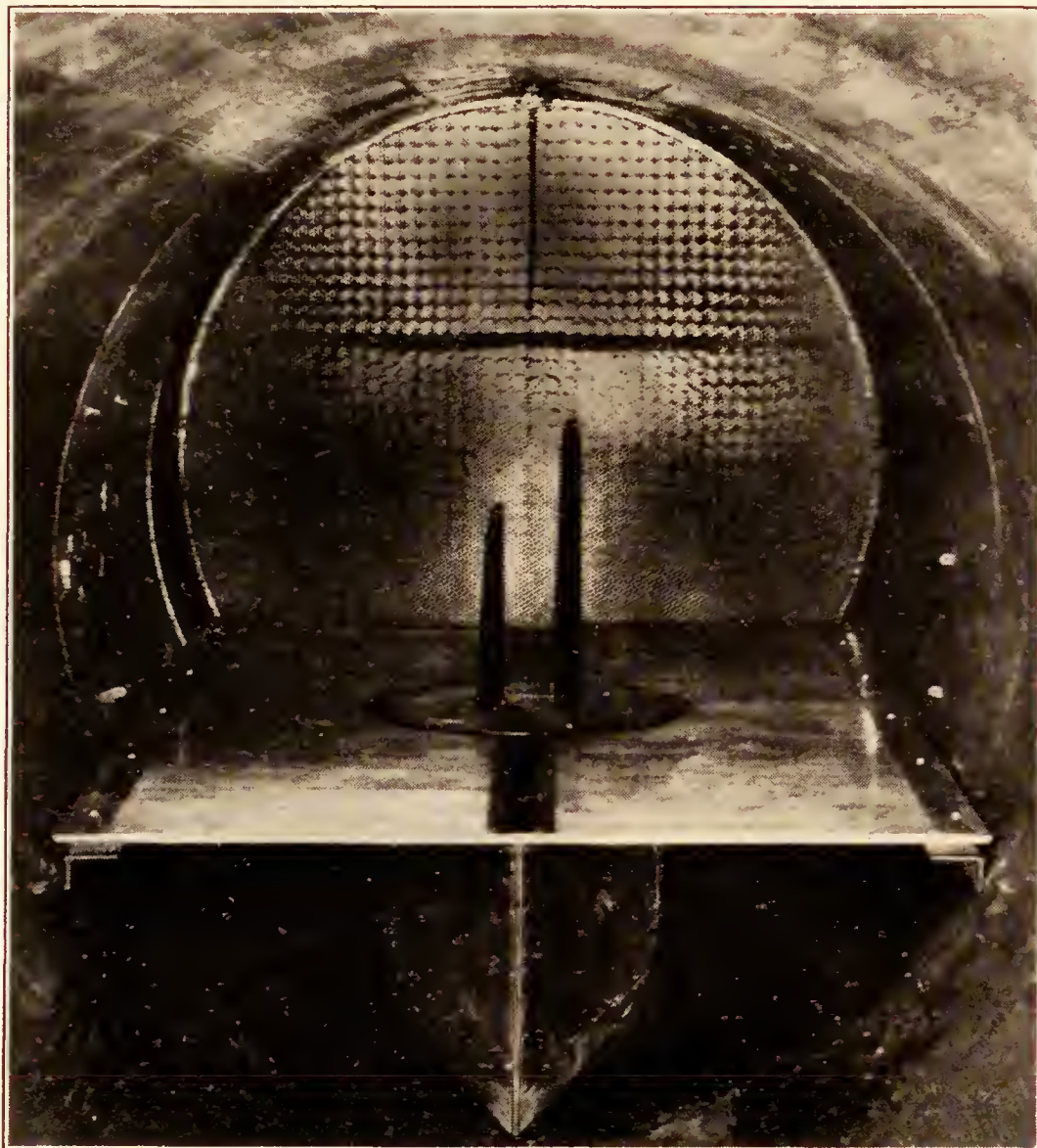


FIG. 4.—PW-9 wing models in wind tunnel

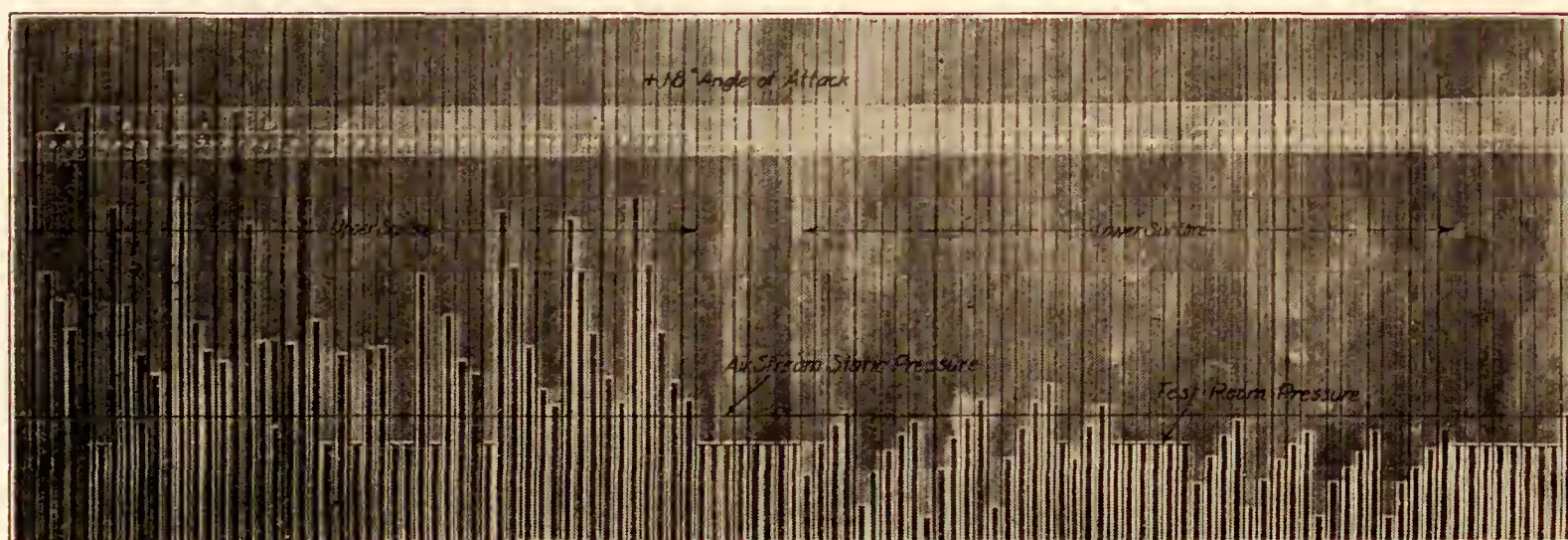


FIG. 5.—Reduced photograph of a manometer record



The final curves are estimated to be accurate to within about  $\pm 3$  per cent, for the planimetry of the pressure distribution curves was held to within 1 per cent, while the fairing of the curves was susceptible to errors of possibly 2 to 3 per cent.

The Reynolds Number based on the weighted mean chord was approximately 300,000.

### RESULTS

It was possible to obtain the resultant normal pressures directly from the algebraic difference of the recorded surface pressures, inasmuch as the upper surface orifices were located directly above the corresponding orifices in the lower surface of each wing. These resultant pressures in terms of dynamic pressure,

$$q = \frac{1}{2} \rho V^2$$

where

$\rho$  = air density

$V$  = air speed

for the wing models separately and in their mutual relation in the biplane cellule, were plotted as ordinates in their respective positions on the isometric projection of the wings. (Figs. 6-18.) The pressure diagrams are drawn through the test points in every case; but in order to avoid congestion these points are not shown. This manner of presentation of pressure distribution offers a direct comparison of pressures between the various test sections over the wing, and also between the monoplane and biplane pressures.

Variation of the coefficient of normal force  $C_{NF_1}$ , at each test section along the semispan, is shown in Figures 19 and 20.  $C_{NF_1}$  is the mean pressure in terms of  $q$  of the individual test sections.

Figure 21 illustrates the variation of coefficient of normal force,  $C_{NF}$ , for each wing and for the biplane cellule; with change of angle of attack. The value of  $C_{NF}$  was obtained from the integrated mean of the respective  $C_{NF_1}$  curves. That for the biplane cellule was obtained from the weighted sum of  $C_{NF}$  for both wings.

$$C_{NF_b} = C_{NF_u} \times \frac{S_u}{S_t} + C_{NF_l} \times \frac{S_l}{S_t}$$

$C_{NF_b}$  = normal force coefficient for the biplane cellule.

$C_{NF_u}$  = normal force coefficient for the biplane upper wing.

$C_{NF_l}$  = normal force coefficient for the biplane lower wing.

$S_u$  = area of upper wing.

$S_l$  = area of lower wing.

$S_t$  = total area of both wings.

The distribution of load along the span, in terms of a nondimensional coefficient  $K$ , is shown in Figures 22 and 23.

$$K = \frac{C_{NF} \times \text{chord}}{\text{mean chord}}$$

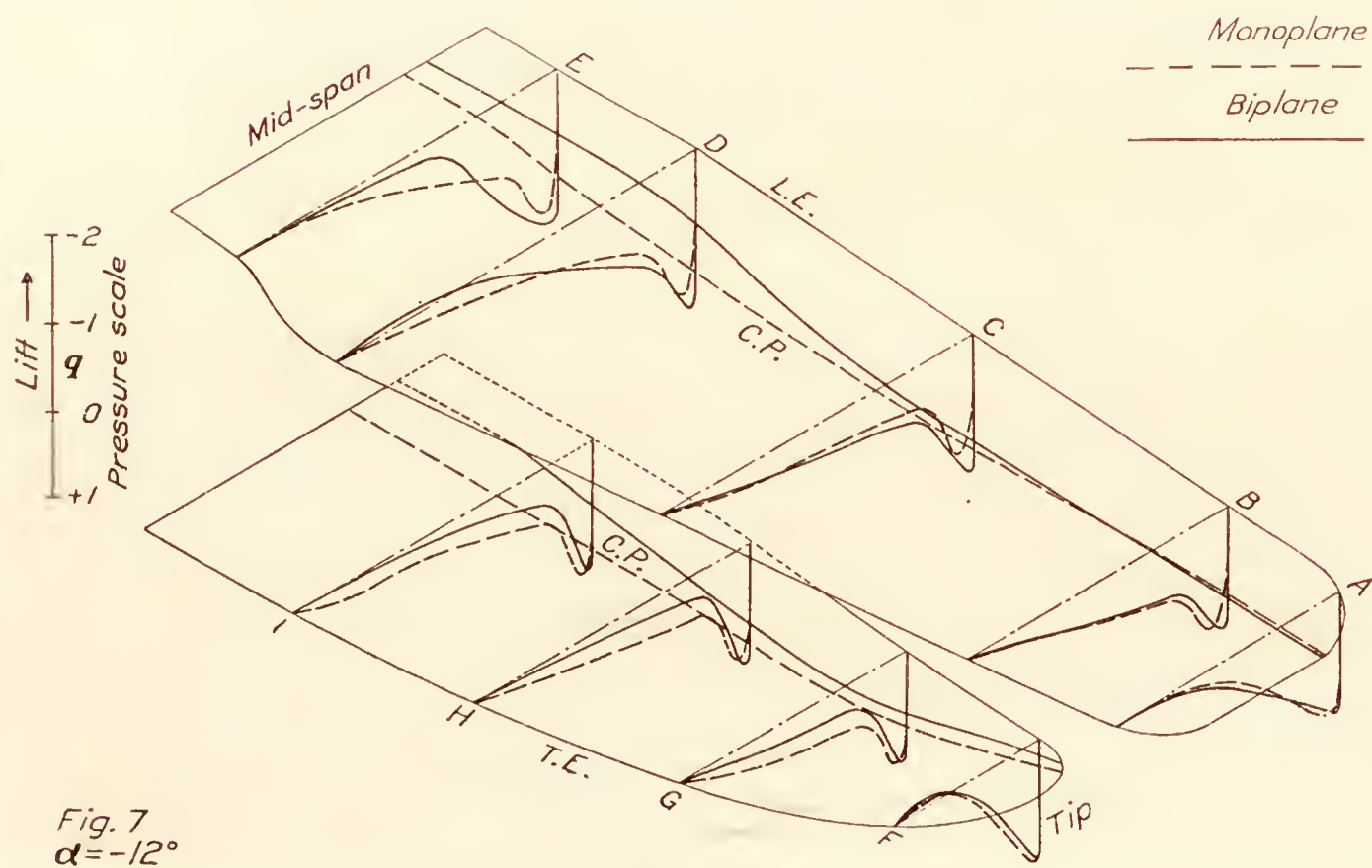
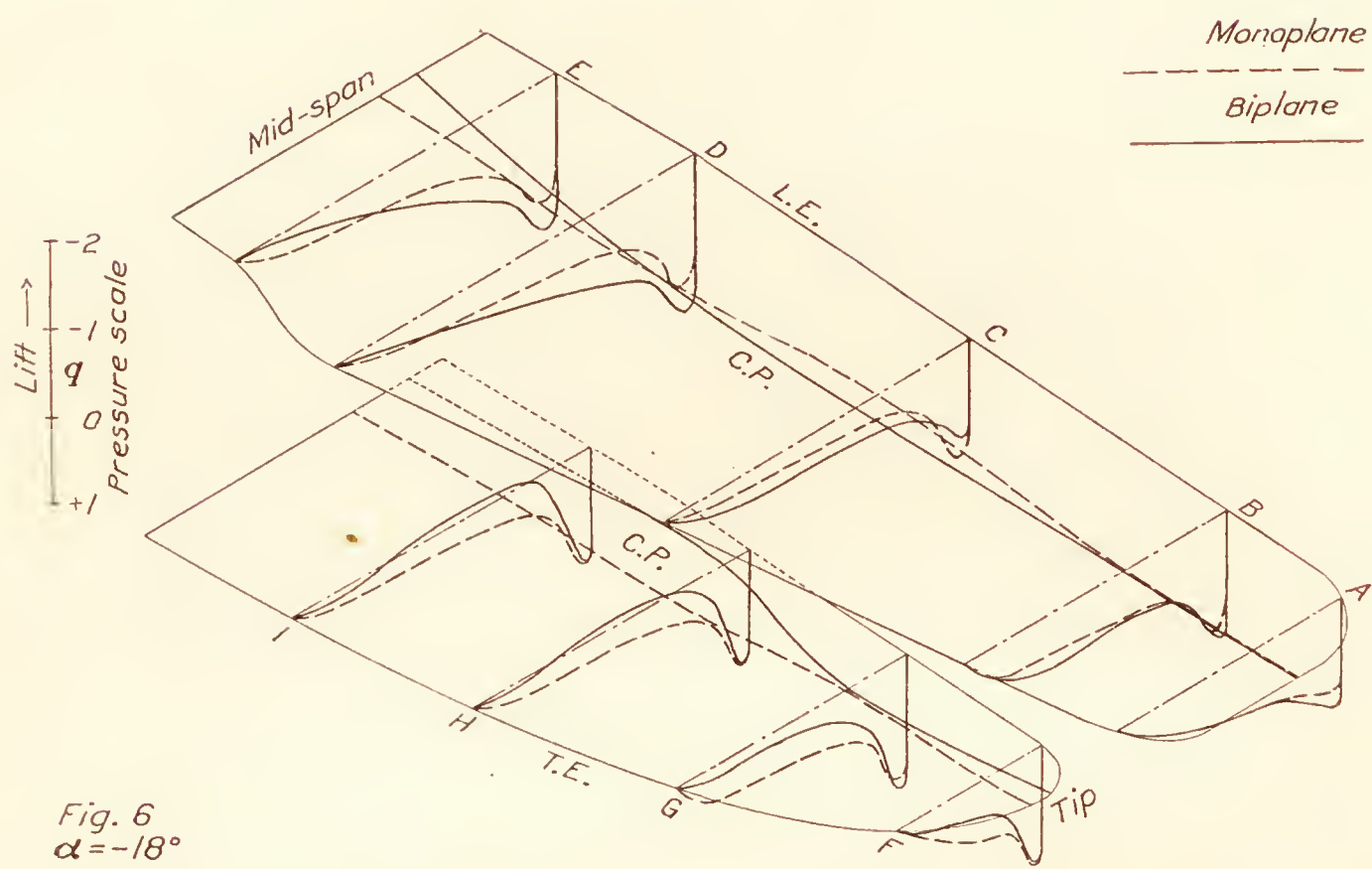
Due to the irregular plan form of the wings, the longitudinal center of pressure  $C_p$ , positions were plotted on the mean chord of each wing in their respective positions in the biplane. (Fig. 24.) The mean chord was obtained by dividing the area by the span, and the mean  $C_p$  was derived from the integrated mean of the  $C_p$  curves as plotted on the isometric diagrams. The biplane cellule center of pressure was computed as the equivalent moment arm of the forces on both wings from the center section leading edge of the upper wing:

$$C_{pb} = \frac{C_{NF_u} \times S_u \times a + C_{NF_l} \times S_l \times b}{C_{NF_u} \times S_u + C_{NF_l} \times S_l}$$

$C_{pb}$  = center of pressure of biplane cellule.

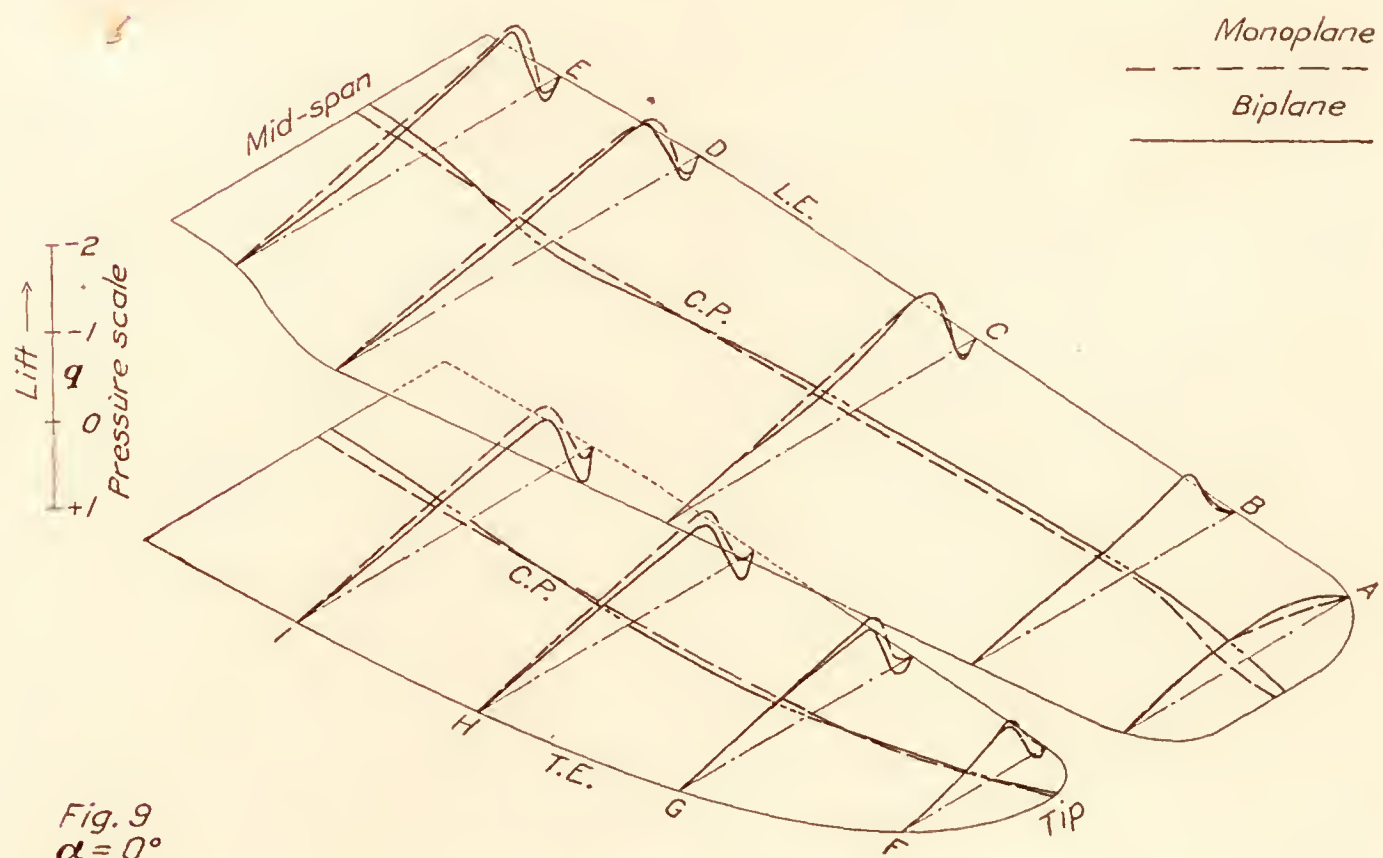
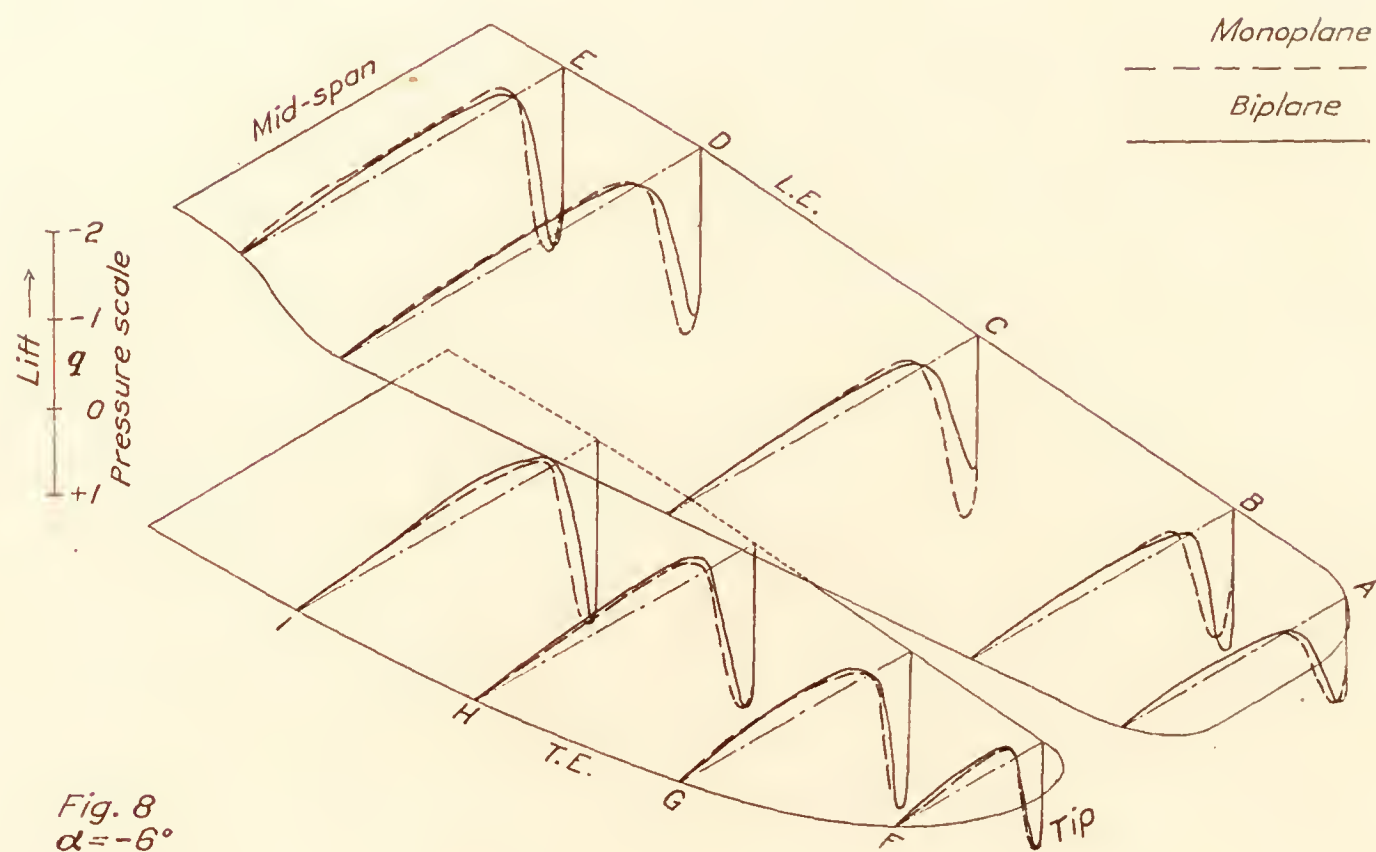
$a$  = position of  $C_p$  of upper wing back of center section leading edge.

$b$  = position of  $C_p$  of lower wing back of upper wing center section leading edge.

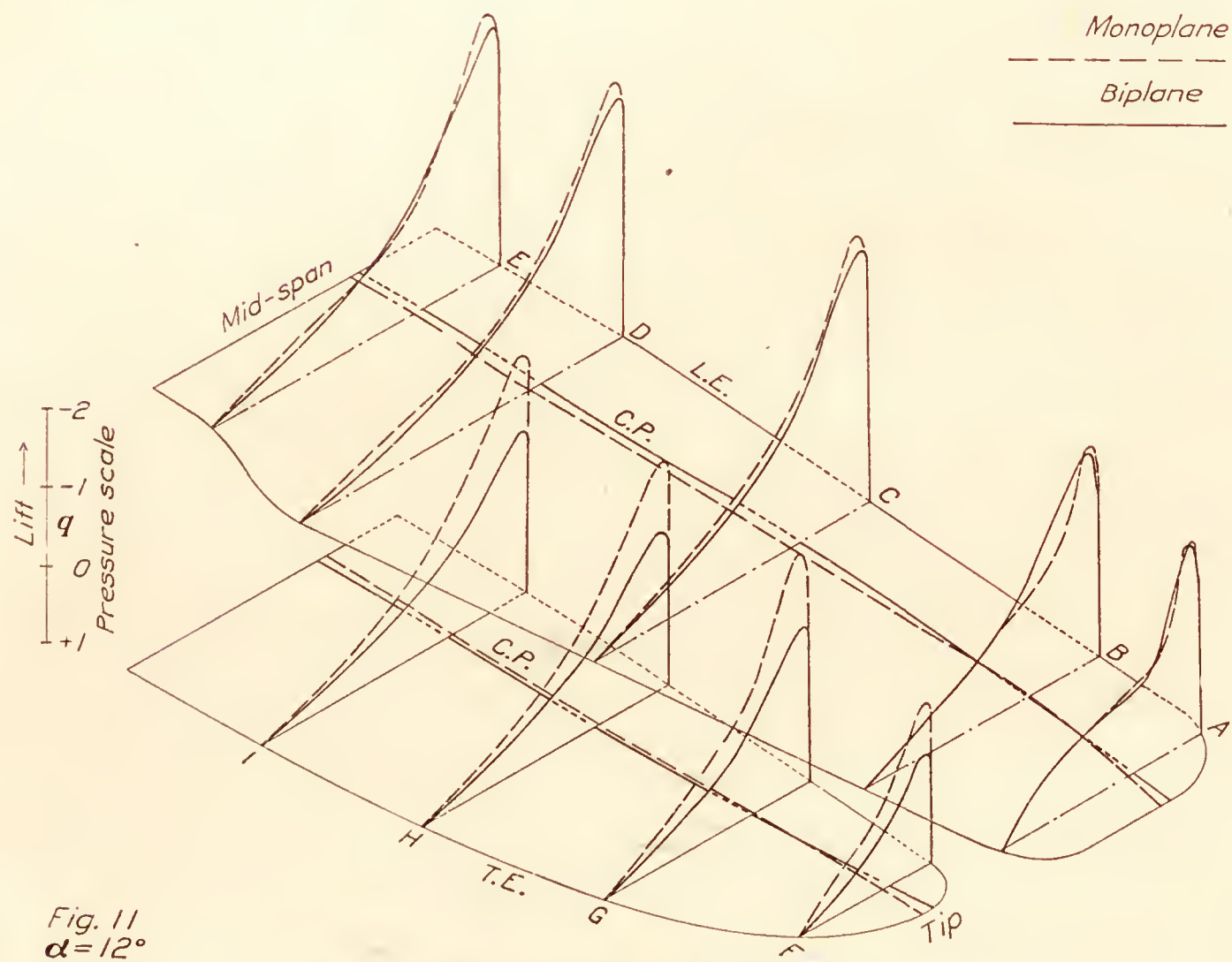
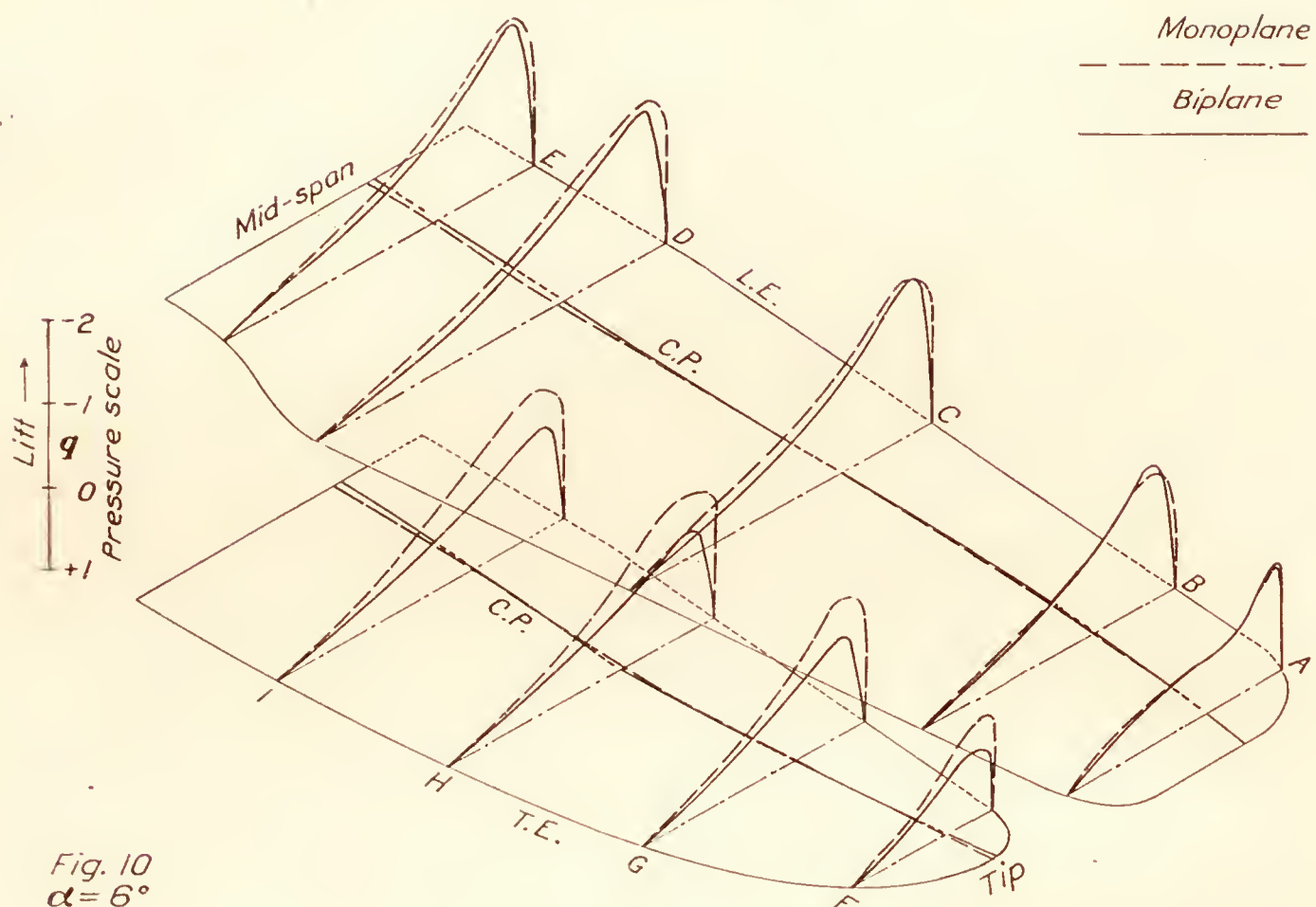


FIGS. 6 and 7.—Total normal pressure distribution



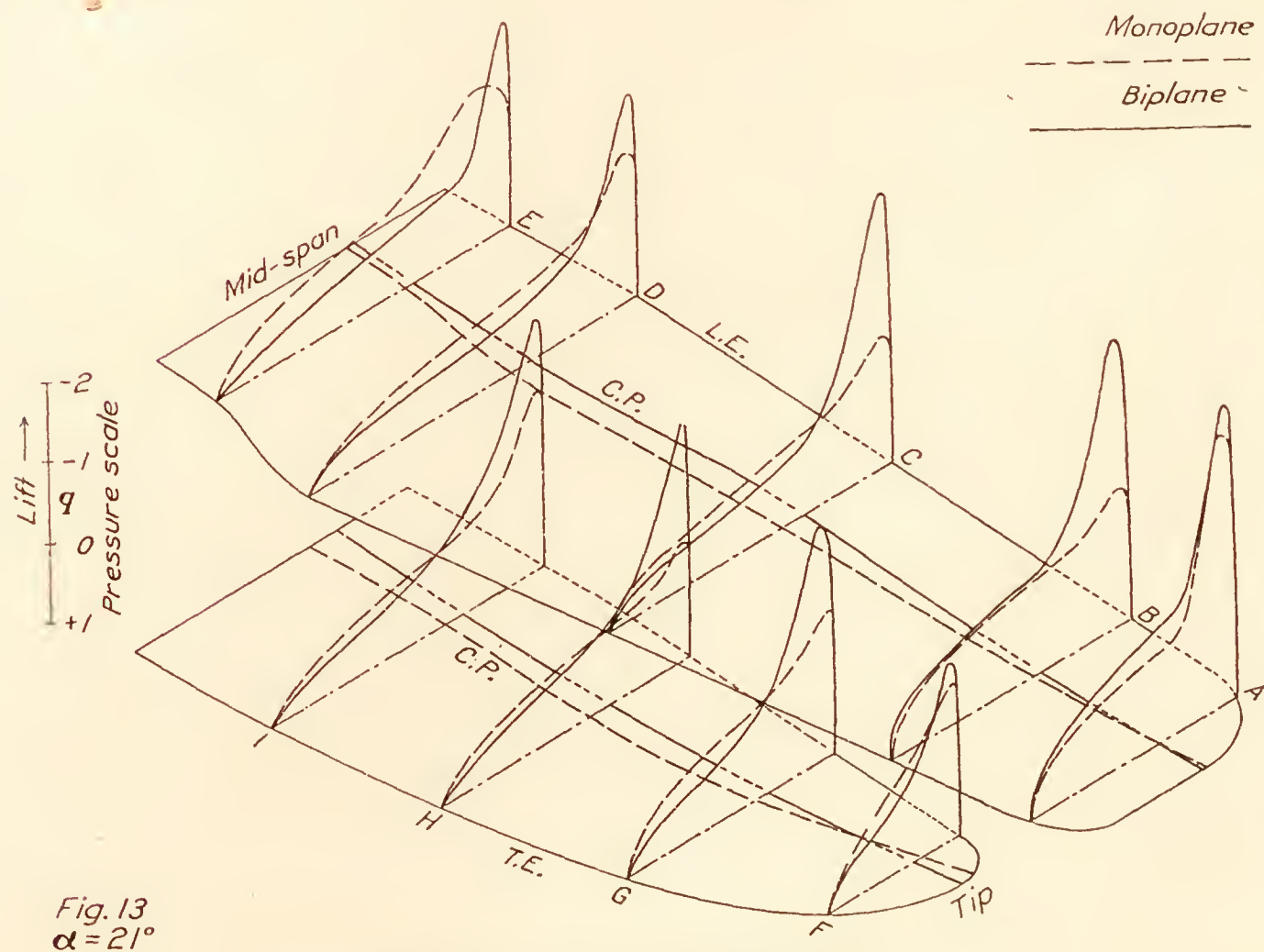
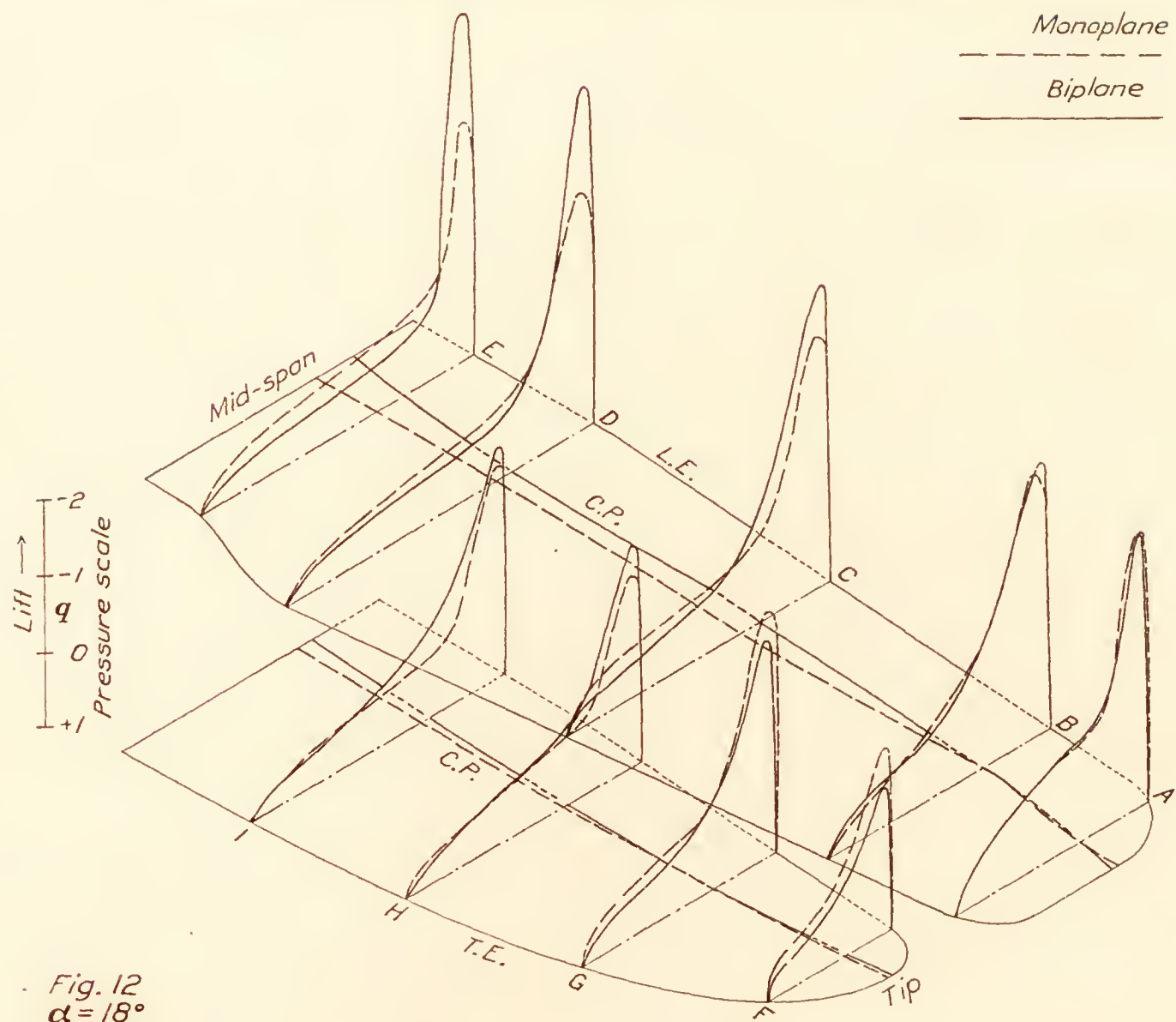


FIGS. 8 and 9.—Total normal pressure distribution



FIGS. 10 and 11.—Total normal pressure distribution





FIGS. 12 and 13.—Total normal pressure distribution

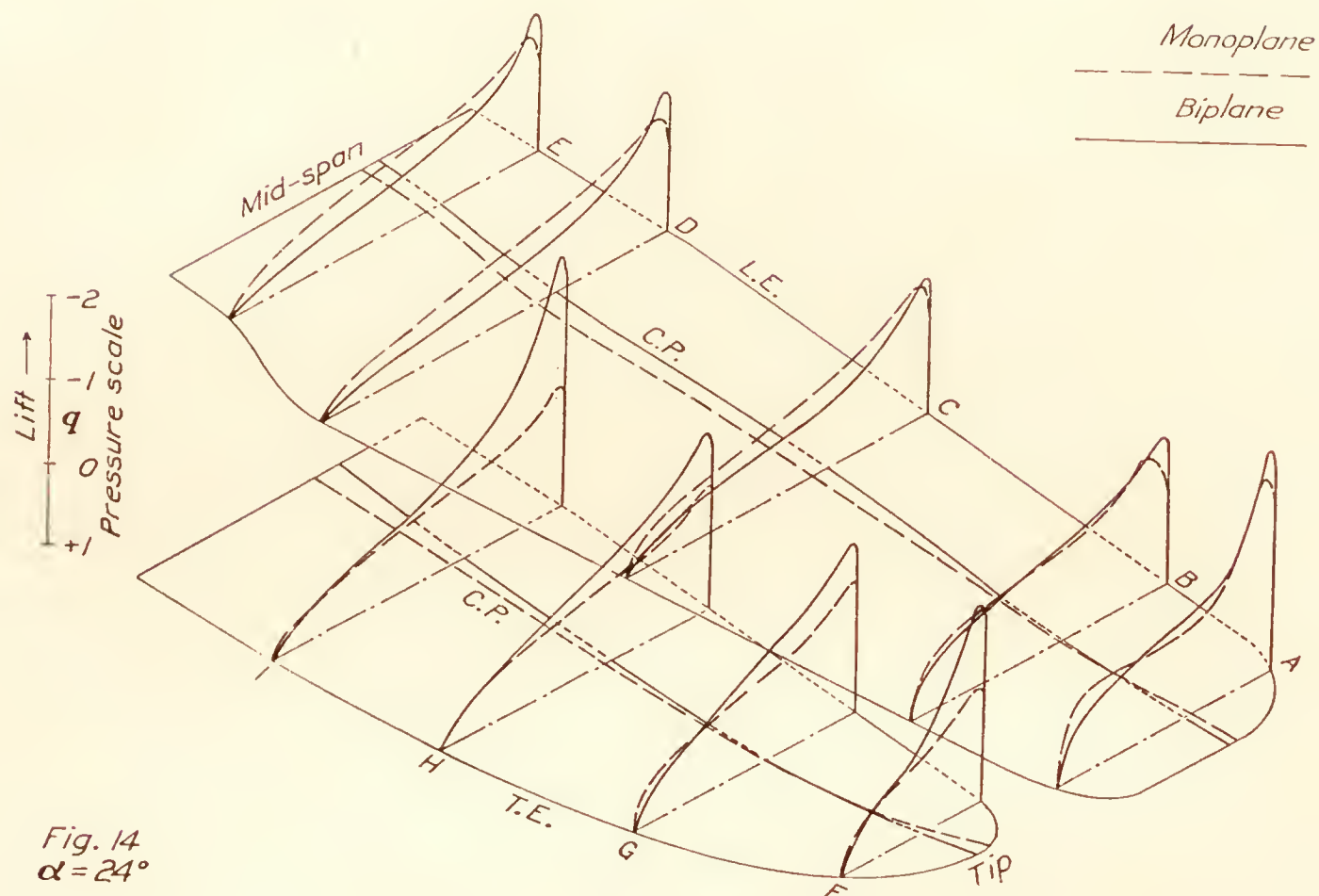


Fig. 14  
 $\alpha = 24^\circ$

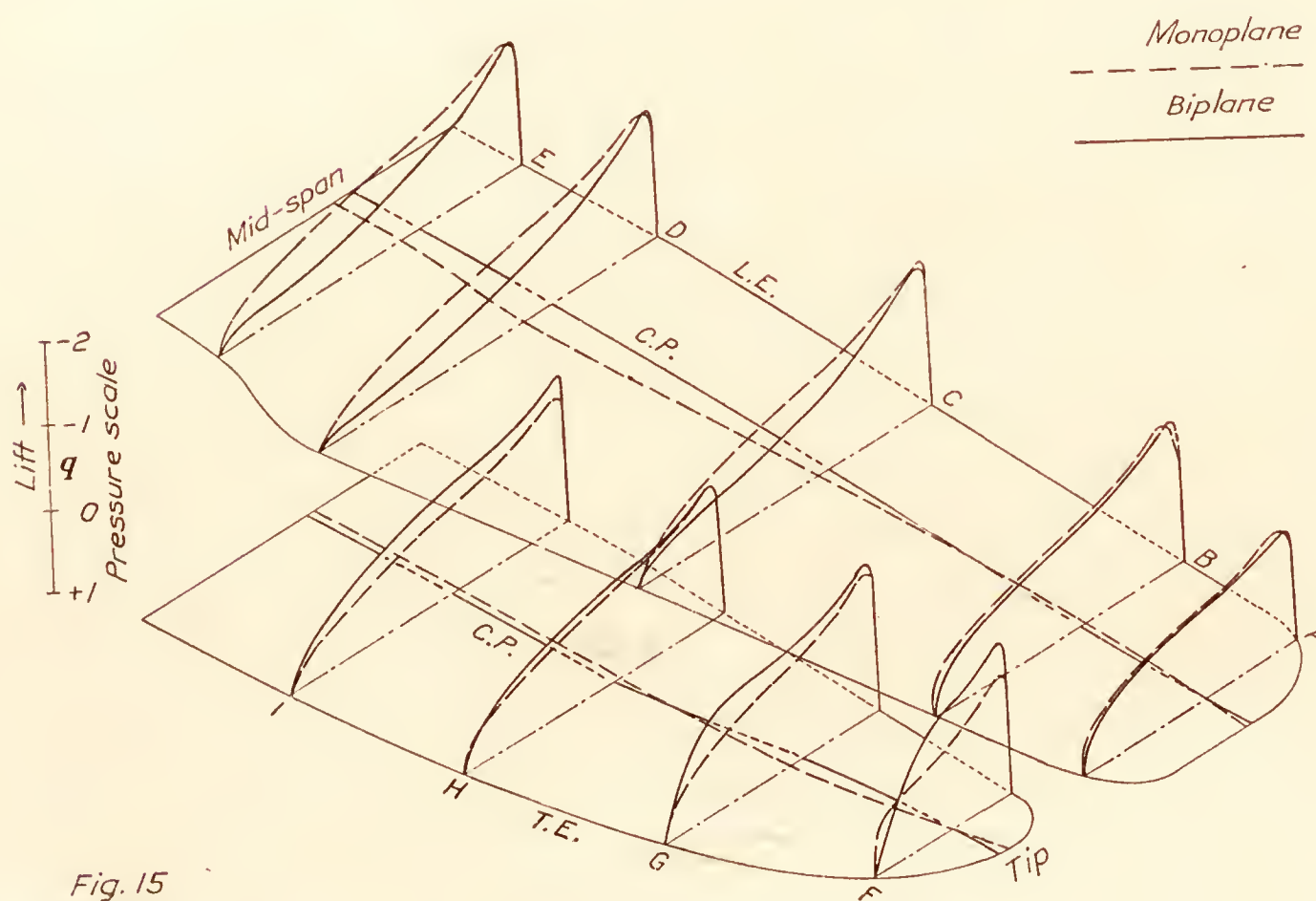


Fig. 15  
 $\alpha = 30^\circ$

FIGS. 14 and 15.—Total normal pressure distribution



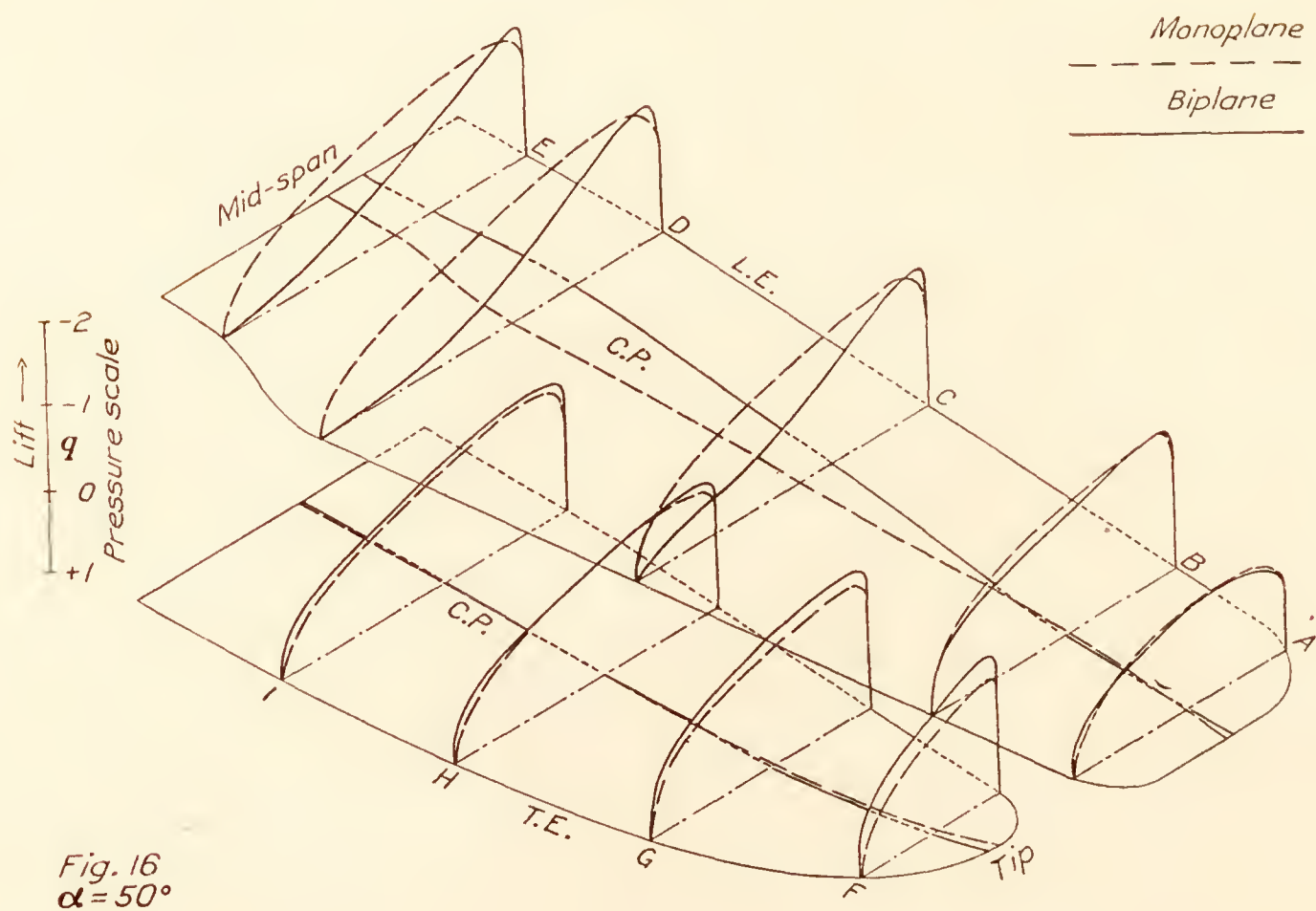


Fig. 16  
 $\alpha = 50^\circ$

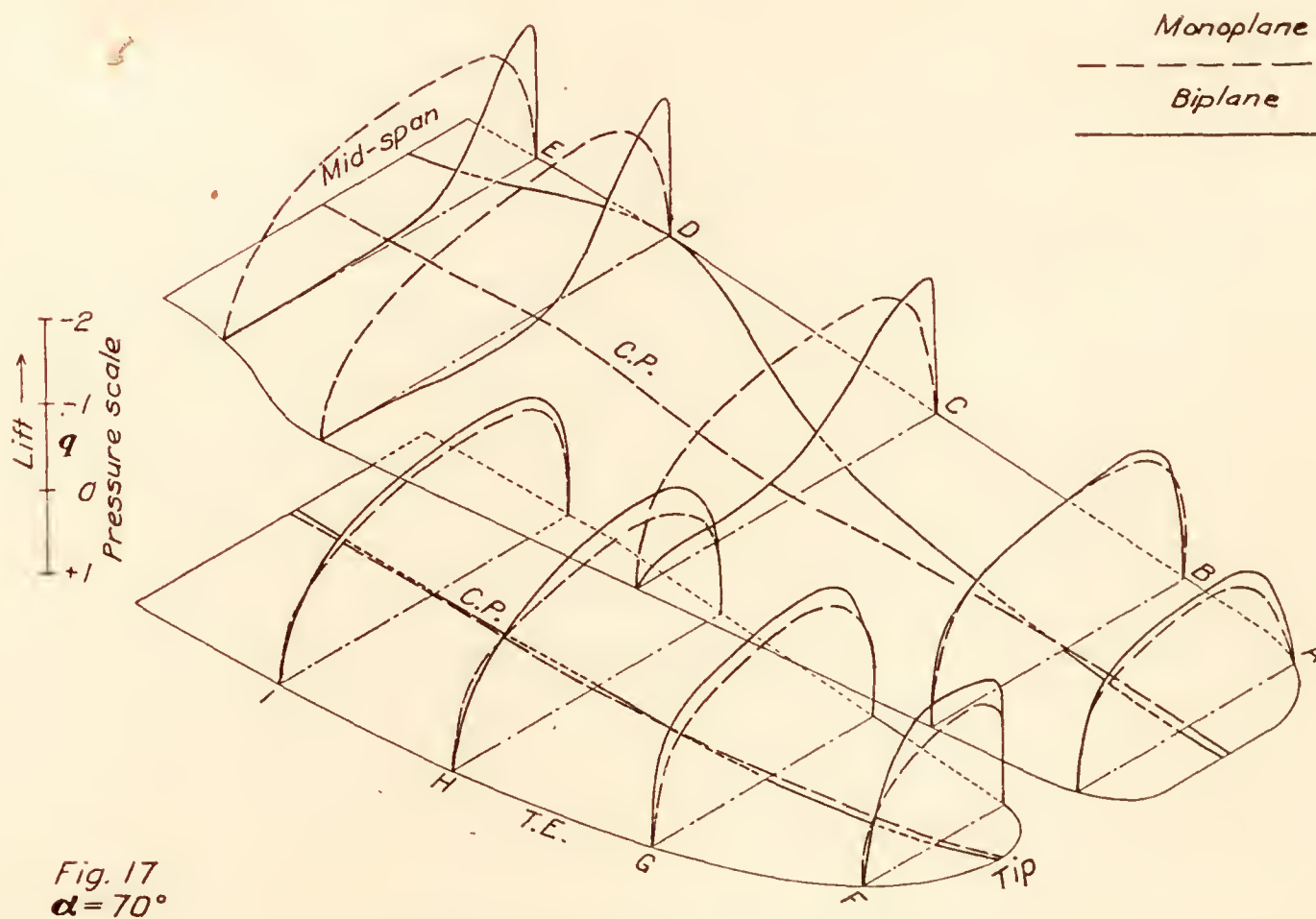


Fig. 17  
 $\alpha = 70^\circ$

Figs. 16 and 17.—Total normal pressure distribution

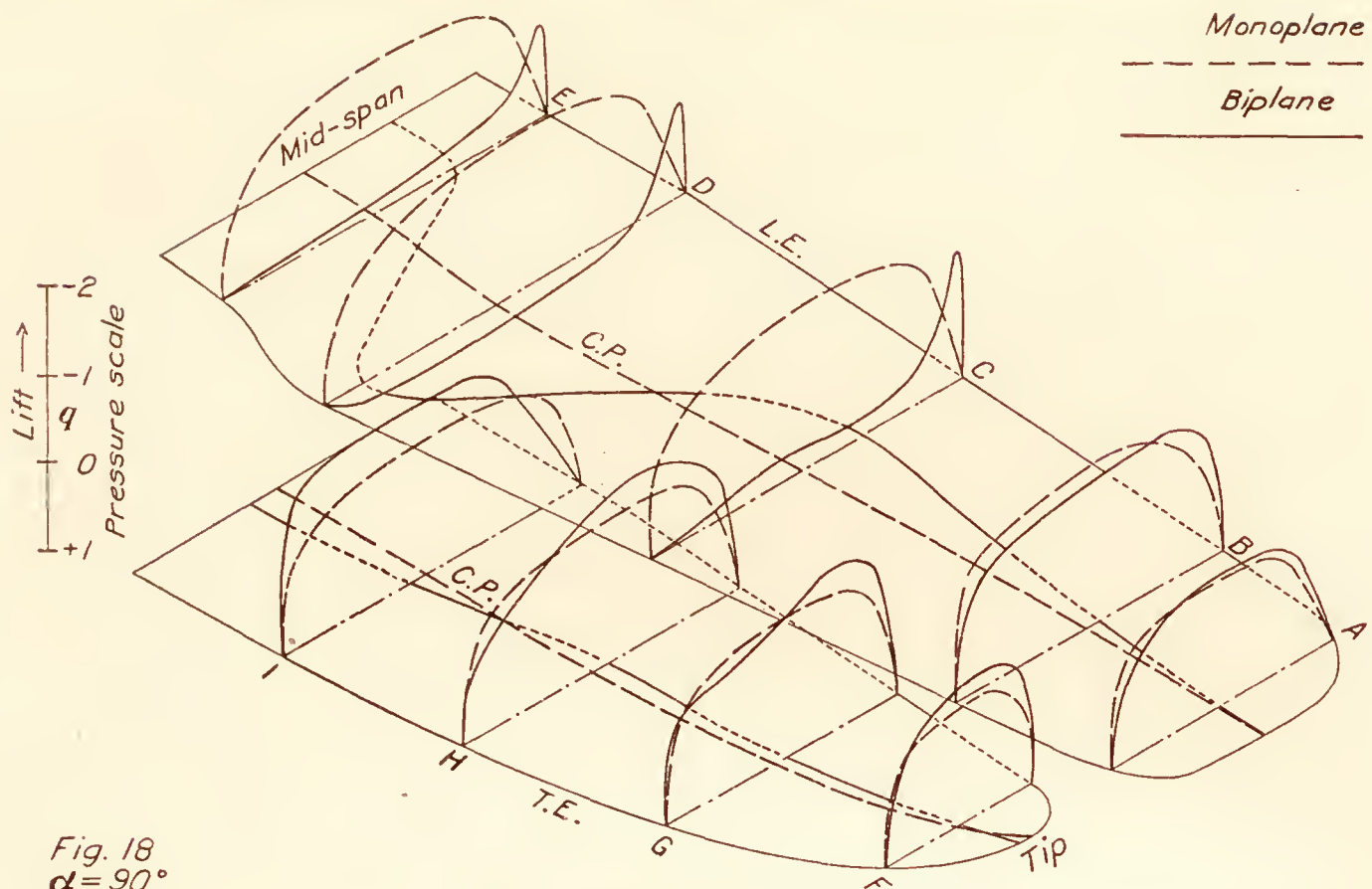
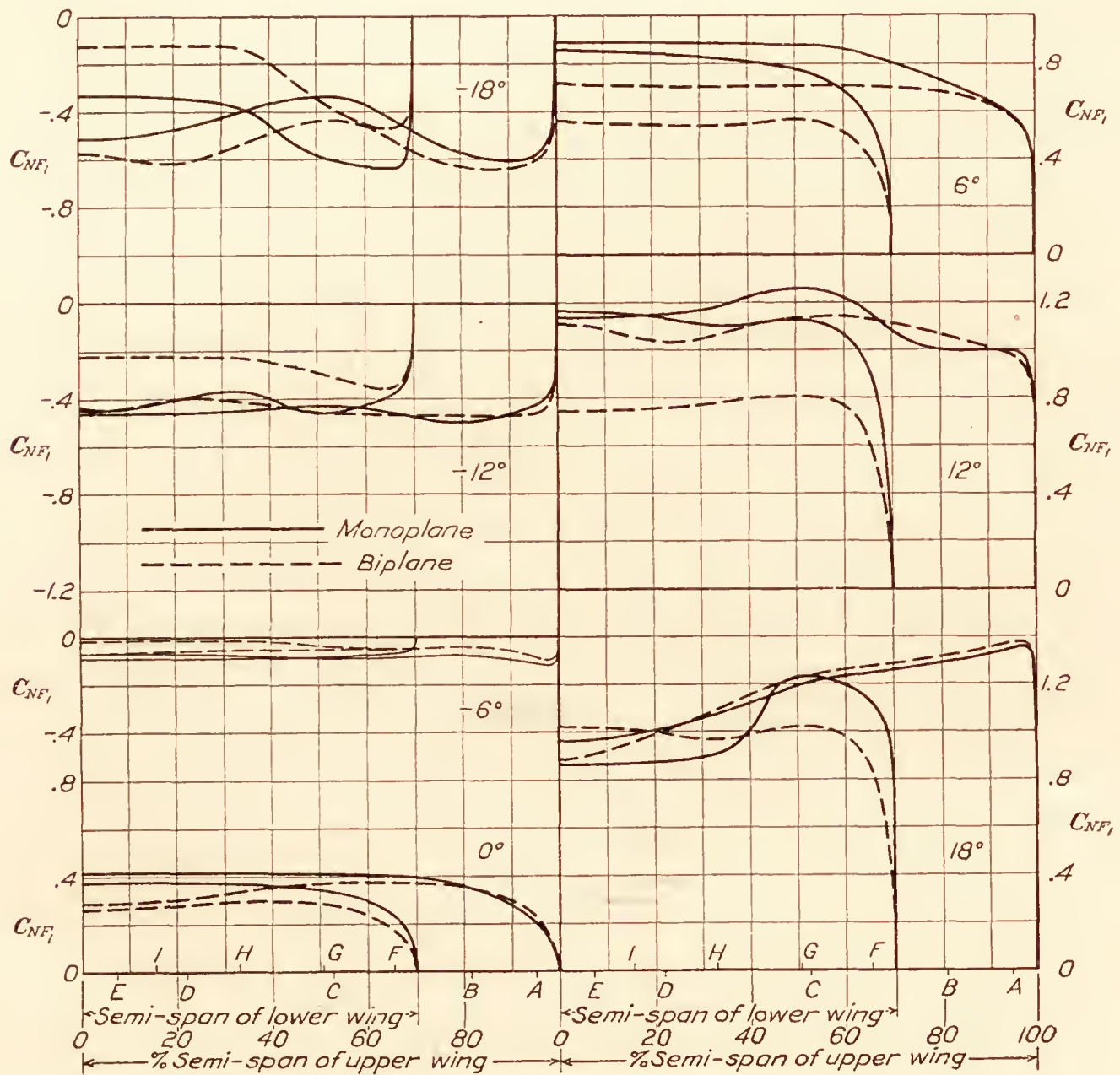


FIG. 18.—Total normal pressure distribution





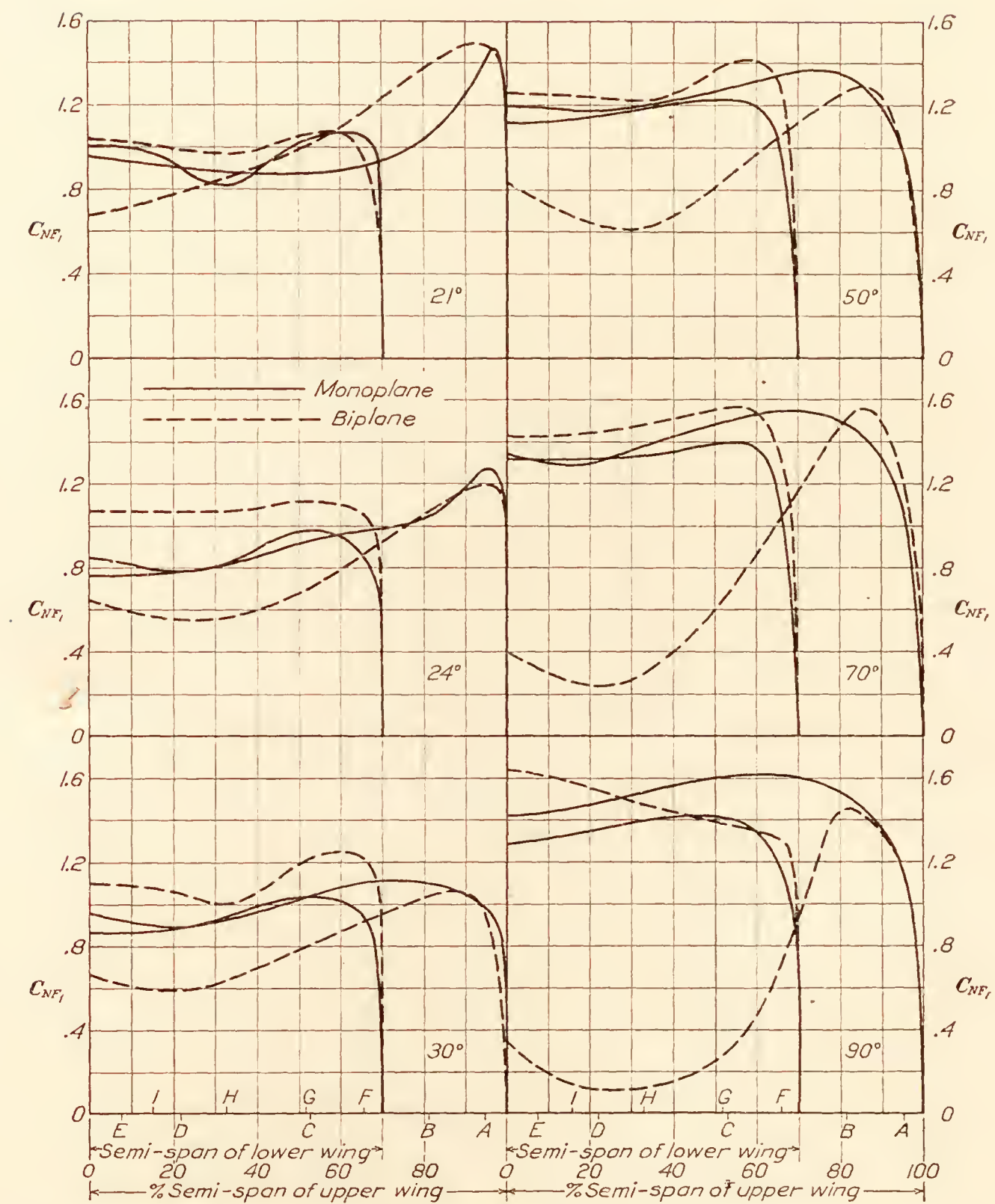


FIG. 20.—Coefficient of normal force vs. semispan

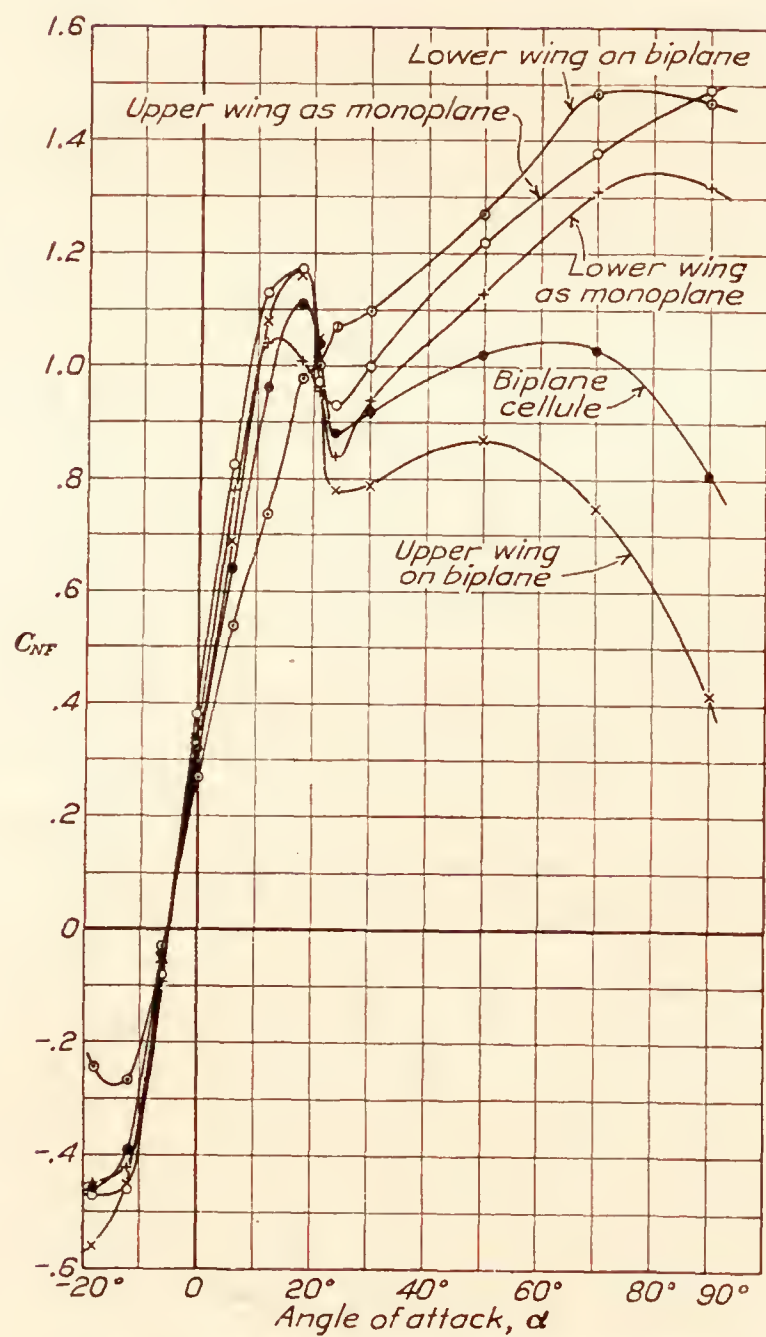


FIG. 21.—Coefficient of normal force vs. angle of attack



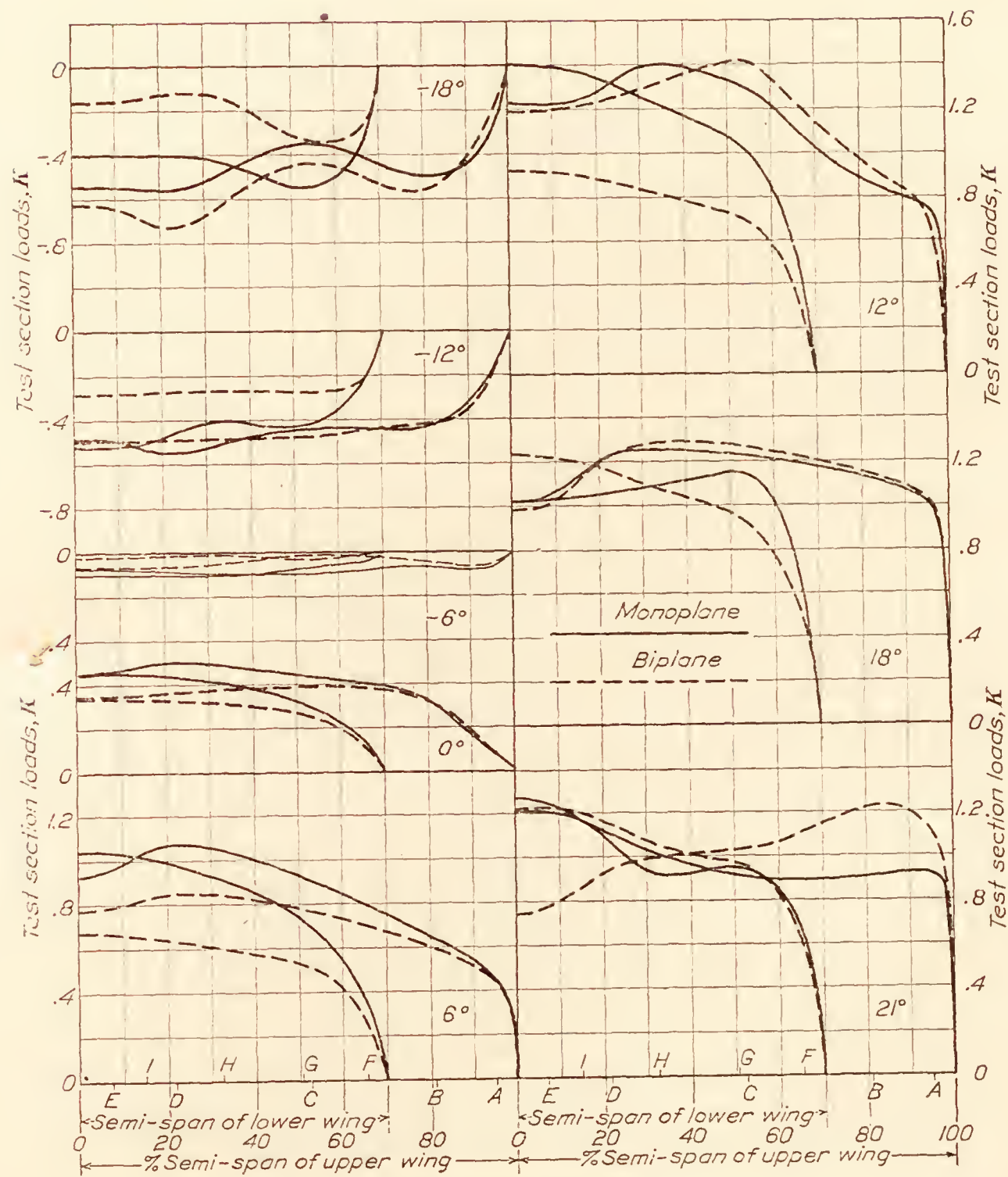


FIG. 22.—Semispan loading

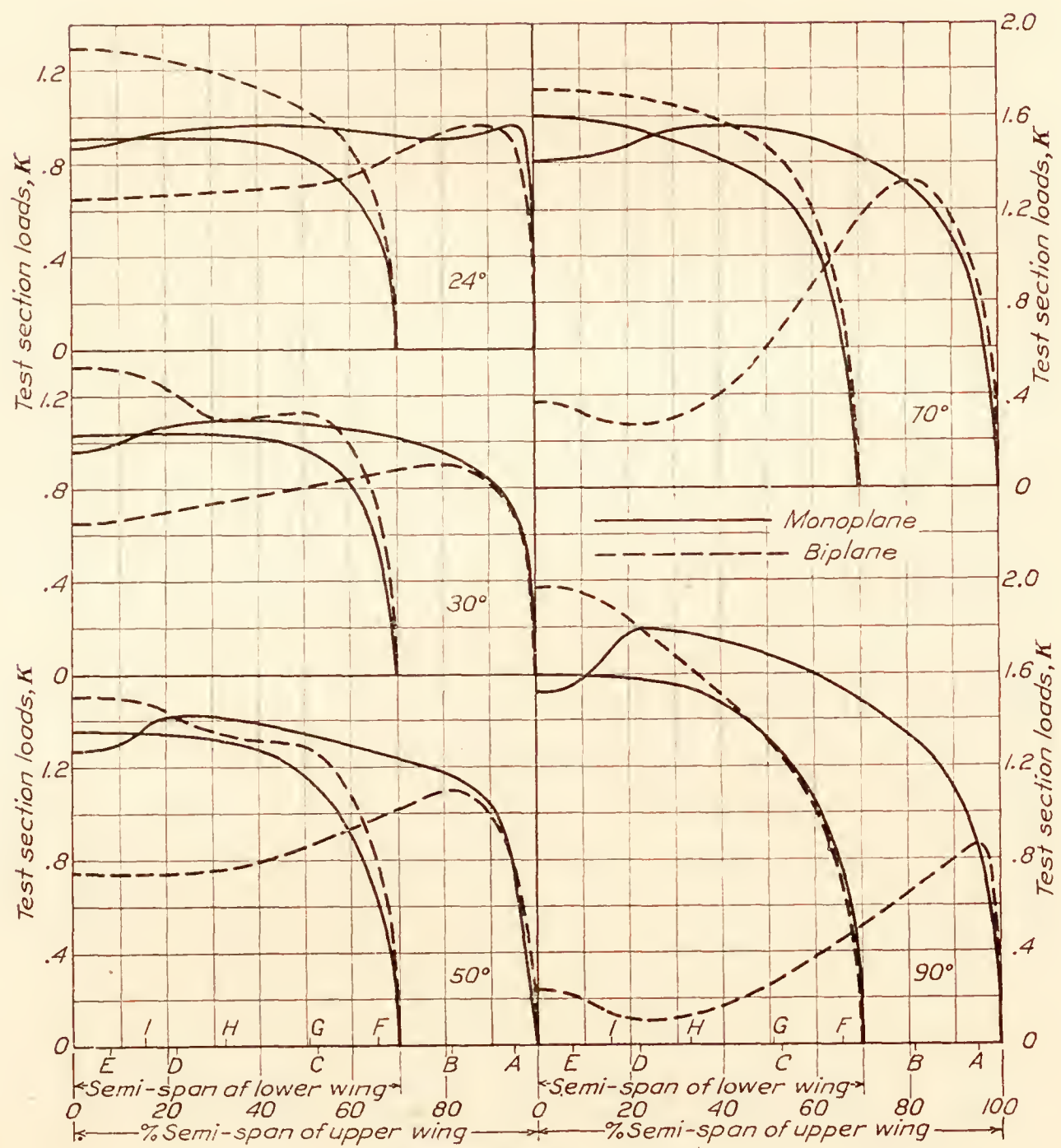


FIG. 23.—Semispan loading



Figure 25 illustrates the lateral  $C_p$  travel. The values for the biplane cellule were obtained from the integrated moments of the span-loading curves, by computing the equivalent moment arm of the forces on the wings measured from the plane of symmetry:

$$C_{pb} = \frac{M_u + M_l}{A_u + A_l}$$

$M_u$  = integrated moment of upper wing span-loading curve about the plane of symmetry.

$M_L$  = integrated moment of the lower wing span-loading curve about the plane of symmetry.

$A_u$  = area under  $K$  curve for upper wing.

$A_L$  = area under  $K$  curve for lower wing.

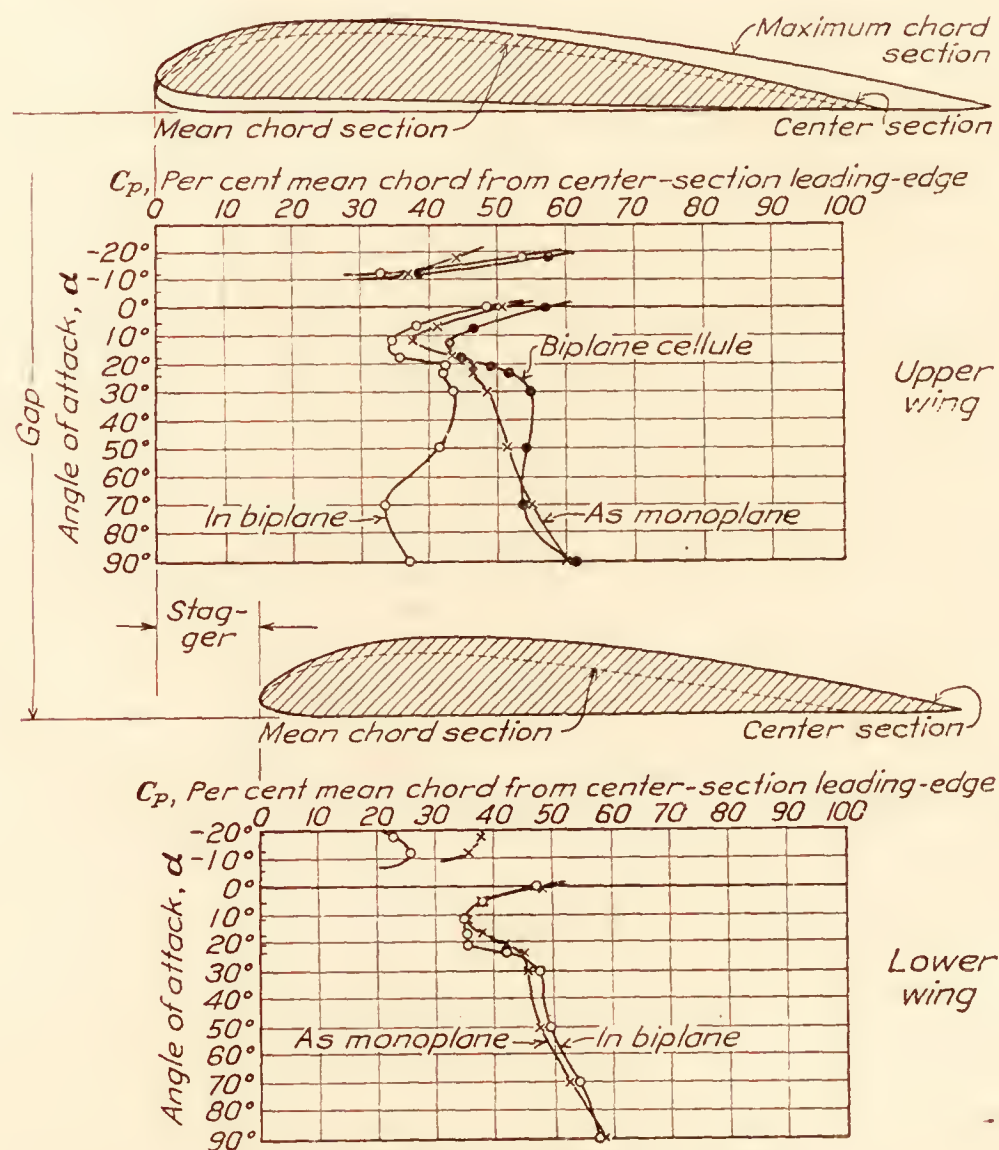


FIG. 24.—Longitudinal  $C_p$  travel vs. angle of attack

### DISCUSSION

At large negative angles of attack ( $\alpha$ ) the biplane upper wing pressures are greater than for the wing as a monoplane. This difference decreases as  $\alpha$  approaches the angle of zero lift, approximately  $-5^\circ$ , above which the monoplane pressures become larger than the biplane pressures. There is but slight difference in pressures between the monoplane and biplane upper wing from zero lift to maximum lift, where the biplane leading edge pressures again become larger. As  $\alpha$  is increased beyond maximum lift, the effect of shielding of the upper wing by the lower becomes apparent and is very marked at the higher angles of attack as shown by the decided decrease in pressure on the biplane upper wing.

The influence of the upper wing on the lower at large negative angles of attack is shown by the decreased pressure on the lower wing. As  $\alpha$  approaches zero lift the lower biplane wing and monoplane pressure diagrams become quite similar. Above zero lift the biplane pressures decrease with reference to the monoplane up to the region of maximum lift, beyond which the lower wing pressures are again higher. As seen from Figures 13, 14, and 21, these increased

pressures are due to the delayed burbling of the lower wing, a result of the influence of the upper wing. At high angles of attack the upper wing of the biplane deflects the air downward over the upper surface of the lower wing, thus tending to prevent the separation of flow from that surface.

In the region above zero lift and below maximum lift the mutual interference of the biplane wings causes decreased pressures on both wings, with the greater effect on the lower wing.

The overhanging portion of the upper wing is little affected by the lower wing of the biplane, except for an increase in pressure on the upper wing leading edge in the region of maximum lift.

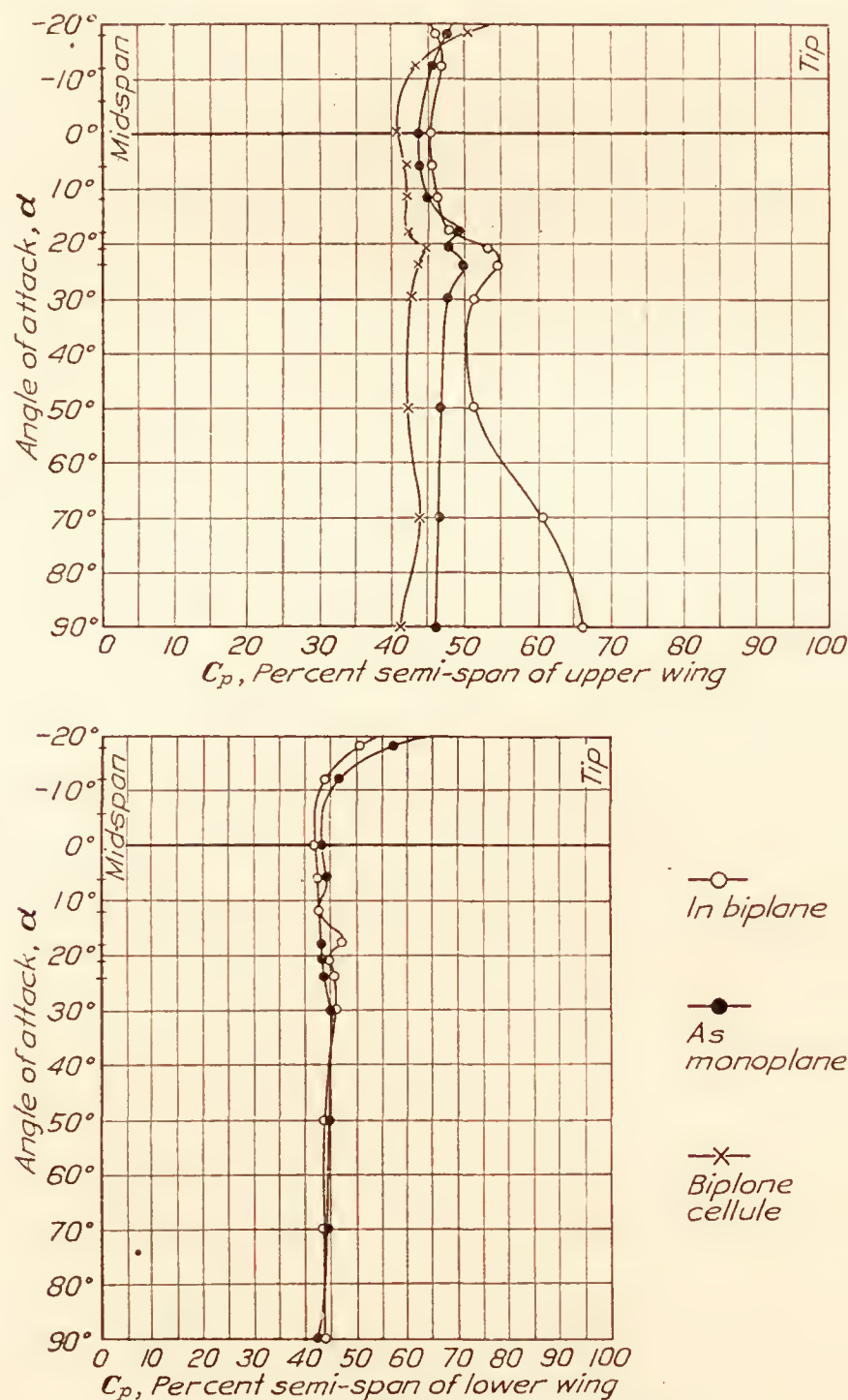


FIG. 25.—Lateral  $C_p$  travel vs. angle of attack

The longitudinal center of pressure position of the biplane upper wing is decidedly forward of that for the monoplane. That for the lower wing is but little affected, except for a slight movement to the rear at large angles of attack. (Fig. 24.)

In the biplane upper wing the lateral  $C_p$  in general moves outward with increase of angle of attack, due to the decreased pressures over the greater part of the wing, while the overhanging portion pressures are little affected by the lower wing. (Fig. 25.) The  $C_p$  of the biplane lower wing differs little from that when taken as a monoplane. Due mainly to the shorter lower wing, the biplane cellule  $C_p$  is nearer the plane of symmetry than that of the upper wing as monoplane.



## CONCLUSIONS

A comparison of the biplane and monoplane results leads to the following conclusions:

1. The biplane upper wing is shielded by the lower at large angles of attack, with resulting decrease in pressures on the upper wing.
2. The influence of the biplane upper wing on the lower is marked at large negative angles of attack by decreased pressures and at large positive angles of attack by the delayed burble of the lower wing.
3. In the region above zero lift and below maximum lift the mutual interference of the biplane wings causes decreased pressures on both wings, with the greater effect on the lower wing.
4. The overhanging portion of the biplane upper wing is little affected by the lower wing, other than for slightly increased leading edge pressures in the region following maximum lift.
5. At angles of attack above maximum lift the biplane upper wing center of pressure moves forward and outward, while the  $C_p$  for the lower wing varies but little from that of the monoplane.

LANGLEY MEMORIAL AERONAUTICAL LABORATORY,  
NATIONAL ADVISORY COMMITTEE FOR AERONAUTICS,  
LANGLEY FIELD, VA., *April 9, 1928.*

### BIBLIOGRAPHY

- Reference 1. Reid, Elliott G.: Standardization Tests of N. A. C. A. No. 1 Wind Tunnel. N. A. C. A. Technical Report No. 195.
- Reference 2. Fairbanks, A. J.: Pressure Distribution Tests on PW-9 Wing Models Showing Effects of Biplane Interference. N. A. C. A. Technical Report No. 271, 1927.
- Reference 3. Warner, E. P.: Airplane Design, Aerodynamics. Pages 41 to 49, 1927.
- Fairbanks, A. J.: Distribution of Pressure Over a Model of the Upper Wing and Aileron of a Fokker D-VII Airplane. N. A. C. A. Technical Report No. 254, 1927.
- Reid, Elliott G.: Pressure Distribution Over Thick Tapered Airfoils, N. A. C. A. 81, U. S. A. 27C Modified, and U. S. A. 35. N. A. C. A. Technical Report No. 229, 1926.
- Norton, F. H., and Bacon, D. L.: Pressure Distribution Over Thick Airfoils—Model Tests. N. A. C. A. Technical Report No. 150, 1922.
- Parkin, J. H., Shortt, J. E. B., and Heard, C. G.: Pressure Distribution Over U. S. A. 27 Aerofoil With Square Wing Tips. University of Toronto Aeronautical Research Paper No. 18, 1925.
- Parkin, J. H., Shortt, J. E. B., and Code, J. G.: Pressure Distribution Over a Göttingen 387 Aerofoil with Square Wing Tips. University of Toronto Aeronautical Research Paper No. 18a, 1926.
- Irving, H. S., and Batson, A. S.: The Distribution of Pressure Over a Biplane of Unequal Chord and Span. British Aeronautical Research Committee Reports and Memoranda No. 997, 1925.



---

---

**REPORT No. 297**

---

**THE  
REDUCTION OF OBSERVED AIRPLANE PERFORMANCE  
TO STANDARD CONDITIONS**

**By WALTER S. DIEHL  
Bureau of Aeronautics**





## REPORT No. 297

---

### THE REDUCTION OF OBSERVED AIRPLANE PERFORMANCE TO STANDARD CONDITIONS

By WALTER S. DIEHL

---

#### SUMMARY

*This report shows how the actual performance of an airplane varies with air temperature when the pressure is held constant. This leads to comparatively simple methods of reducing observed data to standard conditions. The new methods which may be considered exact for all practical purposes, have been used by the Navy Department for about a year, with very satisfactory results.*

*The report also contains a brief historical review of the important papers which have been published on the subject of performance reduction, and traces the development of the standard atmosphere.*

#### INTRODUCTION

The analysis of observed airplane performance is greatly complicated by the fact that the power available and the power required in flight do not vary according to the same law. At constant R. P. M. the engine power is a function of air pressure and air temperature independently, so that the power developed at a given density depends on the combining pressure and temperature. On the other hand, the power absorbed by the propeller at constant R. P. M., and the power required for horizontal flight are constant at a given density regardless of the combining pressure and temperature. Since, on two successive days the pressures and temperatures at given true altitudes or at given densities may vary widely from the average or standard values, it follows that observed performance and in particular the rates of climb at given true altitudes or at given densities also vary widely with the atmospheric conditions. Climbs made on different days rarely agree. The problem is to find some method of reducing observed data to a standard condition by applying corrections such that, regardless of the atmospheric conditions under which the flight tests are made, the reduced data are always in agreement.

There are two basic conditions which must be specified before any accurate method of reduction can be formulated. The first and most important condition is a Standard Atmosphere or a definite set of relations between pressure, temperature, density, and altitude to which the reduced performance may be referred. Arbitrary but definite relations must be used, since the performance is determined by the pressure and temperature and not by the geometric or true altitude. The second condition is the variation of engine power with pressure and temperature.

A standard atmosphere having been adopted, there are two methods of attack. One may assume various relations between engine power and atmospheric pressure and temperature and by trial and error find the relation which gives the best agreement in reducing observed performance, or one may find from test stand data the effect of pressure and temperature on engine power and from this calculate the variation in performance due to variation in atmospheric conditions. The latter method will be used in the present study.

Before taking up the development of an accurate method of performance reduction, a brief historical review of the subject will be made. This review will quote extracts from the more important papers in order to illustrate the steps that have been taken in the improvement of performance reduction, in the adoption of the standard atmosphere, and in the matter of variation of power with altitude.



The terms "pressure altitude" and "density altitude" will occur frequently. These are simply the altitudes in the standard atmosphere defined by a given pressure, or a given density, respectively.

### HISTORICAL REVIEW

Prior to 1915 the performance testing of airplanes was confined to the measurement of high speeds at ground level and to the observation of partial climbs, usually between certain specified aneroid heights such as 3,000 to 5,000 feet, and these climbs were often made with service altimeters. About 1915 the Royal Aircraft Factory made the first definite attempt to place airplane performance testing on a scientific basis. Little is known concerning the initial efforts in this line, but the first paper of any importance on the subject is by Captain H. T. Tizard, R. F. C. This paper, entitled "Methods of Measuring Aircraft Performance," was read before the Royal Aeronautical Society March 7, 1917, and published in the April-May-June issue of the Royal Aeronautical Journal. It opens with a brief historical review followed by a very clear statement of the necessity for reducing observed performance to some standard condition before comparisons are made. The standard condition then employed by the R. A. F. and R. F. C. was obtained from a table of mean atmospheric pressures, temperatures, and densities at various heights, based on observations by Mr. W. H. Dines. A standard density corresponding to  $1.221 \text{ kg/m}^3$  had been adopted and a table of relative densities against altitude prepared from Dines's data. It is interesting to note that the resultant sea-level density ratio 1.026 thus obtained was used more or less generally five years later, although the subject came up in the discussion of Captain Tizard's paper. In view of the general use of the present standard atmosphere the following quotation from the discussion is of historical interest: "Lieut. G. H. Millar, R. N. V. R., said that in his opinion it was a pity that the standard atmosphere which had been adopted was a purely empirical one; he would have preferred one based on a given temperature and pressure at sea level, and a uniform rate of fall of temperature \* \* \*. The advantage of such a standard over the empirical one was that it could be calculated at any time by remembering two constants. He also thought that the unit of density should certainly be the density at zero height for the standard atmosphere adopted." Lieutenant Millar's remarks apparently anticipate by several years the linear temperature gradient usually credited to Toussaint and now used in the standard atmosphere.

In this connection a linear temperature gradient was proposed in the appendix to a report by H. Glauert and S. B. Gates, entitled "Prediction of the Performance and Longitudinal Stability of an Aeroplane, Including the Estimation of the Effect of Small Changes in the Design." This report, dated March, 1917, was published as R. & M. No. 324 by the British Advisory Committee for Aeronautics. According to the author's notes, a linear temperature gradient was also used by Prof. E. P. Warner in a lecture on Airship Design at Massachusetts Institute of Technology, May 28, 1918. The linear temperature gradient now in use  $\frac{dT}{dh} = 0.0065 \text{ }^\circ\text{C/m}$  is based on observations by Professor Gamba at the Padua Observatory between 1906 and 1916. Professor Gamba's data are given in a report published by the experimental section of the Italian Air Service in September, 1918. This report and the linear gradient are discussed in an article entitled "Lois Experimentales des Variations de la Pression Barometrique et du Poids Specifique de l'air avec Altitude," by R. Soreau in the November 1-15 issue of l'Aerophile. Soreau proposes, however, to use a rather complicated empirical formula, which appears to have no advantage other than that of reasonable agreement with observed data. Toussaint's proposal to use a linear temperature gradient was first issued by the S. T. Aé. in March, 1920, as the "Draft of Interallied Agreement on Law Adopted for the Decrease of Temperature with Increase of Altitude." This draft is rather brief, but all essential information is given. It was followed by a more complete definition, together with a quantity of supporting data, in the Bulletin Trimestriel des Etudes, issued by S. T. Aé. in April, 1920. Toussaint's proposal was officially adopted by the S. T. Aé., beginning on May 1, 1920. During the same year England, Belgium, and Spain agreed to adopt the proposal, and in 1921 it was adopted with



one very slight modification by the National Advisory Committee for Aeronautics for use in the United States. Before the adoption in this country a very thorough investigation by the Weather Bureau showed that it was more desirable to use an isothermal temperature of  $-55^{\circ}\text{C}$ . instead of the  $-56.5$  proposed by Toussaint. The difference is negligible in so far as it ever effects any performance reduction. The data supporting this point are given and discussed by Willis Ray Gregg in N. A. C. A. Technical Report No. 147, "Standard Atmosphere" (1922).

Returning to Captain Tizard's paper, the proposed method of reduction was on a density basis. Aneroid altitudes were plotted against time and rates of climb in "aneroid feet" were read from the slope of the curve. These rates of climb were then corrected to "true" rates by multiplying by a correction factor corresponding to the difference between the observed temperature and the  $+10^{\circ}\text{C}$ . constant temperature used in calibrating all aneroids at that time. These "true" rates of climb were then plotted against the standard density heights corresponding to each pressure (aneroid) and temperature reading. Speeds were also plotted against density altitudes after correcting the observed readings for instrumental error and converting to true speeds.

The second paper on performance reduction appears to be Captain Toussaint's "Note sur les Methodes et les Calculs d'essais des Avions Nouveaux," a series of lectures given at l'Ecole Supérieure d'Aeronautique at Paris, January and April, 1918. These lectures were published in mimeographed form by the S. T. Aé. and translated by the Technical Publications Department at McCook Field. A limited number of blue-print copies of this translation, dated September, 1918, were distributed as confidential documents. The method of reduction described by Toussaint is on a density basis quite similar to that outlined by Tizard, except that the standard atmosphere then used was based on Radau's law connecting pressure temperature and pressure

$$\frac{\Delta T}{\Delta P} = \left( \frac{T_o - T}{P_o - P} \right) = 0.08 \quad (1)$$

where  $T$  is in  $^{\circ}\text{C}$  and  $P$  in mm Hg. It is of interest to note that Radau's law dates from 1864. Toussaint's method was used extensively in the United States prior to about 1923.

The first published method of performance reduction on the pressure basis appears to be that outlined in a paper by D. H. Pinsent and H. A. Renwick, "The Variation of Engine Power with Height," which was published in March, 1918, as R. & M. No. 462 by the British Advisory Committee for Aeronautics. The following extract from the summary of this report is of great interest: "The experiments indicate in all cases that the B. HP. can better be expressed as a function of the barometric pressure only, instead of the previous and customary method where it was assumed to be a function of density \* \* \* The above conclusion makes it necessary to reconsider the methods at present in use of reducing climbs and speeds at heights to a standard basis for comparison. It has been customary hitherto in comparing the performances of two airplanes as regards speed to compare their true air speeds at the same density; and as regards climb, to compare their times to climb from one given density to another. If engine power can be better expressed as a function of pressure only, this method of comparison is unduly favorable to airplanes tested in warm weather, and vice versa."

Bairstow in his Applied Aerodynamics, Longmans, Green & Co., 1920, gives a method of reduction on a density basis that is practically the same as Tizard's, but his remarks on the method include the following statement (p. 430); "The standard method of reduction of British performance trials has up to the present date been based on the assumption that the engine horsepower depends only on the density. Questions are now being raised as to the strict validity of this assumption, and the law of dependence of power on pressure and temperature is being examined by means of specially conducted experiments."

The experiments to which Bairstow refers were made during 1919 and 1920, but they were not reported until 1924. The results are given in a paper entitled "Variation of Engine Power with Height," by H. L. Stevens, and published by the British Aeronautical Research Committee in August, 1924, as R. & M. No. 960. This report contains a number of climbs



reduced on both the density basis and the pressure basis, and the conclusion given in the summary is: "For performance reduction it is better to assume that the engine power is proportional to some power of the pressure ( $p^{1.05}$  in this case) than some power of the density." This conclusion is also incorporated in the text and with more emphatic wording: "The direct measurements of performance indicate that for the reduction of climbs to standard conditions a pressure law is definitely better than a density law." An appendix giving brief but complete outlines of the two methods of performance reduction contains under the pressure method the very interesting statement: "\* \* \* It follows that the top speed of level flight of an air plane is such that the indicated speed at a definite aneroid height is independent of the temperature."

A second report, "The Variation of Engine Power with Height," by H. M. Garner and W. G. Jennings, was issued by the British Aeronautical Research Committee in September 1924, as R. & M. No. 961. The conclusion based on flight tests with a torque meter was: "The experiments show that the engine power is very nearly a function of the pressure only, except for low heights, where it depends to a certain extent on the temperature."

In a paper, "Engine Performance and the Determination of Absolute Ceiling," which was published as N. A. C. A. Technical Report No. 171 in September, 1923, the author showed that B. HP. varied as  $p^{1.15}$  when temperature and R. P. M. are held constant and as  $T^{-0.50}$  when pressure and R. P. M. are held constant. At this time the density method of performance reduction was used generally in the United States, as elsewhere, and while it was realized that the pressure method apparently gave more consistent results than the density method, there was considerable opposition to a change. In view of the desirability of having a definite and easily followed method available, the author prepared a simplified approximate density method, and Prof. E. P. Lesley prepared a more elaborate density method of reduction. These methods were published together in 1925 as N. A. C. A. Technical Report No. 216, "The Reduction of Airplane Flight Test Data to Standard Atmosphere Conditions."

A paper by R. S. Capon, "Note on the Reduction of Performance Tests to the Standard Atmosphere," was published by the British Aeronautical Research Committee in January, 1927, as R. & M. No. 1080. Analysis was made of 12 pairs of climbs using special test instruments corrected for temperature effects. The conclusion regarding variation of power with height as given in the summary is: "The law specified by the climbs with corrected instrument calibrations is  $f(p^{2/3}\rho^{1/3})$ . It is indicated that the mean error of the rates of climb determinations is considerably reduced by the use of corrected instruments and is such that the adoption of a power factor which is a function of pressure only will not do justice to the accuracy of the test data." An appendix contains a brief outline of the proposed method of reduction, which states that if any two of the equations:

$$\frac{V'}{V} = \frac{v'_c}{v_c} = \frac{\text{RPM}'}{\text{RPM}} = \frac{f' \text{HP}}{f \text{HP}} = \sqrt{\frac{\rho}{\rho'}} \quad (2)$$

or conditions:

- (1) Angles of climb equal,
- (2) Angles of attack equal,

are satisfied all are satisfied. In the equations  $V$  is true air speed,  $v'_c$  the rate of climb,  $f$  is the power factor, HP is the power at sea-level conditions, and  $\rho$  is the air density. The primed and unprimed letters refer to two flight conditions of different pressure and temperature.

The use of a power factor is treated by H. Glauert in "A Discussion of the Law of Variation of Engine Power with Height," British Aeronautical Research Committee R. & M. No. 1099, issued in March, 1927. The conclusion given in the summary is: "The relative importance of pressure and density in determining the power of an engine appears to vary with height, and different methods of experiment lead to slightly discordant results. The simple pressure law is undoubtedly better than the simple density law, and for greater refinement Mr. Capon's suggestion should give a very close approximation to the truth."



It will be noted that up to this time no great effort has been made to find how the performance of an airplane actually varies with nonstandard conditions. In the pages following a logical method of reduction will be developed from the calculated effect of nonstandard conditions on performance.

#### OUTLINE OF METHODS AND BASIC CALCULATIONS

Preliminary studies indicated that the most direct method of attacking the problem of performance reduction was to calculate the effects of air pressure and temperature on the performance of a given airplane. This requires the adoption of (1) a relation between brake horsepower, air pressure, and air temperature, (2) a standard atmosphere, and (3) a specified variation of thrust horsepower with altitude in standard atmosphere.

In the present study the variation of B. HP. with  $P$  and  $T$  will be assumed to be (reference 1)—

$$\frac{\text{B. HP}}{\text{B. HP}_0} = \left( \frac{P}{P_0} \right)^{1.15} \left( \frac{T}{T_0} \right)^{-0.5} \quad (3)$$

The N. A. C. A. standard atmosphere has been officially adopted for general use in this country. Below 35,000 feet it is identical with the S. T. Ae. standard atmosphere used in Europe. The variation of thrust horsepower with altitude, given in Table I, has been obtained from analysis of flight test data by a simple method based on propeller power coefficients (reference 2). The data in Table I allow for effects of average change in R. P. M., B. HP., and propeller efficiency at constant true air speed.

The performance of a given airplane in standard atmosphere is readily calculated from the data given in Table I. At any given altitude in standard atmosphere for which the power curves have been obtained the pressure may be held constant and the effects of temperature on performance found by calculating new curves of power available from equation (3) and new curves of power required from the usual density relation  $T. HP_2 = T. HP_1 \sqrt{\frac{\rho_1}{\rho_2}}$ . This is equivalent to holding the pressure altitude constant while varying the density altitude. The results so obtained may be compared with the performance in normal standard atmosphere in order to build up an accurate method of performance reduction.

The first part of this investigation is based on the full scale polar for the VE-7 airplane as determined by Professor Lesley (reference 3). The effective aspect ratio of this airplane was taken as 4.8 in calculating the induced and parasite coefficients shown in Figure 1, which is based on Figure 11 of Lesley's report. The full scale data indicates a maximum lift coefficient of  $C_{L \max} = 1.21$ . The VE-7 has the following characteristics:

Wing area.....	289 sq. ft.
Wing section.....	R. A. F.-15.
Span, upper and lower.....	34.11 ft.
Gap.....	4.67 ft.
Chord, upper and lower.....	4.62 ft.

With a wing loading of 7.75 lb./sq. ft. the stalling speed at sea level is 50 mi./hr. This gives a gross weight of 2,230 pounds, which will be used throughout the remainder of the study.

Table II contains the air speeds and thrust horsepowers required at various altitudes, based on the data in Figure 1. Table III contains the calculations for thrust horsepower available at various altitudes, using the power factors from Table I. These data are plotted in Figure 2, from which the performance at altitude is obtained and summarized in Table IV. Figure 3 is a plot of rate of climb against altitude in normal standard atmosphere.

#### EFFECT OF TEMPERATURE ON PERFORMANCE AT 10,000 FEET PRESSURE ALTITUDE

The effect of temperature on performance was first investigated at 10,000 feet pressure altitude by assuming temperatures 83.3, 87.0, 90.9, 95.2, 1.05, 1.10, 1.15, and 1.20 per cent normal and calculating air speeds, powers required, and powers available. The air speeds



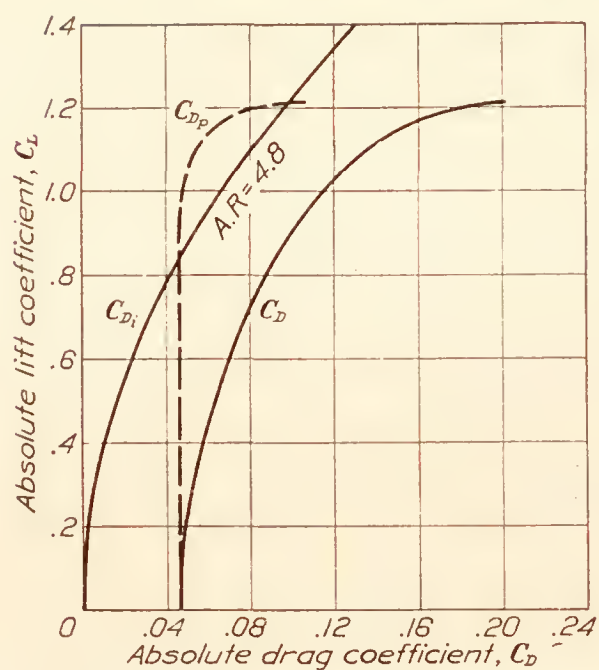


FIG. 1.—Full-scale polars of VE-7 airplane. Taken from Figure 11, N. A. C. A. Technical Report No. 220

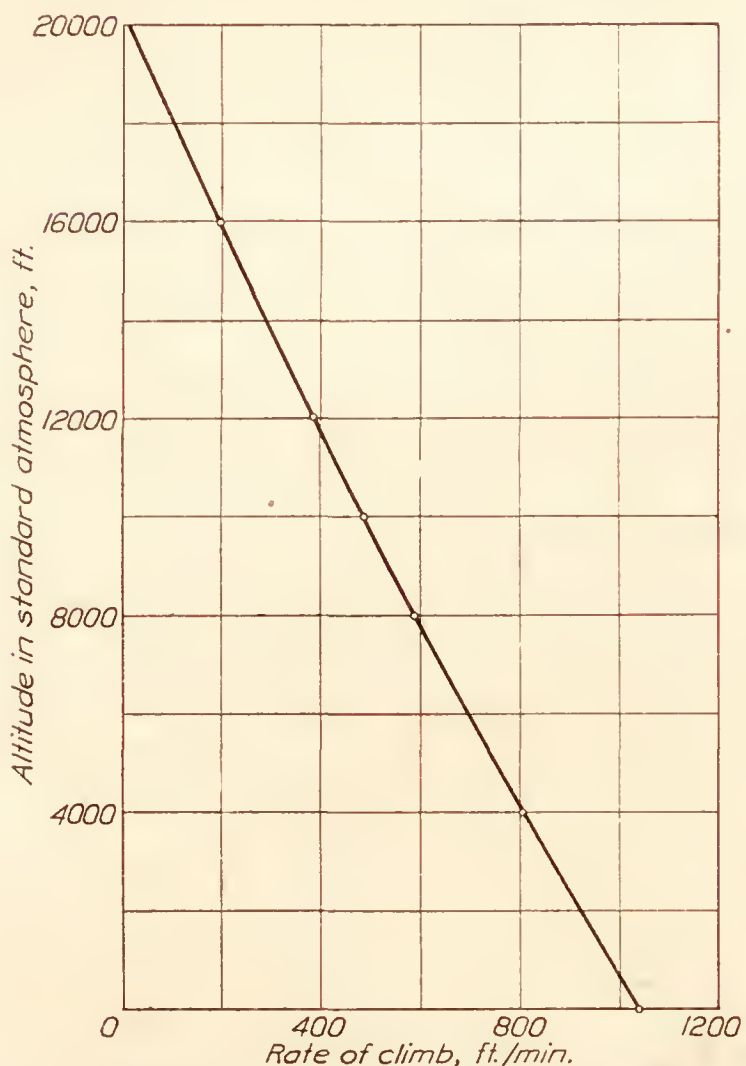


FIG. 3.—Rate of climb in standard atmosphere. Gross weight equals 2,230 pounds. VE-7 airplane

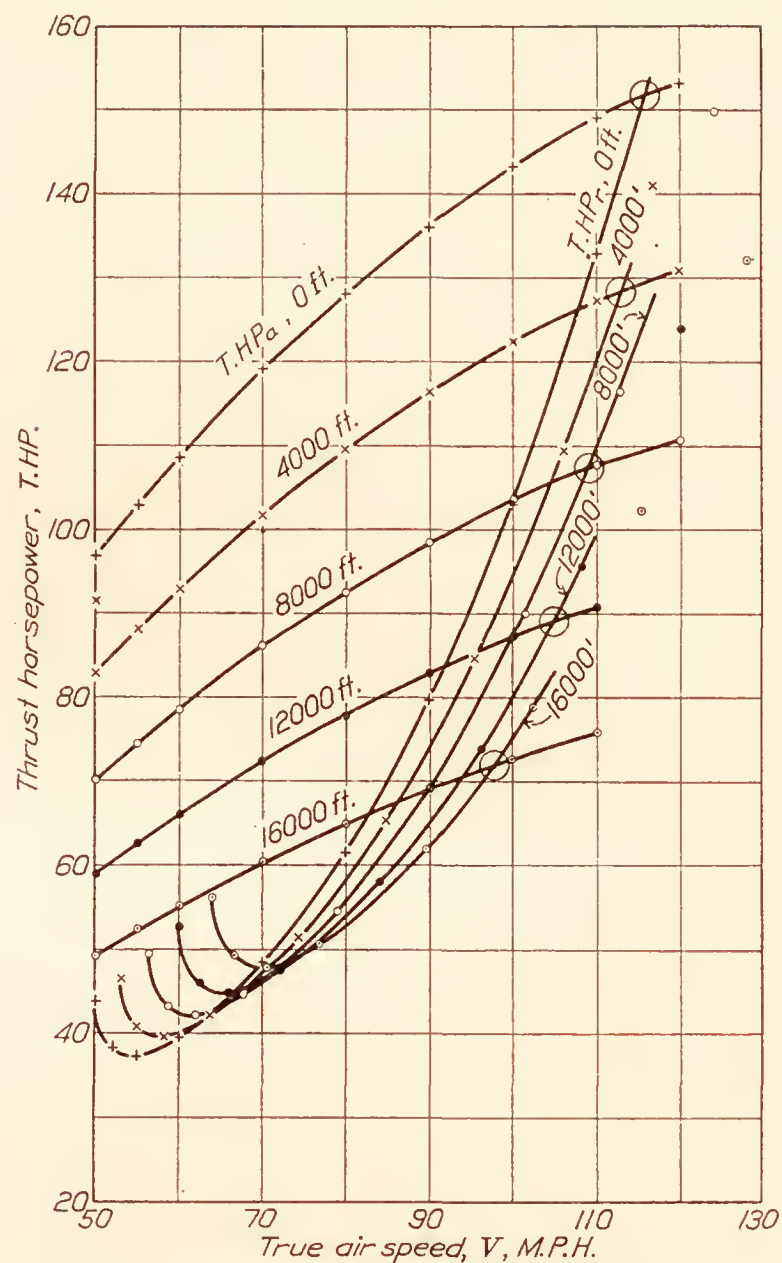


FIG. 2.—Power curves for gross weight of 2,230 pounds. VE-7 airplane. Normal standard atmosphere

and powers required vary inversely as the square root of the density, while the powers available (at constant pressure) vary directly as the square root of the density. The particular low temperature ratios used are reciprocals of the corresponding high temperature ratios and were selected in order to simplify calculations while giving the same percentage change in density. The air speeds and powers required so calculated are given in Table V, and the powers available are given in Table VI. These data are plotted on two figures, 4 and 5, in order to avoid crowding the curves. Table VII contains a summary of the results obtained.

#### CLIMB

The altitude in normal standard atmosphere corresponding to the actual rate of climb for each temperature condition was read from Figure 3, and numerous methods of comparing these with the pressure and density altitudes were studied. The only method giving satisfactory results is that indicated in Table VII. The altitude in normal standard atmosphere at which the rate of climb is identical with that for a nonstandard temperature condition is given by

$$h = h_p - K (h_p - h_d) \quad (4)$$



Where  $h_p$  is the altitude in normal standard atmosphere having the observed pressure,  $h_d$  is the altitude in normal standard atmosphere having the observed density, and  $K$  is constant found in Table VII to be about 0.36.  $h_p$  and  $h_d$  are usually designated as pressure altitude and density altitude, respectively. The constant  $K$  does not show any dependence on the extent to which the temperatures depart from normal. In subsequent calculations, therefore, only the extreme values  $\frac{T}{T_s} = 0.833$  and  $\frac{T}{T_s} = 1.20$  need be considered.

#### MAXIMUM SPEEDS

As shown by Table VII, maximum speeds are not greatly affected by temperature changes. The small change indicated does not appear to bear any definite relation to the pressure altitude and density altitude considered together, as will be shown later. It is obvious, however, that the error involved in plotting true maximum air speeds against pressure altitude is less than the experimental error. It is also obvious that plotting maximum speeds against density altitude may lead to serious errors.

#### CLIMBING SPEEDS

Best climb appears to be at a substantially constant angle of attack or lift coefficient as shown by the slight variation in the ratio  $V_c/V_s$ , which shows a tendency to decrease slowly with increasing temperature. The maximum change in  $V_c/V_s$  likely to be encountered in practice is too small to be considered as a correction. A constant lift coefficient or angle of attack means a constant indicated air speed. Climbing speeds should therefore be specified in terms of indicated air speeds and aneroid pressures if this relation is found to hold for all altitudes.

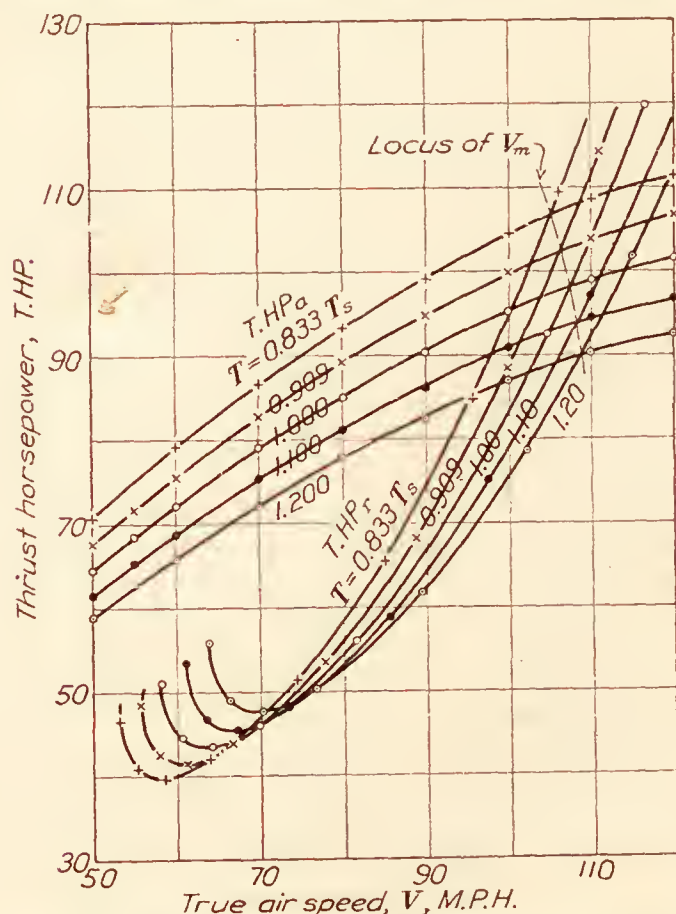


FIG. 4.—Power curves at 10,000-foot pressure altitude. Gross weight equals 2,230 pounds. See Figure 5, VE-7 airplane

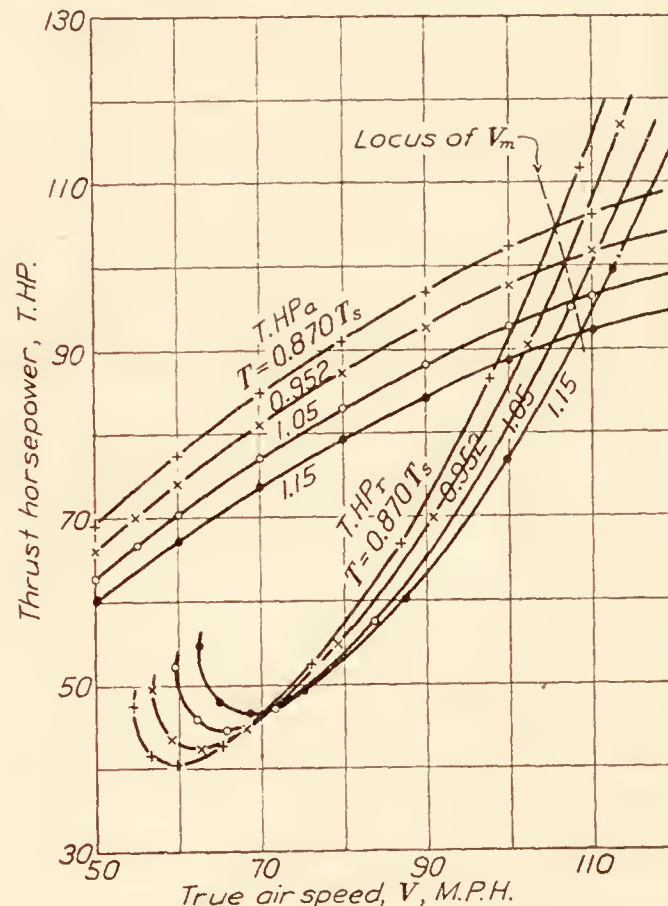


FIG. 5.—Power curves at 10,000-foot pressure altitude. Gross weight equals 2,230 pounds. See Figure 4, VE-7 airplane

#### EFFECT OF TEMPERATURE ON PERFORMANCE AT VARIOUS PRESSURE ALTITUDES

Following the method illustrated in Tables V and VI, powers required and powers available were calculated at pressure altitudes of 4,000, 8,000, 12,000, and 16,000 feet for temperatures 83.3, 90.9, 110, and 120 per cent normal. These calculations are too extensive to be included in the report, but the data are plotted in Figures 6, 7, 8, and 9. The indicated performances from these figures are given in Tables VIII and IX.

#### CLIMB

Values of the constant  $K$  in equation (4) show no marked dependence on altitude. A very slight tendency may be observed for  $K$  to increase with altitude, but the change is not



appreciably greater than the accuracy of the calculations. For all practical purposes  $K$  may be considered independent of altitude.

#### MAXIMUM SPEED

The variation of maximum speed with temperature is slightly greater at low altitudes than at high altitudes, and has no simple dependence on the pressure altitude, density altitude, or any combination of the two. The extreme variation likely to be encountered at a given pressure altitude is about of the same order as the experimental error in determining the maximum speed. Maximum speeds should therefore be plotted against pressure altitude.

#### CLIMBING SPEEDS

At a given pressure altitude the ratio of climbing speed to stalling speed,  $V_c/V_s$ , decreases slightly with increase in temperature. This decrease is greater at low altitudes than at high altitudes, but the maximum change is comparatively small. Therefore at any given pressure altitude the angle of attack, the lift coefficient, and the indicated air speed for best climb are independent of the temperature.

#### VARIATION OF TEMPERATURE EFFECTS WITH CHANGES IN ASPECT RATIO AND PARASITE DRAG

Up to this point the investigation has been concerned with the performance of a single airplane, and some question naturally arises regarding the generality of the results so far obtained. It is proposed to give a convincing demonstration in the form of calculations covering a wide range in effective aspect ratio and parasite drag. For this purpose, a systematic series of 18 fictitious airplanes has been formed by combining 6 effective aspect ratios with 3 parasite drags. The weight, power, and wing area have been held constant at the VE-7 values for convenience, since the absolute values of these factors have no influence on the variation under investigation. The aspect ratios selected—3, 4, 5, 6, 8, and 10—completely cover the practical limits of present design. The parasite drag values adopted are based on the *normal* value of  $C_{DP}=0.046$  shown on Figure 1 and include the *low* value  $C_{DP}=0.031$  and the *high* value  $C_{DP}=0.076$ . The low value corresponds to about a 50 per cent in the structural parasite of the VE-7. The high value corresponds to about double the structural parasite of the VE-7.

Twenty-three groups of power required and power available curves, such as are shown on Figures 10, 11, and 12, were necessary to enable the accurate definition of the rate of climb curves in normal standard atmosphere as shown in Figures 13, 14, and 15. The results obtained in Tables VII, VIII, and IX indicate that calculations for two temperatures, one high and one low, at a single pressure altitude will be sufficient to determine the nature of the variation in  $K$  (equation 4). Accordingly, calculations were made for temperature ratios,  $\frac{T}{T_s}=0.833$  and 1.20 at a pressure altitude of 10,000 feet for the normal and low parasite series, and at 8,000 feet for the high parasite series. The calculations are too extensive to be included in this report, but the power curve plots are given in Figures 16 to 21, inclusive. The data in Tables X, XI, and XII were obtained from Figures 16 to 21, using the same method previously employed. The results follow:

#### CLIMB

The values of  $K$  show a slight but very definite decrease with increase in aspect ratio and an indication of a slight increase with increase in parasite. The values of  $K$  for  $T=1.20 T_s$  are uniformly higher than for  $T=0.833 T_s$  by about 3 per cent. These relations are clearly brought out by the tabulation of  $K$  in Table XIII and the plotting in Figure 22. The data do not enable any definite conclusion to be drawn in regard to the difference between the high and low temperature values of  $K$ , but there is no reason to suspect that it does not exist. The values at aspect ratio 5 check closely with those obtained for 4.8 in the first series, Tables VII, VIII, and IX. Since the maximum deviation from normal standard temperatures is probably less than 10 per cent, the value of  $K$  may be taken as 0.36 without appreciable error for any average airplane. For very high or very low aspect ratios the proper value from Figure 22 should be used.



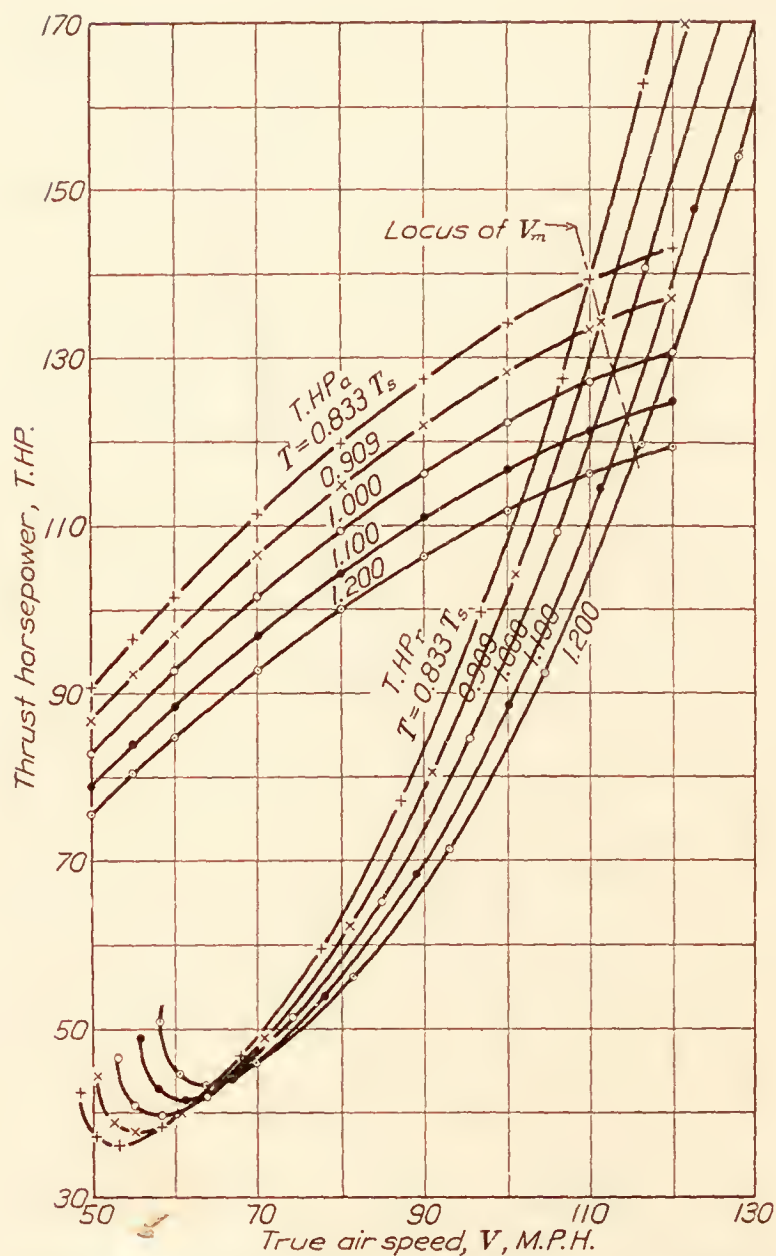


FIG. 6.—Power curves at 4,000-foot pressure altitude. Gross weight equals 2,230 pounds. VE-7 airplane

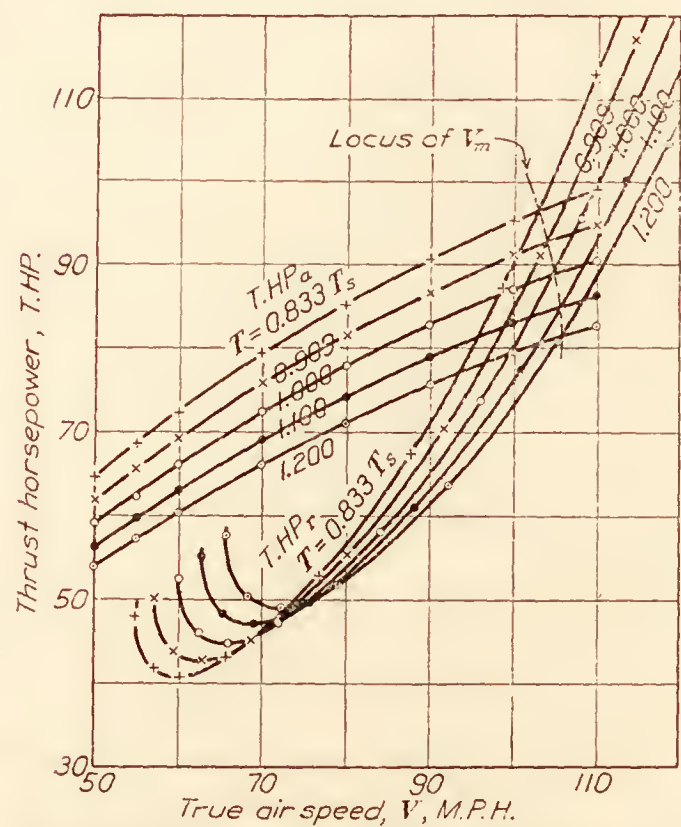


FIG. 8.—Power curves at 12,000-foot pressure altitude. Gross weight equals 2,230 pounds. VE-7 airplane

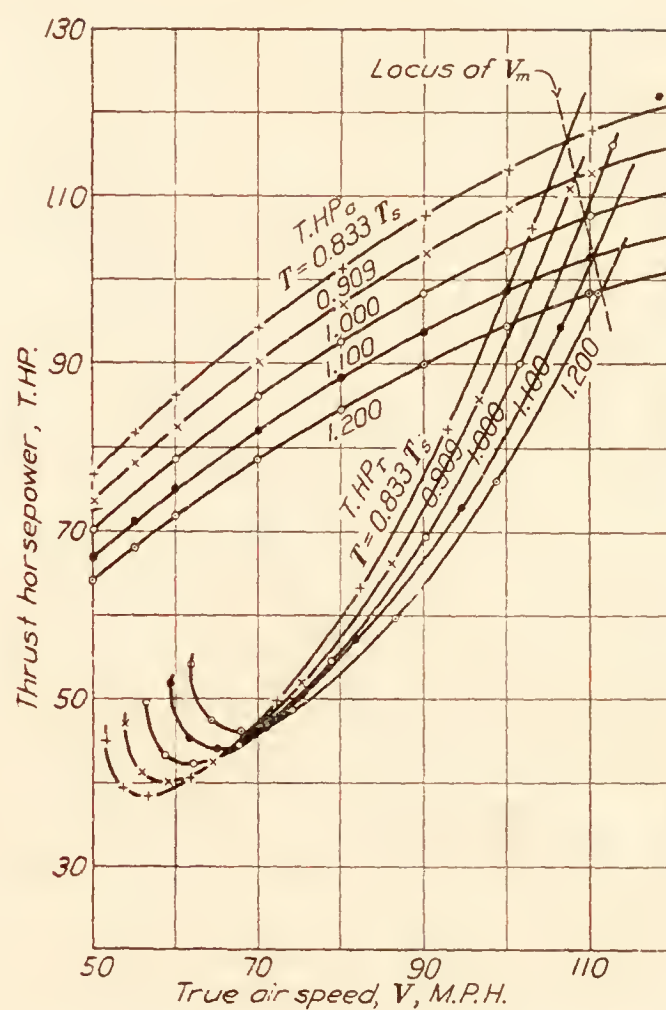


FIG. 7.—Power curves at 8,000-foot pressure altitude. Gross weight equals 2,230 pounds. VE-7 airplane

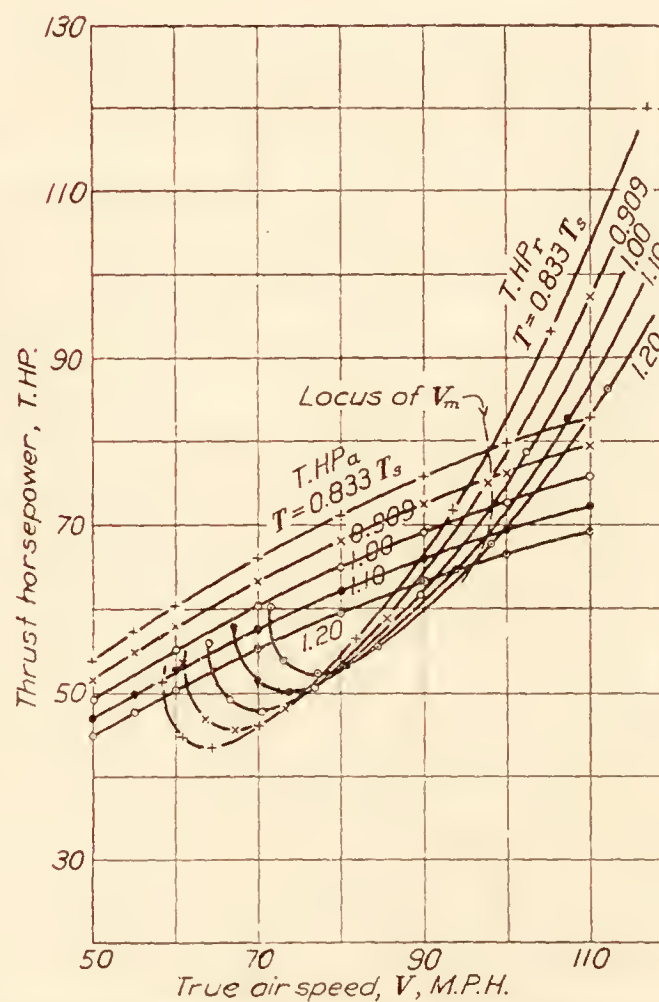


FIG. 9.—Power curves at 16,000-foot pressure altitude. Gross weight equals 2,230 pounds. VE-7 airplane

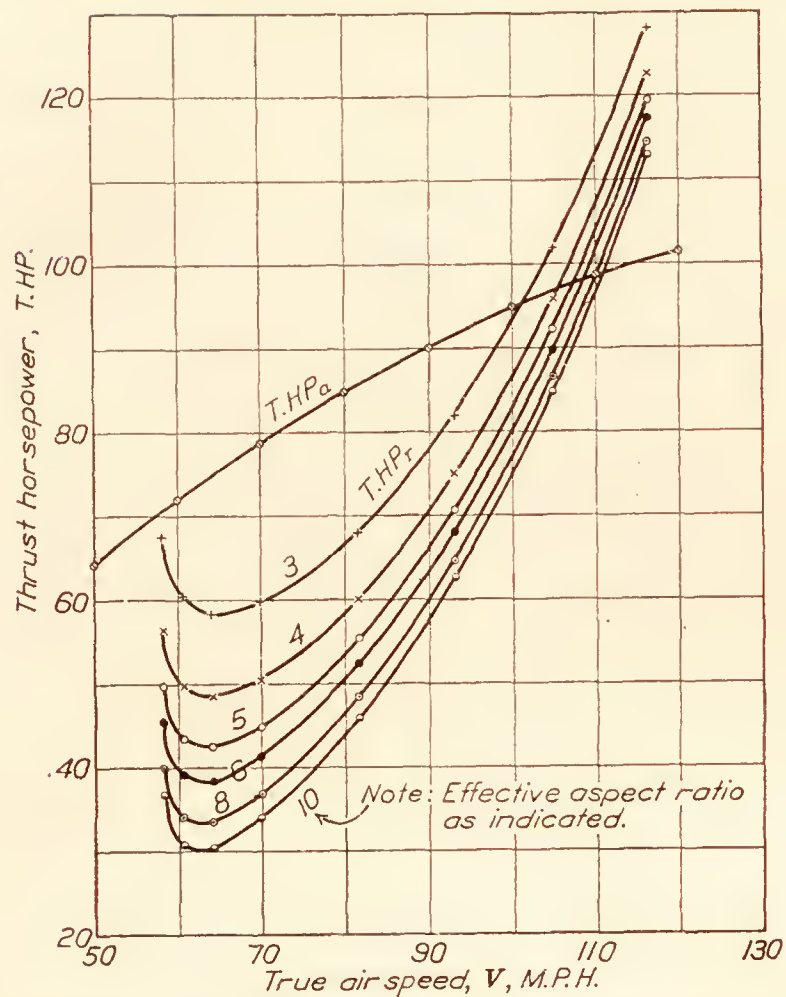


FIG. 10.—Power curves at 10,000 feet in normal standard atmosphere. Normal parasite

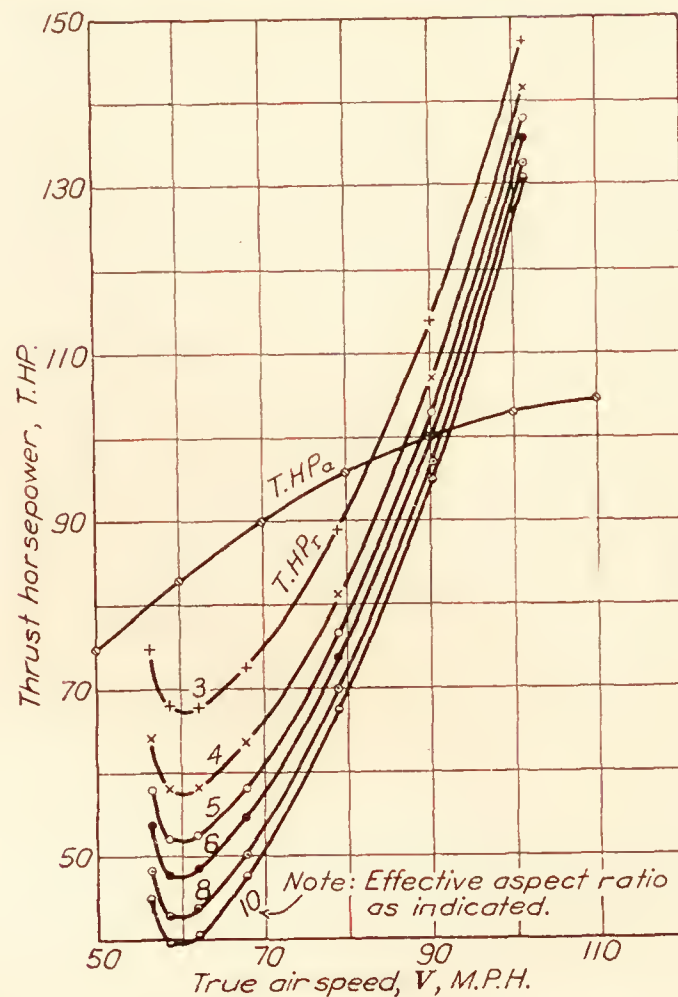


FIG. 12.—Power curves at 8,000 feet in normal standard atmosphere. High parasite

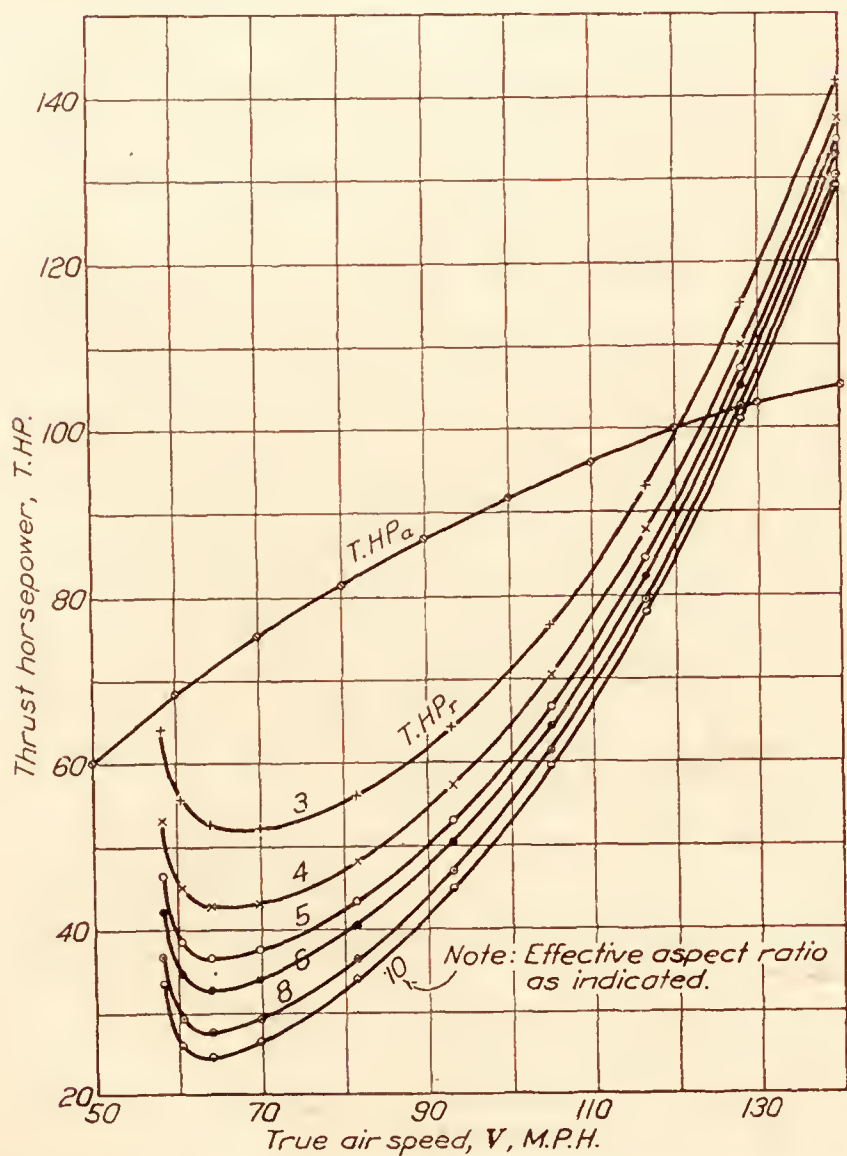


FIG. 11.—Power curves at 10,000 feet in normal standard atmosphere. Low parasite

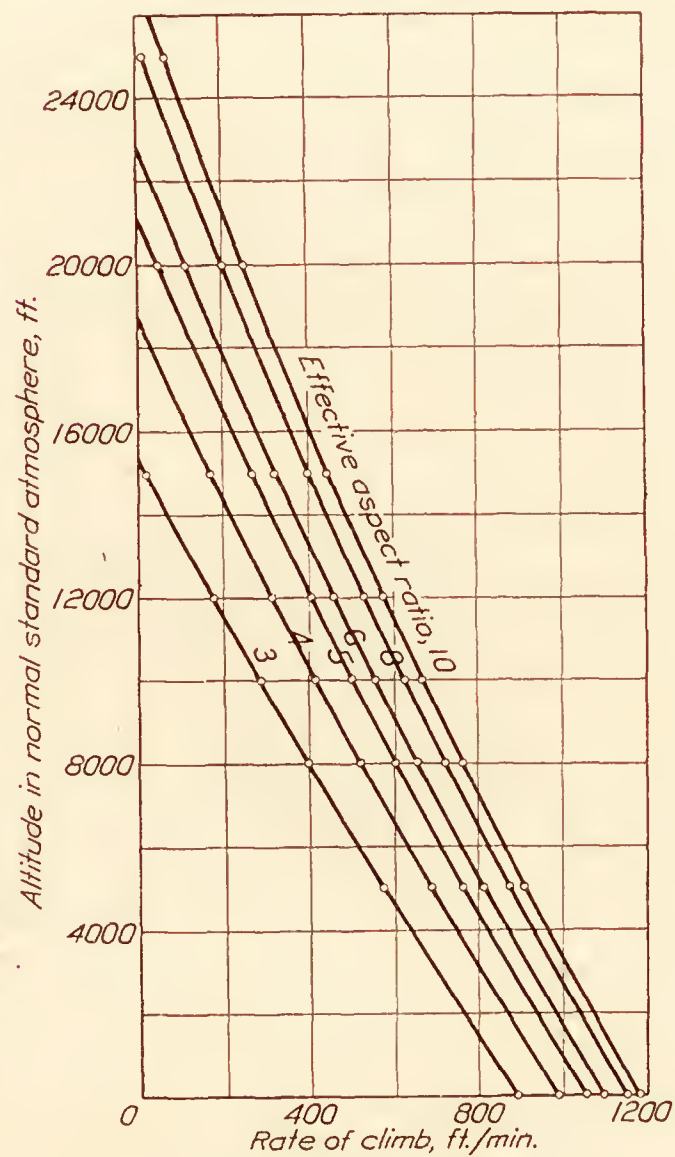


FIG. 13.—Rate of climb curves in normal standard atmosphere. Normal parasite



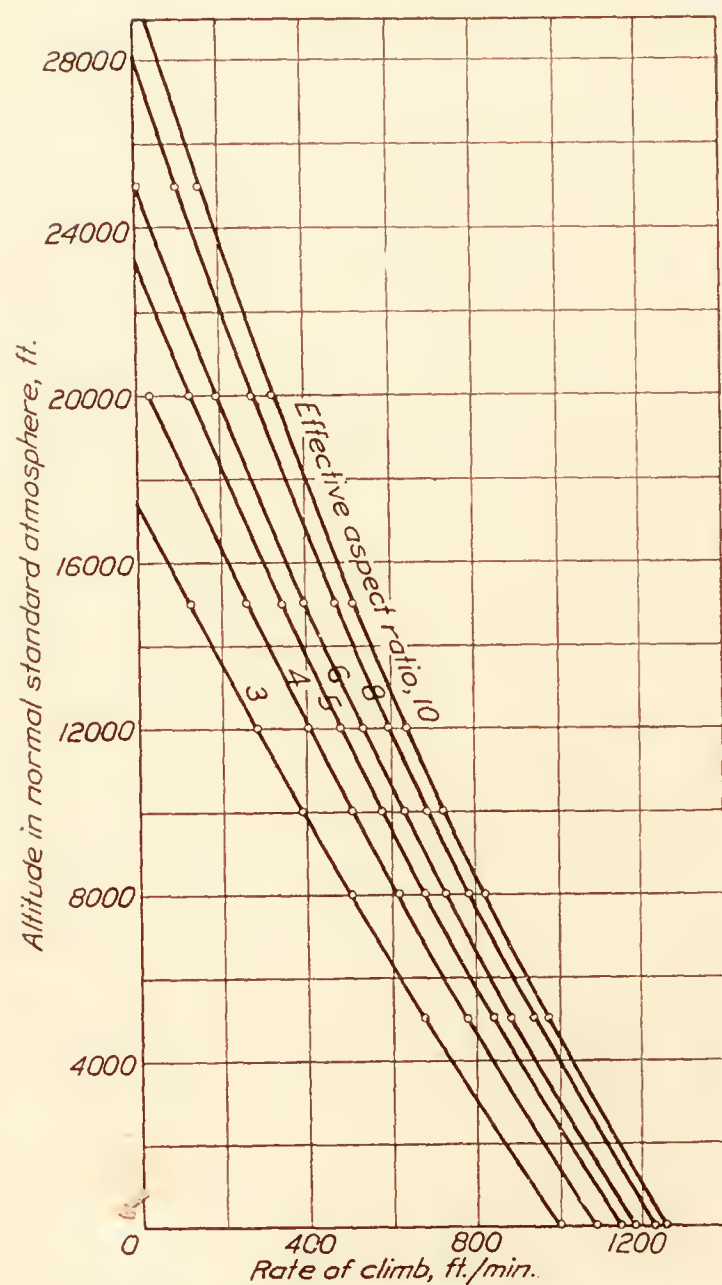


FIG. 14.—Rate of climb curves in normal standard atmosphere.  
Low parasite

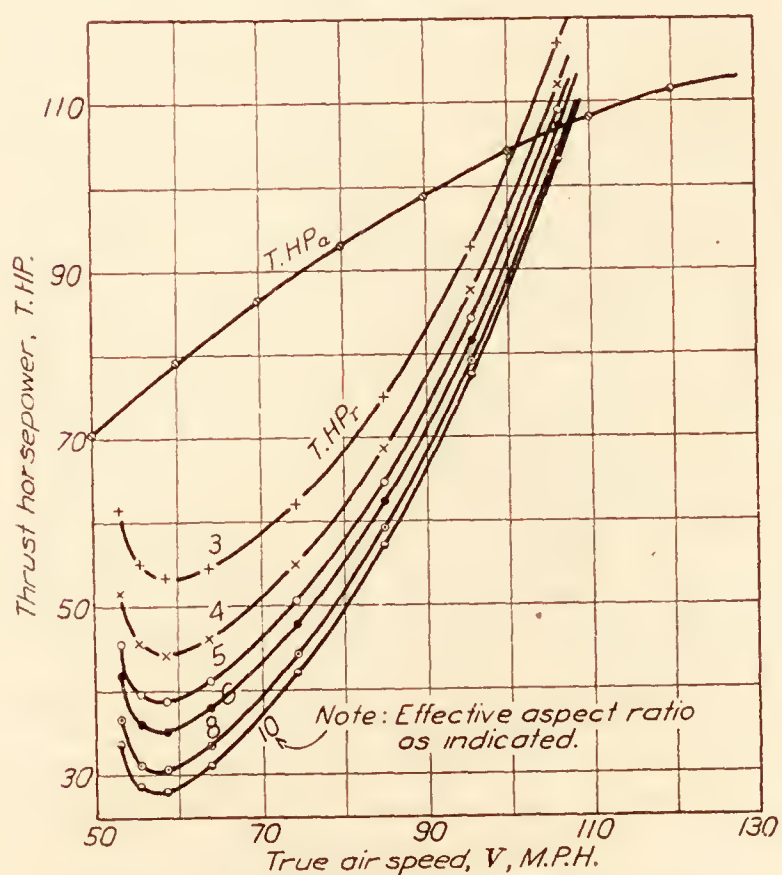


FIG. 16.—Power curves at 10,000-foot pressure altitude with temperature 83.3 per cent normal. Normal parasite.  $T=0.833 T_s$

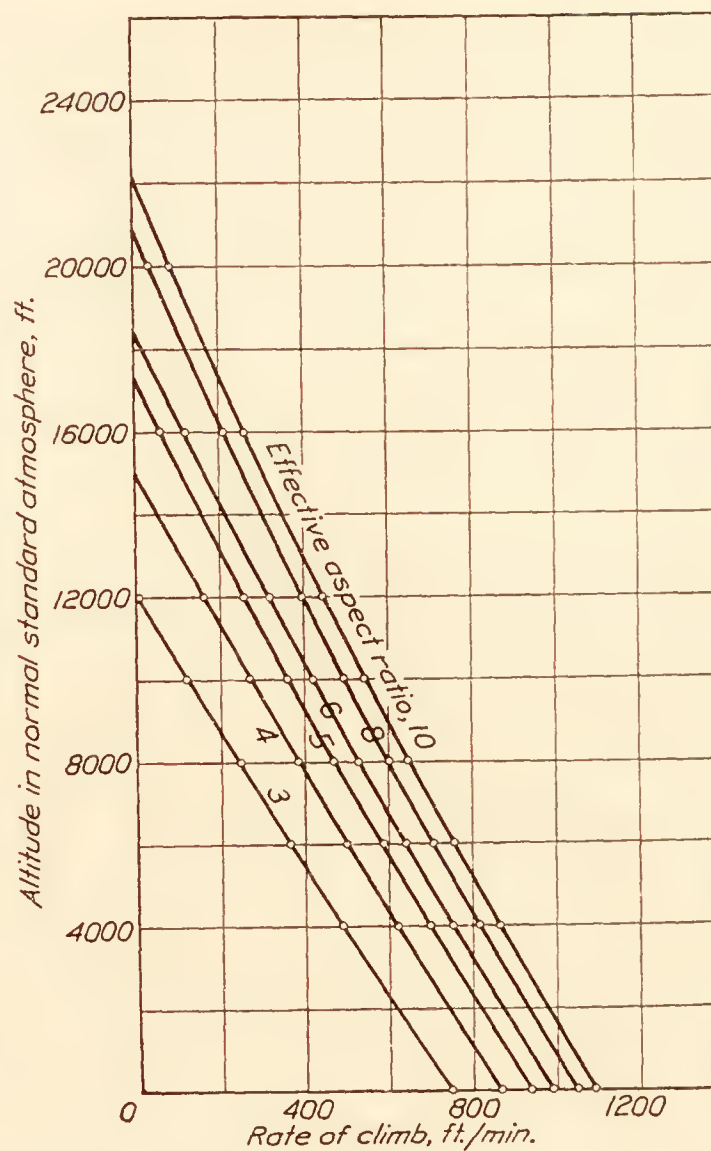


FIG. 15.—Rate of climb curves in normal standard atmosphere.  
High parasite

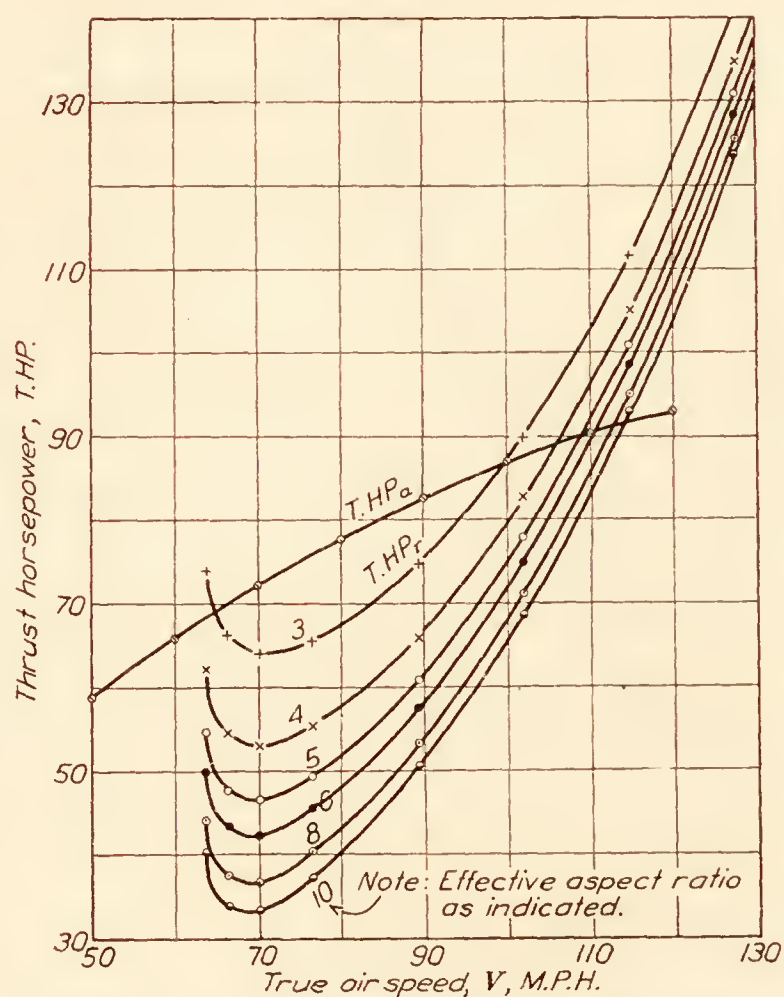


FIG. 17.—Power curves at 10,000-foot pressure altitude with temperature 120 per cent normal. Normal parasite.  $T=1.20 T_s$

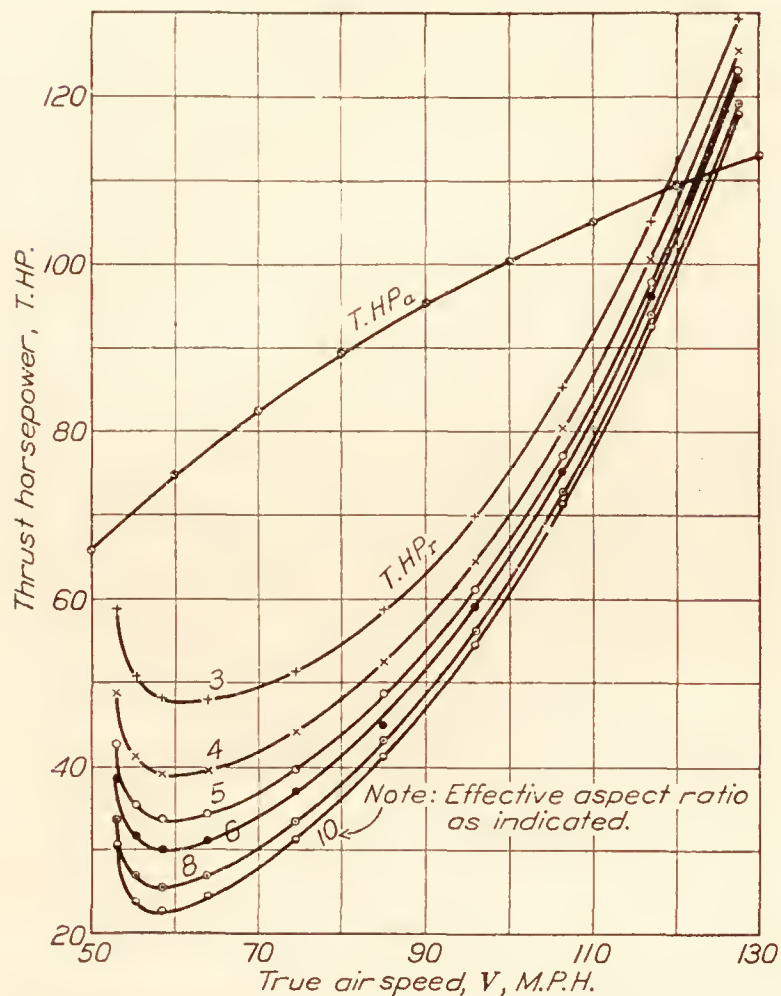


FIG. 18.—Power curves at 10,000-foot pressure altitude with temperature 83.3 per cent normal. Low parasite.  $T=0.833 T_s$ .

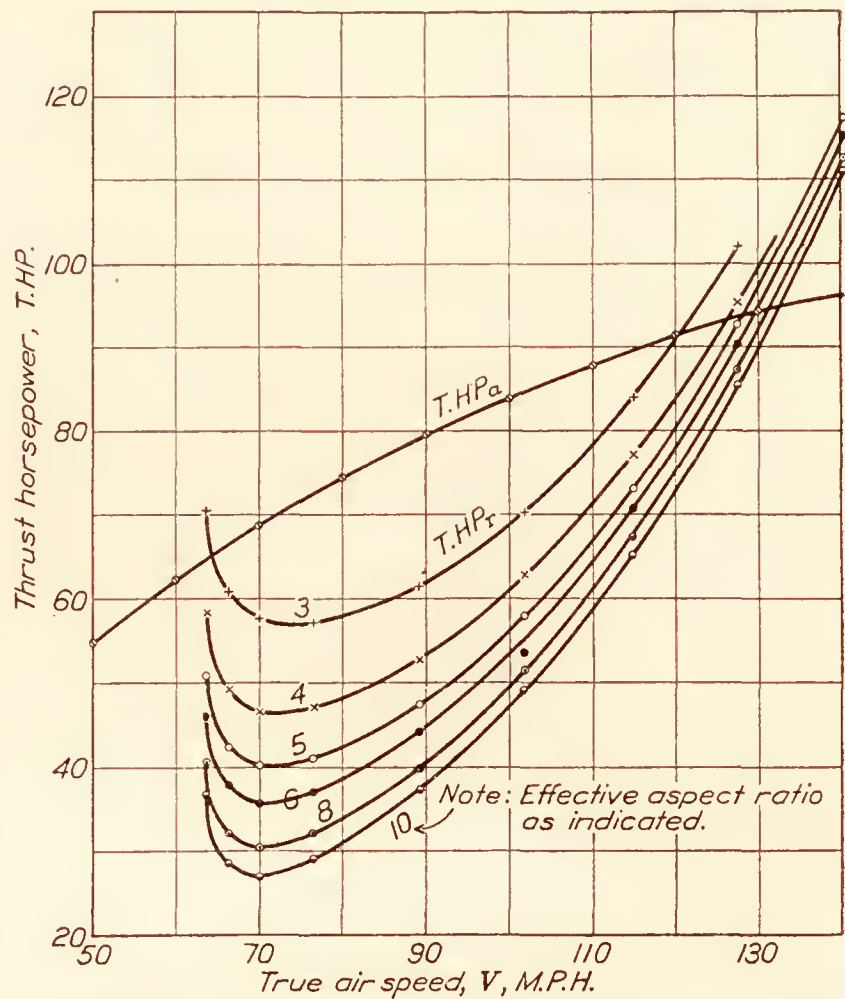


FIG. 19.—Power curves at 10,000-foot pressure altitude with temperature 120 per cent normal. Low parasite.  $T=1.20 T_s$ .

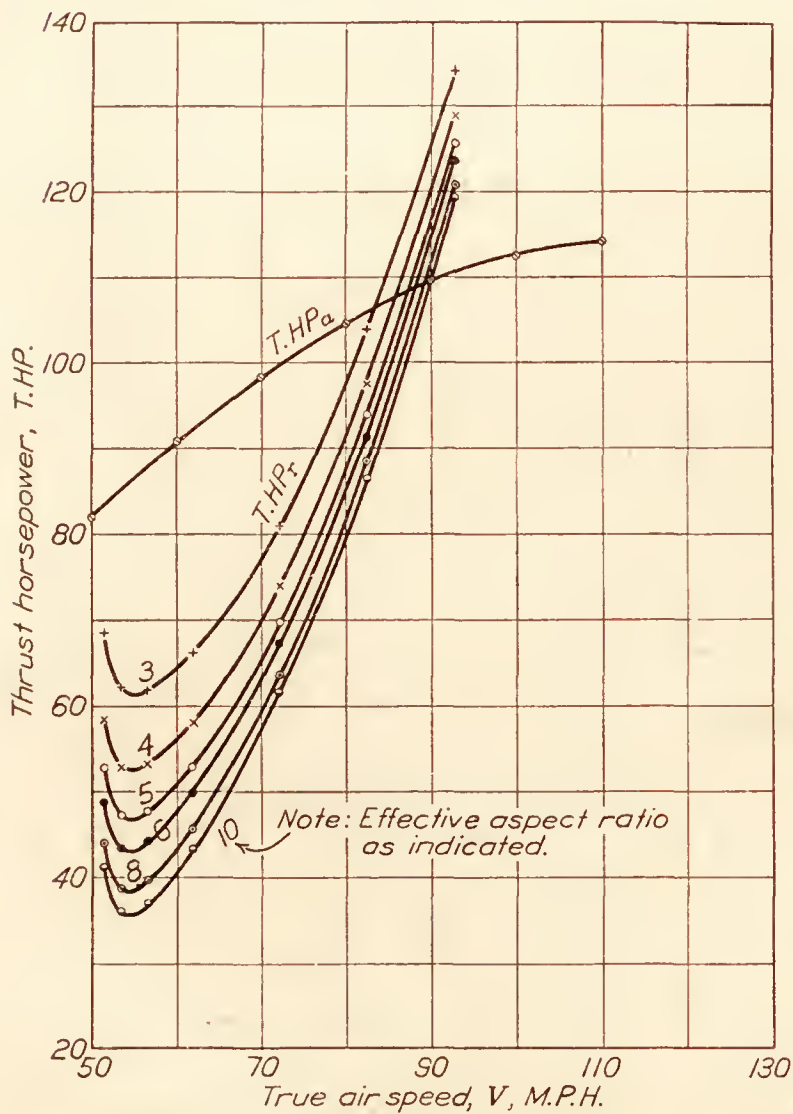


FIG. 20.—Power curves at 8,000-foot pressure altitude with temperature 83.3 per cent normal. High parasite.  $T=0.833 T_s$ .

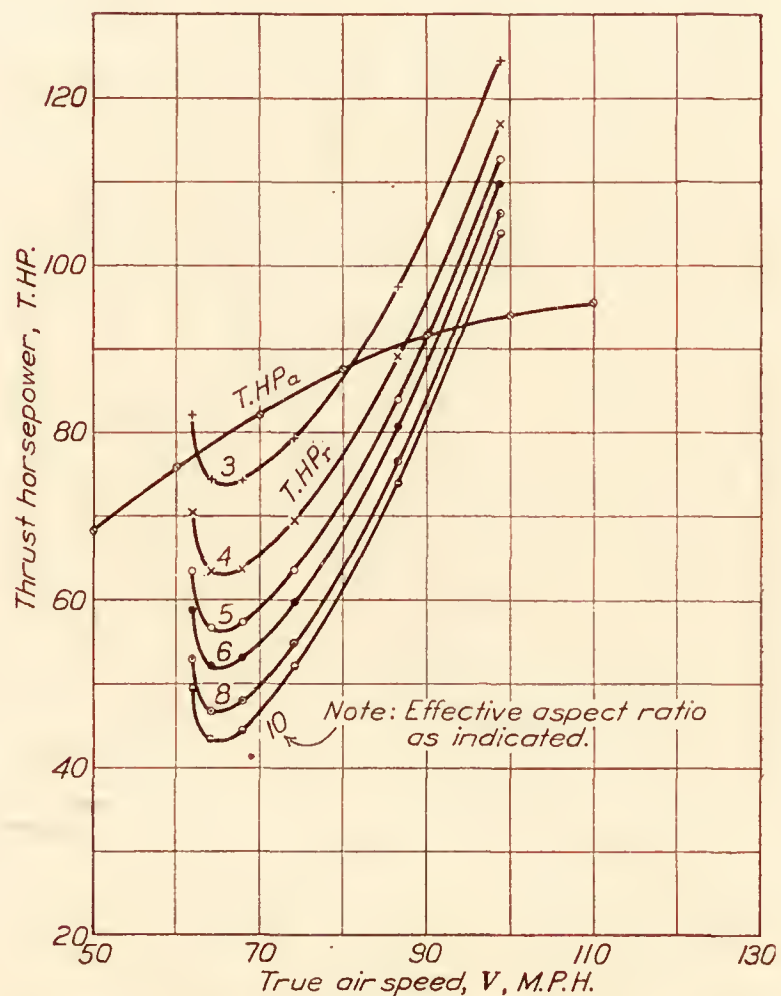


FIG. 21.—Power curves at 8,000-foot pressure altitude with temperature 120 per cent normal. High parasite.  $T=1.20 T_s$ .



## MAXIMUM SPEED

The effect of temperature on maximum speed, at a given pressure altitude, increases with increase in aspect ratio and decreases with increase in parasite drag. The absolute change is always small and in practice the actual maximum speed should be plotted against pressure altitude. When great accuracy is required it would be reasonable to restrict speed runs to days on which the temperatures deviate less than 5 per cent from normal. There appears to be no practical method for applying the small correction to maximum speed.

## CLIMBING SPEED

The effect of temperature on climbing speed at a given pressure altitude decreases with increase in parasite, but the change in indicated speed is so small that it can always be neglected.

## DISCUSSION

It has been shown that the climbing performance of an airplane under nonstandard atmospheric conditions is comparable to the performance under standard conditions at an altitude  $h$  that is between the pressure altitude  $h_p$  and the density altitude  $h_d$  in accordance with the relation

$$h = h_p - K (h_p - h_d). \quad (4)$$

The value of  $K$  has been shown to be practically independent of altitude, temperature departure from normal, and parasite drag, but it is dependent to a noticeable degree on effective aspect ratio.

Two methods of reducing observed climb data to standard conditions are available. The proper value of  $K$  is selected from Table XIII or Figure 22, and the value of the "plotting altitude" or "equivalent altitude"  $h$  is calculated for set of pressure and temperature readings. The calculated rates of climb may then be plotted against  $h$ , or a curve of  $h$  against time may be drawn up and the rates of climb read from the slope of the curve. Both methods have given practically identical results in all cases investigated by the author. The first method appears to be the more accurate, while the second method requires less calculation in the reduction.

It has been shown that maximum speeds should be plotted against pressure altitudes. This entails a slight error, depending in magnitude upon the departure of the temperatures from normal. If great accuracy is desired, maximum speed runs should be restricted to days on which the temperatures are approximately normal.

It has also been shown that for a given airplane the indicated air speed for best climb at a given pressure altitude is practically independent of the temperature. Climbing speeds should therefore be specified as the variation of indicated air speed with pressure.

It is of interest to compare the new methods with the old. Referring to Table VII and Figure 3, it will be seen that for temperatures 10 per cent greater than normal at 10,000 feet pressure altitude the actual rate of climb is 60 ft./min. less than that at the pressure altitude and 95 ft./min. greater than that at the density altitude, while the maximum speed is 1.0 mi./hr. greater than that at the pressure altitude and 4.0 mi./hr. greater than that at the density altitude. The angle of attack for best climb is exactly the same as that at the pressure altitude and slightly less than that at the density altitude. The foregoing comparison shows clearly that the pressure and the density methods of reduction must be discarded as incorrect and unsatisfactory.

An analysis of the British method of reduction defined by equation (2) and accompanying text leads to the conclusion that the assumptions necessary for its validity are not fulfilled. This is particularly true for the condition of "equal angles of climb," since, as shown by Tables VII, VIII, and IX, for example, temperatures greater than normal increase the air speed for best climb but reduce the rate of climb, and vice versa.

Attention is invited to the fact that the methods of reduction developed in this report are based on the N. A. C. A. (or S. T. Ae.) standard atmosphere, which has been officially adopted by all interested Government organizations in this country.



The purpose of performance reduction has been stated before and it will be repeated for emphasis. Observed performance depends greatly on atmospheric conditions, and if the performances of two airplanes are to be compared they must be reduced to a common basis that eliminates the variation in atmospheric conditions. While any arbitrary atmosphere could be used in a reduction, the final results can not be compared in two different standard atmospheres.

An exact method of reduction will result in the same curve of rate of climb against altitude in standard atmosphere for a given airplane, regardless of atmosphere conditions under which the tests are made, provided that the temperatures are not beyond the capacity of the engine-cooling system. This does not mean that two reduced curves of altitude against time will be identical, or even very close together in the usual plotting. However, the reduced curves of altitude against time should differ only in a relative displacement along the time scale. In general, the density method of reduction results in a displacement along the altitude scale, while the pressure method of reduction results in relative rotation indicated by divergence of the two curves. The method outlined in this report appears to eliminate the divergence noted in pressure plotting, but, unfortunately, the author is unable at this time to secure good flight test data obtained under very extreme temperature conditions. However, the tendencies can be illustrated by the flight test data given and reduced in Tables XIV and XV. The data for the two climbs are not strictly comparable owing to a slight difference in the propeller blade setting, which accounts for part of the difference between the two climbs after reduction, but the plotted climbs on Figures 23, 24, and 25 bring out the characteristics of the three methods of reduction. Figure 23 shows the shifting of the curves along the altitude axis when the density method is used; Figure 24 shows the divergence characteristic of the pressure method, and Figure 25 shows how the new method eliminates the divergence observed in Figure 24. The vertical shift remaining in Figure 25 is due largely to the change in propeller blade setting, but the reduction in the vertical shift in comparison with Figure 23 is quite pronounced.

BUREAU OF AERONAUTICS,  
NAVY DEPARTMENT,  
WASHINGTON, D. C., *May 18, 1928.*

#### BIBLIOGRAPHY

- Reference 1. Diehl, W. S.: Engine Performance and the Determination of Absolute Ceiling. N. A. C. A. Technical Report No. 171, 1923.  
Reference 2. Diehl, W. S.: Engineering Aerodynamics, Chapter 6. Ronald Press, 1928.  
Reference 3. Durand, W. F., and Lesley, E. P.: Comparison of Tests on Airplane Propellers in Flight with Wind Tunnel Model Tests on Similar Forms. N. A. C. A. Technical Report No. 220, 1925.

TABLE I  
VARIATION OF THRUST HORSEPOWER WITH ALTITUDE IN STANDARD ATMOSPHERE AT CONSTANT AIR SPEED

Altitude, <i>h</i> feet	$\frac{T. HP}{T. HP_0}$	Altitude, <i>h</i> feet	$\frac{T. HP}{T. HP_0}$
0	1.000	16,000	0.508
2,000	.925	18,000	.465
4,000	.854	20,000	.425
5,000	.820	22,000	.387
6,000	.787	24,000	.352
8,000	.723	25,000	.336
10,000	.663	26,000	.320
12,000	.608	28,000	.291
14,000	.556	30,000	.261
15,000	.532		



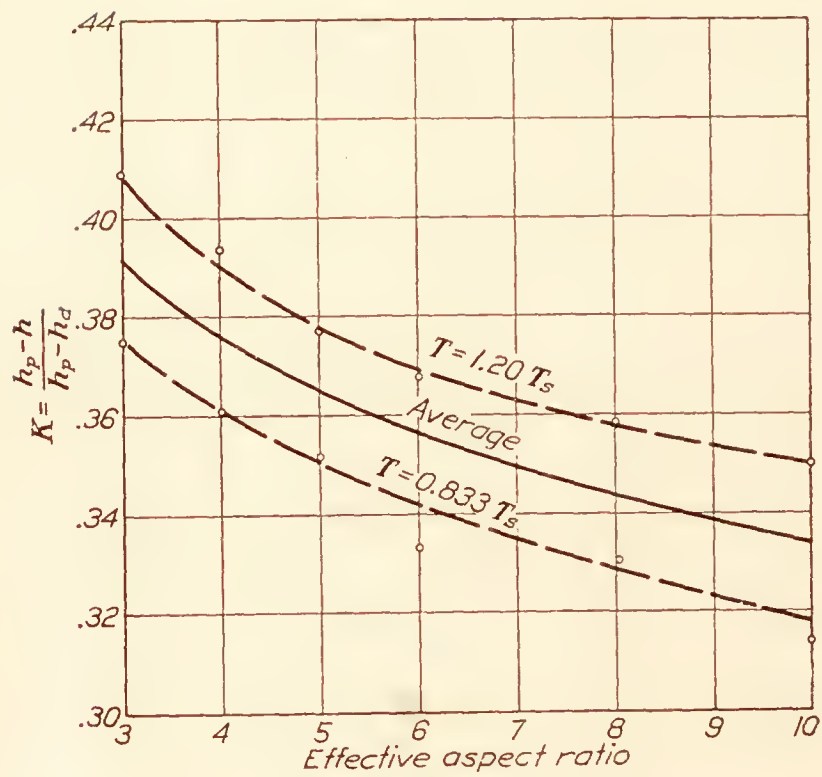


FIG. 22

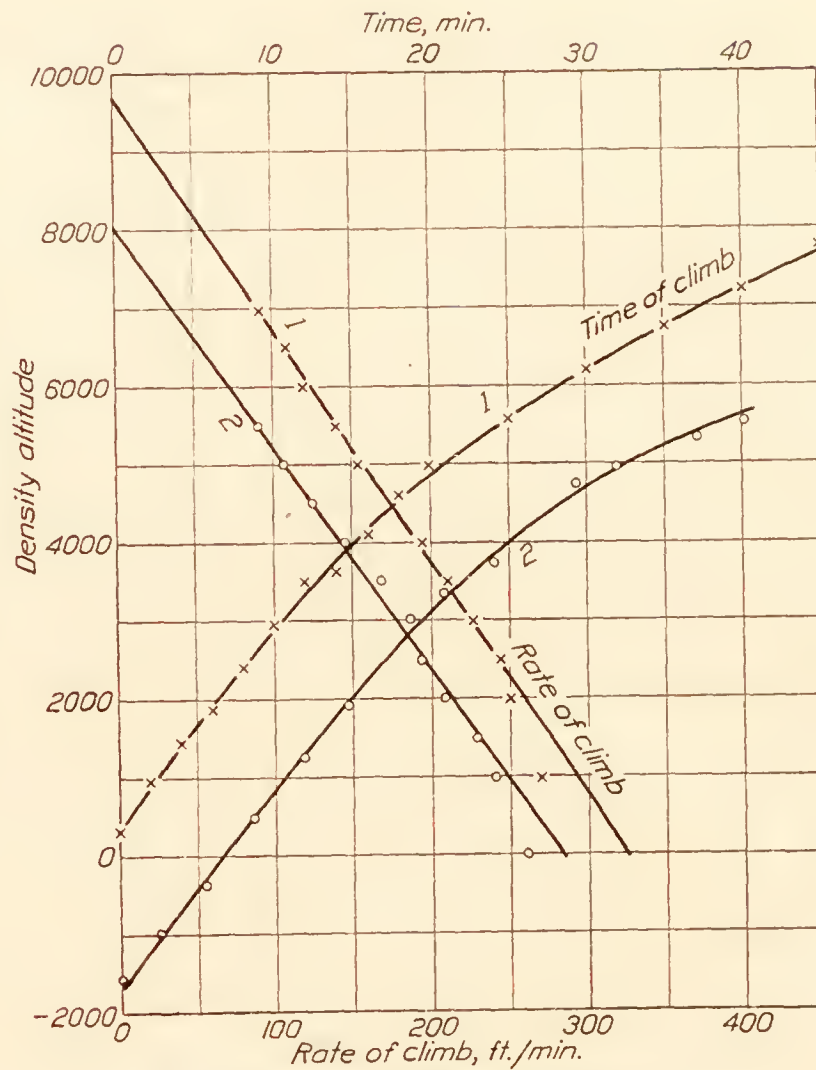


FIG. 23.—Reduction of climb by density method

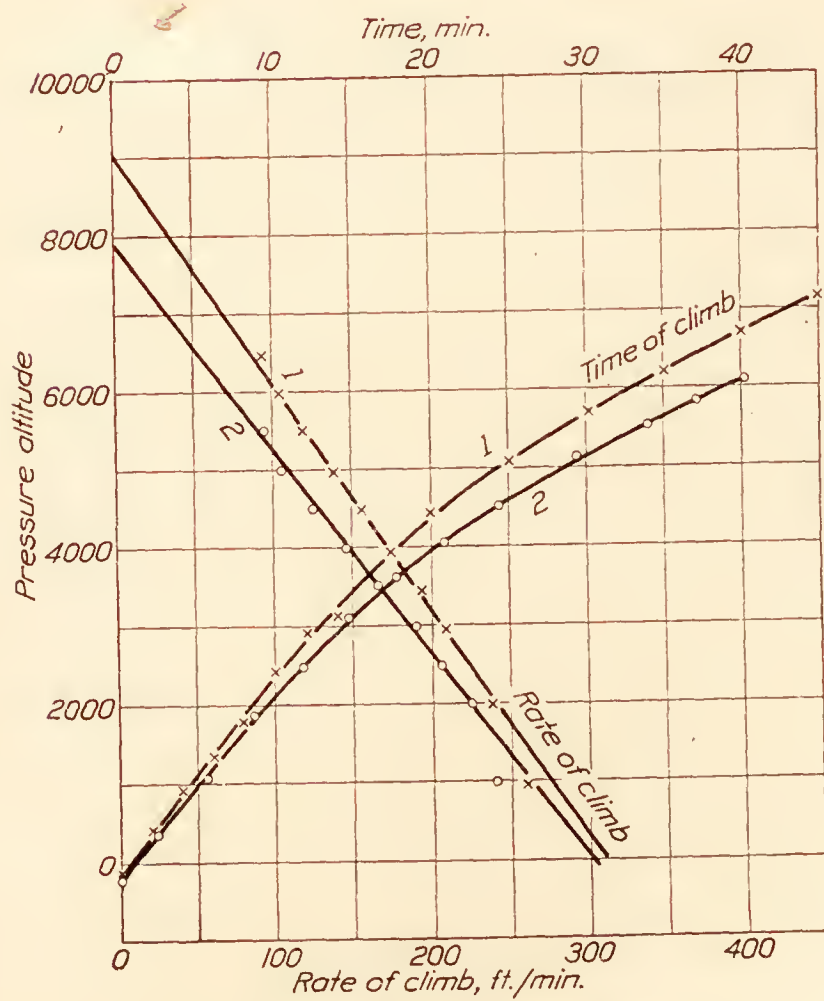


FIG. 24.—Reduction of climb by pressure method

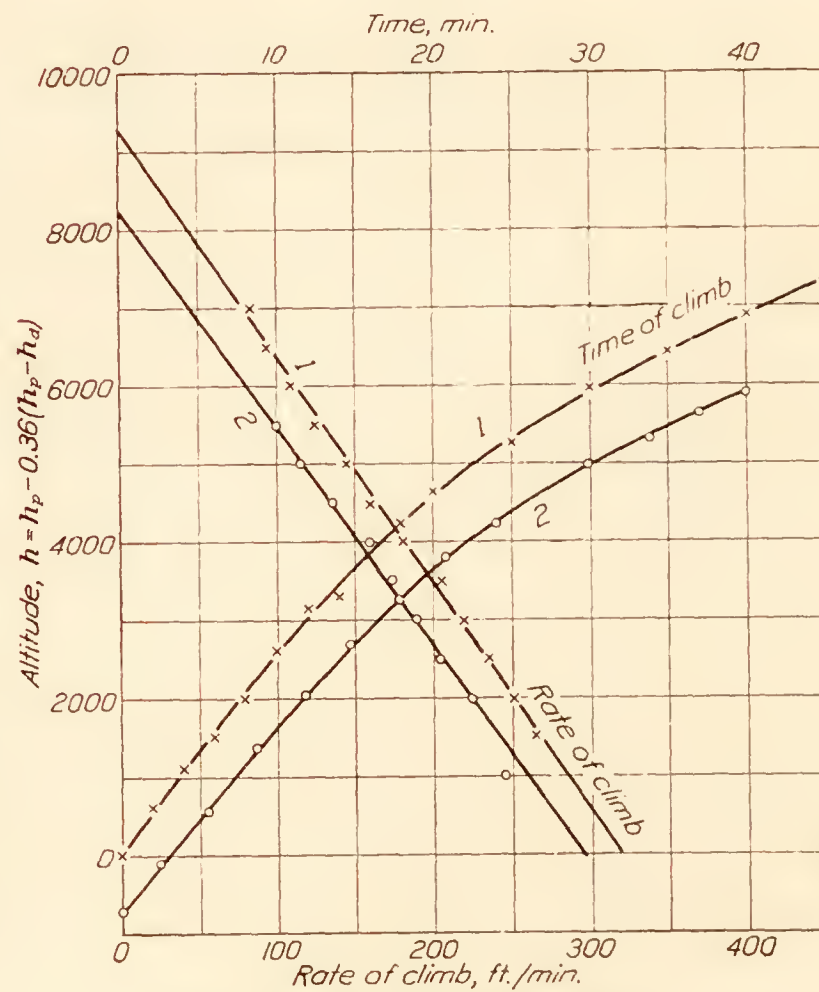


FIG. 25.—Reduction of climb by new method

TABLE II

VE-7 AIRPLANE—POWER REQUIRED FOR HORIZONTAL FLIGHT—GROSS WEIGHT, 2,230 POUNDS

Sea level		4,000 feet		8,000 feet		10,000 feet		12,000 feet		16,000 feet	
Air speed $V$ mi./hr.	T. HP <sub>r</sub>	$V$	T. HP <sub>r</sub>	$V$	T. HP <sub>r</sub>	$V$	T. HP <sub>r</sub>	$V$	T. HP <sub>r</sub>	$V$	T. HP <sub>r</sub>
50	43.8	53.1	46.5	56.4	49.4	58.2	51.0	60.0	52.6	64.0	56.2
52	38.3	55.2	40.7	58.7	43.2	60.5	44.6	62.4	45.9	66.6	49.1
55	37.3	58.3	39.6	62.0	42.1	64.0	43.4	66.0	44.8	70.5	47.8
60	39.5	63.7	41.9	67.7	44.5	69.9	46.0	72.1	47.3	76.8	50.6
70	48.3	74.3	51.3	79.0	54.4	81.5	56.2	84.1	58.0	89.7	61.8
80	61.5	84.9	65.2	90.2	69.3	93.1	71.6	96.2	73.8	102.4	78.8
90	79.7	95.5	84.5	101.5	89.9	104.8	92.8	108.2	95.6	-----	-----
100	103.1	106.1	109.2	112.8	116.3	116.4	120.0	-----	-----	-----	-----
110	132.7	116.8	140.8	-----	-----	-----	-----	-----	-----	-----	-----
120	167.9	-----	-----	-----	-----	-----	-----	-----	-----	-----	-----

TABLE III

VE-7 AIRPLANE—THRUST HORSEPOWER AVAILABLE WITH WRIGHT E-4 ENGINE, 194 B. HP AT 1,800 R. P. M.

Air speed $V$ mi./hr.	$\frac{V}{V_d}$	$\frac{\text{T. HP}}{\text{T. HP}_0}$	T. HP at sea level	T. HP at altitude				
				4,000 feet	8,000 feet	10,000 feet	12,000 feet	16,000 feet
50	0.434	0.640	97.0	82.8	70.1	64.5	59.0	49.2
60	.522	.716	108.6	92.7	78.5	72.2	66.0	55.2
70	.608	.785	119.0	101.6	86.0	79.1	72.4	60.4
80	.695	.845	128.0	109.3	92.5	85.2	77.8	65.0
90	.782	.898	136.0	116.2	98.3	90.4	82.7	69.1
100	.869	.945	143.2	122.3	103.5	95.3	87.1	72.7
110	.957	.985	149.0	127.2	107.7	99.1	90.6	75.7
115	1.000	1.000	151.4	130.7	110.6	101.7	-----	-----

TABLE IV

VE-7 AIRPLANE—CALCULATED PERFORMANCE IN STANDARD ATMOSPHERE—GROSS WEIGHT=2,230 POUNDS

Altitude-----feet-----	0	4,000	8,000	10,000	12,000	16,000
Stalling speed----- $V_s$ mi./hr-----	50.0	53.1	56.4	58.2	60.0	64.0
Max. speed----- $V_m$ mi./hr-----	116.0	113.2	109.2	107.3	105.0	98.6
Air speed for climb----- $V_c$ mi./hr-----	70.0	70.0	70.0	70.0	71.0	73.0
Excess T. HP for climb-----	70.5	54.7	40.0	32.8	26.0	13.0
Rate of climb-----	1,040	.810	590	485	385	190



TABLE V

VE-7 AIRPLANE AT 10,000 FEET PRESSURE ALTITUDE—EFFECT OF TEMPERATURE ON V AND T. HP.

V and T. HP <sub>r</sub> for values of $\frac{T}{T_s}$ given							
0.833		0.870		0.909		0.952	
V	T. HP <sub>r</sub>	V	T. HP <sub>r</sub>	V	T. HP <sub>r</sub>	V	T. HP <sub>r</sub>
53.1	46.6	54.3	47.6	55.5	48.6	56.8	49.8
55.2	40.7	56.4	41.6	57.7	42.5	59.0	43.5
58.4	39.6	59.7	40.5	61.0	41.4	62.5	42.3
63.8	42.0	65.2	42.9	66.6	43.9	68.2	44.9
74.4	51.3	76.0	52.4	77.7	53.6	79.3	54.8
85.0	65.4	86.8	66.8	88.8	68.3	90.8	69.9
95.7	84.7	97.7	86.5	99.9	88.5	102.3	90.6
106.3	109.6	108.5	112.0	111.0	114.6	113.6	117.2
116.9	141.0	119.5	144.1	122.1	147.3	125.0	150.8

V and T. HP <sub>r</sub> for values of $\frac{T}{T_s}$ given									
$\frac{T}{T_s}=1.00$		1.05		1.10		1.15		1.20	
V	T. HP <sub>r</sub>	V	T. HP <sub>r</sub>	V	T. HP <sub>r</sub>	V	T. HP <sub>r</sub>	V	T. HP <sub>r</sub>
58.2	51.0	59.6	52.3	61.0	53.5	62.4	54.7	63.8	55.9
60.5	44.6	62.0	45.7	63.5	46.8	64.9	47.8	66.3	48.9
64.0	43.4	65.6	44.5	67.1	45.5	68.6	46.5	70.1	47.5
69.9	46.0	71.6	47.1	73.3	48.2	75.0	49.3	76.6	50.4
81.5	56.2	83.5	57.6	85.5	58.9	87.4	60.3	89.3	61.6
93.1	71.6	95.4	73.4	97.6	75.1	99.8	76.8	102.0	78.4
104.8	92.8	107.4	95.1	109.9	97.3	112.4	99.5	114.8	101.7
116.4	120.0	119.3	122.8	122.1	125.7	124.8	128.6	127.5	131.3
128.1	154.5								

TABLE VI

VE-7 AIRPLANE AT 10,000 FEET PRESSURE ALTITUDE—EFFECT OF TEMPERATURE ON T. HP AVAILABLE

T. HP <sub>a</sub>									
$\frac{T}{T_s}=$ -----	0.833	0.870	0.909	0.952	Normal 1.000	1.05	1.10	1.15	1.20
True air speed V mi./hr.:									
50-----	70.7	69.2	67.7	66.1	64.5	62.8	61.5	60.2	58.8
60-----	79.2	77.5	75.7	74.1	72.2	70.4	68.8	67.3	65.8
70-----	86.7	84.8	82.9	81.2	79.1	77.1	75.4	73.7	72.2
80-----	93.3	91.3	89.3	87.3	85.2	83.0	81.2	79.3	77.7
90-----	99.2	97.0	94.9	92.7	90.4	88.2	86.1	84.2	82.5
100-----	104.6	102.4	100.1	97.8	95.3	93.0	90.9	88.8	87.0
110-----	108.7	106.3	104.0	101.7	99.1	96.6	94.5	92.3	90.3
115-----	111.5	109.2	106.8	104.3	101.7	99.2	96.8	94.8	92.7

TABLE VII

VE-7 AIRPLANE AT 10,000 PRESSURE ALTITUDE—EFFECT OF AIR TEMPERATURE ON PERFORMANCE—GROSS WEIGHT=2,230 POUNDS

$\frac{T}{T_s}$ -----	0.833	0.870	0.909	0.952	1.00
Max. excess T. HP <sub>a</sub> -----	40. 2	38. 6	36. 7	25. 1	33. 2
Speed for climb, V <sub>c</sub> -----	65. 0	67. 0	68. 0	69. 0	70. 0
Max. speed, V <sub>m</sub> mi./hr-----	105. 2	105. 4	106. 2	106. 8	107. 3
Actual rate of climb, ft./min-----	595	571	543	520	492
Altitude in normal standard atmosphere for actual rate of climb, h ft-----	7, 900	8, 350	8, 900	9, 450	10, 000
Density ratio, $\frac{\rho}{\rho_o}$ -----	0. 8861	0. 8492	0. 8122	0. 7753	0. 7384
Density altitude, h <sub>d</sub> -----	4, 080	5, 480	6, 930	8, 430	10, 000
$\Delta h=h_p-h$ -----	2, 100	1, 650	1, 100	550	0
$\Delta h_d=h_p-h_d$ -----	5, 920	4, 520	3, 070	1, 570	0
$K=\Delta h/\Delta h_d$ -----	0. 355	0. 365	0. 358	0. 351	-----
$\Delta V_m$ -----	-2. 1	-1. 9	-1. 1	- . 5	0
V <sub>s</sub> -----	53. 1	54. 3	55. 5	56. 8	58. 2
V <sub>c</sub> /V <sub>s</sub> -----	1. 22	1. 23	1. 23	1. 22	1. 20

$\frac{T}{T_s}$ -----	1.05	1.10	1.15	1.20
Maximum excess T. HP <sub>a</sub> -----	31. 1	29. 2	27. 3	25. 5
Speed for climb, V <sub>c</sub> -----	72. 0	73. 0	74. 0	75. 0
Maximum speed, V <sub>m</sub> mi./hr-----	107. 8	108. 3	108. 5	108. 8
Actual rate of climb, ft./min-----	460	432	404	377
Altitude in normal standard atmosphere for actual rate of climb, h ft-----	10, 550	11, 100	11, 600	12, 150
Density ratio, $\frac{\rho}{\rho_o}$ -----	0. 7032	0. 6713	0. 6421	0. 6153
Density altitude, h <sub>d</sub> -----	11, 540	12, 990	14, 370	15, 680
$\Delta h=h_p-h$ -----	550	1, 100	1, 600	2, 150
$\Delta h_d=h_p-h_d$ -----	1, 540	2, 990	4, 370	5, 680
$K=\Delta h/\Delta h_d$ -----	0. 357	0. 368	0. 367	0. 378
$\Delta V_m$ -----	+ . 5	+1. 0	+1. 2	+1. 5
V <sub>s</sub> -----	59. 7	61. 0	62. 4	63. 8
V <sub>c</sub> /V <sub>s</sub> -----	1. 21	1. 20	1. 19	1. 18



TABLE VIII

VE-7 AIRPLANE—EFFECT OF AIR TEMPERATURE ON PERFORMANCE AT 4,000 AND 8,000 FEET PRESSURE ALTITUDES

Pressure altitude-----	4,000 feet				
$\frac{T}{T_s}$ -----	0.833	0.909	1.00	1.10	1.20
Maximum excess T. HP <sub>a</sub> -----	62.7	58.8	54.7	50.8	46.8
Speed for climb, $V_c$ -----	65.0	67.5	70.0	71.0	72.0
Max. speed, $V_m$ -----	110.2	111.6	113.2	114.6	115.6
Actual rate of climb, ft./min-----	928	870	810	752	693
Altitude in normal standard atmosphere for actual rate of climb, $h$ ft-----	1,900	2,950	4,000	5,100	6,150
Density ratio, $\frac{\rho}{\rho_o}$ -----	1.0657	0.9769	0.8881	0.8074	0.7400
Density altitude, $h_d$ -----	-2,190	+790	4,000	7,130	9,930
$\Delta h = h_p - h$ -----	2,100	1,050	0	1,100	2,150
$\Delta h_d = h_p - h_d$ -----	6,190	3,220	0	3,130	5,930
$K = \Delta h / \Delta h_d$ -----	0.349	0.326	-----	0.351	0.362
$\Delta V_m$ -----	-3.0	-1.6	0	1.2	2.4
$V_s$ -----	48.5	50.6	53.1	55.7	58.2
$V_c / V_s$ -----	1.34	1.34	1.32	1.28	1.24

Pressure altitude-----	8,000 feet				
$\frac{T}{T_s}$ -----	0.833	0.909	1.00	1.10	1.20
Maximum excess T. HP <sub>a</sub> -----	47.5	43.7	40.0	36.0	32.5
Speed for climb, $V_c$ -----	66.0	68.0	70.0	72.0	74.0
Maximum speed, $V_m$ -----	107.2	108.2	109.2	110.5	111.3
Actual rate of climb, ft./min-----	703	647	592	533	481
Altitude in normal standard atmosphere for actual rate of climb, $h$ ft-----	5,900	6,900	8,000	9,100	10,050
Density ratio, $\frac{\rho}{\rho_o}$ -----	0.9431	0.8645	0.7859	0.7145	0.6549
Density altitude, $h_d$ -----	1,980	4,880	8,000	11,030	13,760
$\Delta h = h_p - h$ -----	2,100	1,100	0	1,100	2,050
$\Delta h_d = h_p - h_d$ -----	6,020	3,120	0	3,030	5,760
$K = \Delta h / \Delta h_d$ -----	0.349	0.352	-----	0.363	0.356
$\Delta V_m$ -----	-2.0	-1.0	0	1.3	2.1
$V_s$ -----	51.5	53.8	56.4	59.2	61.9
$V_c / V_s$ -----	1.28	1.26	1.24	1.22	1.20

TABLE IX

VE-7 AIRPLANE—EFFECT OF AIR TEMPERATURE ON PERFORMANCE AND 12,000 AND 16,000 FOOT PRESSURE ALTITUDES

Pressure altitude-----	12,000 feet				
$\frac{T}{T_s}$ -----	0. 833	0. 909	1. 00	1. 10	1. 20
Maximum excess T. HP <sub>a</sub> -----	33. 3	30. 0	26. 0	22. 6	19. 3
Speed for climb, $V_c$ -----	66. 5	68. 0	71. 0	73. 0	76. 0
Maximum speed, $V_m$ -----	103. 3	104. 2	104. 7	105. 6	105. 7
Actual rate of climb, ft./min-----	493	443	385	334	285
Altitude in normal standard atmosphere for actual rate of climb, $h$ ft-----	9, 850	10, 900	12, 000	13, 050	14, 050
Density ratio, $\frac{\rho}{\rho_o}$ -----	0. 9317	0. 7624	0. 6931	0. 6301	0. 5776
Density altitude, $h_d$ -----	6, 160	8, 970	12, 000	14, 950	17, 590
$\Delta h = h_p - h$ -----	2, 150	1, 100	0	1, 050	2, 050
$\Delta h_d = h_p - h_d$ -----	5, 840	3, 030	0	2, 950	5, 590
$K = \Delta h / \Delta h_d$ -----	0. 368	0. 363	-----	0. 356	0. 367
$\Delta V_m$ -----	-1. 4	- . 5	0	. 9	1. 0
$V_s$ -----	54. 8	57. 2	60. 0	62. 9	65. 7
$V_c / V_s$ -----	1. 19	1. 19	1. 18	1. 16	1. 16

Pressure altitude-----	16,000 feet				
$\frac{T}{T_s}$ -----	0. 833	0. 909	1. 00	1. 10	1. 20
Maximum excess T. HP <sub>a</sub> -----	20. 0	17. 0	13. 0	9. 8	6. 7
Speed for climb, $V_c$ -----	67. 0	70. 0	73. 0	76. 0	79. 0
Maximum speed, $V_m$ -----	97. 8	98. 2	98. 6	97. 5	95. 8
Actual rate of climb, ft./min-----	295	250	197	147	99
Altitude in normal standard atmosphere for actual rate of climb, $h$ ft-----	3, 900	14, 850	16, 000	17, 050	18, 050
Density ratio, $\frac{\rho}{\rho_o}$ -----	0. 7306	0. 6697	0. 6088	0. 5535	0. 5073
Density altitude, $h_d$ -----	10, 340	13, 060	16, 000	18, 860	21, 430
$\Delta h = h_p - h$ -----	2, 100	1, 150	0	1, 100	2, 050
$\Delta h_d = h_p - h_d$ -----	5, 560	2, 940	0	2, 860	5, 430
$K = \Delta h / \Delta h_d$ -----	0. 371	0. 391	-----	0. 384	0. 377
$\Delta V_m$ -----	- . 8	- . 4	0	-1. 1	-2. 8
$V_s$ -----	58. 4	61. 0	64. 0	67. 1	70. 1
$V_c / V_s$ -----	1. 15	1. 15	1. 14	1. 13	1. 13



TABLE X

EFFECT OF AIR TEMPERATURE ON PERFORMANCE OF AIRPLANES WITH NORMAL PARASITE DRAG AT 10,000 FEET  
PRESSURE ALTITUDE

Effective aspect ratio----- $\frac{T}{T_s} =$ -----	3			4		
	0.833	1.00	1.20	0.833	1.00	1.20
Maximum excess T. HP-----	27.7	19.4	10.6	35.7	28.3	20.5
Speed for climb, $V_c$ -----	69.0	73.0	79.0	67.0	72.0	77.0
Maximum speed, $V_m$ -----	101.2	102.2	100.0	103.8	105.7	106.2
Actual rate of climb, ft./min-----	410	287	157	528	418	304
Altitude in normal standard atmosphere, for actual rate of climb, $h$ ft-----	7,800	10,000	12,300	7,850	10,000	12,200
Density ratio-----	0.8861	0.7384	0.6153	0.8861	0.7384	0.6153
Density altitude, $h_d$ -----	4,080	10,000	15,680	4,080	10,000	15,680
$\Delta h_d = h_p - h$ -----	2,200	0	-2,300	2,150	0	-2,200
$\Delta h_d = h_p - h_d$ -----	5,920	0	-5,680	5,920	0	-5,680
$K = \Delta h / \Delta h_d$ -----	0.372	-----	0.405	0.363	-----	0.387
$\Delta V_m$ -----	-1.0	0	-2.2	-1.9	0	+0.5
$V_s$ -----	53.1	58.2	63.7	53.1	58.2	63.7
$V_c / V_s$ -----	1.30	1.25	1.24	1.26	1.24	1.21

Effective aspect ratio----- $\frac{T}{T_s} =$ -----	5			6		
	0.833	1.00	1.20	0.833	1.00	1.20
Maximum excess T. HP-----	40.9	34.3	26.8	44.2	37.8	30.7
Speed for climb, $V_c$ -----	65.0	71.0	75.5	64.5	70.0	74.0
Maximum speed, $V_m$ -----	105.2	107.7	109.1	106.2	108.9	110.8
Actual rate of climb, ft./min-----	605	507	397	654	559	454
Altitude in normal standard atmosphere, for actual rate of climb, $h$ ft-----	7,950	10,000	12,200	8,050	10,000	12,150
Density ratio-----	0.8861	0.7384	0.6153	0.8861	0.7384	0.6153
Density altitude, $h_d$ -----	4,080	10,000	15,680	4,080	10,000	15,680
$\Delta h_d = h_p - h$ -----	2,050	0	-2,200	1,950	0	-2,150
$\Delta h_d = h_p - h_d$ -----	5,920	0	-5,680	5,920	0	-5,680
$K = \Delta h / \Delta h_d$ -----	0.346	-----	0.387	0.329	-----	0.378
$\Delta V_m$ -----	-2.3	0	+1.4	-2.7	0	+1.9
$V_s$ -----	53.1	58.2	63.7	53.1	58.2	63.7
$V_c / V_s$ -----	1.22	1.22	1.19	1.21	1.20	1.16

Effective aspect ratio----- $\frac{T}{T_s} =$ -----	8			10		
	0.833	1.00	1.20	0.833	1.00	1.20
Maximum excess T. HP-----	48.4	42.5	35.8	50.9	45.2	39.2
Speed for climb, $V_c$ -----	63.5	68.0	73.0	63.0	67.0	72.7
Maximum speed, $V_m$ -----	107.6	110.4	112.8	108.2	111.2	114.2
Actual rate of climb, ft./min-----	717	629	530	753	669	580
Altitude in normal standard atmosphere, for actual rate of climb, $h$ ft-----	8,100	10,000	12,050	8,150	10,000	12,050
Density ratio-----	0.8861	0.7384	0.6153	0.8861	0.7384	0.6153
Density altitude, $h_d$ -----	4,080	10,000	15,680	4,080	10,000	15,680
$\Delta h_d = h_p - h$ -----	1,900	0	-2,050	1,850	0	-2,050
$\Delta h_d = h_p - h_d$ -----	5,920	0	-5,680	5,920	0	-5,680
$K = \Delta h / \Delta h_d$ -----	0.321	-----	0.361	0.313	-----	0.361
$\Delta V_m$ -----	-2.8	0	+2.4	-3.0	0	+3.0
$V_s$ -----	53.1	58.2	63.7	53.1	58.2	63.7
$V_c / V_s$ -----	1.20	1.17	1.15	1.19	1.15	1.14

TABLE XI

EFFECT OF AIR TEMPERATURE ON PERFORMANCE OF AIRPLANES WITH LOW PARASITE DRAG AT 10,000 FEET  
PRESSURE ALTITUDE

Effective aspect ratio----- $\frac{T}{T_s}$ -----	3			4		
	0. 833	1. 00	1. 20	0. 833	1. 00	1. 20
Maximum excess T. HP-----	34. 5	26. 2	17. 7	41. 5	34. 3	26. 7
Speed for climb, $V_c$ -----	78. 5	82. 0	88. 5	76. 0	80. 0	86. 0
Maximum speed, $V_m$ -----	118. 7	120. 2	120. 6	121. 0	123. 8	126. 4
Actual rate of climb, ft./min-----	511	387	262	614	507	395
Altitude in normal standard atmosphere, for actual rate of climb, $h$ ft-----	7, 850	10, 000	12, 350	7, 950	10, 000	12, 200
Density ratio-----	0. 8861	0. 7384	0. 6153	0. 8861	0. 7384	0. 6153
Density altitude, $h_d$ -----	4, 080	10, 000	15, 680	4, 080	10, 000	15, 680
$\Delta h = h_p - h$ -----	2, 150	0	-2, 350	2, 050	0	-2, 200
$\Delta h_d = h_p - h_d$ -----	5, 920	0	-5, 680	5, 920	0	-5, 680
$K = \Delta h / \Delta h_d$ -----	0. 363	-----	0. 414	0. 346	-----	0. 387
$\Delta V_m$ -----	-1. 5	0	+0. 4	-2. 8	0	+2. 6
$V_s$ -----	53. 1	58. 2	63. 7	53. 1	58. 2	63. 7
$V_c / V_s$ -----	1. 48	1. 41	1. 39	1. 43	1. 38	1. 35

Effective aspect ratio----- $\frac{T}{T_s}$ -----	5			6		
	0. 833	1. 00	1. 20	0. 833	1. 00	1. 20
Maximum excess T. HP-----	46. 0	39. 0	32. 3	49. 0	42. 8	36. 0
Speed for climb, $V_c$ -----	74. 0	78. 0	85. 0	72. 5	76. 0	82. 0
Maximum speed, $V_m$ -----	122. 5	125. 4	128. 1	123. 1	126. 5	129. 8
Actual rate of climb, ft./min-----	681	577	478	725	633	533
Altitude in normal standard atmosphere, for actual rate of climb, $h$ ft-----	7, 950	10, 000	12, 100	8, 100	10, 000	12, 050
Density ratio-----	0. 8861	0. 7384	0. 6153	0. 8861	0. 7384	0. 6153
Density altitude, $h_d$ -----	4, 080	10, 000	15, 680	4, 080	10, 000	15, 680
$\Delta h = h_p - h$ -----	2, 050	0	-2, 100	1, 900	0	-2, 050
$\Delta h_d = h_p - h_d$ -----	5, 920	0	-5, 680	5, 920	0	-5, 680
$K = \Delta h / \Delta h_d$ -----	0. 346	-----	0. 370	0. 321	-----	0. 361
$\Delta V_m$ -----	-2. 9	0	+2. 7	-3. 4	0	+3. 3
$V_s$ -----	53. 1	58. 2	63. 7	53. 1	58. 2	63. 7
$V_c / V_s$ -----	1. 39	1. 34	1. 33	1. 36	1. 31	1. 29

Effective aspect ratio----- $\frac{T}{T_s}$ -----	8			10		
	0. 833	1. 00	1. 20	0. 833	1. 00	1. 20
Maximum excess T. HP-----	52. 5	46. 5	40. 3	54. 7	49. 0	43. 4
Speed for climb, $V_c$ -----	71. 0	75. 0	80. 0	69. 0	74. 0	79. 0
Maximum speed, $V_m$ -----	124. 4	128. 0	131. 3	125. 0	128. 6	132. 5
Actual rate of climb, ft./min-----	777	688	596	810	725	642
Altitude in normal standard atmosphere, for actual rate of climb, $h$ ft-----	8, 100	10, 000	12, 000	8, 200	10, 000	11, 900
Density ratio-----	0. 8861	0. 7384	0. 6153	0. 8861	0. 7384	0. 6153
Density altitude, $h_d$ -----	4, 080	10, 000	15, 680	4, 080	10, 000	15, 680
$\Delta h = h_p - h$ -----	1, 900	0	-2, 000	1, 800	0	-1, 900
$\Delta h_d = h_p - h_d$ -----	5, 920	0	-5, 680	5, 920	0	-5, 680
$K = \Delta h / \Delta h_d$ -----	0. 321	-----	0. 352	0. 304	-----	0. 335
$\Delta V_m$ -----	-3. 6	0	+3. 3	-3. 6	0	+3. 9
$V_s$ -----	53. 1	58. 2	63. 7	53. 1	58. 2	63. 7
$V_c / V_s$ -----	1. 34	1. 29	1. 26	1. 30	1. 27	1. 24



TABLE XII

EFFECT OF AIR TEMPERATURE ON PERFORMANCE OF AIRPLANES WITH HIGH PARASITE DRAG, 8,000 FEET PRESSURE ALTITUDE

Effective Aspect Ratio----- $\frac{T}{T_s} =$ -----	3			4		
	0. 833	1. 00	1. 20	0. 833	1. 00	1. 20
Maximum excess T. HP-----	26. 3	16. 9	6. 8	34. 8	26. 3	17. 2
Speed for climb, $V_c$ -----	59. 0	64. 0	69. 0	58. 2	64. 0	67. 7
Maximum speed, $V_m$ -----	83. 6	83. 2	81. 1	85. 9	87. 4	87. 5
Actual rate of climb, ft./min-----	389	250	101	51. 5	389	255
Altitude in normal standard atmosphere, for actual rate of climb, $h$ ft-----	5, 650	8, 000	10, 350	5, 750	8, 000	10, 350
Density ratio-----	0. 9431	0. 7859	0. 6549	0. 9431	0. 7859	0. 6549
Density altitude, $h_d$ -----	1, 980	8, 000	13, 760	1, 980	8, 000	13, 760
$\Delta h = h_p - h$ -----	2, 350	0	-2, 350	2, 250	0	-2, 350
$\Delta h_d = h_p - h_d$ -----	6, 020	0	-5, 760	6, 020	0	-5, 760
$K = \Delta h / \Delta h_d$ -----	0. 390	-----	0. 408	0. 374	-----	0. 408
$\Delta V_m$ -----	+0. 4	0	-2. 1	-1. 5	0	+0. 5
$V_s$ -----	51. 5	56. 4	61. 8	51. 5	56. 4	61. 8
$V_c / V_s$ -----	1. 15	1. 13	1. 12	1. 13	1. 13	1. 10

Effective aspect ratio----- $\frac{T}{T_s} =$ -----	5			6		
	0. 833	1. 00	1. 20	0. 833	1. 00	1. 20
Max. excess T. HP-----	40. 2	31. 8	23. 9	43. 7	35. 8	28. 2
Speed for climb, $V_c$ -----	57. 7	63. 5	67. 5	57. 5	62. 5	67. 2
Max. speed, $V_m$ -----	87. 3	89. 3	90. 2	88. 4	90. 6	91. 9
Actual rate of climb, ft./min-----	595	470	354	647	529	418
Altitude in normal standard atmosphere, for actual rate of climb, $h$ ft-----	5, 800	8, 000	10, 150	5, 900	8, 000	10, 100
Density ratio-----	0. 9431	0. 7859	0. 6549	0. 9431	0. 7859	0. 6549
Density altitude, $h_d$ -----	1, 980	8, 000	13, 760	1, 980	8, 000	13, 760
$\Delta h = h_p - h$ -----	2, 200	0	-2, 150	2, 100	0	-2, 100
$\Delta h_d = h_p - h_d$ -----	6, 020	0	-5, 760	6, 020	0	-5, 760
$K = \Delta h / \Delta h_d$ -----	0. 365	-----	0. 373	0. 349	-----	0. 364
$\Delta V_m$ -----	-2. 0	0	+0. 9	-2. 2	0	+1. 3
$V_s$ -----	51. 5	56. 4	61. 8	51. 5	56. 4	61. 8
$V_c / V_s$ -----	1. 12	1. 13	1. 09	1. 12	1. 11	1. 09

Effective aspect ratio----- $\frac{T}{T_s} =$ -----	8			10		
	0. 833	1. 00	1. 20	0. 833	1. 00	1. 20
Max. excess T. HP-----	48. 3	40. 8	33. 3	50. 8	43. 7	36. 7
Speed for climb, $V_c$ -----	56. 5	62. 0	67. 2	56. 0	62. 0	67. 2
Max. speed, $V_m$ -----	89. 4	91. 9	93. 7	90. 0	92. 7	94. 8
Actual rate of climb, ft./min-----	715	603	494	752	646	543
Altitude in normal standard atmosphere, for actual rate of climb, $h$ ft-----	5, 900	8, 000	10, 100	6, 050	8, 000	10, 050
Density ratio-----	0. 9431	0. 7859	0. 6549	0. 9431	0. 7859	0. 6549
Density altitude, $h_d$ -----	1, 980	8, 000	13, 760	1, 980	8, 000	13, 760
$\Delta h = h_p - h$ -----	2, 100	0	-2, 100	1, 950	0	-2, 050
$\Delta h_d = h_p - h_d$ -----	6, 020	0	-5, 760	6, 020	0	-5, 760
$K = \Delta h / \Delta h_d$ -----	0. 349	-----	0. 364	0. 324	-----	0. 356
$\Delta V_m$ -----	-2. 5	0	+1. 8	-2. 7	0	+2. 1
$V_s$ -----	51. 5	56. 4	61. 8	51. 5	56. 4	61. 8
$V_c / V_s$ -----	1. 10	1. 10	1. 09	1. 09	1. 10	1. 09

TABLE XIII

Altitude correction factor  $K=\frac{h_p-h}{h_p-h_d}$

SUMMARY OF RESULTS FROM TABLES X, XI, AND XII

$\frac{\text{Temperature}}{\text{Normal Temperature}}\} = \text{-----}$	0.833			1.20		
Parasite drag	Normal	Low	High	Normal	Low	High
Effective aspect Ratio 3-----	0. 372	0. 363	0. 390	0. 405	0. 414	0. 408
4-----	. 363	. 346	. 374	. 387	. 387	. 408
5-----	. 346	. 346	. 365	. 387	. 370	. 373
6-----	. 329	. 321	. 349	. 378	. 361	. 364
8-----	. 321	. 321	. 349	. 361	. 352	. 364
10-----	. 313	. 305	. 324	. 361	. 335	. 355

TABLE XIV

EXAMPLE OF REDUCTION OF CLIMB DATA—CLIMB NO. 1

Time	Pressure	Temper- ature °C.	Altitudes (feet)				
			Pressure $h_p$	Density $h_d$	$h_p-h_d$ , $\Delta h$	0.36 $\Delta h$	Plotting altitude, $h$
0	765	20	—180	+340	—520	—190	+10
2	749	19	400	970	—570	—210	610
4	735	18	920	1, 460	—540	—190	1, 110
6	724	17	1, 340	1, 880	—540	—190	1, 530
8	712	16. 5	1, 790	2, 420	—640	—230	2, 020
10	696	15	2, 410	2, 970	—560	—200	2, 610
12	683	14	2, 920	3, 520	—600	—220	3, 140
14	678	13	3, 120	3, 630	—510	—180	3, 300
16	668	13	3, 530	4, 110	—580	—210	3, 740
18	656	12	4, 010	4, 610	—600	—220	4, 230
20	646	11	4, 430	4, 980	—550	—200	4, 630
25	630	9	5, 100	5, 570	—470	—170	5, 270
30	616	8	5, 700	6, 190	—490	—186	5, 980
35	604	7	6, 220	6, 740	—520	—190	6, 410
40	593	6	6, 700	7, 230	—530	—190	6, 890
45	583	6	7, 150	7, 790	—640	—230	7, 380



TABLE XV

EXAMPLE OF REDUCTION OF CLIMB DATA—CLIMB NO. 2

Time	Pres- sure	Tem- pera- ture °C.	Altitudes (feet)				
			Pressure altitude, $h_p$	Density altitude, $h_d$	$h_p - h_d$ , $\Delta h$	0.36 $\Delta h$	Plotting altitude, $h$
0	766	4	-220	-1,580	+1,360	490	-710
2.48	750	3	+370	-980	+1,350	490	-120
5.58	731	1	1,070	-370	+1,440	520	+550
8.68	710	0	1,870	+480	+1,390	500	1,370
11.80	694	0	2,490	1,250	+1,240	450	2,040
14.72	678	-1	3,120	1,920	+1,200	430	2,690
17.82	666	+1	3,610	2,820	+990	360	3,250
20.92	655	+1	4,050	3,330	+720	260	3,790
24.02	644	0	4,510	3,730	+780	280	4,230
29.28	629	0	5,140	4,730	+410	150	4,990
33.93	620	-1	5,520	4,950	+570	210	5,310
37.03	613	-1	5,830	5,330	+500	180	5,650
40.14	607	-2	6,090	5,530	+560	200	5,890





---

---

**REPORT No. 298**

---

**EFFECT OF VARIATION OF CHORD AND SPAN OF  
AILERONS ON ROLLING AND YAWING  
MOMENTS IN LEVEL FLIGHT**

**By R. H. HEALD and D. H. STROTHER**

**Bureau of Standards**





## REPORT No. 298

### EFFECT OF VARIATION OF CHORD AND SPAN OF AILERONS ON ROLLING AND YAWING MOMENTS IN LEVEL FLIGHT

By R. H. HEALD and D. H. STROTHER

#### SUMMARY

*This report presents the results of an investigation of the rolling and yawing moments due to ailerons of various chords and spans on two airfoils having the Clark Y and U. S. A. 27 wing sections. Some attention is devoted to a study of the effect of scale on rolling and yawing moments and to the effect of slightly rounding the wing tips.*

*The results apply to level flight with the wing chord set at an angle of attack of  $+4^\circ$  and to conditions of zero pitch, zero yaw, and zero roll of the airplane. It is planned later to extend the investigation to other attitudes for monoplane and biplane combinations.*

*The work was conducted in the 10-foot wind tunnel of the Bureau of Standards (fig. 1) on models of 60-inch span and 10-inch chord.*

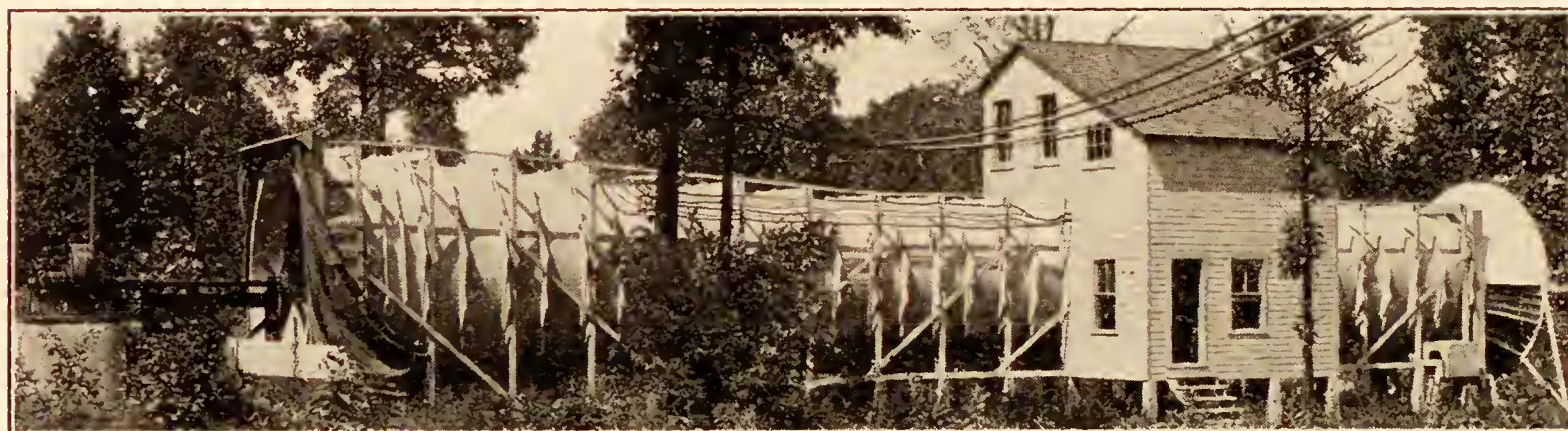


FIG. 1

#### INTRODUCTION

The investigation was undertaken for the Aeronautics Branch of the Department of Commerce in cooperation with the National Advisory Committee for Aeronautics for the purpose of making available to the industry data relative to the rolling and yawing moments due to conventional ailerons on some representative American wing sections. But little systematic work has been done along this line, the outstanding contributions being those of Archer (Reference 1) and Irving, Ower, and Hankins (Reference 2).

#### DESCRIPTION OF APPARATUS AND MODELS

##### THE WIND TUNNEL

The air is drawn through the 10-foot wind tunnel by means of a four-blade 14-foot tractor propeller driven by a 200-HP. direct-current motor. The lower and upper limits of the speeds available are, respectively, 20 feet per second and 100 feet per second. A calibration of the tunnel for speed distribution, which was made in the area subsequently occupied by the model, showed the speed to be uniform within  $\pm 1$  per cent.



## AIRFOILS

The wing models, 60 inches span and 10 inches chord, shown in Figures 2 and 3, were constructed of  $\frac{3}{4}$ -inch mahogany strips and on completion showed a maximum deviation from the templates of  $\pm 0.02$  inch. The metal templates were constructed accurately to the dimensions of the two sections as given in N. A. C. A. Technical Report No. 233. It was felt that this deviation was permissible in wooden models of this size. Two models of each wing were prepared, in order to permit tests in biplane combination.

Figure 3 illustrates the method adopted for obtaining a variation of aileron chord and span. The ailerons of varying chord were built into the right portion of the wing, those of varying span into the left portion of the wing.

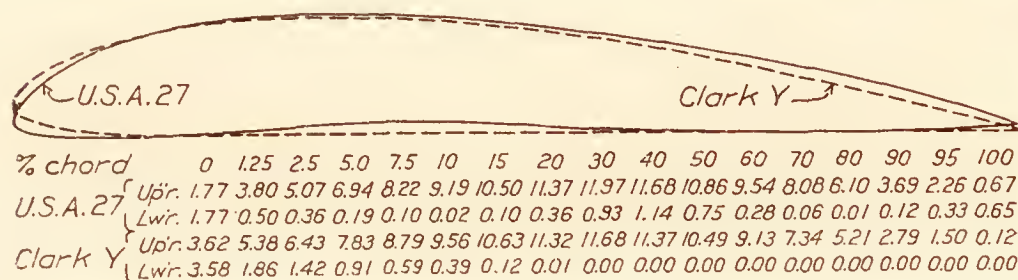


FIG. 2.—Dimensions of wing sections. Source, N. A. C. A. Technical Report No. 233

Thus a study of the characteristics of the individual ailerons was possible through a rather wide range of chord and span variation.

The ailerons were so mounted that their axes of rotation were midway between the upper and lower surfaces of the wing.

When under test, all slots were filled with wax and smoothed. The section of the wing was constant along the span, there being no tapering or feathering.

## FUSELAGE AND UNIVERSAL JOINT

The wings were mounted on a fuselage or fairing which formed the housing for a ball-bearing universal joint from which the whole system was supported by a  $\frac{3}{4}$ -inch mast bolted and

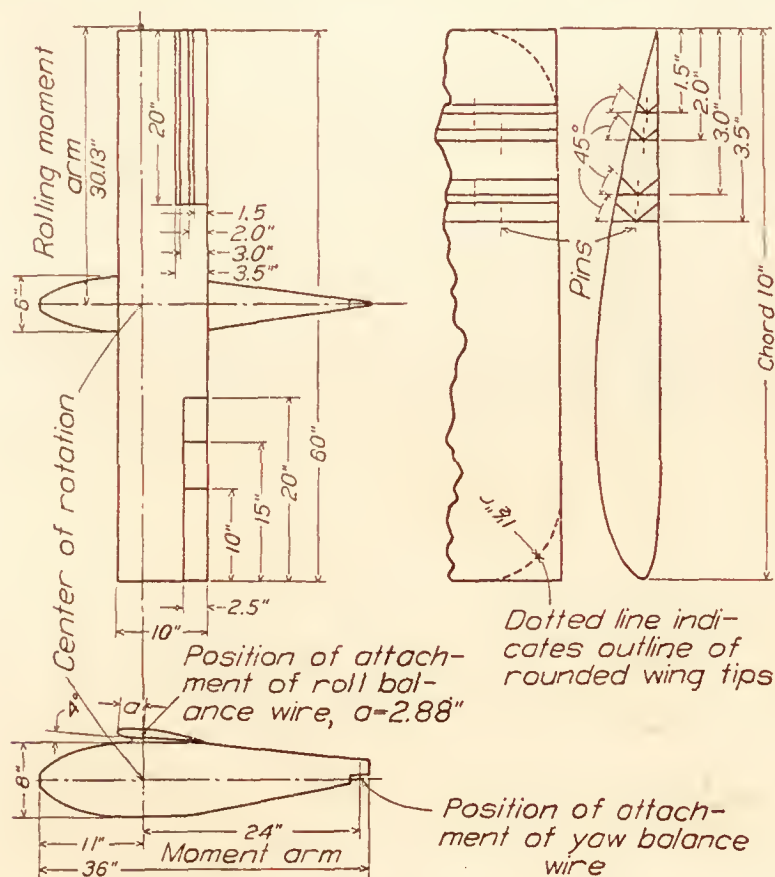


FIG. 3.—Varying aileron chord end of wing, Clark Y section, showing method of hinging ailerons. U. S. A. 27 similarly constructed

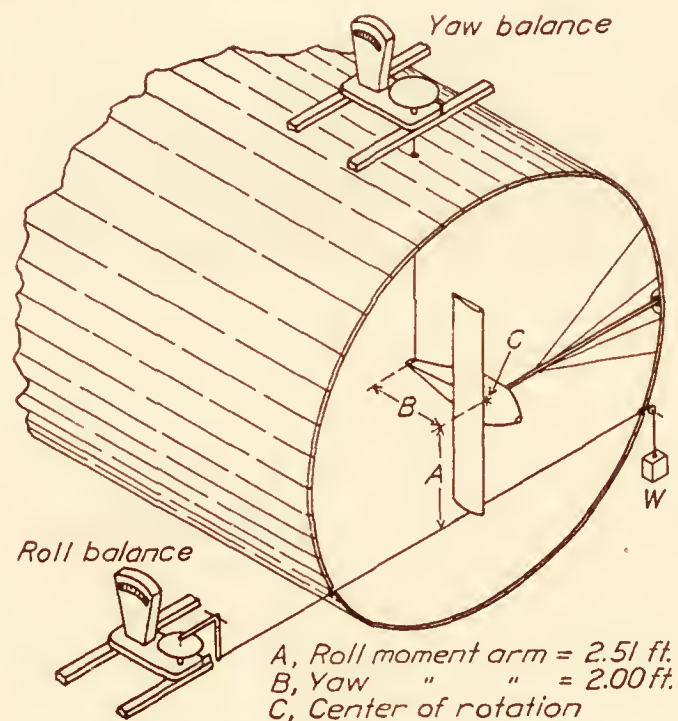


FIG. 4.—Arrangement of rolling and yawing moments

guyed by stay wires to the side of the tunnel. Provision was made for setting the wings at various angles to the axis of the fuselage. The general arrangement of the set-up is shown in Figures 4, 5, and 6.

## ARRANGEMENT OF BALANCES

For convenience in observation, the model was mounted in the tunnel with the span of the wing vertical, and the rolling and yawing forces were read on balances of the pendulum type (fig. 4). Both balances were calibrated before making the observations. A further check was made on the precision of the complete system by applying known moments directly to the model.



## METHOD OF MEASUREMENT

Simultaneous readings of the rolling and yawing moments were made at speeds of 40, 58.7, and 80 feet per second (respectively, 27.3, 40, and 54.5 miles per hour) with the axis of the fuselage parallel to the wind direction and with the angle of incidence of the wing set at  $+4^\circ$ . This setting corresponds to 0.55 of the maximum lift coefficient of the Clark Y wing and 0.52 of the maximum lift coefficient of the U. S. A. 27 wing. (Reference 3.)

Observations were made with the ailerons set at angles of  $8^\circ$  and  $16^\circ$  to the wing chord and at  $4^\circ$  intervals thereafter up to  $44^\circ$ . The aileron angles were set by means of metal templates, but because of a slight warp along the trailing edge of the aileron the precision of setting was  $\pm 1^\circ$ , the values given being the mean of the inclinations at the tip and root of the aileron.

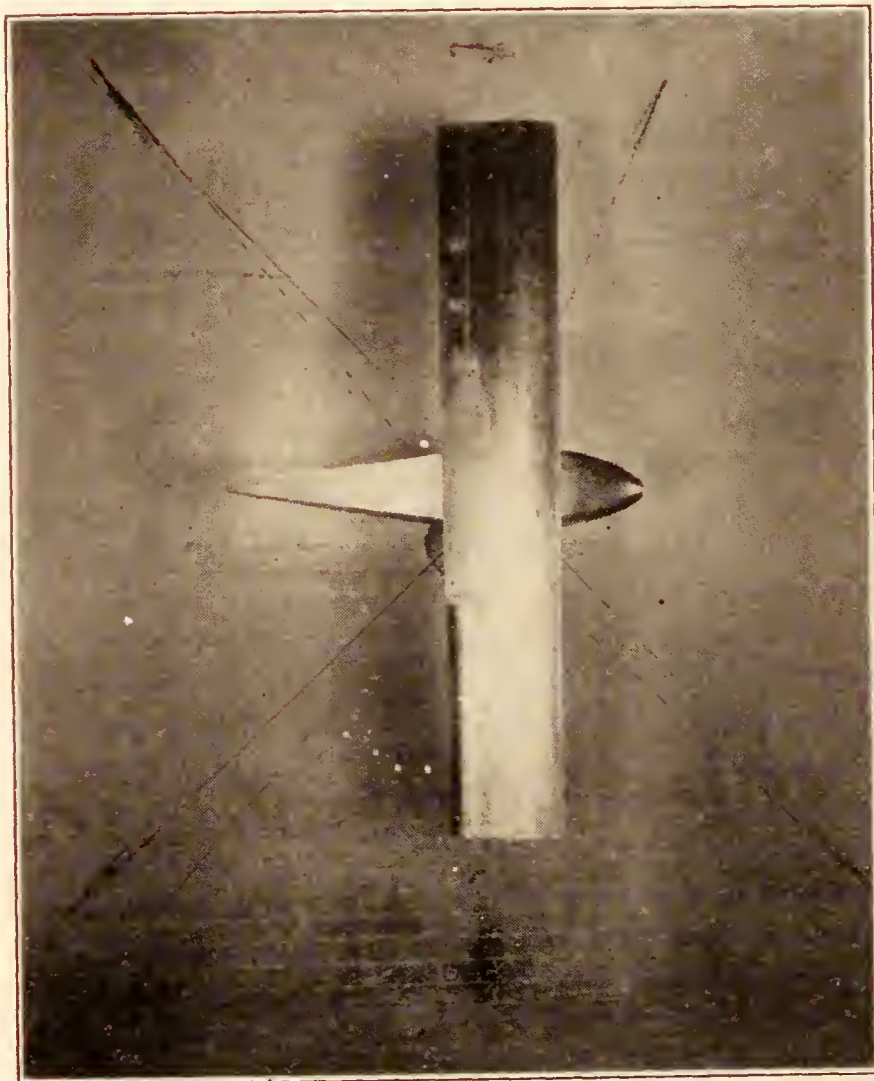


FIG. 5

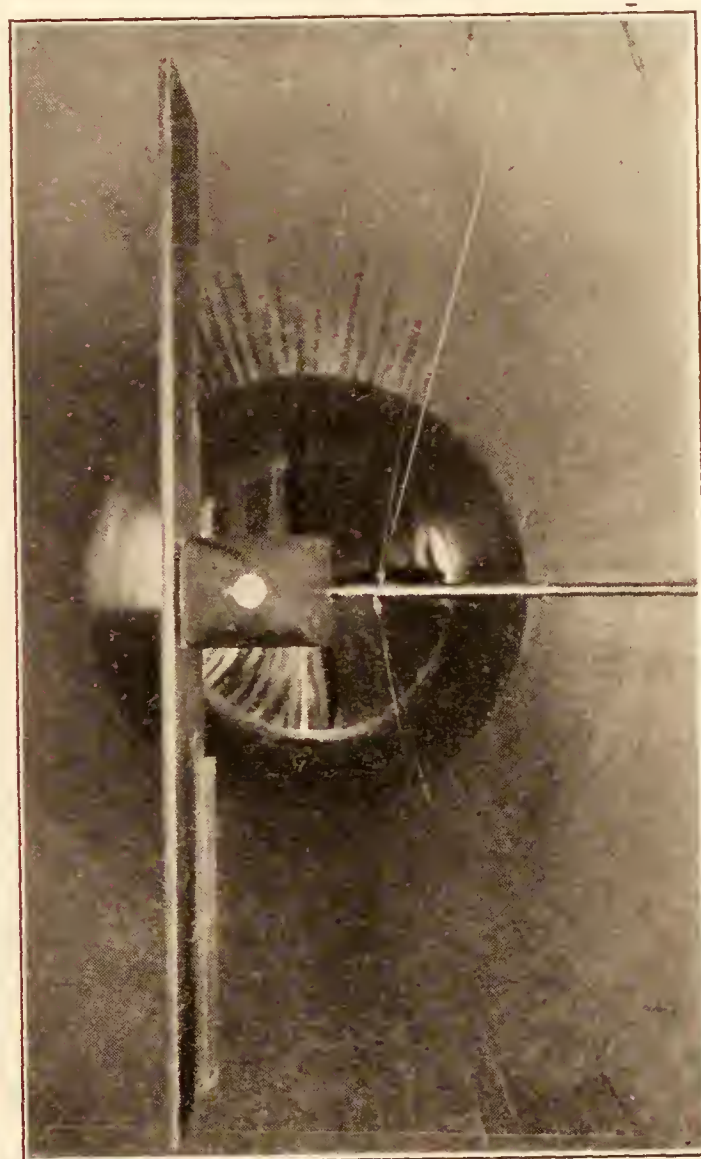


FIG. 6

Indication of unsteady flow about the ailerons was noted early in the investigation in the case of aileron angles greater than  $16^\circ$ . The effect of this burbling flow was so marked on the rolling moment balance that considerably heavier damping was necessary than was used for the yawing moment balance. The region of greatest unsteadiness occurred in the neighborhood of  $24^\circ$  aileron setting. The flow appeared to steady down somewhat for aileron angles greater than  $32^\circ$ .

## REDUCTION OF OBSERVATIONS

Small rolling and yawing forces, which appeared to be due to the drag of the balance wires and possibly to a slight asymmetry in the model, were noted at zero aileron angle in all cases. Correction was made for these forces in the reduction of observations.

The results are expressed in the usual N. A. C. A. form of absolute coefficients given below:<sup>1</sup>

$$C_L = \frac{L}{qbS} \text{ and } C_N = \frac{N}{qfS}$$

where  $C_L$  and  $C_N$  are the absolute rolling and yawing moment coefficients for one aileron.

<sup>1</sup> Note that the coefficients are based on wing dimensions which are held constant throughout the investigation; i. e.—

$L = C_L q \times \text{a constant} = C_L q \times 20.83$   
and  $N = C_N q \times \text{a constant} = C_N q \times 8.68$



$L$  and  $N$  are respectively rolling and yawing moments in pounds-feet.

$$q = \frac{1}{2} \rho V^2 = 0.001189 V^2$$

$b$  = wing span in feet.

$f$  = distance from center of rotation of model to end of tail.

(Note: This distance was chosen as closely representing the distance from the center of gravity of the airplane to the leading edge of the elevator.)

$S$  = wing area in square feet (chord length  $\times$  span.)

$V$  = wind speed in feet per second.

$\rho$  = 0.002378 slugs per cubic foot at 15° C. and 760 mm pressure.

The reference axes are body axes and the directions are conventional, a moment tending to produce clockwise rotation as viewed from the pilot's seat being considered positive. The values given in Tables I-IV and those plotted in Figures 7-20 refer to a single aileron on the right half of the wing.

## RESULTS

### REPRESENTATIVE CURVES

Figures 7 and 8 are representative of plots of the observed values, reduced to the coefficients  $C_L$  and  $C_N$ , for varying aileron angles. Since only a slight scale effect was noted within the range of speeds employed, a faired curve was drawn through all the points, and the values given in Tables I-VIII and subsequently plotted were read from these curves.

### ROUNDED AND RECTANGULAR TIPS

The models were originally made with corners rounded to a radius equal to 15 per cent of the wing chord. These were afterwards filled in to form rectangular tips, as it seemed desirable to use a standard plan form for systematic tests. Some comparative observations were made, and the results are plotted in Figure 9.

The effect of rounding the tips is negligible on the rolling moment coefficient with the aileron up, but is somewhat more pronounced in the case of the yawing moment coefficient. Both rolling and yawing moment coefficients show slight increases when the rounded aileron is put down.

### EFFECT OF VARYING AILERON CHORD AND SPAN

Figures 10-21 and Tables I-IV present the major results of the investigation. The values of  $C_L$  and  $C_N$  are plotted against aileron chord or aileron span expressed in per cent of the corresponding wing dimension. The coefficients due to various differential combinations are obtainable by the use of Tables I-IV, and direct combinations of the values are given in Tables V-VIII and plotted in Figures 23-25.

### ROLLING MOMENT COEFFICIENTS

Comparison of the ratios of the rolling moment coefficients for ailerons in the up and down positions shows that for corresponding angles the rolling moment due to the aileron in the up position exceeds that due to the down aileron by from 2 to 85 per cent, depending on the wing section and the chord, span, and angle of the aileron. The larger ratios of  $\frac{C_{L \text{ up}}}{C_{L \text{ down}}}$  occur in the case of the ailerons having a chord length 35 per cent of that of the wing. The increase of the ratio  $\frac{C_{L \text{ up}}}{C_{L \text{ down}}}$  as the aileron angle is increased is not marked in the case of ailerons of short chord length, but becomes greater as the chord length is increased. For example, in the case of the aileron on the Clark Y wing whose chord length is 15 per cent of that of the wing the ratio of  $\frac{C_{L \text{ up}}}{C_{L \text{ down}}}$  is 1.36 at 8° and 1.20 at 44°. For an aileron having the same span but with a chord length 35 per cent of that of the wing the ratio  $\frac{C_{L \text{ up}}}{C_{L \text{ down}}}$  is 1.24 at 8° and 1.85 at 44°. Lengthening the



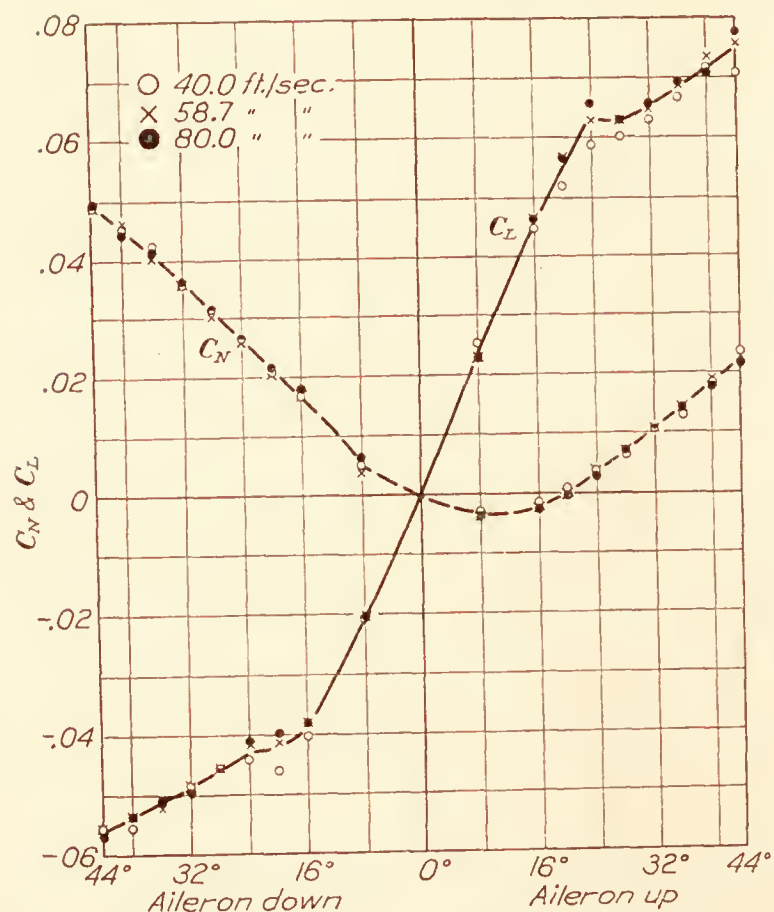


FIG. 7.—Clark Y wing. Aileron span 15 inches. Aileron chord 2.5 inches

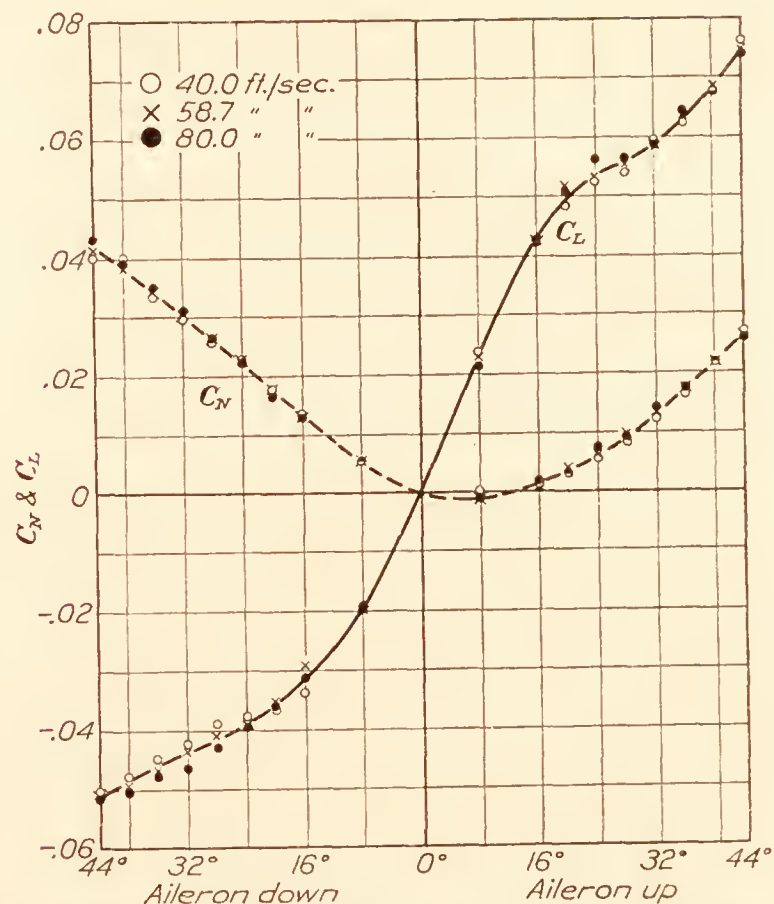


FIG. 8.—U. S. A. 27 wing. Aileron span 15 inches. Aileron chord 2.5 inches

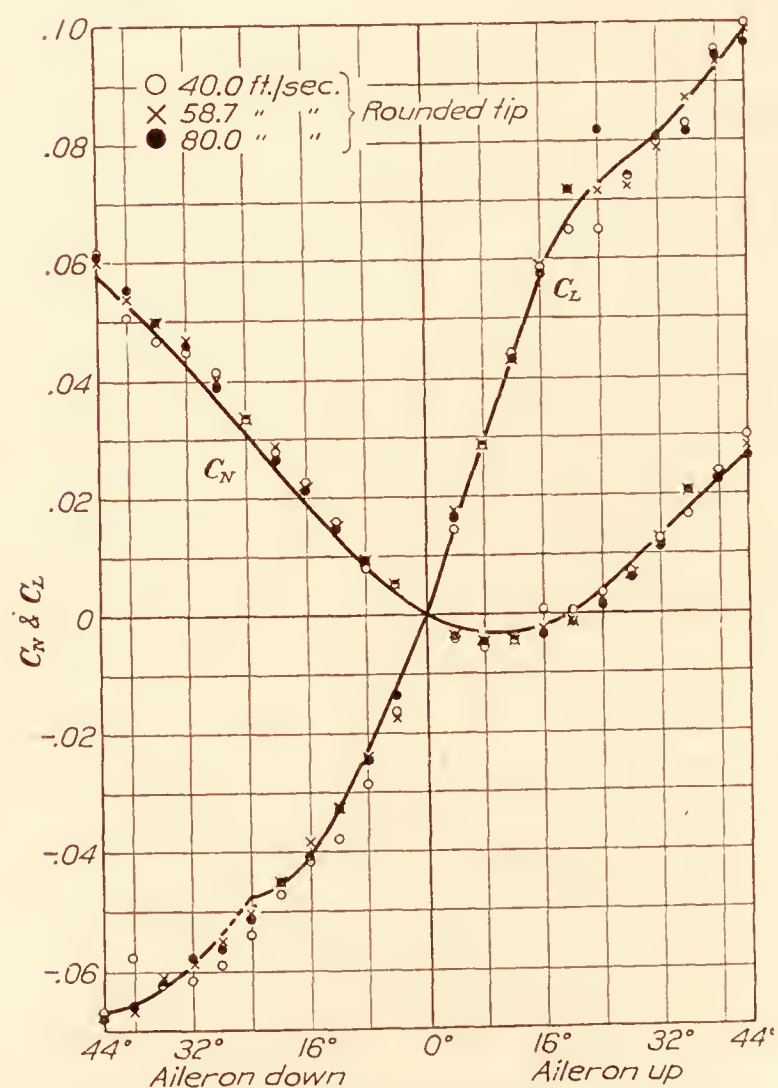


FIG. 9.—Clark Y wing. Aileron span 20 inches. Aileron chord 2.5 inches. Curve line represents rectangular tips—points not shown

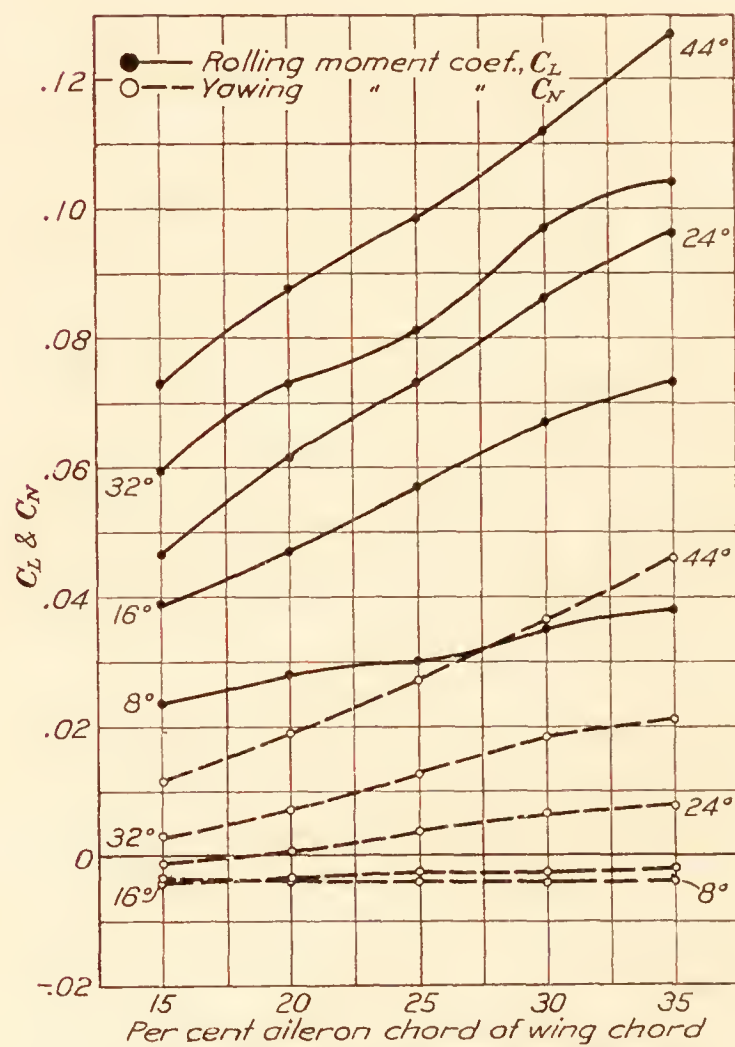


FIG. 10.—Clark Y wing. Aileron span 20 inches. Aileron chord varying. Aileron up

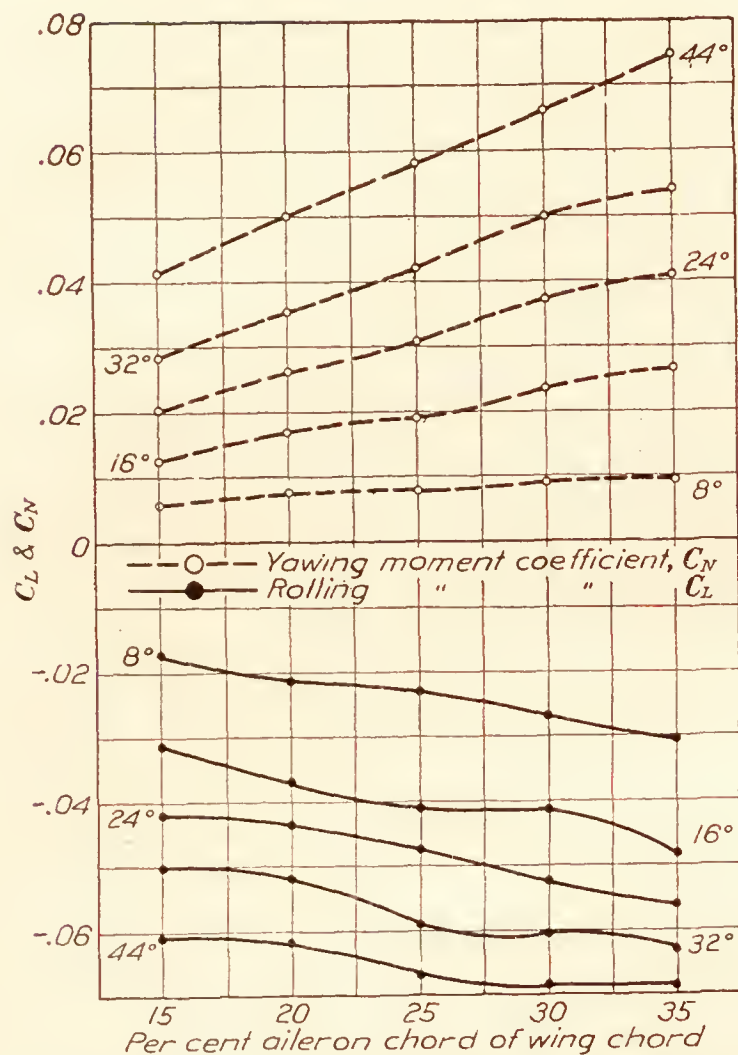


FIG. 11.—Clark Y wing. Aileron span 20 inches. Aileron chord varying. Aileron down

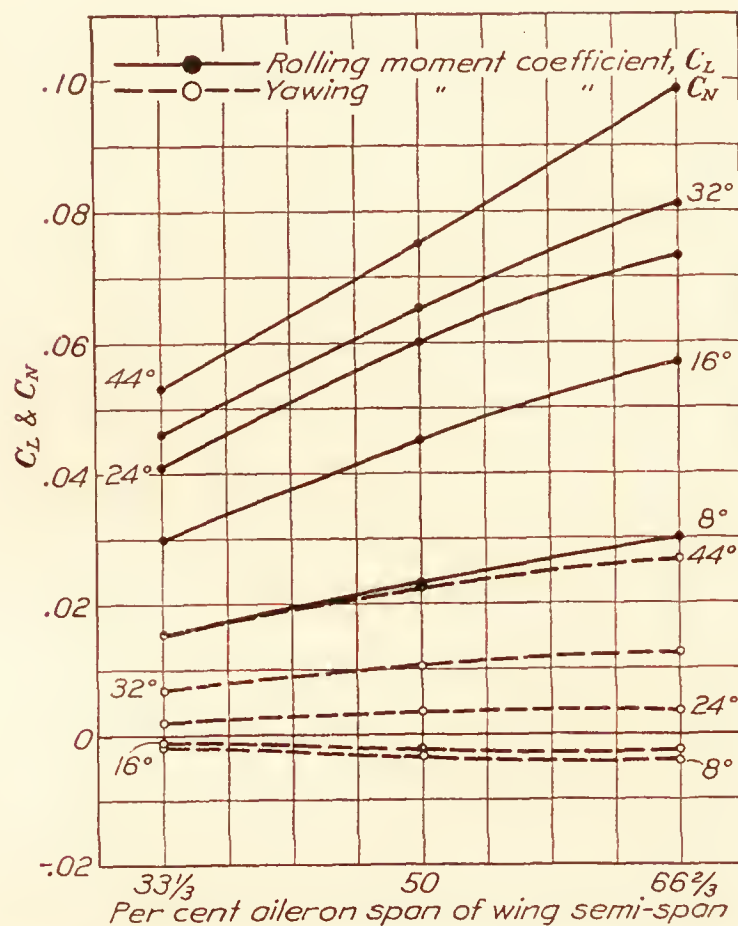


FIG. 12.—Clark Y wing. Aileron span varying. Aileron chord 2.5 inches. Aileron up

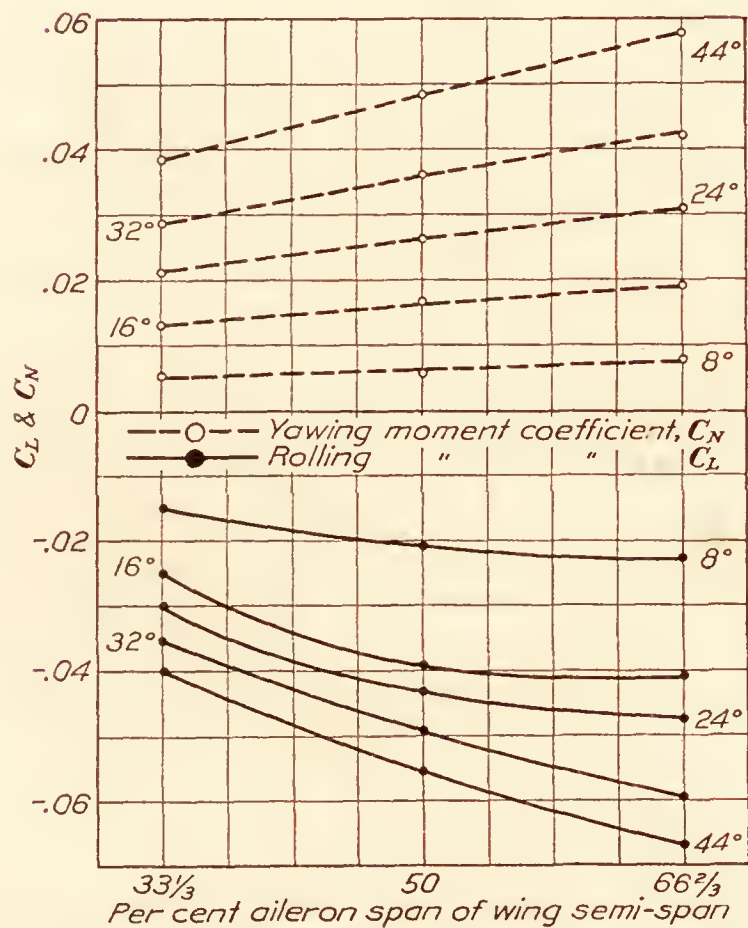


FIG. 13.—Clark Y wing. Aileron span varying. Aileron chord 2.5 inches. Aileron down

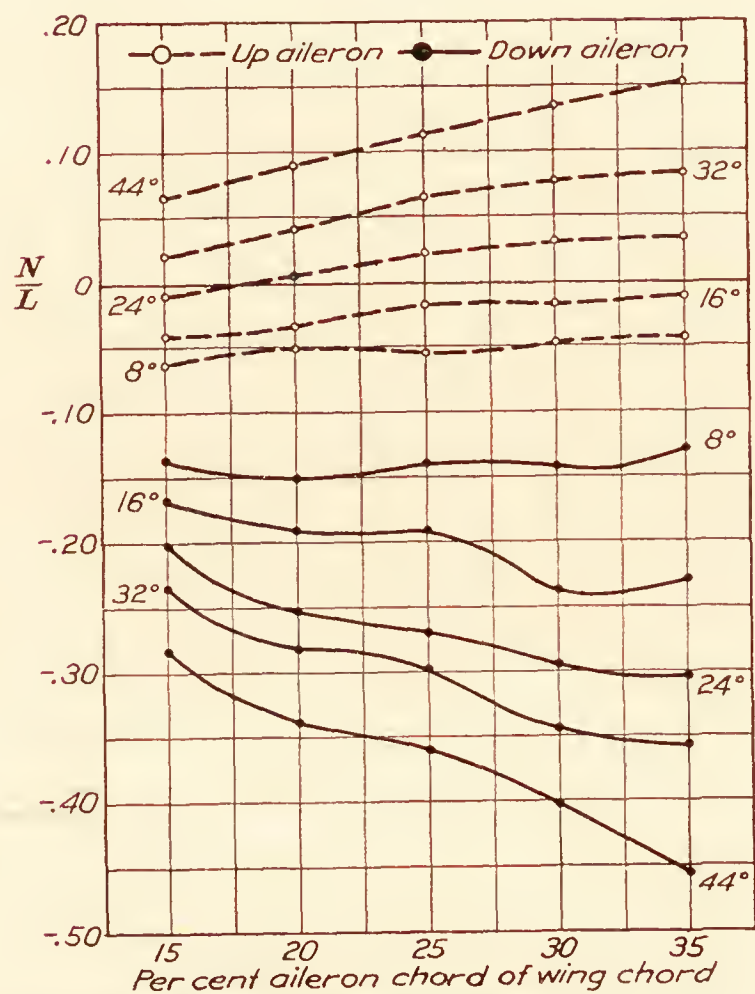


FIG. 14.—Clark Y wing. Aileron span 20 inches.  $N/L = 0.417 C_N / C_L$



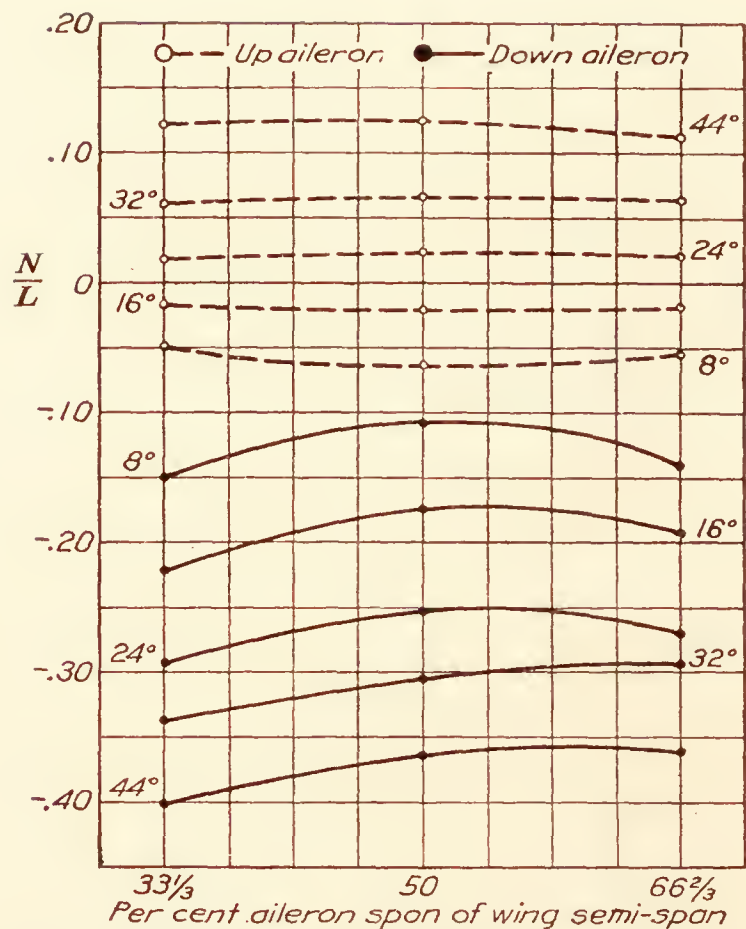


FIG. 15.—Clark Y wing. Aileron span varying. Aileron chord 2.5 inches.  $N/L = 0.417 C_N/C_L$

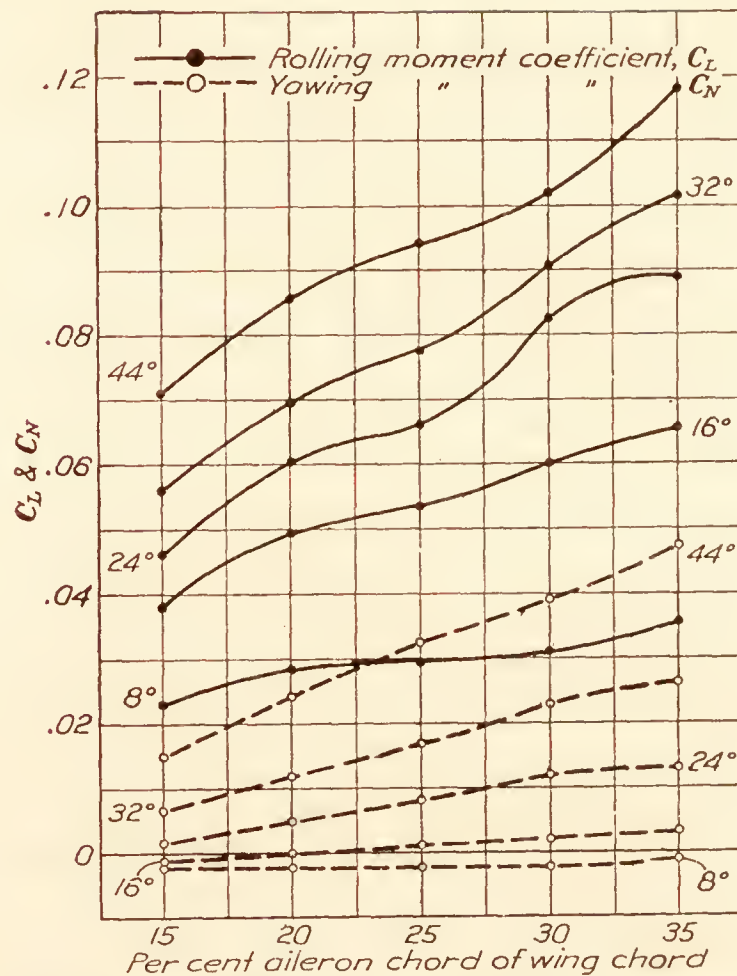


FIG. 16.—U. S. A. 27 wing. Aileron span 20 inches. Aileron chord varying. Aileron up

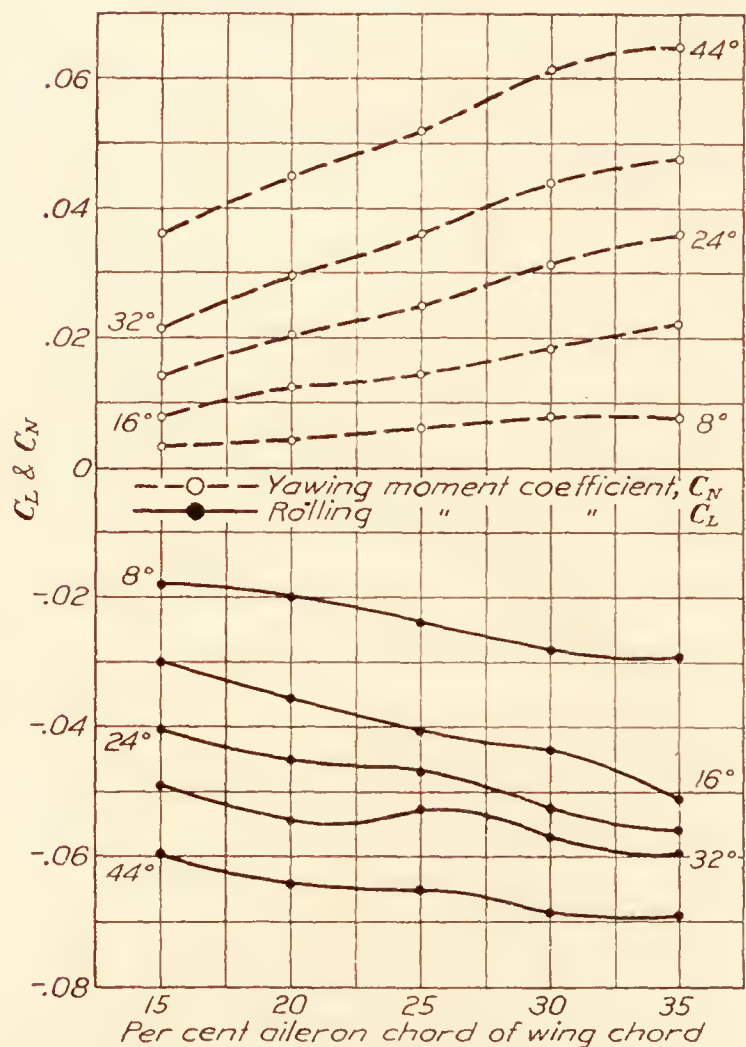


FIG. 17.—U. S. A. 27 wing. Aileron span 20 inches. Aileron chord varying. Aileron down

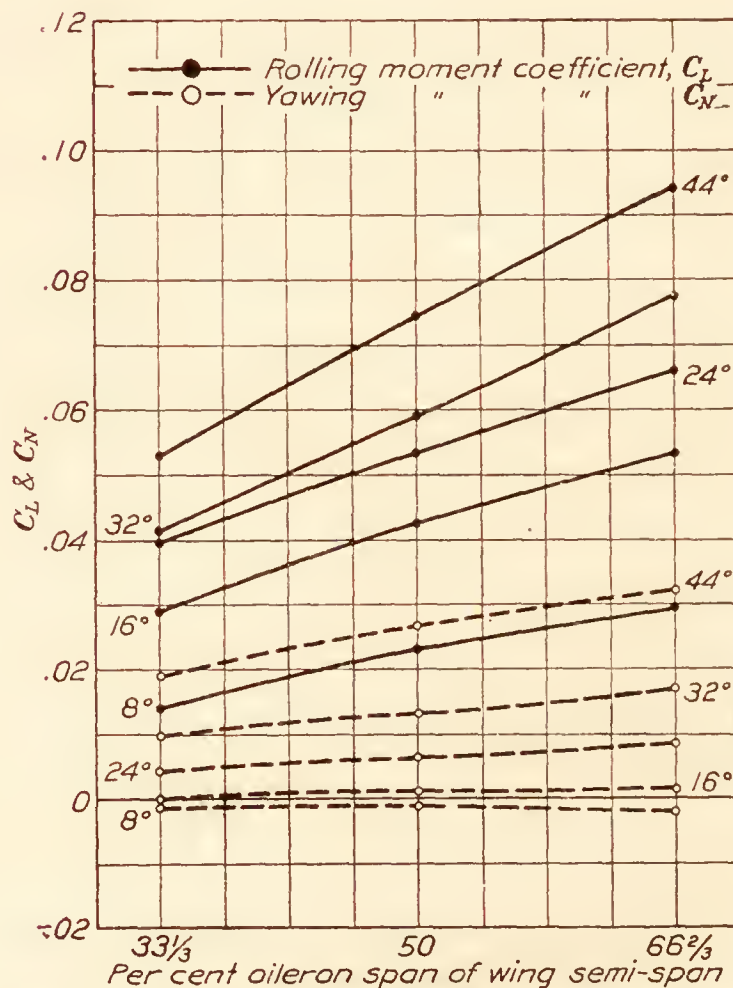


FIG. 18.—U. S. A. 27 wing. Aileron span 20 inches. Aileron chord varying. Aileron up

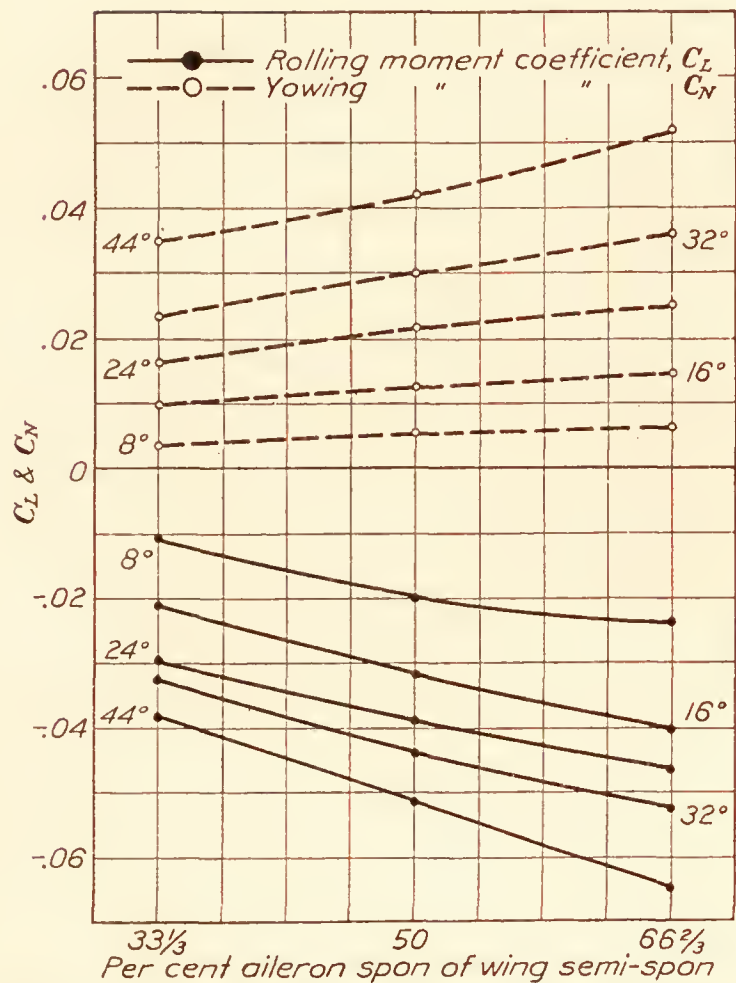


FIG. 19.—U. S. A. 27 wing. Aileron span varying. Aileron chord 2.5 inches. Aileron down

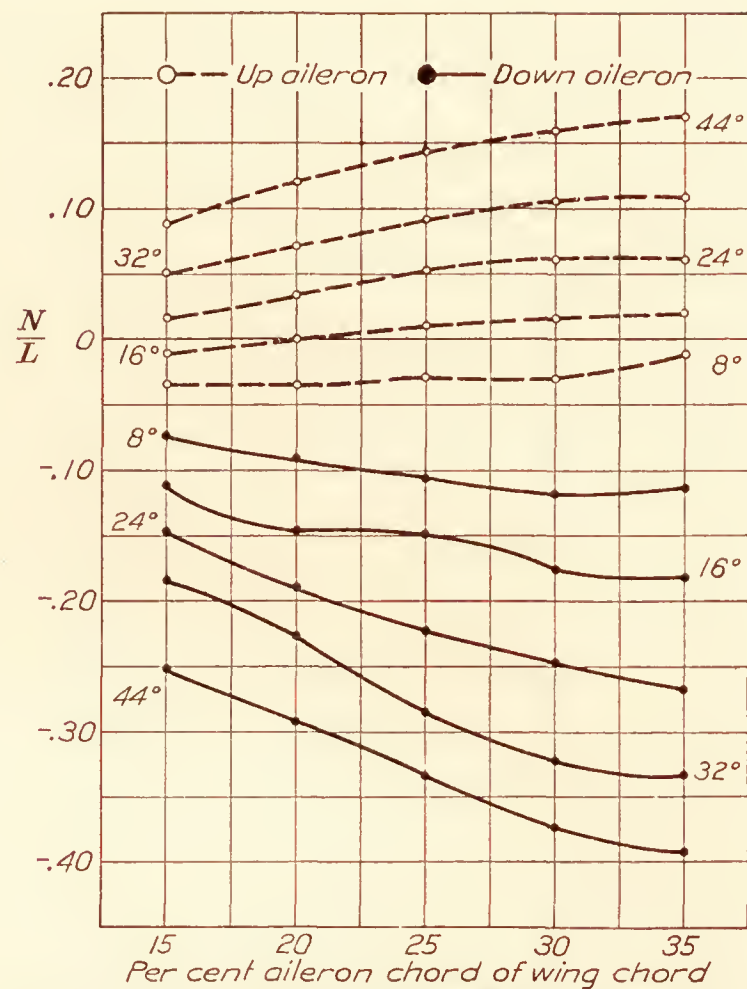


FIG. 20.—U. S. A. 27 wing. Aileron span 20 inches. Aileron chord varying.  $N/L=0.417 C_N/C_L$

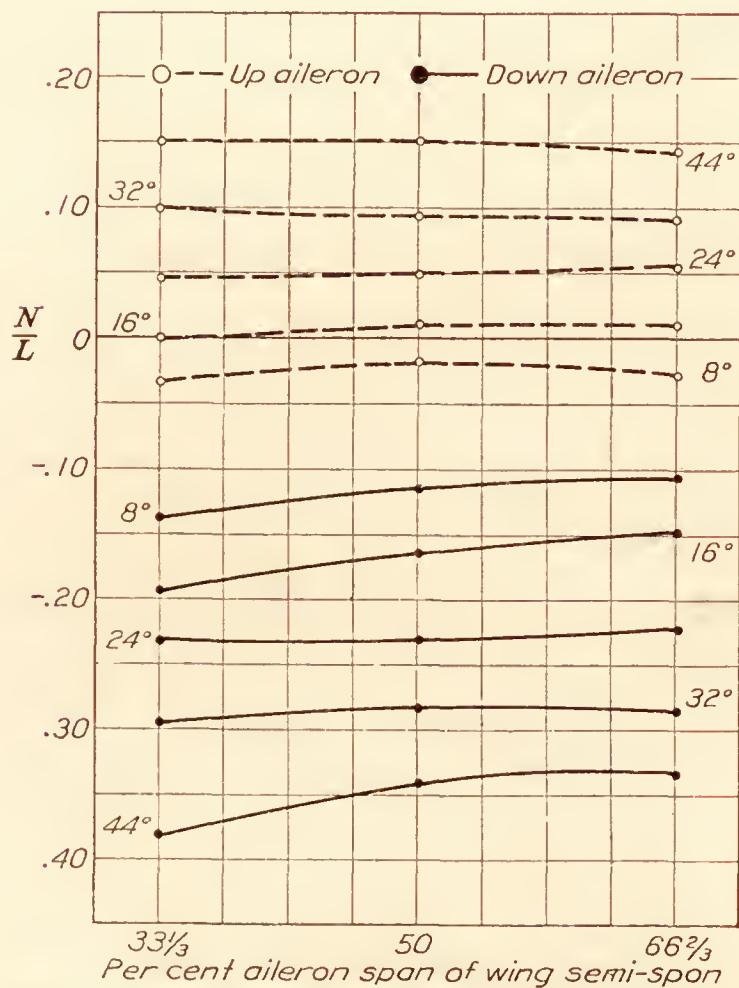


FIG. 21.—U. S. A. 27 wing. Aileron span varying. Aileron chord 2.5 inches.  $N/L=0.417 C_N/C_L$

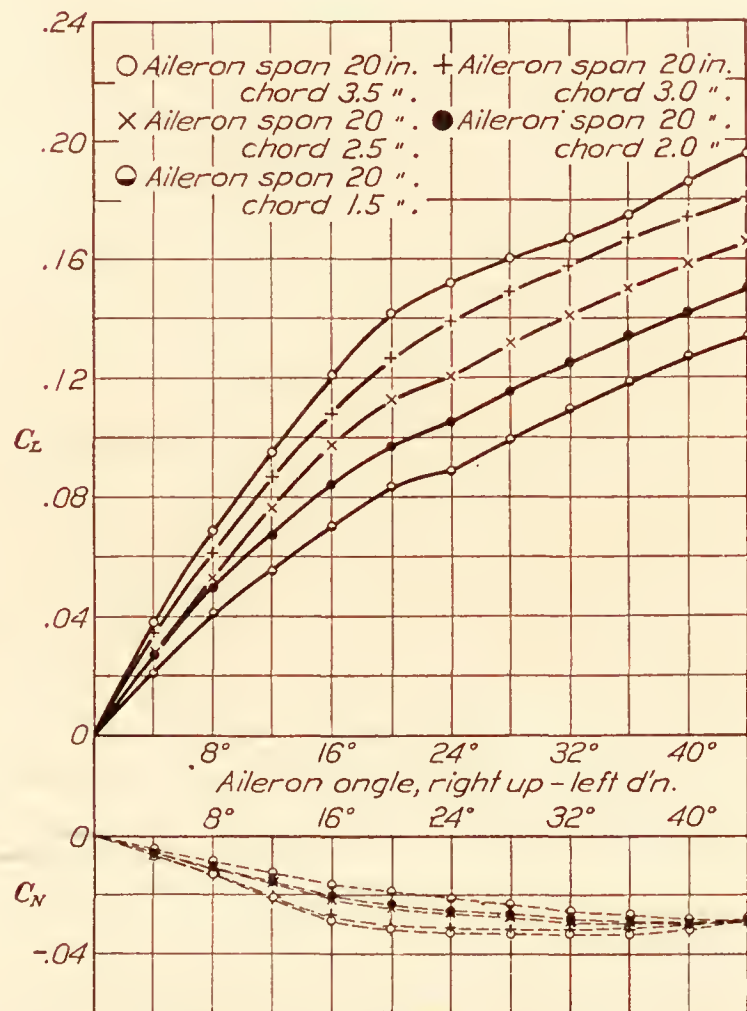


FIG. 22.—Clark Y wing. Combined rolling and yawing moment coefficients.  $N/L=0.417 C_N/C_L$



span of the aileron results in relatively small changes in the ratio  $\frac{C_L \text{ up}}{C_L \text{ down}}$  for corresponding aileron angles. Relationships of the same order occur in the case of the U. S. A. 27 wing.

Comparison of the curves and tables will show that the differences in the rolling moments produced by ailerons of the same size on the two wings are not great. In general, an aileron on the Clark Y wing shows slightly greater rolling moment than the corresponding aileron on the U. S. A. 27 wing for the same setting.

There appears to be no systematic relationship between aileron dimension and rolling moment except that an increased rolling moment accompanies an increase in aileron span or chord, the angle being held constant. In some cases an approximately linear relationship between the two quantities is indicated.

#### YAWING MOMENT COEFFICIENTS

Coincident with the increase of the rolling moment coefficient as the aileron chord is increased there is an increase in the yawing moment coefficient. In the case of the Clark Y wing with an aileron chord 15 per cent of the wing chord the ratio  $\frac{C_N \text{ up}}{C_N \text{ down}}$  is 0.28 for an aileron angle of  $44^\circ$ . This ratio increases to 0.62 for the aileron whose chord is 35 per cent of the wing chord.

The ratio  $\frac{C_N \text{ up}}{C_N \text{ down}}$  decreases in value as the aileron chord is increased, for small angles, and increases as the chord is increased, for large angles, the minimum value occurring in the neighborhood of  $20^\circ$ , depending on the wing section and the dimensions of the aileron.

In all cases a slightly negative yawing moment occurs in the case of both wings for aileron angles below  $12^\circ$ . The angle of zero yawing moment changes somewhat, decreasing as the aileron chord is increased. The effect is more marked in the case of the Clark Y wing, where the angle of the aileron for zero yawing moment is  $26^\circ$  when the aileron chord length is 15 per cent of the chord length of the wing. When the aileron chord length is increased to 35 per cent of that of the wing, the angle of zero yawing moment is decreased to  $18^\circ$ . For the same range of variation in aileron chord length on the U. S. A. 27 wing, the angle of the aileron for zero yawing moment decreases from  $20^\circ$  to  $11^\circ$ .

Within the limits of this investigation the ailerons on both wings show an approximately linear relationship between yawing moment coefficient and aileron chord. The relationship between yawing moment coefficient and aileron span is also approximately linear.

#### RATIO OF YAWING MOMENT ROLLING MOMENT

Inspection of the curves<sup>2</sup> for  $\frac{N}{L}$  (figs. 14, 15, 20, 21) shows that the down aileron is the greater contributing factor to the net yawing moment. The difference is most marked in the case of the Clark Y wing (fig. 14), where the maximum value for  $\frac{N}{L}$  with the aileron up is 0.15, approximately the same as the minimum value with the aileron down.

There appears to be no systematic variation of  $\frac{N}{L}$  with span. The magnitude of the variations in  $\frac{N}{L}$  due to changes in span are small in comparison with those due to changes in chord length.

There is a more nearly linear relationship between  $\frac{N}{L}$  and aileron chord or span for both wings in the case of the up aileron.

#### COMBINED COEFFICIENTS

The values given in Tables I–IV for one aileron in corresponding up and down positions have been combined in Tables V–VIII and are shown plotted in Figures 22–25.

<sup>2</sup> Note that  $\frac{N}{L} = 0.417 \frac{C_N}{C_L}$  due to the differences in the factors  $b$  and  $f$  in the rolling and yawing moment equations.

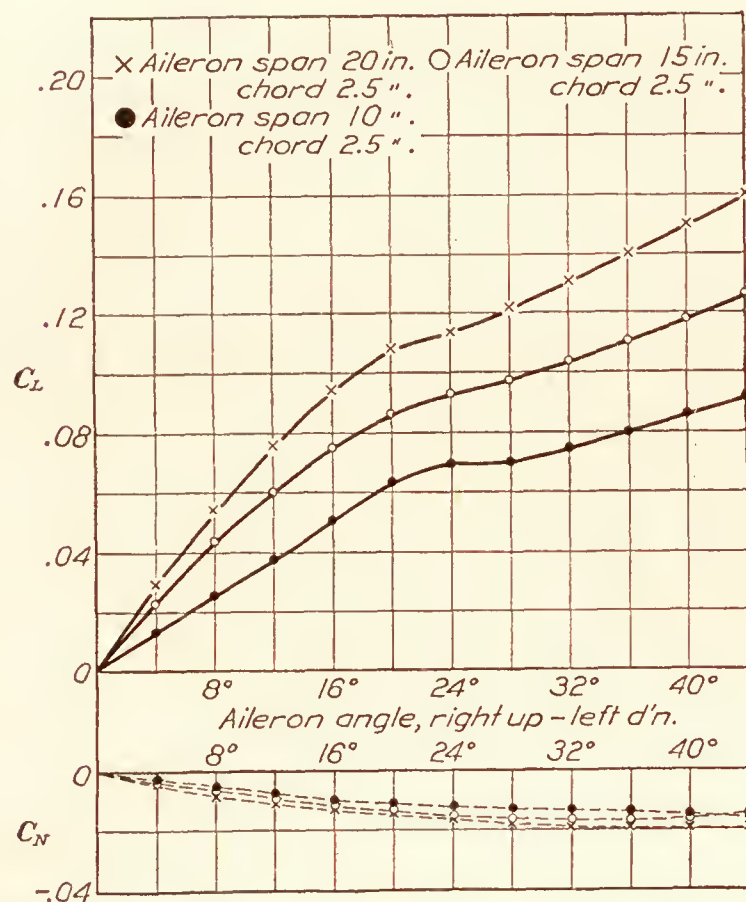


FIG. 23.—Clark Y wing. Combined rolling and yawing moment coefficients.  $N/L=0.417 C_N/C_L$

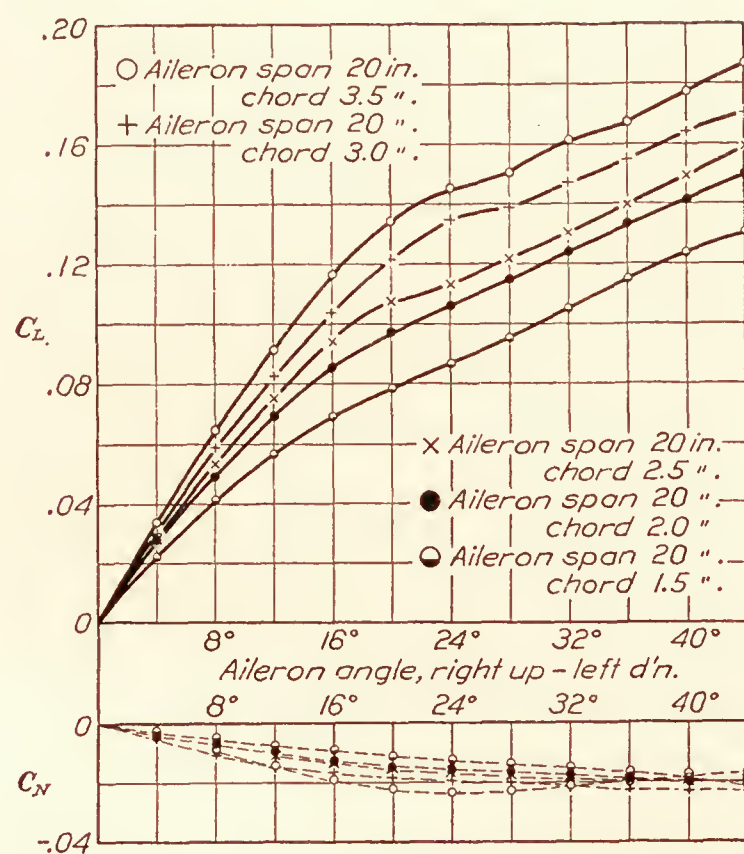


FIG. 24.—U. S. A. 27 wing. Combined rolling and yawing moment coefficients.  $N/L=0.417 C_N/C_L$

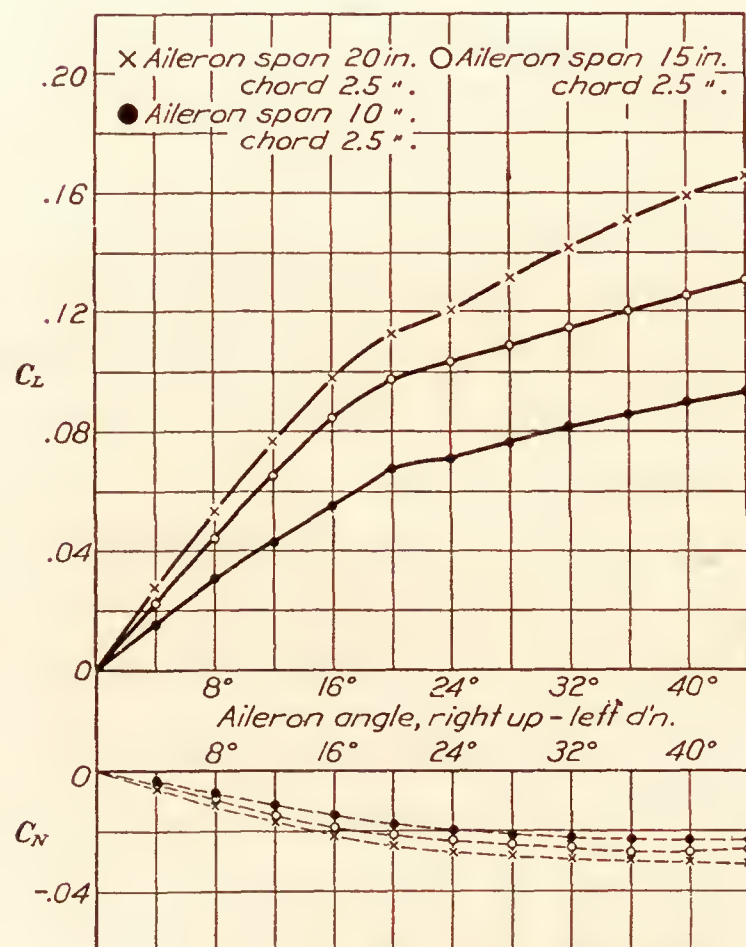


FIG. 25.—U. S. A. 27 wing. Combined rolling and yawing moment coefficients.  $N/L=0.417 C_N/C_L$

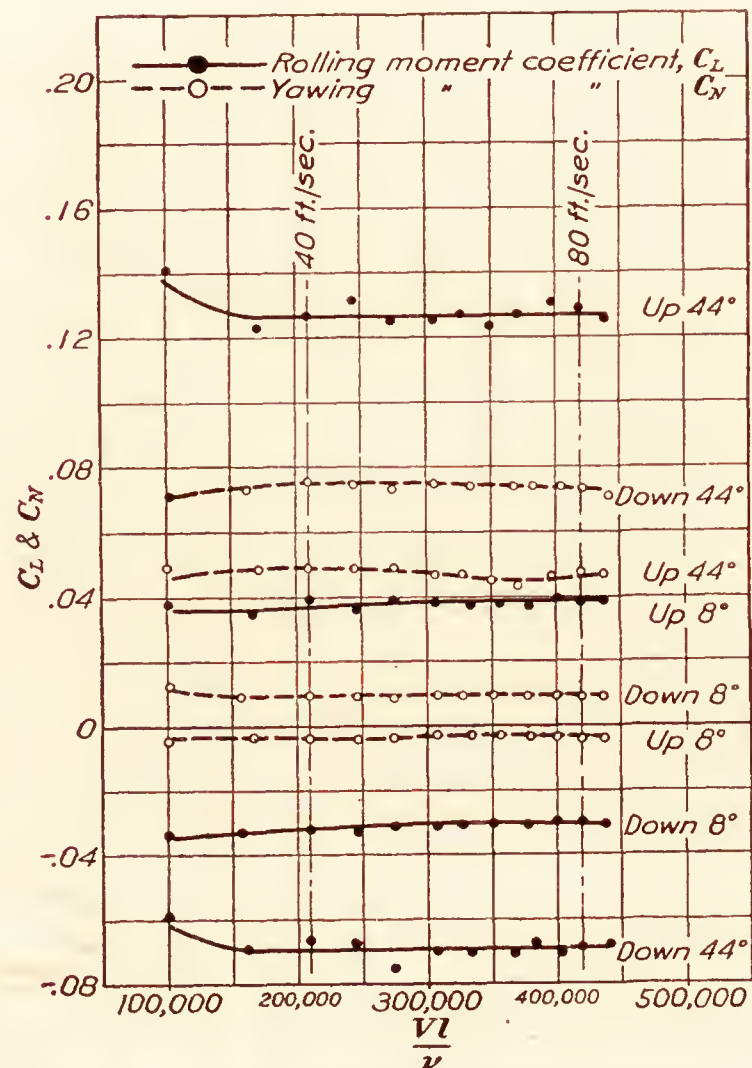


FIG. 26.—Clark Y wing. Aileron span 20 inches. Aileron chord 3.5 inches. Scale effect



There is a continued increase in the value of the combined rolling moment coefficient up to  $44^\circ$  aileron and a decrease in slope of the curves in the neighborhood of  $20^\circ$ .

The curves of combined yawing moment coefficients indicate a tendency toward a common value in the neighborhood of  $44^\circ$ .

#### SCALE EFFECT

Measurements were made for speeds ranging from 20 feet per second to slightly above 80 feet per second on both airfoils and for aileron settings of  $8^\circ$  and  $44^\circ$  up and down. The values of rolling and yawing moment coefficients are shown plotted against Reynolds Number in Figures 26 and 27. The scale effect is slight within the limits of this investigation, the maximum being of the order of 2 per cent.

#### CONCLUSIONS

The greater rolling moment is produced by the up aileron, the magnitude of the ratio  $\frac{C_L \text{ up}}{C_L \text{ down}}$  varying from 1.02 to 1.85, depending on the wing section and the angle and dimensions of the aileron.

There is a slightly negative yawing moment due to the up aileron, which may persist to angles in the neighborhood of  $24^\circ$  (depending on the aileron dimensions and angle) before becoming positive.

The rolling and yawing moment coefficients due to one aileron show a fairly uniform increase with chord or span as the aileron angle is increased to  $44^\circ$ .

The effect of rounding the wing corners to a radius equal to 15 per cent of the chord length of the wing is slight in the cases of both rolling and yawing moments.

The effect of scale on rolling and yawing moments is small between Reynolds Numbers of 200,000 and 440,000.

There is a region of unstable flow set up about the ailerons when inclined at angles to the wing chord in the neighborhood of  $20^\circ$ . The effect is much more marked on the rolling moment than on the yawing moment and is usually more marked in the case of the up aileron.

The occurrence of larger rolling moments and smaller yawing moments in the case of the up aileron suggests the possibility of control by means of large ailerons working through a small range of angles in the up direction. Sufficient control could doubtless be obtained, but whether the proposition would be practicable from a structural standpoint is open to question.

We wish to point out in conclusion that the preceding statements apply only to level flight at a small angle of attack of the wing. The effect of increasing the angle of attack is to modify greatly the relations shown previously, especially in the neighborhood of the stalling angle, as will be shown in a subsequent report.

#### ACKNOWLEDGMENT

The authors wish to acknowledge with thanks the assistance of Messrs. B. H. Monish, W. Hunter Boyd, and P. S. Ballif in this investigation and to express appreciation to Mr. W. H. King for his painstaking workmanship on the exceptionally large models.

BUREAU OF STANDARDS,  
WASHINGTON, D. C., July 10, 1928.

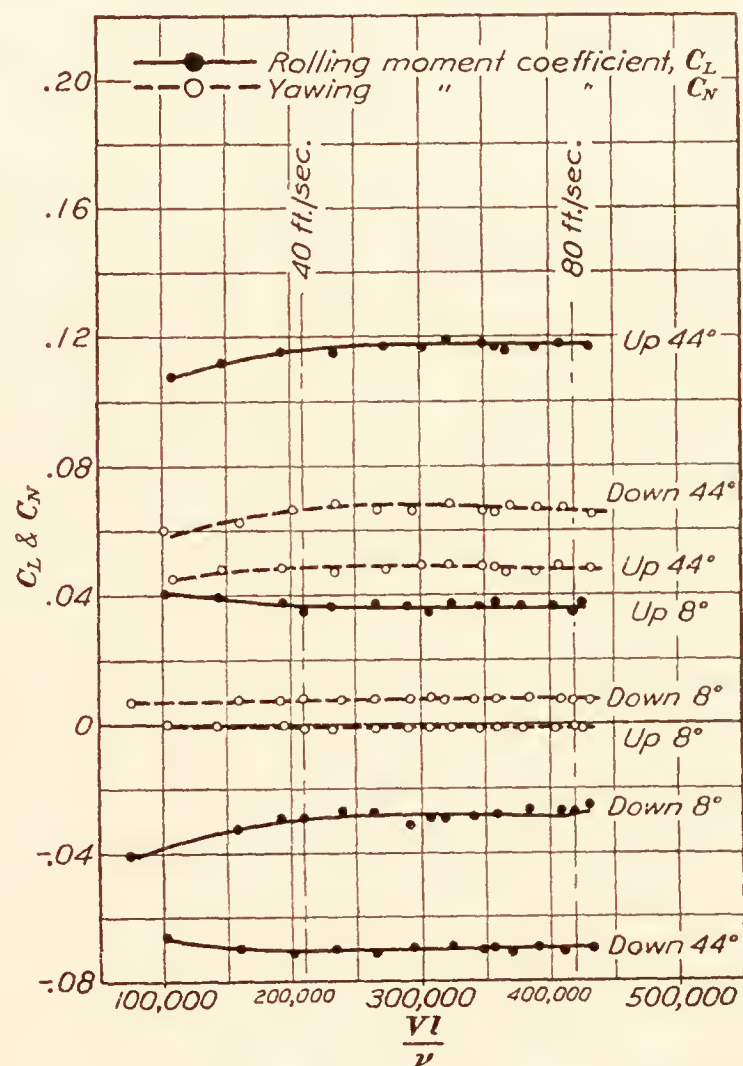


FIG. 27.—U. S. A. 27 wing. Aileron span 20 inches. Aileron chord 3.5 inches. Scale effect

BIBLIOGRAPHY

Reference 1. Archer, Lieut. C. E.: Wind Tunnel Test of Aileron Characteristics as Affected by Design and by Airfoil Thickness. Air Corps Information Circular No. 535, Sept. 1, 1925.

Reference 2. Irving, H. B., Ower, E., and Hankins, G. A.: An Investigation of the Aerodynamic Properties of Wing Ailerons. Part I.—The Effect of Variation of Plan Form of Wing Tip and of Span of Aileron. British Reports & Memoranda No. 550, October, 1918.

Irving, H. B., and Ower, E.: An Investigation of the Aerodynamic Properties of Wing Ailerons. Part II.—The Effect of Variation of Chord of Aileron. The Effect of "Wash-Out" on Ailerons. Tests on Ailerons of the "Panther" Type in which the Ailerons Do Not Extend to the Wing Tips. Effect of Variation in Taper Toward the Tips for Wings of given Plan Form. British Reports & Memoranda No. 615, June, 1919.

Reference 3. National Advisory Committee for Aeronautics: Aerodynamic Characteristics of Airfoils—IV. Technical Report No. 244. N. A. C. A. Sept. 1926.

TABLE I.—CLARK Y WING SECTION— $C_L$  AND  $C_N$  FOR ONE AILERON

[Varying chord of aileron. Angle of attack of airplane, 0°; angle of attack of wing, +4°; angle of yaw, 0°; angle of roll, 0°]

NOTE.—The values apply to either right or left aileron; the signs refer to the right aileron

AILERON SPAN, 20 INCHES

1.5-inch chord					2.0-inch chord				
$\theta$	Aileron up		Aileron down		$\theta$	Aileron up		Aileron down	
	$C_L$	$C_N$	$C_L$	$C_N$		$C_L$	$C_N$	$C_L$	$C_N$
0°	0	0	0	0	0°	0	0	0	0
4°	+. 0115	-. 0020	-. 0090	+. 0028	4°	+. 0150	-. 0024	-. 0120	+. 0040
8°	+. 0235	-. 0035	-. 0173	+. 0057	8°	+. 0280	-. 0035	-. 0212	+. 0076
12°	+. 0305	-. 0042	-. 0249	+. 0090	12°	+. 0382	-. 0040	-. 0290	+. 0125
16°	+. 0390	-. 0040	-. 0313	+. 0125	16°	+. 0470	-. 0038	-. 0370	+. 0170
20°	+. 0465	-. 0029	-. 0370	+. 0163	20°	+. 0545	-. 0020	-. 0430	+. 0215
24°	+. 0465	-. 0011	-. 0420	+. 0203	24°	+. 0614	+. 0008	-. 0436	+. 0262
28°	+. 0530	+. 0008	-. 0465	+. 0243	28°	+. 0678	+. 0040	-. 0479	+. 0307
32°	+. 0595	+. 0030	-. 0503	+. 0285	32°	+. 0730	+. 0070	-. 0519	+. 0353
36°	+. 0646	+. 0057	-. 0538	+. 0328	36°	+. 0785	+. 0110	-. 0555	+. 0400
40°	+. 0691	+. 0085	-. 0580	+. 0371	40°	+. 0830	+. 0148	-. 0589	+. 0450
44°	+. 0730	+. 0114	-. 0610	+. 0415	44°	+. 0876	+. 0190	-. 0618	+. 0500

3.0-inch chord					3.5-inch chord				
$\theta$	Aileron up		Aileron down		$\theta$	Aileron up		Aileron down	
	$C_L$	$C_N$	$C_L$	$C_N$		$C_L$	$C_N$	$C_L$	$C_N$
0°	0	0	0	0	0°	0	0	0	0
4°	+. 0185	-. 0027	-. 0160	+. 0038	4°	+. 0194	-. 0025	-. 0185	+. 0043
8°	+. 0350	-. 0041	-. 0270	+. 0092	8°	+. 0380	-. 0040	-. 0306	+. 0095
12°	+. 0520	-. 0041	-. 0350	+. 0165	12°	+. 0550	-. 0038	-. 0402	+. 0175
16°	+. 0670	-. 0028	-. 0413	+. 0235	16°	+. 0730	-. 0020	-. 0481	+. 0265
20°	+. 0800	+. 0003	-. 0472	+. 0305	20°	+. 0890	+. 0023	-. 0530	+. 0340
24°	+. 0860	+. 0062	-. 0525	+. 0372	24°	+. 0960	+. 0078	-. 0560	+. 0408
28°	+. 0920	+. 0121	-. 0570	+. 0438	28°	+. 1000	+. 0139	-. 0595	+. 0475
32°	+. 0970	+. 0182	-. 0606	+. 0500	32°	+. 1040	+. 0210	-. 0631	+. 0541
36°	+. 1030	+. 0244	-. 0640	+. 0560	36°	+. 1090	+. 0273	-. 0655	+. 0610
40°	+. 1080	+. 0304	-. 0665	+. 0612	40°	+. 1180	+. 0363	-. 0673	+. 0680
44°	+. 1120	+. 0365	-. 0686	+. 0661	44°	+. 1270	+. 0460	-. 0686	+. 0748



TABLE II.—CLARK Y WING SECTION— $C_L$  AND  $C_N$  FOR ONE AILERON[Varying span of aileron. Angle of attack of airplane,  $0^\circ$ ; angle of attack of wing,  $+4^\circ$ ; angle of yaw,  $0^\circ$ ; angle of roll,  $0^\circ$ ]

NOTE.—The values apply to either right or left aileron; the signs refer to the right aileron

AILERON CHORD, 2.5 INCHES

10-inch span					15-inch span				
$\theta$	Aileron up		Aileron down		$\theta$	Aileron up		Aileron down	
	$C_L$	$C_N$	$C_L$	$C_N$		$C_L$	$C_N$	$C_L$	$C_N$
$0^\circ$	0	0	0	0	$0^\circ$	0	0	0	0
$4^\circ$	+. 0080	-. 0013	-. 0078	+. 0022	$4^\circ$	+. 0115	-. 0021	-. 0110	+. 0020
$8^\circ$	+. 0153	-. 0018	-. 0150	+. 0054	$8^\circ$	+. 0230	-. 0035	-. 0210	+. 0055
$12^\circ$	+. 0226	-. 0018	-. 0204	+. 0093	$12^\circ$	+. 0345	-. 0033	-. 0300	+. 0111
$16^\circ$	+. 0300	-. 0012	-. 0250	+. 0133	$16^\circ$	+. 0450	-. 0022	-. 0395	+. 0165
$20^\circ$	+. 0390	-. 0002	-. 0286	+. 0173	$20^\circ$	+. 0550	0	-. 0425	+. 0212
$24^\circ$	+. 0410	+. 0018	-. 0300	+. 0211	$24^\circ$	+. 0600	+. 0035	-. 0432	+. 0262
$28^\circ$	+. 0435	+. 0041	-. 0333	+. 0250	$28^\circ$	+. 0625	+. 0068	-. 0461	+. 0310
$32^\circ$	+. 0460	+. 0068	-. 0356	+. 0288	$32^\circ$	+. 0650	+. 0104	-. 0492	+. 0360
$36^\circ$	+. 0485	+. 0096	-. 0372	+. 0320	$36^\circ$	+. 0680	+. 0140	-. 0520	+. 0410
$40^\circ$	+. 0508	+. 0125	-. 0389	+. 0356	$40^\circ$	+. 0710	+. 0181	-. 0541	+. 0450
$44^\circ$	+. 0530	+. 0155	-. 0400	+. 0385	$44^\circ$	+. 0750	+. 0225	-. 0556	+. 0485

20-inch span				
$\theta$	Aileron up		Aileron down	
	$C_L$	$C_N$	$C_L$	$C_N$
$0^\circ$	0	0	0	0
$4^\circ$	+. 0150	-. 0020	-. 0125	+. 0035
$8^\circ$	+. 0300	-. 0040	-. 0230	+. 0078
$12^\circ$	+. 0440	-. 0030	-. 0325	+. 0131
$16^\circ$	+. 0570	-. 0025	-. 0410	+. 0190
$20^\circ$	+. 0675	-. 0002	-. 0450	+. 0248
$24^\circ$	+. 0730	+. 0038	-. 0475	+. 0308
$28^\circ$	+. 0775	+. 0080	-. 0540	+. 0362
$32^\circ$	+. 0810	+. 0126	-. 0598	+. 0420
$36^\circ$	+. 0870	+. 0175	-. 0632	+. 0474
$40^\circ$	+. 0925	+. 0220	-. 0658	+. 0528
$44^\circ$	+. 0985	+. 0270	-. 0670	+. 0580

TABLE III.—U. S. A. 27 WING SECTION— $C_L$  AND  $C_N$  FOR ONE AILERON

[Varying chord of aileron. Angle of attack of airplane, 0°; angle of attack of wing, +4°; angle of yaw, 0°; angle of roll, 0°]

NOTE.—The values apply to either right or left aileron; the signs refer to the right aileron

AILERON SPAN, 20 INCHES

1.5-inch chord					2.0-inch chord				
$\theta$	Aileron up		Aileron down		$\theta$	Aileron up		Aileron down	
	$C_L$	$C_N$	$C_L$	$C_N$		$C_L$	$C_N$	$C_L$	$C_N$
0°	0	0	0	0	0°	0	0	0	0
4°	+. 0126	-. 0012	-. 0098	+. 0015	4°	+. 0155	-. 0015	-. 0120	+. 0018
8°	+. 0230	-. 0020	-. 0180	+. 0032	8°	+. 0285	-. 0024	-. 0200	+. 0044
12°	+. 0320	-. 0018	-. 0242	+. 0055	12°	+. 0405	-. 0012	-. 0290	+. 0085
16°	+. 0390	-. 0010	-. 0300	+. 0080	16°	+. 0495	0	-. 0355	+. 0125
20°	+. 0430	0	-. 0355	+. 0110	20°	+. 0560	+. 0022	-. 0405	+. 0165
24°	+. 0460	+. 0018	-. 0402	+. 0142	24°	+. 0605	+. 0050	-. 0450	+. 0205
28°	+. 0505	+. 0040	-. 0450	+. 0180	28°	+. 0645	+. 0083	-. 0500	+. 0247
32°	+. 0560	+. 0067	-. 0490	+. 0217	32°	+. 0695	+. 0120	-. 0542	+. 0295
36°	+. 0615	+. 0094	-. 0530	+. 0262	36°	+. 0745	+. 0152	-. 0584	+. 0342
40°	+. 0672	+. 0120	-. 0565	+. 0311	40°	+. 0795	+. 0195	-. 0614	+. 0395
44°	+. 0710	+. 0150	-. 0595	+. 0360	44°	+. 0855	+. 0245	-. 0640	+. 0450

3.0-inch chord					3.5-inch chord				
$\theta$	Aileron up		Aileron down		$\theta$	Aileron up		Aileron down	
	$C_L$	$C_N$	$C_L$	$C_N$		$C_L$	$C_N$	$C_L$	$C_N$
0°	0	0	0	0	0°	0	0	0	0
4°	+. 0155	-. 0020	-. 0145	+. 0035	4°	+. 0177	-. 0010	-. 0159	+. 0035
8°	+. 0310	-. 0022	-. 0280	+. 0080	8°	+. 0353	-. 0010	-. 0290	+. 0079
12°	+. 0460	-. 0010	-. 0368	+. 0130	12°	+. 0510	+. 0004	-. 0405	+. 0149
16°	+. 0600	+. 0022	-. 0435	+. 0185	16°	+. 0655	+. 0033	-. 0510	+. 0222
20°	+. 0720	+. 0065	-. 0495	+. 0250	20°	+. 0790	+. 0076	-. 0553	+. 0298
24°	+. 0825	+. 0120	-. 0525	+. 0312	24°	+. 0890	+. 0130	-. 0560	+. 0360
28°	+. 0860	+. 0175	-. 0530	+. 0372	28°	+. 0961	+. 0195	-. 0545	+. 0419
32°	+. 0904	+. 0230	-. 0568	+. 0440	32°	+. 1016	+. 0265	-. 0595	+. 0476
36°	+. 0945	+. 0280	-. 0608	+. 0500	36°	+. 1058	+. 0335	-. 0617	+. 0533
40°	+. 0985	+. 0335	-. 0660	+. 0558	40°	+. 1116	+. 0406	-. 0660	+. 0592
44°	+. 1020	+. 0390	-. 0685	+. 0615	44°	+. 1180	+. 0477	-. 0690	+. 0650



TABLE IV.—U. S. A. 27 WING SECTION— $C_L$  AND— $C_N$  FOR ONE AILERON

[Varying span of aileron. Angle of attack of airplane, 0°; angle of attack of wing, +4°; angle of yaw, 0°; angle of roll, 0°]

NOTE.—The values apply to either right or left aileron; the signs refer to the right aileron

AILERON CHORD 2.5 INCHES

10-inch span					15-inch span				
$\theta$	Aileron up		Aileron down		$\theta$	Aileron up		Aileron down	
	$C_L$	$C_N$	$C_L$	$C_N$		$C_L$	$C_N$	$C_L$	$C_N$
0°	0	0	0	0	0°	0	0	0	0
4°	+. 0069	−. 0009	−. 0055	+. 0015	4°	+. 0120	−. 0010	−. 0100	+. 0025
8°	+. 0140	−. 0011	−. 0108	+. 0036	8°	+. 0230	−. 0010	−. 0200	+. 0055
12°	+. 0211	−. 0010	−. 0161	+. 0065	12°	+. 0330	−. 0004	−. 0268	+. 0090
16°	+. 0290	0	−. 0211	+. 0098	16°	+. 0426	+. 0010	−. 0318	+. 0127
20°	+. 0375	+. 0021	−. 0257	+. 0130	20°	+. 0500	+. 0036	−. 0358	+. 0171
24°	+. 0397	+. 0044	−. 0295	+. 0163	24°	+. 0534	+. 0063	−. 0390	+. 0218
28°	+. 0385	+. 0069	−. 0310	+. 0198	28°	+. 0557	+. 0095	−. 0414	+. 0260
32°	+. 0412	+. 0098	−. 0328	+. 0232	32°	+. 0590	+. 0131	−. 0440	+. 0300
36°	+. 0450	+. 0128	−. 0348	+. 0270	36°	+. 0630	+. 0172	−. 0465	+. 0343
40°	+. 0490	+. 0159	−. 0368	+. 0310	40°	+. 0685	+. 0219	−. 0490	+. 0382
44°	+. 0530	+. 0191	−. 0382	+. 0350	44°	+. 0745	+. 0269	−. 0514	+. 0420

20-inch span				
$\theta$	Aileron up		Aileron down	
	$C_L$	$C_N$	$C_L$	$C_N$
0°	0	0	0	0
4°	+. 0155	−. 0018	−. 0129	+. 0025
8°	+. 0296	−. 0020	−. 0238	+. 0061
12°	+. 0420	−. 0010	−. 0330	+. 0101
16°	+. 0535	+. 0013	−. 0405	+. 0145
20°	+. 0630	+. 0049	−. 0445	+. 0196
24°	+. 0660	+. 0085	−. 0468	+. 0250
28°	+. 0720	+. 0124	−. 0494	+. 0304
32°	+. 0775	+. 0170	−. 0526	+. 0360
36°	+. 0830	+. 0217	−. 0568	+. 0412
40°	+. 0886	+. 0270	−. 0610	+. 0465
44°	+. 0940	+. 0322	−. 0650	+. 0520

TABLE V.—CLARK Y WING SECTION—COMBINED VALUES OF  $C_L$  AND  $C_N$ , RIGHT AILERON UP, LEFT AILERON DOWN

[Varying chord of aileron. Angle of attack of airplane,  $0^\circ$ ; angle of attack of wing,  $+4^\circ$ ; angle of yaw,  $0^\circ$ ; angle of roll,  $0^\circ$ ]  
AILERON SPAN, 20 INCHES

1.5-inch chord			2.0-inch chord			3.0-inch chord			3.5-inch chord		
$\theta$	$C_L$	$C_N$	$\theta$	$C_L$	$C_N$	$\theta$	$C_L$	$C_N$	$\theta$	$C_L$	$C_N$
$0^\circ$	0	0	$0^\circ$	0	0	$0^\circ$	0	0	$0^\circ$	0	0
$4^\circ$	+. 0205	-. 0048	$4^\circ$	+. 0270	-. 0064	$4^\circ$	+. 0345	-. 0065	$4^\circ$	+. 0379	-. 0068
$8^\circ$	+. 0408	-. 0092	$8^\circ$	+. 0492	-. 0111	$8^\circ$	+. 0620	-. 0133	$8^\circ$	+. 0686	-. 0135
$12^\circ$	+. 0554	-. 0132	$12^\circ$	+. 0672	-. 0165	$12^\circ$	+. 0870	-. 0206	$12^\circ$	+. 0952	-. 0213
$16^\circ$	+. 0703	-. 0165	$16^\circ$	+. 0840	-. 0208	$16^\circ$	+. 1083	-. 0263	$16^\circ$	+. 1211	-. 0285
$20^\circ$	+. 0835	-. 0192	$20^\circ$	+. 0975	-. 0235	$20^\circ$	+. 1272	-. 0302	$20^\circ$	+. 1420	-. 0317
$24^\circ$	+. 0885	-. 0214	$24^\circ$	+. 1050	-. 0254	$24^\circ$	+. 1385	-. 0310	$24^\circ$	+. 1520	-. 0330
$28^\circ$	+. 0995	-. 0235	$28^\circ$	+. 1157	-. 0267	$28^\circ$	+. 1490	-. 0317	$28^\circ$	+. 1595	-. 0336
$32^\circ$	+. 1098	-. 0255	$32^\circ$	+. 1249	-. 0283	$32^\circ$	+. 1576	-. 0318	$32^\circ$	+. 1671	-. 0331
$36^\circ$	+. 1184	-. 0271	$36^\circ$	+. 1340	-. 0290	$36^\circ$	+. 1670	-. 0316	$36^\circ$	+. 1745	-. 0337
$40^\circ$	+. 1271	-. 0286	$40^\circ$	+. 1419	-. 0302	$40^\circ$	+. 1745	-. 0308	$40^\circ$	+. 1853	-. 0317
$44^\circ$	+. 1340	-. 0301	$44^\circ$	+. 1494	-. 0310	$44^\circ$	+. 1806	-. 0296	$44^\circ$	+. 1956	-. 0288

TABLE VI.—CLARK Y WING SECTION—COMBINED VALUES OF  $C_L$  AND  $C_N$ , RIGHT AILERON UP, LEFT AILERON DOWN

[Varying span of aileron. Angle of attack of airplane,  $0^\circ$ ; angle of attack of wing,  $+4^\circ$ ; angle of yaw,  $0^\circ$ ; angle of roll,  $0^\circ$ ]  
AILERON CHORD, 2.5 INCHES

10-inch span			15-inch span			20-inch span		
$\theta$	$C_L$	$C_N$	$\theta$	$C_L$	$C_N$	$\theta$	$C_L$	$C_N$
$0^\circ$	0	0	$0^\circ$	0	0	$0^\circ$	0	0
$4^\circ$	+. 0158	-. 0035	$4^\circ$	+. 0225	-. 0041	$4^\circ$	+. 0275	-. 0055
$8^\circ$	+. 0303	-. 0072	$8^\circ$	+. 0440	-. 0090	$8^\circ$	+. 0530	-. 0118
$12^\circ$	+. 0430	-. 0113	$12^\circ$	+. 0645	-. 0144	$12^\circ$	+. 0765	-. 0161
$16^\circ$	+. 0550	-. 0145	$16^\circ$	+. 0845	-. 0187	$16^\circ$	+. 0980	-. 0215
$20^\circ$	+. 0676	-. 0175	$20^\circ$	+. 0975	-. 0212	$20^\circ$	+. 1125	-. 0250
$24^\circ$	+. 0710	-. 0193	$24^\circ$	+. 1032	-. 0227	$24^\circ$	+. 1205	-. 0270
$28^\circ$	+. 0765	-. 0209	$28^\circ$	+. 1086	-. 0242	$28^\circ$	+. 1315	-. 0282
$32^\circ$	+. 0816	-. 0220	$32^\circ$	+. 1142	-. 0254	$32^\circ$	+. 1408	-. 0294
$36^\circ$	+. 0857	-. 0224	$36^\circ$	+. 1200	-. 0270	$36^\circ$	+. 1502	-. 0299
$40^\circ$	+. 0897	-. 0231	$40^\circ$	+. 1251	-. 0269	$40^\circ$	+. 1583	-. 0306
$44^\circ$	+. 0930	-. 0230	$44^\circ$	+. 1306	-. 0260	$44^\circ$	+. 1655	-. 0310



TABLE VII.—U. S. A. 27 WING SECTION—COMBINED VALUES OF  $C_L$  AND  $C_N$ , RIGHT AILERON UP, LEFT AILERON DOWN[Varying chord of aileron. Angle of attack of airplane,  $0^\circ$ ; angle of attack of wing,  $+4^\circ$ ; angle of yaw,  $0^\circ$ ; angle of roll,  $0^\circ$ ]

AILERON SPAN, 20 INCHES

1.5-inch chord			2.0-inch chord			3.0-inch chord			3.5-inch chord		
$\theta$	$C_L$	$C_N$	$\theta$	$C_L$	$C_N$	$\theta$	$C_L$	$C_N$	$\theta$	$C_L$	$C_N$
$0^\circ$	0	0	$0^\circ$	0	0	$0^\circ$	0	0	$0^\circ$	0	0
$4^\circ$	+. 0224	-. 0027	$4^\circ$	+. 0275	-. 0033	$4^\circ$	+. 0300	-. 0055	$4^\circ$	+. 0336	-. 0045
$8^\circ$	+. 0410	-. 0052	$8^\circ$	+. 0485	-. 0068	$8^\circ$	+. 0590	-. 0102	$8^\circ$	+. 0643	-. 0089
$12^\circ$	+. 0562	-. 0073	$12^\circ$	+. 0695	-. 0097	$12^\circ$	+. 0828	-. 0140	$12^\circ$	+. 0915	-. 0145
$16^\circ$	+. 0690	-. 0090	$16^\circ$	+. 0850	-. 0125	$16^\circ$	+. 1035	-. 0163	$16^\circ$	+. 1165	-. 0189
$20^\circ$	+. 0785	-. 0110	$20^\circ$	+. 0965	-. 0143	$20^\circ$	+. 1215	-. 0185	$20^\circ$	+. 1343	-. 0222
$24^\circ$	+. 0862	-. 0124	$24^\circ$	+. 1055	-. 0155	$24^\circ$	+. 1350	-. 0192	$24^\circ$	+. 1450	-. 0230
$28^\circ$	+. 0955	-. 0140	$28^\circ$	+. 1145	-. 0164	$28^\circ$	+. 1390	-. 0197	$28^\circ$	+. 1506	-. 0224
$32^\circ$	+. 1050	-. 0150	$32^\circ$	+. 1237	-. 0175	$32^\circ$	+. 1472	-. 0210	$32^\circ$	+. 1611	-. 0211
$36^\circ$	+. 1145	-. 0168	$36^\circ$	+. 1329	-. 0190	$36^\circ$	+. 1553	-. 0220	$36^\circ$	+. 1675	-. 0198
$40^\circ$	+. 1237	-. 0191	$40^\circ$	+. 1409	-. 0200	$40^\circ$	+. 1645	-. 0223	$40^\circ$	+. 1776	-. 0186
$44^\circ$	+. 1305	-. 0210	$44^\circ$	+. 1495	-. 0205	$44^\circ$	+. 1705	-. 0225	$44^\circ$	+. 1870	-. 0173

TABLE VIII.—U. S. A. 27 WING SECTION—COMBINED VALUES OF  $C_L$  AND  $C_N$ , RIGHT AILERON UP, LEFT AILERON DOWN[Varying span of aileron. Angle of attack of airplane,  $0^\circ$ ; angle of attack of wing,  $+4^\circ$ ; angle of yaw,  $0^\circ$ ; angle of roll,  $0^\circ$ ]

AILERON CHORD, 2.5 INCHES

10-inch span			15-inch span			20-inch span		
$\theta$	$C_L$	$C_N$	$\theta$	$C_L$	$C_N$	$\theta$	$C_L$	$C_N$
$0^\circ$	0	0	$0^\circ$	0	0	$0^\circ$	0	0
$4^\circ$	+. 0124	-. 0024	$4^\circ$	+. 0220	-. 0035	$4^\circ$	+. 0284	-. 0043
$8^\circ$	+. 0248	-. 0047	$8^\circ$	+. 0430	-. 0065	$8^\circ$	+. 0533	-. 0081
$12^\circ$	+. 0372	-. 0076	$12^\circ$	+. 0598	-. 0094	$12^\circ$	+. 0750	-. 0111
$16^\circ$	+. 0501	-. 0098	$16^\circ$	+. 0744	-. 0117	$16^\circ$	+. 0940	-. 0132
$20^\circ$	+. 0632	-. 0109	$20^\circ$	+. 0858	-. 0135	$20^\circ$	+. 1075	-. 0150
$24^\circ$	+. 0692	-. 0119	$24^\circ$	+. 0924	-. 0155	$24^\circ$	+. 1128	-. 0165
$28^\circ$	+. 0695	-. 0129	$28^\circ$	+. 0971	-. 0165	$28^\circ$	+. 1214	-. 0180
$32^\circ$	+. 0740	-. 0134	$32^\circ$	+. 1030	-. 0169	$32^\circ$	+. 1301	-. 0190
$36^\circ$	+. 0798	-. 0142	$36^\circ$	+. 1095	-. 0171	$36^\circ$	+. 1398	-. 0195
$40^\circ$	+. 0858	-. 0151	$40^\circ$	+. 1175	-. 0163	$40^\circ$	+. 1496	-. 0195
$44^\circ$	+. 0912	-. 0159	$44^\circ$	+. 1259	-. 0151	$44^\circ$	+. 1590	-. 0198





---

**REPORT No. 299**

---

**INVESTIGATION OF DAMPING LIQUIDS  
FOR AIRCRAFT INSTRUMENTS**

**By G. H. KEULEGAN  
Bureau of Standards**





## REPORT No. 299

### INVESTIGATION OF DAMPING LIQUIDS FOR AIRCRAFT INSTRUMENTS

By G. H. KEULEGAN

#### SUMMARY

*This report covers the results of an investigation carried on at the Bureau of Standards with the financial assistance of the National Advisory Committee for Aeronautics.*

*The choice of a damping liquid for aircraft instruments is difficult owing to the range of temperature at which aircraft operate. Temperature changes affect the viscosity tremendously. The investigation was undertaken with the object of finding liquids of various viscosities otherwise suitable which had a minimum change in viscosity with temperature. The new data relate largely to solutions.*

*The effect of temperature on the kinematic viscosity of the following liquids and solutions was determined in the temperature interval  $-18^{\circ}$  to  $+30^{\circ}$  C.*

*(1) Solutions of animal and vegetable oils in xylene. These were poppy seed oil, two samples of neat's-foot oil, castor oil and linseed oil.*

*(2) Solutions of mineral oils in xylene. These were Squibb's petrolatum of naphthene base and transformer oil.*

*(3) Glycerine solutions in ethyl alcohol and in mixture of 50-50 ethyl alcohol and water.*

*(4) Mixtures of normal butyl alcohol with methyl alcohol.*

*(5) Individual liquids; kerosene, mineral spirits, xylene, and recoil oil.*

*The apparatus consisted of four capillary-tube viscometers, which were immersed in a liquid bath in order to secure temperature control. The method of calibration and the related experimental data are presented in detail.*

*The viscosity data for the liquids are given in curves in which  $\log_{10} \frac{t_{\theta}}{t_{30}}$  is plotted against temperature, where  $t_{30}$  and  $t_{\theta}$  are respectively the times of discharge through the viscometer at  $30^{\circ}$  C. and  $\theta^{\circ}$  C. Except for a correction which is usually small, the following relation holds:*

$$\log_{10} \frac{t_{\theta}}{t_{30}} = \log_{10} \frac{\nu_{\theta}}{\nu_{30}}$$

*in which  $\nu_{30}$  and  $\nu_{\theta}$  are respectively the kinematic viscosities at  $30^{\circ}$  C. and  $\theta^{\circ}$  C. The density at  $30^{\circ}$  C., the coefficient of cubical thermal expansion for each solution, and  $\nu_{30}$  are given, together with other data, so that the absolute viscosity may be computed. The accuracy is within 1 per cent.*

#### INTRODUCTION

This investigation was undertaken in order to obtain data on the viscosity and the change in viscosity with temperature of such liquids and solutions as may be suitable for damping purposes in aircraft instruments. Damping liquids in many cases must also have other characteristics, such as invariability with time, low volatility, and constancy of index of refraction and transparency for varying temperatures. These latter characteristics are not dealt with in this paper except incidentally.

Most of the liquids which were chosen for the tests are solutions of mineral, vegetable, and animal oil in xylene. The selection of xylene as a solvent for the heavier oils finds its reason in the fact that it has a low thermal coefficient of viscosity for the thermal range considered in

aircraft instruments, which is the range  $+30^{\circ}\text{C.}$  to  $-30^{\circ}\text{C.}$  The range of temperatures in the tests was somewhat smaller than this and was from  $+30^{\circ}\text{C.}$  to  $-18^{\circ}\text{C.}$

An accuracy of 1 per cent was aimed at in the determination of viscosity at the temperature of  $30^{\circ}$  centigrade. Two considerations have discouraged possible effort for greater precision: First, it is a known fact that most oily solutions age with time, and therefore the viscosity of such solutions need not be accurately determined except for the purpose of showing that the viscosity changes (Reference 1); secondly, more precise determinations of viscosity for the particular range adopted can not be realized with a reasonable amount of attention and effort.

It is desired to acknowledge the valuable assistance of Dr. W. G. Brombacher and the substantial help of Mr. E. R. Melton in obtaining the experimental data.

## APPARATUS AND EXPERIMENTAL PROCEDURE

### VISCOMETERS

Consider the particular Ostwald-type viscometer which is shown in Figure 1. The discharging and receiving bulbs  $A$  and  $B$  are cylinders of equal radius and volume. The timing of the flow is made for the total discharge of liquid in the discharging bulb  $A$ . When this total discharge has taken place, the receiving bulb  $B$  is just full and the discharging bulb  $A$  is empty. Now if liquid flows under its own weight the following expression holds, which is Poiseuille's law applied to the present case (Reference 2):

$$\mu = \frac{\pi r^4 g \rho}{8 l_e Q} \frac{2 h_r}{\log_e \left( \frac{h_o + h_r}{h_o - h_r} \right)} t \quad (1)$$

where

$\mu$  = the absolute viscosity in poises.

$t$  = the time of discharge in seconds.

$Q$  = the volume of the discharging bulb in  $\text{cm.}^3$ .

$h_r$  = the height of  $B$  or of  $A$  (see fig. 1) in cm.

$h_o$  = the vertical distance between the centers of the bulbs  $A$  and  $B$  in cm.

$l_e$  = the effective length of the capillary tube in cm.

$r$  = the radius of the capillary tube in cm.

$\rho$  = the density of the liquid in grams per  $\text{cm.}^3$

$g$  = the acceleration of gravity in  $\text{cm. per sec.}^2$

In practice deviations are made from the viscometer just discussed, particularly in the design of the bulbs. The one which is adopted for the present work is shown in Figure 2. The discharging bulb is a combination of cone frustrums and a cylinder, while, the receiving bulb is a cylinder which has the same radius as the cylinder in the discharging bulb. The volume of the discharging bulb  $A$  is included between the marks  $M_2$  and  $M_1$ , which will be spoken of as the timing marks.

In order to compensate for the slight deviation from the ideal case, equation (1) is modified as follows:

$$\mu = \frac{\pi r^4 g \rho}{8 l_e Q} \frac{2 h_r t}{\log_e \left( \frac{h_o + h_r + C}{h_o - h_r + C} \right)} \quad (2)$$

or putting

$$A_o = \frac{\pi r^4 g}{8 l_e Q}$$

$$\mu = \rho A_o \frac{2 h_r t}{\log_e \left( \frac{h_o + h_r + C}{h_o - h_r + C} \right)} \quad (3)$$

Here all of the quantities except  $h_o$ ,  $h_r$ , and  $C$  have the same meaning as in equation (1).  $C$  is to be determined experimentally, while  $h_o$  and  $h_r$  are defined in the following paragraph.



The quantity  $C$  may involve a constant term and an expression dependent on  $h_o$ . The latter would be small in comparison with the constant term and therefore can be neglected.

It will be supposed that when the liquid in the viscometer is in equilibrium under its own weight its free surface in the receiving tube  $B$  occupies the mark  $m_5$ . (See fig. 2.) Such marks will be spoken of as the filling mark of the viscometer. When the liquid is forced to the level of the timing mark  $M_1$  of the discharging bulb, the free surface of the liquid in the receiving tube will descend to a level  $n_1$ . When the liquid is next forced to the timing mark  $M_2$ , the corresponding level in the receiving tube will be  $n_2$ . Denoting by  $H_1$  and  $H_2$  the vertical distances

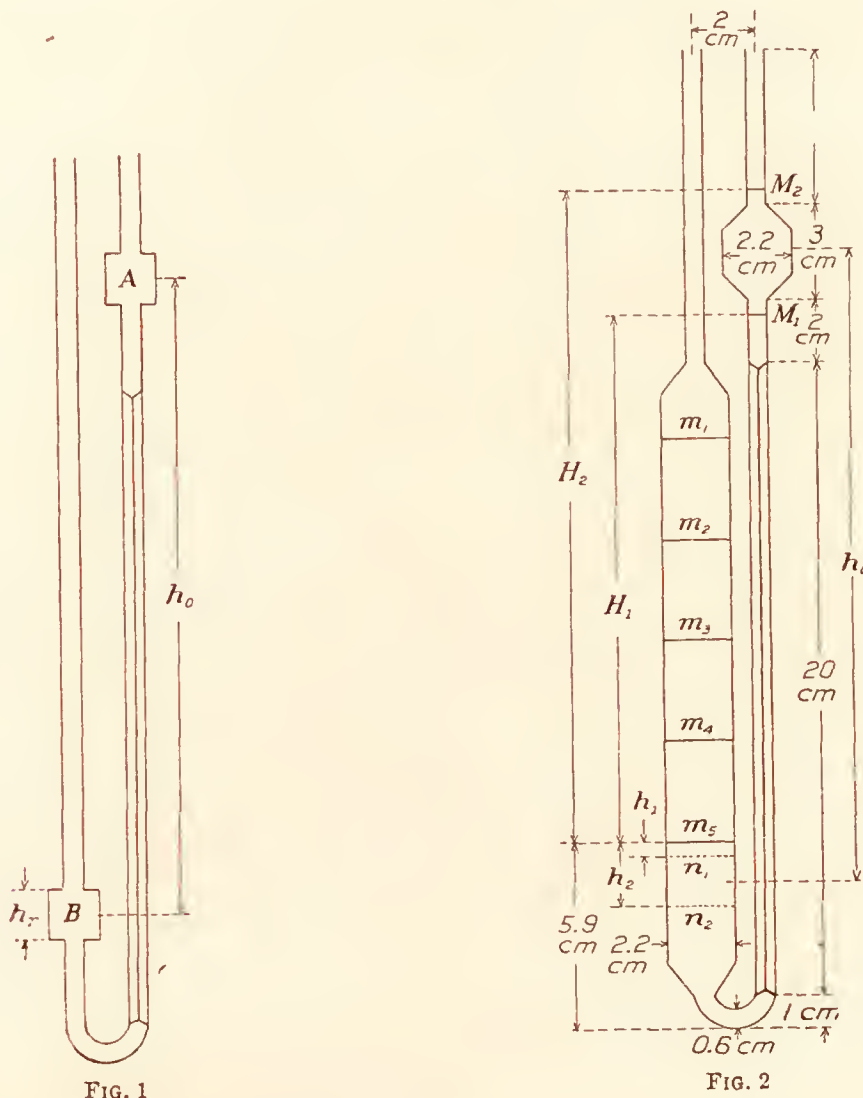


FIG. 1

FIG. 2

of  $M_1$  and  $M_2$  from  $m_5$  and by  $h_2$  and  $h_1$  the vertical distances of  $n_2$  and  $n_1$  from  $m_5$ , the definitions of  $h_o$  and  $h_r$  are

$$h_r = h_2 - h_1$$

$$h_o = \frac{H_1 + H_2 + h_1 + h_2}{2} \quad (4)$$

Equations (2) and (3) hold only for slow rates of flow. If the velocity is fast, the following equation applies:

$$\mu = \rho \left[ A_o \frac{2h_r t}{\log_e \left( \frac{h_o + h_r + C}{h_o - h_r + C} \right)} - \frac{B}{t} \right] \quad (5)$$

where

$$B = \frac{mQ}{8\pi l_e} \quad (6)$$

The term  $\frac{B\rho}{t}$  is known as the inertia term. The quantity  $m$  which appears in the definition of  $B$  is a constant quantity for a given viscometer; its value may vary from 1 to 2, depending on the configuration of the ends. (Reference 4.)

A relation proposed by Bond (Reference 3) is that equation (3) applies when

$$\frac{Q' \rho}{r \mu} = \frac{Q}{r} \frac{\rho}{\mu t} = \frac{Q}{r} B_c \leq 16 \quad (7)$$

and that equation (5) should be used for values in excess of 16.  $Q'$  is the volume rate of flow of the liquid, which is  $Q/t$  for all practical purposes.  $B_c$  may be called Bond's criterion. This relation was shown to hold only for short-length, thick-walled, and square-edged capillaries.

In capillaries with trumpet-shaped ends the quantity  $\frac{Q}{r} B_c$  is larger than 16. (Reference 4.)

It should be noted that multiplying the quantity  $\frac{Q}{r} B_c$  by  $\frac{2}{\pi}$  gives the expression for the more

familiar Reynolds Number; thus the criterion 16 is equivalent to a Reynolds Number of  $\frac{32}{\pi}$ .

The viscometers used during measurements were four in number. They were alike in design, except for the radii of the bores, and conform to the data given in the sketch in Figure 2. In each viscometer there were five filling marks, allowing five different rates of flow. Generally it is the lowest one—that is,  $m_5$ , which was used during the tests. However, use was made of the other filling marks in the calibration of the viscometers. The proportions of the discharging bulb were designed for the smallest error in drainage (Reference 5), which requires that the height of the conical portion is at least equal to the height of the cylindrical portion. The distance between the timing marks was nearly 3.5 cm., while the distances between two consecutive filling marks were nearly 3 cm. Approximate essential dimensions, such as the radii of capillaries  $r$ , the volumes of discharging bulbs  $Q$ , the length of capillaries when the trumpetlike ends are excluded,  $l_2$ , and when they are included,  $l_1$ , are given in Table I. The dimension  $r$  was found by weighing the mercury contained in a measured length of the capillary tube and  $Q$  by weighing mercury both at a temperature of 23° C.

TABLE I

Viscometer	Radius of capillary $r$	Volume of bulb $Q$	Length of capillary	
			$l_2$	$l_1$
V <sub>1</sub> -----	Cm. 0.0519	Cm. <sup>3</sup> 6.37	Cm. 19.6	Cm. 20.2
V <sub>2</sub> -----	.0641	5.84	19.6	20.2
V <sub>3</sub> -----	.1085	6.81	19.5	20.2
V <sub>4</sub> -----	.1283	6.28	19.3	20.0

CALIBRATION OF VISCOMETERS

Equation (5) is the working formula of the viscometers which shall be denoted by  $V_1$ ,  $V_2$ ,  $V_3$ , and  $V_4$ . There are three constants to be determined by calibration; these constants are  $A_o$ ,  $B$ , and  $C$ . The equation (5) can be made linear in these constants if  $C$  is sufficiently small with respect to  $h_o - h_r$ . It will be assumed that this is the case. It can be shown that

$$\log_e \frac{h_o + h_r + C}{h_o - h_r + C} = \log_e \left( \frac{h_o + h_r}{h_o - h_r} \right) - \frac{2h_r C}{h_o^2 - h_r^2} + \frac{2h_r}{h_o^2 - h_r^2} \cdot \frac{h_o}{h_o^2 - h_r^2} C^2$$

or defining

$$N = \log_e \frac{h_o + h_r}{h_o - h_r}$$

$$M = \frac{2h_r}{h_o^2 - h_r^2}$$

$$L = \frac{h_o}{h_o^2 - h_r^2}$$

$$\left( \log_e \frac{h_o + h_r + C}{h_o - h_r + C} \right)^{-1} = \frac{1}{N} + \frac{M}{N^2} C - \frac{M}{N^2} \left( L - \frac{M}{N} \right) C^2 \quad (8)$$



TABLE II  
DATA FOR EVALUATING THE EFFECTIVE HEAD

Viscometer	Filling mark	$h_o$	$h_o$	$\frac{1}{N}$	$M$	$\frac{M}{N^2}$	$L$
V <sub>1</sub> -----	$m_1$	1.73	6.52	1.840	0.0881	0.296	0.1650
	$m_2$		9.59	2.743	.0387	.292	.1078
	$m_3$		12.59	3.621	.0223	.292	.0810
	$m_4$		15.59	4.498	.0143	.292	.0649
	$m_5$		18.60	5.362	.0101	.290	.0542
V <sub>2</sub> -----	$m_1$	1.62	6.94	2.102	.0711	.314	.1524
	$m_2$		9.98	3.051	.0334	.311	.1029
	$m_3$		12.97	3.976	.0196	.309	.0738
	$m_4$		16.01	4.929	.0128	.309	.0631
	$m_5$		19.05	5.862	.0090	.301	.0529
V <sub>3</sub> -----	$m_1$	1.92	6.98	1.771	.0853	.267	.1550
	$m_2$		9.99	2.569	.0399	.263	.1039
	$m_3$		12.98	3.358	.0233	.263	.0788
	$m_4$		15.98	4.142	.0152	.262	.0635
	$m_5$		19.04	4.948	.0107	.262	.0531
V <sub>4</sub> -----	$m_1$	1.99	6.55	1.594	.1022	.260	.1682
	$m_2$		9.63	2.384	.0448	.255	.1085
	$m_3$		12.61	3.141	.0257	.253	.0814
	$m_4$		15.62	3.903	.0166	.253	.0651
	$m_5$		18.56	4.649	.0117	.253	.0545

The values of  $\frac{1}{N} \frac{M}{N^2}$ ,  $M$  and  $L$  for each filling mark of the four viscometers appear in Table II. It is evident from this table that the term containing  $C^2$  in equation (8) is insignificant. Accordingly (5) becomes

$$\frac{\mu}{\rho} = \nu = A'_0 \left[ \frac{1}{N} + \frac{M}{N^2} C \right] t - \frac{B}{t} \quad (9)$$

where  $A'_0 = 2h_r A_0$  and  $\nu$  represent the kinematic viscosity. By definition kinematic viscosity is the ratio of the viscosity in absolute units to the density.

In equation (9) the quantities  $A'_0$ ,  $C$ , and  $B$  are constants for each viscometer, independent of the filling marks. The term  $2h_r g \rho \left( \frac{1}{N} + \frac{M}{N^2} C \right)$  is the effective pressure of which  $2h_r g \rho$  is constant for each viscometer and included in with  $A'_0$ , while  $\frac{1}{N} + \frac{M}{N^2} C$  varies for each filling mark.

Since each viscometer has five filling marks, one standard liquid would be sufficient to determine the three constants,  $A'_0$ ,  $C$ , and  $B$ , providing that  $t$  could be measured with sufficient accuracy. In the determination of these constants at least three appropriate standard liquids were used for each viscometer. The viscosities of these liquids at  $+25^\circ \text{C}$ ., except that of water, were furnished by the friction and lubrication section of the Bureau of Standards. The majority of them were mineral oils, and their viscosity values perhaps had undergone slight variation before use was made of them as calibrating liquids. During the calibrations no particular effort was exerted to observe the flows exactly at  $25^\circ \text{C}$ . as long as the temperature of the liquid remained in the vicinity of  $25^\circ \text{C}$ . By previously determining the thermal coefficient of each standard liquid all the observed values of the time of flow were reduced to that at  $25^\circ \text{C}$ . These reduced values of  $t_{25}$  obtained for the various viscometers are given in Tables IV, V, VI, and VII. When the known values of  $\nu_{25}$  and the observed values of  $t_{25}$  were substituted in equation (9), the substitutions gave concordant values for  $A'_0$  and  $C$  on the supposition that  $m = 1.1$ . The values are given below:

All of the constants in equation (9) are now known for the viscometers.

Viscometer	$C$	$A'_0$
	<i>Cm.</i>	
V <sub>1</sub> -----	-0.09	$0.776 \times 10^{-4}$
V <sub>2</sub> -----	-.30	$1.891 \times 10^{-4}$
V <sub>3</sub> -----	-.24	$1.540 \times 10^{-3}$
V <sub>4</sub> -----	-.34	$3.557 \times 10^{-3}$

The following procedure was adopted in order to study the concordance of the observations given in Figures 5 to 7 and the values of the constants. This will place the results of the calibration in final form for use in measuring viscosities. Define

$$\nu_1 = A_1 t \quad (10)$$

where

$$A_1 = A'_0 \left( \frac{1}{N} + \frac{M}{N^2} C \right)$$

The values of  $A_1$  for each filling mark in each viscometer are given in Table III. Equation (10) gives the value of the kinematic viscosity  $\nu_1$  neglecting the term  $\frac{B}{t}$ . Denoting by  $\nu$  the correct value of the kinematic viscosity, the percentage error of the kinematic viscosities when formula (10) is used becomes  $\frac{\nu_1 - \nu}{\nu} \times 10^2$ . These errors for the calibration are given in Tables IV, V, VI, and VII and in Figures 3, 4, and 5. The ratio  $\frac{1}{t\nu}$  is plotted against these errors. This procedure is substantially that proposed by Herschel (Reference 6), since  $\frac{1}{t\nu}$  is proportional to Reynolds Number, which is in our notation  $\frac{2Q}{\pi r \nu t}$ .

TABLE III  
CALIBRATION OF VISCOMETERS V<sub>1</sub>, V<sub>2</sub>, V<sub>3</sub>, AND V<sub>4</sub>—VALUE OF  $A_1$

Viscometer	Filling mark	$A_1$	Viscometer	Filling mark	$A_1$
V <sub>1</sub> -----	$m_5$	$4.141 \times 10^{-4}$	V <sub>3</sub> -----	$m_5$	$7.524 \times 10^{-3}$
	$m_4$	$3.470 \times 10^{-4}$		$m_4$	$6.283 \times 10^{-3}$
	$m_3$	$2.790 \times 10^{-4}$		$m_3$	$5.074 \times 10^{-3}$
	$m_2$	$2.109 \times 10^{-4}$		$m_2$	$3.859 \times 10^{-3}$
	$m_1$	$1.408 \times 10^{-4}$		$m_1$	$2.630 \times 10^{-3}$
V <sub>2</sub> -----	$m_5$	$1.091 \times 10^{-3}$	V <sub>4</sub> -----	$m_5$	$1.623 \times 10^{-2}$
	$m_4$	$.9145 \times 10^{-3}$		$m_4$	$1.358 \times 10^{-2}$
	$m_3$	$.7343 \times 10^{-3}$		$m_3$	$1.090 \times 10^{-2}$
	$m_2$	$.5594 \times 10^{-3}$		$m_2$	$.8170 \times 10^{-2}$
	$m_1$	$.3799 \times 10^{-3}$		$m_1$	$.5357 \times 10^{-2}$

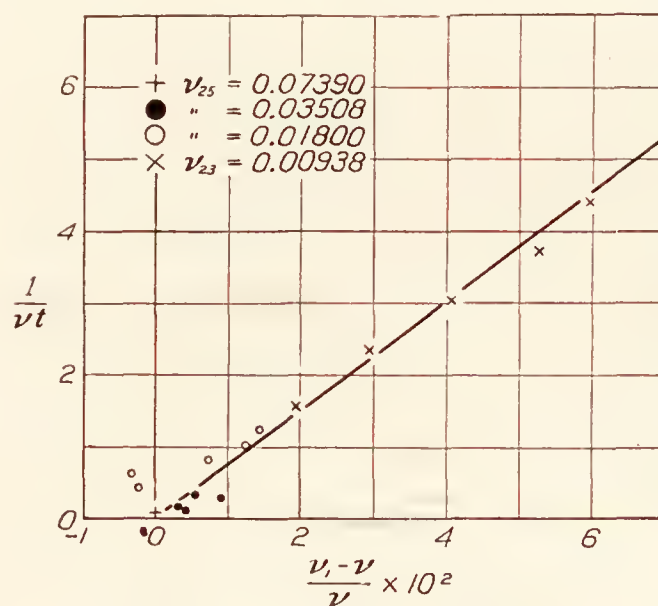


FIG. 3.—Calibration of viscometer No. 1



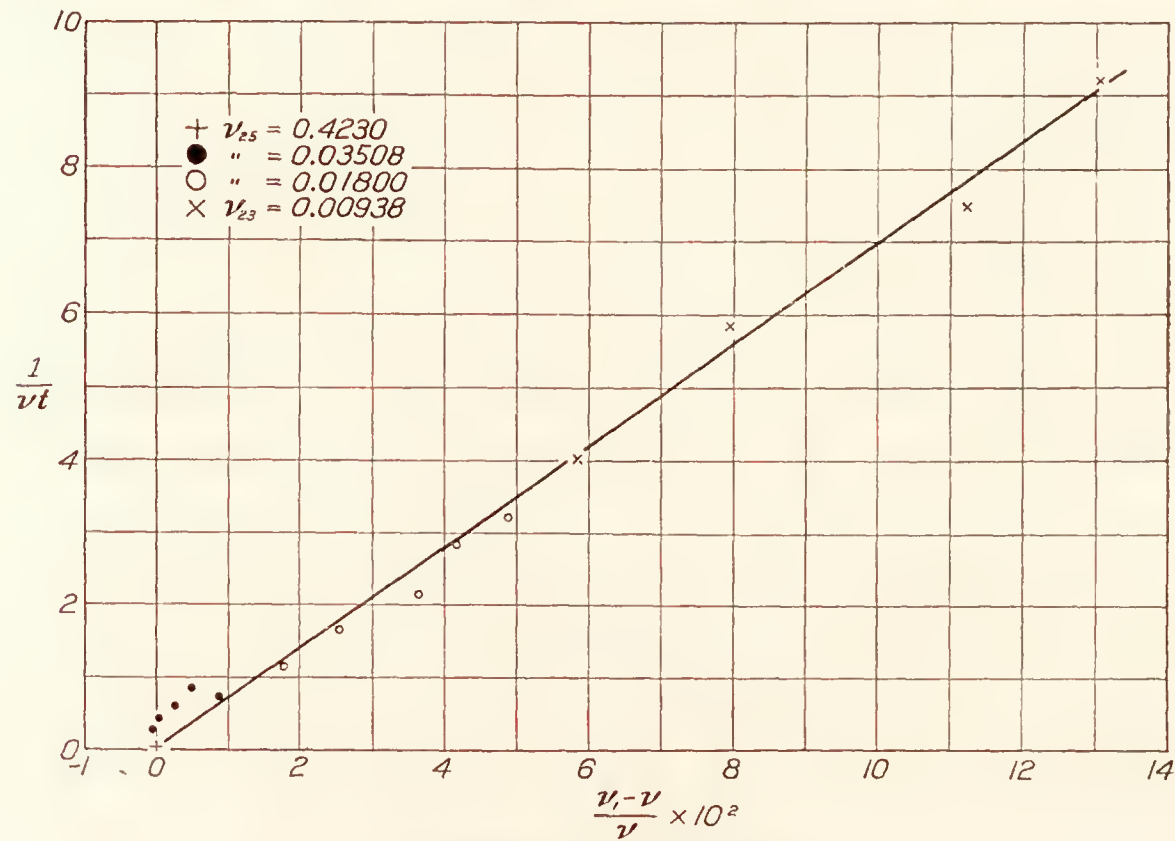


FIG. 4.—Calibration of viscometer No. 2

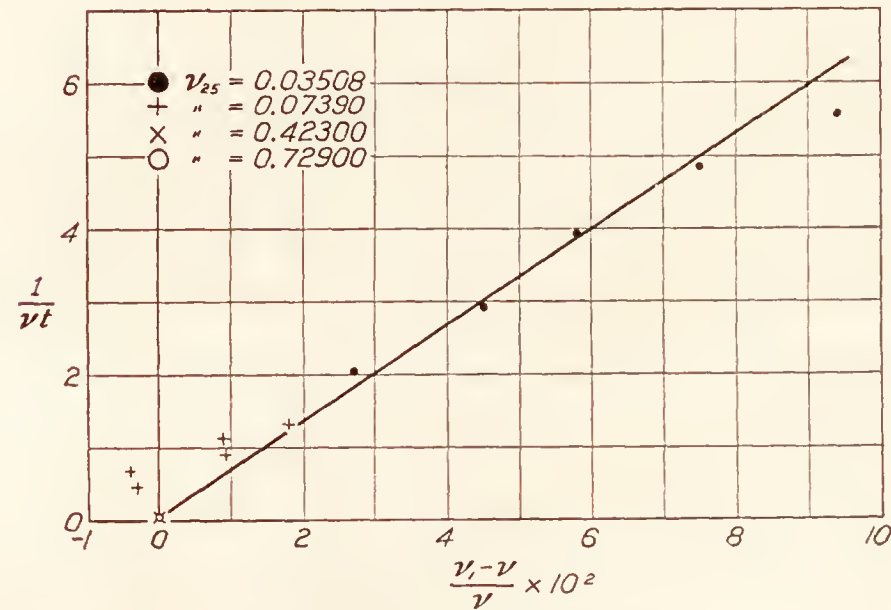


FIG. 5.—Calibration of viscometer No. 3

TABLE IV  
CALIBRATION OF VISCOMETER V₁

Kinematic viscosity of liquid	Filling mark	Time <i>t</i>	Kinematic viscosity <i>ν</i> <sub>1</sub>	Error $\frac{\nu_1 - \nu}{\nu} \times 10^2$	$\frac{1}{t \nu}$
<i>ν</i> <sub>25</sub> = 0. 07390	<i>m</i> <sub>5</sub>	<i>Seconds</i> 178. 8	0. 07404	-----	0. 07
<i>ν</i> <sub>25</sub> = 0. 03508	<i>m</i> <sub>5</sub>	85. 2	. 03528	0. 56	. 33
	<i>m</i> <sub>4</sub>	102. 0	. 03540	. 91	. 28
	<i>m</i> <sub>3</sub>	126. 9	. 03540	. 91	. 22
	<i>m</i> <sub>2</sub>	166. 9	. 03519	. 31	. 17
	<i>m</i> <sub>1</sub>	250. 3	. 03523	. 42	. 11
<i>ν</i> <sub>25</sub> = 0. 01800	<i>m</i> <sub>5</sub>	44. 1	. 01826	1. 44	1. 25
	<i>m</i> <sub>4</sub>	52. 5	. 01822	1. 22	1. 05
	<i>m</i> <sub>3</sub>	65. 0	. 01813	. 72	. 85
	<i>m</i> <sub>2</sub>	85. 1	. 01794	-. 32	. 65
	<i>m</i> <sub>1</sub>	127. 6	. 01796	-. 22	. 43
<i>ν</i> <sub>23</sub> = 0. 00938	<i>m</i> <sub>5</sub>	24. 0	. 00994	5. 96	4. 45
	<i>m</i> <sub>4</sub>	28. 4	. 00986	5. 24	3. 77
	<i>m</i> <sub>3</sub>	35. 0	. 00976	4. 05	3. 07
	<i>m</i> <sub>2</sub>	45. 8	. 00966	2. 98	2. 35
	<i>m</i> <sub>1</sub>	67. 9	. 00956	1. 92	1. 58

TABLE V  
CALIBRATION OF VISCOMETER V<sub>2</sub>

Kinematic viscosity of liquid	Filling mark	Time <i>t</i>	Kinematic viscosity $\nu_1$	Error $\frac{\nu_1 - \nu}{\nu} \times 10^2$	$\frac{1}{t\nu}$
$\nu_{25} = 0.4230$	$m_5$	<i>Seconds</i> 386.6	0.4229	0	0.01
$\nu_{25} = 0.03508$	$m_5$	32.3	.03526	.50	.88
	$m_4$	38.7	.03539	.89	.74
	$m_3$	47.9	.03517	.26	.60
	$m_2$	62.7	.03507	.03	.45
	$m_1$	92.3	.03506	.06	.31
$\nu_{25} = 0.01800$	$m_5$	17.3	.01888	4.89	3.20
	$m_4$	20.5	.01875	4.17	2.72
	$m_3$	25.4	.01865	3.61	2.16
	$m_2$	33.0	.01846	2.55	1.67
	$m_1$	48.2	.01831	1.72	1.16
$\nu_{23} = 0.00938$	$m_5$	9.9	.01080	15.02	10.80
	$m_4$	11.6	.01061	13.02	9.22
	$m_3$	14.2	.01043	11.20	7.50
	$m_2$	18.1	.01012	7.98	5.89
	$m_1$	26.1	.00992	5.81	4.07

TABLE VI  
CALIBRATION OF VISCOMETER V<sub>3</sub>

Kinematic viscosity of liquid	Filling mark	Time <i>t</i>	Kinematic viscosity $\nu_1$	Error $\frac{\nu_1 - \nu}{\nu} \times 10^2$	$\frac{1}{t\nu}$
$\nu_{25} = 0.7290$	$m_5$	<i>Seconds</i> 96.9	0.7290	0.00	0.01
$\nu_{25} = 0.4230$	$m_5$	56.2	.4232	.00	.04
	$m_4$	67.3	.4231	.00	.03
	$m_3$	83.3	.4230	.00	.03
	$m_2$	109.6	.4229	.00	.02
	$m_1$	161.2	.4230	.00	.01
$\nu_{25} = 0.07390$	$m_5$	10.0	.07525	1.83	1.35
	$m_4$	11.9	.07454	.86	1.15
	$m_3$	14.7	.07458	.92	.92
	$m_2$	19.1	.07361	-.39	.71
	$m_1$	28.0	.07370	-.27	.48
$\nu_{25} = 0.03508$	$m_5$	5.1	.03838	9.4	5.53
	$m_4$	6.0	.03771	7.5	4.84
	$m_3$	7.3	.03704	5.8	3.91
	$m_2$	9.5	.03666	4.5	3.00
	$m_1$	13.7	.03604	2.7	2.05



TABLE VII  
CALIBRATION OF VISCOMETER V<sub>4</sub>

Kinematic viscosity of liquid	Filling mark	Time <i>t</i>	Kinematic viscosity $\nu_1$	Error $\frac{\nu_1 - \nu}{\nu} \times 10^2$	$\frac{1}{t \nu}$
$\nu_{25} = 0.729$		<i>Seconds</i>			
	<i>m</i> <sub>5</sub>	44.8	0.727	-0.28	0.030
	<i>m</i> <sub>4</sub>	53.9	.736	+.96	.025
	<i>m</i> <sub>3</sub>	66.3	.720	-1.25	.021
	<i>m</i> <sub>2</sub>	89.1	.728	-.14	.016
	<i>m</i> <sub>1</sub>	135.5	.726	-.42	.009
$\nu_{25} = 0.783$	<i>m</i> <sub>5</sub>	48.0	.780	-.38	.027
	<i>m</i> <sub>4</sub>	57.4	.779	-.51	.022
	<i>m</i> <sub>3</sub>	71.6	.781	-.26	.018
	<i>m</i> <sub>2</sub>	95.2	.778	-.64	.013
	<i>m</i> <sub>1</sub>	145.5	.780	-.38	.009
$\nu_{25} = 0.423$	<i>m</i> <sub>5</sub>	26.2	.425	+.47	.0902
	<i>m</i> <sub>4</sub>	31.3	.425	+.47	.076
	<i>m</i> <sub>3</sub>	39.1	.426	+.71	.062
	<i>m</i> <sub>2</sub>	52.0	.425	+.47	.045
	<i>m</i> <sub>1</sub>	79.3	.425	+.47	.028

The graphs which are straight lines were made to pass through the origin. This procedure of permitting the straight lines to pass through the origin is quantitatively contrary to Bond's criterion. The criterion was ignored purposely in this respect, as the errors of the calibration were sufficiently large to eclipse its importance. For from equation (7) Bond's criterion  $B_c$  for the viscometers V<sub>1</sub>, V<sub>2</sub>, V<sub>3</sub>, and V<sub>4</sub> becomes  $\frac{1}{t \nu} = B_c = 0.13, 0.17, 0.26$ , and  $0.33$ , respectively. As all the observations made with V<sub>4</sub> were below the value of Bond's criterion, the data of Table VII are not plotted.

Now it remains to be seen if the assumed value of  $m = 1.1$  during the determinations of  $A'_0$  and  $C$  is in accordance with the graphs in Figures 2, 3, and 4. As

$$\nu_1 = A_1 t$$

and 
$$\nu = A_1 t - \frac{B}{t}$$

then 
$$\nu_1 - \nu = \frac{B}{t}$$

or 
$$\frac{\nu_1 - \nu}{\nu} = \frac{B}{t \nu} \tag{10A}$$

This gives 
$$B \times 10^2 = \frac{1}{\tan \alpha}$$

where  $\tan \alpha$  is the slope of the straight lines in Figures 3, 4, and 5. (See References 6, 7, and 8.) Finally, if  $l_e$  is supposed not to differ much from  $l_2$ , expression (6) gives

$$m = \frac{8\pi l_2}{Q} \times \frac{10^{-2}}{\tan \alpha} \tag{11}$$

Calculations from the data of the calibration graphs gave  $m = 1.00, 1.18$ , and  $1.11$  for viscometers V<sub>1</sub>, V<sub>2</sub>, and V<sub>3</sub>, respectively. This shows that the values of  $B$  when determined from the calibration graph would have an accuracy of 10 per cent. On the other hand, the values of  $A_1$  which are given in Table III have an accuracy of 0.5 per cent at least as judged from the individual observations of the calibration.

## MEASUREMENT OF KINEMATIC VISCOSITY

The procedure in evaluating  $\nu$  for some particular liquid consisted in determining  $\nu_1$  by means of equation (10) after the time of discharge  $t$  was observed. The values of  $\nu_1$  against temperature are given in graphs, as described later. In order to determine the values of  $\nu$  given in this report, the quantity  $\frac{1}{t\nu_1}$  was computed and the error  $e$  read from the calibration graph for the viscometer used. (Fig. 3 to 5.) The value of  $\nu$  then becomes

$$\nu = \nu_1 (1 - e) \quad (12)$$

## DENSITY AND THERMAL COEFFICIENT OF CUBICAL EXPANSION

When  $t_\theta$  is known for a given liquid, formula (10) gives the kinematic viscosity  $\nu_\theta$  for the temperature  $\theta$ . To obtain the absolute viscosity  $\mu_\theta$  from the known value of  $\nu_\theta$  the density  $\rho_\theta$  at the temperature  $\theta$  must be known. To obtain the density  $\rho_\theta$  in the temperature range  $+30^\circ \text{C.}$  to  $-20^\circ \text{C.}$  with an accuracy adequate for the purpose of the present paper, it suffices to measure  $\rho_{30}$  and the average thermal coefficient of cubical expansion  $\alpha$  for the range  $+30^\circ \text{C.}$  to  $0^\circ \text{C.}$  The definition of  $\alpha$  is

$$\alpha = \frac{V_{30} - V_0}{30 \times V_{30}} \quad (13)$$

where  $V_0$  represents the volume of a given mass of liquid at the temperature  $0^\circ \text{C.}$  Then the density  $\rho_\theta$  is given by

$$\rho_\theta = \rho_{30} [1 + \alpha (30 - \theta)] \quad (14)$$

The determinations of the density  $\rho_{30}$  and the coefficient of expansion were carried out in the well-known orthodox manner; no other comment need be made except the statement that  $\rho_{30}$  is determined with an accuracy of 0.2 per cent and  $\alpha$  with an accuracy of 3 per cent. The results are given in Table VIII, in which  $\alpha$  is the coefficient for temperatures in degrees centigrade.

The values of the change in density per degree centigrade for petroleum oils against specific gravity based on the National Standard Petroleum Oil Tables (Reference 10) are given in convenient form in Reference 9. The data in Table VIII are in agreement within the experimental error.

## TEMPERATURE CONTROL

The four viscometers  $V_1$ ,  $V_2$ ,  $V_3$ , and  $V_4$  arranged in a plane were held parallel to each other by means of two pairs of wooden clamps. To insure fixity of position, a single arm of each clamp was rigidly attached to the two vertical sides of a rectangular brass frame. A heavy rectangular plate was attached to the upper edge of the frame so as to be perpendicular to the vertical plane containing the axis of the viscometers. This plate will be spoken of as the holding plate. When the holding plate is kept horizontal, the axis of the capillaries are in a vertical position. The description so far given relates to the viscometer assembly. Next consider the bath of the viscometers. It consisted of a rectangular glass vessel of over-all dimensions 13 by 22 by 31 centimeters, placed in a wooden frame. The frame embraced the bottom and the two narrow sides of the glass vessel. It also provided a smooth rectangular brim to the glass vessel. The liquid of the bath was a mixture of water and alcohol.

When the viscometer assembly was immersed in the bath, the holding plate rested evenly on the wooden brim of the vessel. Thus if the brim was horizontal, the axis of capillaries would be vertically submerged in the bath. Eight holes in the holding plate allowed the ends of the viscometers to protrude. Two thermometers were employed to measure the temperature of the bath in the lower and upper portion of the vessel. An agitator in the form of a small propeller was placed in the bath for the equalization of temperature.

The viscometer assembly and the bath together constituted the viscometer box of the tests.

In order to control the temperature of the viscometer bath, the viscometer box was placed in a temperature chamber in which the reduction of temperature was effected by the use of an ammonia refrigeration system. An electric heater was the source of heat in the chamber.



Because of the large mass of liquid in the bath, it generally took seven hours to reduce the temperature of the bath from an initial value of  $0^{\circ}\text{C.}$  to  $-18^{\circ}\text{C.}$ , when the temperature of the chamber was held continually at its lowest temperature, that is,  $-23^{\circ}\text{C.}$  This property of the apparatus is the factor limiting the lowest values of the temperature realized during the tests.

#### ERRORS OF THE MEASUREMENTS

Three main sources of experimental error exist; calibration, observation of time of flow, and determination of temperature. As remarked previously, errors of calibration did not appear to be greater than 0.5 per cent. The errors of measurement of time need be considered only in connection with the observation of small values of the time,  $t_{\theta}$ . In the tests the smallest values of  $t_{\theta}$  were in the neighborhood of 10 seconds. To reduce the error, measurements of time for a given temperature were made three times or more and the average noted. Quite generally in runs in which  $t_{30}$  was approximately 10 seconds individual observations of  $t_{\theta}$  did not differ more than 0.1 second from the average. It follows that viscosity determinations for the lowest value of  $t_{30}$  are open to an error of not more than 1 per cent. Temperature errors may arise in two ways: First, that during a flow measurement the temperature of the bath had a temperature gradient along the capillaries; secondly, that the average temperature of the bath was not the same in the beginning of the flow as at the end. However, the temperature error was minimized by taking the averages of the average temperature of the bath at the beginning and at the end of the flow period. For most of the observations the temperature errors were not more than  $\pm 0.5^{\circ}\text{C.}$

#### RESULTS OF INVESTIGATION

##### SAMPLES

The solutions and liquids may be classified as follows:

- (1) Solutions of animal and vegetable oils in xylene. These were poppy-seed oil, two samples of neat's-foot oil, castor oil, and linseed oil.
- (2) Solutions of mineral oil in xylene. These were Squibbs' petrolatum of naphthene base and transformer oil.
- (3) Glycerin solutions in ethyl alcohol and in mixture of 50-50 ethyl alcohol and water.
- (4) Mixtures of normal butyl alcohol with methyl alcohol.
- (5) Individual liquids; kerosene, mineral spirits, xylene, recoil oil.

The following information is available regarding the source, purity, and physical properties of the liquids:

##### XYLENE

The following data were obtained from the label of the container: Chemical composition,  $\text{C}_6\text{H}_4(\text{CH}_3)_2$ ; molecular weight, 106.12; specific gravity, 0.86; boiling point,  $138^{\circ}\text{--}139^{\circ}\text{C.}$  It was found that the freezing point of the sample was below  $-35^{\circ}\text{C.}$  Thorpe and Rodger's values of the viscosity for meta xylol were obtained from the Smithsonian Physical Tables (1920).

Temperature ( $^{\circ}\text{C.}$ )	Viscosity (poise)
0	0.00806
10	.00702
20	.00620
30	.00552

These values are about 2 per cent greater than the values found for the sample.

Xylene has been extensively used as the liquid for bubble levels for use on aircraft sextants and other instruments. Owing to its relatively low viscosity, low rate of change with temperature, and to the fact that the temperature at the melting point is below ordinary conditions of aircraft use, xylene is well adapted for use as a solvent. In this way solutions may be obtained which meet a variety of viscosity requirements.

## POPPY-SEED OIL

A sample was purchased without specifications from a wholesale dealer. This had a density at 15° C. of 0.92 gram per cm.<sup>3</sup> compared with a value of 0.924 to 0.926 given in the International Critical Tables (Vol. II, 1927). The sample was found to have a cloud point of +7° C. and to freeze at -16° C.; the tables give -16° to -18° C. as the freezing point. The coefficient of viscosity of the sample was found to be 0.797 poise at 15.5° C. as compared with the value 0.789 poise given in the International Critical Tables.

The index of refraction of the sample was determined at two temperatures by the optical-instrument section of the Bureau of Standards. The values are given below, including also data on solutions of poppy-seed oil in xylene.

Poppy-seed oil (per cent, by weight)	Xylene (per cent, by weight)	Index of refraction, $n_D$		Temperature coefficient of index per degree C.
		10.0° C.	30.0° C.	
100	0	1.4806	1.4731	-0.00038
75	25	1.4862	1.4779	-.00042
50	50	1.4914	1.4825	-.00045
25	75	1.4964	1.4867	-.00049

Poppy-seed oil and xylene solutions have found some use in dashpots of special aircraft instruments. As poppy-seed oil is a semidrying oil it requires frequent replacement.

## NEAT'S-FOOT OIL

Two samples of neat's-foot oil were furnished through the courtesy of the research department of Armour & Co. The samples are a "wintered" product and are known respectively as 20° and 30° F. (-6.7° C. and -1.1° C.) cold or flow test neat's-foot oil. The 20° F sample became cloudy at -14° C. and froze at about -16.5° C. The 30° F. sample became cloudy at -5° C. and froze at a temperature of -8° C.

The International Critical Tables (Vol. II, 1927) give 0.987 to 1.13 poises for the value of the viscosity at 15.5° C., compared with 1.15 poises for the 30° F. sample and slightly less for the 20° F. sample.

Neat's-foot oil is nonoxidizing in character, which is a desirable property in the selection of a liquid for use in an open dashpot.

## CASTOR OIL

The sample has not been analyzed for purity. The International Critical Tables (Vol. II, 1927) state that castor oil becomes turbid at -12° C. and solid at -17° C. to -18° C. The sample commenced freezing at -15° C. and was solid at -17° C. The density and viscosity are as follows according to the above reference:

Temperature (° C.)	Density (grams/cm. <sup>3</sup> )	Viscosity (poises)
5	0.9707	37.60
10	.9672	24.18
20	.9603	9.86
25	.9569	6.51
30	.9534	4.51

A comparison of the above viscosity data with that for the sample (given later) shows good agreement as regards the change in viscosity with temperature, but the viscosity of the sample is substantially 8 per cent greater.

## LINSEED OIL

The sample was raw linseed oil, purchased under United States Government Master Specification for Raw Linseed Oil. This specification is published as Bureau of Standards Circular No. 82 (third edition, issued April 26, 1927). The density of the sample is 0.932 gram per



cm.<sup>3</sup> at 15.5° C., which is within the specific-gravity tolerance of 0.9300 to 0.935 (15:5°/15:5° C.), which is equivalent to the density interval 0.929 to 0.934 gram per cm.<sup>3</sup> The cloud point of the sample is approximately -7° C., freezing in the interval -14° to -17° C. The International Critical Tables (Vol. II, 1927) give the freezing point as -19° to -27° C. and the viscosity at 15.5° C. as 0.55 poises, while the value found for the sample is 0.585 poises.

#### SQUIBBS' MINERAL OIL (LIQUID PETROLATUM)

This oil is a commercial product sold for medical use. The label on the bottle states that the oil is refined from California crude petroleum (naphthene base) and that it is free from paraffin, inorganic matter, and organic sulphur compounds. The sample froze at a temperature of -21° to -22° C.

#### TRANSFORMER OIL

This oil is a sample of transformer oil which, contrary to expectations, froze in the temperature range -32° to -33° C.

#### GLYCERINE

If the density of the sample is taken as the criterion, then the glycerine of our tests contained 4 per cent water, for, according to the International Critical Tables (Vol. III) the density of 96 per cent aqueous solution of glycerol at 25° C. is 1.2477, and for the same temperature the density of the sample was found to be 1.2480 grams per cm.<sup>3</sup> Shöttner's values of the viscosity of glycerol are given in the Physico-Chemical Tables (Vol. II). According to these tables the viscosity of glycerol at 26.5° C. is 4.939 poises. Our determination of the same quantity gives 3.909 poises. The considerable difference between these two values is due to the water content in our sample.

#### ETHYL ALCOHOL

The sample initially contained less than 2 per cent of water. It should be noted that measurements on a given sample of liquid extended over a period of three days. In the case of hygroscopic liquids and solutions such as alcohol and glycerine some change in water content may have occurred.

#### N. BUTYL ALCOHOL

The sample was purchased from the Eastman Kodak Laboratories. Two grades of the substance are available; one is known as technical and has a boiling point of 114° to 118° C.; the other is a purer product and has a boiling point of 116° to 118° C. The latter product was used in the tests.

The International Critical Tables (Vol. I, 1926) give the melting point as -89.8° C. and the density as 0.810 gram per cm.<sup>3</sup> at 20° C. The values of the viscosity found by Thorpe and Rodger (1894) as given in Landolt-Börnstein Tables (Vol. I, 1923) agree within 1 per cent with the values found for the sample. Thorpe and Rodger's values are:

Temperature (° C.)	Viscosity (poise)
0.27	0.0515
10.69	.0380
21.83	.0280

#### METHYL ALCOHOL

The sample (CH<sub>3</sub>OH) was of reagent quality. The manufacturer's label gave the following analysis:

	Per cent		Per cent
Acetone.....	0	Empyreuma.....	0.001
Aldehyde.....	0	Reaction to litmus.....	Neutral.
Chloroform.....	.01	Reducing matter.....	0

The International Critical Tables (Vol. I, 1926) give the melting point of methyl alcohol as -97.8° C. This alcohol when mixed with butyl alcohol has been proposed for use in rolling ball inclinometers.

## KEROSENE

The sample of kerosene had a density of 0.810 gram per cm.<sup>3</sup> at 30° C. and a freezing point of -15° C.

## MINERAL SPIRITS

This is a petroleum product also known as Varnolene, which is used as a paint thinner. It is generally used as the damping liquid in aircraft compasses. The sample is commercial, most likely a naphthene (asphalt) base. Its density is 0.769 gram per cm.<sup>3</sup> at 30° C. A specification of mineral spirits based on its use as a paint thinner is given in Bureau of Standards Circular No. 98.

The sample was found to remain clear when at a temperature of -35° C.

## RECOIL OIL

This sample conforms to the specification for recoil oil, light grade, given in United States Master Specification for Lubricants and Liquid Fuels, Bureau of Mines Technical Paper 323-B. It was found to remain unfrozen at a temperature of -30° C.

## 2. EXPERIMENTAL RESULTS

Figures 6 to 17, inclusive, show the effect of temperature on the kinematic viscosity of the various solutions and liquids. The concentrations of the solutions are noted in the figures and refer to weight.

The ordinates  $n_\theta$  are the quantities defined by

$$n_\theta = \log_{10} \frac{t_\theta}{t_{30}} \quad (15)$$

where  $t_\theta$  is the observed time of discharge at temperature  $\theta$ . Here  $t_{30}$  was not observed generally but was evaluated from the observed  $t_\theta$  in the temperature range 30° C. to 15° C. Thus the value of  $t_{30}$  is more probable than that of a single observation made at 30° C.

Now, denote by  $n'_\theta$  the quantity

$$n'_\theta = \log_{10} \frac{\nu_\theta}{\nu_{30}} \quad (16)$$

where  $\nu_\theta$  is the kinematic viscosity at the temperature  $\theta$ . The quantity  $n'$  will have the same value as  $n_\theta$  if the inertia term is negligible in the flows of time  $t_\theta$  and  $t_{30}$ . Strictly speaking, this was not the case, particularly for the measurements of  $t_{30}$  made with the viscometer  $V_1$ . For many purposes the differences  $n'_\theta - n_\theta$  being small can be neglected; with this restriction, then, the curves in Figures 6 to 17, inclusive, are representative of the temperature effect on kinematic viscosity.

The magnitudes of the differences  $n'_\theta - n_\theta$  are always less than the value for  $e$  given in the graphs, as is evident from equation (18) below, and therefore the values of  $n_\theta$  are, on the whole, except for the data on Figures 15 and 16, within 1 per cent of  $n'_\theta$ . The data for the 50-50 butyl-methyl alcohol in Figure 15 shows an extreme error  $e$  of 9.5 per cent. If the values of  $n_\theta$  given in the graph are used to compute  $\nu$ , the result is in error 0.5 per cent at + 10° C. and 6.5 per cent at -15° C.

Assuming that the difference of  $n'_\theta - n_\theta$  is negligible, the viscosity  $\nu_\theta$  can be computed from the relation

$$n_\theta = \log \frac{\nu_\theta}{\nu_{30}}$$

in which  $n_\theta$  is read from the proper graph (figs. 6 to 17), and  $\nu_{30}$  is obtained from the tables given in the same figures.

The absolute viscosity  $\mu_\theta$  is given by the relation

$$\mu_\theta = \rho_\theta \nu_\theta$$



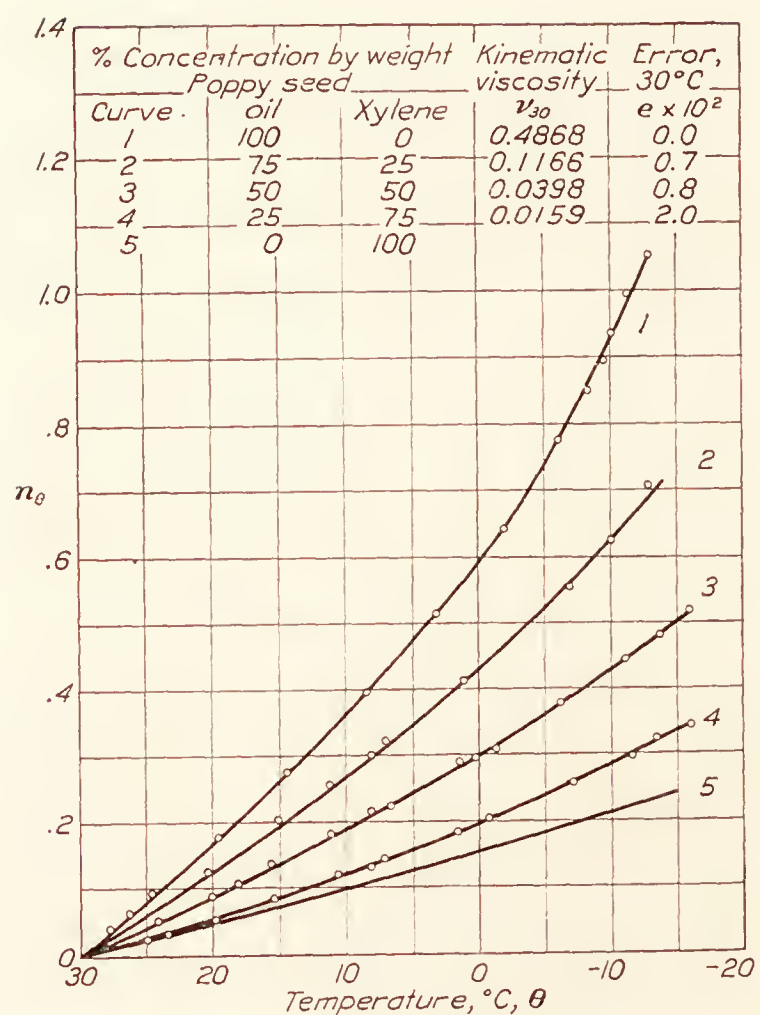


FIG. 6.—Change of kinematic viscosity with temperature. Poppy-seed oil and xylene

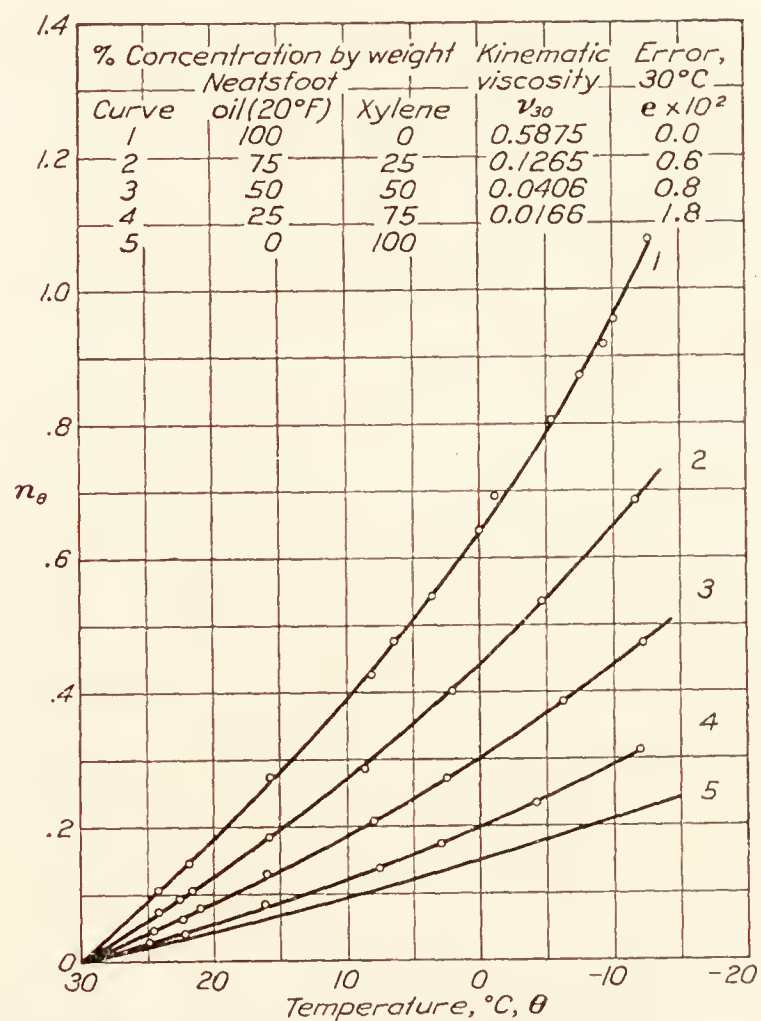


FIG. 7.—Change of kinematic viscosity with temperature. Neat's-foot oil and xylene

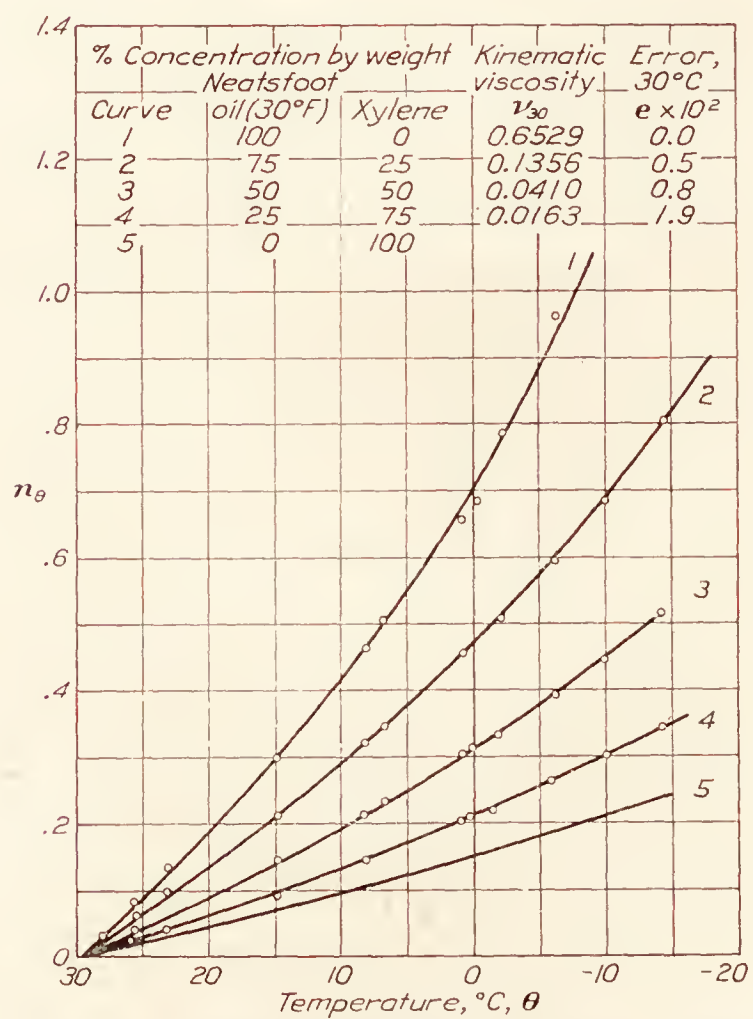


FIG. 8.—Change of kinematic viscosity with temperature. Neat's-foot oil (30° F.) and xylene

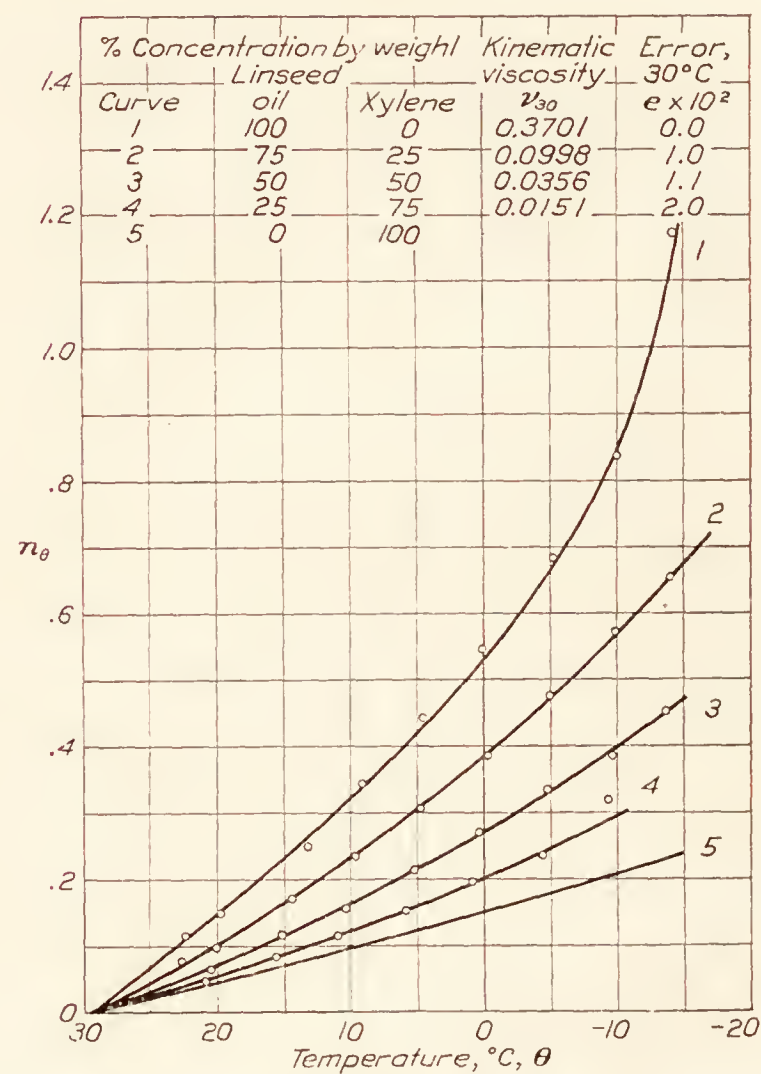


FIG. 9.—Change of kinematic viscosity with temperature. Linseed oil and xylene

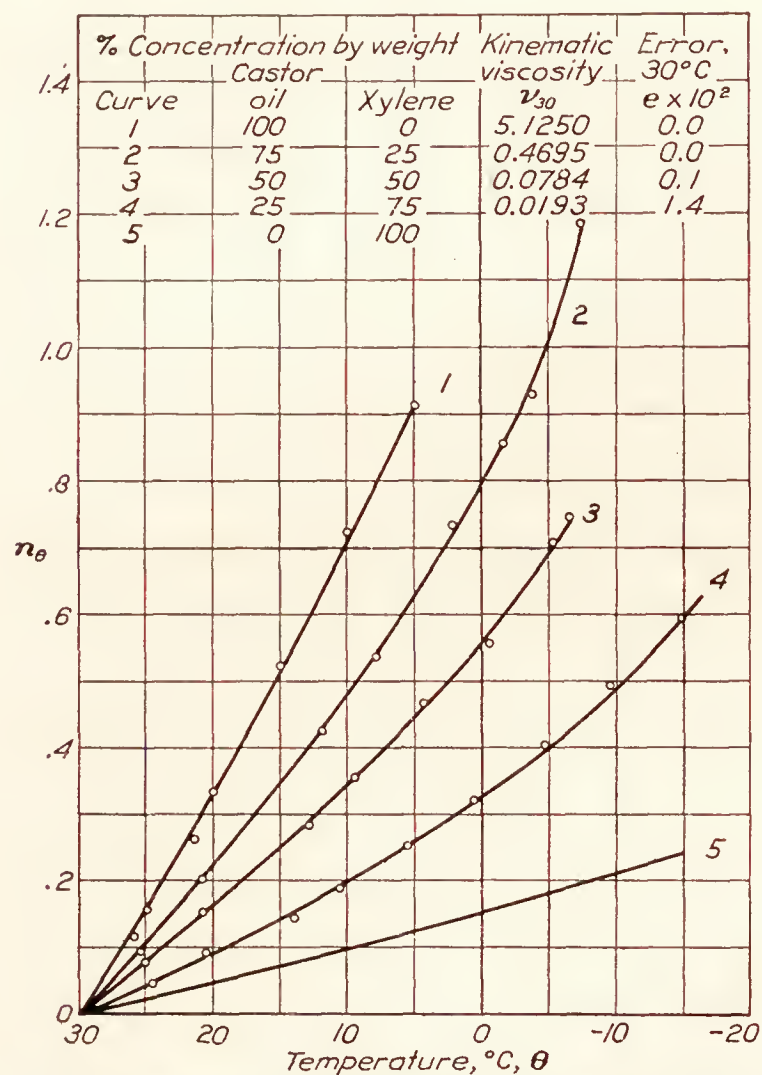


FIG. 10.—Change of kinematic viscosity with temperature. Castor oil and xylene

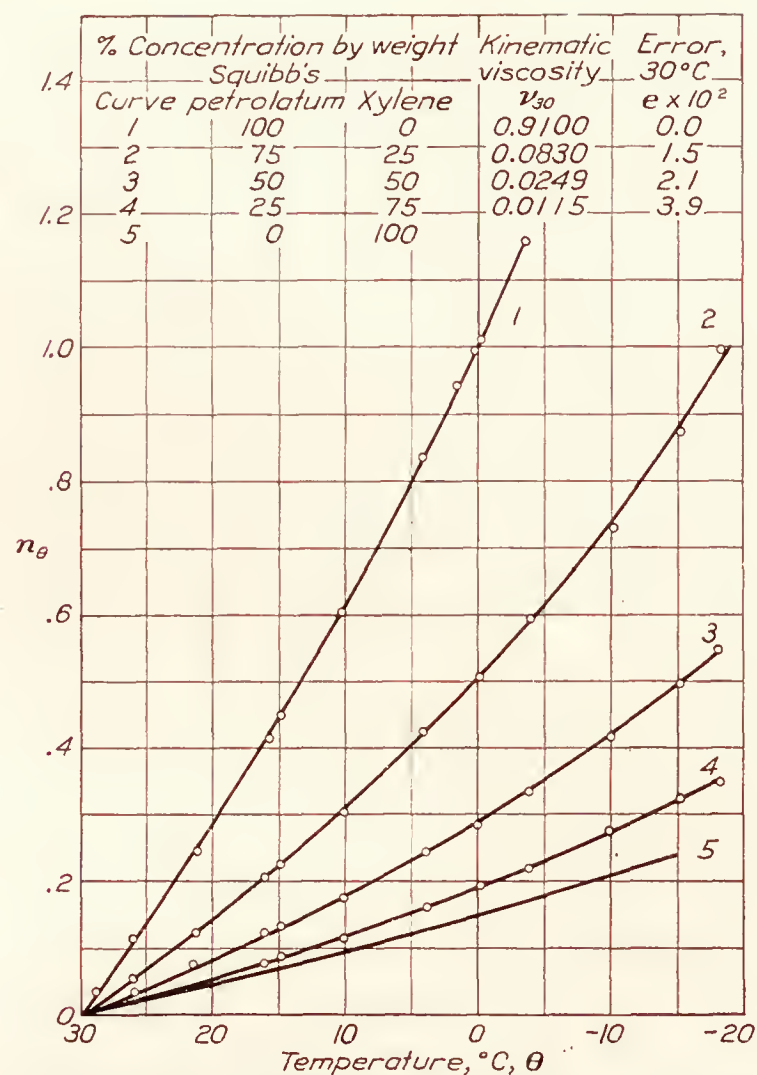


FIG. 11.—Change of kinematic viscosity with temperature. Squibb's petroleum and xylene

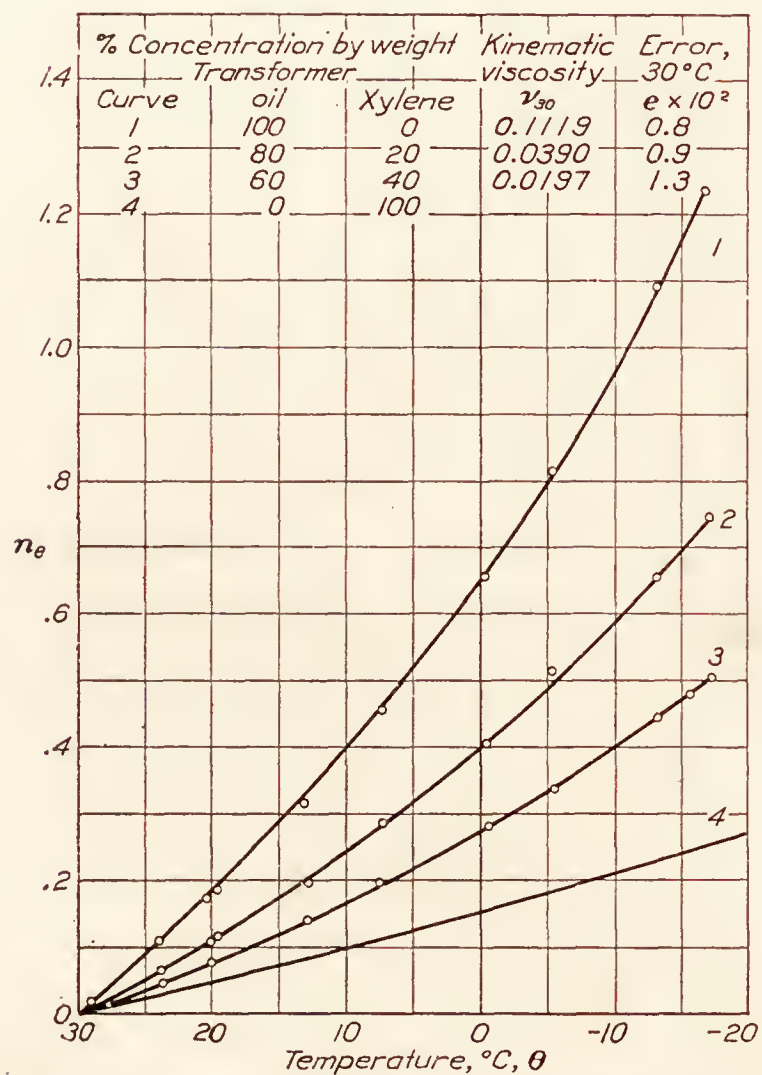


FIG. 12.—Change of kinematic viscosity with temperature. Transformer oil and xylene

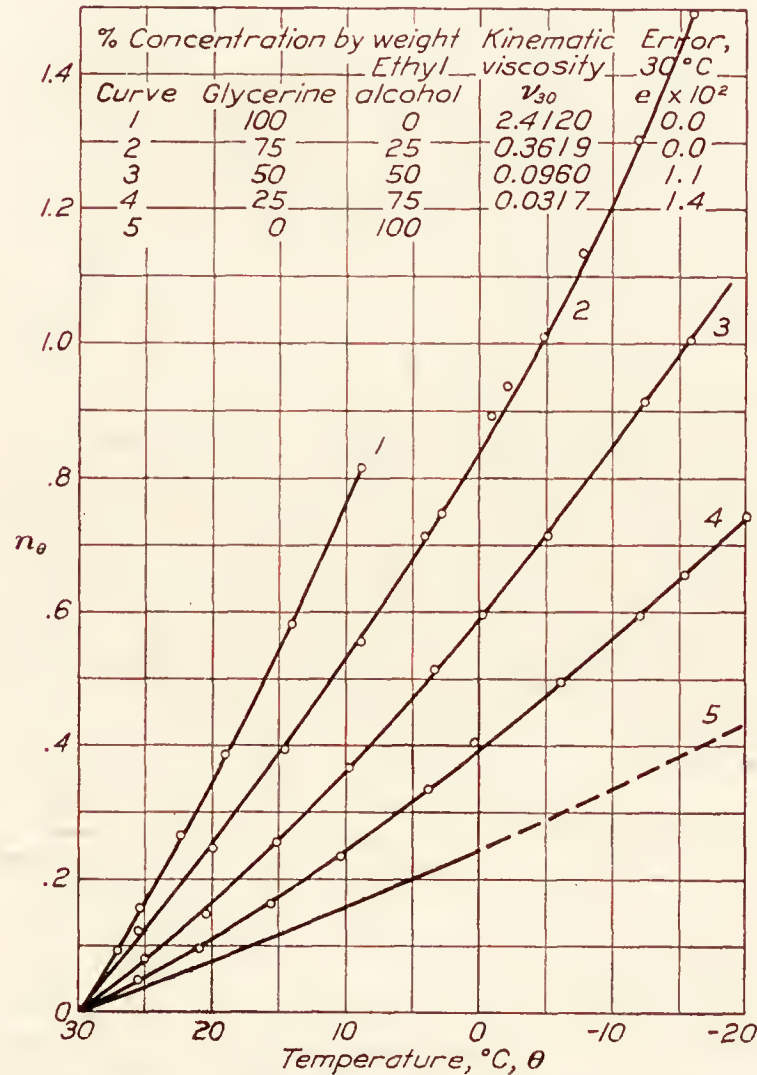


FIG. 13.—Change of kinematic viscosity with temperature. Glycerine and ethyl alcohol



For the purpose of determining the density at  $\theta^\circ \text{C.}$ , the values of  $\rho_{30}$  and the coefficient of volume expansion  $\alpha$  are given in Table VIII. Equation (14) then serves to calculate the value of  $\rho_\theta$ .

In cases such that the difference  $n'_\theta - n_\theta$  can not be ignored, the same procedure given above is followed except that  $n'_\theta$  must be computed and used instead of  $n_\theta$ .

Let  $e_\theta$  as given in equation (10A) represent the proportional error in  $\nu_\theta$ , when  $\nu_\theta$  is evaluated by formula (12). Putting  $e_{30} = e$ , it can be shown that

$$n'_\theta - n_\theta = \log_{10} (1 + e - e_\theta) \quad (17)$$

where  $e_\theta$  satisfies to the first order the relation derived from equation (10A) and the definition of  $n_\theta$

$$\log_{10} e_\theta = \log_{10} e - 2n_\theta \quad (18)$$

Thus to evaluate  $n'_\theta$  one needs to consider only the quantities  $e$  and  $n_\theta$ . The values of  $e$  are given for each liquid in tabular form in Figures 6 to 17, inclusive.

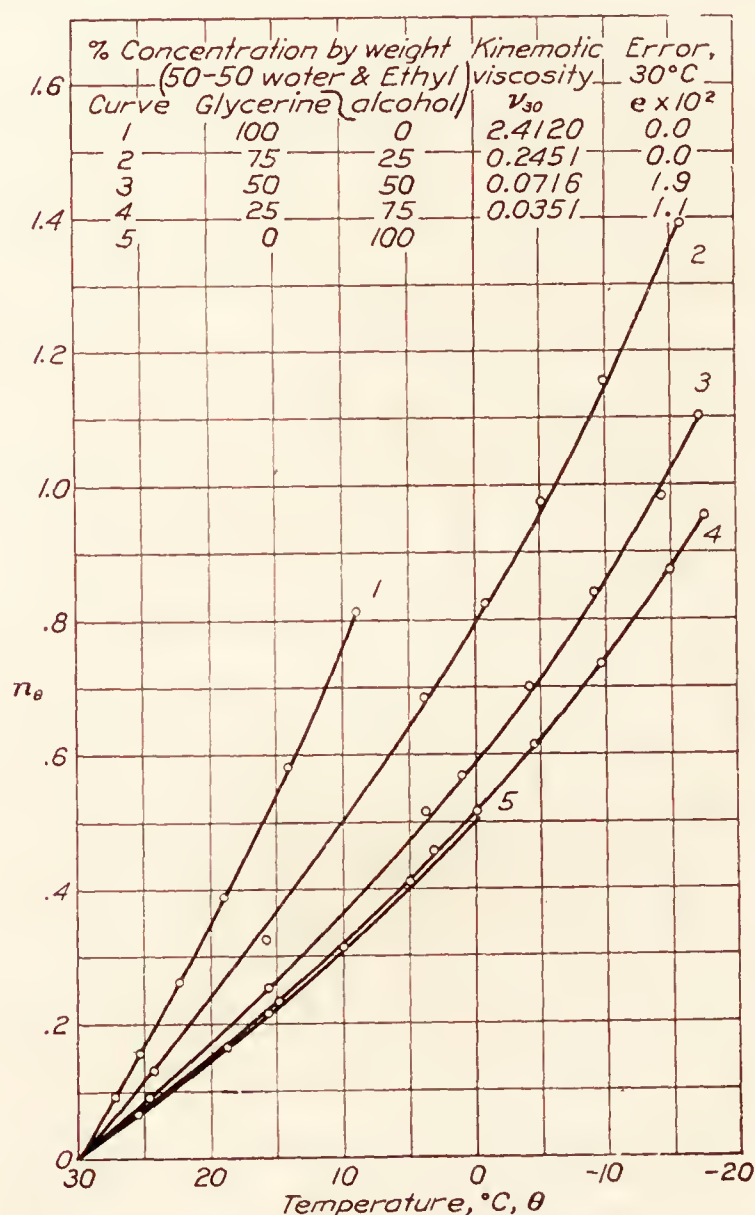


FIG. 14.—Change of kinematic viscosity with temperature. Glycerine and 50-50 water and ethyl alcohol

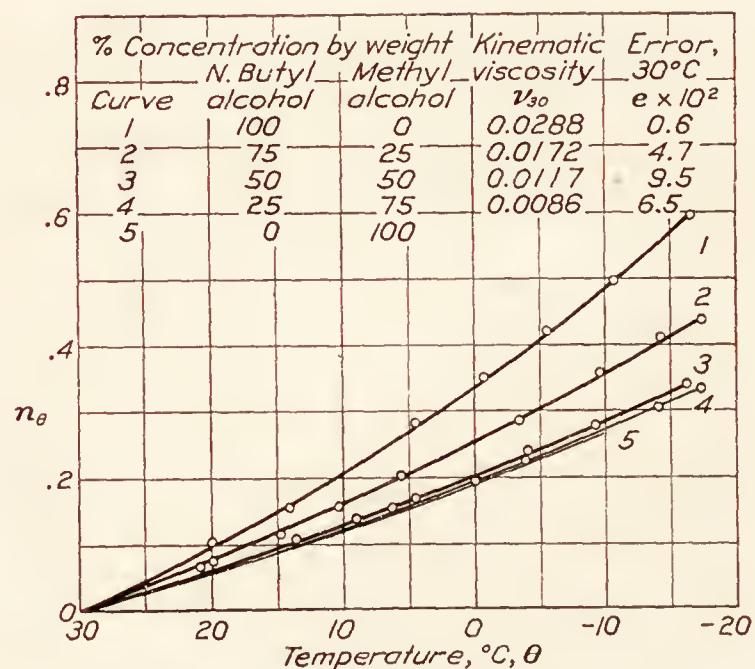


FIG. 15.—Change of kinematic viscosity with temperature. N. butyl alcohol and methyl alcohol

As an illustration, suppose that  $n'_\theta$ ,  $\nu_\theta$ , and  $\mu_\theta$  are required for xylene at  $\theta = -15^\circ \text{C.}$  From the graph for xylene, No. 3, Figure 16, it is seen that  $e = 0.038$  and  $n_\theta = 0.24$ ; then by formula (18)  $e_\theta = 0.013$ , by formula (17)  $n'_\theta - n_\theta = 0.01$ , and  $n'_\theta = 0.25$ . The kinematic viscosity  $\nu_{-15}$  is given by

$$\nu_{-15} = \nu_{30} \text{ antilog } n'_\theta$$

From the table in Figure 16,  $\nu_{30}$  equals 0.0066 and  $\nu_{-15} = 0.0117$ . From Table VIII  $\rho_{30} = 0.855$  and  $\alpha = 0.00095$ . Then  $\rho_{-15} = 0.892$  and  $\mu_{-15} = 0.0104$  poise.

Two tables are presented which summarize the experimental work. Table VIII gives data on the viscometers used coupled with the time of flow at 30° and 25° C. for each individual solution. The data required for determining the density  $\rho_\theta$ , namely,  $\rho_{30}$  and  $\alpha$ , are included in this table.

Table IX gives the viscosity  $\mu$  at 25° C. and the values of the ratio  $n$  at +20° and -15° C. for each solution. This affords a convenient rough comparison of the values of the viscosity  $\mu$  of the liquids at one temperature and of the change of their kinematic viscosity ratio  $n$  in the temperature interval -15° to +20° C. The solution corresponding to any desired value of  $\mu$  may be found by interpolation and then  $n$  at -15° and +20° C. also found by interpolation thus enabling the proper liquid to be selected. The selection should be made bearing in mind the other properties such as given in the description of the samples.

Comparative data on the various solutions is given in Table X. These data are derived by interpolation from Table IX and Figures 6 to 17, inclusive, and give the composition of the solutions against the viscosity at +25° C., varying by convenient steps. The logarithms of the kinematic viscosity ratio are given for five temperatures, neglecting the error  $e$ , and also the

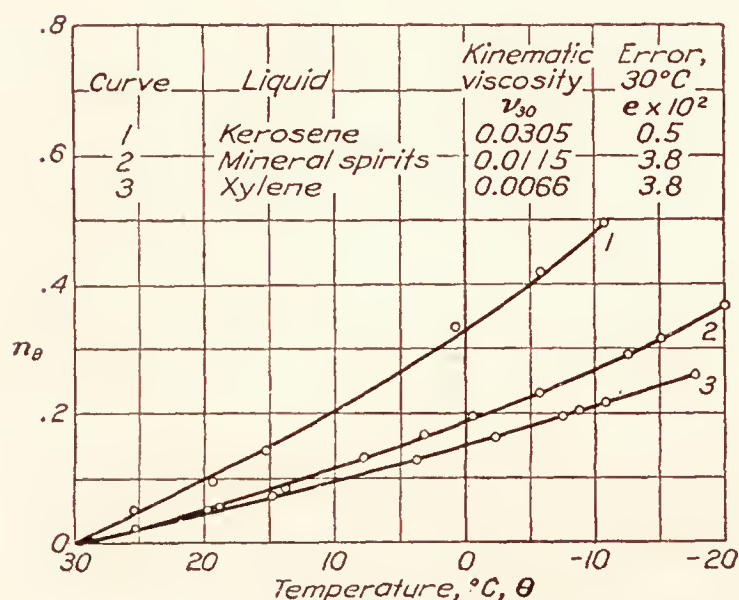


FIG. 16.—Change of kinematic viscosity with temperature. Kerosene, mineral spirits, xylene

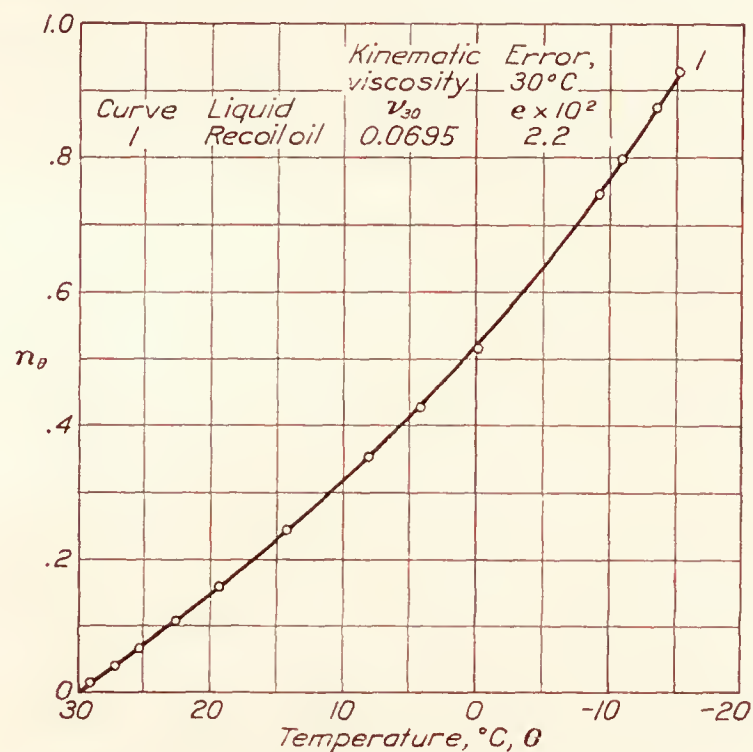


FIG. 17.—Change of kinematic viscosity with temperature. Recoil oil

temperature at which the logarithms of the kinematic viscosity ratio  $n$  equals 0.7. At this temperature the viscosity is very closely five times the value at 30° C., which for many purposes sets the lowest temperature at which the liquid can be used.

### SUMMARY

Table X summarizes the data in convenient form. The solutions and liquids of a given viscosity are compared directly as to lowest temperature at which it is useful and the effect of temperature on the kinematic viscosity.

Inclinometers of the rolling-ball type contain for damping a solution of 40 per cent glycerine and 60 per cent absolute (ethyl) alcohol. This solution is seen to have a viscosity between 0.05 and 0.10 (0.065) poise and to become five times as viscous at about -10° C. as at 30° C. A 50-50 solution of N. butyl and methyl alcohol has been proposed for use in order to secure satisfactory operation at lower temperatures. The data in Table X shows that at -20° C. the solution is less than two and one-half times as viscous as at 30° C., but that the viscosity at +25° C. is only one-sixth that of the glycerine-alcohol solution.

Mineral spirits are used to fill magnetic compasses. Only xylene appears to have better temperature properties.

The uses considered above relate to cases in which the liquid is entirely inclosed. When a liquid is desired for use in an open dashpot, other properties, such as evaporation and oxidation, become as important as the effect of temperature. No oily liquid has been found which is by itself satisfactory at low temperatures. It is seen in Table X that all liquids at 25° C. with a



viscosity greater than 0.05 have an excessive temperature effect, the viscosity at  $-20^{\circ}\text{C}$ . exceeding more than fivefold that at  $30^{\circ}\text{C}$ . Of the liquids investigated the "wintered" neat's-foot-oil solutions appear to be the best. Their temperature properties are substantially as good as those of other solutions of the same viscosity but these solutions have the advantage of being relatively nonoxidizing. The use of xylene as a solvent introduces the factor of evaporation, but possible solvents with the necessary properties of low viscosity and small change with temperature appear to have an appreciable vapor pressure.

TABLE VIII

DATA FOR EVALUATING  $\mu_{25}$  THE VISCOSITY AT  $25^{\circ}\text{C}$ ., THE KINEMATIC VISCOSITY AT  $30^{\circ}\text{C}$ ., AND  $\rho_0$  THE DENSITY AT  $0^{\circ}\text{C}$ .

Proportions, by weight		Viscometer		Time of flow		Density	Thermal coefficient of cubical expansion $\alpha \times 10^3$
		No.	Mark	$t_{30}$ (sec.)	$t_{25}$ (sec.)	$\rho_{30}$ (gr./cm. <sup>3</sup> )	
Poppy-seed oil:	Xylene:						
100	0	V <sub>3</sub>	m <sub>5</sub>	64.7	79.1	0.914	0.70
75	25	V <sub>3</sub>	m <sub>5</sub>	15.6	17.7	.900	.76
50	50	V <sub>2</sub>	m <sub>5</sub>	36.7	41.6	.886	.82
25	75	V <sub>1</sub>	m <sub>5</sub>	39.2	41.6	.871	.89
Neat's-foot oil (20° sample):	Xylene:						
100	0	V <sub>4</sub>	m <sub>5</sub>	36.2	44.5	.905	.66
75	25	V <sub>3</sub>	m <sub>5</sub>	16.9	19.5	.893	.73
50	50	V <sub>2</sub>	m <sub>5</sub>	37.5	41.6	.881	.80
25	75	V <sub>1</sub>	m <sub>5</sub>	40.8	43.5	.869	.87
Neat's-foot oil (30° sample):	Xylene:						
100	0	V <sub>4</sub>	m <sub>5</sub>	40.2	50.1	.909	.70
75	25	V <sub>3</sub>	m <sub>5</sub>	18.1	21.4	.896	.76
50	50	V <sub>2</sub>	m <sub>5</sub>	37.8	41.9	.883	.82
25	75	V <sub>1</sub>	m <sub>5</sub>	40.0	42.9	.870	.89
Castor oil:	Xylene:						
100	0	V <sub>4</sub>	m <sub>5</sub>	31.6	44.7	.954	.74
75	25	V <sub>3</sub>	m <sub>5</sub>	62.4	79.5	.928	.79
50	50	V <sub>2</sub>	m <sub>5</sub>	72.6	87.7	.903	.85
25	75	V <sub>1</sub>	m <sub>5</sub>	47.3	52.7	.879	.89
Linseed oil:	Xylene:						
100	0	V <sub>4</sub>	m <sub>5</sub>	22.8	27.0	.922	.73
75	25	V <sub>3</sub>	m <sub>5</sub>	13.4	15.1	.905	.78
50	50	V <sub>2</sub>	m <sub>5</sub>	33.0	34.8	.889	.84
25	75	V <sub>1</sub>	m <sub>5</sub>	37.1	39.5	.872	.90
Petrolatum:	Xylene:						
100	0	V <sub>4</sub>	m <sub>5</sub>	56.1	78.0	.878	.69
75	25	V <sub>3</sub>	m <sub>5</sub>	11.2	13.3	.871	.75
50	50	V <sub>2</sub>	m <sub>5</sub>	23.3	25.7	.866	.82
25	75	V <sub>1</sub>	m <sub>5</sub>	28.9	30.8	.860	.88
Transformer oil:	Xylene:						
100	0	V <sub>3</sub>	m <sub>5</sub>	15.0	18.4	.896	.73
80	20	V <sub>2</sub>	m <sub>5</sub>	36.0	40.6	.887	.77
60	40	V <sub>1</sub>	m <sub>5</sub>	48.1	52.5	.879	.82
Glycerine:	Ethyl alcohol:						
100	0	V <sub>4</sub>	m <sub>5</sub>	148.6	217.3	1.2455	.45
75	25	V <sub>4</sub>	m <sub>5</sub>	22.3	29.7	1.102	.62
50	50	V <sub>3</sub>	m <sub>5</sub>	12.9	15.5	.993	.75
25	75	V <sub>2</sub>	m <sub>5</sub>	29.4	33.4	.888	.88
Glycerine:	Ethyl alcohol and water (50-50):						
75	25	V <sub>4</sub>	m <sub>5</sub>	15.1	19.6	1.141	.55
50	50	V <sub>3</sub>	m <sub>5</sub>	9.7	11.8	1.052	.61
25	75	V <sub>2</sub>	m <sub>5</sub>	32.5	38.5	.975	.68
N. butyl alcohol:	Methyl alcohol:						
100	0	V <sub>1</sub>	m <sub>5</sub>	70.1	78.0	.811	.82
75	25	V <sub>2</sub>	m <sub>5</sub>	18.5	18.0	.803	.90
50	50	V <sub>2</sub>	m <sub>5</sub>	11.8	12.6	.797	.97
25	75	V <sub>1</sub>	m <sub>5</sub>	22.1	23.6	.789	1.05
Xylene		V <sub>1</sub>	m <sub>5</sub>	49.1	52.1	.855	.95
Kerosene		V <sub>1</sub>	m <sub>5</sub>	74.0	82.8	.810	.80
Mineral spirits		V <sub>1</sub>	m <sub>5</sub>	28.9	30.8	.769	.99
Recoil oil		V <sub>3</sub>	m <sub>5</sub>	9.4	11.1	.883	.74

TABLE IX

DATA FOR COMPARING THE VISCOSITY AND THE EFFECT OF TEMPERATURE ON THE VISCOSITY OF THE VARIOUS SOLUTIONS

Proportions, by weight		Viscosity $\mu_{25}$ (poise)	Logarithm of the kinematic viscosity ratio	
			$n_{20}$	$n_{15}$
Poppy-seed oil: 100 75 50 25	Xylene: 0 25 50 75	0.5460 .1197 .0401 .0148	0.175 .130 .090 .055	>1.20 .735 .500 .335
Neat's-foot oil (20° sam- ple): 100 75 50 25	Xylene: 0 25 50 75	.6560 .1310 .0399 .0156	.180 .125 .085 .055	>1.10 .770 .520 .330
Neat's-foot oil (30° sam- ple): 100 75 50 25	Xylene: 0 25 50 75	.7420 .1433 .0403 .0153	.190 .140 .095 .065	>1.15 .820 .525 .350
Castor oil: 100 75 50 25	Xylene: 0 25 50 75	6.94 .5550 .0867 .0191	.335 .225 .165 .090	>1.50 >1.20 .85 .600
Linseed oil: 100 75 50 25	Xylene: 0 25 50 75	.4060 .1023 .0335 .0140	.150 .100 .070 .055	>1.25 .675 .475 .350
Petrolatum: 100 75 50 25	Xylene: 0 25 50 75	1.1150 .0866 .0239 .0106	.290 .150 .085 .055	>1.25 .880 .495 .325
Transformer oil: 100 80 60	Xylene: 0 20 40	.1238 .0392 .0190	.188 .110 .075	1.16 .695 .475
Glycerine: 100 75 50 25	Ethyl alcohol: 0 25 50 75	4.400 .5325 .1151 .0321	.345 .255 .165 .110	----- 1.44 .985 .650
Glycerine: 75 50 25	Ethyl alcohol and water (50-50): 25 50 75	.3640 .0924 .0408	.240 .175 .155	1.36 1.02 .885
N. butyl alcohol: 100 75 50 25	Methyl alcohol: 0 25 50 75	.0263 .0152 .0101 .00733	.095 .085 .060 .055	.565 .410 .330 .310
Xylene----- Kerosene----- Mineral spirits----- Recoil oil-----	----- ----- ----- -----	.00595 .0278 .00940 .0728	.047 .095 .055 .146	.240 >.500 .315 .918



TABLE X

Absolute viscosity 25° C.	Liquid	Temperature at which $n=0.7$	Logarithm of kinematic viscosity ratio				
			$n_{30}$	$n_{10}$	$n_0$	$n_{-10}$	$n_{-20}$
Poises: 6.0	98 per cent D.....	° C. 9.5	0	0.68	-----	-----	-----
4.0	96 per cent D.....	8.5	0	.66	-----	-----	-----
	98 per cent H.....	11.0	0	-----	-----	-----	-----
	99 per cent K.....	11.0	0	.74	-----	-----	-----
2.0	90 per cent D.....	7.0	0	.60	-----	-----	-----
	90 per cent H.....	8.5	0	.65	-----	-----	-----
	96 per cent K.....	9.5	0	.69	-----	-----	-----
1.0	83 per cent D.....	5.5	0	.53	0.89	-----	-----
	99 per cent F.....	7.5	0	.59	.96	-----	-----
	82 per cent H.....	6.0	0	.58	.91	-----	-----
	90 per cent K.....	8.0	0	.63	-----	-----	-----
.742	30° neat's-foot oil.....	0	0	.42	.70	1.1	-----
.656	20° neat's-foot oil.....	-2.0	0	.39	.64	.96	-----
.6	99 per cent B.....	-2.5	0	.39	.63	.95	-----
	97 per cent C.....	-1.0	0	.40	.68	1.05	-----
	76 per cent D.....	+3.0	0	.48	.80	-----	-----
	77 per cent H.....	5.0	0	.55	.87	-----	-----
	82 per cent K.....	5.5	0	.55	.87	-----	-----
	94 per cent F.....	4.0	0	.50	.81	-----	-----
.546	Poppy-seed oil.....	-4.0	0	.36	.59	.92	-----
.4	94 per cent A.....	-5.8	0	.34	.56	.84	-----
	95 per cent B.....	-4.0	0	.37	.60	.89	-----
	91 per cent C.....	-3.0	0	.38	.62	.94	-----
	71 per cent D.....	+2.0	0	.46	.76	-----	-----
	90 per cent F.....	1.0	0	.48	.80	-----	-----
	70 per cent H.....	2.5	0	.49	.77	-----	-----
	75 per cent K.....	3.0	0	.50	.79	1.14	-----
.4	Linseed oil.....	-6.0	0	.32	.53	.85	-----
.2	82 per cent A.....	-9.8	0	.28	.48	.70	-----
	83 per cent B.....	-8.5	0	.31	.49	.74	-----
	81 per cent C.....	-7.2	0	.33	.53	.78	-----
	63 per cent D.....	-1.0	0	.41	.69	1.05	-----
	87 per cent E.....	-10.0	0	.27	.45	.70	-----
	85 per cent F.....	-2.5	0	.40	.65	.94	-----
	60 per cent H.....	-1.0	0	.41	.67	.96	-----
	62 per cent K.....	-1.0	0	.43	.68	.99	-----
.1238	Transformer oil.....	-3.0	0	.40	.65	.96	1.5
.1	72 per cent A.....	-14.5	0	.25	.41	.60	-----
	70 per cent B.....	-15.0	0	.25	.42	.61	-----
	65 per cent C.....	-15.0	0	.26	.42	.59	.82
	50 per cent D.....	-5.0	0	.34	.56	.90	-----
	75 per cent E.....	-16.0	0	.24	.38	.57	-----
	78 per cent F.....	-6.5	0	.34	.54	.79	-----
	98 per cent G.....	-2.5	0	.39	.63	.93	-----
	48 per cent H.....	-6.0	0	.34	.56	.81	-----
	53 per cent K.....	-3.5	0	.38	.61	.89	-----
.0728	Recoil oil.....	-7.5	0	.32	.52	.76	-----
.05	57 per cent A.....	-20.0	0	.20	.34	.48	.66
	57 per cent B.....	-20.0	0	.21	.34	.50	.69
	52 per cent C.....	-20.0	0	.20	.32	.47	.64
	44 per cent D.....	-8.5	0	.31	.51	.75	-----
	60 per cent E.....	-20.0	0	.20	.32	.46	.64
	63 per cent F.....	-17.0	0	.24	.39	.55	.78
	86 per cent G.....	11.0	0	.28	.45	.67	-----
	35 per cent H.....	-12.5	0	.28	.46	.65	-----
	30 per cent K.....	7.5	0	.33	.53	.77	-----
.0278	Kerosene.....	-15.0	0	.20	.33	.48	-----

TABLE X—Continued

Absolute viscosity 25° C.	Liquid	Temper- ature at which <i>n</i> = 0.7	Logarithm of kinematic viscosity ratio				
			<i>n</i> <sub>30</sub>	<i>n</i> <sub>10</sub>	<i>n</i> <sub>0</sub>	<i>n</i> <sub>-10</sub>	<i>n</i> <sub>-20</sub>
Poises— Contd. 0. 025		° C.					
	38 per cent A-----	<sup>1</sup> —20. 0	0	0. 16	0. 25	0. 36	0. 49
	35 per cent B-----	<sup>1</sup> —20. 0	0	. 15	. 24	. 35	. 49
	38 per cent C-----	<sup>1</sup> —20. 0	0	. 17	. 27	. 38	. 52
	30 per cent D-----	—16. 0	0	. 22	. 37	. 55	0
	42 per cent E-----	<sup>1</sup> —20. 0	0	. 15	. 25	. 37	. 51
	52 per cent F-----	<sup>1</sup> —20. 0	0	. 19	. 31	. 44	. 61
	68 per cent G-----	<sup>1</sup> —20. 0	0	. 19	. 32	. 47	-----
	18 per cent H-----	<sup>1</sup> —20. 0	0	. 20	. 32	. 47	. 63
	15 per cent K-----	—10. 0	0	. 31	. 50	. 70	-----
	98 per cent L-----	—21. 5	0	. 20	. 32	. 46	. 66
. 01	15 per cent C-----	<sup>1</sup> —20. 0	0	. 12	. 19	. 26	. 41
	10 per cent D-----	<sup>1</sup> —20. 0	0	. 13	. 22	. 32	. 44
	20 per cent G-----	<sup>1</sup> —20. 0	0	. 12	. 19	. 26	. 35
	50 per cent L-----	<sup>1</sup> —20. 0	0	. 13	. 20	. 28	. 37
. 01	Ethyl alcohol-----	<sup>1</sup> —20. 0	0	. 16	. 24	. 33	. 43
. 094	Mineral spirits-----	<sup>1</sup> —20. 0	0	. 12	. 19	. 27	. 37
. 00595	Xylene-----	<sup>1</sup> —20. 0	0	. 10	. 15	. 21	. 26

<sup>1</sup> Below.

- A----- Poppy-seed oil and xylene.

B----- Neat's-foot oil (20°F.) and xylene.

C----- Neat's-foot oil (30°F.) and xylene.

D----- Castor oil and xylene.

E----- Linseed oil and xylene.

F----- Petrolatum and xylene.
- G----- Transformer oil and xylene.

H----- Glycerine and ethyl alcohol.

K----- Glycerine and 50-50 solution of ethyl alcohol  
and water.

L----- N. butyl alcohol and methyl alcohol.

The percentage given in the table refers to the amount, by weight, of the first-named liquid.

BUREAU OF STANDARDS,  
WASHINGTON, D. C., May 16, 1928.

BIBLIOGRAPHY

Reference 1. Herschel, W. H.: The Jour. Ind. and Eng. Chemistry, vol. 14, pp. 715-723. (1922.)  
Reference 2. Bingham, E. C., Schlesinger, H. I., and Coleman, A. B.: Jour. Amer. Chem. Soc., vol. 38, p. 27. (1916.)  
Reference 3. Bond, W. N.: Proc. Phys. Soc. (London), vol. 34, pp. 139-144. (1921-22.)  
Reference 4. Dorsey, N. E.: J. O. S. A. & R. S. I., vol. 14, pp. 45-53. (1927.)  
Reference 5. Barr, Guy: Jour. of Scientific Instruments, Vol. I. (1923-24.)  
Reference 6. Herschel, W. H.: Bureau of Standards Technical Paper No. 100, 1927.  
Reference 7. Herschel, W. H.: Bureau of Standards Technical Paper No. 112, 1918.  
Reference 8. Herschel, W. H.: Bureau of Standards Technical Paper No. 125, 1919.  
Reference 9. Herschel, W. H.: Bureau of Standards Technical Paper No. 210, 1922.  
Reference 10. Nat. Std. Pet. Oil Tables, B. S. Circ. 154, 1924.



---

---

**REPORT No. 300**

---

**THE TWENTY-FOOT PROPELLER RESEARCH TUNNEL  
OF THE NATIONAL ADVISORY COMMITTEE  
FOR AERONAUTICS**

**By FRED E. WEICK and DONALD H. WOOD**  
**Langley Memorial Aeronautical Laboratory**





## REPORT No. 300

---

### THE TWENTY-FOOT PROPELLER RESEARCH TUNNEL OF THE NATIONAL ADVISORY COMMITTEE FOR AERONAUTICS

By FRED E. WEICK and DONALD H. WOOD

---

#### SUMMARY

*This report describes in detail the new propeller research tunnel of the National Advisory Committee for Aeronautics at Langley Field, Va. This tunnel has an open jet air stream 20 feet in diameter in which velocities up to 110 M. P. H. are obtained. Although the tunnel was built primarily to make possible accurate full-scale tests on aircraft propellers, it may also be used for making aerodynamic tests on full-size fuselages, landing gears, tail surfaces, and other aircraft parts, and on model wings of large size.*

#### INTRODUCTION

The need of an accurate means for making aerodynamic measurements on full-size aircraft propellers has been realized for some time. Tests on model propellers in wind tunnels are not entirely satisfactory because the deflection of the model is different from that of a similar full-scale propeller, which introduces a rather large error in some cases. The difference in scale and tip speed between the model and full-scale propeller is also a cause of error. Full-scale flight tests on propellers are made, of course, under the correct conditions, but at the present time they can not be made with sufficient accuracy.

In the spring of 1925 the design and construction of a propeller research wind tunnel to fill this need for full-scale tests was started by the National Advisory Committee for Aeronautics. It was completed during the summer of 1927 and testing has been carried on since that time. The tunnel is of the open-jet type with an air stream 20 feet in diameter. This is large enough to permit the mounting of a full-sized airplane fuselage with its engine and propeller. The open-jet type is particularly suitable for testing propellers because no corrections are required for tunnel-wall interference. (References 4 and 5.) Also, since with the open-jet type the inside of the experiment chamber is free from restricting walls, the installation of the objects to be tested is relatively simple.

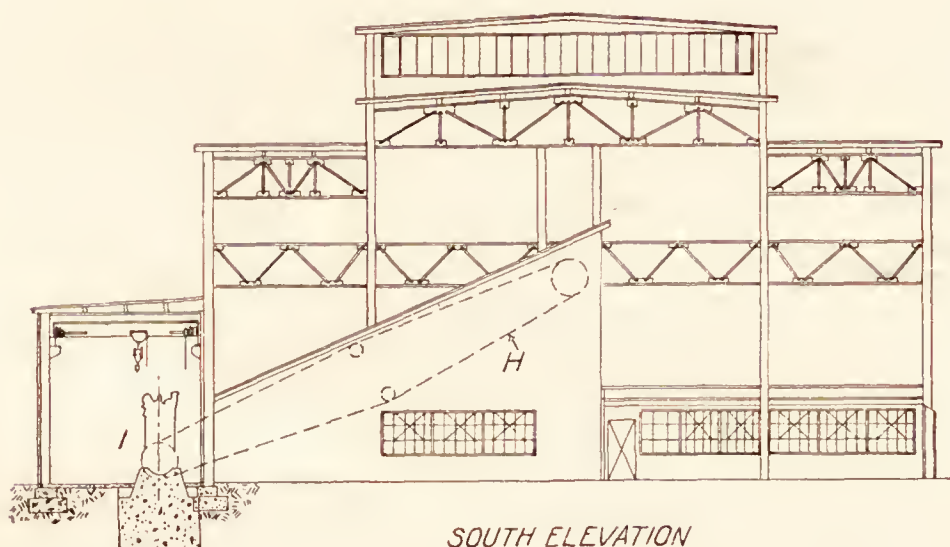
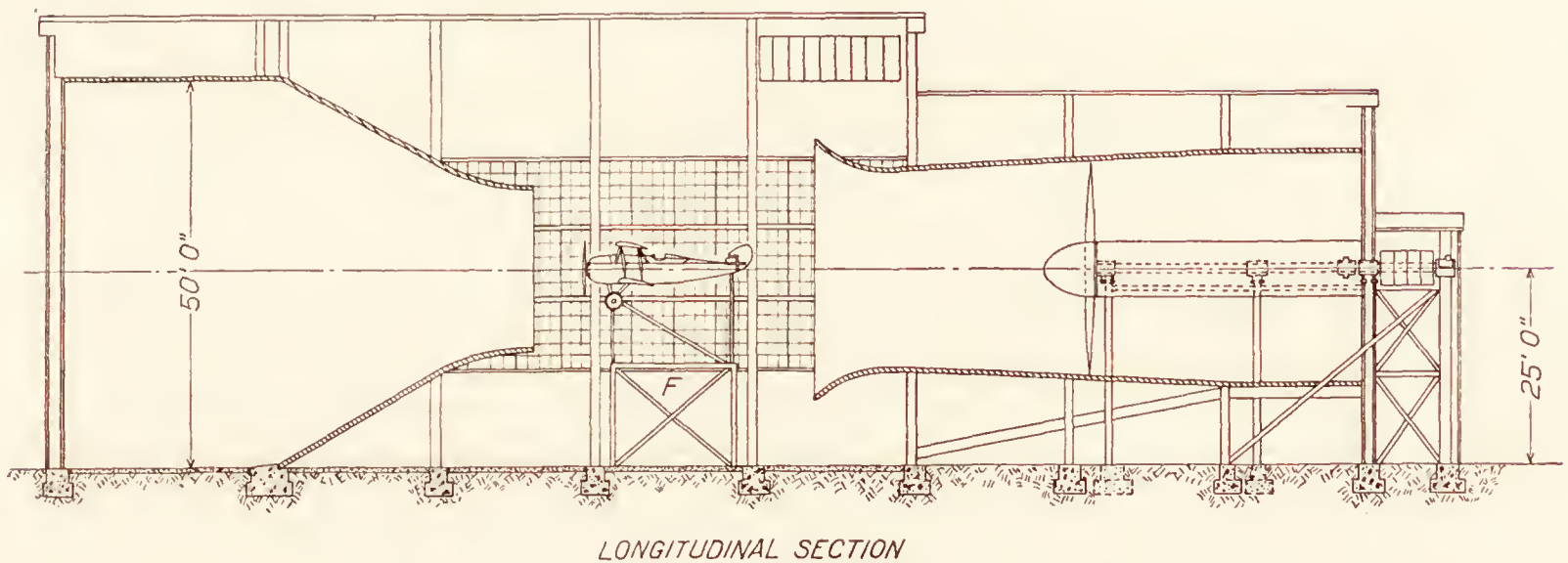
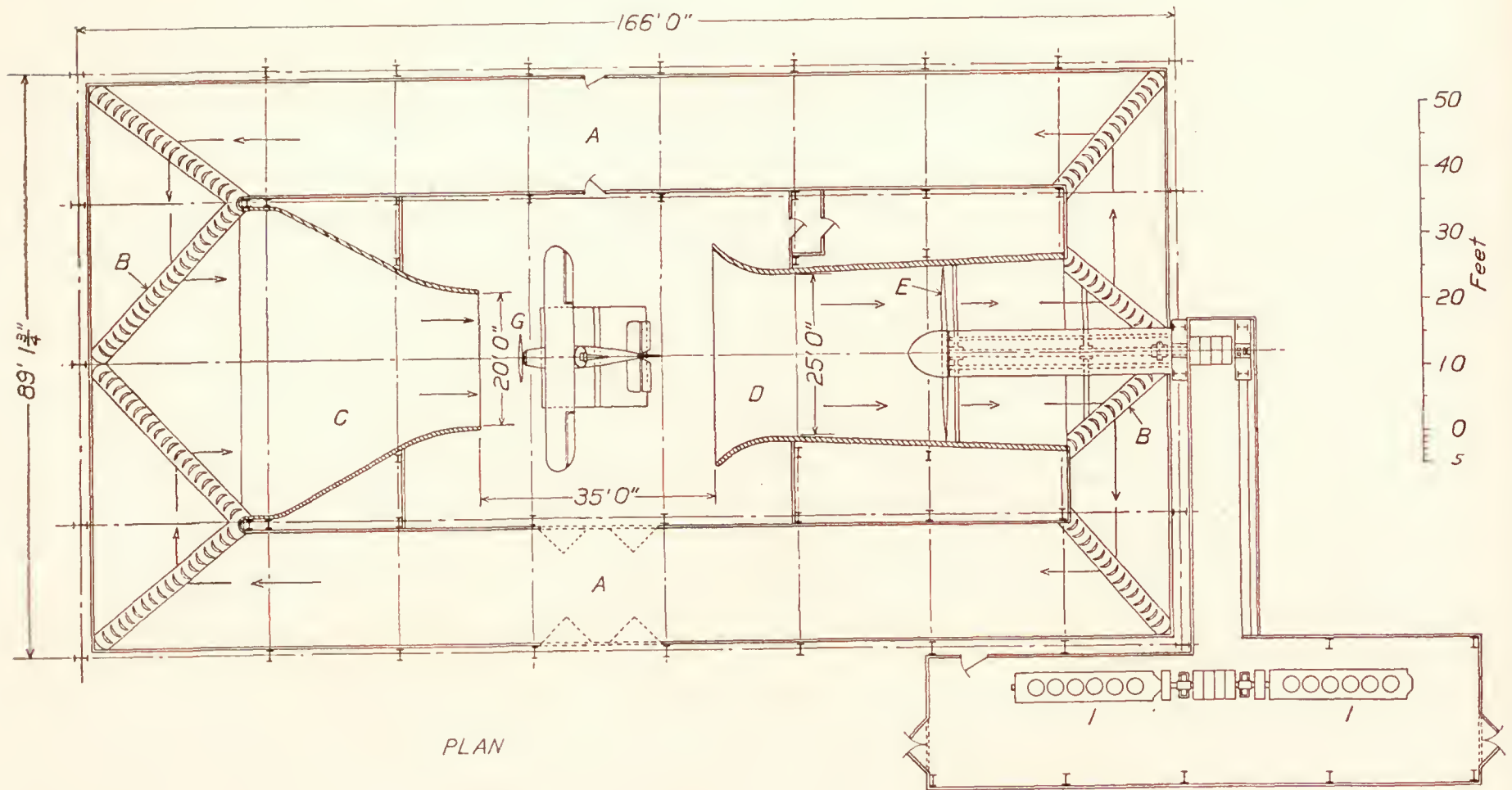
This wind tunnel makes it possible for the first time to make aerodynamic tests with laboratory accuracy on full-scale aircraft propellers and also on full-scale fuselages, engine cowlings, cooling systems, landing gears, tail surfaces and other airplane parts. Full-scale tests of wings are not, of course, possible in a 20-foot air stream, but large model wings (12 feet in span) can be tested at comparatively high values of Reynolds Number.

Dr. Max M. Munk is responsible for the general arrangement of the propeller research tunnel, and the detail design and construction were carried out under the direction of Mr. E. W. Miller of the laboratory staff.

#### DESCRIPTION OF THE TUNNEL

##### GENERAL

The propeller research tunnel of the National Advisory Committee for Aeronautics is located at Langley Field, Va., on a plot adjacent to the committee's other research equipment. Figure 1 is a diagrammatic sketch indicating the general arrangement of the tunnel and Figure 2 illustrates the exterior appearance.



- A, Return passage
- B, Guide vanes
- C, Entrance cone
- D, Exit cone
- E, Circulating fan
- F, Balance
- G, Test propeller
- H, Rope drive
- I, Diesel engines

FIG. 1



The tunnel proper is a wood walled steel-framed structure 166 feet long and 89 feet wide, having a maximum height of 56 feet. The walls are of 2 inch by 6 inch tongued and grooved pine sheathing attached to steel columns with wooden nailers. Except for the fact that the walls are on the inside of the framing only and that the heights vary from point to point, standard structural practice is followed.

The tunnel (fig. 1) is of the open-throat, closed test chamber, return passage type. The direction of the air flow is indicated by arrows. The air is drawn across the test chamber into the exit cone by a propeller fan. After passing through the fan the air column divides, passes through successive sets of guide vanes at the corners, and returns through the side passages to the entrance cone. The areas of the passages are varied in the case of the exit cone by varying the diameter, and of the return passages by sloping the roof and floor, so that the velocity of the moving air is gradually decreased at the large end of the entrance cone to about one-eighth that through the test chamber. It is then rapidly accelerated in passing through the entrance cone.

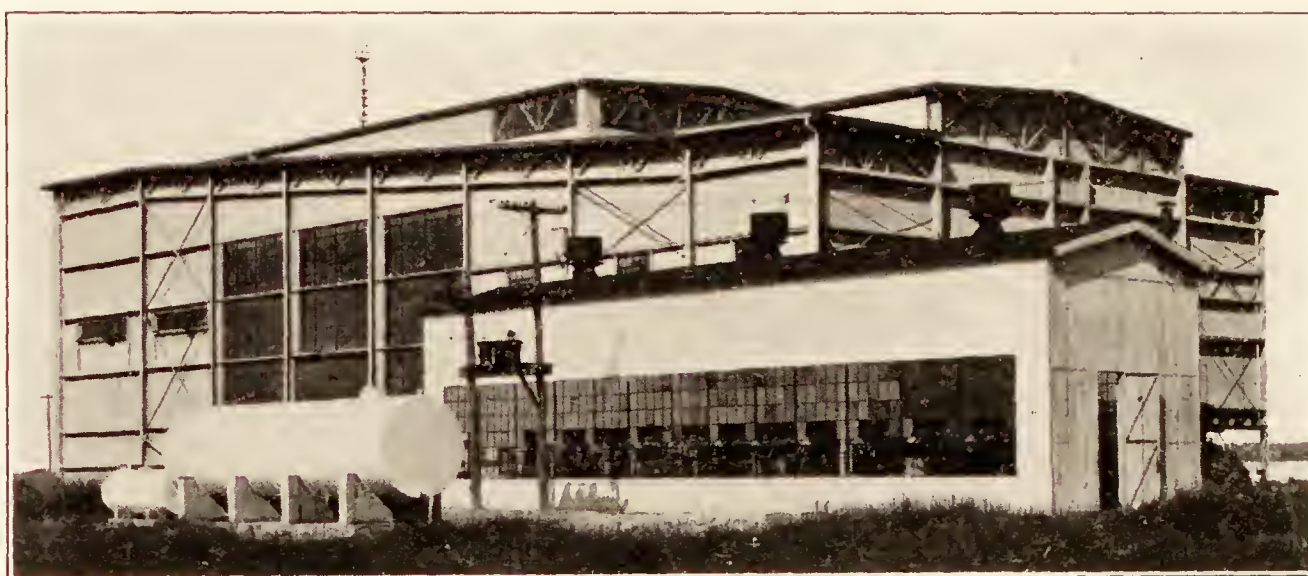


FIG. 2

### TEST CHAMBER

The test chamber is about 50 by 60 by 55 ft., located, as shown in Figure 1, near the center of the tunnel structure. Large windows in the east and west walls afford ample light. Doors open out of the west wall to permit the movement of material to and from the test chamber. An electric crane traveling along a roof truss is useful in lifting loads about the chamber and onto the balance. Electrical outlets for light and power are provided at convenient points.

### ENTRANCE CONE

The entrance cone (fig. 3) is of 50 ft. square section at the large end, changing to 20 ft. diameter in its length of 36 ft. It is constructed of a double layer of  $\frac{3}{4}$  in. by 2 in. sheathing bent, fitted, and nailed to wood forming rings. These, in turn, are bolted to angle clips riveted to I-beams bent to proper shape. A built-up wood ring forms the end of the cone. At the large end the cone runs into the return passage on a gradual curve.

### EXIT CONE

The exit cone (fig. 4) is similar in construction to the entrance cone. It is circular in section from the mouth of the bell in the test chamber to the fan. The cone has a diameter of 33 ft. at the mouth of the bell, reducing to 25 ft. at the test chamber wall and then increasing with a  $7^\circ$  included angle to 28 ft. in diameter at the fan. From the fan a gradual change is made to 30 ft. square at the return passage. The total length of the exit cone is 52 ft.



## GUIDE VANES

Guide vanes (fig. 5) are located, as shown in Figure 1, at each point of change of direction of the air stream. These consist of metal covered wood framed curved shapes built up in sections 5 ft. long. Rounded leading edges and pointed trailing edges are of wood. The vanes are so proportioned that the free area between them is about a mean of the passage areas before and behind them. Streamlined wood separators run diagonally across the corners and act as stiffeners and supports for each tier of vane sections. It may also be noted in Figure 5 that cross bracing in the return passages is streamlined in the direction of flow.

## FAN

Circulation of air is accomplished with a 28 ft. diameter propeller type fan. (Fig. 6 and fig. 1.) It consists of eight cast, heat-treated, aluminum-alloy blades screwed into a cast steel hub and locked in place by means of wedge rings which are forced between the blade shanks

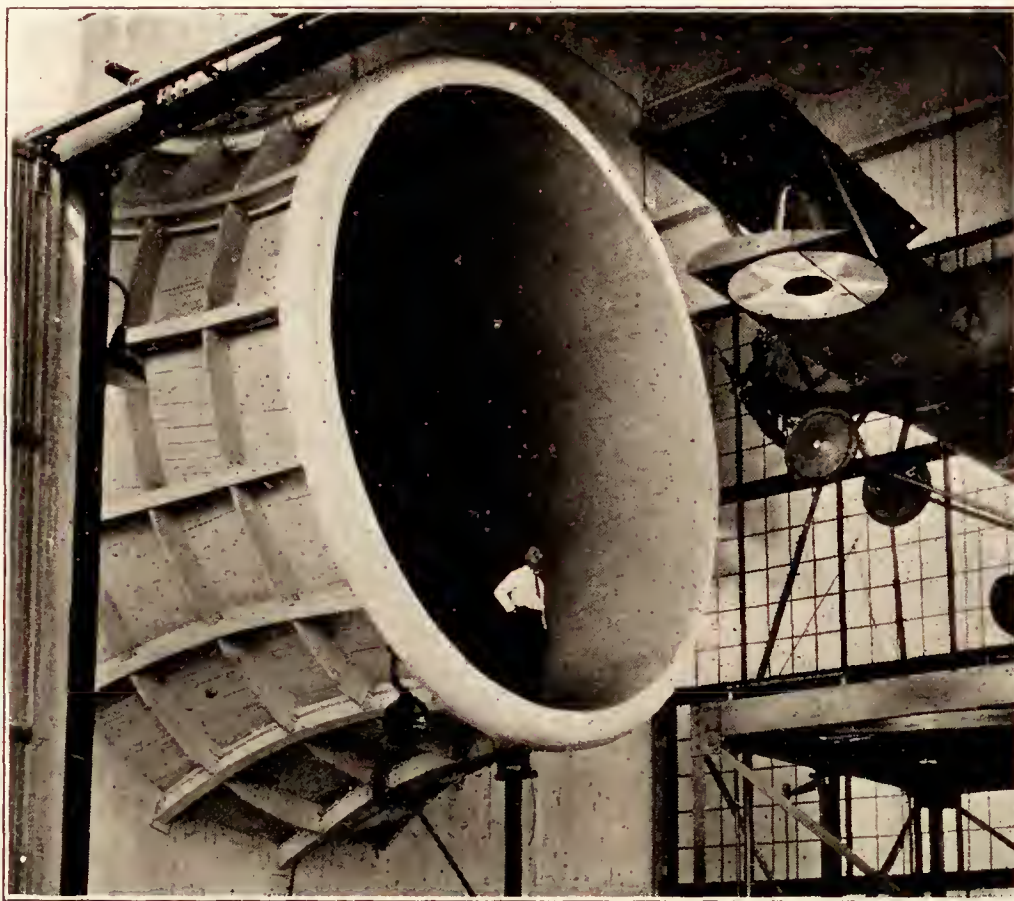


FIG. 3

and the hub. This makes it possible to change the pitch to adapt the fan to the driving engine characteristics or to secure different air speeds with the same engine speed. At present 100 M. P. H. is obtained with 330 R. P. M. of the engines and fan. The weight of each blade is 600 pounds and the total weight of the fan is about  $3\frac{1}{2}$  tons.

A steel framed sheet aluminum spinner 7 ft. in diameter is attached to the hub. This fairs into the cylindrical propeller shaft housing.

## DRIVE SHAFT

The fan hub is keyed on to the tapered end of an 8-in. solid steel shaft running back through the exit cone and return passage. This shaft is supported on four plain, collar oiled, bearings and one combination plain radial bearing and deep groove ball thrust bearing. The latter is located at the end of the shaft opposite the propeller. The bearings are supported, in turn, on steel I-beam A frames resting on spread footings in the ground below the exit cone.



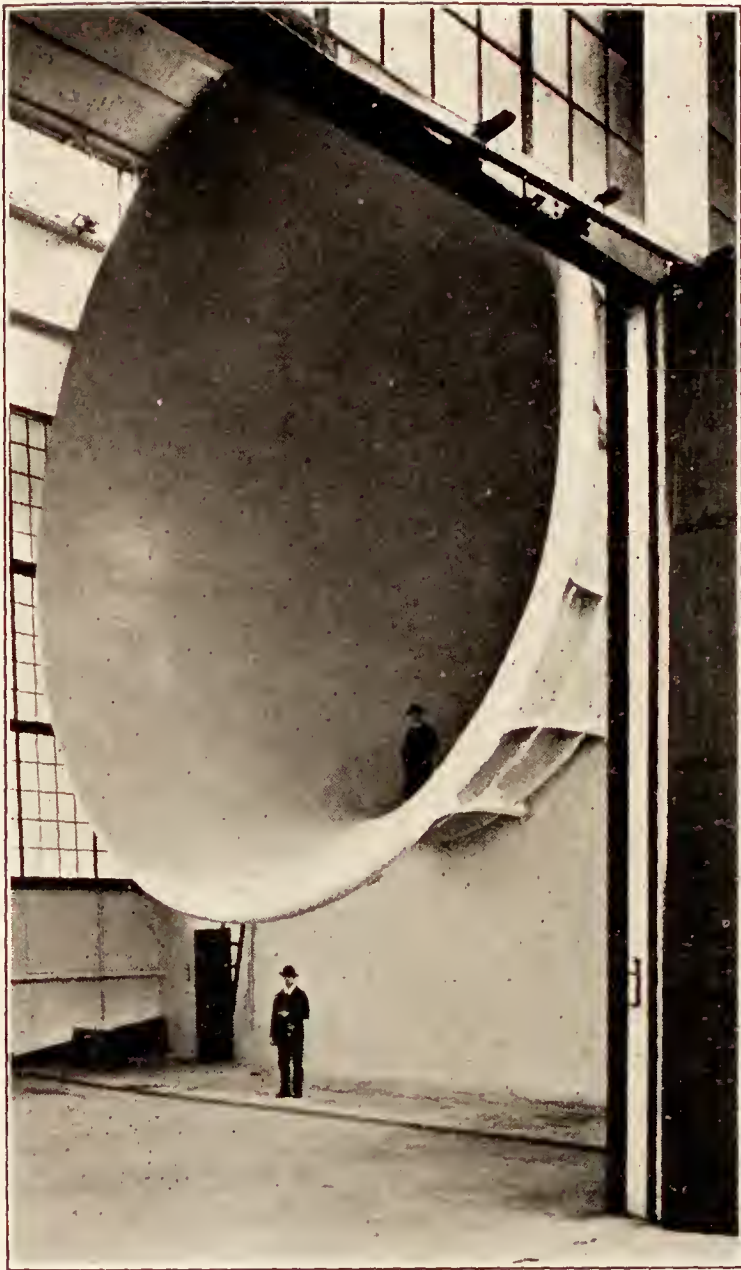


FIG. 4

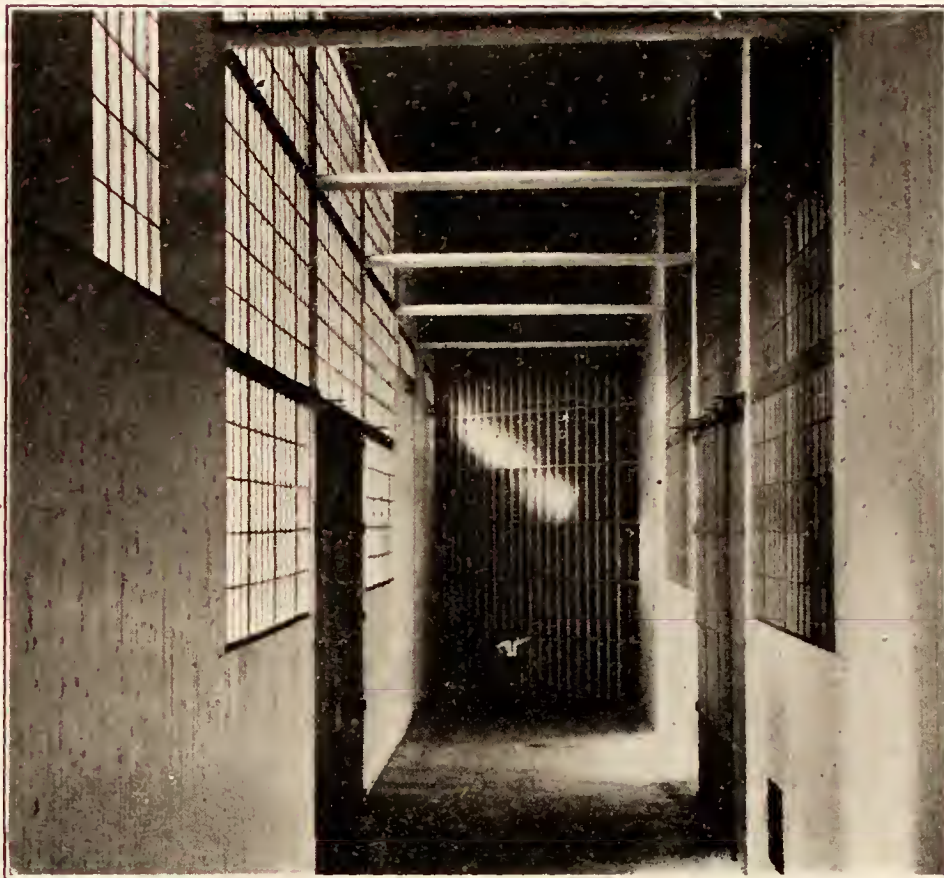


FIG. 5

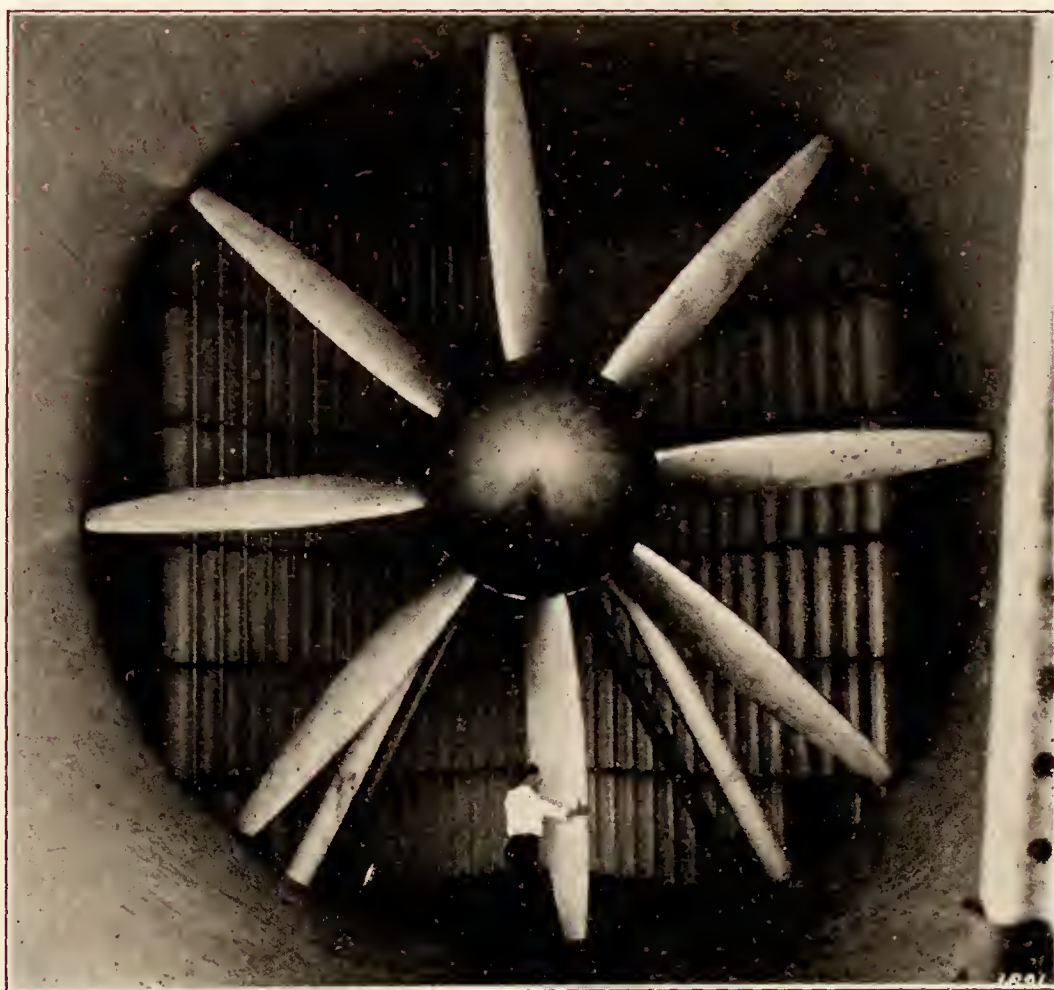


FIG. 6



The shaft and bearing bracing are surrounded by a cylindrical sheet steel fairing on wood formers of the same diameter as the fan spinner. The legs of the A frames are also suitably faired.

#### POWER PLANT AND TRANSMISSION

Because of local conditions it was found advisable to use Diesel engines rather than electric motors to furnish power for circulating the air through the tunnel. Two Diesel engines, which had been removed from a submarine, were furnished by the Navy Department.

These engines are full Diesel M. A. N. type, 6 cylinder, 4 cycle, single acting, rated at 1,000 HP. each at 375 R. P. M. After due consideration, it was decided to install these end to end as they had been in the submarine, using the existing flywheels and clutches, spacing them far enough apart to allow the installation of a driving sheave between. The location of the engine room is shown in Figure 1, with the engine and sheave position indicated. The

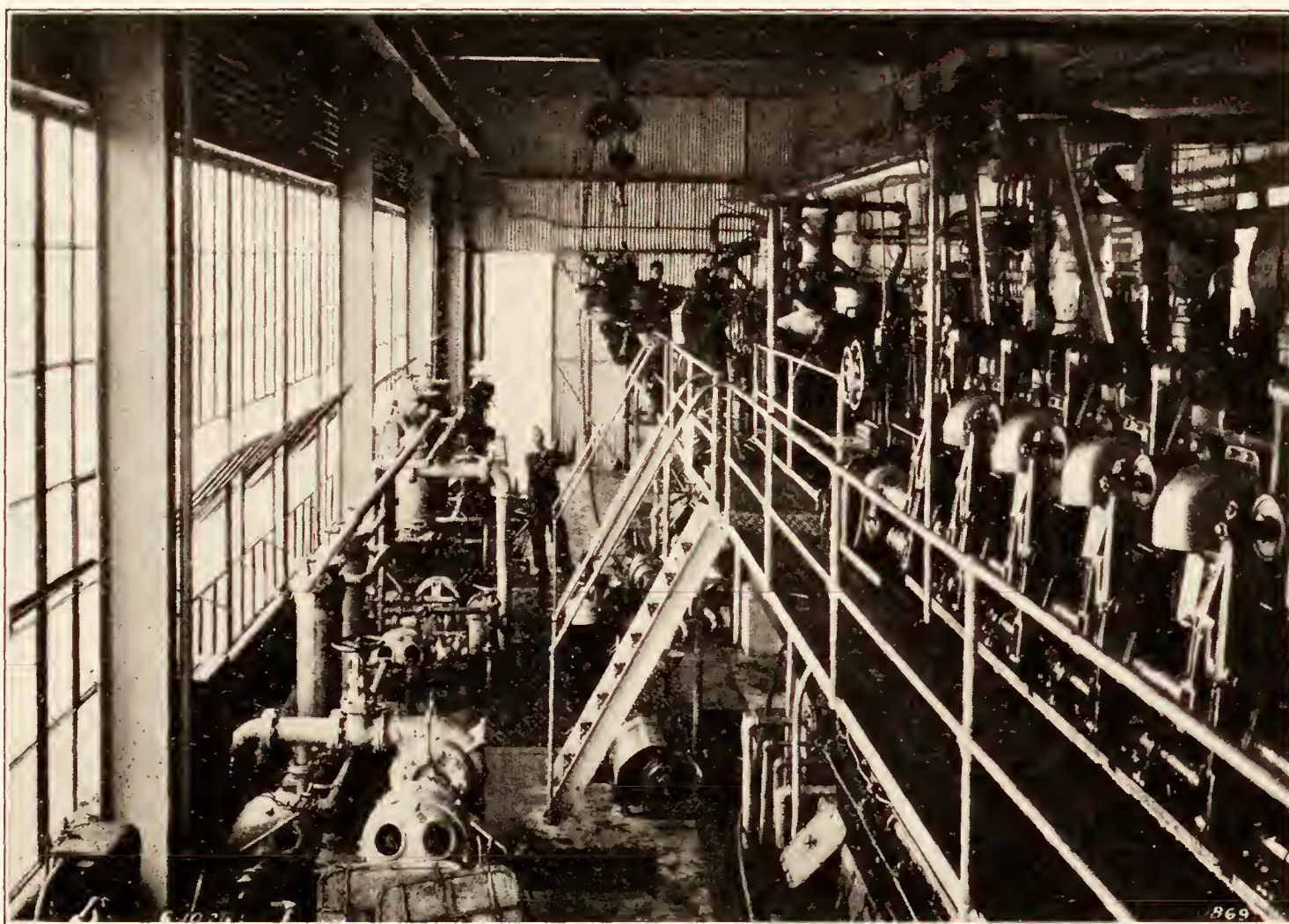


FIG. 7

auxiliary machinery is arranged on the opposite side of the room from the engines. Figure 7 is a general view of the engine room.

Power is transmitted from the driving sheave to a similar sheave located forward of the thrust bearing on a part of the fan shaft extending through the main tunnel wall. Forty-four "Texrope" V-belts are used with two adjustable grooved idler pulleys located as shown in the end view, Figure 1. The transmission ratio is 1 to 1. The belt pull is carried on a suitable steel structure and the whole framing is roofed over and sided with a protected corrugated metal. This same material is a covering for the engine room proper, rendering this part of the installation practically fireproof.

#### BALANCE

The testing of full size airplane fuselages necessitated the design of a new type balance. This, as shown in Figures 8 and 9, consists essentially of a triangular frame A of steel channels and gussets resting on tubular steel posts B, which in turn bear on the platforms of ordinary



beam scales **C**. Double knife edges are provided at both ends of these posts. The rear post of the frame is on the longitudinal center line of the balance and the forward posts are at equal distances (5 ft.) on either side. The sum of the net readings on all three balances is the lift. The pitching moment is computed from the sum of the front balance readings and from the rear balance reading. Since the rear balance is on the longitudinal axis, the rolling moment is computed from the net readings on the front balances.

At **D** are located knife edges connected to tie rods **E** running forward to a bell crank **G** and a counterweight **H**, and aft to a bell crank **F** and a post **I** resting on the scale **T**. A forward pull or thrust on the frame produces a down force on the post or an increase in load on the scale **T**. The counterweight **H** produces an initial load on the scale **T** and consequently a drag or backward force is measured as a diminution of load on the scale. The counterweight

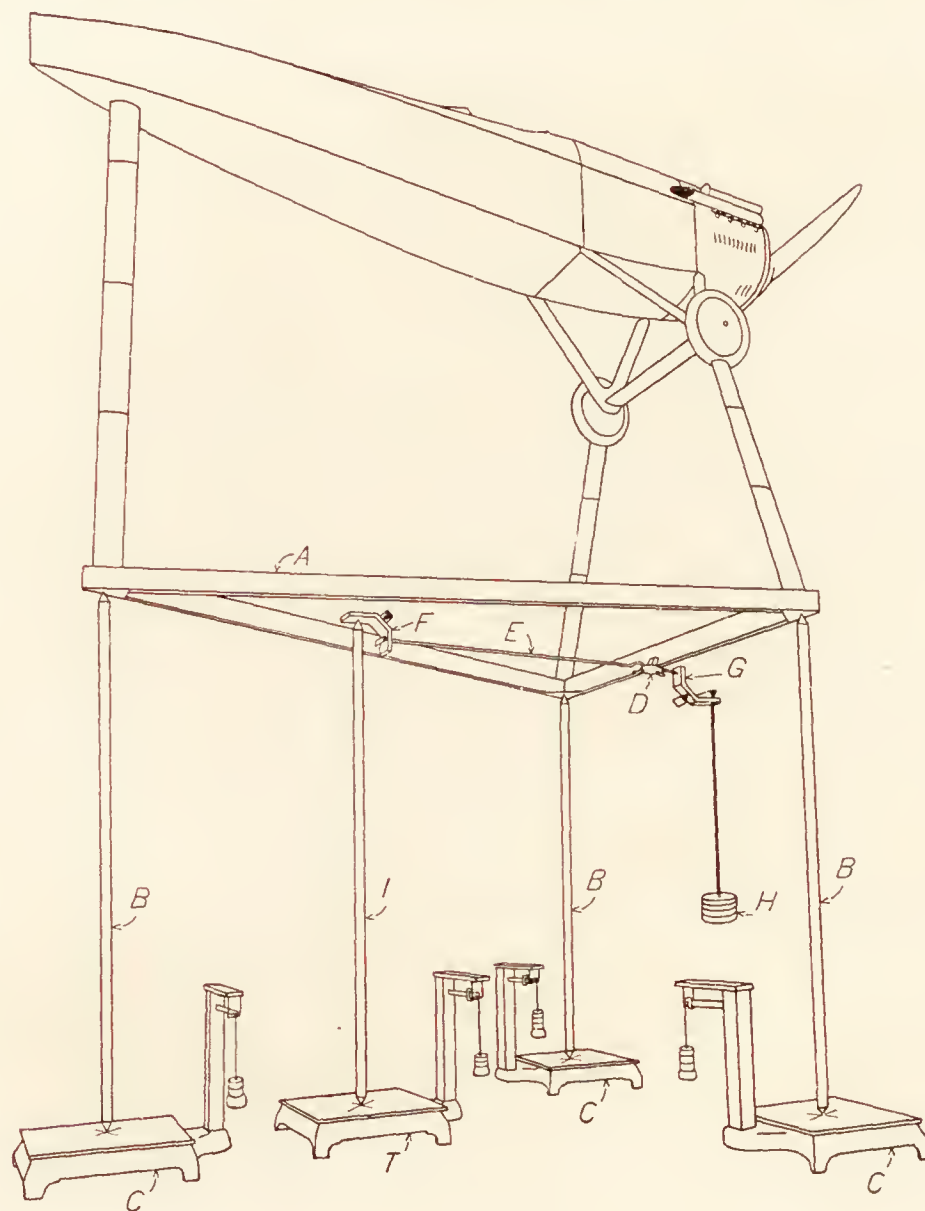


FIG. 8

consists of several 50-lb. units and can be easily adapted to the range of thrusts and drags expected during any one test.

The fixed knife edges on the bell cranks are seated on blocks bolted to a rectangular steel frame rigidly fastened to the floor, as shown in Figure 9. In addition, this frame is provided with knife edges, links, and counterweights which hold the triangular frame in a fixed lateral position. Screws are also provided for raising the triangular frame from the knife edges while working on the attached apparatus. A stairway at the rear and a grating floor facilitate work on the supports and apparatus mounted on the balance.

At each corner of the triangular frame are ball ended steel tubes, adjustable in length and angle, which support the body under test. The forward tubes, in the case of a fuselage with landing gear, have a fitting at the upper end which clamps the axle of the landing gear.



The rear post has a ball-and-socket attachment to the fuselage. The drag of these supports is reduced by streamline fairings which also serve to cover wires and fuel and water lines running to the fuselage.

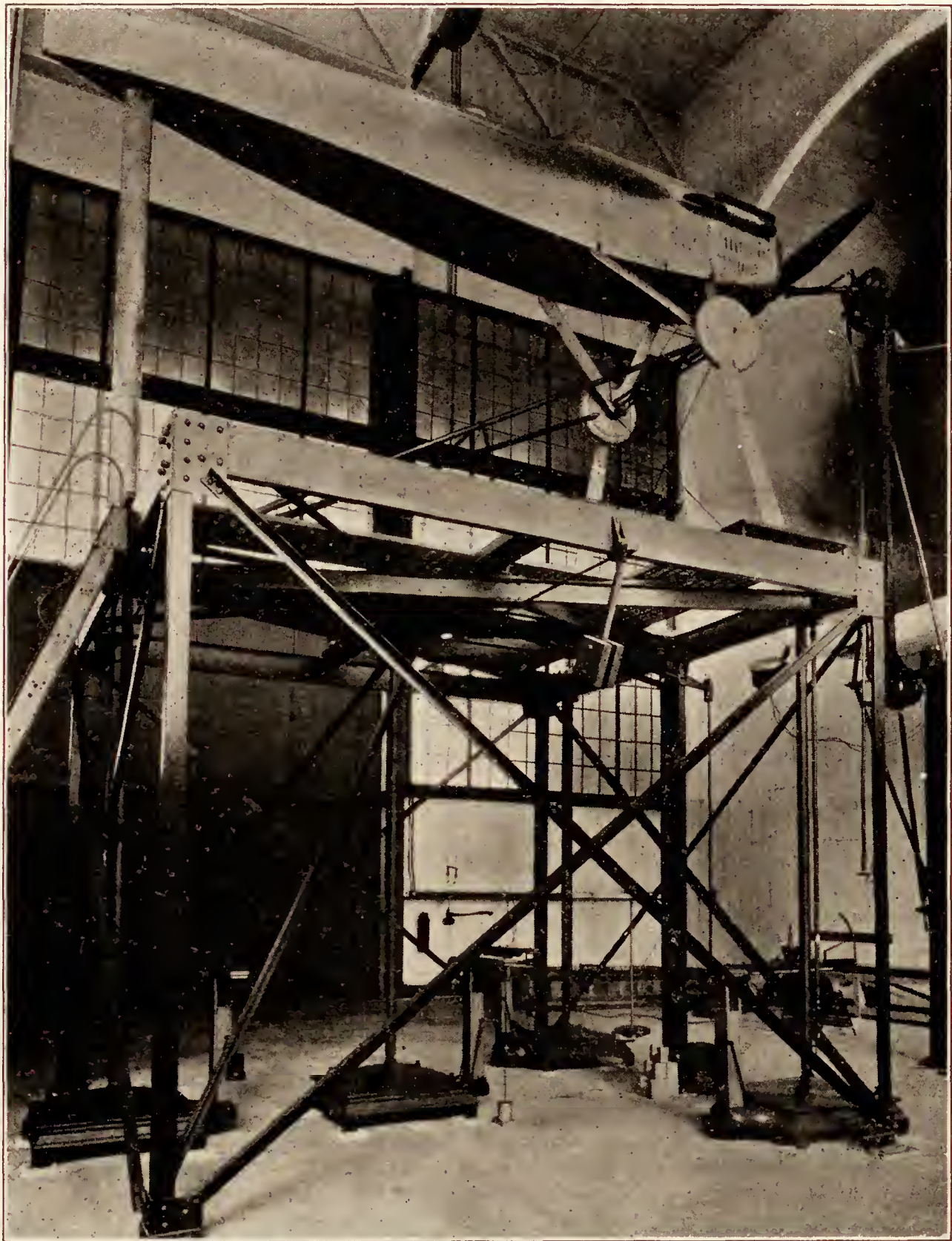


FIG. 9

#### TORQUE DYNAMOMETER

As the engine power is one of the major variables determining the propeller characteristics, a test fuselage has been developed which allows the engine driving the propeller to be mounted on a dynamometer and the torque to be measured directly.

As shown in Figure 10, this is a heavy angle and strap steel frame so shaped that it can be slipped inside a standard airplane fuselage and supported by suitable blocking. At its forward end a steel casting is fixed carrying two large ball bearings and an extension shaft and plate. An airplane engine can be mounted on this plate. Its torque, which is carried through



the plate and shaft and a special linkage, is read on a dial scale mounted farther back in the fuselage. This dial reads directly in lb. ft. up to 2,000 lb. ft. and a total of 4,000 lb. ft. may be obtained with a counterweight. A double link system renders the operation independent of the direction of engine rotation.

Figure 11 shows a VE-7 airplane mounted on the test fuselage with an E-2 engine on the plate. The radiator is mounted independently of the engine and is not used for cooling. Cooling water is supplied and returned through rubber hose running back through the fuselage and down the rear post to the floor. Figure 12 shows the dial in the rear cockpit.

To reduce the fire hazard and to simplify installation, fuel is supplied from a small tank located on the outer wall of the tunnel, feeding by gravity to the engine carburetor. The gravity tank is filled from a large storage tank by an electric gear pump which is started and stopped by an automatic float switch in the gravity tank.



FIG. 10

#### PROPELLER BLADE DEFLECTION

Propeller blade deflections are measured as follows. A telescope with cross hairs, in conjunction with a prism, is mounted on a lathe bed beneath the propeller being tested. One blade of the propeller at a time is painted black and a black background is painted on the ceiling. Two lights are arranged so that their beams strike the propeller blade. On sighting through the telescope no image will be seen when the black blade passes the black background; but when the white or bright metal blade passes, a line of the leading or trailing edge will appear. By locating the cross hairs successively on these lines and reading the distance moved it is possible to compute the angular deflection of the propeller blade at any given radius. Further development of this apparatus is in process.



### MANOMETER

For routine testing, velocities are calculated from the readings of an N. A. C. A. micro-manometer, one side of which is connected to plates set in the walls of the return passage and entrance cone, and the other side open to the air in the test chamber.

### SPEED REGULATOR

An air-speed regulator has been developed to insure a uniform dynamic pressure, but to date its use has not been found necessary.

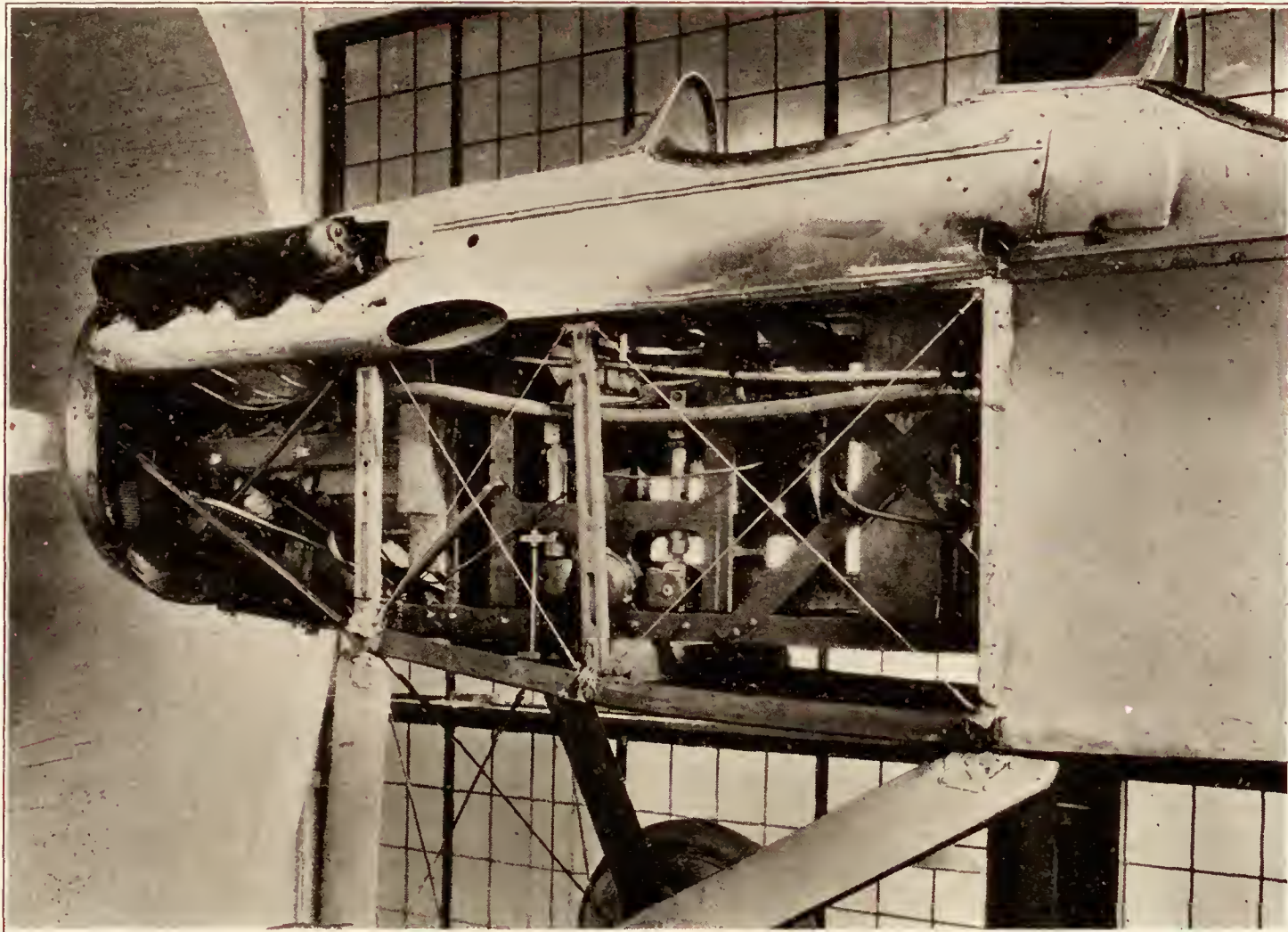


FIG. 11

### ENGINE STARTER

For starting an airplane engine mounted on the balance, an electric starter is secured to the entrance cone shown in Figures 12 and 13. A hollow shaft with a pin meshing with a dog on the propeller shaft is driven by means of a chain from an electric motor. The whole unit is arranged to swing down clear of the air stream during a test.

### CALIBRATIONS

A velocity survey has been made over the entire cross section of the air stream at a point about 6 ft. back of the entrance cone edge. Seventy-nine points were taken at 2 ft. intervals. The velocity without a honeycomb or air straightener was found to be constant within 1 per cent over the test area. This is attributed to the large reduction of area in the entrance cone. Large variations of velocity at the entrance to the cone are greatly reduced by the rapid acceleration through it. In consequence, while provision was made in the structure for the installation of a honeycomb, none has been deemed necessary.

The wall plates and manometer are calibrated from time to time against a group of Pitot tubes set in the air stream. These are attached to a movable frame to which one or more Pitot



tubes may be attached and the velocity at any point in the air stream determined without a special installation. In particular, this apparatus is used to measure the velocities in the plane of the airplane propeller.

The tunnel was designed to give a velocity of 100 M. P. H. with an energy ratio of 1.2 based on the power input to the fan. A velocity of 110 M. P. H. has been obtained indicating an energy ratio higher than that assumed.

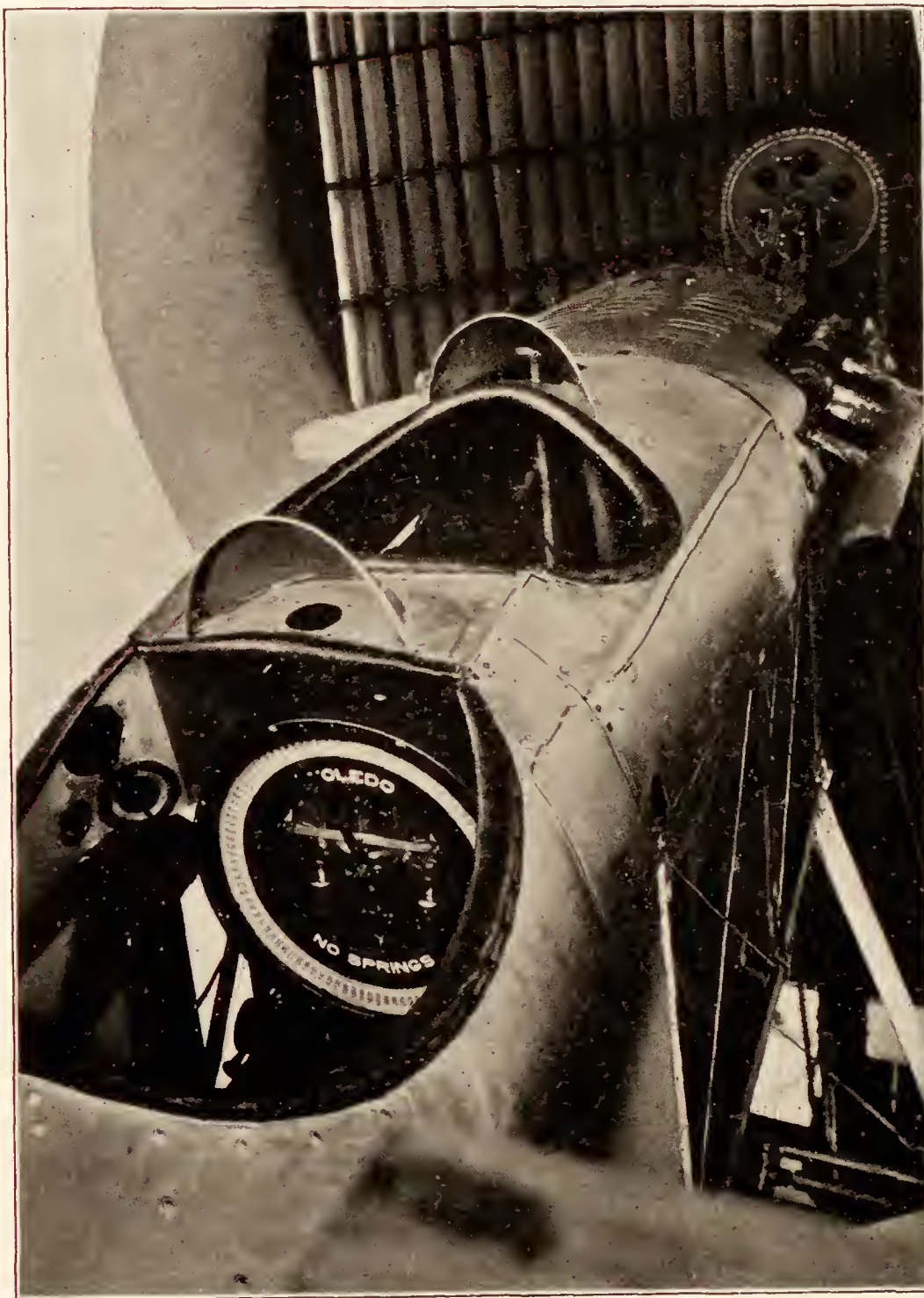


FIG. 12

Figure 13 is a view in the test chamber during a standard propeller test. Balances, manometer and deflection apparatus are shown in operation. An observer stationed in the fuselage to control the engine and read the torque scale does not appear in this view.

#### SOME RESULTS

A considerable amount of testing has already been accomplished since operation began in July, 1927. Figure 14, taken from Technical Note No. 271 (Reference 1), indicates the proportional drag of various parts of the Sperry Messenger airplane fuselage. The propeller research tunnel is particularly adapted to full scale tests of this nature. Figure 15 shows the characteristics of Propeller I, previously tested in model form at Stanford University, and in



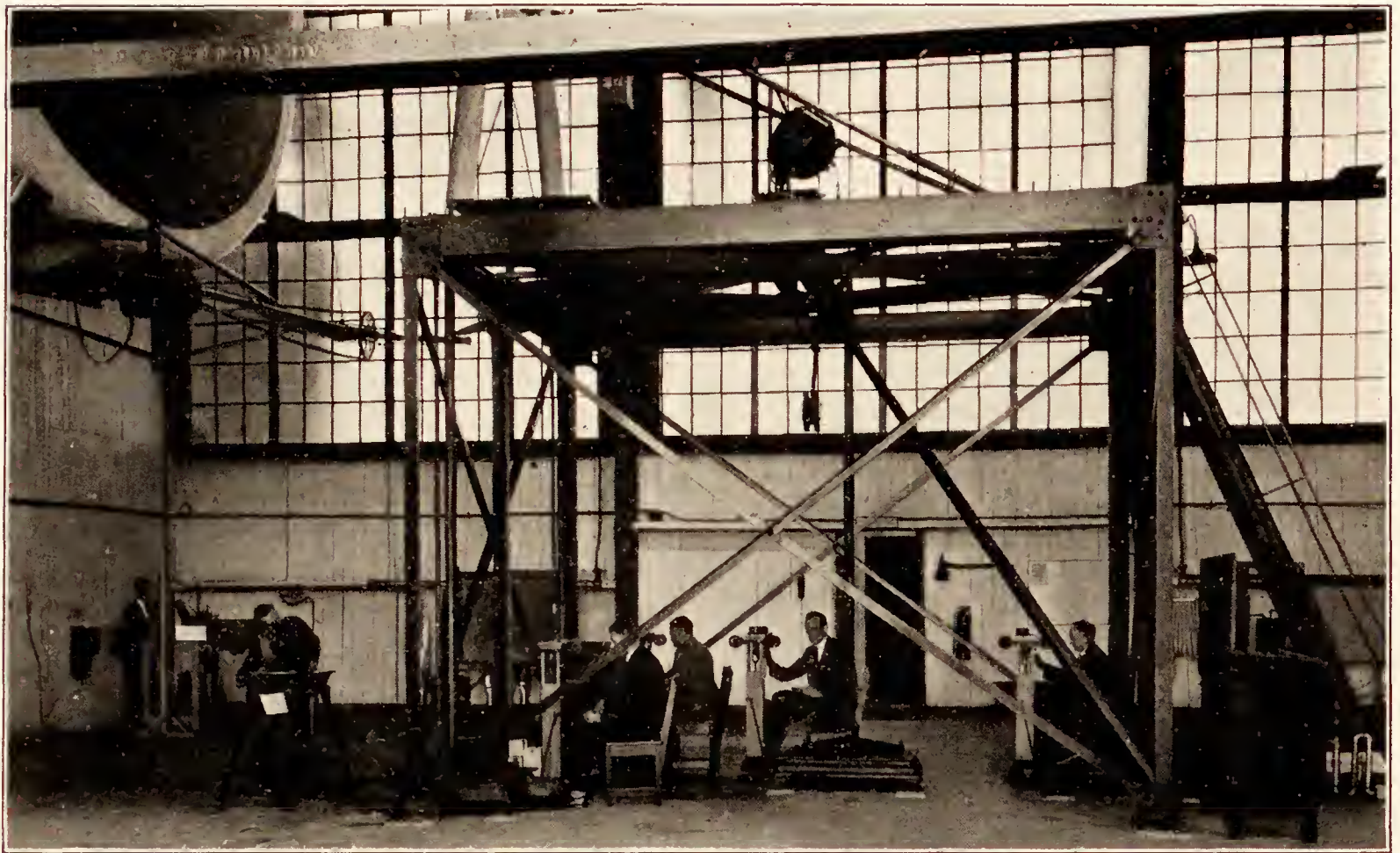


FIG. 13

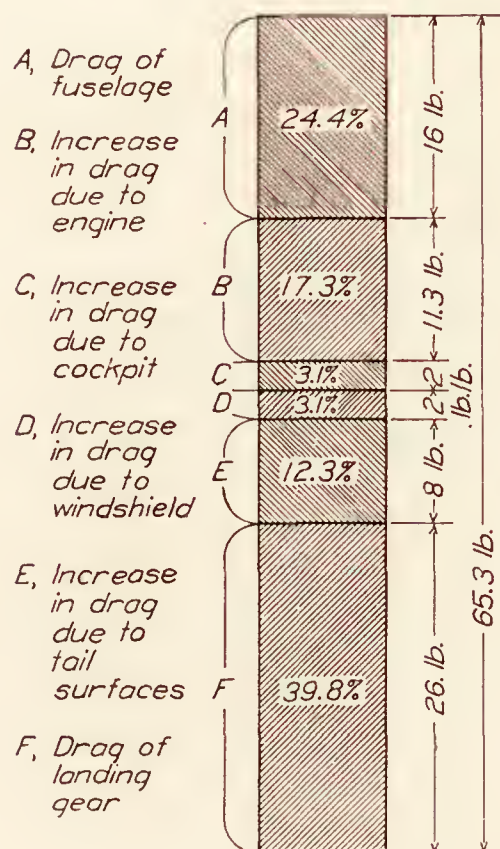


FIG. 14

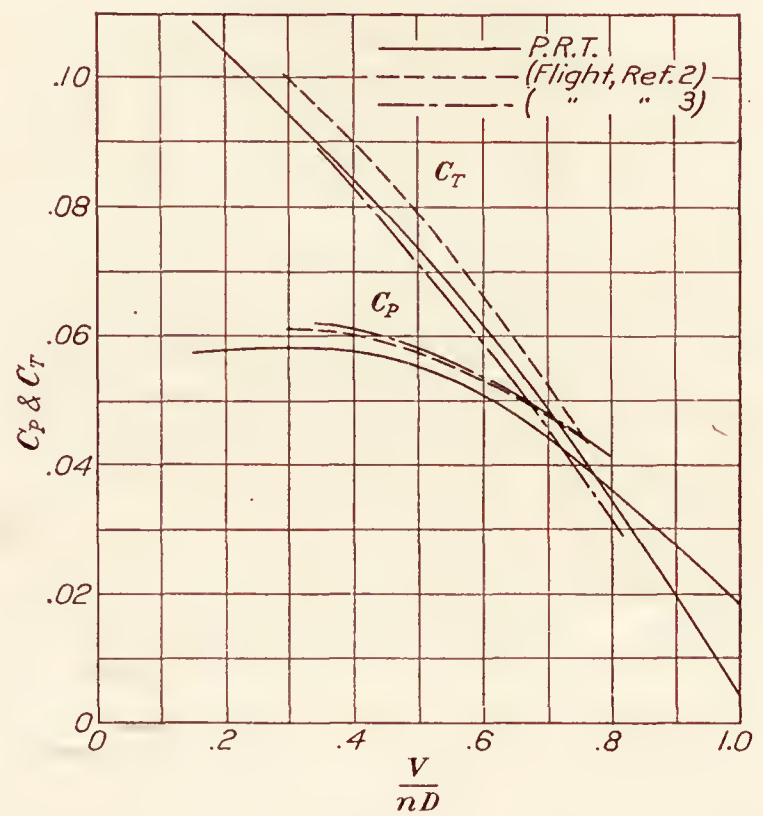


FIG. 15



two separate flight tests. (References 2 and 3.) Curves from these tests are given for comparison. Attention is called to the inaccuracy of flight data mentioned in the introduction to this paper. Tests of wings of 12 ft. span have also been made at speeds up to 100 M. P. H. A comparatively high Reynolds Number is thus attained. Figure 16 is a view of a wing set up for test. A comprehensive program of tests to determine the effect of propellers on air-cooled engines operating in front of various types of fuselages with several shapes of cowling is now in progress. The effect of these bodies on the propeller is also being determined.

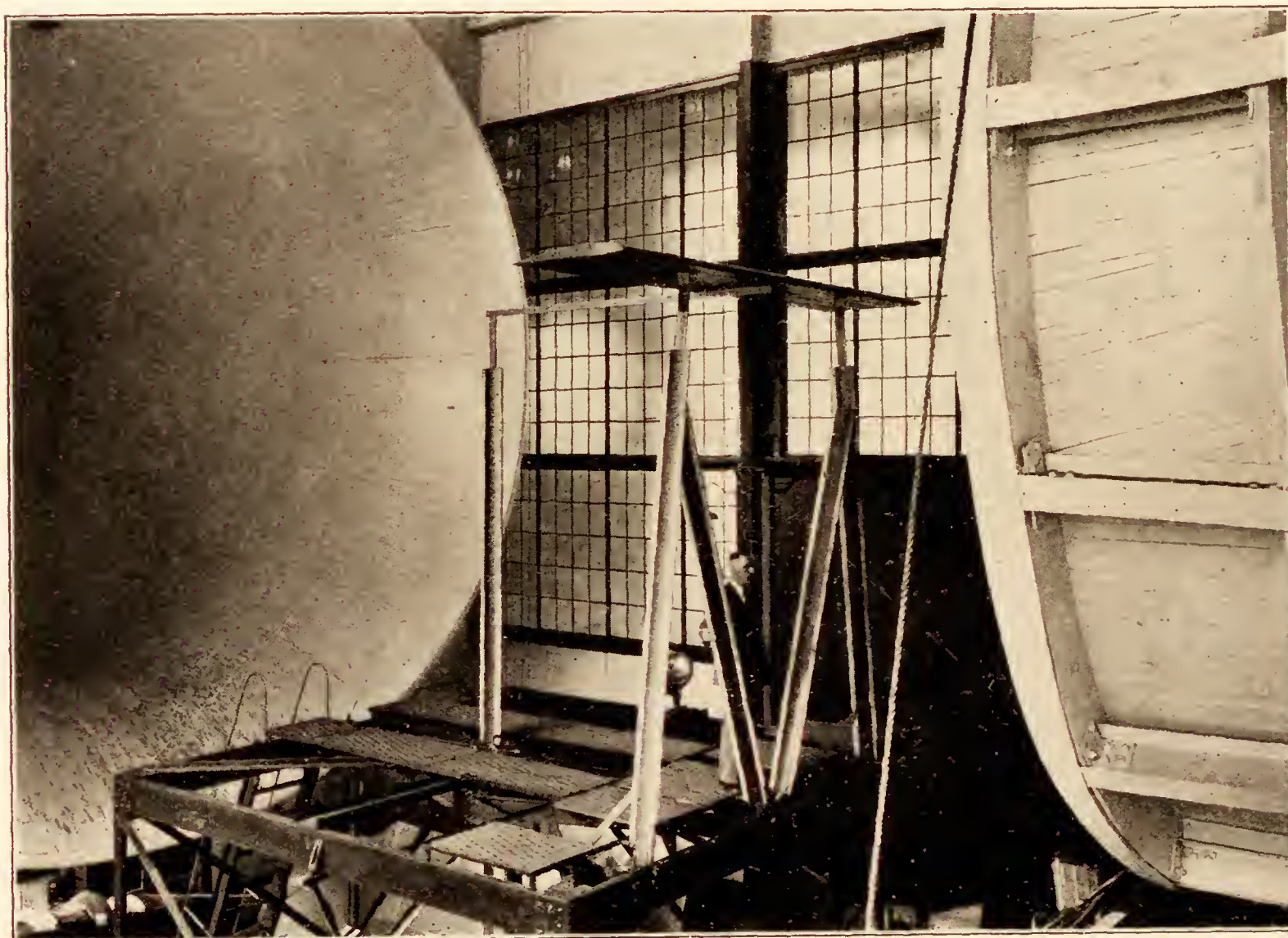


FIG. 16

### ACCURACY

Dynamic pressure, thrust, torque, and R. P. M. are measured with an accuracy of from 1 to 2 per cent. Computed data are, therefore, correct to approximately plus or minus 2 per cent and final faired curves through computed points to about plus or minus 1 per cent. This compares favorably with other engineering measurements. The beam thrust balance is to be replaced with a dial scale which will increase the accuracy and will enable the observers to read more quickly and more nearly simultaneously. A change in the linkage of the torque scale is contemplated which will increase the accuracy of that reading. When these changes are in effect it is hoped that computed points will be correct to plus or minus 1 per cent.

### CONCLUSION

The propeller research tunnel fulfills a long-felt want in aerodynamic research. Propellers can be tested full scale, and with actual engines and bodies in place, with an accuracy not attained in flight tests. The components of the airplane, fuselage, landing gear, and tail surfaces can be tested full scale. While full size wings can not be accommodated, a stub wing can be installed which is sufficient to study the effects of all parts of the airplane on the propulsive

system, and vice versa. Tests thus far made are consistent and reliable and it is increasingly evident that the propeller research tunnel is a useful addition to the extensive research facilities of the National Advisory Committee for Aeronautics.

LANGLEY MEMORIAL AERONAUTICAL LABORATORY,  
NATIONAL ADVISORY COMMITTEE FOR AERONAUTICS,  
LANGLEY FIELD, VA., *June 2, 1928.*

#### REFERENCES

- Reference 1. Weick, Fred E.: Full Scale Drag on Various Parts of Sperry Messenger Airplane. N. A. C. A. Technical Note No. 271, 1928.
- Reference 2. Durand, W. F., and Lesley, E. P.: Comparison of Tests on Air Propellers in Flight with Wind Tunnel Model Tests on Similar Forms. N. A. C. A. Technical Report No. 220, 1926.
- Reference 3. Crowley, J. W., jr., and Mixson, R. E.: Characteristics of Five Propellers in Flight. N. A. C. A. Technical Report No. 292, 1928.
- Reference 4. Glauert, H., and Locke, C. N. H.: On the Advantages of an Open Jet Wind Tunnel for Airscrew Tests. B. A. C. A. R. & M. 1033, 1926.
- Reference 5. Durand, W. F.: Experimental Research on Air Propellers. N. A. C. A. Technical Report No. 14, 1917.



---

# **REPORT No. 301**

---

## **FULL SCALE TESTS OF WOOD PROPELLERS ON A VE-7 AIRPLANE IN THE PROPELLER RESEARCH TUNNEL**

**By FRED E. WEICK**

**Langley Memorial Aeronautical Laboratory**





## REPORT No. 301

---

### FULL SCALE TESTS OF WOOD PROPELLERS ON A VE-7 AIRPLANE IN THE PROPELLER RESEARCH TUNNEL

By FRED E. WEICK

---

#### SUMMARY

*The investigation described in this report was made primarily to afford a comparison between propeller tests in the new Propeller Research Tunnel and flight tests and small model tests on propellers. Three wood propellers which had been previously tested in flight on a VE-7 airplane, and of which models had also been tested in a wind tunnel, were tested again on a VE-7 airplane in the Propeller Research Tunnel. The results of these tests are in fair agreement with those of the flight and model tests.*

*Tests were also made with the tail surfaces removed, and with both the wings and tail surfaces removed. It was found that the effect of the tail surfaces on the propeller characteristics was negligible, but that the wings reduced the maximum propulsive efficiency about 5 per cent.*

#### INTRODUCTION

Heretofore aerodynamic tests on propellers have been made either in flight or on small models in a wind tunnel. Full scale tests are highly desirable, but flight tests to obtain the aerodynamic characteristics of propellers are difficult to make and have not been sufficiently accurate to be useful in bringing out small differences in propellers.

The tests reported in this paper are the first wind-tunnel investigations on full-size propellers. They were made in the 20-foot Propeller Research Tunnel of the National Advisory Committee for Aeronautics, which is described in detail in Reference 1. Three wood propellers of standard Navy form were tested on a Vought VE-7 airplane with a Wright 180 HP. E-2 engine. These particular propellers were selected for this investigation because they had been previously tested on a VE-7 airplane in flight (References 2 and 3) and models of the propellers had also been tested with a model VE-7 airplane in the Stanford University wind tunnel; thus, a direct comparison of the full-scale wind tunnel results with the results of the flight and the model tests was afforded.

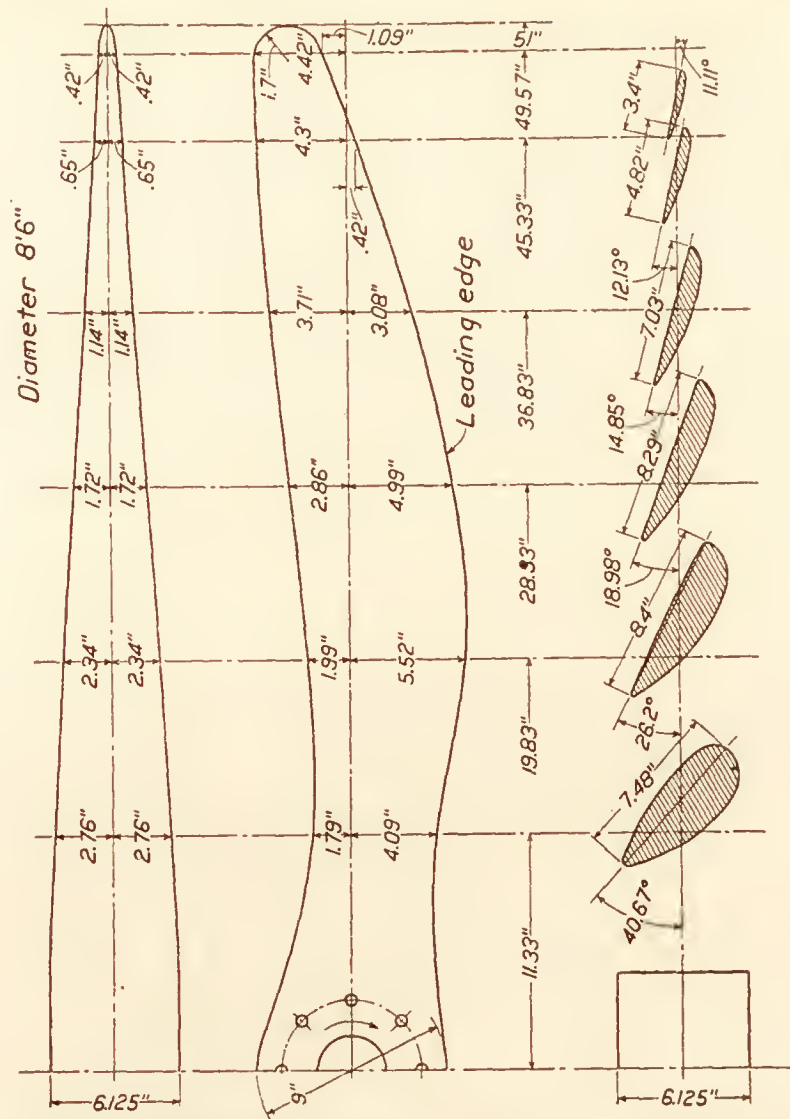
In addition to the aerodynamic characteristics of the three propellers on the complete airplane, the effects of the wings and tail surfaces on the characteristics of one propeller were measured at one angle of attack. Also, the angle of twist of one section of each propeller was measured in operation.

#### METHODS AND APPARATUS

The Propeller Research Wind Tunnel is of the open jet type with an airstream 20 feet in diameter, in which velocities up to 110 M. P. H., can be obtained. A complete description of the tunnel, balances, and other measuring apparatus is given in Reference 1.

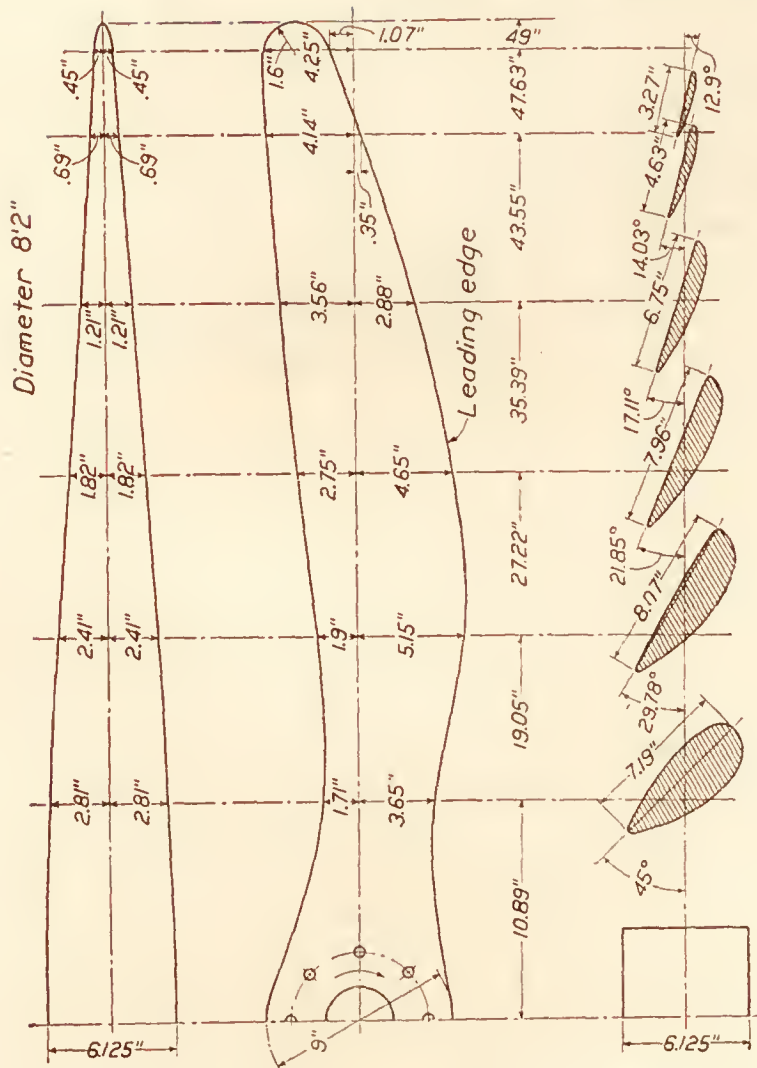






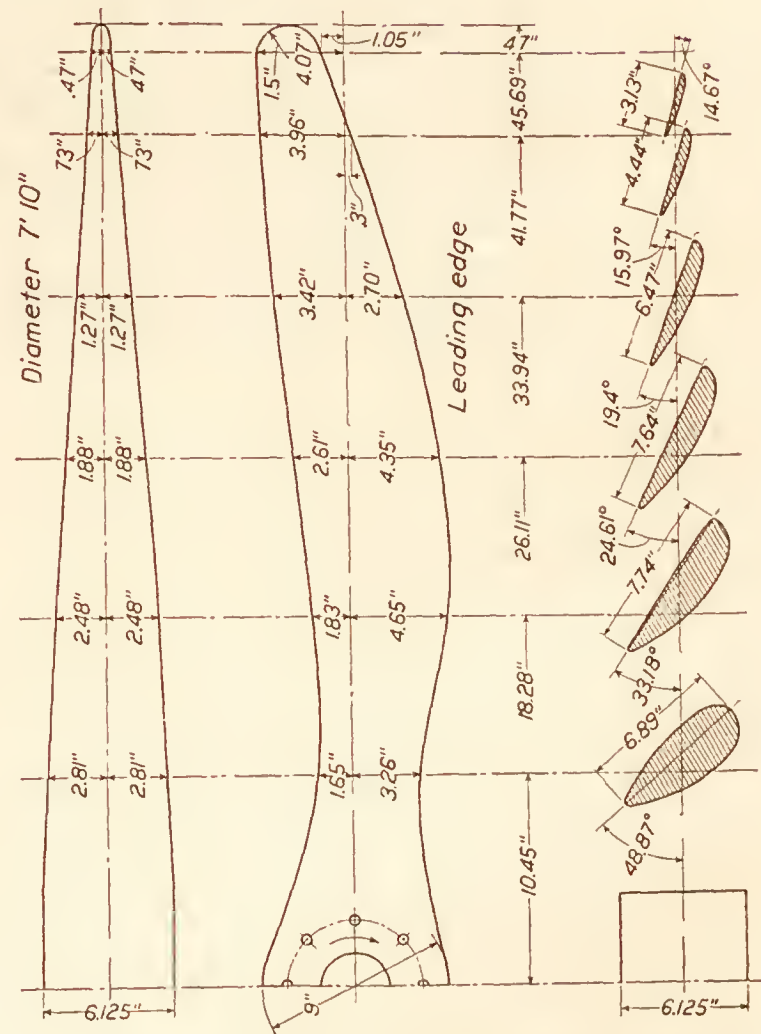
Pitch: 5' 1.2". Pitch ratio: 0.6. Aspect ratio: 6. Camber ratio: Minimum +20 per cent. Rotation: Right hand.

FIG. 3.—Experimental propeller B' for VE-7 airplane



Pitch: 5' 8.6". Pitch ratio: 0.7. Aspect ratio: 6. Camber ratio: Minimum +20 per cent. Rotation: Right hand.

FIG. 4.—Experimental propeller I for VE-7 airplane



Pitch: 6' 3.2". Pitch ratio: 0.8. Aspect ratio: 6. Camber ratio: Minimum +20 per cent. Rotation: Right hand.

FIG. 5.—Experimental propeller D' for VE-7 airplane



The VE-7 airplane (fig. 1) had a span of 34 feet. When mounted in the center of the air stream the wings projected approximately 7 feet outside the air stream. Figure 2 is a photograph of the airplane mounted in the experiment chamber. It is considered that a sufficient portion of the wing structure was in the air stream to include all parts which would react on or be influenced by the propeller.

The general dimensions of the three propellers tested are given in Figures 3, 4, and 5, and the ordinates of the various sections shown in the drawings are given in Table I. The propellers, which are of standard Navy wood type, form a series varying in pitch ratio. Propeller I, the central one of the series, has a ratio of pitch to diameter of 0.7, and the other two propellers, B' and D', have pitch ratios of 0.6 and 0.8, respectively. The blade width, thickness, and angle were measured for each section of each propeller after the tests were completed. In nearly all cases the measured blade widths and thickness were about  $\frac{1}{16}$  inch greater than those shown on the drawings, probably due to the fabric with which the propellers were covered. The measured blade angles over the working section or outer portion of the blade averaged

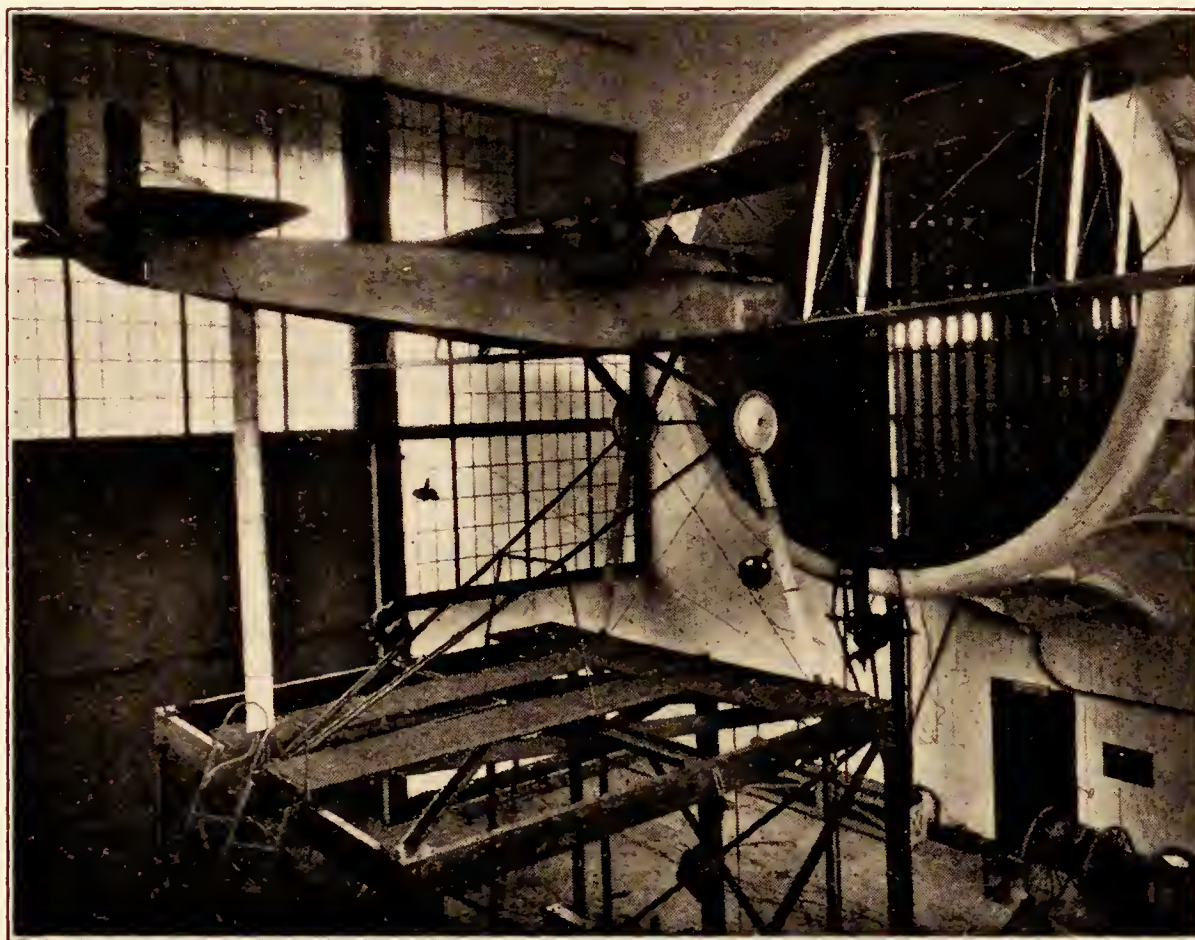


FIG. 2.—The VE-7 airplane mounted on balance of Propeller Research Tunnel

$0.3^\circ$  less than the drawing for propeller B',  $0.5^\circ$  greater than the drawing for propeller I, and the same as the drawing for propeller D'.

The VE-7, as mounted in the tunnel, had inclosed within it a special steel skeleton fuselage with a built-in dynamometer scale to measure the engine and propeller torque directly. (Reference 1.) The engine was mounted in such a manner that it was free to turn about its own axis, but was restrained by means of a torque arm and system of knife-edge linkages leading to a Toledo scale dial, upon which the torque was indicated directly in pound-feet.

The revolution speed of the engine was measured by means of a special Elgin tachometer which, according to calibration, is accurate within  $\pm 2$  R. P. M., although during the present tests it was not possible to read it within less than 5 R. P. M. An observer sat in the rear cockpit throughout the tests to operate the engine and read the torque scale and the tachometer. The velocity of the air stream was obtained by means of calibrated static plates.

In order to know the pitch of the propellers in operation, the deflection of one blade of each propeller was measured at the 36-inch radius, by means of a telescope mounted on a graduated base and sighted on first the leading and then the trailing edge. This was done



while the propeller was standing still and then was repeated for each test point while the propeller was running.

The resultant horizontal force of the propeller-body combination, which may be either a thrust or a drag, was measured on the regular thrust balance (also described in Reference 1).

This resultant horizontal force  $R$  may be thought of as composed of three horizontal components, such that

$$R = T - D - \Delta D,$$

where

$T$  = the thrust of the propeller while operating in front of the body (the tension in the crank shaft).

$D$  = the drag of the airplane alone (without propeller) at the same air velocity and density.

$\Delta D$  = the increase in drag of the airplane with propeller, due to the slip stream.

In order to obtain the propulsive efficiency, which includes the propeller-body interference, an effective thrust is used which is defined as

$$\text{Effective thrust} = T - \Delta D = R + D.$$

The propulsive efficiency is the ratio of the useful power to the input power, or

$$\text{Propulsive efficiency} = \frac{\text{Effective thrust} \times \text{Velocity of advance}}{\text{Input power}}$$

## RESULTS

The results of the tests are given in Figures 6 to 10, inclusive, and in Tables II and III. They are reduced to the usual thrust and power coefficients and plotted against  $\frac{V}{nD}$  for convenience in comparing them with the results of flight and model tests. These coefficients are:

$$C_T = \frac{\text{Effective thrust}}{\rho n^2 D^4}$$

$$C_P = \frac{\text{Power}}{\rho n^3 D^5}$$

$$\eta = \text{Propulsive efficiency}$$

$$= \frac{\text{Effective thrust} \times \text{Velocity}}{\text{Power}}$$

where  $D$  = propeller diameter and  $n$  = revolutions per unit time. Any homogeneous system of units may be used with these coefficients. The propeller characteristics are also given in terms of two other coefficients (sometimes called speed-power coefficients) in Table III.

The points in Figures 6 to 10 have been calculated directly from the observed data. Their dispersion, which it will be noticed is small, is in a general way a measure of the accuracy of the observations.

The angular deflections of one blade of each propeller are plotted against  $\frac{V}{nD}$  in Figures 6, 7, and 8. In general, the deflections of all of the propellers were small. Throughout the working range of  $\frac{V}{nD}$ , propeller B' had an average increase of blade angle of about  $0.4^\circ$  which, with its initial set of  $-0.3^\circ$ , brought the angles in operation very close to the drawing values. The average curve through the points for propeller I shows practically no twist in operation, leaving the blade angles as they were measured,  $0.5^\circ$  too high. Propeller D' checked the drawing without load, and averaged about  $0.2^\circ$  less in operation. The accuracy of the individual deflection measurements is apparently  $\pm 0.5^\circ$ , and the faired curves are probably correct to within  $\pm 0.2^\circ$ .

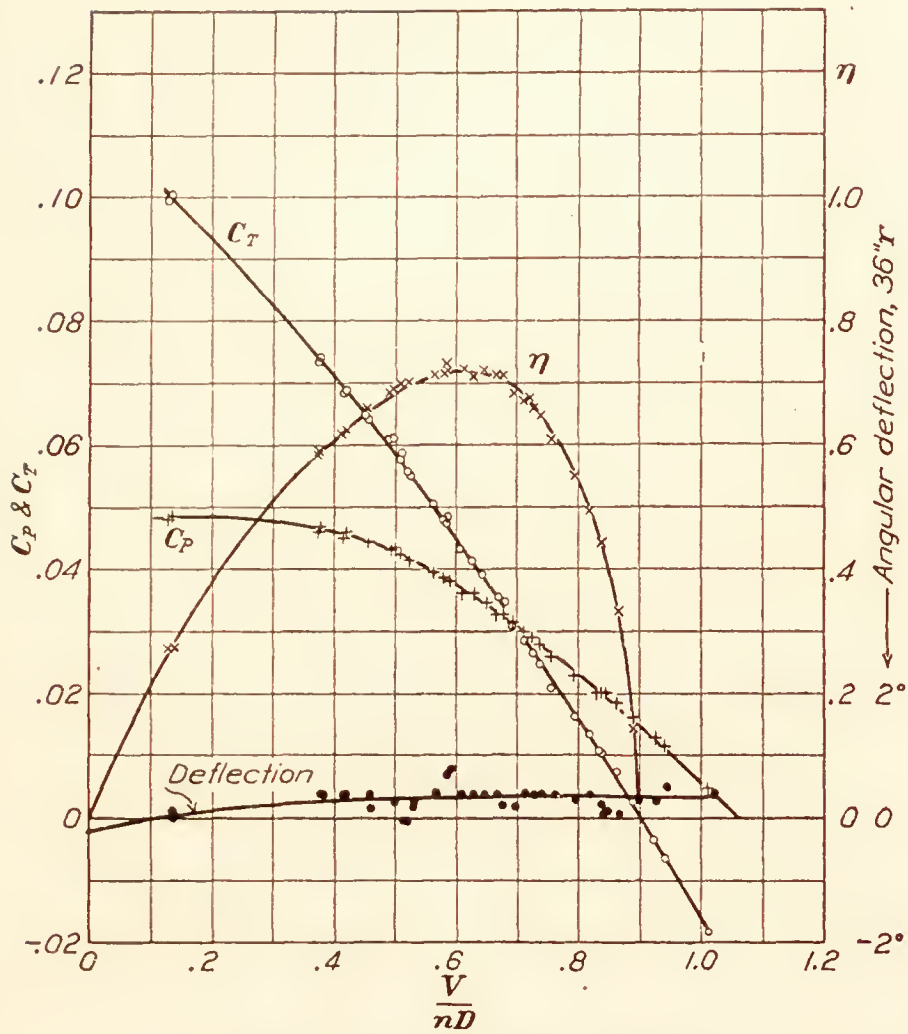


FIG. 6.—Propeller B' with VE-7 airplane

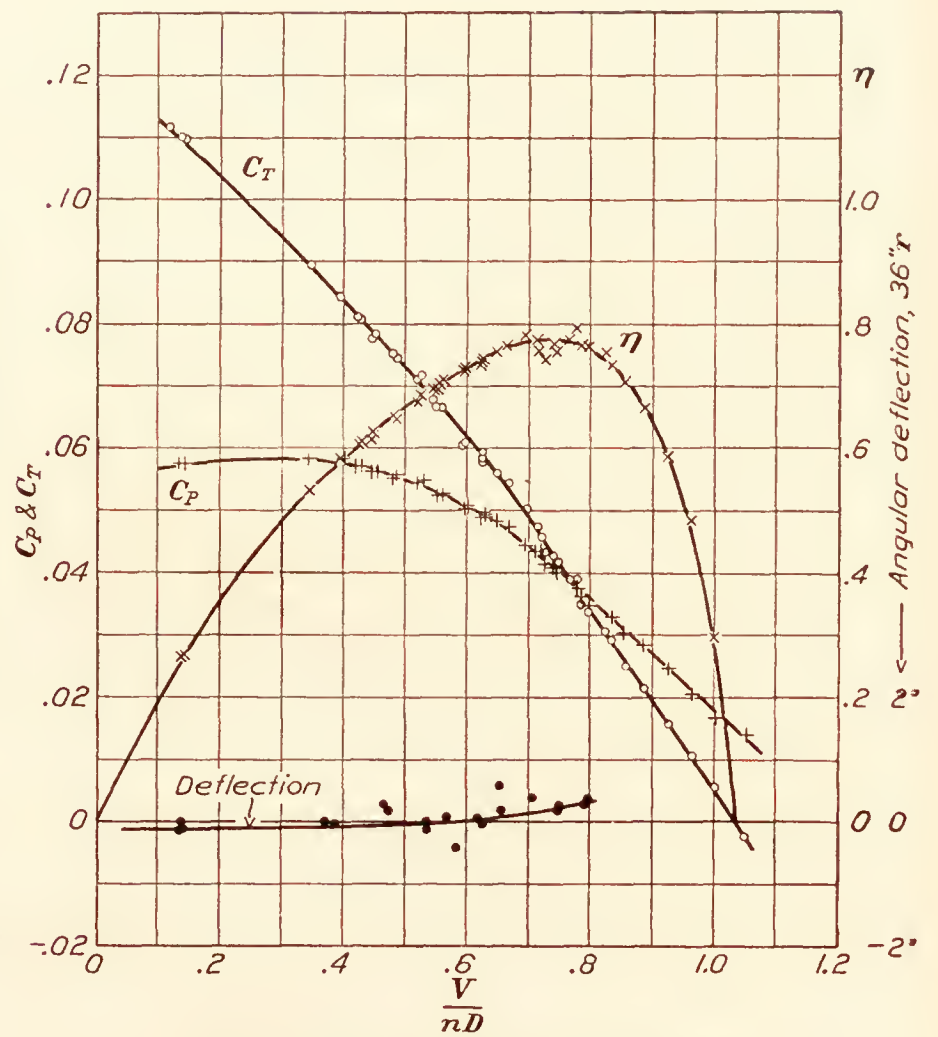


FIG. 7.—Propeller I (3714) with VE-7 airplane

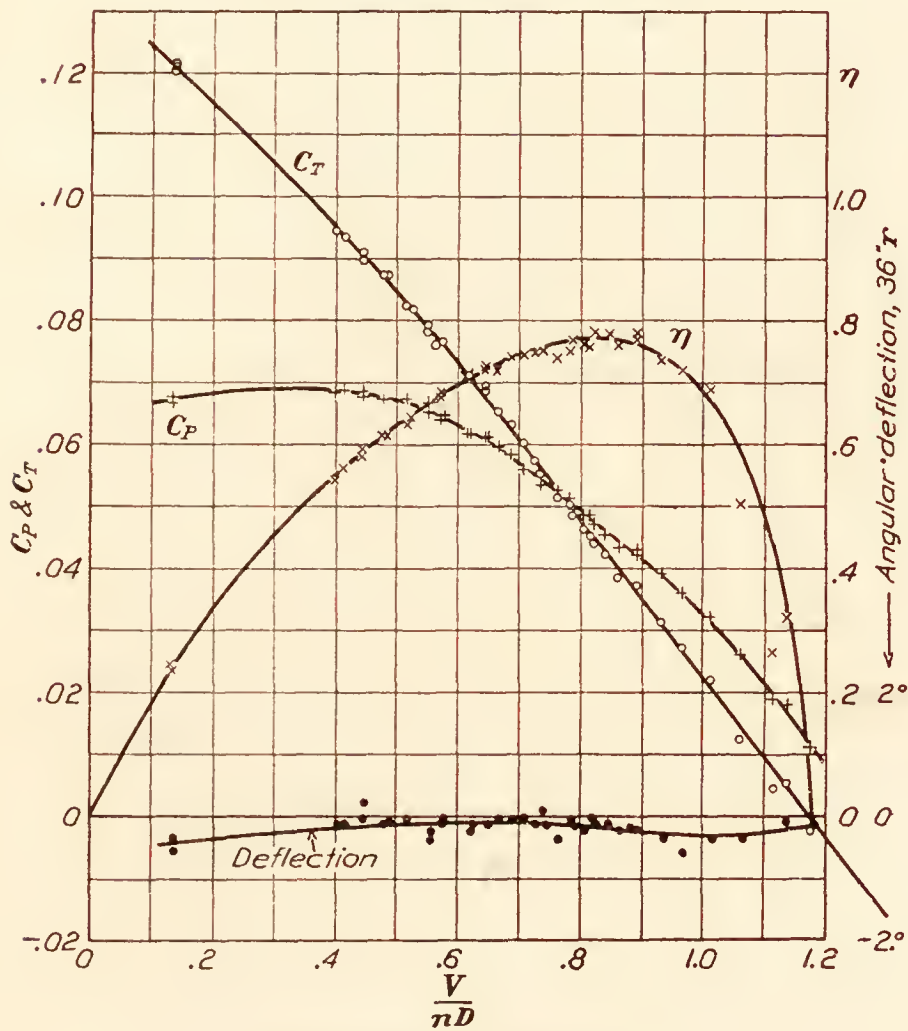


FIG. 8.—Propeller D' with VE-7 airplane

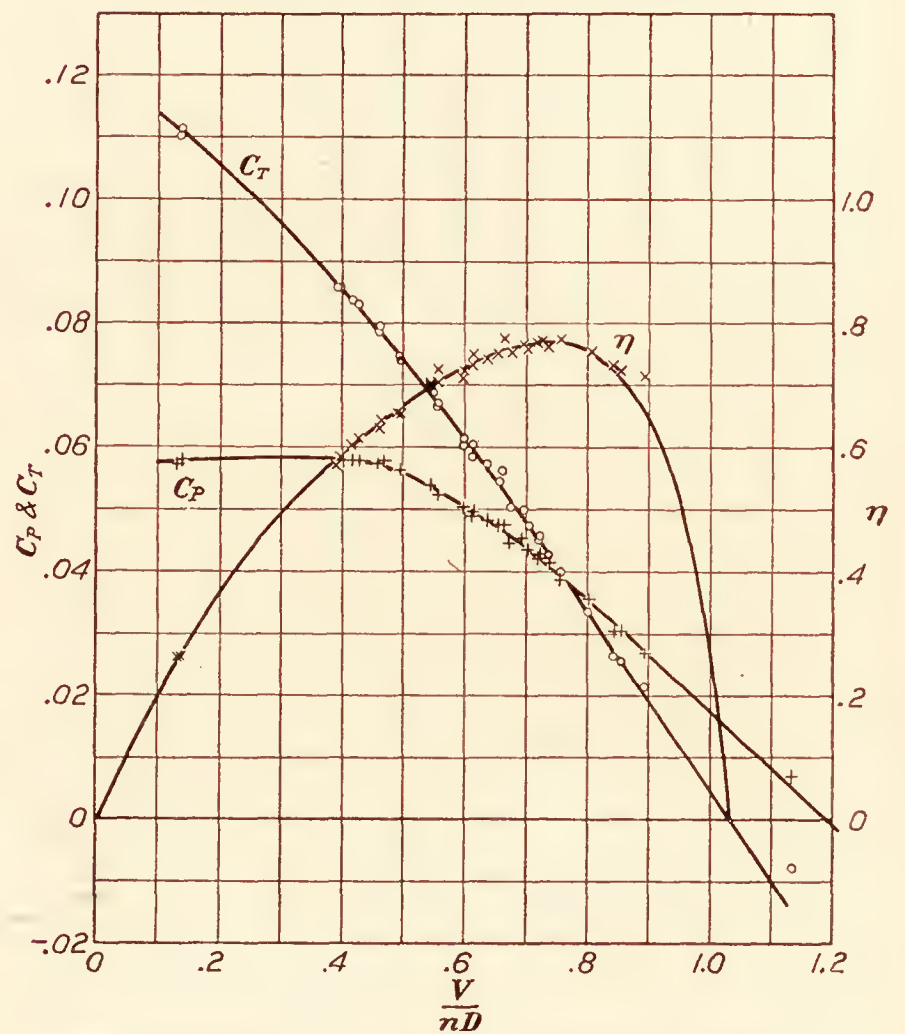


FIG. 9.—Propeller I (3714) with VE-7 airplane, without tail surfaces



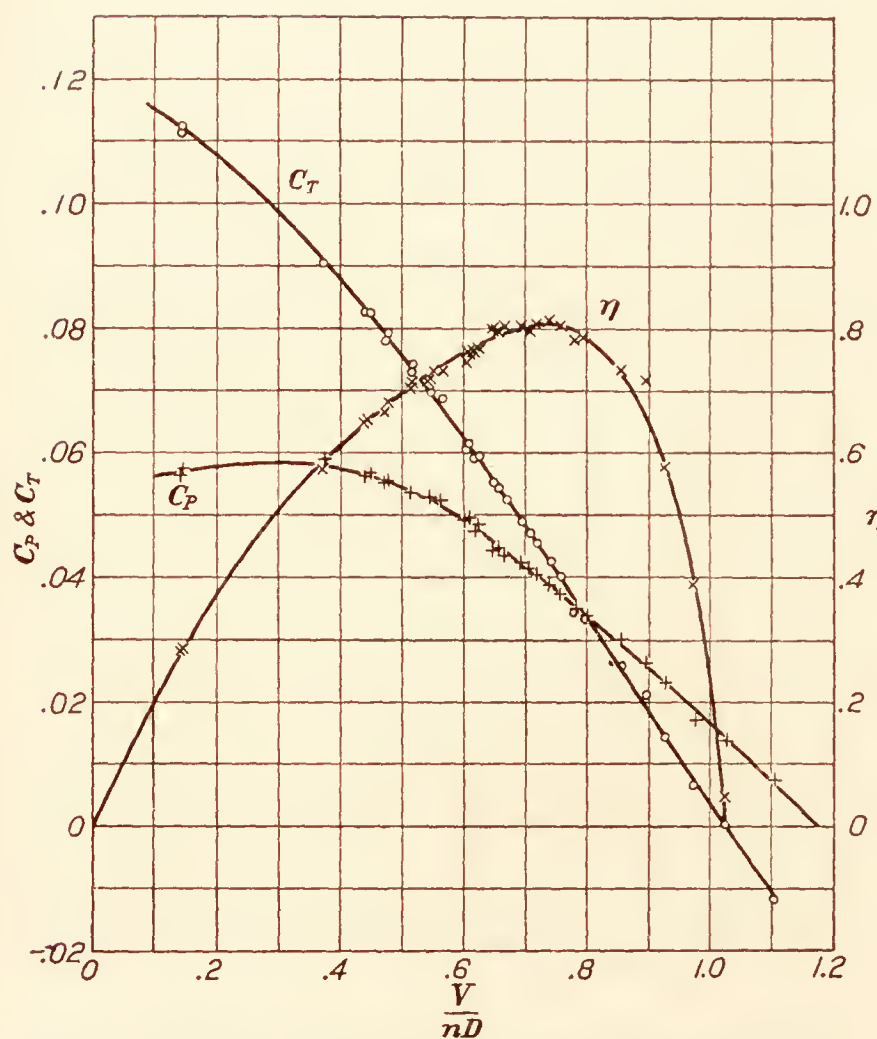


FIG. 10.—Propeller I (3714) with VE-7 airplane, without wings or tail surface

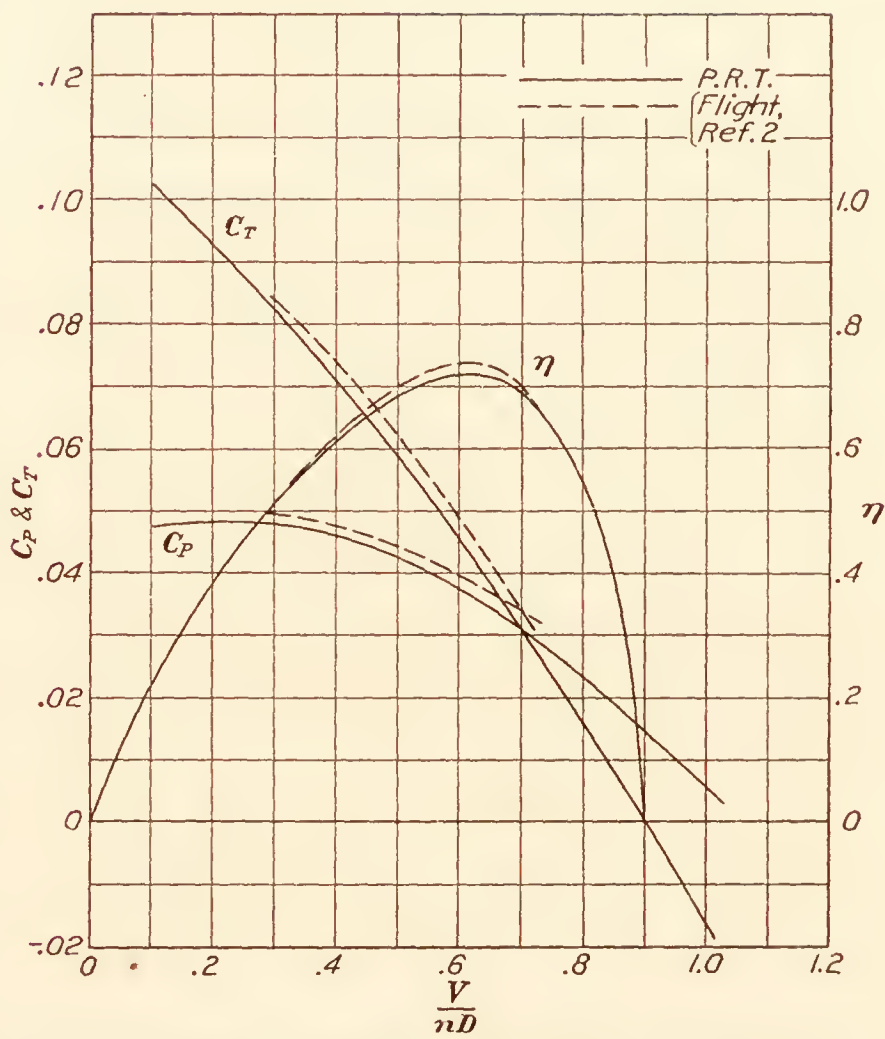


FIG. 11.—Comparison of propeller research tunnel and flight tests on Propeller B'

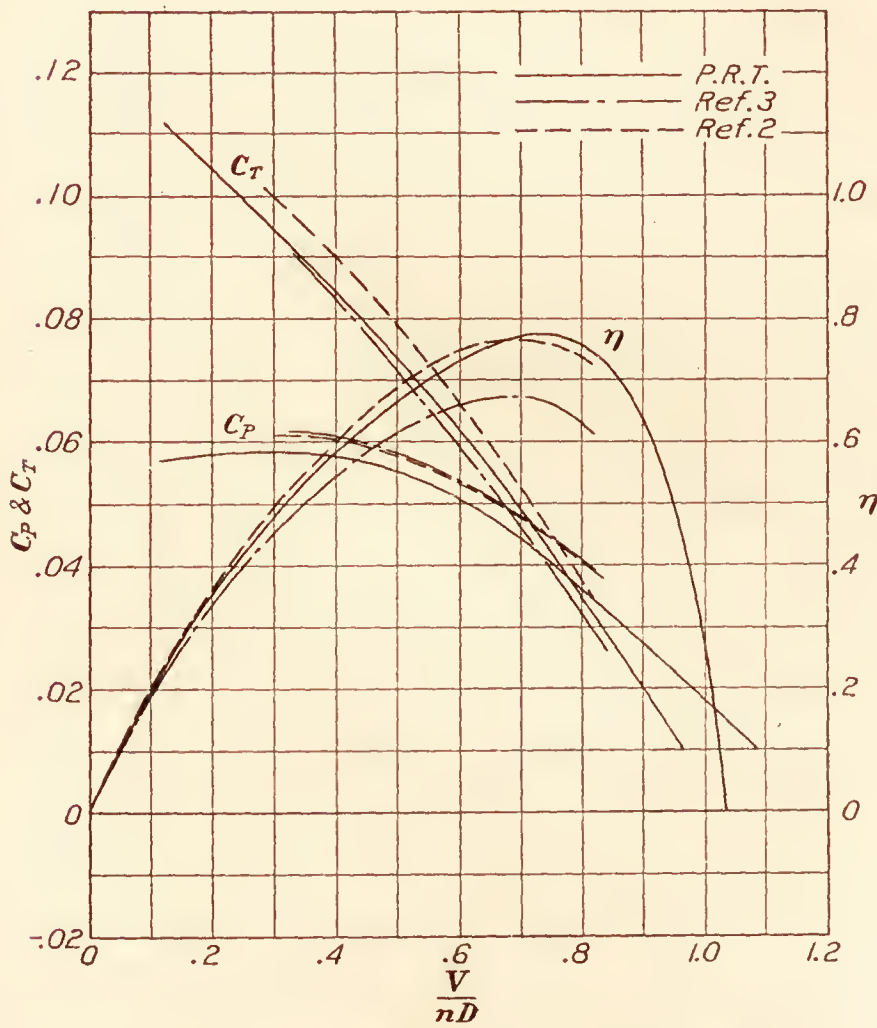


FIG. 12.—Comparison of propeller research tunnel and flight tests on Propeller I (3714)

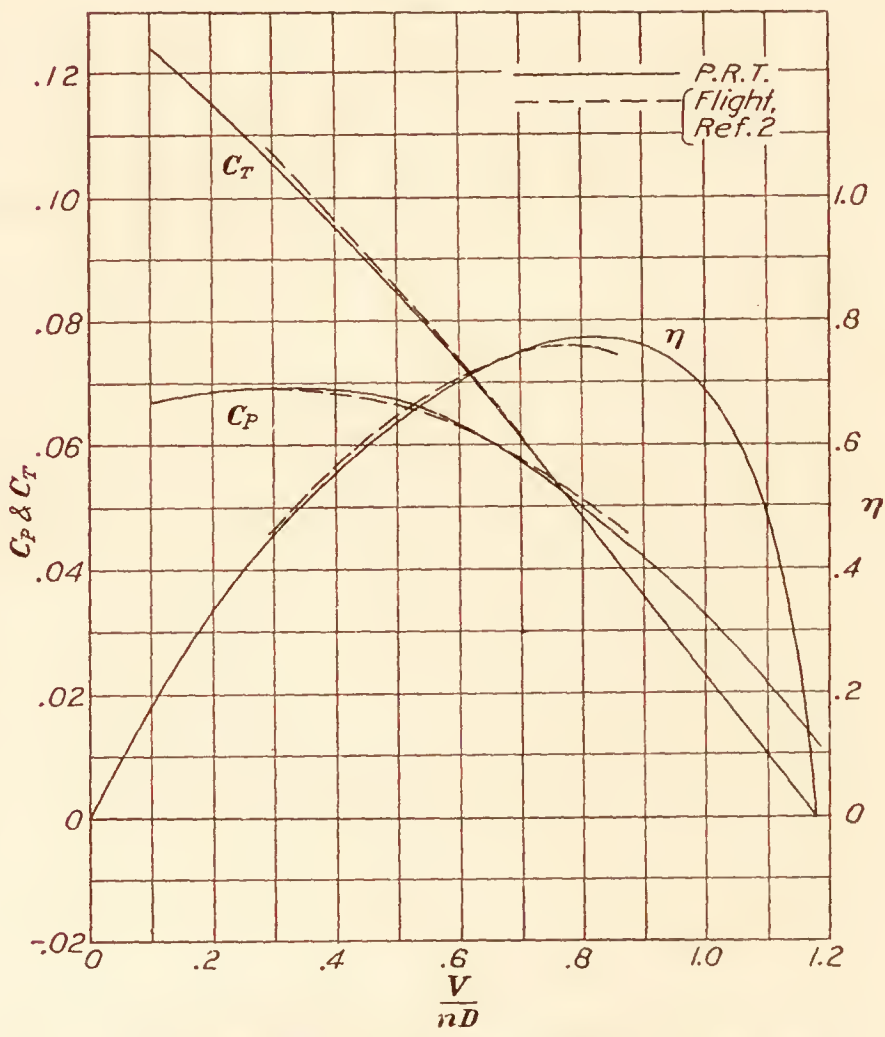


FIG. 13.—Comparison of propeller research tunnel and flight tests on Propeller D'

The present tests on the above three propellers are compared with flight tests on the same propellers (References 2 and 3) in Figures 11, 12, and 13. Propellers B' and D' are the identical ones used in the tests of Reference 2. Propeller I (3714), which is of the same design as I of Reference 2, was used in the tests of Reference 3 (and called 3714) and also in the present tests. Figures 11, 12, and 13 show that in general the agreement between the full-scale Propeller Research Tunnel tests and the flight tests is fair, probably within the limits of accuracy of the flight tests which are quite difficult to make. In three of the four tests the power coefficients from the flight tests are 3 per cent to 5 per cent higher than those obtained from the Propeller Research Tunnel tests. Since the power developed in flight was taken from a calibration of the engine made with an electric dynamometer on the ground, this difference in power coefficients indicates that the engines, when in flight, were probably not actually delivering the full power developed on the dynamometer.

One possible cause for difference between the flight tests and the full-scale wind tunnel tests is the fact that in the latter the propeller axis was kept level at all times, while in the flight tests it assumed various angles to the flight path from about zero degrees at high speed to 10 degrees near stalling speed.

In Figures 14, 15, and 16 the full-scale Propeller Research Tunnel tests are compared with tests on similar model propellers with a model VE-7 airplane (Reference 2). The model tests agree better than the flight tests with those of the Propeller Research Tunnel.

For the full-scale tests the maximum efficiency occurs at a higher  $\frac{V}{nD}$ , and in two of the three cases reaches a noticeably higher value than for the model tests. (In this connection it has been learned that later tests on the same models give somewhat higher efficiencies.) In each case the rate of advance  $\left(\frac{V}{nD}\right)$  at which zero thrust occurs is greater for the full-scale propellers, apparently indicating that the effect of scale is more pronounced in the region of the lower angles of attack of the blade elements. In general, also, the full-scale tests give higher values of the thrust and power coefficients at the lower rates of advance.

The results of the three tests made with propeller I (3714) to obtain the effect of the wings and tail surfaces on the propeller characteristics are plotted in Figure 17. The tail surfaces had no appreciable effect on the propeller characteristics, but the wings increased the power absorbed slightly and decreased the maximum propulsive efficiency approximately 5 per cent. It would naturally be expected, of course, that the effect of the wings would be different at different angles of attack.

#### CONCLUSIONS

1. These, the first complete propeller tests made in the Propeller Research Tunnel, show that the results obtained agree as well as can be expected with both flight tests and model wind tunnel tests.
2. The accuracy of the observations in the Propeller Research Tunnel tests, which are made under full-scale conditions, is apparently of about the same order as that of model propeller tests.
3. From a comparison of these tests with flight tests, it seems likely that the engines used in the flight tests delivered somewhat less power in flight than would have been expected from dynamometer tests.
4. The effect of the tail surfaces on the propeller characteristics is negligible.
5. The effect of the wings on propulsive efficiency is important and deserves further investigation.

LANGLEY MEMORIAL AERONAUTICAL LABORATORY,  
NATIONAL ADVISORY COMMITTEE FOR AERONAUTICS,  
LANGLEY FIELD, VA., *June 18, 1928.*



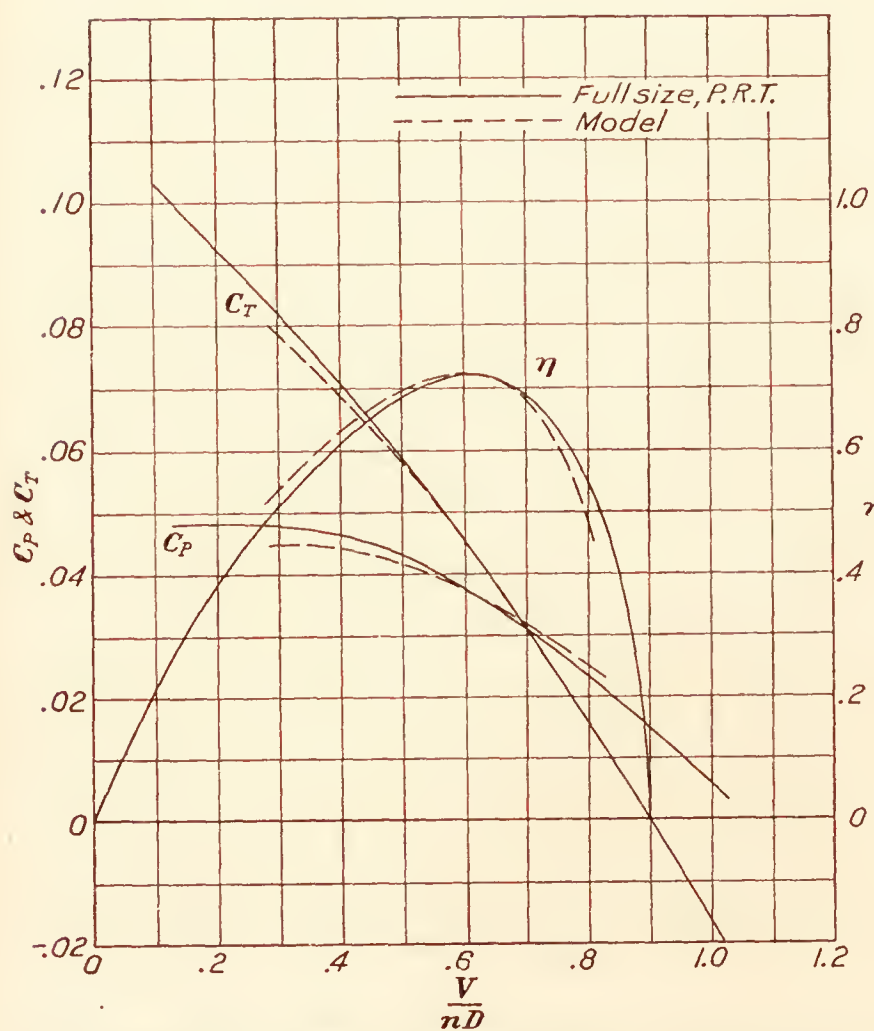


FIG. 14.—Comparison of model and full-size Propeller Research Tunnel tests on Propeller B'

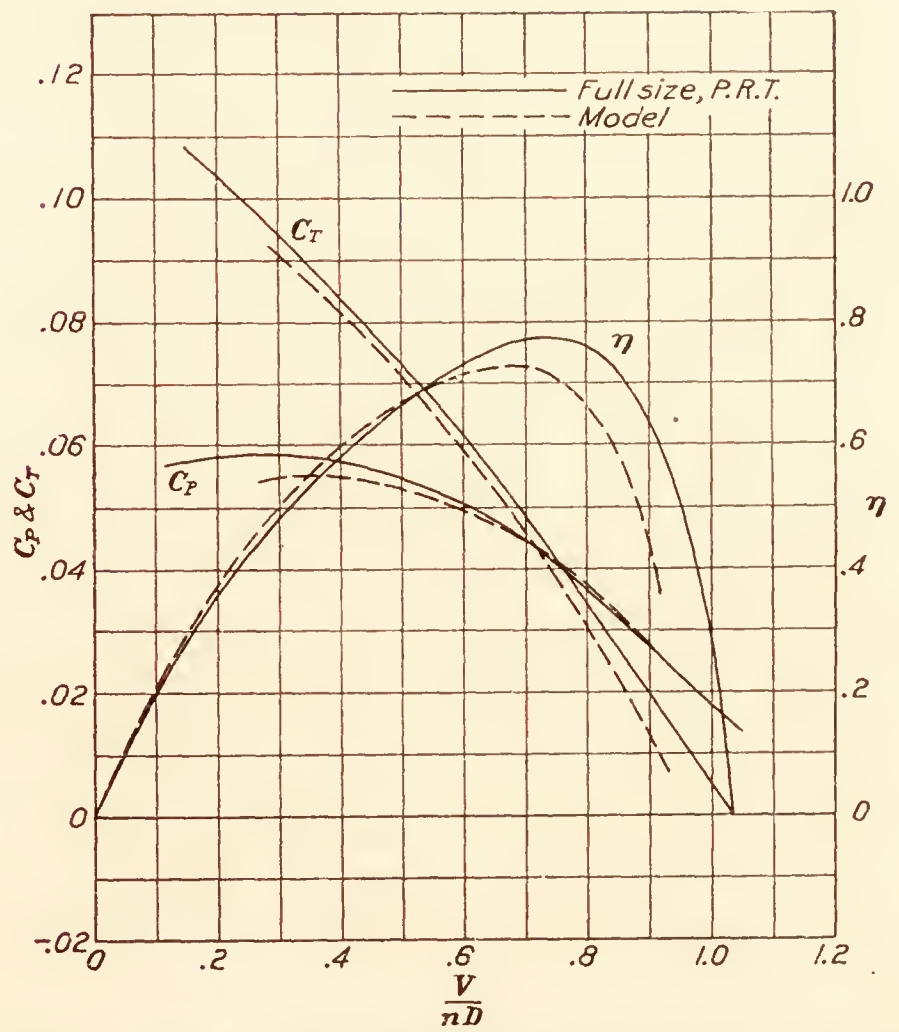


FIG. 15.—Comparison of model and full-size Propeller Research Tunnel tests on Propeller I(3714)

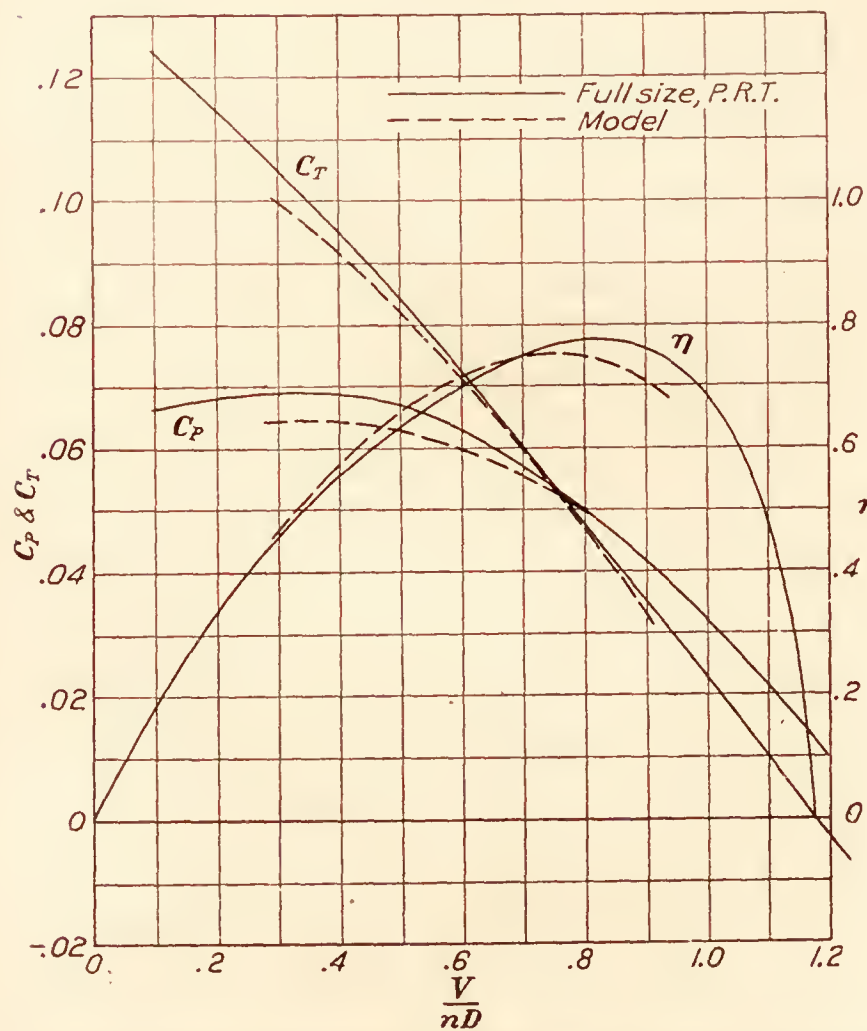


FIG. 16.—Comparison of model and full-size Propeller Research Tunnel tests on Propeller D'

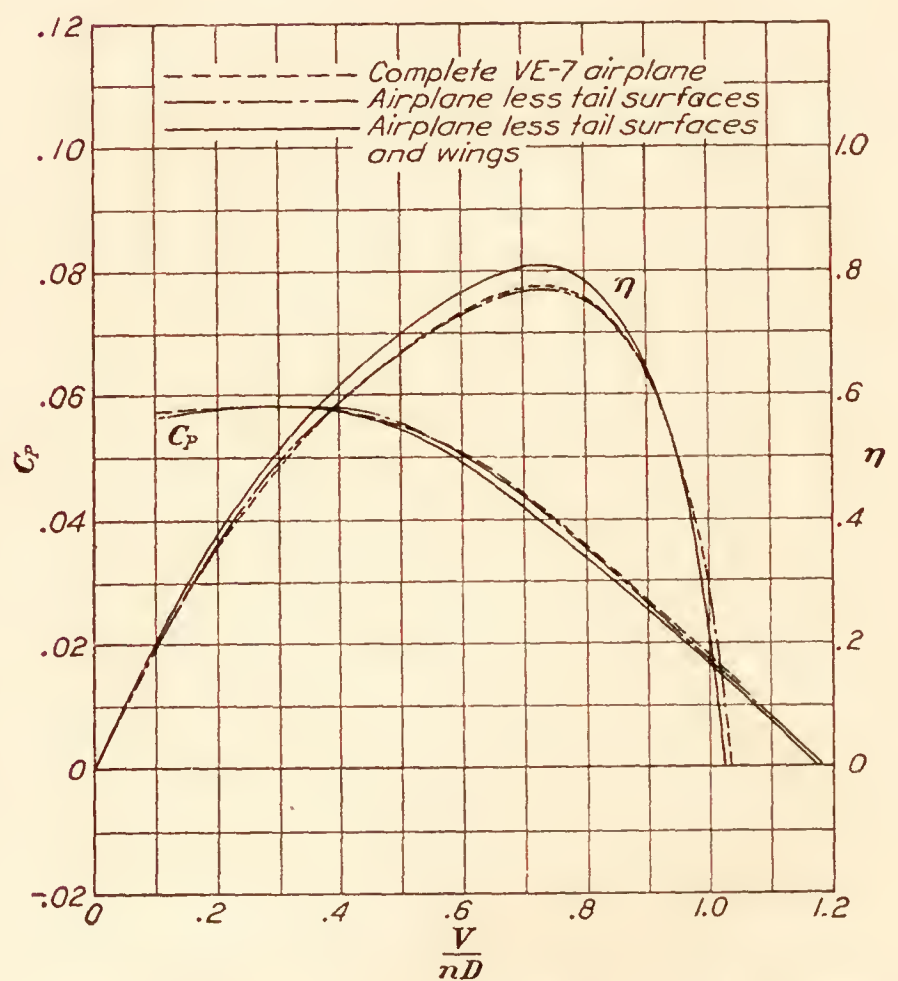


FIG. 17.—Effect of wings and tail surfaces on the performance of Propeller on VE-7 airplane (Propeller Research Tunnel tests)

TABLE I  
ORDINATES FOR SECTIONS OF PROPELLER D' (see fig. 5)

Radius_____	10. 45"		18. 28"		26. 11"	33. 94"	41. 77"	45. 69"
Camber_____	Upper	Lower	Upper	Lower	Upper	Upper	Upper	Upper
Rad. L. E____	0. 877"		0. 282"		0. 128"	0. 083"	0. 047"	0. 031"
2.5_____	0. 686	0. 410	0. 730	0. 047	. 526	. 338	. 194	. 128
5_____	. 987	. 589	1. 053	. 066	. 758	. 489	. 279	. 185
10_____	1. 322	. 790	1. 410	. 088	1. 015	. 655	. 373	. 247
20_____	1. 588	. 949	1. 692	. 106	1. 222	. 786	. 448	. 298
30_____	1. 664	. 996	1. 777	. 113	1. 285	. 830	. 473	. 313
40_____	1. 654	. 990	1. 764	. 113	1. 275	. 821	. 470	. 310
50_____	1. 588	. 949	1. 692	. 106	1. 222	. 786	. 448	. 298
60_____	1. 454	. 868	1. 551	. 097	1. 118	. 720	. 410	. 272
70_____	1. 238	. 739	1. 319	. 085	. 952	. 614	. 351	. 232
80_____	. 937	. 558	. 996	. 063	. 720	. 464	. 266	. 175
90_____	. 586	. 351	. 623	. 041	. 451	. 291	. 166	. 110
Rad. T. E____	0. 26"		0. 125"		. 098"	. 064"	. 036"	. 024"

All ordinates in inches. Station in per cent of chord.

ORDINATES FOR SECTIONS OF PROPELLER B' (see fig. 3)

Radius_____	11. 33"		19. 83"		28. 33"	36. 83"	45. 33"	49. 57"
Camber_____	Upper	Lower	Upper	Lower	Upper	Upper	Upper	Upper
Rad. L. E____	0. 952"		0. 306"		0. 139"	0. 090"	0. 051"	0. 034"
2.5_____	0. 745	0. 445	0. 792	0. 051	. 571	. 367	. 211	. 139
5_____	1. 071	. 639	1. 142	. 071	. 823	. 530	. 303	. 201
10_____	1. 435	. 857	1. 530	. 095	1. 102	. 710	. 405	. 269
20_____	1. 724	1. 030	1. 836	. 115	1. 326	. 854	. 486	. 323
30_____	1. 806	1. 081	1. 928	. 122	1. 394	. 901	. 513	. 340
40_____	1. 795	1. 075	1. 915	. 122	1. 384	. 891	. 510	. 337
50_____	1. 724	1. 030	1. 836	. 115	1. 326	. 854	. 486	. 323
60_____	1. 578	. 942	1. 683	. 105	1. 214	. 782	. 445	. 296
70_____	1. 343	. 802	1. 432	. 092	1. 034	. 667	. 381	. 252
80_____	1. 017	. 605	1. 081	. 068	. 782	. 503	. 289	. 190
90_____	. 636	. 381	. 676	. 044	. 490	. 316	. 180	. 119
Rad. T. E____	0. 280"		0. 115"		. 106"	. 071"	. 039"	. 026"

All ordinates in inches. Stations in per cent of chord.

ORDINATES FOR SECTIONS OF PROPELLER I (see fig. 4)

Radius_____	10. 89"		19. 05"		27. 22"	35. 39"	43. 55"	47. 63"
Camber_____	Upper	Lower	Upper	Lower	Upper	Upper	Upper	Upper
Rad. L. E____	0. 844"		0. 272"		0. 133"	0. 087"	0. 049"	0. 033"
2.5_____	0. 719	0. 427	0. 762	0. 049	. 550	. 357	. 204	. 133
5_____	1. 032	. 615	1. 097	. 068	. 789	. 512	. 291	. 193
10_____	1. 380	. 822	1. 470	. 092	1. 056	. 686	. 392	. 259
20_____	1. 661	. 991	1. 767	. 112	1. 271	. 825	. 471	. 310
30_____	1. 742	1. 040	1. 856	. 117	1. 337	. 866	. 495	. 327
40_____	1. 729	1. 032	1. 840	. 117	1. 326	. 860	. 490	. 324
50_____	1. 661	. 991	1. 767	. 112	1. 271	. 825	. 471	. 310
60_____	1. 522	. 906	1. 617	. 109	1. 165	. 757	. 430	. 283
70_____	1. 293	. 770	1. 377	. 087	. 991	. 642	. 367	. 242
80_____	. 980	. 582	1. 042	. 065	. 748	. 487	. 278	. 182
90_____	. 612	. 365	. 650	. 041	. 468	. 305	. 174	. 114
Rad. T. E____	0. 245"		0. 120"		. 103"	. 068"	. 038"	. 024"

All ordinates in inches. Stations in per cent of chord.



TABLE II

TEST DATA

PROPELLER B',  $\frac{p}{D}=0.6$ 

VE-7 AIRPLANE, COMPLETE

$\rho$	$V$ M. P. H.	$N$ R. P. M.	$Q$ lb. ft.	$T$ lb.	$C_T$	$C_P$	$\frac{V}{nD}$	$\eta$
0. 002289	83. 6	1, 700	556	561	0. 0588	0. 0428	0. 510	0. 700
. 002289	83. 6	1, 705	557	557. 5	. 0579	. 0427	. 509	. 689
. 002289	86. 6	1, 715	552	545	. 0559	. 0417	. 522	. 700
. 002289	86. 7	1, 715	552	541	. 0554	. 0418	. 523	. 695
. 002279	95. 7	1, 755	547	512. 5	. 0505	. 0399	. 564	. 715
. 002279	95. 7	1, 755	547	514. 5	. 0505	. 0399	. 564	. 715
. 002275	100. 6	1, 775	540	490	. 0474	. 0385	. 587	. 722
. 002275	100. 8	1, 780	540	499	. 0479	. 0382	. 585	. 734
. 002279	98. 0	1, 080	62	-27	-. 00676	. 0119	. 939	-. 555
. 002279	97. 7	1, 000	22	-61	-. 0185	. 00493	1. 010	-. 380
. 002279	99. 6	1, 120	73	-15. 5	-. 00374	. 01305	. 921	-. 264
. 002275	99. 7	1, 160	97	11. 5	. 00260	. 0162	. 889	. 1422
. 002275	99. 7	1, 200	120	34. 5	. 00728	. 0188	. 861	. 3335
. 002275	100. 2	1, 245	142	56	. 01095	. 0205	. 834	. 445
. 002275	100. 4	1, 235	137	51. 5	. 01030	. 0202	. 841	. 430
. 002275	99. 8	1, 270	160	72	. 01358	. 0223	. 814	. 496
. 002275	99. 7	1, 300	175	90	. 01615	. 0232	. 792	. 551
. 002275								
. 002275	99. 9	1, 365	215	131	. 02110	. 0260	. 756	. 613
. 002275	99. 9	1, 405	247	162. 5	. 0249	. 0281	. 735	. 651
. 002275	99. 9	1, 460	287	202. 5	. 0285	. 0302	. 709	. 675
. 002270	99. 7	1, 430	263	179. 5	. 0267	. 0292	. 724	. 662
. 002270	99. 7	1, 500	312	229. 5	. 0310	. 0312	. 690	. 685
. 002270	99. 3	1, 550	353	280. 5	. 0356	. 0330	. 664	. 716
. 002265	99. 1	1, 525	339	267	. 0349	. 0329	. 673	. 713
. 002265	99. 5	1, 600	396	329. 5	. 0392	. 0348	. 643	. 723
. 002265	99. 3	1, 645	436	369. 5	. 0416	. 0364	. 624	. 712
. 002265	99. 3	1, 695	467	407. 5	. 0435	. 0365	. 606	. 722
. 002265	99. 5	1, 775	540	496. 5	. 0480	. 0387	. 580	. 720
. 002260	80. 0	1, 690	552	570. 5	. 0610	. 0437	. 491	. 686
. 002260	80. 0	1, 685	550	570	. 0612	. 0438	. 493	. 689
. 002279	72. 9	1, 660	547	583. 5	. 0642	. 0446	. 455	. 654
. 002279	72. 9	1, 665	552	591. 5	. 0651	. 0447	. 453	. 660
. 002279	66. 3	1, 660	562	621. 5	. 0685	. 0457	. 413	. 619
. 002279	66. 7	1, 655	565	622	. 0688	. 0461	. 417	. 622
. 002282	59. 7	1, 645	566	661. 5	. 0740	. 0468	. 375	. 593
. 002282	59. 7	1, 650	565	660	. 0734	. 0467	. 374	. 587
. 002292	20. 8	1, 615	567	867	. 1304	. 0484	. 1332	. 2765
. 002292	20. 8	1, 620	567	866	. 0996	. 0482	. 1328	. 2745

TABLE II—Continued

PROPELLER I (3714),  $\frac{P}{D}=0.7$ 

VE-7 AIRPLANE, COMPLETE

$\rho$	$V$ M. P. H.	$N$ R. P. M.	$Q$ lb. ft.	$T$ lb.	$C_T$	$C_P$	$\frac{V}{nD}$	$\eta$
0.002325	85.2	1,665	545	526.5	0.0663	0.0527	0.550	0.692
.002325	84.3	1,665	550	535.5	.0678	.0532	.545	.694
.002324	86.7	1,675	552	531.5	.0665	.0526	.567	.703
.002324	86.5	1,675	552	530	.0662	.0526	.559	.707
.002324	96.6	1,705	552	506.5	.0609	.0509	.609	.729
.002320	96.1	1,705	549	503.5	.0607	.0504	.605	.729
.002318	99.5	1,720	547	499	.0592	.0497	.623	.742
.002318	99.5	1,720	545	497	.0589	.0496	.623	.741
.002318	100.2	1,720	542	489.5	.0581	.0493	.627	.739
.002318	99.7	1,720	542	487.5	.0578	.0493	.624	.737
.002305	100.1	1,665	495	441	.0560	.0482	.647	.754
.002305	99.5	1,610	455	399	.0543	.0475	.665	.766
.002305	100.1	1,550	397	342.5	.0503	.0447	.694	.780
.002300	100.2	1,520	372	308.5	.0471	.0434	.711	.770
.002305	99.0	1,465	332	260	.0426	.0418	.729	.743
.002305	99.5	1,495	359	289	.0458	.0434	.717	.757
.002300	99.3	1,435	312	243	.0416	.0412	.745	.753
.002300	99.4	1,445	317	252.5	.0427	.0411	.740	.769
.002300	99.3	1,395	277	213.5	.0388	.0385	.766	.771
.002300	98.8	1,365	257	200.5	.0380	.0374	.779	.791
.002300	98.9	1,355	245	184	.0353	.0362	.785	.765
.002300	98.8	1,335	230	168	.0333	.0348	.796	.761
.002300	98.6	1,290	203	143.5	.0304	.0332	.823	.752
.002300	98.6	1,275	197	133.5	.0290	.0328	.832	.736
.002300	98.4	1,240	172	109	.0250	.0304	.854	.703
.002300	98.5	1,200	152	87.5	.0214	.0286	.885	.664
.002300	98.2	1,145	119	58	.0156	.0246	.924	.586
.002300	97.9	1,095	92	36	.0106	.0209	.962	.487
.002300	97.6	1,050	70	16	.00511	.0172	1.001	.298
.002300	97.8	1,000	50	-7.5	-.002657	.0140	1.053	-.200
.002305	80.5	1,665	559	558	.071	.0545	.520	.678
.002305	80.5	1,655	557	557	.0716	.0547	.523	.686
.002305	73.8	1,655	563	582.5	.0750	.0553	.480	.652
.002305	74.3	1,655	565	581.5	.0747	.0557	.483	.649
.002318	68.4	1,645	567	598.5	.0775	.0564	.447	.615
.002318	68.7	1,645	567	603.5	.0781	.0564	.450	.623
.002318	65.0	1,635	567	616.5	.0805	.0572	.428	.603
.002318	64.9	1,635	567	616.5	.0805	.0572	.427	.602
.002318	59.7	1,630	569	641.5	.0845	.0575	.394	.579
.002318	52.4	1,620	571	672.5	.0896	.0585	.348	.533
.002320	21.05	1,625	567	828.5	.110	.0577	.139	.263
.002320	21.05	1,625	567	826.5	.110	.0577	.139	.263



TABLE II—Continued

PROPELLER  $D'$ ,  $\frac{P}{D}=0.8$ 

VE-7 AIRPLANE, COMPLETE

$\rho$	$V$ M. P. H.	$N$ R. P. M.	$Q$ lb. ft.	$T$ lb.	$C_T$	$C_P$	$\frac{V}{nD}$	$\eta$
	0	0						
0. 002305	82. 4	1, 685	555	535	0. 0783	0. 0653	0. 549	0. 658
. 002305	82. 1	1, 675	549	535. 5	. 0795	. 0652	. 550	. 671
. 00230	86. 4	1, 690	550	525	. 0767	. 0645	. 574	. 681
. 00230	86. 4	1, 695	552	525	. 0762	. 0642	. 572	. 679
. 002295	95. 1	1, 725	549	509. 5	. 0715	. 0619	. 619	. 716
. 002295	94. 8	1, 725	550	507	. 0711	. 0619	. 617	. 710
. 002290	99. 5	1, 740	552	499	. 0689	. 0613	. 643	. 723
. 002290	99. 5	1, 735	550	499. 5	. 0693	. 0613	. 645	. 729
. 002295	96. 7	960	50	11. 5	. 00523	. 01815	1. 137	. 327
. 002290	99. 0	940	30	—5	— . 00237	. 0114	1. 175	— . 244
. 002290	99. 0	1, 050	86	33	. 0125	. 0261	1. 060	. 508
. 002285	99. 1	1, 000	57	11	. 00461	. 01915	1. 115	. 269
. 002285	99. 5	1, 105	117	65	. 0222	. 0324	1. 010	. 692
. 002285	99. 5	1, 160	145	88	. 0272	. 0362	. 964	. 724
. 002285	99. 9	1, 205	169	109	. 0312	. 0394	. 930	. 738
. 002285	99. 1	1, 250	201	138	. 0373	. 0431	. 890	. 772
. 002280	99. 5	1, 255	199	140	. 0373	. 0426	. 890	. 781
. 002280	99. 2	1, 295	217	155	. 0388	. 0438	. 861	. 763
. 002280	99. 7	1, 335	242	181	. 0427	. 0459	. 839	. 780
. 002280	99. 7	1, 365	262	196	. 0442	. 0473	. 821	. 784
. 002280	99. 7	1, 375	272	204	. 0453	. 0486	. 815	. 760
. 002280	99. 7	1, 395	282	215	. 0465	. 0489	. 803	. 764
. 002280	99. 9	1, 440	319	248	. 0502	. 0519	. 780	. 756
. 002280	99. 8	1, 425	301	236	. 0488	. 0499	. 787	. 771
. 002275	99. 1	1, 465	335	264	. 0518	. 0530	. 760	. 743
. 002275	99. 5	1, 570	366	300	. 0554	. 0544	. 739	. 753
. 002275	100. 1	1, 525	369	305	. 0554	. 0538	. 736	. 757
. 002275	100. 1	1, 550	392	328	. 0574	. 0552	. 724	. 754
. 002275	100. 2	1, 590	424	361	. 0601	. 0567	. 706	. 750
. 002275	99. 8	1, 640	462	402	. 0631	. 0583	. 685	. 742
. 002270	100. 2	1, 700	507	452	. 0656	. 0598	. 662	. 726
. 002280	77. 0	1, 655	537	535	. 0819	. 0665	. 522	. 644
. 002280	76. 1	1, 655	545	539	. 0825	. 0672	. 516	. 635
. 002280	70. 7	1, 645	543	564	. 0876	. 0676	. 484	. 620
. 002280	69. 8	1, 640	546	565	. 0885	. 0685	. 479	. 618
. 002285	65. 9	1, 640	547	575	. 0898	. 0684	. 445	. 584
. 002285	64. 6	1, 635	542	580	. 0910	. 0682	. 445	. 594
. 002285	60. 0	1, 635	546	599	. 0939	. 0688	. 412	. 562
. 002285	58. 0	1, 635	547	602	. 0944	. 0688	. 400	. 547
. 00230	19. 7	1, 655	556	801	. 1215	. 0678	. 134	. 240
. 00230	19. 7	1, 665	556	801	. 1205	. 0671	. 134	. 240
. 00230	19. 7	1, 660	552	798	. 1210	. 0668	. 134	. 243

TABLE II—Continued

PROPELLER I (3714),  $\frac{P}{D}=0.7$ 

VE-7 WITH WINGS, WITHOUT TAIL

$\rho$	$V$ M. P. H.	$N$ R. P. M.	$Q$ lb. ft.	$T$ lb.	$C_T$	$C_P$	$\frac{V}{nD}$	$\eta$
0.00240	83.4	1,660	572	565.5	0.0694	0.0540	0.542	0.695
.00240	83.4	1,660	572	567.5	.0699	.0540	.542	.701
.002396	86.3	1,660	560	534	.0669	.0529	.557	.702
.002396	86.3	1,660	557	537	.0690	.0526	.557	.728
.002390	95.0	1,705	567	525.5	.0614	.0506	.600	.722
.002390	94.8	1,705	567	520.5	.0607	.0506	.599	.713
.002381	98.8	1,730	567	517.5	.0605	.0495	.615	.753
.002381	98.9	1,735	567	520.5	.0586	.0492	.614	.732
.002378	99.1	1,675	525	471	.0575	.0491	.637	.747
.002378	98.7	1,625	477	421.5	.0545	.0473	.654	.754
.002378	98.7	1,603	470	422	.0564	.0479	.662	.780
.002378	99.9	1,595	435	374.5	.0504	.0448	.673	.757
.002375	99.7	1,545	415	348	.0500	.0455	.695	.764
.002375	99.3	1,525	387	322.5	.0474	.0437	.701	.760
.002375	99.1	1,480	357	294	.0459	.0428	.721	.772
.002375	98.8	1,475	352	288	.0454	.0424	.721	.772
.002370	98.8	1,440	325	259	.0428	.0413	.738	.766
.002370	98.8	1,395	287	223.5	.0394	.0386	.763	.778
.002370	98.5	1,325	237	174.5	.0339	.0360	.801	.755
.002370	98.1	1,250	182	120.5	.0266	.0306	.844	.735
.002370	98.0	1,235	177	115.5	.0260	.0306	.855	.727
.002370	98.0	1,180	143	88.5	.0217	.0270	.894	.716
.002370	98.0	940	25	-22.5	-.00875	.00746	1.137	
.002378	75.5	1,640	575	586	.0745	.0560	.495	.657
.002378	75.4	1,640	575	589	.0746	.0560	.494	.658
.002378	69.7	1,620	573	612.5	.0797	.0574	.465	.644
.002378	69.4	1,625	573	610.5	.0790	.0571	.461	.637
.002381	62.6	1,610	575	636.5	.0837	.0580	.418	.603
.002381	64.4	1,615	575	634.5	.0830	.0578	.429	.617
.00239	59.0	1,620	582	664	.0858	.0578	.392	.581
.00239	59.2	1,620	582	660.5	.0854	.0580	.393	.579
.002396	20.8	1,625	582	860.5	.1105	.0575	.136	.261
.002396	20.8	1,620	583	861.5	.1114	.0578	.138	.266



TABLE II—Continued

PROPELLER I (3714),  $\frac{P}{D}=0.7$ 

VE-7, WITHOUT WINGS OR TAIL

$P$	$V$ M. P. H.	$N$ R. P. M.	$Q$ lb. ft.	$T$ lb.	$C_T$	$C_P$	$\frac{V}{nD}$	$\eta$
0. 002381	83. 7	1, 660	557	564	0. 0698	0. 0528	0. 543	0. 717
. 002381	84. 1	1, 660	557	564. 5	. 0698	. 0528	. 545	. 720
. 002378	87. 3	1, 670	557	556. 6	. 0679	. 0524	. 565	. 732
. 002370	96. 4	1, 720	552	257. 8	. 0610	. 0491	. 603	. 749
. 002370	96. 5	1, 710	550	528	. 0618	. 0494	. 609	. 761
. 002368	100. 4	1, 735	553	524. 6	. 0596	. 0483	. 622	. 768
. 002368	100. 2	1, 745	552	527	. 0591	. 0477	. 619	. 766
. 002368	100. 2	1, 665	472	445. 4	. 0551	. 0447	. 649	. 800
. 002368	100. 0	1, 640	457	429	. 0545	. 0448	. 657	. 798
. 002368	99. 8	1, 615	432	404	. 0529	. 0438	. 665	. 803
. 002363	99. 8	1, 555	387	347. 5	. 0492	. 0423	. 691	. 802
. 002363	99. 8	1, 525	367	320. 5	. 0472	. 0416	. 705	. 799
. 002363	99. 8	1, 495	347	299. 5	. 0459	. 0409	. 719	. 806
. 002363	99. 7	1, 455	312	265. 1	. 0428	. 0388	. 738	. 815
. 002363	99. 3	1, 415	287	234. 2	. 0402	. 0376	. 755	. 806
. 002363	99. 0	1, 370	242	187. 6	. 0342	. 0341	. 780	. 782
. 00236	99. 1	1, 340	232	175. 6	. 0335	. 0340	. 796	. 785
. 00236	98. 8	1, 245	177	116. 3	. 0258	. 0301	. 854	. 731
. 00236	98. 7	1, 190	142	88. 5	. 0214	. 0266	. 894	. 718
. 00236	98. 6	1, 145	117	56	. 0147	. 0236	. 927	. 577
. 00236	98. 3	1, 090	77	23. 7	. 00685	. 0171	. 971	. 390
. 00236	98. 2	1, 030	56	2	. 00065	. 0140	1. 026	. 0476
. 00236	100. 1	980	27	-32	-. 0115	. 00743	1. 102	-----
. 002368	76. 4	1, 590	517	547	. 0741	. 0537	. 517	. 713
. 002368	76. 4	1, 600	520	547	. 0731	. 0534	. 515	. 705
. 00237	70. 5	1, 610	545	592	. 0783	. 0553	. 471	. 666
. 00237	70. 5	1, 600	543	592	. 0793	. 0555	. 476	. 680
. 00237	65. 2	1, 595	545	616. 2	. 0829	. 0562	. 440	. 649
. 00237	65. 8	1, 595	547	614	. 0828	. 0565	. 445	. 652
. 002378	54. 6	1, 585	557	663. 5	. 0903	. 0583	. 371	. 575
. 002381	20. 7	1, 565	527	804. 8	. 1113	. 0563	. 1428	. 282
. 002381	20. 7	1, 555	527	798. 8	. 1124	. 0572	. 1438	. 282

TABLE III

FINAL ADJUSTED COEFFICIENTS

PROPELLER B',  $\frac{p}{D}=0.6$ 

VE-7 AIRPLANE, COMPLETE

$\frac{V}{nD}$	$C_T$	$C_P$	$\eta$	$\sqrt{\frac{\rho V^5}{Pn^2}}$	$\sqrt[5]{\frac{\rho V^5}{Pn^2}}$
0. 15	0. 0982	0. 0485	0. 304	0. 0396	0. 368
. 20	. 0933	. 0485	. 384	. 0814	. 458
. 25	. 0881	. 0483	. 456	. 1423	. 551
. 30	. 0828	. 0479	. 519	. 2260	. 645
. 35	. 0771	. 0470	. 574	. 3345	. 741
. 40	. 0712	. 0462	. 616	. 4720	. 8375
. 45	. 0650	. 0450	. 650	. 6420	. 9390
. 50	. 0586	. 0430	. 681	. 8540	1. 044
. 55	. 0521	. 0405	. 708	1. 1140	1. 155
. 60	. 0451	. 0378	. 715	1. 4350	1. 278
. 65	. 0377	. 0343	. 715	1. 8430	1. 402
. 70	. 0305	. 0310	. 689	2. 3300	1. 544
. 75	. 0234	. 0272	. 645	2. 9600	1. 698
. 80	. 0160	. 0232	. 552	3. 7600	1. 880
. 85	. 0082	. 0190	. 389	4. 8400	2. 090
. 90	. 0000	. 0148	. 000	6. 3200	

PROPELLER I (3714),  $\frac{p}{D}=0.7$ 

VE-7 AIRPLANE, COMPLETE

$\frac{V}{nD}$	$C_T$	$C_P$	$\eta$	$\sqrt{\frac{\rho V^5}{Pn^2}}$	$\sqrt[5]{\frac{\rho V^5}{Pn^2}}$
0. 10					
. 15	0. 1085	0. 0576	0. 282	0. 0364	0. 354
. 20	. 1037	. 0580	. 357	. 0745	. 440
. 25	. 0989	. 0583	. 424	. 1292	. 529
. 30	. 0940	. 0584	. 483	. 204	. 616
. 35	. 0890	. 0583	. 534	. 3002	. 707
. 40	. 0839	. 0578	. 581	. 421	. 800
. 45	. 0785	. 0566	. 624	. 572	. 894
. 50	. 0731	. 0550	. 665	. 755	. 988
. 55	. 0678	. 0530	. 705	. 975	1. 0898
. 60	. 0620	. 0507	. 735	1. 240	1. 194
. 65	. 0558	. 0479	. 758	1. 559	1. 306
. 70	. 0486	. 0442	. 770	1. 95	1. 428
. 75	. 0412	. 0400	. 773	2. 44	1. 555
. 80	. 0340	. 0358	. 759	3. 02	1. 700
. 85	. 0264	. 0312	. 719	3. 78	1. 86
. 90	. 0192	. 0268	. 645	4. 70	2. 04
. 95	. 0120	. 0222	. 513	5. 90	2. 235
1. 00	. 0048	. 0179	. 268	7. 46	



TABLE III—Continued

PROPELLER D',  $\frac{p}{D}=0.8$ 

VE-7 AIRPLANE, COMPLETE

$\frac{V}{nD}$	$C_T$	$C_P$	$\eta$	$\sqrt{\frac{\rho V^5}{Pn^2}}$	$\sqrt[5]{\frac{\rho V^5}{Pn^2}}$
0.10	0.1243	0.0668	0.186	-----	-----
.15	.1197	.0677	.265	0.0336	-----
.20	.1149	.0683	.336	.0685	0.341
.25	.110	.0689	.399	.119	.426
.30	.1051	.0690	.457	.1878	.512
.35	.1002	.0690	.508	.276	.599
.40	.0951	.0689	.554	.386	.684
.45	.0900	.0682	.594	.521	.771
.50	.0847	.0671	.631	.682	.858
.55	.0789	.0654	.664	.876	.948
.60	.0730	.0631	.694	1.11	1.0426
.65	.0671	.0603	.724	1.39	1.141
.70	.0608	.0570	.745	1.72	1.242
.75	.0544	.0534	.765	2.11	1.348
.80	.0478	.0497	.770	2.565	1.457
.85	.0418	.0457	.775	3.12	1.575
.90	.0351	.0416	.759	3.77	1.70
.95	.0288	.0372	.735	4.56	1.836
1.00	.0224	.0325	.689	5.55	1.982
1.05	.0160	.0272	.618	6.85	2.16
1.10	.0096	.0216	.489	8.65	2.37

PROPELLER I (3714),  $\frac{p}{D}=0.7$ 

VE-7, WITH WINGS, WITHOUT TAIL

$\frac{V}{nD}$	$C_T$	$C_P$	$\eta$	$\sqrt{\frac{\rho V^5}{Pn^2}}$	$\sqrt[5]{\frac{\rho V^5}{Pn^2}}$
0.15	0.1099	0.0578	0.285	0.0362	-----
.20	.1054	.0580	.364	.0745	0.354
.25	.1010	.0581	.434	.1298	.440
.30	.09590	.0582	.494	.204	.530
.35	.0908	.0581	.546	.301	.619
.40	.0852	.0580	.588	.421	.708
.45	.0799	.0574	.626	.568	.798
.50	.0740	.0558	.664	.750	.892
.55	.0679	.0532	.702	.974	.987
.60	.0616	.0506	.730	1.240	1.090
.65	.0550	.0475	.754	1.565	1.196
.70	.0482	.0441	.765	1.950	1.306
.75	.0411	.0400	.770	2.44	1.429
.80	.0339	.0358	.757	3.02	1.556
.85	.0264	.0311	.720	3.78	1.700
.90	.0191	.0266	.645	4.71	1.86
.95	.0121	.0221	.520	5.91	2.04
1.00	.0048	.0175	.274	7.62	2.25

TABLE III—Continued

PROPELLER I (3714),  $\frac{P}{D}=0.7$ 

VE-7, WITHOUT WINGS OR TAIL

$\frac{V}{nD}$	$C_T$	$C_P$	$\eta$	$\sqrt{\frac{\rho V^5}{P n^3}}$	$\sqrt[5]{\frac{\rho V^5}{P n^3}}$
0.15	0.1118	0.0571	0.293	0.03645	0.357
.20	.1079	.0579	.372	.0745	.453
.25	.1038	.0582	.445	.1396	.529
.30	.0989	.0585	.507	.204	.620
.35	.0939	.0581	.565	.301	.705
.40	.0881	.0576	.612	.419	.800
.45	.0822	.0563	.656	.574	.896
.50	.0758	.0546	.694	.758	.993
.55	.0690	.0522	.730	.984	1.097
.60	.0623	.0491	.761	1.26	1.204
.65	.0554	.0458	.786	1.59	1.319
.70	.0482	.0420	.803	2.00	1.442
.75	.0409	.0380	.807	2.50	1.574
.80	.0333	.0340	.784	3.105	1.715
.85	.0260	.0298	.740	3.86	1.872
.90	.0185	.0256	.650	4.81	2.058
.95	.0110	.0210	.497	6.07	2.27
1.00	.0037	.0166	.223	7.76	

## REFERENCES

- Reference 1. Weick, Fred E., and Wood, Donald H.: The Twenty-Foot Propeller Research Wind Tunnel of the National Advisory Committee for Aeronautics. N. A. C. A. Technical Report No. 300, 1928.
- Reference 2. Durand, W. F., and Lesley, E. P.: Comparison of Tests on Air Propellers in Flight with Wind Tunnel Model Tests on Similar Forms. N. A. C. A. Technical Report No. 220, 1926.
- Reference 3. Crowley, J. W., jr., and Mixson, R. E.: Characteristics of Five Propellers in Flight. N. A. C. A. Technical Report No. 292, 1928.



---

## **REPORT No. 302**

---

# **FULL SCALE TESTS ON A THIN METAL PROPELLER AT VARIOUS TIP SPEEDS**

**By FRED E. WEICK**  
**Langley Memorial Aeronautical Laboratory**





## REPORT No. 302

---

### FULL SCALE TESTS ON A THIN METAL PROPELLER AT VARIOUS TIP SPEEDS

BY FRED E. WEICK

---

#### SUMMARY

*This report describes an investigation made in order to determine the effect of tip speed on the characteristics of a thin-bladed metal propeller. The propeller was mounted on a VE-7 airplane with a 180-HP. E-2 engine, and tested in the 20-foot propeller research tunnel of the National Advisory Committee for Aeronautics. It was found that the effect of tip speed on the propulsive efficiency was negligible within the range of the tests, which was from 600 to 1,000 ft. per sec. (about 0.5 to 0.9 the velocity of sound in air).*

#### INTRODUCTION

It is known that the nondimensional coefficients of thrust, power, and efficiency, in terms of which propeller characteristics are usually expressed, vary with size and speed; and the size and speed of a propeller are conveniently represented by its tip speed in the plane of rotation.

Tests had been made previously on model propellers at various tip speeds (references 1 to 3) and also on small model airfoils at various air velocities up to and beyond the velocity of sound in air (references 4 and 5). The conditions under which the airfoil tests were made render them purely qualitative in value, but the results of the model propeller tests apparently have some quantitative value. Both sets of tests indicate a serious change in coefficients at the higher speeds, particularly in regard to airfoil drag coefficients (which are higher) and propeller efficiencies (which are very much lower). These tests also indicate that the effect of high speed is less for thin than for thick sections, and, since all of the sections used in these tests were much thicker than the sections of modern metal propellers, it may be inferred that the coefficients for thin metal propellers will be less affected by speed.

The investigation described in this report is the first to obtain the effect of tip speed on the coefficients of a full-scale thin-bladed metal propeller on an actual airplane in a wind tunnel. The tip speeds reached were not quite as high as desirable, but represent the maximum ordinarily found in practice. Even to obtain these tip speeds, it was necessary to set the propeller, which was of the adjustable type, to an unusually low pitch. These tests, therefore, are to be taken as the first step only in a more complete investigation on the effect of tip speeds which is to be made in the near future.

#### METHODS AND APPARATUS

The propeller used in this investigation was of the detachable-blade aluminum-alloy type, made in accordance with Navy drawing No. 4413. (Fig. 1.) The thickness ratio of the section nearest the tip was 0.055 and that of the section at 75 per cent of the tip radius was 0.078. The blades were intended for a propeller 9 ft. 6 in. in diameter, but the only hub available was 1 inch short of the standard length (it had been made so as to save weight), so that the propeller as tested was actually 9 ft. 5 in. in diameter. In order to obtain the highest practicable tip speed with the power available, the blades were set at the comparatively low blade angle of  $7^\circ$  at the 42 in. radius. This, of course, resulted in a propeller of lower pitch than is found in practice, but had the compensating advantage that any tip speed effect would be exaggerated because of the low pitch.



The tests were made in the propeller research tunnel of the National Advisory Committee for Aeronautics, which has an open jet air stream 20 ft. in diameter capable of velocities up to 110 M. P. H. A complete description of the tunnel, balances, and other measuring apparatus is given in reference 6.

A Vought VE-7 airplane with a Wright E-2, 180 HP. engine, which had been mounted in the tunnel for another investigation (reference 7), was also used for these tests. Since the VE-7 airplane has a span of 34 ft., the wings projected about 7 ft. outside of the air stream. Figure 2 is a photograph of the airplane in the experiment chamber. It is considered that a

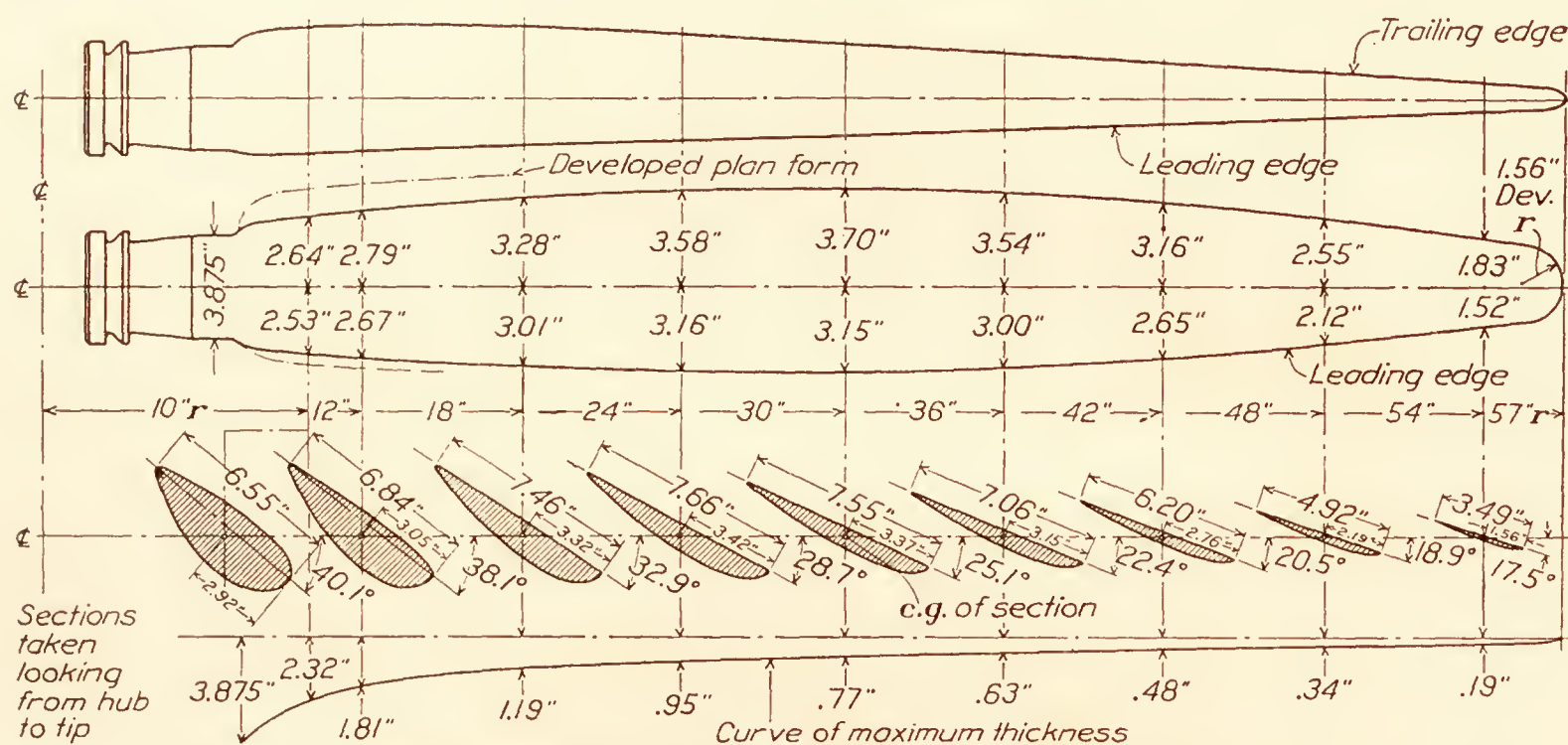


FIG. 1.—Metal propeller blade 9.5 feet in diameter. Right hand. No. 4413

ORDINATES OF SECTIONS AT VARIOUS RADII FOR EXPERIMENTAL METAL PROPELLER BLADE

9.5 ft. diameter, right-hand (fig. 1)

S	10" r		12" r		18" r	24" r	30" r	36" r	42" r	48" r	54" r
	Upper	Lower	Upper	Lower	Upper	Upper	Upper	Upper	Upper	Upper	Upper
2.5	0.62	0.28	0.68	0.14	0.49	0.39	0.32	0.26	0.20	0.14	0.02
5	.84	.44	.86	.21	.70	.56	.46	.37	.28	.20	.08
10	1.13	.59	1.15	.28	.94	.75	.61	.50	.38	.27	.11
20	1.45	.70	1.39	.33	1.13	.90	.73	.60	.46	.32	.15
30	1.53	.74	1.46	.35	1.19	.95	.77	.63	.48	.34	.18
40	1.56	.73	1.45	.35	1.18	.94	.76	.62	.48	.34	.19
50	1.50	.70	1.39	.33	1.13	.90	.73	.60	.46	.32	.19
60	1.38	.64	1.27	.30	1.04	.83	.67	.56	.42	.30	.18
70	1.17	.55	1.08	.26	.88	.70	.57	.47	.36	.23	.17
80	.89	.42	.82	.20	.67	.53	.43	.35	.27	.19	.14
90	.55	.26	.51	.12	.42	.33	.27	.22	.17	.12	.11
Rad. T. E.	0.21		0.16		0.09	0.07	0.06	0.05	0.04	0.03	0.07
Rad. L. E.	.72		.31		.12	.10	.08	.06	.05	.03	.01
Chord	6.55		6.84		7.46	7.66	7.55	7.06	6.20	4.92	3.49

The chord is divided into 10 equal parts, or stations, with the one at the leading edge subdivided into halves and quarters. S equals stations in per cent of chord from the leading edge.

sufficient portion of the airplane was in the air stream to include all parts which would react on or be influenced by the propeller.

In order to determine the pitch of the propeller in operation, the deflection of one blade was measured at the 42 in. radius, by means of a telescope mounted on a graduated base and sighted on first the leading and then the trailing edge. This was done while the propeller was standing still and then was repeated for each test point while the propeller was running.

The air velocity was obtained by means of calibrated static plates in the return passages, leading to a manometer in the experiment chamber. The revolution speed of the propeller was read directly from a specially built and calibrated Elgin chronometric tachometer.



The VE-7, as mounted in the tunnel, had completely enclosed within it a special steel skeleton fuselage with a built-in dynamometer to measure the engine and propeller torque directly. (Reference 6.) An observer sat in the rear cockpit of the airplane throughout the tests to operate the engine and read the torque scale and the tachometer.

The resultant horizontal force of the propeller-body combination, which may be either a thrust or a drag, was measured on the regular thrust balance (also described in reference 6).

This resultant horizontal force  $R$  may be thought of as composed of three horizontal components, such that

$$R = T - D - \Delta D,$$

where

$T$  = the thrust of the propeller while operating in front of the body (the tension in the crank shaft).

$D$  = the drag of the airplane alone (without propeller) at the same air velocity and density.

$\Delta D$  = the increase in drag of the airplane with propeller, due to the slip stream.



FIG. 2.—VE-7 airplane mounted in propeller research tunnel

In order to obtain the propulsive efficiency, which includes the propeller-body interference, an effective thrust is used which is defined as

$$\text{Effective thrust} = T - \Delta D = R + D.$$

### RESULTS

The results of the tests are given in Figures 3 to 7, inclusive, and in Tables I and II. They are reduced to the usual coefficients of thrust, power, and propulsive efficiency,

$$C_T = \frac{\text{Effective thrust}}{\rho n^2 D^4}$$

$$C_P = \frac{\text{Input power}}{\rho n^3 D^5}$$

$$\eta = \frac{\text{Effective thrust} \times \text{velocity of advance}}{\text{Input power}}$$

where  $D$  = propeller diameter and  $n$  = revolutions per unit time. Since the coefficients are dimensionless, any homogeneous system of units may be used.



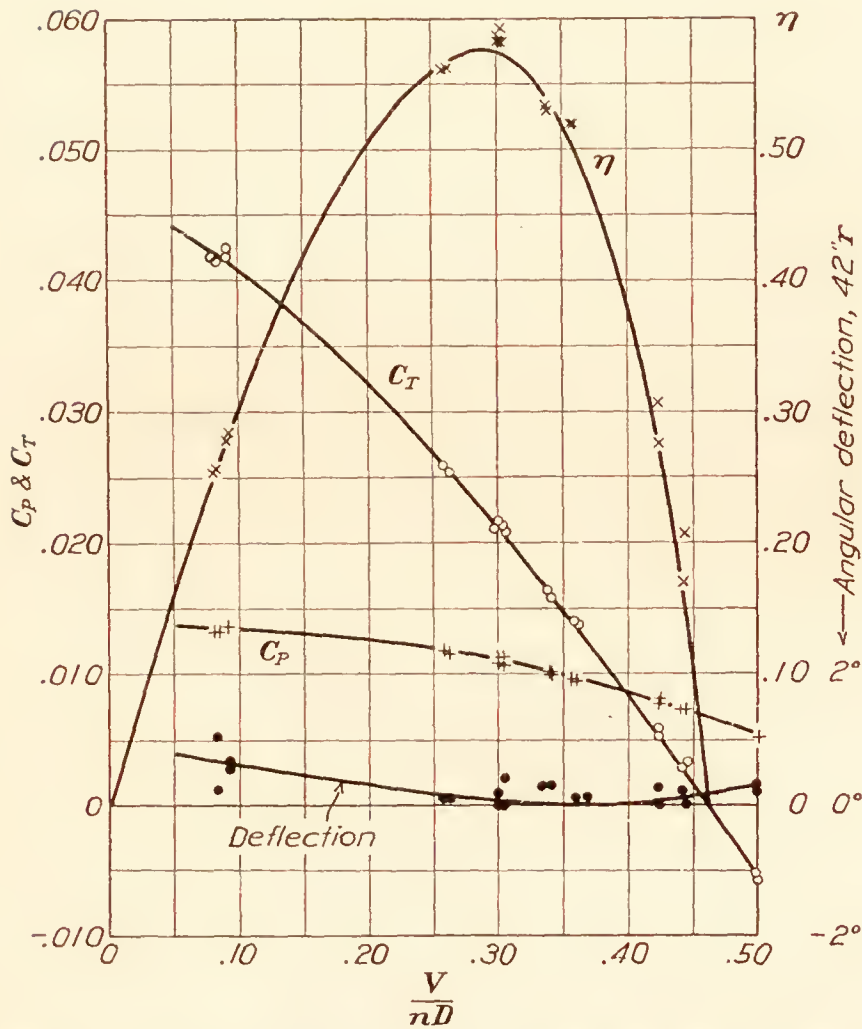


FIG. 3.—Propeller 4413. ( $7^\circ$  at  $42''$ ) on VE-7 airplane. 1,200 R. P. M.  
Tip speed = 591 ft./sec.  $V/c = 0.526$

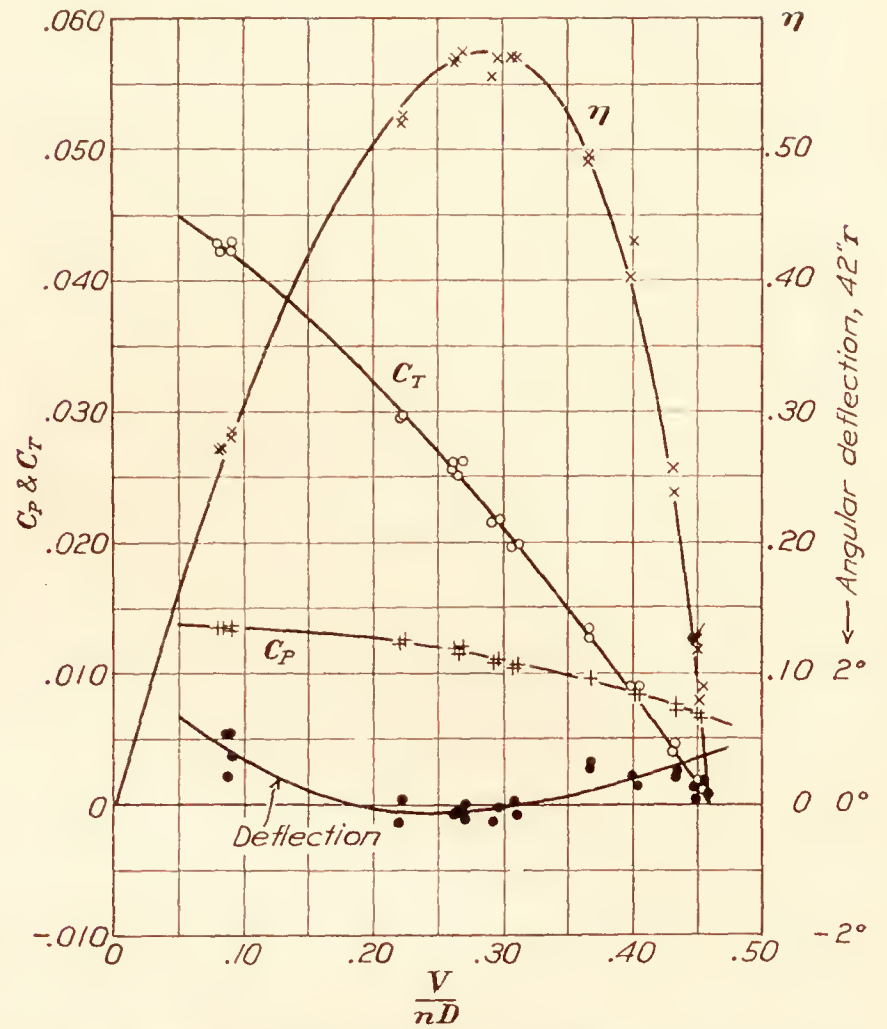


FIG. 4.—Propeller 4413. ( $7^\circ$  at  $42''$ ) on VE-7 airplane. 1,400 R. P. M.  
Tip speed = 690 ft./sec.  $V/c = 0.614$

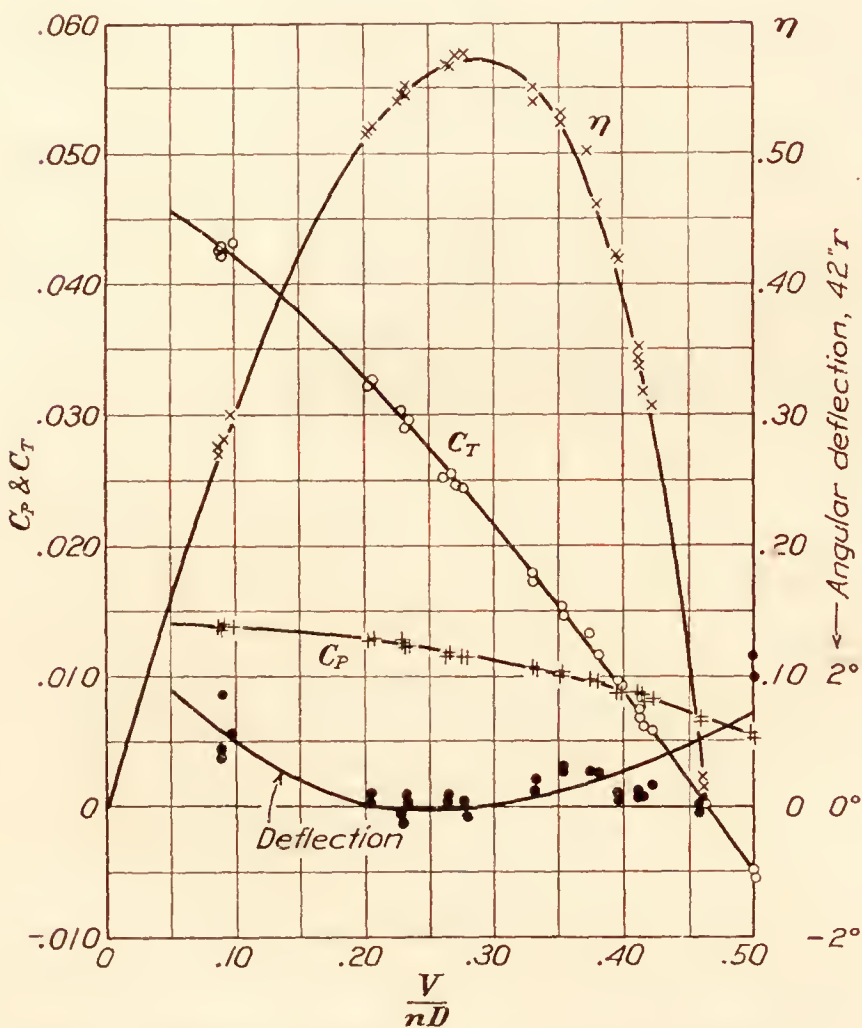


FIG. 5.—Propeller 4413. ( $7^\circ$  at  $42''$ ) on VE-7 airplane. 1,600 R. P. M.  
Tip speed = 788 ft./sec.  $V/c = 0.702$

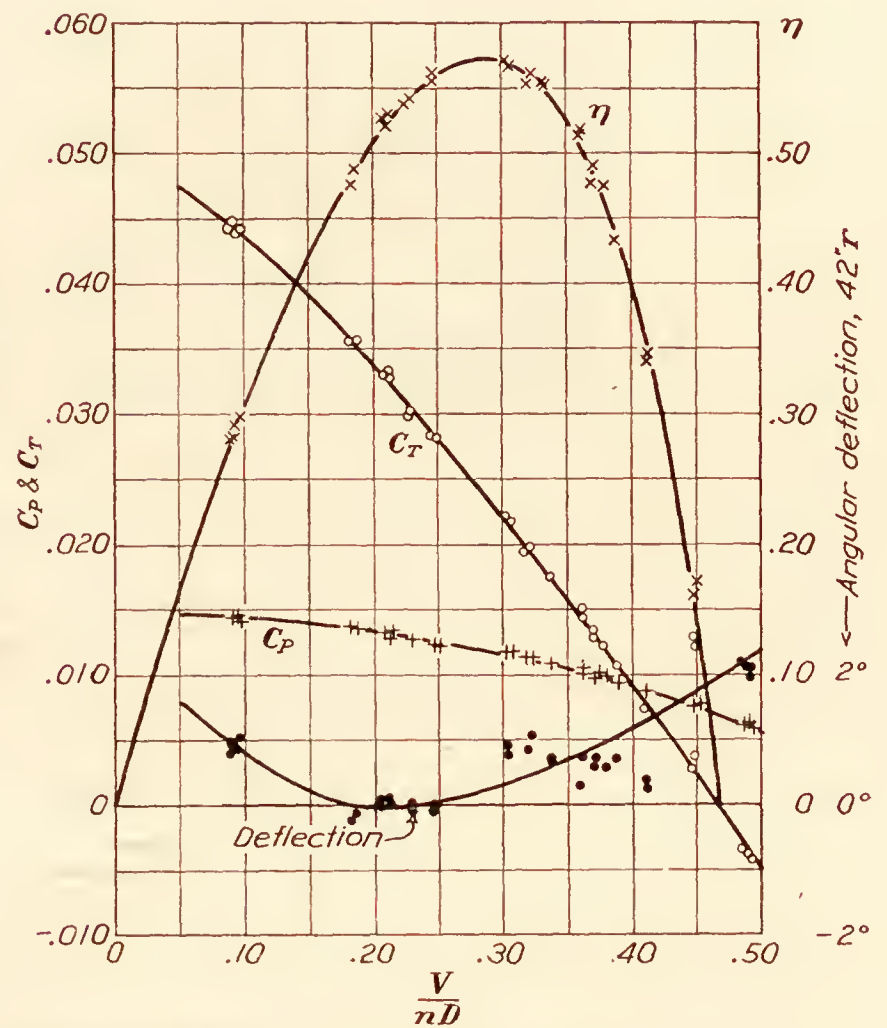


FIG. 6.—Propeller 4413. ( $7^\circ$  at  $42''$ ) on VE-7 airplane. 1,800 R. P. M.  
Tip speed = 887 ft./sec.  $V/c = 0.791$



The angular deflections at the 42 in. radius, which were measured for each test point, are also plotted in Figures 3 to 7. In general, the deflection was very small at the values of  $\frac{V}{nD}$  near maximum efficiency, but at higher and lower values of  $\frac{V}{nD}$  there was an increase in the blade angle, which was greater for the higher rotational speeds than for the lower ones.

A comparison of the thrust coefficients obtained at the various rotational speeds (or tip speeds) is given in Figure 8, and a comparison of the power coefficients in Figure 9. It will be noticed that particularly at the low values of  $\frac{V}{nD}$ , the thrust and power coefficients increase with an increase in tip speed. This can be entirely accounted for by the deflection of the blades in operation, so apparently is not due to scale or compressibility effect to an appreciable extent.

The efficiencies found at the various tip speeds are plotted against  $\frac{V}{nD}$  in Figure 10. The curves for all tip speeds are the same within the limits of accuracy of the experiments, indicating

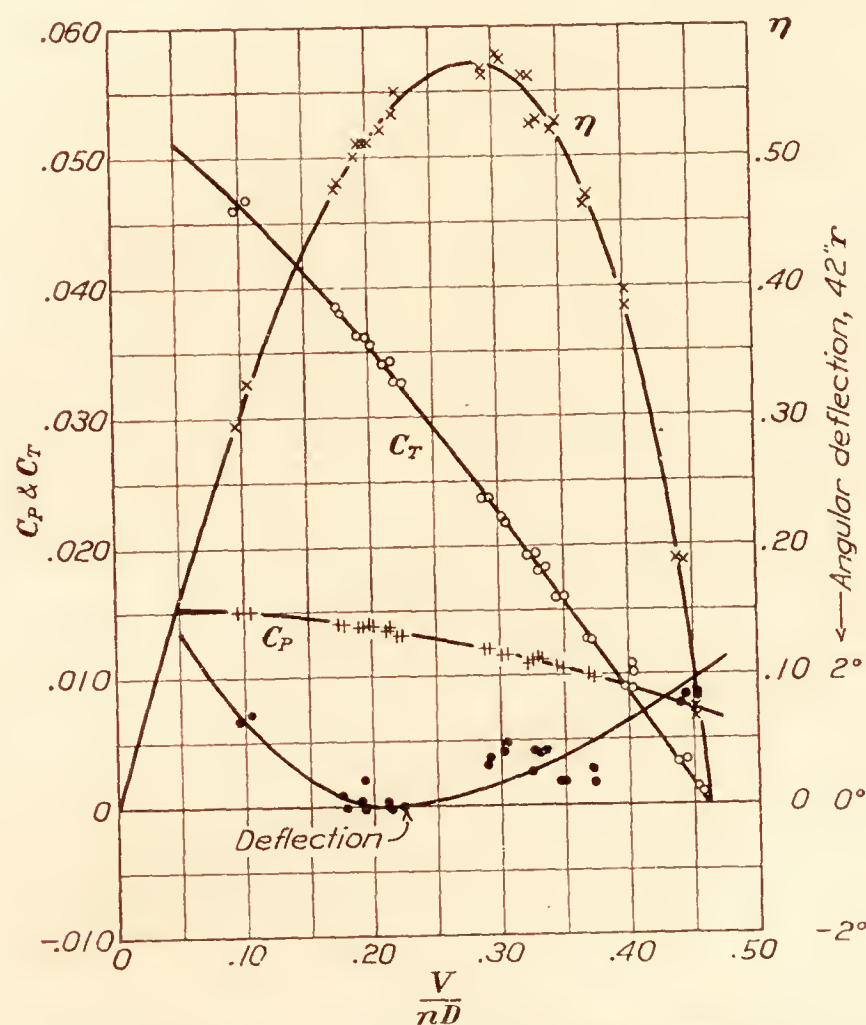


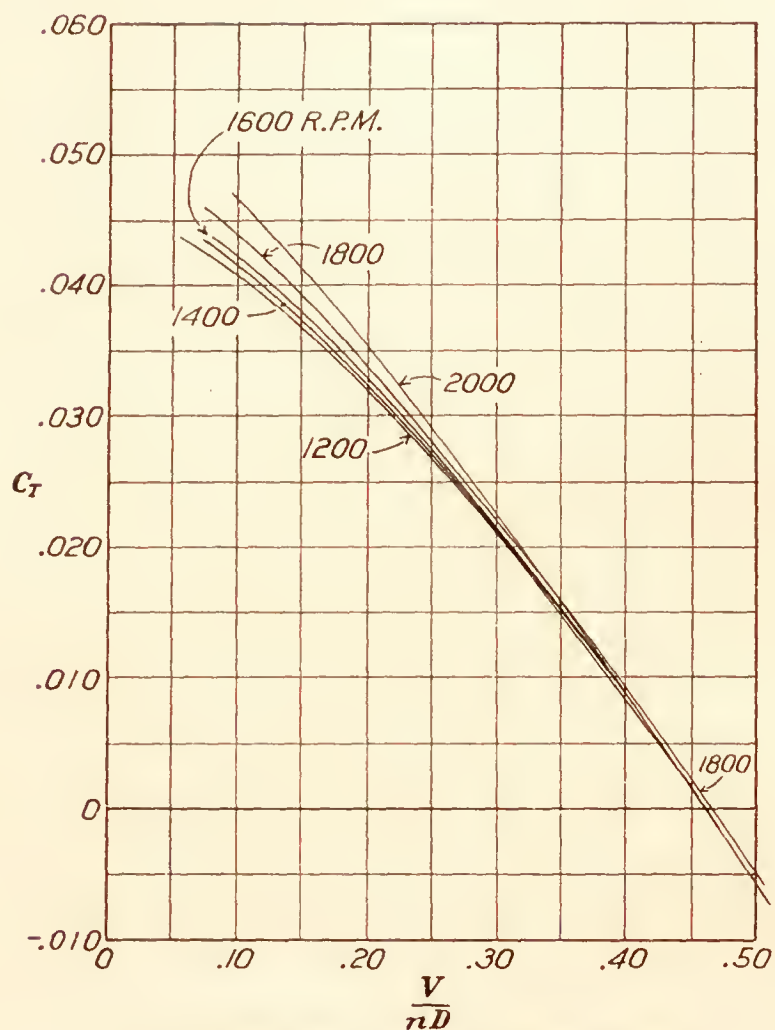
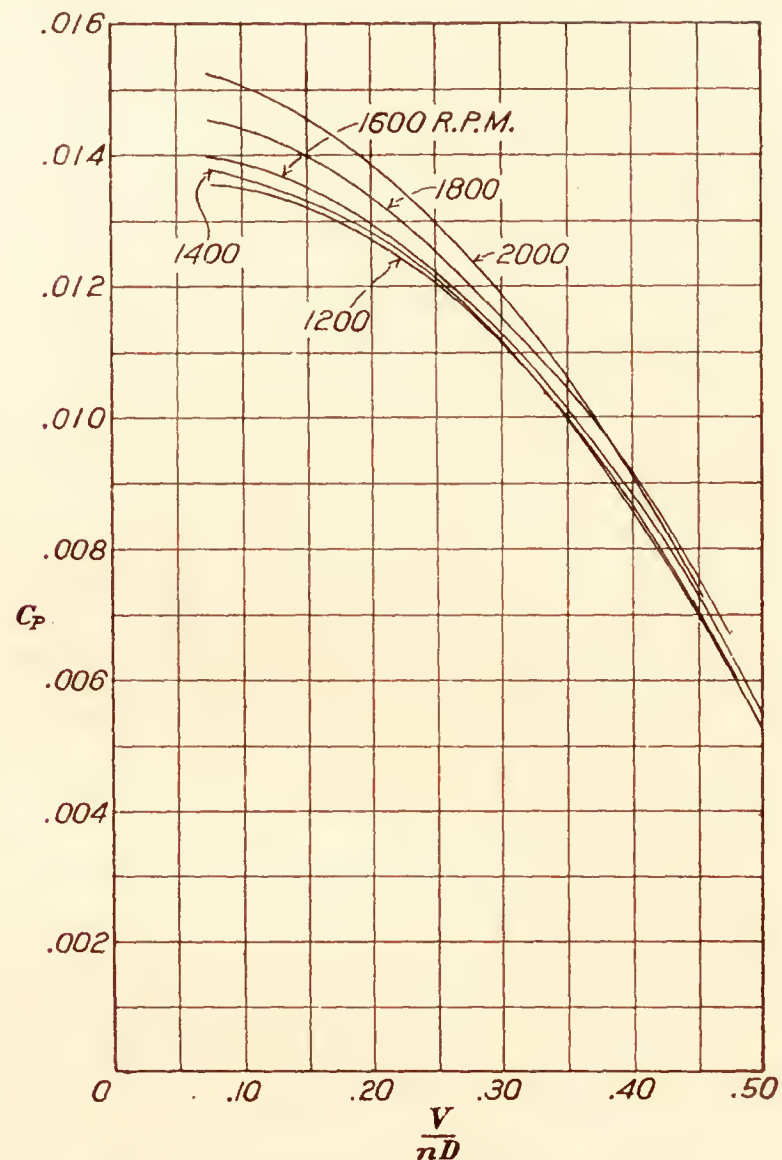
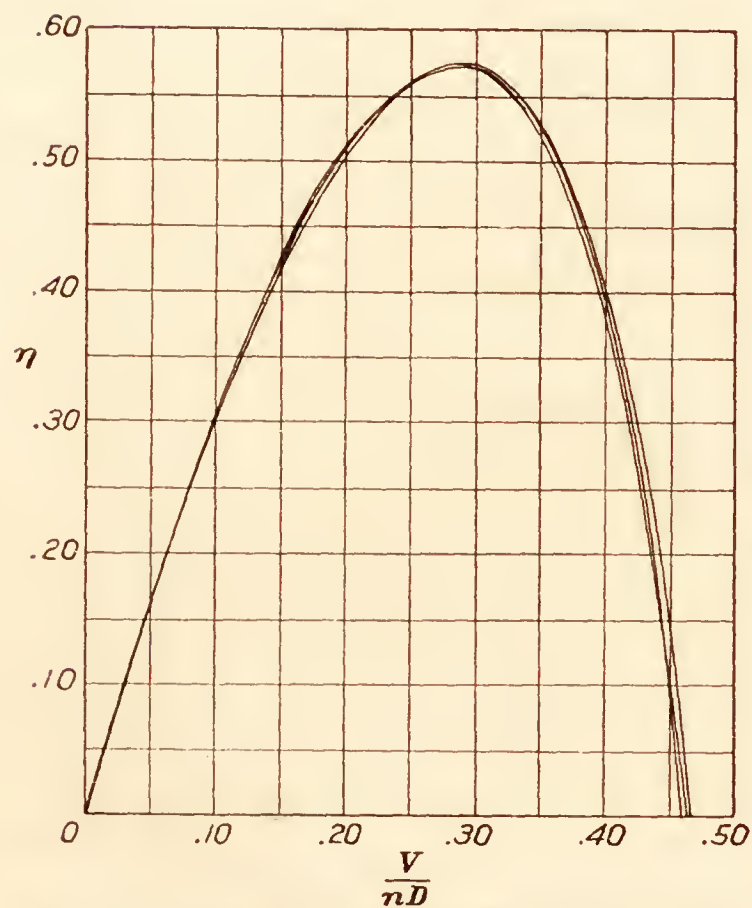
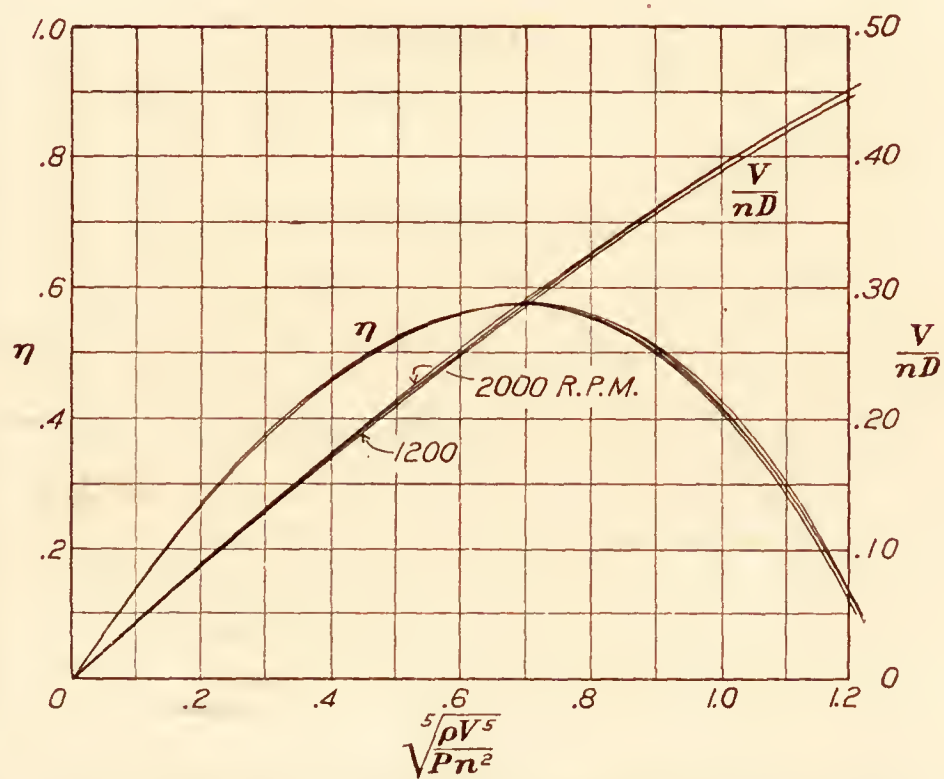
FIG. 7.—Propeller 4413. ( $7^\circ$  at 42") on VE-7 airplane. 2,000 R. P. M.  
Tip speed = 986 ft./sec.  $V/c = 0.878$

that the effect of tip speed on efficiency is negligible for this particular thin-bladed metal propeller within the range of tip speeds tested (from about 0.5 to 0.9, the velocity of sound in air).

In Figure 11 the efficiencies and values of  $\frac{V}{nD}$  are plotted against the factor

$$\sqrt[5]{\frac{\rho V^5}{P n^2}}$$

This is a form of speed-power coefficient which represents the required performance of a propeller on an airplane, since it includes the power absorbed, the revolutions, and the velocity of advance. Propellers operating at the same value of this coefficient are therefore working under similar requirements, and hence a comparison of efficiencies can be made on a fair basis. Figure 11 shows clearly that from the standpoint of effectiveness of operation on an airplane, the tip speed is of no practical importance within the limits of these experiments.

FIG. 8.—Propeller 4413. ( $7^\circ$  at  $42''$ ) on VE-7 airplaneFIG. 9.—Propeller 4413. ( $7^\circ$  at  $42''$ ) on VE-7 airplaneFIG. 10.—Propeller 4413. ( $7^\circ$  at  $42''$ ) on VE-7 airplane. 1,200, 1,400, 1,600, 1,800, and 2,000 R. P. M. Tip speeds, 591 to 986 ft./sec.FIG. 11.—Propeller 4413. ( $7^\circ$  at  $42''$ ) on VE-7 airplane. 1,200, 1,400, 1,600, 1,800, and 2,000 R. P. M. Tip speeds, 591 to 986 ft./sec.



## CONCLUSION

The effect of tip speed on the efficiency and performance coefficients of the propeller tested was negligible throughout the range of the tests, except as the thrust and power coefficients were affected by the slight change of pitch due to deflection. Apparently the coefficients were not affected by scale or compressibility to an appreciable extent.

LANGLEY MEMORIAL AERONAUTICAL LABORATORY,  
NATIONAL ADVISORY COMMITTEE FOR AERONAUTICS,  
LANGLEY FIELD, VA., *June 20, 1928.*

### REFERENCES

- Reference 1. Douglass, G. P., and Wood, R. McKinnon: The Effects of Tip Speed on Airscrew Performance. An Experimental Investigation of the Performance of an Airscrew over a Range of Speeds of Revolution from "Model" Speeds up to Tip Speeds in Excess of the Velocity of Sound in Air. British A. R. C. Reports and Memoranda No. 884, 1923.
- Reference 2. Douglass, G. P., and Perring, W. G. A.: Wind Tunnel Tests with High Tip Speed Airscrews. The Characteristics of the Airfoil Section R. A. F. 31a at High Speeds. British A. R. C. Reports and Memoranda No. 1086, 1927.
- Reference 3. Douglass, G. P., and Perring, W. G. A.: Wind Tunnel Tests with High Tip Speed Airscrews. The Characteristics of a Bi-convex Airfoil at High Speeds. British A. R. C. Reports and Memoranda No. 1091, 1927.
- Reference 4. Briggs, L. J., Hull, G. F., and Dryden, H. L.: The Aerodynamic Characteristics of Airfoils at High Speeds. N. A. C. A. Technical Report No. 207, 1925.
- Reference 5. Briggs, L. J., and Dryden, H. L.: Pressure Distribution over Airfoils at High Speeds. N. A. C. A. Technical Report No. 225, 1927.
- Reference 6. Weick, Fred E., and Wood, Donald H.: The Twenty-Foot Propeller Research Tunnel of the National Advisory Committee for Aeronautics. N. A. C. A. Technical Report No. 300, 1928.
- Reference 7. Weick, Fred E.: Full Scale Tests of Wood Propellers on a VE-7 Airplane in the Propeller Research Tunnel. N. A. C. A. Technical Report No. 301, 1928.



TABLE I  
TEST DATA

Propeller No. 4413—7° at 42 in.

1,200 R. P. M.

(Tip speed 591.7 ft./sec.)

$\rho$	$V$ M. P. H.	$N$ R. P. M.	$Q$ lb. ft.	$T$ lb.	$C_T$	$C_P$	$V/nD$	$\eta$	Def. at 42 in. Rad., deg.
0. 002365	64.0	1,205	57	-40	-0.00540	0.00515	0.498	-0.522	+0.2
.002365	63.8	1,200	57	-41	-.00556	.00519	.499	-.535	.3
.002365	58.2	1,230	83	26	.00336	.00719	.444	.208	.0
.002365	58.2	1,235	85	22	.00281	.00730	.442	.170	.2
.002364	54.3	1,205	88	43	.00577	.00794	.423	.307	.2
.002364	54.1	1,195	87	38	.00520	.00800	.424	.276	.0
.002378	10.7	1,220	152	317	.0414	.0133	.0825	.257	.3
.002378	10.7	1,220	152	317	.0414	.0133	.0825	.257	1.0
.00234	11.65	1,205	149	311	.0424	.01356	.0905	.284	.7
.00234	11.65	1,205	149	307	.0418	.01350	.0905	.281	.6
.002378	39.2	1,210	121	158	.0210	.01078	.304	.591	.4
.002378	39.2	1,210	124	159	.0211	.01104	.304	.581	.0
.002375	43.8	1,215	115	122	.01605	.0101	.338	.535	.3
.002375	43.8	1,215	115	122	.01605	.0101	.338	.535	.3
.002369	45.6	1,195	104	101	.0138	.00954	.358	.519	.1
.002369	45.6	1,195	105	101	.0138	.00961	.358	.514	.1
.002369	38.4	1,200	123	160	.0217	.01118	.300	.582	.0
.002369	38.2	1,195	120	157	.0214	.01096	.300	.586	.2
.002367	32.0	1,165	123	180	.0258	.0118	.258	.563	.1
.002367	32.0	1,155	120	174	.0254	.01174	.2605	.563	.1

1,400 R. P. M.

(Tip speed 690.3 ft./sec.)

0. 002365	68.4	1,410	104	14	0.00138	0.00687	0.453	0.0912	+0.4
.002365	68.2	1,415	106	13	.00127	.00695	.451	.0825	.3
.00237	67.1	1,400	106	20	.00199	.00707	.449	.1265	.5
.00237	66.8	1,395	105	19	.0019	.00705	.449	.121	.1
.002365	64.9	1,410	116	47	.00461	.00765	.432	.260	.5
.002365	64.9	1,405	113	42	.00415	.00747	.433	.241	.4
.002365	59.3	1,395	131	90	.00900	.00883	.399	.406	.4
.002365	59.3	1,385	127	90	.00915	.00852	.402	.432	.3
.002362	55.4	1,425	152	139	.0134	.00983	.365	.496	.7
.002362	55.4	1,425	151	137	.0132	.00973	.365	.494	.6
.002378	13.6	1,405	207	430.5	.0424	.01364	.0909	.283	.8
.002378	13.6	1,405	206	434.5	.0429	.01360	.0909	.287	1.1
.00234	13.25	1,405	204	427	.0428	.0137	.0882	.274	.5
.00234	13.25	1,405	205	422	.0424	.01374	.0882	.272	1.1
.002380	38.3	1,375	175	255	.0262	.01203	.2615	.569	-.1
.002380	38.3	1,375	173	252	.0259	.01190	.2615	.569	-.1
.002375	40.9	1,425	175	229	.0219	.01127	.2955	.573	.0
.002375	44.2	1,420	175	224	.02160	.0113	.292	.557	-.2
.002369	45.8	1,400	160	200	.0199	.01066	.307	.573	+.1
.002369	45.8	1,385	160	197	.0200	.01085	.310	.572	-.1
.002369	39.1	1,365	175	253	.0264	.01229	.269	.578	.0
.002369	38.7	1,375	170	246	.0254	.01172	.264	.572	-.2
.002367	32.9	1,400	187	297	.0296	.01250	.2205	.522	+.1
.002367	32.9	1,390	185	295	.0298	.01252	.222	.528	-.2

TABLE I—Continued  
 TEST DATA—Continued  
 1,600 R. P. M.  
 (Tip speed 788.9 ft./sec.)

$\rho$	$V$ M. P. H.	$N$ R. P. M.	$Q$ lb. ft.	$T$ lb.	$C_T$	$C_P$	$V/nD$	$\eta$	Def. at 42 in. Rad., deg.
0. 00238	83. 8	1, 575	106	-62	-0. 00485	0. 0056	0. 498	-0. 432	+2. 4
. 00238	83. 8	1, 565	102	-69	-. 00546	. 0054	. 500	-. 506	2. 0
. 002365	78. 3	1, 600	133	3	. 000229	. 00678	. 458	. 0155	-. 1
. 002365	78. 4	1, 605	133	4	. 000330	. 00675	. 458	. 0224	+ .1
. 002365	71. 9	1, 595	158	77	. 00593	. 00812	. 422	. 308	. 4
. 002365	70. 7	1, 595	158	81	. 00622	. 00812	. 415	. 318	. 2
. 002365	69. 6	1, 585	167	96	. 00745	. 00867	. 411	. 353	. 2
. 002365	69. 2	1, 575	164	91	. 00715	. 00861	. 412	. 342	. 3
. 00237	67. 2	1, 605	177	127	. 00959	. 00895	. 395	. 423	. 1
. 00237	67. 7	1, 605	177	127	. 00959	. 00895	. 395	. 423	. 2
. 002365	63. 7	1, 600	192	174	. 0133	. 00985	. 373	. 504	. 5
. 002365	65. 0	1, 605	188	153	. 0116	. 00955	. 380	. 462	. 5
. 002365	60. 1	1, 600	199	199	. 0152	. 01018	. 352	. 526	. 5
. 002365	60. 1	1, 600	197	199	. 0152	. 01008	. 352	. 530	. 6
. 002362	56. 1	1, 595	208	233	. 0179	. 01068	. 330	. 552	. 3
. 002362	56. 1	1, 590	207	226	. 0175	. 0107	. 331	. 540	. 5
. 022378	14. 9	1, 600	267	561	. 0426	. 01356	. 0873	. 275	. 9
. 002378	14. 9	1, 595	269	560	. 0428	. 0138	. 0877	. 273	. 8
. 002342	15. 25	1, 585	264	551	. 0432	. 01386	. 0900	. 281	1. 7
. 00234	16. 20	1, 560	257	533	. 0431	. 01395	. 0971	. 300	1. 1
. 00238	40. 3	1, 650	267	427	. 0304	. 01275	. 229	. 546	-. 2
. 00238	40. 2	1, 655	269	427	. 0303	. 01278	. 228	. 541	-. 1
. 002375	45. 3	1, 615	235	340	. 0253	. 01168	. 263	. 568	+ .1
. 002375	45. 3	1, 600	234	334	. 0254	. 01185	. 265	. 567	. 2
. 002369	46. 4	1, 575	223	312	. 0245	. 01172	. 276	. 576	. 1
. 002369	46. 3	1, 575	222	312	. 0245	. 0117	. 276	. 578	-. 1
. 002369	39. 2	1, 585	240	377	. 0292	. 01239	. 232	. 547	+ .2
. 002369	39. 2	1, 585	238	379	. 0294	. 01239	. 232	. 552	. 1
. 002367	34. 3	1, 580	248	417	. 0326	. 01296	. 2035	. 520	. 2
. 002367	33. 9	1, 565	243	406	. 0323	. 01296	. 203	. 516	. 1

1,800 R. P. M.  
 (Tip speed 887.5 ft./sec.)

0. 00238	85. 0	1, 780	187	45. 5	0. 00278	0. 0076	0. 446	0. 163	+2. 6
. 00238	85. 0	1, 775	185	47	. 002895	. 0076	. 449	. 171	2. 5
. 002365	93. 3	1, 800	152	-58	-. 00350	. 0061	. 485	-. 278	2. 2
. 002365	93. 2	1, 790	149	-61	-. 00372	. 0061	. 488	-. 298	2. 1
. 00236	95. 6	1, 820	152	-71	-. 00420	. 0060	. 491	-. 343	2. 0
. 00236	95. 6	1, 825	153	-71	-. 00417	. 0060	. 491	-. 341	2. 1
. 002365	79. 3	1, 810	218	123	. 00733	. 00870	. 411	. 346	. 3
. 00236	78. 9	1, 805	217	120	. 00727	. 00870	. 410	. 342	. 4
. 002365	72. 9	1, 765	223	168	. 01053	. 00936	. 387	. 435	. 7
. 002365	70. 9	1, 750	228	191	. 01220	. 00975	. 379	. 475	. 6
. 002365	71. 2	1, 795	246	217	. 01320	. 0100	. 371	. 490	. 7
. 002365	70. 9	1, 795	244	211	. 01280	. 00991	. 370	. 477	. 6
. 00237	68. 9	1, 795	249	240	. 01455	. 0101	. 360	. 519	. 3
. 00237	68. 5	1, 785	251	240	. 0147	. 0103	. 360	. 514	. 8
. 002365	64. 8	1, 800	266	293	. 01768	. 01075	. 337	. 554	. 6
. 002365	64. 3	1, 795	263	289	. 0175	. 0107	. 336	. 550	. 6
. 002365	61. 4	1, 805	278	324	. 0194	. 01115	. 318	. 554	. 9
. 002365	61. 4	1, 785	275	321	. 01965	. 01128	. 322	. 562	1. 1
. 002362	57. 2	1, 780	281	356	. 02195	. 0116	. 302	. 570	. 9
. 002362	57. 0	1, 770	277	351	. 0219	. 0116	. 302	. 570	. 8
. 002378	18. 0	1, 835	376	769	. 0444	. 0145	. 0919	. 282	. 9
. 002378	18. 0	1, 835	377	779	. 0448	. 01455	. 0919	. 284	. 9
. 002342	18. 45	1, 820	360	741	. 0441	. 0144	. 0947	. 291	. 8
. 002342	18. 85	1, 820	359	742	. 0442	. 01432	. 0967	. 299	1. 0
. 002380	40. 9	1, 800	333	557	. 0333	. 01335	. 213	. 529	. 0
. 002378	40. 8	1, 805	331	554	. 0330	. 01320	. 212	. 530	. 1
. 002375	43. 5	1, 780	308	488	. 0299	. 01270	. 229	. 538	-. 1
. 002375	43. 3	1, 770	305	486	. 0301	. 01268	. 229	. 542	. 0
. 002365	46. 8	1, 775	300	457	. 0283	. 01245	. 247	. 561	-. 1
. 002365	46. 8	1, 775	300	453	. 0282	. 01245	. 247	. 558	. 0
. 002371	39. 5	1, 765	316	528	. 0330	. 01325	. 210	. 523	. 0
. 002371	39. 5	1, 775	315	534	. 0330	. 01308	. 2085	. 527	+ .1
. 002367	35. 9	1, 810	341	598	. 0356	. 01356	. 186	. 488	-. 1
. 002367	35. 3	1, 805	342	597	. 0357	. 0137	. 1836	. 478	-. 2



TABLE I—Continued  
TEST DATA—Continued  
2,000 R. P. M.  
(Tip speed 986.1 ft./sec.)

$\rho$	$V$ M. P. H.	$N$ R. P. M.	$Q$ lb. ft.	$T$ lb.	$C_T$	$C_P$	$V/nD$	$\eta$	Def. at 42 in. Rad., deg.
0.00238	85.8	2,000	285	190	0.00922	0.0093	0.401	0.398	+2.2
.00238	85.8	1,995	282	181	.00881	.0092	.402	.385	2.1
.002365	94.1	2,005	240	69	.00336	.0078	.444	.190	1.7
.002365	94.1	2,010	238	69	.00334	.0078	.440	.190	1.6
.00236	96.1	1,985	217	24	.001194	.0072	.454	.0754	1.7
.00236	96.0	1,980	215	22	.001102	.0072	.454	.0695	1.7
.002365	80.1	2,020	312	264	.01263	.01002	.371	.468	.6
.002365	80.1	2,020	314	266	.01272	.01009	.371	.470	.4
.002365	73.2	1,985	323	328	.01625	.01072	.345	.523	.4
.002365	74.3	1,995	321	327	.01605	.01058	.348	.528	.4
.002365	72.1	2,010	351	376	.0182	.01139	.334	.535	.8
.002365	72.1	2,035	360	382	.01805	.01138	.331	.526	.8
.00237	69.5	1,995	339	397	.0194	.01113	.324	.564	.5
.00237	70.0	2,000	345	398	.0194	.01126	.327	.564	.9
.002365	65.7	2,015	361	457	.0220	.0116	.305	.578	1.0
.002365	65.5	2,015	361	458	.0221	.01160	.304	.580	.9
.002365	62.2	1,995	371	480	.02355	.01218	.292	.565	.8
.002365	62.2	2,005	373	490	.00238	.01215	.290	.569	.6
.002342	20.2	1,960	440	898	.0462	.01512	.0962	.294	1.3
.002342	22.4	1,990	451	941	.0468	.01502	.1052	.327	1.4
.00238	43.0	2,000	431	735	.0357	.0140	.2015	.513	-----
.00238	42.5	2,005	433	748	.0361	.01403	.1985	.511	.4
.002376	45.6	2,010	422	711	.0342	.01363	.212	.532	.1
.002376	45.7	2,010	424	711	.0342	.01373	.214	.531	.0
.00237	47.7	2,000	405	671	.0326	.0132	.223	.551	.0
.00237	47.7	2,010	417	679	.0327	.0135	.221	.535	.0
.002369	41.1	1,985	415	735	.0363	.0138	.1941	.512	.0
.002369	40.3	1,985	416	735	.0363	.01382	.191	.502	.1
.002367	37.1	1,960	415	750	.0381	.01410	.1777	.480	.0
.002367	36.7	1,960	415	755	.0384	.01410	.1758	.478	.2

TABLE II  
FINAL ADJUSTED COEFFICIENTS  
Propeller No. 4413—7° at 42 in. Rad.  
1,200 R. P. M.  
(Tip speed 591.7 ft./sec.)

$\frac{V}{nD}$	$C_T$	$C_P$	$\eta$	$\sqrt{\frac{\rho V^5}{P n^2}}$	$\sqrt[5]{\frac{\rho V^5}{P n^2}}$
0.10	0.0409	0.0135	0.302	0.0272	0.234
.15	.0369	.0132	.419	.0760	.356
.20	.0321	.0127	.504	.158	.479
.25	.0269	.0120	.560	.286	.607
.30	.0211	.0110	.575	.470	.740
.35	.0142	.0100	.519	.725	.879
.40	.00815	.0086	.379	1.09	1.035
.45	.0016	.0070	.103	1.622	1.214

1,400 R. P. M.  
(Tip speed 690.3 ft./sec.)

$\frac{V}{nD}$	$C_T$	$C_P$	$\eta$	$\sqrt{\frac{\rho V^5}{P n^2}}$	$\sqrt[5]{\frac{\rho V^5}{P n^2}}$
0.10	0.0415	0.0136	0.305	0.0271	0.234
.15	.03725	.0133	.420	.0758	.356
.20	.0325	.0129	.503	.1576	.476
.25	.0271	.0121	.560	.284	.604
.30	.0211	.0110	.575	.470	.739
.35	.0150	.0100	.525	.725	.880
.40	.0086	.0087	.396	1.086	1.035
.45	.0015	.0070	.0965	1.622	1.213

TABLE II—Continued  
FINAL ADJUSTED COEFFICIENTS—Continued

1,600 R. P. M.

(Tip speed 788.9 ft./sec.)

$\frac{V}{nD}$	$C_T$	$C_P$	$\eta$	$\sqrt{\frac{\rho V^5}{P n^3}}$	$\sqrt[5]{\frac{\rho V^5}{P n^3}}$
0.10	0.0421	0.0138	0.305	0.02696	0.234
.15	.0380	.0135	.422	.0751	.356
.20	.0330	.0129	.511	.1575	.479
.25	.0274	.0122	.560	.285	.605
.30	.0215	.0113	.571	.464	.735
.35	.0153	.0101	.530	.721	.8775
.40	.0088	.0089	.396	1.071	1.0278
.45	.0018	.0072	.1125	1.601	1.207

1,800 R. P. M.

(Tip speed 887.5 ft./sec.)

0.10	0.0438	0.01445	0.303	0.02635	0.234
.15	.0392	.0140	.420	.0737	.351
.20	.0339	.0133	.509	.1550	.475
.25	.0281	.01255	.560	.2785	.600
.30	.0220	.01155	.570	.459	.733
.35	.0158	.01050	.526	.709	.8715
.40	.0093	.0092	.405	1.052	1.0205
.45	.00245	.0075	.147	1.570	1.196

2,000 R. P. M.

(Tip speed 986.1 ft./sec.)

0.10	0.0467	0.0151	0.309	0.0276	0.234
.15	.0415	.0146	.426	.0721	.349
.20	.0356	.0139	.511	.1520	.471
.25	.0292	.0130	.561	.274	.595
.30	.0226	.0119	.570	.452	.729
.35	.0157	.0106	.518	.705	.8795
.40	.0089	.0092	.388	1.052	1.0205
.45	.0019	.0074	.1154	1.58	1.200



---

## REPORT No. 303

---

# AN INVESTIGATION OF THE USE OF DISCHARGE VALVES AND AN INTAKE CONTROL FOR IMPROVING THE PERFORMANCE OF N. A. C. A. ROOTS TYPE SUPERCHARGER

By OSCAR W. SCHEY and ERNEST E. WILSON

Langley Memorial Aeronautical Laboratory





## REPORT No. 303

---

### AN INVESTIGATION OF THE USE OF DISCHARGE VALVES AND AN INTAKE CONTROL FOR IMPROVING THE PERFORMANCE OF N. A. C. A. ROOTS TYPE SUPERCHARGER

By OSCAR W. SCHEY and ERNEST E. WILSON

---

#### SUMMARY

*This report presents the results of an analytical investigation on the practicability of using mechanically operated discharge valves in conjunction with a manually operated intake control for improving the performance of N. A. C. A. Roots type superchargers. The investigation was conducted by the staff of the National Advisory Committee for Aeronautics at Langley Field, Va.*

*These valves, which may be either of the oscillating or rotating type, are placed in the discharge opening of the supercharger and are so shaped and synchronized with the supercharger impellers that they do not open until the air has been compressed to the delivery pressure. The intake control limits the quantity of air compressed to engine requirements by permitting the excess air to escape from the compression chamber before compression begins.*

*The percentage power saving and the actual horsepower saved were computed for altitudes from 0 to 20,000 feet. These computations are based on the pressure-volume cards for the conventional and the modified Roots type superchargers and on the results of laboratory tests of the conventional type.*

*The use of discharge valves shows a power saving of approximately 26 per cent at a critical altitude of 20,000 feet. In addition, these valves reduce the amplitude of the discharge pulsations and increase the volumetric efficiency. With slow-speed Roots blowers operating at high-pressure differences even better results would be expected. For aircraft engine superchargers operating at high speeds these discharge valves increase the performance as above, but have the disadvantages of increasing the weight and of adding a high-speed mechanism to a simple machine.*

#### INTRODUCTION

The practicability of supercharging aircraft engines as a means of improving their performance at altitude has led to an increasing demand for superchargers of high efficiency, low weight, and low power requirements.

Most of the aircraft engine superchargers in use at the present time are modifications of conventional types of air compressors. The N. A. C. A. Roots type supercharger, which is a modification of the commercial Roots blower, has given very satisfactory results for the supercharging of aircraft engines. (References 1 and 2.) This supercharger is fully described in Report No. 230 of the National Advisory Committee for Aeronautics. (Reference 3.) The reciprocating compressor, which is the most efficient from a theoretical point of view, has met with little success as an aircraft engine supercharger, because of the strict weight limitations imposed by all aircraft service.

A comparison of the pressure-volume cards for the reciprocating and the Roots compressors shows that a considerable saving in power could be effected if the Roots supercharger were modified so that its card, which is rectangular, would approach that of the reciprocating compressor which has an adiabatic compression line. The practicability of using discharge valves and an intake control in obtaining this power saving was investigated by the staff of the National Advisory Committee for Aeronautics at Langley Field, Va.



Pressure-volume cards for conventional and modified Roots superchargers designed for 20,000 feet critical altitude were computed. The percentage saving in power and the actual horsepower saved were calculated for altitudes from 0 to 20,000 feet for a supercharger using rotating discharge valves with and without an intake control.

As far as is known, no experimental work of this nature has been attempted, with the exception of a few preliminary tests on flap valves that were conducted several years ago at this laboratory.

#### DESCRIPTION AND METHODS

The method herein described to improve the performance of a Roots type supercharger involves the use of mechanically operated discharge valves in conjunction with a manually operated intake control. The discharge valves reduce the impeller area subjected to the delivery pressure, prevent the back flow of air that has been compressed in the delivery duct by blocking the discharge passage, and prevent the flow of air from one side of the supercharger case to the other side. The intake control limits the volume of air compressed at any altitude below the critical altitude to the amount required by the engine instead of inducting and compressing more air than required and then by-passing the excess air as is done in the conventional type supercharger.

These discharge valves are synchronized with the impellers and do not open until the intake air has been compressed to the desired pressure, usually 14.7 pounds per square inch. To obtain this condition with a simple driving mechanism, it is necessary that the discharge valves always open at the same time and that the compression pressure be controlled by the amount of air in the compression chamber when compression begins. The amount of air compressed is limited to engine requirements by permitting the excess air to escape from the compression chamber through manually controlled intake ports before compression begins.

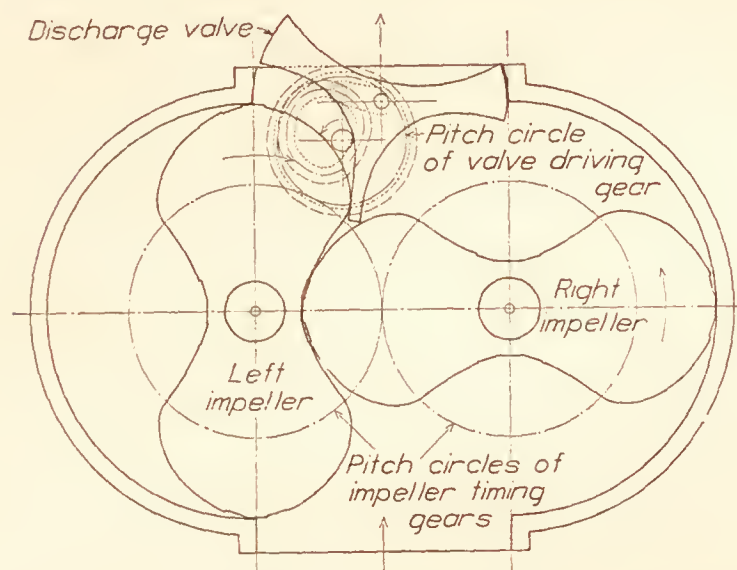


FIG. 1.—Diagrammatic cross section of a Roots type compressor with an oscillating discharge valve

If an intake control is not used in conjunction with the discharge valves, a by-pass valve of normal construction should be added to the upper part of the supercharger case to permit by-passing of the excess compressed air so that the pressures within the modified supercharger will not be greater than those for a normal supercharger.

The principal of operation of the oscillating discharge valve is shown in Figure 1. This valve is located in the center of the discharge opening and is mechanically operated, so that the tongue of the valve, which extends into the case between the impellers, contacts first with one impeller and then with the other. The back flow of air is prevented by the cross member of the valve which closes the discharge passage as soon as the compressed air has been delivered. The tongue prevents the flow of air from one side of the case to the other side and reduces the impeller area subjected to the delivery pressure. As the impeller rotates from the vertical position to the horizontal position, the point of contact between the discharge valve and impeller moves nearer the tip of the impeller. At this point the cross member of the discharge valve contacts with the other side of the impeller lobe. As soon as the impeller has reached the horizontal position the cycle is repeated on the other impeller. For each revolution of the impeller the discharge valve oscillates twice.

The principle of operation of the rotating discharge valves is shown in Figure 2. These valves are synchronized with the impellers by gears which are driven from the impeller timing gears. The discharge valves are so shaped that they contact with the impeller lobe in the vertical position on the high-pressure side, and as the impeller rotates this point of contact



moves to the opposite side of the same impeller lobe. This contact for the rotating valve is maintained until the valve is opened, which, for a 20,000 foot supercharger using  $9\frac{1}{2}$ -inch diameter impellers, corresponds to  $80^\circ$  rotation from the vertical. The air is discharged through the ends of the case with this valve arrangement. A flange is placed on the end of each discharge valve outside of the plane of impeller rotation to prevent the back flow of air. These valves rotate at twice the speed of the impellers.

The intake control shown diagrammatically in conjunction with the rotating discharge valves in Figure 2 is a simple method for limiting the volume of the air compressed. This control is manually operated and replaces the by-pass valve used on other installations where the conventional type supercharger is used. In order that this intake control may best serve its purpose, it must be so constructed that compression does not begin until all the air not required by the engine has escaped from the compression chamber. This control could also be used on a supercharger equipped with an

oscillating discharge valve. The intake control would not be necessary on a supercharger that is always operating at approximately the same altitude and delivering air at a constant rate.

In computing the percentage power saving obtained by the use of discharge valves with and without an intake control it was necessary to assume some definite critical altitude which for this investigation was taken as 20,000 feet. Pressure-volume cards and torque curves corresponding to this critical altitude were prepared for the conventional and the modified Roots type superchargers. The volume and pressure of the air within the compression chamber for

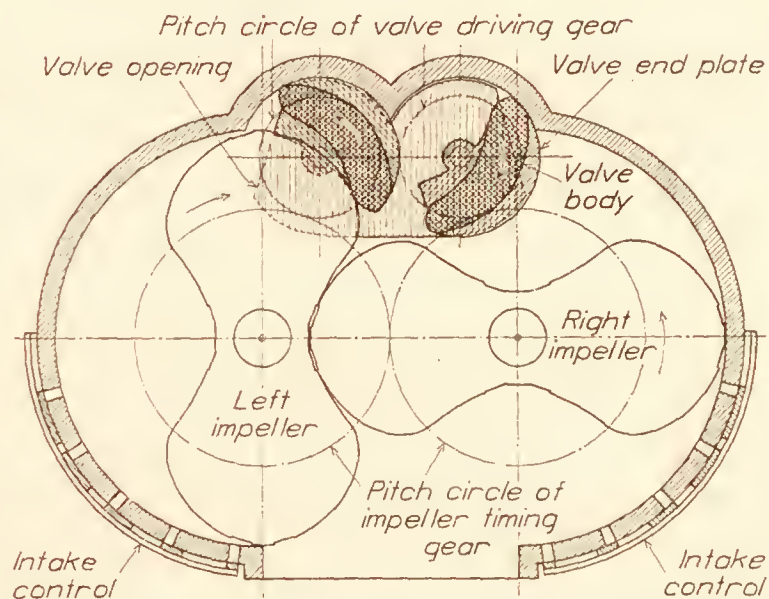


FIG. 2.—Diagrammatic cross section of a Roots type compressor with two rotating discharge valves

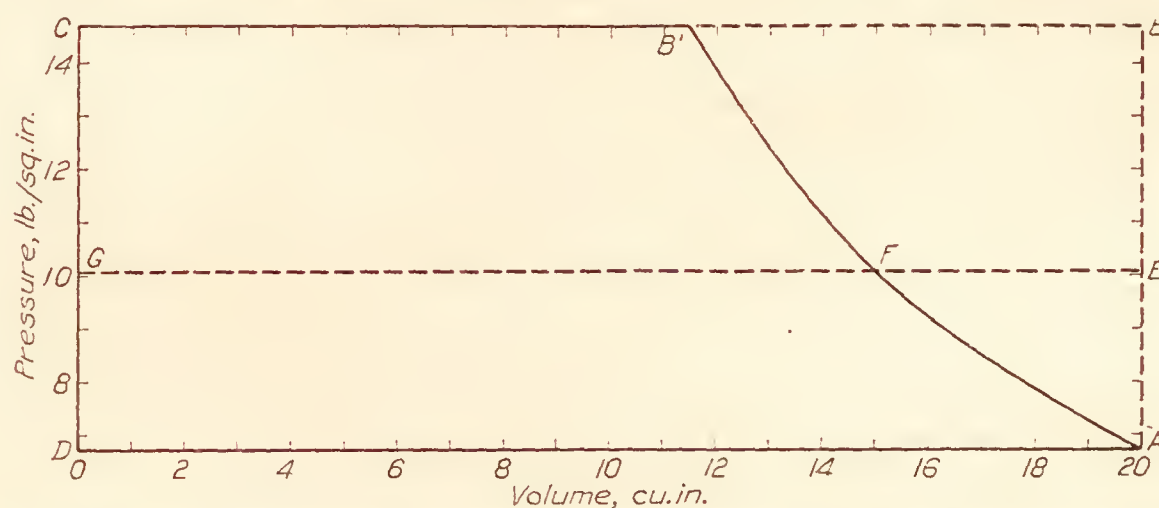


FIG. 3.—Pressure volume cards for the conventional and modified N. A. C. A. Roots type supercharger

each  $10^\circ$  position of the impellers were determined for both the conventional and the modified Roots type superchargers. From the pressures thus obtained torque curves were computed for both superchargers, assuming an impeller length of 1 inch. The torque curves for the conventional and the modified supercharger were compared to obtain the percentage power saving at a critical altitude of 20,000 feet.

The area of the pressure-volume cards ABCD and AB'CD (Fig. 3) for the conventional and the modified Roots superchargers, respectively, were also compared to obtain the per cent saving in power at a critical altitude of 20,000 feet. In a similar manner, the percentage saving in power for all altitudes below 20,000 feet was obtained. For instance, at 10,000 feet the ratio of the areas EBCG and FB'CG gives the ratio of the work in compressing air from intake pressure to discharge pressures and delivering at discharge pressures for the conventional and the modified superchargers, respectively. The actual horsepower saving was calculated from



the percentage power saving determined from the pressure-volume cards and the results of power measurements obtained in laboratory tests on the conventional type of supercharger. (Reference 4.)

### RESULTS

The results of this investigation are presented in the form of pressure-volume cards and curves. The pressure-volume card ABCD, shown in Figure 3, represents the work done in compressing the air by the conventional supercharger which operates against the delivery pressure throughout the complete cycle, and the pressure-volume card AB'CD, also shown in Figure 3, represents the work done by the modified supercharger which compresses the intake air adiabatically to the discharge pressure. The line AB' represents the compression line at a

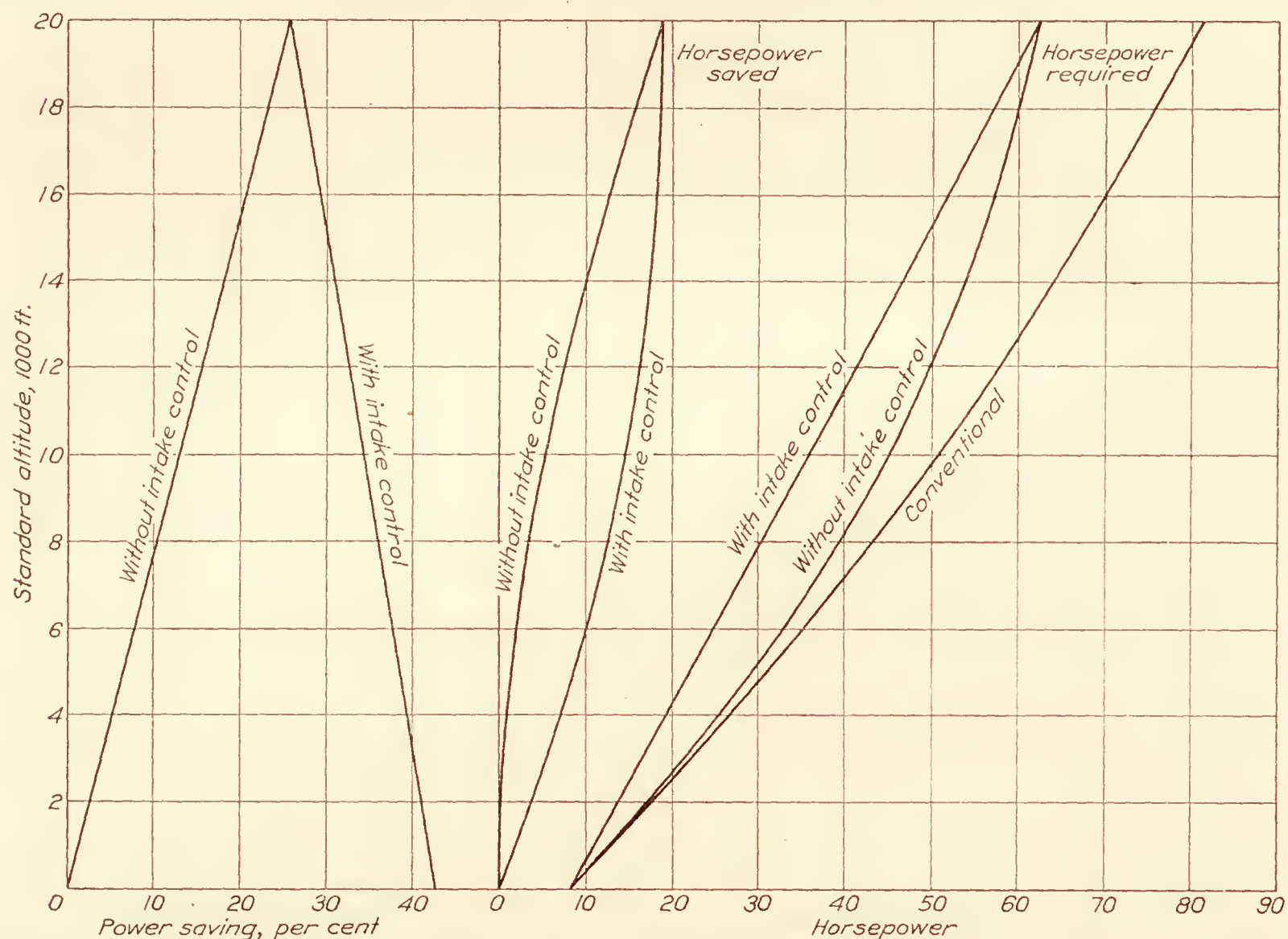


FIG. 4.—The percentage power saving and the power saved for the modified Roots supercharger with and without an intake control and the power required by the modified compared with the conventional

critical altitude of 20,000 feet for a modified Roots supercharger with or without an intake control. For lower altitudes the position where the excess air has escaped from the compression chamber and compression begins moves along the line AB' to a pressure corresponding to the altitude at which the supercharger is operating.

The percentage power saving computed for altitudes up to 20,000 feet, with and without an intake control, is shown by the curves in Figure 4. For the modified type, without an intake control, the percentage power saving increased from zero per cent at sea level to approximately 26 per cent at 20,000 feet. For the same discharge valves with an intake control the percentage power saving varied from approximately 42 per cent at sea level to 26 per cent at 20,000 feet. The torque curves (fig. 5) show a percentage power saving of 24 per cent at 20,000 feet.

The actual horsepower saved by the use of rotating discharge valves, with and without an intake control, is shown in Figure 4. It will be noted that at the critical altitude the percentage power saved and the actual horsepower saved are the same for operation with or without an intake control.



Figure 4 also shows the power required to drive a conventional supercharger of 0.382 cubic feet displacement per revolution at 5,280 revolutions per minute for altitudes from 0 to 20,000 feet. These power measurements were obtained from laboratory tests. (Reference 4.) Similar curves representing the power required to drive the modified supercharger with and without an intake control and for altitudes from 0 to 20,000 feet are shown for comparison with the conventional supercharger.

#### DISCUSSION OF RESULTS

The pressure-volume cards shown in Figure 3 and the curves shown in Figures 4 and 5 give interesting information on the possibilities of using discharge valves in Roots type superchargers, the service for which they may be used, and their limitations.

The pressure-volume cards show that as the critical altitude is increased the percentage power saving will be increased, the line  $AB'$  being transferred to the left, the point  $B'$  moving toward  $C$ , and the point  $A$  moving down to the lower pressure which corresponds to the higher critical altitude. This, however, does not indicate that it would be better to use a 30,000-foot critical altitude supercharger for service in which only a 20,000-foot supercharger is needed because the increased impeller speed of the supercharger for the higher critical altitude would require considerably more power than the increased saving that could be effected on the pressure-volume card. It does, however, indicate that there may be critical altitudes so low that very little if any power saving can be effected.

An examination of the compression chambers of the conventional and the modified Roots superchargers showed that the volume of the compression chamber of the modified supercharger is about 5 per cent greater because of the space around the discharge valves. The difference in the volume caused by this space around the discharge valves has no effect on the results for this method of computing because the energy received during compression by the air trapped around these valves is equal to that given up during expansion on the following cycle. The results presented are based on the volume of a compression chamber of the conventional type supercharger.

A comparison of the results obtained with and without an intake control indicates that very little saving in power can be effected below 10,000 feet without the intake control. The saving of  $5\frac{1}{2}$  horsepower at 10,000 feet without the control corresponds to the power saving at 3,000 feet with the control. The intake control is a satisfactory method of limiting the quantity of air compressed because it shows a large saving in power, is simple to operate, and does not weight more than the by-pass valve which it replaces.

The curves shown in Figure 3 representing the power required to drive the modified superchargers are based on laboratory tests of a conventional supercharger operated at a speed of 5,280 revolutions per minute and on the percentage power saving as determined from the pressure-volume cards. In making these computations the friction and charging losses determined experimentally for a conventional supercharger were used for the modified supercharger so that the only losses that have not been considered in these computations are similar losses in the discharge valves. Inasmuch as the diameter of these valves is small compared to the diameter of the rotors, it is believed that the air friction losses would be small.

Figure 5 shows a graphical comparison between the torques determined for a critical altitude of 20,000 feet for a conventional and a modified supercharger. For the conventional supercharger the mean torque is 102-inch pounds as compared with 78-inch pounds for the modified supercharger. This gives a power saving of 24 per cent. It will be noted that the power saving at a critical altitude of 20,000 feet determined from the torque curves checks within 2 per cent of the power saving determined from the pressure-volume cards. The irregularities in the torque curve for the modified supercharger are caused by the expansion of the air trapped around the discharge valves and the change of the point of contact between the valve and the impeller from one side of the impeller to the other side. As soon as the discharge valves have opened, which is at about  $80^\circ$  for one and  $170^\circ$  for the other, the torque curves for the modified and conventional superchargers are the same for the next  $10^\circ$  of impeller rotation.



Several discharge valve arrangements and different driving mechanisms were considered, but nearly all methods tried required a driving mechanism giving a cyclic variation in speed which usually introduced high inertia stresses. From the various discharge valves considered in a general analysis, the rotating valves were selected as the most desirable for the high impeller speeds necessary in aircraft service and the oscillating valve as a desirable substitute for slower speed machines. Though the best discharge valve location and shape has not been definitely determined, a sufficient number of positions were studied to indicate that the location and shape shown in Figure 2 can not be greatly improved. The valves shown restrict the discharge opening, but this is not a serious objection because at sea level the volume inducted is reduced by the amount ordinarily by-passed and at higher altitudes the volume is reduced by compression.

A supercharger equipped with discharge valves should show an appreciable increase in volumetric efficiency when operating at low speeds and a slight increase in volumetric efficiency at high speeds, because the amount of air that slips back between the case and the impellers is

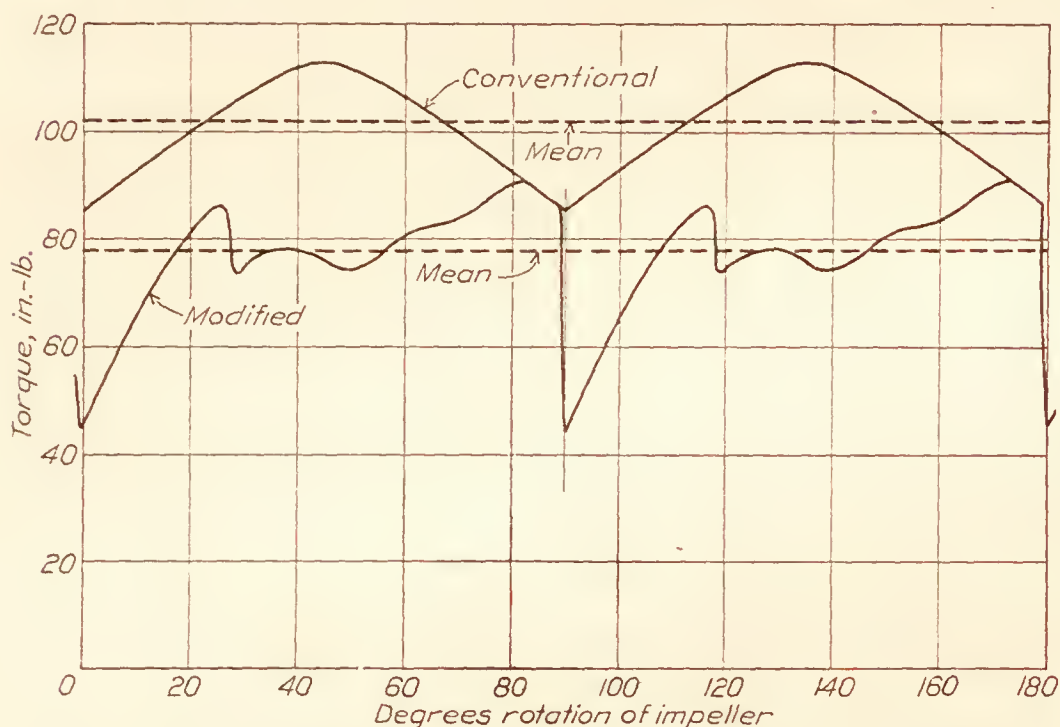


FIG. 5.—Torque curves for conventional and modified N. A. C. A. Roots type supercharger

reduced. The amount of air that slips back for each revolution of the impellers is a function of the time that the impellers are subjected to the delivery pressure. This time depends on both the speed at which the impellers are rotating and the number of degrees of impeller rotation that the discharge valves prevent the high-pressure air from acting on the impellers. Because the amount of air that slips back between the impellers and case is greater in a slow-speed supercharger than in a high-speed supercharger it is evident that the use of discharge valves will prevent a greater amount of air from slipping back in the slow-speed machine. The volumetric efficiency of the slow-speed supercharger will therefore be increased more than that of the high-speed supercharger.

An estimate was made of the increase in supercharger weight necessary in the application of the rotating discharge valves to the supercharger on which the power computations were based. In this estimate the weight of the discharge valves, counterbalance weights on the valves, increase in the length of the supercharger case, increase in length of the impeller shaft, valve gears, and bearings were considered. The increase in weight was estimated to be 17 pounds. Thus, a saving of approximately 20 horsepower may be obtained at a critical altitude of 20,000 feet by adding discharge valves which increase the weight of the supercharger approximately 17 pounds.

#### CONCLUSION

The results of this investigation show that the power saving varies from approximately 42 per cent at sea level to 26 per cent at 20,000 feet altitude by the use of discharge valves and an intake control in a conventional Roots type supercharger. Without the intake control the power saving will vary from 0 per cent at sea level to 26 per cent at 20,000 feet. These valves will reduce the discharge pulsations, because there is only a slight back flow of air, and will increase the volumetric efficiency by reducing the amount of air that slips back between the impellers and case.

For slow-speed Roots compressors operating at high-pressure differences the discharge valves will effect a saving in power greater than 26 per cent and also show a larger increase in volumetric efficiency than that obtained for high-speed compressors.



The application of these discharge valves to aircraft engine superchargers requires a consideration of the disadvantages of increasing the weight and of adding a mechanism operating at high speed to a simple machine.

LANGLEY MEMORIAL AERONAUTICAL LABORATORY,  
NATIONAL ADVISORY COMMITTEE FOR AERONAUTICS,  
LANGLEY FIELD, VA., *June 29, 1928.*

#### BIBLIOGRAPHY

- Reference 1. Gardiner, Arthur W., and Reid, Elliott G.: Preliminary Flight Tests of the N. A. C. A. Roots Type Aircraft Engine Supercharger. N. A. C. A. Technical Report No. 263 (1927).
- Reference 2. Ware, Marsden, and Schey, Oscar W.: A Preliminary Investigation of Supercharging an Air-Cooled Engine in Flight. N. A. C. A. Technical Report No. 283 (1928).
- Reference 3. Ware, Marsden: Description and Laboratory Tests of a Roots Type Aircraft Engine Supercharger. N. A. C. A. Technical Report No. 230 (1926).
- Reference 4. Ware, Marsden, and Wilson, Ernest E.: The Comparative Performance of Roots Type Aircraft Engine Superchargers as Affected by Changes in Impeller Speed and Displacement. N. A. C. A. Technical Report No. 284 (1928).





---

---

**REPORT No. 304**

---

**AN INVESTIGATION  
OF THE AERODYNAMIC CHARACTERISTICS OF  
AN AIRPLANE EQUIPPED WITH SEVERAL  
DIFFERENT SETS OF WINGS**

**By J. W. CROWLEY, Jr., and M. W. GREEN  
Langley Memorial Aeronautical Laboratory**





## REPORT No. 304

### AN INVESTIGATION OF THE AERODYNAMIC CHARACTERISTICS OF AN AIRPLANE EQUIPPED WITH SEVERAL DIFFERENT SETS OF WINGS

By J. W. CROWLEY, Jr., and M. W. GREEN

#### SUMMARY

*This investigation was conducted by the National Advisory Committee for Aeronautics at Langley Field, Va., at the request of the Army Air Corps, for the purpose of comparing the full scale lift and drag characteristics of an airplane equipped with several sets of wings of commonly used airfoil sections. A Sperry Messenger airplane with wings of R. A. F.-15, U. S. A.-5, U. S. A.-27, and Göttingen 387 airfoil sections was flown and the lift and drag characteristics of the airplane with each set of wings were determined by means of glide tests.*

*The results are presented in tabular and curve form.*

#### INTRODUCTION

While there is a very considerable amount of data existent on the aerodynamic characteristics of airplanes and airfoils as obtained in wind tunnel model tests, very little information of this kind has been obtained in full-scale flight test. For the purpose of comparing directly the full-scale lift and drag characteristics of a number of commonly used airfoils and also of providing a basis for comparison with model tests, the present tests on a Sperry Messenger airplane equipped with R. A. F.-15, U. S. A.-5, U. S. A.-27, and Göttingen 387 wings were instituted. The investigation was conducted by the National Advisory Committee for Aeronautics, at Langley Field, Va., at the request of the Army Air Corps. The airplane and wings were furnished by the latter. Six sets of wings of different airfoil section were constructed for the investigation, but during the conduction of the tests this type of airplane was condemned as being structurally unsafe and only the above-mentioned wings were used.

The lift and drag characteristics of the complete airplane with each set of wings were obtained by means of glide tests with the propeller operating at the  $\frac{V}{nD}$  of zero thrust. It is essential in glide tests that the airplane be motivated by its weight only and, consequently, propeller thrust must be eliminated or allowed for. Two general methods are used: (1) Glide tests with the propeller stopped and locked in a definite position, and (2) glide tests with the propeller operating at the  $\frac{V}{nD}$  to produce no thrust. It was necessary to use the latter method in this investigation since the size and loading of the airplane prohibited the use of propeller braking apparatus on the engine.

The  $\frac{V}{nD}$  to be used in flight was determined from the results of a wind tunnel test of a 3-foot model of the Sperry Messenger propeller, tested with no body behind it. It was realized that the value thus obtained would be different from the actual  $\frac{V}{nD}$  of zero thrust in flight since scale effect and the presence of a body behind the propeller would be expected to change this value, and consequently the propeller operating at this  $\frac{V}{nD}$  in flight would be delivering



some thrust. However, since it was a part of the program of these tests to measure the actual  $\frac{V}{nD}$  of zero thrust on the identical airplane and propeller at a later date in the 20-foot propeller research tunnel (then under construction), it was considered satisfactory to conduct the flight tests at the  $\frac{V}{nD}$  determined from the model test, as approximating the true  $\frac{V}{nD}$  of zero thrust, and then correct the flight results for thrust on the basis of the measurements obtained in the propeller research tunnel tests, when the latter were made available. Actually the flight tests were made at a  $\frac{V}{nD}$  of 1.08 while the true  $\frac{V}{nD}$  for zero thrust as determined in the propeller research tunnel was 1.07 to 1.08, making the correction on this account negligible.

#### APPARATUS AND METHOD

**AIRPLANE AND WINGS.**—A standard Sperry Messenger airplane (fig. 1) equipped with United States Air Service propeller No. 048765 and with four interchangeable sets of wings of different airfoil section was used in this investigation. The airfoil sections were R. A. F.-15, U. S. A.-5, U. S. A.-27, and Göttingen 387. The wings were all of rectangular plan form with equal area and aspect ratio (fig. 2) and were constructed in the conventional manner for wooden

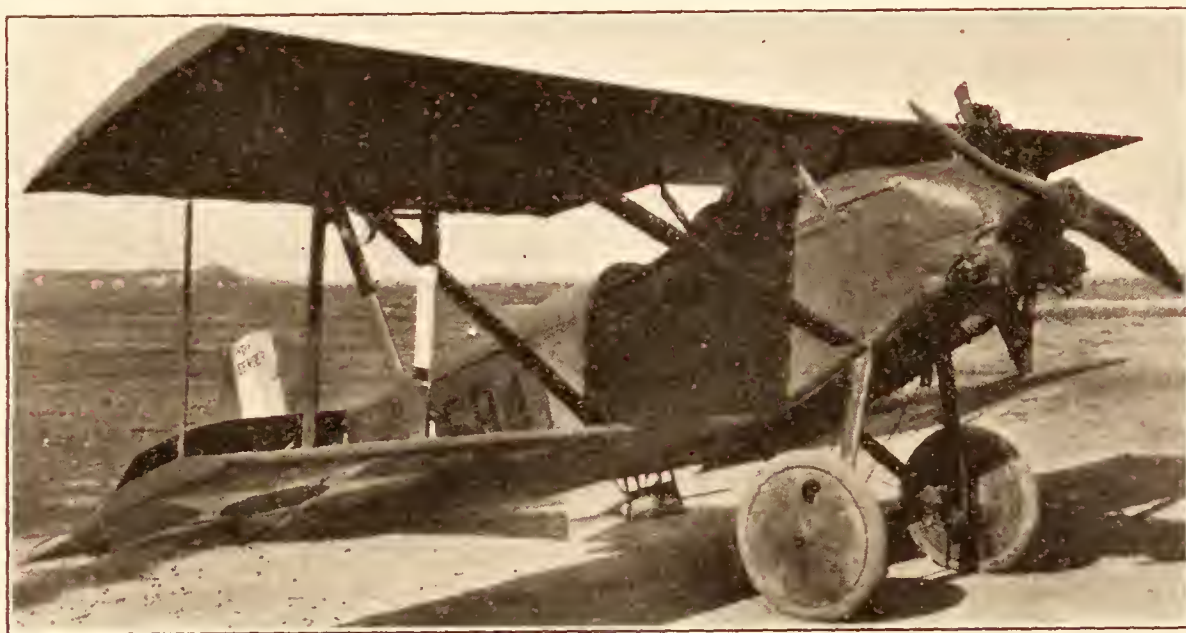


FIG. 1.—Sperry Messenger airplane with flight path angle recorder installed

wings with plywood between the leading edge and the front spar. The dimensions of the biplane cellule were the same for all sets of wings: Span 20 feet, gap 3 feet 10 inches, dihedral  $1\frac{1}{2}^\circ$ , and incidence  $+2^\circ$ . The stabilizer was fixed at  $+1\frac{1}{2}^\circ$  throughout the tests. Including the area of the center section the total wing area was 148.5 square feet.

**INSTRUMENTS.**—The following special test instruments were used:

(1) *N. A. C. A. flight path angle and air-speed recorder* (reference 1).—This instrument, as its name implies, was used for measuring the air speed and the angle of inclination that the airplane's flight path made with the horizontal. It is a suspended type instrument and in these tests was lowered approximately 35 feet below the airplane.

(2) *N. A. C. A. recording inclinometer*.—This instrument consists essentially of an oil-damped pendulum mounted in the standard photographic recording type of instrument used by the N. A. C. A. It was used to record the attitude of the airplane with respect to the horizontal which, together with the flight path angle, determines the angle of attack.

(3) *N. A. C. A. recording altimeter and air-speed meter*.—This instrument is a standard recording air-speed meter (reference 2) with an aneroid mechanism incorporated in it. It was used primarily to measure the barometric pressure during the tests. The air-speed readings provided a check on the air speed recorded by the flight path recorder and the change of altitude with time, together with the air speed, was used to check the flight path angle recorded by the flight path recorder.



(4) *N. A. C. A. control position recorder* (reference 3).—This instrument was used to measure the elevator angle during the tests.

(5) *Revolution counter*.—The revolutions of the engine were recorded by means of a contact-making apparatus which, connected to the service tachometer shaft, completed an electrical circuit every 50 revolutions of the engine and flashed a light in a standard photographic type recording instrument. These light flashes were recorded on a moving film as a series of dots and knowing the film speed enabled the computation of engine revolutions per minute. Film speed was determined from timing lines placed on the record as mentioned below.

(6) *Thermometer*.—An indicating distance thermometer, mounted on the strut, the readings of which were taken by the pilot, gave the air temperatures during the tests.

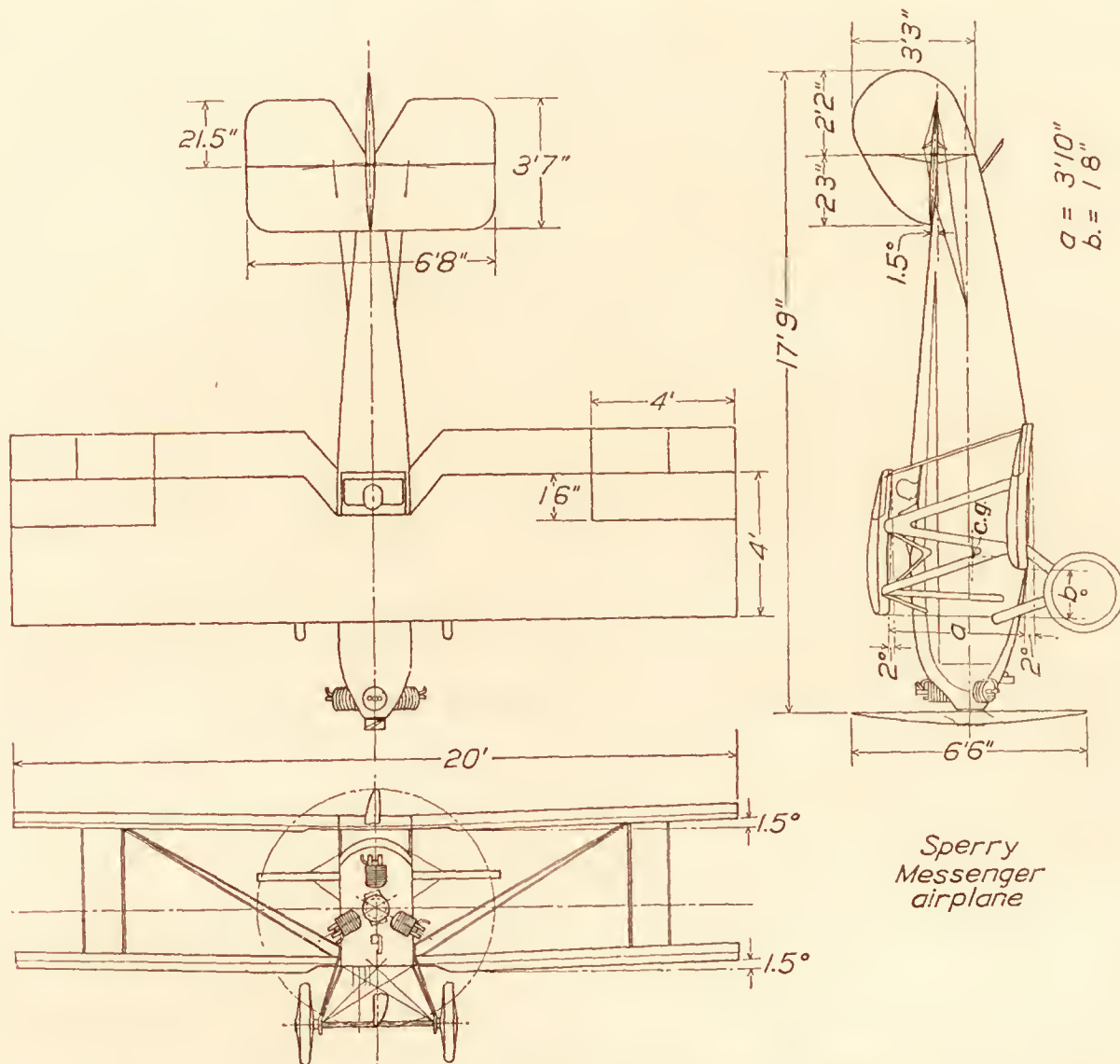


FIG. 2.—Elevations and plan of the Sperry Messenger airplane

The photographic records of all of the above instruments were synchronized by means of timing lines placed simultaneously on all the records at definite time intervals by an N. A. C. A. timer. (Reference 4.)

**FLIGHT TESTS.**—Preliminary tests were made in level flight to determine the airworthiness of each set of wings and the desirability of continuing further tests.

Following the preliminary tests, the lift and drag characteristics of the airplane when equipped with each set of wings were obtained by means of glide tests (reference 5) with the propeller operating at the  $\frac{V}{nD}$  of zero thrust. As previously mentioned, this value of  $\frac{V}{nD}$  determined from the results of a 3-foot model test was 1.08. Glides were made at predetermined air speeds and engine revolutions per minute for a change of altitude of approximately 1,000 feet and records were taken for about one-half minute after the airplane had reached a steady condition. The range of speed covered was approximately 45 to 105 miles per hour. On each glide the following data were obtained: airplane weight, angle of flight path to horizontal, angle of wing chord to horizontal, dynamic pressure, barometric pressure, temperature, propeller revolutions

per minute, and elevator angle. All of these were obtained from the instruments previously mentioned except the weight, which was measured before each flight. An allowance was made for the weight of fuel burned during flight.

**REDUCTION OF DATA.**—The essential observed and computed data for the determination of lift and drag characteristics are given in Tables I, II, III, and IV.

While it was attempted to conduct the glide tests with the propeller operating at the  $\frac{V}{nD}$  of no thrust, this was seldom exactly accomplished since in the first place, as mentioned before, the  $\frac{V}{nD}$  of the model test was not the true  $\frac{V}{nD}$  for zero thrust in flight, and secondly (and most important) because of the difficulties in adjusting the airplane's air speed and engine speed to obtain the exact  $\frac{V}{nD}$  desired. Consequently, there was nearly always a small amount of thrust acting in addition to the weight of the airplane to produce the motion of the airplane, that had to be corrected for as follows:

The apparent drag is equal and opposite to  $W \sin \gamma$ , where  $\gamma$  is the angle of the flight path. Since thrust is present, true drag is equal to apparent drag plus the drag component of thrust

or  $D = W \sin \gamma + T \cos \beta$ , where  $\beta$  is the angle of the thrust axis with the flight path. Since  $\beta$  is small it is possible, within the limits of accuracy of the measurements, to consider  $T \cos \beta = T$  and the true drag is therefore equal to  $W \sin \gamma + T$ .  $T$  is determined for the  $\frac{V}{nD}$  attained in flight from the thrust coefficient

curve for this same propeller and airplane obtained in tests in the propeller research tunnel. (Fig 3)

In a like manner lift is equal to  $W \cos \gamma + T \sin \beta$ . Since  $T \sin \beta$  is negligible, lift is equal to  $W \cos \gamma$ .

The angle of attack given in the tables and curves is the angle of attack of the wing, and the coefficients are given in the absolute form, where

$$C_L = \frac{L}{qS}$$

$$C_D = \frac{D}{qS}$$

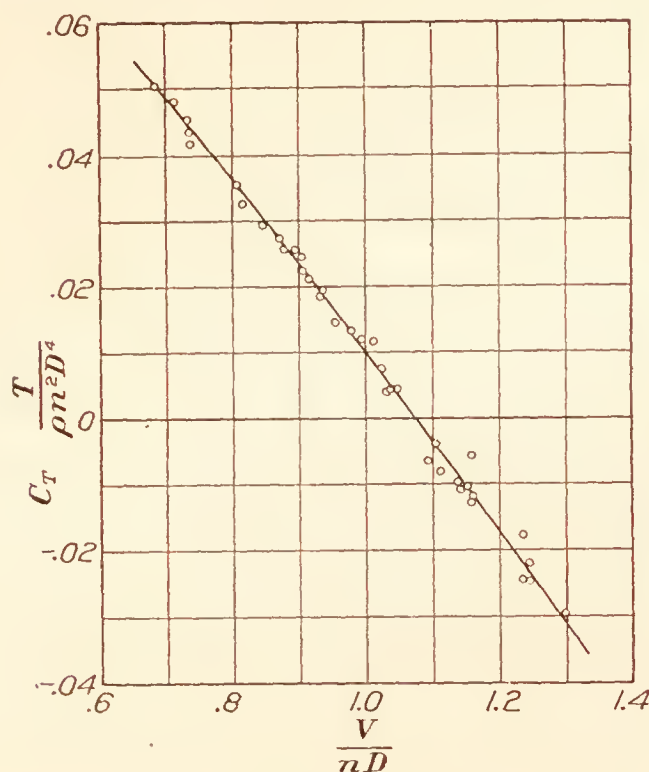


FIG. 3.—Propeller thrust characteristics from propeller research tunnel tests

**PRECISION.**—The greatest sources of error encountered in flight tests of this type are due to accelerations imposed on the airplane and the flight path

recorder by uneven air conditions or the piloting of the airplane during a glide. The instruments used were calibrated frequently during the tests and the errors due to inherent instrumental errors are believed to be negligible in comparison with the others. The tests were made only when the air was found to be unusually smooth and any readings that indicated the presence of accelerations were discarded, but even under these conditions and with the most careful piloting it is probable that accelerations were present to some extent. In general, considering the number and grouping of the experimental points, it is believed that the faired curves of lift and drag coefficients are precise to within  $\pm 2$  per cent. In the determination of angle of attack, accelerations might cause greater errors since this measurement is obtained from the readings of two pendulum type instruments and the angle of attack may, therefore, be in error as much as  $\pm 3$  or  $\pm 4$  per cent.

Another possible source of error lies in the fact that, while the propeller characteristics were determined in the wind tunnel with the propeller axis parallel to the relative wind, in flight the propeller was always operating with its axis at some angle of pitch, and consequently the  $\frac{V}{nD}$  for zero thrust from the wind tunnel tests might not be exactly that obtained in flight. However,



subsequent tests in the propeller research tunnel on a propeller operating with its axis at a pitch of  $5^\circ$ , indicated that the pitch produced no measurable change in the propeller characteristics, and it has been assumed in these tests that errors due to this cause are negligible.

### RESULTS

The results of the investigation are given in Tables I to IV, and Figures 4 to 15. Figures 4, 5, 6, and 7 give the polar diagrams of the airplane when equipped with R. A. F.-15, U. S. A.-5, U. S. A.-27, and Göttingen 387 wings, respectively, with the experimental points shown thereon. The polars for all four sets of wings are plotted together for comparison in Figure 8. In addition, the  $C_L$ ,  $C_D$ , and  $L/D$  versus angle of attack for these wings have been plotted in Figures 9 to 15, where Figures 9, 10, 11, and 12 give these results for each set of wings with the experimental points shown, and Figures 13, 14, and 15 compare the  $C_L$ ,  $C_D$ , and  $L/D$ , respectively.

It will be noted that considerably fewer measurements were obtained with the Göttingen 387 wings than with any of the others and consequently the curves for these are not as definitely established. This was occasioned by the fact that the airplane was condemned while the tests with these wings were in progress.

The results, as shown on the curves, cover the usual flying range of an airplane without reaching maximum lift or minimum drag, although the latter is more closely approached. It is usually difficult to obtain maximum lift in glide tests, and it was almost impossible in these particular tests since the engine could not be throttled sufficiently to give the proper  $\frac{V}{nD}$  at the low air speed required without danger of stopping the propeller. This would have been extremely hazardous because the pilot had to reel in the suspended flight path recorder in addition to piloting the airplane. Even without this difficulty it is believed that only slightly higher lifts could have been reached as the lateral control of the airplane was poor and the difficulties in holding the airplane in a steady glide at low speed were great.

The comparison of the lift and drag characteristics is best shown in Figure 8. This figure indicates that, as would be expected, the use of the thin section, R. A. F.-15, gives the lowest maximum lift and minimum drag, while the thicker section, Göttingen 387, gives the greatest maximum lift and highest minimum drag. The U. S. A.-5 and U. S. A.-27 give quite similar effects in all respects.

The comparisons given in Figures 13 and 14 are mainly of interest in that they show that the slopes of the lift curves (and to a somewhat less extent the slopes of the drag curves) are not greatly different, indicating quite similar characteristics with all sets of wings except, of course, in the region of maximum lift.

The comparison of the  $L/D$  of the airplane with the different wings (fig. 15) shows that the use of the U. S. A.-5 wings gave the highest  $L/D$  and the U. S. A.-27 only a slightly lower value.

In general, the results, particularly as shown in Figure 8, emphasize one fact which it is believed is not sufficiently appreciated and that is, that with the exception of the change in maximum lift, the use of different reasonably good airfoil sections in themselves can not be expected to greatly change the performance of an airplane. When it is considered that the drag of an airplane consists of the airplane's parasite drag, the profile and induced drag of the tail surfaces, the induced drag of the wings, and the profile drag of the wings, it will be more appreciated that different airfoil sections, which change only the wing profile drag, can not be expected to produce any great changes in the airplane's performance.

LANGLEY MEMORIAL AERONAUTICAL LABORATORY,  
NATIONAL ADVISORY COMMITTEE FOR AERONAUTICS,  
LANGLEY FIELD, VA., *July 9, 1928.*

## BIBLIOGRAPHY

- Reference 1. Coleman, D. G.: N. A. C. A. Flight Path Angle and Air-Speed Recorder. N. A. C. A. Technical Note No. 233 (1926).
- Reference 2. Norton, F. H.: N. A. C. A. Recording Air-Speed Meter. N. A. C. A. Technical Note No. 64 (1921).
- Reference 3. Ronan, K. M.: An Instrument for Recording the Position of Airplane Control Surfaces. N. A. C. A. Technical Note No. 154 (1923).
- Reference 4. Brown, W. G.: The Synchronization of N. A. C. A. Flight Records. N. A. C. A. Technical Note No. 117 (1922).
- Reference 5. Green, M. W.: Determination of the Lift and Drag Characteristics of an Airplane in Flight. N. A. C. A. Technical Note No. 223 (1925).



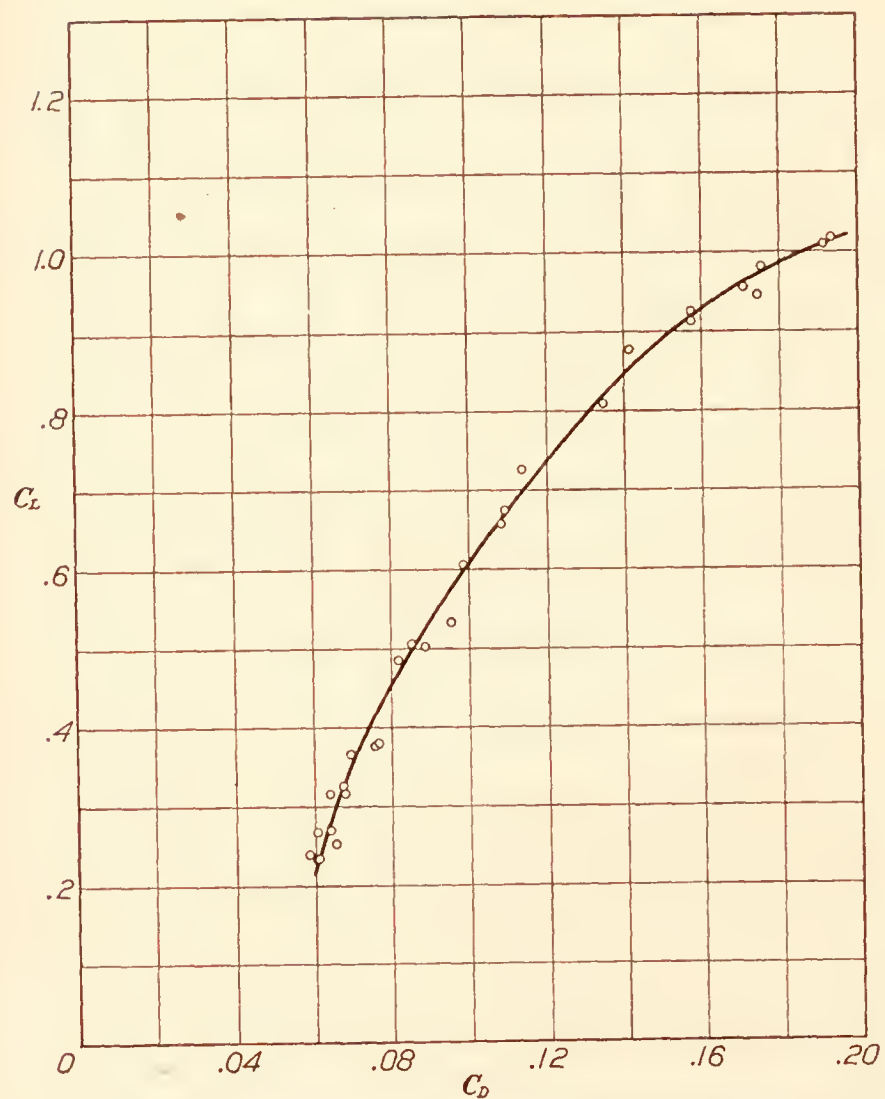


FIG. 4.—Sperry Messenger tests. Characteristics of R. A. F.-15 wings. Glide at  $\frac{V}{nD} = 1.075$

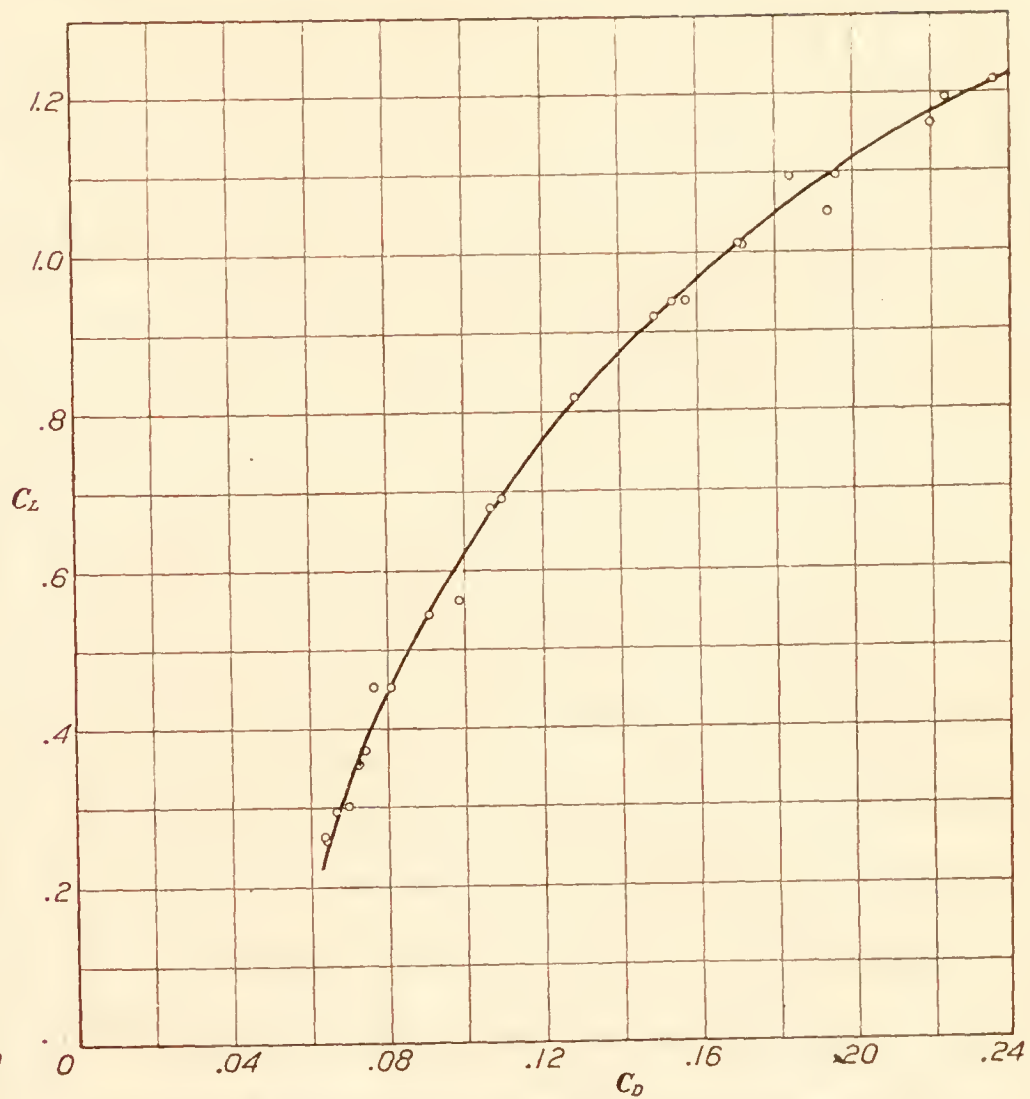


FIG. 6.—Sperry Messenger tests. Characteristics of U. S. A.-27 wings. Glide at  $\frac{V}{nD} = 1.075$

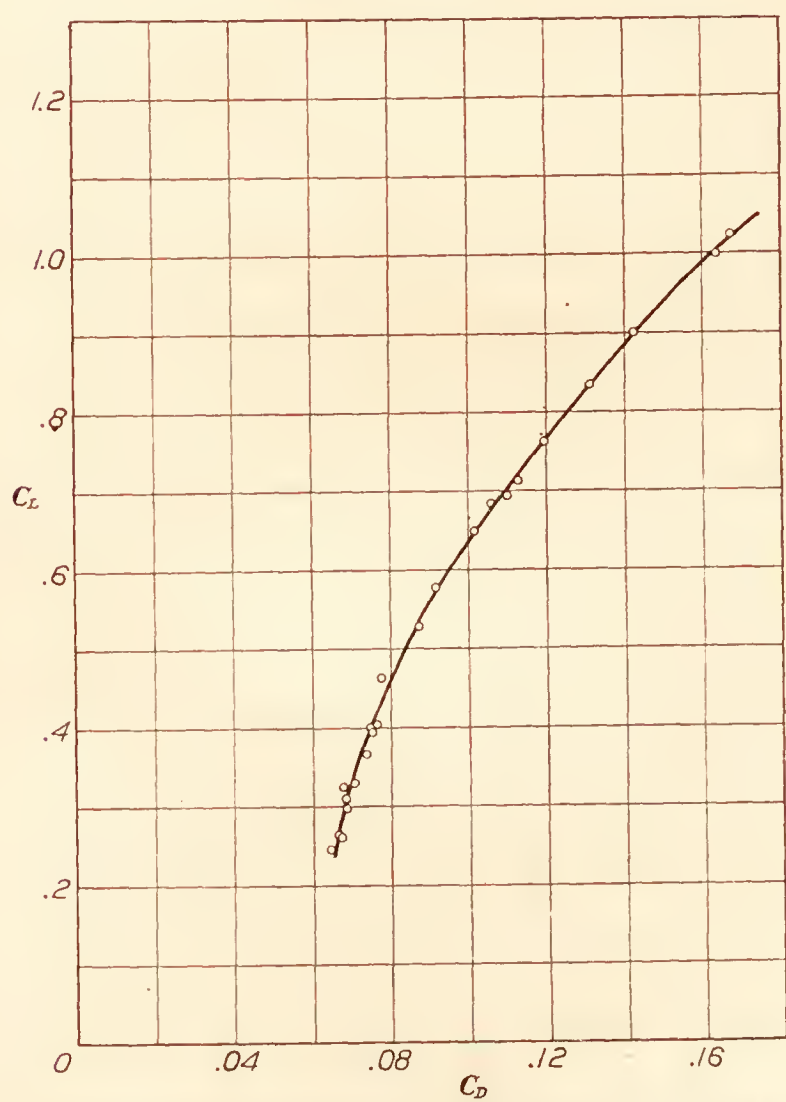


FIG. 5.—Sperry Messenger tests. Characteristics of U. S. A.-5 wings. Glide at  $\frac{V}{nD} = 1.075$

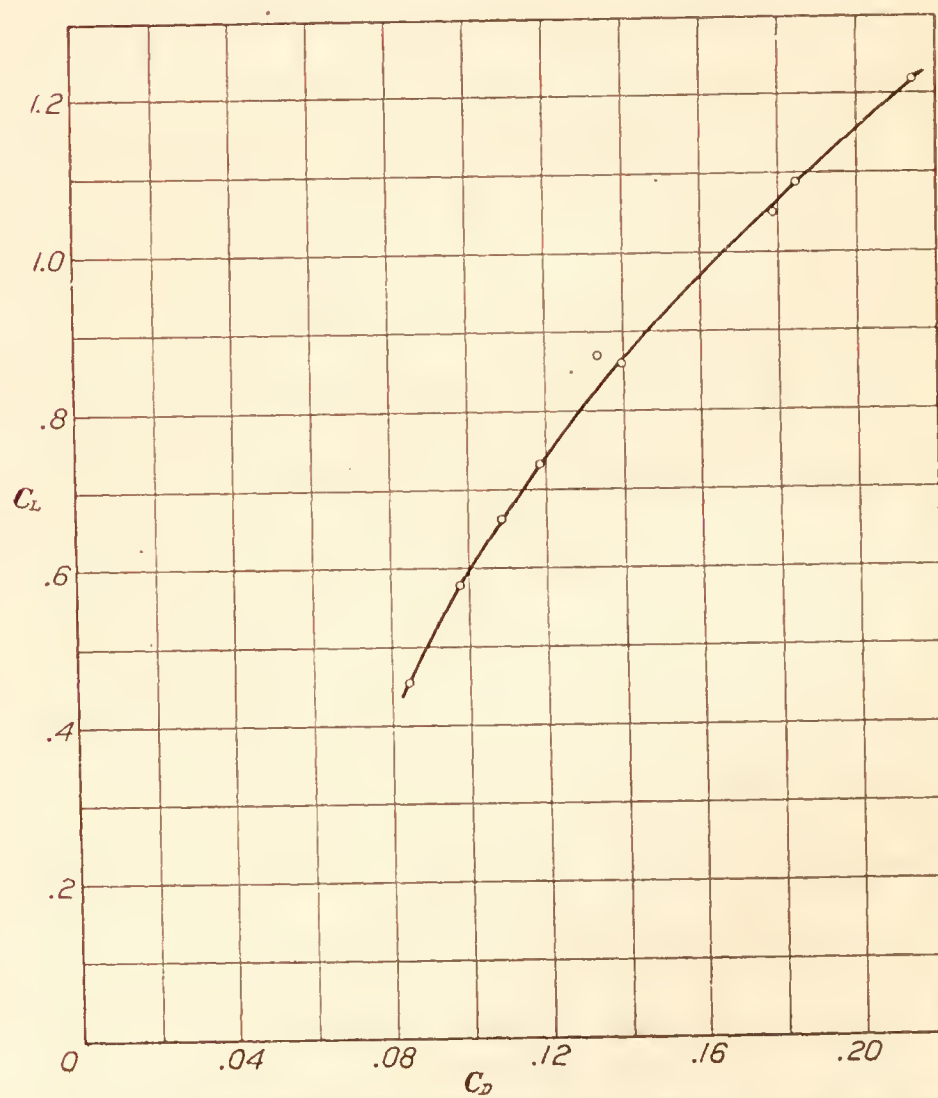


FIG. 7.—Sperry Messenger tests. Characteristics of Göttingen 387 wings. Glide at  $\frac{V}{nD} = 1.075$ . (Limited data)

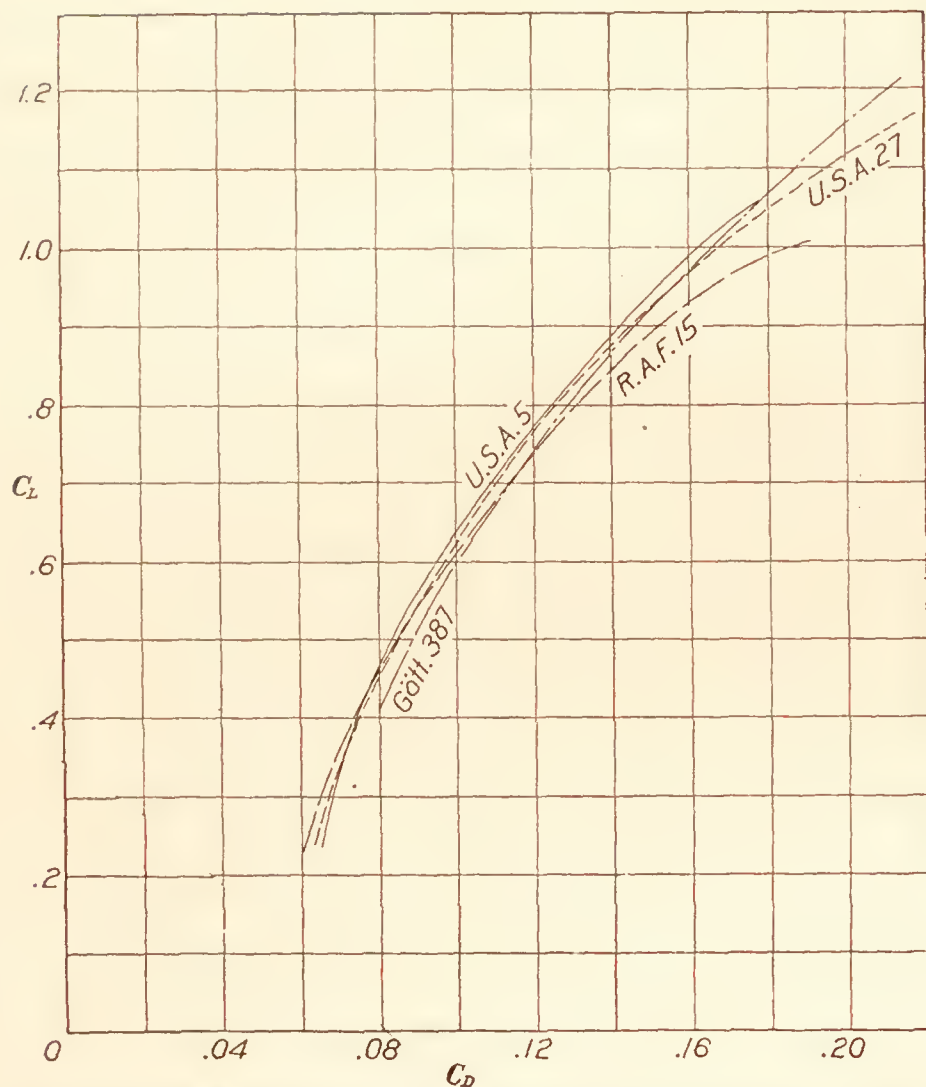


FIG. 8.—Sperry Messenger tests. Characteristics of the various wings. Glide at  $\frac{V}{nD} = 1.075$

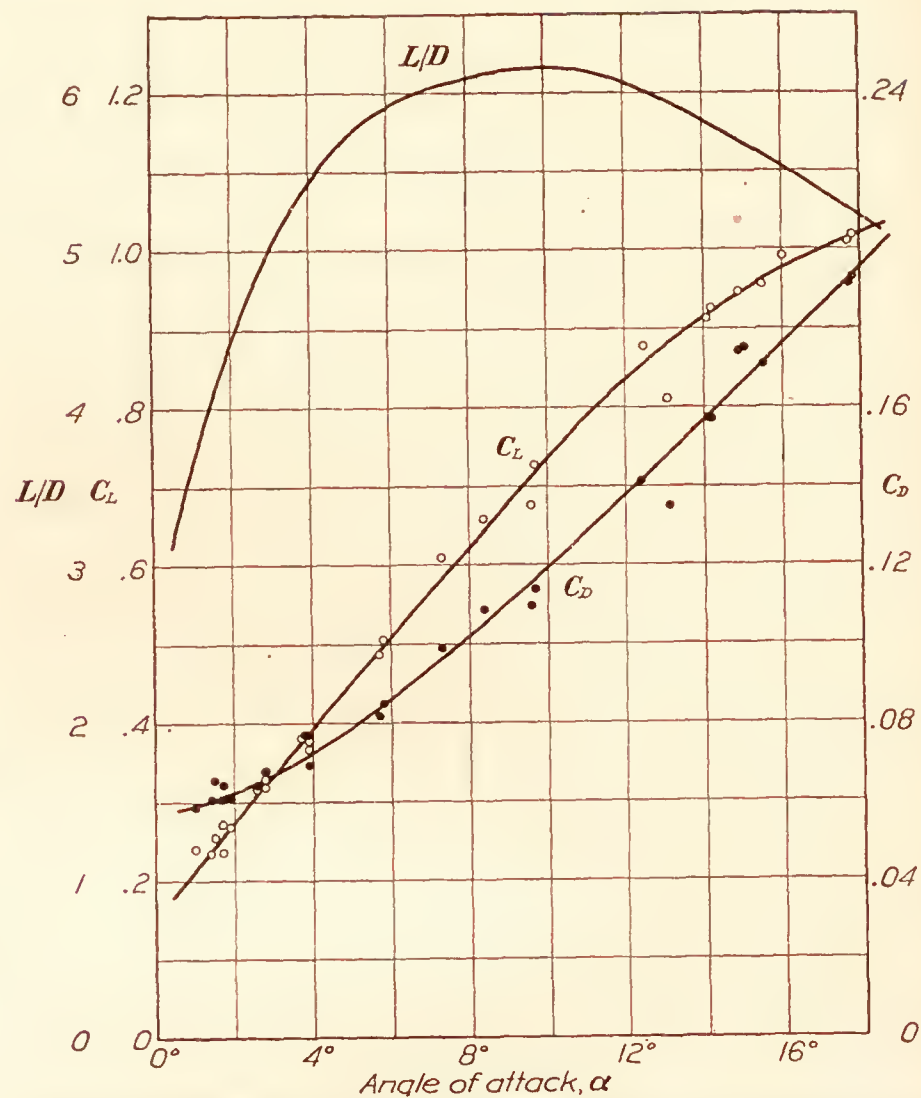


FIG. 9.—Sperry Messenger tests. Characteristics of R. A. F.-15 wings. Glide at  $\frac{V}{nD} = 1.075$

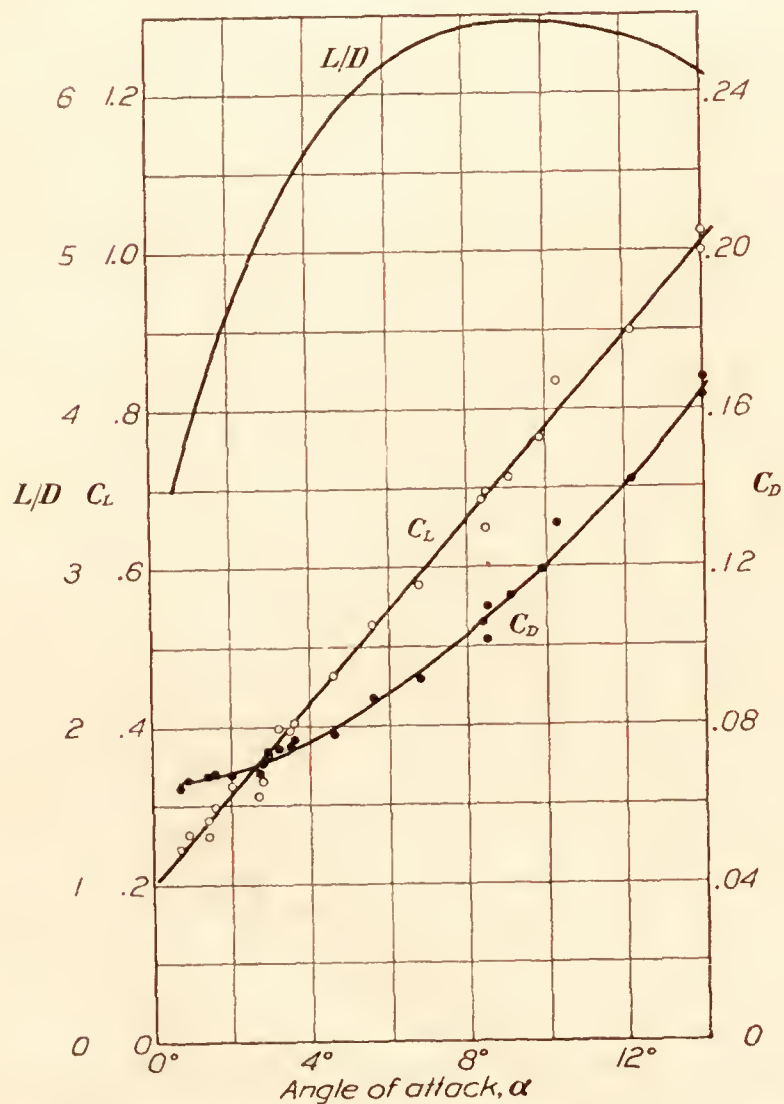


FIG. 10.—Sperry Messenger tests. Characteristics of U. S. A.-5 wings. Glide at  $\frac{V}{nD} = 1.075$

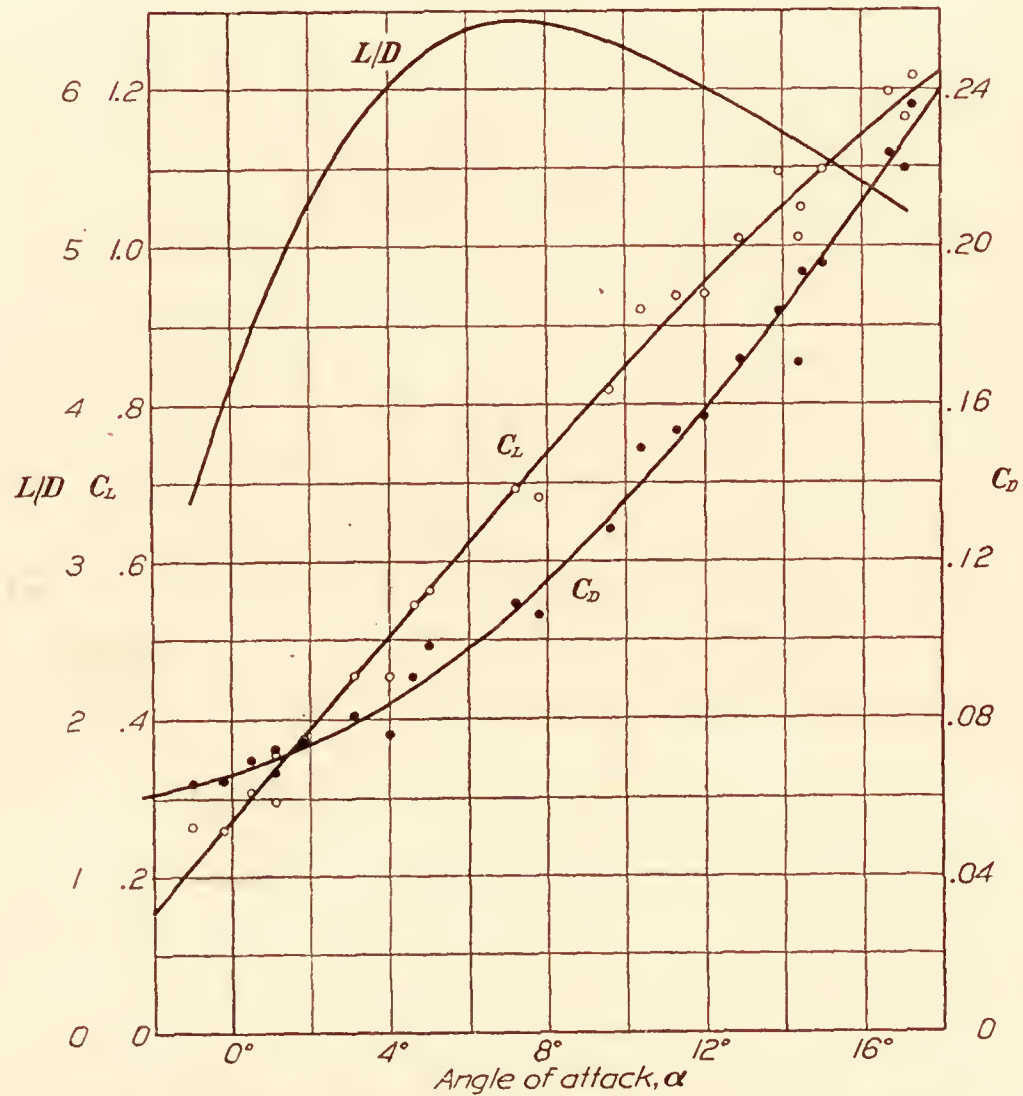


FIG. 11.—Sperry Messenger tests. Characteristics of U. S. A.-27 wings. Glide at  $\frac{V}{nD} = 1.075$



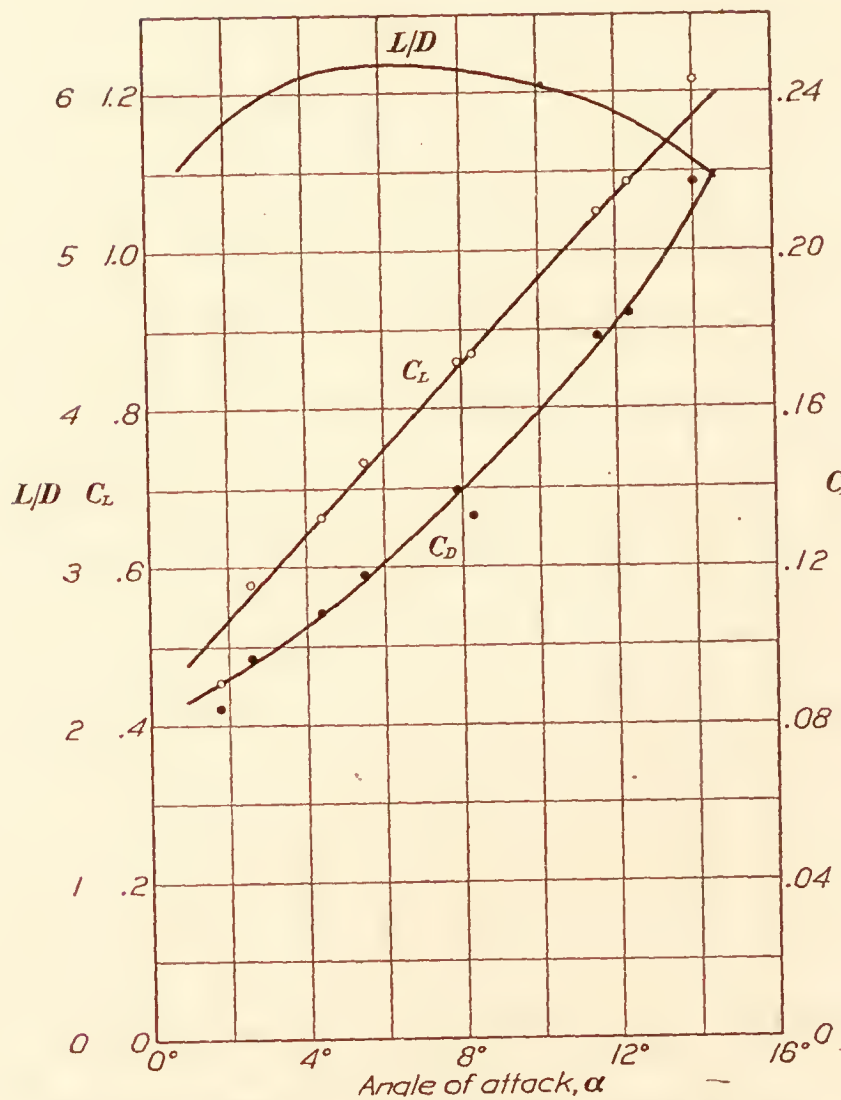


FIG. 12.—Sperry Messenger tests. Characteristics of Göttingen 387 wings. Glide at  $\frac{V}{nD} = 1.075$ . (Limited data)

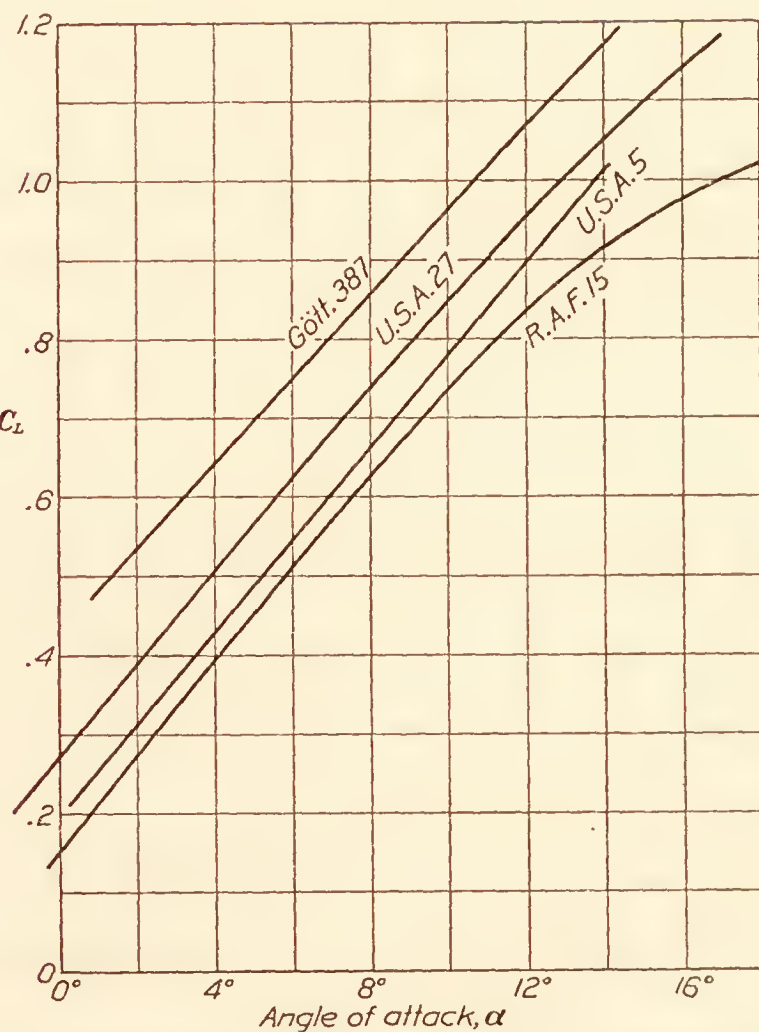


FIG. 13.—Sperry Messenger tests. Lift vs. angle of attack. Glide at  $\frac{V}{nD} = 1.075$

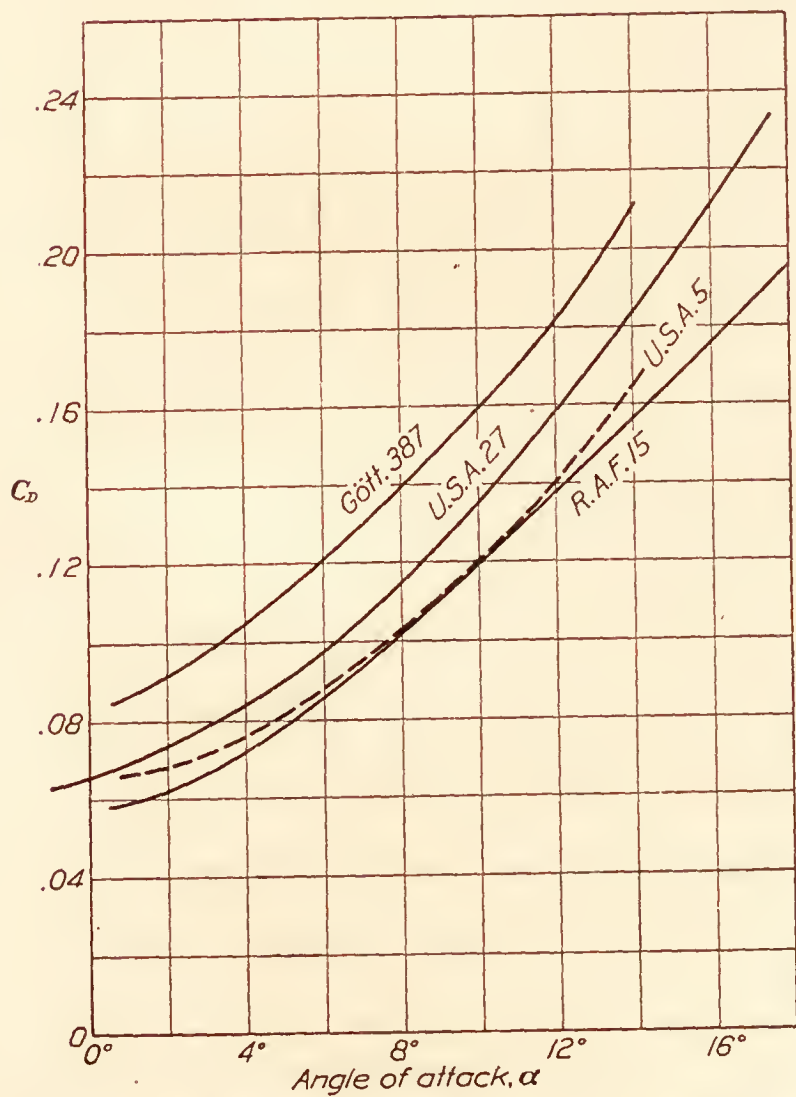


FIG. 14.—Sperry Messenger tests. Drag vs. angle of attack. Glide at  $\frac{V}{nD} = 1.075$

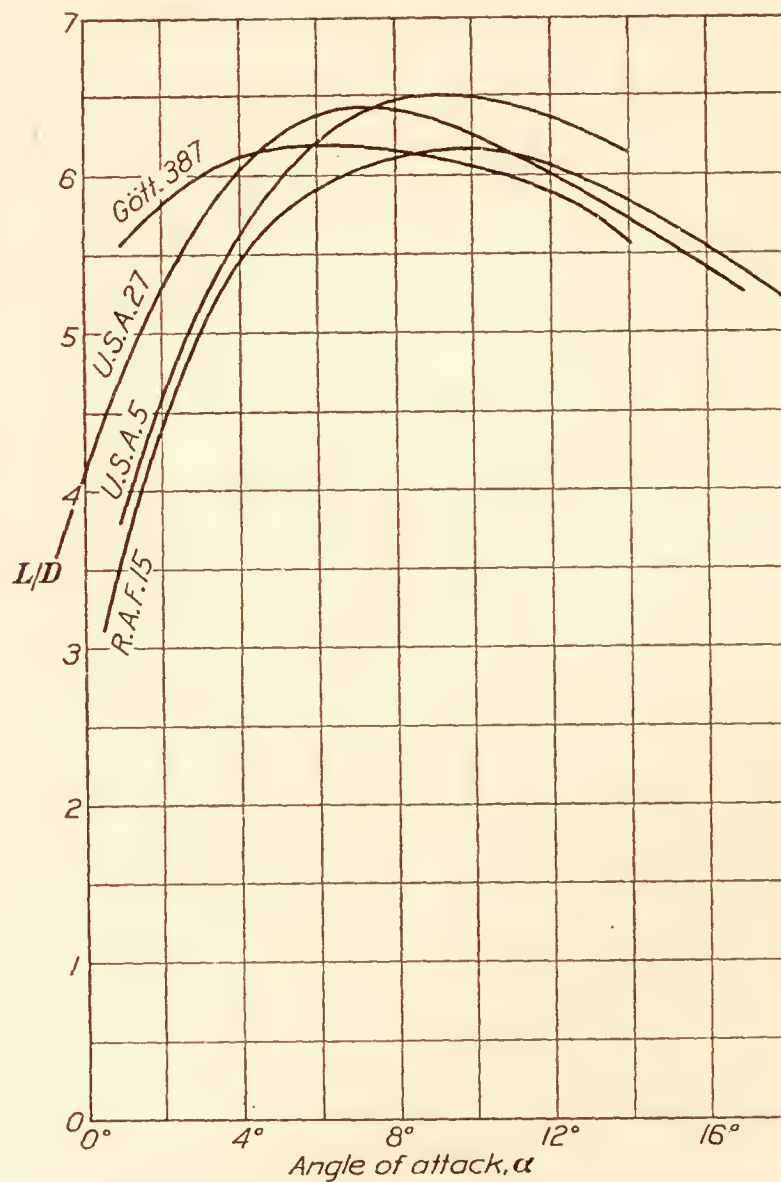


FIG. 15.—Sperry Messenger tests.  $L/D$  vs. angle of attack. Glide at  $\frac{V}{nD} = 1.075$

TABLE I.—DATA FOR U. S. A.-5 WING  
GLIDE TESTS ON SPERRY MESSENGER AIRPLANE

Flight No.	Run No.	$q$ Dy- namic pres- sure	$P$ Baro- metric pres- sure	$T$ Tem- pera- ture	$\rho$ Specific weight	$V_T$ True velocity	$V_{ind}$ Indi- cated velocity	R. P. M.	$V_{T/ND}$	$C_T$ Propeller thrust co- efficient $T/\rho V^2 D^2$	$T$ Thrust	$\gamma$ Flight- path angle	$\sin \gamma$	$\cos \gamma$	$W$ Weight	$D-T$ Appar- ent drag	$D$ True drag	$L$ Lift	$C_D$ $D/qS$	$C_L$ $L/qS$	Inclina- tion	$\alpha$ Angle of attack	$\phi$ Eleva- tor angle
		<i>Lbs. per sq. ft.</i>	<i>Ins. hg.</i>	<i>° C.</i>	<i>Lbs. per cu. ft.</i>	<i>Ft. per sec.</i>	<i>M. p. h.</i>				<i>Lbs.</i>	<i>Deg.</i>			<i>Lbs.</i>	<i>Lbs.</i>	<i>Lbs.</i>	<i>Lbs.</i>			<i>Deg.</i>	<i>Deg.</i>	<i>Deg.</i>
A	1	16.65	27.6	1	0.0740	120.5	80.6	1,020	1.088	-0.0015	-2.1	10.8	0.1874	0.9823	1,019	191.0	188.9	1,000	0.0765	0.404	7.2	3.6	-----
	2	22.35	28.0	-----	.0752	138.2	93.5	1,145	1.112	-.0042	-7.9	13.4	.2317	.9728	1,016	235.0	227.1	986	.0685	.298	11.8	1.6	-----
	3	26.50	27.8	-----	.0746	151.0	102.0	1,242	1.118	-.0048	-10.7	15.2	.2622	.9650	1,013	266.0	255.3	978	.0644	.246	14.5	0.7	-----
	4	16.90	27.3	-----	.0734	122.0	81.2	1,050	1.070	+.0006	+.8	10.7	.1857	.9826	1,010	187.5	188.3	992	.0751	.395	7.2	3.5	-----
B	5	6.76	26.75	-5	.0735	77.0	51.4	632	1.120	-.0050	-2.8	9.4	.1633	.9866	1,019	166.5	163.7	1,005	.1635	1.000	4.6	14.0	1.5
	6	7.54	27.00	-----	.0743	80.8	54.2	660	1.120	-.0050	-3.2	9.2	.1599	.9871	1,016	162.2	159.0	1,002	.1421	.900	3.0	12.2	1.0
	7	8.84	27.50	-----	.0756	86.8	58.8	740	1.080	-.0006	-0.4	8.9	.1547	.9880	1,013	157.0	156.6	1,000	.1195	.764	1.0	9.9	.5
	8	8.06	27.05	-----	.0743	83.6	56.2	716	1.072	+.0003	+0.2	8.9	.1547	.9880	1,010	156.2	156.4	998	.1311	.835	1.4	10.3	.0
C	9	9.36	27.20	-----	.0748	89.6	60.5	745	1.105	-.0034	-2.7	9.1	.1582	.9874	1,007	159.5	156.8	993	.1129	.714	.0	9.1	-3
	10	9.62	27.20	-----	.0748	91.0	61.3	760	1.100	-.0028	-2.3	9.1	.1582	.9874	1,004	159.0	156.7	991	.1100	.696	-.6	8.5	-.5
	11	10.25	26.80	-----	.0736	94.5	63.3	780	1.110	-.0039	-3.4	9.1	.1582	.9874	1,001	158.2	154.8	989	.1018	.650	-.6	8.5	-.7
	12	20.30	27.4	4	.0729	133.8	89.2	1,140	1.080	-.0006	-1.0	12.3	.2130	.9770	1,019	217.0	216.0	995	.0706	.330	9.5	2.8	-----
D	13	25.25	27.4	-----	.0729	149.2	99.4	1,260	1.090	-.0017	-3.6	14.4	.2487	.9686	1,016	252.5	248.9	986	.0666	.264	13.5	1.9	-----
	14	21.30	27.4	-----	.0729	137.2	91.4	1,140	1.100	-.0028	-5.1	12.4	.2147	.9767	1,010	216.5	215.4	986	.0681	.311	9.7	2.7	-----
	15	25.25	28.2	-----	.0750	147.0	99.4	1,260	1.072	+.0003	+.6	14.4	.2487	.9686	1,007	251.0	251.6	975	.0673	.261	13.0	1.4	-----
E	16	11.70	27.30	-5	.0750	100.2	67.6	805	1.145	-.0074	-7.3	9.4	.1633	.9866	1,019	166.5	159.2	1,005	.0918	.578	2.6	6.8	.0
	17	14.58	27.30	-----	.0750	111.5	75.5	900	1.140	-.0069	-8.5	10.0	.1736	.9848	1,016	176.0	167.5	1,000	.0776	.463	5.4	4.6	1.0
	18	18.20	27.65	-----	.0768	123.5	84.4	1,000	1.135	-.0065	+10.0	11.9	.2062	.9785	1,013	208.5	199.5	991	.0739	.367	9.0	2.9	1.5
E	19	6.60	27.00	4	.0718	77.0	50.8	643	1.102	-.0031	1.7	9.4	.1633	.9866	1,019	166.3	164.6	1,005	.1025	.1025	-4.6	14.0	2.4
	20	9.88	27.30	-----	.0726	93.5	62.2	800	1.076	.0000	.0	8.8	.1530	.9882	1,016	155.2	155.2	1,002	.1060	.6850	.4	8.4	.0
	21	12.72	27.55	-----	.0732	106.0	70.6	900	1.082	-.0007	.8	9.4	.1633	.9866	1,013	165.5	164.7	1,000	.0872	.5280	3.8	5.6	.5
	22	16.75	27.80	-----	.0738	121.0	80.9	990	1.125	-.0056	8.0	11.0	.1908	.9816	1,010	193.0	185.0	990	.0745	.3980	7.8	3.2	1.0
	23	20.40	27.50	-----	.0730	134.0	89.2	1,128	1.092	-.0020	3.4	12.0	.2079	.9781	1,007	209.0	205.6	984	.0679	.3250	10.0	2.0	1.8



TABLE II.—DATA FOR R. A. F.-15 WING  
GLIDE TESTS ON SPERRY MESSENGER AIRPLANE

		<i>q</i>	<i>P</i>	<i>T</i>	<i>gρ</i>	<i>V<sub>T</sub></i>	<i>V<sub>ind</sub></i>	R. P. M.	<i>V<sub>T</sub>/nD</i>	<i>C<sub>T</sub></i>	<i>T</i>	<i>γ</i>	Sin <i>γ</i>	Cos <i>γ</i>	<i>W</i>	<i>D-T</i>	<i>D</i>	<i>L</i>	<i>C<sub>D</sub></i>	<i>C<sub>L</sub></i>		<i>α</i>	<i>φ</i>
Flight No.	Run No.	Dy- namic pres- sure	Baro- metric pres- sure	Tem- pera- ture	Specific weight	True velocity	Indi- cated velocity			Propeller thrust co- efficient <i>T/ρ V<sup>2</sup> D<sup>2</sup></i>	Thrust	Flight- path angle			Weight	Appar- ent drag	True drag	Lift	<i>D</i> <i>q S</i>	<i>L</i> <i>q S</i>	Inclina- tion	Angle of attack	Eleva- tor angle
		<i>Lbs. per sq. ft.</i>	<i>Inch. hg.</i>	<i>° C.</i>	<i>Lbs. per cu. ft.</i>	<i>Ft. per sec.</i>	<i>M. p. h.</i>				<i>Lbs.</i>	<i>Deg.</i>			<i>Lbs.</i>	<i>Lbs.</i>	<i>Lbs.</i>	<i>Lbs.</i>			<i>Deg.</i>	<i>Deg.</i>	<i>Deg.</i>
A	1	6.86	27.20	17	0.0690	79.9	51.8	640	1.150	-.0079	-4.6	10.4	0.1805	0.9836	1,016	183.0	178.4	1,000	0.1751	0.982	+4.6	15.0	+4.0
	2	28.10	27.95		.0710	159.8	104.8	1,275	1.150	-.0079	-18.8	15.5	.2672	.9636	1,013	271.0	252.2	975	.0605	.234	-13.8	1.7	-2.5
	3	28.10	28.32		.0719	158.8	104.8	1,280	1.140	-.0074	-17.6	15.6	.2689	.9632	1,010	271.0	253.4	974	.0608	.233	-14.2	1.4	-2.2
	4	24.70	28.10		.0714	149.2	98.3	1,180	1.165	-.0092	-19.2	13.9	.2402	.9707	1,007	242.0	222.8	978	.0608	.267	-12.0	1.9	-2.0
	5	23.90	27.73		.0704	148.2	96.6	1,190	1.148	-.0077	-15.6	13.9	.2402	.9707	1,004	241.6	226.0	976	.0642	.270	-12.2	1.7	-2.0
	6	20.18	27.80		.0707	135.5	88.8	1,080	1.152	-.0081	-13.8	12.4	.2147	.9767	1,001	215.0	201.2	978	.0673	.327	-9.6	2.8	-1.5
	7	20.80	27.87		.0709	137.5	90.2	1,085	1.165	-.0092	-16.2	12.4	.2147	.9767	998	214.0	197.8	975	.0640	.315	-9.8	2.6	-1.6
	8	7.54	27.73		.0704	83.0	54.3	670	1.140	-.0074	-4.7	9.4	.1633	.9866	995	162.8	158.1	982	.1412	.877	+3.0	12.4	+2.0
B	9	9.10	27.87		.0709	90.8	59.6	703	1.190	-.0113	-8.7	9.4	.1633	.9866	992	162.3	153.6	979	.1137	.726	+1.3	9.7	+1.0
	10	17.70	27.10	14	.0696	128.0	83.2	1,118	1.055	+.0032	+4.8	11.2	.1942	.9810	1,016	197.2	202.0	1,000	.0768	.380	-7.4	3.8	-1.5
	11	17.80	27.27		.0701	128.0	83.3	1,138	1.038	+.0047	+7.1	11.1	.1925	.9813	1,013	195.0	202.1	995	.0764	.376	-7.2	3.9	-1.5
	12	13.80	27.42		.0705	112.3	73.4	903	1.140	-.0069	-8.1	10.0	.1736	.9848	1,010	175.5	167.4	994	.0818	.485	-4.3	5.7	-1.9
	13	13.28	27.58		.0709	109.8	72.0	900	1.120	-.0050	-5.6	9.9	.1719	.9851	1,007	173.0	167.4	993	.0850	.505	-4.1	5.8	-1.9
	14	10.15	27.70		.0711	95.7	63.0	795	1.106	-.0035	-3.0	9.2	.1599	.9871	1,004	166.3	163.3	991	.1083	.658	-1.8	8.4	+1.2
	15	10.94	27.62		.0709	99.6	65.4	832	1.102	-.0020	-1.8	9.3	.1616	.9869	1,001	162.0	160.2	989	.0986	.608	-2.0	7.3	.0
	16	27.04	28.25		.0701	158.8	103.0	1,280	1.140	-.0069	-15.8	14.6	.2521	.9677	998	252.0	236.2	965	.0588	.240	-13.6	1.0	-3.4
C	17	26.00	28.85	16	.0735	151.0	101.0	1,275	1.090	-.0018	-4.0	14.6	.2521	.9677	1,016	256.0	252.0	982	.0653	.254	-13.1	1.5	-2.0
	18	21.05	28.25		.0720	137.2	90.6	1,175	1.075	.0000	.0	12.1	.2096	.9778	1,013	212.0	212.0	991	.0679	.317	-9.3	2.8	-1.5
	19	18.20	28.25		.0720	127.6	84.4	1,030	1.140	-.0069	-10.6	11.3	.1959	.9806	1,010	197.8	187.2	990	.0692	.366	-7.4	3.9	-1.0
	20	13.25	28.10		.0716	109.1	72.0	915	1.100	-.0029	-3.3	10.2	.1771	.9842	1,007	178.2	174.9	990	.0888	.502			-1.2
	21	12.48	28.47		.0726	105.2	70.0	875	1.105	-.0034	-3.6	10.0	.1736	.9848	1,004	180.6	177.0	988	.0956	.533			-1.2
	22	9.88	28.25		.0720	93.9	62.2	772	1.114	-.0044	-3.7	9.4	.1633	.9866	1,001	163.8	160.1	988	.1093	.675	+1.2	9.6	+1.6
	23	8.17	28.40		.0724	85.1	56.5	660	1.190	-.0113	-7.8	9.9	.1719	.9851	998	171.2	163.4	982	.1348	.810	+3.2	13.1	+2.2
	24	7.33	27.40	15	.0700	82.0	53.5	664	1.138	-.0067	-4.2	10.0	.1736	.9848	1,016	176.2	172.0	1,000	.1571	.925	+4.2	14.2	
D	25	7.02	28.20		.0721	79.1	52.5	595	1.220	-.0135	-8.0	10.6	.1839	.9829	1,013	186.0	178.0	996	.1708	.955	+4.9	15.5	
	26	6.55	27.77		.0708	77.0	50.6	610	1.160	-.0088	-4.9	11.0	.1908	.9816	1,010	192.5	187.6	990	.1931	1.018	+6.8	17.8	
	27	7.33	27.60		.0706	81.7	53.5	647	1.160	-.0088	-5.5	10.1	.1754	.9845	1,007	176.5	171.0	992	.1572	.913	+4.0	14.1	
	28	7.02	27.83		.0713	79.8	52.5	640	1.145	-.0074	-4.4	10.3	.1788	.9839	1,004	186.0	181.6	988	.1742	.946	+4.6	14.9	
	29	6.55	28.43		.0727	76.1	50.6	618	1.134	-.0064	-3.5	10.9	.1891	.9819	1,001	189.5	186.0	982	.1914	1.010	+6.8	17.7	

AN AIRPLANE EQUIPPED WITH DIFFERENT SETS OF WINGS

TABLE III.—DATA FOR U. S. A.-27 WING  
GLIDE TESTS ON SPERRY MESSENGER AIRPLANE

Flight No.	Run No.	$q$	$P$	$T$	$g\rho$	$V_T$	$V_{ind}$	R. P. M.	$V_T/nD$	$C_T$	$T$	$\gamma$	$\sin \gamma$	$\cos \gamma$	$W$	$D-T$	$D$	$L$	$C_D$	$C_L$		$\alpha$	$\phi$
		Dyn-amic pres-sure	Baro-metric pres-sure	Tem-perature	Specific weight	True velocity	Indi-cated velocity			Propeller thrust co-efficient $T/\rho V^2 D^2$	Thrust	Flight-path angle			Weight	Appar-ent drag	True drag	Lift	$\frac{D}{qS}$	$\frac{L}{qS}$	Inclina-tion	Angle of attack	Eleva-tor angle
		Lbs. per sq. ft.	Ins. hg.	° C.	Lbs. per cu. ft.	Ft. per sec.	M. p. h.				Lbs.	Deg.			Lbs.	Lbs.	Lbs.	Lbs.			Deg.	Deg.	Deg.
A	1	5.72	27.45	15	0.0702	72.4	47.2	600	1.112	-0.0041	-2.0	10.7	0.1857	0.9826	1,033	192.0	190.0	1,016	0.2235	1.195	+6.0	+16.7	+6.0
	2	6.50	27.75	-----	.0710	76.8	50.3	638	1.110	-.0039	-2.1	10.0	.1736	.9848	1,030	179.0	186.9	1,013	.1936	1.050	4.5	14.5	4.8
	3	7.28	27.50	-----	.0704	81.6	53.3	698	1.078	-.0003	-.2	9.3	.1616	.9869	1,027	166.0	165.8	1,012	.1535	.938	2.0	11.3	3.0
	4	18.20	27.22	-----	.0722	127.5	84.2	1,095	1.070	+.0006	+ .9	11.2	.1942	.9816	1,024	199.0	199.9	1,008	.0741	.373	-9.4	+1.8	.5
	5	21.85	27.53	-----	.0705	141.0	92.4	1,210	1.074	.0000	.0	12.8	.2215	.9751	1,021	226.0	226.0	.998	.0698	.308	-12.3	+ .5	.0
	6	25.50	27.96	-----	.0716	151.2	99.8	1,275	1.092	-.0025	-5.4	14.0	.2419	.9703	1,018	246.0	240.6	.999	.0636	.264	-15.0	-1.0	-.7
B	7	5.62	27.82	15	.0711	71.1	46.8	620	1.058	+.0021	+1.0	10.9	.1891	.9820	1,033	196.0	197.0	1,015	.2360	1.216	+6.4	+17.3	+7.5
	8	6.24	27.65	-----	.0707	75.2	49.4	660	1.048	.0033	1.7	9.4	.1633	.9866	1,030	168.5	170.2	1,016	.1838	1.096	4.5	13.9	4.7
	9	6.76	27.52	-----	.0703	78.5	51.4	680	1.062	.0017	1.0	9.6	.1668	.9860	1,027	171.3	172.3	1,013	.1714	1.010	3.3	12.9	3.9
	10	8.06	27.59	-----	.0705	85.8	56.1	760	1.040	.0045	3.1	9.0	.1564	.9877	1,024	160.5	163.6	1,010	.1490	.920	1.4	10.4	2.7
	11	9.98	27.52	-----	.0703	95.5	62.4	800	1.095	-.0023	-1.9	9.0	.1564	.9877	1,021	160.0	158.1	1,010	.1067	.680	-1.2	7.8	1.7
	12	11.95	27.77	-----	.0710	104.0	68.4	900	1.063	+.0015	+1.5	9.2	.1599	.9871	1,018	162.8	164.3	1,006	.0986	.563	-4.2	5.0	1.5
C	13	14.88	27.37	-----	.0700	117.0	76.2	1,000	1.076	.0000	-----	10.3	.1788	.9839	1,015	178.6	178.6	1,000	.0809	.453	-7.2	3.1	1.2
	14	5.88	27.3	9	.0712	73.0	47.9	660	1.020	+.0073	+3.6	10.5	.1822	.9833	1,033	188.5	192.1	1,015	.2198	1.162	+6.6	17.1	5.7
	15	6.76	27.4	-----	.0715	78.1	51.4	720	.998	.0107	6.1	9.2	.1599	.9871	1,030	164.9	171.0	1,016	.1702	1.010	5.2	14.4	3.5
	16	8.32	27.5	-----	.0718	86.3	57.0	780	1.018	.0075	5.3	8.6	.1495	.9888	1,027	153.5	158.8	1,012	.1286	.819	1.0	9.6	2.7
	17	15.00	27.4	-----	.0715	116.2	76.5	1,000	1.070	.0006	.7	9.5	.1650	.9863	1,024	169.0	169.7	1,0106	.0761	.453	-5.5	4.0	.8
	18	22.65	27.5	-----	.0718	142.8	94.0	1,200	1.092	-.0020	-3.8	12.9	.2233	.9748	1,021	228.0	224.2	.99	.0666	.295	-11.8	1.1	.0
D	19	6.24	27.6	9	.0722	74.5	49.4	660	1.040	+.0045	+2.4	10.0	.1736	.9848	1,033	179.0	181.4	1,016	.1959	1.097	+5.0	15.0	5.00
	20	7.28	27.7	-----	.0725	80.4	53.3	700	1.058	.0020	1.2	9.4	.1633	.9865	1,030	168.3	169.5	1,015	.1570	.940	2.6	12.0	3.30
	21	9.88	26.6	-----	.0722	93.8	62.0	800	1.078	-.0005	-.4	9.0	.1564	.9876	1,027	151.0	160.6	1,013	.1094	.692	-1.8	7.2	2.40
	22	12.48	28.2	-----	.0737	104.5	69.8	900	1.070	+.0006	+ .6	9.4	.1633	.9865	1,024	167.3	107.9	1,010	.0907	.545	-4.8	4.6	1.50
	23	19.00	28.2	-----	.0737	129.0	86.0	1,100	1.076	.0000	-----	11.5	.1993	.9799	1,021	204.0	204.6	1,000	.0725	.355	-10.4	1.1	.60
	24	25.75	27.9	-----	.0729	151.0	100.0	1,300	1.068	+.0008	+1.7	13.8	.2385	.9711	1,018	243.0	244.7	.990	.0641	.259	-14.0	-.2	-.60

TABLE IV.—DATA FOR GÖTTINGEN 387 WING  
GLIDE TESTS ON SPERRY MESSENGER AIRPLANE

Flight No.	Run No.	$q$	$P$	$T$	$g\rho$	$V_T$	$V_{ind}$	R. P. M.	$V_T/nD$	$C_T$	$T$	$\gamma$	$\sin \gamma$	$\cos \gamma$	$W$	$D-T$	$D$	$L$	$C_D$	$C_L$		$\alpha$	$\phi$
		Dyn-amic pres-sure	Baro-metric pres-sure	Tem-perature	Specific weight	True velocity	Indi-cated velocity			Propeller thrust co-efficient $T/\rho V^2 D^2$	Thrust	Flight-path angle			Weight	Appar-ent drag	True drag	Lift	$\frac{D}{qS}$	$\frac{L}{qS}$	Inclina-tion	Angle of attack	Eleva-tor angle
		Lbs. per sq. ft.	Ins. hg.	° C.	Lbs. per cu. ft.	Ft. per sec.	M. p. h.				Lbs.	Deg.			Lbs.	Lbs.	Lbs.	Lbs.			Deg.	Deg.	Deg.
A	1	6.86	28.15	25	0.0695	79.8	51.8	670	1.095	-0.0023	-1.33	9.7	0.1685	0.9857	1,082	182.8	181.5	1,068	0.1784	1.050	1.8	11.5	4.0
	2	8.32	28.30	-----	.0698	87.5	57.0	687	1.170	-.0097	-6.82	9.6	.1668	.9860	1,077	179.5	172.7	1,060	.1398	.860	1.7	7.9	1.0
	3	9.72	28.50	-----	.0704	94.2	61.6	765	1.130	-.0059	-4.85	9.4	.1633	.9866	1,072	175.2	170.4	1,058	.1182	.733	3.9	5.5	.3
	4	10.68	28.40	-----	.0702	98.8	64.5	810	1.120	-.0050	-4.50	9.5	.1650	.9863	1,067	176.0	171.5	1,050	.1084	.663	5.1	4.4	-.5
	5	12.20	28.40	-----	.0702	106.0	69.0	884	1.105	-.0034	-3.51	9.8	.1702	.9854	1,062	181.0	177.5	1,048	.0980	.578	7.2	2.6	-1.0
B	6	15.32	28.50	-----	.0704	118.6	77.5	986	1.105	-.0034	-4.41	10.7	.1857	.9826	1,057	196.0	191.6	1,038	.0841	.455	-8.9	1.8	-1.5
	7	5.98	28.40	27	.0696	74.4	48.4	625	1.095	-.0023	-1.16	10.2	.1771	.9842	1,098	194.5	193.3	1,080	.2175	1.218	3.8	14.0	5.3
	8	6.66	28.50	-----	.0700	78.4	51.0	595	1.210	-.0128	-7.20	10.0	.1736	.9848	1,093	189.8	182.6	1,078	.1845	1.088	2.3	12.3	3.5
	9	8.32	28.70	-----	.0704	87.5	57.0	698	1.150	-.0079	-5.50	9.0	.1564	.9877	1,088	169.8	164.3	1,072	.1330	.870	-1.7	8.3	1.9



---

---

**REPORT No. 305**

---

**THE GASEOUS EXPLOSIVE REACTION—A STUDY  
OF THE KINETICS OF COMPOSITE FUELS**

**By F. W. STEVENS**  
**Bureau of Standards**





## REPORT No. 305

### THE GASEOUS EXPLOSIVE REACTION--A STUDY OF THE KINETICS OF COMPOSITE FUELS

By F. W. STEVENS

#### SUMMARY

*This report deals with the results of a series of studies of the kinetics of gaseous explosive reactions where the fuel under observation, instead of being a simple gas, is a known mixture of simple gases. In the practical application of the gaseous explosive reaction as a source of power in the gas engine, the fuels employed are composite, with characteristics that are apt to be due to the characteristics of their components and hence may be somewhat complex. The simplest problem that could be proposed in an investigation either of the thermodynamics or kinetics of the gaseous explosive reaction of a composite fuel would seem to be a separate study of the reaction characteristics of each component of the fuel and then a study of the reaction characteristics of the various known mixtures of those components forming composite fuels more and more complex. This is the order followed in the simple studies herein described.*

The method and device employed in making these studies were a modification, to meet kinetic principles, of those found so effective by Nernst and his students in investigating the thermodynamics of gaseous explosive reactions. Instead of a spherical bomb of constant volume with central ignition made use of by those investigators, a transparent bomb of constant pressure was substituted. This change eliminated irregularities in pressure and in the mass movement of the active gases during the reaction, and maintained the concentrations (partial pressures) of the active gases constant during the reaction—a feature essential to kinetic studies as well as advantageous in thermodynamic investigations. Further, the substitution of a transparent bomb of constant pressure for an opaque one of constant volume, permitted photographic time-volume records to scale to be secured. From these records it was possible to determine the rate of propagation of the reaction zone in space and, much more important, its rate of propagation relative to the active gases it transforms. As a result of these modifications and their application, it was found that the rate  $s$ , at which the zone of explosive reaction moves forward relative to the active gases and effects their transformation is constant, at a constant pressure, and proportional to the product of the partial pressures of the active gases:

$$s = k_1[A]^{n_1}[B]^{n_2}[C]^{n_3} \dots \quad (1)$$

This relationship is the basis of the kinetic studies here made of gaseous reactions, as the equilibrium expression,

$$K = \frac{[A']^{n'_1}[B']^{n'_2}[C']^{n'_3} \dots}{[A]^{n_1}[B]^{n_2}[C]^{n_3} \dots}$$

is the fundamental relation in thermodynamic investigations of gaseous explosive reactions.

The results obtained from the simple specific cases of composite fuels studied would indicate that from a knowledge of the velocity coefficients of the reaction zones of the components of the fuel, the velocity coefficient  $k_F$ , of the fuel F, may be determined; and hence the flame velocity of F with  $O_2$ , since

$$s_F = k_F[F]^{n_1}[O]_2^{n_2},$$



where all of the factors to the right in the equation may be known from the velocity coefficients of the components of F and the mixture ratio of F and  $O_2$ .

### INTRODUCTION

The introduction to the classical investigations of A. Langen (Reference 1) concerning the pressures generated by the explosive reaction of hydrogen and also of carbon monoxide with oxygen in a bomb of constant volume, contains these words: "The necessary physical basis for the thermodynamic determination of the complete cycle for an internal combustion engine is lacking in many fundamental points. Especially has it been impossible up to the present time to determine with certainty from a knowledge of the composition and condition of the working fluid before the explosive reaction what will be its composition and condition—barring heat losses—after the reaction. This lack in our knowledge so often complained of in physico-technical literature of the past few years was the author's incentive to undertake the present investigation."

In this work Langen repeated and analyzed all of the investigations bearing on these reactions that had previously been made. His publication therefore provides a valuable critical review and summary of the work carried out in investigations of the gaseous explosive reaction up till 1903.

His own investigations were directed to the quantitative determination of the available heat energy imparted to the working fluid of the engine and the changes in composition occurring in that fluid as a result of the transformation; to a determination of the specific heats of the fluid and its final composition as expressed in their reaction constants.

In discussing experimental procedure, Langen strongly emphasized two points: The necessity of employing in investigations of the gaseous explosive reaction a spherical bomb with central ignition; and the necessity of securing a manometer as sensitive as possible and with minimum inertia. The use of a spherical bomb with central ignition was found necessary in order to avoid heat losses due to convection and conduction during the reaction process. The reason that a spherical container with central ignition fulfills this condition is due to the fact that the zone of reaction originating at the center of the bomb, remains concentric with the bomb in its spread outward so that the heated products of combustion inclosed within this expanding spherical shell of flame, do not come in contact with the walls of the container till the end of the reaction and the attainment of maximum pressure. By taking advantage in this way of the symmetry of the gross reaction process, the effect of the container on the heat liberated during the reaction was largely eliminated. Langen was not so fortunate in avoiding significant errors introduced by a material manometer of pronounced inertia and disturbing period.

Recognizing the possibilities of the device and method as demonstrated in the work of Langen, Nernst sought to use it as an instrument of precision in thermodynamic studies of gaseous explosive reactions and in particular for the determination of specific heats of gases at the high temperatures possible to attain by means of explosion methods.

As a result of a long series of trials Pier (Reference 2) developed a manometer that overcame to a large degree the objectionable features met with in previous forms. With this improvement of Langen's device he determined the specific heats of a number of gases. His method has been found applicable for this purpose to temperatures exceeding  $3,000^\circ$  absolute and the specific heats of all of the important gases comprising the working fluid of the engine have now been determined at explosion temperatures.

Primarily, a knowledge of the working fluid of an internal combustion engine involves the determination of the equilibrium condition of the fluid under working conditions. The explosion method as developed by Langen and refined by Nernst and his pupils was found particularly suitable to the determination of this constant. The transformation of a hydrocarbon fuel results, for the most part, in the two products of combustion, carbon dioxide and water vapor. These products form an important part of the engine's working fluid. The work of Bjerrum



(Reference 3) and of Siegel (Reference 4), using the explosion method, resulted not only in the determination of the reaction constant  $K$ , but permitted also the determination of the degree of dissociation of these important constituents of the working fluid, over wide ranges of temperature and pressure.

Langen, an automotive engineer, expressed the incentive, born of the gas engine, that led to the development of a method and device of high precision and by its aid to the final solution of the fundamental technical problems he sought. This notable advance was wholly due to the rational application of the principles of thermodynamics as extended to gaseous explosive reactions, and to a clear insight and appreciation of the gross mechanism (the spatial propagation of a definite zone of explosive reaction) by which the transformation of the gases is effected. Commenting on these results, Nernst (Reference 5) called attention to "the specially high value that must be attached to the explosion method, since, by suitable variations of the experimental conditions, it enables both the specific heats and the equilibrium constant to be determined." And in like connection, Partington (Reference 6) offers the following: "To the internal-combustion engine designer this knowledge is vital. It is no less important in the determination of explosive forces which are essentially dependent on specific heats of gases produced by explosive material." The determination of the equilibrium constant makes it possible to ascertain the maximal work of the gaseous transformation involved. It thus provides a more rational standard of reference in the analysis of gas engine performance than is offered by an arbitrary standard that takes no account of molecular changes that occur in the working fluid due to reaction, nor to changes in its physical constants due to the high temperatures and pressures at which the fluid is employed.\*

A significant result due largely to the effect of these important quantitative studies is that the popular conception of a gaseous explosion is fortunately gradually changing from that of a mysterious phenomenon to that of an orderly normal reaction process well enough understood to be used with precision.

In the list of thermodynamic relations that Langen gave as desirable to have determined in order that a complete cycle for an internal-combustion engine might be followed, another important relation naturally not occurring in a thermodynamic list nor bearing directly on a thermodynamic cycle is, however, from the standpoint of the practical technical application of the gaseous explosion as a source of power, quite as important as a knowledge of the thermodynamics of the reaction. This is a knowledge of the kinetics of the gaseous explosive reaction. (Reference 8.)

Unfortunately, a knowledge of the thermodynamics of the reaction furnishes no insight concerning either the mode or the rate at which the transformation proceeds and the final equilibrium is attained. Nevertheless, the lead indicated by the methods and results of the investigations briefly referred to above determined the device and suggested the method made use of by the writer in kinetic studies of gaseous explosive reactions. Some of the features of the thermodynamic investigations made use of in these kinetic studies of the reaction it is necessary to mention and to show how they were adapted to statistical studies of rates.

In the first place it is clear that the accuracy of the results obtained by Langen and his successors, and referred to by Nernst, depends chiefly on the remarkable symmetry of form automatically assumed and maintained, under favorable conditions, by the gross mechanism of the explosive reaction. In the progress of the explosive transformation, the gaseous system, as pointed out by Haber (Reference 9), automatically falls into three well-defined zones: The region occupied by the initial unburned gases, the zone of explosive reaction marked by flame, and the region of reaction products behind the flame. This latter region, he states, "is not from a thermodynamic standpoint free from oxygen, but from an analytical standpoint it is. In this

---

\* "In the steam-world . . . tables of fundamental data are available in which the numerical results have been evolved by a long process of experiment and of critical sifting by the expert engineer. The user of these tables has confidence in the approximate accuracy of the data and makes extensive application of what he finds in them. With the advent of the internal-combustion engine, no similar information has been available. It is true that incomplete summaries have from time to time appeared, but to the eye of the expert they disclose the most serious inaccuracies and uncritical blunders." (Reference 7.)



region no further burning takes place." It is a region of equilibrium depending on temperature and pressure and expressed by the equilibrium constant,

$$K = \frac{[A']^{n'_1}[B']^{n'_2}[C']^{n'_3}\dots}{[A]^{n_1}[B]^{n_2}[C]^{n_3}\dots}$$

It was this feature that formed the basis of the quantitative determinations of Pier, Bjerrum, and Siegel; they took advantage of the natural symmetry and favorable disposition of the three zones by selecting a spherical bomb fired from the center. At the instant the reaction was complete, the volume, temperature, and pressure of the contents of the bomb were the volume, temperature, and pressure corresponding to the equilibrium constant  $K$ . Owing to its symmetrical position within the bomb during the reaction process, the sphere of equilibrium products had suffered a minimum of heat losses.

This most important feature has been retained in the device and methods employed in the kinetic studies made by the writer; it has possibly been somewhat improved upon; for in place of an opaque bomb of constant volume, a transparent bomb of constant pressure (Reference 10) has been substituted, and instead of a material manometer, remote from the seat of reaction, to indicate pressure, direct photographic methods have been employed that permit a continuous and accurate time-volume record of the reaction to be secured. The instant the reaction is complete, the volume, temperature, and pressure of the reaction products are the volume, temperature, and pressure corresponding to the equilibrium constant  $K$ . Owing to the symmetrical position maintained within the gaseous system during the reaction, the sphere of equilibrium products, as in the case of a constant-volume bomb, had suffered a minimum of heat losses from the effect of a material container.

The relationship between the thermodynamic results obtained by the bomb of constant volume and the bomb of constant pressure is expressed by the equation of state

$$pv = nRT^*$$

While it is true that from the standpoint of thermodynamics no insight may be obtained concerning either the mode or rate by which the final equilibrium is attained, it is also true that the expression for the equilibrium constant  $K$  may be derived also from kinetic principles; that is, this expression may carry both the weight of a thermodynamic law and a deduction from statistical mechanics. (Reference 12.) The expression for the equilibrium constant arrived at either from thermodynamic laws or from kinetic theory is

$$K = \frac{[A']^{n'_1}[B']^{n'_2}[C']^{n'_3}}{[A]^{n_1}[B]^{n_2}[C]^{n_3}}$$

The kinetic relation leading to the above expression is written

$$V = k[A]^{n_1}[B]^{n_2}[C]^{n_3}\dots - k'[A']^{n'_1}[B']^{n'_2}[C']^{n'_3} \quad (2)$$

The experimental application of the above-formulated principles may be illustrated by a particular case—the gaseous reaction



Since the equilibrium condition of a reaction for a given temperature and pressure is independent of the way by which it is attained, it may be assumed that the course of the transformation within the zone of explosive reaction is described by equation (2)

$$V = k[\text{CO}]^2[\text{O}_2] - k'[\text{CO}_2]^2 \quad (4)$$

and that the equilibrium condition of this process is expressed by

$$K = \frac{[\text{CO}_2]^2}{[\text{CO}]^2[\text{O}_2]} \quad (5)$$

---

\*"The first attempt at a quantitative kinetic expression is met with in the equation  $pv = RT$ ." (Reference 11.)



Should the reaction proceed almost wholly in one direction, as is usually the case in explosive reactions of gases, the last term in equation (4) may be neglected (Reference 13) and the kinetic expression for the molecular rate of transformation within the reaction zone written

$$V = k[\text{CO}]^2[\text{O}_2] \quad (6)$$

If by some means the successive concentrations of CO and O<sub>2</sub> during the period of transformation from their initial to their final condition, within the reaction zone, could be maintained constant by the introduction into the reaction zone of new initial components *at the same rate* that the reaction products are removed from the reaction zone to the equilibrium zone, then the zone of explosive reaction would represent a constant reaction gradient across it and the relative rate of motion *s* between the reaction zone and the initial gaseous components would remain constant and would express the gross linear rate at which equilibrium was established.

But this imagined process of supplying initial active components to a reaction zone *at the same rate* that the products of equilibrium are formed and removed—an analytical device first made use of by van't Hoff (Reference 14)—is automatically carried out with precision wherever a gaseous explosive reaction is so conditioned that it may run its course in a homogeneous mixture of explosive gases at constant pressure. Observation shows that under these conditions the rate of propagation *s* of the zone of explosive reaction measured relative to the initial active gases remains constant during the reaction and thus expresses the gross constant rate at which an equilibrium is established.

Since the rate of molecular transformation at any instant between the initial and end condition of the reaction process remains proportional to the product of the concentrations of the active gases at that instant, it was assumed that *s*, analogous to *V*, would sustain a like relation to the composition of the explosive gases; the initial composition and concentration of which may be known:

$$s = k_1 [\text{CO}]^2 [\text{O}_2], \quad (7)$$

and since the method employed determines *s* directly,

$$k_1 = \frac{s}{[\text{CO}]^2 [\text{O}_2]}.$$

A further remark in reference to the determination of *k*<sub>1</sub> may be offered here: It seems doubtful if the simplification usually resorted to in the kinetic expression for the rate of molecular transformation occurring at ordinary temperatures and pressures is justifiable in the case of gaseous explosive reactions at high temperatures and moderate pressures. It would seem that in the case of the gaseous explosion (though possibly not for high pressures) the effect of the reverse reaction, represented by the last term in equation (4), would be too significant to be wholly neglected. The degree of dissociation is large for both products of combustion CO<sub>2</sub> and H<sub>2</sub>O, at high temperatures and moderate pressures. It may be seen that the effect of this last term in equation (4) is not wholly wanting in equation (7) since it is involved in the determination of *k*<sub>1</sub>. The final volume, represented by *r'*, is the actual volume of the products of reaction; it therefore includes the effect of the reverse reaction whatever may be its magnitude; and *r'* is a factor in the determination of *k*<sub>1</sub>; for since

$$s = \frac{r^3}{r'^2 t},$$

$$k_1 = \frac{r^3}{r'^2 t [\text{CO}]^2 [\text{O}_2]}.$$

#### EXPERIMENTAL PROCEDURE

Probably the most familiar example that could be cited of the constant rate *s*, at which the zone of explosive reaction moves forward within the active gases and effects their transformation



under the conditions of a constant pressure, is met with in those numerous cases where a homogeneous mixture of the explosive gases is fed through a tube at a constant time-volume rate and ignited. The zone of continuous explosive reaction then automatically adjusts itself to the rate of gas flow through the tube so that its linear rate of advance relative to the active gases is a constant,  $s$ , at any point of the flame surface. If this were not so, the many industrial devices



FIG. 1.—Stationary reaction zone formed by the continuous explosive reaction of a homogeneous mixture of CO and  $3\text{O}_2$  flowing through a tube at a constant time-volume rate. The figure approached that of a cone

based on the reaction as controlled by some form of burner would not be practical. The figure of the stationary reaction zone under these circumstances may simulate more or less closely that of a cone. Its figure would be that of a perfect cone if the rate of gas flow over the entire cross section of the tube were the same and conveniently remained so after leaving the aperture of the tube. Since, however, these velocities vary greatly between the center and the walls of the tube, the figure assumed by the balanced reaction zone becomes, since  $s$  is constant, a figure only approximating more or less closely that of a cone.

A photograph of such a stationary reaction zone produced by the continuous explosive reaction of a homogeneous mixture of CO and  $\text{O}_2$  as it flows through a tube at constant time-volume rate is shown at Figure 1. The figure represents a cross section of the reaction zone through the vertical axis of the tube. Its form resembles that of a cone.

Under favorable conditions, within rather narrow limits, where the gas flow above the tube may be assumed parallel to the axis of the tube, this figure may be used to estimate the value of  $s$  in equation (7); for, between the axis of the tube and its walls, there will exist a zone within which the rate of flow will correspond in value to the time-volume flow  $u$ . Assume this zone to meet the flame surface of the zone of explosive reaction at  $p$ . (Figure 2.) Then the rate  $s$  at which the components CO and  $\text{O}_2$  are entering the reaction zone normal to its surface will be

$$s = u \sin \alpha \quad (8)$$

where  $\alpha$  is the angle made by a tangent to the curve at  $p$ , and the direction of the gas flow assumed parallel to the axis of the tube.

If now a true conical figure be conceived at the top of the tube with the same angle of slant as the tangent at  $p$ , and with base the cross section of the tube, then the surface of this cone will represent the surface of a reaction

zone meeting a gas velocity  $u$  at all points of its surface, so that

$$s = u \sin \alpha$$

will be true for any position taken.

$$s = \frac{ur}{h}, \quad (9)$$

where  $h$  is the slant height of the ideal cone and  $r$  the radius of the tube. Including equation (7)

$$s = \frac{ur}{h} = k_1 [\text{CO}]^2 [\text{O}_2] \quad (10)$$

An experimental estimate of the value of  $s$  in equation (9) was carried out by this device, using flow meters to determine the time-volume rate of flow  $u$ , through the tube as well as to determine the composition, in terms of partial pressures, of the CO,  $\text{O}_2$  mixtures used. From photographic figures similar to that shown at Figure 1, the values of  $h$  were approximated. Some results obtained by the use of this device and method, on the explosive reaction  $2\text{CO} + \text{O}_2 \rightarrow$



FIG. 2



at water vapor saturation, are recorded in Table I and indicated by the mark ● in the coordinate Figure 3. In Figure 3 is also drawn the curve, indicated by open circles and a continuous line, of equation (7).

TABLE I

Showing experimental estimates obtained for the rate of flame propagation in the  $2\text{CO} + \text{O}_2 \rightarrow$  explosive reaction. Burner method

Record 9-12-22 No.	Partial pressures, atmospheres		$\Gamma$ [CO <sup>2</sup> ] [O <sub>2</sub> ]	$s = \frac{ur}{h}$ (cm/sec)	$k_1 = \frac{s}{\Gamma}$
	[CO]	[O <sub>2</sub> ]			
1	0.310	0.690	0.0663	45.6	688
2	.350	.650	.0796	55.0	691
3	.395	.605	.0944	66.5	704
4	.405	.595	.0976	72.5	743
5	.425	.575	.1038	70.0	674
6	.425	.575	.1038	71.5	688
7	.440	.560	.1083	78.0	720
8	.440	.560	.1083	79.5	734
9	.460	.540	.1142	78.5	687
10	.460	.540	.1142	88.0	771
11	.465	.535	.1156	82.5	714
12	.480	.520	.1197	84.5	706
13	.490	.510	.1224	84.0	686
14	.495	.505	.1237	89.0	719
15	.505	.495	.1261	91.5	729
16	.515	.485	.1285	89.0	692
17	.520	.480	.1297	93.0	717
18	.535	.465	.1330	89.5	673
19	.545	.455	.1350	90.5	670
20	.555	.445	.1369	99.5	726
21	.590	.410	.1425	101.0	709
22	.635	.365	.1472	103.0	700
23	.665	.335	.1481	102.0	689
24	.695	.305	.1472	103.0	700
25	.745	.255	.1412	100.0	709
26	.865	.135	.1008	75.0	743
27	.870	.130	.0983	67.0	682
28	.870	.130	.0983	57.0	580
29	.885	.115	.0900	58.0	642
30	.895	.105	.0841	50.0	595
31	.900	.100	.0810	46.0	568
32	.910	.090	.0744	41.0	551
Average $k_1$ -----					688

Besides having very narrow limitations, this device at best can give only approximate estimates of the relative motion between the zone of reaction and the active gases entering it. For thermodynamic studies the condition of equilibrium behind the flame may be only approximately determined by the laborious and uncertain method of sampling and subsequent analysis. (Reference 15.)

The symmetry of the spatial propagation of the zone of reaction when running its course within a transparent bomb of constant pressure is, for moderate velocities below the velocity of sound in the gases, very perfect, being that of a spherical shell of flame expanding at uniform rate. Time-volume photographic figures of the progress of the reaction under these conditions are shown in Figure 4. The method by which they are secured has already been described in previous reports. (Reference 16.)

The initial volume of the gases considered is the sphere  $2r$  determined by the horizontal diameter of the bubble at the ignition gap. The diameter of the sphere of reaction equilibrium products at the instant the reaction is complete is  $2r'$ . Since the rate of propagation of the reaction zone is constant during the reaction, its rate in space  $s'$ , may be determined at any

instant during the reaction; it is equal to any instant radius,  $r_i$ , divided by the time interval  $t$ , between ignition and the attainment of  $r_i$ ;

$$s' = \frac{r_i}{t} \quad (11)$$

The rate of displacement of the reaction zone measured relative to the active gases is, for a sphere expanding at a uniform rate,

$$s = s' \frac{r^3}{r'^3} \quad (12)$$

Including equation (7)

$$s = s' \frac{r^3}{r'^3} = k_1 [\text{CO}^2] [\text{O}_2] \quad (13)$$

for the CO, O<sub>2</sub> explosive reaction.

Whether a simple gas is used or a mixture of a number of simple gases, or a gaseous fuel of quite unknown composition, the gross mechanism of the gaseous explosive reaction remains

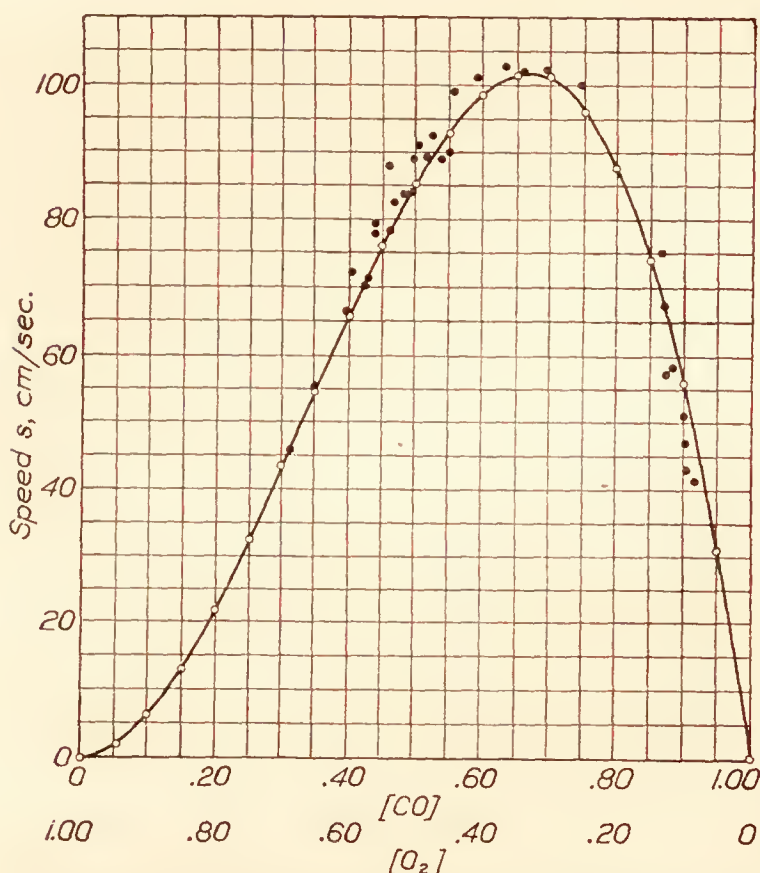
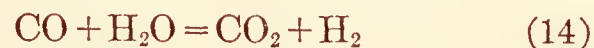


FIG. 3 represents graphically the data given in Table I. The solid circles show observed values,  $s = ur/h$ . The open circles and continuous line show calculated values,  $s = k_1 [\text{CO}]^2 [\text{O}_2]$ . Burner method

the same. There is but one zone of reaction in any case. Within this zone the reaction of the explosive gases proceeds to an equilibrium condition of reaction products  $K$ . The CO, O<sub>2</sub> reaction here used as example, is not supposed to be as simple as indicated by the conventional chemical equation. The actual transformation is believed to depend upon an intermediate reaction, at least for moderate initial temperatures and pressures. The reaction is supposed to involve an active catalyzer, water vapor, and to proceed within the reaction zone as follows (Reference 17):



yet experimental thermodynamic and kinetic results reveal only the final condition as if the reaction had been simply trimolecular,  $2\text{CO} + \text{O}_2 \rightarrow$  with normal maximum for such a reaction,

$$s = k_1 \frac{[\text{CO}]^2 [\text{O}_2]}{[\text{CO}] [\text{O}_2]} \quad (16)$$

The actual microprocess by which the equilibrium  $K$ , is attained within the reaction zone can not be expected to be revealed by a method that takes into account the gross rate only at which an equilibrium condition is attained; that is, the rate at which the pressure at constant volume or the volume at constant pressure increases. The microtransformation within the zone may be very complex or comparatively simple, any knowledge of the actual process of it is limited by the present method to what may be drawn from a knowledge of the initial and final condition of the transformation and its gross rate of progress. For instance, in the case under consideration, some insight may be obtained concerning the effect of the amount of water vapor in the initial components upon the rate of propagation of the reaction zone. Drying the gases to a degree below saturation greatly diminishes the value of the velocity constant  $k_1$ . If the gases are dried as much as possible, they will no longer support a zone of explosive reaction at ordinary initial temperatures and pressures.

The fact that the probable intermediate reaction in the case of the CO, O<sub>2</sub> explosive transformation affected only the rate of propagation by its effect on  $k_1$ , suggested the possibility that



the effect of composite fuels on the rate of propagation might be investigated with some success by the constant pressure method. Some results of that investigation are offered in this report.

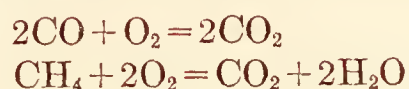
Composite fuels, that will be designated by F, were made up of the gases CO and CH<sub>4</sub> in the following known proportions given in Table II. The characteristics of the explosive reaction of each of the above combinations designated by F were determined over the entire range of mixture ratios of F and O<sub>2</sub> that would ignite and the results tabulated and plotted. Sample records of the results obtained in this study, involving the measurement and calculation of many hundred explosion figures similar to those shown in Figure 4, will be given in this report for those combinations marked \* in Table II.

TABLE II

Showing composition of fuel F; the observed and calculated values of  $k_F$ , and the composition of F and O<sub>2</sub> for maximum flame velocity,  $s$

Partial pressures in fuel mixtures, F		Partial pressures for $s$ maximum		Observed value $k_F$	Calculated value $k_F$
[CO]	[CH <sub>4</sub> ]	[F]	[O <sub>2</sub> ]		
*1.00	0.00	0.667	0.333	691	-----
*.95	.05	.637	.363	1,113	1,051
.90	.10	.625	.375	1,483	1,364
.80	.20	.557	.443	2,054	1,927
.70	.30	.513	.487	2,476	2,412
.60	.40	.476	.524	2,899	2,829
*.50	.50	.444	.556	3,180	3,189
.40	.60	.417	.583	3,505	3,491
.30	.70	.393	.607	3,794	3,775
.20	.80	.370	.630	4,034	4,031
.10	.90	.351	.649	4,177	4,240
*.00	1.00	.333	.667	4,250	-----

The proportion with which the two gaseous components of F unite with oxygen may be taken as that given in their respective stoichiometric equations:



Then for pure CO and O<sub>2</sub>

$$s = k_1 [\text{CO}]^2 [\text{O}_2]$$

The maximum value for  $s$  in this equation should be

$$s = k_1 \frac{[\text{CO}]^2}{[\text{CO}]} \frac{[\text{O}_2]}{[\text{O}_2]} = k_1 [0.667]^2 [0.333]$$

which is confirmed by experimental results. And from the experimental results, the average value of  $k_1$  was found to be

$$k_1 = \frac{s}{[\text{CO}]^2 [\text{O}_2]} = 691 \quad (17)$$

In Table III are set down the results obtained from the photographic records of this explosive reaction. In the lower curve of Figure 5 is shown the plot of these results, marked ●. There is also shown the complete curve, represented by open circles and a continuous line, of the equation

$$s = 691 [\text{CO}]^2 [\text{O}_2]. \quad (18)$$

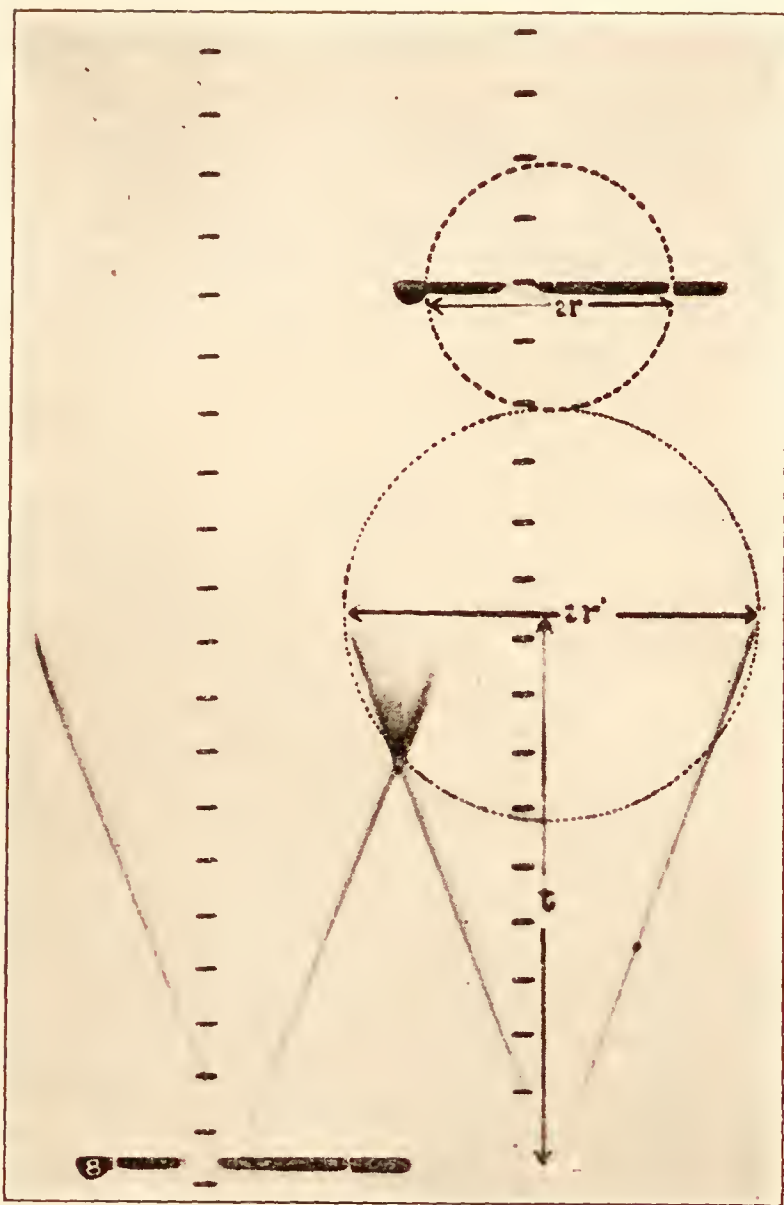


FIG. 4 shows a photographic time-volume record of two gaseous explosive reactions at constant pressure.  $2r$  gives the dimensions of the sphere of active gases whose transformation is to be followed.  $2r'$  gives the dimensions of the sphere of transformed products at the instant the explosive reaction is completed. The uniform rate of motion, in space, of the reaction zone during the transformation is shown by the slant of the flame trace in the photographic figure. The time intervals shown on the figure are 0.002 second

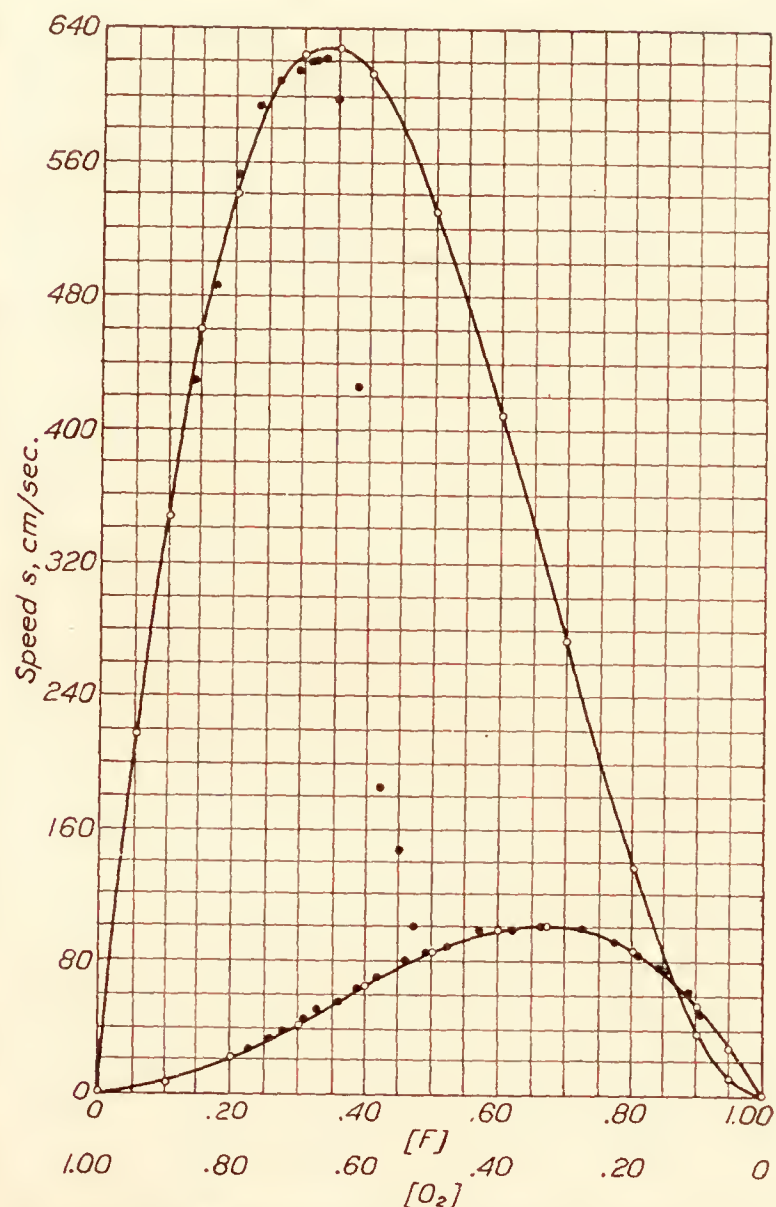


FIG. 5.—The lower curve in this figure represents values of  $s$  in the  $2\text{CO} + \text{O}_2$  explosive reaction at constant pressure. The solid circles give observed values:  $s = s' \frac{r^3}{r'^3}$ . The open circles and continuous line represent calculated values:  $s = k_1 [\text{CO}]^2 [\text{O}_2]$ . In this upper curve the marks have a like significance except that here they refer to the  $\text{CH}_4 + 2\text{O}_2$  explosive reaction at constant pressure

TABLE III

Showing experimental results obtained for the rate of flame propagation in the  $2\text{CO} + \text{O}_2 \rightarrow$  explosive reaction.  
Bubble method

Record 9-7-27 No.	Partial pressure in atmospheres		$\Gamma$ [CO] <sup>2</sup> [O <sub>2</sub> ]	$s' = \frac{r_i}{t}$ cm/sec	$s = s' \frac{r^3}{r'^3}$ cm/sec	$k_1 = \frac{s}{\Gamma}$
	[CO]	[O <sub>2</sub> ]				
1-3	0.224	0.776	0.0389	191	27.6	709
4-7	.260	.740	.0500	226	34.7	694
8-11	.279	.721	.0561	279	37.5	668
12-15	.310	.690	.0663	335	45.3	683
16-19	.325	.675	.0713	365	50.3	705
20-23	.359	.641	.0826	434	55.5	672
24-27	.388	.612	.0921	487	63.3	687
28-31	.416	.584	.1011	561	71.1	703
32-35	.460	.540	.1140	632	80.3	703
36-39	.491	.509	.1227	660	84.3	687
40-43	.523	.477	.1305	715	88.4	678
44-47	.574	.426	.1404	794	99.8	711
48-51	.622	.378	.1463	858	100.6	688
52-55	.668	.332	.1480	870	102.8	694
56-59	.726	.274	.1444	849	101.9	706
60-63	.775	.225	.1351	814	92.2	682
64-67	.810	.190	.1247	733	86.4	693
68-71	.840	.160	.1129	632	79.2	701
72-75	.848	.152	.1093	614	77.7	711
76-79	.883	.117	.0912	463	63.9	700
80-83	.903	.097	.0791	320	50.1	633
Average $k_1$ -----						691



For the methane-oxygen explosive reaction,

$$s = k_1 [\text{CH}_4] [\text{O}_2]^2 \quad (19)$$

the maximum value for  $s$  should be

$$s = k_1 \frac{[0.333]}{\text{CH}_4} \frac{[0.667]^2}{\text{O}_2} \quad (20)$$

This is found to agree well with observed results, and gives for the average value of  $k_1$

$$k_1 = \frac{s}{[\text{CH}_4][\text{O}_2]^2} = 4,250 \quad (21)$$

The experimental results obtained from this reaction are given in Table IV and plotted in the upper curve of Figure 5. They are indicated by the mark  $\bullet$ . This figure also shows the complete curve, marked by open circles and a continuous line, of the equation

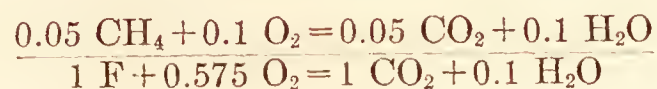
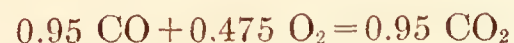
$$s = 4,250[\text{CH}_4] [\text{O}_2]^2 \quad (22)$$

TABLE IV

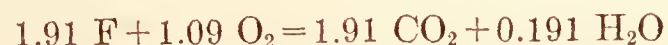
Showing experimental results obtained for the rate of flame propagation in the  $\text{CH}_4 + 2\text{O}_2 \rightarrow$  explosive reaction

Record 11-21-27 No.	Partial pressure in atmospheres		$\Gamma$ [CH <sub>4</sub> ] [O <sub>2</sub> ] <sup>2</sup>	$s' = \frac{r_i}{t}$ (cm/sec)	$s = s' \frac{r^3}{r'^3}$ (cm/sec)	$k_1 = \frac{s}{\Gamma}$
	[CH <sub>4</sub> ]	[O <sub>2</sub> ]				
1-4	0.140	0.860	0.1035	3,347	430	4,155
5-8	.170	.830	.1169	4,536	488	4,172
9-13	.200	.800	.1280	5,156	554	4,326
14-17	.230	.770	.1362	6,048	596	4,375
18-21	.261	.739	.1425	6,098	610	4,280
22-25	.291	.709	.1460	6,359	615	4,212
26-29	.310	.690	.1476	6,586	622	4,212
30-33	.320	.680	.1478	6,636	621	4,200
34-37	.333	.667	.1478	6,714	623	4,213
Average $k_1$ -----						4,240
38-41	.346	.654	.1478	6,586	598	4,044
42-45	.381	.619	.1457	4,988	426	2,903
46-49	.425	.575	.1411	2,808	188	1,333
50-53	.475	.525	.1308	1,308	102	780

For the case where the composition of the fuel F is 0.95 parts by volume of CO and 0.05 parts by volume of CH<sub>4</sub>, the proportion of O<sub>2</sub> necessary to satisfy the conventional formulas of its components for one part F, would be



and for a tri-molecular reaction,



$$s = k_1 [\text{F}]^{1.91} [\text{O}_2]^{1.09} \quad (23)$$

The maximum value of  $s$  in this equation should occur for the composition

$$s = k_1 \frac{[0.637]^{1.91}}{\text{F}} \frac{[0.363]^{1.09}}{\text{O}_2} \quad (24)$$

The average value of  $k_1$  found is

$$k_1 = \frac{s}{[F]^{1.91} [O_2]^{1.09}} = 1,103 \quad (25)$$

The experimental results obtained from the explosive reaction of this combination with  $O_2$  are given in Table V and plotted in Figure 6, together with the complete curve for the equation

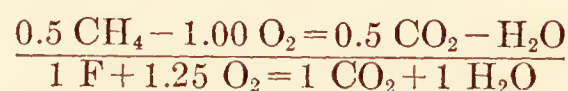
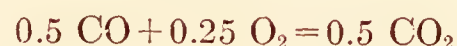
$$s = 1,103 [F]^{1.91} [O_2]^{1.09} \quad (26)$$

TABLE V

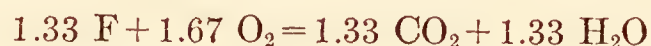
Showing experimental results obtained for the rate of flame propagation in a composite fuel, F, made up of a mixture of 95 parts by volume of carbon monoxide and 5 parts methane, with oxygen

Record 10-11-27 No.	Partial pressures in atmospheres		$\Gamma$ [F] <sup>1.91</sup> [O <sub>2</sub> ] <sup>1.09</sup>	$s' = \frac{r_i}{t}$ (cm/sec)	$s = s' \frac{r^3}{r'^3}$ (cm/sec)	$k_1 = \frac{s}{\Gamma}$
	[F]	[O <sub>2</sub> ]				
1-4	0.226	0.774	0.0442	309	48.8	1,007
5-8	.275	.725	.0598	458	65.2	1,090
9-12	.325	.675	.0761	598	85.4	1,123
13-16	.375	.625	.0920	822	103.2	1,123
17-20	.416	.584	.1042	953	113.0	1,084
21-24	.474	.526	.1194	1,150	130.0	1,090
25-28	.527	.473	.1300	1,320	145.0	1,117
29-32	.578	.422	.1371	1,357	154.0	1,124
33-36	.622	.378	.1397	1,434	155.0	1,108
37-40	.676	.324	.1385	1,426	154.0	1,112
41-44	.724	.276	.1326	1,431	146.0	1,101
45-48	.776	.224	.1206	1,296	136.0	1,127
49-52	.818	.182	.1064	1,097	121.0	1,137
Average $k_1$ -----						1,103

For the case where the composition of the fuel F is 0.5 parts by volume of CO and 0.5 parts by volume of CH<sub>4</sub>, the proportion of O<sub>2</sub> necessary to satisfy the conventional formulas for one part F would be



and for a tri-molecular reaction,



$$s = k_1 [F]^{1.33} [O_2]^{1.67} \quad (27)$$

The average value of  $k_1$  found is

$$k_1 = \frac{s}{[F]^{1.33} [O_2]^{1.67}} = 3,159 \quad (28)$$

In Table VI are recorded the experimental results obtained from the fuel mixture, 0.5 parts carbon monoxide and 0.5 parts methane, with oxygen. These results, marked ●, are plotted in Figure 7, together with the curve for the equation

$$s = 3,159 [F]^{1.33} [O_2]^{1.67} \quad (29)$$

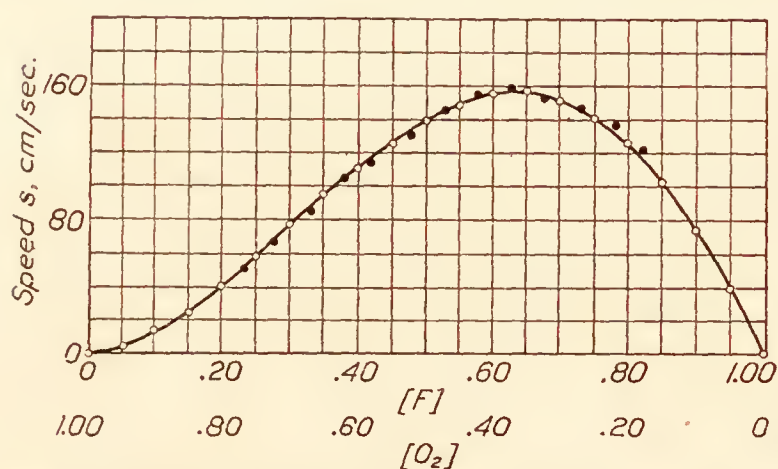


FIG. 6 represents graphically the experimental results given in Table V. The values of  $s = s' \frac{r^3}{r'^3}$  are shown by solid circles. Theoretical values of  $s = k_1 [F]^{1.91} [O_2]^{1.09}$  are shown by open circles and a continuous line



TABLE VI

Showing experimental results obtained for the rate of flame propagation in a composite fuel, F, made up of a mixture of 50 parts by volume of carbon monoxide and 50 parts methane, with oxygen

Record 11-1-27 No.	Partial pressure in atmospheres		$\Gamma$ [F] <sup>1.33</sup> [O <sub>2</sub> ] <sup>1.67</sup>	$s' = \frac{r_i}{t}$ (cm/sec)	$s = s' \frac{r^3}{r'^3}$ (cm/sec)	$k_I = \frac{s}{\Gamma}$
	[F]	[O <sub>2</sub> ]				
1-4	0.175	0.825	0.0714	1,579	223	3,125
5-8	.225	.775	.0898	2,365	281	3,128
9-12	.275	.725	.1050	2,879	325	3,097
13-16	.325	.675	.1163	3,691	372	3,198
17-21	.375	.625	.1238	4,148	395	3,191
22-25	.425	.575	.1272	4,347	409	3,215
26-29	.473	.527	.1268	4,073	400	3,160
Average $k_I$ -----						3,159
30-33	.485	.515	.1262	3,467	340	2,697
34-37	.498	.502	.1253	3,568	336	2,675
38-41	.508	.492	.1243	3,504	330	2,659
42-45	.521	.479	.1229	3,455	311	2,532
46-49	.532	.468	.1215	3,019	263	2,164
50-53	.555	.445	.1182	2,530	219	1,852
54-57	.606	.394	.1084	1,165	104	956

All of the fuel combinations given in Table II were investigated in the same manner as those described above. The results were tabulated and plotted.

In the coordinate Figure 8 the ordinates represent values of the velocity constants of the reaction zone; the abscissas represent partial pressures of F and O<sub>2</sub>. On this figure are plotted the values of  $k_I$  against the corresponding partial pressures for maximum velocity of all of the fuel combinations of CO and CH<sub>4</sub> examined. It may be seen from this plot that these  $k_I$  values follow closely a straight line drawn between the plotted values of  $k_{CH_4}$  and  $k_{CO}$ . This would indicate that the values of  $k_F$  are simple linear functions of the velocity coefficients of the reaction zone of its components  $k_{CH_4}$  and  $k_{CO}$ . The slope of this curve expressed in terms of the factors of the gaseous components is

$$C = \frac{k_{CH_4} - k_{CO}}{\frac{n_{CO}}{n_{CO} + n_{O_2}} - \frac{n_{CH_4}}{n_{CH_4} + n_{O_2}}} \quad (30)$$

where the  $n$ 's represent the coefficients of the active gases in the respective stoichiometrical equations. Hence

$$C = \frac{4,450 - 691}{0.667 - 0.333} = 11,270 \quad (31)$$

The extension of this curve will cut the  $y$ -axis of the coordinate figure at 8206 and the  $x$ -axis at 0.728. The value of  $k_F$  for any composite fuel made up of any mixture of CH<sub>4</sub> and CO may then be written

$$k_F = 11,270 \left( 0.728 - \frac{n_F}{n_F + n_{O_2}} \right) \quad (32)$$

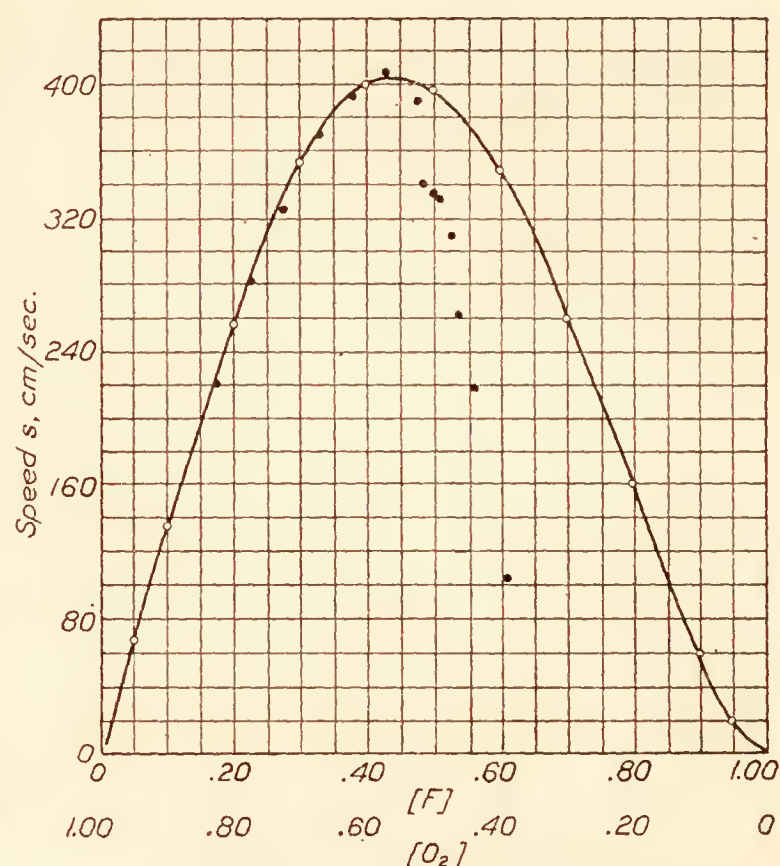


FIG. 7 shows graphically the values obtained for  $s = s' \frac{r^3}{r'^3}$  when the fuel consisted of equal parts by volume of CH<sub>4</sub> and CO. Observed values are indicated by solid circles. Theoretical values of  $s$  computed from  $s = k_I [F]^{1.33} [O_2]^{1.67}$  are shown by open circles and a continuous line

It is therefore possible from a knowledge of the velocity coefficients of the reaction zone of the  $\text{CH}_4$  and  $\text{CO}$  explosive reactions to predict the flame velocity of any composite fuel  $F$ , made up of  $\text{CH}_4$  and  $\text{CO}$ ; and that for any mixture ratio of  $F$  and  $\text{O}_2$  that will ignite, since

$$s = k_F [F]^{n_1} [\text{O}_2]^{n_2}. \quad (33)$$

In the coordinate Figure 9 the curve between the maximal values of  $\text{CH}_4 + 2\text{O}_2 \rightarrow$  and  $2\text{CO} + \text{O}_2 \rightarrow$  is the locus of the maximal values of  $s$  for all possible mixtures of  $\text{CH}_4$  and  $\text{CO}$  with  $\text{O}_2$

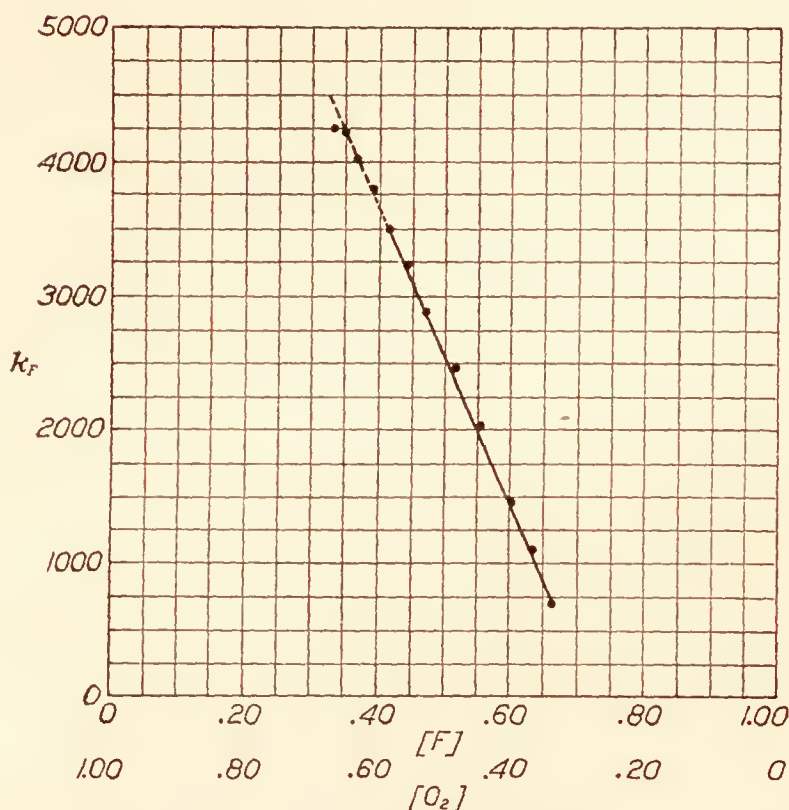


FIG. 8.—The ordinates in this figure represent values of the velocity constants of the reaction zone for those fuel combinations given in Table II. The abscissas represent partial pressures of  $F$  and  $\text{O}_2$ . The values of  $k_F$  in each case are plotted against the corresponding values of  $[F]$  and  $[\text{O}_2]$  representing the maximum value of  $F$ .

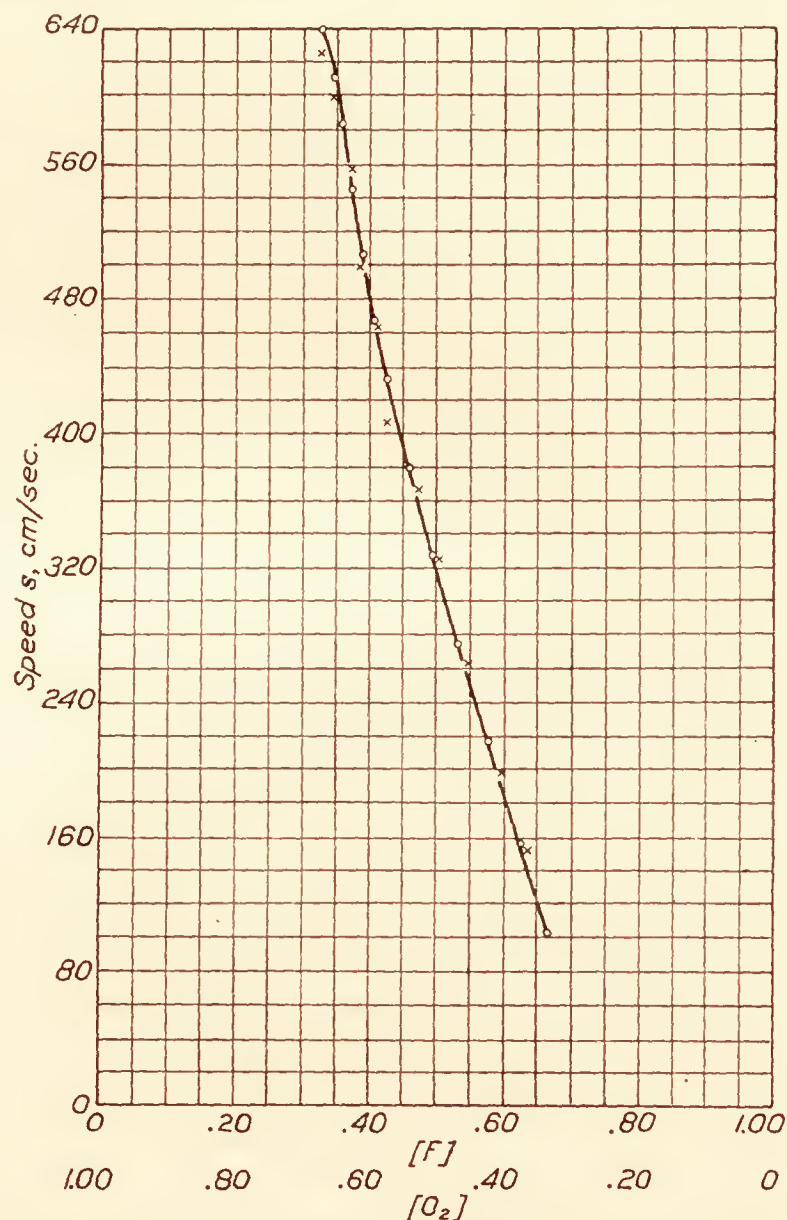


FIG. 9.—The curve represented by open circles and a continuous line in this figure is calculated from equation (33). It is the locus of the maximal values of  $s$  for all possible fuel mixtures of  $\text{CH}_4$  and  $\text{CO}$ . The values represented by the mark  $\times$  in this figure are the observed maximal values of  $s$  found for the fuel combinations given in Table II.

This curve is calculated from equation (33). The points near this curve marked  $\times$  are the observed maxima of the fuel mixtures given in Table II.

#### REMARKS

1. It will be seen by referring to Figure 5 that the observed values of  $s$  for the  $\text{CH}_4 + 2\text{O}_2 \rightarrow$  reaction no longer follow the curve for equation (22) after passing the point for its maximum value,

$$s = 4,250 [0.333] [0.667]^2;$$

$\text{CH}_4 \quad \text{O}_2$

and that the deviation of the observed values of  $s$  from those given by equation (22) are, for those mixture ratios that will ignite the greater, the greater the excess is of  $\text{CH}_4$  over the theoretical amount of  $\text{O}_2$  required to oxidize it. This abrupt decrease in the rate of propaga-



tion of the reaction zone—apparently related to the excess of  $\text{CH}_4$  in the explosive mixture—may or may not be accompanied by a corresponding decrease in the amount of energy liberated. The constant pressure method employed in these studies permits the determination of the actual work done by an explosive reaction. The constant pressure bomb is an efficient experimental gas engine operating with minimum heat losses and negligible friction against the pressure of its surroundings. The photographic figures shown in Figure 4 are engine diagrams to scale;  $r$  and  $r'$  represent the initial and final volumes of the reaction. The actual work accomplished by the transformation of a given charge is

$$W = c (r'^3 - r^3)$$

and for unit charge,

$$\frac{W}{r^3} = c \left( \frac{r'^3}{r^3} - 1 \right).$$

In Figure 10 the ordinates of the curve shown are values of  $\left( \frac{r'^3}{r^3} - 1 \right)$ ; the abscissas represent partial pressures of the active gases. The figure shows that although the rate of reaction has been greatly reduced by an excess of  $\text{CH}_4$ , the total energy liberated has not been affected to the same degree. In fact, the maximum work appears to be obtained with a small excess of the fuel. The rapid decrease in the rate of the explosive reaction, however, due to an increase in the fuel excess, quickly prevents the possibility of maintaining a zone of explosive reaction in the mixture.

2. Composite fuels made up of mixtures of  $\text{CO}$  and  $\text{H}_2$  in different proportions were investigated in the same manner as the  $\text{CO}$ ,  $\text{CH}_4$  mixtures that have been described. The results obtained in the two series of measurements differ only in minor details. The reaction of both components,  $\text{CO}$  and  $\text{H}_2$  with  $\text{O}_2$  is tri-molecular as it is with  $\text{CO}$  and  $\text{CH}_4$  with  $\text{O}_2$ , but with this difference: The maximal value of  $s$  in the  $\text{CH}_4$ ,  $\text{O}_2$  reaction (see Figure 5 upper curve) occurs for the combination

$$s = k_1 \underset{\text{CH}_4}{[0.333]} \underset{\text{O}_2}{[0.667]^2}$$

while the maximal value of  $s$  for the  $\text{CO}$ ,  $\text{O}_2$  reaction (see Figure 5 lower curve) occurs for the combination

$$s = k_1 \underset{\text{CO}}{[0.667]^2} \underset{\text{O}_2}{[0.333]}.$$

The maximal value of  $s$  for any mixture of these components will fall intermediate between these values on the curve shown in Figure 9; but the maximal values of  $s$  for all mixtures of  $\text{CO}$  and  $\text{H}_2$  will be of the form

$$s = k_F \underset{\text{F}}{[0.667]^2} \underset{\text{O}_2}{[0.333]}$$

and will be arranged about the same vertical axis at 0.667 in the coordinate figures.

3. The range of mixtures of hydrogen with oxygen, and mixtures of hydrogen and carbon monoxide with oxygen, will have greatly differing physical properties as heat conductivities, specific heats, etc. The modifying effect of the physical properties of these mixtures on the

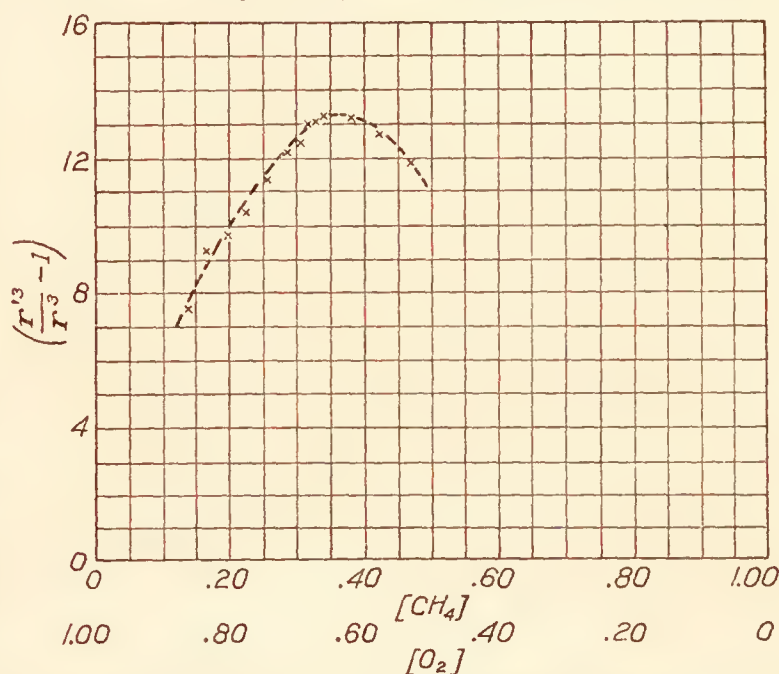


FIG. 10.—This curve shows values proportional to the actual amount of work accomplished by the explosive transformation of unit charge of the various mixture ratios of  $\text{CH}_4$  and  $\text{O}_2$  that would ignite

rate of propagation of the reaction zone within them is found to parallel similar cases observed and described in Report No. 280 of the National Advisory Committee for Aeronautics (Reference 18).

BUREAU OF STANDARDS,  
WASHINGTON, D. C., *April 25, 1928.*

#### REFERENCES

1. Langen, A.: Mitt. ü. Forschungsarbeiten, Heft 8, 1, 1903.
2. Pier, M.: Z. f. Elektrochem. 15, 536, 1909.
3. Bjerrum: Z. f. Physik. Chem. 79, 513, 1912.
4. Siegel: Z. f. Physik. Chem. 87, 614, 1914.
5. Nernst: Theoretical Chemistry, 10th Edition, p. 745, 1923.
6. Partington: The Specific Heats of Gases, p. 6, 1924.
7. Partington: Op. cit.
8. Tolman R. C.: "Statistical Mechanics with Applications to Physics and Chemistry." Chemical Catalog Co., Inc., 1927, p. 239 and 323.
9. Haber: Z. f. Physik. Chem. 68, 726, 1909.
10. Stevens, F. W.: "A Constant Pressure Bomb." N. A. C. A. Technical Report No. 176, 1923. Journal Am. Chem. Soc. 48, 1896 (1926).
11. Ehrenfest, P. and T.: "Die Mechanik der aus sehr zahlreichen diskreten Teilen bestehende Systeme," Encyklop. der Math. Wiessen. 4, 4, 11, 1914.
12. Jourguet, M. E.: "Vitesse de Reaction et Thermodynamique," Ann. d. Physique V, 5-73, 1926. Nernst: Theoretical Chemistry, 10th Edition, p. 521, 1923.
13. Nernst: Op. cit. p. 635; also p. 785.  
Le Chatelier: Z. Physik. Chem. 2, 782, 1888.
14. van't Hoff: Etudes de Dynamique Chimique, Amsterdam, 1884.
15. Haber: Z. f. Elek. Chem. 14, 517, 1908.  
Haber: Thermodynamik technischer Gasreaktionen, p. 585, 1905.  
Hiller: Z. f. Physik. Chem. 81, 591, 1913.
16. Stevens, F. W.: "A Constant Pressure Bomb." N. A. C. A. Technical Report No. 176, 1923. Journal Am. Chem. Soc., 48, 1896 (1926). Zeit. des V. D. I. No. 20 (1926), 659.
17. Nernst: Theoretical Chemistry, 10th Edition, p. 790.
18. Stevens, F. W.: "The Gaseous Explosive Reaction—The Effect of Inert Gases." N. A. C. A. Technical Report No. 280, 1927.



---

**REPORT No. 306**

---

**FULL-SCALE WIND-TUNNEL TESTS OF A SERIES  
OF METAL PROPELLERS ON A  
VE-7 AIRPLANE**

**By FRED E. WEICK**  
**Langley Memorial Aeronautical Laboratory**





# REPORT No. 306

## FULL-SCALE WIND-TUNNEL TESTS OF A SERIES OF METAL PROPELLERS ON A VE-7 AIRPLANE

By FRED E. WEICK

### SUMMARY

An adjustable blade metal propeller was tested at five different angle settings, forming a series varying in pitch. The propeller was mounted on a VE-7 airplane in the Twenty-Foot Propeller Research Tunnel of the National Advisory Committee for Aeronautics. The efficiencies were found to be from 4 to 7 per cent higher than those of standard wood propellers operating under the same conditions. The results are given in convenient form for use in selecting propellers for aircraft.

### INTRODUCTION

It has been known for some time that, in general, thin metal propellers are somewhat more efficient than wooden ones. Actual comparative values have not, however, been available. The present full-scale tests on a series of metal propellers give, for the first time, data on the aerodynamic characteristics of full-size metal propellers, and make possible a direct comparison between the metal propellers and a series of wooden propellers tested under the same conditions.

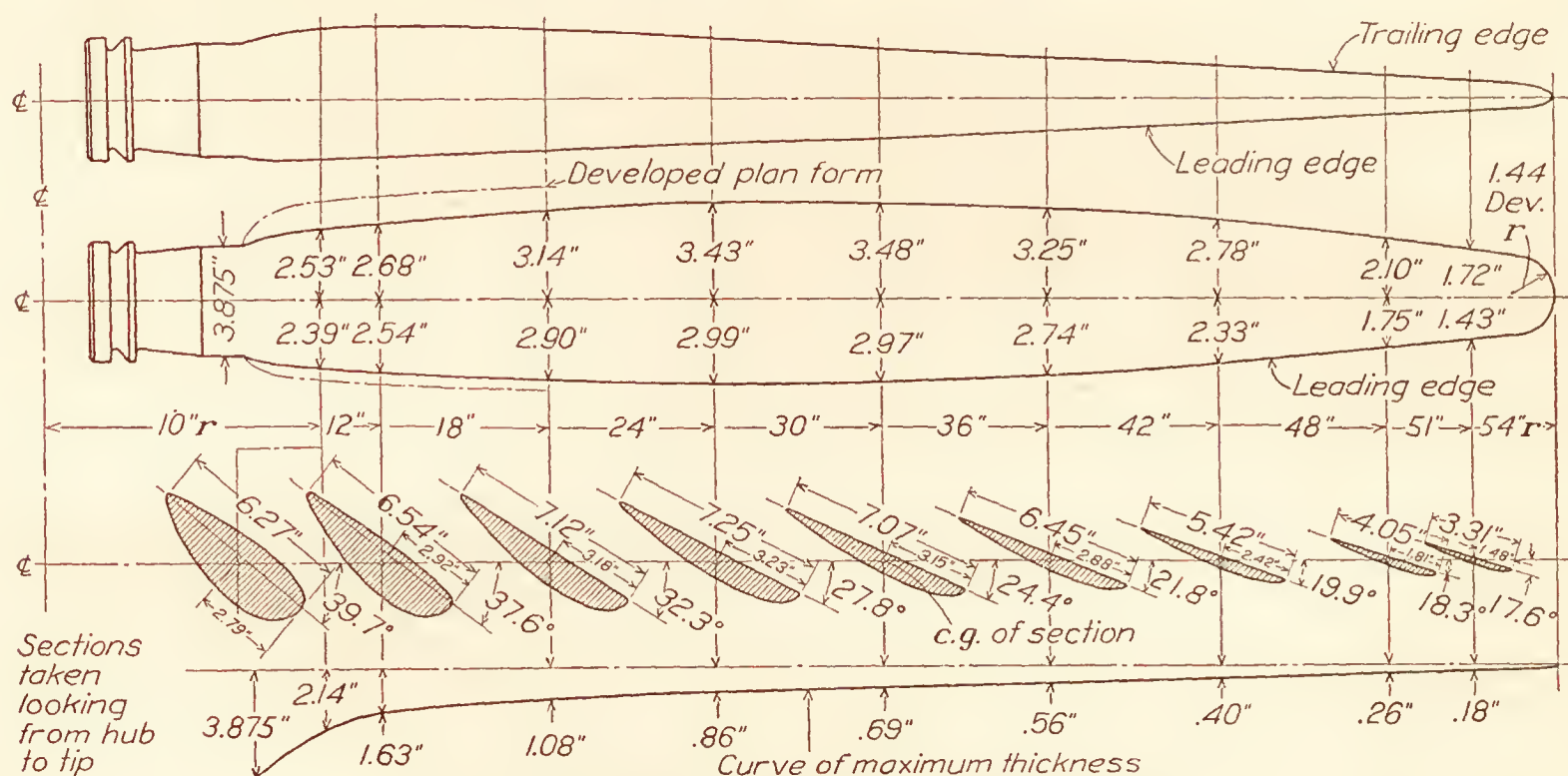


FIG 1.—Metal blade for 9 ft. diameter propeller. Right hand. No. 4412

A two-bladed adjustable pitch metal propeller was tested at five different blade settings, giving in reality a series of propellers varying in pitch. Since each blade as a whole was rotated in the hub to the desired setting, all of the angles along the blade varied the same amount, so that the pitch did not change uniformly. It is, however, common practice to design detachable blade metal propellers with a certain distribution of blade angles and then turn the blades to any pitch required for a particular airplane, thus facilitating production.

The tests were made on a Vought VE-7 airplane with a 180 HP. Wright E-2 engine, in the Twenty-Foot Propeller Research Tunnel of the National Advisory Committee for Aeronautics, at Langley Field, Va.

### METHODS AND APPARATUS

The propeller blades and hub used in this investigation were furnished by the Navy Department. The blades were made of aluminum alloy, according to the drawing in Figure 1. The

hub to which they were fitted was of steel, and in order to save weight, had been made 1 inch shorter than the hub for which the blades had been designed, so that while the drawing shows a 9-foot propeller, the diameter in these tests was actually 8 feet 11 inches. The pitch distribution was unusual and is worthy of note. With the blade set at  $13^\circ$  at the 42-inch radius, the pitch from the 36-inch radius to the tip had the approximately uniform value of 5 feet. From the 36-inch radius toward the hub it gradually reduced so that at the 18-inch radius it was only 4.5

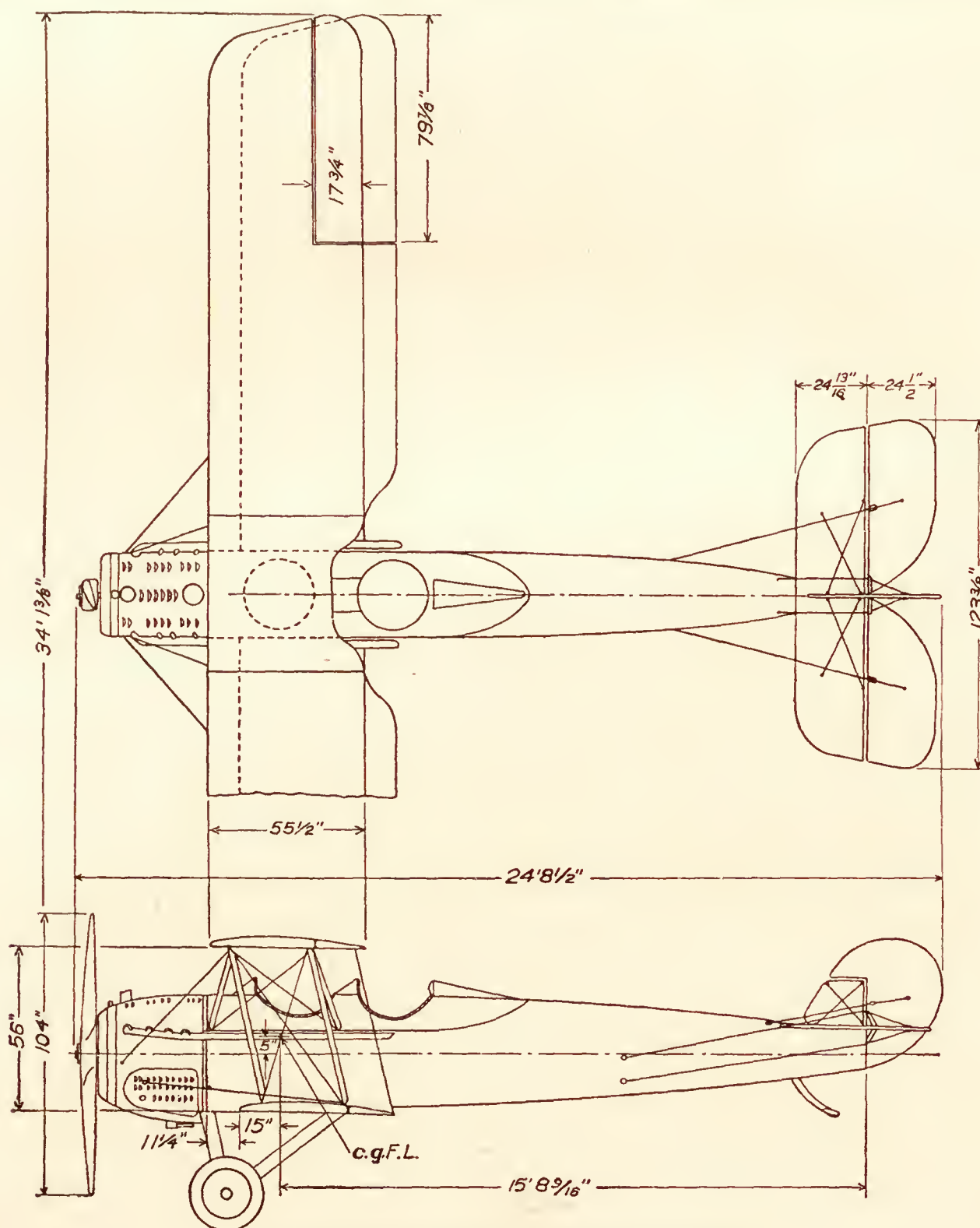


FIG. 2.—Elevational and plan views of the VE-7 airplane

feet. The center line of the propeller, as mounted on the airplane, was 5 inches from the front of the radiator.

The propeller research tunnel is of the open-jet type with an air stream 20 feet in diameter in which velocities up to 110 M. P. H. can be obtained. A complete description of the tunnel, balances, and other measuring devices is given in reference 1.

The VE-7 airplane (fig. 2) had a span of 34 feet, so that when mounted in the air stream the wings projected approximately 7 feet into the relatively still air of the experiment chamber. Figure 3 shows the airplane mounted in the tunnel. It is considered that a sufficient portion of



the wing structure was in the air stream to include all parts which would be influenced by or react on the propeller.

The VE-7, as mounted in the tunnel, had inclosed within it a special steel skeleton fuselage with a built-in dynamometer, including a Toledo scale, to measure the engine and propeller torque directly. (Reference 1.)

The revolution speed of the engine was measured by means of a special calibrated Elgin chronometric tachometer, and the velocity of the air stream was obtained by means of calibrated static plates in the return passages leading to a manometer in the experiment chamber.

In order to know the pitch of the propellers while in operation, the deflection of one blade was measured at the 42-inch radius by means of a telescope mounted on a graduated base and sighted on first the leading and then the trailing edge. This was done while the propeller was standing still and then was repeated for each test point while the propeller was running.

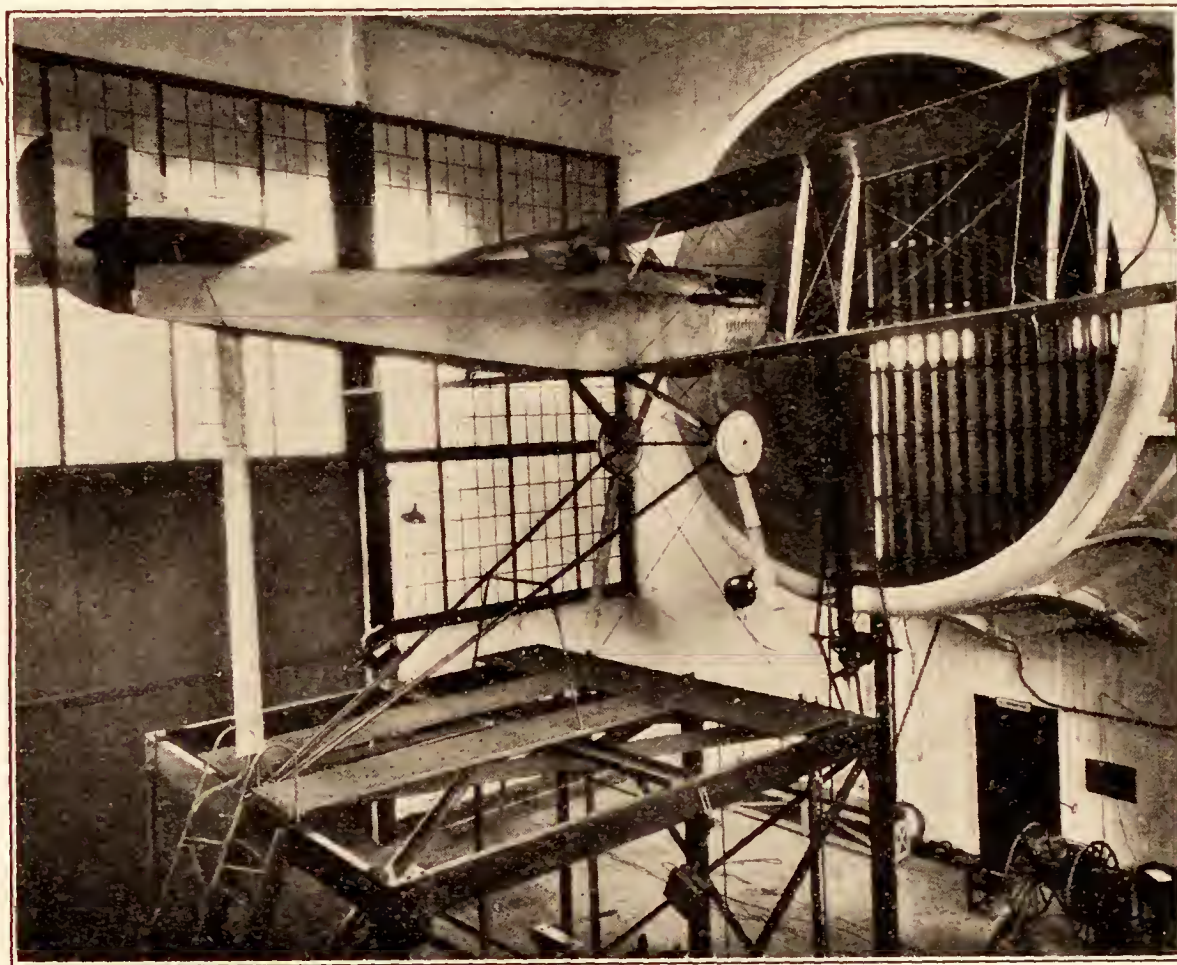


FIG. 3.—VE-7 airplane mounted in Propeller Research Tunnel

The resultant horizontal force of the propeller-body combination, which may be either a thrust or a drag, was measured on the regular thrust balance. (Also described in reference 1.)

This resultant horizontal force,  $R$ , may be thought of as composed of three horizontal components, such that

$$R = T - D - \Delta D,$$

where

$T$  = the thrust of the propeller while operating in front of the body (the tension in the crank shaft).

$D$  = the drag of the airplane alone (without propeller) at the same air velocity and density.

$\Delta D$  = the increase in drag of the airplane with propeller, due to the slip stream.

In order to obtain the propulsive efficiency, which includes the propeller-body interference, an effective thrust is used, which is defined as

$$\text{Effective thrust} = T - \Delta D = R + D.$$

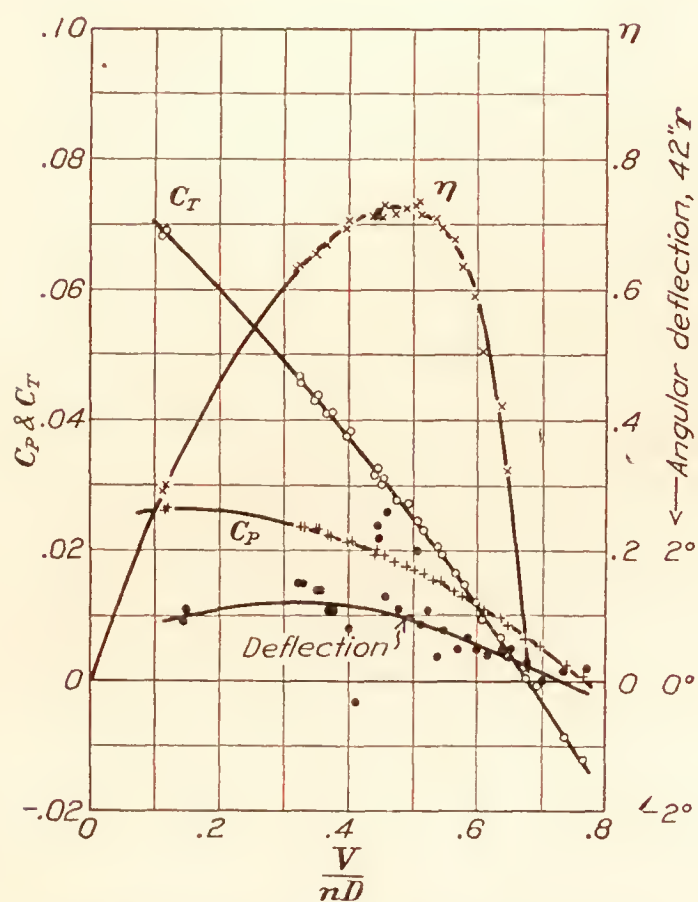


FIG. 4.—Propeller 4412 (11° at 42'') on VE-7 airplane

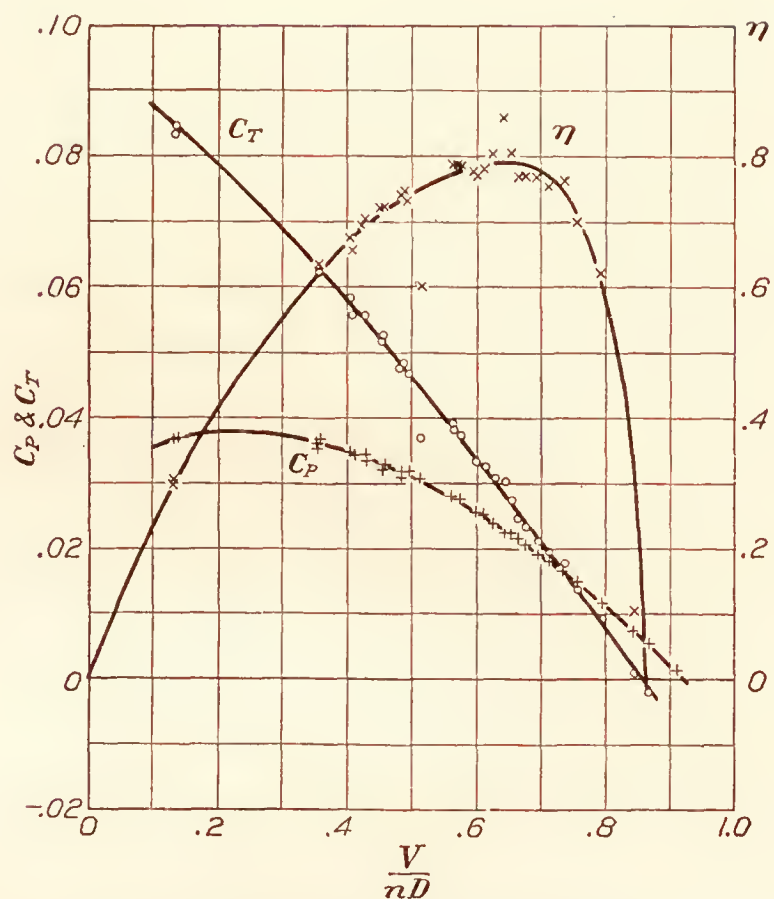


FIG. 5.—Propeller 4412 (15° at 42'') on VE-7 airplane

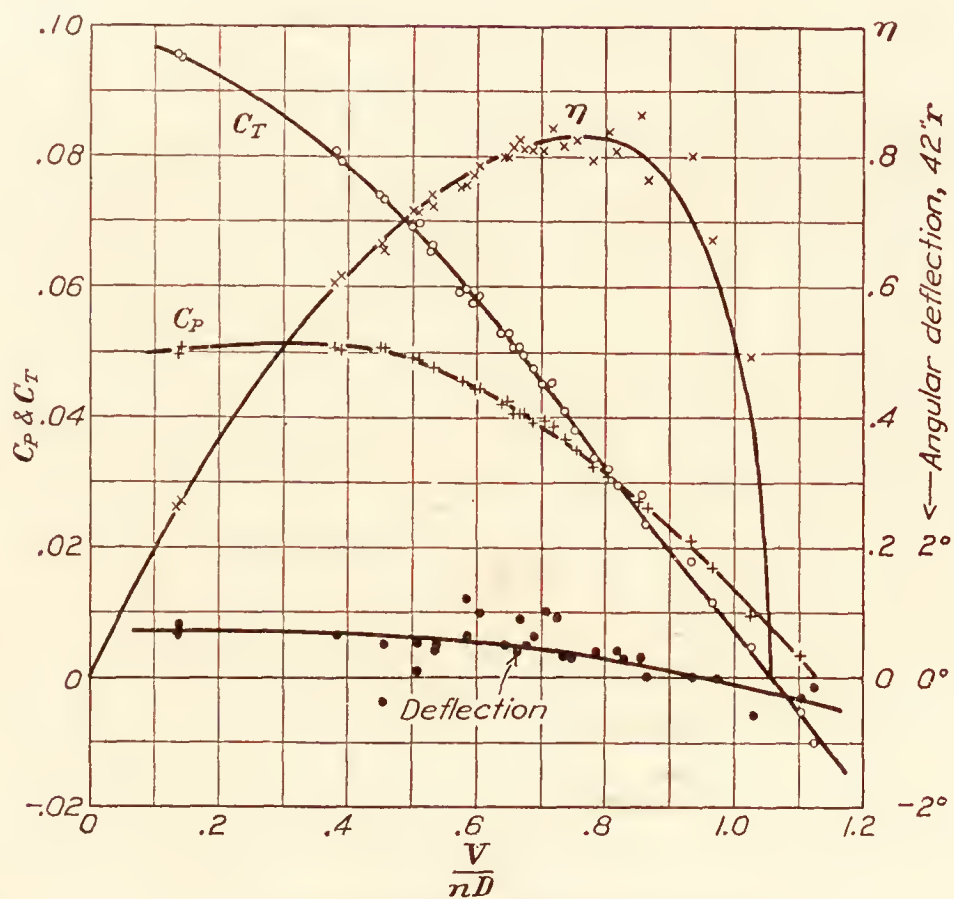


FIG. 6.—Propeller 4412 (19° at 42'') on VE-7 airplane



The propulsive efficiency, then, is the ratio of the useful power to the input power, or

$$\text{Propulsive efficiency} = \frac{\text{effective thrust} \times \text{velocity of advance}}{\text{input power}}.$$

This propulsive efficiency includes the increase in drag of all parts of the airplane affected by the slip stream and also the effect of the body interference on the propeller thrust and power.

### RESULTS

The observed data points are plotted in Figures 4 to 8, inclusive. They are reduced to the usual coefficients of thrust, power, and propulsive efficiency,

$$C_T = \frac{\text{Effective Thrust}}{\rho n^2 D^4},$$

$$C_P = \frac{\text{Input power}}{\rho n^3 D^5},$$

$$\eta = \frac{\text{Effective thrust} \times \text{velocity of advance}}{\text{Input power}},$$

where  $D$  is the propeller diameter and  $n$  represents the revolutions per unit time. Since the coefficients are dimensionless, any homogeneous system of units may be used.

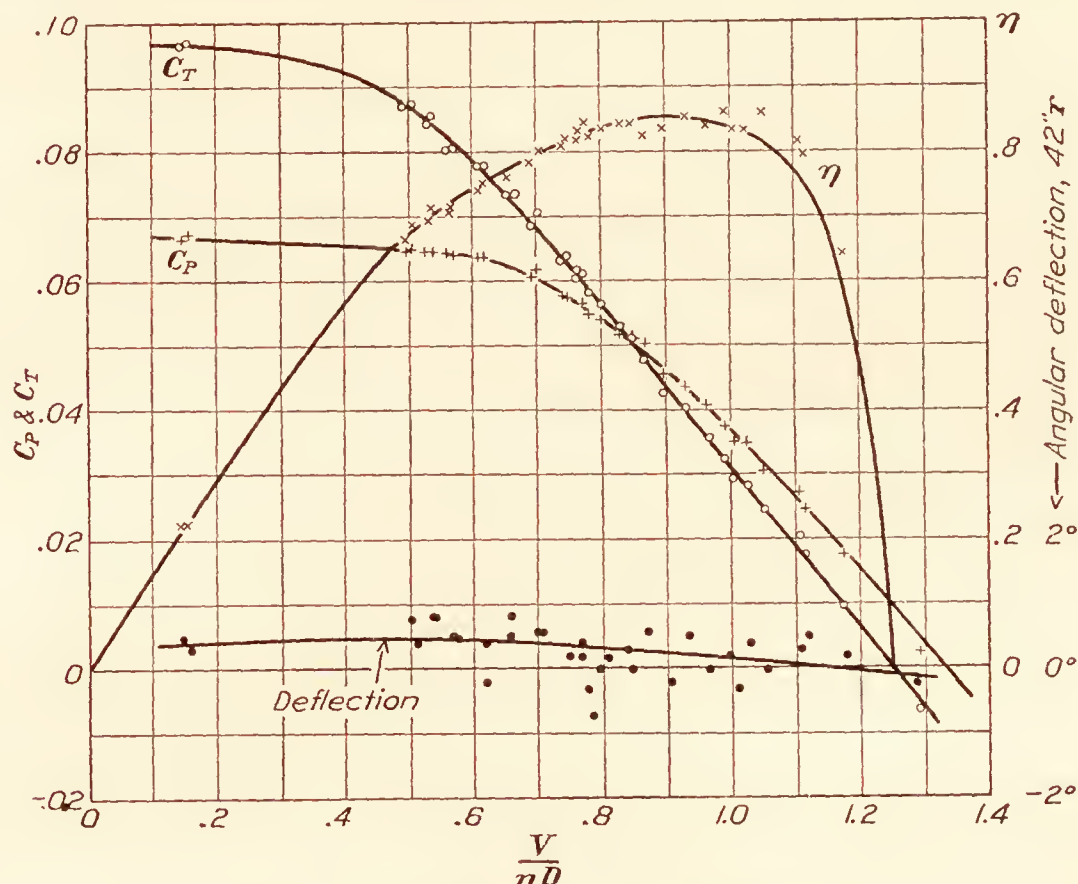


FIG. 7.—Propeller 4412 (23° at 42") on VE-7 airplane

The angular deflections of the propeller blades at the 42-inch radius, which were measured for each test condition, are also plotted in Figures 4 to 8. The blades deflected so as to increase the pitch for all cases excepting the 15° setting. For that setting the deflection readings are evidently erroneous, and have been omitted. For all excepting the 15° setting the twist in operation is greater for the low pitches and the low values of  $\frac{V}{nD}$ . With the highest pitch setting there is practically no twist at any  $\frac{V}{nD}$ .

The curves of thrust coefficients against  $\frac{V}{nD}$  are given for all of the pitch settings in Figure 9, and similar sets of curves for the power coefficients and efficiencies in Figures 10 and 11, respectively. The curves for the various pitch settings form regular series with no unusual features, except for the propulsive efficiencies which are slightly higher than might have been expected from model tests.

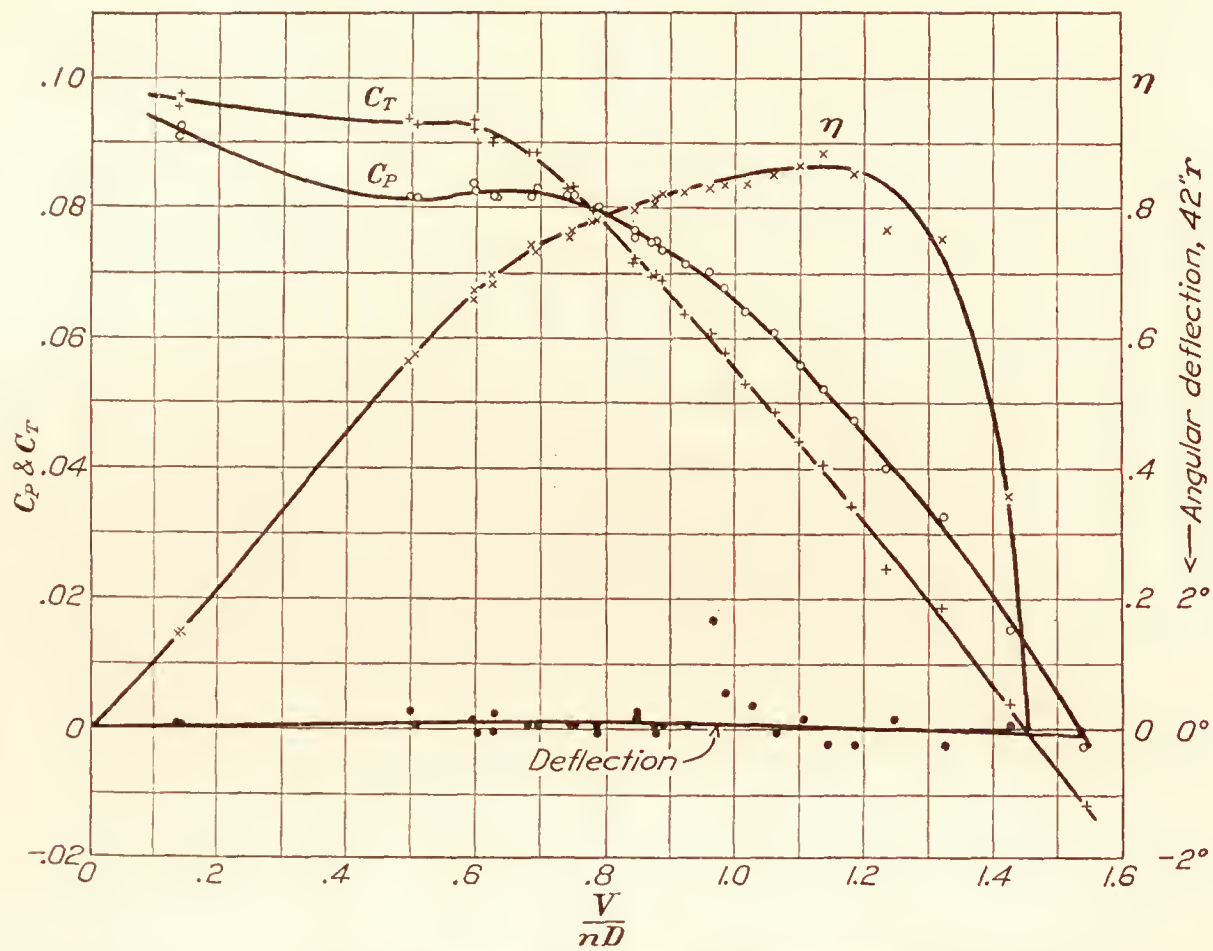


FIG. 8.—Propeller 4412 (27° at 42'') on VE-7 airplane

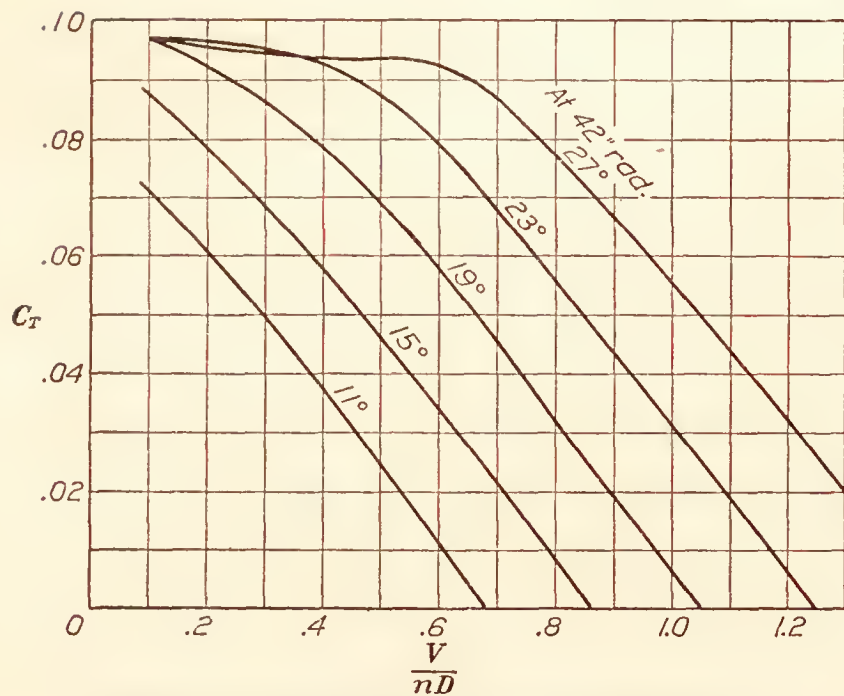


FIG. 9.—Propeller 4412 on VE-7 airplane. Thrust coefficients

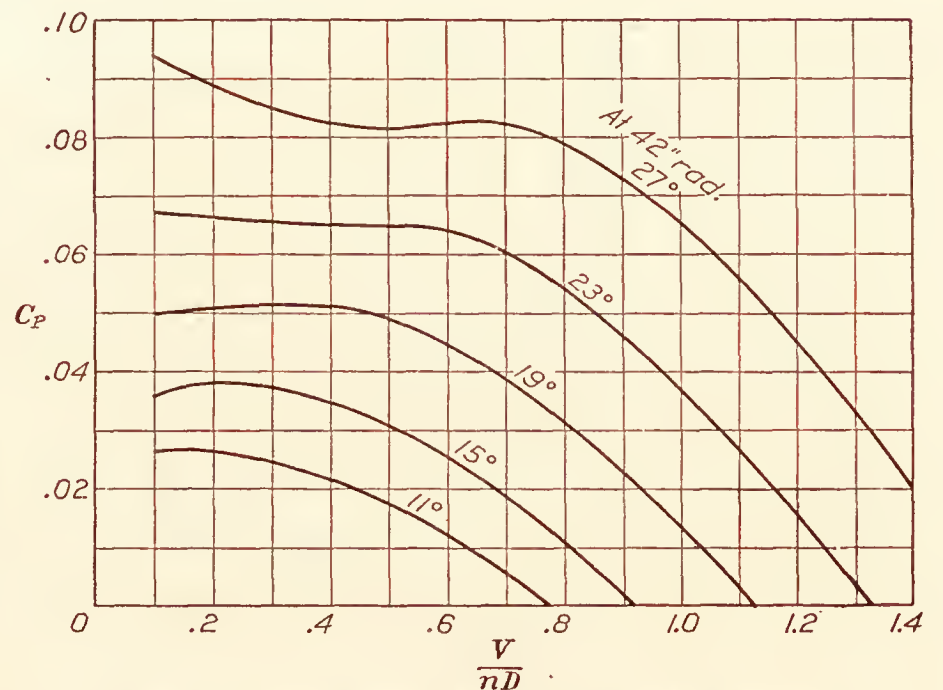


FIG. 10.—Propeller 4412 on VE-7 airplane. Power coefficients

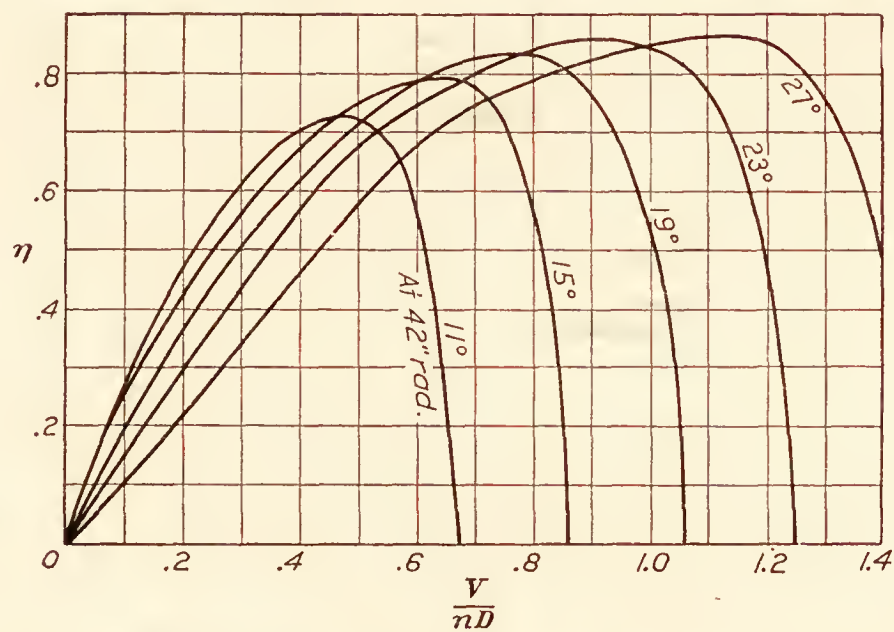


FIG. 11.—Propeller 4412 on VE-7 airplane. Efficiencies



## COMPARISON WITH WOOD PROPELLERS

In Figure 12 the efficiencies of these thin-bladed metal propellers are compared with those of a series of three wood propellers varying in pitch ratio. The wood propellers were of Navy form with uniform pitch, and had pitch ratios of 0.6, 0.7, and 0.8. They were tested (Reference 2) on the same *VE-7* airplane and under the same conditions as the metal propellers. The efficiencies are plotted against the coefficient

$$C_s = \sqrt[5]{\frac{\rho V^5}{P n^2}},$$

where  $P$  represents the power absorbed by the propeller. Propellers operating at the same values of  $C_s$  are fulfilling the same requirements of power, velocity, and revolutions, and are therefore on a fair basis for the comparison of efficiencies.

Figure 12 shows that the metal propellers are from 4 to 7 per cent more efficient than the wood propellers under the same operating conditions.

## USE OF RESULTS IN DESIGNING PROPELLERS

The results of these tests may be used to select the best diameter and pitch setting of propellers of geometrically similar form, to fulfill certain requirements on an airplane having proportions and shape similar to the *VE-7*. The selection can be performed very easily by means of Figure 13, in which the efficiencies and values of  $\frac{V}{nD}$  for the various pitch settings are plotted against the coefficient  $C_s$ . It is merely necessary to (1) calculate the value of  $C_s$  for the power, revolutions, and forward speed at which the propeller is to operate, (2) choose the pitch setting for the propeller operating at the desired portion of the efficiency curve, (3) find the  $\frac{V}{nD}$  for the above  $C_s$  and pitch setting from the lower curves, and (4) knowing  $\frac{V}{nD}$ ,  $n$ , and  $V$ , calculate  $D$ .

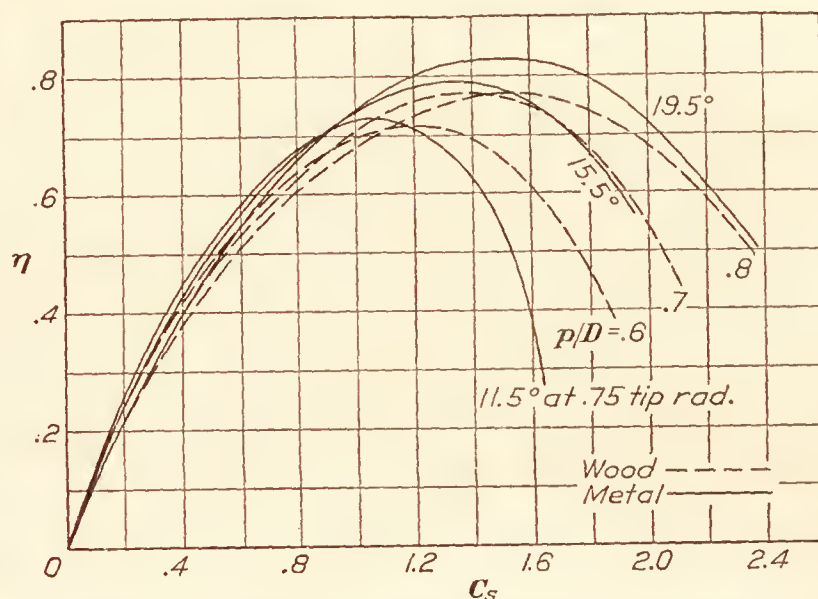


FIG. 12.—Comparison of efficiencies of wood and metal propellers

If the diameter of the propeller is fixed to start with,  $\frac{V}{nD}$  is also fixed, and the pitch setting can be found directly from the curves of  $\frac{V}{nD}$  vs.  $C_s$ .

*Example.*—A propeller is to be selected for an airplane similar in form to the *VE-7*. With an engine developing 300 HP. at 1,800 R. P. M., the maximum horizontal speed is expected to be 150 M. P. H.

(1) In engineering units,

$$\begin{aligned} C_s &= \frac{.638 \times \text{M. P. H.}}{\text{HP}^{\frac{1}{2}} \times \text{R. P. M.}^{\frac{2}{5}}} \\ &= \frac{.638 \times 150}{3.13 \times 20.05} \\ &= 1.52 \end{aligned}$$

The values of  $\text{HP}^{\frac{1}{2}}$  and  $\text{R. P. M.}^{\frac{2}{5}}$  can be easily obtained from scales provided for the purpose in Figure 14.

(2) It will be assumed that it is desirable to have the propeller operate at its maximum efficiency at the high speed of the airplane. Then from the upper or efficiency curves of Figure 13, it will be seen that a setting of  $19.5^\circ$  at 0.75 of the tip radius satisfies this condition (i. e., the efficiency curve for the  $19.5^\circ$  setting peaks at  $C_s =$  approximately 1.52).

(3) From the lower curves in Figure 13, for  $C_s = 1.52$  and a setting of  $19.5^\circ$ ,  $\frac{V}{nD} = 0.77$ .

$$\begin{aligned}
 (4) \quad D &= \frac{88 \times \text{M. P. H.}}{\text{R. P. M.} \left( \frac{V}{nD} \right)} \\
 &= \frac{88 \times 150}{1,800 \times 0.77} \\
 &= 9.52 \text{ ft.}
 \end{aligned}$$

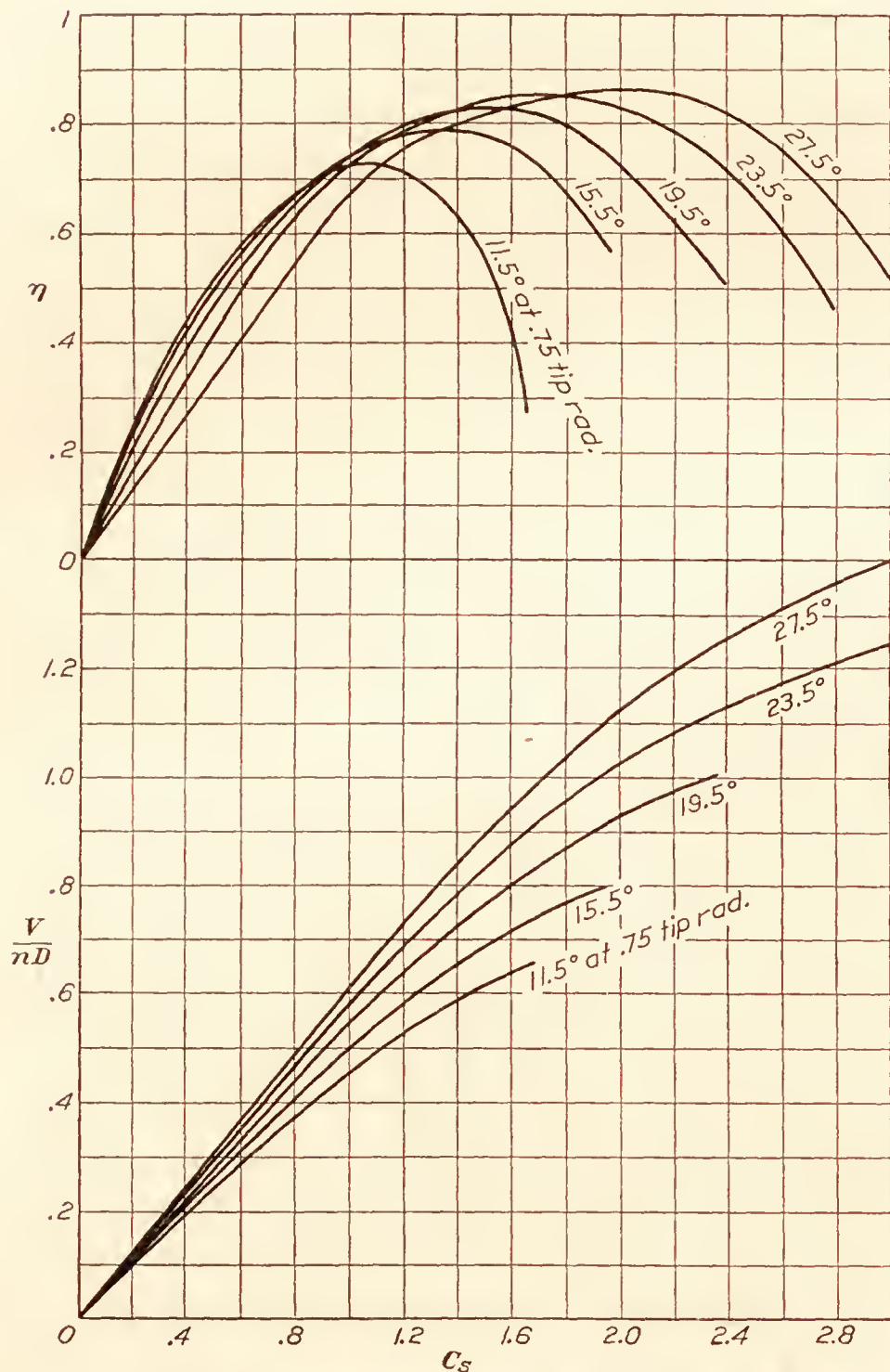


FIG. 13.—Working chart for selecting similar propellers

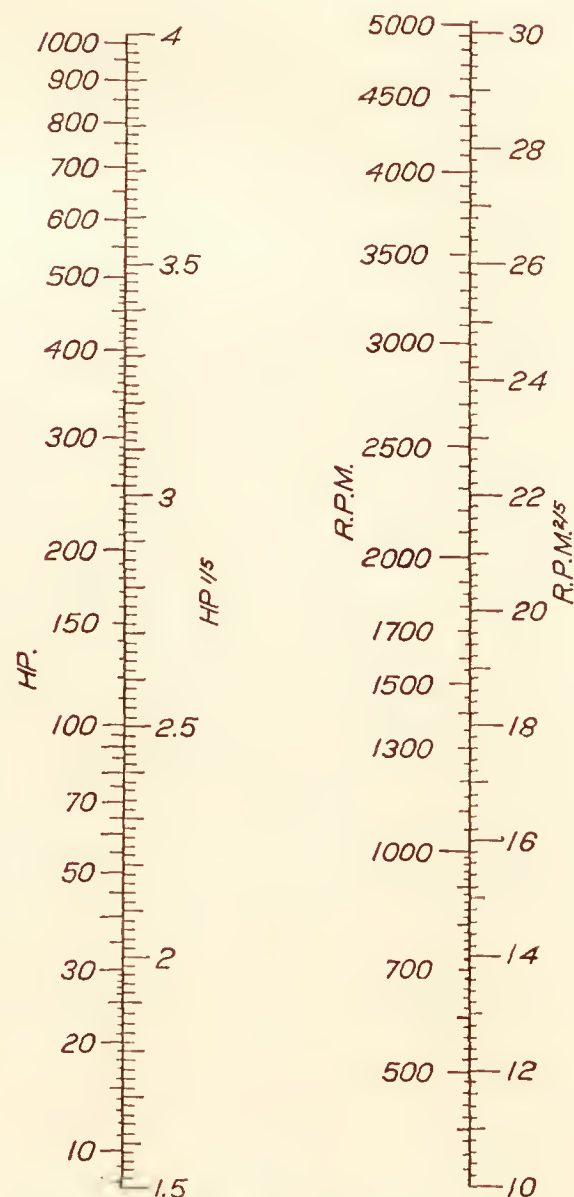


FIG. 14.—Scales for finding  $HP^{1/5}$  and  $R. P. M.^{2/5}$

The propulsive efficiency, which includes the increased drag of the parts of the airplane in the slip stream, is .83.

In case the diameter were fixed from the start at, say, 9 feet, the  $\frac{V}{nD}$  would be fixed at

$$\begin{aligned}
 \frac{V}{nD} &= \frac{88 \times \text{M. P. H.}}{\text{R. P. M.} \times D} \\
 &= \frac{88 \times 150}{1,800 \times 9} \\
 &= .815.
 \end{aligned}$$



Then from the lower curves of Figure 13, for  $C_s=1.52$  and  $\frac{V}{nD}=0.815$ , the blade angle should be set to  $22.0^\circ$  at 0.75 tip radius.

In the application of these results to the selection of a propeller for an airplane it is essential that the actual brake horsepower of the engine under flight conditions be used in the formula for  $C_s$ . The power developed by an engine in service is likely to vary widely from the power developed under ideal conditions on a dynamometer. In a series of 15 flight-performance tests, in which the powers absorbed by the propellers were calculated on the basis of the present full-scale wind-tunnel test data, the computed power averaged about 90 per cent of that credited to the engines by the dynamometer tests on similar engines.

#### CONCLUSIONS

1. The efficiencies of this series of metal propellers range from 4 to 7 per cent higher than those of standard wood propellers operating under the same conditions (tip speeds up to 800 feet per second).

2. The efficiencies of the metal propellers were rather high, reaching 86 per cent for the highest pitch setting, and were apparently not adversely affected by the pitch distributions obtained by turning the whole blade as a unit.

3. The results of the tests, as presented, may be conveniently used for the selection of a propeller to give a certain performance on airplanes similar to the VE-7.

LANGLEY MEMORIAL AERONAUTICAL LABORATORY,  
NATIONAL ADVISORY COMMITTEE FOR AERONAUTICS,  
LANGLEY FIELD, VA., *July 13, 1928.*

#### REFERENCES

1. Weick, Fred E. and Wood,, Donald H.: The Twenty-Foot Propeller Research Tunnel of the National Advisory Committee for Aeronautics. N. A. C. A. Technical Report No. 300 (1928).
2. Weick, Fred E.: Full Scale Tests of Wood Propellers on a VE-7 Airplane in the Propeller Research Tunnel. N. A. C. A. Technical Report No. 301 (1928).

TABLE I  
METAL PROPELLER ON VE-7  
(PROP. No. 4412)  
(BLADE ANGLE  $11^\circ$  AT  $42''$  r.)

$\rho$	$V$ M. P. H.	$N$ R. P. M.	$Q$ lb. ft.	$T$ lb.	$C_T$	$C_P$	$\frac{V}{n D}$	$\eta$	Def. at $42''$ Rad., degrees
0. 002337	80. 7	1820	372	428	0. 0319	0. 0196	0. 440	0. 713	+2. 4
. 002337	81. 4	1825	382	438	. 0325	. 0200	. 441	. 716	2. 2
. 002335	85. 1	1845	377	425	. 0308	. 0193	. 457	. 730	2. 6
. 002335	85. 0	1855	377	423	. 0302	. 0191	. 453	. 716	1. 3
. 002330	94. 5	1910	368	386	. 0262	. 0177	. 491	. 727	1. 0
. 002325	90. 7	1895	373	401	. 0276	. 0182	. 474	. 717	1. 1
. 002323	99. 0	1940	362	370	. 0244	. 0169	. 505	. 731	2. 0
. 002323	99. 4	1940	363	371	. 0245	. 0169	. 507	. 734	. 9
. 002320	99. 3	1900	343	337	. 0232	. 0167	. 517	. 718	1. 1
. 002317	99. 3	1835	296	277	. 0204	. 0154	. 535	. 709	. 4
. 002317	99. 1	1805	280	254	. 0194	. 0151	. 543	. 696	. 8
. 002317	98. 8	1730	237	200	. 0166	. 0139	. 565	. 676	. 5
. 002317	99. 0	1695	213	167	. 0145	. 0131	. 578	. 638	. 7
. 002317	98. 8	1645	187	131	. 0121	. 0123	. 595	. 591	. 5
. 002317	98. 5	1600	159	94	. 0091	. 0110	. 609	. 507	. 4
. 002317	98. 5	1545	135	64	. 0067	. 0100	. 631	. 421	. 5
. 002317	98. 0	1505	112	40	. 0044	. 0087	. 645	. 325	. 5
. 002317	97. 6	1435	77	2	. 0002	. 0066	. 673	. 023	. 3
. 002315	97. 5	1385	56	-26	-. 0030	. 0052	. 696	-----	. 0
. 002315	98. 1	1325	27	-59	-. 0084	. 0027	. 733	-----	. 2
. 002315	98. 8	1285	7	-81	-. 0122	. 0007	. 761	-----	+ . 2
. 002320	75. 5	1865	427	533	. 0381	. 0216	. 401	. 707	- . 3
. 002320	75. 1	1870	426	529	. 0375	. 0215	. 397	. 692	+ . 8
. 002320	68. 5	1845	435	562	. 0410	. 0225	. 368	. 670	1. 1
. 002323	68. 7	1845	436	562	. 0410	. 0226	. 3685	. 670	1. 0
. 002320	64. 6	1815	435	578	. 0437	. 0232	. 352	. 663	1. 4
. 002320	64. 3	1820	435	581	. 0435	. 0232	. 350	. 657	1. 4
. 002325	58. 9	1800	437	604	. 0462	. 0237	. 324	. 632	1. 5
. 002325	58. 9	1800	437	604	. 0462	. 0237	. 324	. 632	1. 5
. 002330	20. 0	1735	449	839	. 0688	. 0262	. 1143	. 300	1. 1
. 002330	19. 9	1740	450	837	. 0684	. 0262	. 1134	. 297	. 9



TABLE I—Continued

15° AT 42''

$\rho$	$V$ M. P. H.	$N$ R. P. M.	$Q$ lb. ft.	$T$ lb.	$C_T$	$C_P$	$\frac{V}{n D}$	$\eta$	Def. at 42'' Rad., degrees
0. 002370	82. 1	1655	496	527	0. 0468	0. 0312	0. 492	0. 737	—0. 1
. 002370	82. 1	1655	499	528	. 0468	. 0315	. 492	. 734	— . 6
. 002370	86. 3	1660	491	407	. 0358	. 0306	. 514	. 601	—1. 4
. 002365	95. 6	1685	464	460	. 0394	. 0282	. 562	. 786	— . 6
. 002360	95. 5	1680	459	448	. 0388	. 0279	. 562	. 788	— . 6
. 002360	99. 2	1710	461	447	. 0373	. 0272	. 574	. 788	— . 4
. 002360	99. 1	1705	462	446	. 0374	. 0274	. 575	. 786	— . 6
. 002355	98. 9	1635	396	364	. 0333	. 0256	. 600	. 780	— . 9
. 002355	98. 8	1600	372	342	. 0327	. 0252	. 612	. 783	— . 8
. 002355	98. 6	1555	336	306	. 0309	. 0240	. 628	. 806	— . 6
. 002355	98. 1	1505	296	279	. 0302	. 0226	. 645	. 862	— . 2
. 002355	98. 4	1495	286	250	. 0272	. 0221	. 652	. 803	+ . 1
. 002355	98. 1	1435	243	196	. 0233	. 0204	. 677	. 773	— . 4
. 002350	98. 4	1465	264	217	. 0248	. 0214	. 665	. 770	— . 3
. 002350	98. 3	1395	216	171	. 0213	. 0193	. 699	. 771	+ . 1
. 002350	98. 3	1365	196	148	. 0195	. 0182	. 712	. 759	— . 3
. 002350	98. 0	1325	171	127	. 0177	. 0169	. 733	. 766	— . 1
. 002350	97. 8	1280	141	92	. 0138	. 0149	. 757	. 700	— . 8
. 002350	97. 8	1225	102	57	. 0093	. 0118	. 791	. 626	— . 3
. 002350	97. 4	1145	56	5	. 0010	. 0074	. 842	. 1071	— . 2
. 002350	97. 2	1110	41	—11	. 0022	. 0058	. 864	-----	— . 8
. 002350	97. 3	1060	9	—36	-----	. 0014	. 910	-----	— . 7
. 002350	97. 0	990	—26	—72	-----	-----	-----	-----	— . 3
. 002360	81. 1	1645	494	537	. 0484	. 0316	. 488	. 748	+ . 1
. 002360	81. 1	1660	497	541	. 0478	. 0311	. 484	. 743	— . 2
. 002360	75. 7	1640	511	576	. 0523	. 0328	. 457	. 729	— . 3
. 002360	75. 7	1645	511	574	. 0517	. 0326	. 456	. 723	— . 4
. 002360	69. 6	1605	506	589	. 0558	. 0339	. 429	. 706	+ . 1
. 002360	69. 5	1605	509	588	. 0557	. 0341	. 428	. 699	— . 8
. 002360	66. 1	1605	515	588	. 0557	. 0345	. 408	. 659	— . 9
. 002360	65. 2	1595	511	605	. 0581	. 0348	. 405	. 677	—1. 2
. 002360	56. 0	1565	515	637	. 0635	. 0363	. 354	. 621	— . 3
. 002360	56. 9	1580	517	651	. 0636	. 0358	. 356	. 633	— . 4
. 002370	20. 1	1565	521	853	. 0847	. 0368	. 135	. 311	— . 4
. 002370	20. 1	1565	521	842	. 0836	. 0368	. 135	. 308	-----

TABLE I—Continued

19° AT 42''

$\rho$	$V$ M. P. H.	$N$ R. P. M.	$Q$ lb. ft.	$T$ lb.	$C_T$	$C_F$	$\frac{V}{n D}$	$\eta$	Def. at 42'' Rad., degrees
0. 002350	82. 0	1405	517	481	0. 0594	0. 0455	0. 578	0. 754	+0. 6
. 002350	82. 2	1405	517	481	. 0594	. 0455	. 579	. 755	1. 2
. 002345	87. 0	1430	527	486	. 0585	. 0448	. 602	. 786	1. 0
. 002345	86. 9	1435	529	483	. 0576	. 0447	. 599	. 772	
. 002340	95. 5	1465	525	462	. 0527	. 0425	. 645	. 799	. 5
. 002340	95. 4	1475	525	464	. 0525	. 0420	. 640	. 799	
. 002340	99. 7	1495	522	460	. 0507	. 0407	. 664	. 826	. 9
. 002340	99. 3	1495	523	457	. 0503	. 0407	. 658	. 814	. 4
. 002340	99. 5	1465	502	431	. 0494	. 0407	. 673	. 815	. 5
. 002335	99. 2	1430	467	392	. 0471	. 0398	. 687	. 811	. 6
. 002335	99. 3	1400	438	358	. 0450	. 0391	. 702	. 809	1. 0
. 002335	99. 1	1365	412	340	. 0451	. 0386	. 719	. 841	. 9
. 002335	98. 4	1325	367	291	. 0407	. 0366	. 734	. 818	. 3
. 002335	98. 9	1295	330	257	. 0377	. 0344	. 754	. 828	. 3
. 002330	98. 5	1200	255	186	. 0319	. 0309	. 813	. 838	. 4
. 002330	98. 7	1250	292	210	. 0332	. 0326	. 781	. 796	. 4
. 002330	97. 9	1120	187	118	. 0231	. 0260	. 864	. 766	0
. 002325	98. 5	1195	244	171	. 0296	. 0300	. 819	. 810	. 3
. 002325	98. 4	1145	202	145	. 0273	. 0270	. 851	. 863	+ . 3
. 002325	97. 9	1040	127	78	. 0179	. 0210	. 931	. 806	0
. 002325	97. 8	1000	97	48	. 0118	. 0170	. 968	. 671	0
. 002325	97. 8	945	50	17	. 0047	. 0098	1. 025	. 494	— . 6
. 002325	97. 8	880	15	—17	— . 0054	. 0034	1. 1055	—1. 636	— . 3
. 002325	97. 1	860	—4	—30	— . 0100	— . 0014	1. 1235	— . 800	— . 1
. 002335	74. 5	1390	527	511	. 0654	. 0477	. 531	. 726	+ . 5
. 002335	74. 7	1395	532	522	. 0664	. 0476	. 530	. 740	. 4
. 002340	70. 2	1385	537	540	. 0692	. 0488	. 502	. 717	. 5
. 002340	70. 5	1385	537	543	. 0695	. 0488	. 507	. 719	. 1
. 002340	62. 9	1375	547	568	. 0738	. 0504	. 453	. 663	+ . 5
. 002340	62. 7	1375	547	564	. 0734	. 0504	. 452	. 658	— . 4
. 002345	52. 7	1370	547	615	. 0804	. 0507	. 381	. 603	+ . 6
. 002345	54. 2	1375	549	609	. 0791	. 0502	. 390	. 616	
. 002350	19. 5	1380	547	736	. 0950	. 0502	. 1400	. 266	. 8
. 002350	19. 2	1375	542	736	. 0955	. 0498	. 1385	. 266	. 6



TABLE I—Continued

23° AT 42''

$\rho$	$V$ M. P. H.	P. M. R.	$Q$ lb. ft.	$T$ lb.	$C_T$	$C_P$	$\frac{V}{n D}$	$\eta$	Def. at 42'' Rad., degrees
0. 002360	81. 2	1230	546	452	0. 0732	0. 0625	0. 653	0. 763	+0. 8
. 002360	81. 0	1230	547	453	. 0733	. 0625	. 652	. 763	. 5
. 002355	87. 6	1235	539	436	. 0704	. 0616	. 701	. 801	. 6
. 002355	87. 3	1250	544	436	. 0685	. 0604	. 690	. 783	. 6
. 002355	96. 0	1275	542	419	. 0635	. 0577	. 745	. 820	. 0
. 002355	95. 5	1275	542	418	. 0630	. 0577	. 741	. 810	. 2
. 002345	99. 5	1290	539	413	. 0611	. 0562	. 763	. 831	. 4
. 002345	99. 5	1295	541	412	. 0605	. 0562	. 761	. 820	+ . 2
. 002345	97. 5			-21					- . 2
. 002345	97. 7	750	7	-14	-. 0063	. 0022	1. 290	-. 378	- . 2
. 002345	98. 0	825	68	+27	. 0098	. 0173	1. 175	. 664	+ . 3
. 002345	98. 5	875	107	54	. 0173	. 0244	1. 115	. 794	. 5
. 002340	98. 8	890	123	64	. 0201	. 0271	1. 105	. 816	+ . 3
. 002340	99. 1	975	192	112	. 0290	. 0350	1. 005	. 834	- . 3
. 002330	96. 2	935	175	101	. 0283	. 0348	1. 025	. 834	+ . 4
. 002335	99. 6	1025	238	151	. 0355	. 0407	. 963	. 840	. 0
. 002335	99. 5	995	213	131	. 0327	. 0375	. 990	. 864	. 2
. 002335	99. 0	1055	277	181	. 0402	. 0436	. 930	. 858	. 5
. 002335	99. 5	1170	397	282	. 0509	. 0509	. 843	. 843	. 0
. 002330	98. 3	1135	367	249	. 0476	. 0500	. 866	. 824	. 6
. 002330	98. 8	1090	307	201	. 0421	. 0452	. 898	. 836	- . 2
. 002330	100. 0	1195	422	305	. 0528	. 0519	. 830	. 846	+ . 3
. 002330	100. 0	1235	467	344	. 0561	. 0538	. 801	. 836	. 2
. 002325	99. 5	1265	502	374	. 0580	. 0550	. 780	. 823	- . 7
. 002325	100. 5	1290	532	413	. 0618	. 0562	. 771	. 849	- . 3
. 002325	98. 3	925	147	85	. 0248	. 0302	1. 050	. 862	. 0
. 002335	75. 0	1215	537	462	. 0777	. 0638	. 612	. 745	- . 2
. 002335	74. 6	1215	537	463	. 0778	. 0638	. 615	. 750	+ . 4
. 002340	69. 1	1210	537	475	. 0801	. 0642	. 565	. 707	. 5
. 002340	69. 4	1210	536	478	. 0805	. 0642	. 568	. 713	. 5
. 002340	64. 5	1205	537	498	. 0846	. 0645	. 530	. 695	. 8
. 002340	65. 1	1205	537	499	. 0858	. 0645	. 534	. 711	. 8
. 002340	61. 6	1200	537	512	. 0875	. 0648	. 508	. 686	. 4
. 002340	60. 5	1205	539	513	. 0870	. 0648	. 498	. 668	. 8
. 002350	18. 5	1180	537	547	. 0968	. 0670	. 155	. 224	. 3
. 002350	17. 7	1185	538	548	. 0962	. 0666	. 148	. 214	. 5

TABLE I—Continued

27° AT 42''

$\rho$	$V$ M. P. H.	$N$ R. P. M.	$Q$ lb. ft.	$T$ lb.	$C_T$	$C_P$	$\frac{V}{n D}$	$\eta$	Def. at 42'' Rad., degrees
0. 002325	81. 2	1075	537	388	0. 0832	0. 0817	0. 748	0. 762	+0. 1
. 002325	80. 9	1075	534	386	. 0829	. 0813	. 744	. 758	+ . 1
. 002325	86. 1	1085	537	380	. 0800	. 0801	. 785	. 783	- . 1
. 002325	86. 1	1090	537	379	. 0792	. 0793	. 781	. 780	+ . 1
. 002320	95. 1	1115	538	361	. 0721	. 0762	. 843	. 798	. 3
. 002320	95. 4	1120	538	361	. 0714	. 0754	. 842	. 797	. 2
. 002315	99. 5	1130	539	356	. 0694	. 0745	. 871	. 810	+ . 1
. 002315	99. 5	1130	539	357	. 0695	. 0745	. 871	. 812	- . 1
. 002315	99. 1	1105	516	337	. 0688	. 0743	. 888	. 821	+ . 1
. 002315	99. 3	1065	457	289	. 0634	. 0711	. 922	. 822	. 1
. 002310	99. 0	1020	412	251	. 0606	. 0700	. 960	. 831	1. 6
. 002305	99. 3	1000	382	231	. 0577	. 0676	. 982	. 837	. 6
. 002305	98. 7	960	333	195	. 0528	. 0640	1. 017	. 839	+ . 4
. 002305	98. 6	920	289	164	. 0484	. 0603	1. 060	. 851	- . 1
. 002305	98. 3	855	215	118	. 0403	. 0520	1. 138	. 884	- . 2
. 002305	98. 1	820	179	91	. 0340	. 0472	1. 184	. 853	- . 2
. 002305	97. 9	780	137	60	. 0246	. 0398	1. 244	. 769	+ . 2
. 002305	97. 3	730	97	39	. 0183	. 0322	1. 321	. 750	- . 2
. 002305	97. 8	680	39	7	. 0038	. 0150	1. 424	. 359	+ . 1
. 002305	97. 8	630	-8	-20	-. 0126	-. 0036	1. 537		- . 1
. 002305	98. 3	885	247	138	. 0440	. 0560	1. 100	. 864	+ . 2
. 002315	75. 0	1075	541	408	. 0881	. 0828	. 691	. 736	. 1
. 002315	74. 5	1075	537	408	. 0881	. 0817	. 686	. 741	+ . 2
. 002317	67. 8	1075	537	418	. 0900	. 0817	. 623	. 687	- . 1
. 002317	67. 8	1075	535	420	. 0904	. 0816	. 623	. 691	+ . 2
. 002317	64. 5	1070	536	424	. 0920	. 0828	. 595	. 660	+ . 2
. 002317	64. 2	1065	536	425	. 0934	. 0830	. 595	. 670	- . 1
. 002317	54. 1	1080	542	438	. 0936	. 0817	. 495	. 567	+ . 2
. 002317	55. 0	1080	542	435	. 0929	. 0817	. 504	. 574	. 1
. 002325	14. 2	1010	535	402	. 0975	. 0921	. 139	. 147	. 1
. 002325	14. 2	1010	538	402	. 0951	. 0907	. 138	. 144	. 1



TABLE II  
FINAL ADJUSTED COEFFICIENTS  
(PROP. NO. 4412)  
(BLADE ANGLE  $11^\circ$  at  $42''$  r.)

$\frac{V}{nD}$	$C_T$	$C_P$	$\eta$	$C_S$
0.15	0.0652	0.0263	0.372	0.309
.20	.0601	.0260	.462	.416
.25	.0549	.0254	.540	.521
.30	.0492	.0243	.607	.631
.35	.0434	.0230	.660	.744
.40	.0373	.0214	.698	.864
.45	.0312	.0194	.724	.990
.50	.0250	.0172	.726	1.125
.55	.0186	.0147	.688	1.279
.60	.0116	.0118	.590	1.458
.65	.0041	.0097	.275	1.644

TABLE II—Continued  
 $15^\circ$  AT  $42''$

$\frac{V}{nD}$	$C_T$	$C_P$	$\eta$	$C_S$
0.15	0.0831	0.0371	0.336	0.295
.20	.0788	.0379	.416	.385
.25	.0740	.0380	.487	.482
.30	.0690	.0373	.555	.580
.35	.0635	.0364	.611	.679
.40	.0580	.0348	.667	.783
.45	.0521	.0330	.711	.891
.50	.0461	.0310	.745	1.002
.55	.0400	.0287	.766	1.118
.60	.0338	.0260	.780	1.248
.65	.0275	.0226	.790	1.388
.70	.0212	.0190	.781	1.546
.75	.0149	.0154	.725	1.726
.80	.0081	.0112	.578	1.96

TABLE II—Continued  
 $19^\circ$  AT  $42''$

$\frac{V}{nD}$	$C_T$	$C_P$	$\eta$	$C_S$
0.15	0.0948	0.0503	0.283	0.269
.20	.0922	.0508	.363	.364
.25	.0896	.0510	.440	.454
.30	.0861	.0510	.506	.544
.35	.0826	.0510	.568	.635
.40	.0785	.0508	.619	.727
.45	.0741	.0501	.666	.819
.50	.0691	.0489	.708	.914
.55	.0639	.0469	.750	1.012
.60	.0581	.0445	.785	1.118
.65	.0520	.0419	.807	1.227
.70	.0455	.0388	.820	1.340
.75	.0389	.0352	.829	1.465
.80	.0322	.0313	.823	1.600
.85	.0259	.0271	.812	1.750
.90	.0194	.0230	.759	1.912
.95	.0131	.0186	.669	2.11
1.00	.0070	.0136	.515	2.36

TABLE II—Continued

23° AT 42''

$\frac{V}{nD}$	$C_T$	$C_P$	$\eta$	$C_S$
0.15	0.0969	0.0669	0.218	0.257
.20	.0963	.0666	.289	.344
.25	.0959	.0663	.361	.431
.30	.0950	.0660	.432	.516
.35	.0940	.0658	.500	.603
.40	.0926	.0654	.567	.690
.45	.0905	.0650	.626	.779
.50	.0876	.0649	.675	.864
.55	.0832	.0645	.710	.952
.60	.0787	.0639	.740	1.040
.65	.0736	.0626	.765	1.131
.70	.0682	.0603	.792	1.236
.75	.0623	.0573	.815	1.329
.80	.0565	.0540	.838	1.434
.85	.0502	.0502	.850	1.545
.90	.0440	.0461	.857	1.665
.95	.0372	.0418	.845	1.790
1.00	.0310	.0369	.840	1.936
1.05	.0249	.0319	.819	2.09
1.10	.0186	.0264	.776	2.27
1.15	.0122	.0209	.671	2.49
1.20	.0060	.0152	.474	2.76

TABLE II—Continued

27° AT 42''

$\frac{V}{nD}$	$C_T$	$C_P$	$\eta$	$C_S$
0.15	0.0962	0.0911	0.158	0.240
.20	.0956	.0890	.215	.324
.25	.0950	.0869	.274	.409
.30	.0944	.0850	.333	.491
.35	.0940	.0834	.394	.576
.40	.0934	.0821	.455	.660
.45	.0932	.0814	.516	.744
.50	.0930	.0812	.572	.826
.55	.0930	.0817	.626	.908
.60	.0925	.0821	.675	.988
.65	.0900	.0823	.711	1.072
.70	.868	.0820	.741	1.154
.75	.826	.0819	.758	1.237
.80	.776	.0789	.788	1.330
.85	.721	.0761	.805	1.425
.90	.666	.0729	.823	1.520
.95	.610	.0694	.835	1.620
1.00	.552	.0655	.844	1.726
1.05	.497	.0611	.855	1.835
1.10	.439	.0560	.862	1.958
1.15	.380	.0507	.861	2.08
1.20	.319	.0450	.852	2.23
1.25	.258	.0393	.822	2.39
1.30	.196	.0334	.762	2.56
1.35	.132	.0271	.658	2.77
1.40	.0068	.0202	.471	3.05



---

## **REPORT No. 307**

---

# **THE PRESSURE DISTRIBUTION OVER THE HORIZONTAL AND VERTICAL TAIL SURFACES OF THE F6C-4 PURSUIT AIRPLANE IN VIOLENT MANEUVERS**

**By R. V. RHODE**

**Langley Memorial Aeronautical Laboratory**





## REPORT No. 307

---

### THE PRESSURE DISTRIBUTION OVER THE HORIZONTAL AND VERTICAL TAIL SURFACES OF THE F6C-4 PURSUIT AIRPLANE IN VIOLENT MANEUVERS

By R. V. RHODE

---

#### SUMMARY

*This investigation of the pressure distribution on the tail surfaces of a pursuit airplane in violent maneuvers was conducted by the National Advisory Committee for Aeronautics at the request of the Navy Bureau of Aeronautics for the purpose of determining the maximum loads likely to be encountered on these surfaces in flight. The information is a part of that needed for a revision of existing loading specifications to bring these into closer agreement with actual flight conditions. A standard F6C-4 airplane was used and the pressure distribution over the right horizontal and complete vertical tail surfaces was recorded throughout violent maneuvers. The results show that the existing loading specifications do not conform satisfactorily to the loadings existent in critical conditions, and in some cases were exceeded by the loads obtained.*

*An acceleration of 10.5 g. was recorded in one maneuver in which the pilot suffered severely; it is therefore indicated that the limits of the physical resistance of the pilot to violent maneuvers are being approached.*

*Navy specifications for the structural design of tail surfaces are included as an appendix.*

#### INTRODUCTION

Due to lack of sufficient data on the loads and load distribution on airplane tail surfaces, specifications of the strength requirements for the empennage are made somewhat arbitrarily and are changed now and then as surfaces which have been designed to meet the requirements fail in some condition of flight. The present specifications are based on certain experimental data obtained in the wind tunnel and in flight (see Bibliography), but this information is quite incomplete and does not furnish a satisfactory basis for the formulation of design rules. The most important of this previous work are the complete pressure distribution measurements on the tail surfaces of a JN-4 in steady and accelerated flight, the pressure measurements on single tail ribs of the VE-7 and TS airplanes at Langley Field, and the pressure distribution measurements on the right stabilizer of the VE-7 at McCook Field. The first of these is becoming less and less useful as airplanes are being made faster and more maneuverable and the others are not sufficiently complete to be of much value.

It was the aim in the present investigation to determine the complete distribution of pressure on all of the tail surfaces of a high-speed airplane in the maneuvers most likely to impose the highest loads on the tail structures, so that the existing specifications could be changed to conform more closely with the conditions likely to be experienced in flight. It was contemplated, further, to determine the loads on several types of balanced rudders and to obtain, simultaneously with the pressure records, accelerations in the  $X$ ,  $Y$ , and  $Z$  directions at the center of gravity and at the tail. Unfortunately, the airplane was available for such a limited time that this program could not be entirely carried out, and the investigation was confined to the measurement of the maximum loads and pressures encountered on the standard tail surfaces in a number of violent maneuvers. Accelerations approaching the design load factor were obtained in several maneuvers and the pilot suffered rather severely at times from these high accelerations. In view, therefore, of this approach to the design load factor and to the limits of the physical resistance of the pilot, the loads obtained on the tail surfaces are indicative of the maximum tail loads which can be safely imposed on this type of airplane.



## APPARATUS

## THE AIRPLANE

The airplane used in these tests was a standard Navy F6C-4 (Curtiss "Hawk" with the Pratt & Whitney "Wasp" engine), (fig. 1), unaltered in any respect as to external form and internal structure. The moments of inertia about the *Y* and the *Z* axes were slightly increased since the recording manometer and the pressure tubes were installed aft of the center of gravity. The center of gravity itself was shifted back a small amount, but both of these alterations were slight, and their effects upon the results are negligible except in the dives, as will be explained



FIG. 1.—The F6C-4 airplane

later, inasmuch as they tend to balance each other in the critical loading condition. The effect, if any, is to decrease the downloads and to increase the uploads on the horizontal surfaces, and to increase the loads on the vertical fin and rudder.

## THE TUBES AND ORIFICES

Pressure orifices of the type illustrated in Figure 2 were mounted on false ribs at the locations shown in Figure 3. There were two orifices at each location shown, one on the lower or right surface, and the other on the upper or left surface of the horizontal or vertical members, respectively. The pressures were transmitted through  $\frac{3}{16}$ -inch I. D. aluminum tubes which

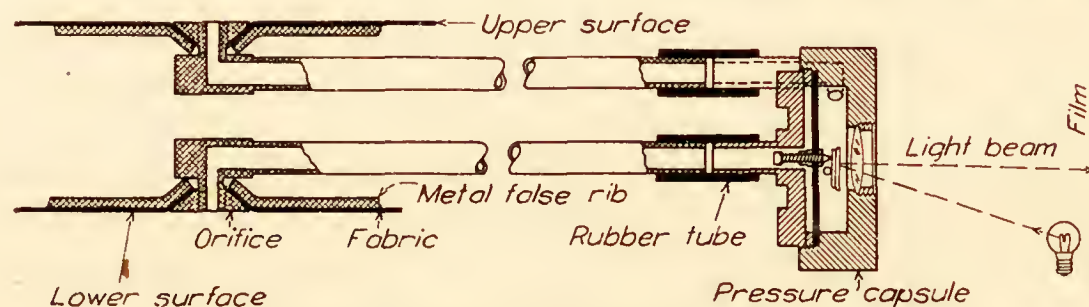


FIG. 2.—Diagram showing type of orifice and connection to capsule

were welded to the orifice blocks and which were connected to the manometer by means of short pieces of rubber tubing. The connections between the tubes in the fixed and movable elements of the tail also were made with rubber tubing so arranged that no kinks occurred at any angular displacement of the controls.

## LOCATION OF ORIFICES

[Inches from center line of hinge]

Rib	G	H	J	K	L	M	B	C	D	E	F
Rib length	28.4''	40.8''	47.4''	58.9''	25.8''	25.8''	52.9''	46.0''	38.8''	33.0''	23.4''
Orifice No. $\left\{ \begin{array}{l} 1 \\ 2 \\ 3 \\ 4 \\ 5 \\ 6 \\ 7 \end{array} \right.$	-7.4	-11.4	-18.2	-29.3	3.3	3.3	-27.0	-22.1	-16.4	-12.4	-6.8
	-2.8	-8.5	-13.9	-23.3	11.8	11.8	-21.8	-17.0	-11.7	-8.1	-3.6
	3.3	-2.8	-3.8	-3.8	21.9	21.9	-14.7	-3.6	-3.6	-3.6	3.6
		3.3	3.3	3.3			-3.6	3.6	3.6	3.6	8.6
		11.8	11.8	11.8			3.6	8.6	8.6	8.6	12.0
		21.9	21.9	21.9			8.6	18.5	16.9	15.3	
							19.7				



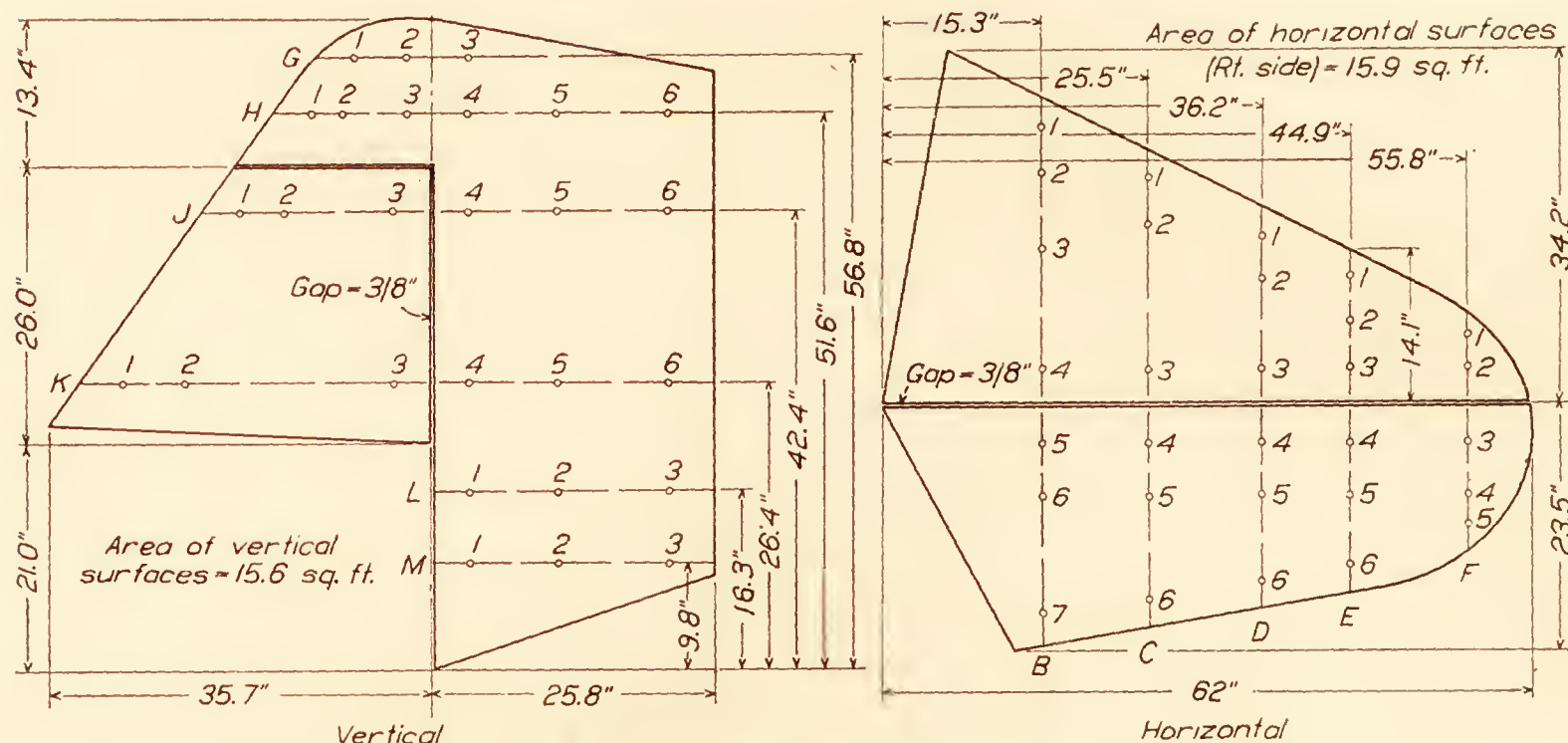


FIG. 3.—Location of orifices on the F6C-4 tail surfaces

## INSTRUMENTS

An N. A. C. A. type 60 recording multiple manometer (photographic type) was used to record the pressures. Briefly, this instrument consists of 60 pressure units or capsules, mounted on a metal case, as shown in Figure 4, and a film holder and driving mechanism. This manometer is the same in principle as the manometers used in previous tests (Reference 1), differing mainly from them in that it is capable of recording pressures from 60 stations instead of only 30.

In addition to the manometer, the following instruments were used: N. A. C. A. recording air-speed meter (Reference 2); N. A. C. A. control position recorder (Reference 3); and N. A. C. A. single component recording accelerometer (Reference 4). These instruments were all operated simultaneously on the same electrical circuit and controlled by the pilot through a button switch

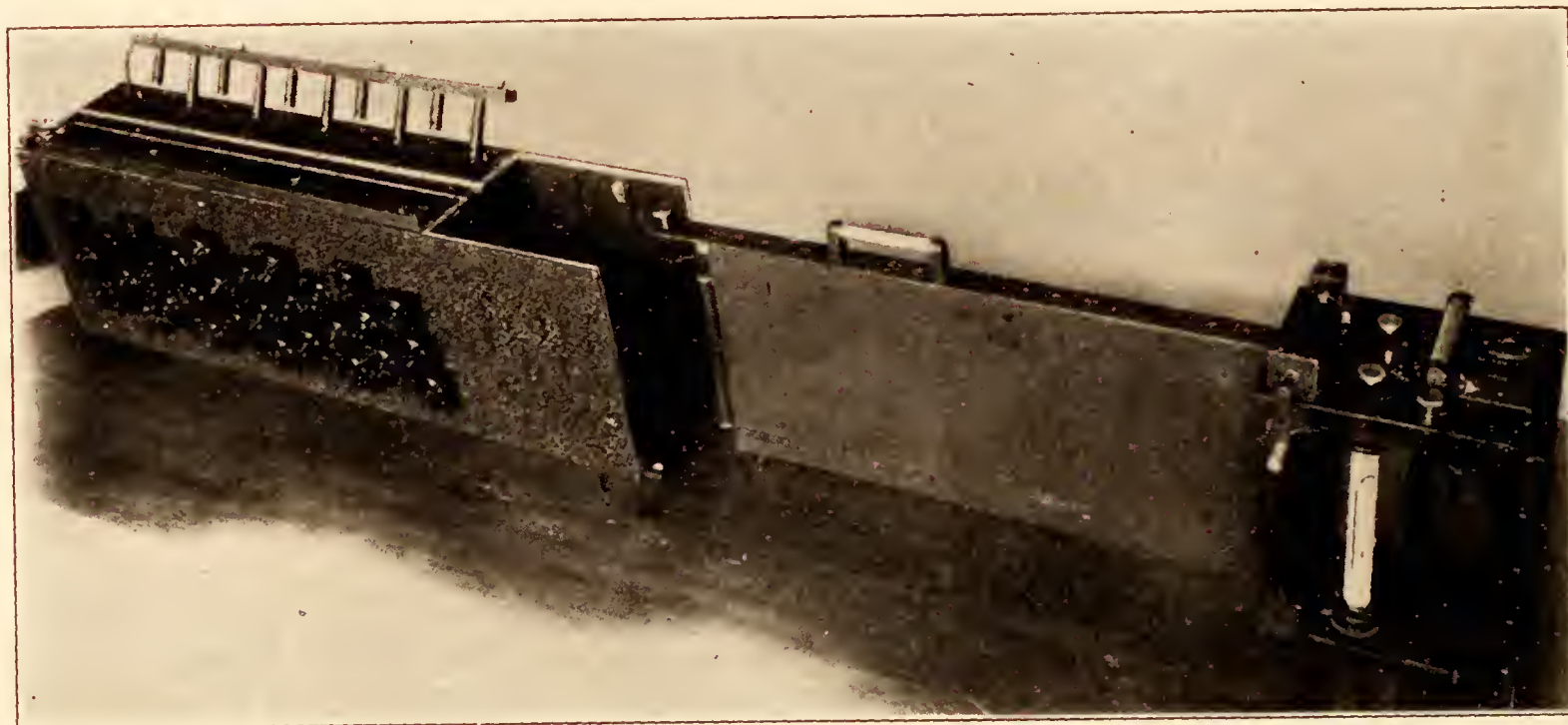


FIG. 4.—N. A. C. A. type 60 recording multiple manometer

mounted on the control column. The instrument records were synchronized by means of timing lines placed simultaneously on all the records by an N. A. C. A. timer (Reference 5).

## METHOD

Since only one manometer was available for these tests (two of the three type 60 manometers possessed by the N. A. C. A. being installed on another airplane), it was possible, in the



time allowed, to investigate the pressure distribution on only one-half of the horizontal tail surfaces in addition to that on the vertical surfaces. The right horizontal surfaces were therefore chosen because a previous investigation on a pursuit type airplane ("Pressure Distribution on the PW-9 Airplane," not yet published) indicated that down loadings are greater than up loadings, in general, and because the effect of the slip stream is to further increase the down loading on the right side. Since, therefore, the maximum loads are obtained on this side, the loads on the left surfaces are within the limits of the loads obtained.

Pressure measurements were made in level flight throughout the speed range; in a number of high-speed dives with stabilizer up, down, and neutral and with power on and off; in a series of abrupt pull-ups at different speeds; and in several of the common maneuvers such as the barrel-roll and tail spin. In addition to the above, two more unusual maneuvers, one of them quite unorthodox, were investigated with the object of obtaining high loads on the vertical surfaces. The first of these, or the "vertical reverse," as it is called in this report, was performed by throwing the airplane from a right or left vertical bank into a vertical bank in the opposite direction, the rudder being the principal control surface used in the maneuver. The second, or "rudder reversal," was made by kicking the rudder right or left while the ship was traveling at high speed, all other controls remaining neutral, and as the ship approached the position of maximum yaw, kicking full opposite rudder. Thus, the vertical surfaces were operating at a high angle of attack at high speed. This maneuver, while not ordinarily performed, probably imposes the highest possible loads on the vertical surfaces, and it is felt that the loads obtained can safely be used as a criterion of the maximum loads obtainable on the surfaces involved.

The pressures obtained were plotted on the chord of each false rib as a base line and curves were drawn through the ordinates giving the pressure diagrams as in Figure 5. In all cases, the difference in pressure between the upper and lower surfaces at each station was measured, no attempt being made to measure individual pressures on the upper or lower surfaces. Integration of the areas under the pressure curves gave the load per foot span and these latter values plotted along the span formed the ordinates of the span-loading curves which, integrated, gave the total loads over the surfaces. In some cases the rib pressure curves were cross-faired to give span-wise pressure curves from which the chord loading for the whole surface could be determined in the same manner as the span loading. Justification for plotting normal to the chord pressures which have been measured normal to the curved surface of an airfoil can be found in Reference 6.

Although the displacements of the controls were measured, they were neglected in working up the data except in the conditions of maximum load.

### PRECISION

A number of possible sources of error are present in work of this nature. In tabular form they are as follows:

#### I. INDIVIDUAL PRESSURES

- (a) Orifice cap not flush with surface.
- (b) Tube stopped or leaking.
- (c) Capsule calibration changed.
- (d) Pressure loss in tube from orifice to manometer.
- (e) "Personal equation" in plotting and reading calibration.
- (f) Excessive width and haziness of record line caused by oil or dust on lens, small rapid pressure fluctuations due to local eddies, or vibration.
- (g) Time lag due to length of tube and hysteresis in capsule diaphragm.
- (h) Shrinkage of film.

#### II. RIB LOADS AND TOTAL LOADS

- (a) Untrue pressure curves caused by errors in individual pressures.
- (b) Plotting—personal errors.
- (c) Fairing curves through relatively few points.
- (d) Integrating—personal errors and necessity of using relatively small scale in plotting.
- (e) Neglect of control surface displacement in plotting pressures on chord line.



The errors due to  $I(a)$  and  $I(b)$  are negligible. Frequent inspection showed no leaks or stoppages in the tubes, and care was taken to make the orifice caps flush with the surface. The duration of the testing period was so short that the capsule calibrations did not change except for a fraction of a per cent in a few cases ( $I(c)$ ). The pressure loss in the tubes,  $I(d)$ , arising from the interference of the pressure impulses within the tube, was less than 2 per cent inasmuch as the tube lengths did not exceed 10 feet (References 7 and 8). Errors due to  $I(e)$  were minimized by checking. It was found that two operators performing the same function checked each other within a half of 1 per cent. Errors due to  $I(f)$  are probably the greatest. In some cases the width of the line was as much as 7 or 8 per cent of the deflection. The mean of this line was always taken as the true line, of course, but as the edges were hazy, how close the mean line could be read is a matter of conjecture. It is probable that the readings are in error not more than 2 per cent from this cause. Time lag (Reference 8) and shrinkage of the film introduce negligible errors.

The principal source of error in the integrated results from the pressure curves is in the curves themselves. Personal errors in plotting and integrating were small, and as the ordinates of the curves, then, are the primary sources of error in the determination of loads, error in the total normal forces depends on the mean error of both the measured pressures and the interpolated pressures. This error is estimated to be within 4 per cent.

In general, then, individual pressures are probably correct to within  $\pm 2$  per cent while total loads are accurate within  $\pm 4$  per cent.

The error introduced by the displacement of the controls is variable. In this investigation the error is neglected in most cases, but this neglect always increases the force, which is on the conservative side. In the worst case, the error caused by the neglect of control displacement would have been 11.7 per cent had the displacement been neglected.

Air speed is correct to within  $\pm 2$  M. P. H. except in the dives, in which case the impact pressures were read on a flattening out portion of the calibration curve and can not be relied upon to within less than 6 M. P. H.

Accelerations are correct to within 0.1 *g*.

## RESULTS

In the tables and pressure plots following, the directions of these pressures and of the loads and moments are in conformity with the standard system used by the National Advisory Committee for Aeronautics; that is, positive loads and pressures on the horizontal surfaces act upwards and positive pressures on the vertical surfaces act from right to left. Therefore, if the pressure or load diagram is plotted on the upper or left surface it is positive, and vice versa. All moments are given with reference to the hinge center lines as the most convenient data and are positive if clockwise when viewed by an observer at the left or from the top of the airplane.

The results are presented in Tables I and II and in Figures 5 to 29. Table I gives the loads, moments, and maximum pressures for the maneuvers investigated except the level flight runs which are omitted because the distribution is the same as in the dives, with pressures of less magnitude.

The most severe loads on the horizontal surfaces were found to occur in the pull-up. In this maneuver a peak down load is experienced which is followed closely by a peak up load of lesser intensity. This sequence always obtains in abrupt pull ups and can easily be explained. The heavy down load is, of course, induced by the sudden upward displacement of the elevator and causes the tail to swing down. The attitude is soon reached where the whole airplane is inclined at a large angle of attack, thus causing the resultant load on the tail surfaces to act upward. The action is so rapid on a highly maneuverable airplane of this type, the time between maximum down and up loads being of the order of a quarter of a second, that there would be no opportunity for the pilot to alter the phenomenon by easing the controls, and hence the condition may be considered entirely automatic and little affected by factors other than the aerodynamic and inertia properties of the airplane. The down loads on this airplane were always at least 100 per cent greater than the corresponding up loads. The values for both



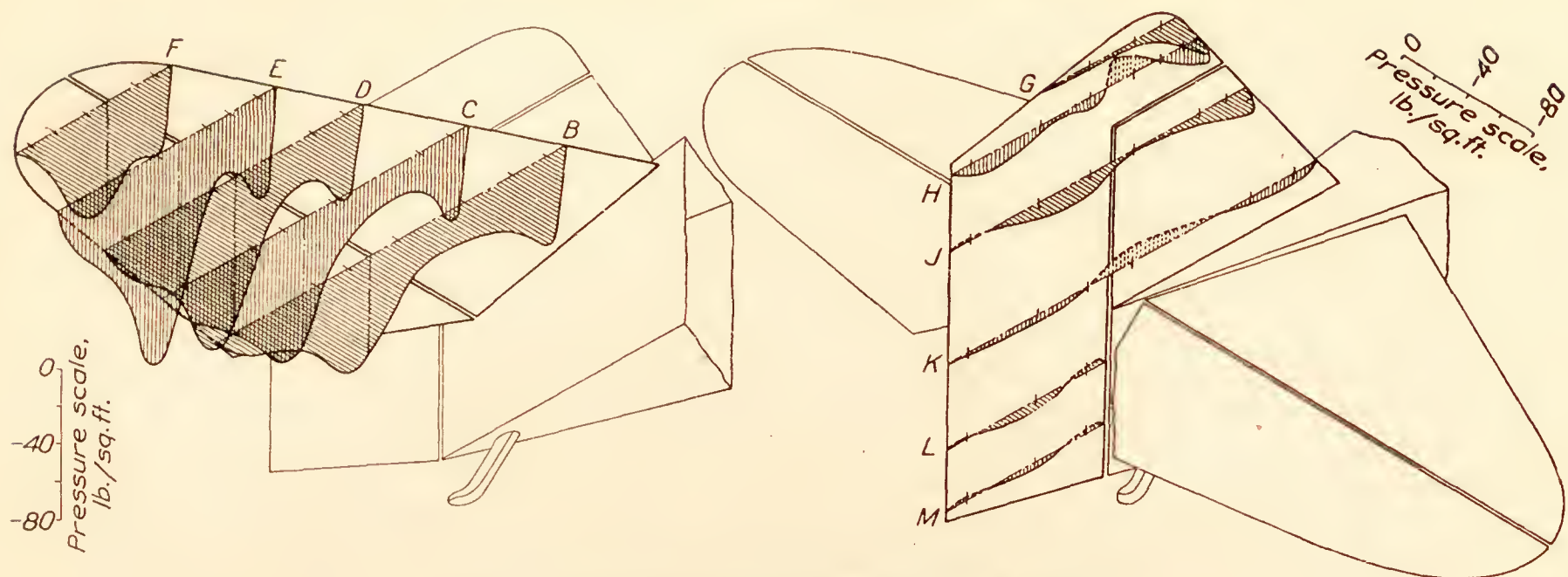


FIG. 5.—Pressure distribution in a pull-up at 163 M. P. H. Run No. 11

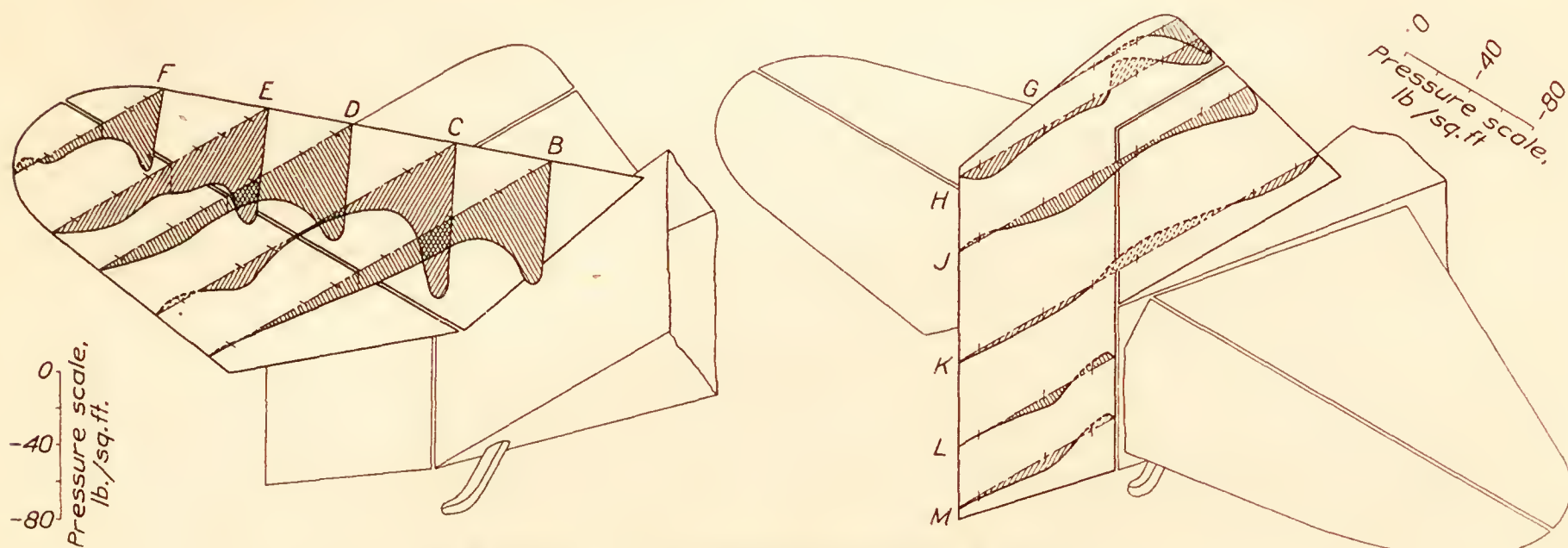


FIG. 6.—Pressure distribution in a dive at 247 M. P. H. Run No. 18

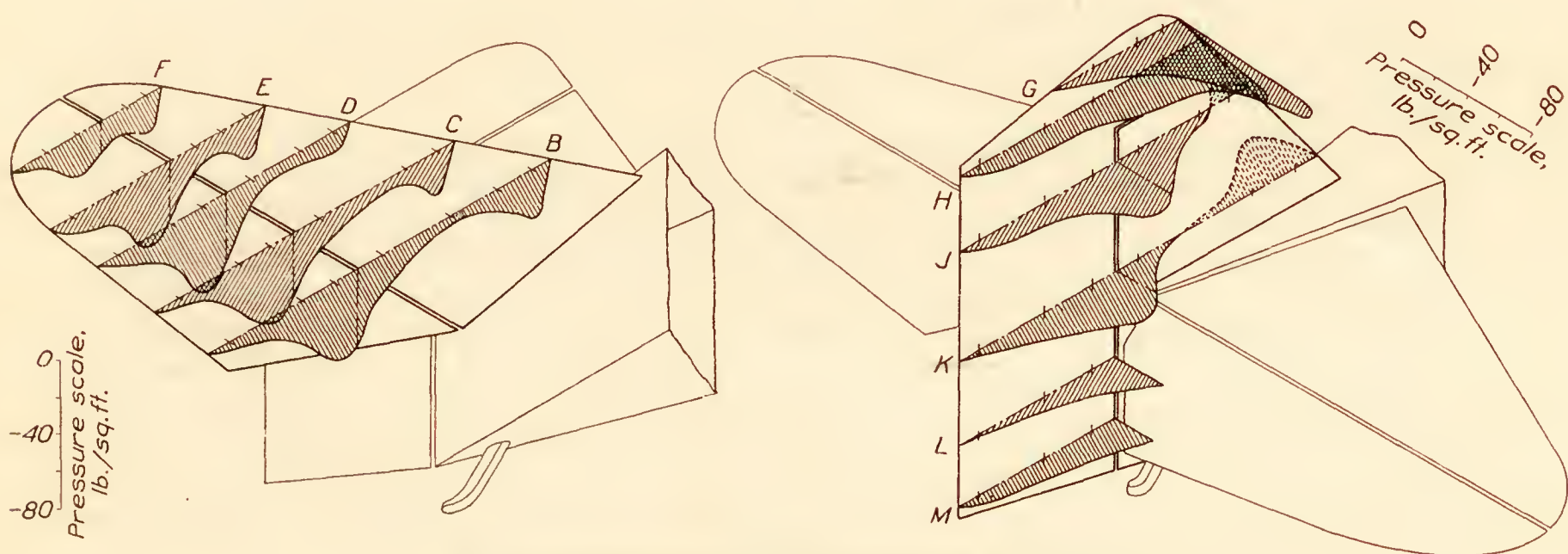


FIG. 7.—Pressure distribution in a right roll at 109 M. P. H. Run No. 57



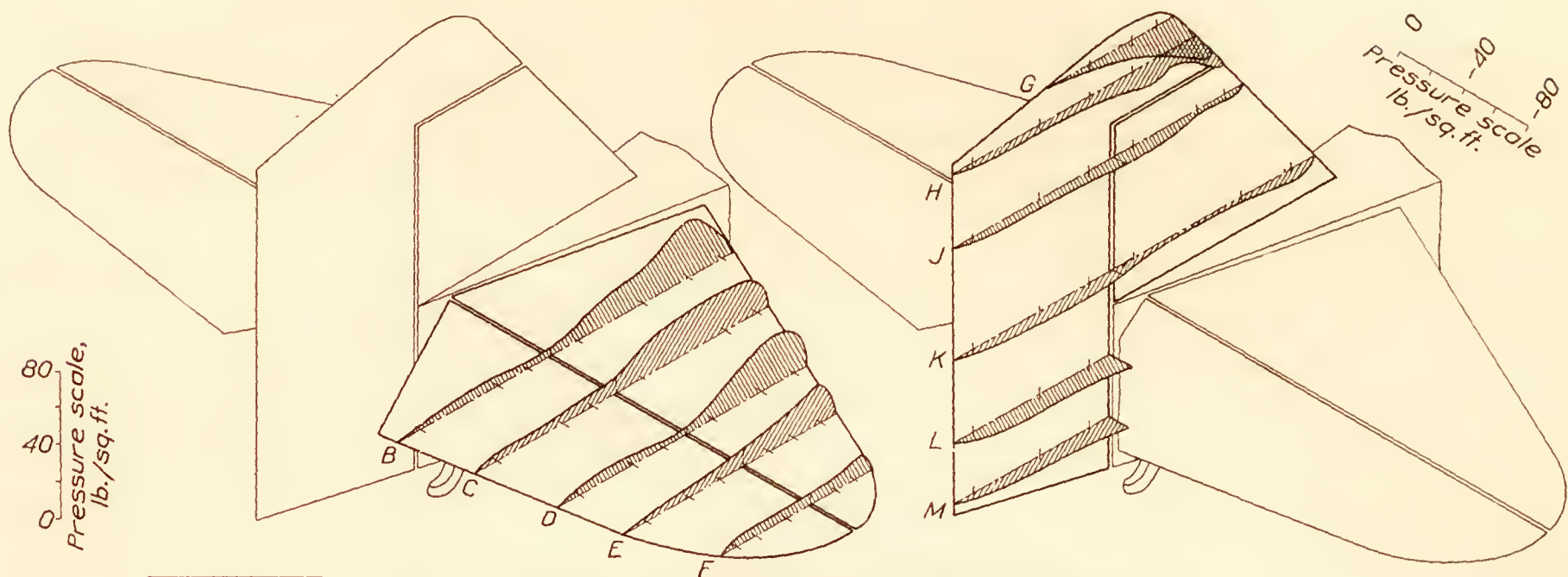


FIG. 8.—Pressure distribution in a left spin. A. S.=43 M. P. H. Run No. 60

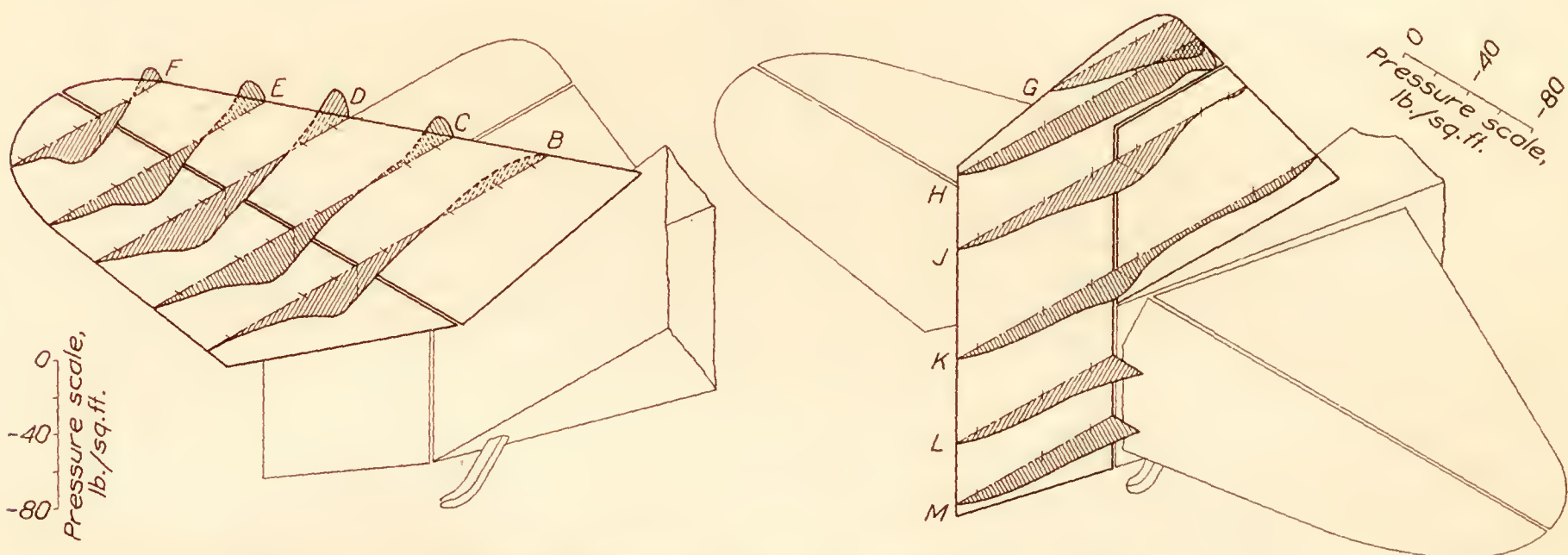


FIG. 9.—Pressure distribution in a left spin. A. S.=74 M. P. H. Run No. 61

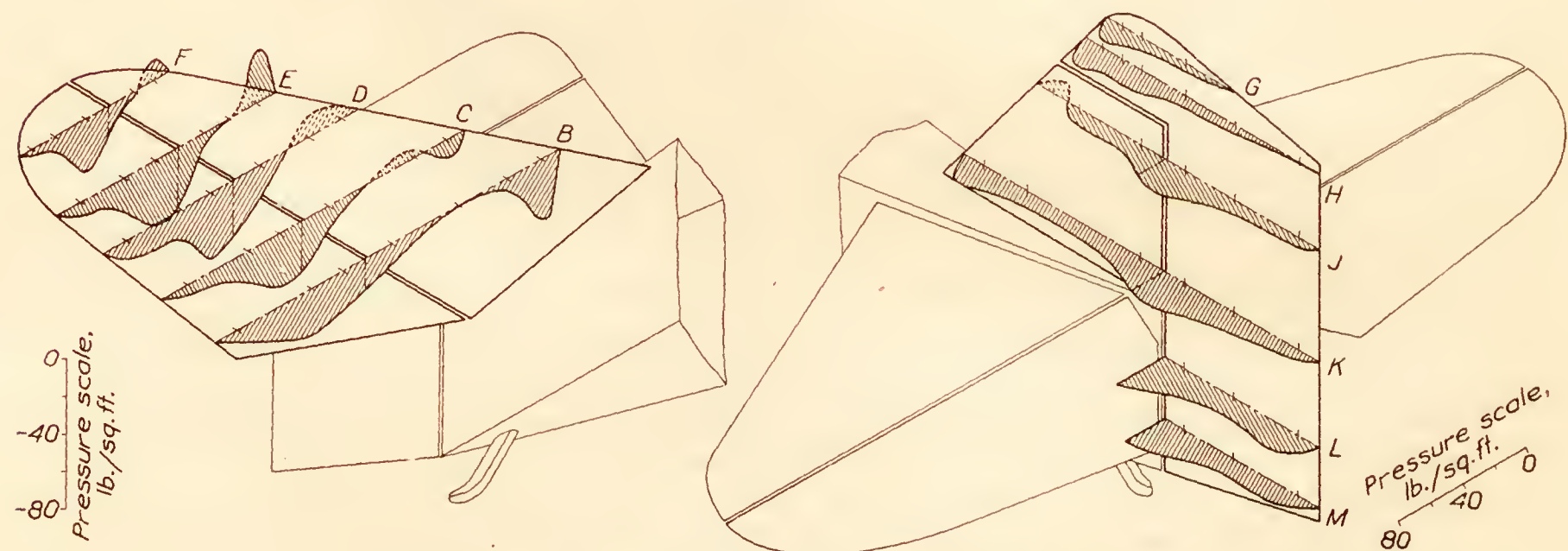


FIG. 10.—Pressure distribution in a vertical reverse at 92 M. P. H. Run No. 62



conditions are given for illustration in Table I, Run No. 7. The maximum total load on the horizontal surfaces occurred in a pull-up at 163 M. P. H. In this maneuver, also, the maximum local pressure and the maximum loads on the stabilizer and elevator occurred simultaneously, the average loading being 34 pounds per square foot acting down. With respect to the load acting normal to the plane of the stabilizer, the tabulated value of -540 pounds

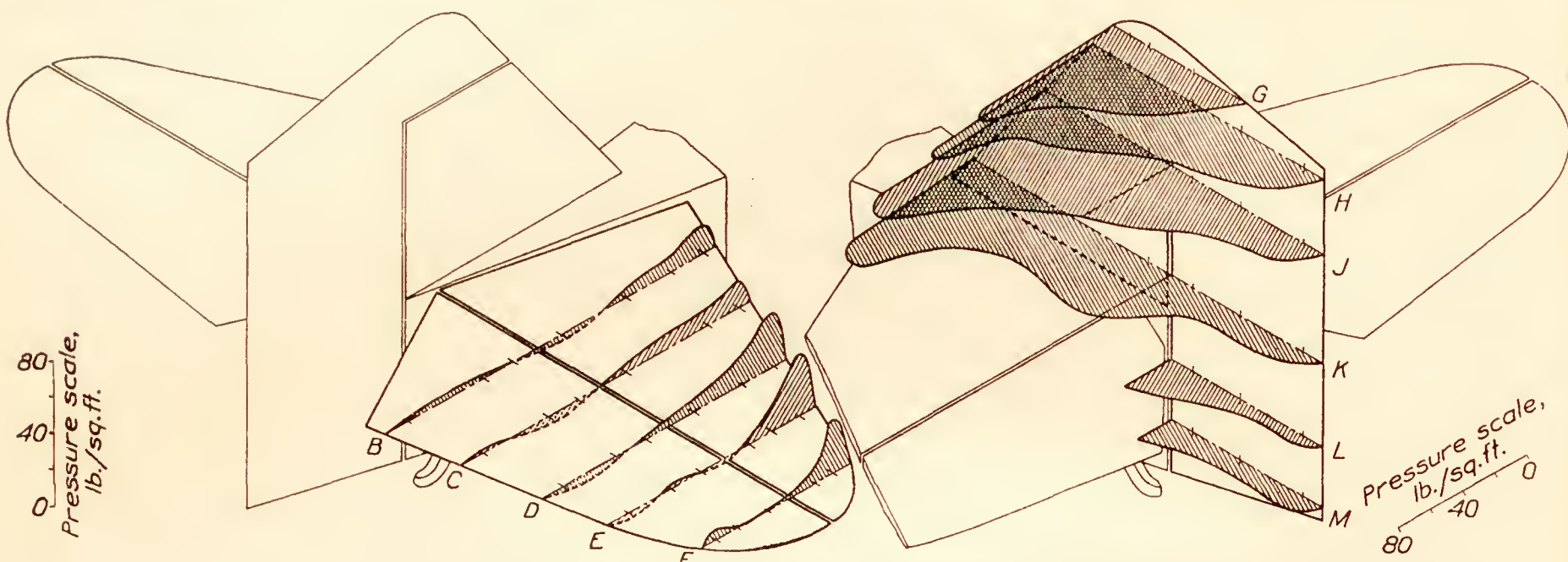


FIG. 11.—Pressure distribution in a rudder reversal at 153 M. P. H. Run No. 70 (a)

is not exact, the true force in this direction, taking into account the elevator angle, which in this case is  $33.3^\circ$ , being -490 pounds, while the component of force on the elevator parallel to the stabilizer chord is 160 pounds. In the pull-up at 173 M. P. H., although the acceleration obtained at the center of gravity was higher (fig. 29), the tail loading was less because the stick was not pulled back so sharply. There is no reason to suppose that had the maneuver been made in the same manner as the preceding ones the tail load would not have been greater.

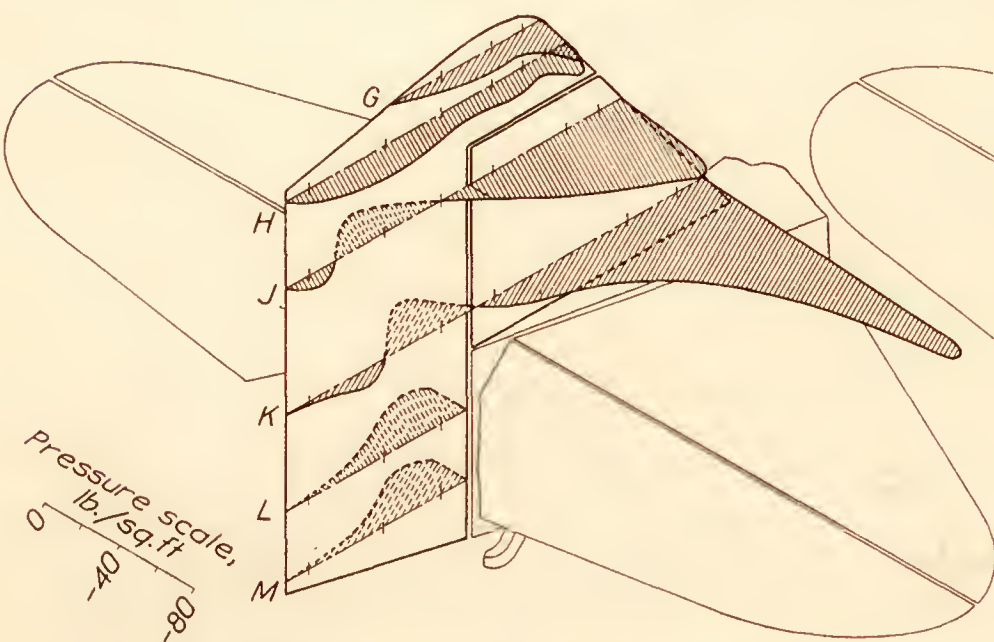


FIG. 12. Pressure distribution in a reversal at 153 M. P. H. Run No. 70 (b)

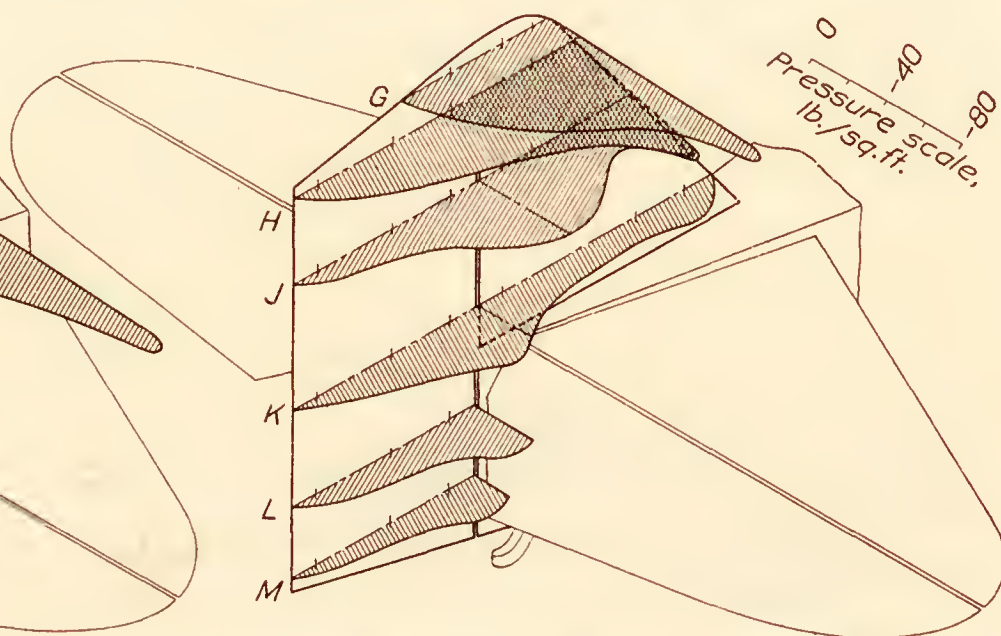


FIG. 13.—Pressure distribution in a reversal at 153 M. P. H. Run No. 70 (c)

The total loads in the dives were relatively small, although the leading edge pressures and stabilizer loads were high. Little difference existed with stabilizer neutral, up, or down and with power on and off. There is some doubt about the position of the stabilizer in the dives. Instructions were given to the pilot to set the stabilizer either up, down, or neutral, as indicated in Table I, but the control position recorder showed a variation of less than  $1^\circ$  from neutral, and it is probable that for some reason the pilot failed to follow instructions. The loads given are the maximum in each case, and the variations are probably due to impact with gusts of air



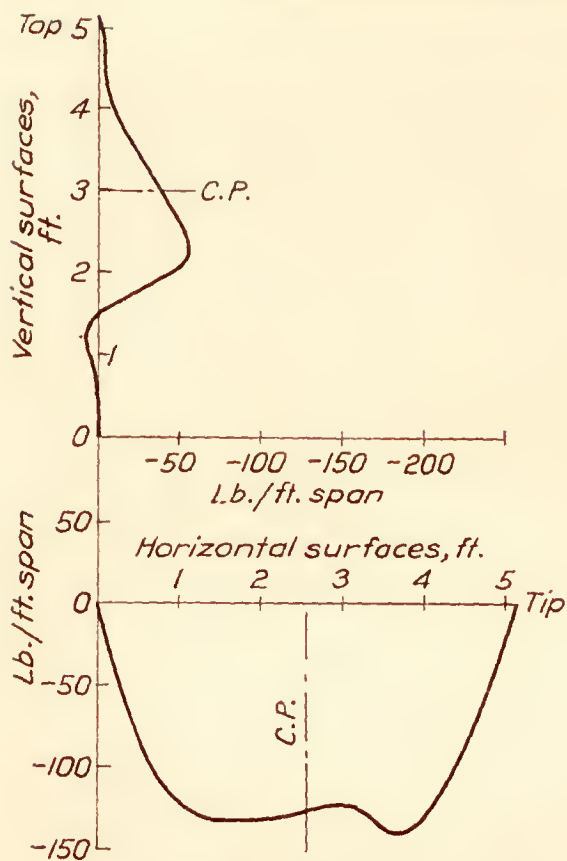


FIG. 14.—Pull-up at 163 M. P. H. Run No. 11

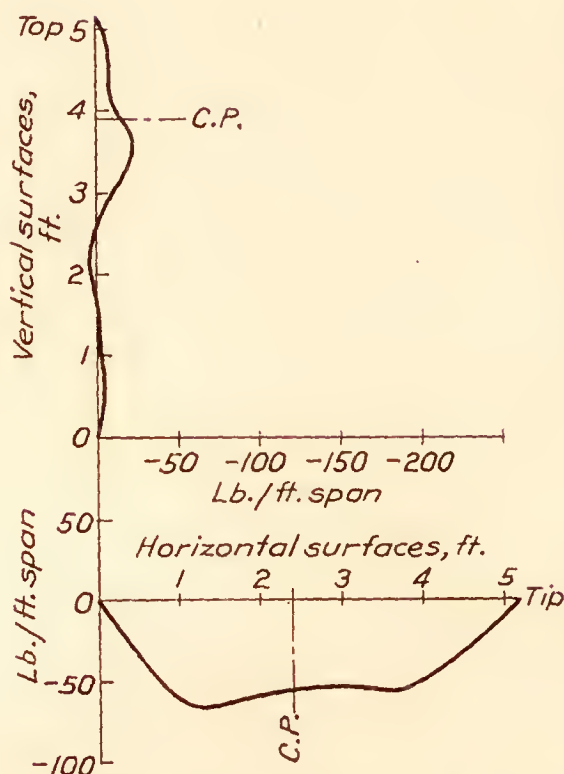


FIG. 15.—Dive at 247 M. P. H. Run No. 18

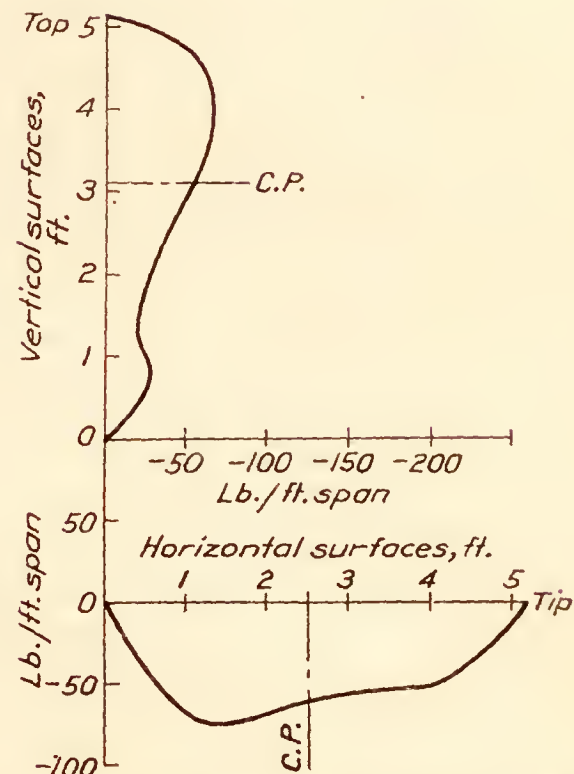


FIG. 16.—Right roll at 109 M. P. H. Run No. 57

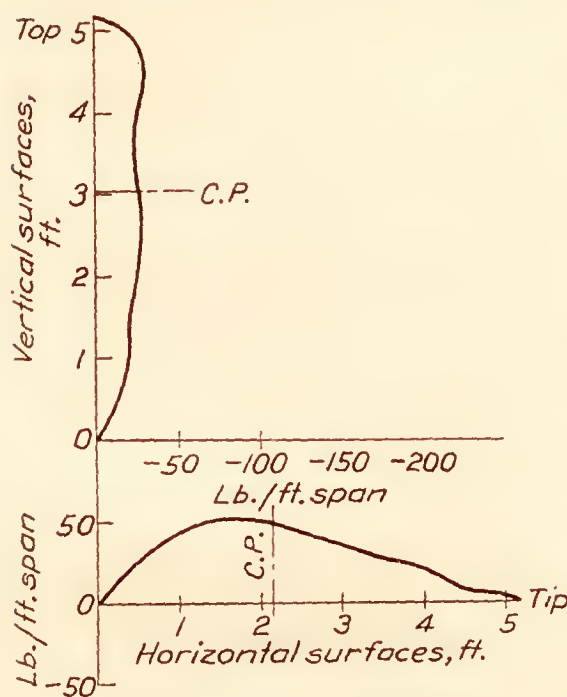


FIG. 17.—Left spin. Run No. 60

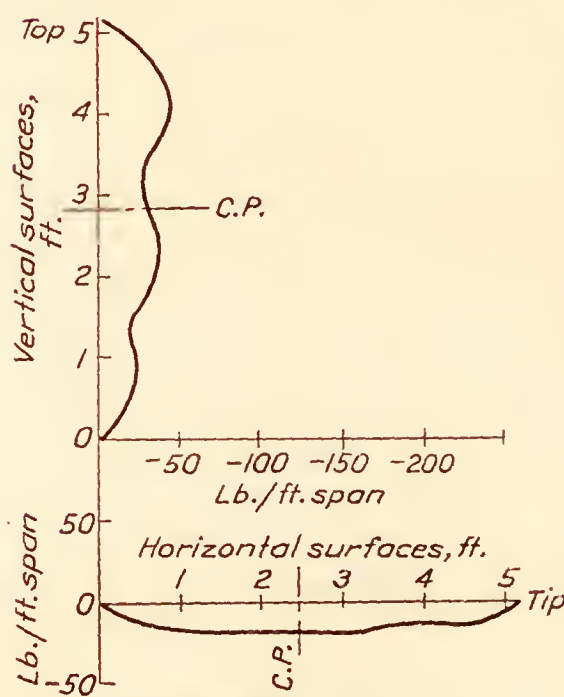


FIG. 18.—Left spin. Run No. 61

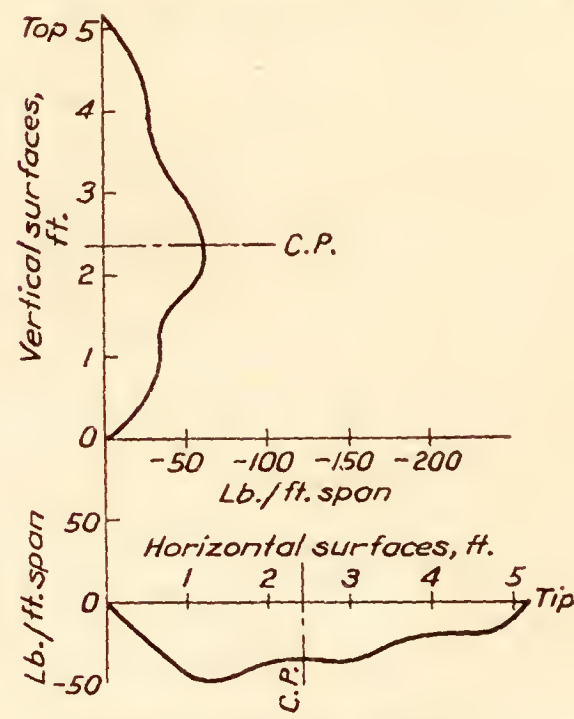


FIG. 19.—Vertical spin. Run No. 62

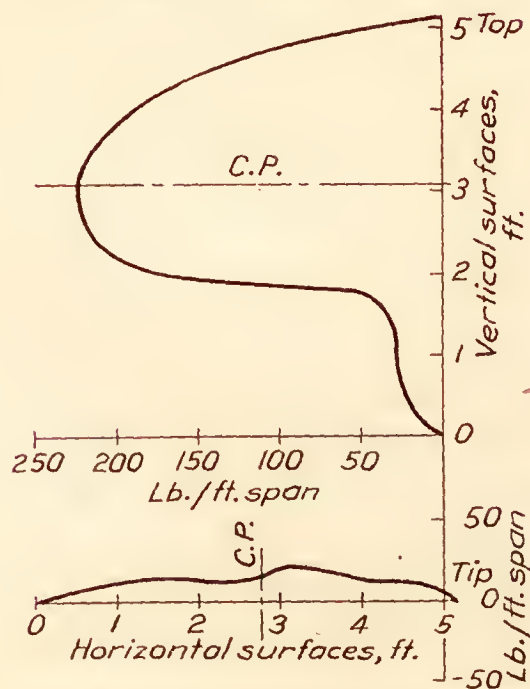


FIG. 20.—Rudder reversal. Run No. 70 (a)

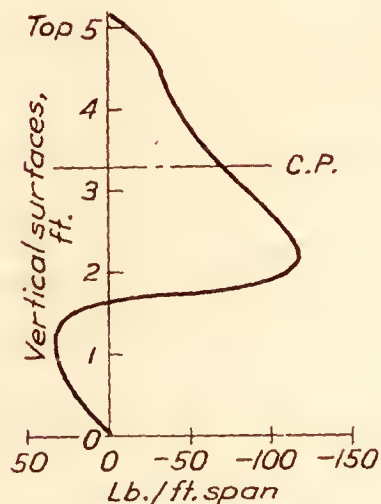


FIG. 21.—Rudder reversal. Run No. 70 (b)

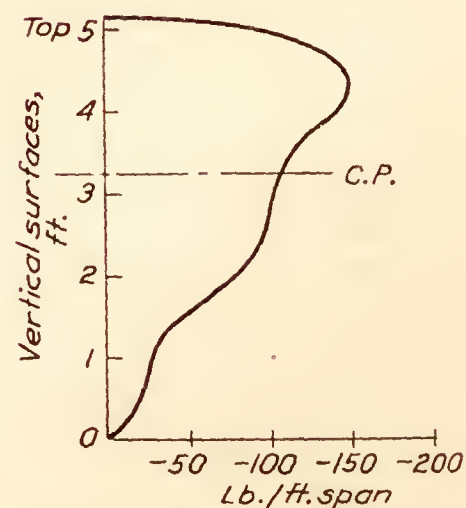


FIG. 22.—Rudder reversal. Run No. 70 (c)

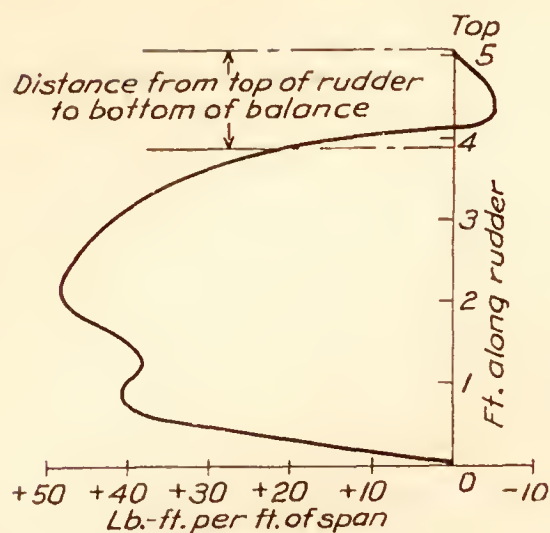


FIG. 23.—Haif roll at 161 M. P. H.

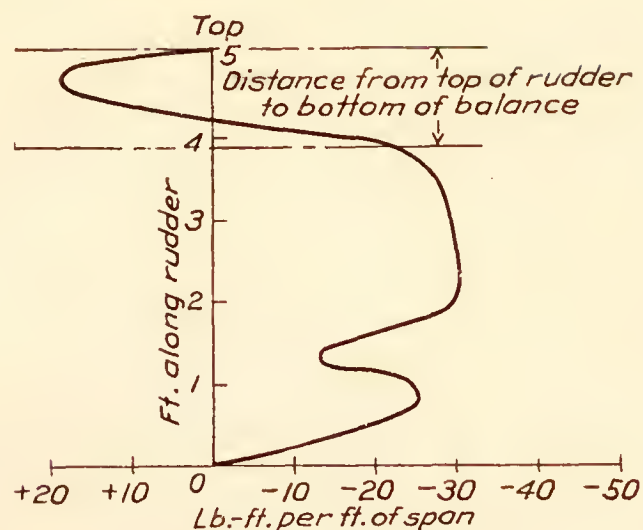


FIG. 24.—Right roll at 109 M. P. H.

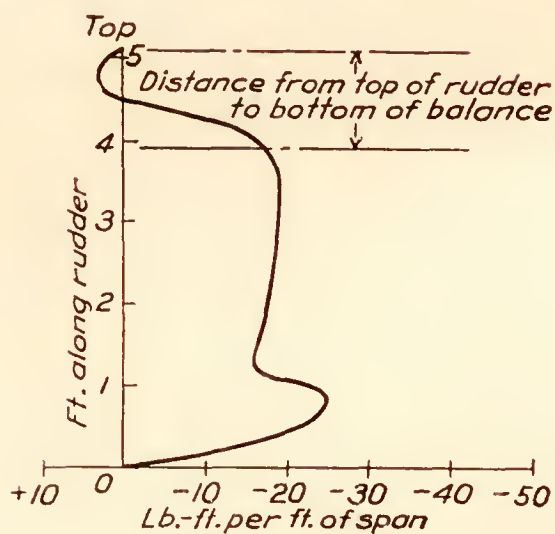


FIG. 25.—Left tail spin

Span-moment curves for the rudder showing effect of balance in reducing hinge moment

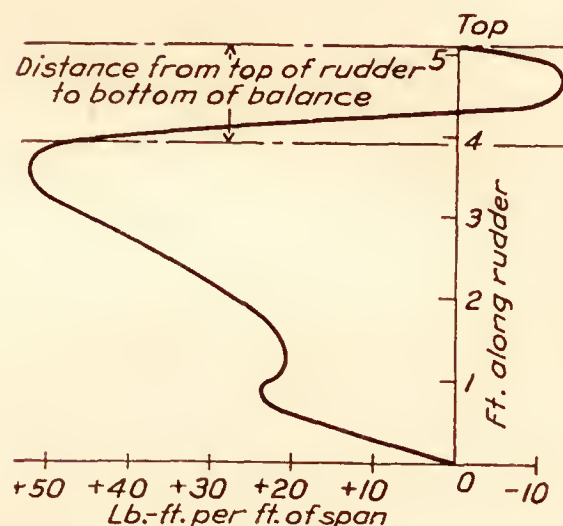
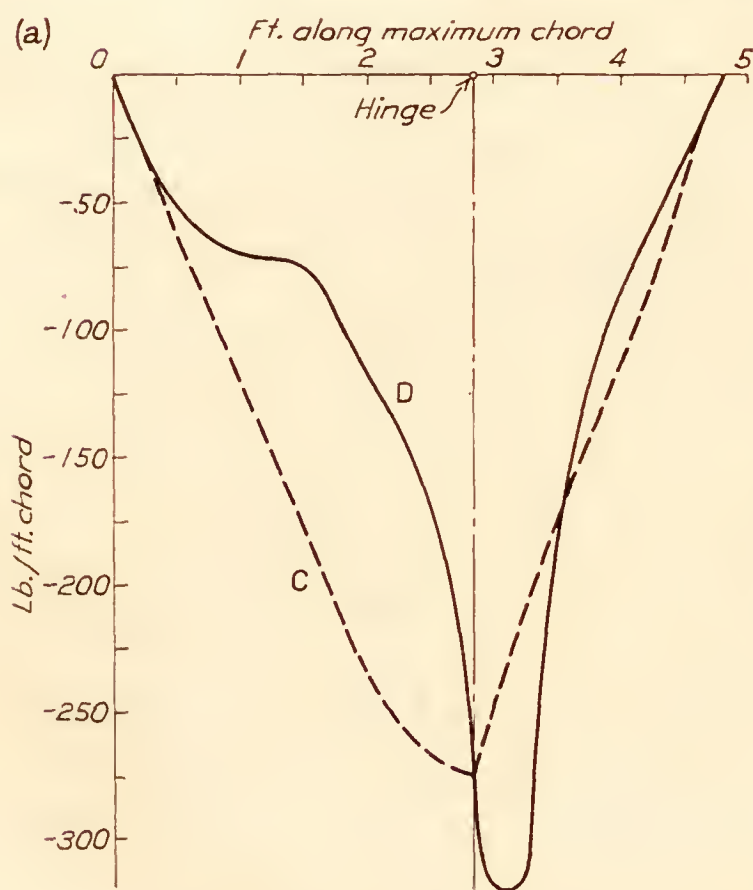
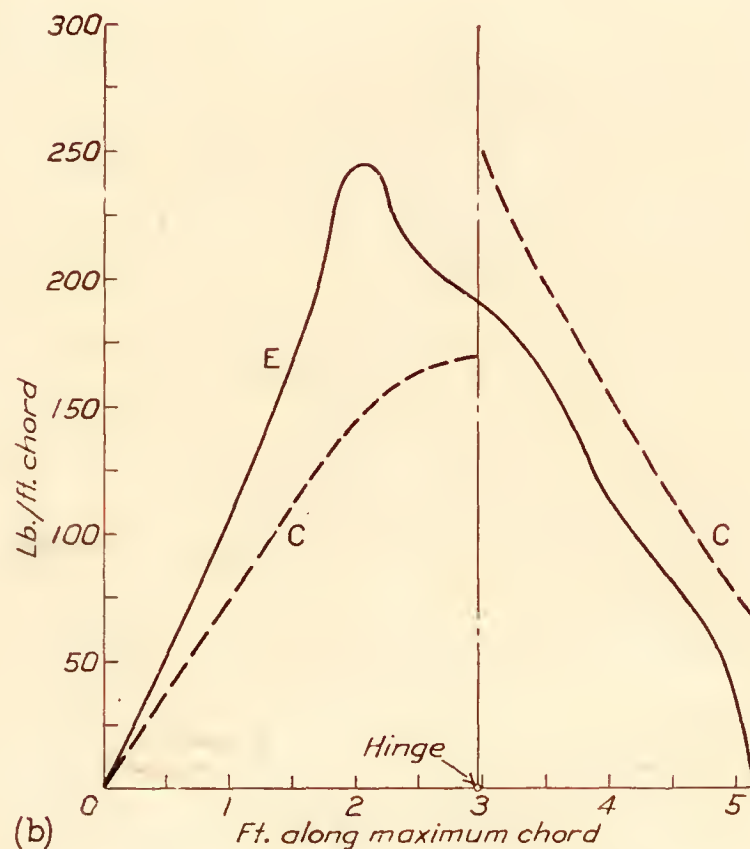


FIG. 26.—Rudder reversal at 153 M. P. H.



(a) Horizontal surfaces, Curve D: Chord loading in the condition of maximum total load on stabilizer and elevator. Run No. 11



(b) Vertical surfaces, Curve E: Chord loading in the condition of maximum total load on fin and rudder. Run No. 70

FIGS. 27 (a) and (b).—Comparison of chord loadings  
Curve C: Chord loading obtained with surfaces loaded as specified for static tests



more than to any other cause. These gusts or bumps are quite noticeable in high-speed dives and produce accelerations of the order of  $2.5 g$ . Table I, it will be noted, indicates down loads on the elevator in all of the dives investigated. This would imply that a pull back on the control column was necessary to hold the airplane in equilibrium and prevent it from going over on its back, which is contrary to normal experience. It is probable that the pilot set the stabilizer neutral for all of the dives (neutral being defined as the position at which the airplane is trimmed at cruising speed), which would really be a slight nose heavy condition for the

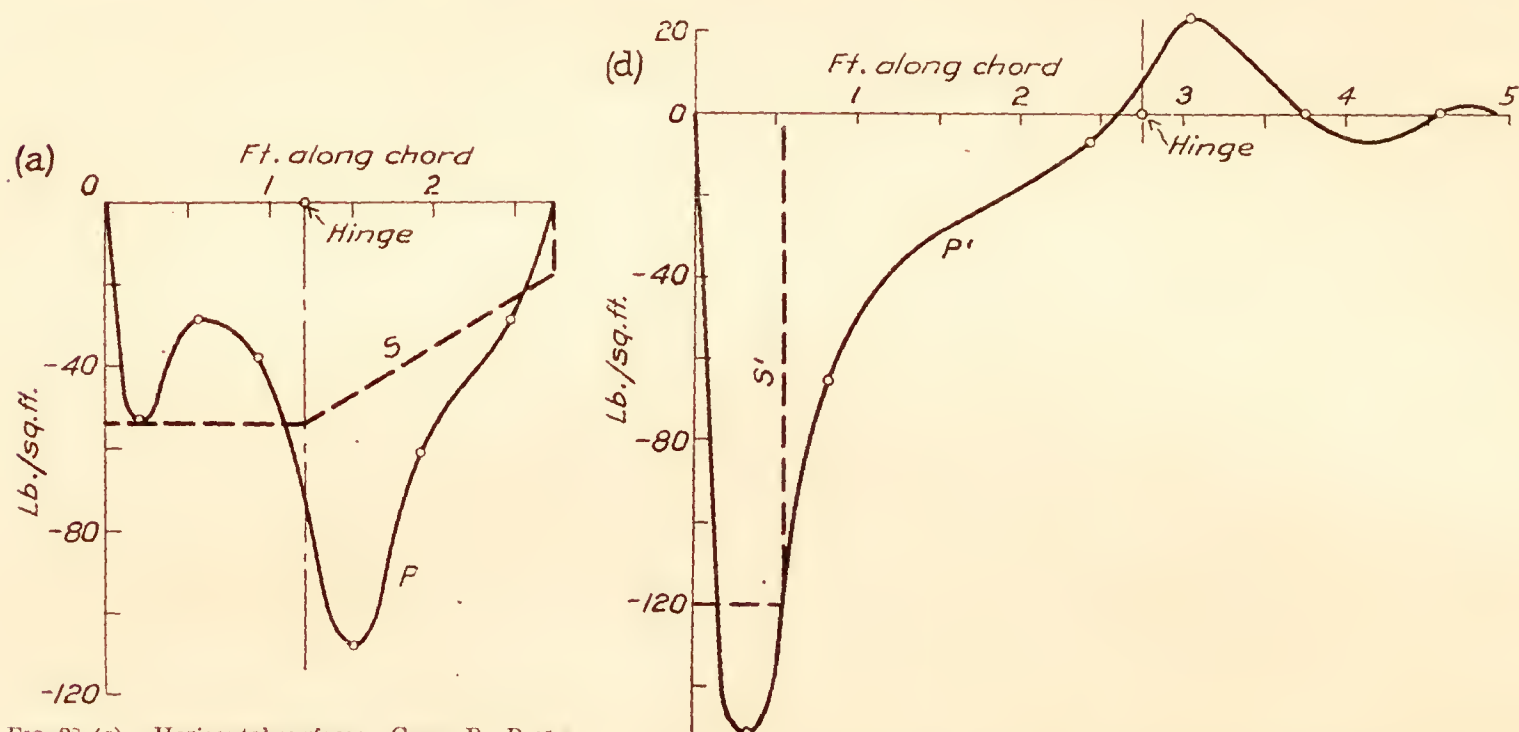


FIG. 28 (a).—Horizontal surfaces. Curve P: Pressure distribution on rib E in a pull-up at 163 M. P. H. Curve S: Specified loading

FIG. 28 (d).—Vertical surfaces. Curve P': Pressure distribution on rib K in a rudder reversal at 153 M. P. H. Curve S': Specified leading edge loading

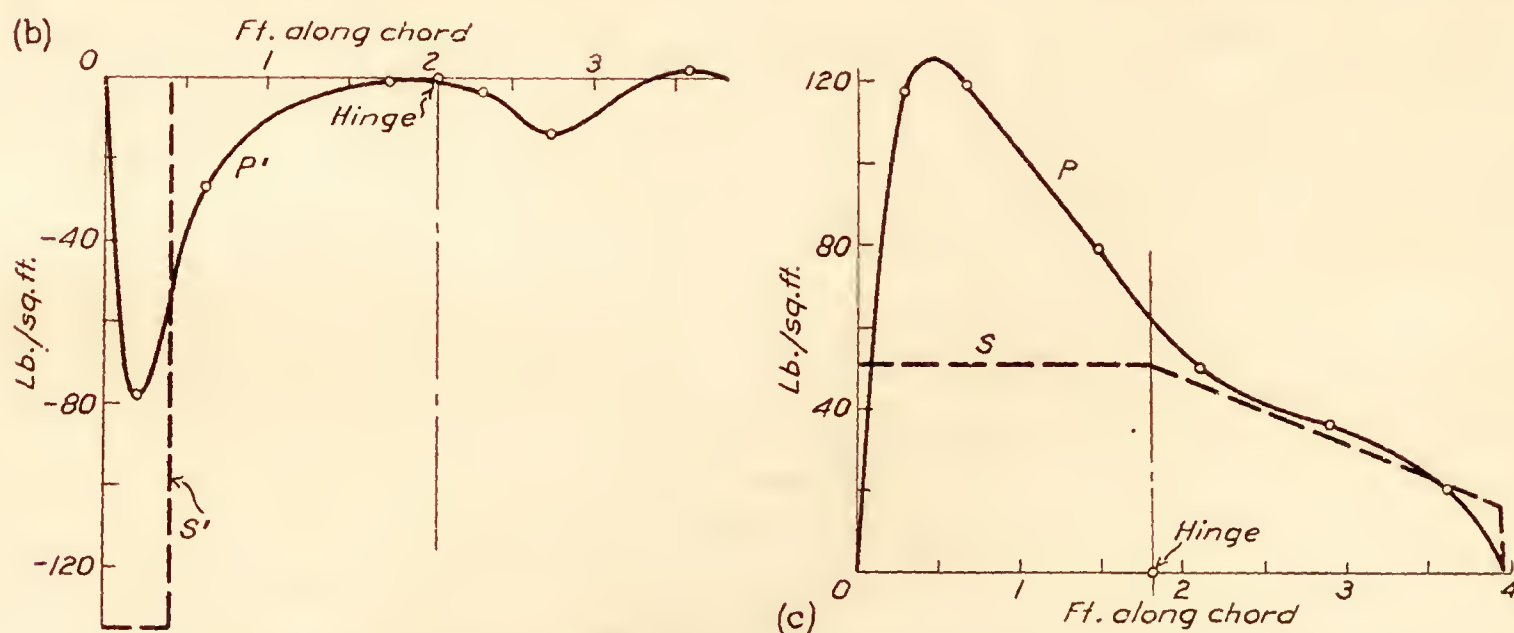


FIG. 28 (b).—Horizontal surfaces. Curve P': Pressure distribution on rib C in a dive at 247 M. P. H. Curve S': Specified leading edge loading

FIG. 28 (c).—Vertical surfaces. Curve P: Pressure distribution on rib J in a rudder reversal at 153 M. H. P. Curve S: Specified loading

#### OBSERVED RIB LOAD DISTRIBUTION COMPARED WITH SPECIFIED LOAD DISTRIBUTION ALONG THE CHORD

airplane with normal location of the center of gravity. (See description of airplane on p. 4.) This would explain the pull-back on the control column, and would mean, too, that the interpretation of the results for the dives should take into consideration that with the stabilizer set down, or tail heavy, as it usually is set in the diving condition, the pressures near the leading edge would be somewhat greater, and the load on the elevator would be reversed in direction, although probably still small in magnitude.

Loads on the horizontal surfaces in the rolls, spin, and vertical reverse and in the rudder maneuvers are comparatively small.

The rudder reversal, as has been stated, is probably the most critical maneuver with reference to the vertical surfaces. In the rudder reversal at 153 M. P. H., the average loading on the vertical tail surfaces was equal, within the experimental error, to the design specification of 40 pounds per square foot. In this case, the maximum load was experienced after the tail swung through zero yaw on the return journey with the rudder practically neutral. Thus, the load given is the true load and requires no correction for control displacement. On the same rudder reversal, at a different part of the maneuver, a maximum pressure of  $-151$  pounds per square foot was experienced on the fin at K-1, which exceeds the leading edge specified

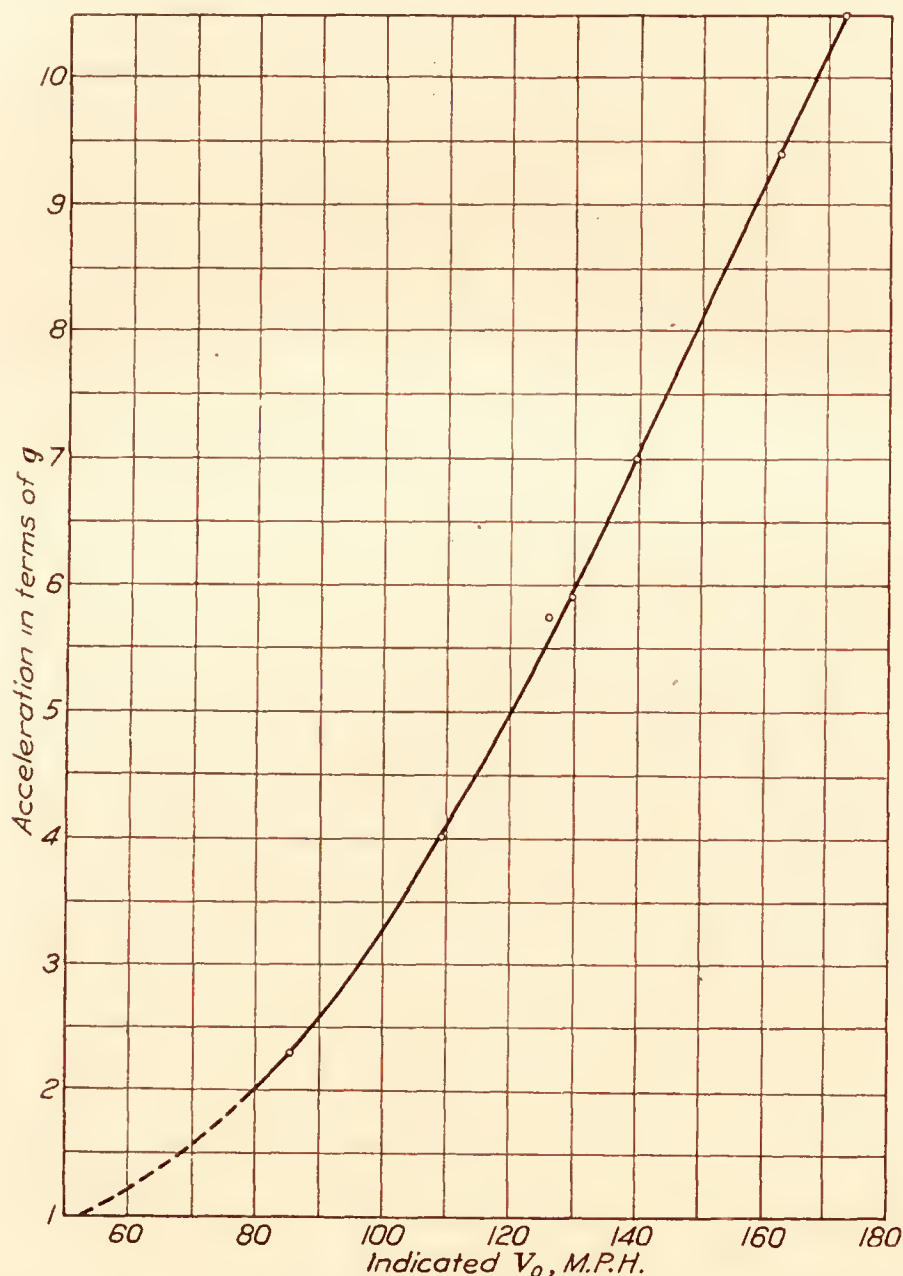


FIG. 29.—Accelerations against  $V_0$  for the F6C-4 airplane in pull-ups

loading at this point. Loads on the balance of the rudder were high in this maneuver, the maximum pressure being 122 pounds per square foot at G-1.

All other loads and pressures on the vertical surfaces were relatively small.

It should be pointed out here again that the rudder reversal is a very unusual maneuver, and, since it imposes extremely high loads on the structure, could very well be prohibited in military maneuvers, particularly inasmuch as it has no known usefulness. It is probable, though, that the distribution obtaining here is similar to that in any other maneuver involving high speed and high angle of attack of the vertical surfaces, such as in a bad side slip. For immediate purposes of design, however, it would probably be better to consider as the worst loads those occurring in the rolls. It will be noted that the loads in the half roll given in Table I are higher than those given for the roll, but the distribution is almost exactly similar for both, the difference being in magnitude only, which would be still different for rolls or half rolls at different speeds.



Pressure curves for several of the more interesting cases are plotted in Figures 5 to 13. The corresponding pressures are tabulated in Table II. Run numbers are given in each case so that the curves and tables can be interconnected readily. The appendices (a), (b), and (c) of Run No. 70 refer to different parts of the same maneuver, not necessarily in chronological order, but in the order of their importance.

Figures 14 to 22 give the span-loading curves for these conditions and are drawn as if viewed from behind the airplane. The load is rather symmetrically disposed on the horizontal surfaces in spite of the considerable taper, which indicates a greater intensity of loading near the tip. The span-loading curves are particularly useful in that they show the lateral and vertical locations of the center of pressure on the horizontal and vertical surfaces, respectively.

Figures 23 to 26 are "span-moment" diagrams for the rudder in several maneuvers in which the rudder moments were high. The curves were constructed from the pressure curves by plotting the moment for each rib, obtained during the integration, along the height of the rudder. The effect of the balance in reducing the rudder hinge moment is shown clearly, and if the curves be faired approximately as they would be if there were no balance present, it will be seen that the difference in area is around 25 per cent. This indicates that the balance could be enlarged without danger of the rudder taking control at the larger angles.

Figure 27 shows the chord-loading curves for the maximum loads on the horizontal and vertical surfaces, respectively, compared with the chord-loading curves obtained with the surfaces loaded as for static test. They indicate that the elevator and fin were overloaded in flight. A glance at the curves discloses that the centers of pressure are both very near the hinge center line, which suggests that the present method of assuming the maximum vertical and horizontal tail surface loads to act at the rudder post in the fuselage analysis is very close to the true conditions.

Several individual chord-pressure curves which indicate high local rib loads and pressures, are compared with the specified loading diagram for these ribs in Figure 28. It will be seen that the measured loads on the elevator greatly exceed the specified, while the stabilizer loads are not dangerous. The rib loading on the unbalanced portion of the rudder in the worst case is about equal to the specified loading and the distribution is very nearly the same. Leading edge pressures on the fin are high and may exceed the specified leading edge load.

When any of the results given herein are compared with the existing specifications, it should be borne in mind that a factor of safety of two is intended to be implied in the latter. Therefore, any load in a legitimate maneuver that exceeds half the design specifications is an indication that the specifications are low.

The curve of accelerations vs. initial air speed for the pull-ups is given in Figure 29. The accelerations show no tendency to fall off as the higher values are approached and it seems evident that it would be quite possible to break the airplane in the air. The "theoretical" acceleration curve (based on the formula  $a = \frac{V_0^2}{V_s^2}$ , where  $V_0$  is initial air speed and  $V_s$  the stalling speed) is not included because the stalling speed of the airplane is not known accurately enough to give a quantitative comparison. However, if a stalling speed of 52.5 M. P. H. be assumed and the theoretical curve plotted, it will be seen that the two curves practically coincide in the range of accelerations measured.

Although the results obtained in these tests are of great value in that they indicate that certain revisions in the design specifications would be desirable, it must not be forgotten that the study of the loads that are likely to be experienced on tail surfaces involves far more than the experimental determination of such loads on one particular airplane. Even the results obtained on one airplane of a particular type are not strictly applicable to other airplanes of the same type, since a considerable number of variables are concerned, the alteration of any one of which will affect the magnitude and distribution of the loads in question. For instance, in steady flight the loads on any combination of horizontal surfaces will vary with the stability characteristics of the wing, the position of the center of gravity, the fuselage length and shape, and the drag-thrust couple. Then, for any given combination of these variables, the load



distribution will change with the tail airfoil section, the plan form, and the slip-stream characteristics at the tail. In accelerated flight conditions are different in that the loads are affected mainly by the resistance of the airplane to rapid changes of direction (exclusive of the stabilizing effect of the tail). It can be seen, therefore, that the present investigation supplies only a relatively small amount of the information that will be necessary before really satisfactory load specifications can be drawn up.

#### EFFECT OF ACCELERATIONS ON THE PILOT

An important though incidental result of these tests is the reaction of the pilot to the instantaneous acceleration of 10.5 *g*. obtained in the sharp pull-up at 173 M. P. H. It has long been a moot question among aeronautical engineers as to whether the design load factor for pursuit airplanes is now set at the proper value, and if not, what the limiting consideration in its determination should be. There have been some attempts to determine the proper load factors for different types from theoretical considerations based on weight and speed range, but the experimental evidence to date (Figure 29, for instance) indicates that for pursuit type airplanes, at least, it is quite possible to break the airplane in the air unless the load factor is made unduly high or the control limited to prevent abrupt maneuvers. Performance in its broad sense is reduced by both of these expedencies. If, however, the physical resistance of the pilot is the limiting factor, there is no need to curtail performance by overstrengthening the airplane structure or by reducing the control.

It has been generally accepted heretofore that instantaneous accelerations as high as 7.8 *g*. cause the pilot no discomfort while "accelerations of the order of 4.5 *g*., continued for any length of time, result in a complete loss of faculties" (Reference 9). This belief has been supported by tests at Langley Field in which short-period accelerations up to 9 *g*. caused no considerable physical reactions. The acceleration of 10.5 *g*., however, resulted in the condition described below, and it seems evident that the limit is being approached. It is not wise, of course, to make conclusions from one instance, but the question would seem to be of considerable importance and warrants further investigation.

The statement of Captain Peak, of the Army Medical Corps, with reference to the case mentioned follows:

STATION HOSPITAL, LANGLEY FIELD, VA.,  
June 8, 1928.

Memorandum to: Richard V. Rhode, N. A. C. A.

Re: Luke Christopher, captain, Air Corps Reserve (N. A. C. A. Pilot).

In September, 1927, Captain Christopher came to the hospital for treatment. On examination he showed a generalized conjunctivitis of both eyes. He also showed generalized systemic neurological symptoms leading me to think that he had a mild cerebral concussion with some generalized cerebral capillary hemorrhage or at least a marked degree of passive traumatic enlargement. Being interested in the case, I wrote complete descriptions to Doctor Schneider, of Wesleyan University, and to Dr. L. H. Bauer, of the Department of Commerce. Both of them agreed with my opinion of the cause and nature of this condition, namely, it was due to sudden changes of centrifugal force while doing high-speed flying in acceleration tests. There was a duty recovery from this condition in about two weeks and a complete recovery in about a month.

I. F. PEAK,  
Captain, Medical Corps.

#### CONCLUSIONS

It is concluded from these tests that:

1. The average loading obtainable on the horizontal tail surfaces in maneuvers involving principally the use of the elevator exceeds half the specified loading, except at very low speeds and in cases where the elevator is used cautiously. Thus, the material factor of safety in these maneuvers is less than two (on the basis of the design specifications and without considering relative distributions), indicating that the specified value of average load should be raised. Also, provision should be made in the specified distribution to take care of the high loads existing on the elevator.



2. The specified average loading on the vertical tail surfaces is probably satisfactory for all legitimate maneuvers, but the specified distribution should be changed to throw the predominance of load on the rudder, except for special leading edge loads.

3. Loads on the balanced portion of the rudder are severe, but with a balance of the size used here they do not approach a value sufficient to balance the loads on the rest of the rudder.

4. Accelerations of the order 10.5 *g*. may cause serious physical disorders in the pilot, and it is recommended that the effect of accelerations upon the pilot be investigated thoroughly by the Army or Navy Medical Corps in conjunction with the National Advisory Committee for Aeronautics or some other agency in a position to measure accelerations in flight.

LANGLEY MEMORIAL AERONAUTICAL LABORATORY,  
NATIONAL ADVISORY COMMITTEE FOR AERONAUTICS,  
LANGLEY FIELD, VA., *July 9, 1928.*

#### REFERENCES

1. Norton, F. H., and Brown, W. G.: The Pressure Distribution Over the Horizontal Tail Surfaces of an Airplane. III. N. A. C. A. Technical Report No. 148. (1922.)
2. Norton, F. H.: N. A. C. A. Recording Air-Speed Meter. N. A. C. A. Technical Note No. 64. (1921.)
3. Norton, F. H.: N. A. C. A. Control Position Recorder. N. A. C. A. Technical Note No. 97. (1922.)
4. Norton, F. H., and Warner, E. P.: Accelerometer Design. N. A. C. A. Technical Report No. 100. (1921.)
5. Brown, W. G.: The Synchronization of N. A. C. A. Flight Records. N. A. C. A. Technical Note No. 117. (1922.)
6. Warner, E. P.: Airplane Design—Aerodynamics. (p. 42) McGraw-Hill Book Co. (1927.)
7. Carroll, T., and Mixson, R. E.: The Effect of Tube Length upon the Recorded Pressures from a Pair of Static Orifices in a Wing Panel. N. A. C. A. Technical Note No. 251. (1926.)
8. Hemke, P. E.: The Measurement of Pressures through Tubes in Pressure Distribution Tests. N. A. C. A. Technical Report No. 270. (1927.)
9. Doolittle, J. H.: Accelerations in Flight. N. A. C. A. Technical Report No. 203. (1925.)

#### BIBLIOGRAPHY

- Norton, F. H.: Pressure Distribution Over the Wings of an MB-3 Airplane in Flight. N. A. C. A. Technical Report No. 193. (1924.)
- Crowley, jr., J. W.: Pressure Distribution Over a Wing and Tail Rib of a VE-7 and of a TS Airplane in Flight. N. A. C. A. Technical Report No. 257. (1927.)
- Haskins, G. W., and Carroll, F. O.: The Pressure Distribution Over the Stabilizer of a Vought VE-7 Airplane. Air Service Information Circular No. 419. (1923.)
- Bryant, L. W., and Batson, A. S.: Pressure Distribution Over the Tail Plane of BE2C. B. A. C. A. Reports and Memoranda No. 661. (1919.)
- Case, J., and Gates, S. B.: Tail Loads in Recovering from a Vertical Dive at Terminal Velocity. B. A. C. A. Reports and Memoranda No. 756. (1922.)
- Niles, jr., A. S.: Airplane Design, Vol. I, 1926. Engineering Division, Air Service, McCook Field.

#### APPENDIX

The Navy requirements for the strength of tail surfaces are given in the following specification excerpted from "General Specification for the Design of Airplanes for the United States Navy," SD-24-B (the specifications of the Army Air Corps are in exact agreement with these):

##### STRENGTH

365. The strength of the tail group shall be demonstrated by static tests to destruction.

366. The design loads for tail surfaces shall be in accordance with Table I.

(Table I gives average loading in pounds per square foot for the horizontal and vertical surfaces of single-seater fighters as 45 and 40, respectively.)

367. The load is to be distributed uniformly over the fixed surface, but for movable surfaces the intensity of loading at the hinges shall be equal to the loading on the fixed surface in front of it and shall decrease uniformly to an intensity of one-third this value at the trailing edge. Portions of the movable surface in front of the hinges shall carry the same loading as the fixed surface. This includes surfaces which are balanced by auxiliary vanes.



368. When auxiliary vanes are used for balancing, they shall be assumed to be subject to the same intensity of loading as the fixed surfaces, when computing the distribution of load and the stresses in the remainder of the movable surface. The vanes themselves and the attachment to the main movable surface shall be strong enough to carry the load required to balance the load on the main portion of the movable surface.

369. The control surfaces must be designed to carry the specified load acting in either direction.

370. Although no load parallel to the chord of the fixed tail surfaces, or torsional load, is specified, provision shall be made to carry a reasonable amount of such load.

371. To determine the unit loading on the fixed surface with trailing control surface, use the following formula:

$$X = \frac{\text{Specified average loading} \times (A_f + A_c + A_b)}{A_f + \frac{2}{3}A_c + A_b}$$

Where  $X$  = unit loading on fixed surface.

$A_f$  = area fixed surface.

$A_c$  = area control surface behind hinges.

$A_b$  = area control surface in front of hinges.

372. In case the control surface is acting alone—i. e., not behind a fixed surface, design for the average load specified above—the distribution is to be uniform from the leading edge to the hinge and from the hinge to the trailing edge shall vary uniformly to one-third this value.

#### LEADING EDGE TEST

373. The stabilizer and fin shall be subjected to leading edge tests. In these tests the surfaces shall be supported at the fuselage and at the hinges along the rear stabilizer beam or the rear fin post. The load shall be uniformly distributed (in pounds per square foot) along the span of the surface and from the leading edge back 20 per cent of the chord of the fixed surface. The intensity of the loading shall be three times the average load specified for the design of horizontal and vertical tail surfaces, respectively.

TABLE I.—MAXIMUM LOADS, MOMENTS, AND PRESSURES

Run No.	Maneuver	Initial air speed	Horizontal surfaces								Vertical surfaces							
			Total normal force	Total moment about hinge	Average loading	Stabilizer load	Elevator load	Elevator hinge moment	Maximum pressure	Location of maximum pressure	Total normal force	Total moment about hinge	Average loading	Fin load	Rudder load	Rudder hinge moment	Maximum pressure	Location of maximum pressure
			Lbs.	Lb./in.	Lbs./sq. ft.	Lbs.	Lbs.	Lb./in.	Lb./sq. ft.		Lbs.	Lb./in.	Lb./sq. ft.	Lbs.	Lbs.	Lb./in.	Lb./sq. ft.	
3	Pull-up.....	86	-337	110	-21.2	-148	-189	1,500	-46	D-4	62	-610	4.0				97	K-1
6	do.....	109	-388	-180	-24.4	-172	-216	1,600	-68	D-4	78	-720	5.0				26	J-1
7	do.....	126	-468	-780	-29.4	-224	-244	1,760	-86	E-4								
7	do.....	126	+202	2,900	12.7	186	16		74	E-1								
10	do.....	140	-481	-180	-30.2	-221	-260	1,920	-93	E-4								
11	do.....	163	-540	-680	-34.0	-245	-295	2,010	-108	E-4	-100	1,100	6.4				-33	K-1
16	do.....	173	-422	380	-26.5	-170	-252	1,700	-89	E-4	243	-530	-15.6				38	K-1
17	Dive, n <sup>1</sup> , power on...	<sup>2</sup> 225	-244	-2,430	-15.3	-192	-52	360	-78	C-1	-34	340	-2.2				-31	G-1
18	do.....	<sup>2</sup> 247	-234	-2,420	-14.7	-189	-45		-78	C-1	-37	-120	-2.4				-29	G-1
19	Dive, n, power off....	<sup>2</sup> 250	-242	-2,680	-15.2	-198	-44		-76	C-1	-41	440	-2.6				-33	G-1
20	Dive, u, power on.....	<sup>2</sup> 253	-205	-2,140	-12.9	-159	-46		-71	C-1								
21	Dive, d, power on.....	<sup>2</sup> 247	-212	-2,900	-13.3	-188	-24		-73	C-1	-22	30	-1.4				-26	G-1
35	Right rudder kick.....	166	-137	-970	-8.6				-41	B-1	260	550	16.7	72	188	1,190	55	G-1
48	Left rudder kick.....	128	-35	660	-2.2				-16	B-5	406	-2,850	26.0	111	295	1,420	49	K-4
51	do.....	169	-81	-470	-5.1				-18	D-4	-339	-570	-21.7	-67	-272		-107	G-1
54	Half roll.....	161	-220	-860	-13.8	-130	-90	700	-37	B-1	315	1,320	-20.2	63	252	1,740	71	K-4
57	Right roll.....	109	-266	-90	-16.7	-107	-159	970	-46	D-4	-198	-1,420	-12.7	-7	-191	-990	92	G-1
61	Left spin.....	<sup>2</sup> 74	-73	930	-4.6	4	-77	470	-22	D-4	-143	-600	-9.2	-27	-116	-876	-26	G-1
62	Vertical reverse.....	92	-148	500	-9.3	-35	-113	820	-35	D-4	164	530	10.5	40	124	960	25	L-1
70(a)	Rudder reversal.....	153	65	940	4.1				34	E-1	630	-3,890	40.4	336	294	1,460	117	J-1
70(b)	do.....	153									-180	4,430	11.9	-212	32		-151	K-1
70(c)	do.....	153									-396	600	25.4	-94	-302		-122	G-1

<sup>1</sup> u, and d (stabilizer neutral, up, and down).

<sup>2</sup> Air speed at the time corresponding to loads given.



TABLE 11.—LOCAL PRESSURES ON F6C-4 TAIL SURFACES IN POUNDS PER SQUARE FOOT

Run No. 11

### Maneuver: Pull-up

Initial A. S. 163 M. P. H.

Condition represented: Maximum load and pressure on horizontal surfaces

[illegible]

Run No. 18.

Maneuver: Dive

Actual A. S. 247 M. P. H.

Condition represented: Representative

[illegible]

Run No. 57.

**Maneuver: Right roll**

Initial A. S. 109 M. P. H.

Condition represented: Peak loads in a roll

[illegible]

Run No. 61.

Maneuver: Left spin

A. S. 74 M. P. H.

Condition represented: Peak load on vertical tail surfaces in a spin

[illegible]

Run No. 62

**Maneuver:** Vertical reverse

Initial A. S. 92 M. P. H.

Condition represented: Peak loads on horizontal and vertical surfaces in vertical reverse

[illegible]

TABLE II.—LOCAL PRESSURES ON F6C-4 TAIL SURFACES IN POUNDS PER SQUARE FOOT—  
Continued

Run No. 70(a).

Maneuver: Rudder reversal

Initial A. S. 153 M. P. H.

Condition Represented: Maximum total load on vertical surfaces; maximum load on fin

Rib		Horizontal surfaces					Vertical surfaces					
		B	C	D	E	F	G	H	J	K	L	M
Orifice	1	+15.6	+15.1	+28.6	+34.3	+29.1	+31.2	+102.0	+117.5	+93.0	+31.2	+19.2
	2	+8.8	+9.4	+15.6	+13.0	+8.8	+71.3	+80.6	+118.6	+61.3	+18.7	
	3	+4.2	+4.7	+6.7	+3.6	+1.6	+49.4	+68.0	+78.0	+48.3	+10.4	+13.5
	4	-3.1	-2.6	+1.6	0	0		+65.0	+49.4	+32.2		
	5	0	-4.2	-1.6	+1.6	+5.7		+53.0	+34.8	+17.7		
	6	+2.1	+1.0	-2.1	-3.1			+27.6	+19.8	+9.4		
	7	+1.6										

Run No. 70(b).

Maneuver: Rudder reversal

Initial A. S. 153 M. P.H.

Condition represented: Maximum pressure on fin

Orifice	1				-31.2	-19.7	-59.8	-151.0	+24.4	+23.4
	2				-10.4	-8.3	-51.5	-65.5	+10.9	
	3				-10.4	-12.5	-26.0	-6.8	+3.6	+2.6
	4					-9.9	0	+23.4		
	5					-14.6	+18.2	0		
	6					-9.3	-6.8	0		
	7									

Run No. 70(c).

Maneuver: Rudder reversal

Initial A. S. 153 M. P. H.

Condition represented: Maximum load and maximum pressure on rudder

[illegible]



---

# **REPORT No. 308**

---

## **AIRCRAFT ACCIDENTS**

### **METHOD OF ANALYSIS**

**Report Prepared by  
Special Committee on the Nomenclature,  
Subdivision, and Classification of Aircraft Accidents**

AUGUST 15, 1928.

THE EXECUTIVE COMMITTEE,  
NATIONAL ADVISORY COMMITTEE FOR AERONAUTICS,  
*Washington, D. C.*

GENTLEMEN: There is submitted herewith the report of the special committee on the nomenclature, subdivision, and classification of aircraft accidents organized in pursuance of resolution adopted by the executive committee on March 1, 1928. Attention is invited to the committee's recommendations at the end of its report.

Respectfully,

SPECIAL COMMITTEE ON THE NOMENCLATURE, SUBDIVISION,  
AND CLASSIFICATION OF AIRCRAFT ACCIDENTS  
GEORGE K. BURGESS, *Chairman.*



# AIRCRAFT ACCIDENTS

## METHOD OF ANALYSIS

---

	Page
INTRODUCTION.....	561
PURPOSE AND ORGANIZATION.	
FOREIGN COOPERATION.	
GENERAL CONSIDERATIONS.....	562
DEFINITION OF AN AIRCRAFT ACCIDENT.	
IMMEDIATE CAUSES.	
CROSS ANALYSIS.	
AIRCRAFT-ACCIDENT ANALYSIS FORM.	
WEIGHTING OF ACCIDENTS.	
CLASSIFICATION OF ACCIDENTS.....	565
I. NATURE OF THE ACCIDENT.	
II. INJURY TO PERSONNEL.	
III. DAMAGE TO MATÉRIEL.	
CAUSES OF ACCIDENTS.....	567
A. IMMEDIATE CAUSES OF AIRCRAFT ACCIDENTS.	
B. UNDERLYING CAUSES OF AIRCRAFT ACCIDENTS.	
DESCRIPTION AND TYPICAL ANALYSIS OF AN ACCIDENT.....	572
CONCLUSION AND RECOMMENDATIONS.....	574





# REPORT No. 308

---

## AIRCRAFT ACCIDENTS

### METHOD OF ANALYSIS

Report Prepared by  
Special Committee on the Nomenclature,  
Subdivision, and Classification of Aircraft Accidents

---

#### INTRODUCTION

##### PURPOSE AND ORGANIZATION

This report on a method of analysis of aircraft accidents has been prepared by a special committee on the nomenclature, subdivision, and classification of aircraft accidents organized by the National Advisory Committee for Aeronautics in response to a request dated February 18, 1928, from the air coordination committee consisting of the Assistant Secretaries for Aeronautics in the Departments of War, Navy, and Commerce. The work was undertaken in recognition of the difficulty of drawing correct conclusions from efforts to analyze and compare reports of aircraft accidents prepared by different organizations using different classifications and definitions. The air coordination committee's request was made "in order that practices used may henceforth conform to a standard and be universally comparable." The purpose of the special committee therefore was to prepare a basis for the classification and comparison of aircraft accidents, both civil and military.

The special committee was organized in pursuance of resolution adopted by the executive committee of the National Advisory Committee for Aeronautics on March 1, 1928, and held its initial meeting on March 19, 1928. Sixteen meetings were held, the last being on July 17, 1928.

Following is the organization of the committee:

*Representatives of the National Advisory Committee for Aeronautics:*

Dr. George K. Burgess, chairman.

Mr. George W. Lewis.

*Representatives of the Army Air Corps:*

Lieut. D. B. Phillips, United States Army.

Lieut. J. D. Barker, United States Army.

*Representatives of the Bureau of Aeronautics of the Navy:*

Lieut. Commander L. C. Stevens, Construction Corps, United States Navy.

Lieut. Charles R. Brown, United States Navy.

*Representatives of the Aeronautics Branch of the Department of Commerce:*

Mr. Daniel deR. Scarritt (succeeded by Mr. Edward P. Howard).

Mr. Lester T. Bradbury.

Mr. Scarritt, having resigned from the Government service, was succeeded by Mr. Howard as a representative of the Department of Commerce at the ninth meeting of the committee. Most of the meetings were attended also by Mr. E. M. Kintz, of the Department of Commerce, and Mr. Starr Truscott, of the National Advisory Committee for Aeronautics, and they assisted the committee in the preparation of this report. In connection with the preparation of the definitions and explanations involving the physiological aspects of aviation Dr. L. H. Bauer, of the Department of Commerce, and Lieut. Commander John R. Poppen, Medical Corps, United States Navy, were also of assistance.



## FOREIGN COOPERATION

The meeting of May 22, 1928, was attended by the following representatives of foreign governments:

Commander Silvio Scaroni, air attaché, Italian Embassy.

Wing Commander T. G. Hetherington, air attaché, British Embassy.

Maj. Georges Thenault, assistant military attaché for aeronautics, French Embassy.

Lieut. Yoshitake Miwa, Imperial Japanese Navy, assistant naval attaché, Japanese Embassy.

At that meeting the proposed method of analyzing aircraft accidents was explained and the value of a uniform system for reporting accidents was discussed. It was suggested that the representatives of the foreign governments consult with the personnel in their governments who were responsible for analyzing and reporting aircraft accidents, regarding the possibility of adopting the proposed method and form.

Great interest was expressed, and it was the opinion of those present that the adoption of a uniform system would be advantageous. The representatives of the foreign governments were invited to submit comments and suggestions regarding changes, but none had been received up to the date of the last meeting of the committee. This was probably due to the necessarily lengthy period of time required for translation, consideration, and approval.

## GENERAL CONSIDERATIONS

## DEFINITION OF AN AIRCRAFT ACCIDENT

An aircraft accident is an occurrence which takes place while an aircraft is being operated as such and as a result of which a person or persons are injured or killed, or the aircraft receives appreciable or marked damage through the forces of external contact or through fire. A collision of two or more aircraft should be analyzed and reported statistically as one accident.

## IMMEDIATE CAUSES

In the course of its meetings the committee considered various methods of analyzing aircraft accidents. These included studies and classification by (a) the immediate causes, (b) the underlying causes, (c) the nature, and (d) the results of the accidents. Each of these methods was considered in detail, and it was finally found possible to reduce their analysis to the methods described in this report and combine the results in the form of a single chart.

A plan devised by Lieutenant Philips, of the Army, and Lieutenant Brown, of the Navy, for the division of the immediate causes of aircraft accidents into four major classes, and providing for the further subdivision of these major classes as seemed desirable, together with proposed definitions of these classes and subdivisions, was submitted to the committee for consideration.

The outline and definitions of the classification of accidents as presented to the committee were carefully considered by the members at a number of meetings, and modifications were made in the plan as originally drafted so as to provide for every type of aircraft accident in the light of the experience of the members in classifying and analyzing accidents in the Government services.

In working out this outline the committee attempted to provide a plan which would permit of the careful analysis of aircraft accidents by the different organizations from the point of view of both personnel and matériel problems. The plan also permits of the analysis of a given accident into two or more distinct causes and makes possible, by the use of percentages, the indication of the relative weight of each cause in any particular accident.

## CROSS ANALYSIS

The plan provides for the analysis of crashes according to the nature of the accident (take-off accidents, tail spins following engine failure, etc.), the degree of seriousness of personnel injuries, and the amount of damage occurring to matériel.



Furthermore, the system, through the use of a cross-analysis method, allows for analyzing pilot errors and matériel failures according to the underlying causes of these errors or failures.

The plan also provides for the analysis of aircraft accidents of different organizations on the same basis, so that the records will be comparable and the preparation of a composite report of all aircraft accidents will be possible. It is the belief of the committee that if all aircraft accidents occurring in all agencies are classified in the manner recommended a composite of all the accidents will offer a basis upon which a study may be made and correct conclusions drawn.

#### AIRCRAFT ACCIDENT ANALYSIS FORM

In drawing up the aircraft accident analysis form and the accompanying definitions the committee had in mind the frequency rate of accidents from the various causes, the logical lines along which studies should be conducted, and the ease with which these studies can be made from this chart. It is recognized that to make a detailed study of accidents due to any one cause a further subdivision may be necessary. However, if all accidents are classified according to this chart the major causes can be easily determined and further investigation can be readily carried out for the purpose of eliminating these causes.

It was also recognized, in working out this chart, that the division of immediate causes between personnel and matériel as set forth in the chart and definitions was more or less arbitrary, since all defects of aircraft can in the last analysis be attributed to errors of personnel, whether in operation, inspection, maintenance, manufacture, or design. Since the purposes of the accident study seemed to be best served by drawing attention to defects of matériel, even though traceable ultimately to personnel errors, the line between personnel and matériel in the immediate causes was drawn at the operating personnel of the aircraft. In other words, under the main heading "Personnel" there are included only those accidents for which personnel engaged in operating the aircraft are responsible. Accidents due to matériel failure are classified under "Matériel" even though personnel charged with design, construction, or operation may be held responsible for the failure. Errors due to personnel other than those immediately accessory to the operation of the aircraft are shown in the "Underlying causes" or "Cross analysis," as set forth hereinafter, rather than in the main headings of immediate causes.

The plan as drawn up by the committee is not in any sense final or complete, but is presented to provide a working basis for the study of aircraft accidents from all sources.

#### WEIGHTING OF ACCIDENTS

Where two or more factors cause an accident, part will be charged to each; for example, in the case of an avoidable accident following an engine failure the responsibility for the accident might be considered to be equally divided between the pilot and the power plant, in which case 50 per cent would be charged to "Personnel" and 50 per cent to "Matériel." If the responsibility for the accident rested largely upon the pilot, "Personnel" would be charged with 60, 70, or 80 per cent of the accident, or even more, depending upon the degree of responsibility decided upon. Conversely in the above cases "Matériel" and "Miscellaneous" would be charged with a total of 40, 30, or 20 per cent of the accident. This same division of responsibility might be carried out under "Personnel" or other subheads. However, in the particular case cited "Errors of pilot" would be the only division of "Personnel" which could be charged with this accident. If 80 per cent of the accident were charged to "Personnel" in the above instance, then 80 per cent of the accident would be charged to "Errors of pilot." Then, assuming that the responsibility for such piloting error rested jointly upon error of judgment and poor technique, a still further subdivision would be made and 40 per cent of an accident would be charged to "Error of judgment" and 40 per cent to "Poor technique." Thus the factors of each crash could be traced down to the last subdivision under any heading and weighted in accordance with their importance.



N.A.C.A. AIRCRAFT ACCIDENT ANALYSIS FORM																													
CLASSIFICATION OF ACCIDENT NATURE: .....				UNDERLYING CAUSES OF ACCIDENT:																									
				ERRORS OF PILOT								MATERIEL FAILURES																	
				LACK OF EXPERIENCE		PHYSICAL AND PSYCHOLOGICAL		FAULTY INSTRUCTIONS		INSPECTION		MATERIALS		DESIGN		INDETERMINATE													
RESULTS: PERSONNEL: CLASS .....				GENERAL		SPECIAL		DISEASE OR DEFECT		POOR REACTION		OPERATING		MAINTENANCE		MANUFACTURING		OVERHAUL		MAINTENANCE		INDETERMINATE		ORIGINAL		MODIFICATION			
				TOTAL	RECENT	TOTAL	RECENT	INHERENT	TEMPORARY	INHERENT	TEMPORARY																		
IMMEDIATE CAUSES OF ACCIDENT																													
%		%		%																									
PERSONNEL				ERRORS OF PILOT		ERROR OF JUDGMENT																							
						POOR TECHNIQUE																							
						DISOBEDIENCE OF ORDERS																							
						CARELESSNESS OR NEGLIGENCE																							
						MISCELLANEOUS																							
				ERRORS OF SUPERVISORY PERSONNEL																									
				ERRORS OF OTHER PERSONNEL																									
MATERIEL				POWER PLANT FAILURE		FUEL SYSTEM																							
						COOLING SYSTEM																							
						IGNITION SYSTEM																							
						LUBRICATION SYSTEM																							
						ENGINE STRUCTURE																							
						PROPELLER AND PROPELLER ACCESSORIES																							
						ENGINE CONTROL SYSTEM																							
						MISCELLANEOUS																							
						UNDETERMINED																							
				STRUCTURAL FAILURE		FLIGHT CONTROL SYSTEM																							
						MOVABLE SURFACES																							
						STABILIZING SURFACES																							
						WINGS, STRUTS, AND BRACINGS																							
						LANDING GEAR																							
						WHEELS, TIRES AND BRAKES																							
						SEAPLANE FLOAT OR BOAT																							
						FUSELAGE, ENGINE MOUNT AND FITTINGS																							
						TAIL SKID OR WHEEL ASSEMBLY																							
						ARRESTING APPLIANCES ON AIRCRAFT																							
						MISCELLANEOUS																							
						UNDETERMINED																							
								HANDLING QUALITIES																					
								INSTRUMENTS																					
								LAUNCHING DEVICES																					
								ARRESTING DEVICES																					
MISCELLANEOUS				WEATHER																									
				DARKNESS																									
				AIRPORT OR TERRAIN																									
				OTHER																									
UNDETERMINED AND DOUBTFUL																													

PREPARED AND RECOMMENDED BY  
 SPECIAL COMMITTEE ON THE NOMENCLATURE, SUBDIVISION  
 AND CLASSIFICATION OF AIRCRAFT ACCIDENTS  
 NATIONAL ADVISORY COMMITTEE  
 FOR AERONAUTICS  
 JULY 17, 1928

FORM-A



## CLASSIFICATION OF ACCIDENTS

For the purpose of comparative study aircraft accidents may be divided into groups of accidents of the same general characteristics. Accident prevention must be regarded as the primary purpose of aircraft study. Studies of accident causes point out needed remedies more clearly when they are supplemented by certain studies based upon the nature and results of the accident.

For example, in both bad landings and tail spins the principal cause is usually errors of the pilot. Statistics based upon the study of causes merely show that pilots' errors are responsible for more than half of all accidents and the formulation of remedies for the situation appears difficult. If, however, the same accidents are classified according to their nature and results, it is found that the tail spin is the kind of accident that is by far the most prevalent among those which produce fatal consequences. It is apparent that new designs which decrease the tendency of airplanes to spin, or new training methods which increase the ability of pilots to avoid falling into spins and to recover from them quickly, will have a marked influence toward the prevention of fatal accidents.

Likewise, the study based upon nature and results indicates, in the case of collisions, that this kind of accident is third in importance among those which produce fatal results, and that these accidents are much more prevalent during winter months than in summer; and while remedies are not so obvious as in the case of tail spins some lines of attack immediately suggest themselves.

The following classifications for study of accidents according to their nature are recommended:

## I. NATURE OF THE ACCIDENT

This consists of dividing accidents into separate classes according to the type of accident which occurs.

1. *Class A—Collisions in full flight with other aircraft.*—This includes all collisions with airplanes, balloons, or other aircraft while the colliding aircraft is at flying speed or at an altitude which permits free maneuvering. It excludes collisions (1) on the ground while taxiing, taking off, or landing, and (2) in the air immediately before landing or after taking off and while the airplane is at or near its minimum flying speed.
2. *Class B—Collisions in full flight with objects other than aircraft.*—This includes collisions while at flying speed and with power plant functioning normally with trees, poles, houses, mountain sides, or other obstacles. It includes collisions with the earth or water by diving. It excludes collisions (1) on the ground while taxiing, taking off, or landing, and (2) in the air immediately before landing or after taking off and while the airplane is at or near its minimum flying speed.
3. *Class C—Tail spins following engine failure.*—This includes spins, stalls, and all collisions with the earth while the airplane is out of control due to loss of flying speed following engine failure.
4. *Class D—Tail spins without engine failure.*—This includes spins, stalls, and all collisions with the earth while the airplane is out of control following loss of flying speed, with the engine functioning normally. It includes spins due to structural failure or defective handling qualities of the airplane.
5. *Class E—Forced landings.*—This covers accidents while making landings necessitated by conditions which could not be overcome while in flight. Such conditions include engine trouble and other defects of the aircraft, loss of knowledge of the direction to the destination or the location on the map of the aircraft's position, bad weather, darkness, and exhaustion of fuel.
6. *Class F—Landing accidents.*—This includes accidents while the pilot is in the act of executing a voluntary landing. It does not include forced landings or accidents while examining a field from the air or approaching it for a landing.
7. *Class G—Take-off accidents.*—This includes accidents occurring between the time of starting a take-off to the time when full flying speed is gained, except those covered under other classifications, as, for instance, tail spins or forced landings.



8. *Class H—Taxying accidents.*—This includes all accidents which occur while the aircraft is maneuvering under its own power on land or water. It excludes accidents while the aircraft is still moving after a landing or while it is getting up speed for a take-off.
9. *Class I—Fires in the air.*—This includes all accidents in which fire breaks out, either as a cause or result of the occurrence, while the aircraft is in flight.
10. *Class J—Carrier, platform, and arresting-gear accidents.*—This includes accidents occurring while the aircraft is landing upon or taking off from (1) the deck of a floating aircraft carrier, or (2) an elevated platform intended for the landing and taking off of aircraft, but excludes launching-gear accidents.
11. *Class K—Launching gear accidents.*—This includes accidents during take-off in which the aircraft is assisted in gaining flying speed by the application of an external force.
12. *Class L—Miscellaneous.*—This includes accidents the nature of which is known but which do not fall into one of the above classifications.
13. *Class M—Indeterminate and doubtful.*—This includes all accidents concerning the nature of which so little is known that any classification can not be intelligently accomplished.

## II. INJURY TO PERSONNEL

This consists of dividing accidents into separate classes according to the injury suffered by personnel in such aircraft.

1. *Class A.*—A "Class A" injury is one resulting in the death of the individual within a period of 90 days.
2. *Class B.*—A "Class B" injury is one resulting in serious injury to the individual. Because of the difficulties of classification, the opinion of a physician should be obtained whenever possible as to whether an injury is severe or minor. When a physician is not available, the following general rules should be followed: Any injury that results in unconsciousness; any fracture of any bone except simple fractures of the fingers and toes; lacerations that involve muscles or cause severe hemorrhage; any injury to any internal organ; or any other injury that it seems probable will incapacitate the individual for more than five days should be classed as a severe injury. All other injuries should be classed as minor.
3. *Class C.*—A "Class C" injury is one resulting in only minor injury to the individual.
4. *Class D.*—Any personnel who experience an aviation accident with no personal injury shall be classified as "Class D."

NOTE.—The classification of an accident according to injury to personnel shall contain a letter for each individual in the aircraft at the time of the accident, the first of these letters representing the pilot of the aircraft. For example, in an accident where the pilot is killed, one passenger seriously injured, and the remaining passenger escapes with only minor injury the accident would be classified as a Class ABC accident. Had the pilot escaped with minor injury and both passengers been killed, it would have been a Class CAA accident.

## III. DAMAGE TO MATÉRIEL

This consists of dividing accidents into separate classes according to the amount of damage which occurs to matériel.

1. *Class A.*—This includes all accidents as a result of which the aircraft is of no further value except for salvage of usable parts.
2. *Class B.*—This includes all accidents as a result of which it is necessary to completely overhaul the aircraft before it would be again airworthy.
3. *Class C.*—This includes all accidents as a result of which it is necessary to replace some major assembly of the aircraft before it would be again airworthy, such as a wing, fuselage, undercarriage, tail, or engine. Accidents in which the damage to the engine or other major assembly was a *cause* and not a *result* are excluded from this category unless the remaining damage warrants such.



4. *Class D.*—This includes all incidents which because of other factors come within the category of an aircraft accident and as a result of which there is only minor and easily repairable damage to the aircraft, such as a broken tail skid, wheel, bent propeller tip, etc.
5. *Class E.*—This includes all incidents similar to Class D accidents above in which there is no damage to matériel.
6. *Class F.*—"Class F" is included in this analysis only because of the interest it may have for the different organizations which may use this method of analyzing. It consists of matériel failures which did not result in an accident, and, strictly speaking, does not actually fit into an accident analysis. However, the methods here used for analyzing matériel failures which did result in accidents can as easily be applied to those which did not, and thus afford a method of studying the potential accidents, which because of other reasons did not occur, such as a successful landing after engine failure, etc.

#### CAUSES OF ACCIDENTS

The following classifications for study of aircraft accidents according to their causes are recommended:

##### A. IMMEDIATE CAUSES OF AIRCRAFT ACCIDENTS

The following is a proposed list of immediate standard causes of aircraft accidents, with definitions where considered necessary for clarity.

- I. *Personnel.*—This includes all accidents which can be traced to persons accessory to the operation of the aircraft, either on the ground or in the air. This does not include accidents due to errors or omissions of personnel charged with the design, manufacture, maintenance, or inspection of aircraft.
  1. **ERRORS OF PILOT.**—This includes all accidents the responsibility for which rests upon the pilot. The pilot is the actual manipulator of the controls or the individual responsible for their correct manipulation.
    - (a) **ERROR OF JUDGMENT.**—This includes all accidents resulting from a decision made by the pilot which was not the best possible under existing circumstances.
    - (b) **POOR TECHNIQUE.**—This includes all accidents resulting from lack of skill, dexterity, or coordination of the senses in handling aircraft controls, whether traceable to inherent inability to attain such or to infrequent flying, lack of experience in flying, lack of experience in flying under particular conditions, or in the particular type of aircraft.
    - (c) **DISOBEDIENCE OF ORDERS.**—This includes all accidents resulting from the violation or disobedience of local or general orders or regulations or provisions of law governing the operation of aircraft, such as low acrobatics, acrobatics in aircraft not to be used for such purposes, or any other type or manner of operation specifically forbidden by orders or regulations issued by competent authorities.
    - (d) **CARELESSNESS OR NEGLIGENCE.**—This includes all accidents resulting from the absence of care on the part of the pilot according to circumstances or the failure to use that degree of care which the circumstances justly demand, either on the ground or in the air, such as careless manipulation of the controls of an aircraft, failure to ascertain the amount of gasoline on board before taking off, failure to ascertain the conditions of the instruments, etc.
    - (e) **MISCELLANEOUS.**—This includes all accidents resulting from errors of the pilot not accounted for above.

I. *Personnel*.—Continued.

2. **ERRORS OF SUPERVISORY PERSONNEL.**—This includes all accidents the responsibility for which rests upon individuals other than the pilot who exercise control over the operation of the aircraft, such as navigators, formation section leaders, ground-operations officers, etc.

3. **ERRORS OF OTHER PERSONNEL.**—This includes all accidents the responsibility for which rests upon other personnel directly concerned with the operation of the aircraft, such as members of the flight and ground crews of the aircraft, aerographers, etc.

II. *Matériel*.—This includes all accidents resulting from failures of the airplane, power plant, accessories, and launching and arresting devices, whether traceable to materials, faulty design, maintenance, or inspection.

1. **POWER-PLANT FAILURE.**—This includes all accidents resulting from failure or malfunctioning of the propelling system and all auxiliaries essential to its proper functioning, exclusive of instruments.

(a) FUEL SYSTEM.

(b) COOLING SYSTEM.

(c) IGNITION SYSTEM.

(d) LUBRICATION SYSTEM.

(e) ENGINE STRUCTURE.

(f) PROPELLER AND PROPELLER ACCESSORIES.

(g) ENGINE CONTROL SYSTEM (THROTTLE ROD, ETC.).

(h) MISCELLANEOUS.

(i) UNDETERMINED.

2. **STRUCTURAL FAILURE.**—This includes all accidents resulting from failures of the airplane exclusive of the propelling system and instruments.

(a) FLIGHT CONTROL SYSTEM.

(b) MOVABLE SURFACES.

(c) STABILIZING SURFACES.

(d) WINGS, STRUTS, AND BRACING.

(e) **LANDING GEAR.**—This includes all accidents resulting from failure of the landing-gear struts and shock-absorbing gear, but does not include accidents resulting from failure of the wheels or floats attached thereto.

(f) WHEELS, TIRES, AND BRAKES.

(g) SEAPLANE FLOAT OR BOAT.

(h) FUSELAGE, ENGINE MOUNT, AND FITTINGS.

(i) TAIL SKID OR WHEEL ASSEMBLY.

(j) ARRESTING APPLIANCES ON AIRCRAFT.

(k) MISCELLANEOUS.

(l) UNDETERMINED.

3. **HANDLING QUALITIES.**—This includes all accidents resulting from those peculiar characteristics of certain types of aircraft affecting their controllability while on the ground or in the air, such as marked tendency to ground loop, inability to recover from a spin, etc.

4. **INSTRUMENTS.**—This includes all accidents resulting from failures of instruments which were essential to operation under the conditions of the flight.

5. **LAUNCHING DEVICES.**—This includes all accidents resulting from failure or malfunctioning of catapults.

6. **ARRESTING DEVICES.**—This includes all accidents resulting from failure or malfunctioning of arresting gear not a part of the aircraft.



III. *Miscellaneous*.—This includes all accidents not accounted for above but those causes are determined.

1. WEATHER.—This includes all accidents resulting from conditions of the weather which could not reasonably have been foreseen and avoided. (Mention may be made on the chart of contributing weather causes, as fog, gale, ice, hail, snow, rain, lightning, etc.)
2. DARKNESS.—This includes all accidents resulting from conditions due to nightfall which could not reasonably have been foreseen and avoided.
3. AIRPORT OR TERRAIN.—This includes all accidents resulting from airports or landing conditions of places which could not reasonably have been detected or avoided. (Forced landings should be charged to power plant, etc., unless report shows that safe landing could have been made, in which case the crash would probably be attributed to error of judgment or poor technique.)
4. OTHER.—This includes all accidents resulting from causes not otherwise accounted for above.

IV. *Undetermined and doubtful*.—This includes all accidents the causes of which are either undetermined or doubtful.

#### B. UNDERLYING CAUSES OF AIRCRAFT ACCIDENTS

The following is a list of standard underlying causes of aircraft accidents, with definitions where considered necessary for clarity.

I. *Errors of pilot*.—Returning to "Errors of pilot," paragraph I, subparagraph 1, above, the subdivisions of this paragraph were made according to the immediate causes of the errors attributed to the pilot, such as an "Error of judgment," "Poor technique," etc. The underlying causes of such errors may frequently be of more interest than the actual causes themselves. These causes may be defined as those elements which contributed to the pilot's mental and physical equipment at the time of the accident or to the deficiencies which existed in such equipment.

1. LACK OF EXPERIENCE.—This includes all accidents resulting from insufficient personal acquaintance with the actual conditions which had to be met under the circumstances.

(a) LACK OF GENERAL EXPERIENCE.—This includes all accidents resulting from a lack of experience in the general problems of aviation, such as landing, taking off, air work, etc.

(1) LACK OF TOTAL GENERAL EXPERIENCE.—This includes all accidents resulting from a lack of general experience due to the fact that the individual concerned has never engaged in such work for a sufficient period of time to acquire the necessary experience to have avoided such accidents.

(2) LACK OF RECENT GENERAL EXPERIENCE.—This includes all accidents resulting from a lack of general ability due to the fact that the individual concerned has too infrequently engaged in general flying activities prior to the accident, and consequently lost the ability he had originally acquired.

(b) LACK OF SPECIAL EXPERIENCE.—This includes all accidents resulting from a lack of experience in special problems of aviation, such as certain features of cross-country flying (which might, for example, require an intimate knowledge of the terrain of a certain section), carrier operations, night flying, blind flying, etc.

(1) LACK OF TOTAL SPECIAL EXPERIENCE.—This includes all accidents resulting from a lack of special experience due to the fact that the individual had never engaged in such special problems for a sufficient period of time to acquire the necessary experience to have avoided such accidents.

I. *Errors of pilot*—Continued.

## 1. LACK OF EXPERIENCE—Continued.

## (b) LACK OF SPECIAL EXPERIENCE—Continued.

(2) LACK OF RECENT SPECIAL EXPERIENCE.—This includes all accidents resulting from a lack of ability in the special problems due to the fact that the individual concerned has too infrequently engaged in special flying activities prior to the accident, and consequently lost the ability he had originally acquired.

## 2. PHYSICAL AND PSYCHOLOGICAL CAUSES.—This includes all accidents resulting from a demonstrable disease or defect or poor reaction.

(a) DISEASE OR DEFECT.—This includes all accidents resulting from a disease or defect, demonstrable by physical (including nervous system) examination.

(1) INHERENT DISEASE OR DEFECT.—This includes all accidents resulting from a disease or defect which is not susceptible to remedy within a reasonable period of time, such as overshooting a field, faulty landings or collision because of defective vision or judgment of distance; unconsciousness; hysterical or epileptic tendency; chronic air sickness; inability to withstand altitude, etc. The history of an individual may often be necessary to determine if a disease or defect is inherent.

(2) TEMPORARY DISEASE OR DEFECT.—This includes all accidents resulting from a disease or defect which is remediable and one which may not be expected to repeat itself with undue frequency in the individual concerned, such as fatigue, either mental or muscular, staleness, temporary illness, incomplete convalescence, etc.

(b) POOR REACTION.—This includes all accidents which result from no demonstrable disease or defect but from psychological causes, making the individual react either erroneously or slowly to a situation, such as selecting what is manifestly the poorer of two fields for an emergency landing, persisting on a course when better judgment would indicate that he should land or turn back, indulging in acrobatics over prohibited areas or at too low altitude, etc.

(1) POOR REACTION, INHERENT.—This includes all accidents resulting from psychological causes which apparently are not susceptible to correction within a reasonable period of time. The history of the individual would be a very important adjunct in determining if such poor reaction were inherent and its repetition to be frequently expected.

(2) POOR REACTION, TEMPORARY.—This includes all accidents resulting from psychological causes which apparently are subject to correction, disciplinary or otherwise, within a reasonable period of time.



II. *Matériel failures*.—The underlying causes of “matériel failures” should also prove of considerable interest in analyzing accidents.

1. FAULTY INSTRUCTIONS.—This includes all accidents resulting from matériel failures which were traceable to errors or omissions in the standard instructions covering the use of such matériel.

(a) FAULTY OPERATING INSTRUCTIONS.—This includes all accidents resulting from matériel failures which were traceable to the operation of such matériel in accordance with standard instructions which prove to be incorrect or incomplete, such as instructions governing the use of the mixture control which when carried out are found to damage the engine, instructions governing the proper engine operating temperature which when carried out are found to damage the engine, etc.

(b) FAULTY MAINTENANCE INSTRUCTIONS.—This includes all accidents resulting from matériel failures which were traceable to the maintenance of such matériel in accordance with standard instructions which prove to be incorrect or incomplete, such as instructions governing the type of protective coating to cover duralumin parts when operating as a seaplane, etc.

2. FAULTY INSPECTION.—This includes all accidents resulting from matériel failures which were traceable to errors or omissions in the inspection of such matériel.

(a) FAULTY MANUFACTURING INSPECTION.—This includes all accidents traceable to faulty inspection of matériel where such errors or omissions occurred prior to the receipt of this matériel by the consumer.

(b) FAULTY OVERHAUL INSPECTION.—This includes all accidents traceable to faulty inspection of matériel where such errors or omissions occurred during overhaul or storage of the matériel.

(c) FAULTY MAINTENANCE INSPECTION.—This includes all accidents traceable to faulty inspection of matériel where such errors or omissions in inspection occurred after the final delivery of this matériel to the operating unit.

(d) FAULTY INSPECTION, INDETERMINATE.—This includes all accidents traceable to faulty inspection of matériel where actual responsibility for the errors or omissions in inspection can not be definitely placed.

3. FAULTY MATERIALS.—This includes all accidents resulting from matériel failures which were traceable to defective materials when such defects in materials could not reasonably have been detected and eliminated by a proper system of inspection.

(a) ORIGINALLY DEFECTIVE MATERIALS.—This includes all accidents traceable to faulty materials where the materials contained such defects when originally delivered.

(b) DETERIORATED MATERIALS.—This includes all accidents traceable to faulty materials where the defects of such materials occurred through deterioration after delivery.

(c) FAULTY MATERIALS, INDETERMINATE.—This includes all accidents traceable to faulty materials where it is not possible to determine the actual time or place when such defects first appeared.



## II. *Material failures.*—Continued.

4. **FAULTY DESIGN.**—This includes all accidents resulting from matériel failures which were traceable to errors or omissions in the original design of such matériel.

(a) **FAULTY DESIGN, ORIGINAL.**—This includes all accidents traceable to faulty design where such errors or omissions in design occurred in the original design of such matériel, or in the course of changes initiated or directed by persons having recognized authority regarding design or construction.

(1) **FAULTY ORIGINAL DESIGN, STRUCTURAL STRENGTH.**

(2) **FAULTY ORIGINAL DESIGN, ARRANGEMENT.**

(3) **FAULTY ORIGINAL DESIGN, AERODYNAMIC.**

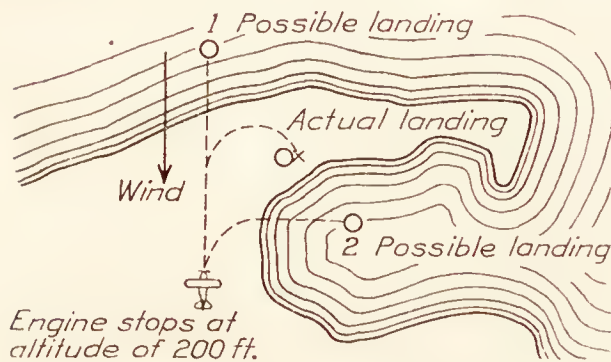
(4) **FAULTY ORIGINAL DESIGN, INDETERMINATE.**

(b) **FAULTY DESIGN, MODIFICATION.**—This includes all accidents traceable to faulty design where such errors or omissions in design occurred in modifications to the original design of such matériel initiated or directed by persons not having recognized authority regarding design or construction (such as jury rigs, emergency repairs, etc.).

5. **INDETERMINATE MATÉRIEL FAILURE.**—This includes all accidents from matériel failures the exact source of which can not be determined.

### DESCRIPTION AND TYPICAL ANALYSIS OF AN ACCIDENT

Pilot John Doe was flying in a seaplane at 200 feet altitude over a point of land between a bay and the open sea when the engine stopped. Pilot Doe had an opportunity to land either directly into the wind in the open sea or cross wind in the bay. He started to land in the ocean, but at 100 feet altitude he changed his mind and attempted to turn so as to land in the bay.



In turning, Doe held the nose of the seaplane up, stalled it, and spun into the land. The seaplane was demolished, the pilot was seriously injured, and the passenger was killed.

Doe, according to his record, was an experienced aviator with 30 hours' flying during the preceding month and with recent experience in stunting seaplanes.

Examination of the engine showed that one of the teeth in the magneto timing gear had stripped, the broken tooth having been drawn into the other teeth, causing the eventual stripping of all teeth. The original break was determined to be a visible hardening crack.

The NATURE of this accident is Class C—Tail spin following engine failure, as defined on page 9. The classification according to RESULTS is Personnel, Class BA (p. 10); Matériel, Class A.

In analyzing this accident the IMMEDIATE CAUSE is charged, as indicated on the analysis chart, as 75 per cent "Personnel" and 25 per cent "Matériel," for the reason that the account of the accident shows that the pilot had two chances to make a safe landing and took advantage of neither of them. Considering the 75 per cent which is charged to "Personnel," it is obvious that this is chargeable neither to "Errors of supervisory personnel" nor to "Errors of other personnel," so that the whole weight, 75 per cent, must be placed under "Errors of pilot." It appears further that the errors of the pilot involved errors of judgment in that he lost altitude while wavering indecisively between landing in the ocean and attempting to land in the bay. It appears that poor technique was the most important single factor in that he continued to pull the nose up, still further stalling the seaplane, when he should have sensed the approaching stall. It is considered that a charge of 35 per cent to "Error of judgment" and 40 per cent to "Poor technique" represents as near an approximation as can be arrived at in this case.



Approved by Executive Committee N. A. C. A., October 3, 1928

On analysis of UNDERLYING CAUSES it would appear that the "Error of judgment" and "Poor technique" were both due to a "Temporary poor reaction" with a strong possibility of such "Poor reaction" being "Inherent" rather than "Temporary." However, in the absence of a history of the individual this would have to be classified as "Temporary."

Considering the 25 per cent charged to "II. Matériel," the entire 25 per cent obviously should be assigned to "1. Power-plant failure," in the second order of subdivision, and again, in the third order of subdivision the entire 25 per cent should be charged to "(c) Ignition system."

The underlying cause of this matériel failure is unquestionably faulty manufacturing and accordingly on the cross analysis it would be placed under the head of "Manufacturing inspection."

#### CONCLUSION AND RECOMMENDATIONS

The special committee on the nomenclature, subdivision, and classification of aircraft accidents, having studied in considerable detail the problem of classifying and analyzing the causes of aircraft accidents, at its final meeting held on July 17, 1928, unanimously adopted a resolution approving this report and recommending that it be published by the National Advisory Committee for Aeronautics and that copies be transmitted to the War, Navy, and Commerce Departments with a recommendation that the proposed method of analysis of aircraft accidents outlined in the report be adopted for use in their respective services. The special committee recommends further that copies of the report be transmitted also to the appropriate representatives of the various interested foreign governments with a request that they cooperate by contributing information from time to time in relation to aircraft accidents.

With the submission of this report the work of the special committee is concluded and it should be discharged. It is probable, however, that the introduction of the proposed chart for the analysis of accidents will result in questions as to interpretation and suggestions for changes, many of which, it is believed, have been considered during the meetings of the committee. It is also probable that study of the information obtained from the application of the method of analysis will indicate that certain features in aircraft construction or operation should be given more detailed study or consideration. The committee therefore at its final meeting adopted a resolution recommending that its present personnel be reorganized into a standing committee on aircraft accidents of the National Advisory Committee for Aeronautics for the purpose of considering from time to time such new matter regarding aircraft accidents as may appear desirable or as may be brought before it.

Respectfully submitted.

23  
SPECIAL COMMITTEE ON THE NOMENCLATURE, SUBDIVISION,  
AND CLASSIFICATION OF AIRCRAFT ACCIDENTS.

GEORGE K. BURGESS, *Chairman*.

WASHINGTON, D. C., August 15, 1928.























SMITHSONIAN LIBRARIES



3 9088 01800 8466